Београд, 6. децембра 2018. године

Научном већу Института за физику

Предмет: Молба за покретање поступка за стицање звања научни саветник

Молим Научно веће Института за физику да, у складу са Правилником о поступку и начину вредновања и квантитативном исказивању научноистраживачких резултата истраживача, покрене поступак за мој избор у звање научни саветник. Сва остала документа потребна за даљи поступак ћу благовремено доставити.

Са поштовањем,

Саша Лазовић

др Саша Лазовић,

научни сарадник

Научном већу Института за физику у Београду

Предмет: Мишљење руководиоца пројекта о избору др Саше Лазовића у звање научни саветник

Др Саша Лазовић је запослен на Институту за физику у Београду од 1.1.2007. године. Руководилац је Лабораторије за биомиметику, у оквиру Националног центра изузетних вредности за изучавање комплексних система и ангажован је на пројекту интегрисаних интердисциплинарних истраживања Министарства просвете, науке и технолошког развоја Републике Србије ИИИ43007 „Истраживање климатских промена и њиховог утицаја на животну средину - праћење утицаја, адаптација и ублажавање“, у оквиру потпројекта 4 под називом "Имплементација нумеричких модела на рачунарским ресурсима високих перформанси", под мојим руководством. На поменутом пројекту ради на темама везаним за пречишћавање вода применом напредних оксидативних процеса, биомедицинске примене плазме, као и за карактеризацију и модификацију нових материјала. С обзиром да испуњава све предвиђене услове у складу са Правилником о поступку, начину вредновања и квантитативном исказивању научноистраживачких резултата истраживача МПНТР, сагласан сам са покретањем поступка за избор др Саше Лазовића у звање научни саветник.

За састав комисије за избор др Саше Лазовића у звање научни саветник предлажем:

(1) др Александар Богојевић, научни саветник, Институт за физику у Београду
(2) др Стеван Стојадиновић, редовни професор, Физички факултет у Београду
(3) др Михајло Мудринић, научни саветник, Институт за нуклеарне науке "Винча"

Руководилац пројекта

др Александар Богојевић
научни саветник

Sasa Lazovic

Institute of Physics Belgrade
, University of Belgrade
Physics

	All	Since 2013
Citations	508	456
h-index	13	13
i10-index	15	14

TITLE	CITED BY	YEAR
Bactericidal efficiency of silver nanoparticles deposited onto radio frequency plasma pretreated polyester fabrics V Ilic, Z Šaponjić, V Vodnik, S Lazović, S Dimitrijevic, P Jovancic, ... Industrial & Engineering Chemistry Research 49 (16), 7287-7293	66	2010
Functionalization of cotton fabrics with corona/air RF plasma and colloidal TiO_2 nanoparticles D Mihailović, Z Šaponjić, M Radoičić, S Lazović, CJ Baily, P Jovančić, ... Cellulose 18 (3), 811-825	65	2011
The effect of a plasma needle on bacteria in planktonic samples and on peripheral blood mesenchymal stem cells S Lazović, N Puač, M Miletić, D Pavlica, M Jovanović, D Bugarski, ... New Journal of Physics 12 (8), 083037	52	2010
Time resolved optical emission images of an atmospheric pressure plasma jet with transparent electrodes N Puač, D Maletić, S Lazović, G Malović, A Đorđević, ZL Petrović Applied Physics Letters 101 (2), 024103	49	2012
Spectroscopic ellipsometry of few-layer graphene G Isic, M Jakovljevic, M Filipovic, DM Jovanovic, B Vasic, S Lazovic, ... Journal of Nanophotonics 5 (1), 051809	30	2011
Effects of non-thermal atmospheric plasma on human periodontal ligament mesenchymal stem cells M Miletić, S Mojsilović, IO Đorđević, D Maletić, N Puač, S Lazović, ... Journal of physics D: Applied physics 46 (34), 345401	29	2013
Time-resolved optical emission imaging of an atmospheric plasma jet for different electrode positions with a constant electrode gap D Maletić, N Puač, N Selaković, S Lazović, G Malović, A Đorđević, ... Plasma Sources Science and Technology 24 (2), 025006	25	2015
Detection of atomic oxygen and nitrogen created in a radio-frequency-driven micro-scale atmospheric pressure plasma jet using mass spectrometry D Maletić, N Puač, S Lazović, G Malović, T Gans, ... Plasma Physics and controlled fusion 54 (12), 124046	25	2012
Characterization and global modelling of low-pressure hydrogen-based RF plasmas suitable for surface cleaning processes N Škoro, N Puač, S Lazović, U Cvelbar, G Kokkoris, E Gogolides Journal of Physics D: Applied Physics 46 (47), 475206	22	2013
Mass analysis of an atmospheric pressure plasma needle discharge G Malović, N Puač, S Lazović, Z Petrović Plasma Sources Science and Technology 19 (3), 034014	22	2010

TITLE	CITED BY	YEAR
WO 3/TiO 2 composite coatings: Structural, optical and photocatalytic properties Z Dohčević-Mitrović, S Stojadinović, L Lozzi, S Aškrabić, M Rosić, ... Materials Research Bulletin 83, 217-224	21	2016
Plasma induced DNA damage: Comparison with the effects of ionizing radiation S Lazović, D Maletić, A Leskovac, J Filipović, N Puač, G Malović, G Joksić, ... Applied Physics Letters 105 (12), 124101	18	2014
Plasma seeds treatment as a promising technique for seed germination improvement I Filatova, V Azharonok, V Lushkevich, A Zhukovsky, G Gadzhieva, ... Proceeding of the 31st International Conference on Phenomena in Ionized Gases	17	2013
Sterilization of bacteria suspensions and identification of radicals deposited during plasma treatment N Puac, M Miletic, M Mojovic, A Popovic-Bijelic, D Vukovic, B Milicic, ... Open Chemistry 13 (1)	13	2015
Biomedical applications and diagnostics of atmospheric pressure plasma ZL Petrović, N Puač, S Lazović, D Maletić, K Spasić, G Malović Journal of Physics: Conference Series 356 (1), 012001	11	2012
Plasma functionalization of titanium surface for repulsion of blood platelets U Cvelbar, M Modic, J Kovač, S Lazović, G Filipič, D Vujošević, I Junkar, ... Surface and Coatings Technology 211, 200-204	8	2012
Realization of Enhanced Magnetoelectric Coupling and Raman Spectroscopic Signatures in 0-0 Type Hybrid Multiferroic Core-Shell Geometric Nanostructures NK Ann Rose Abraham, Balakrishnan Raneesh, Tesfakiros Woldu, Sonja Aškrabić ... The Journal of Physical Chemistry C 121 (8), pp 4352–4362	7	2017
Mass spectrometry of diffuse coplanar surface barrier discharge S Lazovic, N Puac, N Radic, T Hoder, G Malovic, J Ráhel, M Cernak, ... Publications de l'Observatoire Astronomique de Beograd 84, 401-404	5	2008
The impact of concentration and administration time on the radiomodulating properties of undecylprodigiosin in vitro AL Sandra Petrović, Vesna Vasić, Tatjana Mitrović, Saša Lazović Archives of Industrial Hygiene and Toxicology 68 (1), 1-7	4	2017
Plasma properties in a large-volume, cylindrical and asymmetric radio-frequency capacitively coupled industrial-prototype reactor S Lazović, N Puač, K Spasić, G Malović, U Cvelbar, M Mozetič, M Radetić, ... Journal of Physics D: Applied Physics 46 (7), 075201	4	2013
Application of non-equilibrium plasmas in medicine ZL Petrović, N Puač, G Malović, S Lazović, D Maletić, M Miletić, ... Journal of the Serbian Chemical Society 77 (12), 1689-1699	4	2012
Diagnostic of plasma needle properties by using mass spectrometry S Lazovic, N Puac, G Malovic, A Đor-dvic, ZL Petrovic Chem. Listy 102, 1383	4	2008

TITLE	CITED BY	YEAR
Inhibition of methicillin resistant *Staphylococcus aureus* by a plasma needle M Miletić, D Vuković, I Živanović, I Dakić, I Soldatović, D Maletić, ... Central European Journal of Physics 12 (3), 160-167	3	2014
Microplasma Induced Cell Morphological Changes and Apoptosis of Ex Vivo Cultured Human Anterior Lens Epithelial Cells–Relevance to Capsular Opacification N Recek, S Andjelić, N Hojnik, G Filipič, S Lazović, A Vesel, G Primc, ... PloS one 11 (11), e0165883	2	2016
Langmuir probe measurements of a large scale RF asymmetric capacitive coupled plasma S Lazović, N Puač, G Malović, ZL Petrović Cancun, Mexico, 29thICPIG, 12-17	1	2009
Time-resolved images of plasma bullet for different electrode geometries D Maletić, N Puač, N Selaković, S Lazović, G Malović, A Đorđević, ...	1	
Virtual water quality monitoring at inactive monitoring sites using Monte Carlo optimized artificial neural networks: A case study of Danube River (Serbia) T Mitrović, D Antanasijević, S Lazović, A Perić-Grujić, M Ristić Science of The Total Environment		2018
Plasma effects on the bacteria Escherichia coli via two evaluation methods D VUJOŠEVIĆ, U CVELBAR, U REPNIK, M Modic, S LAZOVIĆ, ... Plasma Science and Technology 19 (7), 075504		2017
Utjecaj koncentracije i vremena administracije na radiomodulirajuća svojstva undecilprodigozina in vitro S Petrović, V Vasić, T Mitrović, S Lazović, A Leskovac Arhiv za higijenu rada i toksikologiju 68 (1), 1-7		2017
Biological effects of bacterial pigment undecylprodigiosin on human blood cells treated with atmospheric gas plasma in vitro S Lazović, A Leskovac, S Petrović, L Senerovic, N Krivokapić, T Mitrović, ... Experimental and Toxicologic Pathology 69 (1), 55-62		2017
Effect of dissipated power due to antenna resistive heating on E-to H-mode transition in inductively coupled oxygen plasma N Puač, S Lazović, R Zaplotnik, M Mozetič, ZL Petrović, U Cvelbar Indian Journal of Physics 89 (6), 635-640		2015
PLASMA NEEDLE DECOLOURISATION OF DIRECT RED (DR 28) DIAZO DYE T Mitrović, N Božović, N Tomić, Z Dohčević-Mitrović, D Maletić, S Lazović, ... 20 th Symposium on Application of Plasma Processes, 245		2015
Decolorization of azodyes using the atmospheric pressure plasma jet S Lazovic, D Maletic, N Tomic, G Malovic, U Cvelbar, Z Dohcevic-Mitrovic, ... APS Meeting Abstracts		2013
Diagnostics and applications of high frequency discharges with focus on plasma treatment of human periodontal stem cells N Puač, D Maletić, M Miletić, S Mojsilović, S Lazović, G Malović, ... 31st ICPIG, July, 14-19		2013

TITLE	CITED BY	YEAR
Time resolved images of plasma bullet for different electrode gaps D Maletić, N Puač, N Selaković, S Lazović, G Malović, ZL Petrović Plasma Science (ICOPS), 2012 Abstracts IEEE International Conference on, 1P …		2012
Development of biomedical applications of non-equilibrium plasmas and possibilities for atmospheric pressure nanotechnology applications ZL Petrović, N Puač, D Marić, D Maletić, K Spasić, N Škoro, J Sivoš, ... Microelectronics (MIEL), 2012 28th International Conference on, 31-38		2012
Diagnostics and biomedical applications of radiofrequency plasmas S Lazović Journal of Physics: Conference Series 399 (1), 012015		2012
Time resolved ICCD images of an atmospheric pressure plasma jet N Puac, D Maletic, S Lazovic, G Malovic, A Djordjevic, Z Petrovic APS Meeting Abstracts		2011
Catalytic probe measurements in a large scale CCP reactor S Lazovic, K Spasic, N Puac, G Malovic, U Cvelbar, M Mozetic, Z Petrovic APS Meeting Abstracts		2011
Electrical characteristics of an atmospheric pressure plasma jet with helium flow G Malovic, D Maletic, N Puac, S Lazovic, A Djordjevic, Z Petrovic Bulletin of the American Physical Society 55		2010
Spatial Profiles Of Electron And Ion Concentrations In A Large Size Ccp Discharge Obtained By Using A Langmuir Probe S LAZOVIĆ, N PUAČ, G MALOVIĆ Publications de l'Observatoire Astronomique de Beograd 89, 205-208		2010
Plasma needle treatment of bacteria known to cause infections of the soft tissue of the oral region and bones D Maletic, S Lazovic, N Puac, G Malovic, ZL Petrovic, MP Miletic, ... APS Meeting Abstracts		2009
Mass spectrometry of radicals created in plasma needle discharge S Lazovic, N Puac, G Malovic, A Djordjevic, ZL Petrovic APS Meeting Abstracts		2008
Mass spectrometry of a plasma needle with an external grounded copper ring S Lazovic, N Puac, G Malovic, ZL Petrovic Publications de l'Observatoire Astronomique de Beograd 84, 397-400		2008
Electrical characteristics and comparison of two configurations of plasma needle G Malovic, N Puac, S Lazovic, A Djordjevic, Z Petrovic APS Meeting Abstracts		2007
Non-thermal plasma for revalorization of a complex waste substrate in open lactic acid fermentation A Djukić-Vuković, S Lazović, D Mladenović, Z Knežević-Jugović, J Pejin, ...		
Treatment of Paulownia tomentosa seeds in the low pressure CCP reactor S Lazović, N Puač, D Maletić, S Živković, Z Giba, U Cvelbar, M Mozetič, ... Orléans-France, 207		

TITLE	CITED BY	YEAR

전극물질에 따른 단전극 대기압 제트 플라즈마 스트리머 동역학 연구
SH Park, S Lazovic, HS Jeong, GB Chae, U Cvelbar, WH Choe
Proceedings of the Korean Vacuum Society Conference

Plasma needle treatment of Staphylococcus Aureus (ATCC 25923) biofilms
D Maletić, M Miletić, N Puač, N Selaković, S Lazović, D Vuković, ...
Orléans-France, 194

DIAGNOSTICS AND APPLICATIONS OF HIGH FREQUENCY DISCHARGES IN BIOMEDICAL TREATMENTS AND TREATMENT OF TEXTILES
N Puač, S Lazović, G Malović, M Radetić, M Miletić, S Mojsilović, ...

CURRENT-VOLTAGE CHARACTERISTICS OF μ-APPJ OBTAINED BY USING DERIVATIVE PROBES
S Lazović, D Maletić, N Puač, G Malović, A Đorđević, ZL Petrović

Characterization of a large scale RF CCP reactor using Langmuir and derivative probes
S Lazović, N Puač, K Spasić, G Malović, ZL Petrović

Characterization of plasma needle with an additional grounded ring
S Lazović, N Puač, G Malović, AR Đorđević, ZL Petrović

Time resolved images of an atmospheric pressure plasma bullet
D Maletić, S Lazović, N Puač, G Malović, A Đorđević, ZL Petrović

Mass spectrometric detection of N, O and NO radicals and ions generated by a plasma needle
S Lazović, N Puač, D Maletić, G Malović, ZL Petrović

Characterisation of the plasma needle by using derivative probes and fast ICCD camera
N Puač, S Lazović, G Malović, A Đorđević, ZL Petrović

CURRENT–VOLTAGE CHARACTERISTICS OF ATMOSPHERIC PRESSURE PLASMA JET
N PUAČ, D MALETIĆ, S LAZOVIĆ, G MALOVIĆ, A ĐORĐEVIĆ

MASS-ENERGY SPECTROMETRY DETECTION OF MOLECULE AND ATOMIC RADICALS FORMED BY μ-APPJ
D Maletić, S Lazović, N Puač, G Malović, ZL Petrović

THE INFLUENCE OF THE GAS FLOW ON PROPERTIES OF A PLASMA NEEDLE
S Lazović, N Puač, G Malović, A Đorđević, ZL Petrović

Measurements of atomic oxygen concentrations in a large scale asymmetric capacitively coupled plasma reactor by using catalytic probes
S Lazović, N Puač, K Spasić, G Malović, U Cvelbar, M Mozetič, ...

Spatial profiles of atomic oxygen concentrations in a large scale CCP reactor
S Lazović, K Spasić, N Puač, G Malović, U Cvelbar, M Mozetič, ...

TITLE	CITED BY	YEAR

Plasma modification of titanium for repulsion of blood platelets
U Cvelbar, M Modic, I Junkar, S Lazović, M Mozetic

Sasa Lazovic

Institute of Physics Belgrade

ResearcherID: Q-5056-2016

ORCiD: 0000-0003-1696-9134

PUBLICATIONS	TOTAL TIMES CITED	H-INDEX	VERIFIED REVIEWS
28	359	11	25

Research Fields

PLASMA MEDICINE PLASMA PHYSICS

+ VIEW FULL BIO & INSTITUTIONS

Web of Science

Citation report for 29 results from Web of Science Core Collection between 2008 and 2018 Go

You searched for: **AUTHOR:** (Lazovic S*)
Refined by: AUTHORS: (LAZOVIC S)
Timespan: 2008-2018. **Indexes:** SCI-EXPANDED, SSCI, A&HCI, CPCI-S, CPCI-SSH, ESCI.
...Less

This report reflects citations to source items indexed within Web of Science Core Collection. Perform a Cited Reference Search to include citations to items not indexed within Web of Science Core Collection.

Export Data: Save to Excel File

Total Publications
29 Analyze

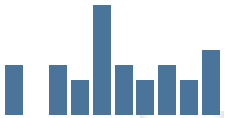

h-index
11

Average citations per item
12.41

Sum of Times Cited
360

Without self citations
309

Citing articles
280 Analyze

Without self citations
263 Analyze

Sum of Times Cited per Year

Close

Web of Science
Page 1 (Records 1 -- 10)
[1 | 2 | 3]

Print

AUTHOR: (Lazovic S*)
Refined by: AUTHORS=(LAZOVIC S)
Timespan=2008-2018. Indexes=SCI-EXPANDED, SSCI, A&HCI, CPCI-S, CPCI-SSH, ESCI.

Total Publications by Year

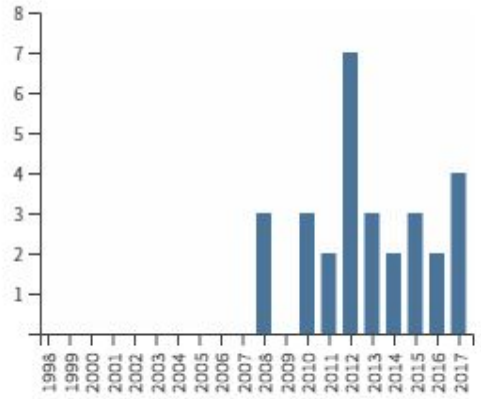

Sum of Times Cited by Year

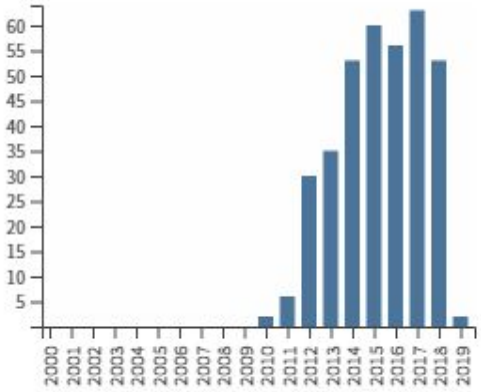

Results found:	29
Sum of the Times Cited:	360
Average Citations per Item:	12.41
h-index:	11

2015	2016	2017	2018	2019	Total	Average Citations per Year

		60 2015	56 2016	63 2017	53 2018	2 2019	360 Total	40.00 Average Citations per Year
		60	**56**	**63**	**53**	**2**	**360**	**40.00**
1.	**Title:** Functionalization of cotton fabrics with corona/air RF plasma and colloidal TiO2 nanoparticles **By:** Mihailovic, D.; Saponjic, Z.; Radoicic, M.; et al. **Source:** CELLULOSE **Volume:** 18 **Issue:** 3 **Pages:** 811-825 **Published:** JUN 2011	11	8	7	6	0	45	5.63
2.	**Title:** Bactericidal Efficiency of Silver Nanoparticles Deposited onto Radio Frequency Plasma Pretreated Polyester Fabrics **By:** Ilic, Vesna; Saponjic, Zoran; Vodnik, Vesna; et al. **Source:** INDUSTRIAL & ENGINEERING CHEMISTRY RESEARCH **Volume:** 49 **Issue:** 16 **Pages:** 7287-7293 **Published:** AUG 18 2010	7	4	3	1	0	42	4.67
3.	**Title:** Time resolved optical emission images of an atmospheric pressure plasma jet with transparent electrodes **By:** Puac, N.; Maletic, D.; Lazovic, S.; et al. **Source:** APPLIED PHYSICS LETTERS **Volume:** 101 **Issue:** 2 **Article Number:** 024103 **Published:** JUL 9 2012	8	8	7	4	0	39	5.57
4.	**Title:** The effect of a plasma needle on bacteria in planktonic samples and on peripheral blood mesenchymal stem cells **By:** Lazovic, Sasa; Puac, Nevena; Miletic, Maja; et al. **Source:** NEW JOURNAL OF PHYSICS **Volume:** 12 **Article Number:** 083037 **Published:** AUG 17 2010	8	5	5	2	0	39	4.33
5.	**Title:** Mass analysis of an atmospheric pressure plasma needle discharge **By:** Malovic, G.; Puac, N.; Lazovic, S.; et al. **Conference:** 29th International Conference on Phenomena in Ionized Gases **Location:** Cancun, MEXICO **Date:** JUL 12-17, 2009 **Sponsor(s):** Univ Nacl Autonoma Mexico; Univ Autonoma Metropolitana; Int Union Pure & Appl Phys **Source:** PLASMA SOURCES SCIENCE & TECHNOLOGY **Volume:** 19 **Issue:** 3 **Article Number:** 034014 **Published:** JUN 2010	3	4	2	2	0	29	3.22

		2015	2016	2017	2018	2019	Total	Average Citations per Year
		60	**56**	**63**	**53**	**2**	**360**	**40.00**
6.	**Title:** Characterization and global modelling of low-pressure hydrogen-based RF plasmas suitable for surface cleaning processes **By:** Skoro, Nikola; Puac, Nevena; Lazovic, Sasa; et al. **Source:** JOURNAL OF PHYSICS D-APPLIED PHYSICS **Volume:** 46 **Issue:** 47 **Article Number:** 475206 **Published:** NOV 27 2013	3	7	2	6	0	20	3.33
7.	**Title:** Detection of atomic oxygen and nitrogen created in a radio-frequency-driven micro-scale atmospheric pressure plasma jet using mass spectrometry **By:** Maletic, D.; Puac, N.; Lazovic, S.; et al. **Conference:** 39th European-Physical-Society Conference on Plasma Physics **Location:** Stockholm, SWEDEN **Date:** JUL 02-06, 2012 **Source:** PLASMA PHYSICS AND CONTROLLED FUSION **Volume:** 54 **Issue:** 12 **Article Number:** 124046 **Part:** 1-2 **Published:** DEC 2012	2	2	6	2	0	19	2.71
8.	**Title:** Spectroscopic ellipsometry of few-layer graphene **By:** Isic, Goran; Jakovljevic, Milka; Filipovic, Marko; et al. **Source:** JOURNAL OF NANOPHOTONICS **Volume:** 5 **Article Number:** 051809 **Published:** JUN 8 2011	1	3	3	4	0	19	2.38
9.	**Title:** Time-resolved optical emission imaging of an atmospheric plasma jet for different electrode positions with a constant electrode gap **By:** Maletic, D.; Puac, N.; Selakovic, N.; et al. **Source:** PLASMA SOURCES SCIENCE & TECHNOLOGY **Volume:** 24 **Issue:** 2 **Article Number:** 025006 **Published:** APR 2015	3	6	2	7	0	18	4.50

		2015	2016	2017	2018	2019	Total	Average Citations per Year
		60	56	63	53	2	360	40.00
10.	**Title:** Effects of non-thermal atmospheric plasma on human periodontal ligament mesenchymal stem cells **By:** Miletic, M.; Mojsilovic, S.; Dordevic, I. Okic; et al. **Source:** JOURNAL OF PHYSICS D-APPLIED PHYSICS **Volume:** 46 **Issue:** 34 **Article Number:** 345401 **Published:** AUG 28 2013	3	3	5	1	0	18	3.00

Close

Web of Science
Page 1 (Records 1 -- 10)
◀ [1 | 2 | 3] ▶

Print

		2015	2016	2017	2018	2019	Total	Average Citations per Year
		60	56	63	53	2	360	40.00
11.	**Title:** Plasma induced DNA damage: Comparison with the effects of ionizing radiation **By:** Lazovic, S.; Maletic, D.; Leskovac, A.; et al. **Source:** APPLIED PHYSICS LETTERS **Volume:** 105 **Issue:** 12 **Article Number:** 124101 **Published:** SEP 22 2014	6	3	5	0	1	16	3.20
12.	**Title:** WO3/TiO2 composite coatings: Structural, optical and photocatalytic properties **By:** Dohcevic-Mitrovic, Zorana; Stojadinovic, Stevan; Lozzi, Luca; et al. **Source:** MATERIALS RESEARCH BULLETIN **Volume:** 83 **Pages:** 217-224 **Published:** NOV 2016	0	0	3	7	0	10	3.33
13.	**Title:** Sterilization of bacteria suspensions and identification of radicals deposited during plasma treatment **By:** Puac, Nevena; Miletic, Maja; Mojovic, Milos; et al. **Source:** OPEN CHEMISTRY **Volume:** 13 **Issue:** 1 **Pages:** 332-338 **Published:** JAN 2015	3	2	3	2	0	10	2.50
14.	**Title:** Plasma functionalization of titanium surface for repulsion of blood platelets **By:** Cvelbar, U.; Modic, M.; Kovac, J.; et al. **Conference:** Symposium K on Protective Coatings and Thin Films held at the European-Materials-Research-Society Spring Meeting (E-MRS) **Location:** Nice, FRANCE **Date:** MAY 09-13, 2011 **Sponsor(s):** European Mat Res Soc (E-MRS); French Minist Educ & Res **Source:** SURFACE & COATINGS TECHNOLOGY **Volume:** 211 **Pages:** 200-204 **Published:** OCT 25 2012	2	1	1	1	0	7	1.00
15.	**Title:** Biomedical applications and diagnostics of atmospheric pressure plasma **By:** Petrovic, Z. Lj; Puac, N.; Lazovic, S.; et al. **Edited by:** VanDeSanden, MCM; Dimitrova, M; Ghelev, C **Conference:** 17th International Summer School on Vacuum, Electron, and Ion Technologies (VEIT) **Location:** BULGARIA **Date:** SEP 19-23, 2011 **Sponsor(s):** Eindhoven Univ Technol, Dept Appl Phys **Source:** 17TH INTERNATIONAL SUMMER SCHOOL ON VACUUM, ELECTRON, AND ION TECHNOLOGIES (VEIT 2011) **Book Series:** Journal of Physics Conference Series **Volume:** 356 **Article Number:** 012001 **Published:** 2012	0	0	2	0	0	7	1.00

		2015	2016	2017	2018	2019	Total	Average Citations per Year
		60	56	63	53	2	360	40.00
16.	**Title:** Realization of Enhanced Magnetoelectric Coupling and Raman Spectroscopic Signatures in 0-0 Type Hybrid Multiferroic Core-Shell Geometric Nanostructures **By:** Abraham, Ann Rose; Raneesh, B.; Woldu, Tesfakiros; et al. **Source:** JOURNAL OF PHYSICAL CHEMISTRY C **Volume:** 121 **Issue:** 8 **Pages:** 4352-4362 **Published:** MAR 2 2017	0	0	1	4	1	6	3.00
17.	**Title:** Plasma properties in a large-volume, cylindrical and asymmetric radio-frequency capacitively coupled industrial-prototype reactor **By:** Lazovic, Sasa; Puac, Nevena; Spasic, Kosta; et al. **Source:** JOURNAL OF PHYSICS D-APPLIED PHYSICS **Volume:** 46 **Issue:** 7 **Article Number:** 075201 **Published:** FEB 20 2013	0	0	1	0	0	4	0.67
18.	**Title:** Application of non-equilibrium plasmas in medicine **By:** Petrovic, Zoran Lj.; Puac, Nevena; Malovic, Gordana; et al. **Source:** JOURNAL OF THE SERBIAN CHEMICAL SOCIETY **Volume:** 77 **Issue:** 12 **Pages:** 1689-1699 **Published:** 2012	0	0	2	0	0	4	0.57
19.	**Title:** The impact of concentration and administration time on the radiomodulating properties of undecylprodigiosin in vitro **By:** Petrovic, Sandra; Vasic, Vesna; Mitrovic, Tatjana; et al. **Source:** ARHIV ZA HIGIJENU RADA I TOKSIKOLOGIJU-ARCHIVES OF INDUSTRIAL HYGIENE AND TOXICOLOGY **Volume:** 68 **Issue:** 1 **Pages:** 1-8 **Published:** MAR 2017	0	0	1	2	0	3	1.50
20.	**Title:** DIAGNOSTIC OF PLASMA NEEDLE PROPERTIES BY USING MASS SPECTROMETRY **By:** Lazovic, Sasa; Puac, Nevena; Malovic, Gordana; et al. **Source:** CHEMICKE LISTY **Volume:** 102 **Special Issue:** SI **Supplement:** 4 **Pages:** S1383-S1387 **Published:** 2008	0	0	1	0	0	2	0.18

Close

Web of Science
Page 2 (Records 11 -- 20)
[1 | 2 | 3]

Print

		60	56	63	53	2	360	40.00
		2015	2016	2017	2018	2019	Total	Average Citations per Year
		60	56	63	53	2	360	40.00
21.	**Title:** Microplasma Induced Cell Morphological Changes and Apoptosis of Ex Vivo Cultured Human Anterior Lens Epithelial Cells - Relevance to Capsular Opacification **By:** Recek, Nina; Andjelic, Sofija; Hojnik, Nataga; et al. **Source:** PLOS ONE **Volume:** 11 **Issue:** 11 **Article Number:** e0165883 **Published:** NOV 10 2016	0	0	0	1	0	1	0.33
22.	**Title:** Inhibition of methicillin resistant Staphylococcus aureus by a plasma needle **By:** Miletic, Maja; Vukovic, Dragana; Zivanovic, Irena; et al. **Source:** CENTRAL EUROPEAN JOURNAL OF PHYSICS **Volume:** 12 **Issue:** 3 **Pages:** 160-167 **Published:** MAR 2014	0	0	1	0	0	1	0.20
23.	**Title:** MASS SPECTROMETRY OF DIFFUSE COPLANAR SURFACE BARRIER DISCHARGE **By:** Lazovic, S.; Puac, N.; Radic, N.; et al. **Edited by:** Malovic, G; Popovic, LC; Dimitrijevic, MS **Conference:** 24th Summer School and International Symposium on Physics of Ionized Gases **Location:** Novi Sad, SERBIA **Date:** AUG 25-29, 2008 **Source:** 24TH SUMMER SCHOOL AND INTERNATIONAL SYMPOSIUM ON THE PHYSICS OF IONIZED GASES, CONTRIBUTED PAPERS **Book Series:** Publications of the Astronomical Observatory of Belgrade Series **Issue:** 84 **Pages:** 401-+ **Published:** 2008	0	0	0	1	0	1	0.09
24.	**Title:** Plasma effects on the bacteria Escherichia coli via two evaluation methods **By:** Vujosevic, Danijela; Cvelbar, Uros; Repnik, Urska; et al. **Source:** PLASMA SCIENCE & TECHNOLOGY **Volume:** 19 **Issue:** 7 **Article Number:** UNSP 075504 **Published:** JUL 1 2017	0	0	0	0	0	0	0.00
25.	**Title:** Biological effects of bacterial pigment undecylprodigiosin on human blood cells treated with atmospheric gas plasma in vitro **By:** Lazovic, Sasa; Leskovac, Andreja; Petrovic, Sandra; et al. **Source:** EXPERIMENTAL AND TOXICOLOGIC PATHOLOGY **Volume:** 69 **Issue:** 1 **Pages:** 55-62 **Published:** JAN 2017	0	0	0	0	0	0	0.00

		2015	2016	2017	2018	2019	Total	Average Citations per Year
		60	56	63	53	2	360	40.00
26.	**Title:** Effect of dissipated power due to antenna resistive heating on E- to H-mode transition in inductively coupled oxygen plasma **By:** Puac, N.; Lazovic, S.; Zaplotnik, R.; et al. **Source:** INDIAN JOURNAL OF PHYSICS **Volume:** 89 **Issue:** 6 **Pages:** 635-640 **Published:** JUN 2015	0	0	0	0	0	0	0.00
27.	**Title:** Diagnostics and biomedical applications of radiofrequency plasmas **By:** Lazovic, Sasa **Edited by:** Kuraica, M; Mijatovic, Z **Conference:** 26th Summer School and International Symposium on the Physics of Ionized Gases (SPIG) **Location:** Zrenjanin, SERBIA **Date:** AUG 27-31, 2012 **Sponsor(s):** Sci & Technol Dev Republ Serbia, Minist Educ; Prov Secretariat Sci & Technol Dev; Inst Francais Serbie; Biser Zrenjanin **Source:** 26TH SUMMER SCHOOL AND INTERNATIONAL SYMPOSIUM ON THE PHYSICS OF IONIZED GASES (SPIG 2012) **Book Series:** Journal of Physics Conference Series **Volume:** 399 **Article Number:** 012015 **Published:** 2012	0	0	0	0	0	0	0.00
28.	**Title:** Development of Biomedical Applications of Non-equilibrium Plasmas and Possibilities for Atmospheric Pressure Nanotechnology Applications **By:** Petrovic, Z. Lj; Puac, N.; Maric, D.; et al. **Conference:** 28th International Conference on Microelectronics (MIEL) **Location:** Nis, SERBIA **Date:** MAY 13-16, 2012 **Sponsor(s):** IEEE; IEEE Serbia & Montenegro Sect - ED/SSC Chapter; IEEE Electron Devices Soc (EDS); IEEE Solid-State Circuits Soc (SSCS) **Source:** 2012 28TH INTERNATIONAL CONFERENCE ON MICROELECTRONICS (MIEL) **Book Series:** International Conference on Microelectronics-MIEL **Pages:** 31-38 **Published:** 2012	0	0	0	0	0	0	0.00

	2015	2016	2017	2018	2019	Total	Average Citations per Year
	60	56	63	53	2	360	40.00
29. **Title:** MASS SPECTROMETRY OF A PLASMA NEEDLE WITH AN EXTERNAL GROUNDED COPPER RING **By:** Lazovic, S.; Puac, N.; Malovic, G.; et al. **Edited by:** Malovic, G; Popovic, LC; Dimitrijevic, MS **Conference:** 24th Summer School and International Symposium on Physics of Ionized Gases **Location:** Novi Sad, SERBIA **Date:** AUG 25-29, 2008 **Source:** 24TH SUMMER SCHOOL AND INTERNATIONAL SYMPOSIUM ON THE PHYSICS OF IONIZED GASES, CONTRIBUTED PAPERS **Book Series:** PUBLICATIONS OF THE ASTRONOMICAL OBSERVATORY OF BELGRADE--SERIES **Issue:** 84 **Pages:** 397-400 **Published:** 2008	0	0	0	0	0	0	0.00

Close

Web of Science
Page 3 (Records 21 -- 29)
[1 | 2 | 3]

Print

Close

Web of Science
Page 1 (Records 1 -- 39)
[1]

Print

Record 1 of 39
Title: Antibacterial activity of Cu-based nanoparticles synthesized on the cotton fabrics modified with polycarboxylic acids
Author(s): Markovic, D (Markovic, Darka); Deeks, C (Deeks, Christopher); Nunney, T (Nunney, Tim); Radovanovic, Z (Radovanovic, Zeljko); Radoicic, M (Radoicic, Marija); Saponjic, Z (Saponjic, Zoran); Radetic, M (Radetic, Maja)
Source: CARBOHYDRATE POLYMERS **Volume:** 200 **Pages:** 173-182 **DOI:** 10.1016/j.carbpol.2018.08.001 **Published:** NOV 15 2018
Accession Number: WOS:000443264400021
PubMed ID: 30177155
ISSN: 0144-8617
eISSN: 1879-1344

Record 2 of 39
Title: The Degradation of Cellulose by Radio Frequency Plasma
Author(s): Shepherd, LM (Shepherd, Larissa Marie); Frey, MW (Frey, Margaret Wilde)
Source: FIBERS **Volume:** 6 **Issue:** 3 **Article Number:** 61 **DOI:** 10.3390/fib6030061 **Published:** SEP 2018
Accession Number: WOS:000448397500019
ISSN: 2079-6439

Record 3 of 39
Title: UV-blocking, superhydrophobic and robust cotton fabrics fabricated using polyvinylsilsesquioxane and nano-TiO2
Author(s): Chen, DZ (Chen, Dongzhi); Mai, ZH (Mai, Zhonghua); Liu, X (Liu, Xin); Ye, DZ (Ye, Deizhan); Zhang, HW (Zhang, Hongwei); Yin, XZ (Yin, Xianze); Zhou, YS (Zhou, Yingshan); Liu, M (Liu, Min); Xu, WL (Xu, Weilin)
Source: CELLULOSE **Volume:** 25 **Issue:** 6 **Pages:** 3635-3647 **DOI:** 10.1007/s10570-018-1790-7 **Published:** JUN 2018
Accession Number: WOS:000432990300037
ISSN: 0969-0239
eISSN: 1572-882X

Record 4 of 39
Title: Development of Cotton Fabrics with Durable UV Protective and Self-cleaning Property by Deposition of Low TiO2 Levels through Sol-gel Process
Author(s): Mishra, A (Mishra, Anu); Butola, BS (Butola, Bhupendra Singh)
Source: PHOTOCHEMISTRY AND PHOTOBIOLOGY **Volume:** 94 **Issue:** 3 **Pages:** 503-511 **DOI:** 10.1111/php.12888 **Published:** MAY-JUN 2018
Accession Number: WOS:000434161500012
PubMed ID: 29349783
ISSN: 0031-8655

eISSN: 1751-1097

Record 5 of 39

Title: Advances in cellulose nanomaterials

Author(s): Kargarzadeh, H (Kargarzadeh, Hanieh); Mariano, M (Mariano, Marcos); Gopakumar, D (Gopakumar, Deepu); Ahmad, I (Ahmad, Ishak); Thomas, S (Thomas, Sabu); Dufresne, A (Dufresne, Alain); Huang, J (Huang, Jin); Lin, N (Lin, Ning)

Source: CELLULOSE **Volume:** 25 **Issue:** 4 **Pages:** 2151-2189 **DOI:** 10.1007/s10570-018-1723-5 **Published:** APR 2018

Accession Number: WOS:000428925300002

Author Identifiers:

Author	ResearcherID Number	ORCID Number
Huang, Jin	E-4537-2011	
Thomas, Prof. Sabu	G-7310-2016	0000-0003-4726-5746
Mariano, Marcos		0000-0003-2374-5198
Gopakumar, Deepu		0000-0001-9394-6302
KARGARZADEH, HANIEH		0000-0003-0137-1463

ISSN: 0969-0239

eISSN: 1572-882X

Record 6 of 39

Title: The influence of corona treatment and impregnation with colloidal TiO2 nanoparticles on biodegradability of cotton fabric

Author(s): Tomsic, B (Tomsic, Brigita); Vasiljevic, J (Vasiljevic, Jelena); Simoncic, B (Simoncic, Barbara); Radoicic, M (Radoicic, Marija); Radetic, M (Radetic, Maja)

Source: CELLULOSE **Volume:** 24 **Issue:** 10 **Pages:** 4533-4545 **DOI:** 10.1007/s10570-017-1415-6 **Published:** OCT 2017

Accession Number: WOS:000410759600032

Author Identifiers:

Author	ResearcherID Number	ORCID Number
VASILJEVIC, JELENA	H-3910-2018	0000-0002-3838-0251

ISSN: 0969-0239

eISSN: 1572-882X

Record 7 of 39

Title: Polyester Composites Reinforced with Corona-Treated Fibers from Pine, Eucalyptus and Sugarcane Bagasse

Author(s): Mesquita, RGD (de Almeida Mesquita, Ricardo Gabriel); Cesar, AAD (da Silva Cesar, Antonia Amanda); Mendes, RF (Mendes, Rafael Farinassi); Mendes, LM (Mendes, Lourival Marin); Marconcini, JM (Marconcini, Jose Manoel); Glenn, G (Glenn, Greg); Tonoli, GHD (Denzin Tonoli, Gustavo Henrique)

Source: JOURNAL OF POLYMERS AND THE ENVIRONMENT **Volume:** 25 **Issue:** 3 **Pages:** 800-811 **DOI:** 10.1007/s10924-016-0864-6 **Published:** SEP 2017

Accession Number: WOS:000407742600028

Author Identifiers:

Author	ResearcherID Number	ORCID Number
AgroNano, Rede	F-5675-2017	
tonoli, gustavo	I-4821-2013	0000-0002-6502-8974

ISSN: 1566-2543
eISSN: 1572-8900

Record 8 of 39
Title: Production of bioethanol from pre-treated cotton fabrics and waste cotton materials
Author(s): Nikolic, S (Nikolic, Svetlana); Lazic, V (Lazic, Vesna); Veljovic, D (Veljovic, Dorde); Mojovic, L (Mojovic, Ljiljana)
Source: CARBOHYDRATE POLYMERS **Volume:** 164 **Pages:** 136-144 **DOI:** 10.1016/j.carbpol.2017.01.090 **Published:** MAY 15 2017
Accession Number: WOS:000398759400017
PubMed ID: 28325310
Author Identifiers:

Author	ResearcherID Number	ORCID Number
Lazic, Vesna	O-1726-2017	0000-0001-6440-6577

ISSN: 0144-8617
eISSN: 1879-1344

Record 9 of 39
Title: Enhancement of durable photocatalytic properties of cotton/polyester fabrics using TiO2/SiO2 via one step sonosynthesis
Author(s): Li, WD (Li, Wan-Di); Gao, J (Gao, Jing); Wang, L (Wang, Lu)
Source: JOURNAL OF INDUSTRIAL TEXTILES **Volume:** 46 **Issue:** 8 **Pages:** 1633-1655 **DOI:** 10.1177/1528083716629138 **Published:** MAY 2017
Accession Number: WOS:000401733500004
ISSN: 1528-0837
eISSN: 1530-8057

Record 10 of 39
Title: Biodegradation of cotton and cotton/polyester with Ag/TiO2 nanoparticles in soil
Author(s): Milosevic, M (Milosevic, Milica); Krkobabic, A (Krkobabic, Ana); Radoicic, M (Radoicic, Marija); Saponjic, Z (Saponjic, Zoran); Radetic, T (Radetic, Tamara); Radetic, M (Radetic, Maja)
Source: CARBOHYDRATE POLYMERS **Volume:** 158 **Pages:** 77-84 **DOI:** 10.1016/j.carbpol.2016.12.006 **Published:** FEB 20 2017
Accession Number: WOS:000393252500010
PubMed ID: 28024545

Author Identifiers:

Author	ResearcherID Number	ORCID Number
Saponjic, Zoran		0000-0001-7848-6715
Radoicic, Marija		0000-0002-2644-5273
Milosevic, Milica		0000-0002-3869-5800

ISSN: 0144-8617
eISSN: 1879-1344

Record 11 of 39
Title: Deposition of nanocomposite coatings on wood using cold discharges at atmospheric pressure
Author(s): Profili, J (Profili, J.); Levasseur, O (Levasseur, O.); Koronai, A (Koronai, A.); Stafford, L (Stafford, L.); Gherardi, N (Gherardi, N.)
Source: SURFACE & COATINGS TECHNOLOGY **Volume:** 309 **Pages:** 729-737 **DOI:** 10.1016/j.surfcoat.2016.10.095 **Published:** JAN 15 2017
Accession Number: WOS:000396184400085
ISSN: 0257-8972

Record 12 of 39
Title: Development of antibacterial fabrics by treatment with Ag-doped TiO2 nanoparticles
Author(s): Aksit, A (Aksit, Aysun); Camlibel, NO (Camlibel, Nurhan Onar); Zeren, ET (Zeren, Esra Topel); Kutlu, B (Kutlu, Bengi)
Source: JOURNAL OF THE TEXTILE INSTITUTE **Volume:** 108 **Issue:** 12 **Pages:** 2046-2056 **DOI:** 10.1080/00405000.2017.1311766 **Published:** 2017
Accession Number: WOS:000410808000004
Author Identifiers:

Author	ResearcherID Number	ORCID Number
Onar, Nurhan		0000-0002-2647-4728

ISSN: 0040-5000
eISSN: 1754-2340

Record 13 of 39
Title: Preparation of highly hydrophobic cotton fabrics by modification with bifunctional silsesquioxanes in the sol-gel process
Author(s): Przybylak, M (Przybylak, Marcin); Maciejewski, H (Maciejewski, Hieronim); Dutkiewicz, A (Dutkiewicz, Agnieszka)
Source: APPLIED SURFACE SCIENCE **Volume:** 387 **Pages:** 163-174 **DOI:** 10.1016/j.apsusc.2016.06.094 **Published:** NOV 30 2016
Accession Number: WOS:000381251100020
Author Identifiers:

Author	ResearcherID Number	ORCID Number

Maciejewski, Hieronim		0000-0003-2771-3089
Przybylak, Marcin		0000-0003-4706-0898

ISSN: 0169-4332

eISSN: 1873-5584

Record 14 of 39

Title: Microwave-assisted TiO2: anatase formation on cotton and viscose fabric surfaces

Author(s): Giesz, P (Giesz, Patrycja); Celichowski, G (Celichowski, Grzegorz); Puchowicz, D (Puchowicz, Dorota); Kaminska, I (Kaminska, Irena); Grobelny, J (Grobelny, Jaroslaw); Batory, D (Batory, Damian); Cieslak, M (Cieslak, Malgorzata)

Source: CELLULOSE **Volume:** 23 **Issue:** 3 **Pages:** 2143-2159 **DOI:** 10.1007/s10570-016-0916-z **Published:** JUN 2016

Accession Number: WOS:000376086900051

Author Identifiers:

Author	ResearcherID Number	ORCID Number
Kaminska, Irena	U-8783-2018	0000-0002-5279-8902
Celichowski, Grzegorz	N-2458-2018	0000-0002-1624-3088
Cieslak, Malgorzata	B-4639-2016	0000-0001-9867-7789
Batory, Damian		0000-0002-6555-7657
Puchowicz, Dorota		0000-0001-5001-9031

ISSN: 0969-0239

eISSN: 1572-882X

Record 15 of 39

Title: Fabrication of superhydrophobic cotton fabrics by a simple chemical modification

Author(s): Przybylak, M (Przybylak, Marcin); Maciejewski, H (Maciejewski, Hieronim); Dutkiewicz, A (Dutkiewicz, Agnieszka); Dabek, I (Dabek, Izabela); Nowicki, M (Nowicki, Marek)

Source: CELLULOSE **Volume:** 23 **Issue:** 3 **Pages:** 2185-2197 **DOI:** 10.1007/s10570-016-0940-z **Published:** JUN 2016

Accession Number: WOS:000376086900054

Author Identifiers:

Author	ResearcherID Number	ORCID Number
Nowicki, Marek	N-7220-2013	
Przybylak, Marcin		0000-0003-4706-0898

ISSN: 0969-0239

eISSN: 1572-882X

Record 16 of 39

Title: Development of multifunctional cotton fabric using atmospheric pressure plasma and nano-finishing
Author(s): Palaskar, SS (Palaskar, S. S.); Desai, AN (Desai, A. N.); Shukla, SR (Shukla, S. R.)
Source: JOURNAL OF THE TEXTILE INSTITUTE **Volume:** 107 **Issue:** 3 **Pages:** 405-412 **DOI:** 10.1080/00405000.2015.1034932 **Published:** MAR 3 2016
Accession Number: WOS:000367899300014
ISSN: 0040-5000
eISSN: 1754-2340

Record 17 of 39
Title: Hybrid cotton-anatase prepared under mild conditions with high photocatalytic activity under sunlight
Author(s): Abid, M (Abid, Marwa); Bouattour, S (Bouattour, Soraa); Conceicao, DS (Conceicao, David S.); Ferraria, AM (Ferraria, Ana Maria); Ferreira, LFV (Vieira Ferreira, Luis Filipe); do Rego, AMB (Botelho do Rego, Ana Maria); Vilar, MR (Vilar, Manuel Rei); Boufi, S (Boufi, Sami)
Source: RSC ADVANCES **Volume:** 6 **Issue:** 64 **Pages:** 58957-58969 **DOI:** 10.1039/c6ra10806g **Published:** 2016
Accession Number: WOS:000379350100013
Author Identifiers:

Author	ResearcherID Number	ORCID Number
Rego, Ana	L-4670-2013	0000-0002-3131-4219
boufi, sami		0000-0002-3153-0288
Ferraria, Ana Maria		0000-0002-6784-6540
Vieira Ferreira, Luis Filipe		0000-0002-1903-5815

ISSN: 2046-2069

Record 18 of 39
Title: Superhydrophobic carbon nanotube/silicon carbide nanowire nanocomposites
Author(s): Yu, HL (Yu, Hailing); Zhu, JQ (Zhu, Jiaqi); Yang, L (Yang, Lei); Dai, B (Dai, Bing); Baraban, L (Baraban, Larysa); Cuniberti, G (Cuniberti, Gianaurelio); Han, JC (Han, Jiecai)
Source: MATERIALS & DESIGN **Volume:** 87 **Pages:** 198-204 **DOI:** 10.1016/j.matdes.2015.08.025 **Published:** DEC 15 2015
Accession Number: WOS:000363816000023
Author Identifiers:

Author	ResearcherID Number	ORCID Number
Baraban, Larysa	C-6244-2011	
Cuniberti, Gianaurelio	B-7192-2008	0000-0002-6574-7848
Dai, Bing		0000-0002-1170-4084

ISSN: 0264-1275
eISSN: 1873-4197

Record 19 of 39

Title: Visible light absorption of surface modified TiO2 powders with bidentate benzene derivatives

Author(s): Milicevic, B (Milicevic, B.); Dordevic, V (Dordevic, V.); Loncarevic, D (Loncarevic, D.); Ahrenkiel, SP (Ahrenkiel, S. P.); Dramicanin, MD (Dramicanin, M. D.); Nedeljkovic, JM (Nedeljkovic, J. M.)

Source: MICROPOROUS AND MESOPOROUS MATERIALS **Volume:** 217 **Pages:** 184-189 **DOI:** 10.1016/j.micromeso.2015.06.028 **Published:** NOV 15 2015

Accession Number: WOS:000360596100025

Author Identifiers:

Author	ResearcherID Number	ORCID Number
Nedeljkovic, Jovan		0000-0003-4347-5236
Milicevic, Bojana		0000-0003-2870-2728
Loncarevic, Davor		0000-0002-2266-337X
Dramicanin, Miroslav		0000-0003-4750-5359

ISSN: 1387-1811

eISSN: 1873-3093

Record 20 of 39

Title: Bacteriostatic photocatalytic properties of cotton modified with TiO2 and TiO2/aminopropyltriethoxysilane

Author(s): Tomsic, B (Tomsic, Brigita); Jovanovski, V (Jovanovski, Vasko); Orel, B (Orel, Boris); Mihelcic, M (Mihelcic, Mohor); Kovac, J (Kovac, Janez); Francetic, V (Francetic, Vojmir); Simoncic, B (Simoncic, Barbara)

Source: CELLULOSE **Volume:** 22 **Issue:** 5 **Pages:** 3441-3463 **DOI:** 10.1007/s10570-015-0696-x **Published:** OCT 2015

Accession Number: WOS:000361002000046

ISSN: 0969-0239

eISSN: 1572-882X

Record 21 of 39

Title: Influence of TiO2 nanoparticles on formation mechanism of PANI/TiO2 nanocomposite coating on PET fabric and its structural and electrical properties

Author(s): Radoicic, MB (Radoicic, Marija B.); Milosevic, MV (Milosevic, Milica V.); Milicevic, DS (Milicevic, Dejan S.); Suljovrujic, EH (Suljovrujic, Edin H.); Ciric-Marjanovic, GN (Ciric-Marjanovic, Gordana N.); Radetic, MM (Radetic, Maja M.); Saponjic, ZV (Saponjic, Zoran V.)

Source: SURFACE & COATINGS TECHNOLOGY **Volume:** 278 **Pages:** 38-47 **DOI:** 10.1016/j.surfcoat.2015.07.070 **Published:** SEP 25 2015

Accession Number: WOS:000361934800006

Author Identifiers:

Author	ResearcherID Number	ORCID Number
CMT, UAntwerpen Group	A-5523-2016	
Suljovrujic, Edin		0000-0001-8774-4341

Milosevic, Milica		0000-0002-3869-5800
Milicevic, Dejan		0000-0001-7746-0708
Radoicic, Marija		0000-0002-2644-5273
Saponjic, Zoran		0000-0001-7848-6715
Ciric-Marjanovic, Gordana		0000-0002-1050-7003

ISSN: 0257-8972

Record 22 of 39

Title: Assimilating the photo-induced functions of TiO2-based compounds in textiles: emphasis on the sol-gel process

Author(s): Pakdel, E (Pakdel, Esfandiar); Daoud, WA (Daoud, Walid A.); Wang, XG (Wang, Xungai)

Source: TEXTILE RESEARCH JOURNAL **Volume:** 85 **Issue:** 13 **Pages:** 1404-1428 **DOI:** 10.1177/0040517514551462 **Published:** AUG 2015

Accession Number: WOS:000354440900008

Author Identifiers:

Author	ResearcherID Number	ORCID Number
Pakdel, Esfandiar	O-6186-2018	0000-0003-1705-0226

ISSN: 0040-5175

eISSN: 1746-7748

Record 23 of 39

Title: Investigating the effect of corona treatment on self-cleaning property of finished cotton fabric with nano titanium dioxide

Author(s): Mirjalili, M (Mirjalili, Mohammad); Karimi, L (Karimi, Loghman); Barari-tari, A (Barari-tari, Amin)

Source: JOURNAL OF THE TEXTILE INSTITUTE **Volume:** 106 **Issue:** 6 **Pages:** 621-628 **DOI:** 10.1080/00405000.2014.932058 **Published:** JUN 3 2015

Accession Number: WOS:000351897500007

Author Identifiers:

Author	ResearcherID Number	ORCID Number
Karimi, Loghman	D-4790-2016	0000-0002-9424-8618
Mirjalili, Mohammad		0000-0002-5307-4535

ISSN: 0040-5000

eISSN: 1754-2340

Record 24 of 39

Title: Effect of dissipated power due to antenna resistive heating on E- to H-mode transition in inductively coupled oxygen plasma

Author(s): Puac, N (Puac, N.); Lazovic, S (Lazovic, S.); Zaplotnik, R (Zaplotnik, R.); Mozetic, M (Mozetic, M.); Petrovic, ZL (Petrovic, Z. Lj); Cvelbar, U (Cvelbar, U.)

Source: INDIAN JOURNAL OF PHYSICS **Volume:** 89 **Issue:** 6 **Pages:** 635-640 **DOI:** 10.1007/s12648-014-0615-2 **Published:** JUN 2015

Accession Number: WOS:000355596700014

Author Identifiers:

Author	ResearcherID Number	ORCID Number
Lazovic, Sasa	Q-5056-2016	0000-0003-1696-9134
Puac, Nevena		0000-0003-1142-8494
Petrovic, Zoran		0000-0001-6569-9447

ISSN: 0973-1458

eISSN: 0974-9845

Record 25 of 39

Title: Sonophotocatalytic degradation of dye CI Acid Orange 7 by TiO2 and Ag nanoparticles immobilized on corona pretreated polypropylene non-woven fabric

Author(s): Markovic, D (Markovic, Darka); Saponjic, Z (Saponjic, Zoran); Radoicic, M (Radoicic, Marija); Radetic, T (Radetic, Tamara); Vodnik, V (Vodnik, Vesna); Potkonjak, B (Potkonjak, Branislav); Radetic, M (Radetic, Maja)

Source: ULTRASONICS SONOCHEMISTRY **Volume:** 24 **Pages:** 221-229 **DOI:** 10.1016/j.ultsonch.2014.11.017 **Published:** MAY 2015

Accession Number: WOS:000349726500029

PubMed ID: 25487219

Author Identifiers:

Author	ResearcherID Number	ORCID Number
Radoicic, Marija		0000-0002-2644-5273
Saponjic, Zoran		0000-0001-7848-6715
Vodnik, Vesna		0000-0003-2944-6957

ISSN: 1350-4177

eISSN: 1873-2828

Record 26 of 39

Title: Negative influence of Ag and TiO2 nanoparticles on biodegradation of cotton fabrics

Author(s): Lazic, V (Lazic, Vesna); Radoicic, M (Radoicic, Marija); Saponjic, Z (Saponjic, Zoran); Radetic, T (Radetic, Tamara); Vodnik, V (Vodnik, Vesna); Nikolic, S (Nikolic, Svetlana); Dimitrijevic, S (Dimitrijevic, Suzana); Radetic, M (Radetic, Maja)

Source: CELLULOSE **Volume:** 22 **Issue:** 2 **Pages:** 1365-1378 **DOI:** 10.1007/s10570-015-0549-7 **Published:** APR 2015

Accession Number: WOS:000350876300033

Author Identifiers:

Author	ResearcherID Number	ORCID Number
Lazic, Vesna	O-1726-2017	0000-0001-6440-6577
Dimitrijevic-Brankovic, Suzana		0000-0001-6849-6936

Radoicic, Marija		0000-0002-2644-5273
Vodnik, Vesna		0000-0003-2944-6957
Saponjic, Zoran		0000-0001-7848-6715

ISSN: 0969-0239

eISSN: 1572-882X

Record 27 of 39

Title: Functionalization of Cellulose Fibres with Oxygen Plasma and ZnO Nanoparticles for Achieving UV Protective Properties

Author(s): Jazbec, K (Jazbec, Katja); Sala, M (Sala, Martin); Mozetic, M (Mozetic, Miran); Vesel, A (Vesel, Alenka); Gorjanc, M (Gorjanc, Marija)

Source: JOURNAL OF NANOMATERIALS **Article Number:** 346739 **DOI:** 10.1155/2015/346739 **Published:** 2015

Accession Number: WOS:000351110800001

Author Identifiers:

Author	ResearcherID Number	ORCID Number
Sala, Martin		0000-0001-7845-860X

ISSN: 1687-4110

eISSN: 1687-4129

Record 28 of 39

Title: Kinetics and mechanism for transparent polyethylene-TiO2 films mediated self-cleaning leading to MB dye discoloration under sunlight irradiation

Author(s): Rtimi, S (Rtimi, S.); Pulgarin, C (Pulgarin, C.); Sanjines, R (Sanjines, R.); Kiwi, J (Kiwi, J.)

Source: APPLIED CATALYSIS B-ENVIRONMENTAL **Volume:** 162 **Pages:** 236-244 **DOI:** 10.1016/j.apcatb.2014.05.039 **Published:** JAN 2015

Accession Number: WOS:000343686900028

Author Identifiers:

Author	ResearcherID Number	ORCID Number
Rtimi, Sami	M-2103-2017	0000-0002-1924-3710
Rtimi, Sami	K-8648-2012	0000-0002-1924-3710

ISSN: 0926-3373

eISSN: 1873-3883

Record 29 of 39

Title: Using graphene/TiO2 nanocomposite as a new route for preparation of electroconductive, self-cleaning, antibacterial and antifungal cotton fabric without toxicity

Author(s): Karimi, L (Karimi, Loghman); Yazdanshenas, ME (Yazdanshenas, Mohammad Esmail); Khajavi, R (Khajavi, Ramin); Rashidi, A (Rashidi, Abosaeed); Mirjalili, M (Mirjalili, Mohammad)

Source: CELLULOSE **Volume:** 21 **Issue:** 5 **Pages:** 3813-3827 **DOI:** 10.1007/s10570-014-0385-1 **Published:** OCT 2014

Accession Number: WOS:000341489300057

Author Identifiers:

Author	ResearcherID Number	ORCID Number
Karimi, Loghman	D-4790-2016	0000-0002-9424-8618
Khajavi, Ramin		0000-0001-6916-4730
Mirjalili, Mohammad		0000-0002-5307-4535

ISSN: 0969-0239

eISSN: 1572-882X

Record 30 of 39

Title: Creating cellulose fibres with excellent UV protective properties using moist CF4 plasma and ZnO nanoparticles

Author(s): Gorjanc, M (Gorjanc, Marija); Jazbec, K (Jazbec, Katja); Sala, M (Sala, Martin); Zaplotnik, R (Zaplotnik, Rok); Vesel, A (Vesel, Alenka); Mozetic, M (Mozetic, Miran)

Source: CELLULOSE **Volume:** 21 **Issue:** 4 **Pages:** 3007-3021 **DOI:** 10.1007/s10570-014-0284-5 **Published:** AUG 2014

Accession Number: WOS:000341490200068

Author Identifiers:

Author	ResearcherID Number	ORCID Number
Sala, Martin	A-3250-2011	0000-0001-7845-860X

ISSN: 0969-0239

eISSN: 1572-882X

Record 31 of 39

Title: UV protective textiles by the deposition of functional ethylcellulose nanoparticles

Author(s): Vilchez-Maldonado, S (Vilchez-Maldonado, S.); Caldero, G (Caldero, G.); Esquena, J (Esquena, J.); Molina, R (Molina, R.)

Source: CELLULOSE **Volume:** 21 **Issue:** 3 **Pages:** 2133-2145 **DOI:** 10.1007/s10570-014-0217-3 **Published:** JUN 2014

Accession Number: WOS:000336322800092

Author Identifiers:

Author	ResearcherID Number	ORCID Number
Molina, Ricardo	F-8597-2016	0000-0001-6324-4983
Caldero, Gabriela		0000-0003-4827-7722
Esquena, Jordi		0000-0002-9188-5259

ISSN: 0969-0239

eISSN: 1572-882X

Record 32 of 39

Title: Structure and Properties of Cotton Fibers Modified with Titanium Sulfate and Urea under Hydrothermal Conditions

Author(s): Zhang, H (Zhang, Hui); Zhu, LL (Zhu, Linlin); Sun, RJ (Sun, Runjun)

Source: JOURNAL OF ENGINEERED FIBERS AND FABRICS **Volume:** 9 **Issue:** 1 **Pages:** 67-75 **Published:** 2014

Accession Number: WOS:000343747100008

ISSN: 1558-9250

Record 33 of 39

Title: Plasma-induced adhesion improvement of cotton/polypropylene-laminated fabrics

Author(s): Armagan, OG (Armagan, Osman Gazi); Kayaoglu, BK (Kayaoglu, Burcak Karaguzel); Karakas, HC (Karakas, Hale Canbaz)

Source: JOURNAL OF ADHESION SCIENCE AND TECHNOLOGY **Volume:** 27 **Issue:** 21 **Pages:** 2326-2339 **DOI:** 10.1080/01694243.2013.774255 **Published:** NOV 1 2013

Accession Number: WOS:000324365300006

Author Identifiers:

Author	ResearcherID Number	ORCID Number
Karaguzel Kayaoglu, Burcak	N-1993-2014	

ISSN: 0169-4243

eISSN: 1568-5616

Record 34 of 39

Title: Functionalization of textile materials with TiO2 nanoparticles

Author(s): Radetic, M (Radetic, Maja)

Source: JOURNAL OF PHOTOCHEMISTRY AND PHOTOBIOLOGY C-PHOTOCHEMISTRY REVIEWS **Volume:** 16 **Pages:** 62-76 **DOI:** 10.1016/j.jphotochemrev.2013.04.002 **Published:** SEP 2013

Accession Number: WOS:000323141600004

ISSN: 1389-5567

eISSN: 1873-2739

Record 35 of 39

Title: Plasma properties in a large-volume, cylindrical and asymmetric radio-frequency capacitively coupled industrial-prototype reactor

Author(s): Lazovic, S (Lazovic, Sasa); Puac, N (Puac, Nevena); Spasic, K (Spasic, Kosta); Malovic, G (Malovic, Gordana); Cvelbar, U (Cvelbar, Uros); Mozetic, M (Mozetic, Miran); Radetic, M (Radetic, Maja); Petrovic, ZL (Petrovic, Zoran Lj)

Source: JOURNAL OF PHYSICS D-APPLIED PHYSICS **Volume:** 46 **Issue:** 7 **Article Number:** 075201 **DOI:** 10.1088/0022-3727/46/7/075201 **Published:** FEB 20 2013

Accession Number: WOS:000314471900014

Author Identifiers:

Author	ResearcherID Number	ORCID Number
Lazovic, Sasa	Q-5056-2016	0000-0003-1696-9134
Mozetic, Miran	K-8784-2014	
Lazovic, Sasa	B-9651-2013	0000-0003-1696-9134
Puac, Nevena		0000-0003-1142-8494
Malovic, Gordana		0000-0003-2356-0652
Petrovic, Zoran		0000-0001-6569-9447

ISSN: 0022-3727

Record 36 of 39

Title: The surface modification of cellulose fibres to create super-hydrophobic, oleophobic and self-cleaning properties

Author(s): Vasiljevic, J (Vasiljevic, Jelena); Gorjanc, M (Gorjanc, Marija); Tomsic, B (Tomsic, Brigita); Orel, B (Orel, Boris); Jerman, I (Jerman, Ivan); Mozetic, M (Mozetic, Miran); Vesel, A (Vesel, Alenka); Simoncic, B (Simoncic, Barbara)

Source: CELLULOSE **Volume:** 20 **Issue:** 1 **Pages:** 277-289 **DOI:** 10.1007/s10570-012-9812-3 **Published:** FEB 2013

Accession Number: WOS:000313365700026

Author Identifiers:

Author	ResearcherID Number	ORCID Number
VASILJEVIC, JELENA	H-3910-2018	0000-0002-3838-0251
Mozetic, Miran	K-8784-2014	
Vesel, Alenka	I-3934-2014	0000-0003-3782-6001

ISSN: 0969-0239

Record 37 of 39

Title: Antimicrobial cotton fibres prepared by in situ synthesis of AgCl into a silica matrix

Author(s): Klemencic, D (Klemencic, Danijela); Tomsic, B (Tomsic, Brigita); Kovac, F (Kovac, Franci); Simoncic, B (Simoncic, Barbara)

Source: CELLULOSE **Volume:** 19 **Issue:** 5 **Pages:** 1715-1729 **DOI:** 10.1007/s10570-012-9735-z **Published:** OCT 2012

Accession Number: WOS:000307768100022

ISSN: 0969-0239

Record 38 of 39

Title: Fabrication and characterization of self-assembled multifunctional coating deposition on a cellulose substrate

Author(s): Yin, YJ (Yin, Yunjie); Wang, CX (Wang, Chaoxia); Wang, YJ (Wang, Youjiang)

Source: COLLOIDS AND SURFACES A-PHYSICOCHEMICAL AND ENGINEERING ASPECTS **Volume:** 399 **Pages:** 92-99 **DOI:** 10.1016/j.colsurfa.2012.02.039 **Published:** APR 5 2012

Accession Number: WOS:000304076500013

ISSN: 0927-7757

Record 39 of 39

Title: Diagnostics and biomedical applications of radiofrequency plasmas

Author(s): Lazovic, S (Lazovic, Sasa)

Edited by: Kuraica M; Mijatovic Z

Source: 26TH SUMMER SCHOOL AND INTERNATIONAL SYMPOSIUM ON THE PHYSICS OF IONIZED GASES (SPIG 2012) **Book Series:** Journal of Physics Conference Series **Volume:** 399 **Article Number:** 012015 **DOI:** 10.1088/1742-6596/399/1/012015 **Published:** 2012

Accession Number: WOS:000312261700015

Conference Title: 26th Summer School and International Symposium on the Physics of Ionized Gases (SPIG)

Conference Date: AUG 27-31, 2012

Conference Location: Zrenjanin, SERBIA

Conference Sponsors: Sci & Technol Dev Republ Serbia, Minist Educ, Prov Secretariat Sci & Technol Dev, Inst Francais Serbie, Biser Zrenjanin

Author Identifiers:

Author	ResearcherID Number	ORCID Number
Lazovic, Sasa	Q-5056-2016	0000-0003-1696-9134
Lazovic, Sasa	B-9651-2013	0000-0003-1696-9134

ISSN: 1742-6588

Close

Web of Science
Page 1 (Records 1 -- 41)
[1]

Print

Record 1 of 41

Title: Biocompatible antimicrobial cotton fibres for healthcare industries: a biogenic approach for synthesis of bio-organic-coated silver nanoparticles

Author(s): Kashid, SB (Kashid, Sahebrao B.); Lakkakula, JR (Lakkakula, Jaya R.); Chauhan, DS (Chauhan, Deepak S.); Srivastava, R (Srivastava, Rohit); Raut, RW (Raut, Rajesh W.)

Source: IET NANOBIOTECHNOLOGY **Volume:** 11 **Issue:** 8 **Pages:** 1046-1051 **DOI:** 10.1049/iet-nbt.2017.0077 **Published:** DEC 2017

Accession Number: WOS:000415945300019

PubMed ID: 29155406

ISSN: 1751-8741

eISSN: 1751-875X

Record 2 of 41

Title: The influence of corona treatment and impregnation with colloidal TiO2 nanoparticles on biodegradability of cotton fabric

Author(s): Tomsic, B (Tomsic, Brigita); Vasiljevic, J (Vasiljevic, Jelena); Simoncic, B (Simoncic, Barbara); Radoicic, M (Radoicic, Marija); Radetic, M (Radetic, Maja)

Source: CELLULOSE **Volume:** 24 **Issue:** 10 **Pages:** 4533-4545 **DOI:** 10.1007/s10570-017-1415-6 **Published:** OCT 2017

Accession Number: WOS:000410759600032

Author Identifiers:

Author	ResearcherID Number	ORCID Number
VASILJEVIC, JELENA	H-3910-2018	0000-0002-3838-0251

ISSN: 0969-0239

eISSN: 1572-882X

Record 3 of 41

Title: Application of nanotechnology in sports clothing and flooring for enhanced sport activities, performance, efficiency and comfort: a review

Author(s): Harifi, T (Harifi, Tina); Montazer, M (Montazer, Majid)

Source: JOURNAL OF INDUSTRIAL TEXTILES **Volume:** 46 **Issue:** 5 **Pages:** 1147-1169 **DOI:** 10.1177/1528083715601512 **Published:** JAN 2017

Accession Number: WOS:000398810900001

Author Identifiers:

Author	ResearcherID Number	ORCID Number
Harifi, Tina		0000-0003-1520-5167

ISSN: 1528-0837

eISSN: 1530-8057

Record 4 of 41

Title: Plasma treatment applied in the pad-dry-cure process for making rechargeable antimicrobial cotton fabric that inhibits S. Aureus

Author(s): Zhou, CE (Zhou, Chang-E); Kan, CW (Kan, Chi-wai); Yuen, CWM (Yuen, Chun-wah Marcus); Matinlinna, JP (Matinlinna, Jukka Pekka); Tsoi, JKH (Tsoi, James Kit-hon); Zhang, Q (Zhang, Qing)

Source: TEXTILE RESEARCH JOURNAL **Volume:** 86 **Issue:** 20 **Pages:** 2202-2215 **DOI:** 10.1177/0040517515622147 **Published:** DEC 2016

Accession Number: WOS:000389335500008

Author Identifiers:

Author	ResearcherID Number	ORCID Number
Kan, Chi-wai		0000-0002-7668-2410

ISSN: 0040-5175

eISSN: 1746-7748

Record 5 of 41

Title: Innovative Self-Cleaning and Biocompatible Polyester Textiles Nano-Decorated with Fe-N-Doped Titanium Dioxide

Author(s): Nica, IC (Nica, Ionela Cristina); Stan, MS (Stan, Miruna Silvia); Dinischiotu, A (Dinischiotu, Anca); Popa, M (Popa, Marcela); Chifiriuc, MC (Chifiriuc, Mariana Carmen); Lazar, V (Lazar, Veronica); Pircalabioru, GG (Pircalabioru, Gratiela G.); Bezirtzoglou, E (Bezirtzoglou, Eugenia); Iordache, OG (Iordache, Ovidiu G.); Varzaru, E (Varzaru, Elena); Dumitrescu, I (Dumitrescu, Iuliana); Feder, M (Feder, Marcel); Vasiliu, F (Vasiliu, Florin); Mercioniu, I (Mercioniu, Ionel); Diamandescu, L (Diamandescu, Lucian)

Source: NANOMATERIALS **Volume:** 6 **Issue:** 11 **Article Number:** 214 **DOI:** 10.3390/nano6110214 **Published:** NOV 2016

Accession Number: WOS:000390103400024

PubMed ID: 28335342

Author Identifiers:

Author	ResearcherID Number	ORCID Number
Diamandescu, Constantin	F-1704-2011	
Mercioniu, Ionel	B-7643-2011	0000-0002-3408-2919

ISSN: 2079-4991

Record 6 of 41

Title: Influence of Silver Loaded Antibacterial Agent on Knitted and Nonwoven Fabrics and Some Fabric Properties

Author(s): Erdem, R (Erdem, Ramazan); Rajendran, S (Rajendran, Subbiyan)

Source: JOURNAL OF ENGINEERED FIBERS AND FABRICS **Volume:** 11 **Issue:** 1 **Pages:** 38-46 **Published:** 2016

Accession Number: WOS:000386648500006

ISSN: 1558-9250

Record 7 of 41

Title: Silver nanomaterials as future colorants and potential antimicrobial agents for natural and synthetic textile materials

Author(s): Shahid-ul-Islam (Shahid-ul-Islam); Butola, BS (Butola, B. S.); Mohammad, F (Mohammad, Faqeer)

Source: RSC ADVANCES **Volume:** 6 **Issue:** 50 **Pages:** 44232-44247 **DOI:** 10.1039/c6ra05799c **Published:** 2016

Accession Number: WOS:000376119000047

ISSN: 2046-2069

Record 8 of 41

Title: Nanomaterials for Functional Textiles and Fibers

Author(s): Rivero, PJ (Rivero, Pedro J.); Urrutia, A (Urrutia, Aitor); Goicoechea, J (Goicoechea, Javier); Arregui, FJ (Arregui, Francisco J.)

Source: NANOSCALE RESEARCH LETTERS **Volume:** 10 **Article Number:** 501 **DOI:** 10.1186/s11671-015-1195-6 **Published:** DEC 29 2015

Accession Number: WOS:000367476300006

PubMed ID: 26714863

Author Identifiers:

Author	ResearcherID Number	ORCID Number
Arregui, Francisco	A-7030-2013	0000-0002-3311-0834
Urrutia, Aitor	B-5295-2015	0000-0002-5087-6778

ISSN: 1556-276X

Record 9 of 41

Title: A facile synthesis of high antibacterial polymer nanocomposite containing uniformly dispersed silver nanoparticles

Author(s): An, J (An, Jing); Luo, QZ (Luo, Qingzhi); Li, MN (Li, Minna); Wang, DS (Wang, Desong); Li, XY (Li, Xueyan); Yin, R (Yin, Rong)

Source: COLLOID AND POLYMER SCIENCE **Volume:** 293 **Issue:** 7 **Pages:** 1997-2008 **DOI:** 10.1007/s00396-015-3589-5 **Published:** JUL 2015

Accession Number: WOS:000356942800015

ISSN: 0303-402X

eISSN: 1435-1536

Record 10 of 41

Title: Effect of dissipated power due to antenna resistive heating on E- to H-mode transition in inductively coupled oxygen plasma

Author(s): Puac, N (Puac, N.); Lazovic, S (Lazovic, S.); Zaplotnik, R (Zaplotnik, R.); Mozetic, M (Mozetic, M.); Petrovic, ZL (Petrovic, Z. Lj); Cvelbar, U (Cvelbar, U.)

Source: INDIAN JOURNAL OF PHYSICS **Volume:** 89 **Issue:** 6 **Pages:** 635-640 **DOI:** 10.1007/s12648-014-0615-2 **Published:** JUN 2015

Accession Number: WOS:000355596700014

Author Identifiers:

Author	ResearcherID Number	ORCID Number
Lazovic, Sasa	Q-5056-2016	0000-0003-1696-9134
Puac, Nevena		0000-0003-1142-8494
Petrovic, Zoran		0000-0001-6569-9447

ISSN: 0973-1458

eISSN: 0974-9845

Record 11 of 41

Title: High-Energy Radiation Induced Sustainable Coloration and Functional Finishing of Textile Materials

Author(s): Shahid-ul-Islam (Shahid-ul-Islam); Mohammad, F (Mohammad, Faqeer)

Source: INDUSTRIAL & ENGINEERING CHEMISTRY RESEARCH **Volume:** 54 **Issue:** 15 **Pages:** 3727-3745 **DOI:** 10.1021/acs.iecr.5b00524 **Published:** APR 22 2015

Accession Number: WOS:000353929300001

ISSN: 0888-5885

Record 12 of 41

Title: Negative influence of Ag and TiO2 nanoparticles on biodegradation of cotton fabrics

Author(s): Lazic, V (Lazic, Vesna); Radoicic, M (Radoicic, Marija); Saponjic, Z (Saponjic, Zoran); Radetic, T (Radetic, Tamara); Vodnik, V (Vodnik, Vesna); Nikolic, S (Nikolic, Svetlana); Dimitrijevic, S (Dimitrijevic, Suzana); Radetic, M (Radetic, Maja)

Source: CELLULOSE **Volume:** 22 **Issue:** 2 **Pages:** 1365-1378 **DOI:** 10.1007/s10570-015-0549-7 **Published:** APR 2015

Accession Number: WOS:000350876300033

Author Identifiers:

Author	ResearcherID Number	ORCID Number
Lazic, Vesna	O-1726-2017	0000-0001-6440-6577
Dimitrijevic-Brankovic, Suzana		0000-0001-6849-6936
Radoicic, Marija		0000-0002-2644-5273
Vodnik, Vesna		0000-0003-2944-6957
Saponjic, Zoran		0000-0001-7848-6715

ISSN: 0969-0239

eISSN: 1572-882X

Record 13 of 41

Title: Release of Engineered Nanomaterials from Polymer Nanocomposites: Diffusion, Dissolution, and Desorption

Author(s): Duncan, TV (Duncan, Timothy V.); Pillai, K (Pillai, Karthik)

Source: ACS APPLIED MATERIALS & INTERFACES **Volume:** 7 **Issue:** 1 **Pages:** 2-19 **DOI:** 10.1021/am5062745 **Published:** JAN 14 2015

Accession Number: WOS:000348085200002

PubMed ID: 25485689

Author Identifiers:

Author	ResearcherID Number	ORCID Number
Duncan, Timothy		0000-0001-6893-2291

ISSN: 1944-8244

Record 14 of 41

Title: Antibacterial and UV protective properties of polyamide fabric impregnated with TiO2/Ag nanoparticles

Author(s): Milosevic, M (Milosevic, Milica); Krkobabic, A (Krkobabic, Ana); Radoicic, M (Radoicic, Marija); Saponjic, Z (Saponjic, Zoran); Lazic, V (Lazic, Vesna); Stoiljkovic, M (Stoiljkovic, Milovan); Radetic, M (Radetic, Maja)

Source: JOURNAL OF THE SERBIAN CHEMICAL SOCIETY **Volume:** 80 **Issue:** 5 **Pages:** 705-715 **DOI:** 10.2298/JSC141104125M **Published:** 2015

Accession Number: WOS:000359987400011

Author Identifiers:

Author	ResearcherID Number	ORCID Number
Lazic, Vesna	O-1726-2017	0000-0001-6440-6577
Saponjic, Zoran		0000-0001-7848-6715
Stoiljkovic, Milovan		0000-0002-2794-3231
Radoicic, Marija		0000-0002-2644-5273
Milosevic, Milica		0000-0002-3869-5800

ISSN: 0352-5139

Record 15 of 41

Title: Silver film on nanocrystalline TiO2 support: Photocatalytic and antimicrobial ability

Author(s): Vukoje, ID (Vukoje, Ivana D.); Tomasevic-Ilic, TD (Tomasevic-Ilic, Tijana D.); Zarubica, AR (Zarubica, Aleksandra R.); Dimitrijevic, S (Dimitrijevic, Suzana); Budimir, MD (Budimir, Milica D.); Vranjes, MR (Vranjes, Mila R.); Saponjic, ZV (Saponjic, Zoran V.); Nedeljkovic, JM (Nedeljkovic, Jovan M.)

Source: MATERIALS RESEARCH BULLETIN **Volume:** 60 **Pages:** 824-829 **DOI:** 10.1016/j.materresbull.2014.09.073 **Published:** DEC 2014

Accession Number: WOS:000347583100120

Author Identifiers:

Author	ResearcherID Number	ORCID Number
Saponjic, Zoran		0000-0001-7848-6715
Dimitrijevic-Brankovic, Suzana		0000-0001-6849-6936
Nedeljkovic, Jovan		0000-0003-4347-5236
Vukoje, Ivana		0000-0001-9364-2616
Budimir, Milica		0000-0003-0742-0983

Vranjes, Mila		0000-0001-6862-7473

ISSN: 0025-5408

eISSN: 1873-4227

Record 16 of 41

Title: Synthesis, characterization, and antimicrobial activity of poly(GMA-co-EGDMA) polymer decorated with silver nanoparticles

Author(s): Vukoje, ID (Vukoje, Ivana D.); Dzunuzovic, ES (Dzunuzovic, Enis S.); Vodnik, VV (Vodnik, Vesna V.); Dimitrijevic, S (Dimitrijevic, Suzana); Ahrenkiel, SP (Ahrenkiel, S. Phillip); Nedeljkovic, JM (Nedeljkovic, Jovan M.)

Source: JOURNAL OF MATERIALS SCIENCE **Volume:** 49 **Issue:** 19 **Pages:** 6838-6844 **DOI:** 10.1007/s10853-014-8386-x **Published:** OCT 2014

Accession Number: WOS:000339337600040

Author Identifiers:

Author	ResearcherID Number	ORCID Number
Nedeljkovic, Jovan		0000-0003-4347-5236
Vukoje, Ivana		0000-0001-9364-2616
Vodnik, Vesna		0000-0003-2944-6957
Dimitrijevic-Brankovic, Suzana		0000-0001-6849-6936

ISSN: 0022-2461

eISSN: 1573-4803

Record 17 of 41

Title: Application of nanotechnology in antimicrobial finishing of biomedical textiles

Author(s): Zille, A (Zille, Andrea); Almeida, L (Almeida, Luis); Amorim, T (Amorim, Teresa); Carneiro, N (Carneiro, Noemia); Esteves, MF (Esteves, Maria Fatima); Silva, CJ (Silva, Carla J.); Souto, AP (Souto, Antonio Pedro)

Source: MATERIALS RESEARCH EXPRESS **Volume:** 1 **Issue:** 3 **Article Number:** 032003 **DOI:** 10.1088/2053-1591/1/3/032003 **Published:** SEP 2014

Accession Number: WOS:000209665200003

Author Identifiers:

Author	ResearcherID Number	ORCID Number
Souto, Antonio	G-8637-2013	0000-0001-6439-4780
Almeida, Luis	B-6341-2009	0000-0002-7781-7743
Zille, Andrea	B-3323-2008	0000-0001-5299-4164
Amorim, Maria		0000-0003-1516-8407
Silva, Carla		0000-0002-7509-9135

ISSN: 2053-1591

Record 18 of 41

Title: The influence of triangular silver nanoplates on antimicrobial activity and color of cotton fabrics pretreated with chitosan

Author(s): Vukoje, I (Vukoje, Ivana); Lazic, V (Lazic, Vesna); Vodnik, V (Vodnik, Vesna); Mitric, M (Mitric, Miodrag); Jokic, B (Jokic, Bojan); Ahrenkiel, SP (Ahrenkiel, S. Phillip); Nedeljkovic, JM (Nedeljkovic, Jovan M.); Radetic, M (Radetic, Maja)

Source: JOURNAL OF MATERIALS SCIENCE **Volume:** 49 **Issue:** 13 **Pages:** 4453-4460 **DOI:** 10.1007/s10853-014-8142-2 **Published:** JUL 2014

Accession Number: WOS:000334492000006

Author Identifiers:

Author	ResearcherID Number	ORCID Number
Lazic, Vesna	O-1726-2017	0000-0001-6440-6577
Vodnik, Vesna		0000-0003-2944-6957
Nedeljkovic, Jovan		0000-0003-4347-5236
Vukoje, Ivana		0000-0001-9364-2616
Mitric, Miodrag		0000-0002-1709-9890

ISSN: 0022-2461

eISSN: 1573-4803

Record 19 of 41

Title: Nanosilver: an inorganic nanoparticle with myriad potential applications

Author(s): Rai, M (Rai, Mahendra); Birla, S (Birla, Sonal); Ingle, AP (Ingle, Avinash P.); Gupta, I (Gupta, Indarchand); Gade, A (Gade, Aniket); Abd-Elsalam, K (Abd-Elsalam, Kamel); Marcato, PD (Marcato, Priscyla D.); Duran, N (Duran, Nelson)

Source: NANOTECHNOLOGY REVIEWS **Volume:** 3 **Issue:** 3 **Pages:** 281-309 **DOI:** 10.1515/ntrev-2014-0001 **Published:** JUN 2014

Accession Number: WOS:000338341800004

Author Identifiers:

Author	ResearcherID Number	ORCID Number
Marcato, Priscyla	D-4371-2012	
Gade, Aniket	C-5656-2016	0000-0002-1966-999X
Rai, Mahendra		0000-0003-0291-0422
Duran, Nelson		0000-0001-8372-5143

ISSN: 2191-9089

eISSN: 2191-9097

Record 20 of 41

Title: Morphology Transformations of Platelets on Plasma Activated Surfaces

Author(s): Modic, M (Modic, Martina); Junkar, I (Junkar, Ita); Stana-Kleinschek, K (Stana-Kleinschek, Karin); Kostanjsek, R (Kostanjsek, Rok); Mozetic, M (Mozetic, Miran)

Source: PLASMA PROCESSES AND POLYMERS **Volume:** 11 **Issue:** 6 **Pages:** 596-605 **DOI:** 10.1002/ppap.201400001 **Published:** JUN 2014
Accession Number: WOS:000337626000010
Author Identifiers:

Author	ResearcherID Number	ORCID Number
Mozetic, Miran	K-8784-2014	

ISSN: 1612-8850
eISSN: 1612-8869

Record 21 of 41
Title: The catalytic decomposition of silver coated cinnamyl alcohol during water exposure and the formation of silver nanoparticles
Author(s): Dahle, S (Dahle, S.); Hofft, O (Hoefft, O.); Viol, W (Vioel, W.); Friedrichs, WM (Friedrichs, W. Maus)
Source: SURFACE SCIENCE **Volume:** 621 **Pages:** 133-139 **DOI:** 10.1016/j.susc.2013.11.009 **Published:** MAR 2014
Accession Number: WOS:000330909300020
Author Identifiers:

Author	ResearcherID Number	ORCID Number
Hofft, Oliver	J-2830-2012	0000-0002-1313-3166
Dahle, Sebastian	O-4064-2015	0000-0001-7568-0483

ISSN: 0039-6028
eISSN: 1879-2758

Record 22 of 41
Title: In situ Synthesis of Silver Nanoparticles on Fabric Attached with Chitosan
Author(s): Peng, JJ (Peng Junjun); Zhang, X (Zhang Xin); Wu, YM (Wu Yiming); Liu, HL (Liu Honglin); Ran, JH (Ran Jianhua); Li, M (Li Ming); Yang, F (Yang Feng)
Source: CHEMICAL JOURNAL OF CHINESE UNIVERSITIES-CHINESE **Volume:** 35 **Issue:** 2 **Pages:** 415-420 **DOI:** 10.7503/cjcu20130678 **Published:** FEB 10 2014
Accession Number: WOS:000332918400035
Author Identifiers:

Author	ResearcherID Number	ORCID Number
Peng, Junjun		0000-0002-3432-9643

ISSN: 0251-0790

Record 23 of 41
Title: Photo-, Bio-, and Magneto-active Colored Polyester Fabric with Hydrophobic/Hydrophilic and Enhanced Mechanical Properties through Synthesis of TiO2/Fe3O4/Ag Nanocomposite

Author(s): Harifi, T (Harifi, Tina); Montazer, M (Montazer, Majid)
Source: INDUSTRIAL & ENGINEERING CHEMISTRY RESEARCH **Volume:** 53 **Issue:** 3 **Pages:** 1119-1129 **DOI:** 10.1021/ie403052m **Published:** JAN 22 2014
Accession Number: WOS:000330203200011
Author Identifiers:

Author	ResearcherID Number	ORCID Number
Harifi, Tina		0000-0003-1520-5167

ISSN: 0888-5885

Record 24 of 41
Title: Biosynthesized Silver Nanoparticles for Antibacterial Treatment of Cellulosic Fabrics Using O-2-Plasma
Author(s): Abdel-Aziz, MS (Abdel-Aziz, M. S.); Eid, BM (Eid, B. M.); Ibrahim, NA (Ibrahim, N. A.)
Source: AATCC JOURNAL OF RESEARCH **Volume:** 1 **Issue:** 1 **Pages:** 6-12 **DOI:** 10.14504/ajr.1.1.2 **Published:** JAN-FEB 2014
Accession Number: WOS:000363609200002
Author Identifiers:

Author	ResearcherID Number	ORCID Number
Eid, Basma		0000-0001-9259-777X
Abdel-Aziz, Mohamed		0000-0001-9151-5920

ISSN: 2330-5517

Record 25 of 41
Title: Increasing Surface Hydrophilicity in Poly(Lactic Acid) Electrospun Fibers by Addition of Pla-b-Peg Co-Polymers
Author(s): Hendrick, E (Hendrick, Erin); Frey, M (Frey, Margaret)
Source: JOURNAL OF ENGINEERED FIBERS AND FABRICS **Volume:** 9 **Issue:** 2 **Pages:** 153-164 **Published:** 2014
Accession Number: WOS:000343747200019
Author Identifiers:

Author	ResearcherID Number	ORCID Number
Frey, Margaret	N-4849-2017	

ISSN: 1558-9250

Record 26 of 41
Title: Screening of Different Fusarium Species to Select Potential Species for the Synthesis of Silver Nanoparticles
Author(s): Gaikwad, SC (Gaikwad, Swapnil C.); Birla, SS (Birla, Sonal S.); Ingle, AP (Ingle, Avinash P.); Gade, AK (Gade, Aniket K.); Marcato, PD (Marcato, Priscyla D.); Rai, M (Rai, Mahendra); Duran, N (Duran, Nelson)

Source: JOURNAL OF THE BRAZILIAN CHEMICAL SOCIETY **Volume:** 24 **Issue:** 12 **Pages:** 1974-+ **DOI:** 10.5935/0103-5053.20130247 **Published:** DEC 2013
Accession Number: WOS:000328703200011
Author Identifiers:

Author	ResearcherID Number	ORCID Number
Marcato, Priscyla	D-4371-2012	
Gade, Aniket	C-5656-2016	0000-0002-1966-999X
Rai, Mahendra		0000-0003-0291-0422
Duran, Nelson		0000-0001-8372-5143

ISSN: 0103-5053
eISSN: 1678-4790

Record 27 of 41
Title: Adsorption of silver on glucose studied with MIES, UPS, XPS and AFM
Author(s): Dahle, S (Dahle, S.); Meuthen, J (Meuthen, J.); Viol, W (Vioel, W.); Maus-Friedrichs, W (Maus-Friedrichs, W.)
Source: APPLIED SURFACE SCIENCE **Volume:** 284 **Pages:** 514-522 **DOI:** 10.1016/j.apsusc.2013.07.126 **Published:** NOV 1 2013
Accession Number: WOS:000324248600072
Author Identifiers:

Author	ResearcherID Number	ORCID Number
Dahle, Sebastian	O-4064-2015	0000-0001-7568-0483

ISSN: 0169-4332

Record 28 of 41
Title: Adsorption of silver on cellobiose and cellulose studied with MIES, UPS, XPS and AFM
Author(s): Dahle, S (Dahle, S.); Meuthen, J (Meuthen, J.); Viol, W (Vioel, W.); Maus-Friedrichs, W (Maus-Friedrichs, W.)
Source: CELLULOSE **Volume:** 20 **Issue:** 5 **Pages:** 2469-2480 **DOI:** 10.1007/s10570-013-0009-1 **Published:** OCT 2013
Accession Number: WOS:000324494200022
Author Identifiers:

Author	ResearcherID Number	ORCID Number
Dahle, Sebastian	O-4064-2015	0000-0001-7568-0483

ISSN: 0969-0239

Record 29 of 41
Title: In situ generation of Ag nanoparticles on polyester fabrics by photoreduction using TiO2 nanoparticles

Author(s): Milosevic, M (Milosevic, Milica); Radoicic, M (Radoicic, Marija); Saponjic, Z (Saponjic, Zoran); Nunney, T (Nunney, Tim); Markovic, D (Markovic, Darka); Nedeljkovic, J (Nedeljkovic, Jovan); Radetic, M (Radetic, Maja)

Source: JOURNAL OF MATERIALS SCIENCE **Volume:** 48 **Issue:** 16 **Pages:** 5447-5455 **DOI:** 10.1007/s10853-013-7338-1 **Published:** AUG 2013

Accession Number: WOS:000319575900006

Author Identifiers:

Author	ResearcherID Number	ORCID Number
Nedeljkovic, Jovan		0000-0003-4347-5236
Milosevic, Milica		0000-0002-3869-5800
Saponjic, Zoran		0000-0001-7848-6715
Radoicic, Marija		0000-0002-2644-5273

ISSN: 0022-2461

eISSN: 1573-4803

Record 30 of 41

Title: Nanobio Silver: Its Interactions with Peptides and Bacteria, and Its Uses in Medicine

Author(s): Eckhardt, S (Eckhardt, Sonja); Brunetto, PS (Brunetto, Priscilla S.); Gagnon, J (Gagnon, Jacinthe); Priebe, M (Priebe, Magdalena); Giese, B (Giese, Bernd); Fromm, KM (Fromm, Katharina M.)

Source: CHEMICAL REVIEWS **Volume:** 113 **Issue:** 7 **Pages:** 4708-4754 **DOI:** 10.1021/cr300288v **Published:** JUL 2013

Accession Number: WOS:000321810600005

PubMed ID: 23488929

ISSN: 0009-2665

eISSN: 1520-6890

Record 31 of 41

Title: In situ synthesis of silver nanoparticles on alkali-treated cotton fabrics

Author(s): Yazdanshenas, ME (Yazdanshenas, Mohammad E.); Shateri-Khalilabad, M (Shateri-Khalilabad, Mohammad)

Source: JOURNAL OF INDUSTRIAL TEXTILES **Volume:** 42 **Issue:** 4 **Pages:** 459-474 **DOI:** 10.1177/1528083712444297 **Published:** APR 2013

Accession Number: WOS:000319132600008

ISSN: 1528-0837

Record 32 of 41

Title: Effect of Particle Size on Silver Nanoparticle Deposition onto Dielectric Barrier Discharge (DBD) Plasma Functionalized Polyamide Fabric

Author(s): Vu, NK (Nguyen Khanh Vu); Zille, A (Zille, Andrea); Oliveira, FR (Oliveira, Fernando Ribeiro); Carneiro, N (Carneiro, Noemia); Souto, AP (Souto, Antonio Pedro)

Source: PLASMA PROCESSES AND POLYMERS **Volume:** 10 **Issue:** 3 **Pages:** 285-296 **DOI:** 10.1002/ppap.201200089 **Published:** MAR 2013

Accession Number: WOS:000315970200012

Author Identifiers:

Author	ResearcherID Number	ORCID Number
Souto, Antonio	G-8637-2013	0000-0001-6439-4780
Carneiro, Noemia	I-3240-2015	0000-0002-9370-2110
Ribeiro Oliveira, Fernando	H-3210-2012	
Zille, Andrea	B-3323-2008	0000-0001-5299-4164

ISSN: 1612-8850

Record 33 of 41

Title: Plasma properties in a large-volume, cylindrical and asymmetric radio-frequency capacitively coupled industrial-prototype reactor

Author(s): Lazovic, S (Lazovic, Sasa); Puac, N (Puac, Nevena); Spasic, K (Spasic, Kosta); Malovic, G (Malovic, Gordana); Cvelbar, U (Cvelbar, Uros); Mozetic, M (Mozetic, Miran); Radetic, M (Radetic, Maja); Petrovic, ZL (Petrovic, Zoran Lj)

Source: JOURNAL OF PHYSICS D-APPLIED PHYSICS **Volume:** 46 **Issue:** 7 **Article Number:** 075201 **DOI:** 10.1088/0022-3727/46/7/075201 **Published:** FEB 20 2013

Accession Number: WOS:000314471900014

Author Identifiers:

Author	ResearcherID Number	ORCID Number
Lazovic, Sasa	Q-5056-2016	0000-0003-1696-9134
Mozetic, Miran	K-8784-2014	
Lazovic, Sasa	B-9651-2013	0000-0003-1696-9134
Puac, Nevena		0000-0003-1142-8494
Malovic, Gordana		0000-0003-2356-0652
Petrovic, Zoran		0000-0001-6569-9447

ISSN: 0022-3727

Record 34 of 41

Title: Functionalization of textile materials with silver nanoparticles

Author(s): Radetic, M (Radetic, M.)

Source: JOURNAL OF MATERIALS SCIENCE **Volume:** 48 **Issue:** 1 **Pages:** 95-107 **DOI:** 10.1007/s10853-012-6677-7 **Published:** JAN 2013

Accession Number: WOS:000312874700006

ISSN: 0022-2461

Record 35 of 41

Title: The Effect of Alkali Pre-treatment on Formation and Adsorption of Silver Nanoparticles on Cotton Surface

Author(s): Yazdanshenas, ME (Yazdanshenas, Mohammad E.); Shateri-Khalilabad, M (Shateri-Khalilabad, Mohammad)

Source: FIBERS AND POLYMERS **Volume:** 13 **Issue:** 9 **Pages:** 1170-1178 **DOI:** 10.1007/s12221-012-1170-0 **Published:** NOV 2012

Accession Number: WOS:000311593100012
ISSN: 1229-9197

Record 36 of 41
Title: Silver nano particle formation on Ar plasma - treated cinnamyl alcohol
Author(s): Dahle, S (Dahle, S.); Marschewski, M (Marschewski, M.); Wegewitz, L (Wegewitz, L.); Viol, W (Vioel, W.); Maus-Friedrichs, W (Maus-Friedrichs, W.)
Source: JOURNAL OF APPLIED PHYSICS **Volume:** 111 **Issue:** 3 **Article Number:** 034902 **DOI:** 10.1063/1.3680883 **Published:** FEB 1 2012
Accession Number: WOS:000301029800122
Author Identifiers:

Author	ResearcherID Number	ORCID Number
Dahle, Sebastian	O-4064-2015	0000-0001-7568-0483

ISSN: 0021-8979

Record 37 of 41
Title: Diagnostics and biomedical applications of radiofrequency plasmas
Author(s): Lazovic, S (Lazovic, Sasa)
Edited by: Kuraica M; Mijatovic Z
Source: 26TH SUMMER SCHOOL AND INTERNATIONAL SYMPOSIUM ON THE PHYSICS OF IONIZED GASES (SPIG 2012) **Book Series:** Journal of Physics Conference Series **Volume:** 399 **Article Number:** 012015 **DOI:** 10.1088/1742-6596/399/1/012015 **Published:** 2012
Accession Number: WOS:000312261700015
Conference Title: 26th Summer School and International Symposium on the Physics of Ionized Gases (SPIG)
Conference Date: AUG 27-31, 2012
Conference Location: Zrenjanin, SERBIA
Conference Sponsors: Sci & Technol Dev Republ Serbia, Minist Educ, Prov Secretariat Sci & Technol Dev, Inst Francais Serbie, Biser Zrenjanin
Author Identifiers:

Author	ResearcherID Number	ORCID Number
Lazovic, Sasa	Q-5056-2016	0000-0003-1696-9134
Lazovic, Sasa	B-9651-2013	0000-0003-1696-9134

ISSN: 1742-6588

Record 38 of 41
Title: Breakdown and discharge regimes in standard and micrometer size dc discharges
Author(s): Skoro, N (Skoro, N.)
Edited by: Kuraica M; Mijatovic Z

Source: 26TH SUMMER SCHOOL AND INTERNATIONAL SYMPOSIUM ON THE PHYSICS OF IONIZED GASES (SPIG 2012) **Book Series:** Journal of Physics Conference Series **Volume:** 399 **Article Number:** 012017 **DOI:** 10.1088/1742-6596/399/1/012017 **Published:** 2012
Accession Number: WOS:000312261700017
Conference Title: 26th Summer School and International Symposium on the Physics of Ionized Gases (SPIG)
Conference Date: AUG 27-31, 2012
Conference Location: Zrenjanin, SERBIA
Conference Sponsors: Sci & Technol Dev Republ Serbia, Minist Educ, Prov Secretariat Sci & Technol Dev, Inst Francais Serbie, Biser Zrenjanin
Author Identifiers:

Author	ResearcherID Number	ORCID Number
Skoro, Nikola		0000-0002-0254-8008

ISSN: 1742-6588

Record 39 of 41
Title: Antimicrobial modification of cellulose fabrics using low-pressure plasma and silver compounds
Author(s): Razic, SE (Razic, Sanja Ercegovic); Cunko, R (Cunko, Ruzica); Bukosek, V (Bukosek, Vili); Matica, B (Matica, Biserka)
Source: TEKSTIL **Volume:** 60 **Issue:** 9 **Pages:** 413-426 **Published:** SEP 2011
Accession Number: WOS:000307628700001
ISSN: 0492-5882

Record 40 of 41
Title: Antimicrobial modification of cellulose fabrics using low-pressure plasma and silver compounds
Author(s): Razic, SE (Razic, Sanja Ercegovic); Cunko, R (Cunko, Ruzica); Bukosek, V (Bukosek, Vili); Matica, B (Matica, Biserka)
Source: TEKSTIL **Volume:** 60 **Issue:** 9 **Pages:** 427-440 **Published:** SEP 2011
Accession Number: WOS:000307628700002
ISSN: 0492-5882

Record 41 of 41
Title: Ellagic acid promoted biomimetic synthesis of shape-controlled silver nanochains
Author(s): Barnaby, SN (Barnaby, Stacey N.); Yu, SM (Yu, Samantha M.); Fath, KR (Fath, Karl R.); Tsiola, A (Tsiola, Areti); Khalpari, O (Khalpari, Omid); Banerjee, IA (Banerjee, Ipsita A.)
Source: NANOTECHNOLOGY **Volume:** 22 **Issue:** 22 **Article Number:** 225605 **DOI:** 10.1088/0957-4484/22/22/225605 **Published:** JUN 3 2011
Accession Number: WOS:000289518000018
PubMed ID: 21454936
Author Identifiers:

Author	ResearcherID Number	ORCID Number
Fath, Karl		0000-0002-6766-2530

ISSN: 0957-4484

Close

Web of Science
Page 1 (Records 1 -- 41)
[1]

Print

Close

Web of Science
Page 1 (Records 1 -- 39)
[1]

Print

Record 1 of 39

Title: Characterisation of a multijet plasma device by means of mass spectrometric detection and iCCD imaging

Author(s): Stancampiano, A (Stancampiano, A.); Selakovic, N (Selakovic, N.); Gherardi, M (Gherardi, M.); Puac, N (Puac, N.); Petrovic, ZL (Petrovic, Z. Lj); Colombo, V (Colombo, V)

Source: JOURNAL OF PHYSICS D-APPLIED PHYSICS **Volume:** 51 **Issue:** 48 **Article Number:** 484004 **DOI:** 10.1088/1361-6463/aae2f2 **Published:** DEC 5 2018

Accession Number: WOS:000446857200001

ISSN: 0022-3727

eISSN: 1361-6463

Record 2 of 39

Title: Atmospheric plasma etching of polymers: A palette of applications in cleaning/ashing, pattern formation, nanotexturing and superhydrophobic surface fabrication

Author(s): Dimitrakellis, P (Dimitrakellis, P.); Gogolides, E (Gogolides, E.)

Source: MICROELECTRONIC ENGINEERING **Volume:** 194 **Pages:** 109-115 **DOI:** 10.1016/j.mee.2018.03.017 **Published:** JUL 5 2018

Accession Number: WOS:000433265900019

ISSN: 0167-9317

eISSN: 1873-5568

Record 3 of 39

Title: Excitation mechanisms in a nonequilibrium helium plasma jet emerging in ambient air at 1 atm

Author(s): Nguyen, T (Tam Nguyen); Hernandez, E (Hernandez, Eduardo); Donnelly, VM (Donnelly, Vincent M.); Economou, DJ (Economou, Demetre J.)

Source: JOURNAL OF VACUUM SCIENCE & TECHNOLOGY A **Volume:** 36 **Issue:** 4 **Article Number:** 04F406 **DOI:** 10.1116/1.5023693 **Published:** JUL 2018

Accession Number: WOS:000438217600006

ISSN: 0734-2101

eISSN: 1520-8559

Record 4 of 39

Title: Destruction of chemical warfare surrogates using a portable atmospheric pressure plasma jet

Author(s): Skoro, N (Skoro, Nikola); Puac, N (Puac, Nevena); Zivkovic, S (Zivkovic, Suzana); Krstic-Milosevic, D (Krstic-Milosevic, Dijana); Cvelbar, U (Cvelbar, Uros); Malovic, G (Malovic, Gordana); Petrovic, ZL (Petrovic, Zoran Lj.)

Source: EUROPEAN PHYSICAL JOURNAL D **Volume:** 72 **Issue:** 1 **Article Number:** 2 **DOI:** 10.1140/epjd/e2017-80329-9 **Published:** JAN 16 2018

Accession Number: WOS:000422899000001

Author Identifiers:

Author	ResearcherID Number	ORCID Number
Puac, Nevena		0000-0003-1142-8494
Cvelbar, Uros		0000-0002-1957-0789
Petrovic, Zoran		0000-0001-6569-9447
Skoro, Nikola		0000-0002-0254-8008

ISSN: 1434-6060

eISSN: 1434-6079

Record 5 of 39

Title: Numerical and experimental study on atmospheric pressure ionization waves propagating through a U-shape channel

Author(s): Yan, W (Yan, Wen); Xia, Y (Xia, Yang); Bi, ZH (Bi, Zhenhua); Song, Y (Song, Ying); Wang, DZ (Wang, Dezhen); Sosnin, EA (Sosnin, Eduard A.); Skakun, VS (Skakun, Victor S.); Liu, DP (Liu, Dongping)

Source: JOURNAL OF PHYSICS D-APPLIED PHYSICS **Volume:** 50 **Issue:** 34 **Pages:** 1-16 **Article Number:** 345201 **DOI:** 10.1088/1361-6463/aa7bc1 **Published:** AUG 31 2017

Accession Number: WOS:000406526400001

ISSN: 0022-3727

eISSN: 1361-6463

Record 6 of 39

Title: Development of a non-equilibrium 60 MHz plasma jet with a long discharge plume

Author(s): Uchida, G (Uchida, Giichiro); Kawabata, K (Kawabata, Kazufumi); Ito, T (Ito, Taiki); Takenaka, K (Takenaka, Kosuke); Setsuhara, Y (Setsuhara, Yuichi)

Source: JOURNAL OF APPLIED PHYSICS **Volume:** 122 **Issue:** 3 **Article Number:** 033301 **DOI:** 10.1063/1.4993715 **Published:** JUL 21 2017

Accession Number: WOS:000406128800005

ISSN: 0021-8979

eISSN: 1089-7550

Record 7 of 39

Title: A diffuse plasma jet generated from the preexisting discharge filament at atmospheric pressure

Author(s): Li, J (Li, Jing); Xu, YG (Xu, Yonggang); Zhang, TY (Zhang, Tongyi); Tang, J (Tang, Jie); Wang, YS (Wang, Yishan); Zhao, W (Zhao, Wei); Duan, YX (Duan, Yixiang)

Source: JOURNAL OF APPLIED PHYSICS **Volume:** 122 **Issue:** 1 **Article Number:** 013301 **DOI:** 10.1063/1.4989975 **Published:** JUL 7 2017

Accession Number: WOS:000405084900008

ISSN: 0021-8979

eISSN: 1089-7550

Record 8 of 39

Title: Transition between stable hydrophilization and fast etching/hydrophilization of poly(methyl) methacrylate polymer using a novel atmospheric pressure

dielectric barrier discharge source

Author(s): Dimitrakellis, P (Dimitrakellis, Panagiotis); Gogolides, E (Gogolides, Evangelos); Zeniou, A (Zeniou, Angelos); Awsiuk, K (Awsiuk, Kamil); Rysz, J (Rysz, Jakub); Marzec, MM (Marzec, Mateusz M.)

Source: JOURNAL OF VACUUM SCIENCE & TECHNOLOGY A **Volume:** 35 **Issue:** 4 **Special Issue:** SI **Article Number:** 041303 **DOI:** 10.1116/1.4984613 **Published:** JUL-AUG 2017

Accession Number: WOS:000405346100006

Conference Title: Pacific Rim Symposium on Surfaces, Coatings and Interfaces (PACSURF)

Conference Date: DEC 11-15, 2016

Conference Location: HI

Author Identifiers:

Author	ResearcherID Number	ORCID Number
Rysz, Jakub	F-1043-2012	0000-0003-1668-3398
Awsiuk, Kamil		0000-0001-9058-4561

ISSN: 0734-2101

eISSN: 1520-8559

Record 9 of 39

Title: The influence of electrode configuration on light emission profiles and electrical characteristics of an atmospheric-pressure plasma jet

Author(s): Maletic, D (Maletic, Dejan); Puac, N (Puac, Nevena); Malovic, G (Malovic, Gordana); Dordevic, A (Dordevic, Antonije); Petrovic, ZL (Petrovic, Zoran Lj)

Source: JOURNAL OF PHYSICS D-APPLIED PHYSICS **Volume:** 50 **Issue:** 14 **Article Number:** 145202 **DOI:** 10.1088/1361-6463/aa5d91 **Published:** APR 12 2017

Accession Number: WOS:000404428200002

Author Identifiers:

Author	ResearcherID Number	ORCID Number
Puac, Nevena		0000-0003-1142-8494
Petrovic, Zoran		0000-0001-6569-9447
Malovic, Gordana		0000-0003-2356-0652

ISSN: 0022-3727

eISSN: 1361-6463

Record 10 of 39

Title: Electrical and optical characterization of an atmospheric pressure, uniform, large-area processing, dielectric barrier discharge

Author(s): Zeniou, A (Zeniou, A.); Puac, N (Puac, N.); Skoro, N (Skoro, N.); Selakovic, N (Selakovic, N.); Dimitrakellis, P (Dimitrakellis, P.); Gogolides, E (Gogolides, E.); Petrovic, ZL (Petrovic, Z. Lj)

Source: JOURNAL OF PHYSICS D-APPLIED PHYSICS **Volume:** 50 **Issue:** 13 **Article Number:** 135204 **DOI:** 10.1088/1361-6463/aa5d69 **Published:** APR 5 2017

Accession Number: WOS:000396058900002

Author Identifiers:

Author	ResearcherID Number	ORCID Number
Petrovic, Zoran		0000-0001-6569-9447
Puac, Nevena		0000-0003-1142-8494
Skoro, Nikola		0000-0002-0254-8008

ISSN: 0022-3727

eISSN: 1361-6463

Record 11 of 39

Title: Study of atmospheric-pressure glow discharge plasma jets based on analysis of electric field

Author(s): Liu, WZ (Liu, Wenzheng); Ma, CL (Ma, Chuanlong); Cui, WS (Cui, Weisheng); Yang, X (Yang, Xiao); Wang, TH (Wang, Tahan); Chen, XY (Chen, Xiuyang)

Source: APPLIED PHYSICS LETTERS **Volume:** 110 **Issue:** 2 **Article Number:** 024102 **DOI:** 10.1063/1.4973815 **Published:** JAN 9 2017

Accession Number: WOS:000392835300064

ISSN: 0003-6951

eISSN: 1077-3118

Record 12 of 39

Title: The plasma footprint of an atmospheric pressure plasma jet on a flat polymer substrate and its relation to surface treatment

Author(s): Onyshchenko, I (Onyshchenko, Iuliia); Nikiforov, AY (Nikiforov, Anton Yu.); De Geyter, N (De Geyter, Nathalie); Morent, R (Morent, Rino)

Source: EUROPEAN PHYSICAL JOURNAL-APPLIED PHYSICS **Volume:** 75 **Issue:** 2 **Special Issue:** SI **Article Number:** 24712 **DOI:** 10.1051/epjap/2016150564 **Published:** AUG 2016

Accession Number: WOS:000380828500012

Conference Title: 6th Central European Symposium on Plasma Chemistry (CESPC)

Conference Date: SEP 06-10, 2015

Conference Location: Bressanone, ITALY

Author Identifiers:

Author	ResearcherID Number	ORCID Number
Morent, Rino	K-7435-2015	0000-0001-6336-1485
Onyshchenko, Iuliia		0000-0001-7449-4961

ISSN: 1286-0042

eISSN: 1286-0050

Record 13 of 39

Title: Atmospheric pressure plasma jet for liquid spray treatment
Author(s): Mitic, S (Mitic, S.); Philipps, J (Philipps, J.); Hofmann, D (Hofmann, D.)
Source: JOURNAL OF PHYSICS D-APPLIED PHYSICS **Volume:** 49 **Issue:** 20 **Article Number:** 205202 **DOI:** 10.1088/0022-3727/49/20/205202 **Published:** MAY 25 2016
Accession Number: WOS:000375255800017
ISSN: 0022-3727
eISSN: 1361-6463

Record 14 of 39
Title: The effect of dielectric tube diameter on the propagation velocity of ionization waves in a He atmospheric-pressure micro-plasma jet
Author(s): Talviste, R (Talviste, Rasmus); Jogi, I (Jogi, Indrek); Raud, J (Raud, Juri); Paris, P (Paris, Peeter)
Source: JOURNAL OF PHYSICS D-APPLIED PHYSICS **Volume:** 49 **Issue:** 19 **Article Number:** 195201 **DOI:** 10.1088/0022-3727/49/19/195201 **Published:** MAY 18 2016
Accession Number: WOS:000375255500015
Author Identifiers:

Author	ResearcherID Number	ORCID Number
Jogi, Indrek	B-4173-2014	0000-0003-0007-8732
Paris, Peeter	O-2330-2017	0000-0002-0829-7510

ISSN: 0022-3727
eISSN: 1361-6463

Record 15 of 39
Title: Reactive species in non-equilibrium atmospheric-pressure plasmas: Generation, transport, and biological effects
Author(s): Lu, X (Lu, X.); Naidis, GV (Naidis, G. V.); Laroussi, M (Laroussi, M.); Reuter, S (Reuter, S.); Graves, DB (Graves, D. B.); Ostrikov, K (Ostrikov, K.)
Source: PHYSICS REPORTS-REVIEW SECTION OF PHYSICS LETTERS **Volume:** 630 **Pages:** 1-84 **DOI:** 10.1016/j.physrep.2016.03.003 **Published:** MAY 4 2016
Accession Number: WOS:000375889900001
Author Identifiers:

Author	ResearcherID Number	ORCID Number
Lu, XinPei	M-5570-2013	0000-0003-0676-9585
Reuter, Stephan	D-2890-2014	0000-0002-4858-1081
Ostrikov, Kostya (Ken)		0000-0001-8672-9297

ISSN: 0370-1573
eISSN: 1873-6270

Record 16 of 39
Title: Radio frequency atmospheric plasma source on a printed circuit board for large area, uniform processing of polymeric materials

Author(s): Dimitrakellis, P (Dimitrakellis, P.); Zeniou, A (Zeniou, A.); Stratakos, Y (Stratakos, Y.); Gogolides, E (Gogolides, E.)
Source: PLASMA SOURCES SCIENCE & TECHNOLOGY **Volume:** 25 **Issue:** 2 **Article Number:** 025015 **DOI:** 10.1088/0963-0252/25/2/025015 **Published:** APR 2016
Accession Number: WOS:000372337900017
ISSN: 0963-0252
eISSN: 1361-6595

Record 17 of 39
Title: Single-electrode He microplasma jets driven by nanosecond voltage pulses
Author(s): Jiang, C (Jiang, C.); Lane, J (Lane, J.); Song, ST (Song, S. T.); Pendelton, SJ (Pendelton, S. J.); Wu, Y (Wu, Y.); Sozer, E (Sozer, E.); Kuthi, A (Kuthi, A.); Gundersen, MA (Gundersen, M. A.)
Source: JOURNAL OF APPLIED PHYSICS **Volume:** 119 **Issue:** 8 **Article Number:** 083301 **DOI:** 10.1063/1.4942624 **Published:** FEB 28 2016
Accession Number: WOS:000371601800009
Author Identifiers:

Author	ResearcherID Number	ORCID Number
Sozer, Esin		0000-0002-6244-3670

ISSN: 0021-8979
eISSN: 1089-7550

Record 18 of 39
Title: Development of Ionization waves in an Atmospheric-Pressure Micro-Plasma Jet
Author(s): Talviste, R (Talviste, R.); Jogi, I (Jogi, I.); Raud, J (Raud, J.); Paris, P (Paris, P.)
Source: CONTRIBUTIONS TO PLASMA PHYSICS **Volume:** 56 **Issue:** 2 **Pages:** 134-145 **DOI:** 10.1002/ctpp.201500050 **Published:** FEB 2016
Accession Number: WOS:000371519600005
Author Identifiers:

Author	ResearcherID Number	ORCID Number
Jogi, Indrek	B-4173-2014	0000-0003-0007-8732
Paris, Peeter	O-2330-2017	0000-0002-0829-7510

ISSN: 0863-1042
eISSN: 1521-3986

Record 19 of 39
Title: Influence of voltage pulse width on the discharge characteristics in an atmospheric dielectric-barrier-discharge plasma jet
Author(s): Uchida, G (Uchida, Giichiro); Takenaka, K (Takenaka, Kosuke); Setsuhara, Y (Setsuhara, Yuichi)
Source: JAPANESE JOURNAL OF APPLIED PHYSICS **Volume:** 55 **Issue:** 1 **Special Issue:** SI **Article Number:** 01AH03 **DOI:** 10.7567/JJAP.55.01AH03 **Published:** JAN

2016

Accession Number: WOS:000369014400085

Author Identifiers:

Author	ResearcherID Number	ORCID Number
Uchida, Giichiro	K-7930-2017	

ISSN: 0021-4922

eISSN: 1347-4065

Record 20 of 39

Title: Practical and theoretical considerations on the use of ICCD imaging for the characterization of non-equilibrium plasmas

Author(s): Gherardi, M (Gherardi, Matteo); Puac, N (Puac, Nevena); Maric, D (Maric, Dragana); Stancampiano, A (Stancampiano, Augusto); Malovic, G (Malovic, Gordana); Colombo, V (Colombo, Vittorio); Petrovic, ZL (Petrovic, Zoran Lj)

Source: PLASMA SOURCES SCIENCE & TECHNOLOGY **Volume:** 24 **Issue:** 6 **Article Number:** 064004 **DOI:** 10.1088/0963-0252/24/6/064004 **Published:** DEC 2015

Accession Number: WOS:000368117100005

Author Identifiers:

Author	ResearcherID Number	ORCID Number
Maric, Dragana		0000-0002-1728-5458
Malovic, Gordana		0000-0003-2356-0652
COLOMBO, VITTORIO		0000-0001-9145-198X
Petrovic, Zoran		0000-0001-6569-9447
Puac, Nevena		0000-0003-1142-8494

ISSN: 0963-0252

eISSN: 1361-6595

Record 21 of 39

Title: Cavity ring-down spectroscopy for atmospheric pressure plasma jet analysis

Author(s): Zaplotnik, R (Zaplotnik, Rok); Biscan, M (Biscan, Marijan); Krstulovic, N (Krstulovic, Niksa); Popovic, D (Popovic, Dean); Milosevic, S (Milosevic, Slobodan)

Source: PLASMA SOURCES SCIENCE & TECHNOLOGY **Volume:** 24 **Issue:** 5 **Article Number:** 054004 **DOI:** 10.1088/0963-0252/24/5/054004 **Published:** OCT 2015

Accession Number: WOS:000364336600007

Author Identifiers:

Author	ResearcherID Number	ORCID Number
Milosevic, Slobodan	A-3408-2010	
Milosevic, Slobodan		0000-0002-4455-7869

ISSN: 0963-0252
eISSN: 1361-6595

Record 22 of 39

Title: Two-dimensional numerical study of an atmospheric pressure helium plasma jet with dual-power electrode

Author(s): Yan, W (Yan Wen); Liu, FC (Liu Fu-Cheng); Sang, CF (Sang Chao-Feng); Wang, DZ (Wang De-Zhen)

Source: CHINESE PHYSICS B **Volume:** 24 **Issue:** 6 **Article Number:** 065203 **DOI:** 10.1088/1674-1056/24/6/065203 **Published:** JUN 2015
Accession Number: WOS:000358130200045

Author Identifiers:

Author	ResearcherID Number	ORCID Number
Sang, Chaofeng	J-6233-2016	0000-0002-6861-5242

ISSN: 1674-1056
eISSN: 1741-4199

Record 23 of 39

Title: Effects of discharge voltage waveform on the discharge characteristics in a helium atmospheric plasma jet

Author(s): Uchida, G (Uchida, Giichiro); Takenaka, K (Takenaka, Kosuke); Setsuhara, Y (Setsuhara, Yuichi)

Source: JOURNAL OF APPLIED PHYSICS **Volume:** 117 **Issue:** 15 **Article Number:** 153301 **DOI:** 10.1063/1.4918546 **Published:** APR 21 2015
Accession Number: WOS:000353306900007

Author Identifiers:

Author	ResearcherID Number	ORCID Number
Uchida, Giichiro	K-7930-2017	

ISSN: 0021-8979
eISSN: 1089-7550

Record 24 of 39

Title: Time-resolved optical emission imaging of an atmospheric plasma jet for different electrode positions with a constant electrode gap

Author(s): Maletic, D (Maletic, D.); Puac, N (Puac, N.); Selakovic, N (Selakovic, N.); Lazovic, S (Lazovic, S.); Malovic, G (Malovic, G.); Dordevic, A (Dordevic, A.); Petrovic, ZL (Petrovic, Z. Lj)

Source: PLASMA SOURCES SCIENCE & TECHNOLOGY **Volume:** 24 **Issue:** 2 **Article Number:** 025006 **DOI:** 10.1088/0963-0252/24/2/025006 **Published:** APR 2015
Accession Number: WOS:000356816200010

Author Identifiers:

Author	ResearcherID Number	ORCID Number

Lazovic, Sasa	Q-5056-2016	0000-0003-1696-9134
Petrovic, Zoran		0000-0001-6569-9447
Puac, Nevena		0000-0003-1142-8494
Malovic, Gordana		0000-0003-2356-0652

ISSN: 0963-0252
eISSN: 1361-6595

Record 25 of 39
Title: Atmospheric-Pressure Gas-Breakdown Characteristics with a Radio-Frequency Voltage
Author(s): Uchida, G (Uchida, Giichiro); Takenaka, K (Takenaka, Kosuke); Miyazaki, A (Miyazaki, Atsushi); Setsuhara, Y (Setsuhara, Yuichi)
Source: JOURNAL OF NANOSCIENCE AND NANOTECHNOLOGY **Volume:** 15 **Issue:** 3 **Pages:** 2192-2196 **DOI:** 10.1166/jnn.2015.10233 **Published:** MAR 2015
Accession Number: WOS:000345054200036
PubMed ID: 26413639
Author Identifiers:

Author	ResearcherID Number	ORCID Number
Uchida, Giichiro	K-7930-2017	

ISSN: 1533-4880
eISSN: 1533-4899

Record 26 of 39
Title: Dynamic Properties of Helium Atmospheric Dielectric-Barrier-Discharge Plasma Jet
Author(s): Uchida, G (Uchida, Giichiro); Takenaka, K (Takenaka, Kosuke); Miyazaki, A (Miyazaki, Atsushi); Kawabata, K (Kawabata, Kazufumi); Setsuhara, Y (Setsuhara, Yuichi)
Source: JOURNAL OF NANOSCIENCE AND NANOTECHNOLOGY **Volume:** 15 **Issue:** 3 **Pages:** 2324-2329 **DOI:** 10.1166/jnn.2015.10232 **Published:** MAR 2015
Accession Number: WOS:000345054200057
PubMed ID: 26413660
Author Identifiers:

Author	ResearcherID Number	ORCID Number
Uchida, Giichiro	K-7930-2017	

ISSN: 1533-4880
eISSN: 1533-4899

Record 27 of 39
Title: Influence of a sample surface on single electrode atmospheric plasma jet parameters

Author(s): Zaplotnik, R (Zaplotnik, Rok); Biscan, M (Biscan, Marijan); Kregar, Z (Kregar, Zlatko); Cvelbar, U (Cvelbar, Uros); Mozetic, M (Mozetic, Miran); Milosevic, S (Milosevic, Slobodan)

Source: SPECTROCHIMICA ACTA PART B-ATOMIC SPECTROSCOPY **Volume:** 103 **Pages:** 124-130 **DOI:** 10.1016/j.sab.2014.12.004 **Published:** JAN-FEB 2015

Accession Number: WOS:000349574200018

Author Identifiers:

Author	ResearcherID Number	ORCID Number
Milosevic, Slobodan	A-3408-2010	
Milosevic, Slobodan		0000-0002-4455-7869

ISSN: 0584-8547

Record 28 of 39

Title: Effects of driving voltage frequency on the discharge characteristics of atmospheric dielectric-barrier-discharge plasma jet

Author(s): Uchida, G (Uchida, Giichiro); Takenaka, K (Takenaka, Kosuke); Kawabata, K (Kawabata, Kazufumi); Miyazaki, A (Miyazaki, Atsushi); Setsuhara, Y (Setsuhara, Yuichi)

Source: JAPANESE JOURNAL OF APPLIED PHYSICS **Volume:** 53 **Issue:** 11 **Special Issue:** SI **Article Number:** 11RA08 **DOI:** 10.7567/JJAP.53.11RA08 **Published:** NOV 2014

Accession Number: WOS:000346597200009

Author Identifiers:

Author	ResearcherID Number	ORCID Number
Uchida, Giichiro	K-7930-2017	

ISSN: 0021-4922

eISSN: 1347-4065

Record 29 of 39

Title: Dynamic Evolution of Helium Atmospheric Pressure Plasma Jet With ITO-PET Electrodes

Author(s): Chang, ZS (Chang, Zheng-Shi); Zhang, GJ (Zhang, Guan-Jun)

Source: IEEE TRANSACTIONS ON PLASMA SCIENCE **Volume:** 42 **Issue:** 10 **Special Issue:** SI **Pages:** 2442-2443 **DOI:** 10.1109/TPS.2014.2332615 **Part:** 1 **Published:** OCT 2014

Accession Number: WOS:000344548300059

Author Identifiers:

Author	ResearcherID Number	ORCID Number
Chang, Zhengshi	J-2517-2018	0000-0002-0024-4553

ISSN: 0093-3813
eISSN: 1939-9375

Record 30 of 39

Title: Microporous N-doped carbon film produced by cold atmospheric plasma jet and its cell compatibility

Author(s): Li, LM (Li, Limin); Zhang, XM (Zhang, Xuming); Zhang, M (Zhang, Ming); Li, PH (Li, Penghui); Chu, PK (Chu, Paul K.)

Source: VACUUM **Volume:** 108 **Pages:** 27-34 **DOI:** 10.1016/j.vacuum.2014.05.019 **Published:** OCT 2014

Accession Number: WOS:000339602200005

Author Identifiers:

Author	ResearcherID Number	ORCID Number
Chu, Paul	B-5923-2013	0000-0002-5581-4883
Li, Penghui	H-9422-2014	0000-0001-7257-6381

ISSN: 0042-207X

Record 31 of 39

Title: Multiple vs. single harmonics AC-driven atmospheric plasma jet

Author(s): Zaplotnik, R (Zaplotnik, R.); Kregar, Z (Kregar, Z.); Biscan, M (Biscan, M.); Vesel, A (Vesel, A.); Cvelbar, U (Cvelbar, U.); Mozetic, M (Mozetic, M.); Milosevic, S (Milosevic, S.)

Source: EPL **Volume:** 106 **Issue:** 2 **Article Number:** 25001 **DOI:** 10.1209/0295-5075/106/25001 **Published:** APR 2014

Accession Number: WOS:000336376100010

Author Identifiers:

Author	ResearcherID Number	ORCID Number
Mozetic, Miran	K-8784-2014	
Vesel, Alenka	I-3934-2014	0000-0003-3782-6001
Milosevic, Slobodan	A-3408-2010	
Milosevic, Slobodan		0000-0002-4455-7869

ISSN: 0295-5075
eISSN: 1286-4854

Record 32 of 39

Title: Spatio-temporally resolved electric field measurements in helium plasma jet

Author(s): Sretenovic, GB (Sretenovic, Goran B.); Krstic, IB (Krstic, Ivan B.); Kovacevic, VV (Kovacevic, Vesna V.); Obradovic, BM (Obradovic, Bratislav M.); Kuraica, MM (Kuraica, Milorad M.)

Source: JOURNAL OF PHYSICS D-APPLIED PHYSICS **Volume:** 47 **Issue:** 10 **Article Number:** 102001 **DOI:** 10.1088/0022-3727/47/10/102001 **Published:** MAR 12 2014

Accession Number: WOS:000332398900001

Author Identifiers:

Author	ResearcherID Number	ORCID Number
Sretenovic, Goran	P-8983-2016	0000-0003-4817-4723
Kovacevic, Vesna		0000-0002-8575-1668
Kuraica, Milorad		0000-0001-8201-8500

ISSN: 0022-3727

eISSN: 1361-6463

Record 33 of 39

Title: Kinetic Phenomena in Transport of Electrons and Positrons in Gases caused by the Properties of Scattering Cross Sections

Author(s): Petrovic, ZL (Petrovic, Zoran Lj); Marjanovic, S (Marjanovic, Srdan); Dujko, S (Dujko, Sasa); Bankovic, A (Bankovic, Ana); Sasic, O (Sasic, Olivera); Bosnjakovic, D (Bosnjakovic, Danko); Stojanovic, V (Stojanovic, Vladimir); Malovic, G (Malovic, Gordana); Buckman, S (Buckman, Stephen); Garcia, G (Garcia, Gustavo); White, R (White, Ron); Sullivan, J (Sullivan, James); Brunger, M (Brunger, Michael)

Book Group Author(s): IOP

Source: XXVIII INTERNATIONAL CONFERENCE ON PHOTONIC, ELECTRONIC AND ATOMIC COLLISIONS (ICPEAC) **Book Series:** Journal of Physics Conference Series **Volume:** 488 **Article Number:** UNSP 012047 **DOI:** 10.1088/1742-6596/488/1/012047 **Published:** 2014

Accession Number: WOS:000338432500047

Conference Title: 28th International Conference on Photonic, Electronic and Atomic Collisions (ICPEAC)

Conference Date: JUL 24-30, 2013

Conference Location: Chinese Acad Sci, Inst Modern Phys, Lanzhou, PEOPLES R CHINA

Conference Sponsors: Natl Nat Sci Fdn China, Chinese Acad Sci, Int Union Pure & Appl Phys, Inst Modern Phys, Youth Innovat Promot Assoc, Inst Modern Phys

Conference Host: Chinese Acad Sci, Inst Modern Phys

Author Identifiers:

Author	ResearcherID Number	ORCID Number
Sullivan, James	F-3040-2011	0000-0003-4489-4926
White, Ron	B-7977-2008	0000-0001-5353-7440
Petrovic, Zoran		0000-0001-6569-9447
Brunger, Michael		0000-0002-7743-2990
Malovic, Gordana		0000-0003-2356-0652

ISSN: 1742-6588

Record 34 of 39

Title: Propagation of plasma bullets in helium within a dielectric capillary-influence of the interaction with surfaces

Author(s): Mussard, MDV (Mussard, M. Dang Van Sung); Guaitella, O (Guaitella, O.); Rousseau, A (Rousseau, A.)

Source: JOURNAL OF PHYSICS D-APPLIED PHYSICS **Volume:** 46 **Issue:** 30 **Article Number:** 302001 **DOI:** 10.1088/0022-3727/46/30/302001 **Published:** JUL 31 2013
Accession Number: WOS:000321611600001
Author Identifiers:

Author	ResearcherID Number	ORCID Number
Guaitella, Olivier	A-1405-2017	0000-0002-6509-6934

ISSN: 0022-3727

Record 35 of 39
Title: Effects of H-2 on Ar plasma jet: From filamentary to diffuse discharge mode
Author(s): Wu, S (Wu, S.); Lu, X (Lu, X.); Zou, D (Zou, D.); Pan, Y (Pan, Y.)
Source: JOURNAL OF APPLIED PHYSICS **Volume:** 114 **Issue:** 4 **Article Number:** 043301 **DOI:** 10.1063/1.4816318 **Published:** JUL 28 2013
Accession Number: WOS:000322539300009
ISSN: 0021-8979
eISSN: 1089-7550

Record 36 of 39
Title: Plasma properties in a large-volume, cylindrical and asymmetric radio-frequency capacitively coupled industrial-prototype reactor
Author(s): Lazovic, S (Lazovic, Sasa); Puac, N (Puac, Nevena); Spasic, K (Spasic, Kosta); Malovic, G (Malovic, Gordana); Cvelbar, U (Cvelbar, Uros); Mozetic, M (Mozetic, Miran); Radetic, M (Radetic, Maja); Petrovic, ZL (Petrovic, Zoran Lj)
Source: JOURNAL OF PHYSICS D-APPLIED PHYSICS **Volume:** 46 **Issue:** 7 **Article Number:** 075201 **DOI:** 10.1088/0022-3727/46/7/075201 **Published:** FEB 20 2013
Accession Number: WOS:000314471900014
Author Identifiers:

Author	ResearcherID Number	ORCID Number
Lazovic, Sasa	Q-5056-2016	0000-0003-1696-9134
Mozetic, Miran	K-8784-2014	
Lazovic, Sasa	B-9651-2013	0000-0003-1696-9134
Puac, Nevena		0000-0003-1142-8494
Malovic, Gordana		0000-0003-2356-0652
Petrovic, Zoran		0000-0001-6569-9447

ISSN: 0022-3727

Record 37 of 39
Title: Parametric study of a cold plasma jet generated at atmospheric pressure
Author(s): Kang, WS (Kang, Woo Seok); Hur, M (Hur, Min); Song, YH (Song, Young-Hoon)
Source: JOURNAL OF THE KOREAN PHYSICAL SOCIETY **Volume:** 62 **Issue:** 3 **Pages:** 453-458 **DOI:** 10.3938/jkps.62.453 **Published:** FEB 2013

Accession Number: WOS:000315351100013
ISSN: 0374-4884

Record 38 of 39
Title: Temporal evolution of dielectric barrier discharge microplasma
Author(s): Blajan, M (Blajan, Marius); Shimizu, K (Shimizu, Kazuo)
Source: APPLIED PHYSICS LETTERS **Volume:** 101 **Issue:** 10 **Article Number:** 104101 **DOI:** 10.1063/1.4749825 **Published:** SEP 3 2012
Accession Number: WOS:000309072800093
ISSN: 0003-6951

Record 39 of 39
Title: Breakdown and discharge regimes in standard and micrometer size dc discharges
Author(s): Skoro, N (Skoro, N.)
Edited by: Kuraica M; Mijatovic Z
Source: 26TH SUMMER SCHOOL AND INTERNATIONAL SYMPOSIUM ON THE PHYSICS OF IONIZED GASES (SPIG 2012) **Book Series:** Journal of Physics Conference Series **Volume:** 399 **Article Number:** 012017 **DOI:** 10.1088/1742-6596/399/1/012017 **Published:** 2012
Accession Number: WOS:000312261700017
Conference Title: 26th Summer School and International Symposium on the Physics of Ionized Gases (SPIG)
Conference Date: AUG 27-31, 2012
Conference Location: Zrenjanin, SERBIA
Conference Sponsors: Sci & Technol Dev Republ Serbia, Minist Educ, Prov Secretariat Sci & Technol Dev, Inst Francais Serbie, Biser Zrenjanin
Author Identifiers:

Author	ResearcherID Number	ORCID Number
Skoro, Nikola		0000-0002-0254-8008

ISSN: 1742-6588

Close

Web of Science
Page 1 (Records 1 -- 39)
◀ [1] ▶

Print

Close

Web of Science
Page 1 (Records 1 -- 39)
[1]

Print

Record 1 of 39

Title: Monte Carlo modeling of radio-frequency breakdown in argon

Author(s): Puac, M (Puac, Marija); Maric, D (Maric, Dragana); Radmilovic-Radjenovic, M (Radmilovic-Radjenovic, Marija); Suvakov, M (Suvakov, Milovan); Petrovic, ZL (Petrovic, Zoran Lj)

Source: PLASMA SOURCES SCIENCE & TECHNOLOGY **Volume:** 27 **Issue:** 7 **Article Number:** 075013 **DOI:** 10.1088/1361-6595/aacc0c **Published:** JUL 2018

Accession Number: WOS:000438601000001

Author Identifiers:

Author	ResearcherID Number	ORCID Number
Suvakov, Milovan		0000-0002-5839-9611

ISSN: 0963-0252

eISSN: 1361-6595

Record 2 of 39

Title: Activity of catalase enzyme in Paulownia tomentosa seeds during the process of germination after treatments with low pressure plasma and plasma activated water

Author(s): Puac, N (Puac, Nevena); Skoro, N (Skoro, Nikola); Spasic, K (Spasic, Kosta); Zivkovic, S (Zivkovic, Suzana); Milutinovic, M (Milutinovic, Milica); Malovic, G (Malovic, Gordana); Petrovic, ZL (Petrovic, Zoran Lj)

Source: PLASMA PROCESSES AND POLYMERS **Volume:** 15 **Issue:** 2 **Article Number:** e1700082 **DOI:** 10.1002/ppap.201700082 **Published:** FEB 2018

Accession Number: WOS:000425453900010

Author Identifiers:

Author	ResearcherID Number	ORCID Number
Puac, Nevena		0000-0003-1142-8494
Malovic, Gordana		0000-0003-2356-0652
Zivkovic, Suzana		0000-0003-0280-5884
Skoro, Nikola		0000-0002-0254-8008
Petrovic, Zoran		0000-0001-6569-9447

ISSN: 1612-8850

eISSN: 1612-8869

Record 3 of 39

Title: An advanced time-dependent collisional-radiative model of helium plasma discharges

Author(s): Claustre, J (Claustre, J.); Boukandou-Mombo, C (Boukandou-Mombo, C.); Margot, J (Margot, J.); Matte, JP (Matte, J-P); Vidal, F (Vidal, F.)
Source: PLASMA SOURCES SCIENCE & TECHNOLOGY **Volume:** 26 **Issue:** 10 **Article Number:** 105005 **DOI:** 10.1088/1361-6595/aa8a16 **Published:** OCT 2017
Accession Number: WOS:000411709600001
ISSN: 0963-0252
eISSN: 1361-6595

Record 4 of 39
Title: Osteogenic Potential of Non Thermal Biocompatible Atmospheric Pressure Plasma Treated Zirconia: In Vitro Study
Author(s): Jha, N (Jha, Nayansi); Choi, JS (Choi, Jin Sung); Kim, JH (Kim, Ji Hye); Jung, R (Jung, Ranju); Choi, EH (Choi, Eun Ha); Ryu, JJ (Ryu, Jae Jun); Han, I (Han, Ihn)
Source: JOURNAL OF BIOMATERIALS AND TISSUE ENGINEERING **Volume:** 7 **Issue:** 8 **Pages:** 662-670 **DOI:** 10.1166/jbt.2017.1626 **Published:** AUG 2017
Accession Number: WOS:000408358800008
ISSN: 2157-9083
eISSN: 2157-9091

Record 5 of 39
Title: Plasma effects on the bacteria Escherichia coli via two evaluation methods
Author(s): Vujosevic, D (Vujosevic, Danijela); Cvelbar, U (Cvelbar, Uros); Repnik, U (Repnik, Urska); Modic, M (Modic, Martina); Lazovic, S (Lazovic, Sasa); Zavasnik-Bergant, T (Zavasnik-Bergant, Tina); Puac, N (Puac, Nevena); Mugosa, B (Mugosa, Boban); Gogolides, E (Gogolides, Evangelos); Petrovic, ZL (Petrovic, Zoran Lj); Mozetic, M (Mozetic, Miran)
Source: PLASMA SCIENCE & TECHNOLOGY **Volume:** 19 **Issue:** 7 **Article Number:** UNSP 075504 **DOI:** 10.1088/2058-6272/aa656b **Published:** JUL 1 2017
Accession Number: WOS:000403264000013
Author Identifiers:

Author	ResearcherID Number	ORCID Number
Lazovic, Sasa	Q-5056-2016	0000-0003-1696-9134
Petrovic, Zoran		0000-0001-6569-9447
Puac, Nevena		0000-0003-1142-8494

ISSN: 1009-0630

Record 6 of 39
Title: The influence of electrode configuration on light emission profiles and electrical characteristics of an atmospheric-pressure plasma jet
Author(s): Maletic, D (Maletic, Dejan); Puac, N (Puac, Nevena); Malovic, G (Malovic, Gordana); Dordevic, A (Dordevic, Antonije); Petrovic, ZL (Petrovic, Zoran Lj)
Source: JOURNAL OF PHYSICS D-APPLIED PHYSICS **Volume:** 50 **Issue:** 14 **Article Number:** 145202 **DOI:** 10.1088/1361-6463/aa5d91 **Published:** APR 12 2017
Accession Number: WOS:000404428200002
Author Identifiers:

Author	ResearcherID Number	ORCID Number
Puac, Nevena		0000-0003-1142-8494
Petrovic, Zoran		0000-0001-6569-9447
Malovic, Gordana		0000-0003-2356-0652

ISSN: 0022-3727

eISSN: 1361-6463

Record 7 of 39

Title: Biological effects of bacterial pigment undecylprodigiosin on human blood cells treated with atmospheric gas plasma in vitro

Author(s): Lazovic, S (Lazovic, Sasa); Leskovac, A (Leskovac, Andreja); Petrovic, S (Petrovic, Sandra); Senerovic, L (Senerovic, Lidija); Krivokapic, N (Krivokapic, Nevena); Mitrovic, T (Mitrovic, Tatjana); Bozovic, N (Bozovic, Nikola); Vasic, V (Vasic, Vesna); Nikodinovic-Runic, J (Nikodinovic-Runic, Jasmina)

Source: EXPERIMENTAL AND TOXICOLOGIC PATHOLOGY **Volume:** 69 **Issue:** 1 **Pages:** 55-62 **DOI:** 10.1016/j.etp.2016.11.003 **Published:** JAN 2017

Accession Number: WOS:000390968000007

PubMed ID: 27843060

Author Identifiers:

Author	ResearcherID Number	ORCID Number
Nikodinovic-Runic, Jasmina	W-1277-2018	0000-0002-2553-977X
Lazovic, Sasa	Q-5056-2016	0000-0003-1696-9134
Senerovic, Lidija		0000-0002-6965-9407
Leskovac, Andreja		0000-0002-6293-5237
Petrovic, Sandra		0000-0003-0930-6455
Vasic, Vesna		0000-0003-1268-2363

ISSN: 0940-2993

eISSN: 1618-1433

Record 8 of 39

Title: Microplasma Induced Cell Morphological Changes and Apoptosis of Ex Vivo Cultured Human Anterior Lens Epithelial Cells - Relevance to Capsular Opacification

Author(s): Recek, N (Recek, Nina); Andjelic, S (Andjelic, Sofija); Hojnik, N (Hojnik, Nataga); Filipic, G (Filipic, Gregor); Lazovic, S (Lazovic, Sasa); Vesel, A (Vesel, Alenka); Primc, G (Primc, Gregor); Mozetic, M (Mozetic, Miran); Hawlina, M (Hawlina, Marko); Petrovski, G (Petrovski, Goran); Cvelbar, U (Cvelbar, Uros)

Source: PLOS ONE **Volume:** 11 **Issue:** 11 **Article Number:** e0165883 **DOI:** 10.1371/journal.pone.0165883 **Published:** NOV 10 2016

Accession Number: WOS:000387725000038

PubMed ID: 27832099

Author Identifiers:

Author	ResearcherID Number	ORCID Number
Filipic, Gregor	T-4900-2018	0000-0003-0153-5181
Lazovic, Sasa	Q-5056-2016	0000-0003-1696-9134

ISSN: 1932-6203

Record 9 of 39

Title: Selective Plasma Etching of Polymeric Substrates for Advanced Applications

Author(s): Puliyalil, H (Puliyalil, Harinarayanan); Cvelbar, U (Cvelbar, Uros)

Source: NANOMATERIALS **Volume:** 6 **Issue:** 6 **Article Number:** UNSP 108 **DOI:** 10.3390/nano6060108 **Published:** JUN 2016

Accession Number: WOS:000378806100014

PubMed ID: 28335238

Author Identifiers:

Author	ResearcherID Number	ORCID Number
Puliyalil, Harinarayanan	I-9180-2016	0000-0002-9749-5307

ISSN: 2079-4991

Record 10 of 39

Title: Metastable helium atom density in a single electrode atmospheric plasma jet during sample treatment

Author(s): Zaplotnik, R (Zaplotnik, R.); Biscan, M (Biscan, M.); Popovic, D (Popovic, D.); Mozetic, M (Mozetic, M.); Milosevic, S (Milosevic, S.)

Source: PLASMA SOURCES SCIENCE & TECHNOLOGY **Volume:** 25 **Issue:** 3 **Article Number:** 035023 **DOI:** 10.1088/0963-0252/25/3/035023 **Published:** JUN 2016

Accession Number: WOS:000376557400031

Author Identifiers:

Author	ResearcherID Number	ORCID Number
Milosevic, Slobodan	A-3408-2010	
Milosevic, Slobodan		0000-0002-4455-7869

ISSN: 0963-0252

eISSN: 1361-6595

Record 11 of 39

Title: Effect of Cold Plasma on Cell Viability and Collagen Synthesis in Cultured Murine Fibroblasts

Author(s): Shi, XM (Shi Xingmin); Cai, JF (Cai Jingfen); Xu, GM (Xu Guimin); Ren, HB (Ren Hongbin); Chen, SL (Chen Sile); Chang, ZS (Chang Zhengshi); Liu, JR (Liu Jinren); Huang, CY (Huang Chongya); Zhang, GJ (Zhang Guanjun); Wu, XL (Wu Xili)

Source: PLASMA SCIENCE & TECHNOLOGY **Volume:** 18 **Issue:** 4 **Pages:** 353-359 **DOI:** 10.1088/1009-0630/18/4/04 **Published:** APR 2016

Accession Number: WOS:000375143300004

Author Identifiers:

Author	ResearcherID Number	ORCID Number
Chang, Zhengshi	J-2517-2018	0000-0002-0024-4553

ISSN: 1009-0630

Record 12 of 39

Title: Cytotoxicity of modified nonequilibrium plasma with chlorhexidine digluconate on primary cultured human gingival fibroblasts

Author(s): Chen, H (Chen, Hui); Shi, Q (Shi, Qi); Qing, Y (Qing, Ying); Yao, YC (Yao, Yi-chen); Cao, YG (Cao, Ying-guang)

Source: JOURNAL OF HUAZHONG UNIVERSITY OF SCIENCE AND TECHNOLOGY-MEDICAL SCIENCES **Volume:** 36 **Issue:** 1 **Pages:** 137-141 **DOI:** 10.1007/s11596-016-1556-0 **Published:** FEB 2016

Accession Number: WOS:000369301700024

PubMed ID: 26838755

ISSN: 1672-0733

eISSN: 1993-1352

Record 13 of 39

Title: Influence of ionic liquid and ionic salt on protein against the reactive species generated using dielectric barrier discharge plasma

Author(s): Attri, P (Attri, Pankaj); Sarinont, T (Sarinont, Thapanut); Kim, M (Kim, Minsup); Amano, T (Amano, Takaaki); Koga, K (Koga, Kazunori); Cho, AE (Cho, Art E.); Choi, EH (Choi, Eun Ha); Shiratani, M (Shiratani, Masaharu)

Source: SCIENTIFIC REPORTS **Volume:** 5 **Article Number:** 17781 **DOI:** 10.1038/srep17781 **Published:** DEC 10 2015

Accession Number: WOS:000366133200001

PubMed ID: 26656857

Author Identifiers:

Author	ResearcherID Number	ORCID Number
Attri, Pankaj		0000-0002-5036-7877
Shiratani, Masaharu		0000-0002-4103-3939

ISSN: 2045-2322

Record 14 of 39

Title: Practical and theoretical considerations on the use of ICCD imaging for the characterization of non-equilibrium plasmas

Author(s): Gherardi, M (Gherardi, Matteo); Puac, N (Puac, Nevena); Maric, D (Maric, Dragana); Stancampiano, A (Stancampiano, Augusto); Malovic, G (Malovic, Gordana); Colombo, V (Colombo, Vittorio); Petrovic, ZL (Petrovic, Zoran Lj)

Source: PLASMA SOURCES SCIENCE & TECHNOLOGY **Volume:** 24 **Issue:** 6 **Article Number:** 064004 **DOI:** 10.1088/0963-0252/24/6/064004 **Published:** DEC 2015

Accession Number: WOS:000368117100005

Author Identifiers:

Author	ResearcherID Number	ORCID Number
Maric, Dragana		0000-0002-1728-5458
Malovic, Gordana		0000-0003-2356-0652
COLOMBO, VITTORIO		0000-0001-9145-198X
Petrovic, Zoran		0000-0001-6569-9447
Puac, Nevena		0000-0003-1142-8494

ISSN: 0963-0252
eISSN: 1361-6595

Record 15 of 39

Title: Research on plasma medicine-relevant plasma-liquid interaction: What happened in the past five years?

Author(s): Jablonowski, H (Jablonowski, Helena); von Woedtke, T (von Woedtke, Thomas)

Source: CLINICAL PLASMA MEDICINE **Volume:** 3 **Issue:** 2 **Pages:** 42-52 **DOI:** 10.1016/j.cpme.2015.11.003 **Published:** DEC 2015
Accession Number: WOS:000433743700002
ISSN: 2452-0896
eISSN: 2212-8166

Record 16 of 39

Title: Effects of air transient spark discharge and helium plasma jet on water, bacteria, cells, and biomolecules

Author(s): Hensel, K (Hensel, Karol); Kucerova, K (Kucerova, Katarina); Tarabova, B (Tarabova, Barbora); Janda, M (Janda, Mario); Machala, Z (Machala, Zdenko); Sano, K (Sano, Kaori); Mihai, CT (Mihai, Cosmin Teodor); Ciorpac, M (Ciorpac, Mitica); Gorgan, LD (Gorgan, Lucian Dragos); Jijie, R (Jijie, Roxana); Pohoata, V (Pohoata, Valentin); Topala, I (Topala, Ionut)

Source: BIOINTERPHASES **Volume:** 10 **Issue:** 2 **Article Number:** 029515 **DOI:** 10.1116/1.4919559 **Published:** JUN 2015
Accession Number: WOS:000357195600033
PubMed ID: 25947389

Author Identifiers:

Author	ResearcherID Number	ORCID Number
Machala, Zdenko	B-6384-2018	0000-0003-1424-1350
Ciorpac, Mitica	C-7790-2015	0000-0001-5374-0908
Mihai, Cosmin-Teodor	F-7815-2011	0000-0002-0945-5437
Tarabova, Barbora	I-7953-2018	0000-0001-9936-1786
Topala, Ionut	A-2305-2009	0000-0002-8954-8106
Janda, Mario	G-5864-2018	0000-0001-9051-4221
Pohoata, Valentin	R-1354-2017	0000-0001-5554-0088

Hensel, Karol	G-5851-2018	0000-0001-6833-681X
Gorgan, Lucian	B-5701-2012	0000-0001-6454-9092
Jijie, Roxana		0000-0003-0354-943X

ISSN: 1934-8630

eISSN: 1559-4106

Record 17 of 39

Title: Time-resolved optical emission imaging of an atmospheric plasma jet for different electrode positions with a constant electrode gap

Author(s): Maletic, D (Maletic, D.); Puac, N (Puac, N.); Selakovic, N (Selakovic, N.); Lazovic, S (Lazovic, S.); Malovic, G (Malovic, G.); Dordevic, A (Dordevic, A.); Petrovic, ZL (Petrovic, Z. Lj)

Source: PLASMA SOURCES SCIENCE & TECHNOLOGY **Volume:** 24 **Issue:** 2 **Article Number:** 025006 **DOI:** 10.1088/0963-0252/24/2/025006 **Published:** APR 2015

Accession Number: WOS:000356816200010

Author Identifiers:

Author	ResearcherID Number	ORCID Number
Lazovic, Sasa	Q-5056-2016	0000-0003-1696-9134
Petrovic, Zoran		0000-0001-6569-9447
Puac, Nevena		0000-0003-1142-8494
Malovic, Gordana		0000-0003-2356-0652

ISSN: 0963-0252

eISSN: 1361-6595

Record 18 of 39

Title: Cross sections and transport of O- in H2O vapour at low pressures

Author(s): Stojanovic, V (Stojanovic, Vladimir); Raspopovic, Z (Raspopovic, Zoran); Maric, D (Maric, Dragana); Petrovic, ZL (Petrovic, Zoran Lj.)

Source: EUROPEAN PHYSICAL JOURNAL D **Volume:** 69 **Issue:** 3 **Article Number:** 63 **DOI:** 10.1140/epjd/e2015-50720-9 **Published:** MAR 6 2015

Accession Number: WOS:000361131200002

Author Identifiers:

Author	ResearcherID Number	ORCID Number
Petrovic, Zoran		0000-0001-6569-9447
Maric, Dragana		0000-0002-1728-5458

ISSN: 1434-6060

eISSN: 1434-6079

Record 19 of 39

Title: Capillary plasma jet: A low volume plasma source for life science applications

Author(s): Topala, I (Topala, I.); Nagatsu, M (Nagatsu, M.)
Source: APPLIED PHYSICS LETTERS **Volume:** 106 **Issue:** 5 **Article Number:** 054105 **DOI:** 10.1063/1.4907349 **Published:** FEB 2 2015
Accession Number: WOS:000349611800091
Author Identifiers:

Author	ResearcherID Number	ORCID Number
Topala, Ionut	A-2305-2009	0000-0002-8954-8106

ISSN: 0003-6951
eISSN: 1077-3118

Record 20 of 39
Title: Sterilization of bacteria suspensions and identification of radicals deposited during plasma treatment
Author(s): Puac, N (Puac, Nevena); Miletic, M (Miletic, Maja); Mojovic, M (Mojovic, Milos); Popovic-Bijelic, A (Popovic-Bijelic, Ana); Vukovic, D (Vukovic, Dragana); Milicic, B (Milicic, Biljana); Maletic, D (Maletic, Dejan); Lazovic, S (Lazovic, Sasa); Malovic, G (Malovic, Gordana); Petrovic, ZL (Petrovic, Zoran Lj)
Source: OPEN CHEMISTRY **Volume:** 13 **Issue:** 1 **Pages:** 332-338 **DOI:** 10.1515/chem-2015-0041 **Published:** JAN 2015
Accession Number: WOS:000355403100040
Author Identifiers:

Author	ResearcherID Number	ORCID Number
Lazovic, Sasa	Q-5056-2016	0000-0003-1696-9134
Popovic Bijelic, Ana	C-6314-2017	0000-0003-3121-2391
Petrovic, Zoran		0000-0001-6569-9447
Mojovic, Milos		0000-0002-1868-9913
Malovic, Gordana		0000-0003-2356-0652
Puac, Nevena		0000-0003-1142-8494

ISSN: 2391-5420

Record 21 of 39
Title: Plasma induced DNA damage: Comparison with the effects of ionizing radiation
Author(s): Lazovic, S (Lazovic, S.); Maletic, D (Maletic, D.); Leskovac, A (Leskovac, A.); Filipovic, J (Filipovic, J.); Puac, N (Puac, N.); Malovic, G (Malovic, G.); Joksic, G (Joksic, G.); Petrovic, ZL (Petrovic, Z. Lj.)
Source: APPLIED PHYSICS LETTERS **Volume:** 105 **Issue:** 12 **Article Number:** 124101 **DOI:** 10.1063/1.4896626 **Published:** SEP 22 2014
Accession Number: WOS:000343004400099
Author Identifiers:

Author	ResearcherID Number	ORCID Number

Lazovic, Sasa	Q-5056-2016	0000-0003-1696-9134
Joksic, Gordana		0000-0002-7186-301X
Petrovic, Zoran		0000-0001-6569-9447
Leskovac, Andreja		0000-0002-6293-5237
Puac, Nevena		0000-0003-1142-8494
Filipovic Trickovic, Jelena		0000-0001-5450-0842
Malovic, Gordana		0000-0003-2356-0652

ISSN: 0003-6951

eISSN: 1077-3118

Record 22 of 39

Title: Microbubble generation by microplasma in water

Author(s): Xiao, P (Xiao, Peng); Staack, D (Staack, David)

Source: JOURNAL OF PHYSICS D-APPLIED PHYSICS **Volume:** 47 **Issue:** 35 **Article Number:** 355203 **DOI:** 10.1088/0022-3727/47/35/355203 **Published:** SEP 3 2014

Accession Number: WOS:000341353800015

ISSN: 0022-3727

eISSN: 1361-6463

Record 23 of 39

Title: Long and short term effects of plasma treatment on meristematic plant cells

Author(s): Puac, N (Puac, N.); Zivkovic, S (Zivkovic, S.); Selakovic, N (Selakovic, N.); Milutinovic, M (Milutinovic, M.); Boljevic, J (Boljevic, J.); Malovic, G (Malovic, G.); Petrovic, ZL (Petrovic, Z. Lj)

Source: APPLIED PHYSICS LETTERS **Volume:** 104 **Issue:** 21 **Article Number:** 214106 **DOI:** 10.1063/1.4880360 **Published:** MAY 26 2014

Accession Number: WOS:000337143000078

Author Identifiers:

Author	ResearcherID Number	ORCID Number
Petrovic, Zoran		0000-0001-6569-9447
Zivkovic, Suzana		0000-0003-0280-5884
Puac, Nevena		0000-0003-1142-8494
Malovic, Gordana		0000-0003-2356-0652

ISSN: 0003-6951

eISSN: 1077-3118

Record 24 of 39

Title: Multiple vs. single harmonics AC-driven atmospheric plasma jet

Author(s): Zaplotnik, R (Zaplotnik, R.); Kregar, Z (Kregar, Z.); Biscan, M (Biscan, M.); Vesel, A (Vesel, A.); Cvelbar, U (Cvelbar, U.); Mozetic, M (Mozetic, M.); Milosevic, S (Milosevic, S.)

Source: EPL **Volume:** 106 **Issue:** 2 **Article Number:** 25001 **DOI:** 10.1209/0295-5075/106/25001 **Published:** APR 2014
Accession Number: WOS:000336376100010
Author Identifiers:

Author	ResearcherID Number	ORCID Number
Mozetic, Miran	K-8784-2014	
Vesel, Alenka	I-3934-2014	0000-0003-3782-6001
Milosevic, Slobodan	A-3408-2010	
Milosevic, Slobodan		0000-0002-4455-7869

ISSN: 0295-5075
eISSN: 1286-4854

Record 25 of 39
Title: Inhibition of methicillin resistant Staphylococcus aureus by a plasma needle
Author(s): Miletic, M (Miletic, Maja); Vukovic, D (Vukovic, Dragana); Zivanovic, I (Zivanovic, Irena); Dakic, I (Dakic, Ivana); Soldatovic, I (Soldatovic, Ivan); Maletic, D (Maletic, Dejan); Lazovic, S (Lazovic, Sasa); Malovic, G (Malovic, Gordana); Petrovic, ZL (Petrovic, Zoran Lj); Puac, N (Puac, Nevena)
Source: CENTRAL EUROPEAN JOURNAL OF PHYSICS **Volume:** 12 **Issue:** 3 **Pages:** 160-167 **DOI:** 10.2478/s11534-014-0437-z **Published:** MAR 2014
Accession Number: WOS:000333023800002
Author Identifiers:

Author	ResearcherID Number	ORCID Number
Lazovic, Sasa	Q-5056-2016	0000-0003-1696-9134
Malovic, Gordana		0000-0003-2356-0652
Petrovic, Zoran		0000-0001-6569-9447
Puac, Nevena		0000-0003-1142-8494
Soldatovic, Ivan		0000-0003-4893-1683

ISSN: 1895-1082
eISSN: 1644-3608

Record 26 of 39
Title: Controlling the oxygen species density distributions in the flowing afterglow of O-2/Ar-O-2 surface-wave microwave discharges
Author(s): Kutasi, K (Kutasi, Kinga); Zaplotnik, R (Zaplotnik, Rok); Primc, G (Primc, Gregor); Mozetic, M (Mozetic, Miran)
Source: JOURNAL OF PHYSICS D-APPLIED PHYSICS **Volume:** 47 **Issue:** 2 **Article Number:** 025203 **DOI:** 10.1088/0022-3727/47/2/025203 **Published:** JAN 15 2014
Accession Number: WOS:000329108000011
Author Identifiers:

Author	ResearcherID Number	ORCID Number
Mozetic, Miran	K-8784-2014	

ISSN: 0022-3727

eISSN: 1361-6463

Record 27 of 39

Title: Quantitative detection of plasma-generated radicals in liquids by electron paramagnetic resonance spectroscopy

Author(s): Tresp, H (Tresp, H.); Hammer, MU (Hammer, M. U.); Winter, J (Winter, J.); Weltmann, KD (Weltmann, K-D); Reuter, S (Reuter, S.)

Source: JOURNAL OF PHYSICS D-APPLIED PHYSICS **Volume:** 46 **Issue:** 43 **Article Number:** 435401 **DOI:** 10.1088/0022-3727/46/43/435401 **Published:** OCT 30 2013

Accession Number: WOS:000325679400013

Author Identifiers:

Author	ResearcherID Number	ORCID Number
Reuter, Stephan	D-2890-2014	0000-0002-4858-1081

ISSN: 0022-3727

eISSN: 1361-6463

Record 28 of 39

Title: Effects of non-thermal atmospheric plasma on human periodontal ligament mesenchymal stem cells

Author(s): Miletic, M (Miletic, M.); Mojsilovic, S (Mojsilovic, S.); Dordevic, IO (Dordevic, I. Okic); Maletic, D (Maletic, D.); Puac, N (Puac, N.); Lazovic, S (Lazovic, S.); Malovic, G (Malovic, G.); Milenkovic, P (Milenkovic, P.); Petrovic, ZL (Petrovic, Z. Lj); Bugarski, D (Bugarski, D.)

Source: JOURNAL OF PHYSICS D-APPLIED PHYSICS **Volume:** 46 **Issue:** 34 **Article Number:** 345401 **DOI:** 10.1088/0022-3727/46/34/345401 **Published:** AUG 28 2013

Accession Number: WOS:000323062400017

Author Identifiers:

Author	ResearcherID Number	ORCID Number
Lazovic, Sasa	Q-5056-2016	0000-0003-1696-9134
Malovic, Gordana		0000-0003-2356-0652
Puac, Nevena		0000-0003-1142-8494

ISSN: 0022-3727

Record 29 of 39

Title: Structured MgO film coated electrodes for glow discharge sustainment

Author(s): Akasaka, H (Akasaka, Hiroki); Matsuda, K (Matsuda, Kuniyuki); Minami, R (Minami, Ryohei); Kiyokawa, T (Kiyokawa, Toshio); Takano, A (Takano, Akihiro); Ohshio, S (Ohshio, Shigeo); Toda, I (Toda, Ikumi); Saitoh, H (Saitoh, Hidetoshi)

Source: THIN SOLID FILMS **Volume:** 534 **Pages:** 465-469 **DOI:** 10.1016/j.tsf.2013.02.006 **Published:** MAY 1 2013

Accession Number: WOS:000317736700076

ISSN: 0040-6090

Record 30 of 39

Title: Plasma properties in a large-volume, cylindrical and asymmetric radio-frequency capacitively coupled industrial-prototype reactor

Author(s): Lazovic, S (Lazovic, Sasa); Puac, N (Puac, Nevena); Spasic, K (Spasic, Kosta); Malovic, G (Malovic, Gordana); Cvelbar, U (Cvelbar, Uros); Mozetic, M (Mozetic, Miran); Radetic, M (Radetic, Maja); Petrovic, ZL (Petrovic, Zoran Lj)

Source: JOURNAL OF PHYSICS D-APPLIED PHYSICS **Volume:** 46 **Issue:** 7 **Article Number:** 075201 **DOI:** 10.1088/0022-3727/46/7/075201 **Published:** FEB 20 2013

Accession Number: WOS:000314471900014

Author Identifiers:

Author	ResearcherID Number	ORCID Number
Lazovic, Sasa	Q-5056-2016	0000-0003-1696-9134
Mozetic, Miran	K-8784-2014	
Lazovic, Sasa	B-9651-2013	0000-0003-1696-9134
Puac, Nevena		0000-0003-1142-8494
Malovic, Gordana		0000-0003-2356-0652
Petrovic, Zoran		0000-0001-6569-9447

ISSN: 0022-3727

Record 31 of 39

Title: Inactivation of Gram-positive biofilms by low-temperature plasma jet at atmospheric pressure

Author(s): Marchal, F (Marchal, F.); Robert, H (Robert, H.); Merbahi, N (Merbahi, N.); Fontagne-Faucher, C (Fontagne-Faucher, C.); Yousfi, M (Yousfi, M.); Romain, CE (Romain, C. E.); Eichwald, O (Eichwald, O.); Rondel, C (Rondel, C.); Gabriel, B (Gabriel, B.)

Source: JOURNAL OF PHYSICS D-APPLIED PHYSICS **Volume:** 45 **Issue:** 34 **Article Number:** 345202 **DOI:** 10.1088/0022-3727/45/34/345202 **Published:** AUG 29 2012

Accession Number: WOS:000307808600005

Author Identifiers:

Author	ResearcherID Number	ORCID Number
Marchal, Frederic		0000-0003-4835-4484
ROBERT, Herve		0000-0002-0561-2781

ISSN: 0022-3727

eISSN: 1361-6463

Record 32 of 39

Title: Complex Responses of Microorganisms as a Community to a Flowing Atmospheric Plasma

Author(s): Bayliss, DL (Bayliss, Danny L.); Walsh, JL (Walsh, James L.); Iza, F (Iza, Felipe); Shama, G (Shama, Gilbert); Holah, J (Holah, John); Kong, MG (Kong, Michael

G.)

Source: PLASMA PROCESSES AND POLYMERS **Volume:** 9 **Issue:** 6 **Special Issue:** SI **Pages:** 597-611 **DOI:** 10.1002/ppap.201100104 **Published:** JUN 2012

Accession Number: WOS:000305476700009

Author Identifiers:

Author	ResearcherID Number	ORCID Number
kong, michael	I-1574-2014	
walsh, james	F-1426-2011	
Shama, Gilbert	E-9008-2011	
Walsh, James		0000-0002-6318-0892

ISSN: 1612-8850

Record 33 of 39

Title: A Monte Carlo simulation of ion transport at finite temperatures

Author(s): Ristivojevic, Z (Ristivojevic, Zoran); Petrovic, ZL (Petrovic, Zoran Lj)

Source: PLASMA SOURCES SCIENCE & TECHNOLOGY **Volume:** 21 **Issue:** 3 **Article Number:** 035001 **DOI:** 10.1088/0963-0252/21/3/035001 **Published:** JUN 2012

Accession Number: WOS:000304781800024

Author Identifiers:

Author	ResearcherID Number	ORCID Number
Petrovic, Zoran		0000-0001-6569-9447

ISSN: 0963-0252

eISSN: 1361-6595

Record 34 of 39

Title: Application of non-equilibrium plasmas in medicine

Author(s): Petrovic, ZL (Petrovic, Zoran Lj.); Puac, N (Puac, Nevena); Malovic, G (Malovic, Gordana); Lazovic, S (Lazovic, Sasa); Maletic, D (Maletic, Dejan); Miletic, M (Miletic, Maja); Mojsilovic, S (Mojsilovic, Slavko); Milenkovic, P (Milenkovic, Pavle); Bugarski, D (Bugarski, Diana)

Source: JOURNAL OF THE SERBIAN CHEMICAL SOCIETY **Volume:** 77 **Issue:** 12 **Pages:** 1689-1699 **DOI:** 10.2298/JSC121020142P **Published:** 2012

Accession Number: WOS:000314080000002

Author Identifiers:

Author	ResearcherID Number	ORCID Number
Lazovic, Sasa	B-9651-2013	0000-0003-1696-9134
Lazovic, Sasa	Q-5056-2016	0000-0003-1696-9134
Petrovic, Zoran		0000-0001-6569-9447

Puac, Nevena		0000-0003-1142-8494
Malovic, Gordana		0000-0003-2356-0652

ISSN: 0352-5139

Record 35 of 39

Title: Diagnostics and biomedical applications of radiofrequency plasmas

Author(s): Lazovic, S (Lazovic, Sasa)

Edited by: Kuraica M; Mijatovic Z

Source: 26TH SUMMER SCHOOL AND INTERNATIONAL SYMPOSIUM ON THE PHYSICS OF IONIZED GASES (SPIG 2012) **Book Series:** Journal of Physics Conference Series **Volume:** 399 **Article Number:** 012015 **DOI:** 10.1088/1742-6596/399/1/012015 **Published:** 2012

Accession Number: WOS:000312261700015

Conference Title: 26th Summer School and International Symposium on the Physics of Ionized Gases (SPIG)

Conference Date: AUG 27-31, 2012

Conference Location: Zrenjanin, SERBIA

Conference Sponsors: Sci & Technol Dev Republ Serbia, Minist Educ, Prov Secretariat Sci & Technol Dev, Inst Francais Serbie, Biser Zrenjanin

Author Identifiers:

Author	ResearcherID Number	ORCID Number
Lazovic, Sasa	Q-5056-2016	0000-0003-1696-9134
Lazovic, Sasa	B-9651-2013	0000-0003-1696-9134

ISSN: 1742-6588

Record 36 of 39

Title: Breakdown and discharge regimes in standard and micrometer size dc discharges

Author(s): Skoro, N (Skoro, N.)

Edited by: Kuraica M; Mijatovic Z

Source: 26TH SUMMER SCHOOL AND INTERNATIONAL SYMPOSIUM ON THE PHYSICS OF IONIZED GASES (SPIG 2012) **Book Series:** Journal of Physics Conference Series **Volume:** 399 **Article Number:** 012017 **DOI:** 10.1088/1742-6596/399/1/012017 **Published:** 2012

Accession Number: WOS:000312261700017

Conference Title: 26th Summer School and International Symposium on the Physics of Ionized Gases (SPIG)

Conference Date: AUG 27-31, 2012

Conference Location: Zrenjanin, SERBIA

Conference Sponsors: Sci & Technol Dev Republ Serbia, Minist Educ, Prov Secretariat Sci & Technol Dev, Inst Francais Serbie, Biser Zrenjanin

Author Identifiers:

Author	ResearcherID Number	ORCID Number

Skoro, Nikola		0000-0002-0254-8008

ISSN: 1742-6588

Record 37 of 39

Title: Development of Biomedical Applications of Non-equilibrium Plasmas and Possibilities for Atmospheric Pressure Nanotechnology Applications

Author(s): Petrovic, ZL (Petrovic, Z. Lj); Puac, N (Puac, N.); Maric, D (Maric, D.); Maletic, D (Maletic, D.); Spasic, K (Spasic, K.); Skoro, N (Skoro, N.); Sivos, J (Sivos, J.); Lazovic, S (Lazovic, S.); Malovic, G (Malovic, G.)

Book Group Author(s): IEEE

Source: 2012 28TH INTERNATIONAL CONFERENCE ON MICROELECTRONICS (MIEL) **Book Series:** International Conference on Microelectronics-MIEL **Pages:** 31-38 **Published:** 2012

Accession Number: WOS:000309119600005

Conference Title: 28th International Conference on Microelectronics (MIEL)

Conference Date: MAY 13-16, 2012

Conference Location: Nis, SERBIA

Conference Sponsors: IEEE, IEEE Serbia & Montenegro Sect - ED/SSC Chapter, IEEE Electron Devices Soc (EDS), IEEE Solid-State Circuits Soc (SSCS)

Author Identifiers:

Author	ResearcherID Number	ORCID Number
Lazovic, Sasa	B-9651-2013	0000-0003-1696-9134
Skoro, Nikola		0000-0002-0254-8008
Malovic, Gordana		0000-0003-2356-0652
Puac, Nevena		0000-0003-1142-8494
Maric, Dragana		0000-0002-1728-5458
Petrovic, Zoran		0000-0001-6569-9447

ISSN: 2159-1660

ISBN: 978-1-4673-0238-8

Record 38 of 39

Title: Biomedical applications and diagnostics of atmospheric pressure plasma

Author(s): Petrovic, ZL (Petrovic, Z. Lj); Puac, N (Puac, N.); Lazovic, S (Lazovic, S.); Maletic, D (Maletic, D.); Spasic, K (Spasic, K.); Malovic, G (Malovic, G.)

Edited by: VanDeSanden MCM; Dimitrova M; Ghelev C

Source: 17TH INTERNATIONAL SUMMER SCHOOL ON VACUUM, ELECTRON, AND ION TECHNOLOGIES (VEIT 2011) **Book Series:** Journal of Physics Conference Series **Volume:** 356 **Article Number:** 012001 **DOI:** 10.1088/1742-6596/356/1/012001 **Published:** 2012

Accession Number: WOS:000307884600002

Conference Title: 17th International Summer School on Vacuum, Electron, and Ion Technologies (VEIT)

Conference Date: SEP 19-23, 2011

Conference Location: BULGARIA
Conference Sponsors: Eindhoven Univ Technol, Dept Appl Phys
Author Identifiers:

Author	ResearcherID Number	ORCID Number
Lazovic, Sasa	B-9651-2013	0000-0003-1696-9134
Lazovic, Sasa	Q-5056-2016	0000-0003-1696-9134
Puac, Nevena		0000-0003-1142-8494
Petrovic, Zoran		0000-0001-6569-9447
Malovic, Gordana		0000-0003-2356-0652

ISSN: 1742-6588

Record 39 of 39
Title: Electrical Breakdown in Water Vapor
Author(s): Skoro, N (Skoro, N.); Maric, D (Maric, D.); Malovic, G (Malovic, G.); Graham, WG (Graham, W. G.); Petrovic, ZL (Petrovic, Z. Lj.)
Source: PHYSICAL REVIEW E **Volume:** 84 **Issue:** 5 **Article Number:** 055401 **DOI:** 10.1103/PhysRevE.84.055401 **Part:** 2 **Published:** NOV 10 2011
Accession Number: WOS:000297418700001
PubMed ID: 22181466
Author Identifiers:

Author	ResearcherID Number	ORCID Number
Maric, Dragana	C-6722-2009	
Skoro, Nikola		0000-0002-0254-8008
Maric, Dragana		0000-0002-1728-5458
Graham, William		0000-0003-2759-4657
Malovic, Gordana		0000-0003-2356-0652
Petrovic, Zoran		0000-0001-6569-9447

ISSN: 1539-3755

Close

Web of Science
Page 1 (Records 1 -- 39)
[1]

Print

Close

Web of Science
Page 1 (Records 1 -- 29)
[1]

Print

Record 1 of 29

Title: Characterisation of a multijet plasma device by means of mass spectrometric detection and iCCD imaging

Author(s): Stancampiano, A (Stancampiano, A.); Selakovic, N (Selakovic, N.); Gherardi, M (Gherardi, M.); Puac, N (Puac, N.); Petrovic, ZL (Petrovic, Z. Lj); Colombo, V (Colombo, V)

Source: JOURNAL OF PHYSICS D-APPLIED PHYSICS **Volume:** 51 **Issue:** 48 **Article Number:** 484004 **DOI:** 10.1088/1361-6463/aae2f2 **Published:** DEC 5 2018

Accession Number: WOS:000446857200001

ISSN: 0022-3727

eISSN: 1361-6463

Record 2 of 29

Title: The effect of ethanol gas impurity on the discharge mode and discharge products of argon plasma jet at atmospheric pressure

Author(s): Xia, WJ (Xia, Wenjie); Liu, DX (Liu, Dingxin); Xu, H (Xu, Han); Wang, XH (Wang, Xiaohua); Liu, ZJ (Liu, Zhijie); Rong, MZ (Rong, Mingzhe); Kong, MG (Kong, Michael G.)

Source: PLASMA SOURCES SCIENCE & TECHNOLOGY **Volume:** 27 **Issue:** 5 **Article Number:** 055001 **DOI:** 10.1088/1361-6595/aabdc1 **Published:** MAY 2018

Accession Number: WOS:000431523300001

Author Identifiers:

Author	ResearcherID Number	ORCID Number
Xu, Han		0000-0002-3525-8904

ISSN: 0963-0252

eISSN: 1361-6595

Record 3 of 29

Title: The influence of electrode configuration on light emission profiles and electrical characteristics of an atmospheric-pressure plasma jet

Author(s): Maletic, D (Maletic, Dejan); Puac, N (Puac, Nevena); Malovic, G (Malovic, Gordana); Dordevic, A (Dordevic, Antonije); Petrovic, ZL (Petrovic, Zoran Lj)

Source: JOURNAL OF PHYSICS D-APPLIED PHYSICS **Volume:** 50 **Issue:** 14 **Article Number:** 145202 **DOI:** 10.1088/1361-6463/aa5d91 **Published:** APR 12 2017

Accession Number: WOS:000404428200002

Author Identifiers:

Author	ResearcherID Number	ORCID Number
Puac, Nevena		0000-0003-1142-8494
Petrovic, Zoran		0000-0001-6569-9447

Malovic, Gordana		0000-0003-2356-0652

ISSN: 0022-3727
eISSN: 1361-6463

Record 4 of 29

Title: Mass spectrometry of diffuse coplanar surface barrier discharge: influence of discharge frequency and oxygen content in N-2/O-2 mixture

Author(s): Cech, J (Cech, Jan); Brablec, A (Brablec, Antonin); Cernak, M (Cernak, Mirko); Puac, N (Puac, Nevena); Selakovic, N (Selakovic, Nenad); Petrovic, ZL (Petrovic, Zoran Lj.)

Source: EUROPEAN PHYSICAL JOURNAL D **Volume:** 71 **Issue:** 2 **Article Number:** 27 **DOI:** 10.1140/epjd/e2016-70607-5 **Published:** FEB 9 2017
Accession Number: WOS:000403477900003

Author Identifiers:

Author	ResearcherID Number	ORCID Number
Cech, Jan	F-8310-2017	0000-0002-4900-6011

ISSN: 1434-6060
eISSN: 1434-6079

Record 5 of 29

Title: Microplasma Induced Cell Morphological Changes and Apoptosis of Ex Vivo Cultured Human Anterior Lens Epithelial Cells - Relevance to Capsular Opacification

Author(s): Recek, N (Recek, Nina); Andjelic, S (Andjelic, Sofija); Hojnik, N (Hojnik, Nataga); Filipic, G (Filipic, Gregor); Lazovic, S (Lazovic, Sasa); Vesel, A (Vesel, Alenka); Primc, G (Primc, Gregor); Mozetic, M (Mozetic, Miran); Hawlina, M (Hawlina, Marko); Petrovski, G (Petrovski, Goran); Cvelbar, U (Cvelbar, Uros)

Source: PLOS ONE **Volume:** 11 **Issue:** 11 **Article Number:** e0165883 **DOI:** 10.1371/journal.pone.0165883 **Published:** NOV 10 2016
Accession Number: WOS:000387725000038
PubMed ID: 27832099

Author Identifiers:

Author	ResearcherID Number	ORCID Number
Filipic, Gregor	T-4900-2018	0000-0003-0153-5181
Lazovic, Sasa	Q-5056-2016	0000-0003-1696-9134

ISSN: 1932-6203

Record 6 of 29

Title: Methods of gas purification and effect on the ion composition in an RF atmospheric pressure plasma jet investigated by mass spectrometry

Author(s): Grosse-Kreul, S (Grosse-Kreul, Simon); Hubner, S (Huebner, Simon); Schneider, S (Schneider, Simon); von Keudell, A (von Keudell, Achim); Benedikt, J (Benedikt, Jan)

Source: EPJ TECHNIQUES AND INSTRUMENTATION **Volume:** 3 **Article Number:** 6 **DOI:** 10.1140/epjti/s40485-016-0034-1 **Published:** SEP 2 2016
Accession Number: WOS:000387282300001
Author Identifiers:

Author	ResearcherID Number	ORCID Number
Benedikt, Jan	A-8463-2016	0000-0002-8954-1908
von Keudell, Achim		0000-0003-3887-9359

ISSN: 2195-7045

Record 7 of 29
Title: The effect of the plasma needle on the human keratinocytes related to the wound healing process
Author(s): Korolov, I (Korolov, Ihor); Fazekas, B (Fazekas, Barbara); Szell, M (Szell, Marta); Kemeny, L (Kemeny, Lajos); Kutasi, K (Kutasi, Kinga)
Source: JOURNAL OF PHYSICS D-APPLIED PHYSICS **Volume:** 49 **Issue:** 3 **Article Number:** 035401 **DOI:** 10.1088/0022-3727/49/3/035401 **Published:** JAN 27 2016
Accession Number: WOS:000368096300019
Author Identifiers:

Author	ResearcherID Number	ORCID Number
Korolov, Ihor	A-2848-2013	0000-0003-2384-1243

ISSN: 0022-3727
eISSN: 1361-6463

Record 8 of 29
Title: Mass Spectrometry of Atmospheric Pressure Surface Wave Discharges
Author(s): Ridenti, MA (Ridenti, M. A.); Souza-Correa, JA (Souza-Correa, J. A.); Amorim, J (Amorim, J.)
Book Group Author(s): IOP
Source: 5TH INTERNATIONAL WORKSHOP & SUMMER SCHOOL ON PLASMA PHYSICS 2012 **Book Series:** Journal of Physics Conference Series **Volume:** 715 **Article Number:** 012003 **DOI:** 10.1088/1742-6596/715/1/012003 **Published:** 2016
Accession Number: WOS:000386609100003
Conference Title: 5th International Workshop and Summer School on Plasma Physics (IWSSPP)
Conference Date: JUN 25-30, 2012
Conference Location: Kiten, BULGARIA
Conference Sponsors: St Kliment Ohridsky Univ Sofia, TCPA Fdn, Assoc EURATOM/IRNRE, Bulgarian Acad Sci
Author Identifiers:

Author	ResearcherID Number	ORCID Number

Amorim, Jayr	M-9794-2014	0000-0002-9250-4681
Ridenti, Marco Antonio		0000-0001-6483-5128
de Souza-Correa, Jorge A.		0000-0002-4365-3920

ISSN: 1742-6588

Record 9 of 29

Title: Use of molecular beacons for the rapid analysis of DNA damage induced by exposure to an atmospheric pressure plasma jet

Author(s): Kurita, H (Kurita, Hirofumi); Miyachika, S (Miyachika, Saki); Yasuda, H (Yasuda, Hachiro); Takashima, K (Takashima, Kazunori); Mizuno, A (Mizuno, Akira)

Source: APPLIED PHYSICS LETTERS **Volume:** 107 **Issue:** 26 **Article Number:** 263702 **DOI:** 10.1063/1.4939044 **Published:** DEC 28 2015

Accession Number: WOS:000368442300042

Author Identifiers:

Author	ResearcherID Number	ORCID Number
Kurita, Hirofumi		0000-0002-2538-6590

ISSN: 0003-6951

eISSN: 1077-3118

Record 10 of 29

Title: Mass spectrometry of atmospheric pressure plasmas

Author(s): Grosse-Kreul, S (Grosse-Kreul, S.); Hubner, S (Huebner, S.); Schneider, S (Schneider, S.); Ellerweg, D (Ellerweg, D.); von Keudell, A (von Keudell, A.); Matejcik, S (Matejcik, S.); Benedikt, J (Benedikt, J.)

Source: PLASMA SOURCES SCIENCE & TECHNOLOGY **Volume:** 24 **Issue:** 4 **Article Number:** 044008 **DOI:** 10.1088/0963-0252/24/4/044008 **Published:** AUG 2015

Accession Number: WOS:000364098900011

Author Identifiers:

Author	ResearcherID Number	ORCID Number
Benedikt, Jan	A-8463-2016	0000-0002-8954-1908
von Keudell, Achim		0000-0003-3887-9359

ISSN: 0963-0252

eISSN: 1361-6595

Record 11 of 29

Title: Sterilization of bacteria suspensions and identification of radicals deposited during plasma treatment

Author(s): Puac, N (Puac, Nevena); Miletic, M (Miletic, Maja); Mojovic, M (Mojovic, Milos); Popovic-Bijelic, A (Popovic-Bijelic, Ana); Vukovic, D (Vukovic, Dragana); Milicic, B (Milicic, Biljana); Maletic, D (Maletic, Dejan); Lazovic, S (Lazovic, Sasa); Malovic, G (Malovic, Gordana); Petrovic, ZL (Petrovic, Zoran Lj)

Source: OPEN CHEMISTRY **Volume:** 13 **Issue:** 1 **Pages:** 332-338 **DOI:** 10.1515/chem-2015-0041 **Published:** JAN 2015

Accession Number: WOS:000355403100040

Author Identifiers:

Author	ResearcherID Number	ORCID Number
Lazovic, Sasa	Q-5056-2016	0000-0003-1696-9134
Popovic Bijelic, Ana	C-6314-2017	0000-0003-3121-2391
Petrovic, Zoran		0000-0001-6569-9447
Mojovic, Milos		0000-0002-1868-9913
Malovic, Gordana		0000-0003-2356-0652
Puac, Nevena		0000-0003-1142-8494

ISSN: 2391-5420

Record 12 of 29

Title: Plasma induced DNA damage: Comparison with the effects of ionizing radiation

Author(s): Lazovic, S (Lazovic, S.); Maletic, D (Maletic, D.); Leskovac, A (Leskovac, A.); Filipovic, J (Filipovic, J.); Puac, N (Puac, N.); Malovic, G (Malovic, G.); Joksic, G (Joksic, G.); Petrovic, ZL (Petrovic, Z. Lj.)

Source: APPLIED PHYSICS LETTERS **Volume:** 105 **Issue:** 12 **Article Number:** 124101 **DOI:** 10.1063/1.4896626 **Published:** SEP 22 2014

Accession Number: WOS:000343004400099

Author Identifiers:

Author	ResearcherID Number	ORCID Number
Lazovic, Sasa	Q-5056-2016	0000-0003-1696-9134
Joksic, Gordana		0000-0002-7186-301X
Petrovic, Zoran		0000-0001-6569-9447
Leskovac, Andreja		0000-0002-6293-5237
Puac, Nevena		0000-0003-1142-8494
Filipovic Trickovic, Jelena		0000-0001-5450-0842
Malovic, Gordana		0000-0003-2356-0652

ISSN: 0003-6951

eISSN: 1077-3118

Record 13 of 29

Title: Long and short term effects of plasma treatment on meristematic plant cells

Author(s): Puac, N (Puac, N.); Zivkovic, S (Zivkovic, S.); Selakovic, N (Selakovic, N.); Milutinovic, M (Milutinovic, M.); Boljevic, J (Boljevic, J.); Malovic, G (Malovic, G.); Petrovic, ZL (Petrovic, Z. Lj)

Source: APPLIED PHYSICS LETTERS **Volume:** 104 **Issue:** 21 **Article Number:** 214106 **DOI:** 10.1063/1.4880360 **Published:** MAY 26 2014

Accession Number: WOS:000337143000078

Author Identifiers:

Author	ResearcherID Number	ORCID Number
Petrovic, Zoran		0000-0001-6569-9447
Zivkovic, Suzana		0000-0003-0280-5884
Puac, Nevena		0000-0003-1142-8494
Malovic, Gordana		0000-0003-2356-0652

ISSN: 0003-6951

eISSN: 1077-3118

Record 14 of 29

Title: Inhibition of methicillin resistant Staphylococcus aureus by a plasma needle

Author(s): Miletic, M (Miletic, Maja); Vukovic, D (Vukovic, Dragana); Zivanovic, I (Zivanovic, Irena); Dakic, I (Dakic, Ivana); Soldatovic, I (Soldatovic, Ivan); Maletic, D (Maletic, Dejan); Lazovic, S (Lazovic, Sasa); Malovic, G (Malovic, Gordana); Petrovic, ZL (Petrovic, Zoran Lj); Puac, N (Puac, Nevena)

Source: CENTRAL EUROPEAN JOURNAL OF PHYSICS **Volume:** 12 **Issue:** 3 **Pages:** 160-167 **DOI:** 10.2478/s11534-014-0437-z **Published:** MAR 2014

Accession Number: WOS:000333023800002

Author Identifiers:

Author	ResearcherID Number	ORCID Number
Lazovic, Sasa	Q-5056-2016	0000-0003-1696-9134
Malovic, Gordana		0000-0003-2356-0652
Petrovic, Zoran		0000-0001-6569-9447
Puac, Nevena		0000-0003-1142-8494
Soldatovic, Ivan		0000-0003-4893-1683

ISSN: 1895-1082

eISSN: 1644-3608

Record 15 of 29

Title: Characterization and global modelling of low-pressure hydrogen-based RF plasmas suitable for surface cleaning processes

Author(s): Skoro, N (Skoro, Nikola); Puac, N (Puac, Nevena); Lazovic, S (Lazovic, Sasa); Cvelbar, U (Cvelbar, Uros); Kokkoris, G (Kokkoris, George); Gogolides, E (Gogolides, Evangelos)

Source: JOURNAL OF PHYSICS D-APPLIED PHYSICS **Volume:** 46 **Issue:** 47 **Article Number:** 475206 **DOI:** 10.1088/0022-3727/46/47/475206 **Published:** NOV 27 2013

Accession Number: WOS:000326984800018

Author Identifiers:

Author	ResearcherID Number	ORCID Number
Lazovic, Sasa	Q-5056-2016	0000-0003-1696-9134
Puac, Nevena		0000-0003-1142-8494

Skoro, Nikola		0000-0002-0254-8008

ISSN: 0022-3727

eISSN: 1361-6463

Record 16 of 29

Title: Atmospheric pressure discharge filaments and microplasmas: physics, chemistry and diagnostics

Author(s): Bruggeman, P (Bruggeman, Peter); Brandenburg, R (Brandenburg, Ronny)

Source: JOURNAL OF PHYSICS D-APPLIED PHYSICS **Volume:** 46 **Issue:** 46 **Special Issue:** SI **Article Number:** 464001 **DOI:** 10.1088/0022-3727/46/46/464001 **Published:** NOV 20 2013

Accession Number: WOS:000326956800002

Author Identifiers:

Author	ResearcherID Number	ORCID Number
Bruggeman, Peter	J-8273-2014	0000-0003-3346-7275
Brandenburg, Ronny	G-6504-2011	0000-0003-3153-8439

ISSN: 0022-3727

eISSN: 1361-6463

Record 17 of 29

Title: Mass spectrometric diagnosis of an atmospheric pressure helium microplasma jet

Author(s): McKay, K (McKay, K.); Oh, JS (Oh, J-S); Walsh, JL (Walsh, J. L.); Bradley, JW (Bradley, J. W.)

Source: JOURNAL OF PHYSICS D-APPLIED PHYSICS **Volume:** 46 **Issue:** 46 **Special Issue:** SI **Article Number:** 464018 **DOI:** 10.1088/0022-3727/46/46/464018 **Published:** NOV 20 2013

Accession Number: WOS:000326956800019

Author Identifiers:

Author	ResearcherID Number	ORCID Number
Bradley, James	M-7577-2018	0000-0002-8833-0180
walsh, james	F-1426-2011	
McKay, Kirsty	F-6445-2011	
Walsh, James		0000-0002-6318-0892

ISSN: 0022-3727

eISSN: 1361-6463

Record 18 of 29

Title: Ambient air particle transport into the effluent of a cold atmospheric-pressure argon plasma jet investigated by molecular beam mass spectrometry

Author(s): Dunnbier, M (Duennbier, M.); Schmidt-Bleker, A (Schmidt-Bleker, A.); Winter, J (Winter, J.); Wolfram, M (Wolfram, M.); Hippler, R (Hippler, R.); Weltmann, KD

(Weltmann, K-D); Reuter, S (Reuter, S.)

Source: JOURNAL OF PHYSICS D-APPLIED PHYSICS **Volume:** 46 **Issue:** 43 **Article Number:** 435203 **DOI:** 10.1088/0022-3727/46/43/435203 **Published:** OCT 30 2013

Accession Number: WOS:000325679400007

Author Identifiers:

Author	ResearcherID Number	ORCID Number
Hippler, Rainer	A-2790-2013	0000-0002-5956-3321
Reuter, Stephan	D-2890-2014	0000-0002-4858-1081

ISSN: 0022-3727

eISSN: 1361-6463

Record 19 of 29

Title: Effects of non-thermal atmospheric plasma on human periodontal ligament mesenchymal stem cells

Author(s): Miletic, M (Miletic, M.); Mojsilovic, S (Mojsilovic, S.); Dordevic, IO (Dordevic, I. Okic); Maletic, D (Maletic, D.); Puac, N (Puac, N.); Lazovic, S (Lazovic, S.); Malovic, G (Malovic, G.); Milenkovic, P (Milenkovic, P.); Petrovic, ZL (Petrovic, Z. Lj); Bugarski, D (Bugarski, D.)

Source: JOURNAL OF PHYSICS D-APPLIED PHYSICS **Volume:** 46 **Issue:** 34 **Article Number:** 345401 **DOI:** 10.1088/0022-3727/46/34/345401 **Published:** AUG 28 2013

Accession Number: WOS:000323062400017

Author Identifiers:

Author	ResearcherID Number	ORCID Number
Lazovic, Sasa	Q-5056-2016	0000-0003-1696-9134
Malovic, Gordana		0000-0003-2356-0652
Puac, Nevena		0000-0003-1142-8494

ISSN: 0022-3727

Record 20 of 29

Title: Observations of ionic species produced in an atmospheric pressure pulse-modulated RF plasma needle

Author(s): Mckay, K (McKay, K.); Walsh, JL (Walsh, J. L.); Bradley, JW (Bradley, J. W.)

Source: PLASMA SOURCES SCIENCE & TECHNOLOGY **Volume:** 22 **Issue:** 3 **Article Number:** 035005 **DOI:** 10.1088/0963-0252/22/3/035005 **Published:** JUN 2013

Accession Number: WOS:000319820100009

Author Identifiers:

Author	ResearcherID Number	ORCID Number
McKay, Kirsty	F-6445-2011	
Bradley, James	M-7577-2018	0000-0002-8833-0180
walsh, james	F-1426-2011	

Walsh, James		0000-0002-6318-0892

ISSN: 0963-0252

Record 21 of 29

Title: Ion mobilities and transport cross sections of daughter negative ions in N2O and N2O-N-2 mixtures

Author(s): de Urquijo, J (de Urquijo, J.); Jovanovic, JV (Jovanovic, J. V.); Bekstein, A (Bekstein, A.); Stojanovic, V (Stojanovic, V.); Petrovic, ZL (Petrovic, Z. Lj)

Source: PLASMA SOURCES SCIENCE & TECHNOLOGY **Volume:** 22 **Issue:** 2 **Article Number:** 025004 **DOI:** 10.1088/0963-0252/22/2/025004 **Published:** APR 2013

Accession Number: WOS:000317275400006

Author Identifiers:

Author	ResearcherID Number	ORCID Number
Jovanovic, Jasmina		0000-0001-6606-5470
Petrovic, Zoran		0000-0001-6569-9447

ISSN: 0963-0252

Record 22 of 29

Title: Plasma properties in a large-volume, cylindrical and asymmetric radio-frequency capacitively coupled industrial-prototype reactor

Author(s): Lazovic, S (Lazovic, Sasa); Puac, N (Puac, Nevena); Spasic, K (Spasic, Kosta); Malovic, G (Malovic, Gordana); Cvelbar, U (Cvelbar, Uros); Mozetic, M (Mozetic, Miran); Radetic, M (Radetic, Maja); Petrovic, ZL (Petrovic, Zoran Lj)

Source: JOURNAL OF PHYSICS D-APPLIED PHYSICS **Volume:** 46 **Issue:** 7 **Article Number:** 075201 **DOI:** 10.1088/0022-3727/46/7/075201 **Published:** FEB 20 2013

Accession Number: WOS:000314471900014

Author Identifiers:

Author	ResearcherID Number	ORCID Number
Lazovic, Sasa	Q-5056-2016	0000-0003-1696-9134
Mozetic, Miran	K-8784-2014	
Lazovic, Sasa	B-9651-2013	0000-0003-1696-9134
Puac, Nevena		0000-0003-1142-8494
Malovic, Gordana		0000-0003-2356-0652
Petrovic, Zoran		0000-0001-6569-9447

ISSN: 0022-3727

Record 23 of 29

Title: Detection of atomic oxygen and nitrogen created in a radio-frequency-driven micro-scale atmospheric pressure plasma jet using mass spectrometry

Author(s): Maletic, D (Maletic, D.); Puac, N (Puac, N.); Lazovic, S (Lazovic, S.); Malovic, G (Malovic, G.); Gans, T (Gans, T.); Schulz-von der Gathen, V (Schulz-von der Gathen, V.); Petrovic, ZL (Petrovic, Z. Lj)

Source: PLASMA PHYSICS AND CONTROLLED FUSION **Volume:** 54 **Issue:** 12 **Article Number:** 124046 **DOI:** 10.1088/0741-3335/54/12/124046 **Part:** 1-2 **Published:**

DEC 2012

Accession Number: WOS:000312579500049

Conference Title: 39th European-Physical-Society Conference on Plasma Physics

Conference Date: JUL 02-06, 2012

Conference Location: Stockholm, SWEDEN

Author Identifiers:

Author	ResearcherID Number	ORCID Number
Gans, Timo	C-5035-2008	0000-0003-1362-8000
Lazovic, Sasa	B-9651-2013	0000-0003-1696-9134
Schulz-von der Gathen, Volker	O-3405-2014	0000-0002-7182-3253
Lazovic, Sasa	Q-5056-2016	0000-0003-1696-9134
Malovic, Gordana		0000-0003-2356-0652
Puac, Nevena		0000-0003-1142-8494
Petrovic, Zoran		0000-0001-6569-9447

ISSN: 0741-3335

eISSN: 1361-6587

Record 24 of 29

Title: Application of non-equilibrium plasmas in medicine

Author(s): Petrovic, ZL (Petrovic, Zoran Lj.); Puac, N (Puac, Nevena); Malovic, G (Malovic, Gordana); Lazovic, S (Lazovic, Sasa); Maletic, D (Maletic, Dejan); Miletic, M (Miletic, Maja); Mojsilovic, S (Mojsilovic, Slavko); Milenkovic, P (Milenkovic, Pavle); Bugarski, D (Bugarski, Diana)

Source: JOURNAL OF THE SERBIAN CHEMICAL SOCIETY **Volume:** 77 **Issue:** 12 **Pages:** 1689-1699 **DOI:** 10.2298/JSC121020142P **Published:** 2012

Accession Number: WOS:000314080000002

Author Identifiers:

Author	ResearcherID Number	ORCID Number
Lazovic, Sasa	B-9651-2013	0000-0003-1696-9134
Lazovic, Sasa	Q-5056-2016	0000-0003-1696-9134
Petrovic, Zoran		0000-0001-6569-9447
Puac, Nevena		0000-0003-1142-8494
Malovic, Gordana		0000-0003-2356-0652

ISSN: 0352-5139

Record 25 of 29

Title: Electrical characterization of an air microplasma jet operated at a low frequency ac voltage

Author(s): Giuliani, L (Giuliani, L.); Grondona, D (Grondona, D.); Kelly, H (Kelly, H.); Minotti, F (Minotti, F.)

Edited by: Bilbao L; Minotti F; Kelly H

Source: 14TH LATIN AMERICAN WORKSHOP ON PLASMA PHYSICS (LAWPP 2011) **Book Series:** Journal of Physics Conference Series **Volume:** 370 **Article Number:** 012011 **DOI:** 10.1088/1742-6596/370/1/012011 **Published:** 2012

Accession Number: WOS:000307752700011

Conference Title: 14th Latin American Workshop on Plasma Physics (LAWPP)

Conference Date: NOV 20-25, 2011

Conference Location: Mar del Plata, ARGENTINA

Conference Sponsors: Inst Fisica Plasma (INFIP), Consejo Nacl Investigaciones Cientificas Tecnicas (CONICET), Comis Nacl Energia Atomica (CNEA), Agencia Nacl Promoc Cientifica Tecnol (ANPCyT), Centro Latino-Americano Fisica (CLAF), Univ Nacl Mar Plata (UNMP), Univ Nacl Ctr Provincia Buenos Aires (UNICEN), Acad Nacl Ciencias Buenos Aires (ANCBA)

ISSN: 1742-6588

Record 26 of 29

Title: Biomedical applications and diagnostics of atmospheric pressure plasma

Author(s): Petrovic, ZL (Petrovic, Z. Lj); Puac, N (Puac, N.); Lazovic, S (Lazovic, S.); Maletic, D (Maletic, D.); Spasic, K (Spasic, K.); Malovic, G (Malovic, G.)

Edited by: VanDeSanden MCM; Dimitrova M; Ghelev C

Source: 17TH INTERNATIONAL SUMMER SCHOOL ON VACUUM, ELECTRON, AND ION TECHNOLOGIES (VEIT 2011) **Book Series:** Journal of Physics Conference Series **Volume:** 356 **Article Number:** 012001 **DOI:** 10.1088/1742-6596/356/1/012001 **Published:** 2012

Accession Number: WOS:000307884600002

Conference Title: 17th International Summer School on Vacuum, Electron, and Ion Technologies (VEIT)

Conference Date: SEP 19-23, 2011

Conference Location: BULGARIA

Conference Sponsors: Eindhoven Univ Technol, Dept Appl Phys

Author Identifiers:

Author	ResearcherID Number	ORCID Number
Lazovic, Sasa	B-9651-2013	0000-0003-1696-9134
Lazovic, Sasa	Q-5056-2016	0000-0003-1696-9134
Puac, Nevena		0000-0003-1142-8494
Petrovic, Zoran		0000-0001-6569-9447
Malovic, Gordana		0000-0003-2356-0652

ISSN: 1742-6588

Record 27 of 29

Title: Time-resolved mass spectroscopic studies of an atmospheric-pressure helium microplasma jet

Author(s): Oh, JS (Oh, Jun-Seok); Aranda-Gonzalvo, Y (Aranda-Gonzalvo, Yolanda); Bradley, JW (Bradley, James W.)

Source: JOURNAL OF PHYSICS D-APPLIED PHYSICS **Volume:** 44 **Issue:** 36 **Article Number:** 365202 **DOI:** 10.1088/0022-3727/44/36/365202 **Published:** SEP 14 2011
Accession Number: WOS:000294770600009

Author Identifiers:

Author	ResearcherID Number	ORCID Number
Bradley, James	M-7577-2018	0000-0002-8833-0180

ISSN: 0022-3727

Record 28 of 29

Title: Microwave discharge as a remote source of neutral oxygen atoms

Author(s): Primc, G (Primc, Gregor); Zaplotnik, R (Zaplotnik, Rok); Vesel, A (Vesel, Alenka); Mozetic, M (Mozetic, Miran)

Source: AIP ADVANCES **Volume:** 1 **Issue:** 2 **Article Number:** 022129 **DOI:** 10.1063/1.3598415 **Published:** JUN 2011
Accession Number: WOS:000302137000027

Author Identifiers:

Author	ResearcherID Number	ORCID Number
Vesel, Alenka	I-3934-2014	0000-0003-3782-6001
Mozetic, Miran	K-8784-2014	

ISSN: 2158-3226

Record 29 of 29

Title: The effect of a plasma needle on bacteria in planktonic samples and on peripheral blood mesenchymal stem cells

Author(s): Lazovic, S (Lazovic, Sasa); Puac, N (Puac, Nevena); Miletic, M (Miletic, Maja); Pavlica, D (Pavlica, Dusan); Jovanovic, M (Jovanovic, Milena); Bugarski, D (Bugarski, Diana); Mojsilovic, S (Mojsilovic, Slavko); Maletic, D (Maletic, Dejan); Malovic, G (Malovic, Gordana); Milenkovic, P (Milenkovic, Pavle); Petrovic, Z (Petrovic, Zoran)

Source: NEW JOURNAL OF PHYSICS **Volume:** 12 **Article Number:** 083037 **DOI:** 10.1088/1367-2630/12/8/083037 **Published:** AUG 17 2010
Accession Number: WOS:000281279700003

Author Identifiers:

Author	ResearcherID Number	ORCID Number
Lazovic, Sasa	Q-5056-2016	0000-0003-1696-9134
Lazovic, Sasa	B-9651-2013	0000-0003-1696-9134
Malovic, Gordana		0000-0003-2356-0652
Puac, Nevena		0000-0003-1142-8494
Petrovic, Zoran		0000-0001-6569-9447

ISSN: 1367-2630

Close

Print

Web of Science
Page 1 (Records 1 -- 29)
[1]

Clarivate
Accelerating innovation

Sign up for the Web of Science newsletter Follow us

Close

Web of Science
Page 1 (Records 1 -- 20)
[1]

Print

Record 1 of 20

Title: Studies on probe measurements in presence of magnetic field in dust containing hydrogen plasma

Author(s): Kalita, D (Kalita, Deiji); Kakati, B (Kakati, Bharat); Kausik, SS (Kausik, Siddhartha Sankar); Siakia, BK (Siakia, Bipul Kumar); Bandyopadhyay, M (Bandyopadhyay, Mainak)

Source: EUROPEAN PHYSICAL JOURNAL D **Volume:** 72 **Issue:** 4 **Article Number:** 74 **DOI:** 10.1140/epjd/e2018-80552-x **Published:** APR 30 2018

Accession Number: WOS:000431919200007

ISSN: 1434-6060

eISSN: 1434-6079

Record 2 of 20

Title: Effects of atmospheric pressure plasma jet operating with DBD on Lavatera thuringiaca L. seeds' germination

Author(s): Pawlat, J (Pawlat, Joanna); Starek, A (Starek, Agnieszka); Sujak, A (Sujak, Agnieszka); Terebun, P (Terebun, Piotr); Kwiatkowski, M (Kwiatkowski, Michal); Budzen, M (Budzen, Malgorzata); Andrejko, D (Andrejko, Dariusz)

Source: PLOS ONE **Volume:** 13 **Issue:** 4 **Article Number:** e0194349 **DOI:** 10.1371/journal.pone.0194349 **Published:** APR 9 2018

Accession Number: WOS:000429505000010

PubMed ID: 29630623

Author Identifiers:

Author	ResearcherID Number	ORCID Number
Sujak, Sujak	U-5538-2018	0000-0001-5616-3827
Terebun, Piotr	D-4825-2017	0000-0002-3947-9552
Pawlat, Joanna	B-3998-2013	0000-0001-8224-0355
Kwiatkowski, Michal	D-4855-2017	0000-0001-5697-3176
Starek, Agnieszka	V-5985-2018	0000-0002-9387-5900

ISSN: 1932-6203

Record 3 of 20

Title: Hydrogen electron cyclotron resonance ion sources plasma characterization based on simple optical emission spectroscopy

Author(s): Feuchtwanger, J (Feuchtwanger, J.); Etxebarria, V (Etxebarria, V.); Portilla, J (Portilla, J.); Jugo, J (Jugo, J.); Badillo, I (Badillo, I.); Arredondo, I (Arredondo, I.)

Source: NUCLEAR INSTRUMENTS & METHODS IN PHYSICS RESEARCH SECTION A-ACCELERATORS SPECTROMETERS DETECTORS AND ASSOCIATED EQUIPMENT **Volume:** 881 **Pages:** 44-47 **DOI:** 10.1016/j.nima.2017.11.008 **Published:** FEB 11 2018

Accession Number: WOS:000418525100006

Author Identifiers:

Author	ResearcherID Number	ORCID Number
Portilla, Joaquin		0000-0001-5531-6131
ARREDONDO LOPEZ DE GUERENU, INIGO		0000-0003-4842-8033

ISSN: 0168-9002

eISSN: 1872-9576

Record 4 of 20

Title: Effects of atmospheric pressure plasma generated in GlidArc reactor on Lavatera thuringiaca L. seeds' germination

Author(s): Pawlat, J (Pawlat, Joanna); Starek, A (Starek, Agnieszka); Sujak, A (Sujak, Agnieszka); Kwiatkowski, M (Kwiatkowski, Michal); Terebun, P (Terebun, Piotr); Budzen, M (Budzen, Malgorzata)

Source: PLASMA PROCESSES AND POLYMERS **Volume:** 15 **Issue:** 2 **Article Number:** e1700064 **DOI:** 10.1002/ppap.201700064 **Published:** FEB 2018

Accession Number: WOS:000425453900006

Author Identifiers:

Author	ResearcherID Number	ORCID Number
Starek, Agnieszka	V-5985-2018	0000-0002-9387-5900
Sujak, Sujak	U-5538-2018	0000-0001-5616-3827
Kwiatkowski, Michal	D-4855-2017	0000-0001-5697-3176
Terebun, Piotr	D-4825-2017	0000-0002-3947-9552
Pawlat, Joanna	B-3998-2013	0000-0001-8224-0355

ISSN: 1612-8850

eISSN: 1612-8869

Record 5 of 20

Title: Activity of catalase enzyme in Paulownia tomentosa seeds during the process of germination after treatments with low pressure plasma and plasma activated water

Author(s): Puac, N (Puac, Nevena); Skoro, N (Skoro, Nikola); Spasic, K (Spasic, Kosta); Zivkovic, S (Zivkovic, Suzana); Milutinovic, M (Milutinovic, Milica); Malovic, G (Malovic, Gordana); Petrovic, ZL (Petrovic, Zoran Lj)

Source: PLASMA PROCESSES AND POLYMERS **Volume:** 15 **Issue:** 2 **Article Number:** e1700082 **DOI:** 10.1002/ppap.201700082 **Published:** FEB 2018

Accession Number: WOS:000425453900010

Author Identifiers:

Author	ResearcherID Number	ORCID Number
Puac, Nevena		0000-0003-1142-8494

Malovic, Gordana		0000-0003-2356-0652
Zivkovic, Suzana		0000-0003-0280-5884
Skoro, Nikola		0000-0002-0254-8008
Petrovic, Zoran		0000-0001-6569-9447

ISSN: 1612-8850

eISSN: 1612-8869

Record 6 of 20

Title: A generalized electron energy probability function for inductively coupled plasmas under conditions of nonlocal electron kinetics

Author(s): Mouchtouris, S (Mouchtouris, S.); Kokkoris, G (Kokkoris, G.)

Source: JOURNAL OF APPLIED PHYSICS **Volume:** 123 **Issue:** 2 **Article Number:** 023301 **DOI:** 10.1063/1.5002653 **Published:** JAN 14 2018

Accession Number: WOS:000422966100010

Author Identifiers:

Author	ResearcherID Number	ORCID Number
Mouchtouris, Sotiris		0000-0001-7580-4554

ISSN: 0021-8979

eISSN: 1089-7550

Record 7 of 20

Title: Hydrogen-plasma patterning of multilayer graphene: Mechanisms and modeling

Author(s): Harpale, A (Harpale, Abhilash); Chew, HB (Chew, Huck Beng)

Source: CARBON **Volume:** 117 **Pages:** 82-91 **DOI:** 10.1016/j.carbon.2017.02.062 **Published:** JUN 2017

Accession Number: WOS:000400212100010

ISSN: 0008-6223

eISSN: 1873-3891

Record 8 of 20

Title: Efficacy of Ozone Fumigation to Control Eupteryx Decemnotata in Rosemary Growing Under Cover

Author(s): Kopacki, M (Kopacki, Marek); Starek, A (Starek, Agnieszka); Kiczorowski, P (Kiczorowski, Piotr); Pawlat, J (Pawlat, Joanna); Diatczyk, J (Diatczyk, Jaroslaw)

Book Group Author(s): IEEE

Source: 2017 INTERNATIONAL CONFERENCE ON ELECTROMAGNETIC DEVICES AND PROCESSES IN ENVIRONMENT PROTECTION WITH SEMINAR APPLICATIONS OF SUPERCONDUCTORS (ELMECO & AOS) **Published:** 2017

Accession Number: WOS:000428142400028

Conference Title: International Conference on Electromagnetic Devices and Processes in Environment Protection with Seminar Applications of Superconductors (ELMECO and AoS)

Conference Date: DEC 03-06, 2017

Conference Location: Naleczow, POLAND

Conference Sponsors: Inst Elect & Elect Engineers, Polish Soc Theoret & Appl Elect Engn, Lab Badan Rozwoju Lublinie, Polish Acad Sci, Lublin Univ Technol, Inst Elect Engn & Electrotechnologies

Author Identifiers:

Author	ResearcherID Number	ORCID Number
Starek, Agnieszka	V-5985-2018	0000-0002-9387-5900

ISBN: 978-1-5386-1943-8

Record 9 of 20

Title: RF atmospheric plasma jet surface treatment of paper

Author(s): Pawlat, J (Pawlat, Joanna); Terebun, P (Terebun, Piotr); Kwiatkowski, M (Kwiatkowski, Michal); Diatczyk, J (Diatczyk, Jaroslaw)

Source: JOURNAL OF PHYSICS D-APPLIED PHYSICS **Volume:** 49 **Issue:** 37 **Article Number:** 374001 **DOI:** 10.1088/0022-3727/49/37/374001 **Published:** SEP 21 2016

Accession Number: WOS:000384093000002

Author Identifiers:

Author	ResearcherID Number	ORCID Number
Pawlat, Joanna	B-3998-2013	0000-0001-8224-0355
Terebun, Piotr	D-4825-2017	0000-0002-3947-9552
Diatczyk, Jaroslaw	B-7554-2013	0000-0001-5827-1485
Kwiatkowski, Michal	D-4855-2017	0000-0001-5697-3176

ISSN: 0022-3727

eISSN: 1361-6463

Record 10 of 20

Title: Diagnostics of low-pressure hydrogen discharge created in a 13.56 MHz RF plasma reactor

Author(s): Kristof, J (Kristof, J.); Annusova, A (Annusova, A.); Angus, M (Angus, M.); Veis, P (Veis, P.); Yang, X (Yang, X.); Angot, T (Angot, T.); Roubin, P (Roubin, P.); Cartry, G (Cartry, G.)

Source: PHYSICA SCRIPTA **Volume:** 91 **Issue:** 7 **Article Number:** 074009 **DOI:** 10.1088/0031-8949/91/7/074009 **Published:** JUL 2016

Accession Number: WOS:000378864400017

Author Identifiers:

Author	ResearcherID Number	ORCID Number
ANGOT, Thierry	Q-8186-2016	
Kristof, Jaroslav	I-3787-2017	0000-0001-8669-7504
Thierry, Angot		0000-0001-9152-6240

Annusova, Adriana		0000-0002-3769-9287

ISSN: 0031-8949
eISSN: 1402-4896

Record 11 of 20
Title: Low-pressure hydrogen plasmas explored using a global model
Author(s): Samuell, CM (Samuell, Cameron M.); Corr, CS (Corr, Cormac S.)
Source: PLASMA SOURCES SCIENCE & TECHNOLOGY **Volume:** 25 **Issue:** 1 **Article Number:** 015014 **DOI:** 10.1088/0963-0252/25/1/015014 **Published:** FEB 2016
Accession Number: WOS:000370974800021
Author Identifiers:

Author	ResearcherID Number	ORCID Number
Corr, Cormac	D-3320-2013	0000-0002-1793-3873

ISSN: 0963-0252
eISSN: 1361-6595

Record 12 of 20
Title: Plasma-graphene interaction and its effects on nanoscale patterning
Author(s): Harpale, A (Harpale, Abhilash); Panesi, M (Panesi, Marco); Chew, HB (Chew, Huck Beng)
Source: PHYSICAL REVIEW B **Volume:** 93 **Issue:** 3 **Article Number:** 035416 **DOI:** 10.1103/PhysRevB.93.035416 **Published:** JAN 11 2016
Accession Number: WOS:000367893400007
ISSN: 2469-9950
eISSN: 2469-9969

Record 13 of 20
Title: CHANGE OF SURFACE CONTACT ANGLE OF POLYMERIC MATERIALS EXPOSED ON PLASMA GENERATED IN DBD PLASMA JET REACTOR
Author(s): Kwiatkowski, M (Kwiatkowski, M.); Terebun, P (Terebun, P.); Diatczyk, J (Diatczyk, J.); Pawlat, J (Pawlat, J.)
Edited by: Cernak M; Hoder T
Source: HAKONE XV: INTERNATIONAL SYMPOSIUM ON HIGH PRESSURE LOW TEMPERATURE PLASMA CHEMISTRY: WITH JOINT COST TD1208 WORKSHOP: NON-EQUILIBRIUM PLASMAS WITH LIQUIDS FOR WATER AND SURFACE TREATMENT **Pages:** 324-325 **Published:** 2016
Accession Number: WOS:000393033200077
Conference Title: 15th International Symposium on High Pressure Low Temperature Plasma Chemistry (HAKONE)
Conference Date: SEP 11-16, 2016
Conference Location: Brno, CZECH REPUBLIC
Conference Sponsors: Masaryk Univ, Fac Sci, Dept Phys Elect, CEPLANT, Union Czech Mathematicians & Physicists
Author Identifiers:

Author	ResearcherID Number	ORCID Number
Pawlat, Joanna	B-3998-2013	0000-0001-8224-0355
Kwiatkowski, Michal	D-4855-2017	0000-0001-5697-3176
Diatczyk, Jaroslaw	B-7554-2013	0000-0001-5827-1485
Terebun, Piotr	D-4825-2017	0000-0002-3947-9552

ISBN: 978-80-210-8318-9

Record 14 of 20

Title: PLASMA PROCESSING OF DRY AND WET CELLULOSE-BASED MATERIALS

Author(s): Pawlat, J (Pawlat, J.); Terebun, P (Terebun, P.); Kwiatkowski, M (Kwiatkowski, M.); Cvelbar, U (Cvelbar, U.); Modic, M (Modic, M.); Puliyalil, H (Puliyalil, H.)

Edited by: Cernak M; Hoder T

Source: HAKONE XV: INTERNATIONAL SYMPOSIUM ON HIGH PRESSURE LOW TEMPERATURE PLASMA CHEMISTRY: WITH JOINT COST TD1208 WORKSHOP: NON-EQUILIBRIUM PLASMAS WITH LIQUIDS FOR WATER AND SURFACE TREATMENT **Pages:** 443-445 **Published:** 2016

Accession Number: WOS:000393033200109

Conference Title: 15th International Symposium on High Pressure Low Temperature Plasma Chemistry (HAKONE)

Conference Date: SEP 11-16, 2016

Conference Location: Brno, CZECH REPUBLIC

Conference Sponsors: Masaryk Univ, Fac Sci, Dept Phys Elect, CEPLANT, Union Czech Mathematicians & Physicists

Author Identifiers:

Author	ResearcherID Number	ORCID Number
Pawlat, Joanna	B-3998-2013	0000-0001-8224-0355
Terebun, Piotr	D-4825-2017	0000-0002-3947-9552
Kwiatkowski, Michal	D-4855-2017	0000-0001-5697-3176

ISBN: 978-80-210-8318-9

Record 15 of 20

Title: Tackling chemical etching and its mechanisms of polyphenolic composites in various reactive low temperature plasmas

Author(s): Puliyalil, H (Puliyalil, H.); Filipic, G (Filipic, G.); Kovac, J (Kovac, J.); Mozetic, M (Mozetic, M.); Thomas, S (Thomas, S.); Cvelbar, U (Cvelbar, U.)

Source: RSC ADVANCES **Volume:** 6 **Issue:** 97 **Pages:** 95120-95128 **DOI:** 10.1039/c6ra15923k **Published:** 2016

Accession Number: WOS:000385632400097

Author Identifiers:

Author	ResearcherID Number	ORCID Number
Filipic, Gregor	T-4900-2018	0000-0003-0153-5181

Thomas, Prof. Sabu	G-7310-2016	0000-0003-4726-5746
PULIYALIL, HARINARAYANAN		0000-0002-9749-5307

ISSN: 2046-2069

Record 16 of 20

Title: Breakdown mechanism in hydrogen microdischarges from direct-current to 13.56 MHz

Author(s): Klas, M (Klas, M.); Moravsky, L (Moravsky, L.); Matejcik, S (Matejcik, S.); Radjenovic, B (Radjenovic, B.); Radmilovic-Radjenovic, M (Radmilovic-Radjenovic, M.)

Source: JOURNAL OF PHYSICS D-APPLIED PHYSICS **Volume:** 48 **Issue:** 40 **Article Number:** 405204 **DOI:** 10.1088/0022-3727/48/40/405204 **Published:** OCT 14 2015

Accession Number: WOS:000362006400014

ISSN: 0022-3727

eISSN: 1361-6463

Record 17 of 20

Title: Effects of gas composition, focus ring and blocking capacitor on capacitively coupled RF Ar/H-2 plasmas

Author(s): Tong, LZ (Tong, Lizhu)

Source: JAPANESE JOURNAL OF APPLIED PHYSICS **Volume:** 54 **Issue:** 6 **Special Issue:** 2 **Article Number:** 06GA01 **DOI:** 10.7567/JJAP.54.06GA01 **Published:** JUN 2015

Accession Number: WOS:000358296000002

Conference Title: International Symposium on Dry Process (DPS)

Conference Date: NOV 27-28, 2014

Conference Location: Yokohama, JAPAN

ISSN: 0021-4922

eISSN: 1347-4065

Record 18 of 20

Title: Studying a low-pressure microwave coaxial discharge in hydrogen using a mixed 2D/3D fluid model

Author(s): Obrusnik, A (Obrusnik, Adam); Bonaventura, Z (Bonaventura, Zdenek)

Source: JOURNAL OF PHYSICS D-APPLIED PHYSICS **Volume:** 48 **Issue:** 6 **Article Number:** 065201 **DOI:** 10.1088/0022-3727/48/6/065201 **Published:** FEB 18 2015

Accession Number: WOS:000348842600006

ISSN: 0022-3727

eISSN: 1361-6463

Record 19 of 20

Title: Insight into hydrogenation of graphene: Effect of hydrogen plasma chemistry

Author(s): Felten, A (Felten, A.); McManus, D (McManus, D.); Rice, C (Rice, C.); Nittler, L (Nittler, L.); Pireaux, JJ (Pireaux, J. -J.); Casiraghi, C (Casiraghi, C.)

Source: APPLIED PHYSICS LETTERS **Volume:** 105 **Issue:** 18 **Article Number:** 183104 **DOI:** 10.1063/1.4901226 **Published:** NOV 3 2014

Accession Number: WOS:000345000000059
Author Identifiers:

Author	ResearcherID Number	ORCID Number
Nittler, Laurent	F-1959-2011	0000-0003-2667-8197
McManus, Daryl		0000-0002-8494-0870

ISSN: 0003-6951
eISSN: 1077-3118

Record 20 of 20
Title: Comparison of spatial distributions of atomic oxygen and hydrogen in ICP by means of catalytic probes and actinometry
Author(s): Kregar, Z (Kregar, Z.); Zaplotnik, R (Zaplotnik, R.); Mozetic, M (Mozetic, M.); Milosevic, S (Milosevic, S.)
Source: VACUUM **Volume:** 109 **Special Issue:** SI **Pages:** 8-14 **DOI:** 10.1016/j.vacuum.2014.06.010 **Published:** NOV 2014
Accession Number: WOS:000342716000002
Author Identifiers:

Author	ResearcherID Number	ORCID Number
Milosevic, Slobodan	A-3408-2010	
Milosevic, Slobodan		0000-0002-4455-7869

ISSN: 0042-207X

Close

Web of Science
Page 1 (Records 1 -- 20)
◀ [1] ▶

Print

Close

Web of Science
Page 1 (Records 1 -- 19)
[1]

Print

Record 1 of 19

Title: Characterisation of a multijet plasma device by means of mass spectrometric detection and iCCD imaging

Author(s): Stancampiano, A (Stancampiano, A.); Selakovic, N (Selakovic, N.); Gherardi, M (Gherardi, M.); Puac, N (Puac, N.); Petrovic, ZL (Petrovic, Z. Lj); Colombo, V (Colombo, V)

Source: JOURNAL OF PHYSICS D-APPLIED PHYSICS **Volume:** 51 **Issue:** 48 **Article Number:** 484004 **DOI:** 10.1088/1361-6463/aae2f2 **Published:** DEC 5 2018

Accession Number: WOS:000446857200001

ISSN: 0022-3727

eISSN: 1361-6463

Record 2 of 19

Title: Microwave micro torch generated in argon based mixtures for biomedical applications

Author(s): Krcma, F (Krcma, Frantisek); Tsonev, I (Tsonev, Ivan); Smejkalova, K (Smejkalova, Katerina); Truchla, D (Truchla, Darina); Kozakova, Z (Kozakova, Zdenka); Zhekova, M (Zhekova, Maya); Marinova, P (Marinova, Plamena); Bogdanov, T (Bogdanov, Todor); Benova, E (Benova, Evgenia)

Source: JOURNAL OF PHYSICS D-APPLIED PHYSICS **Volume:** 51 **Issue:** 41 **Article Number:** 414001 **DOI:** 10.1088/1361-6463/aad82b **Published:** OCT 17 2018

Accession Number: WOS:000442439700001

Author Identifiers:

Author	ResearcherID Number	ORCID Number
Bogdanov, Todor		0000-0002-2808-4280
Benova, Evgenia		0000-0001-6438-0522

ISSN: 0022-3727

eISSN: 1361-6463

Record 3 of 19

Title: Controlled production of atomic oxygen and nitrogen in a pulsed radio-frequency atmospheric-pressure plasma

Author(s): Dedrick, J (Dedrick, J.); Schroter, S (Schroter, S.); Niemi, K (Niemi, K.); Wijaikhum, A (Wijaikhum, A.); Wagenaars, E (Wagenaars, E.); de Oliveira, N (de Oliveira, N.); Nahon, L (Nahon, L.); Booth, JP (Booth, J. P.); O'Connell, D (O'Connell, D.); Gans, T (Gans, T.)

Source: JOURNAL OF PHYSICS D-APPLIED PHYSICS **Volume:** 50 **Issue:** 45 **Article Number:** 455204 **DOI:** 10.1088/1361-6463/aa8da2 **Published:** NOV 15 2017

Accession Number: WOS:000413530400002

Author Identifiers:

Author	ResearcherID Number	ORCID Number

O'Connell, Deborah	D-7967-2018	0000-0002-1457-9004
Gans, Timo	C-5035-2008	0000-0003-1362-8000
Booth, Jean-Paul		0000-0002-0980-3278
Niemi, Kari		0000-0001-6134-1974

ISSN: 0022-3727

eISSN: 1361-6463

Record 4 of 19

Title: Absolute ozone densities in a radio-frequency driven atmospheric pressure plasma using two-beam UV-LED absorption spectroscopy and numerical simulations

Author(s): Wijaikhum, A (Wijaikhum, A.); Schroder, D (Schroeder, D.); Schroter, S (Schroter, S.); Gibson, AR (Gibson, A. R.); Niemi, K (Niemi, K.); Friderich, J (Friderich, J.); Greb, A (Greb, A.); Schulz-von der Gathen, V (Schulz-von der Gathen, V.); O'Connell, D (O'Connell, D.); Gans, T (Gans, T.)

Source: PLASMA SOURCES SCIENCE & TECHNOLOGY **Volume:** 26 **Issue:** 11 **Article Number:** 115004 **DOI:** 10.1088/1361-6595/aa8ebb **Published:** NOV 2017

Accession Number: WOS:000413326300001

Author Identifiers:

Author	ResearcherID Number	ORCID Number
Gans, Timo	C-5035-2008	0000-0003-1362-8000
O'Connell, Deborah	D-7967-2018	0000-0002-1457-9004
Gibson, Andrew		0000-0002-1082-4359
Schulz-von der Gathen, Volker		0000-0002-7182-3253
Niemi, Kari		0000-0001-6134-1974

ISSN: 0963-0252

eISSN: 1361-6595

Record 5 of 19

Title: Field-emission enhanced breakdown in oxygen microdischarges from direct-current to radio-frequencies

Author(s): Klas, M (Klas, M.); Matejcik, S (Matejcik, S.); Moravsky, L (Moravsky, L.); Radjenovic, B (Radjenovic, B.); Radmilovic-Radjenovic, M (Radmilovic-Radjenovic, M.)

Source: EPL **Volume:** 120 **Issue:** 2 **Article Number:** 25002 **DOI:** 10.1209/0295-5075/120/25002 **Published:** OCT 2017

Accession Number: WOS:000423332900013

ISSN: 0295-5075

eISSN: 1286-4854

Record 6 of 19

Title: Time Behaviour of Helium Atmospheric Pressure Plasma Jet Electrical and Optical Parameters

Author(s): Gerber, IC (Gerber, Ioana Cristina); Mihaila, I (Mihaila, Ilarion); Hein, D (Hein, Dennis); Nastuta, AV (Nastuta, Andrei Vasile); Jijie, R (Jijie, Roxana); Pohoata,

V (Pohoata, Valentin); Topala, I (Topala, Ionut)

Source: APPLIED SCIENCES-BASEL **Volume:** 7 **Issue:** 8 **Article Number:** 812 **DOI:** 10.3390/app7080812 **Published:** AUG 2017

Accession Number: WOS:000408905900062

Author Identifiers:

Author	ResearcherID Number	ORCID Number
Topala, Ionut	A-2305-2009	0000-0002-8954-8106
NASTUTA, Andrei Vasile	B-4757-2012	0000-0002-2299-7169
MIHAILA, Ilarion	C-5716-2015	0000-0003-4025-7639
Pohoata, Valentin	R-1354-2017	0000-0001-5554-0088

ISSN: 2076-3417

Record 7 of 19

Title: The influence of electrode configuration on light emission profiles and electrical characteristics of an atmospheric-pressure plasma jet

Author(s): Maletic, D (Maletic, Dejan); Puac, N (Puac, Nevena); Malovic, G (Malovic, Gordana); Dordevic, A (Dordevic, Antonije); Petrovic, ZL (Petrovic, Zoran Lj)

Source: JOURNAL OF PHYSICS D-APPLIED PHYSICS **Volume:** 50 **Issue:** 14 **Article Number:** 145202 **DOI:** 10.1088/1361-6463/aa5d91 **Published:** APR 12 2017

Accession Number: WOS:000404428200002

Author Identifiers:

Author	ResearcherID Number	ORCID Number
Puac, Nevena		0000-0003-1142-8494
Petrovic, Zoran		0000-0001-6569-9447
Malovic, Gordana		0000-0003-2356-0652

ISSN: 0022-3727

eISSN: 1361-6463

Record 8 of 19

Title: Mass spectrometry of diffuse coplanar surface barrier discharge: influence of discharge frequency and oxygen content in N-2/O-2 mixture

Author(s): Cech, J (Cech, Jan); Brablec, A (Brablec, Antonin); Cernak, M (Cernak, Mirko); Puac, N (Puac, Nevena); Selakovic, N (Selakovic, Nenad); Petrovic, ZL (Petrovic, Zoran Lj.)

Source: EUROPEAN PHYSICAL JOURNAL D **Volume:** 71 **Issue:** 2 **Article Number:** 27 **DOI:** 10.1140/epjd/e2016-70607-5 **Published:** FEB 9 2017

Accession Number: WOS:000403477900003

Author Identifiers:

Author	ResearcherID Number	ORCID Number
Cech, Jan	F-8310-2017	0000-0002-4900-6011

ISSN: 1434-6060
eISSN: 1434-6079

Record 9 of 19

Title: Diagnostics of atmospheric-pressure pulsed-dc discharge with metal and liquid anodes by multiple laser-aided methods

Author(s): Urabe, K (Urabe, Keiichiro); Shirai, N (Shirai, Naoki); Tomita, K (Tomita, Kentaro); Akiyama, T (Akiyama, Tsuyoshi); Murakami, T (Murakami, Tomoyuki)

Source: PLASMA SOURCES SCIENCE & TECHNOLOGY **Volume:** 25 **Issue:** 4 **Article Number:** 045004 **DOI:** 10.1088/0963-0252/25/4/045004 **Published:** AUG 2016
Accession Number: WOS:000380380200018

Author Identifiers:

Author	ResearcherID Number	ORCID Number
URABE, Keiichiro	H-6501-2018	0000-0001-9743-3184
Shirai, Naoki		0000-0001-9494-5635

ISSN: 0963-0252
eISSN: 1361-6595

Record 10 of 19

Title: Concepts and characteristics of the 'COST Reference Microplasma Jet'

Author(s): Golda, J (Golda, J.); Held, J (Held, J.); Redeker, B (Redeker, B.); Konkowski, M (Konkowski, M.); Beijer, P (Beijer, P.); Sobota, A (Sobota, A.); Kroesen, G (Kroesen, G.); Braithwaite, NS (Braithwaite, N. St J.); Reuter, S (Reuter, S.); Turner, MM (Turner, M. M.); Gans, T (Gans, T.); O'Connell, D (O'Connell, D.); Schulz-von der Gathen, V (Schulz-von der Gathen, V.)

Source: JOURNAL OF PHYSICS D-APPLIED PHYSICS **Volume:** 49 **Issue:** 8 **Article Number:** 084003 **DOI:** 10.1088/0022-3727/49/8/084003 **Published:** MAR 2 2016
Accession Number: WOS:000369480800006

Author Identifiers:

Author	ResearcherID Number	ORCID Number
Gans, Timo	C-5035-2008	0000-0003-1362-8000
Reuter, Stephan	D-2890-2014	0000-0002-4858-1081
O'Connell, Deborah	D-7967-2018	0000-0002-1457-9004
Sobota, Ana	F-1925-2011	0000-0003-1036-4513
Schulz-von der Gathen, Volker	O-3405-2014	0000-0002-7182-3253
Turner, Miles		0000-0001-9713-6198
Golda, Judith		0000-0003-2344-2146
Held, Julian		0000-0003-1206-7504

ISSN: 0022-3727
eISSN: 1361-6463

Record 11 of 19

Title: Cavity ring-down spectroscopy for atmospheric pressure plasma jet analysis

Author(s): Zaplotnik, R (Zaplotnik, Rok); Biscan, M (Biscan, Marijan); Krstulovic, N (Krstulovic, Niksa); Popovic, D (Popovic, Dean); Milosevic, S (Milosevic, Slobodan)

Source: PLASMA SOURCES SCIENCE & TECHNOLOGY **Volume:** 24 **Issue:** 5 **Article Number:** 054004 **DOI:** 10.1088/0963-0252/24/5/054004 **Published:** OCT 2015

Accession Number: WOS:000364336600007

Author Identifiers:

Author	ResearcherID Number	ORCID Number
Milosevic, Slobodan	A-3408-2010	
Milosevic, Slobodan		0000-0002-4455-7869

ISSN: 0963-0252

eISSN: 1361-6595

Record 12 of 19

Title: Numerical analysis of the effect of nitrogen and oxygen admixtures on the chemistry of an argon plasma jet operating at atmospheric pressure

Author(s): Van Gaens, W (Van Gaens, W.); Iseni, S (Iseni, S.); Schmidt-Bleker, A (Schmidt-Bleker, A.); Weltmann, KD (Weltmann, K-D); Reuter, S (Reuter, S.); Bogaerts, A (Bogaerts, A.)

Source: NEW JOURNAL OF PHYSICS **Volume:** 17 **Article Number:** 033003 **DOI:** 10.1088/1367-2630/17/3/033003 **Published:** MAR 3 2015

Accession Number: WOS:000352898500003

Author Identifiers:

Author	ResearcherID Number	ORCID Number
Bogaerts, Annemie	L-8338-2016	0000-0001-9875-6460
Reuter, Stephan	D-2890-2014	0000-0002-4858-1081
Iseni, Sylvain		0000-0002-4923-1657

ISSN: 1367-2630

Record 13 of 19

Title: Atmospheric pressure plasma jets interacting with liquid covered tissue: touching and not-touching the liquid

Author(s): Norberg, SA (Norberg, Seth A.); Tian, W (Tian, Wei); Johnsen, E (Johnsen, Eric); Kushner, MJ (Kushner, Mark J.)

Source: JOURNAL OF PHYSICS D-APPLIED PHYSICS **Volume:** 47 **Issue:** 47 **Article Number:** 475203 **DOI:** 10.1088/0022-3727/47/47/475203 **Published:** NOV 26 2014

Accession Number: WOS:000344860600007

Author Identifiers:

Author	ResearcherID Number	ORCID Number

Kushner, Mark	D-4547-2015	

ISSN: 0022-3727

eISSN: 1361-6463

Record 14 of 19

Title: Plasma induced DNA damage: Comparison with the effects of ionizing radiation

Author(s): Lazovic, S (Lazovic, S.); Maletic, D (Maletic, D.); Leskovac, A (Leskovac, A.); Filipovic, J (Filipovic, J.); Puac, N (Puac, N.); Malovic, G (Malovic, G.); Joksic, G (Joksic, G.); Petrovic, ZL (Petrovic, Z. Lj.)

Source: APPLIED PHYSICS LETTERS **Volume:** 105 **Issue:** 12 **Article Number:** 124101 **DOI:** 10.1063/1.4896626 **Published:** SEP 22 2014

Accession Number: WOS:000343004400099

Author Identifiers:

Author	ResearcherID Number	ORCID Number
Lazovic, Sasa	Q-5056-2016	0000-0003-1696-9134
Joksic, Gordana		0000-0002-7186-301X
Petrovic, Zoran		0000-0001-6569-9447
Leskovac, Andreja		0000-0002-6293-5237
Puac, Nevena		0000-0003-1142-8494
Filipovic Trickovic, Jelena		0000-0001-5450-0842
Malovic, Gordana		0000-0003-2356-0652

ISSN: 0003-6951

eISSN: 1077-3118

Record 15 of 19

Title: Reaction pathways of biomedically active species in an Ar plasma jet

Author(s): Van Gaens, W (Van Gaens, W.); Bogaerts, A (Bogaerts, A.)

Source: PLASMA SOURCES SCIENCE & TECHNOLOGY **Volume:** 23 **Issue:** 3 **Article Number:** 035015 **DOI:** 10.1088/0963-0252/23/3/035015 **Published:** JUN 2014

Accession Number: WOS:000337891900017

Author Identifiers:

Author	ResearcherID Number	ORCID Number
Bogaerts, Annemie	L-8338-2016	0000-0001-9875-6460

ISSN: 0963-0252

eISSN: 1361-6595

Record 16 of 19

Title: Afterglow chemistry of atmospheric-pressure helium-oxygen plasmas with humid air impurity

Author(s): Murakami, T (Murakami, Tomoyuki); Niemi, K (Niemi, Kari); Gans, T (Gans, Timo); Connell, DO (Connell, Deborah O.); Graham, WG (Graham, William G.)
Source: PLASMA SOURCES SCIENCE & TECHNOLOGY **Volume:** 23 **Issue:** 2 **Article Number:** 025005 **DOI:** 10.1088/0963-0252/23/2/025005 **Published:** APR 2014
Accession Number: WOS:000337890700008
Author Identifiers:

Author	ResearcherID Number	ORCID Number
Gans, Timo	C-5035-2008	0000-0003-1362-8000
Niemi, Kari		0000-0001-6134-1974
Graham, William		0000-0003-2759-4657

ISSN: 0963-0252
eISSN: 1361-6595

Record 17 of 19
Title: Time and spatial resolved optical and electrical characteristics of continuous and time modulated RF plasmas in contact with conductive and dielectric substrates
Author(s): Hofmann, S (Hofmann, Sven); van Gils, K (van Gils, Koen); van der Linden, S (van der Linden, Steven); Iseni, S (Iseni, Sylvain); Bruggeman, P (Bruggeman, Peter)
Source: EUROPEAN PHYSICAL JOURNAL D **Volume:** 68 **Issue:** 3 **Article Number:** 56 **DOI:** 10.1140/epjd/e2014-40430-3 **Published:** MAR 21 2014
Accession Number: WOS:000333400400001
Author Identifiers:

Author	ResearcherID Number	ORCID Number
Bruggeman, Peter	J-8273-2014	0000-0003-3346-7275
van Gils, Koen		0000-0001-8391-0349
Iseni, Sylvain		0000-0002-4923-1657

ISSN: 1434-6060
eISSN: 1434-6079

Record 18 of 19
Title: Ambient air particle transport into the effluent of a cold atmospheric-pressure argon plasma jet investigated by molecular beam mass spectrometry
Author(s): Dunnbier, M (Duennbier, M.); Schmidt-Bleker, A (Schmidt-Bleker, A.); Winter, J (Winter, J.); Wolfram, M (Wolfram, M.); Hippler, R (Hippler, R.); Weltmann, KD (Weltmann, K-D); Reuter, S (Reuter, S.)
Source: JOURNAL OF PHYSICS D-APPLIED PHYSICS **Volume:** 46 **Issue:** 43 **Article Number:** 435203 **DOI:** 10.1088/0022-3727/46/43/435203 **Published:** OCT 30 2013
Accession Number: WOS:000325679400007
Author Identifiers:

Author	ResearcherID Number	ORCID Number
Hippler, Rainer	A-2790-2013	0000-0002-5956-3321
Reuter, Stephan	D-2890-2014	0000-0002-4858-1081

ISSN: 0022-3727

eISSN: 1361-6463

Record 19 of 19

Title: Interacting kinetics of neutral and ionic species in an atmospheric-pressure helium-oxygen plasma with humid air impurities

Author(s): Murakami, T (Murakami, Tomoyuki); Niemi, K (Niemi, Kari); Gans, T (Gans, Timo); O'Connell, D (O'Connell, Deborah); Graham, WG (Graham, William G.)

Source: PLASMA SOURCES SCIENCE & TECHNOLOGY **Volume:** 22 **Issue:** 4 **Article Number:** 045010 **DOI:** 10.1088/0963-0252/22/4/045010 **Published:** AUG 2013

Accession Number: WOS:000322001300011

Author Identifiers:

Author	ResearcherID Number	ORCID Number
O'Connell, Deborah	D-7967-2018	0000-0002-1457-9004
Gans, Timo	C-5035-2008	0000-0003-1362-8000
Niemi, Kari		0000-0001-6134-1974
Graham, William		0000-0003-2759-4657

ISSN: 0963-0252

Close

Web of Science
Page 1 (Records 1 -- 19)
◀ [1] ▶

Print

Close

Web of Science
Page 1 (Records 1 -- 19)
[1]

Print

Record 1 of 19

Title: Ellipsometry of anisotropic graphene-like two-dimensional materials on transparent substrates

Author(s): Adamson, P (Adamson, Peep)

Source: OPTICAL AND QUANTUM ELECTRONICS **Volume:** 50 **Issue:** 11 **Article Number:** 403 **DOI:** 10.1007/s11082-018-1673-z **Published:** NOV 2018

Accession Number: WOS:000448435200003

Author Identifiers:

Author	ResearcherID Number	ORCID Number
Adamson, Peep		0000-0002-2863-5249

ISSN: 0306-8919

eISSN: 1572-817X

Record 2 of 19

Title: Broadband optical properties of graphene and HOPG investigated by spectroscopic Mueller matrix ellipsometry

Author(s): Song, BK (Song, Baokun); Gu, HG (Gu, Honggang); Zhu, SM (Zhu, Simin); Jiang, H (Jiang, Hao); Chen, XG (Chen, Xiuguo); Zhang, CW (Zhang, Chuanwei); Liu, SY (Liu, Shiyuan)

Source: APPLIED SURFACE SCIENCE **Volume:** 439 **Pages:** 1079-1087 **DOI:** 10.1016/j.apsusc.2018.01.051 **Published:** MAY 1 2018

Accession Number: WOS:000427457100130

Author Identifiers:

Author	ResearcherID Number	ORCID Number
Liu, Shiyuan		0000-0002-0756-1439

ISSN: 0169-4332

eISSN: 1873-5584

Record 3 of 19

Title: The optical properties of transferred graphene and the dielectrics grown on it obtained by ellipsometry

Author(s): Kasikov, A (Kasikov, Aarne); Kahro, T (Kahro, Tauno); Matisen, L (Matisen, Leonard); Kodu, M (Kodu, Margus); Tarre, A (Tarre, Aivar); Seemen, H (Seemen, Helina); Alles, H (Alles, Harry)

Source: APPLIED SURFACE SCIENCE **Volume:** 437 **Pages:** 410-417 **DOI:** 10.1016/j.apsusc.2017.08.109 **Published:** APR 15 2018

Accession Number: WOS:000425732700048

Conference Title: 2nd International Conference on Applied Surface Science (ICASS)

Conference Date: JUN 12-15, 2017
Conference Location: Dalian, PEOPLES R CHINA
Author Identifiers:

Author	ResearcherID Number	ORCID Number
Matisen, Leonard	H-9135-2018	0000-0002-6277-8518
Alles, Harry	C-5046-2008	

ISSN: 0169-4332
eISSN: 1873-5584

Record 4 of 19
Title: A Method for Reducing the Effect of Surface Contamination Layers in Reflection Diagnostics of Graphene-like 2D Materials
Author(s): Adamson, P (Adamson, Peep)
Source: NANO **Volume:** 13 **Issue:** 4 **Article Number:** 1850044 **DOI:** 10.1142/S1793292018500443 **Published:** APR 2018
Accession Number: WOS:000431138000011
ISSN: 1793-2920
eISSN: 1793-7094

Record 5 of 19
Title: Spectroscopic ellipsometric investigation of graphene and thin carbon films from the point of view of depolarization effects
Author(s): Papa, Z (Papa, Z.); Csontos, J (Csontos, J.); Smausz, T (Smausz, T.); Toth, Z (Toth, Z.); Budai, J (Budai, J.)
Source: APPLIED SURFACE SCIENCE **Volume:** 421 **Special Issue:** SI **Pages:** 714-721 **DOI:** 10.1016/j.apsusc.2016.11.231 **Part:** B **Published:** NOV 1 2017
Accession Number: WOS:000408756700070
Author Identifiers:

Author	ResearcherID Number	ORCID Number
Budai, Judit		0000-0001-9156-2233

ISSN: 0169-4332
eISSN: 1873-5584

Record 6 of 19
Title: Optical properties of graphene oxide and reduced graphene oxide determined by spectroscopic ellipsometry
Author(s): Schoche, S (Schoche, Stefan); Hong, N (Hong, Nina); Khorasaninejad, M (Khorasaninejad, Mohammadreza); Ambrosio, A (Ambrosio, Antonio); Orabona, E (Orabona, Emanuele); Maddalena, P (Maddalena, Pasqualino); Capasso, F (Capasso, Federico)
Source: APPLIED SURFACE SCIENCE **Volume:** 421 **Special Issue:** SI **Pages:** 778-782 **DOI:** 10.1016/j.apsusc.2017.01.035 **Part:** B **Published:** NOV 1 2017
Accession Number: WOS:000408756700080

Author Identifiers:

Author	ResearcherID Number	ORCID Number
Ambrosio, Antonio		0000-0002-8519-3862

ISSN: 0169-4332
eISSN: 1873-5584

Record 7 of 19
Title: A new heterostructured SERS substrate: free-standing silicon nanowires decorated with graphene-encapsulated gold nanoparticles
Author(s): Li, Y (Li, Yuan); Dykes, J (Dykes, John); Gilliam, T (Gilliam, Todd); Chopra, N (Chopra, Nitin)
Source: NANOSCALE **Volume:** 9 **Issue:** 16 **Pages:** 5263-5272 **DOI:** 10.1039/c6nr09896g **Published:** APR 28 2017
Accession Number: WOS:000399809400026
PubMed ID: 28397912
ISSN: 2040-3364
eISSN: 2040-3372

Record 8 of 19
Title: Ab-initio study of the optical properties of the Li-intercalated graphene and MoS2
Author(s): Pesic, J (Pesic, Jelena); Gajic, R (Gajic, Rados)
Source: OPTICAL AND QUANTUM ELECTRONICS **Volume:** 48 **Issue:** 7 **Article Number:** 368 **DOI:** 10.1007/s11082-016-0635-6 **Published:** JUL 2016
Accession Number: WOS:000379174800024
Author Identifiers:

Author	ResearcherID Number	ORCID Number
Pesic, Jelena	M-2357-2017	

ISSN: 0306-8919
eISSN: 1572-817X

Record 9 of 19
Title: Broadband optical properties of graphene by spectroscopic ellipsometry
Author(s): Li, W (Li, Wei); Cheng, GJ (Cheng, Guangjun); Liang, YR (Liang, Yiran); Tian, BY (Tian, Boyuan); Liang, XL (Liang, Xuelei); Peng, LM (Peng, Lianmao); Walker, ARH (Walker, A. R. Hight); Gundlach, DJ (Gundlach, David J.); Nguyen, NV (Nguyen, Nhan V.)
Source: CARBON **Volume:** 99 **Pages:** 348-353 **DOI:** 10.1016/j.carbon.2015.12.007 **Published:** APR 2016
Accession Number: WOS:000369069800041
Author Identifiers:

Author	ResearcherID Number	ORCID Number
Liang, Xuelei	C-4690-2013	0000-0003-3095-0974
Hight Walker, Angela	C-3373-2009	0000-0003-1385-0672
Peng, Lianmao	E-2089-2011	0000-0003-0754-074X

ISSN: 0008-6223

eISSN: 1873-3891

Record 10 of 19

Title: Plasmonic Indium Nanoparticle-Induced High-Performance Photoswitch for Blue Light Detection

Author(s): Wang, Y (Wang, Yuan); Ge, CW (Ge, Cai-Wang); Zou, YF (Zou, Yi-Feng); Lu, R (Lu, Rui); Zheng, K (Zheng, Kun); Zhang, TF (Zhang, Teng-Fei); Yu, YQ (Yu, Yong-Qiang); Luo, LB (Luo, Lin-Bao)

Source: ADVANCED OPTICAL MATERIALS **Volume:** 4 **Issue:** 2 **Pages:** 291-296 **DOI:** 10.1002/adom.201500360 **Published:** FEB 2016

Accession Number: WOS:000371269300012

Author Identifiers:

Author	ResearcherID Number	ORCID Number
罗, 林保	E-4530-2012	0000-0001-8651-8764

ISSN: 2195-1071

Record 11 of 19

Title: Correlation-free reflection diagnostics of graphene-like surface layers in the infrared region

Author(s): Adamson, P (Adamson, Peep)

Source: SURFACE AND INTERFACE ANALYSIS **Volume:** 47 **Issue:** 13 **Pages:** 1161-1165 **DOI:** 10.1002/sia.5868 **Published:** DEC 2015

Accession Number: WOS:000368298900004

ISSN: 0142-2421

eISSN: 1096-9918

Record 12 of 19

Title: Surface plasmon resonance enhanced highly efficient planar silicon solar cell

Author(s): Luo, LB (Luo, Lin-Bao); Xie, C (Xie, Chao); Wang, XH (Wang, Xian-He); Yu, YQ (Yu, Yong-Qiang); Wu, CY (Wu, Chun-Yan); Hu, H (Hu, Han); Zhou, KY (Zhou, Ke-Ya); Zhang, XW (Zhang, Xi-Wei); Jie, JS (Jie, Jian-Sheng)

Source: NANO ENERGY **Volume:** 9 **Pages:** 112-120 **DOI:** 10.1016/j.nanoen.2014.07.003 **Published:** OCT 2014

Accession Number: WOS:000344632800013

Author Identifiers:

Author	ResearcherID Number	ORCID Number

Jie, Jiansheng	K-8466-2015	0000-0002-2230-4289
罗, 林保	E-4530-2012	0000-0001-8651-8764
Xie, Chao	F-9876-2013	0000-0003-4451-767X

ISSN: 2211-2855
eISSN: 2211-3282

Record 13 of 19
Title: Analytic determination of n, k and d of two-dimensional materials by ellipsometry and reflectivity
Author(s): Adamson, P (Adamson, Peep)
Source: APPLIED OPTICS **Volume:** 53 **Issue:** 21 **Pages:** 4804-4810 **DOI:** 10.1364/AO.53.004804 **Published:** JUL 20 2014
Accession Number: WOS:000339870900025
PubMed ID: 25090221
ISSN: 1559-128X
eISSN: 2155-3165

Record 14 of 19
Title: Influence of transfer residue on the optical properties of chemical vapor deposited graphene investigated through spectroscopic ellipsometry
Author(s): Matkovic, A (Matkovic, Aleksandar); Ralevic, U (Ralevic, Uros); Chhikara, M (Chhikara, Manisha); Jakovljevic, MM (Jakovljevic, Milka M.); Jovanovic, D (Jovanovic, Djordje); Bratina, G (Bratina, Gvido); Gajic, R (Gajic, Rados)
Source: JOURNAL OF APPLIED PHYSICS **Volume:** 114 **Issue:** 9 **Article Number:** 093505 **DOI:** 10.1063/1.4819967 **Published:** SEP 7 2013
Accession Number: WOS:000324386900012
Author Identifiers:

Author	ResearcherID Number	ORCID Number
bratina, gvido		0000-0002-0085-7990

ISSN: 0021-8979
eISSN: 1089-7550

Record 15 of 19
Title: Shifting of surface plasmon resonance due to electromagnetic coupling between graphene and Au nanoparticles
Author(s): Niu, J (Niu, Jing); Shin, YJ (Shin, Young Jun); Son, J (Son, Jaesung); Lee, Y (Lee, Youngbin); Ahn, JH (Ahn, Jong-Hyun); Yang, H (Yang, Hyunsoo)
Source: OPTICS EXPRESS **Volume:** 20 **Issue:** 18 **Pages:** 19690-19696 **DOI:** 10.1364/OE.20.019690 **Published:** AUG 27 2012
Accession Number: WOS:000308414800009
PubMed ID: 23037021
Author Identifiers:

Author	ResearcherID Number	ORCID Number

Ahn, Jong-Hyun	L-9825-2016	0000-0002-8135-7719
Yang, Hyunsoo	F-5149-2010	0000-0003-0907-2898
Ahn, Jong-Hyun	G-7702-2011	

ISSN: 1094-4087

Record 16 of 19

Title: Transport of electrons in Ar/H-2 mixtures

Author(s): Nikitovic, Z (Nikitovic, Z.); Stojanovic, V (Stojanovic, V.); Petrovic, ZL (Petrovic, Z. Lj.)

Source: EPL **Volume:** 99 **Issue:** 3 **Article Number:** 35003 **DOI:** 10.1209/0295-5075/99/35003 **Published:** AUG 2012

Accession Number: WOS:000307868100011

Author Identifiers:

Author	ResearcherID Number	ORCID Number
Petrovic, Zoran		0000-0001-6569-9447

ISSN: 0295-5075

Record 17 of 19

Title: Study of electromagnetic enhancement for surface enhanced Raman spectroscopy of SiC graphene

Author(s): Niu, J (Niu, Jing); Truong, VG (Viet Giang Truong); Huang, H (Huang, Han); Tripathy, S (Tripathy, Sudhiranjan); Qiu, CY (Qiu, Caiyu); Wee, ATS (Wee, Andrew T. S.); Yu, T (Yu, Ting); Yang, H (Yang, Hyunsoo)

Source: APPLIED PHYSICS LETTERS **Volume:** 100 **Issue:** 19 **Article Number:** 191601 **DOI:** 10.1063/1.4712054 **Published:** MAY 7 2012

Accession Number: WOS:000304108000017

Author Identifiers:

Author	ResearcherID Number	ORCID Number
Yang, Hyunsoo	F-5149-2010	0000-0003-0907-2898
Huang, Han	D-9438-2011	
Qiu, Caiyu	E-7064-2013	0000-0001-7784-6141
Wee, Andrew	B-6624-2009	0000-0002-5828-4312
TRUONG, Viet Giang		0000-0003-3589-7850
Yu, Ting		0000-0002-0113-2895
Tripathy, Sudhiranjan		0000-0003-2606-9711

ISSN: 0003-6951

Record 18 of 19

Title: Spectroscopic ellipsometry and the Fano resonance modeling of graphene optical parameters

Author(s): Matkovic, A (Matkovic, A.); Ralevic, U (Ralevic, U.); Isic, G (Isic, G.); Jakovljevic, MM (Jakovljevic, M. M.); Vasic, B (Vasic, B.); Milosevic, I (Milosevic, I.);

Markovic, D (Markovic, D.); Gajic, R (Gajic, R.)

Source: PHYSICA SCRIPTA **Volume:** T149 **Article Number:** 014069 **DOI:** 10.1088/0031-8949/2012/T149/014069 **Published:** APR 2012

Accession Number: WOS:000303523500070

Conference Title: 3rd International School and Conference on Photonics

Conference Date: AUG 29-SEP 02, 2011

Conference Location: Belgrade, SERBIA

Author Identifiers:

Author	ResearcherID Number	ORCID Number
Milosevic, Ivanka		0000-0001-6885-7201

ISSN: 0031-8949

eISSN: 1402-4896

Record 19 of 19

Title: Development of Biomedical Applications of Non-equilibrium Plasmas and Possibilities for Atmospheric Pressure Nanotechnology Applications

Author(s): Petrovic, ZL (Petrovic, Z. Lj); Puac, N (Puac, N.); Maric, D (Maric, D.); Maletic, D (Maletic, D.); Spasic, K (Spasic, K.); Skoro, N (Skoro, N.); Sivos, J (Sivos, J.); Lazovic, S (Lazovic, S.); Malovic, G (Malovic, G.)

Book Group Author(s): IEEE

Source: 2012 28TH INTERNATIONAL CONFERENCE ON MICROELECTRONICS (MIEL) **Book Series:** International Conference on Microelectronics-MIEL **Pages:** 31-38 **Published:** 2012

Accession Number: WOS:000309119600005

Conference Title: 28th International Conference on Microelectronics (MIEL)

Conference Date: MAY 13-16, 2012

Conference Location: Nis, SERBIA

Conference Sponsors: IEEE, IEEE Serbia & Montenegro Sect - ED/SSC Chapter, IEEE Electron Devices Soc (EDS), IEEE Solid-State Circuits Soc (SSCS)

Author Identifiers:

Author	ResearcherID Number	ORCID Number
Lazovic, Sasa	B-9651-2013	0000-0003-1696-9134
Skoro, Nikola		0000-0002-0254-8008
Malovic, Gordana		0000-0003-2356-0652
Puac, Nevena		0000-0003-1142-8494
Maric, Dragana		0000-0002-1728-5458
Petrovic, Zoran		0000-0001-6569-9447

ISSN: 2159-1660

ISBN: 978-1-4673-0238-8

Close

Web of Science
Page 1 (Records 1 -- 18)
[1]

Print

Record 1 of 18

Title: Characterisation of a multijet plasma device by means of mass spectrometric detection and iCCD imaging

Author(s): Stancampiano, A (Stancampiano, A.); Selakovic, N (Selakovic, N.); Gherardi, M (Gherardi, M.); Puac, N (Puac, N.); Petrovic, ZL (Petrovic, Z. Lj); Colombo, V (Colombo, V)

Source: JOURNAL OF PHYSICS D-APPLIED PHYSICS **Volume:** 51 **Issue:** 48 **Article Number:** 484004 **DOI:** 10.1088/1361-6463/aae2f2 **Published:** DEC 5 2018

Accession Number: WOS:000446857200001

ISSN: 0022-3727

eISSN: 1361-6463

Record 2 of 18

Title: Development from dielectric barrier discharge to atmospheric pressure plasma jet in helium: experiment and fluid modeling

Author(s): Zhu, P (Zhu, Ping); Li, B (Li, Ben); Duan, ZC (Duan, Zhengchao); Ouyang, JT (Ouyang, Jiting)

Source: JOURNAL OF PHYSICS D-APPLIED PHYSICS **Volume:** 51 **Issue:** 40 **Article Number:** 405202 **DOI:** 10.1088/1361-6463/aacb12 **Published:** OCT 10 2018

Accession Number: WOS:000443761600001

Author Identifiers:

Author	ResearcherID Number	ORCID Number
Li, Ben		0000-0002-7265-7672

ISSN: 0022-3727

eISSN: 1361-6463

Record 3 of 18

Title: Electrode configurations in atmospheric pressure plasma jets: production of reactive species

Author(s): Lietz, AM (Lietz, Amanda M.); Kushner, MJ (Kushner, Mark J.)

Source: PLASMA SOURCES SCIENCE & TECHNOLOGY **Volume:** 27 **Issue:** 10 **Article Number:** 105020 **DOI:** 10.1088/1361-6595/aadf5b **Published:** OCT 2018

Accession Number: WOS:000448845500001

Author Identifiers:

Author	ResearcherID Number	ORCID Number
Lietz, Amanda		0000-0001-6423-5042

ISSN: 0963-0252

eISSN: 1361-6595

Record 4 of 18

Title: How dielectric, metallic and liquid targets influence the evolution of electron properties in a pulsed He jet measured by Thomson and Raman scattering

Author(s): Klarenaar, BLM (Klarenaar, B. L. M.); Guaitella, O (Guaitella, O.); Engeln, R (Engeln, R.); Sobota, A (Sobota, A.)

Source: PLASMA SOURCES SCIENCE & TECHNOLOGY **Volume:** 27 **Issue:** 8 **Article Number:** 085004 **DOI:** 10.1088/1361-6595/aad4d7 **Published:** AUG 2018

Accession Number: WOS:000440748600001

Author Identifiers:

Author	ResearcherID Number	ORCID Number
Sobota, Ana		0000-0003-1036-4513
Klarenaar, Bart		0000-0003-1544-8011

ISSN: 0963-0252

eISSN: 1361-6595

Record 5 of 18

Title: Interferometry of plasma bursts in helium atmospheric-pressure plasma jets

Author(s): Samara, V (Samara, Vladimir); Ptasinska, S (Ptasinska, Sylwia)

Source: JOURNAL OF VACUUM SCIENCE & TECHNOLOGY A **Volume:** 36 **Issue:** 4 **Article Number:** 04F402 **DOI:** 10.1116/1.5023113 **Published:** JUL 2018

Accession Number: WOS:000438217600002

ISSN: 0734-2101

eISSN: 1520-8559

Record 6 of 18

Title: Activity of catalase enzyme in Paulownia tomentosa seeds during the process of germination after treatments with low pressure plasma and plasma activated water

Author(s): Puac, N (Puac, Nevena); Skoro, N (Skoro, Nikola); Spasic, K (Spasic, Kosta); Zivkovic, S (Zivkovic, Suzana); Milutinovic, M (Milutinovic, Milica); Malovic, G (Malovic, Gordana); Petrovic, ZL (Petrovic, Zoran Lj)

Source: PLASMA PROCESSES AND POLYMERS **Volume:** 15 **Issue:** 2 **Article Number:** e1700082 **DOI:** 10.1002/ppap.201700082 **Published:** FEB 2018

Accession Number: WOS:000425453900010

Author Identifiers:

Author	ResearcherID Number	ORCID Number
Puac, Nevena		0000-0003-1142-8494
Malovic, Gordana		0000-0003-2356-0652
Zivkovic, Suzana		0000-0003-0280-5884
Skoro, Nikola		0000-0002-0254-8008
Petrovic, Zoran		0000-0001-6569-9447

ISSN: 1612-8850
eISSN: 1612-8869

Record 7 of 18

Title: Destruction of chemical warfare surrogates using a portable atmospheric pressure plasma jet

Author(s): Skoro, N (Skoro, Nikola); Puac, N (Puac, Nevena); Zivkovic, S (Zivkovic, Suzana); Krstic-Milosevic, D (Krstic-Milosevic, Dijana); Cvelbar, U (Cvelbar, Uros); Malovic, G (Malovic, Gordana); Petrovic, ZL (Petrovic, Zoran Lj.)

Source: EUROPEAN PHYSICAL JOURNAL D **Volume:** 72 **Issue:** 1 **Article Number:** 2 **DOI:** 10.1140/epjd/e2017-80329-9 **Published:** JAN 16 2018
Accession Number: WOS:000422899000001

Author Identifiers:

Author	ResearcherID Number	ORCID Number
Puac, Nevena		0000-0003-1142-8494
Cvelbar, Uros		0000-0002-1957-0789
Petrovic, Zoran		0000-0001-6569-9447
Skoro, Nikola		0000-0002-0254-8008

ISSN: 1434-6060
eISSN: 1434-6079

Record 8 of 18

Title: Effect of external electric and magnetic field on propagation of atmospheric pressure plasma jet

Author(s): Zhu, P (Zhu, Ping); Meng, ZZ (Meng, Zhaozhong); Hu, HX (Hu, Haixin); Ouyang, JT (Ouyang, Jiting)

Source: PHYSICS OF PLASMAS **Volume:** 24 **Issue:** 10 **Article Number:** 103512 **DOI:** 10.1063/1.5004419 **Published:** OCT 2017
Accession Number: WOS:000414171600145
ISSN: 1070-664X
eISSN: 1089-7674

Record 9 of 18

Title: Electrical and optical characterization of an atmospheric pressure, uniform, large-area processing, dielectric barrier discharge

Author(s): Zeniou, A (Zeniou, A.); Puac, N (Puac, N.); Skoro, N (Skoro, N.); Selakovic, N (Selakovic, N.); Dimitrakellis, P (Dimitrakellis, P.); Gogolides, E (Gogolides, E.); Petrovic, ZL (Petrovic, Z. Lj)

Source: JOURNAL OF PHYSICS D-APPLIED PHYSICS **Volume:** 50 **Issue:** 13 **Article Number:** 135204 **DOI:** 10.1088/1361-6463/aa5d69 **Published:** APR 5 2017
Accession Number: WOS:000396058900002

Author Identifiers:

Author	ResearcherID Number	ORCID Number
Petrovic, Zoran		0000-0001-6569-9447

Puac, Nevena		0000-0003-1142-8494
Skoro, Nikola		0000-0002-0254-8008

ISSN: 0022-3727
eISSN: 1361-6463

Record 10 of 18

Title: Electric field measurements in a kHz-driven He jet-the influence of the gas flow speed

Author(s): Sobota, A (Sobota, A.); Guaitella, O (Guaitella, O.); Sretenovic, GB (Sretenovic, G. B.); Krstic, IB (Krstic, I. B.); Kovacevic, VV (Kovacevic, V. V.); Obrusnik, A (Obrusnik, A.); Nguyen, YN (Nguyen, Y. N.); Zajickova, L (Zajickova, L.); Obradovic, BM (Obradovic, B. M.); Kuraica, MM (Kuraica, M. M.)

Source: PLASMA SOURCES SCIENCE & TECHNOLOGY **Volume:** 25 **Issue:** 6 **Article Number:** 065026 **DOI:** 10.1088/0963-0252/25/6/065026 **Published:** DEC 2016
Accession Number: WOS:000388926700002

Author Identifiers:

Author	ResearcherID Number	ORCID Number
Guaitella, Olivier	A-1405-2017	0000-0002-6509-6934
Sretenovic, Goran	P-8983-2016	0000-0003-4817-4723
Zajickova, Lenka	E-3010-2012	0000-0002-6906-8906
Sobota, Ana	F-1925-2011	0000-0003-1036-4513
Kuraica, Milorad		0000-0001-8201-8500
Kovacevic, Vesna		0000-0002-8575-1668

ISSN: 0963-0252
eISSN: 1361-6595

Record 11 of 18

Title: Dynamics of the gas flow turbulent front in atmospheric pressure plasma jets

Author(s): Pei, X (Pei, X.); Ghasemi, M (Ghasemi, M.); Xu, H (Xu, H.); Hasnain, Q (Hasnain, Q.); Wu, S (Wu, S.); Tu, Y (Tu, Y.); Lu, X (Lu, X.)

Source: PLASMA SOURCES SCIENCE & TECHNOLOGY **Volume:** 25 **Issue:** 3 **Article Number:** 035013 **DOI:** 10.1088/0963-0252/25/3/035013 **Published:** JUN 2016
Accession Number: WOS:000376557400021
ISSN: 0963-0252
eISSN: 1361-6595

Record 12 of 18

Title: Atmospheric pressure plasma jet for liquid spray treatment

Author(s): Mitic, S (Mitic, S.); Philipps, J (Philipps, J.); Hofmann, D (Hofmann, D.)

Source: JOURNAL OF PHYSICS D-APPLIED PHYSICS **Volume:** 49 **Issue:** 20 **Article Number:** 205202 **DOI:** 10.1088/0022-3727/49/20/205202 **Published:** MAY 25 2016
Accession Number: WOS:000375255800017
ISSN: 0022-3727

eISSN: 1361-6463

Record 13 of 18

Title: Helium atmospheric pressure plasma jets interacting with wet cells: delivery of electric fields

Author(s): Norberg, SA (Norberg, Seth A.); Johnsen, E (Johnsen, Eric); Kushner, MJ (Kushner, Mark J.)

Source: JOURNAL OF PHYSICS D-APPLIED PHYSICS **Volume:** 49 **Issue:** 18 **Article Number:** 185201 **DOI:** 10.1088/0022-3727/49/18/185201 **Published:** MAY 11 2016

Accession Number: WOS:000375255300015

ISSN: 0022-3727

eISSN: 1361-6463

Record 14 of 18

Title: Radio frequency atmospheric plasma source on a printed circuit board for large area, uniform processing of polymeric materials

Author(s): Dimitrakellis, P (Dimitrakellis, P.); Zeniou, A (Zeniou, A.); Stratakos, Y (Stratakos, Y.); Gogolides, E (Gogolides, E.)

Source: PLASMA SOURCES SCIENCE & TECHNOLOGY **Volume:** 25 **Issue:** 2 **Article Number:** 025015 **DOI:** 10.1088/0963-0252/25/2/025015 **Published:** APR 2016

Accession Number: WOS:000372337900017

ISSN: 0963-0252

eISSN: 1361-6595

Record 15 of 18

Title: Single-electrode He microplasma jets driven by nanosecond voltage pulses

Author(s): Jiang, C (Jiang, C.); Lane, J (Lane, J.); Song, ST (Song, S. T.); Pendelton, SJ (Pendelton, S. J.); Wu, Y (Wu, Y.); Sozer, E (Sozer, E.); Kuthi, A (Kuthi, A.); Gundersen, MA (Gundersen, M. A.)

Source: JOURNAL OF APPLIED PHYSICS **Volume:** 119 **Issue:** 8 **Article Number:** 083301 **DOI:** 10.1063/1.4942624 **Published:** FEB 28 2016

Accession Number: WOS:000371601800009

Author Identifiers:

Author	ResearcherID Number	ORCID Number
Sozer, Esin		0000-0002-6244-3670

ISSN: 0021-8979

eISSN: 1089-7550

Record 16 of 18

Title: Practical and theoretical considerations on the use of ICCD imaging for the characterization of non-equilibrium plasmas

Author(s): Gherardi, M (Gherardi, Matteo); Puac, N (Puac, Nevena); Maric, D (Maric, Dragana); Stancampiano, A (Stancampiano, Augusto); Malovic, G (Malovic, Gordana); Colombo, V (Colombo, Vittorio); Petrovic, ZL (Petrovic, Zoran Lj)

Source: PLASMA SOURCES SCIENCE & TECHNOLOGY **Volume:** 24 **Issue:** 6 **Article Number:** 064004 **DOI:** 10.1088/0963-0252/24/6/064004 **Published:** DEC 2015

Accession Number: WOS:000368117100005

Author Identifiers:

Author	ResearcherID Number	ORCID Number
Maric, Dragana		0000-0002-1728-5458
Malovic, Gordana		0000-0003-2356-0652
COLOMBO, VITTORIO		0000-0001-9145-198X
Petrovic, Zoran		0000-0001-6569-9447
Puac, Nevena		0000-0003-1142-8494

ISSN: 0963-0252

eISSN: 1361-6595

Record 17 of 18

Title: Atmospheric pressure argon surface discharges propagated in long tubes: physical characterization and application to bio-decontamination

Author(s): Kovalova, Z (Kovalova, Zuzana); Leroy, M (Leroy, Magali); Jacobs, C (Jacobs, Carolyn); Kirkpatrick, MJ (Kirkpatrick, Michael J.); Machala, Z (Machala, Zdenko); Lopes, F (Lopes, Filipa); Laux, CO (Laux, Christophe O.); DuBow, MS (DuBow, Michael S.); Odic, E (Odic, Emmanuel)

Source: JOURNAL OF PHYSICS D-APPLIED PHYSICS **Volume:** 48 **Issue:** 46 **Article Number:** 464003 **DOI:** 10.1088/0022-3727/48/46/464003 **Published:** NOV 25 2015

Accession Number: WOS:000367087600005

Author Identifiers:

Author	ResearcherID Number	ORCID Number
Machala, Zdenko	B-6384-2018	0000-0003-1424-1350
Jacobs, Carolyn		0000-0003-1285-7629

ISSN: 0022-3727

eISSN: 1361-6463

Record 18 of 18

Title: Cavity ring-down spectroscopy for atmospheric pressure plasma jet analysis

Author(s): Zaplotnik, R (Zaplotnik, Rok); Biscan, M (Biscan, Marijan); Krstulovic, N (Krstulovic, Niksa); Popovic, D (Popovic, Dean); Milosevic, S (Milosevic, Slobodan)

Source: PLASMA SOURCES SCIENCE & TECHNOLOGY **Volume:** 24 **Issue:** 5 **Article Number:** 054004 **DOI:** 10.1088/0963-0252/24/5/054004 **Published:** OCT 2015

Accession Number: WOS:000364336600007

Author Identifiers:

Author	ResearcherID Number	ORCID Number
Milosevic, Slobodan	A-3408-2010	
Milosevic, Slobodan		0000-0002-4455-7869

ISSN: 0963-0252

eISSN: 1361-6595

Close

Web of Science
Page 1 (Records 1 -- 18)
[1]

Print

Clarivate
Accelerating innovation

Close

Web of Science
Page 1 (Records 1 -- 17)
[1]

Print

Record 1 of 17

Title: Synergistic effects of plasma-activated medium and chemotherapeutic drugs in cancer treatment

Author(s): Chen, CY (Chen, Chao-Yu); Cheng, YC (Cheng, Yun-Chien); Cheng, YJ (Cheng, Yi-Jing)

Source: JOURNAL OF PHYSICS D-APPLIED PHYSICS **Volume:** 51 **Issue:** 13 **Article Number:** 13LT01 **DOI:** 10.1088/1361-6463/aaafc4 **Published:** APR 4 2018

Accession Number: WOS:000427087700001

Author Identifiers:

Author	ResearcherID Number	ORCID Number
Cheng, Yun-Chien		0000-0002-0803-2053

ISSN: 0022-3727

eISSN: 1361-6463

Record 2 of 17

Title: 6-(2-Fluorobenzoyl)-3-(2-(4-(4-fluorophenyl)piperazin-1-yl)-2-oxoethyl)benzo[d]thiazol-2(3H)-one drug molecule structure and its interaction with atmospheric pressure plasma jet

Author(s): Tanisli, M (Tanisli, Murat); Tasal, E (Tasal, Erol); Sahin, N (Sahin, Neslihan); Arslan, C (Arslan, Cetin)

Source: JOURNAL OF MOLECULAR LIQUIDS **Volume:** 240 **Pages:** 733-751 **DOI:** 10.1016/j.molliq.2017.05.022 **Published:** AUG 2017

Accession Number: WOS:000407654700079

ISSN: 0167-7322

eISSN: 1873-3166

Record 3 of 17

Title: The influence of electrode configuration on light emission profiles and electrical characteristics of an atmospheric-pressure plasma jet

Author(s): Maletic, D (Maletic, Dejan); Puac, N (Puac, Nevena); Malovic, G (Malovic, Gordana); Dordevic, A (Dordevic, Antonije); Petrovic, ZL (Petrovic, Zoran Lj)

Source: JOURNAL OF PHYSICS D-APPLIED PHYSICS **Volume:** 50 **Issue:** 14 **Article Number:** 145202 **DOI:** 10.1088/1361-6463/aa5d91 **Published:** APR 12 2017

Accession Number: WOS:000404428200002

Author Identifiers:

Author	ResearcherID Number	ORCID Number
Puac, Nevena		0000-0003-1142-8494
Petrovic, Zoran		0000-0001-6569-9447
Malovic, Gordana		0000-0003-2356-0652

ISSN: 0022-3727
eISSN: 1361-6463

Record 4 of 17

Title: Plasma Medicine and The Application in Tumor Therapy

Author(s): Xu, DH (Xu De-Hui); Cui, QJ (Cui Qing-Jie); Xu, YJ (Xu Yu-Jing); Liu, DX (Liu Ding-Xin); Kong, GY (Kong Gang-Yu)

Source: PROGRESS IN BIOCHEMISTRY AND BIOPHYSICS **Volume:** 44 **Issue:** 4 **Pages:** 279-292 **DOI:** 10.16476/j.pibb.2016.0371 **Published:** APR 2017
Accession Number: WOS:000399967800002
ISSN: 1000-3282

Record 5 of 17

Title: Treatment of oral hyperpigmentation and gummy smile using lasers and role of plasma as a novel treatment technique in dentistry: An introductory review

Author(s): Jha, N (Jha, Nayansi); Ryu, JJ (Ryu, Jae Jun); Wahab, R (Wahab, Rizwan); Al-Khedhairy, AA (Al-Khedhairy, Abdulaziz A.); Choi, EH (Choi, Eun Ha); Kaushik, NK (Kaushik, Nagendra Kumar)

Source: ONCOTARGET **Volume:** 8 **Issue:** 12 **Pages:** 20496-20509 **DOI:** 10.18632/oncotarget.14887 **Published:** MAR 21 2017
Accession Number: WOS:000396879200149
PubMed ID: 28147333

Author Identifiers:

Author	ResearcherID Number	ORCID Number
Kaushik, Nagendra Kumar		0000-0002-4965-5046

ISSN: 1949-2553

Record 6 of 17

Title: Generation and Role of Reactive Oxygen and Nitrogen Species Induced by Plasma, Lasers, Chemical Agents, and Other Systems in Dentistry

Author(s): Jha, N (Jha, Nayansi); Ryu, JJ (Ryu, Jae Jun); Choi, EH (Choi, Eun Ha); Kaushik, NK (Kaushik, Nagendra Kumar)

Source: OXIDATIVE MEDICINE AND CELLULAR LONGEVITY **Article Number:** 7542540 **DOI:** 10.1155/2017/7542540 **Published:** 2017
Accession Number: WOS:000413554300001
PubMed ID: 29204250

Author Identifiers:

Author	ResearcherID Number	ORCID Number
Kaushik, Nagendra Kumar		0000-0002-4965-5046

ISSN: 1942-0900
eISSN: 1942-0994

Record 7 of 17

Title: Microplasma Induced Cell Morphological Changes and Apoptosis of Ex Vivo Cultured Human Anterior Lens Epithelial Cells - Relevance to Capsular Opacification

Author(s): Recek, N (Recek, Nina); Andjelic, S (Andjelic, Sofija); Hojnik, N (Hojnik, Nataga); Filipic, G (Filipic, Gregor); Lazovic, S (Lazovic, Sasa); Vesel, A (Vesel, Alenka); Primc, G (Primc, Gregor); Mozetic, M (Mozetic, Miran); Hawlina, M (Hawlina, Marko); Petrovski, G (Petrovski, Goran); Cvelbar, U (Cvelbar, Uros)

Source: PLOS ONE **Volume:** 11 **Issue:** 11 **Article Number:** e0165883 **DOI:** 10.1371/journal.pone.0165883 **Published:** NOV 10 2016

Accession Number: WOS:000387725000038

PubMed ID: 27832099

Author Identifiers:

Author	ResearcherID Number	ORCID Number
Filipic, Gregor	T-4900-2018	0000-0003-0153-5181
Lazovic, Sasa	Q-5056-2016	0000-0003-1696-9134

ISSN: 1932-6203

Record 8 of 17

Title: A study of the effect on human mesenchymal stem cells of an atmospheric pressure plasma source driven by different voltage waveforms

Author(s): Laurita, R (Laurita, R.); Alviano, F (Alviano, F.); Marchionni, C (Marchionni, C.); Abruzzo, PM (Abruzzo, P. M.); Bolotta, A (Bolotta, A.); Bonsi, L (Bonsi, L.); Colombo, V (Colombo, V.); Gherardi, M (Gherardi, M.); Liguori, A (Liguori, A.); Ricci, F (Ricci, F.); Rossi, M (Rossi, M.); Stancampiano, A (Stancampiano, A.); Tazzari, PL (Tazzari, P. L.); Marini, M (Marini, M.)

Source: JOURNAL OF PHYSICS D-APPLIED PHYSICS **Volume:** 49 **Issue:** 36 **Article Number:** 364003 **DOI:** 10.1088/0022-3727/49/36/364003 **Published:** SEP 14 2016

Accession Number: WOS:000384052800005

Author Identifiers:

Author	ResearcherID Number	ORCID Number
Marini, Marina	B-1490-2012	0000-0003-1932-7380
Laurita, Romolo	U-6968-2017	0000-0003-1744-3329
Abruzzo, Provvidenza	G-7009-2015	0000-0001-5242-9448
COLOMBO, VITTORIO		0000-0001-9145-198X

ISSN: 0022-3727

eISSN: 1361-6463

Record 9 of 17

Title: The effect of the plasma needle on the human keratinocytes related to the wound healing process

Author(s): Korolov, I (Korolov, Ihor); Fazekas, B (Fazekas, Barbara); Szell, M (Szell, Marta); Kemeny, L (Kemeny, Lajos); Kutasi, K (Kutasi, Kinga)

Source: JOURNAL OF PHYSICS D-APPLIED PHYSICS **Volume:** 49 **Issue:** 3 **Article Number:** 035401 **DOI:** 10.1088/0022-3727/49/3/035401 **Published:** JAN 27 2016

Accession Number: WOS:000368096300019

Author Identifiers:

Author	ResearcherID Number	ORCID Number
Korolov, Ihor	A-2848-2013	0000-0003-2384-1243

ISSN: 0022-3727

eISSN: 1361-6463

Record 10 of 17

Title: The hormesis effect of plasma-elevated intracellular ROS on HaCaT cells

Author(s): Szili, EJ (Szili, Endre J.); Harding, FJ (Harding, Frances J.); Hong, SH (Hong, Sung-Ha); Herrmann, F (Herrmann, Franziska); Voelcker, NH (Voelcker, Nicolas H.); Short, RD (Short, Robert D.)

Source: JOURNAL OF PHYSICS D-APPLIED PHYSICS **Volume:** 48 **Issue:** 49 **Article Number:** 495401 **DOI:** 10.1088/0022-3727/48/49/495401 **Published:** DEC 16 2015

Accession Number: WOS:000368442600020

Author Identifiers:

Author	ResearcherID Number	ORCID Number
Voelcker, Nicolas	D-6199-2012	0000-0002-1536-7804

ISSN: 0022-3727

eISSN: 1361-6463

Record 11 of 17

Title: On the effect of serum on the transport of reactive oxygen species across phospholipid membranes

Author(s): Szili, EJ (Szili, Endre J.); Hong, SH (Hong, Sung-Ha); Short, RD (Short, Robert D.)

Source: BIOINTERPHASES **Volume:** 10 **Issue:** 2 **Article Number:** 029511 **DOI:** 10.1116/1.4918765 **Published:** JUN 2015

Accession Number: WOS:000357195600029

PubMed ID: 25910641

ISSN: 1934-8630

eISSN: 1559-4106

Record 12 of 17

Title: Time-resolved optical emission imaging of an atmospheric plasma jet for different electrode positions with a constant electrode gap

Author(s): Maletic, D (Maletic, D.); Puac, N (Puac, N.); Selakovic, N (Selakovic, N.); Lazovic, S (Lazovic, S.); Malovic, G (Malovic, G.); Dordevic, A (Dordevic, A.); Petrovic, ZL (Petrovic, Z. Lj)

Source: PLASMA SOURCES SCIENCE & TECHNOLOGY **Volume:** 24 **Issue:** 2 **Article Number:** 025006 **DOI:** 10.1088/0963-0252/24/2/025006 **Published:** APR 2015

Accession Number: WOS:000356816200010

Author Identifiers:

Author	ResearcherID Number	ORCID Number
Lazovic, Sasa	Q-5056-2016	0000-0003-1696-9134
Petrovic, Zoran		0000-0001-6569-9447
Puac, Nevena		0000-0003-1142-8494
Malovic, Gordana		0000-0003-2356-0652

ISSN: 0963-0252

eISSN: 1361-6595

Record 13 of 17

Title: Plasma induced DNA damage: Comparison with the effects of ionizing radiation

Author(s): Lazovic, S (Lazovic, S.); Maletic, D (Maletic, D.); Leskovac, A (Leskovac, A.); Filipovic, J (Filipovic, J.); Puac, N (Puac, N.); Malovic, G (Malovic, G.); Joksic, G (Joksic, G.); Petrovic, ZL (Petrovic, Z. Lj.)

Source: APPLIED PHYSICS LETTERS **Volume:** 105 **Issue:** 12 **Article Number:** 124101 **DOI:** 10.1063/1.4896626 **Published:** SEP 22 2014

Accession Number: WOS:000343004400099

Author Identifiers:

Author	ResearcherID Number	ORCID Number
Lazovic, Sasa	Q-5056-2016	0000-0003-1696-9134
Joksic, Gordana		0000-0002-7186-301X
Petrovic, Zoran		0000-0001-6569-9447
Leskovac, Andreja		0000-0002-6293-5237
Puac, Nevena		0000-0003-1142-8494
Filipovic Trickovic, Jelena		0000-0001-5450-0842
Malovic, Gordana		0000-0003-2356-0652

ISSN: 0003-6951

eISSN: 1077-3118

Record 14 of 17

Title: Ionized gas (plasma) delivery of reactive oxygen species (ROS) into artificial cells

Author(s): Hong, SH (Hong, Sung-Ha); Szili, EJ (Szili, Endre J.); Jenkins, ATA (Jenkins, A. Toby A.); Short, RD (Short, Robert D.)

Source: JOURNAL OF PHYSICS D-APPLIED PHYSICS **Volume:** 47 **Issue:** 36 **Article Number:** 362001 **DOI:** 10.1088/0022-3727/47/36/362001 **Published:** SEP 10 2014

Accession Number: WOS:000341769900001

Author Identifiers:

Author	ResearcherID Number	ORCID Number
Jenkins, Toby	C-2124-2009	0000-0002-8981-3029

ISSN: 0022-3727
eISSN: 1361-6463

Record 15 of 17

Title: Microbubble generation by microplasma in water

Author(s): Xiao, P (Xiao, Peng); Staack, D (Staack, David)

Source: JOURNAL OF PHYSICS D-APPLIED PHYSICS **Volume:** 47 **Issue:** 35 **Article Number:** 355203 **DOI:** 10.1088/0022-3727/47/35/355203 **Published:** SEP 3 2014
Accession Number: WOS:000341353800015
ISSN: 0022-3727
eISSN: 1361-6463

Record 16 of 17

Title: Long and short term effects of plasma treatment on meristematic plant cells

Author(s): Puac, N (Puac, N.); Zivkovic, S (Zivkovic, S.); Selakovic, N (Selakovic, N.); Milutinovic, M (Milutinovic, M.); Boljevic, J (Boljevic, J.); Malovic, G (Malovic, G.); Petrovic, ZL (Petrovic, Z. Lj)

Source: APPLIED PHYSICS LETTERS **Volume:** 104 **Issue:** 21 **Article Number:** 214106 **DOI:** 10.1063/1.4880360 **Published:** MAY 26 2014
Accession Number: WOS:000337143000078

Author Identifiers:

Author	ResearcherID Number	ORCID Number
Petrovic, Zoran		0000-0001-6569-9447
Zivkovic, Suzana		0000-0003-0280-5884
Puac, Nevena		0000-0003-1142-8494
Malovic, Gordana		0000-0003-2356-0652

ISSN: 0003-6951
eISSN: 1077-3118

Record 17 of 17

Title: Multiple vs. single harmonics AC-driven atmospheric plasma jet

Author(s): Zaplotnik, R (Zaplotnik, R.); Kregar, Z (Kregar, Z.); Biscan, M (Biscan, M.); Vesel, A (Vesel, A.); Cvelbar, U (Cvelbar, U.); Mozetic, M (Mozetic, M.); Milosevic, S (Milosevic, S.)

Source: EPL **Volume:** 106 **Issue:** 2 **Article Number:** 25001 **DOI:** 10.1209/0295-5075/106/25001 **Published:** APR 2014
Accession Number: WOS:000336376100010

Author Identifiers:

Author	ResearcherID Number	ORCID Number
Mozetic, Miran	K-8784-2014	

Vesel, Alenka	I-3934-2014	0000-0003-3782-6001
Milosevic, Slobodan	A-3408-2010	
Milosevic, Slobodan		0000-0002-4455-7869

ISSN: 0295-5075
eISSN: 1286-4854

Close

Web of Science
Page 1 (Records 1 -- 17)
[1]

Print

Close

Web of Science
Page 1 (Records 1 -- 15)
[1]

Print

Record 1 of 15

Title: Chemistry and biochemistry of cold physical plasma derived reactive species in liquids

Author(s): Wende, K (Wende, Kristian); von Woedtke, T (von Woedtke, Thomas); Weltmann, KD (Weltmann, Klaus-Dieter); Bekeschus, S (Bekeschus, Sander)

Source: BIOLOGICAL CHEMISTRY **Volume:** 400 **Issue:** 1 **Pages:** 19-38 **DOI:** 10.1515/hsz-2018-0242 **Published:** JAN 2019

Accession Number: WOS:000451779300003

PubMed ID: 30403650

Author Identifiers:

Author	ResearcherID Number	ORCID Number
Wende, Kristian		0000-0001-5217-0683

ISSN: 1431-6730

eISSN: 1437-4315

Record 2 of 15

Title: Cross sections and transport coefficients for H-3(+) ions in water vapour

Author(s): Stojanovic, V (Stojanovic, Vladimir); Raspopovic, Z (Raspopovic, Zoran); Jovanovic, J (Jovanovic, Jasmina); Nikitovic, Z (Nikitovic, Zeljka); Maric, D (Maric, Dragana); Petrovic, ZL (Petrovic, Zoran Lj.)

Source: EUROPEAN PHYSICAL JOURNAL D **Volume:** 71 **Issue:** 11 **Article Number:** 283 **DOI:** 10.1140/epjd/e2017-80295-2 **Published:** NOV 14 2017

Accession Number: WOS:000415219300002

Author Identifiers:

Author	ResearcherID Number	ORCID Number
Petrovic, Zoran		0000-0001-6569-9447
Maric, Dragana		0000-0002-1728-5458

ISSN: 1434-6060

eISSN: 1434-6079

Record 3 of 15

Title: The influence of electrode configuration on light emission profiles and electrical characteristics of an atmospheric-pressure plasma jet

Author(s): Maletic, D (Maletic, Dejan); Puac, N (Puac, Nevena); Malovic, G (Malovic, Gordana); Dordevic, A (Dordevic, Antonije); Petrovic, ZL (Petrovic, Zoran Lj)

Source: JOURNAL OF PHYSICS D-APPLIED PHYSICS **Volume:** 50 **Issue:** 14 **Article Number:** 145202 **DOI:** 10.1088/1361-6463/aa5d91 **Published:** APR 12 2017

Accession Number: WOS:000404428200002

Author Identifiers:

Author	ResearcherID Number	ORCID Number
Puac, Nevena		0000-0003-1142-8494
Petrovic, Zoran		0000-0001-6569-9447
Malovic, Gordana		0000-0003-2356-0652

ISSN: 0022-3727

eISSN: 1361-6463

Record 4 of 15

Title: Atmospheric Pressure Pulsed Plasma Induces Cell Death in Photosynthetic Organs via Intracellularly Generated ROS

Author(s): Seol, YB (Seol, You-bin); Kim, J (Kim, Jaewook); Park, SH (Park, Se-hong); Chang, HY (Chang, Hong Young)

Source: SCIENTIFIC REPORTS **Volume:** 7 **Article Number:** 589 **DOI:** 10.1038/s41598-017-00480-6 **Published:** APR 3 2017

Accession Number: WOS:000398136000002

PubMed ID: 28373681

ISSN: 2045-2322

Record 5 of 15

Title: The New Approach for Establishing the Cellular Response Guideline for Medical Applications of Argon-Plasma Jet: Mitochondria and Colorimetric Polydiacetylene as Innovative Parameters

Author(s): Nam, MK (Nam, Min-Kyung); Lee, HC (Lee, Hyo-Chang); Hong, YJ (Hong, Young Joon); Jang, JY (Jang, Ja-Young); Choi, EH (Choi, Eun Ha); Chung, CW (Chung, Chin-Wook); Jeon, S (Jeon, Seongho); Kim, JM (Kim, Jong-Man); Kang, S (Kang, Seongman); Rhim, H (Rhim, Hyangshuk)

Source: JOURNAL OF BIOMEDICAL NANOTECHNOLOGY **Volume:** 13 **Issue:** 1 **Pages:** 77-83 **DOI:** 10.1166/jbn.2017.2311 **Published:** JAN 2017

Accession Number: WOS:000396466900007

PubMed ID: 29372998

Author Identifiers:

Author	ResearcherID Number	ORCID Number
Lee, Hyo-Chang		0000-0003-2754-1512

ISSN: 1550-7033

eISSN: 1550-7041

Record 6 of 15

Title: Biological effects of bacterial pigment undecylprodigiosin on human blood cells treated with atmospheric gas plasma in vitro

Author(s): Lazovic, S (Lazovic, Sasa); Leskovac, A (Leskovac, Andreja); Petrovic, S (Petrovic, Sandra); Senerovic, L (Senerovic, Lidija); Krivokapic, N (Krivokapic, Nevena); Mitrovic, T (Mitrovic, Tatjana); Bozovic, N (Bozovic, Nikola); Vasic, V (Vasic, Vesna); Nikodinovic-Runic, J (Nikodinovic-Runic, Jasmina)

Source: EXPERIMENTAL AND TOXICOLOGIC PATHOLOGY **Volume:** 69 **Issue:** 1 **Pages:** 55-62 **DOI:** 10.1016/j.etp.2016.11.003 **Published:** JAN 2017
Accession Number: WOS:000390968000007
PubMed ID: 27843060
Author Identifiers:

Author	ResearcherID Number	ORCID Number
Nikodinovic-Runic, Jasmina	W-1277-2018	0000-0002-2553-977X
Lazovic, Sasa	Q-5056-2016	0000-0003-1696-9134
Senerovic, Lidija		0000-0002-6965-9407
Leskovac, Andreja		0000-0002-6293-5237
Petrovic, Sandra		0000-0003-0930-6455
Vasic, Vesna		0000-0003-1268-2363

ISSN: 0940-2993
eISSN: 1618-1433

Record 7 of 15
Title: Microplasma Induced Cell Morphological Changes and Apoptosis of Ex Vivo Cultured Human Anterior Lens Epithelial Cells - Relevance to Capsular Opacification
Author(s): Recek, N (Recek, Nina); Andjelic, S (Andjelic, Sofija); Hojnik, N (Hojnik, Nataga); Filipic, G (Filipic, Gregor); Lazovic, S (Lazovic, Sasa); Vesel, A (Vesel, Alenka); Primc, G (Primc, Gregor); Mozetic, M (Mozetic, Miran); Hawlina, M (Hawlina, Marko); Petrovski, G (Petrovski, Goran); Cvelbar, U (Cvelbar, Uros)
Source: PLOS ONE **Volume:** 11 **Issue:** 11 **Article Number:** e0165883 **DOI:** 10.1371/journal.pone.0165883 **Published:** NOV 10 2016
Accession Number: WOS:000387725000038
PubMed ID: 27832099
Author Identifiers:

Author	ResearcherID Number	ORCID Number
Filipic, Gregor	T-4900-2018	0000-0003-0153-5181
Lazovic, Sasa	Q-5056-2016	0000-0003-1696-9134

ISSN: 1932-6203

Record 8 of 15
Title: Metastable helium atom density in a single electrode atmospheric plasma jet during sample treatment
Author(s): Zaplotnik, R (Zaplotnik, R.); Biscan, M (Biscan, M.); Popovic, D (Popovic, D.); Mozetic, M (Mozetic, M.); Milosevic, S (Milosevic, S.)
Source: PLASMA SOURCES SCIENCE & TECHNOLOGY **Volume:** 25 **Issue:** 3 **Article Number:** 035023 **DOI:** 10.1088/0963-0252/25/3/035023 **Published:** JUN 2016
Accession Number: WOS:000376557400031
Author Identifiers:

Author	ResearcherID Number	ORCID Number
Milosevic, Slobodan	A-3408-2010	
Milosevic, Slobodan		0000-0002-4455-7869

ISSN: 0963-0252

eISSN: 1361-6595

Record 9 of 15

Title: Size of silver nanoparticles determines proliferation ability of human circulating lymphocytes in vitro

Author(s): Joksic, G (Joksic, Gordana); Stasic, J (Stasic, Jelena); Filipovic, J (Filipovic, Jelena); Sobot, AV (Sobot, Ana Valenta); Trtica, M (Trtica, Milan)

Source: TOXICOLOGY LETTERS **Volume:** 247 **Pages:** 29-34 **DOI:** 10.1016/j.toxlet.2016.02.007 **Published:** APR 15 2016

Accession Number: WOS:000372432600003

PubMed ID: 26892717

Author Identifiers:

Author	ResearcherID Number	ORCID Number
Joksic, Gordana		0000-0002-7186-301X
Valenta Sobot, Ana		0000-0002-8429-1399
Filipovic Trickovic, Jelena		0000-0001-5450-0842
Trtica, Milan		0000-0001-7157-4907

ISSN: 0378-4274

eISSN: 1879-3169

Record 10 of 15

Title: Use of molecular beacons for the rapid analysis of DNA damage induced by exposure to an atmospheric pressure plasma jet

Author(s): Kurita, H (Kurita, Hirofumi); Miyachika, S (Miyachika, Saki); Yasuda, H (Yasuda, Hachiro); Takashima, K (Takashima, Kazunori); Mizuno, A (Mizuno, Akira)

Source: APPLIED PHYSICS LETTERS **Volume:** 107 **Issue:** 26 **Article Number:** 263702 **DOI:** 10.1063/1.4939044 **Published:** DEC 28 2015

Accession Number: WOS:000368442300042

Author Identifiers:

Author	ResearcherID Number	ORCID Number
Kurita, Hirofumi		0000-0002-2538-6590

ISSN: 0003-6951

eISSN: 1077-3118

Record 11 of 15

Title: Practical and theoretical considerations on the use of ICCD imaging for the characterization of non-equilibrium plasmas

Author(s): Gherardi, M (Gherardi, Matteo); Puac, N (Puac, Nevena); Maric, D (Maric, Dragana); Stancampiano, A (Stancampiano, Augusto); Malovic, G (Malovic, Gordana); Colombo, V (Colombo, Vittorio); Petrovic, ZL (Petrovic, Zoran Lj)

Source: PLASMA SOURCES SCIENCE & TECHNOLOGY **Volume:** 24 **Issue:** 6 **Article Number:** 064004 **DOI:** 10.1088/0963-0252/24/6/064004 **Published:** DEC 2015

Accession Number: WOS:000368117100005

Author Identifiers:

Author	ResearcherID Number	ORCID Number
Maric, Dragana		0000-0002-1728-5458
Malovic, Gordana		0000-0003-2356-0652
COLOMBO, VITTORIO		0000-0001-9145-198X
Petrovic, Zoran		0000-0001-6569-9447
Puac, Nevena		0000-0003-1142-8494

ISSN: 0963-0252

eISSN: 1361-6595

Record 12 of 15

Title: Atmospheric pressure argon surface discharges propagated in long tubes: physical characterization and application to bio-decontamination

Author(s): Kovalova, Z (Kovalova, Zuzana); Leroy, M (Leroy, Magali); Jacobs, C (Jacobs, Carolyn); Kirkpatrick, MJ (Kirkpatrick, Michael J.); Machala, Z (Machala, Zdenko); Lopes, F (Lopes, Filipa); Laux, CO (Laux, Christophe O.); DuBow, MS (DuBow, Michael S.); Odic, E (Odic, Emmanuel)

Source: JOURNAL OF PHYSICS D-APPLIED PHYSICS **Volume:** 48 **Issue:** 46 **Article Number:** 464003 **DOI:** 10.1088/0022-3727/48/46/464003 **Published:** NOV 25 2015

Accession Number: WOS:000367087600005

Author Identifiers:

Author	ResearcherID Number	ORCID Number
Machala, Zdenko	B-6384-2018	0000-0003-1424-1350
Jacobs, Carolyn		0000-0003-1285-7629

ISSN: 0022-3727

eISSN: 1361-6463

Record 13 of 15

Title: Effects of non-thermal plasma on the electrical properties of an erythrocyte membrane

Author(s): Lee, JY (Lee, Jin Young); Baik, KY (Baik, Ku Youn); Kim, TS (Kim, Tae Soo); Lim, J (Lim, Jaekwan); Uhm, HS (Uhm, Han S.); Choi, EH (Choi, Eun Ha)

Source: APPLIED PHYSICS LETTERS **Volume:** 107 **Issue:** 11 **Article Number:** 113701 **DOI:** 10.1063/1.4930872 **Published:** SEP 14 2015

Accession Number: WOS:000361639200058

ISSN: 0003-6951

eISSN: 1077-3118

Record 14 of 15

Title: Effects of air transient spark discharge and helium plasma jet on water, bacteria, cells, and biomolecules

Author(s): Hensel, K (Hensel, Karol); Kucerova, K (Kucerova, Katarina); Tarabova, B (Tarabova, Barbora); Janda, M (Janda, Mario); Machala, Z (Machala, Zdenko); Sano, K (Sano, Kaori); Mihai, CT (Mihai, Cosmin Teodor); Ciorpac, M (Ciorpac, Mitica); Gorgan, LD (Gorgan, Lucian Dragos); Jijie, R (Jijie, Roxana); Pohoata, V (Pohoata, Valentin); Topala, I (Topala, Ionut)

Source: BIOINTERPHASES **Volume:** 10 **Issue:** 2 **Article Number:** 029515 **DOI:** 10.1116/1.4919559 **Published:** JUN 2015

Accession Number: WOS:000357195600033

PubMed ID: 25947389

Author Identifiers:

Author	ResearcherID Number	ORCID Number
Machala, Zdenko	B-6384-2018	0000-0003-1424-1350
Ciorpac, Mitica	C-7790-2015	0000-0001-5374-0908
Mihai, Cosmin-Teodor	F-7815-2011	0000-0002-0945-5437
Tarabova, Barbora	I-7953-2018	0000-0001-9936-1786
Topala, Ionut	A-2305-2009	0000-0002-8954-8106
Janda, Mario	G-5864-2018	0000-0001-9051-4221
Pohoata, Valentin	R-1354-2017	0000-0001-5554-0088
Hensel, Karol	G-5851-2018	0000-0001-6833-681X
Gorgan, Lucian	B-5701-2012	0000-0001-6454-9092
Jijie, Roxana		0000-0003-0354-943X

ISSN: 1934-8630

eISSN: 1559-4106

Record 15 of 15

Title: Effects of Atmospheric Pressure Plasmas on Isolated and Cellular DNA-A Review

Author(s): Arjunan, KP (Arjunan, Krishna Priya); Sharma, VK (Sharma, Virender K.); Ptasinska, S (Ptasinska, Sylwia)

Source: INTERNATIONAL JOURNAL OF MOLECULAR SCIENCES **Volume:** 16 **Issue:** 2 **Pages:** 2971-3016 **DOI:** 10.3390/ijms16022971 **Published:** FEB 2015

Accession Number: WOS:000350333600041

PubMed ID: 25642755

Author Identifiers:

Author	ResearcherID Number	ORCID Number
Sharma, Virender		0000-0002-5980-8675

ISSN: 1422-0067

Close

Page 1 (Records 1 -- 15)

[1]

Print

Clarivate

Accelerating innovation

Close

Web of Science
Page 1 (Records 1 -- 10)
[1]

Print

Record 1 of 10

Title: Enhanced photocatalytic activity of V2O5 nanorods for the photodegradation of organic dyes: A detailed understanding of the mechanism and their antibacterial activity

Author(s): Jayaraj, SK (Jayaraj, Santhosh Kumar); Sadishkumar, V (Sadishkumar, Vishwanathan); Arun, T (Arun, Thirumurugan); Thangadurai, P (Thangadurai, Paramasivam)

Source: MATERIALS SCIENCE IN SEMICONDUCTOR PROCESSING **Volume:** 85 **Pages:** 122-133 **DOI:** 10.1016/j.mssp.2018.06.006 **Published:** OCT 2018

Accession Number: WOS:000436649200016

Author Identifiers:

Author	ResearcherID Number	ORCID Number
Thirumurugan, Arun		0000-0001-7261-988X

ISSN: 1369-8001

eISSN: 1873-4081

Record 2 of 10

Title: Optimization of a nanoparticle ball milling process parameters using the response surface method

Author(s): Petrovic, S (Petrovic, Srdjan); Rozic, L (Rozic, Ljiljana); Jovic, V (Jovic, Vesna); Stojadinovic, S (Stojadinovic, Stevan); Grbic, B (Grbic, Bosko); Radic, N (Radic, Nenad); Lamovec, J (Lamovec, Jelena); Vasilic, R (Vasilic, Rastko)

Source: ADVANCED POWDER TECHNOLOGY **Volume:** 29 **Issue:** 9 **Pages:** 2129-2139 **DOI:** 10.1016/j.apt.2018.05.021 **Published:** SEP 2018

Accession Number: WOS:000437308300018

Author Identifiers:

Author	ResearcherID Number	ORCID Number
Vasilic, Rastko		0000-0003-2476-7516

ISSN: 0921-8831

eISSN: 1568-5527

Record 3 of 10

Title: Narrowing band gap energy of defective black TiO2 fabricated by solution plasma process and its photocatalytic activity on glycerol transformation

Author(s): Jedsukontorn, T (Jedsukontorn, Trin); Ueno, T (Ueno, Tomonaga); Saito, N (Saito, Nagahiro); Hunsom, M (Hunsom, Mali)

Source: JOURNAL OF ALLOYS AND COMPOUNDS **Volume:** 757 **Pages:** 188-199 **DOI:** 10.1016/j.jallcom.2018.05.046 **Published:** AUG 15 2018

Accession Number: WOS:000433609100024

Author Identifiers:

Author	ResearcherID Number	ORCID Number
Ueno, Tomonaga	I-6111-2014	0000-0002-5345-7958

ISSN: 0925-8388

eISSN: 1873-4669

Record 4 of 10

Title: Enhanced photocatalytic hydrogen production of AgMO3 (M = Ta, Nb, V) perovskite materials using CdS and NiO as co-catalysts

Author(s): Carrasco-Jaim, OA (Carrasco-Jaim, Omar A.); Torres-Martinez, LM (Torres-Martinez, Leticia M.); Moctezuma, E (Moctezuma, Edgar)

Source: JOURNAL OF PHOTOCHEMISTRY AND PHOTOBIOLOGY A-CHEMISTRY **Volume:** 358 **Pages:** 167-176 **DOI:** 10.1016/j.jphotochem.2018.03.021 **Published:** MAY 1 2018

Accession Number: WOS:000430883200019

Author Identifiers:

Author	ResearcherID Number	ORCID Number
UANL, FIC-UANL	O-5444-2015	

ISSN: 1010-6030

Record 5 of 10

Title: Investigation of amino-grafted TiO2/reduced graphene oxide hybrids as a novel photocatalyst used for decomposition of selected organic dyes

Author(s): Siwinska-Stefanska, K (Siwinska-Stefanska, Katarzyna); Fluder, M (Fluder, Monika); Tylus, W (Tylus, Wlodzimierz); Jesionowski, T (Jesionowski, Teofil)

Source: JOURNAL OF ENVIRONMENTAL MANAGEMENT **Volume:** 212 **Pages:** 395-404 **DOI:** 10.1016/j.jenvman.2018.02.030 **Published:** APR 15 2018

Accession Number: WOS:000428097500042

PubMed ID: 29455147

Author Identifiers:

Author	ResearcherID Number	ORCID Number
Jesionowski, Teofil	N-1623-2014	
Tylus, Wlodzimierz	I-9225-2018	0000-0001-6780-5100

ISSN: 0301-4797

eISSN: 1095-8630

Record 6 of 10

Title: Cr2O3 nanoparticle-functionalized WO3 nanorods for ethanol gas sensors

Author(s): Choi, S (Choi, Seungbok); Bonyani, M (Bonyani, Maryam); Sun, GJ (Sun, Gun-Joo); Lee, JK (Lee, Jae Kyung); Hyun, SK (Hyun, Soong Keun); Lee, C (Lee,

Chongmu)

Source: APPLIED SURFACE SCIENCE **Volume:** 432 **Pages:** 241-249 **DOI:** 10.1016/j.apsusc.2017.01.245 **Part:** B **Published:** FEB 28 2018

Accession Number: WOS:000416967800028

Conference Title: 20th International Vacuum Congress (IVC)

Conference Date: AUG 21-26, 2016

Conference Location: Busan, SOUTH KOREA

Author Identifiers:

Author	ResearcherID Number	ORCID Number
choi, seungbok		0000-0001-6262-2815

ISSN: 0169-4332

eISSN: 1873-5584

Record 7 of 10

Title: Photocatalytic degradation of sixteen organic dyes by TiO2/WO3-coated magnetic nanoparticles under simulated visible light and solar light

Author(s): Liu, HL (Liu, Hualong); Guo, W (Guo, Wang); Li, YR (Li, Yarong); He, SS (He, Shasha); He, CY (He, Chiyang)

Source: JOURNAL OF ENVIRONMENTAL CHEMICAL ENGINEERING **Volume:** 6 **Issue:** 1 **Pages:** 59-67 **DOI:** 10.1016/j.jece.2017.11.063 **Published:** FEB 2018

Accession Number: WOS:000434777800009

ISSN: 2213-3437

Record 8 of 10

Title: Two-step hydrothermally synthesized carbon nanodots/WO3 photocatalysts with enhanced photocatalytic performance

Author(s): Song, B (Song, Bo); Wang, TT (Wang, Tingting); Sun, HG (Sun, Honggang); Shao, Q (Shao, Qian); Zhao, JK (Zhao, Junkai); Song, KK (Song, Kaikai); Hao, LH (Hao, Luhan); Wang, L (Wang, Li); Guo, ZH (Guo, Zhanhu)

Source: DALTON TRANSACTIONS **Volume:** 46 **Issue:** 45 **Pages:** 15769-15777 **DOI:** 10.1039/c7dt03003g **Published:** DEC 7 2017

Accession Number: WOS:000415989000021

PubMed ID: 29098216

Author Identifiers:

Author	ResearcherID Number	ORCID Number
song, kaikai	G-5908-2011	
Guo, Zhanhu		0000-0003-0134-0210

ISSN: 1477-9226

eISSN: 1477-9234

Record 9 of 10

Title: Photocatalytic removal of gaseous nitrogen oxides using WO3/TiO2 particles under visible light irradiation: Effect of surface modification
Author(s): Mendoza, JA (Mendoza, Joseph Albert); Lee, DH (Lee, Dong Hoon); Kang, JH (Kang, Joo-Hyon)
Source: CHEMOSPHERE **Volume:** 182 **Pages:** 539-546 **DOI:** 10.1016/j.chemosphere.2017.05.069 **Published:** SEP 2017
Accession Number: WOS:000403991700065
PubMed ID: 28521170
Author Identifiers:

Author	ResearcherID Number	ORCID Number
Mendoza, Joseph Albert	Q-8527-2018	0000-0002-2576-3632

ISSN: 0045-6535
eISSN: 1879-1298

Record 10 of 10
Title: Study of Thermal Conductivity of Nanoporous Anodic Alumina Layer Formed in Sulphuric Acid Using Steady-State Heat Flow Technique
Author(s): Andreev, S (Andreev, Svetozar); Chernyakova, K (Chernyakova, Katsiaryna); Tzaneva, B (Tzaneva, Boriana); Videkov, V (Videkov, Valentin); Vrublevsky, I (Vrublevsky, Igor)
Book Group Author(s): IEEE
Source: 2017 XXVI INTERNATIONAL SCIENTIFIC CONFERENCE ELECTRONICS (ET) **Published:** 2017
Accession Number: WOS:000425865800002
Conference Title: 26th International Scientific Conference on Electronics (ET)
Conference Date: SEP 13-15, 2017
Conference Location: Sozopol, BULGARIA
ISBN: 978-1-5386-1753-3

Close

Web of Science
Page 1 (Records 1 -- 10)
◀ [1] ▶

Print

Close

Web of Science
Page 1 (Records 1 -- 10)
[1]

Print

Record 1 of 10

Title: Destruction of chemical warfare surrogates using a portable atmospheric pressure plasma jet

Author(s): Skoro, N (Skoro, Nikola); Puac, N (Puac, Nevena); Zivkovic, S (Zivkovic, Suzana); Krstic-Milosevic, D (Krstic-Milosevic, Dijana); Cvelbar, U (Cvelbar, Uros); Malovic, G (Malovic, Gordana); Petrovic, ZL (Petrovic, Zoran Lj.)

Source: EUROPEAN PHYSICAL JOURNAL D **Volume:** 72 **Issue:** 1 **Article Number:** 2 **DOI:** 10.1140/epjd/e2017-80329-9 **Published:** JAN 16 2018

Accession Number: WOS:000422899000001

Author Identifiers:

Author	ResearcherID Number	ORCID Number
Puac, Nevena		0000-0003-1142-8494
Cvelbar, Uros		0000-0002-1957-0789
Petrovic, Zoran		0000-0001-6569-9447
Skoro, Nikola		0000-0002-0254-8008

ISSN: 1434-6060

eISSN: 1434-6079

Record 2 of 10

Title: Roles of membrane protein damage and intracellular protein damage in death of bacteria induced by atmospheric-pressure air discharge plasmas

Author(s): Zhang, H (Zhang, Hao); Ma, J (Ma, Jie); Shen, J (Shen, Jie); Lan, Y (Lan, Yan); Ding, LL (Ding, Lili); Qian, SL (Qian, Shulou); Xia, WD (Xia, Weidong); Cheng, C (Cheng, Cheng); Chu, PK (Chu, Paul K.)

Source: RSC ADVANCES **Volume:** 8 **Issue:** 38 **Pages:** 21139-21149 **DOI:** 10.1039/c8ra01882k **Published:** 2018

Accession Number: WOS:000435576500009

Author Identifiers:

Author	ResearcherID Number	ORCID Number
Chu, Paul	B-5923-2013	0000-0002-5581-4883
Cheng, Cheng		0000-0002-5007-4695

ISSN: 2046-2069

Record 3 of 10

Title: Analysis of reactive oxygen and nitrogen species generated in three liquid media by low temperature helium plasma jet

Author(s): Chauvin, J (Chauvin, Julie); Judee, F (Judee, Florian); Yousfi, M (Yousfi, Mohammed); Vicendo, P (Vicendo, Patricia); Merbahi, N (Merbahi, Nofel)

Source: SCIENTIFIC REPORTS **Volume:** 7 **Article Number:** 4562 **DOI:** 10.1038/s41598-017-04650-4 **Published:** JUL 4 2017

Accession Number: WOS:000425965100003
PubMed ID: 28676723
ISSN: 2045-2322

Record 4 of 10
Title: Mass spectrometry of diffuse coplanar surface barrier discharge: influence of discharge frequency and oxygen content in N-2/O-2 mixture
Author(s): Cech, J (Cech, Jan); Brablec, A (Brablec, Antonin); Cernak, M (Cernak, Mirko); Puac, N (Puac, Nevena); Selakovic, N (Selakovic, Nenad); Petrovic, ZL (Petrovic, Zoran Lj.)
Source: EUROPEAN PHYSICAL JOURNAL D **Volume:** 71 **Issue:** 2 **Article Number:** 27 **DOI:** 10.1140/epjd/e2016-70607-5 **Published:** FEB 9 2017
Accession Number: WOS:000403477900003
Author Identifiers:

Author	ResearcherID Number	ORCID Number
Cech, Jan	F-8310-2017	0000-0002-4900-6011

ISSN: 1434-6060
eISSN: 1434-6079

Record 5 of 10
Title: Biological effects of bacterial pigment undecylprodigiosin on human blood cells treated with atmospheric gas plasma in vitro
Author(s): Lazovic, S (Lazovic, Sasa); Leskovac, A (Leskovac, Andreja); Petrovic, S (Petrovic, Sandra); Senerovic, L (Senerovic, Lidija); Krivokapic, N (Krivokapic, Nevena); Mitrovic, T (Mitrovic, Tatjana); Bozovic, N (Bozovic, Nikola); Vasic, V (Vasic, Vesna); Nikodinovic-Runic, J (Nikodinovic-Runic, Jasmina)
Source: EXPERIMENTAL AND TOXICOLOGIC PATHOLOGY **Volume:** 69 **Issue:** 1 **Pages:** 55-62 **DOI:** 10.1016/j.etp.2016.11.003 **Published:** JAN 2017
Accession Number: WOS:000390968000007
PubMed ID: 27843060
Author Identifiers:

Author	ResearcherID Number	ORCID Number
Nikodinovic-Runic, Jasmina	W-1277-2018	0000-0002-2553-977X
Lazovic, Sasa	Q-5056-2016	0000-0003-1696-9134
Senerovic, Lidija		0000-0002-6965-9407
Leskovac, Andreja		0000-0002-6293-5237
Petrovic, Sandra		0000-0003-0930-6455
Vasic, Vesna		0000-0003-1268-2363

ISSN: 0940-2993
eISSN: 1618-1433

Record 6 of 10

Title: OH radical production in an atmospheric pressure surface micro-discharge array
Author(s): Li, D (Li, D.); Nikiforov, A (Nikiforov, A.); Britun, N (Britun, N.); Snyders, R (Snyders, R.); Kong, MG (Kong, M. G.); Leys, C (Leys, C.)
Source: JOURNAL OF PHYSICS D-APPLIED PHYSICS **Volume:** 49 **Issue:** 45 **Article Number:** 455202 **DOI:** 10.1088/0022-3727/49/45/455202 **Published:** NOV 16 2016
Accession Number: WOS:000386489700002
ISSN: 0022-3727
eISSN: 1361-6463

Record 7 of 10
Title: Single-electrode He microplasma jets driven by nanosecond voltage pulses
Author(s): Jiang, C (Jiang, C.); Lane, J (Lane, J.); Song, ST (Song, S. T.); Pendelton, SJ (Pendelton, S. J.); Wu, Y (Wu, Y.); Sozer, E (Sozer, E.); Kuthi, A (Kuthi, A.); Gundersen, MA (Gundersen, M. A.)
Source: JOURNAL OF APPLIED PHYSICS **Volume:** 119 **Issue:** 8 **Article Number:** 083301 **DOI:** 10.1063/1.4942624 **Published:** FEB 28 2016
Accession Number: WOS:000371601800009
Author Identifiers:

Author	ResearcherID Number	ORCID Number
Sozer, Esin		0000-0002-6244-3670

ISSN: 0021-8979
eISSN: 1089-7550

Record 8 of 10
Title: Use of molecular beacons for the rapid analysis of DNA damage induced by exposure to an atmospheric pressure plasma jet
Author(s): Kurita, H (Kurita, Hirofumi); Miyachika, S (Miyachika, Saki); Yasuda, H (Yasuda, Hachiro); Takashima, K (Takashima, Kazunori); Mizuno, A (Mizuno, Akira)
Source: APPLIED PHYSICS LETTERS **Volume:** 107 **Issue:** 26 **Article Number:** 263702 **DOI:** 10.1063/1.4939044 **Published:** DEC 28 2015
Accession Number: WOS:000368442300042
Author Identifiers:

Author	ResearcherID Number	ORCID Number
Kurita, Hirofumi		0000-0002-2538-6590

ISSN: 0003-6951
eISSN: 1077-3118

Record 9 of 10
Title: Study of Cold Atmospheric Plasma Jet at the End of Flexible Plastic Tube for Microbial Decontamination
Author(s): Kostov, KG (Kostov, Konstantin G.); Nishime, TMC (Nishime, Thalita M. C.); Machida, M (Machida, Munemasa); Borges, AC (Borges, Aline C.); Prysiazhnyi, V (Prysiazhnyi, Vadym); Koga-Ito, CY (Koga-Ito, Cristiane Y.)

Source: PLASMA PROCESSES AND POLYMERS **Volume:** 12 **Issue:** 12 **Special Issue:** SI **Pages:** 1383-1391 **DOI:** 10.1002/ppap.201500125 **Published:** DEC 2015
Accession Number: WOS:000368449900009
Conference Title: 2nd International Workshop on Plasma for Cancer Treatment (IWPCT)
Conference Date: 2015
Conference Location: Nagoya Univ, Nagoya, JAPAN
Conference Host: Nagoya Univ

Author Identifiers:

Author	ResearcherID Number	ORCID Number
Nishime, Thalita	H-7372-2014	0000-0003-2844-3156
Prysiazhnyi, Vadym	D-2587-2013	0000-0001-7424-5949
Inst. of Physics, Gleb Wataghin	A-9780-2017	
Koga-Ito, Cristiane	D-7999-2012	0000-0002-2416-2173
Kostov, Konstantin	C-2666-2012	
Kostov, Konstantin		0000-0002-9821-8088

ISSN: 1612-8850
eISSN: 1612-8869

Record 10 of 10

Title: Research on plasma medicine-relevant plasma-liquid interaction: What happened in the past five years?
Author(s): Jablonowski, H (Jablonowski, Helena); von Woedtke, T (von Woedtke, Thomas)
Source: CLINICAL PLASMA MEDICINE **Volume:** 3 **Issue:** 2 **Pages:** 42-52 **DOI:** 10.1016/j.cpme.2015.11.003 **Published:** DEC 2015
Accession Number: WOS:000433743700002
ISSN: 2452-0896
eISSN: 2212-8166

Close

Web of Science
Page 1 (Records 1 -- 7)
[1]

Print

Record 1 of 7
Title: Electron beam irradiation impact on surface structure and wettability of ethylene-vinyl alcohol copolymer
Author(s): El-Saftawy, AA (El-Saftawy, A. A.); Ragheb, MS (Ragheb, M. S.); Zakhary, SG (Zakhary, S. G.)
Source: RADIATION PHYSICS AND CHEMISTRY **Volume:** 147 **Pages:** 106-113 **DOI:** 10.1016/j.radphyschem.2018.02.001 **Published:** JUN 2018
Accession Number: WOS:000429394100017
ISSN: 0969-806X

Record 2 of 7
Title: In vitro study of platelet behaviour on titanium surface modified by plasma
Author(s): Vitoriano, JO (Vitoriano, J. O.); Alves, C (Alves, C., Jr.); Braz, DC (Braz, D. C.); Rocha, HA (Rocha, H. A.); da Silva, RCL (Lima da Silva, R. C.)
Source: CIENCIA & TECNOLOGIA DOS MATERIAIS **Volume:** 29 **Issue:** 1 **Pages:** E130-E134 **DOI:** 10.1016/j.ctmat.2016.09.003 **Published:** JAN-APR 2017
Accession Number: WOS:000412098700025
Author Identifiers:

Author	ResearcherID Number	ORCID Number
Alves Junior, Clodomiro	B-7578-2009	0000-0002-5547-5922

ISSN: 0870-8312

Record 3 of 7
Title: Study on a hydrophobic Ti-doped hydroxyapatite coating for corrosion protection of a titanium based alloy
Author(s): Surmeneva, MA (Surmeneva, M. A.); Vladescu, A (Vladescu, A.); Surmenev, RA (Surmenev, R. A.); Pantilimon, CM (Pantilimon, C. M.); Braic, M (Braic, M.); Cotrut, CM (Cotrut, C. M.)
Source: RSC ADVANCES **Volume:** 6 **Issue:** 90 **Pages:** 87665-87674 **DOI:** 10.1039/c6ra03397k **Published:** 2016
Accession Number: WOS:000384232600106
Author Identifiers:

Author	ResearcherID Number	ORCID Number
Cotrut, Mihai Cosmin	G-4505-2011	0000-0002-8991-7485

ISSN: 2046-2069

Record 4 of 7
Title: Plasma treatment for next-generation nanobiointerfaces
Author(s): Levchenko, I (Levchenko, Igor); Keidar, M (Keidar, Michael); Mai-Prochnow, A (Mai-Prochnow, Anne); Modic, M (Modic, Martina); Cvelbar, U (Cvelbar, Uros);

Fang, JH (Fang, Jinghua); Ostrikov, K (Ostrikov, Kostya (Ken))

Source: BIOINTERPHASES **Volume:** 10 **Issue:** 2 **Article Number:** 029405 **DOI:** 10.1116/1.4922237 **Published:** JUN 2015

Accession Number: WOS:000357195600018

PubMed ID: 26104191

Author Identifiers:

Author	ResearcherID Number	ORCID Number
Mai-Prochnow, Anne	D-3954-2013	0000-0003-0136-9144
Ostrikov, Kostya (Ken)		0000-0001-8672-9297
Fang, Jinghua		0000-0002-2214-2902

ISSN: 1934-8630

eISSN: 1559-4106

Record 5 of 7

Title: Titanium nanostructures for biomedical applications

Author(s): Kulkarni, M (Kulkarni, M.); Mazare, A (Mazare, A.); Gongadze, E (Gongadze, E.); Perutkova, S (Perutkova, S.); Kralj-Iglic, V (Kralj-Iglic, V.); Milosev, I (Milosev, I.); Schmuki, P (Schmuki, P.); Iglic, A (Iglic, A.); Mozetic, M (Mozetic, M.)

Source: NANOTECHNOLOGY **Volume:** 26 **Issue:** 6 **Article Number:** 062002 **DOI:** 10.1088/0957-4484/26/6/062002 **Published:** FEB 13 2015

Accession Number: WOS:000348448000003

PubMed ID: 25611515

Author Identifiers:

Author	ResearcherID Number	ORCID Number
Mazare, Anca		0000-0002-4836-946X

ISSN: 0957-4484

eISSN: 1361-6528

Record 6 of 7

Title: Formation of Nanocones on Highly Oriented Pyrolytic Graphite by Oxygen Plasma

Author(s): Vesel, A (Vesel, Alenka); Elersic, K (Elersic, Kristina); Modic, M (Modic, Martina); Junkar, I (Junkar, Ita); Mozetic, M (Mozetic, Miran)

Source: MATERIALS **Volume:** 7 **Issue:** 3 **Pages:** 2014-2029 **DOI:** 10.3390/ma7032014 **Published:** MAR 2014

Accession Number: WOS:000336089500029

PubMed ID: 28788553

Author Identifiers:

Author	ResearcherID Number	ORCID Number

Mozetic, Miran	K-8784-2014	
Vesel, Alenka	I-3934-2014	0000-0003-3782-6001

ISSN: 1996-1944

Record 7 of 7

Title: Application of non-equilibrium plasmas in medicine

Author(s): Petrovic, ZL (Petrovic, Zoran Lj.); Puac, N (Puac, Nevena); Malovic, G (Malovic, Gordana); Lazovic, S (Lazovic, Sasa); Maletic, D (Maletic, Dejan); Miletic, M (Miletic, Maja); Mojsilovic, S (Mojsilovic, Slavko); Milenkovic, P (Milenkovic, Pavle); Bugarski, D (Bugarski, Diana)

Source: JOURNAL OF THE SERBIAN CHEMICAL SOCIETY **Volume:** 77 **Issue:** 12 **Pages:** 1689-1699 **DOI:** 10.2298/JSC121020142P **Published:** 2012

Accession Number: WOS:000314080000002

Author Identifiers:

Author	ResearcherID Number	ORCID Number
Lazovic, Sasa	B-9651-2013	0000-0003-1696-9134
Lazovic, Sasa	Q-5056-2016	0000-0003-1696-9134
Petrovic, Zoran		0000-0001-6569-9447
Puac, Nevena		0000-0003-1142-8494
Malovic, Gordana		0000-0003-2356-0652

ISSN: 0352-5139

Close

Web of Science
Page 1 (Records 1 -- 7)
[1]

Print

Close

Web of Science
Page 1 (Records 1 -- 7)
[1]

Print

Record 1 of 7

Title: The influence of electrode configuration on light emission profiles and electrical characteristics of an atmospheric-pressure plasma jet

Author(s): Maletic, D (Maletic, Dejan); Puac, N (Puac, Nevena); Malovic, G (Malovic, Gordana); Dordevic, A (Dordevic, Antonije); Petrovic, ZL (Petrovic, Zoran Lj)

Source: JOURNAL OF PHYSICS D-APPLIED PHYSICS **Volume:** 50 **Issue:** 14 **Article Number:** 145202 **DOI:** 10.1088/1361-6463/aa5d91 **Published:** APR 12 2017

Accession Number: WOS:000404428200002

Author Identifiers:

Author	ResearcherID Number	ORCID Number
Puac, Nevena		0000-0003-1142-8494
Petrovic, Zoran		0000-0001-6569-9447
Malovic, Gordana		0000-0003-2356-0652

ISSN: 0022-3727

eISSN: 1361-6463

Record 2 of 7

Title: Biological effects of bacterial pigment undecylprodigiosin on human blood cells treated with atmospheric gas plasma in vitro

Author(s): Lazovic, S (Lazovic, Sasa); Leskovac, A (Leskovac, Andreja); Petrovic, S (Petrovic, Sandra); Senerovic, L (Senerovic, Lidija); Krivokapic, N (Krivokapic, Nevena); Mitrovic, T (Mitrovic, Tatjana); Bozovic, N (Bozovic, Nikola); Vasic, V (Vasic, Vesna); Nikodinovic-Runic, J (Nikodinovic-Runic, Jasmina)

Source: EXPERIMENTAL AND TOXICOLOGIC PATHOLOGY **Volume:** 69 **Issue:** 1 **Pages:** 55-62 **DOI:** 10.1016/j.etp.2016.11.003 **Published:** JAN 2017

Accession Number: WOS:000390968000007

PubMed ID: 27843060

Author Identifiers:

Author	ResearcherID Number	ORCID Number
Nikodinovic-Runic, Jasmina	W-1277-2018	0000-0002-2553-977X
Lazovic, Sasa	Q-5056-2016	0000-0003-1696-9134
Senerovic, Lidija		0000-0002-6965-9407
Leskovac, Andreja		0000-0002-6293-5237
Petrovic, Sandra		0000-0003-0930-6455
Vasic, Vesna		0000-0003-1268-2363

ISSN: 0940-2993

eISSN: 1618-1433

Record 3 of 7

Title: Inhibition of methicillin resistant Staphylococcus aureus by a plasma needle

Author(s): Miletic, M (Miletic, Maja); Vukovic, D (Vukovic, Dragana); Zivanovic, I (Zivanovic, Irena); Dakic, I (Dakic, Ivana); Soldatovic, I (Soldatovic, Ivan); Maletic, D (Maletic, Dejan); Lazovic, S (Lazovic, Sasa); Malovic, G (Malovic, Gordana); Petrovic, ZL (Petrovic, Zoran Lj); Puac, N (Puac, Nevena)

Source: CENTRAL EUROPEAN JOURNAL OF PHYSICS **Volume:** 12 **Issue:** 3 **Pages:** 160-167 **DOI:** 10.2478/s11534-014-0437-z **Published:** MAR 2014

Accession Number: WOS:000333023800002

Author Identifiers:

Author	ResearcherID Number	ORCID Number
Lazovic, Sasa	Q-5056-2016	0000-0003-1696-9134
Malovic, Gordana		0000-0003-2356-0652
Petrovic, Zoran		0000-0001-6569-9447
Puac, Nevena		0000-0003-1142-8494
Soldatovic, Ivan		0000-0003-4893-1683

ISSN: 1895-1082

eISSN: 1644-3608

Record 4 of 7

Title: Low Temperature Plasma: A Novel Focal Therapy for Localized Prostate Cancer?

Author(s): Hirst, AM (Hirst, Adam M.); Frame, FM (Frame, Fiona M.); Maitland, NJ (Maitland, Norman J.); O'Connell, D (O'Connell, Deborah)

Source: BIOMED RESEARCH INTERNATIONAL **Article Number:** 878319 **DOI:** 10.1155/2014/878319 **Published:** 2014

Accession Number: WOS:000333309000001

PubMed ID: 24738076

Author Identifiers:

Author	ResearcherID Number	ORCID Number
O'Connell, Deborah	D-7967-2018	0000-0002-1457-9004
Maitland, Norman		0000-0003-1607-9035

ISSN: 2314-6133

eISSN: 2314-6141

Record 5 of 7

Title: Plasma properties in a large-volume, cylindrical and asymmetric radio-frequency capacitively coupled industrial-prototype reactor

Author(s): Lazovic, S (Lazovic, Sasa); Puac, N (Puac, Nevena); Spasic, K (Spasic, Kosta); Malovic, G (Malovic, Gordana); Cvelbar, U (Cvelbar, Uros); Mozetic, M (Mozetic, Miran); Radetic, M (Radetic, Maja); Petrovic, ZL (Petrovic, Zoran Lj)

Source: JOURNAL OF PHYSICS D-APPLIED PHYSICS **Volume:** 46 **Issue:** 7 **Article Number:** 075201 **DOI:** 10.1088/0022-3727/46/7/075201 **Published:** FEB 20 2013

Accession Number: WOS:000314471900014

Author Identifiers:

Author	ResearcherID Number	ORCID Number
Lazovic, Sasa	Q-5056-2016	0000-0003-1696-9134
Mozetic, Miran	K-8784-2014	
Lazovic, Sasa	B-9651-2013	0000-0003-1696-9134
Puac, Nevena		0000-0003-1142-8494
Malovic, Gordana		0000-0003-2356-0652
Petrovic, Zoran		0000-0001-6569-9447

ISSN: 0022-3727

Record 6 of 7

Title: Application of non-equilibrium plasmas in medicine

Author(s): Petrovic, ZL (Petrovic, Zoran Lj.); Puac, N (Puac, Nevena); Malovic, G (Malovic, Gordana); Lazovic, S (Lazovic, Sasa); Maletic, D (Maletic, Dejan); Miletic, M (Miletic, Maja); Mojsilovic, S (Mojsilovic, Slavko); Milenkovic, P (Milenkovic, Pavle); Bugarski, D (Bugarski, Diana)

Source: JOURNAL OF THE SERBIAN CHEMICAL SOCIETY **Volume:** 77 **Issue:** 12 **Pages:** 1689-1699 **DOI:** 10.2298/JSC121020142P **Published:** 2012

Accession Number: WOS:000314080000002

Author Identifiers:

Author	ResearcherID Number	ORCID Number
Lazovic, Sasa	B-9651-2013	0000-0003-1696-9134
Lazovic, Sasa	Q-5056-2016	0000-0003-1696-9134
Petrovic, Zoran		0000-0001-6569-9447
Puac, Nevena		0000-0003-1142-8494
Malovic, Gordana		0000-0003-2356-0652

ISSN: 0352-5139

Record 7 of 7

Title: Diagnostics and biomedical applications of radiofrequency plasmas

Author(s): Lazovic, S (Lazovic, Sasa)

Edited by: Kuraica M; Mijatovic Z

Source: 26TH SUMMER SCHOOL AND INTERNATIONAL SYMPOSIUM ON THE PHYSICS OF IONIZED GASES (SPIG 2012) **Book Series:** Journal of Physics Conference Series **Volume:** 399 **Article Number:** 012015 **DOI:** 10.1088/1742-6596/399/1/012015 **Published:** 2012

Accession Number: WOS:000312261700015

Conference Title: 26th Summer School and International Symposium on the Physics of Ionized Gases (SPIG)

Conference Date: AUG 27-31, 2012

Conference Location: Zrenjanin, SERBIA

Conference Sponsors: Sci & Technol Dev Republ Serbia, Minist Educ, Prov Secretariat Sci & Technol Dev, Inst Francais Serbie, Biser Zrenjanin

Author Identifiers:

Author	ResearcherID Number	ORCID Number
Lazovic, Sasa	Q-5056-2016	0000-0003-1696-9134
Lazovic, Sasa	B-9651-2013	0000-0003-1696-9134

ISSN: 1742-6588

Close

Web of Science
Page 1 (Records 1 -- 6)
[1]

Print

Record 1 of 6

Title: Coexistence of ferromagnetism and ferroelectricity in Mn-doped chromites YCr1-xMnxO3 single crystals

Author(s): Yin, LH (Yin, L. H.); Yang, J (Yang, J.); Tong, P (Tong, P.); Song, WH (Song, W. H.); Dai, JM (Dai, J. M.); Zhu, XB (Zhu, X. B.); Sun, YP (Sun, Y. P.)

Source: JOURNAL OF ALLOYS AND COMPOUNDS **Volume:** 771 **Pages:** 602-606 **DOI:** 10.1016/j.jallcom.2018.09.019 **Published:** JAN 15 2019

Accession Number: WOS:000449621500077

Author Identifiers:

Author	ResearcherID Number	ORCID Number
Yin, Lihua		0000-0002-6993-1140
Tong, Peng		0000-0003-3609-6190

ISSN: 0925-8388

eISSN: 1873-4669

Record 2 of 6

Title: Improving Magnetoelectric Contactless Sensing and Actuation through Anisotropic Nanostructures

Author(s): Fernandes, MM (Fernandes, M. M.); Mora, H (Mora, H.); Barriga-Castro, ED (Barriga-Castro, E. D.); Luna, C (Luna, C.); Mendoza-Resendez, R (Mendoza-Resendez, R.); Ribeiro, C (Ribeiro, C.); Lanceros-Mendez, S (Lanceros-Mendez, S.); Martins, P (Martins, P.)

Source: JOURNAL OF PHYSICAL CHEMISTRY C **Volume:** 122 **Issue:** 33 **Pages:** 19189-19196 **DOI:** 10.1021/acs.jpcc.8b04910 **Published:** AUG 23 2018

Accession Number: WOS:000442960300046

Author Identifiers:

Author	ResearcherID Number	ORCID Number
Ribeiro, Clarisse		0000-0002-9120-4847
Diaz Barriga Castro, Enrique		0000-0003-1971-4030

ISSN: 1932-7447

Record 3 of 6

Title: Optimized Magnetodielectric Coupling on High-Temperature Polymer-Based Nanocomposites

Author(s): Maceiras, A (Maceiras, A.); Marinho, T (Marinho, T.); Vilas, JL (Luis Vilas, Jose); Carbo-Argibay, E (Carbo-Argibay, Enrique); Kolen'ko, YV (Kolen'ko, Yury V.); Martins, P (Martins, P.); Lanceros-Mendez, S (Lanceros-Mendez, S.)

Source: JOURNAL OF PHYSICAL CHEMISTRY C **Volume:** 122 **Issue:** 3 **Pages:** 1821-1827 **DOI:** 10.1021/acs.jpcc.7b09395 **Published:** JAN 25 2018

Accession Number: WOS:000423652700042

Author Identifiers:

Author	ResearcherID Number	ORCID Number
Kolen'ko, Yury	P-5890-2015	0000-0001-7493-1762
Vilas, Jose Luis	L-7178-2015	0000-0002-0188-4579
Andre Rodrigues Marinho, Tiago		0000-0003-4885-5895
Martins, Pedro		0000-0002-9833-9648

ISSN: 1932-7447

Record 4 of 6

Title: Room temperature magnetoelectric coupling effect in CuFe2O4-BaTiO3 core-shell and nanocomposites

Author(s): Thankachan, RM (Thankachan, Rahul Mundiyaniyil); Raneesh, B (Raneesh, B.); Mayeen, A (Mayeen, Anshida); Karthika, S (Karthika, S.); Vivek, S (Vivek, S.); Nair, SS (Nair, Swapna S.); Thomas, S (Thomas, Sabu); Kalarikkal, N (Kalarikkal, Nandakumar)

Source: JOURNAL OF ALLOYS AND COMPOUNDS **Volume:** 731 **Pages:** 288-296 **DOI:** 10.1016/j.jallcom.2017.09.309 **Published:** JAN 15 2018

Accession Number: WOS:000415930900039

Author Identifiers:

Author	ResearcherID Number	ORCID Number
Thomas, Prof. Sabu	G-7310-2016	0000-0003-4726-5746

ISSN: 0925-8388

eISSN: 1873-4669

Record 5 of 6

Title: Interface Engineered Ferrite@Ferroelectric Core-Shell Nanostructures: A Facile Approach to Impart Superior Magneto-electric Coupling

Author(s): Abraham, AR (Abraham, Ann Rose); Raneesh, B (Raneesh, B.); Das, D (Das, Dipankar); Oluwafemi, OS (Oluwafemi, Oluwatobi Samuel); Thomas, S (Thomas, Sabu); Kalarikkal, N (Kalarikkal, Nandakumar)

Book Group Author(s): AIP

Source: 62ND DAE SOLID STATE PHYSICS SYMPOSIUM **Book Series:** AIP Conference Proceedings **Volume:** 1942 **Article Number:** UNSP 020002 **DOI:** 10.1063/1.5028581 **Published:** 2018

Accession Number: WOS:000433118300002

Conference Title: 62nd DAE Solid State Physics Symposium

Conference Date: DEC 26-30, 2017

Conference Location: Mumbai, INDIA

Conference Sponsors: Dept Atom Energy, Board Res Nucl Sci, Dept Atom Energy, Bhabha Atom Res Ctr

ISSN: 0094-243X

ISBN: 978-0-7354-1634-5

Record 6 of 6

Title: Growth Kinetics, Cation Occupancy, and Magnetic Properties of Multimetal Oxide Nanoparticles: A Case Study on Spinel NiFe2O4

Author(s): Wang, Y (Wang, Yan); Li, LP (Li, Liping); Zhang, YL (Zhang, Yuelan); Chen, XQ (Chen, Xianqun); Fang, SF (Fang, Shaofan); Li, GS (Li, Guangshe)

Source: JOURNAL OF PHYSICAL CHEMISTRY C **Volume:** 121 **Issue:** 35 **Pages:** 19467-19477 **DOI:** 10.1021/acs.jpcc.7b05607 **Published:** SEP 7 2017

Accession Number: WOS:000410597600058

ISSN: 1932-7447

Close

Web of Science
Page 1 (Records 1 -- 4)
[1]

Print

Record 1 of 4

Title: Electrical and optical characterization of an atmospheric pressure, uniform, large-area processing, dielectric barrier discharge

Author(s): Zeniou, A (Zeniou, A.); Puac, N (Puac, N.); Skoro, N (Skoro, N.); Selakovic, N (Selakovic, N.); Dimitrakellis, P (Dimitrakellis, P.); Gogolides, E (Gogolides, E.); Petrovic, ZL (Petrovic, Z. Lj)

Source: JOURNAL OF PHYSICS D-APPLIED PHYSICS **Volume:** 50 **Issue:** 13 **Article Number:** 135204 **DOI:** 10.1088/1361-6463/aa5d69 **Published:** APR 5 2017

Accession Number: WOS:000396058900002

Author Identifiers:

Author	ResearcherID Number	ORCID Number
Petrovic, Zoran		0000-0001-6569-9447
Puac, Nevena		0000-0003-1142-8494
Skoro, Nikola		0000-0002-0254-8008

ISSN: 0022-3727

eISSN: 1361-6463

Record 2 of 4

Title: Upscaling plasma deposition: The influence of technological parameters

Author(s): Corbella, C (Corbella, Carles)

Source: SURFACE & COATINGS TECHNOLOGY **Volume:** 242 **Pages:** 237-245 **DOI:** 10.1016/j.surfcoat.2013.12.002 **Published:** MAR 15 2014

Accession Number: WOS:000333782400034

ISSN: 0257-8972

Record 3 of 4

Title: Tailoring surface morphology of cotton fibers using mild tetrafluoromethane plasma treatment

Author(s): Gorjanc, M (Gorjanc, Marija); Jazbec, K (Jazbec, Katja); Zaplotnik, R (Zaplotnik, Rok)

Source: JOURNAL OF THE TEXTILE INSTITUTE **Volume:** 105 **Issue:** 11 **Pages:** 1178-1185 **DOI:** 10.1080/00405000.2013.877190 **Published:** 2014

Accession Number: WOS:000340152600007

ISSN: 0040-5000

eISSN: 1754-2340

Record 4 of 4

Title: Characterization and global modelling of low-pressure hydrogen-based RF plasmas suitable for surface cleaning processes

Author(s): Skoro, N (Skoro, Nikola); Puac, N (Puac, Nevena); Lazovic, S (Lazovic, Sasa); Cvelbar, U (Cvelbar, Uros); Kokkoris, G (Kokkoris, George); Gogolides, E

(Gogolides, Evangelos)

Source: JOURNAL OF PHYSICS D-APPLIED PHYSICS **Volume:** 46 **Issue:** 47 **Article Number:** 475206 **DOI:** 10.1088/0022-3727/46/47/475206 **Published:** NOV 27 2013

Accession Number: WOS:000326984800018

Author Identifiers:

Author	ResearcherID Number	ORCID Number
Lazovic, Sasa	Q-5056-2016	0000-0003-1696-9134
Puac, Nevena		0000-0003-1142-8494
Skoro, Nikola		0000-0002-0254-8008

ISSN: 0022-3727

eISSN: 1361-6463

Close

Web of Science
Page 1 (Records 1 -- 4)
[1]

Print

Record 1 of 4

Title: The influence of electrode configuration on light emission profiles and electrical characteristics of an atmospheric-pressure plasma jet

Author(s): Maletic, D (Maletic, Dejan); Puac, N (Puac, Nevena); Malovic, G (Malovic, Gordana); Dordevic, A (Dordevic, Antonije); Petrovic, ZL (Petrovic, Zoran Lj)

Source: JOURNAL OF PHYSICS D-APPLIED PHYSICS **Volume:** 50 **Issue:** 14 **Article Number:** 145202 **DOI:** 10.1088/1361-6463/aa5d91 **Published:** APR 12 2017

Accession Number: WOS:000404428200002

Author Identifiers:

Author	ResearcherID Number	ORCID Number
Puac, Nevena		0000-0003-1142-8494
Petrovic, Zoran		0000-0001-6569-9447
Malovic, Gordana		0000-0003-2356-0652

ISSN: 0022-3727

eISSN: 1361-6463

Record 2 of 4

Title: Cell Proliferation on Polyethylene Terephthalate Treated in Plasma Created in SO2/O-2 Mixtures

Author(s): Recek, N (Recek, Nina); Resnik, M (Resnik, Matic); Zaplotnik, R (Zaplotnik, Rok); Mozetic, M (Mozetic, Miran); Motaln, H (Motaln, Helena); Lah-Turnsek, T (Lah-Turnsek, Tamara); Vesel, A (Vesel, Alenka)

Source: POLYMERS **Volume:** 9 **Issue:** 3 **Article Number:** 82 **DOI:** 10.3390/polym9030082 **Published:** MAR 2017

Accession Number: WOS:000397231100006

Author Identifiers:

Author	ResearcherID Number	ORCID Number
Recek, Nina		0000-0001-5389-8262

ISSN: 2073-4360

Record 3 of 4

Title: Plasma induced DNA damage: Comparison with the effects of ionizing radiation

Author(s): Lazovic, S (Lazovic, S.); Maletic, D (Maletic, D.); Leskovac, A (Leskovac, A.); Filipovic, J (Filipovic, J.); Puac, N (Puac, N.); Malovic, G (Malovic, G.); Joksic, G (Joksic, G.); Petrovic, ZL (Petrovic, Z. Lj.)

Source: APPLIED PHYSICS LETTERS **Volume:** 105 **Issue:** 12 **Article Number:** 124101 **DOI:** 10.1063/1.4896626 **Published:** SEP 22 2014

Accession Number: WOS:000343004400099

Author Identifiers:

Author	ResearcherID Number	ORCID Number
Lazovic, Sasa	Q-5056-2016	0000-0003-1696-9134
Joksic, Gordana		0000-0002-7186-301X
Petrovic, Zoran		0000-0001-6569-9447
Leskovac, Andreja		0000-0002-6293-5237
Puac, Nevena		0000-0003-1142-8494
Filipovic Trickovic, Jelena		0000-0001-5450-0842
Malovic, Gordana		0000-0003-2356-0652

ISSN: 0003-6951

eISSN: 1077-3118

Record 4 of 4

Title: Inhibition of methicillin resistant Staphylococcus aureus by a plasma needle

Author(s): Miletic, M (Miletic, Maja); Vukovic, D (Vukovic, Dragana); Zivanovic, I (Zivanovic, Irena); Dakic, I (Dakic, Ivana); Soldatovic, I (Soldatovic, Ivan); Maletic, D (Maletic, Dejan); Lazovic, S (Lazovic, Sasa); Malovic, G (Malovic, Gordana); Petrovic, ZL (Petrovic, Zoran Lj); Puac, N (Puac, Nevena)

Source: CENTRAL EUROPEAN JOURNAL OF PHYSICS **Volume:** 12 **Issue:** 3 **Pages:** 160-167 **DOI:** 10.2478/s11534-014-0437-z **Published:** MAR 2014

Accession Number: WOS:000333023800002

Author Identifiers:

Author	ResearcherID Number	ORCID Number
Lazovic, Sasa	Q-5056-2016	0000-0003-1696-9134
Malovic, Gordana		0000-0003-2356-0652
Petrovic, Zoran		0000-0001-6569-9447
Puac, Nevena		0000-0003-1142-8494
Soldatovic, Ivan		0000-0003-4893-1683

ISSN: 1895-1082

eISSN: 1644-3608

Close

Web of Science
Page 1 (Records 1 -- 4)
◀ [1] ▶

Print

Close

Web of Science
Page 1 (Records 1 -- 3)
[1]

Print

Record 1 of 3

Title: In vitro safety assessment of the strawberry tree (Arbutus unedo L.) water leaf extract and arbutin in human peripheral blood lymphocytes

Author(s): Jurica, K (Jurica, K.); Karaconji, IB (Karaconji, I. Brcic); Mikolic, A (Mikolic, A.); Milojkovic-Opsenica, D (Milojkovic-Opsenica, D.); Benkovic, V (Benkovic, V.); Kopjar, N (Kopjar, N.)

Source: CYTOTECHNOLOGY **Volume:** 70 **Issue:** 4 **Pages:** 1261-1278 **DOI:** 10.1007/s10616-018-0218-4 **Published:** AUG 2018

Accession Number: WOS:000440814500014

PubMed ID: 29696482

Author Identifiers:

Author	ResearcherID Number	ORCID Number
Brcic Karaconji, Irena	S-3610-2018	0000-0002-1151-8839
Benkovic, Vesna		0000-0001-5201-3098
Kopjar, Nevenka		0000-0002-3117-2847

ISSN: 0920-9069

eISSN: 1573-0778

Record 2 of 3

Title: Atmospheric Precipitations, Hailstone and Rainwater, as a Novel Source of Streptomyces Producing Bioactive Natural Products

Author(s): Sarmiento-Vizcaino, A (Sarmiento-Vizcaino, Aida); Espadas, J (Espadas, Julia); Martin, J (Martin, Jesus); Brana, AF (Brana, Alfredo F.); Reyes, F (Reyes, Fernando); Garcia, LA (Garcia, Luis A.); Blanco, G (Blanco, Gloria)

Source: FRONTIERS IN MICROBIOLOGY **Volume:** 9 **Article Number:** 773 **DOI:** 10.3389/fmicb.2018.00773 **Published:** APR 23 2018

Accession Number: WOS:000430557800001

PubMed ID: 29740412

Author Identifiers:

Author	ResearcherID Number	ORCID Number
Martin-Serrano, Jesus	M-1937-2014	0000-0001-7487-2790
Reyes, Fernando	G-4027-2013	0000-0003-1607-5106
Garcia, Luis		0000-0003-3233-3582

ISSN: 1664-302X

Record 3 of 3

Title: In vitro assessment of the cytotoxic, DNA damaging, and cytogenetic effects of hydroquinone in human peripheral blood lymphocytes

Author(s): Jurica, K (Jurica, Karlo); Karaconji, IB (Karaconji, Irena Brcic); Benkovic, V (Benkovic, Vesna); Kopjar, N (Kopjar, Nevenka)

Source: ARHIV ZA HIGIJENU RADA I TOKSIKOLOGIJU-ARCHIVES OF INDUSTRIAL HYGIENE AND TOXICOLOGY **Volume:** 68 **Issue:** 4 **Pages:** 322-335 **DOI:** 10.1515/aiht-2017-68-3060 **Published:** DEC 2017

Accession Number: WOS:000423311800009

PubMed ID: 29337680

Author Identifiers:

Author	ResearcherID Number	ORCID Number
Brcic Karaconji, Irena	S-3610-2018	0000-0002-1151-8839
Benkovic, Vesna		0000-0001-5201-3098

ISSN: 0004-1254

eISSN: 1848-6312

Close

Web of Science
Page 1 (Records 1 -- 2)
[1]

Print

Record 1 of 2

Title: Mass spectrometry of diffuse coplanar surface barrier discharge: influence of discharge frequency and oxygen content in N-2/O-2 mixture

Author(s): Cech, J (Cech, Jan); Brablec, A (Brablec, Antonin); Cernak, M (Cernak, Mirko); Puac, N (Puac, Nevena); Selakovic, N (Selakovic, Nenad); Petrovic, ZL (Petrovic, Zoran Lj.)

Source: EUROPEAN PHYSICAL JOURNAL D **Volume:** 71 **Issue:** 2 **Article Number:** 27 **DOI:** 10.1140/epjd/e2016-70607-5 **Published:** FEB 9 2017

Accession Number: WOS:000403477900003

Author Identifiers:

Author	ResearcherID Number	ORCID Number
Cech, Jan	F-8310-2017	0000-0002-4900-6011

ISSN: 1434-6060

eISSN: 1434-6079

Record 2 of 2

Title: The effect of a plasma needle on bacteria in planktonic samples and on peripheral blood mesenchymal stem cells

Author(s): Lazovic, S (Lazovic, Sasa); Puac, N (Puac, Nevena); Miletic, M (Miletic, Maja); Pavlica, D (Pavlica, Dusan); Jovanovic, M (Jovanovic, Milena); Bugarski, D (Bugarski, Diana); Mojsilovic, S (Mojsilovic, Slavko); Maletic, D (Maletic, Dejan); Malovic, G (Malovic, Gordana); Milenkovic, P (Milenkovic, Pavle); Petrovic, Z (Petrovic, Zoran)

Source: NEW JOURNAL OF PHYSICS **Volume:** 12 **Article Number:** 083037 **DOI:** 10.1088/1367-2630/12/8/083037 **Published:** AUG 17 2010

Accession Number: WOS:000281279700003

Author Identifiers:

Author	ResearcherID Number	ORCID Number
Lazovic, Sasa	Q-5056-2016	0000-0003-1696-9134
Lazovic, Sasa	B-9651-2013	0000-0003-1696-9134
Malovic, Gordana		0000-0003-2356-0652
Puac, Nevena		0000-0003-1142-8494
Petrovic, Zoran		0000-0001-6569-9447

ISSN: 1367-2630

Close

Web of Science
Page 1 (Records 1 -- 2)
[1]

Print

Clarivate

Accelerating innovation

Close

Web of Science
Page 1 (Records 1 -- 1)
[1]

Print

Record 1 of 1

Title: High throughput image cytometry micronucleus assay to investigate the presence or absence of mutagenic effects of cold physical plasma

Author(s): Bekeschus, S (Bekeschus, Sander); Schmidt, A (Schmidt, Anke); Kramer, A (Kramer, Axel); Metelmann, HR (Metelmann, Hans-Robert); Adler, F (Adler, Frank); von Woedtke, T (von Woedtke, Thomas); Niessner, F (Niessner, Felix); Weltmann, KD (Weltmann, Klaus-Dieter); Wende, K (Wende, Kristian)

Source: ENVIRONMENTAL AND MOLECULAR MUTAGENESIS **Volume:** 59 **Issue:** 4 **Pages:** 268-277 **DOI:** 10.1002/em.22172 **Published:** MAY 2018

Accession Number: WOS:000430120300001

PubMed ID: 29417643

Author Identifiers:

Author	ResearcherID Number	ORCID Number
von Woedtke, Thomas	U-3604-2018	0000-0002-1097-4832

ISSN: 0893-6692

eISSN: 1098-2280

Close

Web of Science
Page 1 (Records 1 -- 1)
[1]

Print

Close

Web of Science
Page 1 (Records 1 -- 1)
[1]

Print

Record 1 of 1

Title: Biological effects of bacterial pigment undecylprodigiosin on human blood cells treated with atmospheric gas plasma in vitro

Author(s): Lazovic, S (Lazovic, Sasa); Leskovac, A (Leskovac, Andreja); Petrovic, S (Petrovic, Sandra); Senerovic, L (Senerovic, Lidija); Krivokapic, N (Krivokapic, Nevena); Mitrovic, T (Mitrovic, Tatjana); Bozovic, N (Bozovic, Nikola); Vasic, V (Vasic, Vesna); Nikodinovic-Runic, J (Nikodinovic-Runic, Jasmina)

Source: EXPERIMENTAL AND TOXICOLOGIC PATHOLOGY **Volume:** 69 **Issue:** 1 **Pages:** 55-62 **DOI:** 10.1016/j.etp.2016.11.003 **Published:** JAN 2017

Accession Number: WOS:000390968000007

PubMed ID: 27843060

Author Identifiers:

Author	ResearcherID Number	ORCID Number
Nikodinovic-Runic, Jasmina	W-1277-2018	0000-0002-2553-977X
Lazovic, Sasa	Q-5056-2016	0000-0003-1696-9134
Senerovic, Lidija		0000-0002-6965-9407
Leskovac, Andreja		0000-0002-6293-5237
Petrovic, Sandra		0000-0003-0930-6455
Vasic, Vesna		0000-0003-1268-2363

ISSN: 0940-2993

eISSN: 1618-1433

Close

Web of Science
Page 1 (Records 1 -- 1)
[1]

Print

Close

Web of Science
Page 1 (Records 1 -- 1)
[1]

Print

Record 1 of 1

Title: Cold plasma treatment triggers antioxidative defense system and induces changes in hyphal surface and subcellular structures of Aspergillus flavus

Author(s): Simoncicova, J (Simoncicova, Juliana); Kalinakova, B (Kalinakova, Barbora); Kovacik, D (Kovacik, Dusan); Medvecka, V (Medvecka, Veronika); Lakatos, B (Lakatos, Boris); Krystofova, S (Krystofova, Svetlana); Hoppanova, L (Hoppanova, Lucia); Paluskova, V (Paluskova, Veronika); Hudecova, D (Hudecova, Daniela); Durina, P (Durina, Pavol); Zahoranova, A (Zahoranova, Anna)

Source: APPLIED MICROBIOLOGY AND BIOTECHNOLOGY **Volume:** 102 **Issue:** 15 **Pages:** 6647-6658 **DOI:** 10.1007/s00253-018-9118-y **Published:** AUG 2018

Accession Number: WOS:000438606100030

PubMed ID: 29858953

Author Identifiers:

Author	ResearcherID Number	ORCID Number
Kovacik, Dusan	T-5214-2018	

ISSN: 0175-7598

eISSN: 1432-0614

Close

Web of Science
Page 1 (Records 1 -- 1)
[1]

Print

Република Србија

УУБ

Универзитет у Београду
Физички факултет, Београд

Оснивач: Република Србија
Дозволу за рад број 612-00-02666/2010-04 од 10. децембра 2010.
године је издало Министарство просвете и науке Републике Србије

Диплома

Саша, Слободан, Лазовић

рођен 3. фебруара 1980. године у Краљеву, Република Србија, уписан школске 2007/2008. године, а дана 15. децембра 2010. године завршио је докторске академске студије, трећег степена, на студијском програму Физика, обима 180 (сто осамдесет) бодова ЕСПБ са просечном оценом 10,00 (десет и 0/100).

Наслов докторске дисертације је: „Дијагностика радиофреквентних плазма извора и њихове примене у третманима биомедицинских узорака".

На основу тога издаје му се ова диплома о стеченом научном називу

доктор наука - физичке науке

Број: 2504300
У Београду, 3. априла 2014. године

Декан
Проф. др Јаблан Дојчиловић

Ректор
Проф. др Владимир Бумбаширевић

00025176

Република Србија
МИНИСТАРСТВО ПРОСВЕТЕ И НАУКЕ
Комисија за стицање научних звања

Број:06-00-75/379
13.07.2011. године
Б е о г р а д

На основу члана 22. става 2. члана 70. став 5. Закона о научноистраживачкој делатности ("Службени гласник Републике Србије", број 110/05 и 50/06 – исправка и 18/10), члана 2. става 1. и 2. тачке 1 – 4.(прилози) и члана 38. Правилника о поступку и начину вредновања и квантитативном исказивању научноистраживачких резултата истраживача ("Службени гласник Републике Србије", број 38/08) и захтева који је поднео

Институт за физику у Београду

Комисија за стицање научних звања на седници одржаној 13.07.2011. године, донела је

ОДЛУКУ
О СТИЦАЊУ НАУЧНОГ ЗВАЊА

Др Саша Лазовић
стиче научно звање
Научни сарадник

у области природно-математичких наука - физика

О Б Р А З Л О Ж Е Њ Е

Институт за физику у Београду утврдио је предлог број 658/1 од 17.05.2011. године на седници научног већа Института и поднео захтев Комисији за стицање научних звања број 668/1 од 24.05.2011. године за доношење одлуке о испуњености услова за стицање научног звања ***Научни сарадник***.

Комисија за стицање научних звања је по предходно прибављеном позитивном мишљењу Матичног научног одбора за физику на седници одржаној 13.07.2011. године разматрала захтев и утврдила да именовани испуњава услове из члана 70. став 5. Закона о научноистраживачкој делатности ("Службени гласник Републике Србије", број 110/05 и 50/06 – исправка и 18/10), члана 2. става 1. и 2. тачке 1 – 4.(прилози) и члана 38. Правилника о поступку и начину вредновања и квантитативном исказивању научноистраживачких резултата истраживача ("Службени гласник Републике Србије", број 38/08) за стицање научног звања ***Научни сарадник***, па је одлучила као у изреци ове одлуке.

Доношењем ове одлуке именовани стиче сва права која му на основу ње по закону припадају.

Одлуку доставити подносиоцу захтева, именованом и архиви Министарства просвете и науке у Београду.

ПРЕДСЕДНИК КОМИСИЈЕ
др Станислава Стошић-Грујичић,
научни саветник

МИНИСТАР
Проф. др Жарко Обрадовић

The Plasma Science Society Of India

(Regn. No. F-828, Ahmedabad)

Dr. S. Mukherjee
Chairman, Scientific Programme Committee
Plasma-2014

04-Sept-2014
Gandhinagar

To,

Dr. Sasa Lazovic
Assistant Research Professor
Institute of Physics
Pregrevica 118, 11080 Belgrade

SUB : 29th National Symposium On Plasma Science & Technology - Invitation

Dear Professor Lazovic,

On behalf of the Plasma Science Society of India, and the Scientific Programme Committee, it is my pleasure to invite you to the 29th National Symposium on Plasma Science & Technology and the International Conference on Plasma & Nanotechnology will be held at the Mahatma Gandhi University, Kottayam, Kerala, India from 8-11 December, 2014

The Scientific Programme Committee of Plasma 2014 is also pleased to invite you to deliver an INVITED TALK in the **Other Areas Session** (Session 13) of the meeting.

Tentatively, your talk is scheduled to be held in the afternoon (09:00 - 11:30) of 11th December 2014. The duration of your talk would be 20 mins + 5 mins for discussion. The final schedule of your talk will be communicated to you soon. I would greatly appreciate if you could kindly confirm your acceptance of the talk to the Convener, Plasma 2014 and submit an abstract (maximum 1 A4 size page) of your proposed talk to the Conference email ID on or before 15th October, 2014.

Details of the conference are available on the website www.ipr.res.in/plasma2014

Looking forward to meeting you at Kottayam, Kerala !

Thanking you,

Warm regards,

Plasma Science Society Of India
Reg. No. F-828, Ahmedabad

(Dr. S. Mukherjee)

All You Need to Know About Plasmas & Liquids and Never Dared to Ask

Location: INP Greifswald, Felix-Hausdorff Str. 2, 17489 Greifswald

Web: INP Greifswald http://www.inp-greifswald.de

Web:Greifswald http://www.greifswald.de

Programm of the 2015 Training School

Arrival: Sunday 4th of Octobre

Sunday, 4th Oct.			
	16:30 - 19:00	**Registration**	
Monday, 5th Oct.		Applications and First Steps	
	08:30 - 08:50	Registration & Coffee	
	08:50 - 09:00	Welcome	F. Krcma, S. Reuter
1	09:00 - 10:30	**Applications of Plasmas in Liquids I** Applications in water treatment and advanced oxidation processes	**Joanna Pawlat** *IEEE - Lublin University of Technology*
		Coffee Break	
2	10:45 - 12:15	**Dos and Don'ts of Electrical Characterization**	**Nick Braithwaithe** *Open University Milton Keynes, UK*
	12:30 - 14:00	Lunch	
3	14:00 - 15:30	**Alternatives to Plasma Liquid Treatment - Bioelectrics**	**Jürgen Kolb** *INP Greifswald, Germany*
		Coffee Break	
4	15:45 - 17:15	**My Research - Pathways to Impact**	**Saša Lazovic** *Institute of Physics Belgrade Serbia*
	18:00 - 20:00	**Poster Session and Finger Food**	
Tuesday, 6th Oct		Applications and Technical Tricks	
	08:30 - 09:00	Coffee	
5	09:00 - 10:30	**Applications of Plasmas in Liquids III** Organic chemistry applications	**Felipe Iza** *Univ. Loughbrough, UK*
		Coffee Break	
6	10:45 - 12:15	**Applications of Plasmas in Liquids II** *Applications in surface treatment and in nanosciences*	**Nikolai Tarasenko** *Institute of Physics National Academy of Science, Belarus*
	12:30 - 14:00	Lunch	
7	14:00 - 15:30	**Applications of Plasmas in Liquids IV** *Biological Applications of Plasmas*	**Thomas von Woedtke** *INP Greifswald, Germany*
		Coffee Break	
8	15:45 - 16:30	**Technical Tricks they normally don't tell you**	**Volker Schulz-von der Gathen** *Ruhr Universität Bochum, Germany*
9	16:45 - 17:30	**Technical Tricks they normally don't tell you / Hands on experience**	**Judith Golda** *Ruhr Universität Bochum, Germany*
	19:00	**Social Dinner**	
Wednesday, 7th Oct. Plasma and Liquid Systems - Fundamentals and Diagnostics			
	08:30 - 09:00	Coffee	
10	09:00 - 10:30	**Diagnostics of chemical species in plasma treated liquids**	**Petr Lukes** *Institute of Plasma Physics Prague, Czech Republic*
ee Break			
11	10:45 - 12:15	**Fundamentals of Plasma and Liquid Systems**	**Antoine Rosseau** *LPP, Ecole Polytechnique Paris, France*
	12:30 - 14:00	Lunch	
	14:00 - 18:00	**Excursion to Stralsund or free time**	
	19:00 - 21:00	**Dinner in Stralsund**	
Thursday, 8th Oct. Plasma Sources and Their Diagnostics			
	08:30 - 09:00	Coffee	
12	09:00 - 10:30	**Plasma Sources at the INP**	**Torsten Gerling** *INP Greifswald, Germany*
ee Break			
13	10:45 - 12:15	**Gas Phase/Plasma diagnostics**	**Stephan Reuter** *INP Greifswald, Germany*
	12:30 - 13:30	Lunch	
	13:30	**Closure & Departure**	

PRELIMINARY LIST OF INVITED LECTURERS

1. Atomic Collision Processes

General Lectures

M.Charlton, Swansea University, UK
Transport and Collision Phenomena Involving Antiparticles and Antihydrogen

D. Gerlich, Techische Universitat Chemnitz,Germany
Experimental Studies on HnDm+ collision systems n+m≤5

M. Stockli, Oak Ridge National Lab, USA
Plasma-Wall Interactions in Cesiated H^- Ion Sources

Topical Lectures

J-M. Bizau, Université Paris-Sud, France
Photoionization of Atomic and Molecurar Positively Charged Ions

R. Čurik, J. Heyrovský Institute of Physical Chemistry of the ASCR, v.v.i., Czech Republic
Vibrationally inelastic collisions of slow electrons with molecules

F.Penent, LCPMR, CNRS (UMR 7614) and Université Paris 06, France
Single Photon Double K-shell ionization of Small Molecules

2. Particle and Laser Beam Interactions with Solids

General Lectures

D. Batani, CELIA, University of Bordeaux, France
Preliminary results from recent experiments and future roadmap to Shock Ignition of Fusion Targets

U. Cvelbar, Jozef Stefan Institute, Slovenia
The Origin of the Plasma Grown Nanostructures at the Solid-Solid Interface

J. Hermann, Université Aix-Marseille II, France
Properties of plasmas produced by laser ablation with single and double pulses

Topical Lectures

T. Ikeda, Atomic Physics Laboratory, Japan
Guiding of Slow Highly Charged Ions through Tapered glass caillaries

V. Milosavljević, University of Belgrade, Serbia
Comprehensive Plasma Diagnostics for an ECR Etcher

Juana L. Gervasoni, Centro Atómico Bariloche, Argentina
Title pending

3. Low Temperature Plasmas

General Lectures

A. Bogaerts, University of Antwerp, Belgium
Modeling of Plasma and Plasma-Surface Interactions for Environmental, Medical and Nano Applications

U. Ebert, Eindhoven University of Technologi, Netherlands
Extremely far from Equilibrium: the Multiscale Dynamics of Streamers

M. Kushner, University of Michigen, USA
Model Based Design of Low Temperature Plasma Reaactors

J-M. Pouvesle, GREMI University of Orleans, France
Antitumoral effect of non thermal plasmas alone or in combination with chemotherapy

H. E. Wagner, Ernst-Moritz-Arndt-Universität Greifswald, Germany
The Complex Diagnostics of Barrier Discharges – an Experimental Challenge

Topical Lectures

J. A. Aparicio, Universidad de Valladolid, Spain
Experimental transition probability measurements in Pulsed lamps: Critical points

A. Bultel, Université de Rouen, France
Physico-Chemistry of Planetary Atmospheric Entry Plasmas

E. Kovačević, GREMI University of Orleans, France
Plasma based formation and activation of nanoparticles and nanocomposite materials

Đ. Spasojević, Faculty of Physics, Serbia
Cathode sheath and hydrogen Balmer lines modeling in a micro-hollow gas discharge

4. General Plasmas

General Lectures

V. M. Astashinski, National Academy ofSciences of Belarus, Republic of Belarus
Ion-Drift Acceleration of Magnetized Plasma in Quasi-Stationary
Plasma Accelerators

G. Ferland, University of Kentucky, USA
Plasma simulations of general interest in astrophysics

Hideo Nagatomo, Institute of Laser Engineering, Osaka University, Japan
Integrated Simulations for Laser Fusion

Topical Lectures

L. Campbell, Flinders University, Australia
Electron Impact Excitation in Planetary and Cometary Atmospheres

N. B. Nassib, INSAT, University of Carthage, Tunisia
Ab Initio Determinations of Stark Broadening Parameters and Applications in Astrophysics

T. Popov, St. Kliment Ohridski University of Sofia, Bulgaria
Evaluation of Plasma Potential and Electron Energy Distribution Function by Langmuir Probes in Magnetized Plasma

J. Rosato, Aix Marseille University, France
Plasma Spectriscopy in the Conditions of the Iter Tokamak

T. Watanabe, National Institute for Fusion Science, Japan
Kinetic Transport Simulation Studies for Helical Plasma Confinement

Progress Reports

A. Antoniou, University of Athens, Greece
The Structure of Si IV Region in Be Stars; a Study of Si IV Spectral Lines in 68 Be Stars

N. Cvetanović, Faculty of Transport and Traffic Engineering, Serbia
Investigation of Energetic Hydrogen Atoms in Glow Discharges

M. Coreno, Elettra Sincrotrone Trieste and CNR, Italy
On the Work that we're Carrying out at Elettra on the Novel Ultrafast VUV sources CITIUS and FERMI FEL

S. M. D. Galijaš, Faculty of Physics, Serbia
Two-State Vector Model of the Nonresonant Population of the Rydberg States of Multiply Charged Ions Interacting with Solid Surfaces

N. Gavrilović-Bon, Astronomical Observatory Belgrade, Serbia
Stellar Population in the sample of Type 2 Active Galactic Nuclei

J. Kovačević, Astronomical Observatory Belgrade, Serbia
The properties of the emission lines and their correlations in the spectra of Active Galactic Nuclei

D. Kubala, University of Fribourg, Switzerland
Dissociative Electron Attachment to Small Model Molecules

S. Lazović, Institute of Physics, Serbia
Diagnostics and Biomedical Applications of Radiofrequency Plasma

M. Majkić, Faculty of Physics, Serbia
Intermediate Stages of the Neutralization of Multiply Charged Slow Ions Interacting with Solid Surfaces

A. Mihelič, Jožef Stefan Institute, Slovenia
Studies of Multiphoton Processes in Noble Gas Atoms

S. Petrović, Vinča Institute of Nuclear Sciences, Serbia
Composition and structure modification of a WTi/Si system by nanosecond and picosecond laser pulses

M. Radović, Vinča Institute of Nuclear Sciences, Serbia
Low Dimensional Ti-Oxide Based Structure: From SrTiO3 to TiO2

M. Ristić, Faculty of Physical Chemistry, Serbia
Differential Cross Sections at 0^o and 180^o for Electron Impact Excitation of H_2 and CO

N. Šišović, Faculty of Physics, Serbia
Spectroscopic study of hydrogen Balmer line shapes in a hollow cathode glow discharge in NH3, Ar/NH3, Ar/CH4 and Ar/C2H2 mixtures

N. Škoro, Institute of Physics, Serbia
Breakdown and discharge regimes in standard and micrometer size DC discharges

D. Tankosić, USRA/NASA – Marshal space Fight Center, USA
Laboratory Studies of Charging Properties of Dust Grains in Astrophysical/Planetary Environments

S. Tošić, Institute of Physics, Serbia
Measurements of Differential Cross Sections for Elastic Electron Scattering and Electronic Excitation of Metal atoms

G. Wachter, Vienna University of Technology, Austria
Electron emission from a metal nanotip by ultrashort laser pulses

M. Zlatar, Institute of Chemistry, Technology and Metallurgy, Serbia
Dissociative Electron Attachment Measurements and TDDFT Calculations of the Excitation Energies in $Pt(PF_3)_4$: Sinergy Between Experiment and Theory

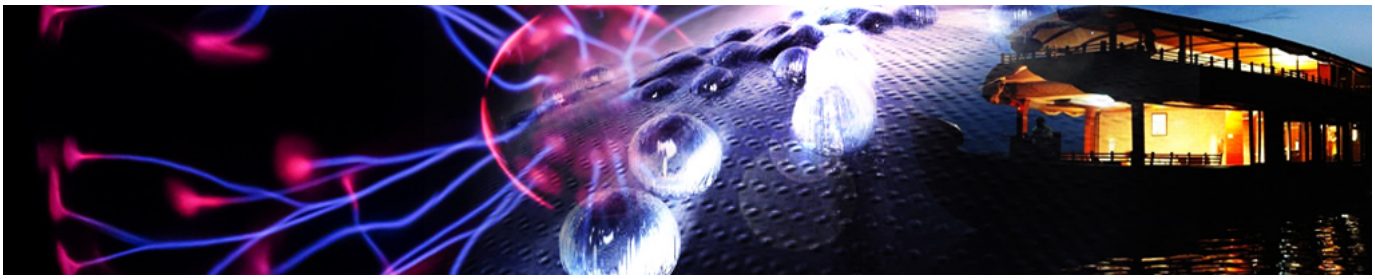

INDIAN DELEGATES

PLASMA 2014 POSTER ▶

FIRST CALL FOR ABSTRACTS ➡

IMPORTANT DATES

Conference on 8,9,10 and 11 Dec 2014

Extended Date for Submission of Abstracts :

25th Sept 2014

Intimation to Authors : **30th Sept 2014**

Deadline for the Registration : **30th Oct 2014**

Deadline for the Submission of Full Papers :

15th Nov 2014

Register Now! Click Here

TRAVELS ➤

Mahatma Gandhi University, Kottayam, Kerala, india - 686560

The 29th National Symposium on Plasma Science & Technology and the International Conference on Plasma & Nanotechnology will be held at the Mahatma Gandhi University, Kottayam, Kerala, India from 8-11 December, 2014

Background & Objectives

We are extremely happy to inform you that we are organising the International Conference on Plasma & Nanotechnology (PLASMA- 2014) and 29th National Symposium on Plasma Science & Technology on December 8-11, 2014, Kottayam, Kerala, India.

This conference will be immensely rewarding for every scientist, researcher and students alike as it is being organized together with the 29th National Symposium Plasma Science & Technology. The conference will hence be attended by more than 500 delegates prominent in the field. The goal of the conference emphasizes interdisciplinary research on plasma science and Nanotechnology.

VICE CHANCELLOR

Mahatma Gandhi University
Kottayam, Kerala
India- 686560.

CHAIRPERSON OF INTERNATIONAL CONFERENCE

Prof.Dr.Sabu Thomas Ph.D, FRSC
Director International and Inter University Centre for Nanoscience and Nanotechnology (IIUCNN) Mahatma Gandhi University
Kottayam, Kerala, India- 686560.

Prof.dr. Uros Cvelbar
Jozef Stefan Institute,
Jamova cesta 39,
SI-1000 Ljubljana, Slovenia, EU

Prof. Miran Mozetič
Jozef Stefan Institute,
Jamova cesta 39, SI-1000 Ljubljana,
Slovenia, EU

CONVENER

Dr. Nandakumar Kalarikkal
Joint Director International and Inter University Centre for Nanoscience and Nanotechnology (IIUCNN) & School of Pure and Applied Physics
Mahatma Gandhi University Kottayam, Kerala,
India- 686560.

International and Inter University Centre for Nanoscience and Nanotechnology (IIUCNN) & School of Pure and Applied Physics,
Mahatma Gandhi University & The Plasma Science Society of India

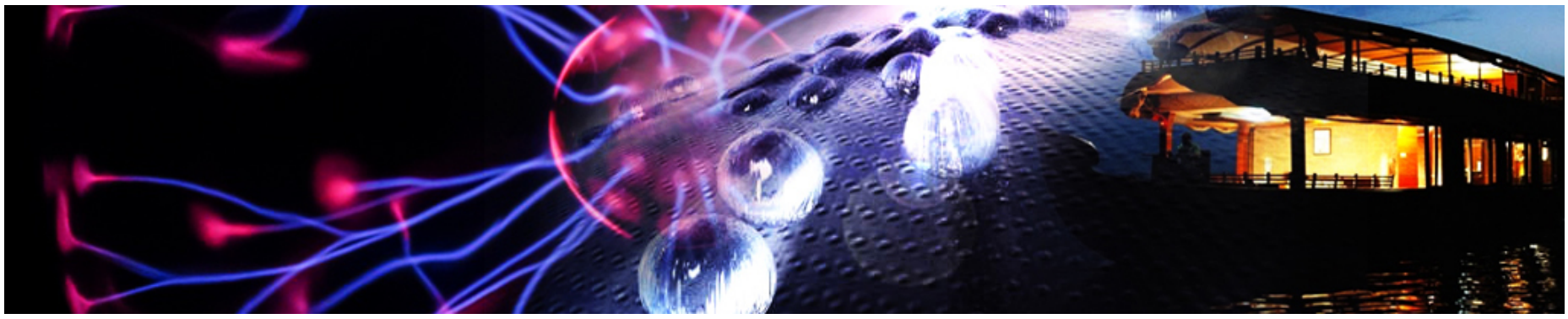

Committee

INTERNATIONAL ADVISORY COMMITTEE

- Prof. Petr Spatenka, Czech Technical University, Czech Republic
- Prof. Vladimer Cech, Brno University of Technology, Czech Republic
- Dr.Mariusz Ozimek, Electrotechnical Institute Wroclaw, Poland
- Prof. M.C.M. van de Sanden, DIFFER, Netherlands
- Prof. Tamio Endo, Mie University, Japan
- Prof. Dr. D. Depla, Ghent University, Belgium
- Dr. Murukeshan Vadakke Matham, Nanyang Technological University, Singapore
- Dr. Chin Han Chan, UIT Mara, Malasyia
- Dr. SasaLazovic, Institute of Physics, Serbia
- Prof. Dzaraini Kamarun, UIT Mara, Malaysia

INTERNATIONAL ADVISORY COMMITTEE

- Vice-Chancellor, M. G.University
- Dhiraj Bora, IPR Gandhinagar
- Abhijit Sen, IPR, Gandhinagar
- Amita Das, IPR Gandhinagar
- Das A. K, BARC Mumbai
- Ganguli A, IIT Delhi
- Goswami J.N, PRL Ahmedabad
- Gupta P.D, RRCAT Indore
- Kaw P. K, IPR Gandhinagar
- Krishan Vinod, IIAP Bangalore
- Padmanabhan P. V. A, BARC Mumbai
- Ravindrakumar G, TIFR Mumbai
- Sabu Thomas, M G University, Kottayam
- Saxena Y. C, IPR ,Gandhinagar
- Sekar Iyengar A. N, SINP, Kolkata

INTERNATIONAL ADVISORY COMMITTEE

- Mukherjee S, IPR Gandhinagar
- Ganesh Rajaraman, IPR Gandhinagar
- Joydeep Ghosh, IPR Gandhinagar
- Nandakumar K, M G Univertity, Kottayam
- Padmanabhan P. V. A, BARC Mumbai
- Sita Janaki, SINP Kolkata
- Sukthisama Ghosh, IIGM, Mumbai

» Dr. Murukeshan Vadakke Matham

LOCAL ADVISORY COMMITTEE

» Prof. Sabu Thomas, MGU

» Dr. Nandakumar Kalarikkal, MGU

» Dr. Latha M.S, MGU

» Prof. C. SudarshanaKumar, MGU

» Prof. N. V. Unnikrishnan, MGU

» Prof. Chandu Venugopal, MGU

» Prof. C. T Aravind Kumar, MGU

» Dr. M. S Kala, MGU

» Prof. Jacob, Philip CUSAT

» Prof. M. K Jayraj, CUSAT

» Dr. Shubha, University of Calicut

» Dr. Raji. V, MGU

XX ESCAMPIG Scientific Committee

W. G. Graham	*chair*	United Kingdom / Ireland
A. Bogaerts		Benelux
J. Glosik		Czech Rep. / Slovakia
J. P. Boeuf		France
J. Meichsner		Germany
P. Hartmann		Hungary / Austria
G. Dilecce		Italy
V. Guerra		Portugal
G. Dinescu		Romania
Yu. Akishev		Russia
D. Marić		Serbia
F. Gordillo Vázquez		Spain

Local Organizing Committee

Zoran Lj. Petrović	*co-chair*	Institute of Physics, Belgrade
Gordana Malović	*co-chair*	Institute of Physics, Belgrade
Nikola Konjević	*honorary co-chair*	Faculty of Physics, Belgrade
Dragana Marić	*secretary*	Institute of Physics, Belgrade
Bratislav Marinković		Institute of Physics, Belgrade
Saša Dujko		Institute of Physics, Belgrade

Nevena Puač	Institute of Physics, Belgrade
Nikola Škoro	Institute of Physics, Belgrade
Saša Lazović	Institute of Physics, Belgrade
Milovan Šuvakov	Institute of Physics, Belgrade
Zoran Mijatović	Faculty of Sciences, Novi Sad
Željka Nikitović	Institute of Physics, Belgrade
Marija Radmilović-Rađenović	Institute of Physics, Belgrade

LOC Contact info

Zoran Lj. Petrović (Chair of the LOC)
Gordana Malović (Chair of the LOC)
Dragana Marić (General Secretary)

Institute of Physics
Pregrevica 118
11080 Zemun, Belgrade
Serbia

Tel: +381 11 3713 056
Fax: +381 11 3162 190

E-mail: escampig2010@ipb.ac.rs
Web: www.escampig2010.ipb.ac.rs

- # Proceedings

  - General Lectures
  - Topical Lectures
  - Hot Topics
  - All Papers

- Author Index

Conference Info

- About Conference
- Committees
- Scientific Program
- Workshops
- Prizes
- Sponsors
- Exhibitors

69TH IUVSTA WORKSHOP ON OXIDATION OF ORGANIC MATERIALS BY EXCITED RADICALS CREATED IN NON-EQUILIBRIUM GASEOUS PLASMA

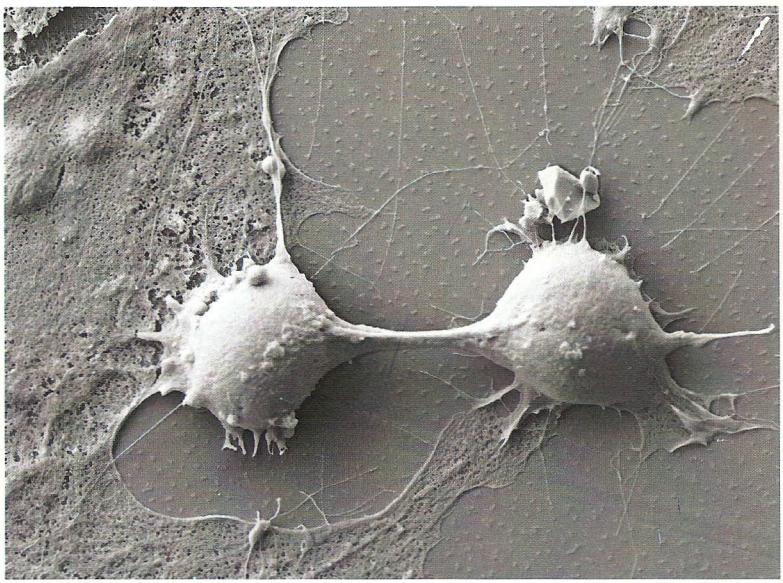

Book of abstracts

69TH IUVSTA WORKSHOP ON OXIDATION OF ORGANIC MATERIALS BY EXCITED RADICALS CREATED IN NON-EQUILIBRIUM GASEOUS PLASMA

ABSTRACTS

December 9th — December 13th 2012, Crklje na Gorenjeskem, Slovenia

Editors of Proceedings: Miran Mozetič and Uroš Cvelbar

Published by: Slovenian Society for Vacuum Technique (DVTS Društvo za vakuumsko tehniko Slovenije), Teslova 30, SI-1000 Ljubljana, Slovenia

Conference Chair:

Miran Mozetič (Slovenia)

Program Committee :

Miran Mozetič, Slovenia (Program chair)
Giorgos Evangelakis, Greece (Program vice chair)
Igor Levchenko, Australia
Primoz Eiselt, Austria
Xiaoxia Zhong, PR China
Masaharu Shiratani, Japan
Mohan R. Sankaran, USA
Mahendra K. Sunkara, USA
Francisco Tabares, Spain
Slobodan Milosevic, Croatia
JJ Shi, PR China
Petr Slobodian, Czech Republic
Shuyan Xu, Singapore

Organizing Committee:

Uroš Cvelbar, Slovenia (Organizing chair)
Ita Junkar , Slovenia (Secretary)
Kristina Eleršič, Slovenia
Saša Lazović, Slovenia
Gregor Filipič, Slovenia
Martina Modic, Slovenia
Gregor Primc, Slovenia
Aleksander Drenik, Slovenia

Organizer:

Društvo za vakuumsko tehniko slovenije (DVTS) - Slovenian Society for Vacuum Technique, Teslova 30, SI-1000 Ljubljana, Slovenia

Sponsors:

International Union for Vacuum Science, Technique and Applications (IUVSTA)
Slovenian Research Agency (ARRS)
Jožef Stefan Institute, Ljubljana, Slovenia
Plasmait

Monday	Dec. 10th	
7:30 - 9:20	Breakfast	
9:20 – 9:30	Opening	
9:30 - 10:00	F. Poncin-Epaillard (invited)	Towards a comprehensive approach of plasma-degradation of polymers
10:00 - 10:30	T. Belmonte (invited)	Oxidation of organic materials by excited radicals created in non-equilibrium gaseous plasma
10:30 - 12:00	Topical discussions: The basic mechanisms on plasma interaction with organic materials	
12:00 - 14:00	Lunch	
14:00 -14:30	M. Hori (invited)	Comprehensive study of atmospheric pressure plasma oxidation on organic materials and organisms
14:30 - 15:00	T. Gans (invited)	Diagnostics and simulations of reactive oxygen species in cold non-equilibrium atmospheric pressure plasmas for healthcare technologies
15:00 - 15:30	S. Lazović (invited)	Properties and bio-medical applications of non-thermal plasma
15:30 - 16:00	D. O'Connell (invited)	Cold atmospheric pressure plasma jet interactions with different biological materials
16:30 - 17:00	Coffee break	
17:00 - 17:30	H. Kersten (invited)	On the energy balance during removal of organic compounds by oxygen-containing plasmas
17:30 - 18:00	S. Tajima (invited)	The effect of active species in the plasma on the change in nanomechanical properties of polymers
18:00 - 18:30	C. Canal (invited)	Plasmas in organic biomaterials: a case study of polypropylene meshes for soft tissue repair
19:00 - 20:00	Dinner	
20:00 - 22:00	Poster section 1	

Tuesday	Dec. 11th	
7:30 - 9:30	Breakfast	
9:30 - 10:45	Topical discussions: Low-pressure plasmas for oxidation of organic materials	
10:45 - 12:00	Topical discussions: Atmospheric-pressure plasmas for oxidation of organic materials	
12:00 - 14:00	Lunch	
14:00 -14:30	D. N. Ruzic (invited)	Ozone generation with atmospheric pressure microplasma array
14:30 - 15:00	V. Guerra (invited)	Afterglow kinetics in oxygen pulsed discharges
15:00 - 15:30	K. Kutasi (invited)	Characteristics of a small volume Ar-O2 afterglow
15:30 - 16:00	D. Mariotti (invited)	Plasma-liquid interactions for nanoscale engineering
16:30 - 17:00	Z. Lj. Petrović (invited)	Electrical breakdown in water vapor and ethanol
17:00 - 17:30	Coffee break	
17:30 - 18:00	V. Švrček (invited)	Non-equilibrium plasmas for engineering composition bandgap, build-in-charge and interface of silicon nanocrystals with conjugated polymers
18:00 - 18:30	G. Uchida (invited)	Application of Si nanoparticles to energy devices: quantum-dot solar cells and Li ion batteries
19:00 - 20:00	Dinner	
20:00 - 22:00	Poster section 2	

Wednesday	Dec. 12th	
7:30 - 9:30	Breakfast	
9:30 - 10:00	W. Choe (invited)	Tomographic and lens optical diagnostics of filtered emissivity and excitation temperature (as an alternative to electron temperature) profiles for large area plasmas
10:00 - 10:30	K. Ostrikov (invited)	Effects of atmospheric-pressure plasma-generated species in functionalization of organic nanomaterials and organic-inorganic nanocomposites
10:30 - 11:00	M. Lehocky (invited)	Allylamine grafting, attachment and antibacterial agent and antibacterial activity assessment of plasma pre-treated LDPE
11:00 - 12:00	Conclusions on future perspectives	
12:00 - 14:00	Lunch	
14:00 -14:30	Departures	

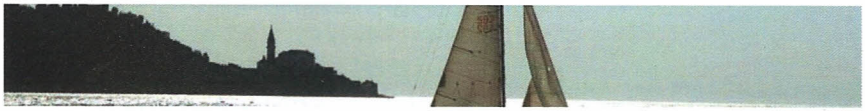

ECM 112
ICAPT2011

112 IUVSTA Executive Council Meeting and 4th International Conference on Advanced Plasma Technologies with Workshop

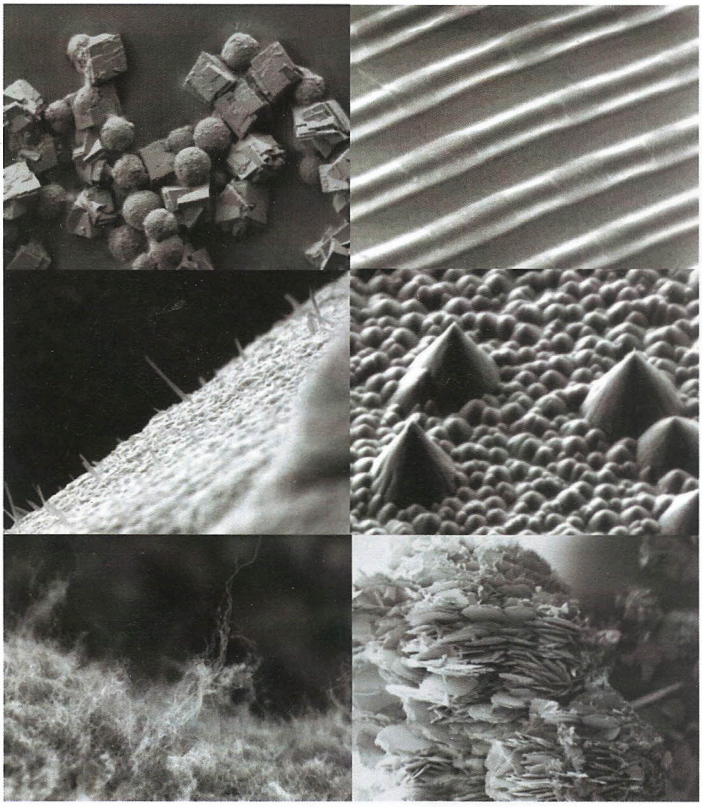

CONFERENCE PROCEEDINGS

Sep 9th-13th 2011 | Strunjan, Slovenia, EU

4th International Conference on Advanced Plasma Technologies (iCAPT-IV) with Workshop on Plasma Synthesis and Applications of Nanomaterials & 112th IUVSTA Executive Council Meeting

CONFERENCE PROCEEDINGS

September 9th — September 13th 2011, Strunjan, Slovenia

Editors of Proceedings: Miran Mozetič and Uroš Cvelbar

Published by: Slovenian Society for Vacuum Technique (DVTS Društvo za vakuumsko tehniko Slovenije), Teslova 30, SI-1000 Ljubljana, Slovenia

Graphic design: Kristina Eleršič

Printed by: Infokart d.o.o., Ljubljana

Ljubljana, September 2011

CIP - Kataložni zapis o publikaciji
Narodna in univerzitetna knjižnica, Ljubljana

533.9(082)
620.3(082)

INTERNATIONAL Conference on Advanced Plasma Technologies (4 ; 2011 ; Strunjan)

Conference proceedings / 4th International Conference on Advanced Plasma Technologies (iCAPT-IV), September 11th - Aeptember 13th 2011, Strunjan, Slovenia ; [editor Miran Mozetič]. - Ljubljana : Slovenian Society for Vacuum Technique = DVTS - Društvo za vakuumsko tehniko Slovenije, 2011

ISBN 978-961-92989-3-0
1. Mozetič, Miran, 1961-

257634560

Conference scope

The International Conference on Advanced Plasma Technologies (iCAPT) focuses on scientific and technological topics related to fundamental science and applications of low-temperature plasmas, ion beams, lasers and related approaches to plasma processing, reactor design as well as micro- and nanofabrication.

This conference aims to provide forum for extensive and in-depth discussions related to specific problems and create more opportunities for collaborations between the leaders and experts in the field and developing an international leadership for the next-generation plasma-based technologies. One of the motivations to organize this Conference is an everincreasing and more and more widespread use of plasma-based tools and techniques for processing and replacement of ecologically benign technologies like wet chemical treatments. The number of publications in the field has experienced an exceptionally strong growth due to many advantages offered by plasma technologies.

The conference is planned as a small-scale expert meeting with open participation to early-career researchers and students and will include overviews of some of the most important research directions in this field followed by the comments and detailed discussions of the main challenges and strategic directions for the future development given by leaders in relevant areas. It is also planned to develop a coordinated international approach towards achieving stronger impact of this research field on the emerging advanced plasma technologies that offer the use of effective, cheap, and environmentally-friendly plasma-based devices and processes.

Research topics:

- Fundamental topics related processing using non-equilibrium plasmas, thermal plasma, ion beams, lasers, etc.
- Elementary processes of plasma-surface interactions and processing
- Physical and chemical mechanisms using plasma-based and related processes
- Self-assembly and self-organization on plasma-exposed surfaces
- Surface science of plasma-exposed surfaces
- Plasma processing of soft matter and polymers
- Plasma treatment of waste
- Discharges and plasma processes in liquid medium
- Plasma synthesis of quantum dots, nanowires, nanotubes and nanorods
- Plasma designed nanodevices
- Present and future industrial applications of plasma-based processing
- Design of plasma processes, reactors, and associated tools and instrumentation processing
- Diagnostics of plasma species and related tools
- Multiscale modelling and numerical simulations of associated processes in the plasma, plasma sheath, solid and nanostructure surfaces
- Analysis of industrial viability and competitive advantages of plasma-based and related nanotools with any other existing approaches
- Plasma treated material characterization and surface analysis
- Comparative analysis of performance of different plasma types and sources (e.g., low- vs atmospheric pressure, thermal vs non-equilibrium plasmas etc.)
- Etching and selective etching processes in plasmas
- Plasma technologies in health care, biology, medicine, environmental remediation,
- Plasma sterilization and improvement of biocompatibility of materials with plasma
- Any other relevant topics

Organizer:

Društvo za vakuumsko tehniko slovenije (DVTS) - Slovenian Society for Vacuum Technique, Teslova 30, SI-1000 Ljubljana, Slovenia

Plasmabull

Workshop orgainzed by CO Polimat

Sponsors:

Slovenian Resarch Agency (ARRS), Slovenia

Jožef Stefan Institute, Ljubljana, Slovenia

Vacutech d.o.o.

Conference Chairs:

Miran Mozetič (Slovenia) - Chair

Uroš Cvelbar (Slovenia) - Convenor and Workshop co-chair

Makoto Sekine (Japan) – Workshop chair

Program Committee :

Miran Mozetič, Jožef Stefan Institute, Slovenia (Chair)

Francisco L. Tabares, CIEMAT, Madrid, Spain

Fabienne Poncin-Epaillard, University du Maine, France

Kostya Ostrikov, CSIRO, Australia

Primoz Eiselt, Plasmait, Austria

Kinga Kutashi, Hungarian Academy of Sciences, Hungary

Davide Ruzic, University of Illnois, Urbana, USA

Mohan R. Sankaran, Case Western Reserve University, USA

Meyya Meyyppan, NASA Ames, CA, USA

Davide Mariotti, University of Ulster, UK

Ales Mracek, Tomas Bata University, Czech Republic

Nikola Radič, Institute of Phisics, Croatia

Xiaoxia Zhong, Shanghai Jiao Tong Universtity, PR China

Masaru Hori, Nagoya University, Japan

Adrijana Skapin Sever, ZAG, Slovenia

Organizing Committee:

Uroš Cvelbar, Jožef Stefan Institute, Slovenia (LOC Chair)

Kristina Eleršič, Jožef Stefan Institute, Slovenia

Ita Junkar, Jožef Stefan Institute, Slovenia

Martina Modic, Jožef Stefan Institute, Slovenia

Aleksander Drenik, Jožef Stefan Institute, Slovenia

Alenka Vesel, Jožef Stefan Institute, Slovenia

Zdenka Perše, University of Maribor, Slovenija

Gregor Primc, Jožef Stefan Institute, Slovenia

Gregor Filipič, Jožef Stefan Institute, Slovenia

Rok Zaplotnik, Jožef Stefan Institute, Slovenia

Saša Lazović, Jožef Stefan Institute, Slovenia

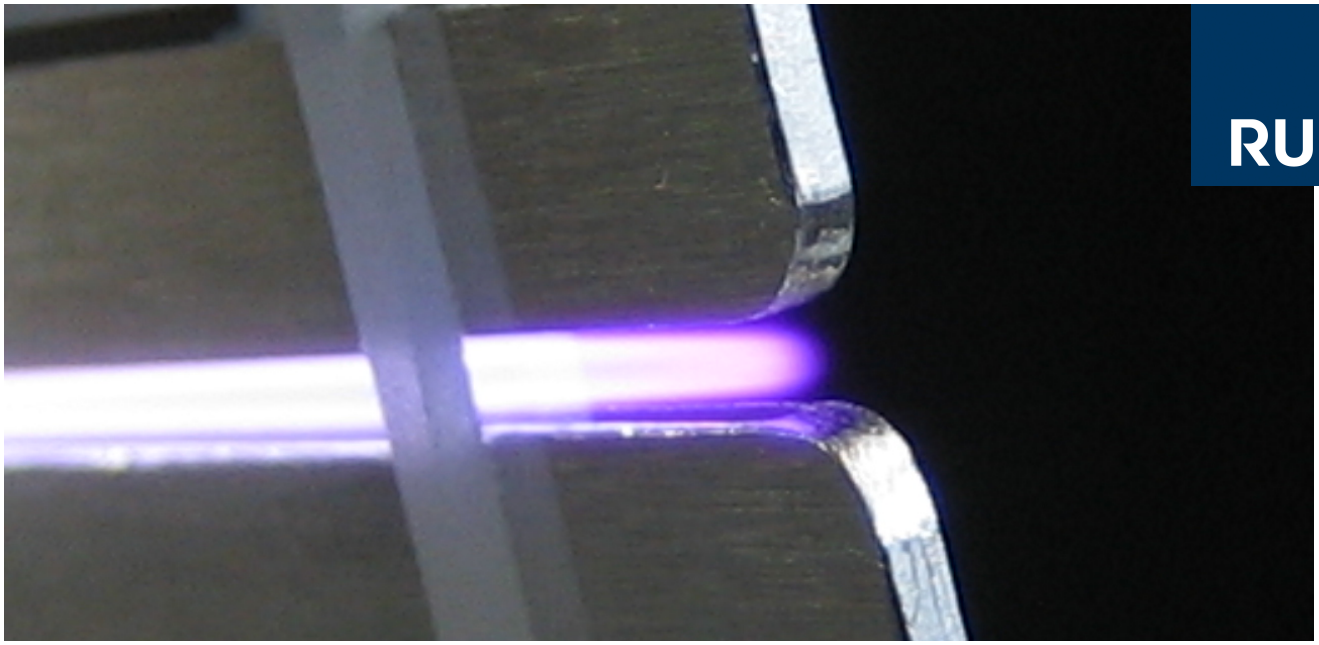

International Workshop

Young Professionals in Microplasma Research

Nov. 24-26th, 2014

Venue: Conference Center, Room 3,
Ruhr-University Bochum (RUB), Bochum, Germany

The aim of this Workshop is to bring together **young professionals in the field of non-equilibrium atmospheric plasmas**. Young researchers are encouraged to exchange their expertise and knowledge in the field of microplasmas, reactive plasma jets, plasma simulation and modelling in a conference format organized and led by young researchers.

A special session will be devoted to materials processing using microplasmas.

The workshop is supported by the German Science Foundation under the framework of the research unit "FOR 1123: Physics of Microplasmas", the Research Department "Plasmas with Complex Interctions", and by the Leverhulme International Network "Atmospheric Plasma Materials processing for Energy application". Therefore, no conference fee will be asked.

For more information please visit

www.for1123.rub.de* or *www.plasmamate.net

RESEARCH DEPARTMENT
Plasmas with Complex Interactions
DFG FORSCHERGRUPPE 1123
Physics of Microplasmas

The Leverhulme Trust

First Name	Surname	Institution / Company	Department / Division	City	Country
Konstantin	Artem'ev	Prokhorov General Physics Institute, Russian Academy of Sciences	Plasma Physics Department	Moscow	Russian Federation
Thierry	Belmonte	Institut Jean Lamour	CP2S	Nancy	France
Jan	Benedikt	Ruhr-Universität Bochum	Coupled Plasma-Solid State Systems	Bochum	Germany
Beatrix	Biskup	Ruhr-Universität Bochum	Experimentalphysik V	40468 Düsseldorf	Deutschland
Patrick	Boehm	Ruhr-University Bochum	Institute for Experimental Physics V	Bochum	Germany
Marc	Böke	Ruhr-Universität Bochum	Experimentalphysics II	Bochum	Germany
Jerome	Bredin	University of York	York Plasma Institute	York	UK
Sebastian	Burhenn	Ruhr-Universität Bochum	Institut für Experimentalphysik II	Bochum	Germany
Jan	Čech	Masaryk University	CEPLANT	Brno	Czech Republic
Uwe	Czarnetzki	Ruhr-Universität Bochum	Experimentalphysik V	Bochum	Germany
Aleksey	Davydov	Prokhorov General Physics Institute, Russian Academy of Sciences		Moscow	Russia
Valentin	Felix	GREMI		45067 Orléans	France
Torsten	Gerling	INP Greifswald	Plasma Sources	17489 Greifswald	Germany
Willems	Gert	Ruhr-Universität Bochum	Experimental Physics II	Bochum	Germany
Judith	Golda	Ruhr-Universität Bochum	Experimentalphysics II	Bochum	Germany
Yury	Gorbanev	University of York	Department of Chemistry	York	North Yorkshire
Arthur	Greb	University of York	Department of Physics	York	United Kingdom
Simon	Große-Kreul	Ruhr-Universität Bochum	Experimentalphysik II	Bochum	Germany
Magamou	Gueye	Institut Jean Lamour		Nancy	France
Mohamed	Hefny	Ruhr-Universität Bochum	coupled plasma solid state physics	Bochum	Germany
Hans	Höft	INP Greifswald		17489 Greifswald	Germany
Simon	Hübner	Ruhr Universität Bochum	APPLICATION-ORIENTED PLASMA PHYSICS	Bochum	Deutschland
Abdallah	Imam	Jean Lamour institute		Nancy	France
Ivaylo	Ivanov	Technical University - Sofia	Electrical Apparatus / Faculty of Electrical Engineering	Sofia 1000	Bulgaria
Felix David	Klute	Ruhr-Universität Bochum	Institut für Experimentalphysik V	Bochum	Deutschland
Saša	Lazović	Institute of Physics		Belgrade	Serbia
Li	Li	Gent university	faculty of applied physics	Gent	Belgium
Dirk	Luggenhölscher	Ruhr-University Bochum	Institute for Experimental Physics V	Bochum	Germany
Daniil	Marinov	LPP Ecole Polytechnique		Palaiseau	France
Plamena	Marinova	Sofia University "St. Kliment Ohridski"	Faculty of Physics	Sofia	Bulgaria
Davide	Mariotti	University of Ulster	NIBEC	Newtownabbey	United Kingdom
Calum	McDonald	University of Ulster	NIBEC	Belfast	Northern Ireland
Steffen Marius	Meier	Ruhr-Universität Bochum	Institute for Experimental Physics V, Chair for Plasma and Atomic Physics	Bochum	Germany
Thomas	Mussenbrock	Ruhr-Universität Bochum	Department of Electrical Engineering and Information Science	Bochum	Germany
Alexandre	Nominé	Institut Jean Lamour UMR CNRS 7198	Dpt. Chimie et Physique des Solides et Surfaces	54011 NANCY Cedex	France
Adam	Obrusnik	Masaryk University	Department of Physical Electronics	Brno, CZ-61137	Czech Republic
Jenish	Patel	University of Ulster	Nanotechnology and Integrated BioEngineering Centre (NIBEC)	Belfast	United Kingdom
David	Pavlinak	Masaryk University	Department of Physical Electronic	Brno	Czech Republic
Branislav	Pongrác	Faculty of Mathematics, Physics and Informatics, Comenius University Bratislava	Division of Environmental Physics	Bratislava	Slovakia
Ramasamy	Pothiraja	Institute for Electrical Engineering and Plasma Technology	Ruhr University Bochum	Bochum	Germany
Katja	Rügner	Ruhr-Universität Bochum	Research Department Plasmas with Complex Interactions	Bochum	Deutschland
Verena M.	Scharf	Ruhr-Universität Bochum	RD Plasma	Bochum	Deutschland
Christian-Georg	Schregel	Ruhr-Universität Bochum	Experimentalphysik V	Bochum	Germany
Daniel	Schroeder	Ruhr-Universität Bochum	Experimental Physics II	Bochum	Germany
Volker	Schulz-von der Gathen	Ruhr-Universität Bochum	Experimentalphysics II	Bochum	Germany
Dana	Skacelova	Masaryk University	Department of Physical Electronics	Brno	Czech Republic
Jiri	Sperka	Masaryk University	Department of Physical Electronics	Brno	Czech Republic
Stefan	Spiekermeier	Ruhr-Universität Bochum	Experimental Physics II	Bochum	Germany
Vlasta	Štěpánová	Masaryk University	Faculty of Science, Department of Physical Electronics	Brno	Czech Republic
Vladimir	Svrcek	National Institute of Advanced Industrial Science and Technology (AIST)	Research Center for Photovoltaic Technologies	Tsukuba	JAPAN
Tamilselvan	Velusamy	University of Ulster	Nanotechnology and Integrated Bioengineering Centre	Newtownabbey	Antrim
Achim	von Keudell	Ruhr-Universität Bochum	Experimentalphysics II	Bochum	Germany
Andrew	West	York Plasma Institute	Department of Physics	York	United Kingdom
Jörg	Winter	Ruhr-Universität Bochum	EP II	Bochum	Germany
shiqiang	zhang	TU/e	Apllied physics, EPG group	Eindhoven	Netherlands

Monday, Nov. 24th 2014

10:00-10:10	**Welcome** *Jan Benedikt* *Ruhr-Universität Bochum*

Session: Diagnostics / Laser (Steffen Marius Meier)

10:10-10:40	**Constricted, 'y-mode-like' discharge in the self-pulsing operation regime of the *μ*-APPJ** *Daniel Schröder* *Ruhr-Universität Bochum*
10:40-11:05	**Non-thermal Atmospheric Pressure Plasma Jet Operated in Noble Gases** *Jiri Sperka* *Masaryk University*
11:05-11:30	**He-Metastable Densities and N2 Afterglow in the pulsed constricted mode of the *μ*APPJ RF Microjet (*μ*APPJ)** *Stefan Spiekermeier* *Ruhr-Universität Bochum*
11:30-11:55	**Thomson scattering measurments in a ns pulsed atmospheric pressure plasma jet** *Christian Schregel* *Ruhr-Universität Bochum*
11:55-13:00	Lunch at Mensa

Session: Diagnostics general (Daniel Schröder)

13:00-13:30	**Power coupling and electrical characterization of a radio-frequency micro-APPJ** *Daniil Marinov* *LPP Ecole Polytechnique*
13:30-13:55	**Controlling inception and breakdown characteristics in pulsed dielectric barrier discharges by variable pulse width - influence of the pre-phase** *Hans Höft* *INP Greifswald*
13:55-14:20	**Pulse microwave capillary discharge in atmospheric presure argon** *Aleksey Davydov* *Prokhorov General Physics Institute, Russian Academy of Sciences*
14:20-14:40	Break

Session: Plasma / Liquid (Jan Benedikt)

14:40-15:05	**Influence of the water electrospray on the DC corona discharge** *Branislav Pongrác* *Faculty of Mathematics, Physics and Informatics, Comenius University Bratislava*
15:05-15:30	**Imaging of Sparks and Streamers in Water** *Simon Hübner* *Ruhr-Universität Bochum*
15:30-15:55	**Electron paramagnetic resonance spectroscopy: A valuable tool for the analysis of plasma-induced species in liquids** *Yury Gorbanev* *University of York*
15:55-16:10	walk to NB
16:00-18:30	**Labtours EP2, EP5**
18:30	**Informal welcome reception at VZ**

Tuesday, Nov. 25th 2014

Session: Application I (Ramasamy Pothiraja)

9:00-9:30	**The study of thin film and nanocrystals synthesis by means of non-equilibrium atmospheric pressure plasmas** *Jan Benedikt* *Ruhr-Universität Bochum*
9:30-9:55	**Origin of Microplasma instabilities during DC operation of silicon based MHCDs** *Valentin Felix* *GREMI*
9:55-10:20	**Surface modification due to atmospheric pressure plasma treatment during film growth of silicon dioxide like and amorphous hydrogenated carbon material** *Katja Rügner* *Ruhr-Universität Bochum*
10:20-10:40	Break

Session: Application II (Katja Rügner)

10:40-11:05	**Atmospheric-pressure plasma source for high-speed low-cost surface treatments** *Dana Skácelová* *Masaryk University*
11:05-11:30	**Photoresist Removal Using An Atmospheric Pressure Plasma Jet** *Andrew West* *York Plasma Institute*
11:30-11:55	**Dielectric Barrier Discharge (DBD) aided capillary impregnation** *Ivaylo Ivanov* *Technical University - Sofia*
11:55-13:00	Lunch at Mensa

Session: Nanoparticles (Jan Benedikt)

13:00-13:10	**LINet** *Davide Mariotti* *University of Ulster*
13:10-13:35	**Microplasma induced silicon quantum dots surface and energy band gap engineering.** *Vladimir Svrcek* *National Institute of Advanced Industrial Science and Technology (AIST)*
13:35-14:00	**Differing Microplasma-Induced Surface Chemistries on P-type and N-type Colloidal Silicon Nanocrystals** *Velusamy Tamilselvan* *University of Ulster*
14:00-14:25	**Gas phase interaction between 3-Aminopropyltriethoxysilane (APTES) and Ar-N2 afterglow: application to nanoparticles synthesis** *Magamou Gueye* *Institut Jean Lamour*
14:25-14:45	Break

Session: Nanoparticles + Surface (Davide Mariotti)

14:45-15:10	**Diamond micro-crystals and graphitic micro-balls formation in plasmoids under atmospheric pressure** *Ramasamy Pothiraja* *Ruhr-Universität Bochum*
15:10-15:35	**Silicon NPs by Atmospheric Pressure Plasma for Solar Cell Devices** *Calum McDonald* *University of Ulster*
15:35-16:00	**Combined characterisation of micro-discharges and oxide layers grown by Plasma Electrolytic Oxidation (PEO)** *Alexandre Nominé* *Institut Jean Lamour UMR CNRS 7198*
16:00-16:10	Break
16:10-18:30	**Poster session**

19:00	**Dinner @ Henrichs/Hattingen**

Wednesday, Nov. 26th 2014

Session: Fast Diagnostics (Stefan Spiekermeier)

9:00-9:30	**Using ps-TALIF to probe an atmospheric pressure plasma jet** *Jerome Bredin* *University of York*
9:30-9:55	**Optical and electrical investigation of a transient spark discharge in argon at atmospheric pressure** *Torsten Gerling* *INP Greifswald*
9:55-10:20	**Plasma diagnostics by Terahertz Time Domain Spectroscopy** *Steffen Marius Meier* *Ruhr-Universität Bochum*
10:20-10:40	Break

Session: Modeling (Simon Hübner)

10:40-11:05	**A pragmatic approach to numerical simulations of high-frequency laboratory discharges** *Adam Obrusnik* *Masaryk University*
11:05-11:30	**Characterization of Micro-discharges at atmospheric pressure with a Particle-In-Cell/Monte Carlo model** *Ya Zhang* *University of Antwerp*
11:30-11:55	**Effect of Gas Discharge Conditions on Argon Surface-Wave-Sustained Plasma Torch** *Plamena Marinova* *Sofia University "St. Kliment Ohridski"*
11:55-13:00	Lunch at Mensa

Session: Diagnostics / Afterglow (Christian Schregel)

13:00-13:30	**Mass spectrometry of ions originating from atmospheric pressure plasmas** *Simon Große-Kreul* *Ruhr-Universität Bochum*
13:30-13:55	**Plasma needle for localized biomedical applications** *Saša Lazović* *Institute of Physics, Belgrade*
13:55-14:20	**Active spectroscopic methods monitoring of active species in atmospheric radio frequency plasma** *Li Li* *Gent university*
14:20-14:40	**Diagnostics of surface dielectric barrier discharges generated above solid or liquid surfaces** *Jan Cech* *CEPLANT, Masaryk University Brno*
14:40-15:05	Break

Session: Diagnostics / OES (Simon Große-Kreul)

15:05-15:30	**The effect of air admixture in the argon flow on ozone absorption in a time modulated atmospheric pressure plasma jet** *Shiqiang Zhang* *TU/e*
15:30-15:55	**Transient emission from a ns-discharge** *Beatrix Biskup* *Ruhr-Universität Bochum*
15:55-16:10	**Break/End of the Workshop**

ISBN 978-86-7031-242-5

SPIG 2012

26th Summer School and International Symposium on the Physics of Ionized Gases

August 27th -31st, 2012, Zrenjanin Serbia

CONTRIBUTED PAPERS & ABSTRACTS OF INVITED LECTURES AND PROGRESS REPORTS

Editors
M. Kuraica, Z. Mijatović

University of Novi Sad, Faculty of Sciences
Department of Physics
Novi Sad, Serbia

SPIG 2012

26th Summer School and International Symposium on the Physics of Ionized Gases

August 27th -31st, 2012, Zrenjanin Serbia

CONTRIBUTED PAPERS & ABSTRACTS OF INVITED LECTURES AND PROGRESS REPORTS

Editors
M. Kuraica, Z. Mijatović

University of Novi Sad, Faculty of Sciences
Department of Physics
Novi Sad, Serbia

ISBN 978-86-7031-242-5

CONTRIBUTED PAPERS & ABSTRACTS OF INVITED LECTURES AND PROGRESS REPORTS of the 26th SUMMER SCHOOL AND INTERNATIONAL SYMPOSIUM ON THE PHYSICS OF IONIZED GASES

August 27th - 31st, Zrenjanin, Serbia

Editors: Milorad Kuraica
Zoran Mijatović

Publisher:

University of Novi Sad
Faculty of Sciences
Department of Physics
Trg Dositeja Obradovića 3
21000 Novi Sad, Serbia

CIP - Каталогизација у публикацији
Библиотека Матице Српске, Нови Сад

537.56(082)
539.186.2(082)
539.121.7(082)
533.9(082)

SUMMER School and International Symposium on the Physics of Ionized Gases (26 ; 2012 ; Zrenjanin)
Contributed papers & abstracts of invited lectures and progress reports / SPIG 2012 - 26th Summer School and International Symposium on the Physics of Ionized Gases, August 27th-31st, 2012, Zrenjanin Serbia ; editor Z. Mijatović. - Novi Sad : Faculty of sciences, Department of physics, 2012 (Novi Sad : Stojkov). - XVII, 403 str. : ilustr. ; 24 cm

Str. III: Preface / editors. - Napomene i bibliografske reference uz tekst. - Bibliografija uz svaki rad. - Registar.

ISBN 978-86-7031-242-5
I. SPIG (26 ; 2012 ; Zrenjanin) v. Summer School and International Symposium on the Physics of Ionized Gases (26 ; 2012 ; Zrenjanin)
a) Јонизовани гасови - Зборници b) Атоми - Интеракција - Зборници c) Плазма - Зборници
COBISS.SR-ID 272861703

Printed by:
Štamparija "Stojkov", Novi Sad, Serbia

PREFACE

This publication of Department of Physics, Faculty of Sciences, University of Novi Sad contains the Contribution Papers and the abstracts of Invited Lectures (General/Topical and Progress Reports) to be presented at the 26th Summer School and Symposium on the Physics of Ionized Gases – SPIG 2012. The symposium shall be held in Zrenjanin, Serbia, from August 27th – 31st, 2012. It is organized by Department of Physics, Faculty of Sciences, University of Novi Sad under the auspices and with support of Provincial Secretariat for Science and Technological development, Autonomous Province of Vojvodina, Ministry of Education and Science, Republic of Serbia, Institute Français Serbia and with sponsorship of European Physical Society (EPS).

The Invited Lectures and Contributed Papers are related to the following research fields: (i) Atomic Collision Processes (Electron and Photon Interactions with Atomic Particles, Heavy Particles Collisions, Swarms and Transport Phenomena); (ii) Particle and Laser Beam Interactions with Solids (Atomic Collisions in Solids, Sputtering and Deposition, Laser and Plasma Interaction with Surfaces); (iii) Low Temperature Plasmas (Plasma Spectroscopy and Other Diagnostics Methods, Gas Discharges, Plasma Applications and Devices); (iv) General Plasmas (Fusion Plasmas, Astrophysical Plasmas and Collective Phenomena). These four disciplines have strong interaction in numerous applications, however, due to the development of specialized international conferences, it has become increasingly rare that such a wide range of topics are covered at a single conference. Except the abstracts of invited lectures this book includes 78 contributed papers from which one can have impression about state-of-art of investigations in these four research fields.

The Editors would like to thank to the members of the Scientific and Advisory Committees of SPIG 2012 for their efforts in proposing the invited lectures and review of the contributed papers. Especially we acknowledge the support of all of the members of the Organizing Committee for a huge work in organization of the Conference.

Editors
Milorad M. Kuraica and Zoran Mijatović

26th SPIG

Scientific Committee

M. Kuraica (Chairmen) Serbia

S. Buckman, Australia
J. Burgdoerfer, Austria
Z. Donko, Hungary
V. Guerra, Portugal
D. Jovanović, Serbia
K. Lieb, Germany
G. Malović, Serbia
I. Mančev, Serbia
A. Milosavljević, Serbia
N. J. Mason, USA
M. Danezis, Greece
Z. Mijatović, Serbia
K. Mima, Japan
Z. Mišković, USA
G. Poparić, Serbia
L. Č. Popović, Serbia
Z. Rakočević, Serbia
Y. Serruys, France
N. Simonović, Serbia
M. Škorić, Serbia

Advisory Committee

D. Belić
N. Konjević
J. Labat
B. P. Marinković
S. Đurović
M. S. Dimitrijević
N. Bibić
M. Milosavljević
Z. Lj. Petrović
J. Purić
B. Stanić

Organizing Committee

Z. Mijatović (Chairmen)

I. Savić (Secretary)
S. Đurović
N. Cvetanović
R. Kobilarov
T. Gajo
Z. Nađ
L. Gavanski

CONTENT

SECTION 1.

Invited Lectures

Contributed papers

SECTION 2.

Invited Lectures

Contributed papers

SECTION 3.

Invited Lectures

Contributed Papers

SECTION 4.

Invited Lectures

Contributed Papers

27th Summer School and International Symposium on the Physics of Ionized Gases

August 26-29, 2014, Belgrade, Serbia

CONTRIBUTED PAPERS

&

ABSTRACTS OF INVITED LECTURES, TOPICAL INVITED LECTURES, PROGRESS REPORTS AND WORKSHOP LECTURES

Editors:
Dragana Marić
Aleksandar R. Milosavljević
Zoran Mijatović

Institute of Physics, Belgrade
University of Belgrade

Serbian Academy
of Sciences and Arts

www.spig2014.ipb.ac.rs

Nevena

27th Summer School and International Symposium on the Physics of Ionized Gases

SPIG 2014

CONTRIBUTED PAPERS

&

ABSTRACTS OF INVITED LECTURES,
TOPICAL INVITED LECTURES, PROGRESS REPORTS
AND WORKSHOP LECTURES

Editors

Dragana Marić, Aleksandar R. Milosavljević and
Zoran Mijatović

Institute of Physics, Belgrade
University of Belgrade

Serbian Academy
of Sciences and Art

Belgrade, 2014

CONTRIBUTED PAPERS & ABSTRACTS OF INVITED LECTURES, TOPICAL INVITED LECTURES, PROGRESS REPORTS AND WORKSHOP LECTURES
of the 27th Summer School and International Symposium on the Physics of Ionized Gases

August 26 – 29, 2014, Belgrade, Serbia

Editors:

Dragana Marić, Aleksandar R. Milosavljević and Zoran Mijatović

Publishers:

Institute of Physics,Belgrade
Pregrevica 118, P. O. Box 68
11080 Belgrade, Serbia

Klett izdavačka kuća d.o.o.
Maršala Birjuzova 3-5, IV sprat
11000 Belgrade

Computer processing:

Sanja D. Tošić, Nikola Škoro and Miloš Ranković

Printed by

CICERO
Belgrade

Number of copies

300

ISBN 978-86-7762-600-6

SPIG 2014

SCIENTIFIC COMMITTEE

Z. Mijatović (Chair), Serbia
S. Buckman, Australia
J. Burgdörfer, Austria
M. Danezis, Greece
Z. Donko, Hungary
V. Guerra, Portugal
M. Ivković, Serbia
D. Jovanović, Serbia
K. Lieb, Germany
I. Mančev, Serbia
D. Marić, Serbia
N. J. Mason, UK
A. R. Milosavljević, Serbia
K. Mima, Japan
Z. Mišković, Canada
B. Obradović, Serbia
G. Poparić, Serbia
L. C. Popović, Serbia
Z. Rakočević, Serbia
Y. Serruys, France
N. Simonović, Serbia
M. Škorić, Japan
M. Trtica, Serbia

ADVISORY COMMITTEE

D. Belić
N. Bibić
M. S. Dimitrijević
S. Đurović
N. Konjević
J. Labat
B. P. Marinković
M. Milosavljević
Z. LJ. Petrović
J. Purić
B. Stanić

ORGANIZING COMMITTEE

Institute of Physics Belgrade

D. Marić (Co-chair)
A. R. Milosavljević (Co-chair)
S. D. Tošić (Co-Secretary)
N. Škoro (Co-Secretary)
B. P. Marinković
M. Cvejić
J. Sivoš
K. Spasić
M. Ranković

Serbian Academy of Sciences and Arts

Z. Lj. Petrović
M. Ivanović

SPIG 2014 CONFERENCE TOPICS

Section 1.
ATOMIC COLLISION PROCESSES

1.1. Electron and Photon Interactions with Atomic Particles
1.2. Heavy Particle Collisions
1.3. Swarms and Transport Phenomena

Section 2.
PARTICLE AND LASER BEAM INTERACTION WITH SOLIDS

2.1. Atomic Collisions in Solids
2.2. Sputtering and Deposition
2.3. Laser and Plasma Interaction with Surfaces

Section 3.
LOW TEMPERATURE PLASMAS

3.1. Plasma Spectroscopy and Other Diagnostics Methods
3.2. Gas Discharges
3.3. Plasma Applications and Devices

Section 4.
GENERAL PLASMAS

4.1. Fusion Plasmas
4.2. Astrophysical Plasmas
4.3. Collective Phenomena

REMOVAL OF REACTIVE ORANGE 16 FROM WATER BY PLASMA NEEDLE

Tatjana Mitrović[1,2], Dejan Maletić[1], Nataša Tomić[1], Saša Lazović[1], Gordana Malović[1], Tanja Nenin[2], Uroš Cvelbar[3], Zorana Dohčević-Mitrović[1] and Zoran Lj. Petrović[1]

[1]*Institute of Physics, University of Belgrade, Pregrevica 118, 11080 Belgrade, Serbia*
[2]*Institute for development of water recources "Jaroslav Černi", Jaroslava Černog 80, 11226 Belgrade, Serbia*
[3]*Jožef Stefan Insitute, Jamova Cesta 39, Ljubljana, SI-1000, Slovenia*
email:lazovic@ipb.ac.rs

Abstract. In this article we present the results of decolourisation and degradation of Reactive Orange 16 dye in the water by a plasma needle. Argon flow rates are varied in order to improve the removal efficiency. We find that the complete decolourization and a considerable percent of mineralization are achieved after 60 min of plasma treatment for the flow rates higher than 4 slm. The decolourisation and mineralization effects are measured by UV/VIS spectrophotometry and total organic carbon content.

1. INTRODUCTION

Plasma technologies are used in wastewater treatment because of a high removal efficiency of organic pollutants. Besides the capability to abundantly generate chemically active species, plasma is used for water decontamination because of convenient operating conditions (atmospheric pressure and relatively low temperature) [1].

There are various types of non-thermal plasma devices such as plasma jets, plasma needle, gliding arc, etc. [2-4]. These plasmas can produce high concentrations of radicals [5]. Plasma generated radicals enable numerous biomedical applications. In our previous research we have used plasma needle for treatment of biological samples like bacteria, human stem cells, plant stem cells (calli) [2, 6-8]. Besides the biomedical applications, radicals are important in advanced oxidation processes [1]. OH radicals have a particularly large oxidation potential. They interact with organic pollutants and can decompose them into less or non-harmful components.

In this paper we present the results of decolourisation of Reactive Orange 16 (RO 16) azo dye recorded using the UV/VIS spectroscopy.

Furthermore, we present degradation curves for two different argon flow rates (4 and 8 slm) obtained by total organic carbon measurements (TOC).

2. EXPERIMENTAL SETUP

The experimental setup is given on Figure 1. Plasma needle consists of a body made of Teflon, a central electrode made of copper, and a glass tube. A dye sample is prepared with distilled water (50 mg/l, 25 ml). The needle tip is immersed into the solution as presented in Figure 1. Magnetic stirrer (300 rpm) preserved the homogeneity of the sample. We use different argon flow rates (1, 4, and 8 slm). Decolourisation is monitored by measuring absorbance after plasma treatments at 493.7 nm (which corresponds to the -N=N- bond). A complete dye spectra and absorbance at a fixed wavelength are measured by UV/VIS spectrophotometry. Degradation is recorded based on the total organic carbon content.

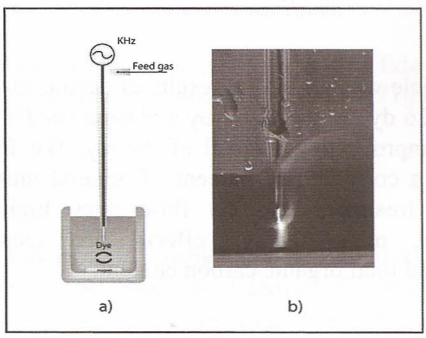

Figure 1. a) Experimental setup, b) Plasma in the dye solution.

3. RESULTS AND DISCUSSION

The degradation rate of RO 16 is determined following two different processes: the colour loss and oxidation. The colour loss gives evidence that the chromophore group which is responsible for the absorption of the dye molecule in the visible region of the spectral range is eliminated. This colorant is characterized by azo group as a chromophore (–N=N–) which has a maximum absorption at 493.7 nm. Decolourisation is presented on Figure 2. For the given set of experimental conditions we observe a decrease of absorbance and that the total decolourisation is achieved after 60 min of plasma treatment for the flow rates of 4 and 8 slm. However, for the lowest flow rate of 1 slm the colour loss is not complete even after 60 min of treatment, but it is obvious that there is a decreasing trend. In this case, longer treatment times could lead to the total decolourisation. It is very interesting to compare the decolourisation kinetics for 4 and 8 slm flow rates in the first 30 min and beyond that time. We can see that when we double the flow rate, the degradation rate significantly increases for the

first 30 min. For example, after 10 min of treatment the absorbance ratio (A/A_0) is reduced to 20 and 40 % for 8 and 4 slm flow rates of argon, respectively. However, after 30 min, the increase in flow rate does not contribute that much to the decolourisation rate as compared to the previous case.

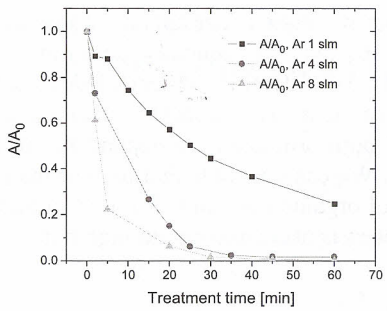

Figure 2. Decolourisation of Reactive orange 16 for three different argon flow rates (1, 4, 8 slm).

In order to demonstrate that the colorant is not just decolourised, but also degraded to some extent, we have performed TOC measurements. Although a full decolourisation is achieved after 60 min of plasma treatment, there is a possibility that hazardous by-products may appear as a result of incomplete decomposition of the molecule. To verify this, total organic carbon content, which concerns bond breaking in the aromatic part of the dye (C–C, C=C, C–N, C–S) is measured.

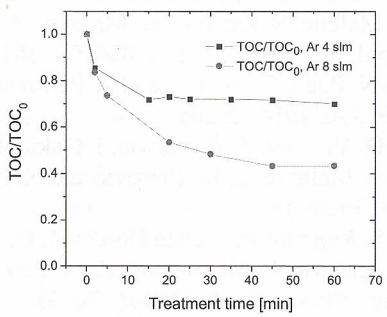

Figure 3. Degradation of Reactive Orange 16 for two different argon flow rates (4 and 8 slm)

We can see that the total organic carbon is reduced by about 60 % for 8 slm and only 30 % for 4 slm after 60 minutes of plasma treatment (Figure 3). As in the case of decolourisation, mineralisation rate also depends on the flow rate. For smaller flow rates the oxidation process is typically slower as compared to the

higher flow rates. Unlike decolourisation, full degradation was not reached after 60 min of plasma treatment.

4. CONCLUSION

In this paper we show the results of decolourisation and degradation of Reactive Orange 16 dye in aqueous solution. We find that complete decolourisation and a considerable percent of degradation are achieved after 1 hour of plasma treatment. As expected, degradation is much slower than decolourisation and both processes are dependent on treatment conditions such as the gas flow rate. We can conclude that the plasma needle can be a promising device for removal of organic pollutants from water and that further optimization of treatment parameters is needed to obtain high removal rates.

Acknowledgements

MESTD, Republic of Serbia, project no. III 41011 and ON 171037.

REFERENCES

[1] B. Jiang, J. Zheng, S. Qiu, M. Wu, Q. Zhang, Z. Yan and Q. Xue, Chem. Eng. J., 236, 348–368 (2014).

[2] S. Lazović, N. Puač, M. Miletić, D. Pavlica, M. Jovanović, D. Bugarski, S. Mojsilović, D. Maletić, G. Malović, P. Milenković and Z. Petrović, New J. Phys., 12, 8, 083037 (2010).

[3] M. R. Ghezzar, F. Abdelmalek, M. Belhadj, N. Benderdouche and a Addou, J. Hazard. Mater., 164, 2–3, 1266–74 (2009).

[4] N. Puač, D. Maletić, S. Lazović, G. Malović, A. Đorđević and Z. Lj. Petrović, Appl. Phys. Lett., 101, 2, 024103 (2012).

[5] G. Malović, N. Puač, S. Lazović and Z. Petrović, Plasma Sources Sci. Technol., 19, 3, 034014 (2010).

[6] M. Miletić, D. Vuković, I. Živanović, I. Dakić, I. Soldatović, D. Maletić, S. Lazović, G. Malović, Z. Lj. Petrović and N. Puač, Cent. Eur. J. Phys., 12, 3, 160–167 (2014).

[7] M. Miletić, S. Mojsilović, I. Okić Đorđević, D. Maletić, N. Puač, S. Lazović, G. Malović, P. Milenković, Z. Lj. Petrović and D. Bugarski, J. Phys. D. Appl. Phys., 46, 34, 345401 (2013).

[8] N. Puač, S. Živković, N. Selaković, M. Milutinović, J. Boljević, G. Malović and Z. Lj. Petrović, Appl. Phys. Lett., 104, 21, 214106 (2014).

Univerzitet u Beogradu

Fakultet za fizičku hemiju

Diplomski rad

Određivanje koncentracije neutrala i jona energetsko masenim spektrometrom u atmosferskom radiofrekventnom pražnjenju malih dimenzija

Dejan Maletić

Beograd, 2008.

Diplomski rad pod nazivom "Određivanje koncentracije neutrala i jona energetsko masenim spektrometrom u atmosferskom radiofrekventnom pražnjenju malih dimenzija " je rađen u Laboratoriji za neravnotežnu plazmu Instituta za fiziku u Zemunu, pod rukovodstvom dr. Nevene Puač.

Zahvalio bih se mentoru dr. Neveni Puač i Saši Lazoviću na pomoći oko izbora teme diplomskog rada, kao i na obezbeđivanju uslova za izvođenje eksperimenata, pomoći prilikom merenja i na sugestijama pri pisanju diplomskog rada.

Takođe bih se zahvalio mentoru dr. Ivanki Holclajtner Antunović profesoru Fakulteta za fizičku hemiju na jasnim i preciznim savetima prilikom pisanja i sređivanja diplomskog rada.

Sadržaj

Fizički fakultet

Univerzitet u Beogradu

Aktivacija Langmuirove sonde i merenje koncentracije elektrona i jona u niskotemperaturnim plazmama u argonu

Student

Kosta Spasić

Br. Indeksa 3030046

Mentor

dr Nevena Puač

Beograd, 2010

Diplomski rad pod nazivom "Aktivacija Langmuirove sonde i merenje koncentracije elektrona i jona u niskotemperaturnim plazmama u argonu" je urađen pod rukovodstvom dr Nevene Puač u Laboratoriji za gasnu elektroniku, Instituta za fiziku u Beogradu kojom rukovodi prof. dr Zoran Lj. Petrović.

Svoju zahvalnost dugujem pre svega prof. dr Zoranu Lj. Petroviću koji me je zainteresovao za ovu oblast fizike i omogućio izradu diplomskog rada u okviru njegove grupe na Institutu za fiziku. Posebno bih se zahvalio svom mentoru dr Neveni Puač na pomoći pri izboru teme, uputstvima i savetima pri izradi kao i na velikom strpljenu i nesebičnosti. Zahvalio bih se još i dr Saši Lazoviću za uspešno rukovođenje eksperimentima, pomoći pri obradi rezultata merenja i korisnim sugestijama pri izradi rada. Takođe veliku zahvalnost dugujem i dr Gordani Malović koja je svojim znanjem i iskustvom doprinela izradi i uobličavanju ovog rada.

Na kraju, zahvalio bih se svim članovima Laboratorije za gasnu elektroniku na svojoj nesebičnosti i pruženoj pomoći.

Sadržaj

Advisory Panel

Outside the Editorial Board, the journal heavily relies on a selection of physicists and other scientists who regularly provide us with constructive and careful analysis of those papers submitted to the journal. We are keen to offer recognition to these outstanding referees, who currently remain largely unrecognised by the community. Therefore, it is with pleasure that we announce the installation of our Advisory Panel, which will be made up of these outstanding referees, and thus publicly recognise, for the first time, their contribution to the journal.

Advisory Panel Members

04 -11- 2015

РЕПУБЛИКА СРБИЈА
ЗАВОД ЗА ИНТЕЛЕКТУАЛНУ СВОЈИНУ

990 број 2015/10418-П-2012/0550
Датум: 20.10.2015. године
Београд, Кнегиње Љубице 5

2-1/7

Завод за интелектуалну својину је, на основу члана 31. Закона о министарствима („Службени гласник РС”, бр. 44/14, 14/15 и 54/15), чл. 67, 69, 70. и 107. Закона о патентима („Службени гласник РС”, број 99/11) и решења о специјалним овлашћењима за потпис аката Завода за интелектуалну својину број 4/1299 од 31.12.2014. године, у управном поступку по пријави патента број П-2012/0550, подносилаца ЛАЗОВИЋ Слободан, Милке Трајловић 38, 36000 Краљево, RS и ЛАЗОВИЋ Саша, Милке Трајловић 38, 36000 Краљево, RS, које заступа PLAVŠA & PLAVŠA patentna kancelarija, Струмичка 51, 11050 Београд, RS, ради признања патента, донео следеће

Р Е Ш Е Њ Е

I **ПРИЗНАЈЕ СЕ** патент по пријави број П-2012/0550 од 12.12.2012. године, за проналазак под називом: „**ХРАНИЛИЦА ЗА ПЧЕЛЕ СА КОНТРОЛИСАНИМ ДНЕВНИМ УНОСОМ ТЕЧНЕ ХРАНЕ**”, према опису, патентним захтевима и цртежима из патентног списа.

II **УПИСУЈЕ СЕ** у Регистар патената Завода за интелектуалну својину, признато право из тачке I диспозитива овог решења под бројем

54246

Носилац (оци) патента:

ЛАЗОВИЋ проф. Слободан
Милке Трајловић 38,
36000 Краљево, RS;

ЛАЗОВИЋ др Саша
Милке Трајловић 38,
36000 Краљево, RS

Проналазач(и):

ЛАЗОВИЋ проф. Слободан
Милке Трајловић 38,
36000 Краљево, RS;

ЛАЗОВИЋ др Саша
Милке Трајловић 38,
36000 Краљево, RS

Признаје се право
првенства по пријави:

III Податке о признатом праву и први патентни захтев објавити у „Гласнику интелектуалне својине” број 6/2015.

О б р а з л о ж е њ е

ЛАЗОВИЋ Слободан, Милке Трајловић 38, 36000 Краљево, RS и ЛАЗОВИЋ Саша, Милке Трајловић 38, 36000 Краљево, RS, поднели су дана 12.12.2012. године, пријаву патента број П-2012/0550, за проналазак под називом: „ХРАНИЛИЦА ЗА ПЧЕЛЕ СА КОНТРОЛИСАНИМ ДНЕВНИМ УНОСОМ ТЕЧНЕ ХРАНЕ".

У спроведеном поступку суштинског испитивања пријаве патента, у смислу члана 104. Закона о патентима („Службени гласник РС", број 99/11), утврђено је да су испуњени сви услови за признање патента прописани овим законом.

Имајући у виду наведено, Завод је, на основу чл. 107, 109. и 111. Закона о патентима, одлучио као у диспозитиву овог решења.

Такса за исправу о признатом праву плаћена је у складу са Тарифним бројем 123. Тарифе републичких административних такси, која је саставни део Закона о републичким административним таксама („Службени гласник РС", бр. 43/03, 51/03-исправка, 53/04, 42/05, 61/05, 101/05-др. закон, 42/06, 47/07, 54/08, 5/09, 54/09, 35/10, 50/11, 70/11, 55/12, 93/12, 47/13, 65/13-др. закон, 57/14 и 45/15-усклађени дин. износи), док су накнада трошкова за објаву података о признатом праву и накнада трошкова за штампање патентног списа плаћене у складу са Тарифним бр. 1. и 2 Тарифе накнада посебних трошкова поступка који води Завод за интелектуалну својину и трошкова за пружање информационих услуга Завода, која је саставни део Одлуке о висини посебних трошкова поступка који води Завод за интелектуалну својину и накнада трошкова за пружање информационих услуга Завода („Службени гласник РС", број 113/13), а доказ о уплати приложен уз поднесак број RS/E/2015/5226-П-2012/0550 од 2.10.2015. године.

Упутство о правном средству:
Против овог решења може се изјавити жалба Влади Републике Србије у року од 15 дана од дана пријема решења, а преко овог Завода. Уз жалбу треба доставити доказ о уплати административне таксе у износу од 440,00 динара.

Решење доставити:
- подносиоцу пријаве/заступнику
PLAVŠA & PLAVŠA patentna kancelarija
Струмичка 51
11050 Београд
- регистру
- издаваштву преко информационог система
- документацији
- у спис

Самостални саветник

Милан Миљевић

New Journal of Physics

The open-access journal for physics

www.njp.org

100 years of superconductivity

Best of 2010

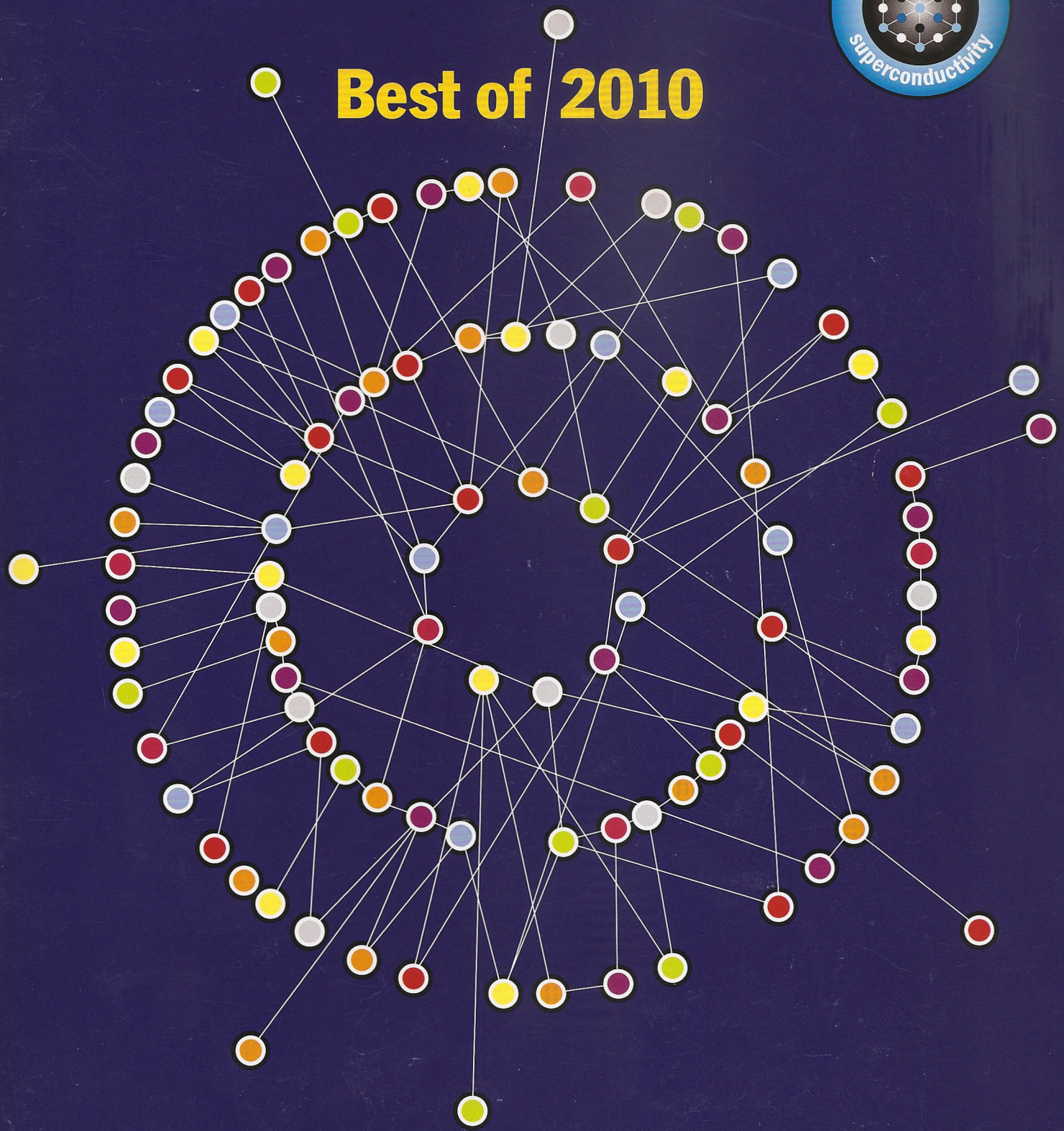

Deutsche Physikalische Gesellschaft DPG | IOP Institute of Physics

PLASMA PHYSICS

CONDENSED MATTER

NANOPHYSICS

SURFACE SCIENCE AND THIN FILMS

SURFACE SCIENCE AND THIN FILMS *(continued)*

SOFT MATTER AND BIOLOGICAL PHYSICS

STATISTICAL PHYSICS AND COMPLEX SYSTEMS

LIST OF EDITORS

CONTENTS

→

ATOMIC AND MOLECULAR PHYSICS

OPTICS AND IMAGING

QUANTUM OPTICS AND LASERS

→

Orsay, France
[6] Institute of Modern Physics, Chinese Academy of Science, 730000 Lanzhou, People's Republic of China

Intense heavy ion beams offer a unique tool for generating samples of high energy density matter with extreme conditions of density and pressure that are believed to exist in the interiors of giant planets. An international accelerator facility named FAIR (Facility for Antiprotons and Ion Research) is being constructed at Darmstadt, which will be completed around the year 2015. It is expected that this accelerator facility will deliver a bunched uranium beam with an intensity of 5×10^{11} ions per spill with a bunch length of 50–100 ns. An experiment named LAPLAS (Laboratory Planetary Sciences) has been proposed to achieve a low-entropy compression of a sample material like hydrogen or water (which are believed to be abundant in giant planets) that is imploded in a multi-layered target by the ion beam. Detailed numerical simulations have shown that using parameters of the heavy ion beam that will be available at FAIR, one can generate physical conditions that have been predicted to exist in the interior of giant planets. In the present paper, we report simulations of compression of water that show that one can generate a plasma phase as well as a superionic phase of water in the LAPLAS experiments.

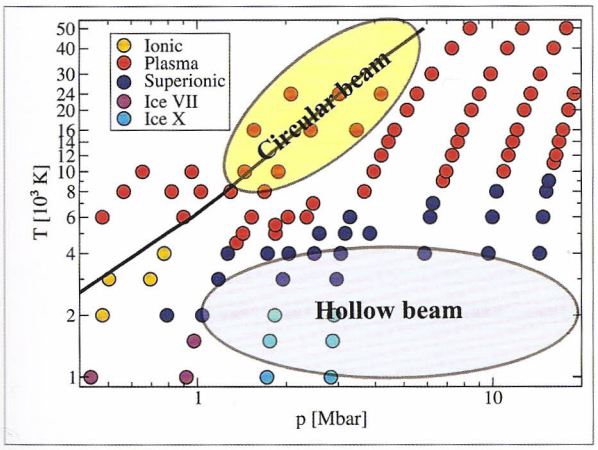

Each colored point corresponds to a quantum molecular dynamics simulation in thermodynamic equilibrium. When the electronic conductivity exceeds 100 (ohm cm)$^{-1}$, the ionic (dissociated) fluid is labeled as plasma. The solid line is the principal Hugoniot curve.

The effect of a plasma needle on bacteria in planktonic samples and on peripheral blood mesenchymal stem cells

General Scientific Summary

Saša Lazović *et al* 2010 *New J. Phys.* **12** 083037

Saša Lazović[1], Nevena Puač[1], Maja Miletić[2], Dušan Pavlica[2], Milena Jovanović[2], Diana Bugarski[3], Slavko Mojsilović[3], Dejan Maletić[1], Gordana Malović[1], Pavle Milenković[2] and Zoran Petrović[1]
[1] Institute of Physics, Pregrevica 118, 11080 Belgrade, Serbia
[2] Faculty of Stomatology, Dr SubotiÐa 8, 11000 Belgrade, Serbia
[3] Institute for Medical Research, Dr SubotiÐa–starijeg 4, 11000 Belgrade, Serbia

In this paper, we study the application of a plasma needle to induce necrosis in planktonic samples containing a single breed of bacteria. Two different types of bacteria, *Staphylococcus aureus* (ATCC 25923) and *Escherichia coli* (ATCC 25922), were covered in this study. In all experiments with bacteria, the samples were liquid suspensions of several different concentrations of bacteria prepared according to the McFarland standard. The second system studied in this paper was human peripheral blood mesenchymal stem cells (hPB-MSC). In the case of hPB-MSC, two sets of experiments were performed: when cells were covered with a certain amount of liquid (indirect) and when the cell sample was in direct contact with the plasma. Most importantly, the study is made with the aim to see the effects when the living cells are in a liquid medium, which normally acts as protection against the many agents that may be released by plasmas. It was found that a good effect may be expected for a wide range of initial cell densities and operating conditions causing destruction of several orders of magnitude even under the protection of a liquid. It was established independently that a temperature increase could not affect the cells under the conditions of our experiment, so the effect could originate only from the active species produced by the plasma. In the case of those hPB-MSC that were not protected by a liquid, gas flow proved to produce a considerable effect, presumably due to poor adhesion of the cells, but in a liquid the effect was only due to the plasma. Further optimization of the operation may be attempted, opening up the possibility of localized *in vivo* sterilization.

Staphylococcus aureus treated by plasma. The flow rate of He was 0.5 slm and the power was 1.6 W. Four different starting concentrations of bacteria were used: (1) 12×10^8 colony-forming units (CFU) ml^{-1}; (2) 12×10^7 CFU ml-1; (3) 12×10^6 CFU ml^{-1}; (4) 12×10^5 CFU ml^{-1}.

CONDENSED MATTER

Advanced spectroscopic synchrotron techniques to unravel the intrinsic properties of dilute magnetic oxides: the case of Co:ZnO

A Ney *et al* 2010 *New J. Phys.* **12** 013020

A Ney[1], M Opel[2], T C Kaspar[3], V Ney[1], S Ye[1], K Ollefs[1], T Kammermeier[1], S Bauer[2], K-W Nielsen[2], S T B Goennenwein[2], M H Engelhard[3], S Zhou[4], K Potzger[4], J Simon[5], W Mader[5], S M Heald[6], J C Cezar[7], F Wilhelm[7], A Rogalev[7], R Gross[2] and S A Chambers[3]
[1] Fakultät für Physik and CeNIDE, Universität Duisburg-Essen, 47057 Duisburg, Germany
[2] Walther-Meißner-Institut, Bayerische Akademie der Wissenschaften, 85748 Garching, Germany
[3] Fundamental and Computational Sciences Directorate, Pacific Northwest National Laboratory, Richland, WA 99352, USA
[4] Institut für Ionenstrahlphysik und Materialforschung, Forschungszentrum Dresden-Rossendorf e.V., 01328 Dresden, Germany
[5] Institut für Anorganische Chemie, Rheinische Friedrich-Wilhelms-Universität, 53117 Bonn, Germany
[6] Advanced Photon Source, Argonne National Laboratory Argonne, IL 60439, USA
[7] European Synchrotron Radiation Facility (ESRF), 38043 Grenoble, France

Video abstracts can be very useful because often the evolution of natural systems can be more clearly depicted using videos rather than a set of figures. Also, videos typically do not require as much effort as reading written abstracts and figure captions.

Joaquim Fort, Universitat de Girona, Spain

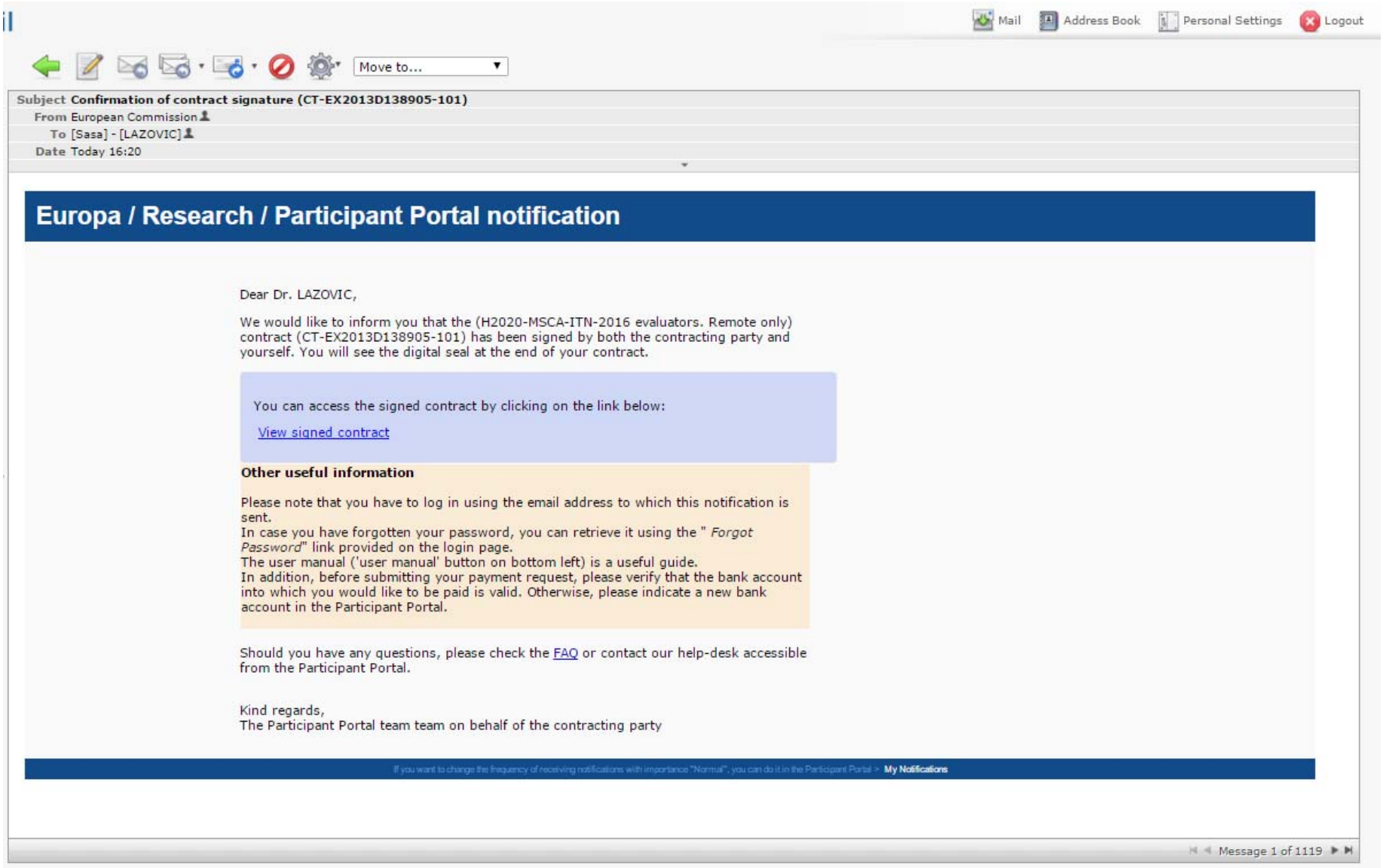
Mail
Address Book
Personal Settings
Logout
Move to...
Subject Confirmation of contract signature (CT-EX2013D138905-101)
From European Commission
To [Sasa] - [LAZOVIC]
Date Today 16:20
Europa / Research / Participant Portal notification
Dear Dr. LAZOVIC,
We would like to inform you that the (H2020-MSCA-ITN-2016 evaluators. Remote only) contract (CT-EX2013D138905-101) has been signed by both the contracting party and yourself. You will see the digital seal at the end of your contract.
You can access the signed contract by clicking on the link below:
View signed contract
Other useful information
Please note that you have to log in using the email address to which this notification is sent.
In case you have forgotten your password, you can retrieve it using the " Forgot Password" link provided on the login page.
The user manual ('user manual' button on bottom left) is a useful guide.
In addition, before submitting your payment request, please verify that the bank account into which you would like to be paid is valid. Otherwise, please indicate a new bank account in the Participant Portal.
Should you have any questions, please check the FAQ or contact our help-desk accessible from the Participant Portal.
Kind regards,
The Participant Portal team team on behalf of the contracting party
If you want to change the frequency of receiving notifications with importance "Normal", you can do it in the Participant Portal > My Notifications
Message 1 of 1119

JAVNI SKLAD
REPUBLIKE SLOVENIJE
ZA RAZVOJ KADROV
IN ŠTIPENDIJE

Dunajska 22, SI - 1000 Ljubljana | telefon (01) 434 10 80 | faks (01) 434 58 99
info@sklad-kadri.si | www.sklad-kadri.si

Številka: 11013-56/2010-9
Datum: 19. januar 2011

Skladno s 207. členom Zakona o splošnem upravnem postopku (Ur.l. RS, št. 24/2006-UPB2, 105/2006-ZUS-1, 126/2007, 65/2008, 47/2009 Odl. US: U-I-54/06-32 (48-2009 popr.), 8/2010, v nadaljevanju: ZUP), Splošnimi pogoji poslovanja Javnega sklada Republike Slovenije za razvoj kadrov in štipendije (Ur.l. RS, št. 91/2009) in na zahtevo prijavitelja **Institut Jožef Stefan, Jamova cesta 39, 1000 Ljubljana** (v nadaljevanju: prijavitelj), v zvezi s prijavo na »Javni razpis za sofinanciranje pedagoškega ali raziskovalnega sodelovanja tujih državljanov v Sloveniji v letu 2010/2011« (Ur.l. RS, št. 72/2010; v nadaljevanju: javni razpis), Javni sklad Republike Slovenije za razvoj kadrov in štipendije izdaja naslednjo

O D L O Č B O

1. Vlogi prijavitelja **Institut Jožef Stefan** za sofinanciranje stroškov 12-mesečnega raziskovalnega dela Saša Lazovića, roj. 3.2.1980, stalno prebivališče Bulevar Arsenija Čarnojevića 209/19, 11070 Novi Beograd, Srbija, v Sloveniji **se ugodi.**

2. Prijavitelju se za sofinanciranje stroškov raziskovalnega sodelovanja iz prejšnjega odstavka dodelijo finančna sredstva v višini [redacted].

3. Prijavitelj mora za podpis pogodbe o sofinanciranju javnemu skladu predložiti obvestilo o prihodu tujega gostujočega znanstvenika Saša Lazovića, ki mora vključevati izjavo o pridobitvi ustreznega dovoljenja za prebivanje za tujega gostujočega znanstvenika s številko in datumom izdaje tega dovoljenja ter datumi njegove veljavnosti ter izjavo o datumu začetka raziskovalnega sodelovanja glede na veljavnost dovoljenja za prebivanje.

4. Posebni stroški v tem postopku niso nastali.

O b r a z l o ž i t e v

Institut Jožef Stefan (v nadaljevanju: prijavitelj) je dne 29.10.2010 vložil vlogo na razpis za sofinanciranje pedagoškega ali raziskovalnega sodelovanja tujih državljanov v Sloveniji v letu 2010/2011 Javnega sklada Republike Slovenije za razvoj kadrov in štipendije, ki je bil objavljen v Uradnem listu RS, št. 72/2010, in sicer za sofinanciranje stroškov 12-mesečnega raziskovalnega dela tujega znanstvenika Saša Lazovića (v nadaljevanju: gostujoči znanstvenik). Vloga je bila pravočasna, vložil jo je upravičen prijavitelj.

Prijavitelj je prijavnici priložil izjavo gostujočega znanstvenika, s katero ta soglaša, da ga prijavitelj prijavi na razpis, fotokopijo veljavnega potnega lista ter fotokopijo potrdila o pridobljenem doktorskem nazivu.

Vloga ob prijavi ni bila popolna, vendar je prijavitelj vlogo pravočasno in v celoti dopolnil skladno s pozivom k dopolnitvi vloge.

Pravočasna in popolna vloga se je uvrstila v nadaljnji postopek ugotavljanja izpolnjevanja razpisnih pogojev.

Javni razpis določa, da se za sofinanciranje stroškov raziskovalnega sodelovanja tujih državljanov v Sloveniji lahko prijavijo izobraževalne ali raziskovalne ustanove s sedežem v Republiki Sloveniji, vpisane v evidenco izvajalcev raziskovalne in razvojne dejavnosti pri Javni agenciji za raziskovalno dejavnost Republike Slovenije (v nadaljevanju: ARRS), za raziskovalno sodelovanje gostujočega znanstvenika na raziskovalnem projektu ali programih, ki so predhodno odobreni s strani ARRS oziroma se izvajajo v okviru odobrenih mednarodnih projektov (npr. sodelovanje v okvirnih programih Evropske unije na področju raziskav in tehnološkega razvoja) in zagotavljajo osnovni vir financiranja raziskav. Javni razpis nadalje določa pogoje, ki jih mora izpolnjevati gostujoči znanstvenik, ki ga prijavi prijavitelj, in sicer mora imeti dosežen naziv doktor znanosti, ne sme biti državljan Republike Slovenije, imeti mora stalno prebivališče izven Republike Slovenije ter v času pedagoškega oziroma raziskovalnega sodelovanja urejeno začasno prebivanje v Republiki Sloveniji iz namena pedagoškega ali raziskovalnega sodelovanja.

Javni sklad Republike Slovenije za razvoj kadrov in štipendije je na podlagi prijavnice in dostavljenih dokazil ugotovil, da prijavitelj in gostujoči znanstvenik izpolnjujeta pogoje, določene v razpisu, zato se je vloga uvrstila v postopek točkovanja, v okviru katerega je vloga prejela skupno 50 točk in sicer po merilu področja pedagoškega ali raziskovalnega sodelovanja 30 točk, saj se je raziskovalno sodelovanje uvrstilo v področje tehnike, po merilu vrste sodelovanja 0 točk, saj gre za raziskovalno sodelovanje ter po merilu predhodnega sofinanciranja sodelovanja 20 točk, saj prijavitelju za prijavljenega gostujočega znanstvenika še niso bila podeljena sredstva po predhodnih razpisih sklada.

Vrednost zaprošenih sredstev vseh prijaviteljev na javnem razpisu, katerih vloge so bile pravočasne, popolne in so izpolnjevale pogoje razpisa, je znašala 331.000,00 EUR in je presegla vrednost razpisanih sredstev. Vloge prijaviteljev, ki so izpolnjevale pogoje javnega razpisa, so se ocenile na podlagi meril, ki jih določa javni razpis. Seznam upravičencev se je določil na podlagi prednostnega seznama, v katerem so se vloge prijaviteljev razvrstile po vrstnem redu glede na prejeto oceno vloge od najvišje do najnižje ocenjene vloge. Ker je več vlog prejelo enako število točk, so se za razvrstitev teh vlog uporabila razmejitvena merila, določena z javnim razpisom. Iz prednostnega seznama so se na seznam upravičencev do sredstev uvrstile vloge, ki so bile ocenjene z vključno 30 točkami, pri čemer se za vlogo, uvrščeno na zadnje mesto na seznamu upravičencev, sredstva dodelijo v znesku do porabe razpisanih sredstev.

Ker se je vloga prijavitelja uvrstila na prednostni seznam s 50 točkami, se je prijavitelj nadalje uvrstil tudi na seznam upravičencev do sofinanciranja. Vlogi prijavitelja se tako ugodi, kot je navedeno v izreku te odločbe.

Pravica, pridobljena s to odločbo, bo učinkovala po podpisu pogodbe o sofinanciranju. Podpis pogodbe je možen po dokončnosti te odločbe in po prejemu s strani prijavitelja predloženega obvestila o prihodu tujega gostujočega znanstvenika, kot je določeno v 3. točki izreka te odločbe.

Nakazilo sredstev bo izvršeno skladno s sklenjeno pogodbo.

Upravna taksa je bila plačana ob vložitvi vloge skladno z Zakonom o upravnih taksah (Ur.l. RS, št. 42/2007–UPB3, 126/2007) v skupnem znesku 17,73 EUR, in sicer 3,55 EUR za vlogo po tar. št. 1 in 14,18 EUR za odločbo po tar. št. 3.

Pravni pouk: Zoper to odločbo je dopustna pritožba v roku 15 dni od vročitve odločbe. Pritožba se vloži pisno ali da ustno na zapisnik pri Javnem skladu Republike Slovenije za razvoj kadrov in štipendije, Dunajska 22, Ljubljana. Če je pritožba poslana priporočeno po pošti, se šteje, da je pravočasna, če je oddana na pošto zadnji dan pritožbenega roka. O pritožbi bo odločalo Ministrstvo za delo, družino in socialne zadeve.

Za pritožbo zoper odločbo je potrebno ob vložitvi pritožbe po tar. št. 2 Zakona o upravnih taksah (Uradni list RS, št. 106/10 – uradno prečiščeno besedilo) plačati upravno takso v znesku 15,49 EUR na račun Ministrstva RS za finance pri Upravi za javna plačila št. 01100-1000315637, sklic 11, številka sklica 96091-7111002-110093, o čemer je potrebno k pritožbi priložiti dokazilo o plačilu.

Prijavitelj se lahko do izteka roka za pritožbo odpove pravici do pritožbe. Izjava o odpovedi pravici do pritožbe se da pisno ali ustno na zapisnik. Odpoved pravici do pritožbe učinkuje od dneva, ko Javni sklad Republike Slovenije za razvoj kadrov in štipendije dobi pisno izjavo oziroma ko stranka da izjavo ustno na zapisnik.

REPUBLIKA SLOVENIJA Nosilec javnega pooblastila JAVNI SKLAD REPUBLIKE SLOVENIJE ZA RAZVOJ KADROV IN ŠTIPENDIJE Dunajska cesta 22, 1000 Ljubljana 1

Pripravila:
Darinka Trček
področna svetovalka I

Romana Tomc
direktorica

Prejme:
- Institut Jožef Stefan, Jamova cesta 39, 1000 Ljubljana, z vročilnico po ZUP

The Intellectual Property Office of the Republic of Serbia

Center for technology transfer
University of Belgrade

WIPO
WORLD INTELLECTUAL PROPERTY ORGANIZATION

WIPO NATIONAL TRAINING PROGRAM

CERTIFICATE

We hereby certify that

Saša Lazović

Successfully completed the

NATIONAL TRAINING PROGRAM ON
IP MARKETING AND VALUATION

Organized by

the World Intellectual Property Organization (WIPO)
in cooperation with
the Intellectual Property Office of the Republic of Serbia
and the Center for Technology Transfer, University of Belgrade

Belgrade, Serbia
October 12 to 14, 2015

Nevenka Novaković
Acting Director
Intellectual Property Office
of the Republic of Serbia

Michal SVANTNER

Michal Svantner, Director,
Department for Transition
and Developed Countries,
World Intellectual Property
Organisation

Center for technology transfer

European IPR Helpdesk

CERTIFICATE OF PARTICIPATION

the Center for Technology Transfer, University of Belgrade and EU IPR Helpdesk confirm that

Mr. Saša Lazović

has taken part in the full day training regarding:

- Strategic Uses of IP by Researchers and Business IP for Business
- IP Management in International Research and Innovation Initiatives
- IP Commercialisation and Licensing

held in Belgrade, Serbia
June 13th , 2014

DIRECTOR

Dr. Nedeljko Milosavljević
Center for Technology Transfer,
University of Belgrade

HEAD OF TRAINING

Mr. Jörg Scherer
EU IPR Helpdesk

European Commission

Certificate of Participation

I hereby certify that

Saša Lazović

Successfully completed the

"Danube Innovation Partnership Summer School on Knowledge and Technology Transfer"

organised by the the European Commission Joint Research Centre, the World Intellectual Property Organisation, the Center for Technology Transfer of University of Belgrade and the Intellectual Property Office of the Republic of Serbia

Held in Belgrade, Serbia 17-24 September 2014

Giancarlo Caratti

Head of Unit, Intellectual Property and Technology Transfer,
Joint Research Centre, European Commission

WIPO WORLD INTELLECTUAL PROPERTY ORGANIZATION

The Intellectual Property Office of the Republic of Serbia

Joint Research Centre

Center for technology transfer

CERTIFICATE OF ATTENDANCE

This is to certify that

SAŠA LAZOVIĆ

Attended the 2nd Annual Meeting COST Action TD1208
held in BARCELONA, SPAIN from 23th to 26th February 2015

Cristina Canal

2nd Annual Meeting COST Action TD1208 Chair

MAHATMA GANDHI UNIVERSITY · KOTTAYAM ·

विद्यया अमृतमश्नुते

International Conference on Plasma & Nanotechnology
&
29th National Symposium on Plasma Science and Technology

PSSI ESTD 1978

Plasma-2014

Certificate

This is to certify that Mr./Ms./Dr./Prof. SAŠA LAZOVIĆ *affiliated to* UNIVERSITY OF BELGRADE, SERBIA *has given an invited talk/* ~~*chaired session*~~ *in the* ***International Conference on Plasma and Nanotechnology (PLASMA- 2014) & 29th National Symposium on Plasma Science and Technology,*** *jointly organized by Plasma Science Society of India (PSSI), International & Inter University Centre for Nanoscience & Nanotechnology (IIUCNN) and School of Pure and Applied Physics, Mahatma Gandhi University, from 8-11 December, 2014 at Kottayam, Kerala, India.*

Organized by PLASMA 2014 8-11-Dec. 2014 Kottayam Kerala, India IIUCNN, SPAP, PSSI

11th December, 2014
Kottayam, Kerala

Dr. Nandakumar Kalarikkal
Convener, PLASMA-2014

INTERNATIONAL CONFERENCE ON ADVANCED NANOSTRUCTURES (ICAN-2018)

ICAN 2018

12-14th March 2018

Organized by

Post Graduate and Research Department of Physics
Catholicate College, Pathanamthitta, Kerala, 689645

Supported By

KSCSTE

SERB INDIA

Ministry of Electronics and Information Technology Government of India

BRNS

Certificate

This is to Certify that Prof./Dr./Ms./Mrs./Mr. **Prof. Dr. Saša Lazović,** Institute of Physics Belgrade University of Belgrade, Serbia

has presented a paper plenary/invited/short invited/oral/poster/Participated at the INTERNATIONAL CONFERENCE ON ADVANCED NANOSTRUCTURES (ICAN-2018) held at Catholicate College, Pathanamthitta, Kerala, India from 12-14 March 2018.

CATHOLICATE COLLEGE KERALA PATHANAMTHITTA

Dr. Raneesh B.
(Convenor, ICAN 2018)

Dr. George Thomas
(Co-Convenor, ICAN 2018)

Dr. Mathew P Joseph
(Principal, Catholicate College)

INTERNATIONAL CONFERENCE ON ADVANCED NANOSTRUCTURES (ICAN-2018)

12-14th March 2018

Organized by

Post Graduate and Research Department of Physics

Catholicate College, Pathanamthitta, Kerala, 689645

Supported By

KSCSTE

iNSERB INDIA

Ministry of Electronics and Information Technology Government of India

CSIR INDIA

BRNS

Certificate

This is to Certify that Prof./Dr./~~Ms./Mrs./Mr.~~ SASA LAZOVIC

UNIVERSITY OF BELGRADE, SERBIA

has Chaired a Session at the INTERNATIONAL CONFERENCE ON ADVANCED NANOSTRUCTURES (ICAN-2018) held at Catholicate College, Pathanamthitta, Kerala, India from 12-14 March 2018.

CATHOLICATE COLLEGE KERALA PATHANAMTHITTA

Dr. Raneesh B.
(Convenor, ICAN 2018)

Dr. George Thomas
(Co-convenor, ICAN 2018)

Dr. Mathew P Joseph
(Principal, Catholicate College)

Univerzitet u Beogradu
Tehnološko-metalurški fakultet

Nataša M. Vasić

Mogućnost primene netermalne plazme za inaktivaciju *Candida albicans* u destilerijskoj džibri

Završni master rad

Beograd
septembar 2017.

Zahvalnica

Zahvaljujem se mentoru ovog rada Dr Ljiljani Mojović, na pruženoj prilici i mogućnosti realizacije ovog rada u njenoj laboratoriji!

Veliku zahvalnost dugujem Dr Aleksandri Đukić-Vuković, naučnom saradniku TMF-a, koja je rukovodila izradom i pisanjem ovog rada, na nesebičnoj pomoći, podršci i posvećenosti!

Hvala Dragani Mladenović, istraživaču saradniku TMF-a, za pomoć u eksperimentalnom radu, za svaki savet i podršku!

Hvala Dr Saši Lazović, naučnom saradniku Instituta za fiziku, Beograd, za pomoć u eksperimentalnom radu!

Hvala prijateljima za sve zajedničke suze i osmehe!

Hvala mojoj porodici koja me je podržavala i verovala u mene!

ДП

На основу чл. 40. став 3. Закона о високом образовању, чл. 104. став 3. Статута Универзитета у Београду, чл.40. Статута ТМФ-а и чл. 32. Правилника о докторским студијама ТМФ-а, на седници Наставно-научног већа Технолошко-металуршког факултета од 06.07.2018. године, донета је

О Д Л У К А
о прихватању Реферата Комисије за оцену подобности теме и кандидата за израду докторске дисертације

Прихвата се Реферат Комисије за оцену подобности теме и кандидата и одобрава израда докторске дисертације **Татјане Митровић**, дипломираног инжењера технологије, под називом: **„Хемометријске методе за предвиђање параметара квалитета речних вода и разградње загађујућих материја“**.

Одлуку о давању сагласности на предлог теме докторске дисертације доноси Универзитет у Београду.

За менторе се одређују др Мирјана Ристић, редовни професор Универзитета у Београду, Технолошко-металуршки факултет и др Саша Лазовић, научни сарадник Универзитета у Београду, *Институт за физику*.

Одлуку доставити: Универзитету у Београду на сагласност, кандидату, менторима, Служби за наставно студентске послове и архиви Факултета.

ДЕКАН

Проф. др Ђорђе Јанаћковић

УНИВЕРЗИТЕТ У БЕОГРАДУ

Студентски трг 1, 11000 Београд, Република Србија
Тел.: 011 3207400; Факс: 011 2638912; E-mail: officebu@rect.bg.ac.rs

ВЕЋЕ НАУЧНИХ ОБЛАСТИ
ТЕХНИЧКИХ НАУКА

Београд, 27.8.2018. године
02 број: 61206-3476/2-18
ЛД

На основу члана 48. став 5. тачка. 3. Статута Универзитета у Београду ("Гласник Универзитета у Београду", број 201/18) и чл. 14. – 21. Правилника о већима научних области на Универзитету у Београду ("Гласник Универзитета у Београду", број 134/07, 150/09, 158/10, 164/11, 165/11, 180/14, 195/16 и 197/17), а на захтев Технолошко-металуршког факултета, број: 35/240 од 15.8.2018. године, Веће научних области техничких наука, на седници одржаној 27.8.2018. године, донело је

О Д Л У К У

ДАЈЕ СЕ САГЛАСНОСТ на предлог теме докторске дисертације Татјане Митровић, под називом: „Хемометријске методе за предвиђање параметара квалитета речних вода и разградње загађујућих материја".

ПРЕДСЕДНИК ВЕЋА

Проф. др Јован Филиповић

Доставити:
- Факултету,
- Архиви Универзитета.

УНИВЕРЗИТЕТ У БЕОГРАДУ
ИНСТИТУТ ЗА ФИЗИКУ БЕОГРАД
Прегревица 118, 11080 Земун - Београд, Србија
Телефон: +381 11 3713000, Факс: +381 11 3162190, www.ipb.ac.rs
ПИБ: 100105980, Матични број: 07018029, Текући рачун: 205-66984-23

Београд, 19.10.2016.

На основу члана 27. Статута Института за физику 0801 бр. 285/4 од 30. маја 2011. године (измене и допуне на седницама 17.06.2013. год. и 23.12.2014. год.) и важећег Правилника о организацији и систематизацији рада (радних места) на Институтут за физику, а у циљу испуњавања законских обавеза Института везаних за рад и безбедност на раду, директор Института за физику доноси следећу

О Д Л У К У

Сви запослени научни радници на Институту за физику се једнозначно распоређују у следеће лабораторије (истраживачке групе):

1. Лабораторија за нелинеарну фотонику
2. Лабораторија за спектроскопију плазме и ласере
3. Лабораторија за холографију, оптичке материјале и фотоничке кристале
4. Лабораторија за квантну и нелинеарну оптику
5. Лабораторија за ласерску интеракцију са материјалима и ласере
6. Лабораторија за биофизику
7. Лабораторија за метаматеријале
8. Лабораторија за фотоакустику
9. Лабораторија за примену рачунара у науци
10. Лабораторија за грануларне материјале
11. Лабораторија за биомиметику
12. Лабораторија за физику материјала под екстремним условима
13. Лабораторија за гасну електронику
14. Лабораторија за нелинеарну физику
15. Лабораторија за истраживања у области електронских материјала
16. Лабораторија за физику нано-композитних структура и био-вибрационих спектара
17. Лабораторија за чврсто стање
18. Лабораторија за графен, друге 2Д материјале и уређене наноструктуре
19. Лабораторија за мезоскопску физику
20. Лабораторја за физику високих енергија
21. Група за гравитацију, честице и поља
22. Лабораторија за физику атомских сударних процеса
23. Лабораторија за физику животне средине
24. Нискофонска лабораторија за нуклеарну физику
25. Лабораторија за астрофизику и физику јоносфере

За сваку од наведених лабораторија се доноси посебна одлука којом се утврђује списак истраживача чланова, даје кратак опис области деловања, и поставља руководилац лабораторије у наредном једногодишњем периоду.

Ова одлука ступа на снагу даном доношења.

ДИРЕКТОР ИНСТИТУТА ЗА ФИЗИКУ

др Александар Богојевић

УНИВЕРЗИТЕТ У БЕОГРАДУ
ИНСТИТУТ ЗА ФИЗИКУ БЕОГРАД
Прегревица 118, 11080 Земун - Београд, Србија
Телефон: +381 11 3713000, Факс: +381 11 3162190, www.ipb.ac.rs
ПИБ: 100105980, Матични број: 07018029, Текући рачун: 205-66984-23

Београд, 20.10.2016.

На основу члана 27. Статута Института за физику 0801 бр. 285/4 од 30. маја 2011. године (измене и допуне на седницама 17.06.2013. год. и 23.12.2014. год.), директор Института за физику доноси

О Д Л У К У

У Лабораторију за биомиметику Института за физику се распоређују следећи истраживачи:

1. др Саша Лазовић, научни сарадник
2. Александар Бојаров, истраживач сарадник

Област деловања лабораторије:

Лабораторија за биомиметику се бави решавањем актуелних друштвених проблема тражећи идеје, инспирацију и решења у природи и њеним јединственим биолошким процесима, понашањима и системима. Лабораторија тежи да комбинујући приступ и методологију више научних и истраживачких дисциплина као што су физика, хемија, биологија, медицина, социологија, програмирање, електротехника, машинство, и др., даје конкретан допринос развоју нових технологија.

За руководиоца лабораторије се именује др Саша Лазовић, научни сарадник.

Одлука ступа на снагу даном доношења.

ДИРЕКТОР ИНСТИТУТА ЗА ФИЗИКУ

др Александар Богојевић

УНИВЕРЗИТЕТ У БЕОГРАДУ
ИНСТИТУТ ЗА ФИЗИКУ | БЕОГРАД
Прегревица 118, 11080 Земун - Београд, Србија
Телефон: +381 11 3713000, Факс: +381 11 3162190, www.ipb.ac.rs
ПИБ: 100105980, Матични број: 07018029, Текући рачун: 205-66984-23

Београд, 03.07.2018.

На основу члана 27. Статута Института за физику 0801 бр. 285/4 од 30. маја 2011. године (измене и допуне на седницама 17.06.2013. год. и 23.12.2014. год.), директор Института за физику доноси

О Д Л У К У

У Лабораторију за биомиметику Института за физику се распоређују следећи истраживачи:

1. др Саша Лазовић, научни сарадник
2. др Драган Драмлић, научни саветник

Област деловања лабораторије:

Лабораторија за биомиметику се бави решавањем актуелних друштвених проблема тражећи идеје, инспирацију и решења у природи и њеним јединственим биолошким процесима, понашањима и системима. Лабораторија тежи да комбинујући приступ и методологију више научних и истраживачких дисциплина као што су физика, хемија, биологија, медицина, социологија, програмирање, електротехника, машинство, и др., даје конкретан допринос развоју нових технологија.

За руководиоца лабораторије се именује др Саша Лазовић, научни сарадник.

Одлука ступа на снагу даном доношења.

ДИРЕКТОР ИНСТИТУТА ЗА ФИЗИКУ

др Александар Богојевић

РЕПУБЛИКА СРБИЈА
УНИВЕРЗИТЕТ У БЕОГРАДУ
ИНСТИТУТ ЗА ФИЗИКУ
0801 Бр. 1014/1
10. 07. 2018 год.

Plasma induced DNA damage: Comparison with the effects of ionizing radiation

Article *in* Applied Physics Letters · September 2014

Impact Factor: 3.3 · DOI: 10.1063/1.4896626

Plasma induced DNA damage: Comparison with the effects of ionizing radiation

S. Lazovi, D. Maleti, A. Leskovac, J. Filipovi, N. Pua, G. Malovi, G. Joksi, and Z. Lj. Petrovi

Citation: Applied Physics Letters **105**, 124101 (2014); doi: 10.1063/1.4896626
View online: http://dx.doi.org/10.1063/1.4896626
View Table of Contents: http://scitation.aip.org/content/aip/journal/apl/105/12?ver=pdfcov
Published by the AIP Publishing

Plasma induced DNA damage: Comparison with the effects of ionizing radiation

S. Lazović,[1] D. Maletić,[1] A. Leskovac,[2] J. Filipović,[2] N. Puač,[1] G. Malović,[1] G. Joksić,[2] and Z. Lj. Petrović[1]
[1]*Institute of Physics, University of Belgrade, Pregrevica 118, 11080 Belgrade, Serbia*
[2]*Department of Physical Chemistry, Vinča Institute of Nuclear Sciences, University of Belgrade, 11001 Belgrade, Serbia*

(Received 20 June 2014; accepted 15 September 2014; published online 24 September 2014)

We use human primary fibroblasts for comparing plasma and gamma rays induced DNA damage. In both cases, DNA strand breaks occur, but of fundamentally different nature. Unlike gamma exposure, contact with plasma predominantly leads to single strand breaks and base-damages, while double strand breaks are mainly consequence of the cell repair mechanisms. Different cell signaling mechanisms are detected confirming this (ataxia telangiectasia mutated - ATM and ataxia telangiectasia and Rad3 related - ATR, respectively). The effective plasma doses can be tuned to match the typical therapeutic doses of 2 Gy. Tailoring the effective dose through plasma power and duration of the treatment enables safety precautions mainly by inducing apoptosis and consequently reduced frequency of micronuclei. © *2014 AIP Publishing LLC*. [http://dx.doi.org/10.1063/1.4896626]

Plasma medicine is maturing as a research field by advancing from unadorned applications such as bacteria sterilization[1–3] to the more sophisticated ones including the cancer treatment.[4,5] Contrary to the relatively young and developing research field of plasma medicine,[6–8] radiation biology is a well-established discipline which has been collecting data on safe doses of different types of irradiation for decades now.[9,10]

Improved blood coagulation, wound healing and sterilization even for diabetes chronic wounds and Hailey-Hailey disease[11–15] are confirming maturity and good prospects of cold plasma based plasma medicine but also raise a question of the safety of the use and of the long term effects.

Plasma needle is a well-studied atmospheric pressure non-equilibrium plasma[16] often used for bacteria sterilization, medical treatments, and fine surface treatment of biomaterials.[17] Due to its small size and mild nature, the needle has been used for subtle stem cell manipulations as well.[18,19] Plasma sources of different designs but of very similar properties are known to be able to interact not only with the cell membranes, but the plasma effects can penetrate the cell interior and reach the DNA itself. Authors report single and double strand breaks (SSBs and DSBs) following plasma irradiation.[20–23] Furthermore, repair kinetics and recovery is monitored hours after the plasma treatment. O'Connell *et al.*[20] report on quantitative determination of the rates of single and double strand breaks formation in the plasmid DNA and also correlate the formation of double strand breaks with the atomic oxygen density.[20] The importance for biomedical applications of plasma generated reactive oxygen and nitrogen species (RONS) is explained elsewhere.[24] Detection of reactive species generated by plasma operating in an open-air environment typically requires sophisticated diagnostics such as triple stage mass spectrometry enabling detection of plasma generated ions and neutrals.[16,25–28] Those as well as the data on two-photon absorption laser-induced fluorescence (TALIF) spectroscopy or tunable diode-laser absorption spectroscopy (TDLAS)[29,30] should be compared to the simulation results in order to evaluate absolute densities of relevant species and understand the underlying phenomena. The complexity of physical and chemical processes induced by the high density plasma environment can be further promoted by the presence of air impurities such as water vapor.[31–33] The observed effects on the DNA presented here are direct outcome of the plasma treatment. It is necessary to observe them in context of modeling and diagnostics of plasma chemical products and their interaction with the living tissue. It is well known that DSBs are the primary lesions responsible for biological effects of ionizing radiation; when miss repaired lead to formation of complex chromosomal aberrations and micronuclei (MN) lead to cell death. Residual, unrepaired DSBs induce genomic instability representing an early event in carcinogenesis.

We use human primary fibroblasts to compare the effects of cold plasma and gamma irradiation (Co^{60} γ-ray) on cell DNA in order to determine the effective plasma irradiation doses. Dose-response was established by CBMN and γ-H2AX phosphorylation assays. Irradiation was acute, employed radiation doses were in range of 0.5–4 Gy. Alongside γ-H2AX phosphorylation assay was used for the dose-response and assessment of repair kinetics of the DSBs. All biomarkers were monitored to precisely distinguish peculiarities of two interactions. Furthermore, effective doses are correlated with the power delivered to the plasma.

A variety of atmospheric pressure plasma sources provide an extreme flexibility of use through a wide span of applicable parameters but also raises a question of unification of the results, especially in terms of comparison and reproducibility. Our plasma source is the so-called plasma needle, a 13.56 MHz capacitively coupled discharge around the central wire inside a narrow glass tube in the flow of helium mixing with the air. We have developed a special high sensitivity power measurement technique (using derivative probes) allowing us to detect powers even in the range below 0.1 W. Apart from allowing us control of gas heating and avoiding thermal necrosis it is applicable to small size plasma (down

to mm^3 scale).[34] Another feature is that we know very well the chemically active products stemming from the plasma due to detailed diagnostics by atmospheric pressure mass analyzer. The details of plasma experimental setup, gamma irradiation, primary fibroblast preparation, micronucleus test, and γ-H2AX assay are explained elsewhere.[18,19,35]

The effect of different kinds of irradiation is mostly based on the generation of radicals in the vicinity of DNA.[36,37] Even small concentrations of radicals can be sufficient to induce DNA damage. Therefore, it is of great importance that the therapeutic exposures are accommodated and controlled to avoid extensive damage of genetic material. In the case of gamma irradiation, the exposure is easily controlled by controlling the exposure time at fixed rates (in this case 0.45 Gy/min), radiation field, and the distance. However, in the case of plasma exposure, the control is not that simple due to the small size, multi-parameter dependence, and stochastic component of plasma.

In order to compare the effects of gamma irradiation and cold plasma, we have measured the incidence of DSBs employing γ-H2AX phosphorylation assay in both cases at different time-periods after irradiation: 30 min, 2 h, and 24 h. The maximum induction of DBSs is detected 30 min after irradiation with γ rays, whereas plasma treatment induces maximum DSBs 2 h after the treatment. The dependence of number of γ-H2AX foci per cell is linear for the applied range of radiation doses of 0.5–4 Gy (see Fig. 1(a)). In the case of plasma, the number increases both with the treatment time and power (Fig. 1(b)). The effects can be controlled by adjusting either of the two or both.

High resolution power measurements are employed to determine the power delivered to the plasma (see Fig. 2(a)). The values are obtained by subtracting the power obtained without the plasma (no Helium flow) from the powers when plasma is on. In this way, the power losses in the rest of the plasma needle electrical circuit are eliminated achieving high accuracy.

A numerical procedure following the waveform acquisition from the derivative probes is further adapted to support the high resolution measurements and treatment reproducibility. The power is calculated as follows:

$$P = \frac{1}{T}\int_{O}^{T} v(t)i(t)dt, \tag{1}$$

where v(t) and i(t) are time dependent waveforms of voltage and current, respectively, and T is the integration interval, usually taken to be an integer multiple of the fundamental period of the 13.56 MHz signal in the present case. If the integration time is set to be equal to the treatment time, any changes induced by the stochastic nature of the discharge and/or by any variation of the parameters would be taken into account therefore supporting high sensitivity measurements and treatment reproducibility. The powers of 0.4, 0.6, and 1.4 W correspond to voltages of 337, 357, and 393 V, respectively, and are used for all treatments (Fig. 2(a)).

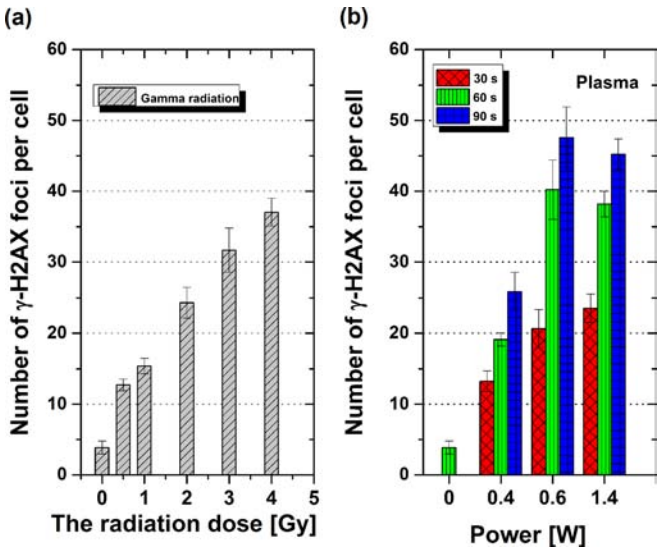

FIG. 1. The number of γ-H2AX foci per cell after irradiation with gamma rays (a); and after the treatment with cold plasma (b) at the time of maximal induction.

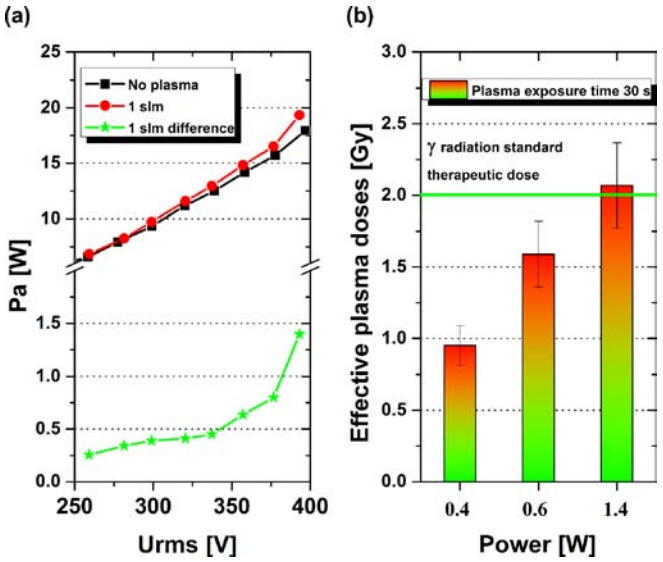

FIG. 2. (a) Power delivered to the plasma. (b) Effective doses of plasma irradiation.

Based on data from Figure 1, the effective doses of plasma irradiation are presented in Figure 2(b). Depending on the power and exposure time, the doses range from 0.96 Gy (0.4 W and 30 s) to 4.69 Gy (1.4 W and 90 s). They are calculated by comparing to the number of γ-H2AX foci per cell after the gamma rays irradiation (see Figs. 1(b) and 1(c)). For example, gamma irradiation of 2 Gy induces 25 γ-H2AX foci per cell, same as 0.6 W, 90 s plasma treatment. Linear data interpolation and extrapolation are used where necessary to obtain other values (Fig. 2(b)). For 30 s plasma treatments, the calculated effective doses are 0.96 Gy, 1.56 Gy, and 2 Gy for the powers of 0.4 W, 0.6 W, and 1.4 W, respectively. In this particular case, 2 Gy can be reached either by 90 s treatment with 0.6 W or by 30 s treatment with 1.4 W. Therefore, the desired effective dose can be reached either by adjusting the power or the treatment time or both.

In order to provide in-depth understanding of the nature of two irradiations, finding that maximal number of Co^{60} γ-ray induced DSBs is seen 30 min after irradiation, while in case of plasma treatment it appeared 2.5 h later, we

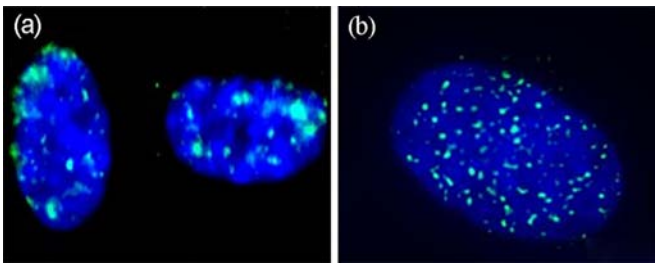

FIG. 3. (a) γ-H2AX foci induced by ionizing radiation 30 min after irradiation (typical ATM signaling); (b) cold plasma source induces ATR signalization, which is recognized as small green foci all over the nuclei.

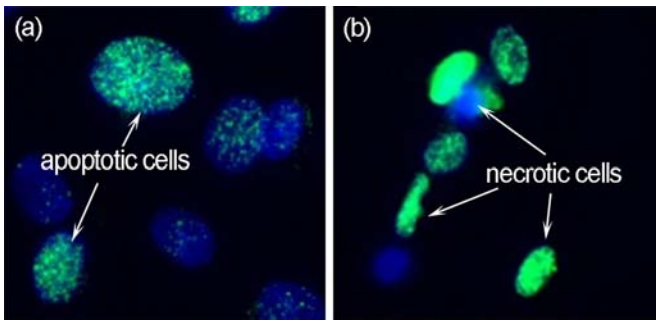

FIG. 4. Examples of cells undergoing early apoptosis (a) and necrosis (b).

investigate the cell signaling processes and appearance of early and late apoptosis (Fig. 3). Phosphorylation of H2AX histones occurs via action of ATM (ataxia telangiectasia mutated) protein which recognizes DSBs. Subsequently, γ-H2AX recruits DNA repair proteins to the breaks visible as fluorescent foci. ATM ensures retention of recruited DNA repair proteins at the site of break. If ATM is dysfunctional or aberrant its role is taken over by ATR (ataxia telangiectasia and Rad3 related) protein. ATR signaling responds to the stalled replication fork and operates more slowly than ATM.[38] Ionizing radiation typically induces ATM signaling in DNA damage response.[39]

The most interesting observation is that cold plasma induces ATR signal pathway, which is never observed after the treatment by ionizing radiation. ATR signaling reflects staled replication fork demonstrating that cold plasma induces bulky lesions leading to replication fork arrest, and consequently cell death by apoptosis or necrosis (Figure 4). Plasma simultaneously induces SSBs and BD, base damages, which compose DSBs due to action of base excision repair. Because of that the peak of the γ -H2AX foci appeared 2 h later when compared to ionizing radiation.

ATR signaling induced by plasma treatment is a phenomenon which deserves further investigation.

Besides the high incidence of γ-H2AX surprisingly low incidence of micronuclei was found indicating that plasma induces bulky lesions on the DNA (see Figure 5). Reduced micronuclei formation could be explained by massive cell death via late apoptosis. In study of the micronuclei incidence we use binucleated cells (BN). For most of the cells analyzed for micronuclei incidence, apoptotic BN cells were found (see micrograph panel b) which is not seen in gamma irradiated cells (panels (e)–(f)), even for the highest doses applied. Moreover, heavily damaged nuclei, nuclear buddings, basophilic granules frequently were observed only in plasma treated samples illustrating complex nuclei damages (panels (a)–(d)). However, these effects were only observed for powers of 0.6 W and 1.4 W when cell death is rapidly induced. For short exposure times (30 s) and lower powers (0.4 W) no such effects were observed suggesting that lower power and shorter plasma exposures are non-toxic to the fibroblasts.

The effective doses of cold plasma irradiation are found based on the comparative effects on DNA damage of primary human fibroblast cells with gamma irradiation. Power delivered to the plasma measured by advanced high resolution derivative probes is found to be an excellent parameter for precise tailoring of plasma effective doses. The values

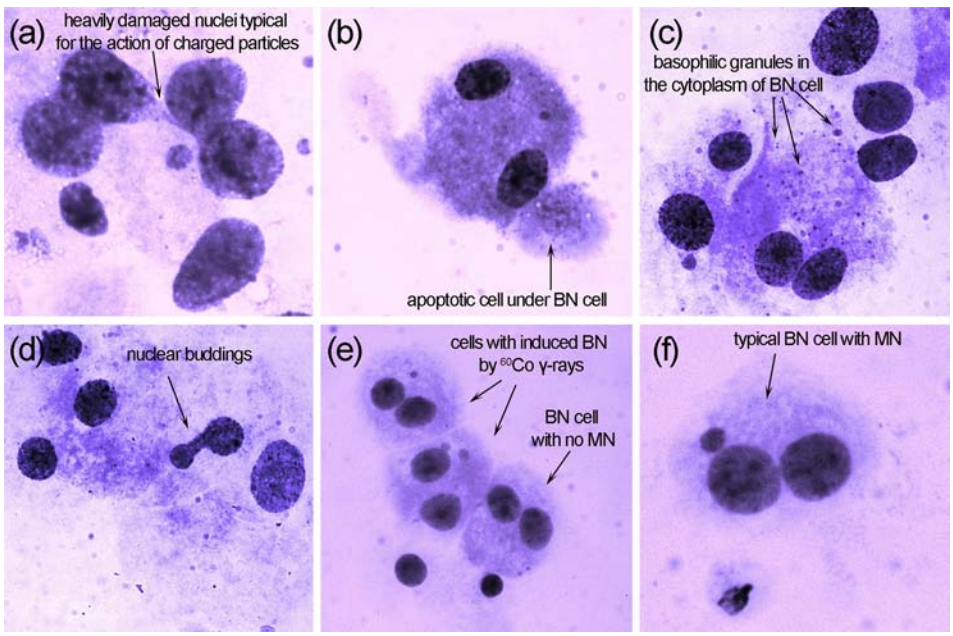

FIG. 5. Cell damage induced by plasma treatment −1.4 W, 90 s ((a)–(d)): heavily damaged nuclei typical for the action of charged particles (a); apoptotic cell under BN cell carrying MN (b); basophilic granules in the cytoplasm of BN cell (c); nuclear buddings in BN cell (d). Cell damage induced by ^{60}Co γ-rays ((e)–(f)): BN cells with and without MN (e); typical BN cell with MN (f).

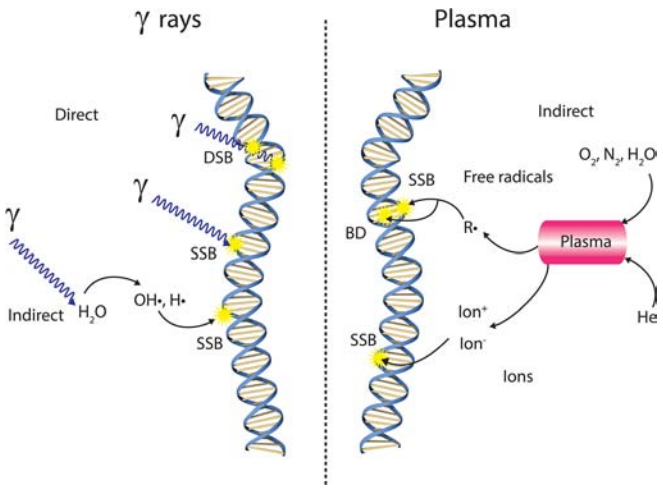

FIG. 6. Schematic representation of the γ ray and plasma effects on DNA.

can be adjusted to match the standard therapeutic dose of 2 Gy. Plasma can be tailored to induce apoptosis rather than necrosis avoiding inflammation and other undesirable effects by controlling dose and time of exposure.

Difference of gamma irradiation and cold plasma are presented in Figure 6. It is known that gamma rays manifest their effects all along the propagation path, while plasma has the capacity for localized application. Gamma irradiation can cause both SSB and DSB through direct or indirect interaction mechanisms. Gamma irradiation directly induces mainly DSBs (seen as typical γ-H2AX foci).

On the other hand plasma induces directly only the SSB. By monitoring the intrinsic lesions induced by treatment, their repair phenotype and cell signaling processes occurring during the DNA repair, we distinguish the origin of plasma induced DSBs and find that most of DSBs are not directly induced by the plasma but are the consequence of cell repair mechanisms. The appearance of DSBs in plasma treatments is attributed to the cell repair mechanisms based on the different cell signaling pathways making a clear distinction from the gamma irradiation (ATM vs. ATR). However, larger powers and exposure times lead sometimes to the damage of the nuclei with typical apoptotic cell death scenario. Another very important distinction is that the small scale plasma can be very precisely applied locally avoiding the "along the path" damage typical for the gamma irradiation. The results support the flow of expertise from the well-established field of radiobiology towards the younger and rapidly growing field of plasma medicine in terms of safety precautions and long term effects. Comparisons like this one may also speed up the application of plasma medicine in clinical trials based on prior experience with radiation exposure and therapy.

This work has been supported by the Ministry of Education, Science and Technological Development of the Republic of Serbia, Project No. III41011, ON 171037, and ON 173046. S.L. would also like to acknowledge COST action MP1101—Biomedical Applications of Atmospheric Pressure Plasma Technology.

[1]M. Laroussi, J. P. Richardson, and F. C. Dobbs, Appl. Phys. Lett. **81**(4), 772 (2002).
[2]B. Kim, H. Yun, S. Jung, Y. Jung, H. Jung, W. Choe, and C. Jo, Food Microbiol. **28**(1), 9 (2011).
[3]U. Cvelbar, M. Mozetic, N. Hauptman, and M. Klanjšek-Gunde, J. Appl. Phys. **106**(10), 103303 (2009).
[4]T. von Woedtke, H. R. Metelmann, and K. D. Weltmann, Contrib. Plasma Phys. **54**(2), 104 (2014).
[5]E. Robert, M. Vandamme, J. Sobilo, V. Sarron, D. Ries, S. Dozias, L. Brulle, S. Lerondel, A. Le Pape, and J. M. Pouvesle, in *Plasma for Bio-Decontamination, Medicine and Food Security*, edited by Z. Machala K. Hensel, and Y. Akishev (Springer Netherlands, 2012), p. 381.
[6]M. G. Kong, G. Kroesen, G. Morfill, T. Nosenko, T. Shimizu, J. van Dijk, and J. L. Zimmermann, New J. Phys. **11**(11), 115012 (2009).
[7]Z. Lj Petrović, N. Puač, S. Lazović, D. Maletić, K. Spasić, and G. Malović, J. Phys.: Conf. Ser. **356**, 012001 (2012).
[8]Z. Petrovic, N. Puac, G. Malovic, S. Lazovic, D. Maletic, M. Miletic, S. Mojsilovic, P. Milenkovic, and D. Bugarski, J. Serb. Chem. Soc. **77**(12), 1689 (2012).
[9]G. Joksic, S. B. Pajovic, M. Stankovic, S. Pejic, J. Kasapovic, G. Cuttone, N. Calonghi, L. Masotti, and D. T. Kanazir, Cell. Mol. Life Sci. **57**(5), 842 (2000).
[10]R. J. Preston, Health Phys. **88**(6), 545 (2005).
[11]T. Nosenko, T. Shimizu, and G. E. Morfill, New J. Phys. **11**(11), 115013 (2009).
[12]G. Isbary, G. Morfill, H. U. Schmidt, M. Georgi, K. Ramrath, J. Heinlin, S. Karrer, M. Landthaler, T. Shimizu, B. Steffes, W. Bunk, R. Monetti, J. L. Zimmermann, R. Pompl, and W. Stolz, Br. J. Dermatol. **163**(1), 78 (2010).
[13]J. Heinlin, G. Isbary, W. Stolz, G. Morfill, M. Landthaler, T. Shimizu, B. Steffes, T. Nosenko, J. L. Zimmermann, and S. Karrer, J. Eur. Acad. Dermatol. Venereol. **25**(1), 1 (2011).
[14]D. Dobrynin, G. Fridman, G. Friedman, and A. Fridman, New J. Phys. **11**(11), 115020 (2009).
[15]G. Isbary, G. Morfill, J. Zimmermann, T. Shimizu, and W. Stolz, Arch. Dermatol. **147**, 388 (2011).
[16]G. Malovic, N. Puac, S. Lazovic, and Z. Petrovic, Plasma Sources Sci. Technol. **19**(3), 034014 (2010).
[17]E. Stoffels, I. E. Kieft, R. E. J. Sladek, L. J. M. van den Bedem, E. P. van der Laan, and M. Steinbuch, Plasma Sources Sci. Technol. **15**(4), S169 (2006).
[18]S. Lazović, N. Puač, M. Miletić, D. Pavlica, M. Jovanović, D. Bugarski, S. Mojsilović, D. Maletić, G. Malović, P. Milenković, and Z. Petrović, New J. Phys. **12**(8), 083037 (2010).
[19]M. Miletić, S. Mojsilović, I. Okić Đorđević, D. Maletić, N. Puač, S. Lazović, G. Malović, P. Milenković, Z. Lj Petrović, and D. Bugarski, J. Phys. D: Appl. Phys. **46**(34), 345401 (2013).
[20]D. O'Connell, L. J. Cox, W. B. Hyland, S. J. McMahon, S. Reuter, W. G. Graham, T. Gans, and F. J. Currell, Appl. Phys. Lett. **98**(4), 043701 (2011).
[21]G. Li, H.-P. Li, L.-Y. Wang, S. Wang, H.-X. Zhao, W.-T. Sun, X.-H. Xing, and C.-Y. Bao, Appl. Phys. Lett. **92**(22), 221504 (2008).
[22]M. Leduc, D. Guay, R. L. Leask, and S. Coulombe, New J. Phys. **11**(11), 115021 (2009).
[23]H. Kurita, T. Nakajima, H. Yasuda, K. Takashima, A. Mizuno, J. I. B. Wilson, and S. Cunningham, Appl. Phys. Lett. **99**(19), 191504 (2011).
[24]D. B. Graves, J. Phys. D: Appl. Phys. **45**(26), 263001 (2012).
[25]E. Stoffels, Y. Aranda Gonzalvo, T. D. Whitmore, D. L. Seymour, and J. A. Rees, Plasma Sources Sci. Technol. **15**(3), 501 (2006).
[26]D. Maletić, N. Puač, S. Lazović, G. Malović, T. Gans, V. Schulz-von der Gathen, and Z. Lj Petrović, Plasma Phys. Controlled Fusion **54**(12), 124046 (2012).
[27]P. Bruggeman, F. Iza, D. Lauwers, and Y. Aranda Gonzalvo, J. Phys. D: Appl. Phys. **43**(1), 012003 (2010).
[28]D. Ellerweg, J. Benedikt, A. von Keudell, N. Knake, and V. Schulz-von der Gathen, New J. Phys. **12**(1), 013021 (2010).
[29]N. Knake, S. Reuter, K. Niemi, V. Schulz-von der Gathen, and J. Winter, J. Phys. D: Appl. Phys. **41**(19), 194006 (2008).
[30]J. S. Sousa and V. Puech, J. Phys. D: Appl. Phys. **46**(46), 464005 (2013).
[31]S. Zhang, W. van Gaens, B. van Gessel, S. Hofmann, E. van Veldhuizen, A. Bogaerts, and P. Bruggeman, J. Phys. D: Appl. Phys. **46**(20), 205202 (2013).
[32]T. Murakami, K. Niemi, T. Gans, D. O'Connell, and W. G. Graham, Plasma Sources Sci. Technol. **22**(1), 015003 (2013).
[33]T. Murakami, K. Niemi, T. Gans, D. O'Connell, and W. G. Graham, Plasma Sources Sci. Technol. **22**(4), 045010 (2013).
[34]N. Puač, Z. Lj Petrović, G. Malović, A. Dordević, S. Živković, Z. Giba, and D. Grubišić, J. Phys. D: Appl. Phys. **39**(16), 3514 (2006).

[35]See supplementary material at http://dx.doi.org/10.1063/1.4896626 for details about plasma treatment, gamma irradiation, primary fibroblast preparation, micronucleus test, and γ-H2AX assay.
[36]R. P. Rastogi, Richa, A. Kumar, M. B. Tyagi, and R. P. Sinha, J. Nucleic Acids **2010**, 592980 (2010).
[37]J. F. Ward, E. Cohn Waldo, and M. Kivie, in *Progress in Nucleic Acid Research and Molecular Biology* (Academic Press, 1988), Vol. 35, p. 95.
[38]B. B. Zhou and S. J. Elledge, Nature **408**(6811), 433 (2000).
[39]P. A. Jeggo, Adv. Genet. **38**, 185 (1998).

Characterization and global modelling of low-pressure hydrogen-based RF plasmas suitable for surface cleaning processes Characterization and global modelling of low-pressure hydrog...

Article *in* Journal of Physics D Applied Physics · November 2013

Impact Factor: 2.72 · DOI: 10.1088/0022-3727/46/47/475206

Characterization and global modelling of low-pressure hydrogen-based RF plasmas suitable for surface cleaning processes

2013 J. Phys. D: Appl. Phys. 46 475206

(http://iopscience.iop.org/0022-3727/46/47/475206)

J. Phys. D: Appl. Phys. **46** (2013) 475206 (13pp) doi:10.1088/0022-3727/46/47/475206

Characterization and global modelling of low-pressure hydrogen-based RF plasmas suitable for surface cleaning processes

Nikola Škoro[1,4,5], Nevena Puač[2], Saša Lazović[2,3], Uroš Cvelbar[3], George Kokkoris[1] and Evangelos Gogolides[1,5]

[1] Institute of Microelectronics, NCSR Demokritos, Aghia Paraskevi, Attiki, 15310, Greece
[2] Institute of Physics, University of Belgrade, Pregrevica 118, 11080 Belgrade, Serbia
[3] Jožef Stefan Institute, Jamova cesta 39, 1000 Ljubljana, Slovenia

E-mail: nskoro@ipb.ac.rs and evgog@imel.demokritos.gr

Received 10 April 2013, in final form 24 August 2013
Published 5 November 2013
Online at stacks.iop.org/JPhysD/46/475206

Abstract
In this paper we present results of measurements and global modelling of low-pressure inductively coupled H_2 plasma which is suitable for surface cleaning applications. The plasma is ignited at 1 Pa in a helicon-type reactor and is characterized using optical emission measurements (optical actinometry) and electrical measurements, namely Langmuir and catalytic probe. By comparing catalytic probe data obtained at the centre of the chamber with optical actinometry results, an approximate calibration of the actinometry method as a semi-quantititative measure of H density was achieved. Coefficients for conversion of actinometric ratios to H densities are tabulated and provided. The approximate validity region of the simple actinometry formula for low-pressure H_2 plasma is discussed in the online supplementary data (stacks.iop.org/JPhysD/46/475206/mmedia). Best agreement with catalytic probe results was obtained for ($H\beta$, Ar750) and ($H\beta$, Ar811) actinometric line pairs. Additionally, concentrations of electrons and ions as well as plasma potential, electron temperature and ion fluxes were measured in the chamber centre at different plasma powers using a Langmuir probe. Moreover, a global model of an inductively coupled plasma was formulated using a compiled reaction set for H_2/Ar gas mixture. The model results compared reasonably well with the results on H atom and charge particle densities and a sensitivity analysis of important input parameters was conducted. The influence of the surface recombination, ionization, and dissociation coefficients, and the ion–neutral collision cross-section on model results was demonstrated.

(Some figures may appear in colour only in the online journal)

S Online supplementary data available from stacks.iop.org/JPhysD/46/475206/mmedia

1. Introduction

Radio-frequency plasmas in molecular gases at low pressures have been used for many technological applications such as etching [1], deposition [2, 3], microelectronics fabrication [4, 5] and many others [6, 7]. The majority of etching applications have employed plasmas as tools for anisotropic etching [8, 9]. However, recent investigations have looked into isotropic etching, since this process is important, when it comes to understanding dust formation and removal in fusion devices [10], and cleaning of different contamination layers formed on various types of optical elements [11]. The latter application is usually connected to optical elements used in synchrotrons [12] and extreme ultraviolet lithography (EUVL) tools [13], where the main threats to optics efficiency are carbon contamination and oxidation on the surfaces. As a remedy for optics efficiency degradation, cleaning in O_2 plasmas was often used [14]. Although efficient, this treatment may cause oxidation and

[4] Permanent address: Institute of Physics, University of Belgrade.
[5] Authors to whom any correspondence should be addressed.

roughening of multilayer mirrors producing non-recoverable damage of the optics. Thus, several investigators have recently studied the possibility of carbon contamination removal in H_2 RF plasmas [13, 15–18] or only in atomic H environment [17]. The carbon layer was removed from the surfaces almost without any change of surface properties, with H atoms playing an important role in the removal [11]. Therefore, H_2 plasmas appear to be good candidates for cleaning applications.

When it comes to cleaning applications, important issues for the use of plasma process are cost, availability and safety. Since H_2 plasma can be ignited in all RF plasma sources, generally used for material treatment, and since the pressure is low (up to a few Pa) these three issues can be satisfied. Nevertheless, in order to compare processes done in different reactors and understand mechanisms taking place at the surfaces, complete characterization of the plasma should be performed. Knowledge of plasma parameters becomes even more necessary when it comes to comparing surface treatments in plasmas generated in different ways, e.g. in the case of laser-induced plasmas, which can be produced inside lithography tools permitting *in situ* optics cleaning.

As a first step in a wider investigation of hydrogen plasmas for processing of materials, we performed here characterization of H_2 plasmas in the diffusion region of a helicon reactor (Adixen Micromachining Etching Tool–MET), where samples are positioned [7]. Several experimental techniques have been used in order to characterize the discharge: (a) electron and ion density, electron temperature, plasma potential and ion flux have been measured with commercial RF compensated Langmuir probe (ESPion HIDEN). Since this is considered as one of the simplest measurement techniques, its application in various types of discharges and its theory are extensively studied and given in details by various authors [5, 8, 19–21]. (b) A combination of optical emission spectroscopy with catalytic probes provided real-time monitoring of the neutral atom density with better quantification of the results, and allowed validation of the actinometric technique for H. Indeed, reliable procedures for measuring atomic densities require the combination of two or more diagnostic methods. Mass spectrometry is applicable at low [22, 23] and nowadays even at atmospheric pressure [24] with the addition of differential pumping systems. The method based on chemical titration is reliable, but time consuming, destructive and lacks the capability for real time measurements [25, 26]. Laser-induced fluorescence (LIF), two-photon laser induced fluorescence (TALIF) [27] or cavity ring-down spectroscopy (CRDS) [28] require expensive equipment. Optical emission spectroscopy (OES) is easy to use; it requires inexpensive equipment and allows real time measurements. Nevertheless, it is still regarded semi-qualitative since quantification of the results is difficult [29]. Moreover, in the case of diatomic molecules (H_2, O_2, Cl_2), their atomic optical emission may originate not only from direct atom excitation, but also from dissociative excitation of the parent gas, thus questioning the validity of optical actinometry as a measure of atomic density [30, 31]. Another very simple quantitative method for obtaining atom densities is the use of catalytic probes, which were so far successfully employed in various types of discharges [32–35]. Therefore, in this case, a combination of OES with catalytic probes was used.

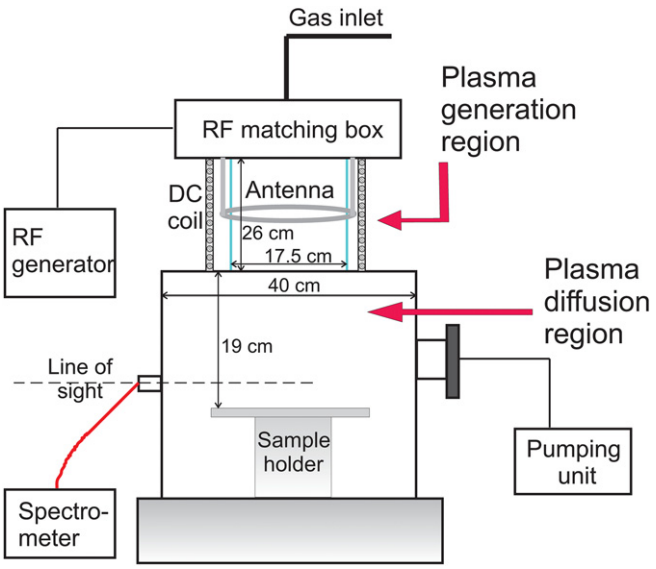

Figure 1. A schematic diagram of the experimental setup.

This paper is organized as follows: first, we describe the plasma chamber and diagnostics used. After that, an overview of a compiled reaction set used in the global model is given. In continuation, a comparison between densities of hydrogen atoms obtained from optical actinometry calculations and catalytic probe measurements is presented and the validity of the actinometric method is discussed. Finally, measurements of plasma parameters obtained by Langmuir and catalytic probes are given and compared to global modelling results in order to validate the model. The critical role of surface recombination coefficient of H atoms, and other parameters is discussed in a sensitivity analysis.

2. Experimental setup

The plasma processing system investigated is a helicon-type micromachining etching tool (MET) from Adixen-Alcatel. The etcher consists of two chambers: the upper part is the plasma generation region with a quartz cylinder 26 cm high and 17.5 cm in diameter surrounded by one-turn coil-antenna. Below the plasma generation chamber is a cylindrical processing region with stainless steel walls 40 cm in diameter and a centrally located sample holder positioned 19 cm beneath the bottom of the generation chamber cylinder, as shown in figure 1. Such a large distance between the production region and the wafer is necessary in order to have a radial uniformity of the plasma in front of the substrate [4]. The plasma generation region is surrounded by an electromagnet producing a constant magnetic field of 1 mT (10 G). Power from a RF 13.56 MHz generator, shown on a power meter built-in the generator, was forwarded to the antenna through a matching box. The plasma produced in this region diffused in the water-cooled processing chamber, which was surrounded by 14 permanent magnets from the outer side with alternating orientation (NS-SN). The

rows of magnets generate a magnetic configuration in which the magnetic field strength has a maximum near the magnets and decays with the distance into the chamber [8]. Hence, the measurements of the plasma parameters obtained at the centre of the processing chamber can be considered as measurements in a magnetic field-free plasma volume. Blank aluminum wafer holders (10 cm (4″) in diameter) entered the chamber through a load-lock and were mechanically clamped on the floating sample holder which was cooled with He-backside pressure (the sample holder can be biased with a separate RF source, but this was not done in these experiments). The process chamber was not vented to atmosphere for wafer transport and was kept at base pressure of approximately 5×10^{-5} mbar.

Plasma emission from the processing region was guided through 1 mm thick optical fibre (Ocean Optics UV–VIS fibre 300–1100 nm) with an acceptance angle of 25.4° in air terminated with standard SMA 905 connectors. Next, the light entered an Acton Research Corporation Spectra-Pro 500 monochromator with 0.5 m focal length and a 1200 g mm^{-1} grating blazed at 750 nm. Light emission at the exit was detected with a thermoelectrically cooled CCD camera (SBIG ST-6I) gated up to 10 s exposure time and connected to a computer for signal detection and processing of obtained spectra. The resolution of the spectrometer used for the measurements is 0.04 nm which was enough for precise determination of different lines in visual spectra from time-integrated recordings.

A single Langmuir probe with passive RF compensation was used for measurement of plasma parameters: electron density (N_e), ion density (N_i), plasma potential (V_p), electron temperature (T_e) and ion current (flux) (J_i, I_{flux}). The probe system consisted of a tungsten probe tip, a high-frequency compensation electrode made of hard anodized aluminum, and a stainless steel reference electrode fastened at a ceramic probe body close to the compensation electrode. It was fastened at one of the side chamber windows with a flange which provided vacuum-tight connection with the chamber.

During all measurements the probe tip was positioned in the centre of the chamber, 5 cm above the sample holder. This position for the probe was chosen so that the point of collecting data for ion and electron concentration would be as close as possible to the position where the samples are positioned during treatments, given that in our commercial system the closest to the sample set of windows is 5 cm above the sample holder. We note than in large-volume diffusion chambers, such as the one used in the experiment, a non-equilibrium plasma formed at low pressures in the source (upstream) is homogeneous enough in a down-stream region, a fact verified by almost constant etching rates at different sample height and diameter. The probe tip dimensions were 10 mm in length and 0.15 mm in diameter. Measured impedance of the probe was 6 Ω. The voltage-sampling interval was set from −40 to 90 V with a step of 0.1 V. Prior to each scan the probe was cleaned *in situ* by applying a voltage of −40 V for a period of 200 ms. For a particular set of plasma parameters, the current–voltage (I–V) characteristic was obtained by averaging 20 scans. Recording of the characteristics, storing and data processing was done by using the Hiden Analytical software ESPsoft. The theory of Langmuir probes and approaches for data processing have been described in detail elsewhere [5, 20].

For measurement of the concentrations of hydrogen atoms, a catalytic probe was employed. Details about probe design and operation are given elsewhere [26, 36]. Gold was used as catalytic material, since it has a high and stable recombination coefficient for the surface recombination of H atoms. Change of the thermocouple voltage versus time was monitored with a voltmeter connected to a computer. The probe was introduced into the processing chamber using a leak-proof flare-through flange on one of the side windows and positioned in such a way that the tip was at the chamber centre, a few centimeters above the bottom electrode close to the position where usually a sample is placed.

The plasma was ignited at the pressure of 1 Pa. All measurements except actinometry were done in pure H_2 (5.5 purity) with a gas flow of 50 sccm (standard cubic centimeters). For actinometry measurements, 5% of Ar (purity of 5.0) was added keeping the total pressure at 1 Pa by slightly opening the chamber valve. Due to the low sensitivity of the built-in flow meters we were not able to use less than 5% of argon in the admixtures. Adding Ar to H_2 plasma may result in the appearance of another dissociation channel that influences broadening of line wings, and can also lead to an increase of the overall number of excited hydrogen. However, these effects are pronounced for Ar admixtures larger than 5% [37]. Furthermore, addition of Ar leads to quenching of hydrogen states excited in plasma, but this effect is not significant at low pressures [38]. The forward powers measured at the power source used in experiments were 800–1900 W with reflected power that never exceeded 5 W. Before each measurement, reflected power was checked and adjusted to minimum value if necessary.

The data obtained in all the measurements (Langmuir probe, catalytic probe, actinometry) are time-averaged values. Moreover, the actinometry results are also spatially averaged due to the fact that the collection of data was performed along the radial axis of the discharge chamber.

Since the same reactor was used for different kinds of processes involving fluorine (e.g. silicon etching in F- and CFx-containing plasmas), special attention was devoted to clean the chamber from different impurities that may be deposited on the walls. Periodically, after several processing events involving fluorine, the chamber was cleaned in oxygen plasma, for 45 min at 1.5 Pa at high power (1800 W). In the beginning of the cleaning process, immediately after plasma ignition, pressure rose significantly and then its decrease was monitored until stabilization. Additionally, at the beginning of every hydrogen plasma measurement day, the chamber was seasoned with hydrogen plasma at a pressure of 1 Pa and power of 1000 W for 30 min. Very small pressure rise in the beginning and subsequent drop was detected during the period of 30 min cleaning. Hence, during measurements, pressure changes after plasma ignition were negligible. Moreover, spectroscopic scans performed throughout hydrogen cleaning process did not reveal the presence of typical fluorine lines in the plasma.

3. Reaction set for H_2 and global model

In order to gain a first estimate on plasma parameters a global model for ICP plasma was used. Details about zero-dimensional global models, previously developed and tested with gases C_4F_8 and SF_6, can be found in earlier publications [39, 40]. This model was supplied with sets of gas phase (homogeneous) reactions as well as surface (heterogeneous) reactions for hydrogen and argon. Based on these data sets the mass balances of charged and neutral species in the gas phase, the mass balances of the species on the surface and the power balance are formulated averaged in space and at the steady state. The equation set is complemented with the charge neutrality equation. In order to solve the aforementioned equation set, the temperature of the gas (T_g) and the ion temperature (T_i) ought to be defined. In our case we assumed that T_g is equal to 315 K, which is slightly higher than the temperature of the walls. Generally speaking, there could be an increase in the gas temperature due to elastic collisions between electrons and gas molecules [41]. At low pressures this effect would appear during prolonged plasma operation. Nevertheless, for all measurements plasma-on time did not exceed 5 min, and as a result this increase was considered small enough to be neglected. Ion temperature is calculated by the empirical equation proposed by Lee and Liebermann [42]. Other input parameters for the model are reactor dimensions, gas pressure and flow and power forwarded to the plasma. The model calculates all densities of species in the plasma and the electron temperature.

The set of gas phase (homogeneous) reactions in hydrogen and argon used in the model is given in table 1. For a particular reaction considered in the model, its threshold energy and the reference used are given as well. Reactions were compiled following already well-established models of low-temperature hydrogen plasmas [43, 44] and recommendations from the literature [45]. However, attention was also paid to taking into account only the most probable reactions in order to construct a model that will realistically describe the plasma with particular parameters, but with a reasonable number of reactions included. Test runs of the model with negative ions included proved that changes in concentrations of particles were negligible compared to the case without negative ions, since the probability for these reactions is low [46]. Therefore, channels of creation and recombination of negative ions were not included in the reaction set. Reaction rate coefficients for the model were derived assuming Maxwell distribution of electron energy using the software Bolsig+ [47] and cross-sections included therein or using other cross-sections from the literature (data sources shown in table 1). In addition, electron excitation of species to radiative states, except in the case of metastables, is treated only as an energy loss, i.e. no mass balances for excited state species are considered in the model. For the ion–neutral reactions of table 1, the rate coefficients are taken from the literature. Where a cross-section and not a coefficient is given in the literature, they are calculated by multiplying the cross-sections (data sources shown in table 1) with the velocity corresponding to the average ion energy between the bulk and the presheath. Ion

Table 1. The set of gas phase and surface reactions, threshold energies (E_{th}), comments (Com.) and sources of data (Ref.) for H_2/Ar low-pressure plasma.

Index	Reaction	E_{th} (eV)	Com.	Ref.
	Electrons and H_2			
	Electronic excitation			
(G1)	$H_2(X\,^1\Sigma_g^+) + e \rightarrow H_2(b\,^3\Sigma_u^+) + e \rightarrow 2H + e$	8.9	a	[47]
(G2)	$H_2 + e \rightarrow H_2(B\,^1\Sigma_u^+) + e$	11.37		[47]
(G3)	$H_2 + e \rightarrow H_2(C\,^1\Pi_u) + e$	12.4		[47]
(G4)	$H_2 + e \rightarrow H_2(c\,^3\Pi_u) + e \rightarrow 2H + e$	11.75	a	[47]
	Vibrational excitation			
(G5)	$H_2(X\,^1\Sigma_g^+, v = 0) + e \rightarrow H_2(X\,^1\Sigma_g^+, v = 1) + e$	0.52		[47]
(G6)	$H_2 + e \rightarrow H_2(v = 2) + e$	1.0		[47]
(G7)	$H_2 + e \rightarrow H_2(v = 3) + e$	1.5		[47]
	Dissociative excitation			
(G8)	$H_2 + e \rightarrow H(n = 3) + H + e$	16.6		[51]
	Ionization			
(G9)	$H_2 + e \rightarrow H_2^+ + 2e$	15.4		[47]
(G10)	$H_2 + e \rightarrow H + H^+ + 2e$	34.8		[52]
	Elastic			
(G11)	$H_2 + e \rightarrow H_2 + e$			[47]
	Electrons and H_2^+			
	Dissociative ionization			
(G12)	$H_2^+ + e \rightarrow H^+ + H + e$	4	b	[53]
(G13)	$H_2^+ + e \rightarrow 2H^+ + 2e$	19.4		[52]
	Dissociative recombination			
(G14)	$H_2^+ + e \rightarrow 2H$	0.01		[52]
	Electrons and H_3^+			
	Dissociative excitation			
(G15)	$H_3^+ + e \rightarrow H^+ + 2H + e$	14.3		[52]
	Dissociative recombination			
(G16)	$H_3^+ + e \rightarrow H_2 + H$	0.01		[52]
	Electrons and H			
	Ionization			
(G17)	$H + e \rightarrow H^+ + 2e$	13.6		[52]
	Electrons and Ar			
	Electronic excitation			
(G18)	$Ar + e \rightarrow Ar + e$	11.5	c	[54]
(G19)	$Ar + e \rightarrow Ar(met) + e$	13.08 13.27	d	[55]
	Ionization			
(G20)	$Ar + e \rightarrow Ar^+ + 2e$	15.8		[47]
	Elastic			
(G21)	$Ar + e \rightarrow Ar + e$			[47]
	Metastable quenching			
(G22)	$Ar(met) + e \rightarrow Ar + e$			[47]
	Electrons and heavyparticles			
	Recombination			
(G23)	$ArH^+ + e \rightarrow Ar + H$			[54]
	Heavy-particle interaction			
	Proton transfer			
(G24)	$H_2^+ + H_2 \rightarrow H_3^+ + H$			[43]
	H_2 quenching of Ar(met)			
(G25)	$Ar(met) + H_2 \rightarrow Ar + 2H$			[54]
	Ar quenching of Ar(met)			
(G26)	$Ar(met) + Ar \rightarrow 2Ar$			[56]
	Charge transfer			
(G27)	$Ar^+ + H_2 \rightarrow Ar + H_2^+$			[54]
	Proton transfer			
(G28)	$Ar^+ + H_2 \rightarrow ArH^+ + H$			[54]

Proton transfer			
(G29)	$ArH^+ + H_2 \rightarrow H_3^+ + Ar$		[54]
Momentum transfer			
(G30)	$H_3^+ + H_2 \rightarrow H_3^+ + H_2$		[50]
	$\sigma = 8.5 \times 10^{-15}$ cm^2 at 0.1 eV		
	$\sigma = 2.5 \times 10^{-15}$ cm^2 at 1 eV		
Atom–surface interaction			
Stainless steel		0.13	[49]
Quartz		0.003	[48]
Realistic case—quartz and stainless steel (weighted by areas)			
(S1)	$H \rightarrow 1/2\ H_2$	0.097	

[a] Excitation to triple states leads to dissociation [43].
[b] Threshold for the process established from [52].
[c] Total excitation.
[d] States 2p9 and 2p4 (in paschen notation), respectively.

temperature in the bulk is calculated to be close to 0.1 eV by the empirical relation [42] proposed by Lee and Liebermann (equation (5) in [40]), while presheath ion energy is half the electron temperature [8].

The set of reactions between gas species and chamber walls (heterogeneous reactions) consists of wall surface recombination of hydrogen atoms and the recombination of hydrogen molecular and atomic ions and Ar ions in collisions with chamber walls. The probability of recombination of atoms on surfaces for the reaction $H \rightarrow 1/2\ H_2$ was important for the agreement of the model results with experimental measurements (see section 4.4 on global model validation). Hence, value of the recombination probability was calculated using the values for quartz [48] and stainless steel [49] weighted by areas of the dome and the processing chamber (all coefficients for atom recombination on surfaces are shown in table 1). The rate coefficient for the loss of an ion in a surface reaction (see equation (9) in [40]) is analogous to the Bohm velocity and to a factor h; a different factor h is calculated for each wall surface of the reactor. h is the ratio of the sheath edge density to the average bulk density of the ion and depends [42] on several quantities (see equations (13) and (14) in [42]): the ratio of negative ion density to electron density, the ratio of the ion to electron temperature, the dimensions of the reactor, the Bohm velocity, the ambipolar diffusion coefficient, and the mean free path of ions. The mean free path is inversely proportional to the total ion–neutral cross-section. This total cross-section is required for the calculations of the global model and affects strongly the factor h, and as a consequence the loss of ions at the wall surfaces. For that cross-section, a value corresponding to the collision cross-section between H_3^+ ions (that are dominant ions) and H_2 neutrals is considered at the ion energy of 1 eV [50].

4. Results and discussion

4.1. Emission spectroscopy of a hydrogen plasma

A typical spectrum from a H_2/Ar plasma recorded in a wide range of wavelengths is shown in figure 2. Some hydrogen and argon lines are designated in the plot: lines from different transitions in atomic H and Ar and Fulcher α bands of lines coming from electronic transitions in H_2 molecule.

In figure 3 the variation of maximal intensity of four lines from optical emission spectra with power is shown. Two lines of atomic hydrogen: Hα—656.3 nm and Hβ—486.1 nm and two Ar lines: 750.4 nm and 811.5 nm all show increase in peak values with power increase. At powers higher than 1400–1600 W, when electron energies increase (see supporting data for electron temperature) Hα line exhibits larger increase in intensity compared to other lines. This is due to the fact that direct and dissociative excitation cross-section of this line is higher compared to other lines, and in addition the cross-section increases with increasing energy. The intensities of these lines were used for actinometric calculations.

4.2. Densities and the dissociation degree of hydrogen

The degree of dissociation of molecular hydrogen is a very important parameter in H_2 and H_2-containing low-temperature plasmas for understanding surface processes. For hydrogen, when an initial concentration of hydrogen molecules $N_{H_2}^0$ dissociates into a certain concentration of hydrogen atoms N_H, the dissociation degree x can be expressed as

$$x = \frac{1}{2} \cdot \frac{N_H}{N_{H_2}^0} = \frac{N_H/2}{N_{H_2} + (N_H/2)}. \quad (1)$$

Actinometry is one of the emission spectroscopy methods which relate the relative concentrations of two ground state atom species in the plasma with their emission intensity measurements. The method requires an addition of a small amount of noble gas (actinometer) in the feed gas and subsequent observation of lines belonging to the de-excitation transitions in atoms of both gases. The method proved to be an effective diagnostic technique to measure the densities of the various species [57–62] under conditions that fulfil the following assumptions: (i) the addition of a known small amount of an actinometer, A (Ar or other noble gas) should not affect the emissions of the feed gas atomic species G; (ii) the monitored optical emission should originate from excited states of the actinometer and the atomic species, A* and G*, which are dominantly produced through direct electron-impact excitation from ground states; (iii) the excitation cross-sections of A* and G* should have similar threshold energies and similar shapes as a function of energy; and (iv) the loss of A* and G* species should be dominated by radiative processes. Condition (iii) actually underlines that the same group of electrons in the electron energy distribution will take part in the excitation of A and G radiative states, making the method independent of the energy distribution function. Except in few cases [59, 61], these conditions prove to be over limiting since they neglect many processes such as cascading processes from higher excited states, dissociative excitation, collisions between heavy particles and quenching.

Particularly, in the case of H_2 plasmas, conditions (ii) and (iv) are not fulfilled. Detailed analysis of the kinetics of hydrogen excited species [31, 37] showed that in many conditions one has to include electron-impact dissociation of hydrogen molecules as an origin of excited H atoms and, at pressures higher than 100 Pa, the quenching of excited

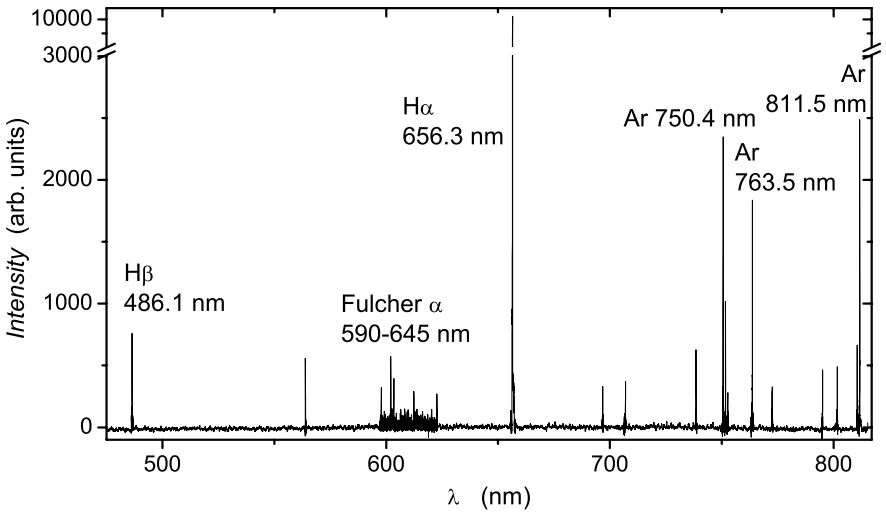

Figure 2. Spectra of a H_2/Ar plasma at 1 Pa recorded at 1200 W. Line intensities are relatively scaled.

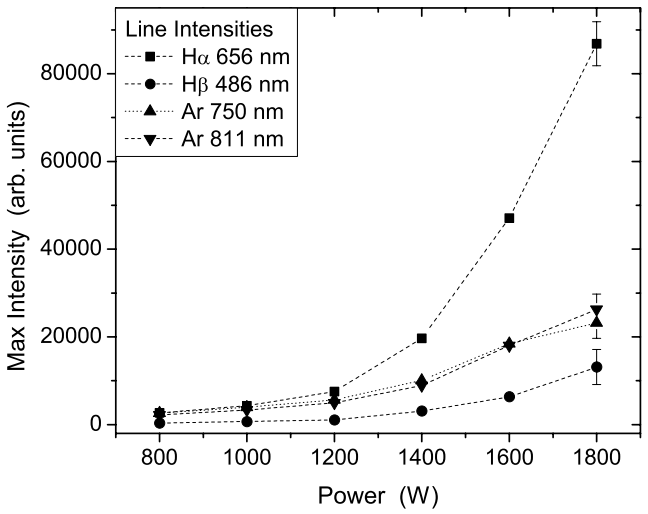

Figure 3. Maximal intensities of Hα, Hβ, Ar-750 and Ar-811 lines in H_2/Ar plasma at 1 Pa versus power. Line intensities are relatively scaled so that they can be compared.

states by other species [38]. In the case of Ar lines, apart from direct excitation from a ground level, excitation of upper levels may be achieved through a metastable state [31]. However, at the low pressures used in this work the density of Ar metastables is a few orders of magnitude lower than the density of Ar atoms, allowing one to disregard this excitation channel. All reactions taken into account for the actinometry are summarized in table 2. One should note that the reactions and corresponding cross-section data in table 2 consider electron-impact excitation to a particular level, while the reactions used in the global model (table 1) do not consider excited states. The rate coefficients used in all calculations were obtained by taking into account the cross-sections for the direct and dissociative excitation for Hα, Hβ taken from Lavrov and Pipa [63] and direct excitation for Ar lines using a set of Hayashi cross-sections [55] and calculated using Maxwell electron energy distribution function with mean electron energy obtained from Langmuir probe measurements.

From the reactions in the table 2, balance equations for atomic H and Ar excited species (H_j and Ar_p, respectively) can be written and are detailed in the online supplementary data section S1 (stacks.iop.org/JPhysD/46/475206/mmedia). From these equations and for steady-state plasma, the density ratios of H and Ar can be calculated as:

$$\frac{N_{\mathrm{H}}}{N_{\mathrm{Ar}}} = \frac{I_{\mathrm{H}}}{I_{\mathrm{Ar}}}\gamma\frac{k_{\mathrm{Ar}}^{\mathrm{dir}}}{k_{\mathrm{H}}^{\mathrm{dir}}(1+Ds)} \tag{2}$$

where

$$\gamma = \frac{C(\lambda_{\mathrm{Ar}})\,\lambda_H A_{\mathrm{Ar}p}(\sum_j A_{\mathrm{H}ji})}{C(\lambda_{\mathrm{H}})\,\lambda_{\mathrm{Ar}} A_{\mathrm{H}j}(\sum_p A_{\mathrm{Ar}pq})}$$

and

$$Ds = \frac{N_{\mathrm{H_2}} k_{\mathrm{H}}^{\mathrm{dis}}}{N_{\mathrm{H}} k_{\mathrm{H}}^{\mathrm{dir}}}$$

A_{ji} and A_{pq} are the spontaneous emission coefficients (in s^{-1}) between j and i states for atomic hydrogen and from p to q for Ar. λ_{H} and λ_{Ar} are the emission wavelengths corresponding to these two transitions and $C(\lambda_x)$ is the total optical detection efficiency of the spectroscopic system at λ_x.

Formula (2) shows a relation which links the line emission intensity ratio to the concentration ratios of atomic hydrogen and actinometer. Ds is the ratio of dissociative to direct excitation and the factor $(1+Ds)$ modifies the 'classical' actinometry formula by adding an electron-impact dissociation contributon. Rearranging formula (2) in the way that can fit expression (1), the dissociation degree of hydrogen can be obtained

$$x = \left(\frac{N_{\mathrm{Ar}}}{N_{\mathrm{H_2}}^0}\frac{I_{\mathrm{H}}}{I_{\mathrm{Ar}}}\gamma\frac{k_{\mathrm{Ar}}^{\mathrm{dir}}}{k_{\mathrm{H}}^{\mathrm{dir}}} - \frac{k_{\mathrm{H}}^{\mathrm{dis}}}{k_{\mathrm{H}}^{\mathrm{dir}}}\right) \Big/ \left(2 - \frac{k_{\mathrm{H}}^{\mathrm{dis}}}{k_{\mathrm{H}}^{\mathrm{dir}}}\right) \tag{3}$$

and thus the H densities.

The density of hydrogen atoms in the chamber centre was also determined using a catalytic probe, from the time dependence of temperature recorded from a thermocouple located at the probe tip and merged to catalytic material.

Table 2. Processes occurring in H_2/Ar low-pressure plasmas used for actinometry calculations. The reference data is given in the far right column.

	Process		E_{th} (eV)	Rate coef. at 3 eV (10^{-18} m^3 s^{-1})		Ref.
1a	H atom excitation	$H(n=1) + e \rightarrow H(n=3) + e$	12.09	k_H^{dir}	41.4	[63]
1b		$H(n=1) + e \rightarrow H(n=4) + e$	12.75		8.86	
2	H_2 dissociative excitation	$H_2 + e \rightarrow H(n=3) + H(n=1) + e$	16.57	k_H^{dis}	0.53	[63]
		$H_2 + e \rightarrow H(n=4) + H(n=1) + e$	17.23		0.01	
3	Ar direct excitation	$Ar(3p) + e \rightarrow Ar(4p'[1/2]0) + e$	13.48	k_{Ar}^{dir}	10.7	[55]
		$Ar(3p) + e \rightarrow Ar(4p[5/2]3) + e$	13.08		11.2	
4	Radiative de-excitation		A_{ij} (10^6 s^{-1})		$\sum A_{ij}$	
4a		$H(n=3) \rightarrow H(n=2) + h\nu(H\alpha - 656\,nm)$	44.1		99.8	[64]
		$H(n=4) \rightarrow H(n=2) + h\nu(H\beta - 486\,nm)$	8.4		30.2	
4b		$Ar(4p'[1/2]0) \rightarrow Ar(4s) + h\nu(750\,nm)$	44.5		44.7	[64]
		$Ar(4p[5/2]3) \rightarrow Ar(4s) + h\nu(811\,nm)$	33.1		33.1	

Namely, after plasma ignition the thermocouple registers a temperature increase until it saturates at some constant value. Indeed, due to extensive recombination of hydrogen atoms at the surface of the catalyst, energy dissipation of the reaction (heating term) makes the recorded temperature above the ambient temperature. A typical temperature curve is shown in the online supplementary data (see figure S2 (stacks.iop.org/JPhysD/46/475206/mmedia)). The temperature saturates when the contribution of heating and cooling terms become equal [26]. Immediately after turning the plasma off, the catalytic material of the probe starts to cool down, the temperature drops and dT/dt describes the cooling term. The full physical formalism and precision of the method is discussed elsewhere [65, 66], while details of the calculation are described in the online supplementary data section S3 (stacks.iop.org/JPhysD/46/475206/mmedia). The result of the calculation is an equation for the density of H atoms obtained by equating the heating and the cooling terms at the dropping edge of the temperature curve:

$$n = \frac{8\,m C_p}{\nu W_D \gamma_{cat} A}\left(\frac{dT}{dt}\right), \qquad (4)$$

where ν is the average thermal velocity of H atoms at room temperature (2520 m s^{-1}), W_D is 7.24×10^{-19} J or 4.52 eV. γ_{cat} is assumed to be constant and equal to 0.18. The probe area A was 21 mm^2, mass m was 0.0203 g and the specific heat capacity C_p of gold is 130 J kg^{-1} K^{-1}.

In figure 4, densities of H atom in the centre of the reactor for different powers measured with the catalytic probe are shown (green diamonds). Together with probe measurements, absolute atom densities calculated from actinometry are also plotted (squares and circles). Calculations were performed using the constants shown in table 2, electron temperature of 3 eV measured with a Langmuir probe (see section 4.3) and assuming a gas temperature of $T_g = 315$ K. In figure 4(*a*) calculations were performed employing formula (3), while results in figure 4(*b*) are obtained using the 'classical' actinomery formula, disregarding the dissociation contribution term Ds in equation (2). The densities were calculated using four different actinometric line pairs: (Hα, Ar750), (Hα, Ar811), (Hβ, Ar750) and (Hβ, Ar811). All results show an increase of the density of atomic hydrogen with power. In the case of actinometry including Ds term, comparisons show very good agreement of probe measurements with actinometric results using (Hβ, Ar750) and (Hβ, Ar811) line pairs, while calculations with (Hα, Ar750) and (Hα, Ar811) pairs produced values which are about three times lower than probe measurements.

Similar results are also observed for the classical actinometry formula (with $Ds = 0$), with values only slightly increased at low powers (where the Ds term is larger). The accuracy of the catalytic probe is typically about 30%. The actinometric measurements have an accuracy of 15%. The discrepancy between the (Hβ, Ar750), (Hβ, Ar811) and the catalytic probe results falls within the accuracy of both techniques.

The discrepancy in actinometry results obtained with different line pair has been noticed before [67], and it may come from atomic data differences (i.e. cross-sections and/or transition constants) [37] or from the fact that the excited levels are not populated only by direct electron-impact from the ground state [67]. Moreover, when threshold energy for an excitation process lies in the tail of an electron energy distribution function, differences in threshold energies become important since different electron groups take part in the excitation processes of hydrogen and Ar. This may be the reason for better agreement of the catalytic probe data with actinometry calculations with Hβ line, since the difference in threshold energies between hydrogen and argon is smaller in this case (see table 2). Anyhow, small differences between results obtained from the formula including the dissociation term and the one without it, show that in this case the dissociation contribution can be neglected. Despite the differences between absolute values coming from the actinometry and experimental measurements, all data obtained with the actinometric method have the same tendency as the results from the catalytic probe. However, since H densities in actinometry are obtained from integrated line intensities along the full diameter of the chamber and the catalytic probe is collecting atoms from the one point, at the centre of the chamber 5 cm above the wafer holder, some disagreement could be expected.

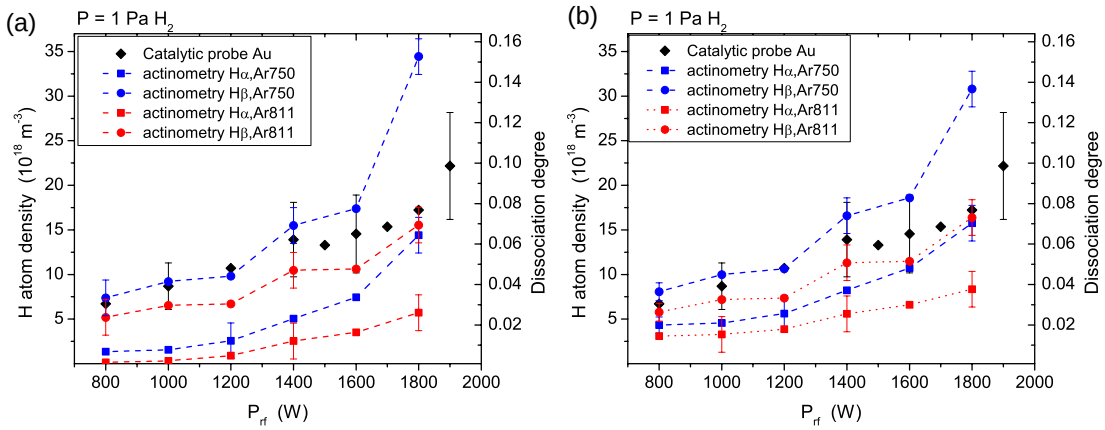

Figure 4. Measurements of H atom densities using a catalytic probe (diamonds) and optical actinometry employing different ratios of lines: (Hα, Ar750) (blue squares), (Hα, Ar811) (red squares), (Hβ, Ar750) (blue circles) and (Hβ, Ar811) (red circles). (*a*) shows results using a complete actinometry formula taking into account dissociative ionization (e.g. see equation (3)). (*b*) shows the results from 'classical actinometry' (i.e. neglecting the dissociation term see equation (2) with *D*s neglected, i.e. *D*s < 0.1). Catalytic measurements were done at hydrogen pressure of 1 Pa, and flowrate 50 sccm, while for actinometry measurements 5% of Ar (2.5 sccm) was added at constant pressure.

Table 3. Coefficients used for actinometric calculations.

Actinometry ratio used	λ-involved (nm)	Detector response ratio in our system	Ratio of A coefficients	γ	Actinometric conversion coefficient $\gamma^* k_{\mathrm{Ar}}^{\mathrm{dir}}/k_{\mathrm{H}}^{\mathrm{dir}}$ to convert intensity to concentration ratio of $N_{\mathrm{H}}/N_{\mathrm{Ar}}$.					
					2 eV	2.5	3 eV	3.5	4 eV	4.5
Hα/Ar750	656/750	0.7	2.2	1.4	0.25	0.31	0.36	0.41	0.44	0.48
Hα/Ar811	656/811	0.4	2.3	0.8	0.19	0.20	0.22	0.22	0.23	0.23
Hβ/Ar750	486/750	1.7	3.6	3.9	3.55	4.16	4.70	5.19	5.60	5.99
Hβ/Ar811	486/811	1.1	3.6	2.2	2.62	2.71	2.78	2.83	2.85	2.87

In order to evaluate the approximate limits of validity of actinometry for all combination of line pairs used, an analysis of actinometric formula (equation (3)) was performed and is presented in the online supplementary data section S2 (stacks.iop.org/JPhysD/46/475206/mmedia). For the Hα line, the dissociation term can be neglected (i.e. *D*s $\leqslant$ 0.1) for density ratios larger than 5% (dissociation $>\sim$2.5%) for any electron temperature (figure S1a (stacks.iop.org/JPhysD/46/475206/mmedia)). In the case of Hβ line, neglecting the term *D*s (i.e. *D*s $\leqslant 0.1$) is justified only for electron temperatures lower than 3 eV and density ratios larger than 10% (dissociation $>\sim$ 5%) (figure S1b (stacks.iop.org/JPhysD/46/475206/mmedia)). Nevertheless, for our experiments it seems that even for Hβ line it is safe to neglect dissociative excitation except at low powers (below 1200 W see figure 4). Since Hβ lines better compare with experiments if the conditions discussed above and detailed in the online supplementary data are met, it is best to use the Hβ line.

Finally, in table 3 we present values of the actinometric conversion coefficient, i.e. the coefficient to convert intensity ratios to density ratios in the case of 'classical actinometry' for several electron temperatures. Using the conversion coefficient allows simple conversion of actinometric line intensity ratio to absolute H density, assuming that the dissociation term can be neglected. Additionally, spectrometric constants of the system used in our experiment and ratios of atomic transition probabilities are also given. Spectral efficiency constants are obtained using a standard calibration lamp. Rate coefficients entering (3) are calculated using reference data given in table 2 and assuming a Maxwellian energy distribution of electrons. It is hoped that this table can be of use to people doing H actinometry as an approximate semi-quantitative guide to convert actinometric data to densities.

4.3. Densities of electrons and ions, plasma potential and ion flux

We used a cylindrical Langmuir probe to measure the *I*–*V* characteristics of the plasma and extract the ion and electron saturation current, the plasma potential, the electron temperature and ion flux using the ESPion software [68].

In figure 5, in the left hand-side axis, the change in densities of electrons and ions for different powers forwarded to plasma is presented. Measured densities exhibit slow increase towards higher powers, with nearly parallel slopes. However, for powers higher than 1600 W electron density seems to saturate and slightly decrease, while ion density continues to increase. Measured electron densities are in the range 0.4–0.7 $\times$ 10^{16} m^{-3} and measured ion densities are 2–4 times higher ((0.9–1.7) $\times$ 10^{16} m^{-3}) depending on the power forwarded to the plasma. One has to take into account the fact that determination of the ion densities by using ion saturation current can lead to errors that could easily go up to 20–30% [5].

Measurements of plasma potential are shown in figure 5, in the right hand-side axis. For powers below 1700 W,

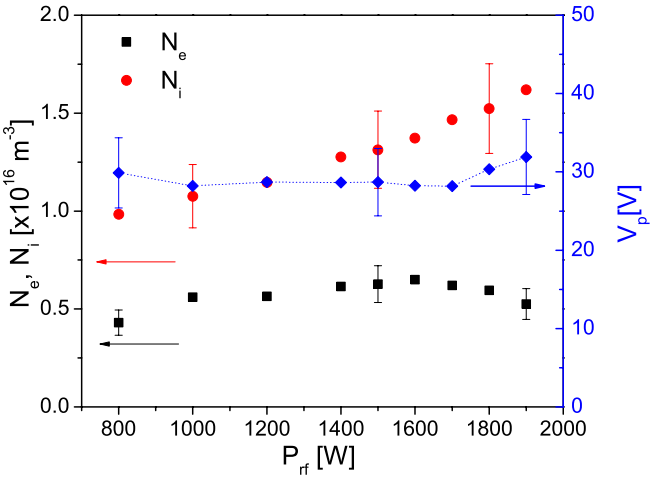

Figure 5. Electron and ion densities (left hand-side axis) and plasma potential (right hand-side axis) in H_2 plasma at 1 Pa at different powers.

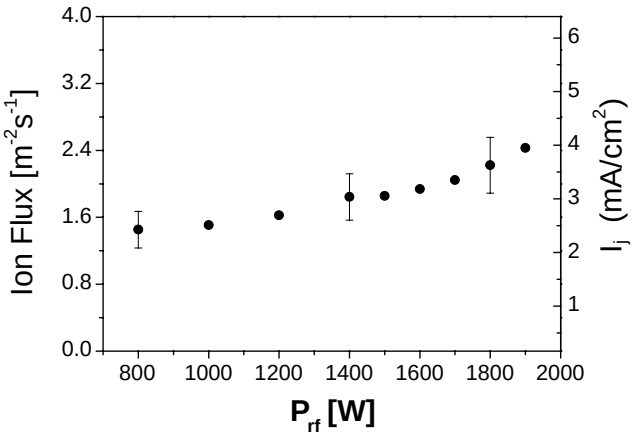

Figure 6. Change of ion flux (left axis) and ion current density (right axis) with power in H_2 plasma at 1 Pa.

the potential in the centre of the chamber shows almost no change with power, staying around 29 V. At higher powers V_p rises up to 32 V. At the same time measured electron temperature at the centre of the chamber is almost constant (3 eV) up to 1700 W of forwarded power, when it increases and reaches 4.5 eV at the maximum power of 1900 W (see figure S3 in the supplementary data (stacks.iop.org/JPhysD/46/475206/mmedia)). At the same time, for the same powers, there is a decrease in electron density. Sudit and Chen [69] stated that mean electron energy and density of electrons are coupled (in order to have constant pressure ($N_e k T_e$)). The coupling of these two values can be seen also in our case.

The increase in the mean electron energy for the higher powers is also consistent with the increase of the Hα and Hβ line intensities (figure 3) as well an increase in hydrogen atom density (figure 4).

The flux of ions at the centre of the chamber is shown in figure 6. In the right axis, values of ion current density values are presented. The flux rises with an increase in power, as expected.

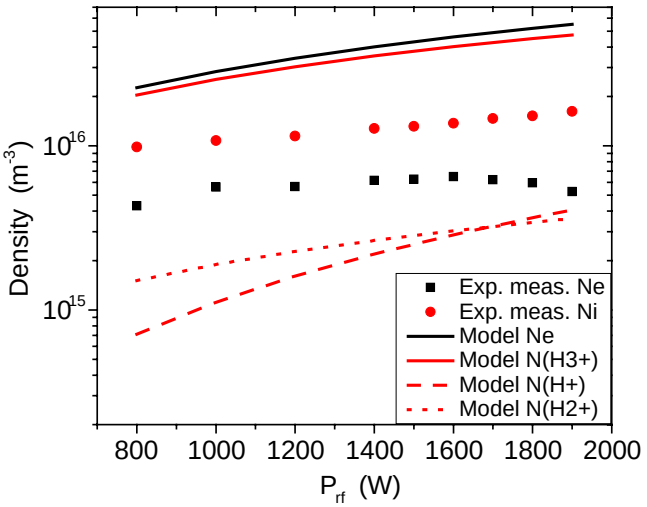

Figure 7. Electron (and total ion) density (full line), H_3^+ ions (dash-dot line), H_2^+ ions (dotted line) and H^+ ions (dashed line) calculated in the model for different powers compared with Langmuir probe measurements (N_e—black squares, N_i—red dots).

Therefore,it is evident that all plasma parameters presented (N_i, V_p, I_{flux}, N_H) exhibit similar dependency changes versus RF power.

4.4. Comparison with the global model

The obtained experimental results allowed us to make a comparison with the results from a zero-dimensional (0d), global model, supplied with the gas reaction set for hydrogen and the realistically calculated surface recombination coefficient (section 3). We focus our discussion on the results for the electron temperature (T_e), the electron density (N_e), and the density of H (N_H).

The electron temperature is calculated 3.58 eV from the global model; it does not change versus power. It is 19% greater than the measured electron temperature for power from 800 to 1700 W.

In figure 7 the densities of charged particles coming from the model are compared to the experimental results. The calculated density for H_3^+ and electron density is (2–4) $\times 10^{17}$ m^{-3} which is approximately 2 to 4 times higher than the experimental values. Electron density calculated by the model is around 6 times greater than the measured one. However, the relative increase of calculated densities with power follows the experimental results.

In figure 8 the density of H obtained from the model are shown together with the catalytic probe data measured at the chamber centre and actinometry results from (Hβ, Ar750) and (Hβ, Ar811) lines. The results attained with a surface recombination coefficient (k_r) equal to 0.097 (black line) agree well with the experimental data: the calculated density of H is 1.2–2 times greater than the measured one. The recombination coefficients for quartz glass [48] and stainless steel [49] are weighted according to the contribution of these materials to the surface area in the reactor chamber. The obtained value of 0.097 for k_r depicts a physically realistic situation, since it takes into account both materials present inside the reactor

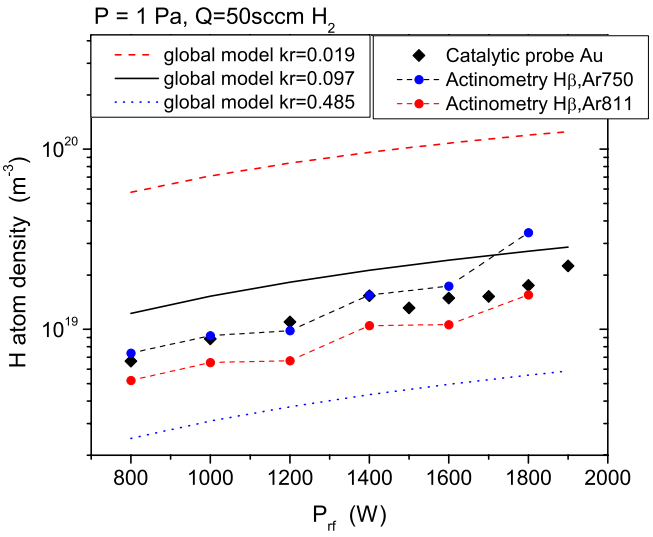

Figure 8. Comparison of H density obtained from the global model for three different values of surface recombination coefficient and the catalytic probe and actinometry data.

(quartz and stainless steel) with their respective areas. All density curves in figure 8 have the same slope, thus the change of H atoms is independent of the recombination coefficient. Densities of Ar neutrals, metastables and ions were also calculated in the model. Since initial Ar atom density is low, densities of produced ions and metastables are a few orders of magnitude lower.

When comparing modelling with experimental results one should have in mind that modelling results are coming from a global, 0d or volume-averaged model aiming to capture the complex phenomena occurring in 3d in a plasma reactor. There are works referring to global models where the plasma generation region is treated separately from the processing (diffusion) chamber (see for example [70]). In the global model used here, there was no separate treatment of the two regions; this may be an additional source for differences between experimental and simulation results.

In order to further investigate the potential origin of differences in uncertainties of the model parameters, a sensitivity analysis was performed (see supplementary data). All model parameters (reaction rate coefficients, recombination coefficient and cross-section for ion–neutral collisions) were increased 5 times and decreased 5 times. When a model parameter changed, all others were kept constant. It should be noted that we changed the pre-exponential factor of the reaction rate coefficients. The reaction rate coefficients are functions of T_e, thus a change of the pre-exponential factor, through its effect on the balances, may result into a change of T_e. The sign of the change of the rate coefficient depends on the changes of both the pre-exponential factor and T_e. It is not impossible that an increase of the pre-exponential factor will finally result in a decrease of the reaction rate coefficient through a decrease of T_e. We focused on the effect of model parameters on T_e, N_e, and N_H. A parameter was identified as important if the absolute value of the % change of T_e, N_e, or N_H is greater than 50% or less than −33%, i.e. when the value of T_e, N_e, or N_H is multiplied or divided by 1.5. The results for the important parameters are summarized in table 4.

Table 4. Sensitivity analysis for the results of the model: the % change of N_H, N_e, and T_e when the important (see supplementary information for the full sensitivity table) model parameters are multiplied and divided by 5. When one parameter changes the rest of them remain constant. The base case conditions are 50 sccm of H_2 feed, pressure of 1 Pa, and power of 1400 W. The indices of k in the first column correspond to the indices of the reactions in table 1.

Model parameter	$\%\Delta N_H$	$\%\Delta N_e$	$\%\Delta T_e$
$k_1\times5$	79.24	−48.29	−0.53
$k_1/5$	−40.34	23.66	0.27
$k_2\times5$	−35.39	−36.64	0.09
$k_2/5$	12.15	12.91	−0.03
$k_9\times5$	−9.89	97.85	−26.28
$k_9/5$	−8.48	−57.01	49.31
$k_r\times5$	−79.61	−3.21	0.41
$k_r/5$	352.69	16.36	−1.75
$\sigma_{\text{ion-neutral}}\times5$	7.45	85.03	−15.67
$\sigma_{\text{ion-neutral}}/5$	−7.53	−30.25	10.70

The important model parameters are the rate coefficients of reactions (G1) (electronic excitation leading to H_2 dissociation, see table 1), (G2) (electronic excitation) and (G9) (ionization of H_2), the surface recombination coefficient (reaction (S1), see table 1) and the cross-section for ion–neutral collisions in plasma (reaction (G30), see table 1); the latter parameter plays an important role to the losses of ions at the wall surfaces by affecting the parameter h (see section 3).

When the rate coefficient for the dissociation reaction (G1) (k_1) increases (decreases), the density of H increases (decreases) and the electron density decreases (increases), while the electron temperature remains constant. The increase (decrease) of the rate coefficient for the electronic excitation reaction (G2) (k_2) causes a decrease (small increase) of both the electron and H density; the electron temperature is not affected by the change of k_2. The increase (decrease) of the rate coefficient for the ionization reaction (G9) (k_9) induces an increase (decrease) of the electron density and a decrease (increase) of the electron temperature; the density of H is slightly decreased with the change of k_9.

Enriching the sensitivity analysis, the effect of the surface recombination coefficient (k_r) on the density of H is shown in figure 8 for the whole power range investigated. Figure 8 includes the densities of H obtained from the model for different surface recombination coefficient together with the catalytic probe data measured at the chamber centre. The results of the model obtained with $k_r = 0.485$ ($0.097 \cdot 5$) are far below the experimental data (dots in figure 8). In this case, the value of the coefficient is high, well above the value for stainless steel [49], the recombination seems to be overestimated, and the density of H is lower by a factor of 2 compared to the measured density. The model results acquired with lower recombination coefficient, $k_r = 0.019$, yielded 3 to 4 times higher H densities compared to the base case ($k_r = 0.097$, compare the dashed line with the black line in figure 8). Such low recombination coefficients could be present in the case of glass-type surfaces [48].

Finally, the increase (decrease) of the cross-section for ion–neutral collisions ($\sigma_{\text{ion-neutral}}$) causes an increase

(decrease) of the electron density and a small decrease (increase) of the electron temperature; the change of $\sigma_{\text{ion-neutral}}$ slightly affects the density of H.

The main discrepancy between the modelling and the experimental results is in the value of the electron density; the electron density is calculated to be 6 times greater. The sensitivity analysis shows that this discrepancy could have been reduced if k_1 and/or k_2 were greater. It could have been also reduced if k_9 was lower; however, in the latter case the electron temperature would have been increased (see table 4).

Regarding k_1 (rate coefficient for the dissociation of H_2), it is rather greater than the value we used: some paths to dissociation coming from vibrational excitations [45, 71] were not taken into account. Sawada and Fujimoto [72] calculated an effective rate coefficient for the H_2 dissociation which is greater than the one used in this work; in particular, for an electron temperature equal to 3.5 eV, they report an effective rate coefficient which is about 4 times greater (figure 5 of [72]) than the one we used. Indeed, the sensitivity analysis shows that a multiplication of k_1 with 5 will result in an electron density 3 (and not 6) times greater than the experimental result.

Regarding k_2 (rate coefficient for electronic excitation reaction), we have no evidence that it has an underestimated value. However, what the sensitivity analysis shows us is that omitted excitation reactions (even if they do not join the mass balances as reaction (G2)) potentially affect the electron density; the addition of more excitation reactions in the reaction set of table 1, will increase the energy loss rate per electron which will subsequently result in a decrease of the electron density. Regarding the reaction set of table 1, the omission of excitation reactions, e.g. vibrational excitations [45, 71] or metastable atoms [43], could result into an overestimation of the electron density. We are working on a 2d plasma model for H_2 discharges, where all these potential sources of discrepancies will be further investigated in conjunction with a more detailed model. In addition, we will also check the effect of using the experimentally obtained EEDF (and not a Maxwellian EEDF) on the rate coefficients of electron-impact reactions and as a consequence on the model results.

5. Conclusions

Low-pressure hydrogen plasma characterization was performed in the helicon-type RF source in the region close to the wafer holder position using experimental measurements and a global model. Density of atomic hydrogen was determined using two independent diagnostic methods, namely catalytic probes and actinometry. We have found that in general there is a good agreement in the results, within the measurement error. In the case of (Hβ, Ar750) and (Hβ, Ar811) line pairs, the consistency was even better than in the case of (Hα, Ar750), (Hα, Ar811). The reason for this is that both the sensitivity of the method on cross-section data and the differences in threshold energies may influence the actinometric calculations.

Furthermore, we have investigated the domain of applicability of 'classical' actinometic formula by looking at the magnitude of the dissosiative excitation term (see supplementary data). We have defined the range of conditions where the dissociative excitation term can be neglected. For such conditions we have calculated and tabulated the proportionality constant for several actinometric lines, and hope that this calculation may be useful for quick real-time measurements of H densities at least in a semi-quantitative way, given the uncertainties in cross-sections and the possibility of non-Maxwellian electron energy distributions.

We have used Langmuir probe simultaneously with other diagnostics to record the plasma parameters such as N_i, N_e and ion flux for standard material processing conditions. The obtained results fall in the range of typical values for such reactor. Densities of electrons and ions in hydrogen plasma of around $10^{16}\,m^{-3}$ were slowly changing with plasma power. Ion flux was found to rise steadily with increasing power from 1.5 to $2.5 \times 10^{20}\,m^{-2}\,s^{-1}$. The established global model of hydrogen plasma included both gas phase reactions and surface reactions. We have shown that H atom concentration depends considerably on the surface recombination coefficient, i.e. material of the reactor walls. The best agreement with the catalytic probe results was obtained when a realistic surface recombination coefficient of stainless steel/quartz walls was used. The global model shows that there is a reasonable agreement with experimentally measured electron temperature, and the charged particle densities measured by Langmuir probe. In order to test the model and provide an explanation for the differences observed in the comparison, a detailed sensitivity analysis was performed by changing input parameters of the model. The important model parameters are the rate coefficients of electronic excitation leading to H_2 dissociation and ionization of H_2, the surface recombination coefficient of H, and the cross-section for ion–neutral collisions in the plasma (reaction (G30), see table 1), which plays an important role to the losses of ions at the wall surfaces.

For successful material processing in an industrial reactor like ours, detailed characterization of the discharge parameters, plasma–surface interactions and plasma behaviour needs to be employed. Even though the reactor has a relatively complex geometry, the global model provided good insight into plasma behaviour. Detailed plasma parameter measurements give a firm ground for optimization of material surface cleaning processes.

Acknowledgments

The main funding of this work (EG, NŠ) came from the EU FP7 Marie Curie Initial Training Network Surface Physics for Advanced Manufacturing—S.P.A.M, grant n° 215723. NP gratefully acknowledges the support of Ministry of Science and Technological Development, Serbia, for scholarship and projects under the contract numbers ON171037 and III41011. SL and UC acknowledge the support of ARRS, AdFutura and COST action MP1011. GK was funded by the project CORSED (PE-844) under the program 'Supporting post-doctoral researchers' of the National Strategic Reference Framework; the source of funding is the European Social Fund (ESF)-European Union and National Resources.

References

[1] Manos D M and Flamm D L 1989 *Plasma Etching: An Introduction* (New York: Academic)

[2] Mahan J E 2000 *Physical Vapor Deposition of Thin Films* (New York: Wiley)

[3] Ostrikov K 2007 Plasma nanoscience: from nature's mastery to deterministic plasma-aided nanofabrication *IEEE Trans. Plasma Sci.* **35** 127

[4] Makabe T and Petrovic Z Lj 2006 *Plasma Electronics* (New York: Taylor and Francis)

[5] Francis C F and Chang J P 2002 *Lecture Notes on Principles of Plasma Processing* (New York/Dordrecht: Plenum/Kluwer)

[6] Fridman A 2008 *Plasma Chemistry* (New York: Cambridge University Press)

[7] Gogolides E, Constantoudis V, Kokkoris G, Kontziampasis D, Tsougeni K, Boulousis G, Vlachopoulou M and Tserepi A 2011 Controlling roughness: from etching to nanotexturing and plasma-directed organization on organic and inorganic materials *J. Phys. D: Appl. Phys.* **44** 174021

[8] Liberman M A and Lichtenberg A J 2005 *Principles of Plasma Discharges and Materials Processing* (Hoboken, NJ: Wiley)

[9] Samukawa S *et al* 2012 The 2012 plasma roadmap *J. Phys. D: Appl. Phys.* **45** 253001

[10] Sharpe J P, Petti D A and Bartels H-W 2002 A review of dust in fusion devices: Implications for safety and operational performance *Fusion Eng. Des.* **63/64** 153

[11] Graham S, Steinhaus C, Clift M and Klebanoff L 2002 Radio-frequency discharge cleaning of silicon-capped Mo/Si multilayer extreme ultraviolet optics *J. Vac. Sci. Technol.* B **20** 2393

[12] Koide T, Yanagihara M, Aiura Y, Sato S, Shidara T, Fujimori A, Fukutani H, Niwano M and Kato H 1987 Resuscitation of carbon-contaminated mirrors and gratings by oxygen-discharge cleaning. in the 4–40 eV range *Appl. Opt.* **26** 3884

[13] Malinowski M E, Steinhaus C, Clift W M, Klebanoff L E, Mrowka S and Soufli R 2002 Controlling contamination in Mo/Si multilayer mirrors by Si surface capping modifications *Proc. SPIE* **4688** 442

[14] Morgan C G and Vane R 2012 Carbon contamination removal in larger chambers with low-power downstream plasma cleaning *Proc. SPIE* **8324** 83242F

[15] Wurm S and Gwyn C W 2007 *Microlithography* (Boca Raton, FL: CRC Press/Taylor and Francis Informa Group)

[16] Nishiyama I, Oizumi H, Motai K, Izumi A, Ueno T, Akiyama H and Namiki A 2005 Reduction of oxide layer on Ru surface by atomic-hydrogen treatment *J. Vac. Sci. Technol.* B **23** 3129

[17] Graham S Jr, Steinhaus C A, Clift W M, Klebanoff L E and Bajt S 2003 Atomic hydrogen cleaning of EUV multilayer optics *Proc. SPIE* **5037** 460

[18] Braginsky O V *et al* 2012 Removal of amorphous C and Sn on Mo : Si multilayer mirror surface in Hydrogen plasma and afterglow *J. Appl. Phys.* **111** 093304

[19] Braithwaite N S J and Franklin R N 2009 Reflections on electrical probes *Plasma Sources Sci. Technol.* **18** 014008

[20] Chen F F 2009 Langmuir probes in RF plasma: surprising validity of OML theory *Plasma Sources Sci. Technol.* **18** 035012

[21] Godyak V A, Piejak R B and Alexandrovich B M 1992 Measurement of electron energy distribution in low-pressure RF discharges *Plasma Sources Sci. Technol.* **1** 36

[22] Ferreira J A and Tabareìs F L 2007 Cryotrapping assisted mass spectrometry for the analysis of complex gas mixtures *J. Vac. Sci. Technol.* A **25** 246

[23] Gaboriau F, Cartry G, Peignon M-C and Cardinaud C 2006 Etching mechanisms of Si and SiO_2 in fluorocarbon ICP plasmas: analysis of the plasma by mass spectrometry, Langmuir probe and optical emission spectroscopy *J. Phys. D: Appl.Phys.* **39** 1830

[24] Malovic G, Puac N, Lazovic S and Petrovic Z 2010 Mass analysis of an atmospheric pressure plasma needle discharge *Plasma Sources Sci Technol.* **19** 034014

[25] Mozetić M, Ricard A, Babić D, Poberaj I, Levaton J, Monna V and Cvelbar U 2003 Comparison of NO titration and fiber optics catalytic probes for determination of neutral oxygen atom concentration in plasmas and postglows *J. Vac. Sci. Technol.* A **21** 369

[26] Mozetic M, Cvelbar U, Vesel A, Ricard A, Babic D and Poberaj I 2005 A diagnostic method for real-time measurements of the density of nitrogen atoms in the postglow of an Ar–N_2 discharge using a catalytic probe *J. Appl. Phys.* **97** 103308

[27] Gaboriau F, Cvelbar U, Mozetic M, Erradi A and Rouffet B 2009 Comparison of TALIF and catalytic probes for the determination of nitrogen atom density in a nitrogen plasma afterglow *J. Phys. D: Appl. Phys.* **42** 055204

[28] Labazan I and Milošević S 2004 Determination of electron density in a laser-induced lithium plume using cavity ring-down spectroscopy *J. Phys. D: Appl. Phys.* **37** 2975

[29] Makabe T and Petrović Z L 2002 Development of optical computerized tomography in capacitively coupled plasmas and inductively coupled plasmas for plasma etching *Appl. Surf. Sci.* **192** 88

[30] Booth J-P, Joubert O, Pelletier J and Sadeghi N 1991 Oxygen atom actinometry reinvestigated: Comparison with absolute measurements by resonance absorption at 130 nm *J. Appl. Phys.* **69** 618

[31] Gicquel A, Chenevier M, Hassouni K, Tserepi A and Dubus M 1998 Validation of actinometry for estimating relative hydrogen atom densities and electron energy evolution in plasma assisted diamond deposition reactors *J. Appl. Phys.* **83** 7504

[32] Mozetic M, Vesel A, Cvelbar U and Ricard A 2006 An iron catalytic probe for determination of the O-atom density in an Ar/O_2 afterglow *Plasma Chem. Plasma Proc.* **26** 103

[33] Primc G, Zaplotnik R, Vesel A and Mozetic M 2011 Microwave discharge as a remote source of neutral oxygen atoms *AIP Adv.* **1** 022129

[34] Vrlinic T, Mille C, Debarnot D and Poncin-Epaillard F 2009 Oxygen atom density in capacitively coupled RF oxygen plasma *Vacuum* **83** 792

[35] Lazović S, Puač N, Spasić K, Malović G, Cvelbar U, Mozetič M, Radetić M and Petrović Z Lj 2013 Plasma properties in a large-volume, cylindrical and asymmetric radio-frequency capacitively coupled industrial-prototype reactor *J. Phys. D: Appl. Phys.* **46** 075201

[36] Mozetic M, Vesel A, Drenik A, Poberaj I and Babic D 2007 Catalytic probes for measuring H distribution in remote parts of hydrogen plasma reactors *J. Nucl. Mater.* **363–365** 1457

[37] Schulz-von der Gathen V and Döbele H F 1996 Critical comparison of emission spectroscopic determination of dissociation in hydrogen RF discharges *Plasma Chem. Plasma Process.* **16** 461

[38] Wouters M J, Khachan J, Falconer I S and James B W 1999 Quenching of excited Ar I and H by H_2 in a gas discharge *J. Phys. B: At. Mol. Opt. Phys.* **32** 2869

[39] Kokkoris G, Panagiotopoulos A, Goodyear A, Cooke M and Gogolides E 2009 A global model for SF_6 plasmas coupling reaction kinetics in the gas phase and on the surface of the reactor walls *J. Phys. D: Appl. Phys.* **42** 055209

[40] Kokkoris G, Goodyear A, Cooke M and Gogolides E 2008 A global model for C_4F_8 plasmas coupling gas phase and wall surface reaction kinetics *J. Phys. D: Appl. Phys.* **41** 195211

[41] Chabert P and Braithwaite N 2011 *Physics of Radio-Frequency Plasmas* (Cambridge: Cambridge University Press)
[42] Lee C and Lieberman M A 1995 Global model of Ar, O_2, Cl_2, and Ar/O_2 high-density plasma discharges *J. Vac. Sci. Technol.* A **13** 368
[43] Bogaerts A and Gijbels R 2000 Effects of adding hydrogen to an argon glow discharge: overview of relevant processes and some qualitative explanations *J. Anal. At. Spectrom.* **15** 441
[44] Zorat R and Vender D 2000 Global model for an rf hydrogen inductive plasma discharge in the deuterium negative ion source experiment including negative ions *J. Phys. D: Appl. Phys.* **33** 1728
[45] Capitelli M, Celiberto R, Esposito F, Laricchiuta A, Hassouni K and Longo S 2002 Elementary processes and kinetics of H_2 plasmas for different technological applications *Plasma Sources Sci. Technol.* **11** A7
[46] Wadehra J M and Bardsley J N 1978 Vibrational- and rotational-state dependence of dissociative attachment in e-H_2 collisions *Phys. Rev. Lett.* **41** 1795
[47] Hagelaar G J M, Bolsig+, www.codiciel.fr/plateforme/plasma/bolsig/ (2012)
[48] Wood B J and Wise H 1958 Diffusion and heterogeneous reaction: II. Catalytic activity of solids for hydrogen-atom recombination *J. Chem. Phys.* **29** 1416
[49] Jolly J and Booth J-P 1990 Atomic hydrogen densities in capacitively coupled very high-frequency plasmas in H_2: effect of excitation frequency *J. Appl. Phys.* **97** 103305
[50] Phelps A V 1990 Cross sections and swarm coefficients for H^+, H_2^+, H_3^+, H, H_2, and H^- in H_2 for energies from 0.1 eV to 10 keV *J. Phys. Chem. Ref. Data* **19** 653
[51] Buckman S and Phelps A 1985 Vibrational excitation of D_2 by low energy electrons *J. Chem. Phys.* **82** 4999
[52] Tawara H, Itikawa Y, Nishimura H and Toshino M 1990 Cross sections and related data for electron collisions with hydrogen molecules and molecular ions *J. Phys. Chem. Ref. Data* **19** 617
[53] Peart B and Dolder K T 1972 Collisions between electrons and H_2^+ ions: II. Measurements of cross sections for dissociative excitation *J. Phys. B: At. Mol. Phys.* **5** 860
[54] Kimura T and Kasugai H 2010 Properties of inductively coupled rf Ar/H_2 plasmas: experiment and global model *J. Appl. Phys.* **107** 083308
[55] Hayashi M 2003 *Report No* NIFS-DATA-72, National Institute For Fusion Science
[56] Tachibana K 1986 Excitation of the $1s_5$, $1s_4$, $1s_3$, and $1s_2$ levels of argon by low-energy electrons *Phys. Rev.* A **34** 1007
[57] Ray P P, Dutta Gupta N and Chaudhuri P 2002 Calculation of the precursor flux from optical emission spectroscopy data in plasma enhanced chemical vapour deposition of silane and its correlation with the deposition rate *Japan. J. Appl. Phys.* **41** 3955
[58] Welzel Th, Dani I and Richter F 2002 Determination of radical densities by optical emission spectroscopy during the ECR plasma deposition of Si–C–N : H films using TMS as a precursor *Plasma Sources Sci. Technol.* **11** 351
[59] Coburn J W and Chen M 1980 Optical emission spectroscopy of reactive plasmas: a method for correlating emission intensities to reactive particle density *J. Appl. Phys.* **51** 3134
[60] Radovanov S B, Tomcik B, Petrovic Z Lj and Jelenkovic B M 1990 Optical emission spectroscopy of rf discharge in SF_6 *J. Appl. Phys.* **67** 97
[61] Fuller N C M, Donnelly V M and Herman I P 2002 Electron temperatures of inductively coupled Cl_2–Ar plasmas *J. Vac. Sci. Technol.* A **20** 170
[62] Geng Z-C, Xu Y, Yang X-F, Wang W-G and Zhu A-M 2005 Atomic hydrogen determination in medium-pressure microwave discharge hydrogen plasmas via emission actinometry *Plasma Sources Sci. Technol.* **14** 76
[63] Lavrov B P and Pipa A V 2002 Account of the fine structure of hydrogen atom levels in the effective emission cross sections of Balmer lines excited by electron impact in gases and plasma *Opt. Spectrosc.* **92** 647
[64] NIST Database 2012 NIST Database: www.nist.gov/pml/data/asd.cfm
[65] Mozetic M, Drobnic M, Pregelj A and Zupan K 1996 Determination of density of hydrogen atoms in the ground state *Vacuum* **47** 943
[66] Babic D, Poberaj I and Mozetic M 2001 Fiber optic catalytic probe for weakly ionized oxygen plasma characterization *Rev. Sci. Instrum.* **72** 4110
[67] Iordanova S, Koleva I and Paunska T 2011 Hydrogen degree of dissociation in a low pressure tandem plasma source *Spectrosc. Lett.* **44** 8
[68] HIDEN Analytical: www.hidenanalytical.com/
[69] Sudit I and Chen F 1996 Discharge equilibrium of a helicon plasma *Plasma Sources Sci. Technol.* **5** 43
[70] Sakiyama Y, Graves D B, Chang H-W, Shimizu T and Morfill G E 2012 Plasma chemistry model of surface microdischarge in humid air and dynamics of reactive neutral species *J. Phys D: Appl. Phys.* **45** 425201
[71] Hjartarson A T, Thorsteinsson E G and Gudmundsson J T 2010 Low pressure hydrogen discharges diluted with argon explored using a global model *Plasma Sources Sci. Technol.* **19** 065008
[72] Sawada K and Fujimoto T 1995 Effective ionization and dissociation rate coefficients of molecular hydrogen in plasma *J. Appl. Phys.* **78** 2913

Plasma properties in a large-volume, cylindrical and asymmetric radio-frequency capacitively coupled industrial-prototype reactor

Article *in* Journal of Physics D Applied Physics · January 2013

Impact Factor: 2.72 · DOI: 10.1088/0022-3727/46/7/075201

8 authors, including:

Kosta Spasic
University of Belgrade
10 PUBLICATIONS **12** CITATIONS
SEE PROFILE

Gordana Malovic
Institute of Physics Belgrade
157 PUBLICATIONS **932** CITATIONS
SEE PROFILE

Miran Mozetic
Jožef Stefan Institute
287 PUBLICATIONS **3,708** CITATIONS
SEE PROFILE

Maja Radetić
University of Belgrade
89 PUBLICATIONS **1,083** CITATIONS
SEE PROFILE

Plasma properties in a large-volume, cylindrical and asymmetric radio-frequency capacitively coupled industrial-prototype reactor

2013 J. Phys. D: Appl. Phys. 46 075201

(http://iopscience.iop.org/0022-3727/46/7/075201)

J. Phys. D: Appl. Phys. **46** (2013) 075201 (8pp) doi:10.1088/0022-3727/46/7/075201

Plasma properties in a large-volume, cylindrical and asymmetric radio-frequency capacitively coupled industrial-prototype reactor

Saša Lazović[1,2], Nevena Puač[1], Kosta Spasić[1], Gordana Malović[1], Uroš Cvelbar[2], Miran Mozetič[2], Maja Radetić[3] and Zoran Lj Petrović[1]

[1] Institute of Physics, University of Belgrade, Pregrevica 118, Belgrade, Serbia
[2] Jožef Stefan Institute, Jamova cesta 39, 1000 Ljubljana, Slovenia
[3] Faculty of Technology and Metallurgy, University of Belgrade, Karnegijeva 4, 11000 Belgrade, Serbia

E-mail: lazovic@ipb.ac.rs

Received 22 October 2012, in final form 10 December 2012
Published 23 January 2013
Online at stacks.iop.org/JPhysD/46/075201

Abstract
We have developed a large-volume low-pressure cylindrical plasma reactor with a size that matches industrial reactors for treatment of textiles. It was shown that it efficiently produces plasmas with only a small increase in power as compared with a similar reactor with 50 times smaller volume. Plasma generated at 13.56 MHz was stable from transition to streamers and capable of long-term continuous operation. An industrial-scale asymmetric cylindrical reactor of simple design and construction enabled good control over a wide range of active plasma species and ion concentrations. Detailed characterization of the discharge was performed using derivative, Langmuir and catalytic probes which enabled determination of the optimal sets of plasma parameters necessary for successful industry implementation and process control. Since neutral atomic oxygen plays a major role in many of the material processing applications, its spatial profile was measured using nickel catalytic probe over a wide range of plasma parameters. The spatial profiles show diffusion profiles with particle production close to the powered electrode and significant wall losses due to surface recombination. Oxygen atom densities range from 10^{19} m^{-3} near the powered electrode to 10^{17} m^{-3} near the wall. The concentrations of ions at the same time are changing from 10^{16} to the 10^{15} m^{-3} at the grounded chamber wall.

(Some figures may appear in colour only in the online journal)

1. Introduction

Low-temperature plasmas represent an irreplaceable tool for many industrial processes due to a variety of chemical reactions that can be induced and controlled, even at low gas temperatures. Most of the energy delivered to non-equilibrium plasmas is transferred to electrons and not to the heating of the background gas or walls of the vessel. Therefore, the electrons are determining the nature of chemical processes in the plasma as well as at the plasma–sample interfaces. Energetic electrons in plasma can produce active species (ions, radicals, metastables and new electrons) in very high concentrations that can hardly be matched by traditional chemical or other methods. In addition, non-equilibrium plasmas may be easily modified and controlled by changing the composition, pressure, current density and flow, thus allowing a wide range of variation of a number of parameters and allowing optimization and even on-line control of some technological plasma based processes.

However, the interaction between the plasma created active species and the substrate is also depending on the material properties of the substrate. Intrinsic surface properties

and desired treatment effects are setting the requirements for the plasma source design, defining the range of applicable internal and external plasma parameters. From the point of practical use, the crucial aim is to determine the optimal range of applicable plasma parameters and proper plasma operating regime [1–5]. Controllable plasma chemical reactions are widely used in the processing of materials of different origins and properties [6, 7]. For example, field of microelectronics is strongly influenced by the development of plasma devices, i.e. by improved results on plasma deposition, etching, ashing, implantation, surface cleaning and other surface modification processes [8, 9]. Another rapidly growing research field is biomedical plasma applications [10–13]. Related to this, low-pressure plasmas also find their place in the sterilization of medical instruments, processing of biocompatible materials and, for example, in increasing antibacterial properties of textiles later used in medical, military or food preparation purposes. While it was expected that atmospheric pressure plasmas would replace the low-pressure reactors, the complexity of vacuum system is replaced by other complexities, such as small gap, instability of operation and usage of helium as a buffer gas [14, 15]. Thus, low pressure plasmas are still an option for applications of materials and samples that can be placed in vacuum.

In order to measure plasma parameters and effectively control the plasma process, we need to apply different diagnostic techniques. Typically, we are looking for quantitative results which can be monitored as an indication of the plasma processing and also in order to compare with models that are required to understand plasmas, to optimize the equipment and even to control processing in real time.

Several methods have been developed for measurement of neutral atom density. The mass spectroscopy is suitable as long as plasma is created at low pressures; however, in many plasmas partial pressure may be as high as 100 Pa [16, 17]. For these cases and the cases of atmospheric pressure discharges, differential pumping of the mass spectrometer is obligatory, which significantly increases the cost of the technique and introduces some problems [18]. A similar problem occurs when measuring plasma ions. In any case, mass spectrometry, while providing detailed results, has a limitation due to difficulty in making absolute calibration. Chemical titration using NO is a reliable method, but it tends to be time consuming and destructive so it is not suitable for real time measurements [19, 20]. Laser absorption spectroscopy such as laser-induced fluorescence (LIF), two-photon laser-induced fluorescence (TALIF) [21] or cavity ring-down spectroscopy (CRDS) [22] are reliable methods, but require expensive equipment and are therefore of little interest for industry. On the other hand, optical emission spectroscopy (OES) is easy to use; it requires inexpensive equipment and allows real time measurements. Nevertheless it is still nowadays regarded as semi-qualitative since quantification of the results is difficult (see [23]).

Catalytic probes are simple, easy to use and allow real-time monitoring of the neutral atom density as long as the neutral gas temperature is close to the room temperature, and the dissociation fraction is many orders of magnitude larger than the ionization fraction [24]. Until now, catalytic probes were used to measure atomic oxygen species in inductively coupled radiofrequency and microwave discharges [25, 26]. Some measurements were also performed in capacitively coupled radiofrequency plan parallel reactors [27–29]. Reports show that atomic oxygen concentrations are of the order of 10^{21} m^{-3} except for the capacitively coupled plasma (CCP) reactor where densities are lower, 10^{19} m^{-3}.

In this paper we apply several diagnostic techniques to study plasma of a large-scale asymmetric capacitive plasma reactor. We have developed an industrial reactor of a simple design where homogeneous, stable plasma capable of long term operation is generated. The main objective was to limit the energy of the ions bombarding the sample surfaces while still having sufficient densities of active plasma species.

The large size reactor was built to demonstrate the properties of plasma of a large size that can reasonably handle on-line textile treatment. This would require an additional differential pumping stage so that the textile would be introduced through a slit at one side of the reactor wall, continuously moved through the plasma and finally the treated textile would be rolled after exiting. Additionally, the intensity of the treatment can also be controlled by adjusting the distance between the power electrode and the samples. Our previous studies of plasma treatment of textile [30] were carried out in a similar asymmetric reactor of a much smaller volume. In this paper, we present results on characterization of the large volume plasma. Langmuir and catalytic probes were used to measure spatial profiles of concentration of ions and of atomic oxygen. Detailed electrical characterization of the reactor was performed using home-made derivative probes which proved to be superior to commercial probes and power meters, overcoming problems with operating frequency ranges and calibration. The current–voltage characteristics of the discharge, as well as, the real power delivered to the plasma by the generator will be presented. All measurements were carried out in air plasma for several different pressures and powers.

The ion energies and concentrations can be independently controlled using two RF sources operating at different frequencies [31, 32], but due to simplicity and reduced cost, we have chosen asymmetrical (cylindrical) geometry of the reactor [33]. This asymmetry provides a very large ratio of areas of the grounded to the powered electrode and consequently pronounced differences between voltage drops in the sheaths. This leads to differences in energies of ions bombarding the two electrodes. In addition, relatively large atomic oxygen densities are present. Oxygen atoms are necessary for plasma modification of seeds, polymers and textiles [34–37] for which the reactor was already used, as well as, many other treatments. However, a detailed characterization of plasma species, especially of ions, neutral atoms as well as proper input powers, is not yet available including correlations between those species and plasma properties. One of the most common problems in microelectronic manufacturing [38] is temporal variation of plasma properties due to modification of surfaces of the vessel. We have thus developed a simple real time monitoring plasma processes based on the catalytic probes that may be easily applied in large-scale industrial processes.

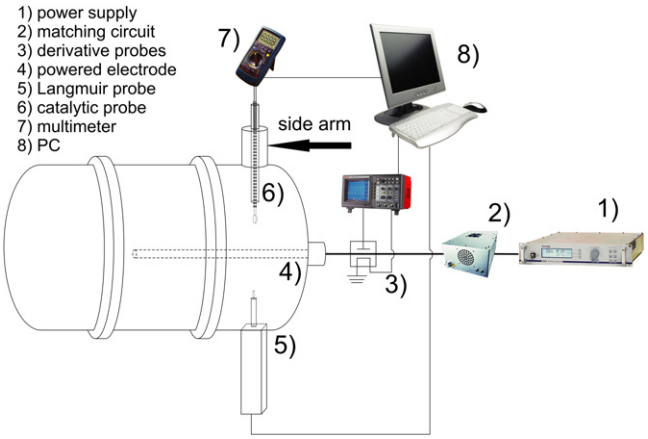

Figure 1. Schematics of the experimental setup.

2. Experimental setup

A CCP reactor powered at 13.56 MHz and operated at low pressures with a large volume in which uniform plasma can be created was used for experiments. The discharge chamber made of stainless steel was 2.5 m long and 1.17 m in diameter. The powered electrode was 1.5 m long (and could be extended to fully 2.5 m), 3 cm in diameter and made of aluminum. It is placed axially at the centre of the chamber. The chamber has a platform at the bottom where samples can be placed. The distance between the platform and the powered electrode is adjustable by moving the platform. The outer chamber wall is the grounded electrode and the sample platform is grounded as well.

The electrical circuit consists of an RF power generator Dressler Cesar 1310 in combination with Variomatch matching network. Derivative probes were placed as close as possible to the powered electrode. Langmuir and catalytic probe were placed side-on to the reactor wall (as presented in figure 1). The reduced pressure is maintained using a two-stage rotary pump (60 $m^3\,h^{-1}$). Ambient air is introduced into the chamber through a needle valve.

In the regime with flowing working gas, the pumping system can also affect the way atomic oxygen recombines at the catalytic probe surface [39]. Due to this reason, we measured densities in both fluent and stationary regime, with and without pumping. Our results showed that in the present setup the effect of pumping on results was negligible.

Knowledge of power introduced into the plasma is essential in characterizing plasmas and controlling operating conditions in plasma processing. Non-linear impedance of the plasma imposes harmonics of the drive frequency. Asymmetry of the discharge chamber also affects the way harmonics are generated. Due to this non-linearity, the change in external circuitry leads to unpredictable variation of the plasma properties. For example, the auto-tune feature on the matching network can result in different reflected power minima for several apparently identical measurements which will result in different values of power deposited into the plasma [40]. Therefore, the power measured at the RF generator is not the best parameter.

Disadvantages of using commercial power meters lie in the fact that the power is usually measured only at a single frequency or in a very narrow range of frequencies, thus leaving out the information about power delivered to the load at the frequencies of the higher harmonics. There are also commercial probes available for current and voltage measurements at radio frequencies but their disadvantage is that in most of the cases their frequency response is not characterized properly. Derivative probes which are calibrated in a wide range of frequencies (from an order of magnitude lower to an order of magnitude higher) overcome these problems. Such probes can be placed close to the powered electrode reducing the error introduced by the losses in the part of external electrical circuit from the probes to the powered electrode. We have used previously described derivative probes [41] in order to measure the power transmitted to the plasma and analyse harmonic composition of the signals.

Both probes were placed into a stainless steel box opposite each other and as close as possible to the powered electrode. Instantaneous voltages and currents were monitored using derivative probes which were connected to the oscilloscope with cables of identical length (so there would be no additional phase differences between current and voltage signals introduced). All waveforms were collected by the computer for further analysis. Numerical processing of the acquired data consists of a fast Fourier transform (FFT), calibration in the frequency domain of both amplitude and phase and inverse fast Fourier transform (IFFT) after which the real calibrated waveforms are obtained. Measurements using derivative probes were carried out for the whole range of powers delivered by the RF generator. Before every measurement reflected power was checked and, if needed, adjusted to be less than 1% of the forward power.

Spatial profiles of the ion concentrations were measured using Hiden Analytical ESPION advanced Langmuir probe system which was placed side-on. The system has a linear motion drive which enables probe positioning with the minimal spatial resolution of 0.1 mm. Measurements were made in air at 100 mTorr. We have used a platinum probe tip, 5 mm long and 0.15 mm in diameter. Linear motion drive was used to position the probe at distances from 50.5 to 20.5 cm measured from the powered electrode. Measurements of V–I curves were made for all those positions of the Langmuir probe. At every position 50 measurements were made each consisting on average of 10 scans with pre-cleaning for each measurement. Afterwards, the V–I curves were smoothed and data were processed using HidenESPSoft. Orbit motion-limited theory implemented in the standard HIDEN ESPion software was applied. Mass of N_2^+ ion was assumed in the analysis thus giving an effective density where contributions of other ions are projected onto that of N_2^+.

Spatial profiles of the neutral oxygen atoms were measured using nickel catalytic probe (polycrystalline nickel disc with purity ∼99.8%). The probe covered the same distances from the powered electrode where the ion concentrations were measured. The catalytic probe was moved even further away from the powered electrode than the reactor

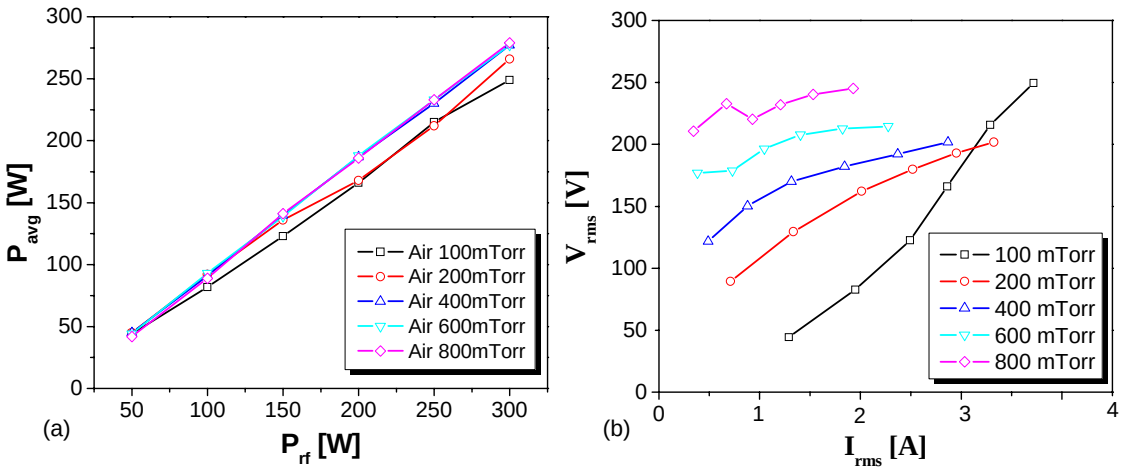

Figure 2. (*a*) Average power delivered to the plasma measured by derivative probes (P_{avg}) as a function of power given by the RF generator (P_{rf}). (*b*) Volt–ampere characteristics of the discharge measured by derivative probes. Gas was air at 100, 200, 400, 600 and 800 mTorr.

walls. Namely, it was necessary to mount a cylindrical, stainless steel, side chamber (arm) which is perpendicular to the chamber wall in order to mount the probe and allow its movement. The chamber wall is 57.5 cm away from the electrode, and the catalytic probe was moved up to 6 cm inside the side tube. Measurements of oxygen concentrations were extended into the reactor side arm.

The asymmetry of the reactor introduces large differences in ion energies and fluxes near the powered electrode and near the grounded chamber wall due to different values of sheath potential drops:

$$\left(\frac{U_p}{U_g}\right) = \left(\frac{A_g}{A_p}\right)^k, \qquad (1)$$

where U_p and U_g are sheath voltages and A_p and A_g are the areas of powered and grounded electrodes, respectively. Theoretically, k ranges from 1.25 to 4, and experimentally it is less than 2.5 [42]. The smaller the electrode area, the smaller is its capacitance, and therefore the corresponding potential drop is larger. On the other hand, the sheath thickness, which will also affect the capacitance and the voltage drops, may depend on the voltage across it, through Child's law. The problem needs to be solved self-consistently to obtain the voltages [43]. Pronounced gradients of ion energies and concentration appear at different distances from the powered electrode in our reactor. Therefore, the position of the substrate or the measuring probe will strongly affect the intensity of the positive ion bombardment of the substrate surface. The highest flux of ions and the highest energies will be associated with the bombardment of the smaller electrode (1) [42, 44].

3. Results and discussion

3.1. Electrical characterization of the reactor: power measurements and current–voltage characteristics

We first recorded current and voltage waveforms and then calculated the mean power as the time integral of their product. Dependence of the average power, measured by the derivative probes, on the power produced by the RF generator in air for several pressures is given in figure 2(*a*). We can see that the dependence is linear and that most of the power is indeed delivered to the reactor. With the changing of pressure, the delivered power does not change significantly. The discrepancy increases with an increase in the power.

From the volt–ampere (V–A) characteristics shown in figure 2(*b*) we can conclude that the plasma is operating in the α regime judged by the almost linear V–A dependence. The differential impedance magnitude is decreasing with an increase in pressure (from 100 Ω down to 30 Ω). We can also see that the root mean square values (rms) of voltage are ranging from about 50 up to 250 V and that working voltages are increased with an increase in pressure of the working gas. On the other hand, rms values of current are decreased with an increase in the pressure, remaining in the range from 0.2 to 3.8 A.

As mentioned above, the dimensions of the reactor were selected to be such that it could accommodate processing of a standard width of the textile as used in the industry. It turned out that it was possible to achieve uniformity over the entire width of the textile and stable operation for hours without any sparking that often occurs at atmospheric pressure. Our experimental device that was used in our previous studies of textile treatment [30, 34, 35, 45] had 0.37 m diameter and length of 0.5 m. Thus, its volume is about 50 times smaller than the volume of the large size reactor. Nevertheless the large volume reactor was able to provide the same level of treatment of the surface with only an increase in 30–50% in power.

3.2. Influence of ion bombardment on heating of the catalytic probe and samples

There are two major reasons for performing Langmuir probe measurements in the main reactor chamber. The first one is to establish the flux of ions which determines the basic effect but if allowed to be excessive may damage the sample. Secondly, we need to estimate the contribution of ion bombardment to the heating of the catalytic probe. For that purpose we have measured spatial profiles in air at 100 mTorr at different

distances from the powered electrode. Ion bombardment, light quanta, radiation, accommodation of gaseous molecules, relaxation of metastable oxygen and ion recombination can significantly contribute to the heating of the probe, depending on the type of the discharge and operating conditions.

If we assume that the heating of the probe is only due to recombination of atomic oxygen and ion bombardment, then the heat dissipated at the probe surface is given by

$$P_{\text{heat}} = P_{\text{O}} + P_{\text{i}} = j_{\text{O}}\gamma W_{\text{d}}\pi r^2 + j_{\text{i}}W_{\text{i}}\pi r^2 \qquad (2)$$

where P_{O} is the contribution due to the neutral oxygen atom recombination, P_{i} is the ion bombardment term, j_{O} is the neutral oxygen atom flux and j_{i} is the ion flux, γ is the coefficient for heterogeneous surface recombination of O atoms on the nickel surface with the value of 0.27 [46], W_{d} and W_{i} are the dissociation and first ionization energy of oxygen molecules and r is the nickel probe disc radius. Here, it is worth noting that our discharge is created in air, which can also produce neutral nitrogen atoms and other species including metastables. However, one should have in mind that the dissociation energy of N_2 is 9.75 eV, as compared with 5.12 eV for O_2. Additionally, the recombination coefficient for N atoms is also lower and is 0.1. Due to this reason, the dissociation of O molecules with dissociation energy of 5.12 eV is the most probable channel, and contributions of N atoms can be neglected in first approximation.

Neutral oxygen atom flux and ion flux are then given by

$$j_{\text{O}} = \tfrac{1}{4}n_{\text{O}}v_{\text{O}}; \qquad j_{\text{i}} = n_{\text{i}}v_{\text{i}}, \qquad (3)$$

where n_{O} and n_{i} are the O atom and ion density, in the probe vicinity, respectively. v_{O} is the average of the absolute value of thermal velocity of O atoms, v_{i} is the Bohm velocity. The probe is being heated until the temperature saturates and then the discharge is turned off. At this moment heating and cooling rates of the probe are equal. The cooling rate is given by

$$P = mc_p\frac{\Delta T}{\Delta t}, \qquad (4)$$

where m is the nickel disc mass, c_p its specific thermal capacity and $\Delta T/\Delta t$ is the absolute value of the temperature derivative just after turning off the discharge. It is important to note that by equating the heating and the cooling terms and taking into account only the neutral atom contribution, the concentrations are calculated as follows:

$$n = \frac{4mC_p}{v\gamma W_{\text{d}}\pi r^2}\frac{\Delta T}{\Delta t}. \qquad (5)$$

Another important fact is that from the ratio of $j_{\text{i}}W_{\text{i}}/j_{\text{O}}\gamma W_{\text{d}}$ we can calculate the upper limit for the ion contribution to the heating of the electrode. The ion contribution to the energy of the electrode W_{i} is the sum of the kinetic energy which is gained in the sheaths and the ionization energy (the first ionization energy for O_2 molecule is 12 eV) [27]. Obviously, the ion kinetic energy in a strongly asymmetric discharge of this kind is going to be significantly different at different distances from the powered electrode, as mentioned before (1). From figures 3 and 4, we can see that the

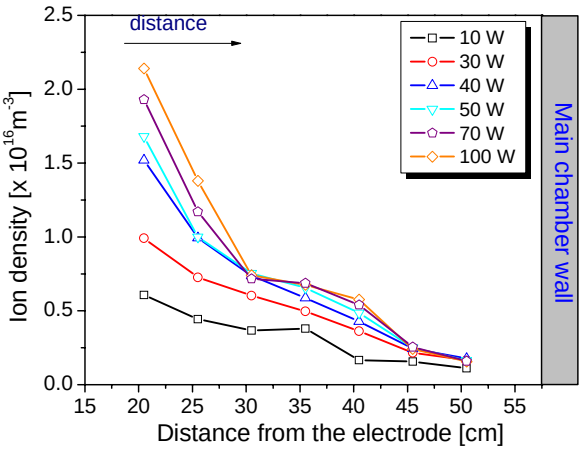

Figure 3. Spatial profiles of ions measured by the Langmuir probe in air at 100 mTorr and at different powers.

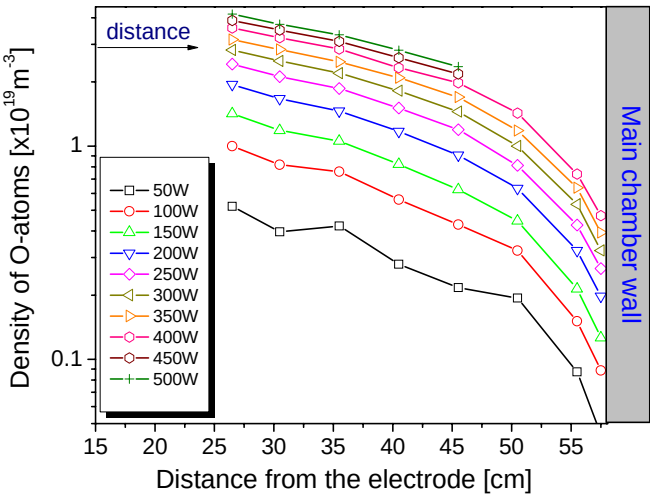

Figure 4. Concentrations of oxygen atoms measured by the catalytic probe in air at 100 mTorr at different powers.

ion concentrations are three orders of magnitude lower than the measured neutral atomic oxygen concentrations for low generator powers up to 100 W. We were not able to conduct proper Langmuir probe measurements for higher powers due to additional secondary discharge developing at the tip of the probe influencing our results, but we expect the same ratio to be maintained for powers higher than 100 W.

Ion measurements were performed in air plasma at 100 mTorr and at distances from the powered electrode of 20.5 cm up to 50.5 cm. Measured ion densities are between 10^{15} and 10^{16} m^{-3} (figure 3), whereas concentrations of neutral oxygen atoms were of the order of 10^{18}–10^{19} m^{-3} (figure 4). Ion and atomic oxygen concentrations are typically decreasing with the distance from the powered electrode, and increasing with the power.

Recombination coefficient of nickel is 0.27 for neutral atomic oxygen recombination while almost every ion (for example O^+, N^+, N_2^+, O_2^+, NO^+) reaching the probe surface recombines with probability 100% and contributes to the probe's heating. In the case of the symmetric CCP, the authors report that the ion contribution is about 2%, when

taking W_i to be 12 eV + 18 eV [26]. Having in mind that in the region close to the grounded electrode of the asymmetric CCP, the ion energies are lower than 18 eV [30], we can conclude that the contribution to heating of the catalytic probe due to ions is even lower than for the symmetric CCP. More precisely, the upper limit to the contribution to heating of the catalytic probe surface due to ions in our case ranges from 1.2% to 2%, as previously estimated. Unfortunately, due to the limited length of the catalytic probe we were not able to go very close to the powered electrode.

From the above results we can conclude that in our experiments the ion contribution to the heating of the catalytic probe surface is not substantial. In the same light, we can see that close to the main chamber wall neither ion energies (1) nor ion concentrations (see figure 3) are high and that the wall represents a drain for both species.

3.3. Radial dependence of atomic oxygen in cylindrical chamber and chamber extension

The dependence of oxygen atom densities with the distance from the powered electrode is influenced by the balance of production and losses. Having in mind cylindrical geometry of the reactor, atomic oxygen is produced in the plasma at close proximity to the powered electrode, while on the other hand recombination takes place predominantly at the surface of reactor walls. Atom recombination at the probe surface may, amongst other things, be affected by the vicinity and area of the reactor walls in the main chamber and the side tube.

The spatial profiles of oxygen atom densities in the main reactor and in the side arm are shown in figure 5. We cannot guarantee whether the reading of the atom density at the position of the chamber wall is the same as it is at the wall where there is neither side arm nor catalytic probe. Nevertheless the profiles are consistent with diffusion profiles with a small but appreciable reflection. As expected, at lower pressures the density is lower which is consistent with a longer mean free path.

The densities in the small tube continue decreasing but faster than in the main chamber. This is consistent with increased losses due to smaller size vessel and larger probability of reaching the walls. The observed profiles offer a possibility to control fluxes of reactive particles by placing samples at different distances from the powered electrode, even placing them inside the sidearm.

4. Conclusion

Plasma behaviour was studied in a large-volume (2.6 m^3) asymmetric CCP (industrial prototype) reactor of a simple design (with a side arm that is needed to mount probes). Two key properties of plasma for application in textile treatment, densities of ions (physical sputtering and damage to the surface) and oxygen atoms (chemical functionalization of surfaces) and electrical characteristics were measured. The wetting time achieved by this system was dramatically reduced. Since the wetting time after plasma treatment is extremely short and difficult to measure, we could not quantify these results,

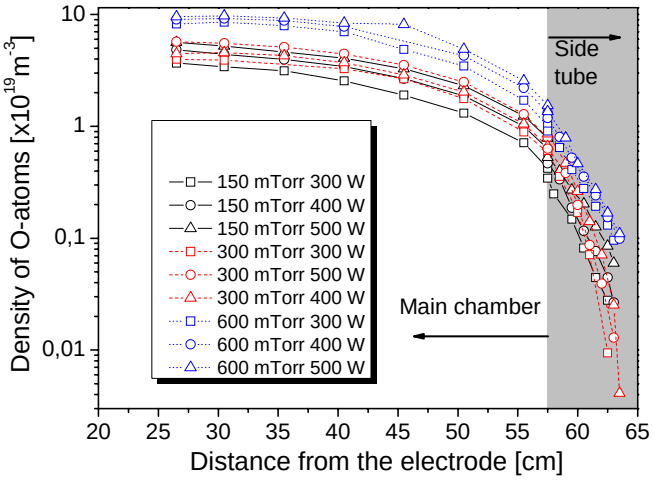

Figure 5. Spatial profiles of oxygen atoms measured by the catalytic probe in air in the main reactor vessel and in the side arm (tube positioned perpendicular to the chamber wall) in which the probe is mounted (the main chamber wall distance from the powered electrode is 57.5 cm). Measurements were made at different powers and gas pressures.

i.e. we could not compare the two treated samples. Although, we can state that the reduction in wetting time is similar and causes very fast wetting of the samples whereas plasma non-treated samples are very hydrophobic and water as well as dye solution does not penetrate the textile. Size of the reactor would allow continuous treatment of textile from the rolls of the standard width used in the industry.

Derivative probes used for electrical characterization of the reactor and plasma power measurement proved to provide reliable results. We found that our plasma operates in alpha mode and most of the generated power is dissipated inside the plasma [47]. Due to reactor design and its cylindrical asymmetric geometry, spatial distributions of ions and atomic oxygen are changing significantly as we move away from the powered electrode. Langmuir probe was used to measure the spatial profiles of ion densities in order to make sure that samples will not be damaged by ion bombardment and to calculate the ion contribution to the heating of the catalytic probe. Ion densities were of the order of $10^{16}\,m^{-3}$. A nickel catalytic probe was used to measure the spatial profiles of atomic oxygen in air for a wide range of pressures. It is determined that in the main reactor vessel the atomic oxygen densities are of the order of $10^{19}\,m^{-3}$ and are almost linearly decreasing as we move away from the powered electrode. In the small side reactor the densities are $10^{18}\,m^{-3}$ or even $10^{17}\,m^{-3}$ depending on the proximity to the walls and pressure. Therefore, there is a wide range of atomic oxygen concentrations which can be delivered to the samples based on the position of treated material, inside the main vessel or perpendicular side arm. The results indicate that the diffusion is the mechanism governing profiles of neutral atoms. Atomic oxygen loss processes are dominantly affected by the recombination of atoms at the vessel/tube walls. Taking into account the power measured by the derivative probes, spatial profiles of ion densities measured by the Langmuir probe and spatial profiles of atomic oxygen optimal set of

important plasma parameters can be obtained for optimization of sensitive material treatment according to required flux of ions or atoms to its surface. It is shown that high atomic density can be achieved even for lower powers, and therefore lower processing costs, by placing the sample close to the powered electrode but in that case one has to deal with somewhat higher ion energies.

Compared with other plasma sources investigated by the catalytic probes (MW and ICP for example) here we have two to four orders of magnitude lower oxygen atom densities due to its large size and smaller volume where the atoms are produced [48]. This property makes the cylindrical reactor appropriate for treatment of sensitive samples such as seeds, polymers and textile. The primary reason for the low measured densities is the distance from the powered electrode and a very large volume. At the same time one may select the geometry and position of the sample to control the fluxes. The energy of ions may also be controlled by selecting position (1) and also by biasing.

Acknowledgments

This research is sponsored by the Ministry of Education and Science, Republic of Serbia, project no OI 171037 and III 41011, Slovenian Research Agency (ARRS) and Slovenian Human Resources Development and Scholarship Fund (AdFutura). This paper has also been facilitated by the bilateral programme of scientific cooperation between Slovenia and Serbia.

References

[1] Fridman A and Kennedy L A 2004 *Plasma Physics and Engineering* (New York: Taylor and Francis)
[2] Mahony C M O, Maguire P D and Graham W G 2005 Electrical characterization of radio frequency discharges *Plasma Sources Sci. Technol.* **14** S60–7
[3] Godyak V A 2011 Electrical and plasma parameters of ICP with high coupling efficiency *Plasma Sources Sci. Technol.* **20** 025004
[4] Kieft I E, Laan E P v d and Stoffels E 2004 Electrical and optical characterization of the plasma needle *New J. Phys.* **6** 149–63
[5] Gahan D, Daniels S, Hayden C, Scullin P, O'Sullivan D, Pei Y T and Hopkins M B 2012 Ion energy distribution measurements in rf and pulsed dc plasma discharges *Plasma Sources Sci. Technol.* **21** 024004
[6] Makabe T and Yagisawa T 2011 Low-pressure nonequilibrium plasma for a top-down nanoprocess *Plasma Sources Sci. Technol.* **20** 024011
[7] Roth C, Oberbossel G and Rudolf von Rohr P 2012 Electron temperature, ion density and energy influx measurements in a tubular plasma reactor for powder surface modification *J. Phys. D: Appl. Phys.* **45** 355202
[8] Chen F F and Chang J P 2003 *Lecture Notes on Principles of Plasma Processing* (Dordrecht/New York: Kluwer/Plenum)
[9] Makabe T and Petrović Z L 2006 *Plasma Electronics: Applications in Microelectronic Device Fabrication* (New York: Taylor and Francis)
[10] Dobrynin D, Fridman G, Friedman G and Fridman A 2009 Physical and biological mechanisms of direct plasma interaction with living tissue *New J. Phys.* **11** 115020
[11] Kong M G, Kroesen G, Morfill G, Nosenko T, Shimizu T, van Dijk J and Zimmermann J L 2009 Plasma medicine: an introductory review *New J. Phys.* **11** 115012
[12] Lazović S *et al* 2010 The effect of a plasma needle on bacteria in planktonic samples and on peripheral blood mesenchymal stem cells *New J. Phys.* **12** 083037
[13] Petrović Z L, Puač N, Lazović S, Maletić D, Spasić K and Malović G 2012 Biomedical applications and diagnostics of atmospheric pressure plasma *J. Phys.: Conf. Ser.* **356** 012001
[14] Puač N, Maletić D, Lazović S, Malović G, Đordević A and Petrović Z L 2012 Time resolved optical emission images of an atmospheric pressure plasma jet with transparent electrodes *Appl. Phys. Lett.* **101** 024103
[15] Stefanović I, Kuschel T, Škoro N, Marić D, Petrović Z L and Winter J 2011 Oscillation modes of direct current microdischarges with parallel-plate geometry *J. Appl. Phys.* **110** 083310
[16] Ferreira J A and Tabarés F L 2007 Cryotrapping assisted mass spectrometry for the analysis of complex gas mixtures *J. Vac. Sci. Technol.* A **25** 246
[17] Gaboriau F, Cartry G, Peignon M-C and Cardinaud C 2006 Etching mechanisms of Si and SiO 2 in fluorocarbon ICP plasmas: analysis of the plasma by mass spectrometry, Langmuir probe and optical emission spectroscopy *J. Phys. D: Appl. Phys.* **39** 1830–45
[18] Malović G, Puač N, Lazović S and Petrović Z 2010 Mass analysis of an atmospheric pressure plasma needle discharge *Plasma Sources Sci. Technol.* **19** 034014
[19] Mozetić M, Ricard A, Babić D, Poberaj I, Levaton J, Monna V and Cvelbar U 2003 Comparison of NO titration and fiber optics catalytic probes for determination of neutral oxygen atom concentration in plasmas and postglows *J. Vac. Sci. Technol.* A **21** 369
[20] Mozetič M, Cvelbar U, Vesel A, Ricard A, Babic D and Poberaj I 2005 A diagnostic method for real-time measurements of the density of nitrogen atoms in the postglow of an Ar–N_2 discharge using a catalytic probe *J. Appl. Phys.* **97** 103308
[21] Gaboriau F, Cvelbar U, Mozetic M, Erradi A and Rouffet B 2009 Comparison of TALIF and catalytic probes for the determination of nitrogen atom density in a nitrogen plasma afterglow *J. Phys. D: Appl. Phys.* **42** 055204
[22] Labazan I and Milošević S 2004 Determination of electron density in a laser-induced lithium plume using cavity ring-down spectroscopy *J. Phys. D: Appl. Phys.* **37** 2975–80
[23] Makabe T and Petrović Z L 2002 Development of optical computerized tomography in capacitively coupled plasmas and inductively coupled plasmas for plasma etching *Appl. Surf. Sci.* **192** 88–114
[24] Drenik A C U, Vesel A and Mozetič M 2005 *Inform. MIDEM* **35** 85
[25] Mozetič M, Vesel A, Cvelbar U and Ricard A 2006 An iron catalytic probe for determination of the O-atom density in an Ar/O_2 afterglow *Plasma Chem. Plasma Process.* **26** 103–17
[26] Primc G, Zaplotnik R, Vesel A and Mozetič M 2011 Microwave discharge as a remote source of neutral oxygen atoms *AIP Adv.* **1** 022129
[27] Vrlinic T, Mille C, Debarnot D and Poncin-Epaillard F 2009 Oxygen atom density in capacitively coupled RF oxygen plasma *Vacuum* **83** 792–6
[28] Gomez S, Steen P G and Graham W G 2002 Atomic oxygen surface loss coefficient measurements in a capacitive/inductive radio-frequency plasma *Appl. Phys. Lett.* **81** 19

[29] Kitajima T, Noro K, Nakano T and Makabe T 2004 Influence of driving frequency on oxygen atom density in O_2 radio frequency capacitively coupled plasma *J. Phys. D: Appl. Phys.* **37** 2670–6
[30] Puač N, Petrović Z L, Radetić M and Djordjevic A 2005 Low pressure RF capacitively coupled plasma reactor for modification of seeds, polymers and textile fabrics *Mater. Sci. Forum* **494** 291–6
[31] Kitajima T, Takeo Y, Nakano N and Makabe T 1998 Effects of frequency on the two-dimensional structure of capacitively coupled plasma in Ar *J. Appl. Phys.* **84** 5928
[32] Kitajima T, Takeo Y, Petrović Z L and Makabe T 2000 Functional separation of biasing and sustaining voltages in two-frequency capacitively coupled plasma *Appl. Phys. Lett.* **77** 489
[33] Gahan D, Daniels S, Hayden C, Sullivan D O and Hopkins M B 2012 Characterization of an asymmetric parallel plate radio-frequency discharge using a retarding field energy analyzer *Plasma Sources Sci. Technol.* **21** 015002
[34] Ilić V, Šaponjić Z, Vodnik V, Lazović S, Dimitrijević S, Jovančić P, Nedeljković J M and Radetić M 2010 Bactericidal efficiency of silver nanoparticles deposited onto radio frequency plasma pretreated polyester fabrics *Indust. Eng. Chem. Res.* **49** 7287–93
[35] Mihailović D, Šaponjić Z, Radoičić M, Lazović S, Baily C J, Jovančić P, Nedeljković J and Radetić M 2011 Functionalization of cotton fabrics with corona/air RF plasma and colloidal TiO(2) nanoparticles *Cellulose* **18** 811–25
[36] Živković S, Puač N, Giba Z, Grubišić D and Petrović Z L 2004 The stimulatory effect of non-equilibrium (low temperature) air plasma pretreatment on light-induced germination of *Paulownia tomentosa* seeds *Seed Sci. Technol.* **32** 693–701
[37] Morent R, De Geyter N, Verschuren J, De Clerck K, Kiekens P and Leys C 2008 Non-thermal plasma treatment of textiles *Surf. Coat. Technol.* **202** 3427–49
[38] Hrunski D, Grählert W, Beese H, Kilper T, Gordijn a and Appenzeller W 2009 Control of plasma process instabilities during thin silicon film deposition *Thin Solid Films* **517** 4188–91
[39] Cvelbar U, Mozetič M, Babič D, Poberaj I and Ricard A 2006 Influence of effective pumping speed on oxygen atom density in a plasma post-glow reactor *Vacuum* **80** 904–7
[40] Miller P A, Anderson H and Splichal M P 1992 Electrical isolation of radiofrequency plasma discharges *J. Appl. Phys.* **71** 1171–6
[41] Puač N, Petrović Z, Živković S, Giba Z, Grubišić D and Đordević A 2005 *Plasma Processes and Polymers* ed R d'Agostino *et al* (Weinheim: Wiley)
[42] Koenig H R and Maissel L I 1970 Application of Rf discharges to sputtering *IBM J. Res. Dev.* **14** 168–71
[43] Lieberman M A and Lichtenberg A J 2005 *Principles of Plasma Discharge and Materials Processing* (Hoboken, NJ: Wiley)
[44] d'Agostino R, Favia P and Fracassi F 1997 *Plasma Processing and Polymers* vol 346 (Dordrecht: Kluwer)
[45] Gorenšek M, Gorjanc M, Bukošek V, Kovač J, Petrović Z and Puač N 2010 Functionalization of Polyester Fabric by Ar/N_2 Plasma and Silver *Textile Res. J.* **80** 1633–42
[46] Šorli I and Ročak R 2000 Determination of atomic oxygen density with a nickel catalytic probe *J. Vac. Sci. Technol.* A **18** 338
[47] Savić M, Radmilović Radenović M, Šuvakov M, Marjanović S, Marić D and Petrović Z L 2011 On explanation of the double-valued Paschen-like curve for RF breakdown in argon *IEEE Trans. Plasma Sci.* **39** 2556–7
[48] Balat-Pichelin M and Vesel A 2006 Neutral oxygen atom density in the MESOX air plasma solar furnace facility *Chem. Phys.* **327** 112–8

Bactericidal Efficiency of Silver Nanoparticles Deposited onto Radio Frequency Plasma Pretreated Polyester Fabrics

Article *in* Industrial & Engineering Chemistry Research · July 2010

Impact Factor: 2.59 · DOI: 10.1021/ie1001313

8 authors, including:

Vesna V Vodnik
Vinča Institute of Nuclear Sciences
79 PUBLICATIONS **696** CITATIONS
SEE PROFILE

Suzana I, Dimitrijevic-Brankovic
University of Belgrade
103 PUBLICATIONS **1,043** CITATIONS
SEE PROFILE

Jovan M Nedeljković
Vinča Institute of Nuclear Sciences
197 PUBLICATIONS **3,758** CITATIONS
SEE PROFILE

Maja Radetić
University of Belgrade
89 PUBLICATIONS **1,083** CITATIONS
SEE PROFILE

Bactericidal Efficiency of Silver Nanoparticles Deposited onto Radio Frequency Plasma Pretreated Polyester Fabrics

Vesna Ilić,[†] Zoran Šaponjić,[‡] Vesna Vodnik,[‡] Saša Lazović,[§] Suzana Dimitrijević,[||] Petar Jovančić,[†] Jovan M. Nedeljković,[‡] and Maja Radetić*,[†]

Textile Engineering Department, Faculty of Technology and Metallurgy, University of Belgrade, Karnegijeva 4, 11120 Belgrade, Serbia, Vinča Institute of Nuclear Sciences, P. O. Box 522, 11001 Belgrade, Serbia, Institute of Physics, Pregrevica 118, 11080 Zemun, Serbia, and Department of Bioengineering and Biotechnology, Faculty of Technology and Metallurgy, University of Belgrade, Karnegijeva 4, 11120 Belgrade, Serbia

The potential application of low-temperature radio frequency (RF) plasma for fiber surface activation in order to enhance the binding efficiency of colloidal silver nanoparticles onto the polyester fabrics and improve the stability of antibacterial effects was studied. Antibacterial activity and laundering durability were tested against gram-negative bacterium *Escherichia coli* and gram-positive bacterium *Staphylococcus aureus.* Plasma treatment positively affected the loading of silver nanoparticles as well as antibacterial activity and laundering durability of these textile nanocomposite materials. In spite of good laundering durability after five washing cycles, it was found that silver leached from the fabric into the bath during washing. Released silver from the washing effluent was efficiently removed by recycled wool-based nonwoven sorbent modified with hydrogen peroxide and biopolymer alginate.

1. Introduction

Textile materials have been recognized as media that can easily support the growth of different microbes.[1] Hence, the growing production of advanced medical, protective, and hygiene textiles requires efficient antimicrobial finishing. A wide range of antimicrobial agents have been employed so far in the antimicrobial finishing of textile materials: metals and metal compounds, quaternary ammonium salts, poly(hexamethylene biguanide), triclosan, chitosan, dyes, regenerable *N*-halamine compounds, and peroxyacids.[1] Relatively poor efficiency and/or high toxicity made most of them unsuitable for long-term use. However, silver in different forms exhibits outstanding antimicrobial activity with low toxic impact to mammalian cells.[2] It is a powerful biocide for more than 650 various microbes.[3] In particular silver nitrate has been widely used as an antimicrobial agent.[4,5] Despite its excellent antimicrobial properties, silver nitrate is not convenient for the treatment of textile materials as it stains to black-brown when exposed to air and light, due to uncontrolled reduction processes.[6] On the other hand, the deposition of engineered silver nanoparticles (Ag NPs) onto textile materials can provide an adequate level of antimicrobial efficiency without considerable color change.[3]

Recently developed simple procedures for synthesis of Ag NPs and their high antimicrobial efficiency make them a viable substitute to conventional antimicrobial agents. Consequently, the treatment of different textile materials with Ag NPs is receiving remarkable, not only scientific but also industrial, attention.[2,7–11] Numerous methods have been developed for the loading of textile substrates with Ag NPs. In addition to the most commonly applied dip-coating methods,[7,8,10,11] sonochemical coating using ultrasound irradiation[12,13] as well as the sputter deposition[14,15] of Ag NPs onto textile surfaces, were performed. Vigneshwaran et al. proposed in situ synthesis of Ag NPs on cotton fabrics where the aldehyde terminal of starch made possible the reduction of the silver nitrate to silver metal, simultaneously stabilizing the NPs on the fabric.[9] Durán et al. reported that good antibacterial efficiency can be achieved using the Ag NPs produced by a fungal process on cotton fabrics.[16] Ag NPs can be also efficiently incorporated into fibers by electrospinning.[17]

However, the latest trends are more oriented toward obtaining stable and durable nanocomposite textile materials with Ag NPs.[2,18] Plasma activation of textile materials, in particular hydrophobic polyester (PES) fabrics, appears to be beneficial for Ag NPs loading from colloids.[2,18] Conventional chemical treatments that can increase the surface energy of PES fibers, and, hence, improve their wettability and adhesion properties, are recognized as ecologically unacceptable as they require huge amounts of water and chemicals.[19] Unlike them, plasma processing is dry, clean, simple, multifunctional, environmentally friendly, and an economically feasible treatment. Additionally, it is not time-consuming, and it provides superficial modification of a fiber surface, leaving the bulk properties unaltered. The desired surface chemistry, i.e., plasma functionalization, can be achieved by adequate control of plasma parameters (treatment time, power, gas type, pressure, and gas flow).

It has been shown that pretreatment of PES fabrics by corona discharge at atmospheric pressure improves the loading of Ag NPs, providing the enhanced antimicrobial activity and laundering durability.[20–22] The main advantage of corona systems is that they operate at atmospheric pressure. Although corona systems principally meet the demands of the textile industry from the standpoint of speed and width, generated type of plasma cannot provide the desired spectrum of surface functionalizations on textile materials.[23] Plasma particles cannot penetrate deeply into yarns, and, hence, achieved effects are short-lived. Additionally, the thickness of the textile materials is limited due to small interelectrode spacing.[23] However, low-pressure devices, in particular radio frequency (RF) powered plasma sources, allow easier control of properties and provide

* To whom correspondence should be addressed. Fax: +381 11 3370387. Tel.: +381 11 3303 857. E-mail: maja@tmf.bg.ac.rs.
[†] Textile Engineering Department, University of Belgrade.
[‡] Vinča Institute of Nuclear Sciences.
[§] Institute of Physics.
[||] Department of Bioengineering and Biotechnology, University of Belgrade.

10.1021/ie1001313
Published on Web 07/12/2010

a greater stability and uniformity at the cost of a more complex handling of fabric through the vacuum system.[24–26] Therefore, the first part of this study discusses the potential application of low-temperature air RF plasma for fiber surface activation that can facilitate the deposition of colloidal Ag NPs onto the PES fabrics and, thus, enhance their antibacterial properties. Antibacterial activity and laundering durability were tested against gram-negative bacterium *Escherichia coli* (*E. coli*) and gram-positive bacterium *Staphylococcus aureus* (*S. aureus*).

In spite of growing commercialization of Ag NPs in general, little is known about the environmental impact of the products containing these species.[27] It is well-established that ionic silver is very toxic to aquatic organisms, and its concentration in water is strictly regulated by water quality criteria.[28,29] In contrast, data corresponding to toxicity and exposure of Ag NPs are still lacking.[28] To our knowledge, there are only a few studies on silver release during washing of textile materials and possible treatments of these effluents.[28–30] Benn and Westerhoff analyzed the form and amount of silver released from different sorts of commercial socks into water and its fate in wastewater treatment plants.[28] This study clearly indicates that silver is released either in the form of NPs or as ions. Additionally, the amount and rate of silver release strongly depends on the sock type, suggesting that the manufacturing process may control silver release.[28] Durán et al. studied the bioremediation process of Ag NPs released from cotton fabrics with the bacterium *Chromobacterium violaceum* (*C. violaceum*).[29] This treatment based on biosorption seems to be efficient for removal of released Ag NPs in water. However, both studies reported the leaching of silver in ultrapure or tap water; i.e., the effect of washing agents on silver release from textile materials into the washing effluents was not addressed in their work. Geranio et al. followed the effect of pH, surfactants, and oxidizing agents on the amount and the form of released silver during washing from nine different fabrics with silver bound to the fiber surface or incorporated into the fiber.[30] Again, they came to the same conclusion that the release of silver either in ionic or particulate form varies remarkably among the products (from less than 1 to 45%). However, particulate silver seems to be the predominant form of silver released under conditions relevant to washing.

Hence, the second part of this study considers silver release from the PES fabrics during washing in the presence of washing agent and the possibility of silver removal by recycled wool-based nonwoven sorbent from washing effluent. Extensive research on potentials of this sorbent for removal of metal ions (Pb^{2+}, Cu^{2+}, and Zn^{2+}), different dyes, and oils from water indicated its multifunctionality and high sorption efficiency.[31–33] It is well-known that Ag^{+} is bound to the wool primarily via carboxylic groups.[34] Thus, in order to introduce new carboxylic groups to the wool fiber surface, the recycled wool-based nonwoven sorbent was modified with hydrogen peroxide and biopolymer alginate.

2. Materials and Methods

2.1. Materials. 2.1.1. Treatment of PES Fabrics. Desized and bleached polyester (PES, 115 g/m^2) fabrics were cleaned in a bath containing 0.50% nonionic washing agent Felosan RG-N (Bezema) at a liquor-to-fabric ratio of 50:1.[20] After 15 min of washing at 50 °C, the fabrics were rinsed once with warm water (50 °C) for 3 min and three times (3 min) with cold water. The samples were dried at room temperature.

Low-temperature plasma treatment of fabrics was carried out in capacitively coupled, radio frequency (13.56 MHz) air induced plasma. This capacitively coupled plasma (CCP) reactor was previously used for treatment of polymers and different textile materials.[24,26,35] The apparatus consisted of a constant RF power supply (Dressler Caesar 1010), matching box (Variomatch matching network), vacuum pump, chamber, gas supply with appropriate pressure gauges, current and voltage probes, digital oscilloscope, and a computer. To keep the reflected power at the minimum, the impedance was adjusted by tuning the matching box. With reduction of the reflected power, the power transmitted to the system increased and a stable operation was achieved.

The chamber was cylindrical (37 cm in diameter, 50 cm in length) with a central electrode (14 mm in diameter) that was powered through the matching box. Plasma formed between the central electrode and the wall of the chamber that was grounded. The samples were placed on the platform at the bottom of the chamber. Such an asymmetric system was intentionally constructed in order to provide operating conditions under which the sheath potential is not too high[36] but sufficient for optimum modification of different textile materials, avoiding their permanent damage. Preliminary studies indicated that plasma parameters which showed optimum effects in previous work seemed to be also adequate for PES fabrics. Therefore, the power applied to the CCP reactor was 100 W; treatment time was 2.5 min, while the pressure was maintained at a constant level of 0.27 mbar.

$AgNO_3$ (Kemika) and $NaBH_4$ (Fluka) of p.a. grade were used without any further purification for the synthesis of colloidal Ag NPs. Briefly, 8.5 mg of $AgNO_3$ was dissolved in 250 mL of water purged by argon for 30 min.[37,38] Under vigorous stirring, reducing agent $NaBH_4$ (125 mg) was added to the solution and left for 1 h in argon atmosphere. The concentration of Ag colloid was 50 ppm.

A 1 g amount of PES fabric was immersed in 65 mL of colloid of Ag NPs for 5 min and dried at room temperature. After 5 min of curing at 100 °C, the samples were rinsed twice (5 min) with deionized water and dried at room temperature. To investigate the influence of the colloid concentration, the whole procedure was repeated on certain fabrics.

2.1.2. Treatment of Sorbent. The possibility of silver removal from the washing effluent by sorption was tested on the recycled wool-based nonwoven material (78/22 wool/polyester). This sorbent was produced from second-hand military knitted pullovers. A procedure for the production of recycled wool-based nonwoven material is described elsewhere in detail.[32]

The recycled wool-based nonwoven material was treated with hydrogen peroxide and biopolymer alginate in order to improve its sorption properties. Hydrogen peroxide treatment (H_2O_2, 20 mL/L; $Na_4P_2O_7$, 1.5 g/L; NH_3(aq), 2.5 mL/L) was carried out in static conditions (without shaking). Samples were treated in the solution for 1 h (liquor ratio, 30:1) at 70 °C and pH 9.4, washed with water, and dried at room temperature.

Low-viscosity sodium alginate (CHT-alginat NVS, Bezema) was used for the preparation of 0.5% alginate solution. Sodium alginate was dissolved in deionized water and stirred for 30 min. A 1 g amount of sorbent was dipped into 50 mL of freshly prepared 0.5% alginate solution for 10 min. After 10 min of curing at 100 °C, the fabrics were rinsed twice (5 min) with deionized water and dried at room temperature.

2.2. Methods. 2.2.1. Scanning Electron Microscopy. Fiber morphology was investigated by scanning electron microscopy (SEM, JEOL JSM 6460 LV). A golden layer was deposited on the samples before the analysis.

2.2.2. Atomic Absorption Spectroscopy. The content of silver in the washing bath after each washing cycle and in the fabrics after the fifth washing cycle was determined by a Perkin-Elmer 403 atomic absorption spectrometer.

2.2.3. Antibacterial Efficiency. The antibacterial efficiency of PES fabrics was quantitatively assessed using a gram-negative bacterium *E. coli* ATCC 25922 and gram-positive bacterium *S. aureus* ATCC 25923. Bacterial inoculum was prepared in the Tryptone soya broth (Torlak, Serbia), which was used as a growing medium for bacteria, and potassium hydrogen phosphate buffer solution (pH 7.2) as a testing medium. Bacteria were cultivated in 3 mL of Tryptone soya broth at 37 °C and left overnight (late exponential stage of growth). Sterile potassium hydrogen phosphate buffer solution (70 mL) was added to a sterile Erlenmeyer flask (300 mL), which was then inoculated with 0.7 mL of bacterial inoculum. A 1 g amount of sterile fabric cut into small pieces (1×1 cm^2) was placed in the flask and shaked for 1 h.

Time zero counts were made by removing 1 mL aliquots from the inoculum which were diluted with physiological saline solution (8.5 g of NaCl in 1 L of water). A 0.1 mL aliquot of the solution was placed onto a Tryptone soya agar, and after 24 h of incubation at 37 °C, the zero time counts (initial number of bacterial colonies) of viable bacteria were made. Counts of 1 h each were made in accordance with the previously described procedure.

The percentage of bacterial reduction (R, %) was calculated using the following equation:

$$R = \frac{C_0 - C}{C_0} \times 100\% \quad (1)$$

where C_0 (CFU, colony forming units) is the number of bacterial colonies on the control fabric (untreated fabric without Ag) and C (CFU) is the number of bacterial colonies on the fabric loaded with Ag NPs.[7,8,39]

2.2.4. Laundering Durability. Laundering durability of antibacterial effects was evaluated after five washing cycles in Polycolor (Werner Mathis AG) laboratory beaker dyer at 45 rpm. The fabrics were washed in the bath containing 0.5% Felosan RG-N (Bezema) at a liquor-to-fabric ratio of 40:1. After 30 min of washing at 40 °C, the fabrics were rinsed once with warm water (40 °C) for 3 min and three times (3 min) with cold water. Afterward, the fabrics were dried at 70 °C.[8] The percentage of bacterial reduction after five washing cycles was determined in accordance with eq 1.

2.2.5. Sorption of Silver. The effluents collected after the first two cycles of washing of all studied samples were mixed, and silver concentration was measured by atomic absorption spectroscopy (AAS). The measured pH value of the effluent was pH 4.5. Subsequently, 0.50 g of recycled wool-based nonwoven material was shaken in 25 mL of effluent for 3 and 24 h. Ag concentration after the sorption was also followed by AAS.

3. Results and Discussion

3.1. Characterization of PES Fabrics Modified by Plasma Treatment and Ag NPs. To enhance the interaction between hydrophilic colloidal Ag NPs and hydrophobic PES fibers, the surface of the substrate was modified by air RF plasma. Plasma induced morphological changes of PES fibers were analyzed by SEM. SEM images of untreated (UPES) and plasma treated PES (PPES) fibers are shown in Figure 1. Figure 1a reveals the smooth surface of the UPES fiber. The topography

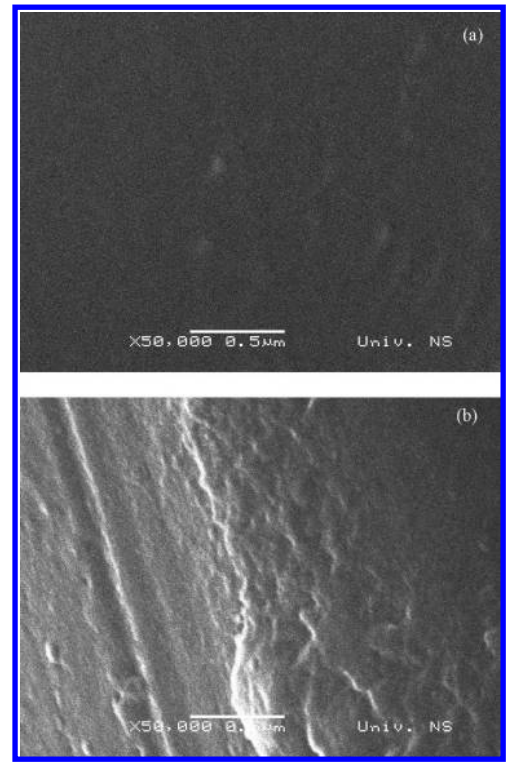

Figure 1. SEM images of UPES (a) and PPES fibers (b).

of the fiber was considerably altered after plasma treatment due to plasma etching (Figure 1b). Namely, energetic and highly reactive plasma species attacked the fiber surface and triggered the fiber ablation. Consequently, uneven cracks, pits, and striations running parallel to the fiber axis appeared, inducing the increase in fiber surface roughness.[20,40,41]

In addition to morphological changes, the chemical composition of the outer layers of the PES fibers was significantly altered. The XPS measurements in our previous study showed that air plasma treatment of PES fabrics resulted in an increase of the O/C ratio.[42] The formation of new oxygen-containing groups on the fiber surface is suggested to be due to the presence of extremely reactive atomic oxygen species in discharge during the air plasma processing and/or post-plasma chemical reactions when the activated fiber surface reacts with environmental species.[43–45] The rise of oxygen content ensures the improvement of PES fiber surface hydrophilicity and better accessibility of hydrophilic species.

UPES and PPES fabrics were loaded once or twice with colloidal Ag NPs. For this purpose, uniform nearly spherical Ag NPs with an average diameter of approximately 10 nm, synthesized without using any stabilizer, were applied.[20] The changes in fiber surface morphology after deposition of Ag NPs was also followed by SEM. SEM images of the PES fabrics loaded once and twice with Ag NPs (UPES + Ag and UPES + Ag × 2) as well as of the PPES fabrics loaded once and twice with Ag NPs (PPES + Ag and PPES + Ag × 2) are shown in Figure 2. Only a few almost spherical aggregates of Ag NPs with dimensions around 100 nm are observed on the surface of the UPES + Ag fiber (Figure 2a). On the contrary, a higher amount of smaller aggregates of Ag NPs with dimensions ranging from 40 to 70 nm was deposited on the surface of the UPES + Ag × 2 fibers (Figure 2b). As expected, plasma treatment positively affected the deposition of Ag NPs onto PES fibers (Figure 2c,d). Aggregates of Ag NPs (from 40 to 70 nm) were more uniformly distributed particularly over the surface of the PPES + Ag × 2 fibers (Figure 2d). Namely,

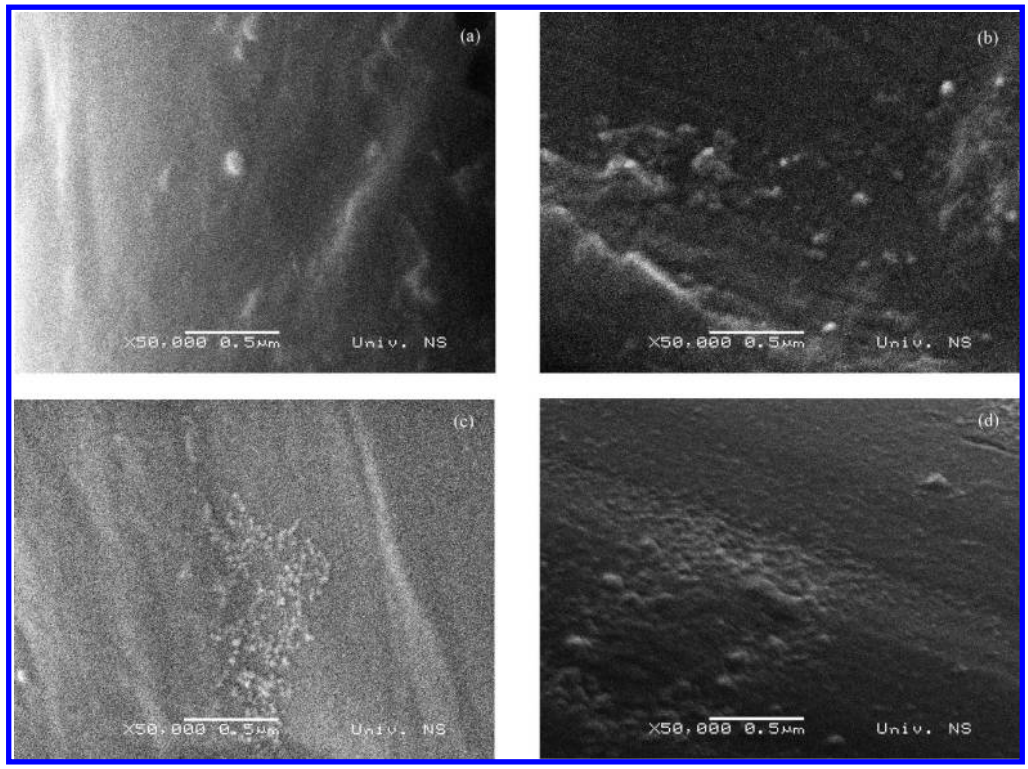

Figure 2. SEM images of UPES fabrics loaded with Ag NPs once (a) and twice (b) and PPES fabrics loaded with Ag NPs once (c) and twice (d).

Table 1. Antibacterial Efficiency of Ag Loaded UPES and PPES Fabrics

sample	bacteria	initial no. of bacterial colonies (CFU)	no. of bacterial colonies on the fabric (CFU)	*R* (%)
control	*E. coli*	5.6×10^5	3.4×10^4	
UPES + Ag			<10	99.9
UPES + Ag × 2			<10	99.9
PPES + Ag			<10	99.9
PPES + Ag × 2			<10	99.9
control	*S. aureus*	1.7×10^5	1.0×10^4	
UPES + Ag			<10	99.9
UPES + Ag × 2			<10	99.9
PPES + Ag			<10	99.9
PPES + Ag × 2			<10	99.9

Table 2. Antibacterial Efficiency of Ag Loaded UPES and PPES Fabrics after Five Washing Cycles

sample	bacteria	initial no. of bacterial colonies (CFU)	no. of bacterial colonies on the fabric (CFU)	*R* (%)
control	*E. coli*	2.4×10^5	1.7×10^4	
UPES + Ag			2.0×10^2	98.9
UPES + Ag × 2			10	99.9
control		5.6×10^5	7.4×10^4	
PPES + Ag			<10	99.9
PPES + Ag × 2			<10	99.9
control	*S. aureus*	1.4×10^5	4.0×10^4	
UPES + Ag			2.8×10^2	99.3
UPES + Ag × 2			55	99.9
control		1.0×10^4	4.5×10^3	
PPES + Ag			<10	99.9
PPES + Ag × 2			<10	99.9

plasma-induced hydrophilicity of PES fiber surface in conjunction with increased fiber surface roughness makes the PES fibers remarkably more accessible to colloidal Ag NPs. Hence, better deposition of Ag NPs is provided on PPES fabrics.

AAS measurements also confirmed higher Ag content in the PPES fabrics. It was found that 1 g of the UPES + Ag, UPES + Ag × 2, PPES + Ag, and PPES + Ag × 2 contains 79.7, 61.8, 155.7, and 145.5 μg of Ag, respectively. Unlike plasma pretreatment, double loading of colloidal Ag NPs did not enhance the deposition of Ag NPs onto the UPES and PPES fabrics.

3.2. Antibacterial Efficiency and Laundering Durability of PES Fabrics Loaded with Ag NPs. Antibacterial activity of UPES and PPES fabrics loaded with Ag NPs was tested against gram-negative bacterium *E. coli* and gram-positive bacterium *S. aureus*. The values of bacterial reduction of the UPES and PPES fabrics loaded once and twice with Ag NPs are given in Table 1. All PES fabrics loaded with Ag NPs reached the maximum bacterial reduction, independently of treatment. The results in Table 2 demonstrate that after five washing cycles the PPES fabrics loaded with Ag NPs once and twice, preserved the initial antibacterial activity, indicating an excellent laundering durability. A similar effect was achieved by corona treatment at atmospheric pressure in our previous work.[20] To obtain the same level of antibacterial efficiency after five washing cycles, the UPES fabrics have to be loaded with Ag NPs twice. In other words, the UPES + Ag fabric exhibited poorer laundering durability. It is interesting to note that laundering durability of the UPES + Ag × 2 fabrics in our previous study[20] was not as good as the data in Table 2 imply. The discrepancy between previous and current results is very likely due to different construction of the studied PES fabrics. Obtained results reveal that the fabric parameters should be also taken into consideration since they indirectly determine the macroscopic accessibility of fibers to colloidal Ag NPs.

The exact mechanism by which Ag NPs interact with bacteria is not totally clear yet. One approach relies on the hypothesis that Ag ions released from Ag NPs are responsible for killing the bacteria[46–48] Lok et al. suggested that antibacterial activity of Ag NPs depends on the chemisorbed Ag^+ that is formed on the nanoparticle surface.[49] However, another approach is oriented toward the work of Morones et

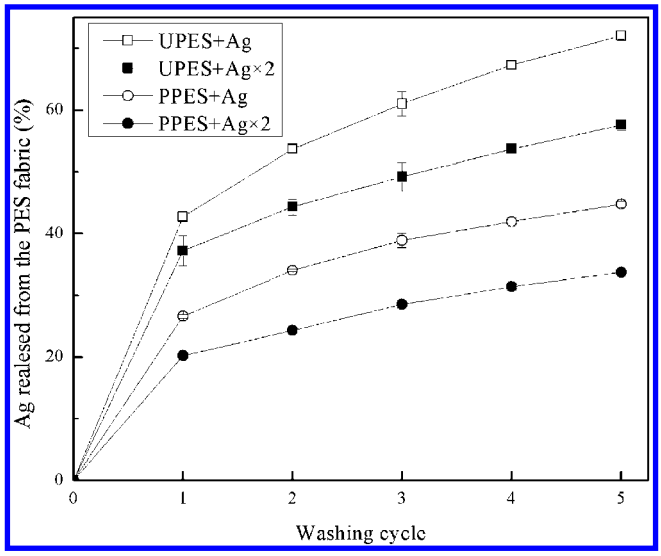

Figure 3. Silver release from the PES fabrics loaded with Ag NPs during washing.

al. who reported the presence of small-sized Ag NPs attached to the cell membrane and inside the bacteria that are crucial findings for understanding the bactericidal mechanism of Ag NPs.[46] Because silver shows high affinity to react with sulfur and phosphorus compounds,[50] it can be expected that Ag NPs react with sulfur reach protein in the bacteria cell membrane and interior of the cell or with phosphorus-containing compounds such as DNA.[51,52] Therefore, the morphological changes in the cell membrane of bacteria and possible damage of DNA triggered by reaction with Ag NPs negatively affect the respiratory chain or cell division processes, inducing a cell death.[46]

The amount of Ag released from the PES fabrics loaded with Ag NPs into the washing bath after each washing cycle was evaluated by AAS measurements. The total amount of Ag initially deposited onto PPES fabrics was approximately two times higher compared to equivalent UPES fabrics. As predicted, Ag leaching from the PES fabrics occurred during the washing. The results in Figure 3 indicate that the amount of Ag released from the PES fabrics decreases in each subsequent washing cycle. After a high initial rate of Ag release, the Ag leaching slowed down already in the second washing cycle for all samples. A similar trend of Ag release was observed on cotton fabrics.[3] The fabrics were burned after the last washing cycle, and the amount of Ag retained on the fabrics was determined. It was found that 22.3, 26.2, 86.1, and 96.4 μg of Ag is left in 1 g of the UPES + Ag, UPES + Ag × 2, PPES + Ag and PPES + Ag × 2 fabric, respectively. It can be noticed that Ag contents in the UPES + Ag and UPES + Ag × 2 after washing only slightly differ. Taking into account that the UPES + Ag fabric exhibited poor laundering durability unlike UPES + Ag × 2, it could be assumed that the critical amount of Ag necessary to provide desirable antibacterial activity in our systems should be within 22.3 and 26.2 μg/(g of fabric). It is also evident that a larger amount of Ag is left on the double-loaded PES fabrics compared to single-loaded PES fabrics. It appears that PPES fabrics retained almost four times more Ag compared to equivalent UPES samples. These results along with obtained antibacterial effects clearly confirm the positive effect of air RF plasma treatment on the deposition of Ag NPs onto PES fibers.

This study implies that silver leaching occurs during washing, but it cannot answer in what form silver is released from the PES fabrics. One assumption relies on the simple detachment of Ag NPs from the fiber surface and release into the washing bath. Another one involves the oxidation of silver since it was found out that, in contact with water and dissolved oxygen, Ag NPs release small amounts of silver ions according to[53]

$$O_2(aq) + 4H_3O^+ + 4Ag(s) \rightarrow 4Ag^+(aq) + 6H_2O \quad (2)$$

Benn and Westerhoff reported the presence of both forms of silver in the ultrapure water after simulated washing of commercial socks.[28] However, it is known that colloidal Ag NPs oxidize in aqueous medium on a long time scale (days).[37]

3.3. Sorption of Silver on the Recycled Wool-Based Nonwoven Material. To diminish the possible risk of ionic silver impact on the aquatic environment, the sorption of silver from the effluent collected after the first two washing cycles was tested using the recycled wool-based nonwoven material. AAS measurement indicated that the initial concentration of silver in the effluent was 0.5 mg/L. This value is in excellent agreement with the one calculated on the basis of results from Figure 3 corresponding to the amount of released silver in a certain volume of effluent. After 3 h of sorption about 70% of silver was removed from the effluent. The removal of silver increased to 84% after 24 h of sorption. Modification of sorbent with hydrogen peroxide and particularly biopolymer alginate positively influenced the removal of silver from the effluent. Already after 3 h of sorption, material modified with hydrogen peroxide removed 90% while with alginate 92% of silver. The good sorption properties of the material treated with hydrogen peroxide are likely due to modification of the surface of the wool fibers, i.e., oxidation and formation of appropriate groups that are potential sites for the binding of metal cations.[54,55] The abundance of carboxylic groups existing in alginates[56,57] makes this biopolymer a potential modifier of textile fiber surfaces, which may provide additional sites for complexation of ionic silver.

Presented results along with published data clearly imply that silver in concentrations existing in the washing effluents can be successfully treated.

4. Conclusions

Untreated and air RF plasma treated polyester fabrics loaded with silver nanoparticles once or twice from 50 ppm colloid exhibited excellent antibacterial activity against gram-negative bacterium *E. coli* and gram-positive bacterium *S. aureus*. Plasma pretreated polyester fabrics preserved excellent antibacterial activity even after five washing cycles. Untreated polyester fabric has to be loaded twice with silver nanoparticles to reach the equal antibacterial activity after washing. For the same goal, plasma pretreated PES fabric required only one loading of silver nanoparticles. Greater antibacterial efficiency of plasma treated fabrics is attributed to a larger amount of deposited silver. On the other hand, double loading did not improve the deposition of the silver nanoparticles. The results also demonstrated that a similar amount of silver was released from both untreated and plasma treated fabrics during washing. However, a much higher amount of silver was retained on the plasma pretreated fabrics after five washing cycles, indicating that plasma pretreatment positively affected the silver nanoparticle deposition, but it did not provide enhanced stability of the textile nanocomposite system. Released silver from the washing effluent was

efficiently removed by recycled wool-based nonwoven sorbent modified with hydrogen peroxide and biopolymer alginate.

Acknowledgment

This study was supported by the Ministry of Science of the Republic of Serbia—Project TR19007, 142066 and Eureka Project E !4043—NANOVISION. We gratefully acknowledge M. Bokorov (University of Novi Sad, Serbia) for performing SEM measurements.

Literature Cited

(1) Gao, Y.; Cranston, R. Recent Advances in Antimicrobial Treatments of Textiles. *Text. Res. J.* **2005**, *78*, 60.

(2) Yuranova, T.; Rincon, A. G.; Bozzi, A.; Parra, S.; Pulgarin, C.; Alberts, P.; Kiwi, J. Antibacterial Textiles Prepared by RF-plasma and Vacuum-UV Mediated Deposition of Silver. *J. Photochem. Photobiol., A* **2003**, *161*, 27.

(3) Ilić, V.; Šaponjić, Z.; Vodnik, V.; Potkonjak, B.; Jovančić, P.; Nedeljković, J.; Radetić, M. The Influence of Silver Content on Antimicrobial Activity and Color of Cotton Fabrics Functionalized with Ag Nanoparticles. *Carbohydr. Polym.* **2009**, *78*, 564.

(4) Feng, Q. L.; Wu, J.; Chen, G. Q.; Cui, F. Z.; Kim, T. N.; Kim, J. O. A Mechanism Study of Antibacterial Effect of Silver Ions on Escherichia coli and Staphylococcus aureus. *J. Biomed. Mater. Res.* **2000**, *52*, 662.

(5) Kostić, M.; Radić, N.; Obradović, B. M.; Dimitrijević, S.; Kuraica, M. M.; Škundrić, P. Silver Loaded Cotton/Polyester Fabric Modified by Dielectric Barrier Discharge Treatment. *Plasma Process. Polym.* **2009**, *6*, 58.

(6) Vigneshwaran, N.; Kumar, S.; Kathe, A. A.; Vradarajan, P. V.; Prasad, V. Functional Finishing of Cotton Fabrics Using Zinc Oxide-Soluble Starch Nanocomposites. *Nanotechnology* **2006**, *17*, 5087.

(7) Jeong, H. S.; Hwang, Y. H.; Yi, S. C. Antibacterial Properties of Padded PP/PE Nonwovens Incorporating Nano-Sized Silver Colloids. *J. Mater. Sci.* **2005**, *40*, 5413.

(8) Lee, H. J.; Yeo, S. Y.; Jeong, S. H. Antibacterial Effect of Nanosized Silver Colloidal Solution on Textiles Fabrics. *J. Mater. Sci.* **2003**, *38*, 2199.

(9) Vigneshwaran, N.; Kathe, A. A.; Varadarajan, P. V.; Nachane, R. P.; Balasubramanya, R. H. Functional Finishing of Cotton Fabrics Using Silver Nanoparticles. *J. Nanosci. Nanotechnol.* **2007**, *7*, 1893.

(10) Lee, H. J.; Jeong, S. H. Bacteriostasis of Nanosized Colloidal Silver on Polyester Nonwovens. *Text. Res. J.* **2004**, *74*, 442.

(11) Yuranova, T.; Rincon, A. G.; Pulgarin, C.; Laub, D.; Xantopoulos, N.; Mathieu, H. J.; Kiwi, J. Performance and Characterization of Ag-cotton and Ag/TiO_2 Loaded Textiles During the Abatement of *E. coli*. *J. Photochem. Photobiol., A* **2006**, *181*, 363.

(12) Perelshtein, I.; Applerot, G.; Perkas, N.; Guibert, G.; Mikhailov, S.; Gedanken, A. Sonochemical Coating of Silver Nanoparticles on Textile Fabrics (Nylon, Polyester and Cotton) and Their Antibacterial Activity. *Nanotechnology* **2008**, *19*, 255705.

(13) Hadad, L.; Perkas, N.; Gofer, Y.; Calderon-Moreno, J.; Hule, A.; Gedanken, A. Sonochemical Deposition of Silver Nanoparticles on Wool Fibers. *J. Appl. Polym. Sci.* **2007**, *104*, 1732.

(14) Wang, H. B.; Wei, Q. F.; Wang, J. Y.; Hong, J. H.; Zhao, X. Y. Sputter Deposition of Nanostructured Antibacterial Silver on Polypropylene Non-wovens. *Surf. Eng.* **2008**, *24*, 70.

(15) Mejia, M. I.; Restrepo, G.; Marin, J. M.; Sanjines, R.; Pulgarin, C.; Mielzarski, E.; Mielzarski, J.; Kiwi, J. Magnetron-Sputtered Ag Surfaces. New Evidence for the Nature of the Ag Ions Intervaning in Bacterial Inactivation. *ACS Appl. Mater. Interfaces* **2010**, *2*, 230.

(16) Durán, N.; Marcato, P. D.; De Souza, G. I. H.; Alves, O. L.; Esposito, E. Antibacterial Effect of Silver Nanoparticles Produced by Fungal Process on Textile Fabrics and Their Effluent Treatment. *J. Biomed. Nanotechnol.* **2007**, *3*, 203.

(17) Xu, X.; Yang, Q.; Wang, Y.; Yu, H.; Chen, X.; Jing, X. Biodegradable Electrospun Poly (L-lactide) Fibers Containing Antibacterial Silver Nanoparticles. *Eur. Polym. J.* **2006**, *42*, 2081.

(18) Jiang, S. Q.; Yuen, C. W. M.; Tao, X. M.; Kan, C. W.; Choi, P. S. R. Low-Temperature Plasma Pre-treatment of Polyester Fabric for Chemical Silver Plating. Presented at the 6th AUTEX Conference, Raleigh, NC, June 2006.

(19) Morent, R.; De Geyter, N.; Leys, C.; Gengembre, L.; Payen, E. Surface Modification of Non-woven Textiles using a Dielectric Barrier Discharge Operating in Air, Helium and Argon at Medium Pressure. *Text. Res. J.* **2007**, *77*, 471.

(20) Radetić, M.; Ilić, V.; Vodnik, V.; Dimitrijević, S.; Jovančić, P.; Šaponjić, Z.; Nedeljković, J. Antibacterial Effect of Silver Nanoparticles Deposited on Corona Treated Polyester and Polyamide Fabrics. *Polym. Adv. Technol.* **2008**, *19*, 1816.

(21) Ilić, V.; Šaponjić, Z.; Vodnik, V.; Mihailović, D.; Jovančić, P.; Nedeljković, J.; Radetić, M. The Study of Coloration and Antibacterial Efficiency of Corona Activated Dyed Polyamide and Polyester Fabrics Loaded with Ag Nanoparticles. *Fiber Polym.* **2009**, *10*, 650.

(22) Ilić, V.; Šaponjić, Z.; Vodnik, V.; Molina, R.; Dimitrijević, S.; Jovančić, P.; Nedeljković, J.; Radetić, M. Antifungal Efficiency of Corona Pretreated Polyester and Polyamide Fabrics Loaded with Ag Nanoparticles. *J. Mater. Sci.* **2009**, *44*, 3983.

(23) Shishoo, R. Introduction—The Potential of Plasma Technology in the Textile Industry. In *Plasma Technologies for Textiles*; Shishoo, R., Ed.; Woodhead: Cambridge, U.K., 2007.

(24) Radetić, M.; Jocić, D.; Jovančić, P.; Trajković, R.; Petrović, Z. Lj. The Effect of Low-Temperature Plasma Pretreatment on Wool Printing. *Text. Chem. Color. Am. Dyest. Rep.* **2000**, *32*, 55.

(25) Riccardi, C.; Barni, R.; Fontanesi, M.; Marcandalli, B.; Massafra, M.; Selli, E.; Mazzone, G. ASF6 RF Plasma Reactor for Research on Textile Treatment. *Plasma Sources Sci. Technol.* **2001**, *10*, 92.

(26) Puač, N.; Petrović, Z. Lj.; Radetić, M.; Djordjević, A. Low Pressure RF Capacitively Coupled Plasma Reactor for Modification of Seeds, Polymers and Textile Fabrics. *Mater. Sci. Forum* **2005**, *494*, 291.

(27) Morris, J.; Willis, J. *U.S. Environmental Protection Agency Nanotechnology White Paper*, EPA 100/B-07/001; Science Policy Council, U.S. Environmental Protection Agency: Washington, DC, 2007.

(28) Benn, T. M.; Westerhoff, P. Nanoparticle Silver Released into Water from Commercially Available Sock Fabrics. *Environ. Sci. Technol.* **2008**, *42*, 4133.

(29) Durán, N.; Marcato, P. D.; Alves, O. L.; Da Silva, J. P. S.; De Souza, G. I. H.; Rodrigues, F. A.; Esposito, E. Ecosystem Protection by Effluent Bioremediation: Silver Nanoparticles Impregnation in a Textile Fabrics Process. *J. Nanopart. Res.*, in press.

(30) Geranio, L.; Heuberger, M.; Nowack, B. The Behavior of Silver Nanotextiles during Washing. *Environ. Sci. Technol.* **2009**, *43*, 8113.

(31) Radetić, M.; Ilić, V.; Radojević, D.; Miladinović, R.; Jocić, D.; Jovančić, P. Efficiency of Recycled Wool-Based Nonwoven Material for the Removal of Oils from Water. *Chemosphere* **2008**, *70*, 525.

(32) Radetić, M.; Radojević, D.; Ilić, V.; Jocić, D.; Povrenović, D.; Potkonjak, B.; Puač, N.; Jovančić, P. Removal of Metal Cations from Wastewater Using Recycled Wool-Based Non-woven Material. *J. Serb. Chem. Soc.* **2007**, *72*, 605.

(33) Radetić, M.; Radojević, D.; Ilić, V.; Mihailović, D.; Jovančić, P. Recycled Wool-Based Nonwoven Material for Decolorisation of Dyehouse Effluents. *Int. J. Cloth. Sci. Tech.* **2009**, *21*, 109.

(34) Masri, M. S.; Friedman, M. Effect of Chemical Modification of Wool on Metal Ion Binding. *J. Appl. Polym. Sci.* **1974**, *18*, 2367.

(35) Tomčik, B.; Popović, D. R.; Jovanović, I. V.; Petrović, Z. Lj. Modification of Wettability of Polymer Surface by Microwave Plasma. *J. Polym. Res.* **2001**, *8*, 259.

(36) Lieberman, M. A.; Lichtenberg, A. J. *Principles of Plasma Discharge and Materials Processing*; Wiley: Hoboken, NJ, and New York, 2005.

(37) Vuković, V. V.; Nedeljković, J. M. Surface Modification of Nanometer-Scale Silver Particles by Imidazole. *Langmuir* **1993**, *9*, 980.

(38) Šaponjić, Z. V.; Csencsits, R.; Rajh, T.; Dimitrijević, N. Self-Assembly of Topo-Derivatized Silver Nanoparticles Into Multilayered Film. *Chem. Mater.* **2003**, *15*, 4521.

(39) Ki, H. Y.; Kim, J. H.; Kwon, S. C. Antibacterial Activity of Ag^+ Ion-Containing Silver Nanoparticles Prepared Using the Alcohol Reduction Method. *J. Mater. Sci.* **2007**, *42*, 8020.

(40) Qi, K.; Xin, J. H.; Daoud, W. A. Functionalizing Polyester Fiber with a Self-Cleaning Property Using Anatase TiO_2 and Low-Temperature Plasma Treatment. *Int. J. Appl. Ceram. Technol.* **2007**, *4*, 554.

(41) Zhang, C.; Fang, K. Surface Modification of Polyester Fabrics for Inkjet Printing with Atmospheric-Pressure Air/Ar plasma. *Surf. Coat. Technol.* **2009**, *203*, 2058.

(42) Mihailović, D.; Radetić, M.; Radoičić, M.; Molina, R.; Puač, N.; Jovančić, P.; Nedeljković, J.; Šaponjić, Z. *Specific Properties of Polyester Fabrics Functionalized by RF Plasma and Colloidal TiO_2 Nanoparticles*. Presented at the International Conference: Latest Advances in High Tech Textiles and Textile-Based Materials, Ghent, Belgium, September 2009, 213.

(43) Pappas, D.; Bujanda, A.; Demaree, J. D.; Hirvonen, J. K.; Kosik, W.; Jensen, R.; McKnight, S. Surface Modification of Polyamide Fibers and Films Using Atmospheric Plasmas. *Surf. Coat. Technol*. **2006**, *201*, 4384.

(44) Dai, X. J.; Hamberger, S. M.; Bean, R. A. Reactive Plasma Species in the Modification of Wool Fibre. *Aust. J. Phys*. **1995**, *48*, 939.

(45) De Geyter, N.; Morent, R.; Leys, C. Penetration of a Dielectric Barrier Discharge Plasma into Textile Structures at Medium Pressure. *Plasma Sources Sci. Technol*. **2006**, *15*, 78.

(46) Morones, J. R.; Elechiguerra, J. L.; Camacho, A.; Holt, K.; Kouri, J. N.; Ramirez, J. T.; Yacaman, M. J. The Antibactericidal Effect of Silver Nanoparticles. *Nanotechnology* **2005**, *16*, 2346.

(47) Xu, X.; Yang, Q.; Wang, Y.; Yu, H.; Chen, X.; Jing, X. Biodegradable Electrospun Poly(L-lactide) Fibers Containing Antibacterial Silver Nanoparticles. *Eur. Polym. J*. **2006**, *42*, 2081.

(48) Damm, C.; Muenstedt, H.; Roesch, A. Long-Term Antimicrobial Polyamide 6/Silver-Nanocomposites. *J. Mater. Sci*. **2007**, *42*, 6067.

(49) Lok, C. N.; Ho, C. M.; Chen, R.; He, Q. Y.; Yu, W. Y.; Sun, H.; Tam, P. K. H.; Chiu, J. F.; Che, C. M. Silver Nanoparticles: Partial Oxidation and Antibacterial Activities. *J. Biol. Inorg. Chem*. **2007**, *12*, 527.

(50) Hatchett, D. W.; Henry, S. Electrochemistry of Sulfur Adlayers on the Low-Index Faces Silver. *J. Phys. Chem*. **1996**, *100*, 9854.

(51) Feng, Q. L.; Wu, J.; Chen, G. Q.; Cui, F. Z.; Kim, T. N.; Kim, J. O. A Mechanism Study of Antibacterial Effect of Silver Ions on Escherichia coli and Staphylococcus aureus. *J. Biomed. Mater. Res*. **2000**, *52*, 662.

(52) Kim, J. S. Antibacterial Activity of Ag^{+} Ion-Containing Silver Nanoparticles Prepared Using the Alcohol Reduction Method. *J. Ind. Eng. Chem*. **2007**, *13*, 718.

(53) Hoskins, J. S.; Karanfil, T.; Serkiz, S. M. Removal and Sequestation of Iodide Using Silver-Impregnated Activated Carbon. *Environ. Sci. Technol*. **2002**, *36*, 784.

(54) Jovančić, P.; Jocić, D.; Molina, R.; Juliá, M. R.; Erra, P. Shrinkage Properties of Peroxide-Enzyme-Biopolymer Treated Wool. *Text. Res. J*. **2001**, *71*, 948.

(55) Julià, M. R.; Erra, P.; Jocić, D.; Canal, J. M. The Use of Chitosan on Hydrogen Peroxide Pretreated Wool. *Text. Chem. Color*. **1998**, *30*, 78.

(56) Mihailović, D.; Šaponjić, Z.; Radoičić, M.; Radetić, T.; Jovančić, P.; Nedeljković, J.; Radetić, M. Functionalization of Polyester Fabrics with Alginates and TiO_2 Nanoparticles. *Carbohydr. Polym*. **2010**, *79*, 526.

(57) Fernandez, J.; Dhananjeyan, M. R.; Kiwi, J.; Senuma, Y.; Hilborn, J. Evidence for Fenton Photoassisted Processes Mediated by Encapsulated Fe Ions at Biocompatible pH Values. *J. Phys. Chem. B* **2000**, *104*, 5298.

Received for review January 20, 2010
Revised manuscript received June 28, 2010
Accepted June 28, 2010

IE1001313

Characterization of plasma needle with an additional grounded ring

Article

4 authors, including:

Saša Lazović
Institute of Physics Belgrade
70 PUBLICATIONS **212** CITATIONS
SEE PROFILE

Nevena Puač
Institute of Physics Belgrade
98 PUBLICATIONS **390** CITATIONS
SEE PROFILE

Gordana Malovic
Institute of Physics Belgrade
157 PUBLICATIONS **932** CITATIONS
SEE PROFILE

Characterization of plasma needle with an additional grounded ring

S. Lazović[1], N. Puač[1], G. Malović[1], A.R. Đorđević[2] and Z.Lj. Petrović[1]

[1] *Institute of Physics, Pregrevica 118, 11080 Belgrade, Serbia*
[2] *School of Electrical Engineering, Bulevar kralja Aleksandra 73, 11000, Belgrade, Serbia*

In this paper we present voltage–current–power characteristics of a plasma needle operating in the flow of helium at atmospheric pressure. In the characterization of the plasma needle, current and voltage waveforms were recorded by two derivative probes. These two probes are similar to the probes previously used by Puač *et al.* for measuring transmitted power in low pressure CCP RF discharge. The instantaneous power was calculated from current and voltage waveforms and mean values of the power delivered to plasma needle were calculated. Regime of operation with the grounding copper ring at the tip of the needle was considered. In addition, we will show emission intensity of the discharge obtained by using fast ICCD camera.

1. Introduction

Nonequilibrium plasmas proved to be able to produce chemically reactive species at a low gas temperature while maintaining uniform reaction rates over relatively large areas [1-3]. One of the advantages of working at atmospheric pressure is that no vacuum system is needed. The other is possibility to treat materials that cannot be treated at all under the low-pressure conditions. Treatment of organic materials and living tissues falls under that category. The need for 'bio-compatible' plasma sources nowadays is increasing and much effort is invested in creating such sources. Nevertheless, some requirements are to be met: such sources must produce non-thermal plasmas, operating at ambient pressure and temperature, and should not pose any electrical or chemical hazards.

One of the newly developed sources, which satisfies majority of the conditions that have to be fulfilled in order to treat sensitive samples, is the plasma needle. Before any application, it is necessary to examine the properties of such source as well as possible and define the optimum conditions for the specific treatment. So far, biological tissues of mammalian origin were treated [4, 5]. For that purpose, it is particularly important to know electrical characteristics of the plasma needle, i.e., the power transmitted to the plasma. In order to achieve that, we have developed derivative probes. In this paper we will show some of the electrical characteristics of the plasma needle (with additional copper ring) and, also, plasma emission intensity obtained by using ICCD camera.

2. Experimental setup

The plasma needle consists of the central tungsten wire (0.7 mm in diameter) which is placed in a ceramic (OD 2 mm) tube and then inside a glass tube (OD 6 mm). The body of the plasma needle is made of a stainless steel cylinder 20 mm in diameter. The tungsten wire is connected to a BNC connector placed at the end of the plasma needle body and acts as the powered electrode.

In our experiments we have used two different configurations of plasma needle. The configuration of the plasma needle without the grounded ring is described in more detail in [6]. In this paper we will present results obtained by using configuration with an additional copper ring. The grounded ring was introduced in order to improve the efficiency and the stability of the entire system. The ring was positioned at the tip of the needle around the glass tube. Helium was used as the feeding gas and it was introduced into the glass cylinder with a fixed flow rate. Flow rate was 110 sccm in all experiments.

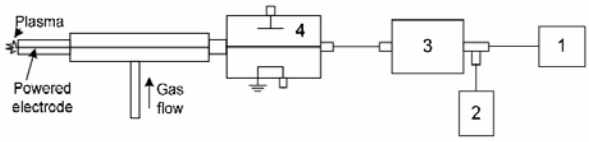

Fig.1. Schematic representation of the plasma needle setup: (1) RF power supply and matching network; (2) dummy load 50Ω; (3) home-made voltage transformer; (4) stainless steel box with derivative probes.

Electrical circuit of the experimental setup is shown in Fig. 1. Dressler Caeser 1010 power supply in combination with Variomatch matching network is used to generate low-temperature RF discharge at 13.56 MHz. Home-made transformer inserted between the plasma needle and the RF matching network is used to increase the peak-to-peak voltage. Dummy load is implemented to make the discharge more stable and to be sure that only a small amount of power supplied by the RF power supply is

transmitted to the discharge. So, it serves as a 'power divider'.

Instantaneous voltage and current are monitored using two derivative probes developed previously [1], somewhat different from the probes proposed in the literature. Both probes were placed inside a stainless steel box opposite to each other. The box was placed as close as possible to the plasma needle. The output of the probes was connected to a digital oscilloscope (Tektronix TDS220) by cables of equal length. The computer was used for collecting all waveforms and for further manipulation. In addition to derivative probes, we used a fast ICCD camera in order to see emission intensity of the discharge. Emission of the discharge was recorded side-on and for the time interval of 5 ms.

3. Results and discussion

Powers from 30 W to 100 W given by the RF power supply were used to generate plasma at the tip of the plasma needle. Plasma ignites as a glow on the tip of the needle (fig.2) with the power increase at the RF power supply.

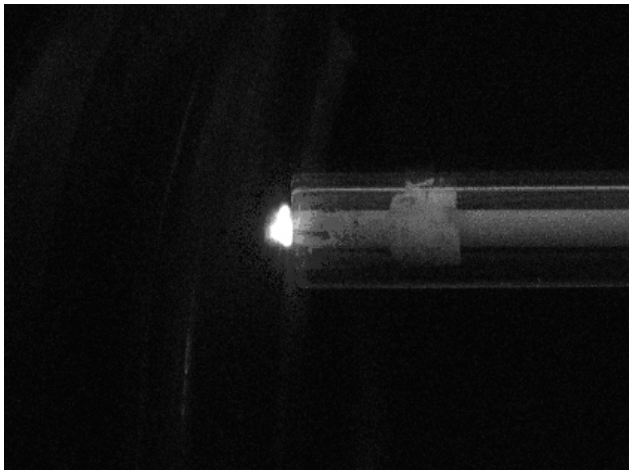

Fig. 2. Plasma glow at the tip of the needle.

The needle operates in a bipolar mode when the tip of the needle is brought close to the target object and the glow spreads over the object's surface. When there are no objects in the vicinity of the tip, remote surroundings serve as a grounded electrode and plasma works in unipolar mode.

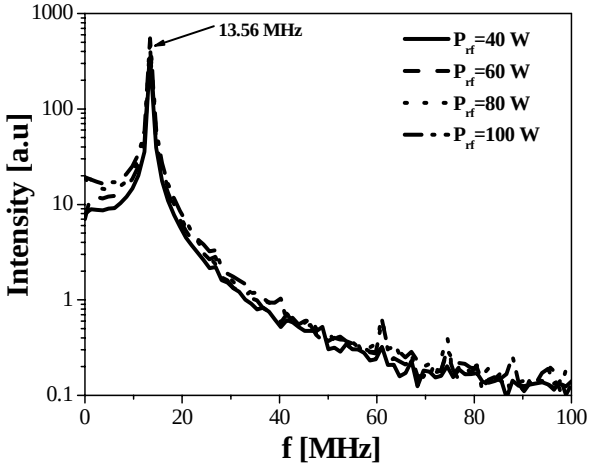

Fig. 3. Current harmonics for different values of power supplied by the RF source.

For the same range of powers (30 W to 100 W) instantaneous current and voltage waveforms were recorded by using derivative probes. All current and voltage waveforms gathered by the computer were transferred from time to the frequency domain by using FFT (Fast Fourier Transform).

We can see that only the first harmonic is relevant, both for the current and voltage (see fig. 3 and fig. 4). This indicates the symmetry of the discharge and stability of its regime of operation.

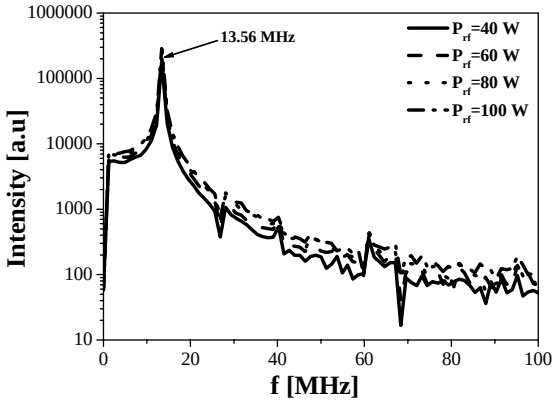

Fig. 4. Voltage harmonics for different values of power supplied by the RF source.

Also, the correction of current and voltage waveforms according to their calibration curves was done in the frequency domain. Current and voltage waveforms, before and after corrections, are shown in fig. 5 and fig. 6.

In fig. 7, current, voltage and power waveforms are shown. All waveforms are obtained by using configuration of plasma needle with additional copper ring placed at the tip of the glass tube.

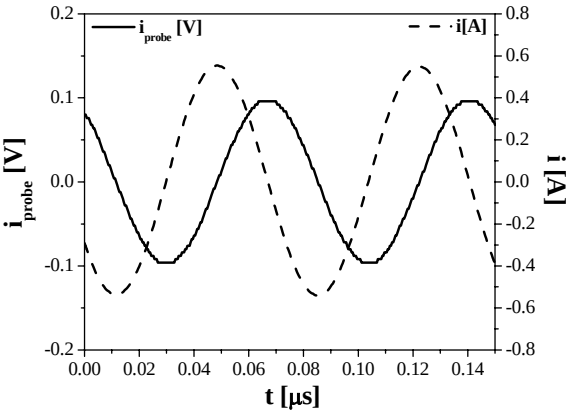

Fig. 5. Current waveforms before (i_{probe}) and after calibration and phase correction.

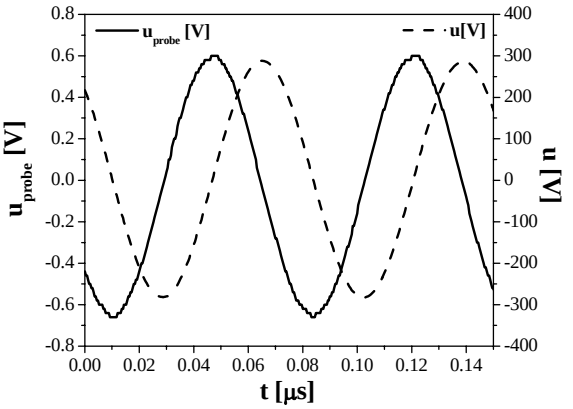

Fig. 6. Voltage waveforms before (u_{probe}) and after calibration and phase correction.

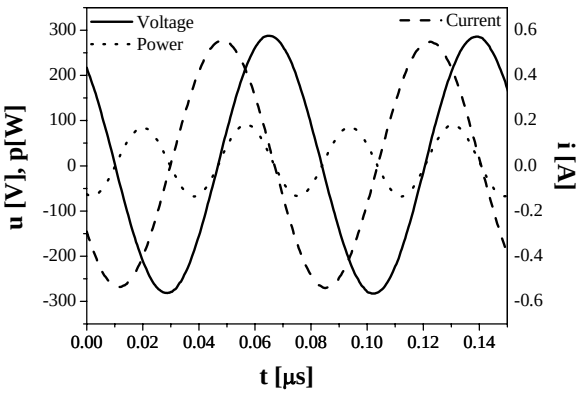

Fig. 7. Instantaneous current, voltage and power waveforms for 100 W given by RF power source.

Only about 10% of the total power is supplied to the branch of the electrical circuit with plasma needle. The rest goes to the dummy load and this branch of electrical circuit serves as 'power divider'. The mean power was calculated by integrating 6T (T=1/(13.56e6 Hz)) interval of instantaneous power waveforms. In fig 8, mean power values are shown as function of power given by RF power supply when there is ignited plasma at the tip of the needle and without it. We can see that less then 1% is delivered to the plasma itself (fig 9), and the rest is converted to heat in conductors and dielectrics. With the increase of the power given by RF power supply, we observed a significant increase in the value of the power transmitted to the plasma (inside circle in fig 8).

This effect was also observed by ICCD camera as an increase in intensity of plasma emission (see fig 10).

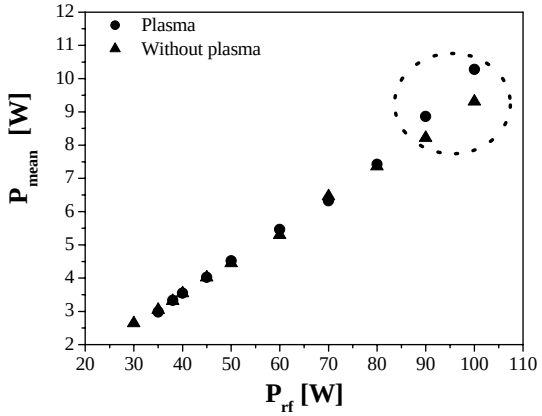

Fig. 8. Mean power as function of the power given by RF power source.

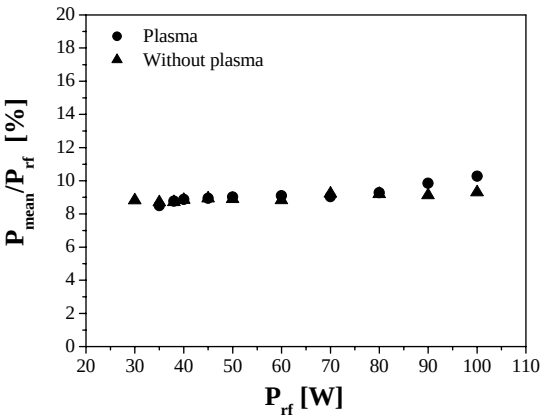

Fig. 9. Percentage of the power delivered to the plasma as function of the power given by RF power source.

If we decrease the power delivered into the system by RF power supply, we were able to observe the hysteresis effect. From emission intensities we can see (fig. 11) that the discharge stays ignited even if we reduce the power below the value where originally plasma was ignited (in this case, 60 W given by RF power supply). This can be explained by the fact that the ignition voltage is

much higher then the working voltage of the discharge.

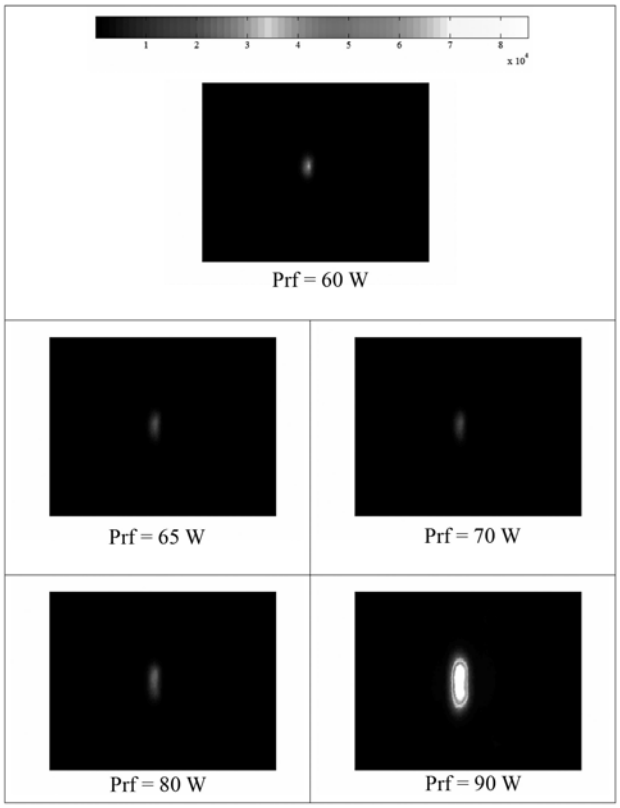

Fig. 10. Intensity of plasma emission as a function of the **increasing** power given by the RF power source. Emission of the discharge was recorded for the time interval of 5 ms.

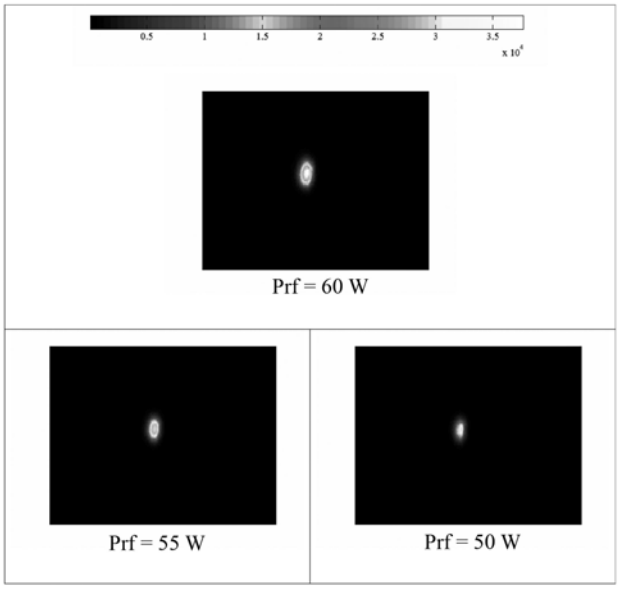

Fig. 11. Intensity of plasma emission as a function of the **decreasing** power given by the RF power source. Emission of the discharge was recorded for the time interval of 5 ms.

4. Conclusion

We have developed a plasma needle similar to that of Stoffels and co-workers [4, 5]. It looks like that if there is a plasma discharge on the tip of the needle and we decrease the power given by the RF power supply, hysteresis appears. Thus, there is still a plasma glow even for the power lower than the ignition power. The reason for this can be that the working voltage of plasma needle is much lower than the breakdown voltage. The hysteresis effect was, also, detected in configuration without grounded ring [6].

It can be seen from the results shown here that the configuration of the plasma needle with the additional grounded copper ring is a much more efficient system than without it [6]. The ignition power (power given by RF power supply) is lower with the ring, and after the ignition, plasma can operate on lower power values than without the ring. This can be important issue when applying plasma needle for treatment of biological materials. The destruction of treated tissues is less when using 'low power plasmas'.

On the other hand, it is observed that with the increase of power above certain values, sharp rise of emission intensity appears. This rise of intensity is followed by the rise of mean power delivered to the plasma needle. When increasing the power of the RF generator above 80 W, a significant rise of the mean power delivered to the plasma needle is recorded. This effect was not observed in the configuration without the additional ring.

5. References

[1] N. Puač, Z.Lj. Petrović, S.Živković, Z Giba, D. Grubišić and A. Đorđević, “Low-temperature Plasma Treatment of Dry Empress-Tree Seeds” in Plasma Processes and Polymers edited by R d’Agostino, P Favia, C Oehr, M R Wertheimer, Berlin: Wilez-VCH (2005) 193-203

[2] T. Makabe and Z.Lj. Petrović, Plasma Electronics, New York: Taylor and Francis, (2006).

[3] J.R. Roth, Industrial Plasma Engineering, Bristol UK Institute of Physics (1995)

[4] R.E.J. Sladek and E. Stoffels, J.Phys.D: Appl. Phys. **38** (2005) 1716-1721

[5] E. Stoffels, A. J. Flikweert, W. W. Stoffels and G. M. W. Kroesen, Plasma Sources Sci. Technol. **11** (2002) 383-388

[6] N. Puač, Z.Lj. Petrović, G. Malović, A. Đorđević, S. Živković, Z. Giba and D. Grubišić, J.of Phys.D: Appl. Phys., **39**, (2006) 3514-3519

Langmuir probe measurements of a large scale RF asymmetric capacitive coupled plasma

3 authors:

Saša Lazović
Institute of Physics Belgrade
70 PUBLICATIONS **212** CITATIONS
SEE PROFILE

Nevena Puač
Institute of Physics Belgrade
98 PUBLICATIONS **390** CITATIONS
SEE PROFILE

Gordana Malovic
Institute of Physics Belgrade
157 PUBLICATIONS **932** CITATIONS
SEE PROFILE

Topic number

Langmuir probe measurements of a large scale RF asymmetric capacitive coupled plasma

S.Lazović[1], N. Puač[1], G.Malović[1] and Z.Lj. Petrović[1]

[1] *Institute of Physics, Pregrevica 118, 11080 Belgrade, Serbia*

Hiden Analytical ESPION Langmuir probe and derivative probes were used to diagnose large-volume asymmetric RF CCP in air at 100mTorr. Electron and ion concentrations were measured for several distances from the powered electrode. Radial profiles of charged particle densities have been followed across the radius of the cylindrical vessel and with the change of power. Values of power transferred to the plasma were obtained from derivative probes as well as the harmonic composition of the RF signal. It was determined from the shape of voltage-current characteristics that this discharge operates in alpha mode. Large scale discharge chamber investigated in this experiment was previously used in treatments of textile

1. Introduction

The applications of the capacitively coupled plasmas (CCPs) in the industry are various. Processes like etching, deposition, sputtering using CCPs are irreplaceable in treatment of many different kinds of conductive and non-conductive materials like microelectronics devices [1-3], biological samples [4] and textiles [5].

We have constructed a large scale discharge chamber in our laboratory in order to be able to diagnose and study plasma that can be used directly in the textile industry. When having electrically and geometrically asymmetric discharge chamber, the distance between the treated sample and the powered electrode plays an important role. The fluxes and energies of particles coming to the sample surface depend strongly on this distance. Therefore, measuring these values is important for the characterisation of the treatments of different samples. While the system was shown empirically to give excellent quality of treatment, with uniformity and stability from mode transitions to streamers and sparks it is important to perform a complete diagnostics of such a system in order to provide space for further optimizations especially in the speed of treatment. Convenient way to measure concentrations of ions and electrons, electron temperatures, electron energy distribution functions and ion fluxes, floating and plasma potentials is by using Langmuir probes.

Main advantages of Langmuir probes include ability to cover a wide range of plasma parameters that can be measured, spatially and temporally resolved results, simplicity of construction and relatively low price. Its disadvantages are that it perturbs the plasma, contamination of the probe tip, and that the results are sometimes very hard to interpret. Misinterpretation of current-voltage characteristics of Langmuir probes in RF discharges is due to the effects of RF time averaging, ionization near the probe, and expansion of the probe sheath [6, 7].

Another important parameter for the treatment of samples is power deposited in the plasma. Non-linear impedance characteristics of the plasma impose harmonics of the drive frequency generated at the external circuitry conductors. Asymmetry of the discharge chamber also affects the way harmonics are generated. Due to this non-linearity the change in external circuitry leads to unpredictable variation of plasma properties. For example, the auto-tune feature on the matching network can result in different reflected power minima for several apparently identical measurements which will result in different values of power deposited into the plasma [8]. In this manner the power measured on the RF generator itself is not the best parameter. Therefore, we have used previously developed derivative probes [4] in order to measure the power transmitted to plasma and analyze harmonic composition of the signals.

In this paper we will present results obtained in large scale asymmetric CCP discharge obtained by using Langmuir and derivative probes. U-I characteristics of the discharge for 100 mTorr in air is determined as well as concentration of electrons and ions at several distances from the powered electrode.

2. Experimental setup

The discharge chamber is 2.5 m long and 1.17 m in diameter and made of stainless steel. Powered electrode is placed axially in the centre of the chamber and is 1.5 m long, 3 cm in diameter and

made of aluminium. Outer chamber wall is the grounded electrode. The rest of the electrical circuit consists of RF power generator Dressler Cesar 1010 in combination with Variomatch matching network. Derivative probes are placed into a stainless steel box opposite to each other. The box is placed as close as possible to the powered electrode. Low pressures are maintained using mechanical vacuum pump with a constant flow of gas air (see Fig.1).

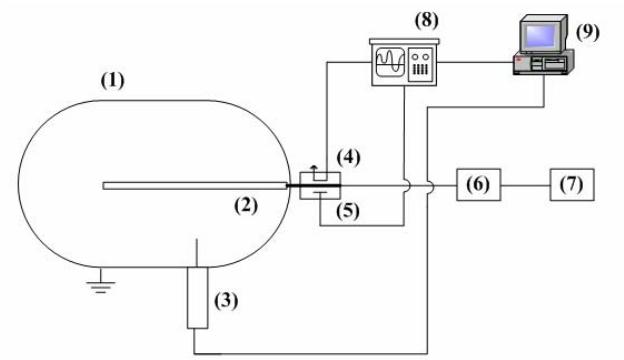

Figure 1. Experimental set-up: (1) Chamber, (2) Powered electrode, (3) ESPION system, (4) Current probe, (5) Voltage probe, (6) Variomatch, (7) Power supply, (8) Oscilloscope, (9) Computer

Instantaneous voltages and currents are monitored using derivative probes which were connected to the oscilloscope Agilent 6052A with the cables of identical length. All waveforms are collected by the computer for further analyzes.

Hiden Analytical ESPION advanced Langmuir probe system is placed side-on. The system has a linear motion drive which enables probe positioning with the spatial resolution of 0.1 mm. The chamber has a platform at the bottom where samples are placed. The distance between the platform and the powered electrode is adjustable by moving the platform. We have chosen distances for Langmuir probe measurements within this range. All measurements were done in air at 100 mTorr. We have used platinum probe tip, 10 mm long and 0.15 mm in diameter. Linear motion drive was used to position the probe at the distances 50.5 cm to 20.5 cm from the powered electrode. Measurements of U-I curves were made for all those positions of Langmuir probe.

At every position 10 measurements were made each being an average of 100 scans with pre-cleaning for each measurement. It was observed that even with pre-cleaning it is better to neglect first few measurements because of the probe contamination until results become stable. After that, the U-I curves were smoothed and data was processed using Hiden ESPSoft.

3. Results and discussion

3.1. Derivative probe measurements

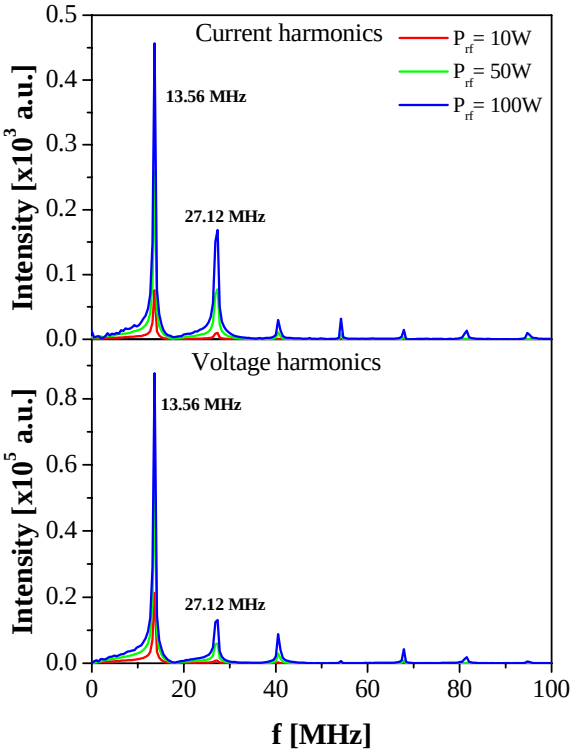

Figure 2. Current and voltage harmonics for three different powers given by RF power supply.

Voltage and current waveforms for a range of powers given by the RF source (10W-100W) are acquired by the derivative probes and transferred to computer for numerical processing. First, Fast Fourier Transform is performed. We can see that the presence of higher harmonics is increasing with the increase of power (see Fig. 2).

In frequency domain, voltage and current signals are multiplied by their calibration curves. After that the signals are converted back to time domain using Inverse Fast Fourier Transform and instantaneous values of power are calculated. Figure 3. shows instantaneous values of current, voltage and power.

Peak to peak values for voltage are between 80 V and 400 V while for current these values are from 0.35 A to 2.5 A. By calculating root-mean-square values of voltage and current we were able to obtain U-I characteristics (see Fig. 4). From the shape of this curve we can conclude that our discharge operates in alpha mode.

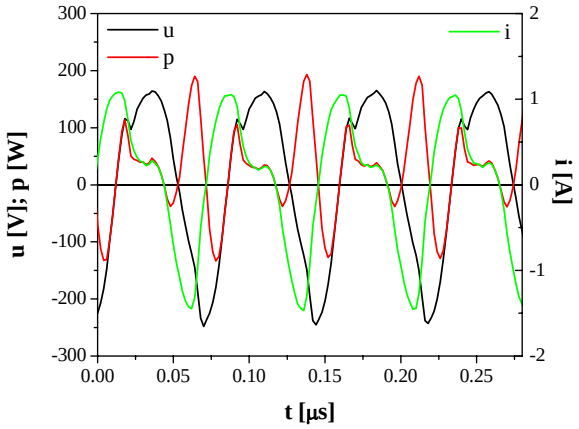

Figure 3. Instantaneous voltage, current and power curves.

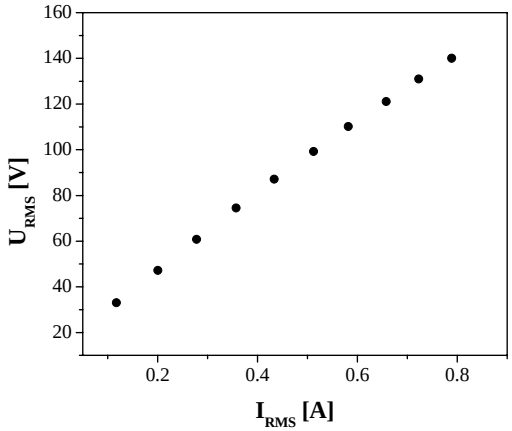

Figure 4. U-I characteristic of the discharge for 100 mTorr.

3.2. Langmuir probe measurements

Langmuir probe was placed perpendicular to the powered electrode (side on). We have recorded U-I curves for different powers given by RF power supply and different positions of Langmuir probe. From U-I characteristics one can obtain floating and plasma potentials, electron temperature and concentration as well as ion concentration and ion fluxes.

Main purpose of asymmetric CCP discharge used in this experiment is application in treatment of different kind of samples (textile, polymers, seeds etc.). Therefore, knowledge of concentration of ions and electrons, as well as their distribution at the various distances from the powered electrode, is of importance. In Figures 5. and 6. concentration of electrons and ions for different distances from the powered electrode are shown. We can see that with the increase of RMS voltage, therefore power transmitted to the plasma, concentration of electrons increases (see Fig 5.). Also, N_e does not change significantly when approaching powered electrode.

On the other hand, concentrations of ions (see Fig 6.) stay nearly constant with the RMS voltage increase even when approaching powered electrode. We can observe rise in ion concentration with applied RMS voltage only for two closest positions of the Langmuir probe to the powered electrode. Since ions play important role in plasma treatment, depending on sensitivity of the sample, one can determine optimal position for their placement from ion concentration and their energies.

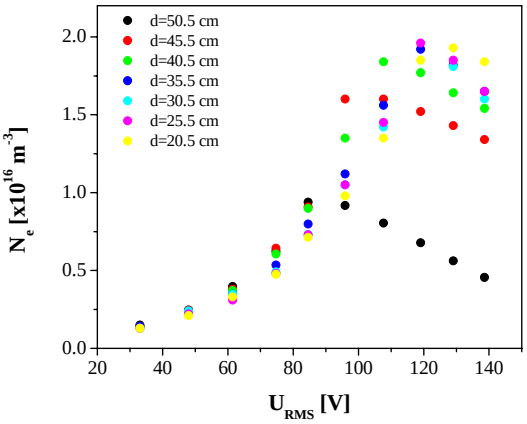

Figure 5. Electron concentrations at different distances from the powered electrode and different applied RMS voltages

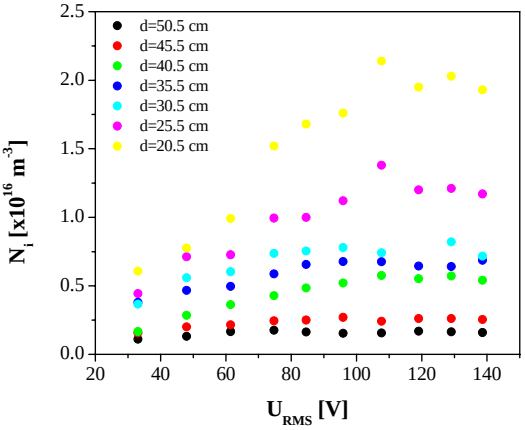

Figure 6. Ion concentrations at different distances from the powered electrode and different applied RMS voltages.

4. Conclusion

Large volume radio frequency asymmetric capacitive coupled plasma in air at 100 mTorr was diagnosed by using Langmuir probe and derivative probes. Power delivered to plasma was measured using derivative probes. From the shape of the

U_{rms}-I_{rms} characteristics it was determined that discharge operates in alpha mode. Electron and ion concentrations were measured at the several distances from the powered electrode at which the treated samples could be placed.

With the increase of RMS voltage, therefore power transmitted to the plasma, concentration of electrons increases, but it does not change significantly when approaching the powered electrode. On the other hand, concentrations of positive ions remain nearly constant with the RMS voltage increase and start to increase only for the distances less than 30 cm.

From the presently obtained results one can see a complex development of spatial profiles of ions and electrons. One could perhaps elucidate how is continuity of current maintained as the area increases towards the grounded electrode.

5. References

[1] M.A. Lieberman, A.J. Lichtenberg, Principles of Plasma Discharge and Materials Processing, (2005) (Wiley:Hoboken);
[2] T. Makabe, Z.Lj. Petrović, Plasma Electronics, (2006) (Taylor and Francis:New York);
[3] U. Cvelbar, K. (Ken) Ostrikov and M. Mozetic, Nanotechnology **19** (2008) 405605.
[4] N. Puač, Z.Lj. Petrović, S. Živković, Z. Giba, D. Grubišić and A.R. Đorđević, Plasma Processes and Polymers, (2005) 193, (Whiley)
[5] M. Radetić, P. Jovančić, N. Puač and Z.Lj. Petrović, Workshop on Nonequilibrium Processes in Plasma Physics and Studies of the Environment, SPIG 2006, Journal of Physics: Conference Series **71** (2007) 012017
[6] N. St. J. Braithwaite, R. N. Franklin, Plasma Sources Sci. Technol. **18** (2009) 014008
[7] N. Hershkowitz, M. H. Cho, C. H. Nam, T. Intraor, Plasma Chemistry and Plasma Processing **8** (1988) 35
[8] P.A. Miller, H. Anderson, M.P. Splichal, J. App. Phys. **71** (1992) 1171

The effect of a plasma needle on bacteria in planktonic samples and on peripheral blood mesenchymal stem cells

Article *in* New Journal of Physics · August 2010

Impact Factor: 3.56 · DOI: 10.1088/1367-2630/12/8/083037

11 authors, including:

Diana Bugarski
Institute for Medical Research - Belgrade
60 PUBLICATIONS **421** CITATIONS
SEE PROFILE

Slavko Mojsilović
University of Belgrade
59 PUBLICATIONS **298** CITATIONS
SEE PROFILE

Gordana Malovic
Institute of Physics Belgrade
157 PUBLICATIONS **932** CITATIONS
SEE PROFILE

Zoran Lj Petrović
Institute of Physics Belgrade
510 PUBLICATIONS **5,652** CITATIONS
SEE PROFILE

The effect of a plasma needle on bacteria in planktonic samples and on peripheral blood mesenchymal stem cells

2010 New J. Phys. 12 083037

(http://iopscience.iop.org/1367-2630/12/8/083037)

New Journal of Physics
The open-access journal for physics

The effect of a plasma needle on bacteria in planktonic samples and on peripheral blood mesenchymal stem cells

Saša Lazović[1,4], Nevena Puač[1], Maja Miletić[2], Dušan Pavlica[2], Milena Jovanović[2], Diana Bugarski[3], Slavko Mojsilović[3], Dejan Maletić[1], Gordana Malović[1], Pavle Milenković[2] and Zoran Petrović[1]

[1] Institute of Physics, Pregrevica 118, 11080 Belgrade, Serbia
[2] Faculty of Stomatology, Dr Subotića 8, 11000 Belgrade, Serbia
[3] Institute for Medical Research, Dr Subotića—starijeg 4, 11000 Belgrade, Serbia
E-mail: lazovic@ipb.ac.rs

New Journal of Physics **12** (2010) 083037 (21pp)
Received 11 January 2010
Published 17 August 2010
Online at http://www.njp.org/
doi:10.1088/1367-2630/12/8/083037

Abstract. In this paper, we study the application of a plasma needle to induce necrosis in planktonic samples containing a single breed of bacteria. Two different types of bacteria, *Staphylococcus aureus* (ATCC 25923) and *Escherichia coli* (ATCC 25922), were covered in this study. In all experiments with bacteria, the samples were liquid suspensions of several different concentrations of bacteria prepared according to the McFarland standard. The second system studied in this paper was human peripheral blood mesenchymal stem cells (hPB-MSC). In the case of hPB-MSC, two sets of experiments were performed: when cells were covered with a certain amount of liquid (indirect) and when the cell sample was in direct contact with the plasma.

Most importantly, the study is made with the aim to see the effects when the living cells are in a liquid medium, which normally acts as protection against the many agents that may be released by plasmas. It was found that a good effect may be expected for a wide range of initial cell densities and operating conditions causing destruction of several orders of magnitude even under the protection of a liquid. It was established independently that a temperature increase could not affect the cells under the conditions of our experiment, so the effect could

[4] Author to whom any correspondence should be addressed.

originate only from the active species produced by the plasma. In the case of those hPB-MSC that were not protected by a liquid, gas flow proved to produce a considerable effect, presumably due to poor adhesion of the cells, but in a liquid the effect was only due to the plasma. Further optimization of the operation may be attempted, opening up the possibility of localized *in vivo* sterilization.

Contents

1. Introduction

One of the leading techniques for material engineering is plasma treatment, irreplaceable in the fabrication of semiconductor devices, integrated circuits, optical devices and solar cells. The possibilities of plasma treatment surely do not end here. The constantly growing field of biomedical applications is a new frontier that drives the field [1, 2]. Sterilization of medical equipment and treatment of wounds and dental caries are only segments of that field, and they show the breadth of potential applications. The desire to use plasma for *in vivo* treatments has made several requirements for plasma sources to be met. It is obvious that for this kind of application, a plasma has to operate at atmospheric pressure. On the positive side, no expensive vacuum systems are needed; on the other hand, it is much more difficult to achieve a non-equilibrium (non-thermal) mode of operation, which is equally essential. The heat sensitivity of biomedical samples narrows the choice to non-thermal plasmas. There are many types of plasmas that can be generated under ambient pressure and temperature conditions; the need for precise and localized treatments qualifies the plasma needle as a good candidate [3].

The path to understanding the interaction between plasma and living tissues is a long one. A lot of effort has been invested in understanding the details of the basic mechanisms of this interaction. Aspects of plasma-generated heat [4], UV radiation, radicals and charge particle interactions with different kinds of bacteria and cells have been studied [5]–[15]. Nevertheless, many of the questions remain open.

Mass spectrometry of plasma generated by the needle, as well as derivative probe measurements of power delivered to it, has already been presented in our previous work [16]–[18]. The plasma needle generates radicals like N, O, O_3 and especially NO, which

plays an important role in cell metabolism. Measurements of the power delivered to the plasma itself as a parameter provides the information needed to control the heating of the target and enables us to repeat treatments with the same or very similar plasmas every time. This is much more difficult to achieve if power is measured directly at the power source, so one needs to perform direct measurements of the local heating in that case [4].

The wide potential usage of plasma technology in the biomedical sciences, besides the plasma requirements, also directs the biological effect testing. To investigate the possible applications and the ways in which the plasma needle can affect various kinds of cells in this study, we performed experiments on two model cell systems. The first one was treatment of *Escherichia coli* and *Staphylococcus aureus* bacteria in order to study the deactivation of harmful bacteria, since the plasma needle can be applied in the treatment of light bacterial infections, such as *in vivo* sterilization of skin and dental cavities. For other potential applications, including the high-precision removal of pathological cells or tissues (cancer, peeling and removal of scars), but without excessive damage to the body, or the improvement of wound healing by controlling cell adhesion, we analyzed the plasma interaction with normal, living cells. For these experiments, we have used human peripheral blood mesenchymal stem cells (hPB-MSC) as a model system to predict the degree of possible damage to the cell responses. The plasma needle has been used to induce the killing of *Streptococcus mutans* and *E. coli* bacteria [19, 20]. Its application for the sterilization of bacteria inside the tooth to cure caries without conventional mechanical preparation and loss of tooth structure has been proposed and studied [4]. *S. aureus* (ATCC 25923) has been a subject of OAUGDP plasma treatment [21] as well as of other types of plasma sources [8, 9, 22]. *E. coli* (ATCC 25922) has been used in numerous studies, and here we mention only a few [7, 9, 20], [22]–[26].

On the other hand, the plasma needle has been used to induce apoptosis and necrosis of cultured eukaryotic cells [27], rat aortic smooth muscle cells, bovine aortic endothelial cells [28] and human (epithelial cells—MR65 cells originating from non-small cell lung carcinoma [29]) tissues. Studies of the plasma treatment of human mesenchymal stem cells (MSCs) have not been performed before, and only recently we heard of the first attempt [30]. Adult MSCs are defined as multipotent cells able to differentiate into various types of end-stage, specialized mesenchymal cells, such as osteoblasts, chondrocytes, adipocytes, tenocytes and others [31]. These cells are located in and around different organs and tissues of the body. The possibility of growing these cells and their progeny in cultures offers a shortcut to test the toxicity of various chemical or physical agents on various cells and tissues of the adult organism [32, 33].

In this paper, we will present the results of plasma needle treatments of two types of bacteria. Under normal circumstances, bacteria would most likely be present either in a liquid or as a part of a biofilm. We have treated samples that were in the form of a suspension with different concentrations of bacteria. Changes in bacteria concentration after the treatments will be presented. We covered one example of Gram-positive and one of Gram-negative bacteria. The second system that was studied was mesenchymal cells (hPB-MSC). These samples were treated with and without the liquid environment. Results of the 3-(4,5-dimethylthiazol-2-yl)-2,5-diphenyltetrazolium bromide (MTT) viability and Crystal Violet (CV) adhesion tests performed with hPB-MSC will be presented. These represent the first step on the route to developing, optimizing, understanding and using the plasma needle for the *in vivo* treatment of periodontal pockets.

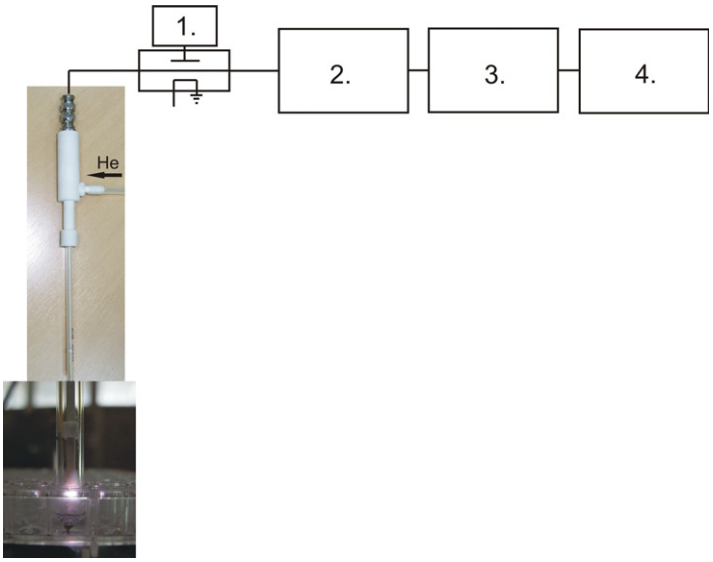

Figure 1. The experimental setup used in treatments: 1, oscilloscope connected to current and voltage derivative probes; 2, matching network; 3, amplifier; 4, signal generator.

2. Experimental setup

2.1. Setup

Non-equilibrium plasma generated by a plasma needle was used for the treatment of bacteria and cells. In this research, standard strains of two bacterial species were used: *S. aureus* (ATCC 25923) and *E. coli* (ATCC 25922). These species were used because of their regular use in protocols for the testing of antibiotics and disinfecting agents. Also, these species of bacteria are frequently found in later stages of many oro-pharyngeal infections. The other cells used in the experiments for cell toxicity were hPB-MSC obtained from a healthy volunteer. The experimental setup used for these treatments is shown in figure 1.

The needle consists of a central electrode that is made of wolfram and is 0.5 mm in diameter, covered almost to the tip by a slightly larger ceramic tube and both placed in a glass tube with a 6 mm inside diameter. The needle body is made of Teflon. Helium is flowing between the ceramic and glass tubes. We used flow rates of 0.5 and 1 slm (standard liters per minute). The central electrode is powered by a 13.56 MHz signal generator (Agilent N9310A) through an amplifier (Barthel RFA-0.1/50–100 B00) and a matching network. The grounded electrode is copper foil placed beneath the plastic plate. Plasma can ignite even without an additional grounding, but in this way we can obtain higher intensities and focus plasma better towards the bacteria suspension. The distance between the surface of the suspension containing bacteria and the tip of the electrode is 3 mm.

In order to measure the power delivered to the plasma, we use derivative probes placed as close as possible to the needle tip. Probe signals are transferred from the oscilloscope to the computer for further manipulation. Firstly, fast Fourier transform is performed followed by calibration of the signals in the frequency domain and subtraction of the displacement current. Finally, converting back to the time domain using inverse fast Fourier transform is carried out.

The difference in signals when the plasma is on and off (no helium flow) carries information about the power delivered to the plasma. Application of probes allows us to gain a direct knowledge of the actual power transmitted to the plasma. Choosing the measured power as a basic parameter provides more direct knowledge of some of the conditions in a plasma and a better control of whether all treatments are done using the same or very similar plasmas every time. This may not be the case when power is measured from the power supply. A suspension containing bacteria was placed inside 96 wells of a microtiter plate and exposed to the plasma generated by the needle. The sample exposure to a severe gas flow can lead to cell injury and contribute to killing [19, 34, 35]. Therefore, to ensure that this was not the case with the gas flows we used during these experiments, we always had control samples that were exposed only to a gas jet without ignition of the plasma.

2.2. Bacteria treatment

Standard strains of bacteria were obtained from American Type Culture Collection (ATCC). These were kept in a deep freeze at a temperature of −76 °C. They were activated by cultivating in dextrose broth (Torlak Institute of Immunology and Virology, Serbia), and incubated in a thermostat for 20 h at 37 °C. After incubation, the strains were sub-cultivated in solid nutritional media. *S. aureus* was sub-cultivated on blood agar (Torlak Institute of Immunology and Virology, Serbia) and *E. coli* was sub-cultivated on endo agar (Torlak Institute of Immunology and Virology, Serbia). Sub-cultures on solid nutritional media were incubated under the same conditions (20 h at 37 °C).

Further, suspensions with different numbers of bacteria were made. This was done according to 4 McFarland standards whose density corresponds to an approximate cell density of 12×10^8 CFU ml^{-1}. From this initial suspension, other suspensions were made with cell density 1:10, 1:100 and 1:1000 of the original. The suspensions were made in a microtiter plate with 96 wells. Each well contained 0.18 ml of suspension.

After the treatment of bacterial suspensions with the plasma needle, 0.05 ml of the suspension sample was taken from each well and cultivated on the corresponding solid nutritional media. These solid media were then incubated for 20 h at 37 °C, after which the results were analysed. The effect of the plasma needle treatment was graded according to the number of bacterial colonies formed, which are described using arbitrarily defined units 0–5 (0, no growth; 1, sparse growth ($\leqslant$ 50 colonies per plate); 2, moderate growth (50–200 per plate); 3, abundant growth (200–500 per plate); 4, very abundant growth (>500 colonies per plate with areas of confluent growth); 5, confluent growth) [36].

The effect of bacteria sterilization using high temperatures is well known [37]. For the purpose of measuring temperature increase during the plasma treatment, we placed a chromel–alumel thermocouple into the suspension 1 mm from the bottom of the well. Measurements were done for both helium flows (0.5 and 1 slm). It is shown that there was no significant increase in sample temperature during the treatment and so the effects of sterilization are only due to the plasma influence.

2.3. MSC treatment

Human MSCs were isolated from mononuclear peripheral blood cells using the methodology described by Kuznetsov *et al* [38], and characterized as plastic adherent cells that display

fibroblastic morphology. After several successive passages, we generated a homogeneous population of MSCs with the capacity to differentiate into osteocytes, adipocytes and myocytes when cultured in the corresponding specific differentiation media [39].

The cells were cultivated in polystyrene flasks at 37 °C in a humidified atmosphere with 5% CO_2. The culture medium was Dulbecco's modified eagle medium (DMEM) with 4.5 g l^{-1} glucose, supplemented with 10% fetal bovine serum (FCS), 0.1 M Hepes buffer, 100 IU ml^{-1} penicillin and 100 mg ml^{-1} streptomycin. About 48 h before treatment with the plasma (the time needed for the cells to reach confluence), cells were seeded in multi-well plates (24- or 48-well plates) at 25 000 cells cm^{-2}, and incubated in a culture medium at 37 °C in a humidified atmosphere with 5% CO_2.

The treatment of hPB-MSC with the plasma needle was done in a similar way to the bacteria treatment, and after the treatments, MSC viability and adhesion were tested using the MTT and CV assays, respectively.

2.4. MTT assay

Cell viability was assessed by using the MTT assay. After the treatment, the medium in the wells was replaced by a fresh one and the MTT substrate was added to the final concentration of 0.5 mg ml^{-1}. The cells were incubated for 3 h at 37 °C in a humidified atmosphere with 5% CO_2. In the mitochondria of living cells, yellow MTT is reduced to water-insoluble purple formazan. The formazan dye was dissolved in absolute isopropanol acidified with 0.1 N HCl and the absorbance of the colored solution was measured by a spectrophotometer at 540 nm [40].

2.5. Adhesion assay

After the treatment, the cells were washed with phosphate-buffered saline (PBS) and fixed with ice-cold methanol for 10 min. The adherent cells were then stained by 0.2% solution of CV in PBS for 10 min at room temperature and washed thoroughly with tap water. The stain was dissolved in 33% acetic acid and the absorbance of the colored solution was measured by a spectrophotometer at 540 nm [41]. Photographs of the plasma-treated cells remaining at the bottom of plate wells were also taken, from which areas of cell adhesion and detachment could be determined.

3. Results and discussion

3.1. Plasma treatment of E. coli and S. aureus bacteria

Many factors are responsible for bacterial inactivation. Direct exposure of the bacterial samples to the plasma is always more effective than remote exposure. Even in the case of remote exposure, significant killing can be obtained as well [42]. Another factor that determines the efficiency of the specific treatment is the bacteria sample type [43]. All our samples were prepared as planktonic samples [4, 44]. These are liquid samples with inoculated bacteria, with varying concentrations of bacterial colony-forming units per ml (CFU/ml).

We treated all the samples for three different time periods, three different powers and two different flows of the buffer gas in the needle. For every treatment set, two types of control were used: completely untreated samples and samples treated only by the flow of the buffer gas (He)

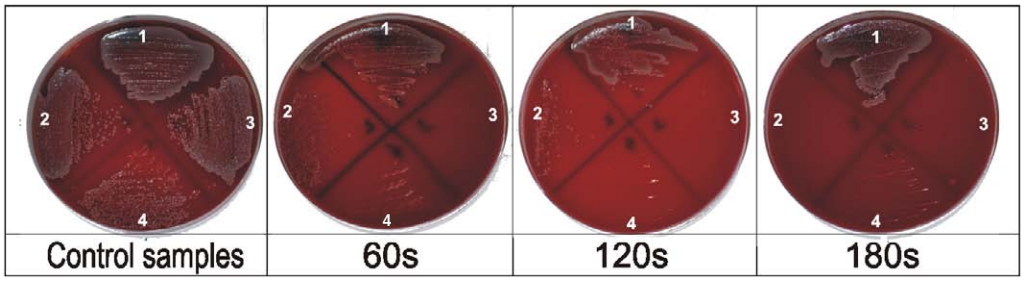

Figure 2. *S. aureus* treated by plasma. The flow rate of He was 0.5 slm and the power was 1.6 W. Four different starting concentrations of bacteria were used: **1**, 12×10^8 CFU ml^{-1}; **2**, 12×10^7 CFU ml^{-1}; **3**, 12×10^6 CFU ml^{-1}; **4**, 12×10^5 CFU ml^{-1}.

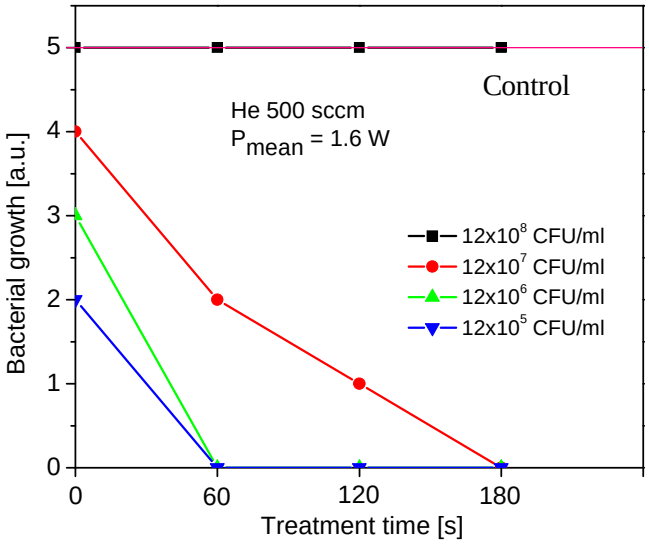

Figure 3. Arbitrarily defined units describing the number of bacterial colonies of *S. aureus* (ATCC 25923) after treatment with plasma. Four samples with different starting concentrations were used; the power was 1.6 W and the He flow rate was 0.5 slm.

but without plasma ignition. In cases where only He flow was present, none of the bacteria were destroyed. After sub-cultivation in solid nutritional media, the bacteria colonies were counted.

In figure 2, photographs of the cultivated bacteria *S. aureus* (ATCC 25923) are shown. The different starting concentrations presented in the figure are marked by numbers (**1**, 12×10^8 CFU ml^{-1}; **2**, 12×10^7 CFU ml^{-1}; **3**, 12×10^6 CFU ml^{-1}; **4**, 12×10^5 CFU ml^{-1}). The flow rate of the buffer gas was 0.5 slm. We can see that for the highest power used almost all bacteria are destroyed except for the highest starting concentration (**1** in figure 2). This pertains only to the conditions that we set here and we did not seek extended treatment to achieve full sterilization for all concentrations.

After the 12 h incubation, bacterial colonies were counted and the results for all four concentrations are shown in figure 3. The effect of the plasma needle treatment was graded according to the number of bacterial colonies formed, which are described using arbitrarily defined units 0–5 (0, no growth; 1, sparse growth; 2, moderate growth; 3, abundant growth;

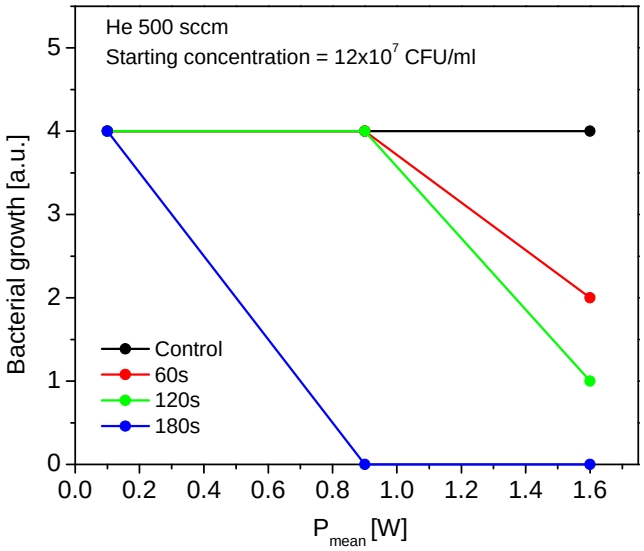

Figure 4. Arbitrarily defined units describing the number of bacterial colonies of *S. aureus* (ATCC 25923) after treatment with the plasma needle as a function of the applied mean power.

4, very abundant growth; 5, confluent growth). The units are chosen to correspond to the growth related to different densities without treatment. In this respect, the results shown in these units may be perceived as a logarithmic representation of the concentration. The results presented in this graph are obtained for the highest power used (1.6 W) and a flow rate of He of 0.5 slm. We can see that with an increase in the treatment time, the number of bacterial colonies formed is significantly reduced. For the longest treatment time except for the highest concentration, practically all the bacteria are killed in the treated sample. For smaller concentrations, even the shortest treatment times were sufficient to destroy the bacteria.

In figure 4, the final concentration of bacteria as a function of applied power in the treatments is shown. Data were obtained for samples with the starting concentration of 12×10^7 CFU ml^{-1}. With an increase in the applied power and with an increase in the time period of treatment, the number of bacterial colonies can be reduced by a factor of 10^4. This means that more than 99% of the bacteria that were contained in the initial sample were killed. By looking at the photographs of the treated samples (see figure 2) visually, we can see that almost no colonies were formed for this set of parameters (highest power/longest treatment time). Most importantly, one can see that for higher initial concentrations, the treatment time proved to be more important than merely the power, which could be related to the fact that our samples were in solution. For example, the 180 s treatment proves to be efficient after a sufficient power level is reached, even at lower powers, whereas higher powers appear to be less efficient for shorter treatment times.

The same set of treatments was performed also for a flow rate of the buffer gas of 1 slm. All other parameters, such as applied power and treatment times, were the same as those for the flow rate of 0.5 slm. Photographs of the cultivated bacteria for a flow rate of 1 slm are shown in figure 5. Again, as in the case of a smaller gas flow, the highest applied power and longest treatment time result in the highest killing of the bacteria. For the two smallest starting concentrations of bacteria, almost no colonies manifest after the treatments.

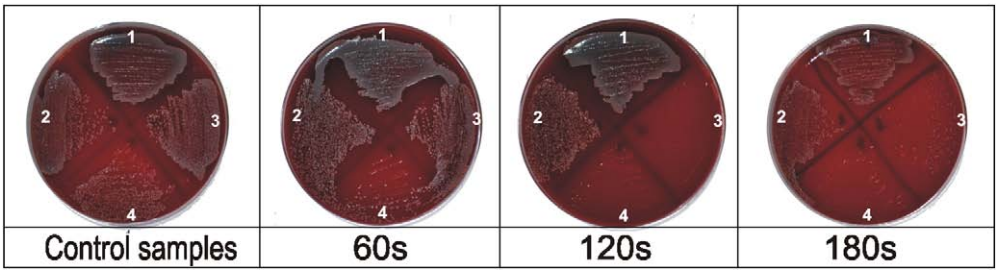

Figure 5. *S. aureus* treated by plasma. Flow of He was 1 slm and the power was 1.6 W. Four different initial concentrations of bacteria were used: **1**, 12×10^8 CFU ml^{-1}; **2**, 12×10^7 CFU ml^{-1}; **3**, 12×10^6 CFU ml^{-1}; **4**, 12×10^5 CFU ml^{-1}.

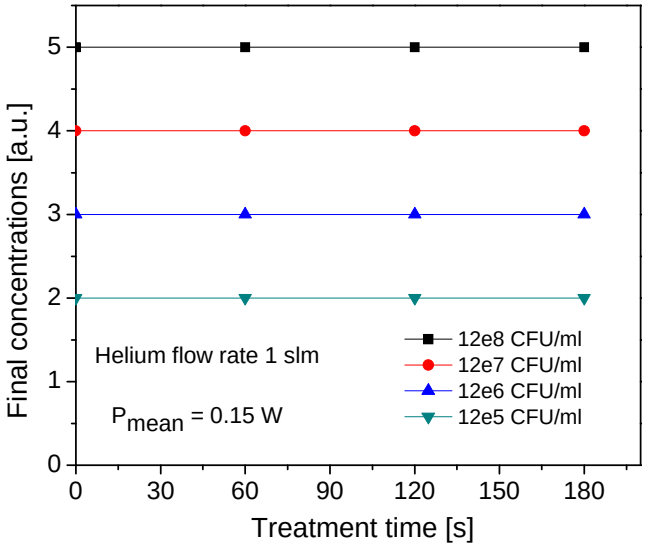

Figure 6. Arbitrarily defined units describing the number of bacterial colonies of *S. aureus* (ATCC 25923) after the treatment as a function of treatment duration for four different starting concentrations.

On the other hand, for the smallest applied power (0.15 W), we could not see any change in bacteria number even after extended treatment times (see figure 6). As in the case of the 0.5 slm flow rate, the lowest power did not reduce the concentration of bacteria in the treated samples.

The flow of the buffer gas plays an important role in the resulting concentrations of bacteria [34]. This is presumably due to different resulting concentrations of reactive particles (radicals) where the flow of the inert buffer gas pushes atmospheric gases further away from the plasma core, and while the densities of UV photons and ions could remain unperturbed, the densities of chemically active radicals would be reduced because of the increasing gas flow. This is, on the other hand, a simplified explanation as operating conditions may be quite different depending on the percentage of atmospheric gases. Thus, an increased flow may result in reduced operating voltage, thereby reducing the efficiency of the production as well.

In figures 7 and 8, the concentration of bacteria after treatment for two different treatment times (60 and 120 s) are shown for several initial densities. The applied power in all cases was

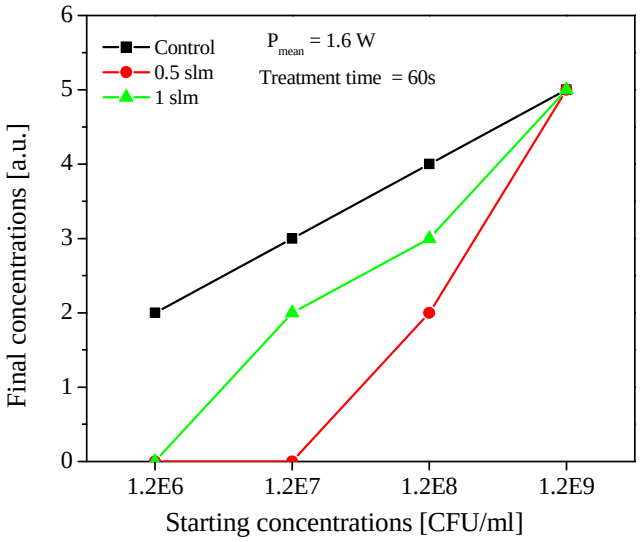

Figure 7. Arbitrarily defined units describing the number of bacterial colonies of *S. aureus* (ATCC 25923) after the plasma treatment for two different gas flows. The treatment time was 60 s and the applied power was 1.6 W.

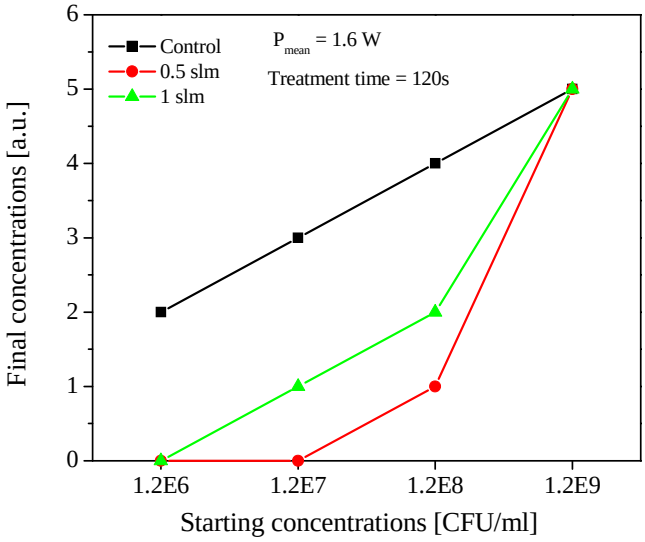

Figure 8. Arbitrarily defined units describing the number of bacterial colonies of *S. aureus* (ATCC 25923) after plasma treatment for two different gas flows. The treatment time was 120 s and the applied power was 1.6 W.

1.6 W. From these figures, it can be concluded that the plasma created when the flow rate of the buffer gas was 0.5 slm was more effective than in the case of the He flow of 1 slm. It is important to note that for both flows of the buffer gas, plasma did not have any effect on the bacteria count in the case of the highest initial concentration. It is perceivable that we could find conditions where this could be achieved, but we decided to operate under conditions where we had a full dynamic range that is accessible to us. Nevertheless, one should be warned that extended treatment times may have to be used for very high densities of bacteria.

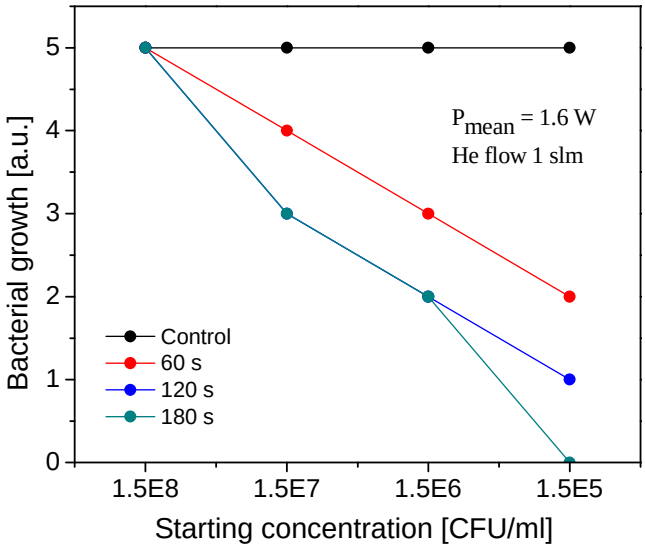

Figure 9. Concentration of the bacteria *E. coli* (ATCC 25922) after plasma treatment for three different treatment times.

We have also done some preliminary treatments of planktonic samples containing *E. coli* (ATCC 25922). *E. coli* is a Gram-negative bacteria, which means that it has an additional outer membrane made of lipopolysaccharides and protein. If mechanical erosion of the bacterial membrane is one of the factors responsible for its inactivation, we can assume that *E. coli* will suffer less damage in the same treatment conditions, as compared to *S. aureus*. Park *et al* [45, 46] showed that damage induced by plasma in the case of *E. coli* consisted of punctured, eroded and morphologically transformed bacteria, while for *S. aureus*, the bacteria were ruptured with their cellular contents released onto the substrate surface. This, according to the authors, demonstrates that a strong etching process is responsible for the observed micro-organism inactivation [45, 46].

In the case of *E. coli*, our starting concentrations were somewhat smaller than in the treatments of *S. aureus*. In figure 9, the concentration of *E. coli* (ATCC 25922) after plasma treatment is shown. Again, even though the highest initial concentration is smaller than in the case of *S. aureus* (1.5×10^8 CFU ml^{-1}), we did not notice any change in bacteria count after the treatments. Better results are obtained for lower initial concentrations. With an increase in the treatment time, the number of bacteria colonies can be reduced even by a factor of 10^4 (almost 99% of the initial concentration).

Some of the agents from the chemical (plasma) point of view that can cause bacterial death or injury include heat, stress, UV radiation, free radicals and charging [43]. Heat-based sterilization methods use either moist heat or dry heat. In the case of moist heat, such as in an autoclave, a temperature of 121 °C at a pressure of 15 psi is used. Dry heat sterilization requires temperatures close to 170 °C and treatment times of about 1 h [37]. For obvious reasons, thermal sterilization cannot be applied to local sterilization of living organisms.

In the case of plasma treatment of the contaminated samples, thermal damage is usually not an important mechanism of injury, considering that most (including plasma needle) discharges at atmospheric pressure operate at room temperature. Since temperature can be one of the possible agents that causes bacterial death or injury, we wanted to check the changes in temperature of

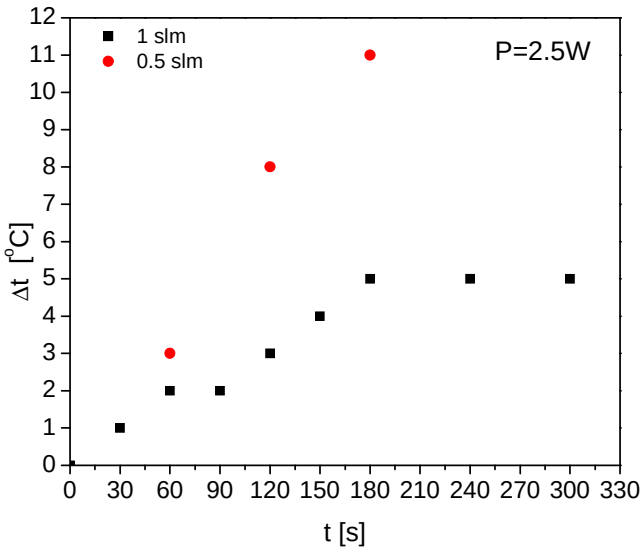

Figure 10. Temperature change of the treated sample as a function of duration of treatment. The flow rates of the buffer gas were 0.5 and 1 slm, and the distance from the tip of the needle to the bacteria-containing liquid was 3 mm.

the sample during treatment. Temperature measurements were done in the same experimental setup used for treatments of bacteria samples. The chromel–alumel thermocouple was used for temperature measurements and it was placed at the bottom of the treated well. The same quantity of saline solution (180 μl) as used in bacteria inactivation was placed in the well.

Temperature measurements were done for several different powers transmitted to the plasma, and the temperature difference for the highest power is shown in figure 10. We can see that for the longest treatment times the increase in temperature is less than 5.5 °C (from the room temperature of 21 °C) in the case of 1 slm gas flow and not more than 10 °C for the plasma with 0.5 slm He flow. In order to show significant effects of the heating, we had to go to a power of 2.5 W, which is considerably higher than the power used in this experiment. In this figure, only the highest power used in temperature measurements is shown because the results for some of the lower powers (<1 W) did not show any increase in the measured temperature, but even the sample temperature decreases. This decrease in the sample temperature can be explained by cooling due to flow of the inert gas. In these cases, heating by the plasma is not enough to raise the temperature of the treated samples and the equilibrium temperature is lower than the starting temperature of the sample (room temperature of 21 °C). Most importantly, saturation was reached after 180 s, indicating that a balance between the released heat and the heat that is taken out by losses has been reached, and further increases in the temperature may be controlled by thermal balance in the broader area that can be controlled.

In all our experiments, power was much lower than the power where we could actually record an increase in the temperature, and treatment times in all our experiments did not exceed 3 min. We can conclude that in our case, heat, as one of the agents that can be responsible for bacteria inactivation or death, does not play an important role.

Another very strong disinfectant is UV radiation [44, 47, 48], but its role in atmospheric plasma sterilization goes from modest [2], [49]–[51] to highly effective [8, 24, 46, 52], depending on the type and concentration of bacteria or spores, the amount and composition

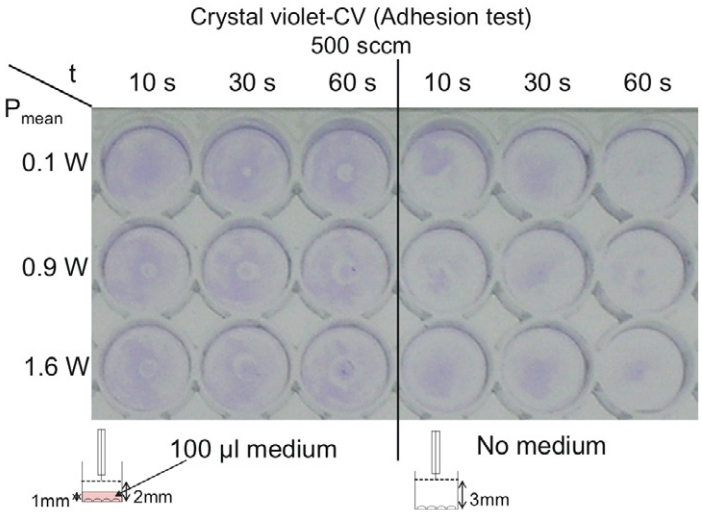

Figure 11. A photograph of a microtiter plate with treated cells after the CV test. Cells are treated using exposure times of 10, 30 and 60 s and mean powers of 0.1, 0.9 and 1.6 W. Wells on the left-hand side contained cells covered by 100 μl of medium and those on the right-hand side contained directly exposed cells.

of the medium containing bacteria and the UV radiation power. Besides local heating and UV photons that can be responsible for killing of bacteria, we also have ions created in the discharge, radicals and the effect of charging of the cell membrane.

We have shown that heating of the cells did not exceed the normal conditions. It is very difficult to find a simple mechanism that would allow the effect of radicals and energetic ions to penetrate the liquid. On the other hand, the effect of UV photons would depend strongly on the absorption of UV radiation, and some recent measurements have confirmed that there is a correlation between the effect of plasma and the transparency of the liquid [8]. However, we cannot give a final conclusion on this mechanism in our system without further studies. The negative charging of the cell wall by plasma electrons was considered by Laroussi *et al* [43, 53]. In certain conditions, mechanical stress induced by charging can be sufficient to cause rupture in G− (*E. coli*) but not in G+ (*S. aureus*) bacteria. Furthermore, inflicting mechanical damage caused by charging is not the only way to destroy cells. If the surface charge equilibrium [54]–[58] is disturbed, cells can be killed without actually tearing them apart. Charging of the bacteria cell wall by electrons in our case is highly improbable because of the fact that bacteria are diluted in saline solution that cannot be penetrated by charged particles from plasmas, and also any charge accumulation is conducted away.

3.2. Plasma treatment of human peripheral blood-derived MSC

Along with the plasma treatment of bacteria, we have also performed plasma treatment of hPB-MSC to test the possible harmful effect of plasmas on normal, living cells. Plasma parameters in these experiments were the same as those when bacteria samples were treated. After the cell treatment, two types of tests were performed: the MTT assay for cell viability, and the CV staining assay as a measure of the cells' adhesion.

In figure 11, a photograph of the adhesion test after the plasma treatment is shown. On the left-hand side (3×3) are wells in which the cells were covered with 100 μl of DMEM during the

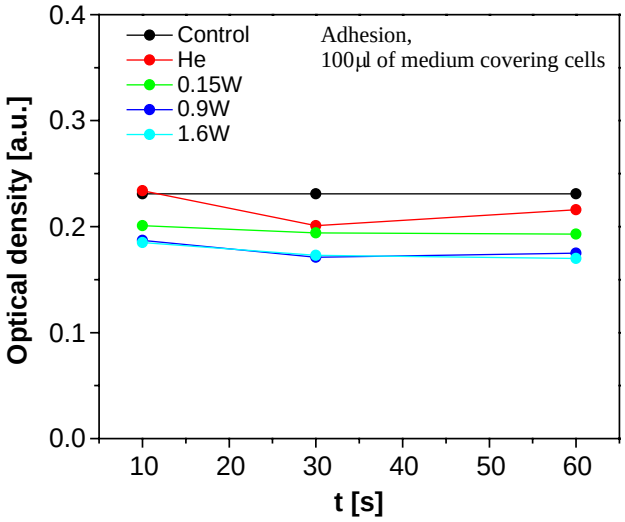

Figure 12. Optical densities of treated cells covered by 100 μl of medium obtained by a spectrophotometer at 540 nm (CV tests).

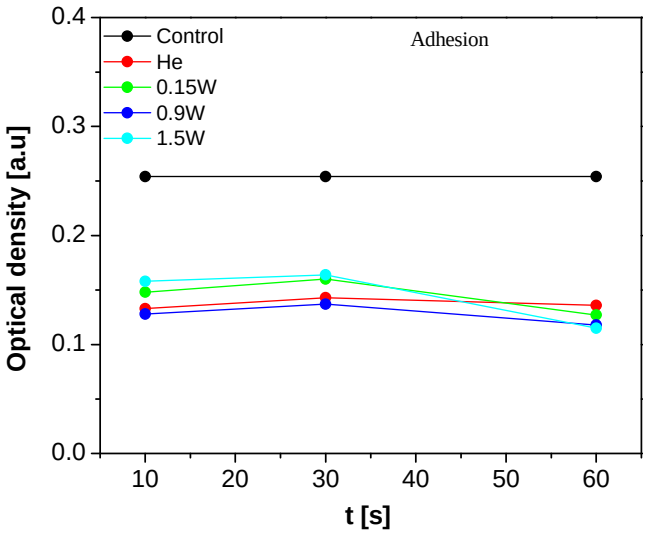

Figure 13. Optical densities of directly treated cells obtained by a spectrophotometer at 540 nm (CV tests).

treatment. As shown in both figures 11 and 12, it can be seen that during the plasma treatment, only a small number of cells were detached. With an increase in the applied power, only a small change is noticeable, while there is almost no change in the number of attached cells with a variation in the treatment time. In all cases, He control was performed where there was an He flow (in this case 0.5 slm), but the plasma was not ignited, and we noticed a certain amount of cells that were detached even in this case when flow was present in the absence of plasma.

On the other hand, in the well in which there was no medium covering treated cells (3×3—right-hand side of figure 11), detachment of the cells during the treatment was quite high and He flow played the most important role in this case (see figure 13). Here, one cannot distinguish between the effect of plasma and the effect of He flow.

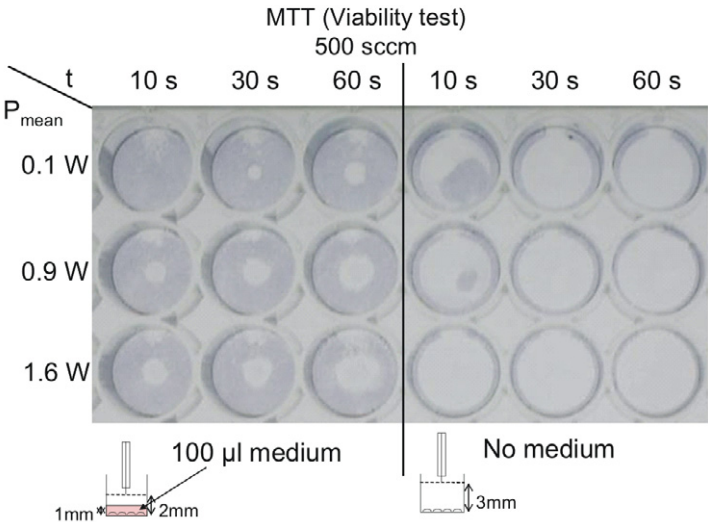

Figure 14. A photograph of a microtiter plate containing treated cells after the MTT (viability) test. Cells are treated using exposure times of 10, 30 and 60 s and mean powers of 0.1, 0.9 and 1.6 W. The left-hand side wells contained cells covered by 100 μl of medium, while the right-hand side wells contained directly exposed cells.

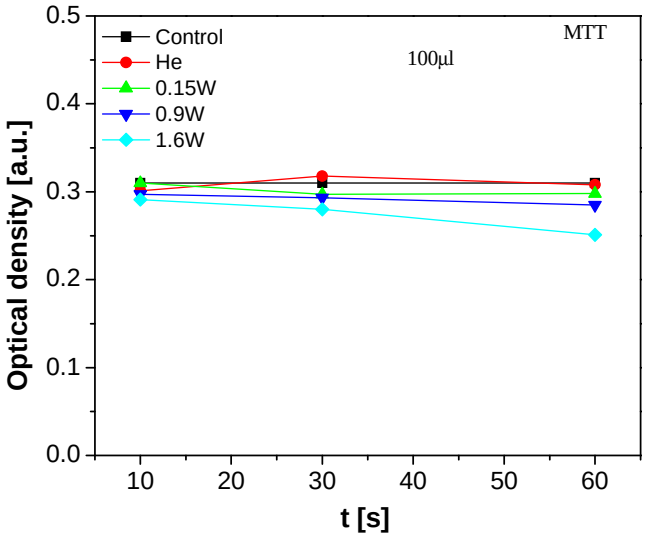

Figure 15. Optical densities of treated cells covered by 100 μl of medium obtained by a spectrophotometer at 540 nm (MTT tests).

The results of the viability tests performed are presented in figure 14, showing the photograph of the wells after the plasma treatment and MTT test coloring. Again, on the left-hand side of the photograph (3×3) are wells in which the cells were covered with 100 μl of medium during the treatment. In this case, we could notice that more cells were dead with an increase in the applied power and treatment time. Control with only He flow shows no changes at all (see figure 15).

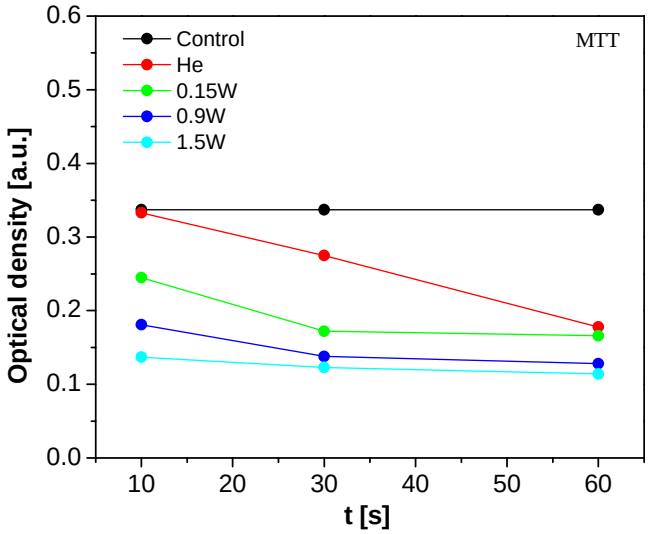

Figure 16. Optical densities of directly treated cells obtained by a spectrophotometer at 540 nm (MTT tests).

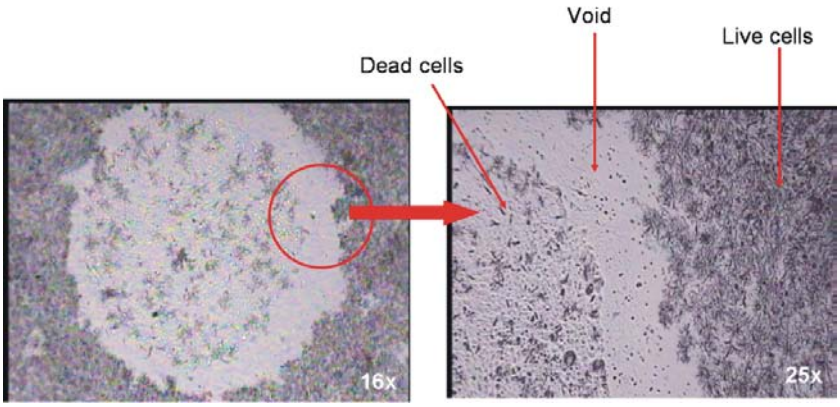

Figure 17. Photographs of the representative well containing hPB-MSC covered by 100 μl of medium after plasma treatment and the MTT test.

The right-hand side of the photograph (3×3 wells; see figure 14) shows the wells in which there was no medium covering the cells during treatment. Again, control of He flow was done, and with an increase in treatment time more cells were destroyed, even if no plasma was ignited (see figure 16). By increasing the power and treatment time, drastic changes in viability percentage of the cells were observed.

The photograph of the plasma-treated hPB-MSC after the MTT test, shown in figure 17, points to the 'track' of the plasma left on the mesenchymal cell sample in the plate wells. It can clearly be seen that there are three separate regions with cells exhibiting different responsiveness. The first region is at the center of the well, where the cells were placed directly under the tip of the needle during treatment. All the cells in this area were destroyed, although some of their debris still adheres to the surface. At the edge of this region, there is an annular area, a gap without any cell present. Living cells can be observed only outside this area towards the wall of the well.

Both the viability and the adhesion tests demonstrated that the effect of plasma+He treatment was somewhat milder when the cells during the treatment were covered with medium as compared to the case when the cells were without medium, i.e. in direct contact with the plasma, which makes its effect stronger and more efficient in terms of cell removal. Under these conditions, however, it was shown that the gas flow played an even more important role, which is not the case when liquid medium is present over the cell samples. This result indicates that the plasma parameters should be adjusted according to the treatment desired. Namely, because in the human body the cells are within a liquid microenvironment, the plasma parameters when plasma is applied for pathological cell or tissue removal or for wound healing have to be somewhat different from those in the case of direct contact with the tissue, for example skin peeling. Further work on optimization of the plasma parameters should include experiments on MSCs differentiated toward specific tissues, along with defining mechanisms underlying the cell responses.

4. Conclusion

This work continues our earlier work on plasma-induced sterilization at low pressures [59], plasma treatment of seeds at low and atmospheric pressures [60, 61] and the effects of a plasma needle on the calli *Fritillaria imperialis* (family Lilliaceae) [62]. The main goal of this paper was to study the effects of plasma treatment on two cell systems. The treatment of *E. coli* and *S. aureus* bacteria was performed in order to study the deactivation of harmful bacteria, while the MSCs were a model system to predict the degree of possible damage to cell responses.

In the treatment of *S. aureus* (ATCC 25923), we see a very good effect of plasma, practically no effect of the gas flow and sterilization of the order of five orders of magnitude in some cases. At very low powers there is no effect, but at higher powers the effect increases dramatically with treatment time. Finally, very little effect was found when the initial densities were relatively high for the choice of powers that were selected in this study. We have also verified that in addition to gas flow, the heating was low and played no role in the sterilization of samples. Similar but somewhat less impressive results were found for *E. coli* (ATCC 25922). This reduction in efficiency may be expected for Gram-negative bacteria but still the results in both cases support very efficient sterilization and give a promise of applications in sterilization of living tissues and cavities. For very high initial densities in both cases, the effect of plasma was not observed, requiring higher powers, or perhaps more optimal choice of flow and proximity. Independent of our work, a study with *E. coli* and *S. aureus* in planktonic samples was recently published by Joshi *et al* [9], reaching similar conclusions.

For hPB-MSC, measurements were made when the cells were covered with medium as well as when the cells were without medium. In the case of direct cell exposure, without medium cover, although the effect of the plasma was observable, its impact was diminished in the context of the desiccation caused by the gas flow. When the cells were covered by medium, gas flow did not affect the results, and the effect of the plasma was more obvious. The effect differed in three regions. The central circle of the plasma-treated area consisted of dead cells; the annular region with no cell debris, perhaps defined by the anatomy of the plasma in a plasma needle, due to the combined effect of gas flow, mixing with the atmosphere and the central core of plasma with energetic and reactive particles; and finally, the outside region consisted of the viable cells. Since the region with dead cells could be controlled by defined plasma parameters (power, duration of treatment), their optimization can lead to refined cell removal.

Comparisons of the effects of plasmas on bacteria and on human cells may be justified by the search for selectivity that may be necessary for the treatment of live tissues. As far as plasma goes, some further optimization may be achieved for localized accurate treatment of cells or sterilization. Further work needs to be done to achieve optimal operation and uniformity over large areas. With a good knowledge of the power deposited into the plasma, and control of the radicals that are produced, together with spatial emission profiles indicating changes to the regime of operation, sufficient control of the reproducibility of plasma needle operation is achieved. Other sources may be sought for more refined interaction with living cells.

Acknowledgments

The work at the Institute of Physics was supported by MNTRS project no. 141025 (ZLP, NP, SL, DM and GM). The authors are grateful to E Stoffels and M Kong for useful discussion and A Djordjevic for the development and calibration of probes.

References

[1] Fridman A and Kennedy L A 2004 *Plasma Physics and Engineering* (New York: Taylor and Francis)
[2] Iza F, Kim G J, Lee S M, Lee J K, Walsh J L, Zhang Y T and Kong M G 2008 Microplasmas: sources, particle kinetics, and biomedical applications *Plasma Process. Polym.* **5** 322–44
[3] Stoffels E, Flikweert A J, Stoffels W W and Kroesen G M W 2002 Plasma needle: a nondestructive atmospheric plasma source for fine surface treatment of (bio)materials *Plasma Sources Sci. Technol.* **11** 383–8
[4] Sladek R E J, Stoffels E, Walraven R, Tielbeek P J A and Koolhoven R A 2004 Plasma treatment of dental cavities: a feasibility study *IEEE Trans. Plasma Sci.* **32** 1540–3
[5] Moisan M, Barbea J, Crevier M C, Pelletie J, Philip N and Saoudi B 2002 Plasma sterilization. Methods and mechanisms *Pure Appl. Chem.* **74** 349–58
[6] Kutasi K, Pintassilgo C D and Loureiro J 2009 An overview of modelling of low-pressure post-discharge systems used for plasma sterilization *J. Phys.: Conf. Ser.* **162** 012008
[7] Dobrynin D, Fridman G, Friedman G and Fridman A 2009 Physical and biological mechanisms of direct interaction with living tissue *New J. Phys.* **11** 115020–46
[8] Nosenko T, Shimizu T and Morfill G E 2009 Designing plasmas for chronic wound disinfection *New J. Phys.* **11** 115013–32
[9] Joshi S G, Paff M, Friedman G, Fridman G, Fridman A and Brooks A D 2010 *Am. J. Inf. Control* **38** 293–301
[10] Fridman G, Friedman G, Gutsol A, Shekhter A B, Vasilets V N and Fridman A 2008 Applied plasma medicine *Plasma Process. Polym.* **5** 503–33
[11] Fridman G, Shereshevsky A, Jost M M, Brooks A D, Fridman A, Gutsol A, Vasilets V and Friedman G 2007 Floating electrode dielectric barrier discharge plasma in air promoting apoptotic behavior in melanoma skin cancer cell lines *Plasma Chem. Plasma Process.* **27** 163–76
[12] Lee M H, Park B J, Jin S C, Kim D, Han I, Kim J, Hyun S O, Chung K-H and Park J-C 2009 Removal and sterilization of biofilms and planktonic bacteria by microwave-induced argon plasma at atmospheric pressure *New J. Phys.* **11** 115022–33
[13] Morfill G E, Kong M G and Zimmermann J L 2009 Focus on plasma medicine *New J. Phys.* **11** 115011–9
[14] Kim G C, Kim G J, Park S R, Jeon S M, Seo H J, Iza F and Lee J K 2009 Air plasma coupled with antibody-conjugated nanoparticles: a new weapon against cancer *J. Phys. D: Appl. Phys.* **42** 032005–10

[15] Kim G J, Kim W, Kim K T and Lee J K 2010 DNA damage and mitochondria dysfunction in cell apoptosis induced by non-thermal air plasma *Appl. Phys. Lett.* **96** 021502–5
[16] Lazović S, Puač N, Malović G, Đorđvić A and Petrović Z Lj 2008 Diagnostic of plasma needle properties by using mass spectrometry *Chem. Listy* **102** s1383–7
[17] Malović G, Puač N, Lazović S and Petrović Z Lj 2010 Mass analysis of an atmospheric pressure plasma needle discharge *Plasma Sources Sci. Technol.* **19** 034014
[18] Puač N 2008 Development, diagnostic and applications of radio-frequency plasma reactor *J. Phys.: Conf. Ser.* **133** 012007
[19] Goree J, Liu B, Drake D and Stoffels E 2006 Killing of *S. mutans* bacteria using a plasma needle at atmospheric pressure *IEEE Trans. Plasma Sci.* **34** 1317–24
[20] Sladek R E J and Stoffels E 2005 Deactivation of *Escherichia coli* by the plasma needle *J. Phys. D: Appl. Phys.* **38** 1716–21
[21] Kelly-Wintenberg K, Hodge A, Montie T C, Deleanu L, Sherman D, Reece Roth J, Tsai P and Wadsworth L 1999 Use of a one atmosphere uniform glow discharge plasma to kill a broad spectrum of microorganisms *J. Vac. Sci. Technol.* A **17** 1539–44
[22] Heinlin J, Isbary G, Stolz W, Morfill G, Landthaler M, Shimizu T, Steffes B, Nosenko T, Zimmermann J L and Karrer S 2010 Plasma applications in medicine with a special focus on dermatology *J. Eur. Acad. Dermatol. Venereol.* published online: 17 May 2010, DOI: 10.1111/j.1468-3083.2010.03702.x
[23] Morfill G E, Shimizu T, Steffes B and Schmidt H-U 2009 Nosocomial infections—a new approach towards preventive medicine using plasmas *New J. Phys.* **11** 115019–29
[24] Sato T, Miyahara T, Doi A, Ochiai S, Urayama T and Nakatani T 2006 Sterilization mechanism for *Escherichia coli* by plasma flow at atmospheric pressure *Appl. Phys. Lett.* **89** 073902
[25] Laroussi M 2002 Nonthermal decontamination of biological media by atmospheric-pressure plasmas: review, analysis, and prospects *IEEE Trans. Plasma Sci.* **30** 1409–15
[26] Yu Q S, Huang C, Hsieh F H, Huff H and Duan Y 2006 Sterilization effects of atmospheric cold plasma brush *Appl. Phys. Lett.* **88** 013903
[27] Kieft I E, Kurdi M and Stoffels E 2006 Reattachment and apoptosis after plasma-needle treatment of cultured cells *IEEE Trans. Plasma Sci.* **34** 1331–6
[28] Stoffels E, Kieft I E, Sladek R E J, van den Bedem L J M, van der Laan E P and Steinbuch M 2006 Plasma needle for *in vivo* medical treatment: recent developments and perspectives *Plasma Sources Sci. Technol.* **15** S169–80
[29] Kieft I E, Dvinskikh N A, Broers J L V, Slaaf D W and Stoffels E 2004 *Proc. SPIE* **5483** 247
[30] Kong M 2009 personal communication
[31] Chamberlain G, Fox J, Ashton B and Middleton J 2007 Concise review: mesenchymal stem cells: their phenotype, differentiation capacity, immunological features, and potential for homing *Stem Cells* **25** 2739–49
[32] Chang J K, Li C J, Wu S C, Yeh C H, Chen C H, Fu Y C, Wang G J and Ho M L 2007 Effects of anti-inflammatory drugs on proliferation, cytotoxicity and osteogenesis in bone marrow mesenchymal stem cells *Biochem. Pharmacol.* **74** 1371–82
[33] Dai Z Q, Wang R, Ling S K, Wan Y M and Li Y H 2007 Simulated microgravity inhibits the proliferation and osteogenesis of rat bone marrow mesenchymal stem cells *Cell Prolif.* **40** 671–84
[34] Goree J, Liu B and Drake D 2006 Gas flow dependence for plasma-needle disinfection of *S. mutans* bacteria *J. Phys. D: Appl. Phys.* **39** 3479–86
[35] Laroussi M and Akan T 2007 Arc-free atmospheric pressure cold plasma jets: a review *Plasma Process. Polym.* **4** 777–88
[36] Miller P H, Wiggs L S and Miller J M 1995 Evaluation of anaerogen system for growth of anaerobic bacteria *J. Clin. Microbiol.* **33** 2388–91
[37] Block S S 1992 Sterilization *Encyclopedia of Microbiology* vol 4 ed J Lederberg (San Diego, CA: Academic) p 87

[38] Kuznetsov S A, Mankani M H, Gronthos S, Satomura K, Bianco P and Robey P G 2001 Circulating skeletal stem cells *J. Cell Biol.* **153** 1133–40
[39] Kocic J unpublished results
[40] Mosmann T 1983 Rapid colorimetric assay for cellular growth and survival: application to proliferation and cytotoxicity assay *J. Immunol Methods* **65** 55–63
[41] Oez S, Welte K, Platzer E and Kalden J R 1990 A simple assay for quantifying the inducible adherence of neutrophyls *Immunobiology* **180** 308–15
[42] Stolz W, Georgi M, Schmidt H U, Ramrath K, Pompl R, Shimizu T, Steffes B, Bunk W, Peters B, Jamitzky F and Morfill G 2007 Low-temperature argon plasma for sterilization of chronic wounds: from bench to bedside *Proc. 1st Int. Conf. on Plasma Med. (Corpus Christi, TX, 15–18 October 2007)* p. 15
[43] Stoffels E, Sakiyama Y and Graves D B 2008 Cold atmospheric plasma: charged species and their interactions with cells and tissues *IEEE Trans. Plasma Sci.* **36** 1441
[44] Kamgang J O, Briandet R, Herry J M, Brisset J L and Naitali M 2007 Destruction of planktonic, adherent and biofilm cells of *Staphylococcus epidermidis* using a gliding discharge in humid air *J. Appl. Microbiol.* **103** 621–8
[45] Park B J, Lee D H, Park J C, Lee I S, Lee K Y, Hyun S O, Chun M S and Chung K H 2003 Sterilization using a microwave-induced argon plasma system at atmospheric pressure *Phys. Plasmas* **10** 4539–44
[46] Lee K Y, Joo Park B, Hee Lee D, Lee I S, Hyun O S, Chung K H and Park J C 2005 Sterilization of *Escherichia coli* and MRSA using microwave-induced argon plasma at atmospheric pressure *Surf. Coat. Technol.* **193** 35–8
[47] Sosnin E A, Stoffels E, Erofeev M V, Kieft I E and Kunts S E 2004 The effects of UV irradiation and gas plasma treatment on living mammalian cells and bacteria: a comparative approach *IEEE Trans. Plasma Sci.* **32** 1544–50
[48] Moisan M, Barbeau J, Moreau S, Pelletier J, Tabrizian M and Yahia L'H 2001 Low-temperature sterilization using gas plasmas: a review of the experiments and an analysis of the inactivation mechanisms *Int. J. Pharm.* **226** 1–21
[49] Laroussi M and Leipold F 2004 Evaluation of the roles of reactive species, heat, and UV radiation in the inactivation of bacterial cells by air plasmas at atmospheric pressure *Int. J. Mass Spectrom.* **233** 81–6
[50] Laroussi M 2005 Low temperature plasma-based sterilization: overview and state-of-the-art *Plasma Process. Polym.* **2** 391–400
[51] Gaunt L F, Beggs C B and Georghiou G E 2006 Bactericidal action of the reactive species produced by gas-discharge nonthermal plasma at atmospheric pressure: a review *IEEE Trans. Plasma Sci.* **34** 1257–69
[52] Moisan M, Saoudi B, Crevier M C, Philip N, Fafard E, Barbeau J and Pelletier J 2003 Recent development in the application of microwave discharges to the sterilization of medical devices *5th Int. Workshop on Microwave Discharges (Greifswald, Germany)* pp 210–21
[53] Laroussi M, Mendis D A and Rosenberg M 2003 Plasma interaction with microbes *New J. Phys.* **5** 41
[54] Bayat O, Arslan V, Bayat B and Poole C 2004 Application of a flocculation–ultrafiltration process for bacteria (*Desulfovibrio desulfuricans*) removal from industrial plant process water *Biochem. Eng. J.* **18** 105–10
[55] Wasserman E and Felmy A R 1998 Computation of the electrical double layer properties of semipermeable membranes in multicomponent electrolytes *Appl. Environ. Microbiol.* **64** 2295–300
[56] West R J, Stephens G M and Cilliers J J 1998 Zeta potential of silver absorbing *Thiobacillus ferrooxidans Minerals Eng.* **11** 189–94
[57] Campanhã M T, Mamizuka E M and Carmona-Ribeiro A M 1999 Interactions between cationic liposomes and bacteria: the physical chemistry of the bactericidal action *J. Lipid Res.* **40** 1495–500
[58] Kuyyakanond T and Quesnel L B 1992 The mechanism of action of chlorhexidine *FEMS Microbiol. Lett.* **100** 211–5

[59] Manola S, Petrović Z Lj and Jankov R M 1993 Application of microwave discharges for sterilization of medical instruments *16th SPIG XVI Summer School and Int. Symp. on Physics of Ionized Gases* (*Belgrade*) ed M Milosavljević p 285

[60] Puač N, Petrović Z Lj, Živković S, Giba Z, Grubišić D and Đorđević A R 2005 Low temperature treatment of dry Empress-tree seeds *Plasma Processes and Polymers* ed R d'Agostino, P Favia, C Oehr and M R Wertheimer (New York: Wiley) pp 193–203

[61] Živković S, Puač N, Giba Z, Grubišić D and Petrović Z Lj 2004 The stimulatory effect of non-equilibrium (low temperature) air plasma pretreatment on light-induced germination of *Paulownia tomentosa* seeds *Seed Sci. Technol.* **32** 693–701

[62] Puač N, Petrović Z Lj, Malović G, Đorđević A, Živković S, Giba Z and Grubišić D 2006 Measurements of voltage–current characteristics of a plasma needle and its effect on plant cells *J. Phys. D: Appl. Phys.* **39** 3514–9

Spatial Profiles Of Electron And Ion Concentrations In A Large Size Ccp Discharge Obtained By Using A Langmuir Probe

Article · July 2010

4 authors, including:

Gordana Malovic
Institute of Physics Belgrade
157 PUBLICATIONS **932** CITATIONS
SEE PROFILE

Zoran Lj Petrović
Institute of Physics Belgrade
510 PUBLICATIONS **5,652** CITATIONS
SEE PROFILE

Publ. Astron. Obs. Belgrade No. 89 (2010), 205-208 *Contributed Paper*

SPATIAL PROFILES OF ELECTRON AND ION CONCENTRATIONS IN A LARGE SIZE CCP DISCHARGE OBTAINED BY USING A LANGMUIR PROBE

SAŠA LAZOVIĆ, NEVENA PUAČ, GORDANA MALOVIĆ
and ZORAN Lj. PETROVIĆ
Institute of Physics, University of Belgrade, 118 Pregrevica,
11080 Belgrade, Serbia
E-mail: lazovic@ipb.ac.rs

Abstract. Electron and ion concentrations in a large scale capacitively coupled plasma are measured using Hiden ESPION Langmuir probe system for different distances from the powered electrode. The reactor is cylindrical and has a radius of 60 cm. Derivative probes were used to measure rms Volte/Ampere characteristics and from these curves it was possible to determine that plasma runs in the alpha mode. From the spatial profiles of ion concentrations optimum distance can be found for treatment of samples of different sensitivity.

1. INTRODUCTION

Langmuir probe techniques can provide useful information on plasma and floating potentials, concentrations of ions and electrons, electron temperature and energy distribution functions, ion fluxes. Low cost, simplicity in construction and operation and the fact that plasma parameters can be measured in very wide ranges recommend this technique for application in research and industry as well.

Major disadvantages of Langmuir probes are contamination of the probe tip, perturbation of plasma and in most cases complexity of the theory that is needed to interpret the results. Nevertheless, for the industrial application, in many situations, it is only needed to check that plasma parameters are not changing significantly during the process and exact measurement of parameters is not always necessary. Langmuir probe measurements in RF discharges draw another set of problems due to the effects of RF time averaging, ionization near the probe, and expansion of the probe sheath (see Braithwaite et al. 2009 and Hershkowitz et al. 1988).

Main advantage of RF plasmas is that they can be used for treatment of both conductive and non-conductive materials (see Lieberman and Lichtenberg 2005 and Makabe and Petrović 2006). Treatment of textiles in RF low pressure discharges leads to several effects (see Radetić et al. 2007). For example, affinity to water of treated sample can be changed from hydrophobic to hydrophilic. Fat ac-

ids covering thread can be removed by plasma. Dying of textile can be done much more efficiently, compared to conventional methods, with prior plasma treatment.

A large scale discharge chamber has been made and studied in our laboratory with the objective to optimize plasma for low pressure textile treatment. Uniform and stable low-pressure, capacitively coupled plasma, safe from mode transitions to streamers and sparks was diagnosed using a Langmuir probe. The aim was to optimize plasma parameters for fast and reliable textile treatment. In that manner, concentrations of charged particles arriving at the sample surface play major role and are strongly dependent on the distance from the powered electrode for the cylindrical system.

In this paper we present spatial profiles of ion and electron concentrations obtained using Hiden Analytical ESPION Langmuir probe system on asymmetric large scale low-pressure capacitive coupled plasma.

2. EXPERIMENTAL SETUP

Experimental setup can be seen at Fig. 1. The setup consists of discharge chamber (1) in which powered electrode is placed axially (2) and Langmuir probe (3) perpendicular to the powered electrode. Current and voltage waveforms are obtained using derivative probes (4 and 5) connected with oscilloscope (8) and the computer (9). Discharge is run by an RF generator Dressler Cesar 1010 (7) through Variomatch matching network (6). The discharge chamber is 2.5 m long and 1.17 m in diameter and made of stainless steel. Powered electrode is placed in the centre of the chamber and is 1.5 m long, 3 cm in diameter and made of aluminum. Outer chamber wall is the grounded electrode.

Derivative probes are placed into a stainless steel box opposite to each other. The box is placed as close as possible to the powered electrode. Derivative probes were connected to the oscilloscope Agilent 6052A with the cables of identical length. All waveforms are collected by the computer for further analysis. Low pressure is maintained using mechanical vacuum pump with a constant flow of feeding gas (air).

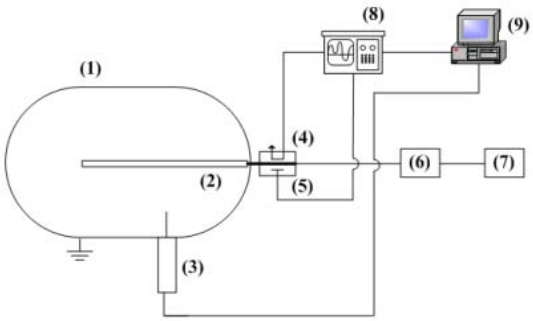

Figure 1: Experimental setup.

Hiden Analytical ESPION advanced Langmuir probe system is placed side-on. The system has a linear motion drive which enables probe positioning with the spatial resolution of 0.1 mm. The chamber has a platform at the bottom where samples are placed. The distance between the platform and the powered electrode is adjustable by moving the platform. We have chosen distances for Langmuir probe measurements within this range. All measurements were done in air at 100 mTorr. We have used platinum probe tip, 10 mm long and 0.15 mm in diameter. Linear motion drive was used to position the probe at the distances from 20.5 cm to 50.5 cm from the powered electrode. Measurements of U-I curves were made for all those positions of Langmuir probe.

At every position 10 measurements were made each being an average of 100 scans with pre-cleaning for each measurement. Prior to each acquisition, probe tip was cleaned for 120 ms providing -50 V to it. Voltage range was from -50 V to 85 V with resolution of 1 V. U-I curves were smoothed using 25 point Savitzky-Golay algorithm and data was further processed using Hiden ESPSoft.

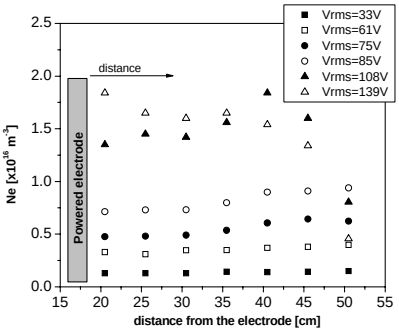

Figure 2: Electron concentrations at different distances from the powered electrode and different applied RMS voltages.

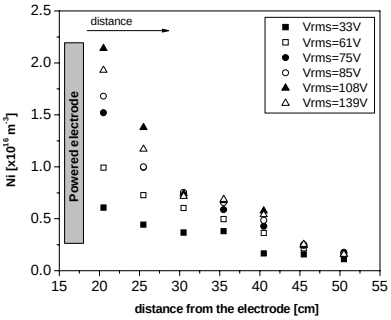

Figure 3: Ion concentrations at different distances from the powered electrode and different applied RMS voltages.

3. RESULTS AND DISCUSSION

Derivative probes were used to obtain RMS voltage and current values and from obtained V_{RMS}-I_{RMS} curves we can see that our discharge operates in the alpha mode. By using Langmuir probe we have recorded V-I curves for the range from 10W to 100W of powers given by RF power supply. In Figs. 2. and 3. dependences of concentration of electrons and ions on distance from the powered electrode are shown. We can see that with the increase of the distance electron concentrations do not change significantly. On the other hand, with an increase of the RMS voltage, and consequently power transmitted to the plasma, concentration of electrons increases (see Fig. 2). Also, *Ne* does not change significantly even when approaching powered electrode.

On the other hand, concentrations of ions (see Fig. 3) decrease with the increase of the distance from the powered electrode. Also, for the longest distances ion concentrations do not change even with the increase of the V_{rms} i.e. of the power transmitted to the plasma. This change is only significant for two closest positions of the Langmuir probe, where ion concentration rises with applied RMS voltage. Since ions play important role in plasma treatment, depending on sensitivity of the sample, one can determine optimal position for their placement from ion concentration and their energies.

4. CONCLUSION

Large scale 13.56 MHz asymmetric capacitive coupled plasma in air at 100 mTorr was diagnosed by using Langmuir probe and derivative probes. From the shape of the Urms-Irms characteristics it was determined that discharge operates in alpha mode. Electron and ion concentrations were measured at the several distances from the powered electrode at which the treated samples could be placed.

With the increase of RMS voltage, therefore power transmitted to the plasma, concentration of electrons increases, but it does not change significantly when approaching the powered electrode. On the other hand, concentrations of positive ions remain nearly constant with the RMS voltage increase and start to increase only for the distances less than 30 cm.

From the presently obtained results one can see a complex development of spatial profiles of ions and electrons. One could perhaps elucidate how is continuity of current maintained as the area increases towards the grounded electrode.

Acknowledgements

This work was supported in part by MNTRS project 141025.

References

Braithwaite, N. St. J., Franklin, R. N.: 2009, *Plasma Sources Sci. Technol.*, **18**, 014008.

Hershkowitz, N., Cho, M. H., Nam, C. H., Intraor, T.: 1988, *Plasma Chemistry and Plasma Processing,* **8**, 35.

Lieberman, M. A., Lichtenberg, A. J.: 2005, *Principles of Plasma Discharge and Materials Processing* (Wiley:Hoboken).

Makabe, T., Petrović, Z. Lj.: 2006, *Plasma Electronics* (Taylor and Francis: New York).

Radetić, M., Jovančić, P., Puač, N. and Petrović, Z. Lj.: 2007, *Workshop on Nonequilibrium Processes in Plasma Physics and Studies of the Environment, SPIG 2006, Journal of Physics: Conference Series,* **71**, 012017.

Application of non-equilibrium plasmas in medicine

Article *in* Journal of the Serbian Chemical Society · December 2012

Impact Factor: 0.87 · DOI: 10.2298/JSC121020142P

Journal of the Serbian Chemical Society
JSCS-info@shd.org.rs • www.shd.org.rs/JSCS
J. Serb. Chem. Soc. 77 (12) 1689–1699 (2012)
JSCS–4381
UDC 544.558:61:576:61.088:614.48.014.4:539.12
Original scientific paper

Application of non-equilibrium plasmas in medicine

ZORAN LJ. PETROVIĆ[1]*, NEVENA PUAČ[1], GORDANA MALOVIĆ[1], SAŠA LAZOVIĆ[1], DEJAN MALETIĆ[1], MAJA MILETIĆ[2], SLAVKO MOJSILOVIĆ[3], PAVLE MILENKOVIĆ[2] and DIANA BUGARSKI[3]

[1]*Institute of Physics, University of Belgrade, Pregrevica 118, 11080 Zemun, Serbia,* [2]*Faculty of Dental Medicine, University of Belgrade, Dr Subotića 8, Serbia and* [3]*Institute for Medical Research, University of Belgrade, Dr Subotića - starijeg 4, Serbia*

(Received 20 October, revised 10 December 2012)

Abstract: The potential of plasma applications medicine, the connections to nanotechnologies and the results obtained by our group are reviewed. A special issue in plasma medicine is the development of the plasma sources that would achieve non-equilibrium at atmospheric pressure in an atmospheric gas mixture with no or only marginal heating of the gas, and with desired properties and mechanisms that may be controlled. Our studies have shown that control of radicals or chemically active products of the discharge, such as ROS (reactive oxygen species) and/or NO, may be used to control the growth of the seeds. Simultaneously, a specially designed plasma needle and other sources were shown to be efficient to sterilize not only colonies of bacteria but also planktonic samples (microorganisms protected by water) or bio films. Finally, it was shown that a plasma might induce differentiation of stem cells. Non-equilibrium plasmas may be used in detection of different specific markers in medicine. For example proton transfer mass spectroscopy may be employed in the detection of volatile organic compounds without their dissociation and thus as a technique for instantaneous measurement of the presence of markers for numerous diseases.

Keywords: low temperature plasmas; plasma technologies; sterilization; functionalization; stem cells.

INTRODUCTION

This paper provides a survey of current plasma medical research/applications in the context of nanotechnologies, in particular, some of the research that was realized in our laboratory.

Low temperature, non-thermal or more precisely non-equilibrium plasmas have shown extraordinary range of applications and range of targets that may be

* Corresponding author. E-mail: zoran@ipb.ac.rs
doi: 10.2298/JSC121020142P

treated. Some of the applications, such as plasma etching for integrated circuit production plasma sources of light, gas lasers and deposition of thin films, have already shaped the existing civilization,[1–5] some on the other hand promise to make a similar impact in the future. Medical applications are at the forefront of future technologies associated with low temperature plasmas and the most active front of present day research.[6–9]

Non-thermal plasmas are being widely used in nano-technological and biomedical applications due to several distinctive properties.[1,2,10,11] The key feature is that it is possible to achieve dramatic changes of surface chemistry at low temperatures. Most of the generator power is absorbed by the electrons in the discharge, which then become hot, typically of the order of 10000 K or more, while, at the same time, ions and neutral molecules maintain room temperature, or close to it. The gas composition, the electron energy distribution function and the cross sections for the dominant interactions between electrons and the background gas particles dictate the production of huge amounts of chemically active species. If the gas composition is chosen properly and if the applied fields are designed efficiently and appropriately, the effects required by a certain application may be achieved while simultaneously fulfilling the criterion of maintaining a low temperature of the background gas.[12]

For the nano-technological applications, the main advantage is the anisotropic ion bombardment of surfaces (Fig. 1). Namely, sheaths are formed near surfaces due to the difference in particle masses. These high field regions conveniently accelerate ions, often with no collisions, to allow (nearly) normal incidence impacts at the surfaces, converting the potential energy in the sheath into kinetic energy at the surface.[14] A normal incidence angle is a crucial factor for contact holes to be obtained and interconnects with high aspect ratios. It is thought that the technology of combined photolithography and plasma etching is the most widely employed nanotechnology (belonging to the top down group) ever since the barrier in miniaturization of 200 nm was broken. The present day resolution of 32 nm in manufacture and aspect ratios of up to 20 (and much smaller dimensions achieved in laboratories) truly challenge even the bottom up technologies.

Furthermore, ion impacts on the sample surface are isolated because the time between impacts onto an area of ≈1 nm^2 is about 10^{-3} s. This should be compared to the time of 10^{-12} s required for the energy of a single impact to dissipate to the background heat. In unison, a single ion impact dissipates several hundreds of eV locally, which is sufficient to make a significant albeit localized modification of the surface. A typical flux of 10^{17} ions cm^{-2} s^{-1}, on average, dissipates power densities of the order of 1 W cm^{-2}. Thus, significant local and superficial changes of the surface structure are obtained while the overall temperature is not

increased significantly. The point here is that the peak power is sufficiently high to break chemical bonds easily and to perform functionalization of the surface.

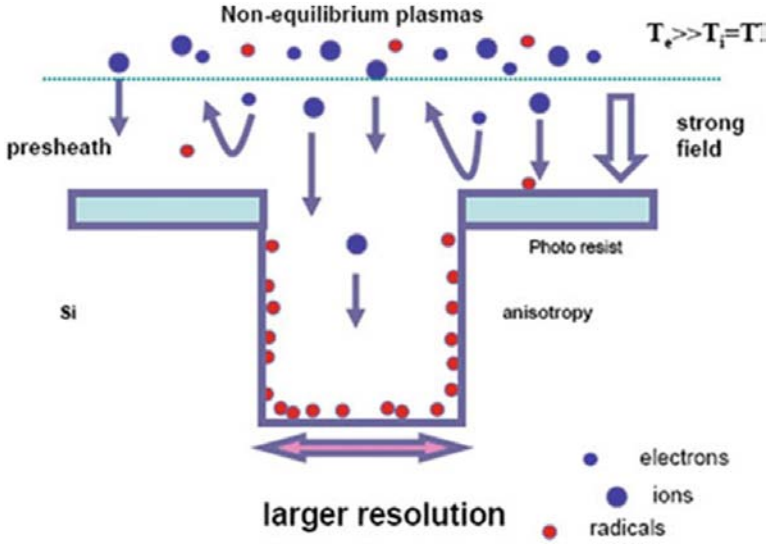

Fig. 1. Schematics of anisotropic plasma etching in non-equilibrium plasmas. The bulk of the plasma produces low energy ions and somewhat higher energy electrons that produce new ions and chemically active radicals. The sheath slows down the electrons and accelerates the ions, thus giving them energies of the order of several 100 eV. Hence, when they hit the surface they do so at a right angle and they facilitate anisotropic etching without sidewall undercutting. Electrons hit the surface with an almost isotropic distribution. The combined effect of the ions and radicals is much greater than the sum of the individual effects of the two species.[13]

It is also well known that the individual effects of ions and neutral chemically active species can be dramatically increased[13] when they both impact surfaces. This kind of synergy of the plasma agents is another crucial property in nano-technological applications.

Neutral, chemically active radicals are created in large numbers by electron-impact dissociation in molecular gas plasmas. It could easily be assumed that the surface flux of reactive particles (density) scales with pressure but gas phase collisions and slower diffusion as well as three body processes, which may change the chemistry entirely, have to be taken into consideration. The higher fluxes of active particles are one of the main arguments for atmospheric pressure non-thermal plasma sources over the low-pressure sources. This was one of the driving forces towards replacing low-pressure plasmas with atmospheric pressure/gas composition plasmas, together with the increased simplicity and decreased cost of atmospheric pressure systems. Thus, the needs of modern nano-technologies gave impetus for the development of more efficient and varied at-

mospheric pressure sources of low temperature plasmas. With the opportunity for such a development, a new front easily opened - that of medical applications.

Another advantage of atmospheric pressure, non-equilibrium plasmas is, of course, the fact that most biomedical systems cannot be subjected to vacuum. Moreover, for most biomedical applications, the temperature of the background gas should not exceed 42 °C, when cell death due to the overheating is induced. Hence, the ultimate conditions for biomedical applications would be not to overheat the sample but rather to induce subtle and selective cell and tissue responses to the plasma-generated chemicals and other species. Similar to nano-technological applications, but probably even more important is the understanding of the synergetic effects of the plasma agents, namely ions, electrons, electric fields and currents, light, neutrals, radicals and metastables. It can be concluded that common goals together with a common need for a localized synergistic effect of several agents drive the applications in both nanotechnologies and plasma medicine. Sometimes plasma medical effects that may be observed over a larger area are in essence due to very localized and specific effects that are fully in tune with nanotechnologies, their criteria and needs.

A BRIEF HISTORY OF PLASMA MEDICINE AND ITS CURRENT STATUS

The history of atmospheric pressure plasma applications in medicine can be divided into several periods. The first generation of plasma devices dating back to 1900 were those when heat was mainly used for tissue removal (plasma cutter). This period was followed by the second generation (since 1970) where thermal plasma energy was used for the surface treatment of tissues (argon plasma coagulator). In addition, there were numerous associated applications such as those using dielectric barrier discharges (DBD) for water purification, electrostatic precipitators to cleanse the air in hospitals and plasma activated hydrogen peroxide as sterilizer. At the same time, low-pressure plasmas were efficiently used in the early 1990s to sterilize equipment.[15] The third generation commenced in the late 1990s when plasmas were used, mainly at atmospheric pressures, for surface treatment with charged particles, reactive UV photons and electric fields.

The first commercial plasma devices date back to the beginning of the 20th century and those were aimed at surgery.[16] At present, there are numerous surgical devices but one has to be aware of the distinction between whether a plasma is just a conducting medium between an electrode and the treated tissue while the effect is due to thermal heating that is the result of the passage of the current or whether the surgical effects are due to plasma-created particles and their interaction with the fields and surface. One of the most successful devices associated with surgical interventions are plasma related devices for stopping bleeding, both by thermal effects and/or by plasma influence on the surface.

These devices include the endoscopic usage of APC (argon plasma coagulation) developed in 1995.[17]

Another front of medical applications that proved to be very successful expanded from low pressures[15] to atmospheric pressures in the late 90s. Very efficient sterilization of bacteria *Escherichia coli* was demonstrated by Laroussi in 1999 using a helium DBD.[18] This line of studies was pursued either directly in Petri dishes[19] or in planktonic samples (in liquid)[20] or even in biofilms.[21] More importantly, sterilization by a plasma was shown to be one of the benefits in the treatment of wounds.[22]

In addition to sterilization, plasmas were shown to benefit proliferation of new cells and the removal of scar tissue.[23] Thus, numerous wounds were treated including burns and chronic wounds, such as diabetic foot.[23] One of the recent applications of microwave plasma applications in dermatology for the treatment of chronic wounds is the application of the plasma torch MicroPlaSter®.[22]

In vitro treatment of cancer cells was demonstrated in 2007 using a floating electrode dielectric barrier discharge (FE-DBD) plasma.[24]. With this device, it was possible to induce programmed death of cells, so-called apoptosis. The Plasma acts directly on the cell without poisoning the solution in which they are located, even when the cells are covered with a medium.

The ion source of a proton transfer mass spectrometer (PTR-MS) operates using a non-thermal plasma. PTR-MS, compared to other analyzing devices, is more sensitive and can detect volatile organic compounds (VOC) down to parts per trillion in real time sampling. Breath sampling and analysis can provide data on VOC for the early stage detection of various diseases, such as breast and lung cancer, diabetes *etc*. Breath is a very complex mixture of various organic compounds.[25] For lung cancer, VOC-31 (m/z = 31), tentatively protonated formaldehyde, and VOC-43 (m/z = 43), tentatively a fragment of protonated 2-propanol, were found at significantly higher concentrations in the breath of cancer patients than in the breath of the control group.[26] One of the biomarkers for diabetes is acetone[27] and its higher concentration in breath, as well as the dynamics of its removal can be an indicator for the disease.

EXPERIMENTAL SETUP AND PROCEDURE

The main reason for the application of plasmas in medicine is that they can replace old conventional procedures in surgery and wound sterilization. Another important feature is the simplicity and low production cost of these plasma devices. Various plasma sources are used in plasma medicine, such as plasma jets, plasma needle, APC and FE-DBD (Fig. 2). Most of the plasma devices have low working gas temperatures because of the great non-equilibrium between the energies of the electrons and heavy particles. This feature is crucial for treatment without damaging the sample. In order to ignite and maintain a discharge at atmospheric

pressure, a noble gas is often used (usually helium or argon). The main role of the noble gas is to lower the breakdown voltage and with its flow, the treated area is also cooled. The complex chemistry and reactions in a plasma produce a unique mixture of particles, for instance atomic species, radicals, UV photons and electrons, important for the efficiency of the treatment of a biological sample. In order to produce higher concentration of the reactive species, a mixture of the noble and a molecular gas, usually oxygen, can be used.

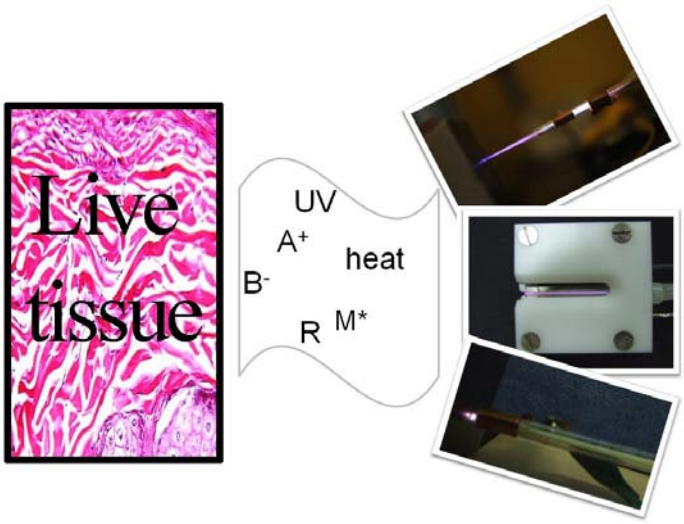

Fig. 2. Photographs of several atmospheric plasma devices that are used in our laboratory for biomedical applications. From the top, a plasma jet, a micro atmospheric pressure plasma jet and a plasma needle are shown.

In our laboratory, low-pressure plasma reactors are accessible that have been used mainly for the treatment of surfaces (textile, polymers, graphene, silicon dioxide surfaces, *etc*.). Atmospheric pressure non-equilibrium plasmas that are available include plasma needle, micro atmospheric pressure plasma jet, plasma jet (operating in the plasma bullet mode), corona and dielectric barrier discharge.

Our principal plasma device that was used to date in the studies of plasma medicine is the plasma needle, which was first applied for the treatment of mammalian cells reported in 2003.[28] The operating power was low and the frequency of the driving current was 13.56 MHz in atmosphere of helium. The plasma needle can be used for the treatment of small areas covered by cells. The plasma needle at higher power kills cells, usually causing necrosis, but at smaller powers either apoptosis may be induced or cells could be just separated.

This plasma device was shown to be suitable for bacteria sterilization[20] of bacteria colonies, planktonic samples and bio films. In addition, this source was

shown to be able to destroy cancer cells, affect but to a much lesser degree human stem cells and even cause differentiation of the stem cells.[29]

DIAGNOSTICS OF PLASMAS

In order to determine the pertinent plasma properties and optimize the desired effects, we use several diagnostic methods. In principle, the basic electrical properties are determined by probes (including derivative probes for higher frequencies that have been calibrated to determine the powers delivered to a plasma of less than 1 W). Optical emission spectroscopy is applied with a limited range of interesting effects that may be covered unless time resolved measurements are made. Spatial profiles of emission recorded by an ultra fast ICCD are employed to determine the time dependent anatomy of the discharge. Finally, a mass analyzer with triple differential pumping is employed, which enables sample ions or radicals from atmospheric pressure discharges to be sampled.[30,31]

MECHANISMS

The interactions between a plasma and cells are hard to investigate due to the complexity of both systems. A plasma is a cocktail of active agents (radicals, UV light, heat, ions, electric fields, energetic particles, *etc*.) with strong synergetic effects. The proper diagnostics and optimization of plasma treatment is of vital importance. On the other hand, the biological samples being treated have a complex sub-structure of their own, so plasma usually targets and affects several of them if not all. The character and the selectivity of the interaction are determined by the plasma properties and the structure of the bio-sample. For example, UV light can easily penetrate and reach DNA introducing single and double strand breaks (directly and/or by creating radicals in the vicinity of the DNA).[32] In the case of bacteria, the DNA is in the nucleoid and is circular while the eukaryotic cells have their DNA better protected in the nucleus. The same intensity of UV light exposure can lead to the destruction of bacteria without long-term effects on the eukaryotic cell, which is just one of the examples of the selectivity mechanism. Other examples worth discussing can be drawn from the differences in the surface to volume ratios, the structure of cell walls, the existence of cell enzymes, *etc*.[33] Bacteria have a higher surface to volume ratio meaning that the same dose of plasma exposure can be sufficient for deactivation while no negative effects to surrounding tissue is caused. The cell wall is usually directly exposed to the plasma treatment. Due to ion bombardment (or to the strong electric fields), pores are being created in the cell wall.[34] Through these pores, the cell can exchange its content with the surrounding. The cell content can leak out and cause cell stress and eventually cell death, as often happens. Bacteria cell wall is made of polysaccharides. Eukaryotic cells have walls made of phospholipids. Exposed to the plasma, lipid peroxidation process occurs. In the process of peroxidation of polysaccharides and phospholipids, the presence of water is important as well as

the composition of the media surrounding the cells and the ions play a catalytic role. One of the products of the lipid peroxidation process of the cell wall is the malondialdehyde. Formed at the cell wall by the plasma, malondialdehyde can be transported to the vicinity of DNA where it can introduce DNA mutation.[35] All this shows the indirect effects of the plasma as well as the complexity of the cell reactions. The enzymes are also able to regulate the stress dealt to the cell. They also regulate the cell radical levels, which on the other hand are massively produced by the plasma. The importance of reactive oxygen and nitrogen species through cell redox processes is evidently crucial but not sufficiently understood.[36] Some of the reactive oxygen species are listed in Table I.[37] The balance between the free radicals and the antioxidants is necessary for proper cell functioning. The conclusion is general and valid for plant cells also.[37]

TABLE I. Reactive oxygen species, ROS[37]

Radicals	Non-radicals
Superoxide, $O_2^{\bullet -}$	H_2O_2
Hydroxyl, $OH^{\bullet}$	Hypobromous acid, HOBr
Hydroperoxyl, $HO_2^{\bullet}$ (protonated superoxide)	Hypochlorous acid, HOCl
Carbonate, $CO_2^{\bullet -}$	Ozone, O_3
Peroxyl, $RO_2^{\bullet}$	Singlet oxygen ($O_2{}^1\Delta_g$)
Alkoxyl, $RO^{\bullet}$	Organic peroxides, ROOH
Carbon dioxide radical, $CO_2^{\bullet -}$	Peroxynitrite, ONOO
Singlet $O_2{}^1\Sigma_g^+$	Peroxynitrate, O_2NOO

PARALLELS WITH PLASMA NANOTECHNOLOGIES

Plasmas have been used in top down plasma technologies for many years, especially through synergistic process of plasma etching that is presently massively used in production with resolutions of 32 nm. Several plasma applications in nanotechnology may be associated with medicine. These include coating of biocompatible thin films, functionalization of surfaces to allow binding of bactericidal nanoparticles of TiO_2 or silver, thus allowing the development of germ free clothes for surgeons and other medical personnel.[38–45]

Furthermore, a more direct parallel lies in the fact that most plasma medical processes are very local over areas that are small parts of a cell and thus compatible with nano-dimensions. Besides the plasma needle and micro atmospheric pressure plasma jet, the capillary microplasmas used for nanostructuring have similar potentials for biomedical applications.[46,47] In a similar way, non-equilibrium plasmas are used to achieve thermodynamically unlikely structures/effects and in the same way surfaces are bombarded by a cocktail of ions and neutrals, electrons, chemically active radicals and are subjected to the effects of local fields. Finally, the need for atmospheric pressure for plasma medicine is also a

motivating factor for the development of cheaper nano-technologies not employing expensive vacuum procedures. Thus, the development of plasma medicine may be associated with the advances in non-equilibrium plasmas for micro (nano) electronics that have occurred over the past two decades.

CONCLUSIONS

Recent advances in plasma medical applications have left very little doubt that this application will be the main driving force for the future developments of non-equilibrium collisional plasmas. The main trick in achieving the non-equilibrium operation and no gas heating is the control of the electron multiplication. For this purpose, inhomogeneous fields (corona), dielectric barrier, RF and pulsed operation and breakdown in rare gas flow may be employed.

Plasma medicine is a new and fast developing field of both medicine and plasma physics, introduced in the last decade. The non-thermal atmospheric pressure plasmas were recently used for the treatment of diverse thermo sensitive biological samples.

Acknowledgements. This research was supported by the Ministry of Education, Science and Technological Development of the Republic of Serbia, under the contract numbers ON171037 and III41011.

И З В О Д

ПРИМЕНА НЕРАВНОТЕЖНЕ ПЛАЗМЕ У МЕДИЦИНИ

ЗОРАН Љ. ПЕТРОВИЋ[1], НЕВЕНА ПУАЧ[1], ГОРДАНА МАЛОВИЋ[1], САША ЛАЗОВИЋ[1], ДЕЈАН МАЛЕТИЋ[1], МАЈА МИЛЕТИЋ[2], СЛАВКО МОЈСИЛОВИЋ[2], ПАВЛЕ МИЛЕНКОВИЋ[2] и ДИАНА БУГАРСКИ[3]

[1]Институт за физику, Универзитет у Београду, Прегревица 118, 11080 Земун, [2]Стоматолошки факултет, Универзитет у Београду, Др Суботића 8, Београд и [3]Институт за медицинска истраживања, Универзитет у Београду, Др Суботића-старијег 4, Београд

У овом раду дат је преглед примене плазме у медицини, повезаност са нанотехнологијама и резултате на овом пољу које је постигла наша група. Посебан проблем у плазма медицини је развој извора плазме који би радили у неравнотежним условима на атмосферском притиску и у смеши гасова каква је у атмосфери уз занемарљиво грејање гаса и са жељеним карактеристикама које се могу подешавати по жељи. Наша истраживања су показала да се контрола присуства радикала и других хемијски активних честица као што су реактивне кисеоничне честице (ROS) и/или NO, може користити за контролу клијања семенки. У исто време је доказано за посебно конструисану плазма иглу да може ефикасно да стерилише не само колоније бактерија већ и планктонске узорке (микроорганизме заштићене водом) па и биофилмове. На крају, ми смо показали да плазма може да индукује диференцијацију матичних ћелија. Неравнотежна плазма се може користити за детекцију разних специфичних маркера у медицини. На пример масена спектроскопија на бази измене протона може да се користи за детекцију испаривих органских једињења без њихове дисоцијације и на тај начин се може оставрити тренутна детекција маркера за бројне болести из даха.

(Примљено 20. октобра, ревидирано 10. децембра 2012)

REFERENCES

1. M. A. Lieberman, A. J. Lichtenberg *Principles of Plasma Discharge and Materials Processing*,Wiley, Hoboken, NJ, 2005
2. T. Makabe, Z. L. Petrović, *Plasma electronics: applications in microelectronic device fabrication*, Taylor and Francis, New York, 2006
3. M. G. Kong, G. Kroesen, G. Morfill, T. Nosenko, T. Shimizu, J. Van Dijk, J. L. Zimmermann, *New J. Phys.* **11** (2009) 115012
4. K. Ostrikov, U. Cvelbar, A. B. Murphy, *J. Phys. D: Appl. Phys.* **44** (2011) 174001
5. Z. Lj. Petrović, B. Radjenović, M. Radmilović-Rađenović, in *Proceedings 26th International Conference on Microelectronics MIEL, the Production of Integrated Circuits and Surface Modification of Materials*, Niš, Serbia, 2008, p. 19
6. K. D. Weltmann, Th. Von Woedtke, *Eur. Phys. J. Appl. Phys.* **55** (2011) 13807
7. J. Heinlin, G. Isbary, W. Stolz, G. Morfill, M. Landthaler, T. Shimizu, B. Steffes, T. Nosenko, J. L. Zimmermann, S. Karrer, *J. Eur. Acad. Dermatol.* **25** (2011) 1
8. R. Sensenig, S. Kalghatgi, E. Cerchar, G. Fridman, A. Shereshevsky, B. Torabi, K. Priya Arjunan, E. Podolsky, A. Fridman, G. Friedman, J. Azizkhan-Clifford, A. D. Brooks, *Ann. Biomed. Eng.* **39** (2011) 674
9. R. Wang, H. Zhou, P. Sun, H. Wu, J. Pan, W Zhu, J Zhang, J Fang, *Plasma Med.* **1** (2011) 143
10. *Non-equilibrium air plasmas at atmospheric pressure*, K. H. Becker, U. Kogelschatz, K. H. Schoenbach, R. J. Barker, Eds., Taylor & Francis, New York, 2004,
11. *Plasma for bio-decontamination, medicine and food security*, Z. Machala, K. Hensel, Y. Akishev, Eds., Springer, Dordrecht, The Netherlands, 2012
12. Z. L. Petrović, N. Puač, S. Lazović, D. Maletić, K. Spasić, G. Malović, *J. Phys. Conf. Ser.* **356** (2012) 012001
13. H. F. Winters, J. W. Coburn, *J. Vac. Sci. Technol., B* **3** (1985) 1376
14. T. Makabe, T. Yagisawa, *Plasma Sources Sci. Technol.* **18** (2009) 014016
15. S. Manola, Z. Lj. Petrović, R. M. Jankov, in *Proceedings of 16th SPIG XVI Summer School and International Symposium on the Physics of Ionized Gases*, Belgrade, 1993, p. 285
16. W. Bovie, H. Cushing, *Surg. Gynecol. Obstet.* **47** (1928) 751
17. J. Sessler, H. D. Becker, I. Flesch, K. E. Grund, *J. Cancer. Res. Clin. Oncol.* **121** (1995) 235
18. M. Laroussi, G. S. Sayler, B. B. Glascock, B. Mccurdy, M. E. Pearce, N. G. Bright, C. M. Malott, *IEEE Trans. Plasma Sci.* **27** (1999) 34
19. G. Fridman, A. D. Brooks, M. Balasubramanian, A. Fridman, A. Gutsol, V. N. Vasilets, H. Ayan, G. Friedman, *Plasma Processes Polym.* **4** (2007) 370
20. S. Lazović, N. Puač, M. Miletić, D. Pavlica, M. Jovanović, D. Bugarski, S. Mojsilović, D. Maletić, G. Malović, P. Milenković, Z. L. Petrović, *New J. Phys.* **12** (2010) 083037
21. S. A. Ermolaeva, A. F. Varfolomeev, M. Y. Chernukha, D. S. Yurov, M. M. Vasiliev, A. A. Kaminskaya, M. M. Moisenovich, J. M. Romanova, A. N. Murashev, I. Selezneva , T. Shimizu, E. V. Sysolyatina, I. A. Shaginyan, O. F. Petrov, E. I. Mayevsky, V. E. Fortov, G. E. Morfill, B. S. Naroditsky, A. L. Gintsburg, *J. Med. Microbiol.* **60** (2011) 75
22. J. Heinlin, G. Morfill, M. Landthaler, W. Stolz, G. Isbary, J. L. Zimmermann, T. Shimizu, S. Karrer, *J. Dtsch. Dermatol. Ges.* **8** (2010) 968

23. G. Fridman, G. Friedman, A. Gutsol, A. B. Shekhter, V. N. Vasilets, A. Fridman, *Plasma Processes Polym.* **5** (2008) 5033
24. G. Fridman, A. Shereshevsky, M. M. Jost, A. D. Brooks, A. Fridman, A. Gutsol, V. Vasilets, G. Friedman, *Plasma Chem. Plasma Process.* **27** (2007) 163
25. K. Schwarz, W. Filipiak, A. Amann, *J. Breath Res.* **3** (2009) 027002
26. A. Wehinger, A. Schmid, S. Mechtcheriakov, M. Ledochowski, C. Grabmer, G. A. Gastl, A. Amann, *Int. J. Mass Spectrom*. **265** (2007) 49
27. D. Smith, P. Španěl, A. A. Fryer, F. Hanna, G. A. A. Ferns, *J. Breath Res.* **5** (2011) 022001ss
28. E. Stoffels, I. E. Kieft, R. E. J. Sladek, *J. Phys., D* **36** (2003) 2908
29. M. Miletić, S. Mojsilović, I. Okić Đorđević, D. Maletić, N. Puač, S. Lazović, G. Malović, P. Milenković, Z. Petrović, D. Bugarski, unpublished results
30. S. Lazović, N. Puač, G. Malović, A. Đorđević, Z. L., Petrović *Chem. Listy* **102** (2008) 1383
31. G. Malović, N. Puač, S. Lazović, Z. Petrović, *Plasma Sources Sci. Technol.* **19** (2010) 034014
32. D. O' Connell, L. J. Cox, W. B. Hyland, S. J. Mcmahon, S. Reuter, W. G. Graham, T. Gans, F. J. Currell, *Appl. Phys. Lett.* **98** (2011) 043701
33. D. Dobrynin, G. Fridman, G. Friedman, A. Fridman, *New J. Phys.* **11** (2009) 115020
34. K. H. Schoenbach, F. E. Peterkin, R. W. Alden, S. J Beebe. *IEEE Trans. Plasma. Sci.* **25** (1997) 284
35. L. J. Marnett, *Mutat. Res.* **424** (1999) 83
36. D. B. Graves, *J. Phys., D* **45** (2012) 263001
37. B. Halliwell, *Plant Physiol.* **141** (2006) 312
38. X. Liu, P. K. Chu, C. Ding, *Mat. Sci. Eng., R* **70** (2010) 275
39. P. Uhlmanna, L. Ionov, N. Houbenov, M. Nitschke, K. Grundke, M. Motornov, S. Minko, M. Stamma, *Prog. Org. Coat.* **55** (2006) 168
40. U. Cvelbar, M. Modic, J. Kovač, S. Lazović, G. Filipič, D. Vujošević, I. Junkar, K. Eleršič, S. P. Brühl, C. Canal, T. Belmonte, M. Mozetič, *Surf. Coat. Technol.* **211** (2012) 200
41. U. Cvelbar, Z. Chen, I. Levchenko, R. M. Sheetz, J. B. Jasinski, M. Menon, M. K. Sunkar, K.(Ken) Ostrikov, *Chem. Commun.* **48** (2012) 11070
42. U. Cvelbar, Z. Chen, M. K. Sunkara, M. Mozetič, *Small* **4** (2008) 1610
43. K. (Ken) Ostrikov, U. Cvelbar, A. B Murphy, *J. Phys. D: Appl. Phys.* **44** (2011) 174001
44. G Arnoult, T Belmonte, F Kosior, M Dossot, G Henrion, *J. Phys., D* **44** (2011) 174022
45. M. Hiramatsu, M. Hori *Carbon Nanowalls: Synthesis and Emerging Applications* Springer, Wein, 2009
46. A. C. Bose, Y. Shimizu, D. Mariotti, T. Sasaki, K. Terashima, N. Koshizaki, *Nanotechnol.* **17** (2006) 5976
47. Y. Shimizu, T. Sasaki, A. C. Bose, K. Terashima, N. Koshizaki, *Surf. Coat. Tech.* **200** (2006) 4251.

Biomedical applications and diagnostics of atmospheric pressure plasma

Article *in* Journal of Physics Conference Series · March 2012

DOI: 10.1088/1742-6596/356/1/012001

6 authors, including:

Zoran Lj Petrović
Institute of Physics Belgrade
510 PUBLICATIONS **5,652** CITATIONS
SEE PROFILE

Saša Lazović
Institute of Physics Belgrade
70 PUBLICATIONS **212** CITATIONS
SEE PROFILE

Kosta Spasic
University of Belgrade
10 PUBLICATIONS **12** CITATIONS
SEE PROFILE

Gordana Malovic
Institute of Physics Belgrade
157 PUBLICATIONS **932** CITATIONS
SEE PROFILE

Biomedical applications and diagnostics of atmospheric pressure plasma

2012 J. Phys.: Conf. Ser. 356 012001

(http://iopscience.iop.org/1742-6596/356/1/012001)

Journal of Physics: Conference Series **356** (2012) 012001 doi:10.1088/1742-6596/356/1/012001

Biomedical applications and diagnostics of atmospheric pressure plasma

Z Lj Petrović[1], N Puač, S Lazović, D Maletić, K Spasić and G Malović

Institute of Physics, University of Belgrade, Pregrevica 118, 11080 Belgrade, Serbia

E-mail: zoran@ipb.ac.rs

Abstract. Numerous applications of non-equilibrium (cold, low temperature) plasmas require those plasmas to operate at atmospheric pressure. Achieving non-equilibrium at atmospheric pressure is difficult since the ionization growth is very fast at such a high pressure. High degree of ionization on the other hand enables transfer of energy between electrons and ions and further heating of the background neutral gas through collisions between ions and neutrals. Thus, all schemes to produce non-equilibrium plasmas revolve around some form of control of ionization growth. Diagnostics of atmospheric pressure plasmas is difficult and some of the techniques cannot be employed at all. The difficulties stem mostly from the small size. Optical emission spectroscopy and laser absorption spectroscopy require very high resolution in order to resolve the anatomy of the discharges. Mass analysis is not normally applicable for atmospheric pressure plasmas, but recently systems with triple differential pumping have been developed that allow analysis of plasma chemistry at atmospheric pressures which is essential for numerous applications. Application of such systems is, however, not free from problems. Applications in biomedicine require minimum heating of the ambient air. The gas temperature should not exceed 40 ^{o}C to avoid thermal damage to the living tissues. Thus, plasmas should operate at very low powers and power control is essential. We developed unique derivative probes that allow control of power well below 1 W and studied four different sources, including dielectric barrier discharges, plasma needle, atmospheric pressure jet and micro atmospheric pressure jet. The jet operates in plasma bullet regime if proper conditions are met. Finally, we cover results on treatment of bacteria and human cells as well as treatment of plants by plasmas. Localized delivery of active species by plasmas may lead to a number of medical procedures that may also involve removal of bacteria, fungi and spores.

1. Introduction

The choice of the plasma system used for treatment is usually guided by the kind of samples that are treated and the effect these plasmas are intended to have on the samples. The desire to use plasma for in-vivo treatments have made it necessary that several requirements for plasma sources be met. Necessarily, plasmas have to operate at atmospheric pressure if they are to be used for medical treatment of living organisms. At the same time, one needs non-equilibrium plasmas in order to achieve separation of electrons on the one side, and ions and neutrals, on the other. It is an advantage that no expensive vacuum systems are needed, while, on the other hand, it is much more difficult to achieve non-equilibrium (non-thermal) mode of operation at higher pressures.

[1] To whom any correspondence shoul be addressed.

The sensitivity to heat of biomedical samples narrows the choice of non-thermal plasmas. There are many types of plasmas that can be generated under ambient pressure and temperature conditions suitable for treatment of sensitive samples [1, 2, 3]. The motivation is to develop new medical techniques, as plasma offers some possibilities for inducing desired processes with minimum damage to the living tissue [1, 2, 3, 4]. While the first results seemed quite impressive, including effects on tumor cells and even active tumors [5], tooth decay treatment and tooth cleaning [6], wound healing [5], treatment of fungi and spores and even treatment of ulcers and blood vessels, one can still not rule out negative effects that have not been studied over a sufficiently long time scale. Th preliminary results, however, show a large degree of selectivity.

Some of the well-known small-size atmospheric-pressure plasma sources are: plasma needle [7, 4], μAPPJ [8], plasma bullet [9], plasma torch [10] and floating electrode dielectric barrier discharge plasma [11]. Their electrode configuration, voltages and excitation frequencies are very different; some of them work at microwave frequencies, some at 13.56 MHz and others at 5-120 kHz in sine or pulse regime. Yet, all is not understood about their physics and while models are being developed mainly based on low pressure plasmas, the reliable experimental data are limited due to the limited availability of diagnostic techniques that are suited for such plasmas.

Here we will present several diagnostics techniques suited for atmospheric pressure plasmas and the operation of several different plasma systems working at atmospheric pressure. We will also summarize our results in treating living organisms and give examples of results mainly on sterilization of bacteria and biofilms.

2. Atmospheric pressure discharges – different experimental set-ups

Achieving non-equilibrium at atmospheric pressure is difficult since the ionization growth is very fast at such a high pressure. The high degree of ionization on the other hand enables transfer of energy between electrons and ions through Coulomb collisions. Furthermore, heating of the background neutral gas is achieved through collisions between ions and neutrals. Thus, all schemes to produce non-equilibrium plasmas revolve around some form of control of the ionization growth. It can be achieved either by an inhomogeneous field as in corona or by employment of a dielectric barrier which turns the field off after a space charge is deposited on the dielectric. Ionization growth limiting may also be achieved by a time-varying field. Another approach is to operate at the *pd* value corresponding to the Paschen minimum, i.e. at microscopic dimensions and high pressures. In that case, the breakdown voltage is below the threshold for streamer development and thus a glow discharge may be achieved. If the electronegative nature of the gas is increasing the breakdown and operating voltages, one may mix in an inert gas. The discharge is thus initiated in the inert gas and then the atmospheric gas is mixed to produce chemically active radicals. In most cases, however, atmospheric pressure plasmas have small dimensions making it very difficult to perform standard diagnostics.

Some of the plasma devices designed for in-vivo treatments are the μ-APPJ and the plasma needle, which operate at 13.56 MHz at atmospheric pressure. A micro-atmospheric plasma jet was developed by Schultz van der Gathen and coworkers [12]; this plasma source is interesting both for applications as well as for the study of its basic properties.

The micro-atmospheric pressure plasma jet [μ-APPJ] consists of two symmetrical electrodes of equal length (34 mm) made of stainless steel. The distance between the electrodes can be adjusted with good precision from a few mm up to several hundred micrometers. In all our experiments, the distance between the powered and the grounded electrode was 1 mm. One of the electrodes was powered by a signal generator at 13.56 MHz while the other electrode was grounded. The measurements were made at powers of 40-80 W fed by a RF power supply.

Plasma is ignited along the entire length of the electrodes (figure 1); for certain combinations of power/gas-flow parameters, effluent of plasma coming out of the cuvette can be formed. The main advantage of this design is that both the discharge volume (plasma core) and effluent region are accessible for diagnostics, such as optical emission spectroscopy (OES) and two-photon absorption

laser-induced fluorescence (TALIF) [8]. Also, the plane parallel geometry of the electrodes adds to the simplicity when it comes to modeling this type of discharge.

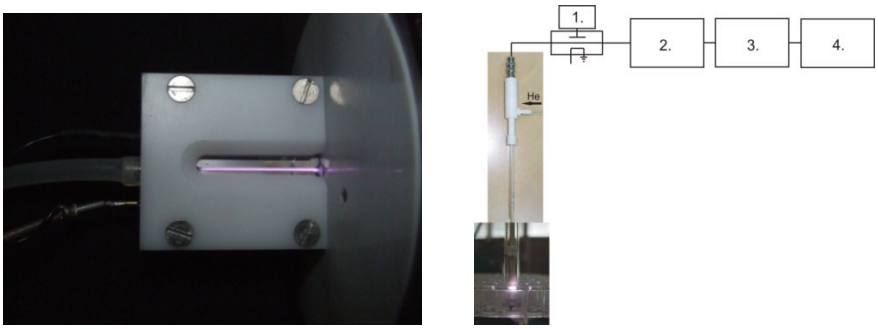

Figure 1. μ-APPJ with formed plasma and plasma needle system set-up.

Another plasma source that meets all the necessary conditions for treatment of organic materials and living tissues is the plasma needle (figure 1, picture on the right-hand side). Most importantly, in such a discharge gas the heating is minimized, while th effects on the tissue and bacteria have been clearly shown to be significant. The needle consists of a central electrode made of tungsten insulated almost to the tip by a slightly larger ceramic tube, both being placed inside a glass tube. The needle body is made of Teflon. We used helium as a buffer gas at several different flow rates. The central electrode is powered by a 13.56 MHz signal generator through an amplifier and a matching network. Both for the plasma needle and for thee μ-APPJ, we have derivative probes and a Hiden HPR60 mass/energy analyzer in order to determine the power applied to plasma and the composition of the discharge, respectively. In both of these systems, inert gas is used to reduce the breakdown voltage and achieve stable non-equilibrium plasma formation. Yet these plasmas have shown several modes of operation and further studies are required to fully understand their operation and make further optimizations.

Another type of atmospheric pressure plasma relies on mixing the inert gas carrying the plasma created by external electrodes with atmospheric gas mixture. It is the so-called plasma jet. The operating frequencies of plasma jets are in the region of several tens of kHz which are much lower frequencies then those used for the plasma needle and μ-APPJ (in MHz). It has been shown that micro jet plasma is not always continuous but often is formed by a train of fast travelling bullets which only appear to be continuous to the human eye. The atmospheric pressure plasma jet/bullet that we constructed was made of a Pyrex glass tube with the electrodes made of a thin copper foil wrapped around the glass tube. The distance between the powered and the grounded electrode was 13.5 mm and their width was 13 mm. One of the electrodes (the left electrode, see figure 2) was grounded. The other electrode, closer to the end of the glass tube, was the powered one (see figure 2). In all experiments the buffer gas was helium. We used a signal generator connected to the custom-made amplifier to power the micro jet. The highest voltages that we could obtain from the amplifier were up to 1 kV, which was not enough to ignite the plasma. In order to the increase the applied voltages to more than 5-6 kV, we had to use an additional homemade transformer. The operating frequency was 80 kHz and the applied voltage was sinusoidal in the range of 6-10 $kV_{peak\text{-}to\text{-}peak}$. Micro jets with plasma bullets have been constructed with a range of different

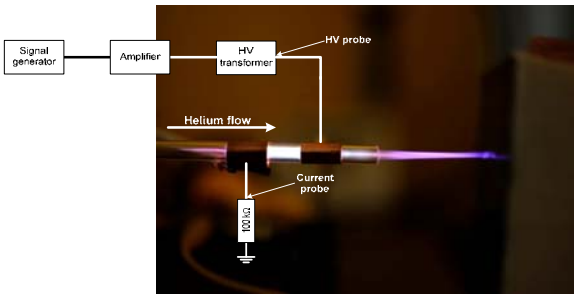

Figure 2. Atmospheric plasma bullet.

geometries, frequencies and shapes of applied voltage. The effect of bullets seems to be quite universal for an optimum range of electrode sizes and flows, while the frequencies and voltage shapes vary a lot. Plasma bullets, however, still need to be fully understood and properly modelled. We will focus here on the plasma jet diagnostics, while at the same time showing some results on the sterilization achieved by a plasma needle.

3. Plasma diagnostics

It has been reported only quite recently that the plasma jets formed by the source operating at low excitation frequency is not continuous. Instead it consists of small plasma packages that are formed in positive and/or negative half cycle of the period [13]. Amazingly these little bullets are formed and travel outside the plasma jet where there is no applied electric field. The velocity of these packages are larger than the speed of the flowing feed gas by several orders of magnitude. Several theories of bullet formation have been proposed [13, 14, 15, 16, 17, 18] but to date a definite explanation of the physical mechanisms involved in creation and propagation of plasma bullet are still not fully understood.

For the current and voltage measurements, we used two commercial probes. The current and voltage waveforms when the plasma is formed and without discharge are shown in figure 3. When the plasma is off, the phase difference between the current and voltage is close to 90˚. In this case, we have a capacitive impedance of several MΩ, corresponding to a capacitance of about 0.5 pF. On the other hand, when the plasma is formed, the current signal is larger, deformed and shifted in phase overlapping more with the voltage signal. The plasma ignition changes the slopes of the V_{RMS}–I_{RMS} curves (see figure 4). The mean power calculated increases with the increase of the applied voltage; it was in the range from 1 to 8 W in all measurements.

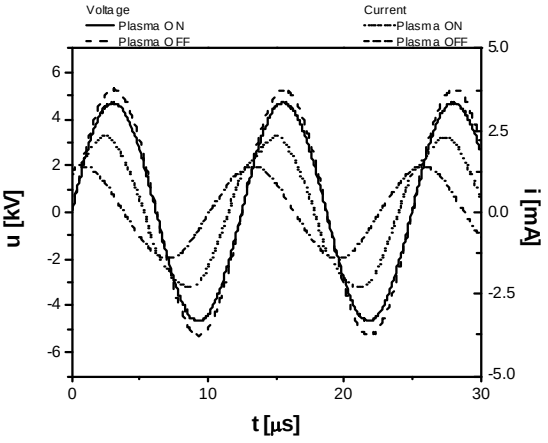

Figure 3. Current and voltage waveforms for helium flow rate of 3 slm. The dashed lines represent the case when discharge is OFF, the solid lines, when discharge is ignited [19].

Integral and time-resolved images of the plasma jet system were obtained by an ICCD camera. For exposure times larger than the cycle period (12.5 μs), the plasma appears to be continuous, like a plume (see figure 1 LHS picture). The length of the plasma plume is up to five centimeters, depending of the flow rate and the voltage applied. For the time-resolved images, we had to use integration on the chip because the light emission in a single shot is not sufficient to obtain clear images with gate widths less than 50 ns. This was facilitated by the high reproducibility of the pulses and the small jitter. Figure 5 shows the plasma bullet images obtained for several different flows of working gas. We can see that with the decrease in the He flow, the plasma bullet starts to be elongated, deformed and its intensity is much smaller. Eventually, bullets are not formed at the very small flows.

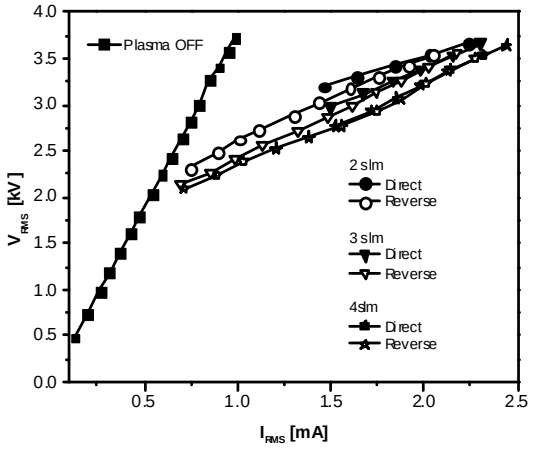

Figure 4. Current-voltage characteristics for three different flows of helium [19].

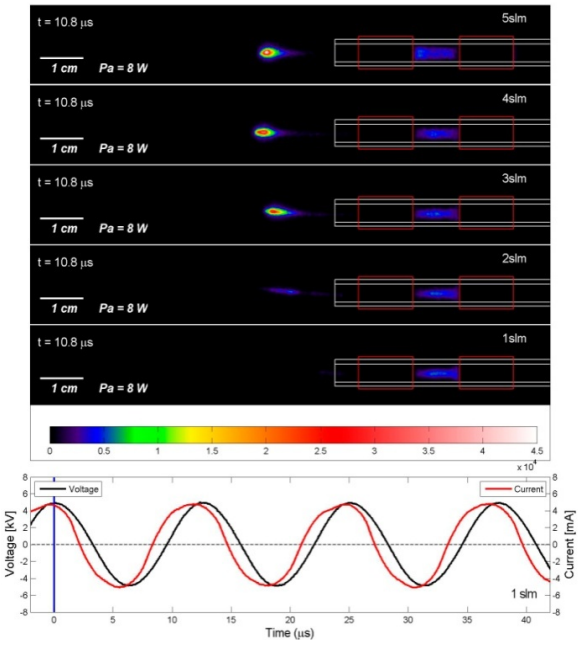

Figure 5. Plasma jet for 1, 2, 3, 4 and 5 slm of He flow. Exposure time 2 ms, gate width 25 ns, gate delay 10.8 µs [19].

Figure 6 shows the development of the plasma over the entire period of applied voltage (12.5 µs). All images are scaled to the same maximum intensity and thus can be compared. One can see that when the current and voltage signals are close to zero, the plasma is not visible. In the negative part of the current and voltage waveforms, the plasma is confined between the electrodes. During the positive part of the waveforms, the plasma is first confined between the electrodes (rising slope) and then, near the maximum of the curves, it leaves the glass tube in the form of a bullet. The dimensions of the bullet are of the order of a few millimeters. We calculated the speed of the bullet at ~20 km/s, depending on the position away from the end of the glass tube. The plasma bullet is much faster than the speed of the buffer gas flow (1 to 7 m/s). Thus we can conclude that our plasma source was not continuous, it consisted of very small plasma packages that traveled at a high speed. By varying the plasma parameters, the length and intensity of the plasma coming out of the tube can be adjusted.

For the two plasma devices operating at a much

Figure 6. Plasma jet at 5 slm, exposure time 2 ms, gate width 25 ns and gate delay from 0.4 to 12.4 µs [19].

higher frequency (13.56 MHz), the diagnostics was made by using homemade derivative probes in order to determine the power transmitted to the plasma and the operation mode of the discharge. The derivative probes were very sensitive; a numerical procedure for subtracting the displacement current based on accurate calibration of the system was performed so that it was possible to measure powers of the order of 0.1 W or less even with displacement current a couple of orders of magnitude larger than the plasma current.

Besides derivative probes, we used mass spectrometry to analyze the plasma products formed by a μ-APPJ [19] and by a plasma needle [20]. Several problems occurred during the setting up of the experiment; they are described in detail elsewhere [19, 20].

The analysis of the composition of neutrals and ions was motivated by the need to check which species are formed in the discharge. These results may be used as a test of plasma chemical models, to identify radicals and ions (that may be used after acceleration to induce damage to the tissue). The performance of the mass analyzer was tested and techniques were developed to produce data without the uncertainty induced by a contribution of the ionizer to possible dissociation. It was found that the predominant ions created by the plasma are O_2^+, O^+, H_3O^+, N_2^+, N^+, NO^+, OH^+ [19]. When it comes to plasma treatment of samples of biological origin, the chemically active species that are of interest are O, metastables O and O_2, OH, N, H_2O_2 and NO.

4. Plasma sterilization

The entry point for most groups dealing with plasma medicine is a study of sterilization. The effects on bacteria may be shown quickly, although it requires expertise in biomedicine. The benefit is that direct potential applications may be developed outside the realms of strict medical regulations. Yet, in situ sterilization, for example, treatment of wounds to prevent infection, would be a much more important goal. Following preliminary work on sterilization in microwave plasma, albeit at low pressure, we reinitiated the studies of plasma sterilization as a part of our plasma medical project. So far, a plasma needle has been used to induce killing of Streptococcus mutans and Escherichia coli bacteria in the form of planktonic samples. Also, we have the plasma interaction with normal, living cells; for these experiments we used human peripheral blood mesenchymal stem cells (hPB-MSC) as a model system to predict the degree of possible damage to the cell responses [21]. Many factors are responsible for bacterial inactivation. Direct exposure of the bacterial samples to the plasma appears to be more effective than remote exposure. Another factor that determines the efficiency of the specific treatment is the type [22] of bacteria, gram positive or gram negative. Very importantly, we studied the sterilization of bacteria in planktonic samples, where bacteria are dissolved in a small amount of liquid that would otherwise give it some protection from other agents. We showed that efficient sterilization of planktonic samples is not only possible, but may be efficient depending on the initial population [21].

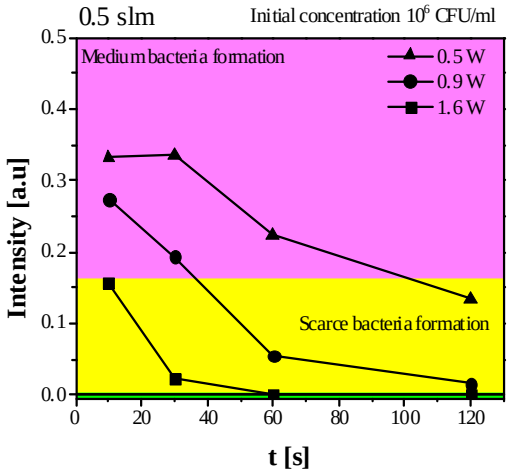

Figure 7. Treatment of MRSA biofilms of Staphylococcus aureus (ATCC 25923) by using plasma needle. Untreated sample showed STRONG bacteria formation (control intensity 0.65 a.u). Initial concentration of bacteria used was 10^6 CFU/ml.

One of the most serious problems in the hospital environment is bacterial contamination of surfaces with methicillin-resistant Staphylococcus aureus (MRSA) responsible for significant nosocomial infections. The pathogenic contaminants form biofilms, which are difficult to treat with routine biocides. The biofilm is not just a secured shelter

but a defense mechanism and a nutrition depot for pathogens. We show below the preliminary results of plasma treatment of the MRSA bacteria samples in the form of a biofilm.

In figure 7, we show the optical density of bacteria samples after plasma treatment for several different treatment times (10, 30, 60 and 120 s). The initial concentration of the samples was 10^6 CFU/ml, which corresponds to a measured optical density of 0.65 a.u. The buffer gas flow was 0.5 slm, but studies were also made as a function of the flow rate. The treatment efficiency increases with the increase of the treatment time and the mean power deposited to the plasma. For the highest power and only for the shortest treatment time of 10 s, there was scarcely bacteria formation; for the longer treatment, no bacteria formation was observed after the plasma treatment and yet there was very little or no heating of the gas.

Conclusions

We reviewed shortly our studies of atmospheric pressure plasmas and their application in biomedicine. In particular, we covered new results obtained with a plasma jet showing formation of plasma bullets and their properties as a function of geometry of electrodes and gas flow. In addition, we showd some practical results of sterilization using a plasma needle. The treatment of biofilms is essential, as are the studies of treatment of fungi, spores, prions and viruses. At the same time, one needs to extend the studies to specific medical problems associated with treatment of living organisms, including humans.

As far as plasma goes, some further optimization may be made for localized accurate treatment of cells or sterilization. With good knowledge of the power deposited into the plasma and control of the radicals that are produced, together with spatial emission profiles indicating changing of the regime of operation, a sufficient control over the reproducibility of the plasma needle operation was achieved. Other sources may be sought for more refined interaction with living cells. Different applications may seek more uniform sources extended over larger areas or even more localized treatment, which is all within the reach of the present day techniques.

Acknowledgements

This research has been supported by the MES, Serbia, under contract numbers ON171037 and III41011.

References

[1] Fridman A and Kennedy L A 2004 *Plasma Phys. Eng.* (New York: Taylor and Francis)
[2] Iza F, Kim G J A, Lee S M A, Lee J K A, Walsh A J, Zhang A Y and Kong M 2008 *Plasma Process. Polym.* **5** 322
[3] Stoffels E, Flikweert A J, Stoffels W W, and Kroesen G M W 2002 *Plasma Sources Sci. Technol.* **11**/4 383
[4] Puač N, Petrović Z Lj, Malović G, Đorđević A, Živković S, Giba Z and Grubišić D 2006 *J. Phys.* D: *Appl. Phys.* **39** 3514-19
[5] Fridman G, Friedman G, Gutsol A, Shekhter A B, Vasilets V N and Fridman A 2008 *Plasma Process. Polym.* **5** 503–33
[6] Sladek R E J, Stoffels E, Walraven R, Tielbeek P J A and Koolhoven R A 2004 *IEEE Trans. Plasma Sci.* **32**/4 1540-3
[7] Kieft I E, v d Laan E P and Stoffels E 2004 *New J. Phys.* **6** 149
[8] v d Gathen S V, Schaper L, Knake N, Reuter S, Niemi K, Gans T and Winter J 2008 Spatially resolved diagnostics on a microscale atmospheric pressure plasma jet *J. Phys.* D: *Appl. Phys.* **41** 194004
[9] Shi J, Zhong F, Zhang J, Liu D W and Kong M G 2008 *Phys. Plasmas* **15** 013504
[10] Yonson S, Coulombe S, Leveille V and Leask R L 2006 *J. Phys.* D: *Appl. Phys.* **39** 3508–13
[11] Fridman G, Shereshevsky A, Jost M M, Brooks A D, Fridman A, Gutsol A, Vasilets V and Friedman G 2007 *Plasma Chem. Plasma Process.* **27** 163–176
[12] v d Gathen S V, Buck V, Gans T, Knake N, Niemi K, Reuter St, Schaper L and Winter J 2007

Contrib. Plasma Phys. **47**/7 510
[13] Walsh J L and Kong M G 2008 *IEEE Trans. Plasma Sci.* **36** 1314
[14] Lu X and Laroussi M 2006 *J. Appl. Phys.* **100** 063302
[15] Walsh J L, Iza F, Janson N B, Law V J, Kong M G and Shi J 2010 *J. Phys.* D: *Appl. Phys.* **43** 075201
[16] Zhong F, Zhang J, Liu D W and Kong M G 2008 *Phys. Plasmas* **15** 013504
[17] Mericam-Bourdet N, Laroussi M, Begum A and Karakas E 2009 *J. Phys. D*: *Appl. Phys.* **42** 055207
[18] Shashurin A A, Shneider M N, Dogariu A, Miles R B and Keidar M 2009 *Appl. Phys. Lett.* **94** 231504
[19] Maletić D, Puač N, Malović G and Petrović Z Lj *unpublished*
[20] Malović G, Puač N, Lazović S and Petrović Z Lj 2010 Mass analysis of an atmospheric pressure plasma needle discharge *Plasma Sources Sci. Technol.* **19** 034014
[21] Lazović S, Puač N, Miletić M, Pavlica D, Jovanović M, Bugarski D, Mojsilović S, Maletić D, Malović G, Milenković P and Petrović Z Lj 2010 *New J. Phys.* **12** 083037
[22] Stoffels E, Sakiyama Y and Graves D B 2008 *IEEE Trans. Plasma Sci.* **36**/4 1441

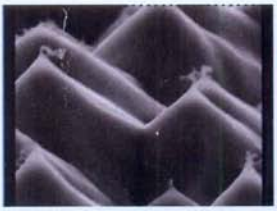
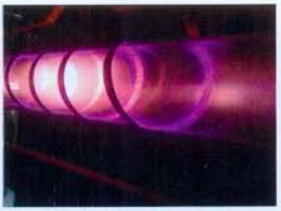


2wPNI

2ND INTERNATIONAL WORKSHOP ON PLASMA NANO-INTERFACES AND PLASMA CHARACTERIZATION

WORKSHOP PROCEEDINGS

March 1st-March 4th 2011 | Cerklje, Slovenia (EU)

2nd International Workshop on Plasma Nano-Interfaces and Plasma Characterization

Abstract book

March 1st — March 4th 2011, Cerklje, Slovenia

Editor: Uroš Cvelbar

Published by: Slovenian Society for Vacuum Technique (DVTS Društvo za vakuumsko tehniko Slovenije), Teslova 30, SI-1000 Ljubljana, Slovenia

Graphic design: Martina Modic

Printed by: Plasmabull

www: http://plazma.ijs.si/2wPNI/

Ljubljana, February 2011

Characterization of a large scale RF CCP reactor using derivative probes

S. Lazović[1], N. Puač[1], K. Spasić[1], G. Malović[1], Z. L. Petrović[1]

[1]Institute of Physics, Pregrevica 118, 11080 Belgrade, Serbia

lazovic@ipb.ac.rs

A large scale cylindrical CCP reactor was developed as a prototype of an industrial device, aiming to show that continuous treatment of textile rolls is possible. Discharge is large in volume (~2 m_3), homogeneous and stable from transitions to streamers and treatment effects are strongly dependant on the distance between the central electrode and the textile sample. Powered electrode is made of aluminum (1.13 m long) while chamber walls are the grounded electrode. Current and voltage derivative probes are used to obtain U-I characteristics as well as power delivered to the plasma, providing useful information on plasma operation mode. Measurements are performed in Argon at 400, 600, 800 and 1000 mTorr, for different powers given by the RF generator.

Langmuir probe measurements of a large scale RF CCP reactor

S. Lazović[1], N. Puač[1], K. Spasić[1], G. Malović[1], Z. L. Petrović[1]

[1]Institute of Physics, Pregrevica 118, 11080 Belgrade, Serbia

lazovic@ipb.ac.rs

A large scale cylindrical CCP reactor was developed as a prototype of an industrial device, aiming to show that continuous treatment of textile rolls is possible. Discharge is large in volume (~2 m_3), homogeneous and stable from transitions to streamers and treatment effects are strongly dependant on the distance between the central electrode and the textile sample. Powered electrode is made of aluminum (1.13 m long) while chamber walls are the grounded electrode. In this type of asymmetric discharge, concentrations of ions coming to the surface are decreasing when samples are placed further away from the powered electrode. Langmuir single probe (Hiden ESPION) which was placed side-on was used to perform measurements of the spatial profiles of ions and electrons. Measurements are performed in Argon at 400, 600, 800 and 1000 mTorr, for several distances from the powered electrode and for different powers delivered to the plasma.

Electrical probe measurements of an atmospheric pressure plasma bullet

D. Maletić[1], S. Lazović[1], N. Puač[1], G. Malović[1], A. Đorđević[2], Z. Lj. Petrović[1]

[1]Institute of Physics, Pregrevica 118, 11080 Belgrade, Serbia
[2]Faculty of Electrical Engineering, University of Belgrade, Bulevar kralja Aleksandra 73, 11000 Belgrade, Serbia

In the last few years atmospheric non-thermal plasmas increasingly attract interest. Potential use of the plasma bullet is very broad, biomedical application, material modification and as the ionization source for some analytical techniques. Plasma bullet operates in the range of 5-10 kV and 25-150 kHz. It is made of Pyrex glass tube (I.D. 4 mm; O.D. 6 mm) with two cylindrical electrodes made of copper foil (13 mm wide). We used helium as a buffer gas with flow of 2 to 7 slm. With high voltage probe we obtain voltage waveforms while current waveforms were measured at the resistor (100 kΩ) placed in the grounded branch of the electrical circuit. Measurements are performed for increasing and decreasing applied voltage and we observed hysteresis effect. RMS voltage/current values and mean power values are calculated from the signals acquired with the oscilloscope. It was possible to control the mean power and in all cases it is below 10 W. Low power is essential for biomedical applications and the treatment of temperature sensitive materials.

Time resolved ICCD images of an atmospheric pressure plasma bullet

D. Maletić[1], S. Lazović[1], N. Puač[1], G. Malović[1], A. Đorđević[2], Z. Lj. Petrović[1]

[1]Institute of Physics, Pregrevica 118, 11080 Belgrade, Serbia
[2]Faculty of Electrical Engineering, University of Belgrade, Bulevar kralja Aleksandra 73, 11000 Belgrade, Serbia

Plasma bullet is relatively new plasma source with wide specter of possible applications. Our plasma bullet is made of Pyrex glass tube (i. d. 4 mm and o. d. 6 mm), the electrodes were made of thin copper foil (13 mm wide) and the gap between the electrodes was 10 mm. Power supply was waveform generator connected to the LF amplifier and custom made HV transformer. The frequency that we used was 80 kHz and the applied voltage was in the range of 6-10 kVpeak-to-peak. In this paper we will show time resolved ICCD images of our plasma bullet device and how the emission changes with applied power and flow of working gas. Camera is synchronized with the excitation signal. In images plasma is consisted of a small plasma packages that leave the glass tube only in the positive peak of current. Power was calculated from the signal obtained from the probes, transmitted power to the plasma was lower than 10 W in all cases.

Plasma needle treatment of planctonic bacteria samples

D. Maletić[1], S. Lazović[1], N. Puač[1], M. Miletić[2], D. Pavlica[2], M. Jovanovic[2], G. Malović[1], P. Milenković[2], Z. Lj. Petrović[1]

[1]Institute of Physics, Pregrevica 118, 11080 Belgrade, Serbia
[2]Faculty of Stomatology, Dr. Subotića 8, 11000 Belgrade, Serbia

Because of its mild plasma, low gas temperature and geometry, the plasma needle is especially convenient for medical applications. This device can be used for non-contact disinfection of dental cavities and wounds, minimum-destructive precise treatment, as well as the removal of damaged tissue. Our measurements were performed on a standard size plasma needle that we originally used for the treatment of plant cells.

The bacteria cultures used are bacterial reference culture species *Staphycoccus aureus* ATCC (American Type Culture Collection) 25923, *Enterococcus faecalis* ATCC 29212, *Pseudomonas aeruginosa* ATCC 27853, and *Esherichia coli* ATCC 25922. We investigated the effect of the plasma needle discharge on different concentration of bacteria using several exposure times and power transmitted to the plasma. It was found that excellent removal of this and other bacteria may be achieved by the plasma needle treatment.

Diagnostics and applications of high frequency discharges

Conference Paper · January 2012

10 authors, including:

Slavko Mojsilović
University of Belgrade
59 PUBLICATIONS **298** CITATIONS
SEE PROFILE

Kosta Spasic
University of Belgrade
10 PUBLICATIONS **12** CITATIONS
SEE PROFILE

Gordana Malovic
Institute of Physics Belgrade
157 PUBLICATIONS **932** CITATIONS
SEE PROFILE

Diana Bugarski
Institute for Medical Research - Belgrade
60 PUBLICATIONS **421** CITATIONS
SEE PROFILE

Diagnostics and applications of high frequency discharges

N. Puač[1], M. Miletić[2], S. Mojsilović[3], S. Lazović[1], D. Maletić[1], K. Spasić[1], G. Malović[1], D. Bugarski[3], P. Milenković[2] and Z.Lj. Petrović[1]

[1]*Institute of Physics, University of Belgrade, Pregrevica 118, 11080 Belgrade, Serbia*

[2]*Faculty of Stomatology, University of Belgrade, Dr Subotića 8, 11000 Belgrade, Serbia*

[3]*Institute for Medical Research, University of Belgrade, Dr Subotića-starijeg 4, 11000 Belgrade, Serbia*

Non-equilibrium plasmas proved to be able to produce large variety of chemically reactive species at a low gas temperature while maintaining uniform reaction rates over relatively large areas. The choice of the plasma system used for treatment is usually guided by the type of samples that are treated and effect these plasmas are intended to have on the samples. Some of the samples cannot undergo vacuum and due to this fact non-thermal atmospheric pressure plasmas lately have drawn considerable attention with their enormous potential for technological applications in surface modifications and biomedical applications. So far we have used several different high frequency plasma sources operating from low to atmospheric pressure for treatments of polymer, textiles [1], graphene [2], seeds [3], sterilization of bacteria and treatment of plant and stem cells [4, 5]. In order to be able to effectively use these plasma systems in treatments that demand different conditions it was necessary to make detailed diagnostics of these systems. We have used home-made derivative probes, Langmuir and catalytic probe, ICCD camera and mass-energy analyser that works both in low and atmospheric pressures to determine the optimal treatment parameters for various samples.

This research has been supported by the MES Serbia, project III41011 and ON171037.

References

[1] M. Gorenšek, M. Gorjanc, V. Bukošek, J. Kovač, Z. Petrović and N. Puač, Textile Research Journal, 80(16), pp. 1633-1642, (2010)

[2] G. Isić, M. Jakovljević, M. Filipović, Đ. Jovanović, B. Vasić, S. Lazović, N. Puač, Z. Lj. Petrović, R. Kostić, R. Gajić, J. Humlček, M. Losurdo, G. Bruno, I. Bergmair and K. Hingerlf, Journal of Nanophotonics, 5, 051809(7pp), (2011)

[3] N. Puač, Z.Lj. Petrović, S. Živković, Z. Giba, D. Grubišić and A.R. Đorđević, Plasma Processes and Polymers, Eds. R. d'Agostino, P. Favia, C. Oehr and M.R. Wertheimer, Whiley-VCH, p 193-203, (2005)

[4] N. Puač, Z.Lj. Petrović, G. Malović, A. Đorđević, S. Živković, Z. Giba and D. Grubišić, Journal of Physics D: Applied Physics, 39, p 3514-3519, (2006)

[5] S. Lazović, N. Puač, M. Miletić, D. Pavlica, M. Jovanović, D. Bugarski, S. Mojsilović, D. Maletić, G. Malović, P. Milenković and Z. Lj. Petrović, New Journal of Physics, 12, 083037 (21pp), (2010)

Characterization of a large scale RF CCP reactor using Langmuir and derivative probes

Article

6 authors, including:

Saša Lazović
Institute of Physics Belgrade
70 PUBLICATIONS **212** CITATIONS
SEE PROFILE

Kosta Spasic
University of Belgrade
10 PUBLICATIONS **12** CITATIONS
SEE PROFILE

Gordana Malovic
Institute of Physics Belgrade
157 PUBLICATIONS **932** CITATIONS
SEE PROFILE

Zoran Lj Petrović
Institute of Physics Belgrade
510 PUBLICATIONS **5,652** CITATIONS
SEE PROFILE

Characterization of a large scale RF CCP reactor using Langmuir and derivative probes

Saša Lazović, Nevena Puač, Kosta Spasić, Gordana Malović and Zoran Lj. Petrović

Institute of Physics, Pregrevica 118,11080 Belgrade, Serbia

University of Belgrade, Studentski trg 1, 11080 Belgrade, Serbia

Abstract: A large scale cylindrical CCP reactor was developed as a prototype of an industrial device, aiming to show that continuous plasma treatment of textile rolls at low pressures is possible. Discharge is large in volume (~3 m^3), homogeneous and free from transitions to streamers. Treatment effects are strongly dependant on the distance between the central electrode and the textile sample. Powered electrode is made of aluminum (1.5 m long) while chamber walls are the grounded electrode. In this type of asymmetric discharge, concentrations of ions coming to the surface are decreasing when samples are placed further away from the powered electrode. Langmuir probe (Hiden ESPION) which was placed side-on was used to perform measurements of the spatial profiles of ions and electrons. Current and voltage derivative probes are used to obtain U-I characteristics as well as power delivered to the plasma, providing useful information on plasma operation mode. Measurements are performed in Argon at 400, 600, 800 and 1000 mTorr, for several distances from the powered electrode and for different powers delivered to the plasma.

Keywords: large scale asymmetric cylindrical RF CCP reactor, Langmuir probe, current and voltage derivative probes

1. Introduction

Radiofrequency discharges are necessary for treatment of isolators and semiconductors [1]. Different kinds of conductive and non-conductive materials like microelectronics devices [2-4], biological samples [5] and textiles [6] can be treated using capacitively coupled RF plasmas. In our laboratory a large scale CCP RF reactor was developed in order to cheaply and uniformly treat textile rolls without damaging the surface of the fibers. Homogeneous and stable plasma, without transition to streamers, capable of long term stable operation (i.e. treatments) was achieved. Detailed electrical characterization of the plasma reactor is however required because it can provide information on the relations between external discharge properties (current and voltage waveforms, impedance) and plasma parameters (densities, energies, fluxes of charged particles).

Textile samples can be placed in the chamber on several distances from the powered electrode providing various intensities of treatment. Langmuir probe measurements are performed in argon, for different distances, powers and pressures of the working gas. Ion and electron concentrations are obtained at the places were textile sample would be placed. These measurements show complex spatial dependences of the concentrations and are important

for proper characterization of treating procedures. Current-voltage properties and power delivered to plasma can be measured using derivative probes.

2. Experimental setup

The discharge chamber is 2.5 m long and 1.17 m in diameter and made of stainless steel. Powered electrode is placed axially in the centre of the chamber and is 1.5 m long, 3 cm in diameter and made of aluminium. The chamber has a platform at the bottom where samples are placed. The distance between the platform and the powered electrode is adjustable by moving the platform. Distances for the Langmuir probe measurements were chosen within this range. Outer chamber wall is the grounded electrode. The rest of the electrical circuit consists of RF power generator Dressler Cesar 1010 in combination with Variomatch matching network. Derivative probes are placed into a stainless steel box opposite to each other. The box is placed as close as possible to the powered electrode. Low pressures are maintained using mechanical vacuum pump with a constant flow of gas air (see Fig.1).

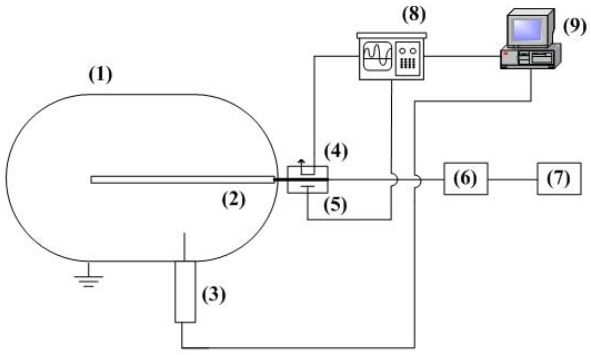

Figure 1. Experimental set-up: (1) Chamber, (2) Powered electrode, (3) ESPION system, (4) Current probe, (5) Voltage probe, (6) Variomatch, (7) Power supply, (8) Oscilloscope, (9) Computer

Instantaneous voltages and currents are monitored using derivative probes which were connected to the oscilloscope with cables of identical length. All waveforms are collected by the computer for further analysis.

Hiden Analytical ESPION advanced Langmuir probe system is placed side-on. The system has a linear motion drive which enables probe positioning with the minimal spatial resolution of 0.1 mm. Measurements were made in the range of pressures from 400 mTorr to 1 Torr. We have used platinum probe tip, 5 mm long and 0.15 mm in diameter. Linear motion drive was used to position the probe at the distances 50.5 cm to 20.5 cm from the powered electrode. Measurements of U-I curves were made for all those positions of Langmuir probe.

At every position 50 measurements were made each being an average of 10 scans with pre-cleaning for each measurement. It was observed that even with pre-cleaning it is better to neglect the first few measurements because of the probe contamination until results become stable. After that, the U-I curves were smoothed and data was processed using Hiden ESPSoft.

3. Results and discussion

3.1. Derivative probes measurements

Waveforms acquired by current and voltage derivative probes are further processed using Fast Fourier Transform procedure. Signals are then calibrated in the frequency domain and converted back to time domain using Inverse Fast Fourier Transform showing the real signal shapes. Figure 2. shows current and voltage signals after numerical procedures (for Argon at different pressures 400, 600, 800 and 1000 mTorr). Power at RF generator was 200 W (forward minus reflected power).

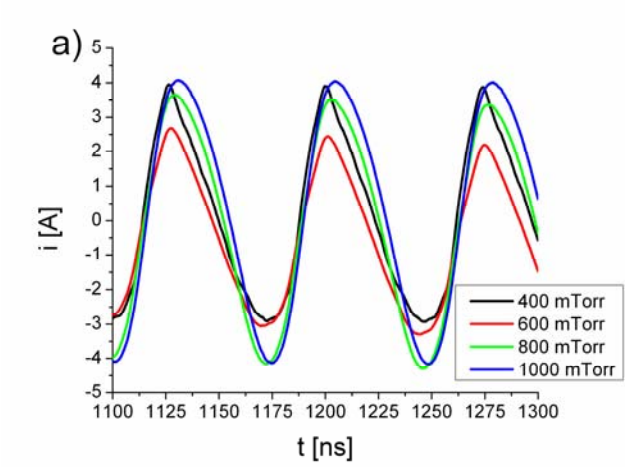

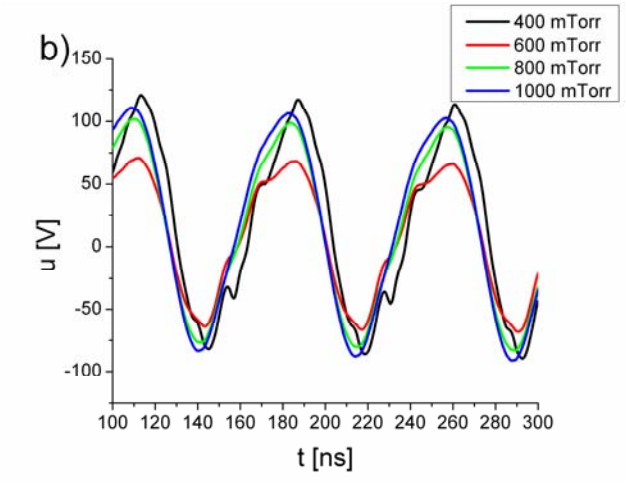

Figure 2. Derivative probe measurements of a) current and b) voltage waveforms for Argon discharge at 400, 600, 800 and 1000 mTorr. Power at the RF generator was 200 W.

Current signals are in the range of 5.5 A to 8.5 A peak to peak, and voltage is ranging from 130 V to 200 V peak to peak. At lower pressures (400 and 600 mTorr) current waveform has a saw tooth like shape and at higher pressures (800 and 1000 mTorr) it becomes more sinusoidal.

Voltage waveforms clearly indicate a presence of higher harmonics, especially at 400 and 600 mTorr. At higher pressures, waveforms become more sinusoidal. Generation of higher harmonics is due to geometrical asymmetry of the discharge chamber and due to the nonlinear nature of plasma impedance. In this configuration, having grounded electrode with a large area, and metal platform at the bottom for placing the samples, current paths can be very different in different parts of the chamber [7]. More detailed derivative probe and Langmuir probe measurements in different current branches would prove useful in an attempt to determine equivalent discharge chamber circuit, putting more light on the links between external and internal plasma parameters. Our main objective was to obtain homogeneous and stable plasma, find optimal treatment conditions and provide reproducible treatments based on electrical measurements. Power delivered to plasma, V-I characteristic and impedance of the discharge can also be calculated.

3.2. Langmuir probe measurements

Langmuir probe (Hiden ESPION) was placed perpendicular to the powered electrode. Measurements were performed for distances of 20.5 cm, 30.5 cm, 40.5 cm and 50.5 cm from the powered electrode in Argon at 400 mTorr and 1000 mTorr and powers at RF generator in range from 100 W to 300 W. At the lowest pressure (400 mTorr) both electron and ion concentrations are slightly lower than at 1000 mTorr (compare Figure 3. a) and b)). Electron concentrations are almost constant for all probe positions (see Figure 3.), while ion concentrations are decreasing by more than an order of magnitude as probe is placed closer to the grounded chamber wall (40.5 cm and 50.5 cm).

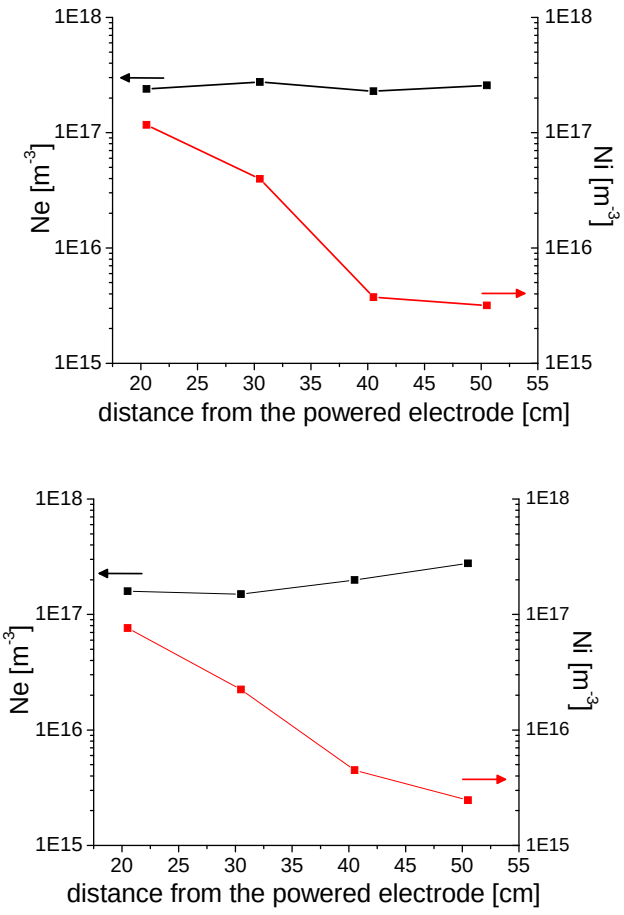

Figure 3. Electron and ion concentrations in Argon discharge at a) 400 mTorr and b) 1000 mTorr. Power at the RF generator was 300 W for both pressures.

Treatment effects of different kinds of materials strongly depend on ion concentrations and energies.

We can see that by placing the samples at different positions from the powered electrode we can control the concentrations of ions coming to the sample surface and therefore achieve different treating effects. Fine ion concentration adjustment in a range of almost two orders of magnitude (from $1e^{15}$ to $1e^{17}$ m^{-3}) can be achieved by precise positioning of the samples without changing power or pressure.

4. Conclusion

A large scale asymmetric RF CCP reactor at 13.56 MHz has been diagnosed by using derivative and Langmuir probes. Working gas was Argon and measurements by using derivative probes were committed for pressures of 400, 600, 800 and 1000 mTorr. Presented Langmuir probe results are obtained at 400 and 1000 mTorr for the power of 300 W given by the RF generator. Electron and ion concentrations were measured for several distances from the powered electrode (20.5, 30.5, 40.5 and 50.5 cm). It was found that shape of the current and voltage waveforms is changing with changing the gas pressure due to changing in plasma impedance and generation of higher harmonics. Current signals are in the range from 5.5 A to 8.5 A and voltage from 130 V to 200 V peak to peak.

For proper plasma treatment characterization and reproducibility, electron and ion concentrations were measured. Electron concentrations are found to be almost constant with changing the distance between the Langmuir probe and the powered electrode. Ion concentrations are changing in the range from $1e^{15}$ to $1e^{17}$ m^{-3} and are decreasing rapidly when moving away from the powered electrode. Changing of the distance between the sample and the powered electrode, ma be used to control ion concentrations and treatment of the surfaces.

References

[1] A. Bogaerts et al. / Spectrochimica Acta Part B 57 (2002) 609–658

[2] M.A. Lieberman, A.J. Lichtenberg, Principles of Plasma Discharge and Materials Processing, (2005) (Wiley:Hoboken);

[3] T. Makabe, Z.Lj. Petrović, Plasma Electronics, (2006) (Taylor and Francis:New York);

[4] U. Cvelbar, K. (Ken) Ostrikov and M. Mozetic, Nanotechnology 19 (2008) 405605.

[5] N. Puač, Z.Lj. Petrović, S. Živković, Z. Giba, D. Grubišić and A.R. Đorđević, Plasma Processes and Polymers, (2005) 193, (Whiley)

[6] M. Radetić, P. Jovančić, N. Puač and Z.Lj. Petrović, Workshop on Nonequilibrium Processes in Plasma Physics and Studies of the Environment, SPIG 2006, Journal of Physics: Conference Series 71 (2007) 012017

[7] M. A. Sobolewski, IEEE Transactions on Plasma Science 23 (1995) 1006

Spatial profiles of atomic oxygen concentrations in a large scale CCP reactor

Article

7 authors, including:

Kosta Spasic
University of Belgrade
10 PUBLICATIONS **12** CITATIONS
SEE PROFILE

Gordana Malovic
Institute of Physics Belgrade
157 PUBLICATIONS **932** CITATIONS
SEE PROFILE

Miran Mozetic
Jožef Stefan Institute
287 PUBLICATIONS **3,708** CITATIONS
SEE PROFILE

Zoran Lj Petrović
Institute of Physics Belgrade
510 PUBLICATIONS **5,652** CITATIONS
SEE PROFILE

Spatial profiles of atomic oxygen concentrations in a large scale CCP reactor

S. Lazović[(*)1,2], K. Spasić[1], N. Puač[1], G. Malović[1], U. Cvelbar[2], M. Mozetič[2], Z. LJ. Petrović[1]

[1] *Institute of Physics, University of Belgrade, Pregrevica 118, 11080 Belgrade, Serbia*
[2] *Jozef Stefan Institute, Jamova 39, 1000 Ljubljana, Slovenia*
[(*)] lazovic@ipb.ac.rs

Nickel catalytic probe was used to measure atomic oxygen concentrations in a large scale cylindrical asymmetrical capacitively coupled plasma reactor. We have measured O concentrations in the main chamber of the reactor as well as in the side tube placed perpendicular to the chamber wall. The spatial profiles in these two regions differ both in magnitude (10^{19} m^{-3}vs. 10^{18} m^{-3} or even 10^{17} m^{-3}) and in the way the concentrations decrease when moving away from the powered electrode. This is explained by the different chamber wall configuration around the probe and its proximity because the grounded walls are also O atom drain due to the recombination. Working gas was air at 300 and 600 mTorr and the power was fixed at 500W.

Low temperature plasmas at sub-atmospheric pressures are an essential tool in many industrial processes due to variety of chemical reactions that can be induced and controlled while maintaining low gas temperatures. Low pressure radiofrequency plasmas are irreplaceable in the semiconductor industry but this is hardly the only field of their application [1, 2]. A large scale cylindrical asymmetrical 13.56 MHz CCP reactor was developed in our laboratory for the purpose of textile, polymer and seeds modification [3, 4]. Sensitive material treatment requires low ion energy bombardment and high concentrations of active species like O. For instance the formation of new oxygen-containing groups on the fiber surface is suggested to be due to the presence of extremely reactive atomic oxygen species in discharge during the air plasma processing and/or post-plasma chemical reactions when the activated fiber surface reacts with environmental species [5]. The asymmetric design of the reactor was chosen to provide low energies of ions bombarding the surfaces of the samples in order to avoid excessive damage of the samples.

We have used nickel catalytic probe positioned side-on to the powered electrode to measure O concentrations in the main chamber and in the small side tube (see Fig 1.).

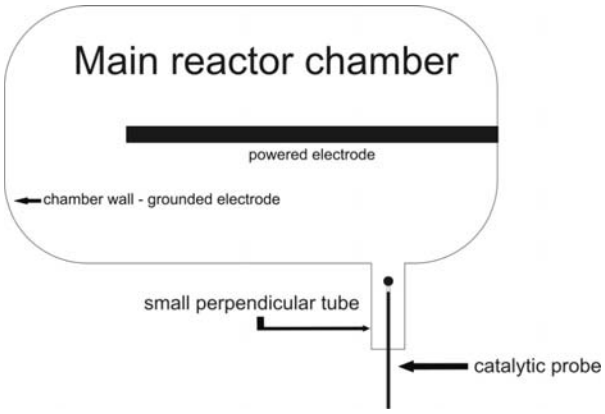

Fig. 1: Catalytic probe position in the reactor.

Detailed experimental setup details can be found elsewhere [6] as well as the design and the operation of the catalytic probe [7, 8]. Measurements are performed in air at 300 and 600 mTorr. The power was fixed at 500 W.

Spatial profiles of O concentrations are shown at Fig 2. We can see that the concentrations are higher at higher pressure and are decreasing faster in the side tube compared to the main chamber when moving away from the powered electrode. This is due to the difference in the vicinity and the area of the grounded wall which is closest to the probe at certain position.

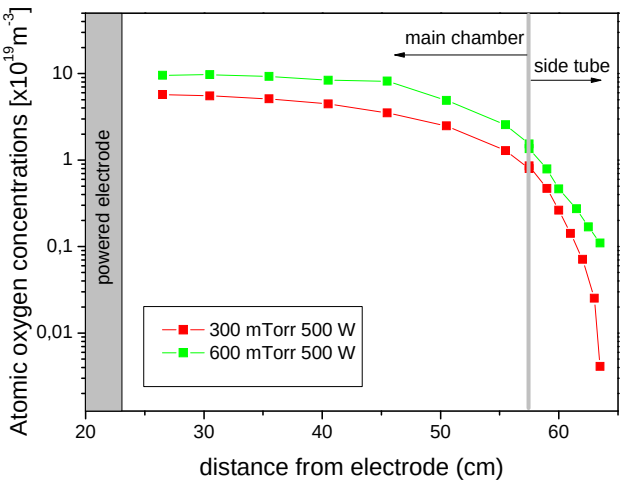

Fig. 2: Atomic oxygen spatial profiles in the main reactor chamber and in the side tube. Working gas was air at 300 and 600 mTorr and the power was fixed at 500 W.

The surface recombination of O atoms is taking place at the surface of both the nickel catalytic probe and at the chamber wall. In the tube, the wall is a stronger O atom drain both because it is closer and because the effective area is larger. By placing the sample at different distances from the powered electrode O concentrations can be controlled in the range from 10^{17} m^{-3} to $10^{19}m^{-3}$. Depending on the intrinsic properties of the material being treated and on the modification effects that are desired we can tune the O concentrations at the sample surface simply by putting the sample in one of two regions of the reactor (main chamber and side tube) and adjusting its position. Adjustment can also be achieved by changing the pressure, power and gas composition.

References

[1] T. Makabe, Z.Lj. Petrović, *Plasma Electronics*, (2006) (*Taylor and Francis, New York*).
[2] M.A. Lieberman, A.J. Lichtenberg, *Principles of Plasma Discharge and Materials Processing*, (2005) (*Wiley, Hoboken*).
[3] N. Puač, Z.Lj. Petrović, M. Radetić and A. Đorđević, *Materials Science Forum*, **494** (2005) 291-296.
[4] M. Radetić, P. Jovančić, N. Puač and Z.Lj. Petrović, *Workshop on Nonequilibrium Processes in Plasma Physics and Studies of the Environment*, SPIG 2006, *Journal of Physics: Conference Series* **71** (2007) 012017.
[5] V. Ilić, Z. Šaponjić, V. Vodnik, S. Lazović, S. Dimitrijević, P. Jovančić, J. M. Nedeljković and M. Radetić, *Ind. Eng. Chem. Res.* **49** (2010) 7287–7293.
[6] S. Lazović, N. Puač, K. Spasić, G. Malović, U. Cvelbar, M. Mozetič, Z. Lj. Petrović, *30th ICPIG*, August 28th – September 2nd (2011).
[7] T.Vrlinic, C. Mille, D. Debarnot, F. Poncin-Epaillard, *Vacuum* **83** 5 (2009) 792–796.
[8] M. Mozetic, A. Vesel, U. Cvelbar, A. Ricard, *Plasma Chem Plasma P* **26** (2006) 103–117.

IUVSTA62 Workshop

62ND IUVSTA WORKSHOP ON PLASMA SYNTHESIS AND MODIFICATION OF NANOMATERIALS

June14th-June18th 2010 | Lake Bohinj, Slovenia (EU)

62ND IUVSTA WORKSHOP

ON

PLASMA SYNTHESIS AND MODIFICATION OF NANOMATERIALS

Invited talks

June 14th — June 18th 2010, Lake Bohinj, Slovenia

Editors: Uroš Cvelbar and Miran Mozetič

Published by: Slovenian Society for Vacuum Technique (DVTS Društvo za vakuumsko tehniko Slovenije), Teslova 30, SI-1000 Ljubljana, Slovenia

Graphic design: Kristina Eleršič

Printed by: Infokart d.o.o., Ljubljana

Cover image: Prof. M.K.Sunkara group, University of Lousiville, USA

www: http://plazma.ijs.si/iuvsta62/

Ljubljana, June 2010

18.30		
19.00-20.30		Dinner

Thursday

7.30-9.30		Breakfast
9.30-12.20	Vogel alt. 1600 m - cable car	
12.20-15.00		Lunch
15.00-15.40	W. Choe	TiO2 catalyst assisted atmospheric pressure plasma for inactivation enhancement of bacterial spores (invited)
15.40-16.20	Z. Lj. Petrović	Diagnostics of atmospheric pressure discharges from biomedical applications and treatment of sensitive materials (invited)
16.20-17.00	J. Kovač	Surface characterization of air-plasma activated textile surfaces and deposition of nanoscale functional coatings for packaging (invited)
17.00-17.10		Break
17.10-17.50	M.K. Sunkara	Bulk production of nanowires in atmospheric microwave plasma reactor (invited)
17.50-18.30	S. Xu	Reactive plasmas: from custom-designed nanoclusters to next generation of renewable energy (invited)
19.00-22.00		Dinner

Friday

7.30-9.30	Breakfast
9.30-12.20	Discussion on Plasma Nanoscience for Renewable Energy
12.20-15.00	Lunch
15.00-16.00	Departure

Diagnostics of atmospheric pressure discharges for biomedical applications and treatment of sensitive materials

Z. Lj. Petrović[1], N. Puač[1], S. Lazović[1], M. Miletić[2], D. Pavlica[2], M. Jovanović[2], D. Bugarski[3], S. Mojsilović[3], D. Maletić[1], P. Milenković[2] and G. Malović[1]

[1] Institute of Physics, Pregrevica 118, 11000 Belgrade, Serbia
[2] Faculty of Stomatology, Dr Subotića 8, 11000 Belgrade, Serbia
[3] Institute for the Medical Research, Dr Subotića - starijeg 4

zoran@ipb.ac.rs

Constantly growing field of biomedical applications is a new frontier that drives the the development of plasma sources [1-3]. Sterilization of medical equipment, treatment of wounds and dental caries are only examples of well established applications that indicate an even wider breadth of potential applications that may be offered by cold plasmas.

The necessity to use plasma for *in-vivo* treatments/procedures has led to several requirements for plasma sources to meet. The most obvious one is that biomedical plasmas have to operate at atmospheric pressure in most cases. The other requirement is that the gas temperature should not exceed 40 °C. The secret of generating atmospheric pressure non-equilibrium plasma is in control of ionization before density of the charged particles starts favoring momentum transfer from electrons to heavy particles through Coulomb interaction. Apart from inhomogeneous fields, dielectric barriers and pulsed or high frequency fields a popular technique that is often combined with some of the previously mentioned modes of supplying power is that to mix a flow of rare gas with the atmosphere thus allowing the discharge to be generated at lower voltages. At the same time mixing with the atmospheric gases in the region of the discharge leads to production of a number of radicals.

We have studied the following plasma sources: corona discharge, plasma needle, micro atmospheric pressure plasma jet, atmospheric pressure jet and wide area dielectric barrier discharge for treatment of textiles. At the same time we have employed different diagnostics methods: atmospheric pressure mass/energy analyzer to establish which radicals and ions are formed and their energies as sample by the system, derivative probes to determine the power given to the plasma and help control heating of the gas, ICCD camera to analyze the anatomy and modes of operation and we analyzed the effect of plasmas on textile fibers or living micro organisms as another technique to compare effects and processes due to different sources.

Most of our studies so far focused on the plasma needle. There are many types of plasmas that can be generated under ambient pressure and temperature conditions, plasma needle is best suited for the need for precise and localized treatments [4]. Because of its mild plasma, low gas temperature and geometry, the plasma needle is especially convenient for medical applications (see Figure 1). This device can be used for non-contact disinfection of dental cavities and wounds, minimum-destructive precise treatment, as well as the removal of damaged tissue. Our measurements were performed on a standard size plasma needle that we originally used for the treatment of plant cells [3].

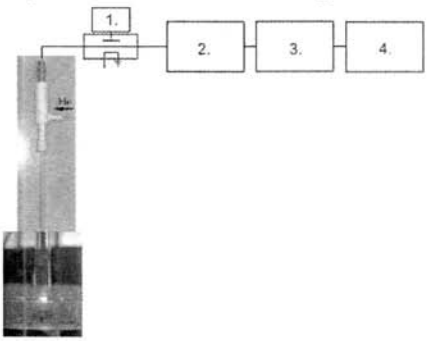

Figure 1. Experimental setup used in treatments: 1. oscilloscope connected to current and voltage derivative probes; 2. matching network; 3. amplifier; 4. signal generator.

Mass spectrometry of the plasma needle was performed by using Hiden HPR60 mass-energy spectrometer [5-7]. We present the measured densities of all particles as yields (percentage in the total detected flux of ions or neutrals) to avoid misrepresentation of fluctuations in the flux. When it comes to plasma treatment of samples of biological origin ions that are of interest are O^+, N^+ and NO^+ while the most important radicals are N, O and NO. We can see that the most abundant ions created in the plasma are NO^+ ions which are believed to be among the key factors in treatment of cells or tissues (see Figure 2). The observed NO^+ ions are definitely the result of chemical reactions rather than ionization of NO, while both N^+ and O^+ may be created directly from the more abundant molecules in dissociative ionization. Only a small amount of O_3 was observed but following a technique shown here one could work towards reducing the amount of ozone even further. On the other hand significant amounts of O,N and NO were detected. Dependence of the radicals and NO on power may reveal the relevant chemical processes.

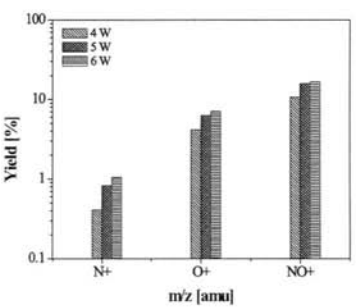

Figure 2. Yields of N^+, O^+ and NO^+ ions created in the discharge for 3 different powers.

Measurements of power delivered to the plasma itself were performed by using derivative voltage and current probes [3]. Power as a parameter provides information needed to control the heating of the target and enables us to repeated treatments with the same or very similar plasmas every time.

ICCD camera was used in order to obtain light emission from the discharge and to detect under which conditions transition in operating modes of plasma needle occurs [8]. So far, Sakiyama and Graves showed that this mode transition does not correspond to α-γ transition, but that this is only transition from corona to glow mode [9]. Initially, discharge is ignited in 'corona' mode where there is no grounded electrode and the discharge itself is contained at the tip of the needle. With the power increase we can observe transition of discharge to the glow mode where target's surface acts as grounded electrode. In this case discharge spreads itself over a larger area. The corona mode may be more suitable for surface processing in which we need to localize the treatment to a region as small as possible. On the other hand, more rapid and uniform treatment is expected under glow mode conditions.

We have studied effect of the plasma needle on different living cells, from plants [3] through microorganisms such as Escherichia coli and Staphylococcus aureus to the human peripheral blood mesenchymal stem cells (hPB-MSC), as a model system to predict the degree of possible damage to the human cells. The results support application of the plasma needle in treatments of light bacterial infections, such as in vivo sterilization of skin and dental cavities. We also considered other potential applications, including high-precision removal of pathological cells or tissues (cancer, peeling, removal of scars), but without excessive damage to the body, or the improvement of wound healing by controlling cell adhesion.

Results using corona discharge, micro atmospheric pressure plasma jet, atmospheric pressure jet and wide area dielectric barrier discharge will also be shown. Recently, several investigators reported on various means of generating cold plasma jets at atmospheric pressure. More interestingly, these jets turned out not to be a continuous plasmas but trains of small high velocity plasma packets-bullets. We have constructed plasma jet (see Figure 3) that can operate in the frequency range form 25-100 kHz. Helium gas flow was varied from 1 up to 7 slm was used as the basis and some preliminary results will be shown.

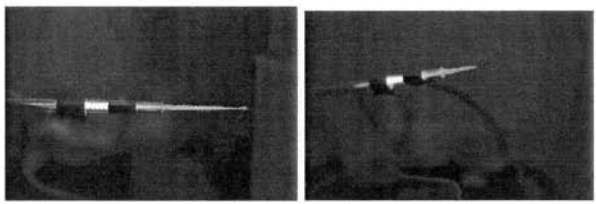

Figure 3. Atmospheric pressure plasma jets with a possibility of operating in the plasma bullet regime.

Finally we shall consider the applicability of all the above mentioned plasmas and micro discharges in general for nanotechnologies and nanomaterial generation or modifications [10].

References

[1] A. Fridman and L. A. Kennedy. *Plasma Physics and Engineering*. Taylor and Francis, 2004.

[2] F. Iza, G. J. Kim , S. M. Lee, J. K. Lee, J. L. Walsh, Y. T. Zhang and M. G. Kong. Microplasmas: Sources, particle kinetics, and biomedical applications. *Plasma Process. Polym.*, 5: 322–344, 2008

[3] N. Puač, Z.Lj. Petrović, G. Malović, A. Đorđević, S. Živković, Z. Giba and D. Grubišić, Measurements of voltage–current characteristics of a plasma needle and its effect on plant cells, Journal of Physics D: Applied Physics, 39, 3514'3519, 2006

[4] E. Stoffels, A. J. Flikweert, W. W. Stoffels, and G. M. W. Kroesen. Plasma needle: a non-destructive atmospheric plasma source for fine surface treatment of (bio)materials. *Plasma Sources Sci. Technol.*, 11: 383 2002

[5] G. Malović, N. Puač, S Lazović, Z. Lj. Petrović. Mass analysis of atmospheric pressure plasma needle discharge. *Plasma Sources Sci. Technol.*, accepted 2010

[6] S. Lazović, N. Puač, G. Malović, A. Đorđević and Z. Lj. Petrović. Diagnostics of plasma needle properties by using mass spectrometry. *Chem. Listy*, 102: s1383-s1387, 2008

[7] N.Puač. Development, diagnostic and applications of radio-frequency plasma reactor. *Journal of Physics: Conference Series,* 133(1): 012007 2008

[8] N. Puač, S. Lazović, G.Malović, A. Đorđević and Z. Lj. Petrović, unpublished

[9] Y. Sakiyama and D. B. Graves. Corona-glow transition in the atmospheric pressure RF-excited plasma needle. *J. Phys. D: Appl. Phys.* 39: 3644–3652, 2006

[10] Z. Lj. Petrović, P. Maguire, M. Radmilović-Rađenović, M. Radetić, N. Puač, D. Marić, C. Mahony, G. Malović, On application of plasmas in nanotechnologies, In "Nanoscale Science and Technology Applications in Electronics, Photonics, Sensing and Renewable Energy" Ed. A. Korkin, P.Krstic and J. Wells,, Springer verlag 2010.

Electrical characteristics of an atmospheric pressure plasma jet with helium flow

Conference Paper · October 2010

READS
30

6 authors, including:

Gordana Malovic
Institute of Physics Belgrade
157 PUBLICATIONS **932** CITATIONS
SEE PROFILE

Dejan Maletic
Institute of Physics Belgrade
53 PUBLICATIONS **97** CITATIONS
SEE PROFILE

Saša Lazović
Institute of Physics Belgrade
70 PUBLICATIONS **212** CITATIONS
SEE PROFILE

Zoran Lj Petrović
Institute of Physics Belgrade
510 PUBLICATIONS **5,652** CITATIONS
SEE PROFILE

BULLETIN

OF THE AMERICAN PHYSICAL SOCIETY

63rd Gaseous Electronics Conference & 7th International Conference on Reactive Plasmas

October 4 – 8, 2010, Paris, France

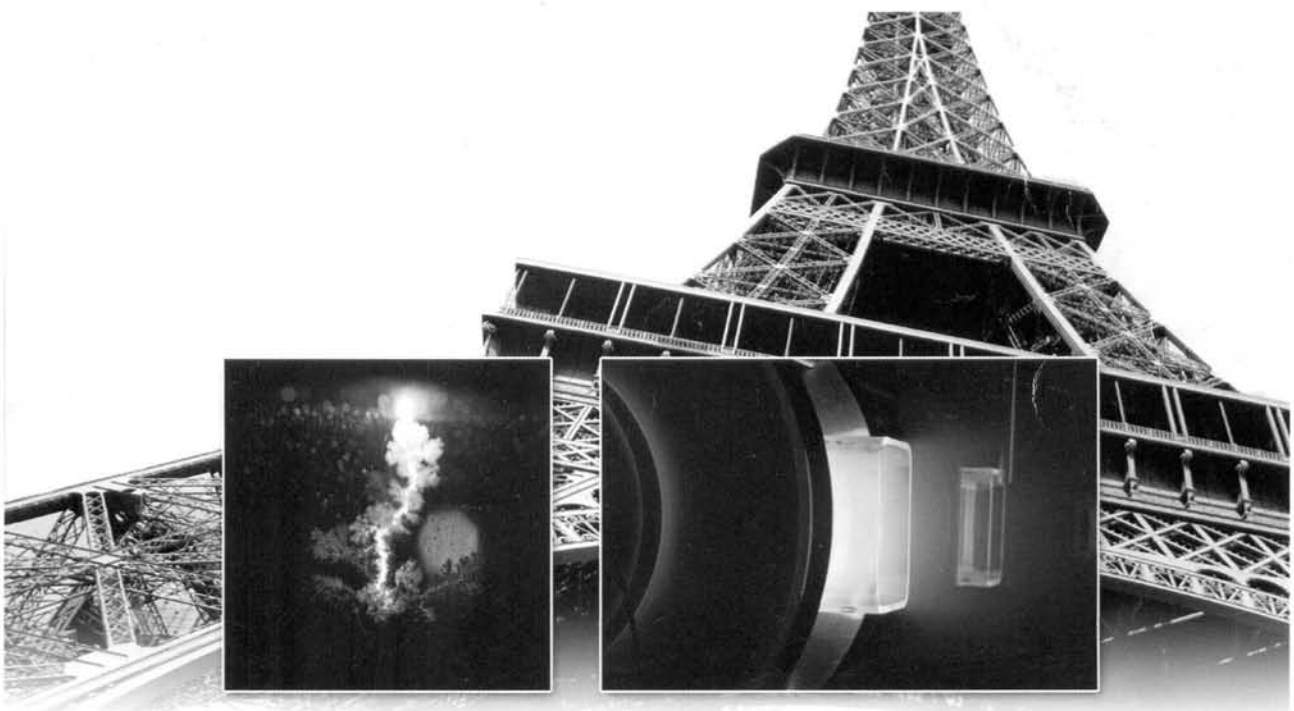

Laboratoire de Physique des Plasmas, École Polytechnique - CNRS

October 2010

Volume 55, No. 7

APS physics

BULLETIN
OF THE AMERICAN PHYSICAL SOCIETY

Coden BAPSA6 ISSN: 0003-0503
Series II, Vol. 55, No. 7 **October 2010**

APS COUNCIL 2010

President
Curtis G. Callan, Jr.,* *Princeton University*

President-Elect
Barry C. Barish,* *California Institute of Technology*

Vice President
Robert L. Byer,* *Stanford University*

Executive Officer
Kate P. Kirby,* *Harvard-Smithsonian Center for Astrophysics (Retired)*

Treasurer
Joseph W. Serene,* *Georgetown University (Emeritus)*

Editor in Chief
Gene D. Sprouse,* *State University of New York, Stony Brook (On Leave)*

Past-President
Cherry A. Murray,* *Harvard University*

General Councillors
Robert Austin, Elizabeth Beise,* Marcela Carena, Marta Dark McNeese, Katherine Freese, Nergis Mavalvala, Warren Mori, Jorge Pullin

Division, Forum and Section Councillors
Neil Cornish (*Astrophysics*), P. Julienne (*Atomic, Molecular & Optical Physics*), Mark Reeves (*Biological*), Nancy Levinger (*Chemical*), Arthur Epstein (*Condensed Matter Physics*), David Landau (*Computational*), James Brasseur* (*Fluid Dynamics*), Gay Stewart (*Forum on Education*), Amber Stuver* (*Forum on Graduate Student Affairs*), Michael Riordan (*Forum on History of Physics*), Stefan Zolner* (*Forum on Industrial and Applied Physics*), Herman Winick (*Forum on International Physics*), Philip "Bo" Hammer (*Forum on Physics and Society*), Steven Rolston (*Laser Science*), Ted Einstein (*Materials*), Wick Haxton (*Nuclear*), Marjorie Corcoran (*Particles & Fields*), John Galayda (*Physics of Beams*), David Hammer* (*Plasma*), Scott Milner (*Polymer Physics*), Heather Galloway* (*Texas Section*), Bruce Barrett (*Four Corners Section*)

Members of the APS Executive Board

Scientific Program Coordinator:
Vinaya K. Sathyasheelappa

APS MEETINGS DEPARTMENT
One Physics Ellipse
College Park, MD 20740-3844
Telephone: (301) 209-3286
Fax: (301) 209-0866
Email: meetings@aps.org
Donna Baudrau, *Director of Meetings & Conventions*
Terri Gaier, *Assistant Director of Meetings & Conventions*
Don Wise, *Registrar*
Christine Lenihan, *Meetings Program Coordinator*

International Councillor
Belita Koiler

Chair, Nominating Committee
Angela Olinto

Chair, Panel on Public Affairs
Robert Socolow

ADVISORS

Representatives from other Societies
Fred Dylla, *AIP*; David M. Cook, *AAPT*

International Advisors
Louis Felipe Rodriguez Jorge, *Mexican Physical Society*; Robert Mann, *Canadian Association of Physicists*

Staff Representatives
Alan Chodos, *Associate Executive Officer*; Amy Flatten, *Director of International Affairs*; Ted Hodapp, *Director of Education and Outreach*; Michael Lubell, *Director, Public Affairs*; Dan Kulp, *Editorial Director*; Christine Giaccone, *Director, Journal Operations*; Michael Stephens, *Controller and Assistant Treasurer*

Administrator for Governing Committees
Ken Cole

Please Note: APS has made every effort to provide accurate and complete information in this *Bulletin*. However, changes or corrections may occasionally be necessary and may be made without notice after the date of publication. To ensure that you receive the most up-to-date information, please check the meeting Corrigenda distributed with this *Bulletin*.

perature and sheath voltage as the ion sheath is. However, electron sheath is about 1.6 times thicker than ion sheath at same conditions. The calculated sheath thicknesses are verified by probe diagnostics as well as particle simulation. Monitoring the variation of ion saturation current of Langmuir probe with tiny tip with respect to sheath voltage, locations of sheath edge are measured at different plasma densities and electron temperatures. Using the 1D particle-in cell code, thickness of electron sheath are investigated, as well. Outbreak voltages of the breakdown in the electron sheath are gauged at various pressures and powers. Regarding the plasma as a cathode, biased electrode as an anode and electron sheath thickness as a discharge gap respectively, one-dimensional breakdown model is suggested. Applying Townsend's criteria of DC discharge to this breakdown model, a nonlinear equation for breakdown voltages is derived. Comparison of model-based numerical calculations to experimental results shows a good agreement between them.

✓

DTP 12 Electrical characteristics of an atmospheric pressure plasma jet with helium flow GORDANA MALOVIC, DEJAN MALETIC, NEVENA PUAC, *Institute of Physics Belgrade Serbia* SASA LAZOVIC, ANTONIJE DJORDJEVIC, *Faculty of Electrical Engineering Belgrade* ZORAN PETROVIC, *Institute of Physics Belgrade Serbia* INSTITUTE OF PHYSICS TEAM, FACULTY OF ELECTRICAL ENGINEERING BELGRADE TEAM, In the last few years atmospheric nonthermal plasma jet increasingly attracts interest because of its potential in biomedical applications. We have constructed a plasma jet that operates in the range of 5-10 kV and 25-150 kHz. It is made of Pyrex glass tube (I.D. 4 mm; O.D. 6 mm) with two cylindrical electrodes made of copper foil (13 mm wide). The buffer gas was helium with a flow of 2-7 slm. High voltage probe was used to obtain voltage waveforms while current waveforms were measured at the resistor (100 kOhm) placed in the grounded branch of the electrical circuit. Measurements are performed for increasing and decreasing applied voltage in order to observe hysteresis. RMS voltage/current values and mean power values are calculated. Our results show that plasma is a nonlinear load in the electrical circuit and that there is a significant hysteresis. It was possible to control the mean power in all cases to be below 10 W which is required for biomedical applications. The electrical measurements are coupled to ICCD measurements of the plasma profile and motion.

✓

DTP 13 Modeling of heavy particle collisions in high E/N discharges in helium ZORAN PETROVIC, ZELJKA NIKITOVIC, *Institute of Physics Belgrade Serbia* SVETLANA RADOVANOV, *Varian Semiconductor Equipment Associates, 35 Dory Road, Gloucester, MA 01930 USA* VLADIMIR STOJANOVIC, *Institute of Physics Belgrade Serbia* We have compiled a set of collision cross sections for electrons, ions and fast neutrals in helium. The sat has been used as the basis for modeling of heavy particle excitation and other effects that occur at very high E/N. As a first step modeling was performed for Townsend discharges in uniform electric field. We calculate spatial profiles of emission with imprints of both electron and heavy particle excitation and compare them to the experiment. Non-hydrodynamic transport close to electrodes at low pressures is illustrated and effects of reflection of particles, secondary particle emission and surface excitation are included in the model. We also present the spatial profile of fluxes of all particles and we calculate line profiles that show Doppler broadening that may be detected in gas discharges. We also analyze kinetics of electrons, ions and fast neutrals in helium discharges with inhomogeneous electric field.

DTP 14 New Method for Homogeneous Plasma Production at Gas Pressure 0.005 – 5 Pa Used for Substrate Etching, Nitriding, Ion Implantation and Coating Deposition ALEXANDER METEL, SERGEI GRIGORIEV, YURIY MELNIK, VLADIMIR PRUDNIKOV, *Moscow State University of Technology "Stankin"* DC glow discharge with electrostatic confinement of electrons is used for homogeneous plasma production inside working vacuum chamber of technological system "Bulat-6" at argon or nitrogen pressure p ranging from 0.005 Pa to 5 Pa. Plasma nonuniformity at $p < 0.05$ Pa does not exceed $\sim$ 10% and rises to $\sim$ 20% at $p = 0.5 - 5$ Pa. The argon plasma enables conductive substrates etching and targets sputtering with energetic ions as well as heating and melting metals and dielectrics with energetic electrons. The nitrogen plasma enables cost-effective ion implantation and nitriding of conductive substrates, which are negatively biased using a simple DC high-voltage power supply.

DTP 15 Characterization of high-power atmospheric pressure transient micro-glow discharge using double-pulsed high-voltages SHINJI IBUKA, JUN KIKUCHI, NAOAKI YOSHIDA, KOICHI IGARASHI, SHOZO ISHII, *Tokyo Institute of Technology* A high-power transient micro-glow discharge is a promising candidate for atmospheric pressure plasma processes. Although the utilization of a highly repetitive pulsed high-voltage is effective to generate the spatially uniform transient micro-glow discharge without a glow-to-arc transition, its stabilization mechanism has not been fully understood yet. In this study, the transient micro-glow discharges powered by double-pulsed voltages were investigated for various pulse-intervals and helium flow rates. The electrical and the optical emission spectroscopic characterizations illustrated the important roll of the metastable species with long excitation lifetime for stability enhancement. The helium flow rate had also remarkable effect on the plasma parameters. According to the Stark broadening of the hydrogen Balmer lines, the electron density reached over 10^{15}cm^{-3} during the high-voltage applied period and maintained above 10^{14}cm^{-3} for several microseconds. The results show the feasibility of the atmospheric pressure reactive plasma generation having high electron density using MHz order repetitive pulsed voltages.

DTP 16 Qualitative theory of multi-hollow microwave plasma source IVAN GANACHEV, *Shibaura Mechatronics Corporation* IJI LIANG, HIDEO SUGAI, *Chubu University* The performance, in particular uniformity, of planar surface- wave plasma sources can be enhanced by modifying the dielectric- plasma interface to include an array of hollows cut into the dielectric ("multi-hollow plasma source"). Recently[1] we found that with increasing overall power the number of ignited hollows increases, but the power absorbed by each one of them remains almost constant for fixed gas type and pressure (about 7 Watt per hollow in Ar at 1.3 Pa and 2.45 GHz). In the present contribution we propose an explanation to this behavior: We show that small plasma-filled hollows have a discrete spectrum of resonance densities. In the particular case of small hemispherical hollows, the electron density of the n-th mode is $n_e(n) = n_c[1 + \epsilon_d(2n + 1)/2n]$, $n = 1,2,\ldots$, where n_c is the cut-off density and ϵ_d is the dielectric constant of the plate

PLASMA NEEDLE TREATMENT OF STAPHYLOCOCCUS AUREUS IN PLANCTONIC FORM

Conference Paper · April 2010

READS
31

9 authors, including:

Saša Lazović
Institute of Physics Belgrade
70 PUBLICATIONS **212** CITATIONS
SEE PROFILE

Dejan Maletic
Institute of Physics Belgrade
53 PUBLICATIONS **97** CITATIONS
SEE PROFILE

Gordana Malovic
Institute of Physics Belgrade
157 PUBLICATIONS **932** CITATIONS
SEE PROFILE

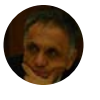

Zoran Lj Petrović
Institute of Physics Belgrade
510 PUBLICATIONS **5,652** CITATIONS
SEE PROFILE

BALKAN BaSS

15th thessaloniki BaSS

Hosting the Annual Meeting of the E C G

Proceedings of the 15th Congress of the BaSS 2010

hosting the Annual Meeting of the European College of Gerodontology

22-25 April 2010

Thessaloniki, Greece

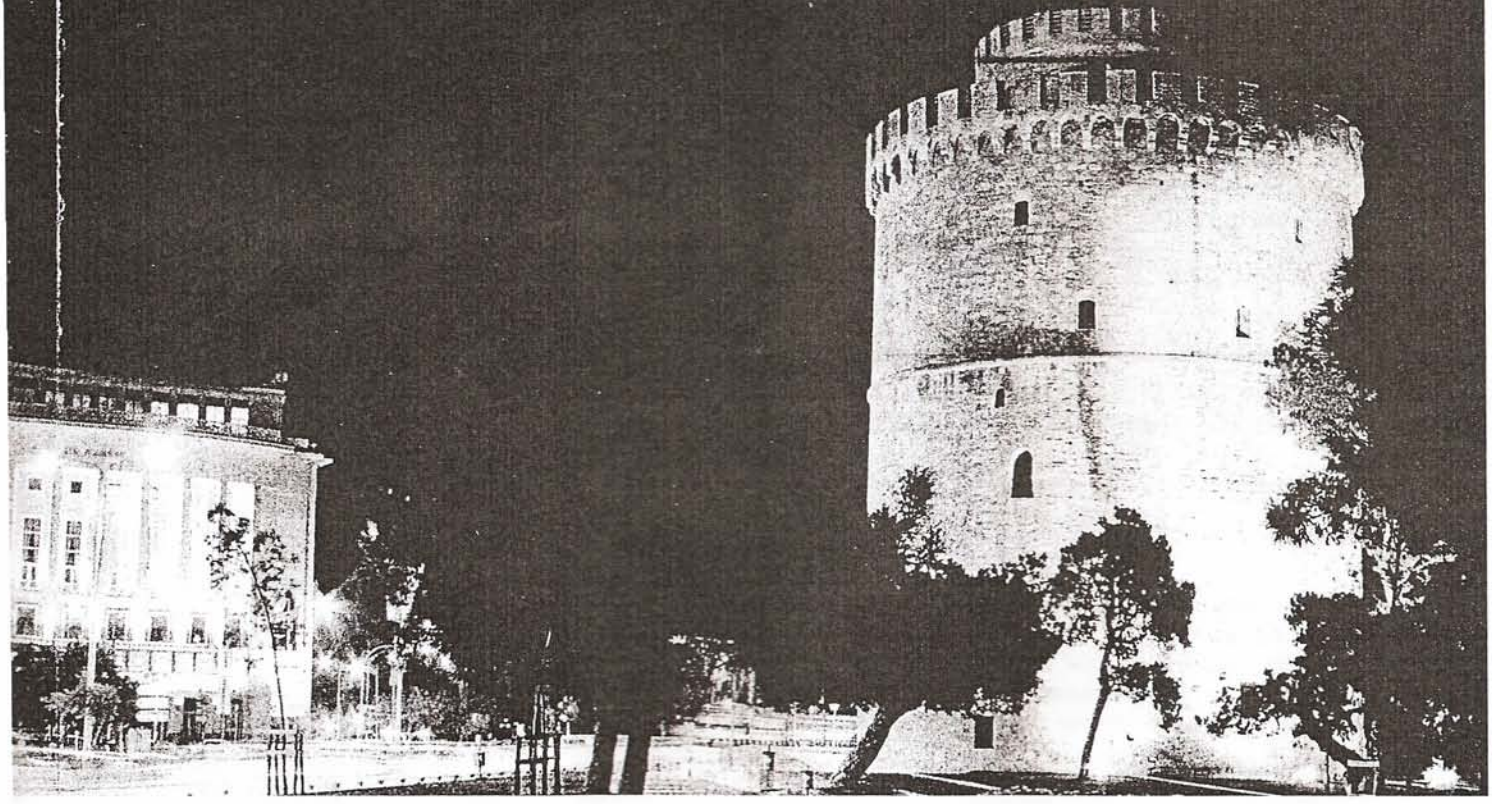

CONCLUSIONS: Interpatient microbiological cross-contamination can occur between routine radiographic examinations, therefore microbial contamination during radiographic processing is a serious problem of dentistry. So effective cleaning regimens and method of the disinfection are of fundamental importance in controlling and preventing potential microbiological cross-contamination at the dentistry.

PP 115

PLASMA NEEDLE TREATMENT OF STAPHYLOCOCCUS AUREUS IN PLANCTONIC FORM

Miletic Maja, Lazovic Sasa, Puac Nevena, Maletic Dejan, Jovanovic Milena,Pavlica Dusan, Malovic Gordana, Milenkovic Pavle, Petrovic Zoran
Serbia

INTRODUCTION: Atmospheric non-thermal plasmas, generated by a plasma needle, are suitable for the treatment of heat-sensitive biomedical samples. High-precision surgery, improvement of wound healing, and non-contact disinfection of dental cavities and wounds are only segment of potential applications of plasma technology. We studied the effects of the plasma needle discharge on a suspension containing different concentrations of Staphylococcus aureus (ATCC 25923).

METHODS: Suspensions of bacteria were made according to 0,5 McFarland standard. From this initial suspension other suspensions were made with cell density 1:10, 1:100, 1:1000 of the original. We treated all samples for three different exposure times, three different powers and two different flows of buffer gas in the needle. The effect of the plasma needle treatment was graded according to the number of bacterial colonies formed after incubation, which are described using arbitrary defined units (0-5).

RESULTS: The results of this investigation indicated that with an increase of the applied power and with an increase of the time of treatment, the number of bacterial colonies can be reduces by factor of 104. For the longest treatment time (180s) and highest applied power (1.6 W), except for the highest concentration of bacteria, practically all the bacteria are killed in the treated sample. For smaller concentrations even the shortest treatment times (60, 120s) were sufficient to destroy the bacteria. For the smallest applied power (0.15 W) we couldn't see any change in bacteria number even after extended treatment times. The results shown that the plasma created when the flow buffer gas was 0.5 slam was more effective then in the case of He flow of 1 slam.

CONCLUSIONS: These results represent the first step of the route of developing, optimizing, understanding and using the plasma needle for in-vivo deactivation of harmful bacteria

PP 116

PROS AND CONS OF ROUTINE ANTIBIOTIC PROPHYLAXIS

Aranitasi Loreta Pojani, Aranitasi Luela, Disha Valbona
Albania

INTRODUCTION: Antibiotic prophylaxis is used in dental practice to minimize infectious complications resulting from daily interventions. It has no direct influence on the control of pain, swelling or postoperative trismus, but it seems that preventing postoperative infection may have an indirect influence on these parameters. Side-effects and development of microbial resistance patterns are risks of the use of antibiotics.
Therefore, the use should be well considered and based on high levels of evidence.

METHODS: A systematic literature review was conducted, searching Medline, the Cochrane Library and other relevant studies found in internet.

RESULTS: The prescription to prevent surgical site infection after lower third molar removal are well studied and have a high and moderate to high level of evidence in favor of using antibiotic prophylaxis. Antibiotic prevention in implant surgery and joint procedures are well studied and all authors agree that prophylaxis in these cases is necessary. Other oral interventions are not well studied. The moderate to low evidence suggests no need for antibiotic prophylaxis in routine tooth extraction, pulp inflammation, no complicated pulpitis, or crown restorations. Antibiotic prophylaxis is not advised in scaling or prosthetic procedures.

CONCLUSIONS: Correct practice urges the dentist to consider using narrow-spectrum antibacterial drugs in simple infections to minimize disturbance of the normal microflora, and to preserve the use of broad-spectrum drugs for more complex infections
The professional should balance the low risk of wound infection against the adverse risk from the antibiotic. Factors which need to be considered are the tissue trauma, the extent of host compromise, difficult bone impactions with previous history of recurrent infections and other medical comorbidities. In the few cases where antibiotic prophylaxis is considered, a single high preoperative dose should be given.

PP 117

SALIVARY IGA AND MUTANS STREPTOCOCCI IN SEVERE EARLY CHILDHOOD CARIES

Cvetković Andrijana, Ivanović Mirjana, Matvijenko Vladimir, Martinović Brankica
Serbia

INTRODUCTION: The aim of this study was to examine the relationship between level of whole IgA in saliva, mutans streptococci in saliva and plaque, and the presence serotype (c, e, f) mutans streptococci in dental plaque at children with severe early childhood caries (S-ECC).

Mass-energy spectrometry of atmospheric pressure RF discharges

Conference Paper · June 2011

READS
12

7 authors, including:

Saša Lazović
Institute of Physics Belgrade
70 PUBLICATIONS **212** CITATIONS
SEE PROFILE

Gordana Malovic
Institute of Physics Belgrade
157 PUBLICATIONS **932** CITATIONS
SEE PROFILE

Miran Mozetic
Jožef Stefan Institute
287 PUBLICATIONS **3,708** CITATIONS
SEE PROFILE

Zoran Lj Petrović
Institute of Physics Belgrade
510 PUBLICATIONS **5,652** CITATIONS
SEE PROFILE

18. MEDNARODNO ZNANSTVENO SREČANJE VAKUUMSKA ZNANOST IN TEHNIKA
18th INTERNATIONAL SCIENTIFIC MEETING ON VACUUM SCIENCE AND TECHNIQUES

PROGRAM IN KNJIGA POVZETKOV
PROGRAMME AND BOOK OF ABSTRACTS

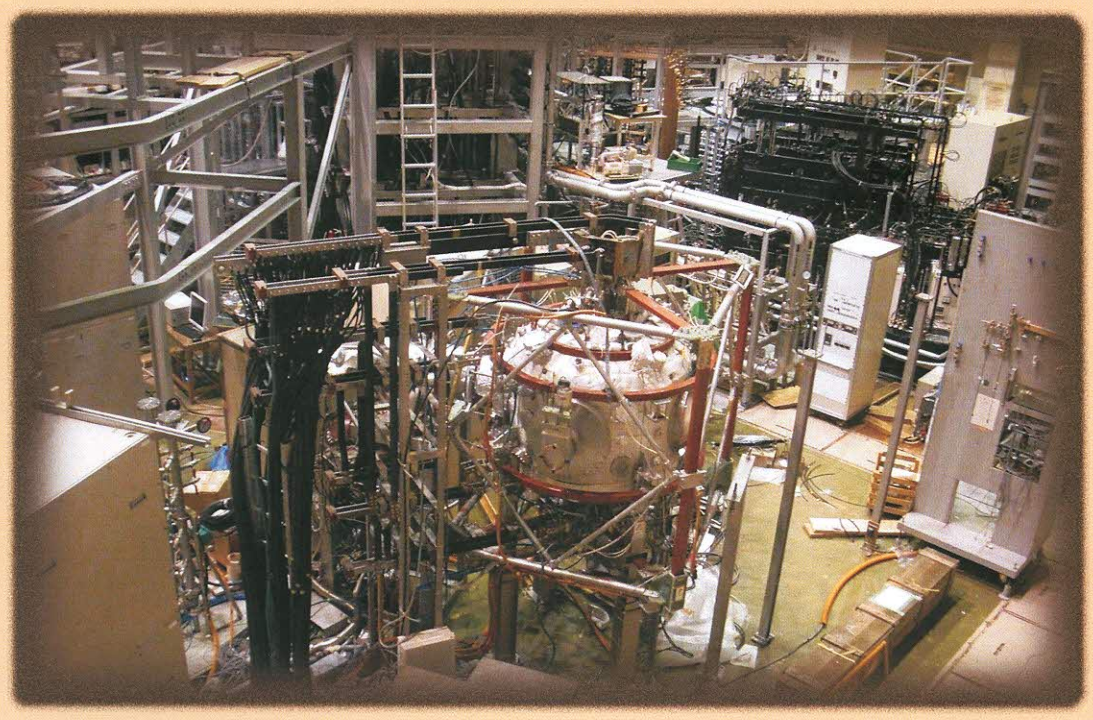

Bohinjsko Jezero
2.–3. Junij 2011 / 2–3 June 2011

18. MEDNARODNO ZNANSTVENO SREČANJE VAKUUMSKA ZNANOST IN TEHNIKA

Bohinjsko Jezero, 2.–3. JUNIJ 2011

18th INTERNATIONAL SCIENTIFIC MEETING ON VACUUM SCIENCE AND TECHNIQUES

Bohinjsko Jezero, 2–3 JUNE 2011

PROGRAM IN KNJIGA POVZETKOV
PROGRAMME AND BOOK OF ABSTRACTS

UREDNIKA / EDITORS

Miran Mozetič, Alenka Vesel

Društvo za vakuumsko tehniko Slovenije

Slovenian Society for Vacuum Technique

2011

18. MEDNARODNO ZNANSTVENO SREČANJE VAKUUMSKA ZNANOST IN TEHNIKA
18th INTERNATIONAL SCIENTIFIC MEETING ON VACUUM SCIENCE AND TECHNIQUES
Program in knjiga povzetkov / Programme and book of abstracts

Izdal in založil / Published by
Društvo za vakuumsko tehniko Slovenije

Za založnika / For the publisher
Miran Mozetič

Organizatorji / Organized by
Društvo za vakuumsko tehniko Slovenije

Urednika / Editors
Miran Mozetič, Alenka Vesel

Računalniški prelom / Prepress
Miro Pečar

Tisk / Printed by
Infokart, d. o. o., Ljubljana

Naklada / Issue
80 izvodov

Ljubljana 2011

ISBN 978-961-92989-2-3

General sponsor:
Slovenian Research Agency

CIP - Kataložni zapis o publikaciji
Narodna in univerzitetna knjižnica, Ljubljana

533.5(082)
621.52(082)

MEDNARODNO znanstveno srečanje Vakuumska znanost in tehnika (18 ; 2011 ; Bohinjsko Jezero)
Program in knjiga povzetkov = Programme and book of abstracts / 18. mednarodno znanstveno srečanje Vakuumska znanost in tehnika, Bohinjsko Jezero, 2.-3. junij 2011 = 18th International Scientific Meeting on Vacuum Science and Techniques, Bohinjsko Jezero, 2-3 June 2011 ; urednika, editors Miran Mozetič, Alenka Vesel ; [organizator Društvo za vakuumsko tehniko Slovenije]. - Ljubljana : Društvo za vakuumsko tehniko Slovenije = Slovenian Society for Vacuum Technique, 2011

ISBN 978-961-92989-2-3
1. Vakuumska znanost in tehnika 2. Vacuum science and techniques 3. Mozetič, Miran, 1961- 4. Društvo za vakuumsko tehniko Slovenije
256236800

Programski odbor / Programme Committee:

- Miran Mozetič
- Janez Kovač
- Monika Jenko
- Peter Panjan
- Slobodan Milošević
- Nikola Radić
- Branko Pivac
- Petar Pervan

Organizacijski odbor / Organizing Committee:

- Alenka Vesel
- Janez Šetina
- Miha Čekada
- Kristina Eleršič
- Ita Junkar
- Rok Zaplotnik
- Tomaž Semenič
- Damir Šokčević
- Ognjen Milat
- Ivana Capan
- Marko Kralj

MASS-ENERGY SPECTROMETRY OF ATMOSPHERIC PRESSURE RF DISCHARGES

Saša Lazović[1,2], Nevena Puač[1], Dejan Maletić[1], Gordana Malović[1], Uroš Cvelbar[2], Miran Mozetič[2], Zoran Lj. Petrović[1]
[1]Institute of Physics, Pregrevica 118, 11080 Belgrade, Serbia
[2]Jožef Stefan Institute, Jamova cesta 39, 1000 Ljubljana Slovenia

Two different atmospheric pressure plasma sources suitable for biomedical applications and sensitive material treatment were diagnosed by using mass-energy analyzer Hiden HPR60 which operates at atmospheric pressure. Both sources (plasma needle and Micro Atmospheric Pressure Plasma Jet – μAPPJ) are 13.56 MHz driven, capacitively coupled and operated in a mixture of laboratory air with the addition of Helium (in case of μAPPJ 1% of O_2 was added to Helium). Due to the difference in electrode construction and therefore configuration of electrical field, we were able to record both neutral and ion spectra of the plasma needle and just the neutral spectra of the μAPPJ. From the biomedical point of view it is very important to study the influence of the atomic and molecule radicals like N, O, NO, O_3. We were, also, able to deal with and overcome several problems which are specific for mass spectrometry measurements in RF plasmas at atmospheric pressure.

Detection of atomic species in micro atmospheric pressure discharge by using mass spectrometry

Conference Paper · June 2011

READS
18

5 authors, including:

Dejan Maletic
Institute of Physics Belgrade
53 PUBLICATIONS **97** CITATIONS
SEE PROFILE

Saša Lazović
Institute of Physics Belgrade
70 PUBLICATIONS **212** CITATIONS
SEE PROFILE

Gordana Malovic
Institute of Physics Belgrade
157 PUBLICATIONS **932** CITATIONS
SEE PROFILE

Zoran Lj Petrović
Institute of Physics Belgrade
510 PUBLICATIONS **5,652** CITATIONS
SEE PROFILE

BELGRADE CEPAS 2011

5th Conference on Elementary Processes in Atomic Systems

CEPAS 2011 & CEAMPP 2011

CONTRIBUTED PAPERS
&
ABSTRACTS OF INVITED LECTURES

Editors
Aleksandar R. Milosavljević
Saša Dujko
Bratislav P. Marinković

Institute of Physics
Belgrade - Serbia

2nd National Conference on Electronic, Atomic,Molecular and Photonic Physics

CEAMPP 2011

5th Conference on Elementary Processes in Atomic Systems

2nd National Conference on Electronic, Atomic, Molecular and Photonic Physics

CEPAS 2011 & CEAMPP 2011

CONTRIBUTED PAPERS
&
ABSTRACTS OF INVITED LECTURES

Editors

Aleksandar R. Milosavljević, Saša Dujko and Bratislav P. Marinković

Institute of Physics
Belgrade, Serbia

Belgrade, 2011

CONTRIBUTED PAPERS & ABSTRACTS OF INVITED LECTURES
of the
5th CONFERENCE ON ELEMENTARY PROCESSES IN ATOMIC SYSTEMS
and the satellite meeting
2nd NATIONAL CONFERENCE ON ELECTRONIC, ATOMIC, MOLECULAR AND PHOTONIC PHYSICS

21st – 25th June 2011
Belgrade, Serbia

Editors

Aleksandar R. Milosavljević, Saša Dujko and Bratislav P. Marinković

Publisher
Institute of Physics
Pregrevica 118, P. O. Box 68
11080 Belgrade, Serbia

Computer processing
Aleksandar R. Milosavljević, Sanja D. Tošić, Nikola Škoro, Maja Rabasović and Saša Dujko

Printed by

SZR "Kragulj"
Kneza Višeslava 88, Belgrade

Number of copies
150

ISBN 978-86-82441-32-8

Detection of atomic species in micro atmospheric pressure discharge by using mass spectrometry

D. Maletić, S. Lazović, N. Puač, G. Malović and Z. Lj. Petrović

Institute of Physics, University of Belgrade, Pregrevica 118, 11080 Belgrade, Serbia

Large concentrations of radicals, low gas temperatures, absence of vacuum systems and possibility of localized treatment make atmospheric plasmas suitable for modification of sensitive surfaces and for biomedical applications [1, 2, 3]. Here we will present results obtained by mass spectrometry measurements of micro atmospheric pressure plasma jet [4].

Measurements were made for the electron energies below the threshold energy for the dissociation of the O_2 and N_2 molecules (see Fig.1). From these distributions one can identify processes that are pertinent in creation of neutral atoms. In order to eliminate contribution of atoms produced by dissociation of O_2 inside the mass analyzer, the electron energy range was varied from 13.6 eV (required for direct ionization of O) up to 19 eV (less then O_2 dissociation threshold). The counts for atomic O increase with the applied power as well as with the increase in the buffer gas flow. This can be explained by the increase of the electron densities with the applied power. With the increase in the applied power depletion of the molecular oxygen also increases. In case of atomic nitrogen counts stay almost constant with increasing of the applied power.

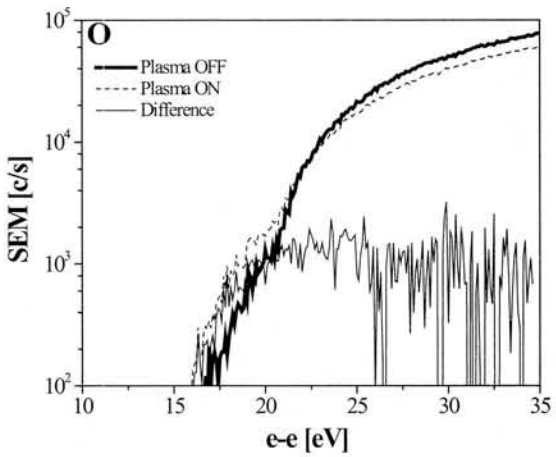

Fig.1. Filament electron energy dependence of oxygen signal (2 slm 1% O_2 70 W).

Acknowledgments: This research has been supported by the MNTR, Serbia, under the contract numbers ON171037 and III41011.

REFERENCES

[1] M. G. Kong, G. Kroesen, G. Morfill, T. Nosenko, T. Shimizu, J. van Dijk and J. L. Zimmermann, New J. Phys., 11 (2009) 115012.

[2] G. Fridman, G. Friedman, A. Gutsol, A. B. Shekhter, V. N. Vasilets and Alexander Fridman, Plasma Process. Polym., 5 (2008) 000.

[3] N. Puač, Z. Lj. Petrović, G. Malović, AĐordević, S. Živković, Z. Giba and D. Grubišić, J. Phys. D: Applied Physics, 39 (2006) 3514.

[4] V. Schulz-von der Gathen, V. Buck, T. Gans, N. Knake, K. Niemi, St. Reuter, L. Schaper, and J.Winter, Contrib.Plasma Phys., 47 (2007) 510.c

Inhibition of methicillin resistant Staphylococcus aureus by a plasma needle

Article *in* Central European Journal of Physics · March 2014

Impact Factor: 1.09 · DOI: 10.2478/s11534-014-0437-z

10 authors, including:

Ivan Soldatovic
University of Belgrade
112 PUBLICATIONS **251** CITATIONS
SEE PROFILE

Saša Lazović
Institute of Physics Belgrade
70 PUBLICATIONS **212** CITATIONS
SEE PROFILE

Gordana Malovic
Institute of Physics Belgrade
157 PUBLICATIONS **932** CITATIONS
SEE PROFILE

Zoran Lj Petrović
Institute of Physics Belgrade
510 PUBLICATIONS **5,652** CITATIONS
SEE PROFILE

Cent. Eur. J. Phys. • 12(3) • 2014 • 160-167
DOI: 10.2478/s11534-014-0437-z

VERSITA

Central European Journal of **Physics**

Inhibition of methicillin resistant *Staphylococcus aureus* by a plasma needle

Research Article

Maja Miletić[1]*, Dragana Vuković[2], Irena Živanović[2], Ivana Dakić[2], Ivan Soldatović[3], Dejan Maletić[4], Saša Lazović[4], Gordana Malović[4], Zoran Lj. Petrović[4], Nevena Puač [4†]

1 *Faculty of Dental Medicine, University of Belgrade, dr Subotica 8, 11000 Belgrade, Serbia*

2 *Institute of Microbiology and Immunology, Faculty of Medicine, University of Belgrade, dr Subotica 1, 11000 Belgrade, Serbia*

3 *Institute for Medical Statistics and Informatics, Faculty of Medicine, University of Belgrade, dr Subotica 1, 11000 Belgrade, Serbia*

4 *Institute of Physics, University of Belgrade, Pregrevica 118, 11080 Belgrade, Serbia*

Received 19 July 2013; accepted 30 December 2013

Abstract: In numerous recent papers plasma chemistry of non equilibrium plasma sources operating at atmospheric pressure has been linked to plasma medical effects including sterilization. In this paper we present a study of the effectiveness of an atmospheric pressure plasma source, known as plasma needle, in inhibition of the growth of biofilm produced by methicillin resistant *Staphylococcus aureus* (MRSA). Even at the lowest powers the biofilms formed by inoculi of MRSA of 10^4 and 10^5 CFU have been strongly affected by plasma and growth in biofilms was inhibited. The eradication of the already formed biofilm was not achieved and it is required to go to more effective sources.

PACS (2008): 52.80.Pi, 87.18.Fx, 92.20.jb

Keywords: non-thermal atmospheric plasmas • plasma needle • antimicrobial • methicillin resistant *Staphylococcus aureus* • biofilm

1. Introduction

The majority of bacteria in nature have a tendency to interact and grow in close association with surfaces, forming biofilms. A biofilm can be defined as a surface-attached community of bacteria growing embedded in a self-produced matrix composed of extracellular polymeric substances (EPS) [1, 2]. Bacteria within biofilms have metabolic and physiological capabilities which are not associated with individual, unattached cells. Notable amongst these unique properties is high level of resistance to antibiotics and chemical/physical decontamination procedures. Therefore, bacteria living in biofilms are

*E-mail: maja.miletic@stomf.bg.ac.rs (Corresponding author)
†E-mail: nevena@ipb.ac.rs

difficult or even impossible to eradicate [1, 2]. The aim of this investigation was to evaluate the antimicrobial activity of a non-thermal atmospheric plasma, generated by a specifically designed plasma needle device, against biofilms produced by methicillin resistant *Staphylococcus aureus* (MRSA). Recently atmospheric pressure discharges have been developed as sources of low temperature plasmas at atmospheric pressure and, thus, it became possible to develop plasma medical applications [3, 4]. Most studies have shown very good results [5–8] in direct contact of plasmas with microorganisms. However sterilization of planktonic samples and biofilms proved to be more difficult [9–13]. In this paper we extend the application of a plasma needle that has been tested in direct contact with plant and mammalian cells [14, 15] and for planktonic samples of bacteria [15] to study sterilization of biofilms. It is estimated that up to 80% of human bacterial infections are actually biofilm-associated. Biofilm formation has typically been implicated in persistent tissue infections and medical device-related infections [16], although the role of biofilm has recently been recognized in acute infections as well [17]. Species of the genus *Staphylococcus*, in particular *S. aureus* and *S. epidermidis*, are among the most frequent causative agents of biofilm-mediated infections [18, 19]. The most important *S. aureus* diseases that have a demonstrated biofilm component are osteomyelitis, medical device-related infections, wound infections and endocarditis. Worldwide dissemination of MRSA strains that display resistance to all beta-lactam antibiotics, further complicates prevention and treatment of these diseases [18, 19]. Since antibiotic treatment often fails to overcome biofilm-associated infections, particularly those caused by multidrug resistant bacteria, it is apparent that development of alternative strategies for preventing and/or treating these infections is of great importance. Further research is needed to understand molecular mechanisms of biofilm formation by bacteria. For example, it has recently been shown that *S. aureus* cysteine proteases ScpA and SspB, so called Staphopains, are the key modulators of biofilm production by this bacterium and that development of strategies to up-regulate the Staphopains could be a novel approach to treating *S. aureus* biofilm infections [20]. Lately, it was shown that low-temperature gas plasma presents a powerful medical tool in general [3, 4, 21]. Cold plasma can successfully eradicate microorganisms [22–24] and this fact is exploited in plasma sterilization of medical equipment and instruments [25, 26]. Compared to common methods used in health-care facilities like steam under pressure, dry heat, ethylene oxide gas and liquid chemicals, plasma offers non-toxicity and treatment of heat sensitive instruments without rapid degradation. Plasmas can offer different principles of inactivation mechanisms like etching or sputtering of membranes of bacteria or endospore coat, charging of the bacterial cell membrane, DNA modifications based on strand breaks [27]. For all inactivation mechanisms maximum result is obtained through synergistic effects of all plasma agents (electrons, ions, photons, electric fields, radicals and metastables) [28] that target many cellular components and metabolic processes in bacteria. This explains one of the major advantages of cold atmospheric plasmas *i.e.* multiple targets in bacterial cells make the emergence of resistance mechanisms less likely [9]. In addition, plasma chemistry is important as generation of radicals or active molecules at the surface in very small quantities may trigger a biological response with only a small amount of reactive species that would otherwise be very toxic. The effectiveness of the sterilization process depends not only on plasma composition, but also on intrinsic properties of the sample. For example, individual bacteria are easily inactivated by UV radiation at a timescale of seconds [29]. On the other hand, only UV radiation is not sufficient when bacteria are contained in some surrounding medium, especially if this medium has a supporting structure. Good examples are bacteria in suspensions and bioflims [30]. Our previous work showed plasma sterilization of bacteria in planktonic sample despite the obvious "shielding" by the liquid medium [15]. Independent of our work, Joshi *et al.* reached similar conclusions [13]. A large number of papers followed [31–33]. In this sense, biofilms represent an even more challenging task because bacteria are shielded by the polymeric matrix. Plasma cannot easily penetrate complex porous and hollow structures and, in addition, a synergetic effect of agents is needed for biomaterial removal and in-depth effects on multilayer stacks. As we move towards the *in-vivo* applications, the situation gets more complicated due to the presence of biofilms containing several species of bacteria, blood, fat, and other body products like sweat or saliva. Despite the problems, application of low-temperature plasmas at atmospheric pressure presents a promising antibiofilm approach according to the literature.

2. Experimental

2.1. Bacterial strain and growth conditions

The MRSA isolate used in this study was recovered from a surgical wound and identified as MRSA by BD Phoenix Automated Microbiology System (Becton Dickinson Diagnostic Systems, Sparks, MD). Identification to the species level was confirmed by detection of the *nuc* gene [34] whilst resistance to meticillin was established by polymerase chain reaction (PCR) for the *mecA* gene [35]. Pre-

vious evaluation identified the strain as a strong biofilm producer [36]. The MRSA strain was transferred from a frozen stock culture onto tryptic soy agar and incubated aerobically for 24 hours at 35 – 37°C. The bacterial suspensions were prepared as follows: a few colonies were suspended in physiological saline and the turbidity of the suspension was adjusted to 0.5 McFarland standard ($\approx 10^8$ CFU mL^{-1}) by using a Densimat photometer (BioMerieux, France). The final testing inocula used in this study ranged from 10^6 to 10^4 CFU per well of a sterile 96 well-flat bottom polystyrene microtiter plate.

2.2. Plasma source

In this study we used a plasma needle device (developed in our laboratory at the Institute of Physics of the University of Belgrade) that was designed for biomedical applications and tested with numerous diagnostic procedures [14, 37]. The device is similar in concept to the one developed by Stoffels *et al.* [38, 39]. The plasma needle consists of a central wolfram electrode (0.5 mm in diameter) covered by a ceramic tube. The ceramic tube serves to insulate the central electrode from the working gas [14]. The powered electrode and the ceramic tube are placed in a glass tube with a 4 mm inner and 6 mm outer diameter. Helium is flowing between the ceramic and the glass tube and allows plasma formation only at the tip of the electrode. The body of the plasma needle is made of Teflon. Plasma needle operates at 13.56 MHz with the electrical circuit consisting of a signal generator, amplifier and matching network.

Electrical characterization of the system is performed by using derivative probes. The probes are placed as close as possible to the tip of the needle in order to obtain the actual power transmitted to the plasma. An oscilloscope and a computer are used to capture and process the signals. The collected signals are transferred to the frequency domain by using Fast Fourier transform. In this domain current and voltage signals are corrected according to calibration curves. Conversion back to the time domain by inverse fast Fourier transform is carried out in the final stage. The difference between signals when plasma is lit and without the plasma (no helium flow) contains the information about the power transferred to the plasma. Knowledge of power transmitted to the plasma gives us a good control of treatment conditions.

2.3. Biofilm growth

Microtiter biofilm assay was carried out in accordance with the protocol described by Stepanović *et al.* [40]. Each well contained 180 µL of brain heart infusion broth (BHI) supplemented with 1% glucose and 20 µL of bacterial suspension. The negative control wells contained 200 µL BHI supplemented with 1% glucose, only. In order to assess the inhibitory effects of non-thermal plasma on growth of MRSA biofilm, the bacteria were exposed to the plasma 5 h after the addition of bacterial suspension to medium. After plasma treatment the biofilms were allowed to grow for 24 h at 35 – 37°C and then quantified. To evaluate possible effects of non-thermal plasma on the formed MRSA biofilm, the inoculated plates were first incubated for 24 h at 35 – 37°C and then exposed to plasma treatment. Quantification of the biofilm was performed after the plasma treatment.

2.4. Plasma treatment conditions

The same set of conditions was applied both to freshly inoculated plates and plates with already developed biofilms. The plasma needle was placed vertically above the microtiter plate in line with the upper edge of each well (Figure 1).

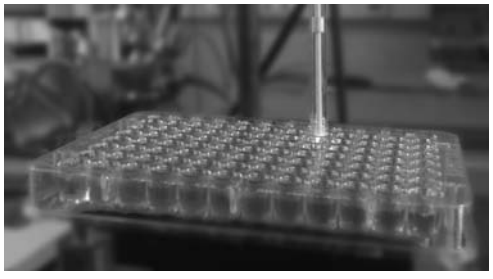

Figure 1. Plasma needle with microtiter plate.

The distance between the tip of the plasma needle and the surface of the sample in each well was fixed to 3 mm. The samples were treated by plasma operating at three different powers (0.15, 0.9 and 1.6 W), and two flows of helium (0.5 and 1 slm) during three exposure times (30, 60 and 120 s). The untreated wells were used as positive controls. All treatments were performed in triplicate and repeated at least two times for each bacterial inoculum tested.

2.5. Quantification of biofilm

The content of a microplate was poured off and each well was washed three times with 300 µL of sterile phosphate-buffered saline (PBS; pH 7.2) to remove free floating bacteria. After fixation of adherent biofilm with 150 µL of methanol per well for 20 min, the plates were emptied by flicking and left to air dry overnight in an inverted position at room temperature. The biofilms were

stained with 150 µL of 2% crystal violet for 15 min. Excess stain was washed under running tap water. After the plates were air dried, the dye bound to the adherent cells was resolubilized with 150 µL of 95% ethanol. The optical density (OD) of each well was measured at 570 nm using Multiskan EX reader (Labsystems). The results obtained were averaged and expressed as numbers. The cut-off OD (ODc) was defined as three standard deviations (SD) above the mean OD of the negative control [40]. The results were classified as follows: OD≤ODc no biofilm production; ODc≤OD≤2xODc weak biofilm production; 2xODc≤OD≤4xODc moderate biofilm production; 4xODc≤OD strong biofilm production. Statistical analysis (One-way ANOVA, Dunett test) was performed using SPSS statistical software package (SPSS 15.0 (Chicago, Illinois)). Statistical significance was declared as $p < 0.05$.

3. Results

The study evaluated efficacy of the low-temperature plasma at atmospheric pressure generated by an in-house designed plasma needle device against biofilm formation by a MRSA strain. Summarized results of the microtiter biofilm assays are expressed as qualitative categories in Table 1.

Table 1. Qualitative evaluation of efficacy of low-temperature plasma against biofilm formation by MRSA . Notations: No biofilm formation (0); Weak biofilm formation (+); Moderate biofilm formation (++); Strong biofilm formation (+++); Flow 1 (flow rate of He of 0.5 slm); Flow 2 (flow rate of He of 1 slm).

Power [W]	Exposure time [s]	10^4 *CFU*		10^5 *CFU*		10^6 *CFU*	
		flow 1	flow 2	flow 1	flow 2	flow 1	flow 2
0.15	30	++	+	++	++	++	++
	60	+	+	++	+	++	+
	120	++	+	+	+	+	+
0.9	30	+	+	+	+	++	++
	60	+	+	+	+	+	+
	120	0	0	0	0	+	+
1.6	30	0	0	+	+	+	+
	60	0	0	0	0	+	+
	120	0	0	0	0	+	0

The experimental design included four major variables: three different bacterial inocula were exposed to three different powers of plasma and two flows of helium during three exposure times.

It is obvious that the powers of 0.9 W and 1.6 W achieved a complete inhibition of biofilm growth for testing inocula of 10^4 and 10^5 CFU. The highest power, 1.6 W, exhibited this effect irrespective of the treatment time, while the power of 0.9 W completely prevented biofilm formation only after the longest exposure of 120 s. On the other hand, total inhibition of biofilm production by 10^6 CFU required maximal plasma parameters, namely power of 1.6 W, flow rate of 1 slm and exposure for 120 s.

In order to quantitatively assess the antibiofilm activity of the non-thermal atmospheric plasma, the mean OD values of treated samples were compared to those of untreated controls. The mean OD values with standard deviations obtained at the flow rates of 0.5 slm and 1 slm are shown in Figures 2 and 3, respectively. All OD values equal to or lower than ODc values shown in Figures 2 and 3 indicate absence of biofilm since ODc was defined as three SDs above the mean OD of the negative control, i.e. wells containing growth medium only.

Combination of lower flow rate and minimal plasma power of 0.15 W was ineffective for all inocula and exposure times (Fig. 2). Higher plasma powers (0.9 W, 1.6 W) significantly decreased biofilm production by 10^4 MRSA cells regardless of the exposure time (Fig. 2A), while a decrease in biofilm production by 10^5 MRSA cells required a longer exposure, i.e. 60 and 120 s (Fig. 2B). The biofilm production by the highest bacterial inoculum was not affected by the plasma treatments at the flow rate of 0.5 slm (Fig. 2C).

At the flow rate of 1 slm, plasma significantly reduced biofilm formation in samples with 10^4 CFU, even when the smallest power of plasma was applied, during all treatment times (Fig. 3A). As far as larger inocula are concerned, 10^5 and 10^6 CFU, higher plasma powers of 0.9 and 1.6 W and exposure time of at least 60 s were needed for significant reduction in biofilm growth (Fig. 3B and 3C). The effects of non-thermal plasma on formed MRSA biofilm were evaluated by using the same set of plasma treatments. No significant reduction in biofilm was noted, even with maximal plasma parameters applied (data not shown).

4. Discussion

The use of atmospheric pressure non-thermal plasma has been evaluated for many potential biomedical applications, including eradication of microorganisms [8, 11]. The cold plasma has been proven to be effective in terms of microbial inactivation and surface decontamination and sterilization [41, 42]. Numerous studies showed activity of non-thermal plasma against different Gram-negative and Gram-positive bacteria [13, 15, 43–46]. However, data on activity of cold atmospheric pressure plasma for eradication of biofilm produced by MRSA are still lim-

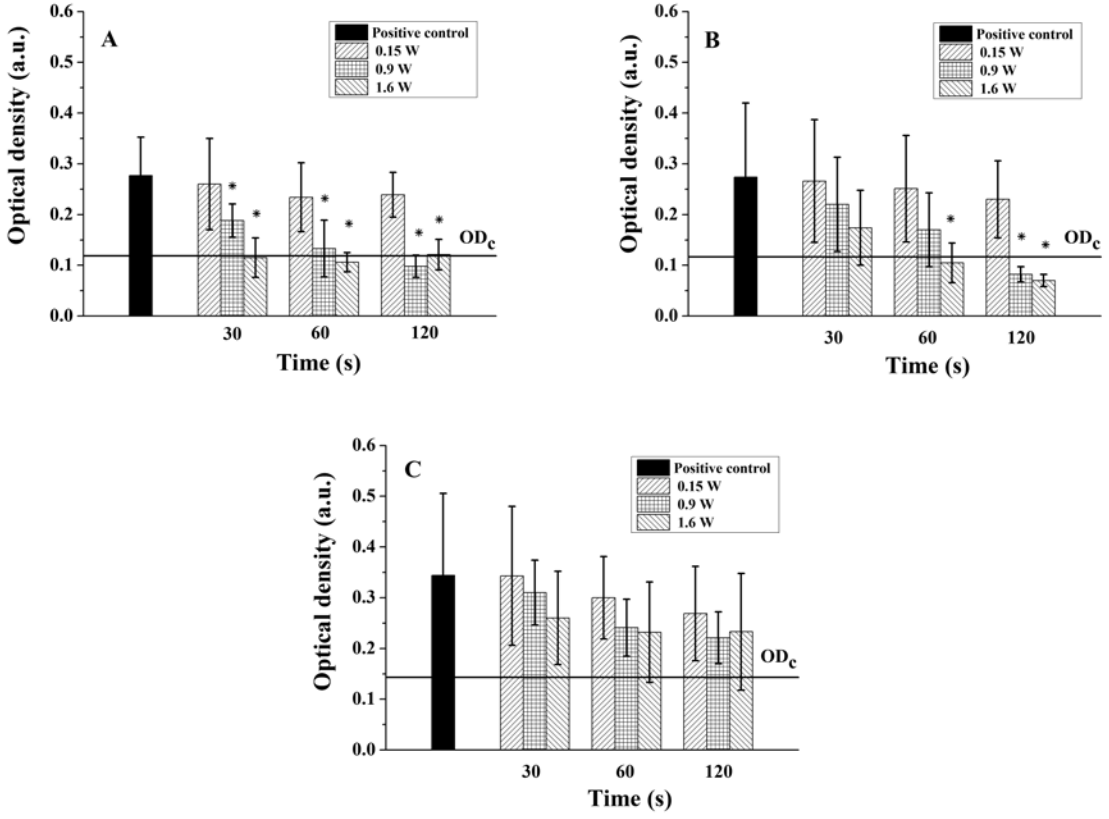

Figure 2. Efect of non-thermal atmospheric plasma on MRSA biofilm for helium flow of 0.5 slm. Samples with different inoculum size of MRSA ((A) 10^4 CFU; (B) 10^5 CFU; (C) 10^6 CFU) were treated for three plasma powers (0.15 W, 0.9 W, 1.6 W) and three exposure times (30 s, 60 s, 120 s). Control samples were untreated cells. The results are presented as mean OD values of triplicates $\pm SD$ of two separate experiments. ODc was defined as 3 SDs above the mean OD of the negative control. $*p < 0.05$ compared to untreated, control cells (Dunett test).

ited [13, 47]. MRSA strains are among the leading causes of healthcare-associated infections and are a major concern for infection control programs. It is also generally appreciated that the staphylococci, including MRSA, have the ability to adhere to many types of surfaces and develop biofilms. MRSA biofilms, in addition to the multiresistance of the bacterium, have innate resistance to antimicrobial agents, and, thus, new treatment strategies that target MRSA biofilm are needed. We carried out a comprehensive *in vitro* investigation of the activity of atmospheric pressure non-thermal plasma generated by an in-house designed plasma needle against biofilm produced by a clinically relevant MRSA strain. Assessment of a particular plasma source is important since the working parameters for the application of different low-temperature sources of the atmospheric plasma are difficult to be standardized, and are defined separately for every single source.

The MRSA cell densities varied from 10^4 to 10^6 per well and the effects of changing the plasma parameters such as power and flow rate at three different exposure times were evaluated. The results obtained clearly show that the low temperature atmospheric pressure plasma generated by a plasma needle exhibited inhibitory effects against MRSA biofilm growth. In general, inhibitory effects of the plasma tested were positively correlated to the plasma parameters. We found that effectiveness of the plasma was time and power dependent and that enhanced anti-biofilm activity was also accomplished by a higher helium gas flow. Namely, with a higher flow rate more reactive plasma agents come in contact with bacterial cells. The higher power delivered to the plasma means that concentration of the radicals and ions is increased compared to the lower powers while still staying well within the limits of negligible temperature change. As a plasma needle produces negligible amount of ozone, in this case the most important radical is NO which is

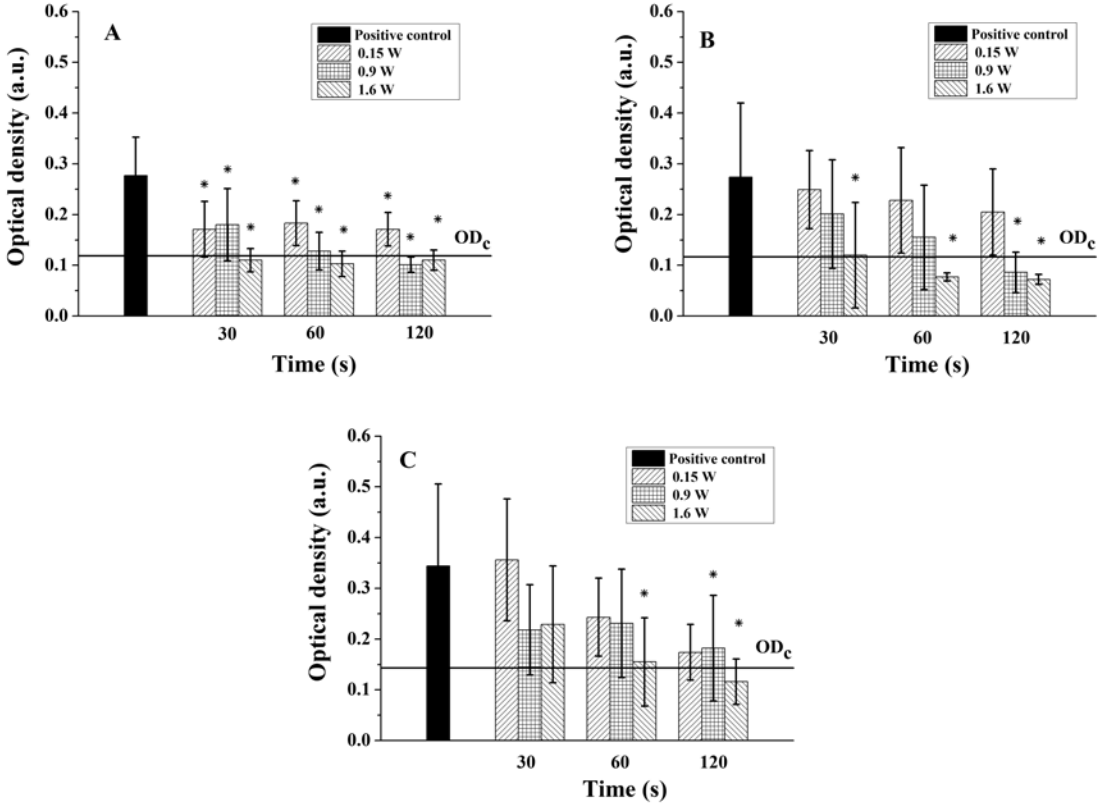

Figure 3. Efect of non-thermal plasma on MRSA biofilm for helium flow of 1 slm. Samples with different inoculum of MRSA ((A) 10^4 CFU; (B) 10^5 CFU; (C) 10^6 CFU) were treated for three plasma powers (0.15 W, 0.9 W, 1.6 W) and three exposure times (30 s, 60 s, 120 s). Control samples were untreated cells. The results are presented as mean OD values of triplicates $\pm SD$ of two separate experiments. ODc was defined as 3 SDs above the mean OD of the negative control. $*p < 0.05$ compared to untreated, control cells (Dunett test).

a potent antimicrobial agent, effective against a range of Gram-negative and Gram-positive bacteria, including *S. aureus* [48]. In our previous work we have shown that plasma needle generates NO radicals and that amount of generated NO is highly dependent on the power delivered to the plasma [37]. It was shown that with an increase in power delivered to the plasma concentration of NO increases. As another point we have to mention the abundance of ions created by a plasma needle whose concentration also increases with power. An increase in power means a larger plasma volume and, thus, larger area is in direct contact with the plasma. The exact composition of bactericidal agents produced by plasma varies depending on geometry, composition of working gas, humidity, power, etc. The antimicrobial properties of NO may be elicited by direct modification of biomacromolecules or by formation of reactive nitrogen oxide species (RNOS) such as peroxynitrite ($OONO^-$), S-nitrosothiols (RSNO), nitrogen dioxide (NO_2), dinitrogen trioxide (N_2O_3), and dinitrogen tetroxide (N_2O_4). These reactive intermediates exert antimicrobial effects by inducing lipid peroxidation or altering DNA according to Schairer *et al.* [49] RNOS can cause nitrosation of protein thiols and the nitrosylation of metal centres (Fe-S), ultimately modifying the functions of proteins that are essential to cellular processes [50, 51].

The results of the present study show that biofilm inhibition by the plasma, in addition to the plasma parameters, was also closely dependent on the inoculum size. For the largest inoculum of bacteria, plasma treatment did not afect biofilm formation at the flow rate of 0.5 slm, even with the maximum power and the longest exposure. Inhibitory effects of the plasma against biofilm produced by 10^6 bacteria were observed only at the flow rate of 1 slm, in combination with other plasma parameters. Consistently high level of biofilm inhibition obtained for the smallest inoculum of 10^4 MRSA cells was not sensitive to the changes in treatment times. At the flow rate of 0.5 slm, plasma power of 0.9 W was sufficient to decrease significantly biofilm formation by this inoculum, irrespective of the exposure

time. At the higher flow rate, all combinations of plasma parameters were effective in biofilm growth inhibition.

While the inhibitory effects of the cold plasma on biofilm formation by the MRSA strain tested in the present study were apparent, the plasma treatments of formed biofilms, *i.e.* biofilms grown after 24 hours of incubation were ineffective. This may be related to the thickness of the biofilm and the inability of bactericidal agents produced by plasma to penetrate a thick biofilm. Since eradication of biofilm is essential for possible practical application of the nonthermal atmospheric plasma, further evaluation of its effects on biofilm formed after 24 h as well as longer incubation periods is needed. In addition to the biofilm incubation period, all parameters of the plasma treatment should be optimized in the context of biofilm eradication. It opens a possibility of further tests depending on the targeted substrates which would include extended period and repeated treatments, higher powers, a different more energetic plasma (perhaps for non living substrates) and combined treatment with other techniques. It is noteworthy that we have shown that even with a higher power the thermal heating of the target is negligible and, thus, going to a higher power would lead to some effects.

5. Conclusion

In this study the in-house plasma needle device has been proven to generate cold atmospheric pressure plasma that is highly efficient for an *in vitro* prevention of MRSA biofilm development. Under the specific conditions, complete inhibition of biofilm formation was noted even for the inoculum as high as 10^6 MRSA cells. Therefore, the plasma application suggested by this study lies within the area of inanimate surface decontamination/sterilization. As far as *in vivo* application is concerned, it should be noted that the same plasma treatments utilized against MRSA biofilm had been previously tested for cytotoxicity on peripheral blood-derived mesenchymal stem cells and no cytotoxic effects were established [15].

We are well aware that the study provided results based upon an *in vitro* experimental model, and that further research is needed for practical application within the area of *in vivo* desinfection. In addition, further research into eradication of formed biofilms by plasmas that produce more effects on surfaces is planned, such as a micro atmospheric pressure plasma jet and an atmospheric pressure plasma jet.

Acknowledgement

This study was supported by Grants No. III41011, ON175039 and ON171037 from the Ministry of Education, Science and Technological Development of the Republic of Serbia.

References

[1] P. Cos, K. Toté, T. Horemans, L. Meas, Curr. Pharm. Des. 16, 2279 (2010)
[2] U. Römling, C. Balsalobre, J. Intern. Med. 272, 541 (2012)
[3] Z. Lj. Petrović et al., Journal of Physics: Conference Series 356, 012001 (2012)
[4] Z. Lj. Petrović et al., J. Serb. Chem. Soc. 77, 1689 (2012)
[5] M. Moreau, N. Orange, M. G. J. Feuilloley, Biotechnol. Adv. 26, 610 (2008)
[6] J. Goree, B. Liu, D. Drake, E. Stoffels, IEEE T. Plasma Sci. 34, 1317 (2006)
[7] B. Kim,et al., Food microbial. 28, 9 (2011)
[8] G. Fridman et al., Plasma Process. Polym. 5, 503 (2008)
[9] T. Maisch et al., PloS One 7, e34610 (2012)
[10] J. L. Zimmermann et al., New J. Phys. 14, 073037 (2012)
[11] M. G. Kong et al., New J. Phys. 11, 115012 (2009)
[12] M. Hee Lee et al., New J. Phys. 11, 115022 (2009)
[13] S. G. Joshi et al., Am. J. Infect. Control 38, 293 (2010)
[14] N. Puač et al., J. Phys. D Appl. Phys. 39, 3514 (2006)
[15] S. Lazović et al., New J. Phys. 12, 083037 (2010)
[16] N. Hoiby et al., Int. J. Oral. Sci. 3, 55 (2011)
[17] T. J. Hannan et al., FEMS Microbiol. Rev. 36, 616 (2012)
[18] C. J. Sanchez et al., BMC Infect. Dis. 13, 47 (2013)
[19] N. K. Archer et al., Virulence 2, 445 (2011)
[20] J. M. Mootz et al., Infect. Immun. 81, 3227 (2013)
[21] K. D. Weltmann et al., Pure Appl. Chem. 82, 1223 (2010)
[22] M. Laroussi, Plasma Process. Polym. 2, 391 (2005)
[23] M. Moisan et al., Int. J. Pharmaceut. 226, 1 (2001)
[24] U. Cvelbar, M. Mozetič, N. Hauptman, M. Klanjsek-Gunde, J. Appl. Phys. 106, 103303 (2009)
[25] S. Manola, Z. Lj. Petrović, R. M. Jankov, In: M. Milosavljević (Ed.), 16th SPIG XVI Summer School and International Symposium on the Physics of Ionized Gases, Serbia (Belgrade 1993) 285
[26] K. Stapelmann, O. Kylián, B. Denis, F. Rossi, J. Phys. D: Appl. Phys. 41, 192005 (2008)
[27] D. O'Connell et al., Appl. Phys. Lett. 98, 043701

(2011)
[28] A. von Keudell et al., Plasma Process. Polym. 7, 327 (2010)
[29] N. Philip et al., IEEE T. Plasma Sci. 30, 1429 (2002)
[30] M. Y. Alkawareek et al., FEMS Immunol. Med. Microbiol. 65, 381 (2012)
[31] E. Kvam, B. Davis, F. Mondello, A. L. Garner, Antimicrob. Agents Ch. 56, 2028 (2012)
[32] R. Matthes et al., Plasma Process. Polym. 10, 161 (2013)
[33] T. Maisch et al., J. Ind. Microbiol. Biot. 39, 1367 (2012)
[34] O. G. Brakstad, K. Aasbakk, J. A. Maeland, J. Clin. Microbiol. 30, 1654 (1992)
[35] Y. Kondo et al., Antimicrob Agents Chemother 51, 264 (2007)
[36] I. Ćirković, Ph.D. thesis, University of Belgrade (Belgrade, Serbia, 2009)
[37] G. Malović, N. Puač, S. Lazović, Z. Lj. Petrović, Plasma Sources Sci. T. 19, 034014 (2010)
[38] I. E. Kieft and E. Stoffels, New J. Phys. 6, 149 (2004)
[39] E. Stoffels, J. Flikweert, W. W. Stoffels, G. M. W. Kroesen, Plasma Sources Sci. T. 11, 383 (2002)
[40] S. Stepanović et al., APMIS 115, 891 (2007)
[41] A. G. Whittaker et al., J. Hosp. Infect. 56, 37 (2004)
[42] H. Halfmann, N. Bibinov, J. Wunderlich, P. Awakowicz, J. Phys. D., Appl.Phys. 40, 4145 (2007)
[43] Y. F. Hong et al., Lett. Appl. Microbiol. 48, 33 (2009)
[44] K. Lee, K. H. Peak, W. T. Ju, Y. Lee, J. Microbiol. 44, 269 (2006)
[45] H. Yu et al., J. Appl. Microbiol. 101, 1323 (2006)
[46] M. H. Lee et al., New J. Phys. 11, 115022 (2009)
[47] J. J. Cotter et al., J. Hosp. Infect. 78, 204 (2011)
[48] A. Ghaffari, C. C. Miller, B. McMullin, A. Ghahary, Nitric oxide 14, 21 (2006)
[49] D. O. Schairer, J. S. Chouake, J. D. Nosanchuk, A. J. Friedman, Virulence 3, 271 (2012)
[50] A. Friedman et al., Virulence 2, 217 (2011)
[51] G. Han et al., PloS One 4, e7804 (2009)

Functionalization of cotton fabrics with corona/air RF plasma and colloidal TiO2 nanoparticles

Article *in* Cellulose · June 2011

Impact Factor: 3.57 · DOI: 10.1007/s10570-011-9510-6

Cellulose (2011) 18:811–825
DOI 10.1007/s10570-011-9510-6

Functionalization of cotton fabrics with corona/air RF plasma and colloidal TiO_2 nanoparticles

D. Mihailović · Z. Šaponjić · M. Radoičić · S. Lazović · C. J. Baily · P. Jovančić · J. Nedeljković · M. Radetić

Received: 10 December 2010 / Accepted: 4 February 2011 / Published online: 16 February 2011

Abstract This study discusses the possibility of using a corona discharge at atmospheric pressure and air RF plasma at low pressure for the cotton fibre activation prior to deposition of colloidal TiO_2 nanoparticles in order to enhance antibacterial, UV protective and self-cleaning properties. X-ray photoelectron spectroscopy (XPS) analysis confirmed the presence of TiO_2 nanoparticles on the surface of cotton fibres. XPS elemental mapping indicated that TiO_2 nanoparticles were more evenly distributed across the surface of untreated and corona pre-treated cotton fabrics in comparison with RF plasma pre-treated fabric. Atomic absorption spectroscopy measurements revealed that the equivalent total content of TiO_2 in the cotton fabrics pre-treated by corona and RF plasma was 31% higher than in the fabric that did not undergo any treatment prior to loading of TiO_2 nanoparticles. In order to achieve maximum bacteria (Gram-negative bacteria *Escherichia coli*) reduction, untreated cotton fabric had to be loaded with colloidal TiO_2 nanoparticles twice, but only once following corona or RF plasma pre-treatment. Deposition of TiO_2 nanoparticles onto cotton fabrics provided maximum UV protective rating of 50+. Extraordinary photocatalytic activity of TiO_2 nanoparticles deposited onto cotton fabrics was proved by self-cleaning of blueberry juice stains and photodegradation of methylene blue in aqueous solution under UV illumination.

Keywords Cotton · TiO_2 nanoparticles · Corona · RF plasma · Photocatalytic activity

D. Mihailović · P. Jovančić · M. Radetić (✉)
Textile Engineering Department, Faculty of Technology and Metallurgy, University of Belgrade, Belgrade, Serbia
e-mail: maja@tmf.bg.ac.rs

Z. Šaponjić · M. Radoičić · J. Nedeljković
Vinča Institute of Nuclear Sciences, Belgrade, Serbia

S. Lazović
Institute of Physics, Zemun, Serbia

C. J. Baily
Thermo Fisher Scientific, West Sussex, UK

Introduction

The extensive work in last two decades on the possible application of plasma to different textile materials indicated that this technology can be efficiently exploited for obtaining plenty of advantageous effects. High efficiency, economic feasibility, environmental acceptability and flexibility make plasma processing a viable alternative to conventional wet finishing processes. Major work so far was focused on plasma modification of wool due to its complex structure and specific properties (Ueda and Tokino 1996; Wakida and Tokino 1996; Thomas 2007; Morent et al. 2008). However, plasma

modification of cellulosic and particularly cotton fibres also gained much scientific attention (Ueda and Tokino 1996; Johansson 2007). While the early research was oriented more towards improvement of the cotton fibres spinnability, and strength of the yarns and fabrics (Ueda and Tokino 1996), recent studies have been predominantly exploring the wetting, dyeing and printing properties of plasma treated cotton fibres (Sun and Stylos 2004; Yuen and Kan 2007; Karahan and Özdoğan 2008; Navaneetha Pandiyaraj and Selvarajan 2008). It was also suggested that plasma treatment could efficiently replace conventional high energy- and water-consuming desizing of polyvinyl alcohol from cotton fabrics (Cai et al. 2003). Additionally, novel application of plasma treatment for obtaining "worn look" effect on indigo-dyed denim fabrics was also proposed (Ghoranneviss et al. 2006; Radetić et al. 2009).

Latest studies opened up some new perspectives on plasma that could be utilized for engineering of multifunctional, stable and durable textile nanocomposite materials. Namely, interest in the application of metal and metal oxide nanoparticles to textile materials has been growing and many efforts have been already done to impart some specific effects (antimicrobial, self-cleaning, antielectrostatic, UV protective, fire retardancy, etc.) and produce high added-value textile products (Lee et al. 2003; Xin et al. 2004; Bozzi et al. 2005a; Daoud et al. 2005; Yuranova et al. 2006; Qi et al. 2007; Uddin et al. 2007; Mejía et al. 2009; Wu et al. 2009; Clemencic et al. 2010; Kiwi and Pulgarin 2010). Several reports suggested that the problem of stability and durability of such nanocomposite materials can be overcome by plasma functionalization i.e. introduction of new functional groups to fibre surface (Bozzi et al. 2005a; Qi et al. 2007; Mejía et al. 2009). Plasma-induced activation of fibre surface facilitates the binding of colloidal nanoparticles to fibres. Although potential utilities of plasma were primarily examined on hydrophobic synthetic fibres prior to deposition of Ag or TiO_2 nanoparticles (NPs) (Bozzi et al. 2005a; Qi et al. 2007), Bozzi et al. suggested that radio-frequency (RF) and microwave (MW) plasma can also be efficiently used for the modification of cotton fibres (Bozzi et al. 2005b). It is well known that low-pressure plasma systems provide high stability, uniformity and control of properties, but these devices also require expensive vacuum pumps and complex handling of textile materials. This can be avoided by applying the systems operating at atmospheric pressure (corona discharge and dielectric barrier discharge). Mejía et al. demonstrated that fabrics pre-treated by air RF plasma at atmospheric pressure were able to bind TiO_2 due to the extreme localized heating of cotton (Mejía et al. 2009). We reported that corona treatment at atmospheric pressure ensures equally good results as RF plasma treatment of polyester fabrics prior to deposition of colloidal TiO_2 NPs (Mihailović et al. 2010a, b).

Taking into account the potentials of both, corona discharge at atmospheric pressure and RF plasma at low pressure, the aim of this study was to discuss the possibility of using these systems for the activation of cotton fibre surface in order to enhance the deposition of colloidal TiO_2 NPs. The changes in the chemical composition were followed by X-ray photoelectron spectroscopy and atomic absorption spectrometry. Antibacterial activity of cotton fabrics was tested against Gram-negative bacterium *Escherichia coli*. UV protective properties were evaluated by determining the UV protective factor (UPF). Photocatalytic activity of TiO_2 NPs deposited onto cotton fabric was tested by degradation of methylene blue as a model compound in aqueous solution while the self-cleaning efficiency was assessed with blueberry juice stains.

Experimental part

Materials

Desized and bleached cotton woven fabric (Co, 168 g/m^2) has been used as a substrate in this study. To eliminate the surface impurities, the fabric was washed in the bath (liquor-to-fabric ratio of 50:1) containing 0.5% nonionic washing agent Felosan RG-N (Bezema) for 15 min at 50 °C. After the single rinsing with warm water (50 °C) for 3 min and triple rinsing (3 min) with cold water, the samples were dried at room temperature.

Corona treatment of cotton fabric

Corona treatment of Co fabric was performed at atmospheric pressure using a commercial device Vetaphone CP-Lab MK II. Samples were placed on

the electrode roll covered with silicon coating, rotating at the minimum speed of 4 m/min. The distance between electrodes was 2 mm. The power was 900 W and the number of passages was set to 30.

RF plasma treatment of cotton fabric

Glow-discharge treatment of Co fabric was carried out in low-pressure RF induced (13.56 MHz) air plasma. The plasma reactor is described in detail elsewhere (Radetić et al. 2009). The power applied to capacitively-coupled reactor was 100 W. The exposure time was 2.5 min, the gas flow rate 150 sccm and the pressure 0.27 mbar.

Loading of cotton fabric with colloidal TiO_2 NPs

The colloid containing TiO_2 NPs was synthesized by acid hydrolysis of $TiCl_4$ according to procedure thoroughly described in our earlier work (Mihailović et al. 2010c). The synthesized colloid comprises of faceted, single crystalline, anatase NPs with an average size of 6 nm (Mihailović et al. 2010c).

Untreated Co fabric and Co fabrics pre-treated by corona or RF plasma were dipped into the 0.1 M TiO_2 colloid (liquor-to-fabric ratio of 1:20) for 5 min and dried at room temperature. After 30 min of curing at 100 °C, the samples were rinsed twice (5 min) with deionized water and dried at room temperature.

Methods

The total content of Ti in the Co fabrics was quantitatively determined using a Perkin Elmer 403 atomic absorption spectrometer (AAS).

X-ray photoelectron spectroscopy (XPS) was used to assess the chemistry and bonding variations of the cotton samples. The XPS studies were carried out using a K-Alpha spectrometer (Thermo Scientific, UK) utilising a monochromated Al Kα ($h\nu = 1{,}486.6$ eV) X-ray source. The system base pressure was less than 5×10^{-9} mbar, however the pressure in the chamber during analysis was 2×10^{-7} mbar due to use of the charge neutralization system which employs a combination of low energy electrons and low energy argon ions to compensate for the loss of photoelectrons from an insulating sample.

The antibacterial efficiency of fabrics was tested against Gram-negative bacterium *E. coli* ATCC 25922. Bacterial inoculum was prepared in the tripton soy broth (Torlak, Serbia), which was used as a growth medium for bacteria. The physiological saline solution (pH 7.0) was applied as a testing medium. Bacteria were cultivated in 3 mL of tripton soy broth at 37 °C and left overnight (late exponential stage of growth). Subsequently, 70 mL of sterile physiological saline solution was added to sterile beaker (400 mL) that was then inoculated with 0.7 mL of the bacterial inoculum. The zero counts were made by removing 1 mL aliquots from the flask with inoculum, and making 1:10 and 1:100 dilutions in physiological saline solution. 0.1 mL of the 1:100 solution was put on the tripton soy agar (Torlak, Serbia) and after 24 h of incubation at 37 °C, the zero time counts (initial number of bacterial colonies) of viable bacteria were made.

A 1 g of the sterile Co fabric cut into small pieces was put into the beaker (70 mL of sterile physiological saline solution inoculated with 0.7 mL of the bacterial inoculum) and shaken for 2 h under UV illumination (TL-D lamp, 18 W, Philips). Two-hour counts were made according to above described procedure.

The percentage of bacteria reduction (R, %) was calculated using Eq. 1:

$$R = \frac{C_0 - C}{C_0} \times 100 \quad (1)$$

where: C_0 (CFU—colony forming units) is the number of bacterial colonies on the control fabric (Co fabric without TiO_2 NPs) and C (CFU) is the number of bacterial colonies on the Co fabric with deposited TiO_2 NPs (Lee et al. 2003).

The UV protection factor (UPF value) of the PES fabrics was determined by UV/VIS spectrophotometer Cary 100 Scan (Varian). The UV protection factor (UPF) values were automatically calculated on the basis of recorded data in accordance with Australia/New Zealand standard AS/NZS 4399:1996 using a Startek UV fabric protection application software version 3.0 (Startek Technology).

Laundering durability of antibacterial and UV protective effects was checked after five washing cycles in Polycolor (Werner Mathis AG) laboratory beaker dyer at 45 rpm. The samples were washed in the bath containing 0.5% Felosan RG-N (Bezema) at

liquor-to-fabric ratio of 40:1. After 30 min of washing at 40 °C, fabrics were soaked once in warm water (40 °C) for 3 min and three times (3 min) in cold water. The fabrics were subsequently dried at 70 °C. The percentage of bacteria reduction after five washing cycles was determined according to Eq. 1.

The self-cleaning effects were examined on the Co fabrics that were stained with blueberry juice. Untreated and corona/RF plasma pre-treated Co fabrics loaded with TiO_2 NPs were cut into 5 × 5 cm^2 pieces and stained with 50 μL of blueberry juice. After drying at room temperature, the fabrics were illuminated using ULTRA-VITALUX lamp (300 W, Osram) for 24 h. The applied lamp provides sun-like irradiation with a spectral radiation power distribution at wavelengths between 300 and 1,700 nm.

Photocatalytic activity of TiO_2 NPs deposited onto the untreated and corona/RF plasma pre-treated Co fabrics was examined by degradation of methylene blue (MB) in aqueous solution under UV illumination (ULTRA-VITALUX lamp, 300 W, Osram). A 0.5 g of Co fabric was dipped into 25 mL of MB solution (10 mg L^{-1}, pH 5.81) and illuminated for 2, 4, 6, 8 and 24 h. The MB concentration was calculated on the basis of spectrophotometric measurements at 664 nm (UV/VIS spectrophotometer Cary 100 Scan, Varian).

In order to establish whether the MB completely degraded on the Co fabrics after 24 h of illumination, the samples were dried at room temperature and their colour coordinates (CIE L^*, a^*, b^*) were determined by Datacolor SF300 spectrophotometer under illuminant D_{65} using the 10° standard observer. On the basis of measured CIE colour coordinates, colour difference (ΔE^*) between the control Co fabric (as supplied) and Co fabrics exposed to MB solution after 24 h of illumination was determined as:

$$\Delta E^* = \sqrt{(\Delta a^*)^2 + (\Delta b^*)^2 + (\Delta L^*)^2} \quad (2)$$

where: ΔL^*—the lightness difference; Δa^*—red/green difference; Δb^*—yellow/blue difference.

Results and discussion

The changes in chemical structure on the surface of Co fabrics induced by deposition of colloidal TiO_2 NPs were analysed by XPS. The XPS survey spectra of the untreated Co fabric (Co), Co fabric loaded with TiO_2 NPs (Co + TiO_2), Co fabric activated by corona and subsequently loaded with TiO_2 NPs (CCo + TiO_2), and Co fabric activated by air RF plasma and subsequently loaded with TiO_2 NPS (AIRCo + TiO_2) are shown in Fig. 1. The O/C ratio of the Co fibre of 0.45 is considerably lower compared to theoretically calculated value of 0.83, implying that the outer layer of studied Co fibres was not composed of pure cellulose (Tourrette et al. 2009). Generally, cotton fibres are comprised of α-cellulose (88.0–96.5%) and non-cellulosic components such as waxes, pectin, proteins and inorganic matter. Unlike proteins, inorganic salts and colouring matter that are located in the fibre lumen, the rest of the non-cellulosic compounds are found in the cuticle layer and the primary wall, which are considered as outer layers of cotton fibre (Topalovic et al. 2007). Waxes are mixture of hydrocarbons, alcohols, esters and free acids with long alkyl chains (Chung et al. 2004). Thus, they contain significant amount of carbon atoms without oxygen neighbours (Fras et al. 2005). On the other hand, pectins are complex polysaccharides that are composed of the linear chains of α-(1-4)-linked D-galacturonic acid (Tourrette et al. 2009) with mostly methylated carboxyl groups (Chung et al. 2004). Along with expected C1s and O1s signals, some other weak signals (Si2p, N1s, Cu2p, Ca2p, Cl2p) were detected in Co fibres which can be associated with impurities that likely originate from the cotton growing, fabric production and sample preparation.

After the deposition of TiO_2 NPs onto Co fabrics, Ti2p signals were clearly noticeable. As could be anticipated, the O/C ratio increased due to the presence of TiO_2 NPs.

In order to get better insight into the chemical composition of all studied samples, a high resolution scan was accomplished in C1s, O1s and Ti2p regions. Relative amounts of differently bound carbon atoms established by deconvolution of C1s peak are presented in Table 1. Cellulose is made up of a linear chain of β (1-4) D-glucose units. Hence, it is expected that the C1s spectrum of pure cellulose should be deconvoluted with three components: C–O, O–C–O and C–O–C groups. According to recorded spectra, additional peak corresponding to C–C/C–H groups appeared. Taking into account that C–C/C–H groups are supposed to be detected in cotton waxes it can be assumed that identified peaks originate exactly

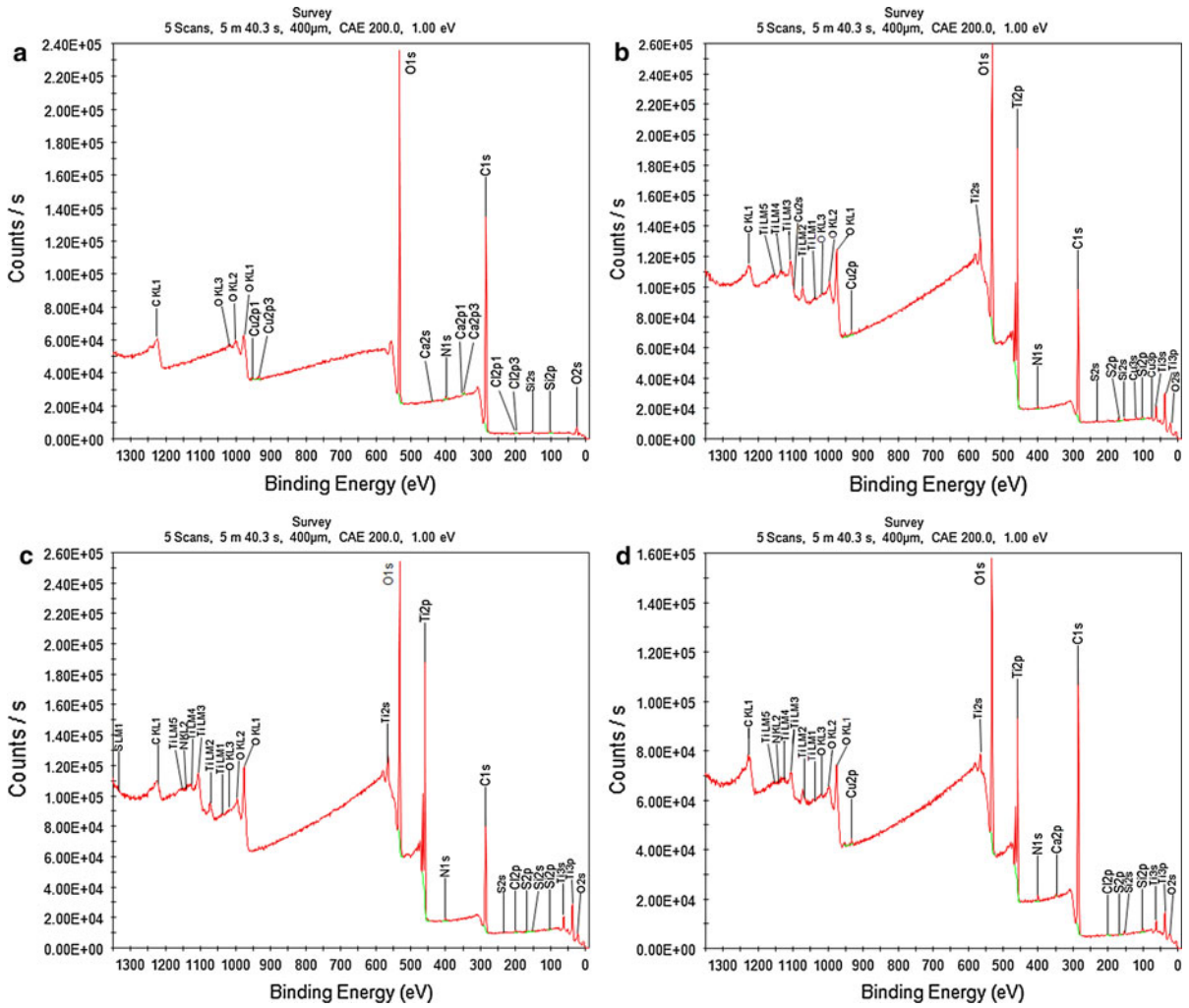

Fig. 1 The XPS survey spectra of Co (**a**), Co+TiO_2 (**b**), CCo+TiO_2 (**c**) and AIRCo+TiO_2 (**d**) fibres

from these impurities. The O–C–O groups might partially originate from pectic substances. Similar results can be found in literature (Chung et al. 2004; Topalovic et al. 2007; Tourrette et al. 2009). However, it is also common for carbon to be absorbed onto the surfaces of polymers, metals and oxides when exposed to air (Johansson and Campbell 2004). Therefore, it is very likely that detected C–C/C–H peaks appear partially due to adventitious contamination. The intensity of C–C/C–H peaks depends on the laboratory conditions during the sample preparation and the conditions in the spectrophotometer itself (Kontturi et al. 2003). The results from Table 1 also demonstrate that the amount of C–OH, C–O–C and O–C–O groups significantly decreased after corona or RF plasma pre-treatment and subsequent deposition of TiO_2 NPs.

The high resolution XPS spectra of O1s and Ti2p photoelectron peaks for the Co + TiO_2, CCo + TiO_2 and AIRCo + TiO_2 fibres are presented in Fig. 2. The $Ti2p_{1/2}$ and $Ti2p_{3/2}$ spin-orbital splitting electrons are located at binding energies of 464.2 and 458.5 eV, respectively. The O1s spectrum of analyzed fibres was deconvoluted with two components (Table 1) assigned to TiO_2 and C–O groups, respectively. The clear peak that appears in each spectrum at 529.8 eV confirms the presence of TiO_2 NPs on the surface of each sample.

The results from Table 1 also reveal that within experimental error (±10% of atomic percent value)

Table 1 Comparison of chemical composition of untreated and differently modified Co fibres derived from high resolution XPS spectra

	Atom %			
	Co	Co + TiO_2	CCo + TiO_2	AIRCo + TiO_2
Si2p (organic)	0.5	0.5	0.3	0.5
S2p (sulfate)	0.0	0.4	0.2	0.1
Cl2p	0.1	0.2	0.2	0.2
C1s (C–C/C–H)	24.8	29.1	27.2	26.2
C1s (C–OH)	35.8	12.2	13.8	20.5
C1s (C–O–C)	6.0	4.3	2.9	4.2
C1s (O–C–O)	5.8	3.0	3.3	4.1
$Ca2p_{3/2}$	0.2	0.0	0.0	0.1
N1s (organic)	0.4	0.5	0.5	0.4
$Ti2p_{3/2}$ (TiO_2)	0.0	10.2	9.3	4.1
O1s (TiO_2)	0.0	20.7	23.9	14.0
O1s (O–C)	26.2	19.1	18.4	25.5
Cu2p	0.1	0.0	0.0	0.1

the Co + TiO_2 and CCo + TiO_2 fibres have the same TiO_2 content. Unexpectedly, the AIRCo + TiO_2 fabric has about half as much TiO_2 as the other two samples.

7 × 6, 8 × 6.5 and 9.5 × 7 mm^2 areas of Co + TiO_2, CCo + TiO_2 and AIRCo + TiO_2 samples respectively were mapped in steps of 200 μm and the C1s, O1s and $Ti2p_{3/2}$ signals were measured at each point. From this, the percentage of TiO_2 was determined across the Co fibre surface. The results on mapping of the Co + TiO_2, CCo + TiO_2 and AIRCo + TiO_2 fabric surfaces are shown in Fig. 3. Figure 3a reveals the relatively uniform distribution of TiO_2 across the surface of the Co + TiO_2 fabric. Similar tendency is observed in the case of the CCo + TiO_2 fabric (Fig. 3b), where the lined patterning in the distribution can be attributed to the weave of the Co fabric. The TiO_2 on the fabric that was pre-treated by air RF plasma shows non-uniform distribution with most of the TiO_2 concentrated in the top right corner of the Fig. 3c.

The difference in TiO_2 NPs distribution across the surface of the CCo + TiO_2 and AIRCo + TiO_2 samples is suggested to be due to changes of fibres morphology induced by corona or air RF plasma. SEM images of the untreated, air RF plasma treated (AIRCo) and corona treated (CCo) fibres are shown in Fig. 4. The presence of characteristic folds running parallel to the elongation direction of the pristine cotton fiber is evident in Fig. 4a (Uddin et al. 2007). Severe bombardment of Co fibre surface by different energetic and reactive plasma species leads to an ablation of the fibre. Consequently, the surface roughness increases. The changes in fibre topography are highly affected by the plasma type and treatment conditions. Figure 4c demonstrates that air RF plasma brought about the formation of uneven pits and micro-cracks due to certain degree of plasma etching. This is in good correlation with literature data (Sun and Stylios 2006; Yuen and Kan 2007). In contrast, corona treatment led to a creation of uniform nano-sized grain-like fibre topography. Such structure might explain more uniform anchoring of TiO_2 NPs across the surface of CCo as detected by elemental mapping (Fig. 3b).

The total TiO_2 content in the Co fabrics was calculated on the basis of Ti content measured by AAS. The Co + TiO_2, CCo + TiO_2 and AIRCo + TiO_2 samples contained 1.3, 1.7 and 1.7 wt% of TiO_2. Unlike AAS which gives information on the total Ti content, XPS analysis is confined to the thin surface layer of Co fibres. This explains the difference between the results of XPS and AAS measurements. Although the X-rays penetrate a long way into the sample, the emitted photoelectrons have a strong interaction with the solid. Typically they can only travel around 10 nm before losing too much energy to be detected. Therefore the detected signal comes within 10 nm of the surface. Keeping in mind that the average dimension of the TiO_2 NPs in colloidal solution was 6 nm as well as that the nanoparticles are prone to agglomeration on the fabric surface, it is very likely that XPS supply us only with data corresponding to outer surface of agglomerated particles. This in turn also means that the composition that is detected by XPS will be biased towards the surface species, and will not be the same as the bulk analysis by AAS.

Greater content of TiO_2 in the CCo + TiO_2 and AIRCo + TiO_2 samples compared to the Co + TiO_2 found by AAS indicate the real advantage of fibre surface activation prior to TiO_2 NPs deposition. It is well known that corona and RF plasma cause morphological and chemical changes of the Co fibre surface (Johansson 2007; Tourrette et al. 2009). The interaction of plasma particles with cotton often

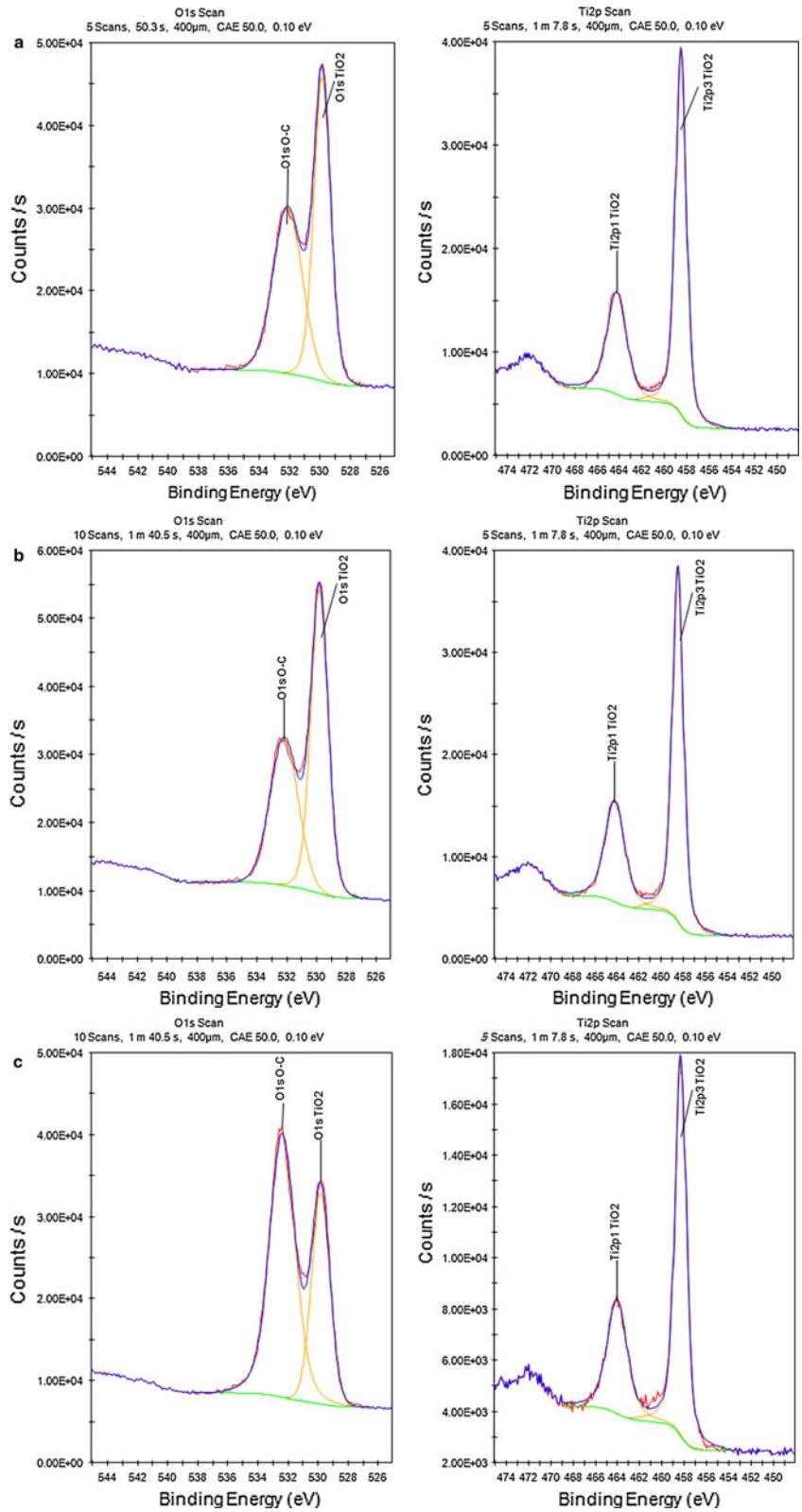

Fig. 2 High resolution XPS O1s and Ti2p spectra of Co+TiO_2 (**a**), CCo+TiO_2 (**b**) and AIRCo+TiO_2 (**c**) fibre

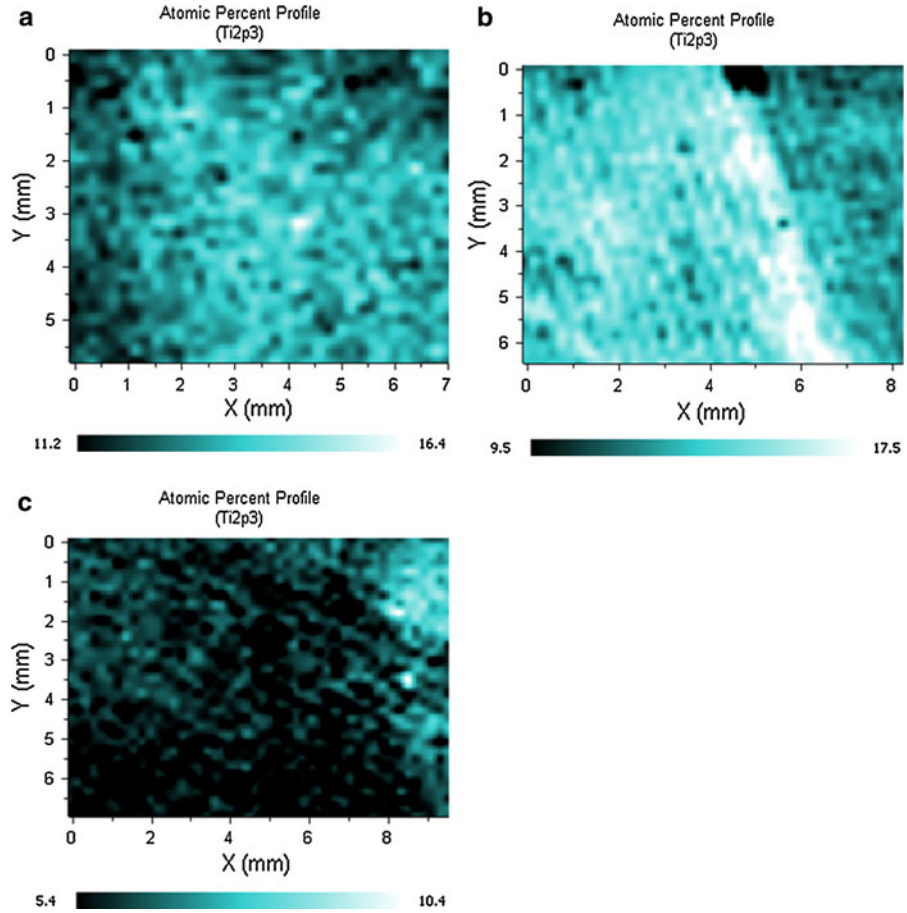

Fig. 3 TiO_2 mapping of the surfaces of the Co+TiO_2 (**a**), CCo+TiO_2 (**b**) and AIRCo+TiO_2 (**c**) fabrics

results in homolytic bond cleavage and generation of extremely instable and reactive free radicals on the fibre surface (Johansson 2007). Generated free radicals can react with certain species in oxygen or oxygen containing plasmas or species from atmospheric environment after plasma treatment. Hence, different new functionalities such as C–O, O–C–O, O = C–O, C = O and O–CO–O can be formed (Johansson 2007; Tourrette et al. 2009) the generation of which is highly influenced by the nature of the gas and plasma operating conditions. Altered chemical structure along with morphological changes of the Co fibre surface (Fig. 4) improved the fibre accessibility to TiO_2 NPs and consequently, the amount of deposited TiO_2 NPs increased as proved by AAS.

The advantages of plasma activation prior to TiO_2 NPs loading were illustrated by testing some specific practical effects. Bactericidal efficiency of Co fabrics loaded with TiO_2 NPs was evaluated against Gram-negative bacterium *E. coli*. Although the AAS and XPS measurements proved the presence of TiO_2 NPs on the Co + TiO_2 fabric, this sample did not exhibit any antibacterial activity. In order to obtain maximum bacteria reduction ($R = 99.9\%$), the deposition of TiO_2 NPs onto Co fabric had to be carried out twice (Co + TiO_2 × 2, Table 2). Excellent bactericidal efficiency of the Co + TiO_2 × 2 fabric is ascribed to higher content of deposited TiO_2 NPs. Precisely, AAS measurements revealed that the double loading of Co fabric with TiO_2 NPs led to an increase in the TiO_2 content (2.3 wt%) by 77%. However, optimum bactericidal efficiency can also be achieved by corona or RF plasma activation of Co fabrics and only one loading of TiO_2 NPs. In both cases maximum bacteria reduction was attained and even preserved after five washing cycles. Taking into account that the Co + TiO_2 fabric did not demonstrate any antibacterial activity unlike the CCo + TiO_2 and AIRCo + TiO_2 fabrics, it could be assumed

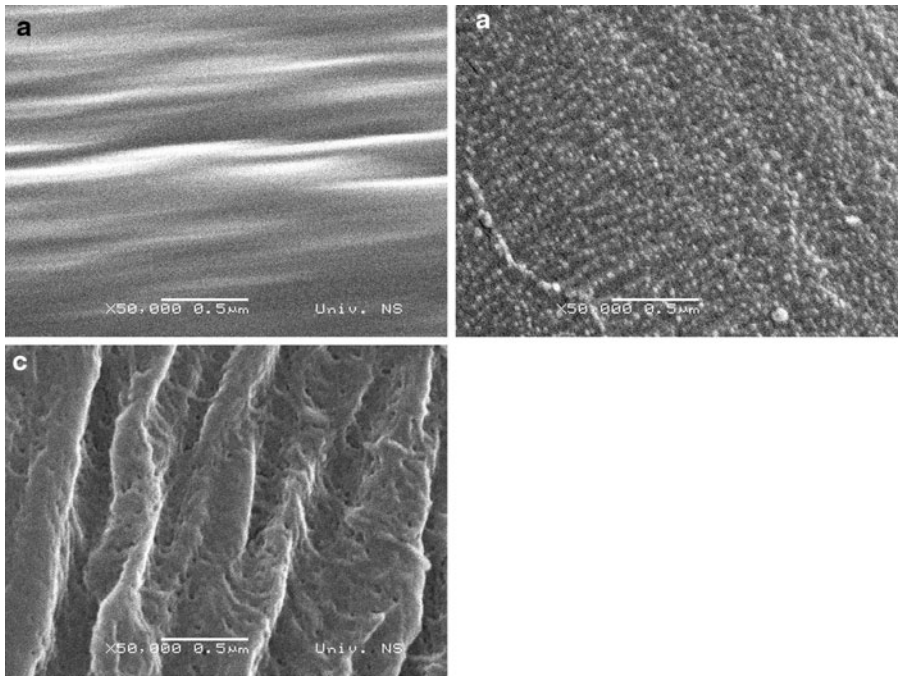

Fig. 4 SEM images of untreated Co (**a**), CCo (**b**) and AIRCo (**c**) fibres

Table 2 Bactericidal efficiency of Co fabrics modified with TiO_2 NPs before and after washing

Sample	Initial number of bacterial colonies (CFU)	Number of bacterial colonies (CFU)	*R*%
Control Co	2.1×10^5	9.6×10^4	
Co + TiO_2 × 2		90	99.9
Control Co	1.0×10^5	1.4×10^5	
CCo + TiO_2		20	99.9
Control Co	3.0×10^5	7.4×10^4	
AIRCo + TiO_2		10	99.9
After washing			
Control Co	4.5×10^5	1.6×10^5	
Co + TiO_2 × 2		55	99.9
Control Co	1.4×10^5	1.8×10^5	
CCo + TiO_2		65	99.9
Control Co	3.7×10^5	1.8×10^5	
AIRCo + TiO_2		25	99.9

that the critical amount of TiO_2 necessary to provide desirable antibacterial activity in our systems should be within 1.3 and 1.7 wt%.

The property of TiO_2 NPs to absorb well the UV light can be efficiently utilized for the reduction or elimination of negative impact of UV radiation on the human skin. The UV protective properties of textile materials are commonly evaluated via UPF values and corresponding UPF rating. It is recommended that UPF rating for garments should not be less than 40–50+. As can be seen in Table 3 control Co fabric posses extremely low UPF and non-rateable UPF rating of five (Qi et al. 2006). However, loading of Co fabrics with TiO_2 NPs led to a drastic increase of UPF values and accordingly, desired UPF rating of 50+ was reached. Taking into consideration the standard deviations of performed measurements, it can be deduced that the Co + TiO_2 × 2 and CCo + TiO_2 fabrics had almost the same UPF values and the best UV protective properties. Excellent UV protection efficacy is consistent with the amount of deposited TiO_2 NPs on the Co + TiO_2 × 2 fabric. Despite the equal content of TiO_2 in the CCo + TiO_2 and AIRCo + TiO_2 fabrics, apparently the CCo + TiO_2 fabric demonstrated better UV protective properties. This might be caused by more evenly distributed TiO_2 NPs across the surface of the fabric as indicated by elemental mapping (Fig. 3).

The UPF values decreased after five washing cycles, but UPF rating was maintained at 50+. The

Table 3 UPF rating of untreated and differently modified Co fabrics

Sample	UPF value	SD	UPF rating
Co	7.3	0.6	5
Co + TiO_2	134.3	47.2	50+
Co + TiO_2 × 2	208.3	72.2	50+
CCo + TiO_2	230.8	44.2	50+
AIRCo + TiO_2	173.2	42.1	50+
After washing			
Co + TiO_2	100.0	31.2	50+
Co + TiO_2 × 2	236.8	58.0	50+
CCo + TiO_2	164.0	17.9	50+
AIRCo + TiO_2	147.1	27.9	50+

peculiar rise of the UPF value for the Co + TiO_2 × 2 fabric after washing can be also found in literature and it is assigned to morphological change of textile nano-composite that occurred after washing (Paul et al. 2010). Daoud and co-workers suggested that the good laundering durability of Co fabrics loaded with TiO_2 NPs can be attributed to the formation of covalent bonding resulting from a dehydratation reaction between the hydroxyl groups of cotton and the hydroxyl groups of TiO_2 (Daoud and Xin 2004; Xin et al. 2004).

The ability of TiO_2 NPs to absorb the UV light and generate reactive chemical species can be exploited for photodegradation of stains on different textile materials (Bozzi et al. 2005a, b; Qi et al. 2007; Yuranova et al. 2007; Tung and Daoud 2009; Kiwi and Pulgarin 2010). In order to investigate a self-cleaning efficiency of studied samples, Co fabrics stained with blueberry juice were exposed to UV lamp for 24 h. Figure 5 clearly implies that Co fabric alone does not posses photocatalytic properties. The deposition of TiO_2 NPs onto Co fabric brought about only slight photodegradation of blueberry juice stain. However, the self-cleaning effect was considerably more prominent on the Co + TiO_2 × 2, CCo + TiO_2 and AIRCo + TiO_2 fabrics due to larger amount of deposited TiO_2 NPs. Higher content of TiO_2 NPs provides stronger UV absorption intensity and thus, greater photocatalytic activity.

The photodegradation activity of TiO_2-based substrates is commonly tested on dye methylene blue (MB) as a pollutant. The samples placed in the aqueous solution of MB were illuminated with UV lamp for 24 h. As predicted, the deposition of TiO_2 NPs imparted photocatalytic activity i.e. self-cleaning properties to Co fabrics. The dependence of C/C_0 versus time of UV illumination for the Co + TiO_2, Co + TiO_2 × 2, CCo + TiO_2 and AIRCo + TiO_2 fabrics is shown in Fig. 6. Presented results evidently indicate that the rate of MB discolouration increases with a rise of the TiO_2 content in the Co fabrics. Hence, the rate of MB discolouration particularly in the first 6 h of UV illumination increased in the following order: Co + TiO_2 × 2 > AIRCo + TiO_2 > CCo + TiO_2 > Co + TiO_2. Although the equal content of TiO_2 was detected by AAS in the AIRCo + TiO_2 and CCo + TiO_2 samples, the AIR-Co + TiO_2 fabric exhibited slightly faster MB discolouration. The complete discolouration of the MB solution was achieved after 24 h of UV illumination independently of the former modification of the fabric. Obtained results confirmed that the amount of deposited TiO_2 NPs was sufficient for efficient decomposition of MB in aqueous solution.

In order to examine the durability of photodegradation efficiency, applied procedure was repeated two more times under the same experimental conditions. Changes in relative MB concentration after repeated photodegradation processes under the UV illumination for the Co, Co + TiO_2, Co + TiO_2 × 2, CCo + TiO_2 and AIRCo + TiO_2 fabrics are also presented in Fig. 6. It is evident that the rate of MB discolouration increased in each subsequent cycle in the presence of the Co + TiO_2, CCo + TiO_2 and AIRCo + TiO_2 fabrics in the solution. The CCo + TiO_2 and AIRCo + TiO_2 fabrics accomplished the complete MB removal from the solution already after 8 h of UV lamp exposure in the third photodegradation cycle. Such behaviour was also observed on the polyester fabrics loaded with TiO_2 NPs that were studied in detail in our earlier research (Mihailović et al. 2010a, b). Equivalent results were also reported by other research groups (Uddin et al. 2007). Higher photocatalytic activity of TiO_2 NPs in repeated cycles is attributed to surface cleaning from impurities during the first photodegradation cycle. Unexpectedly, the Co + TiO_2 × 2 fabric did not follow this trend, though the MB was completely eliminated from the solution after 24 h of photodegradation in all three cycles.

Spectrophotometric measurements of the MB solutions confirmed that the MB solution was

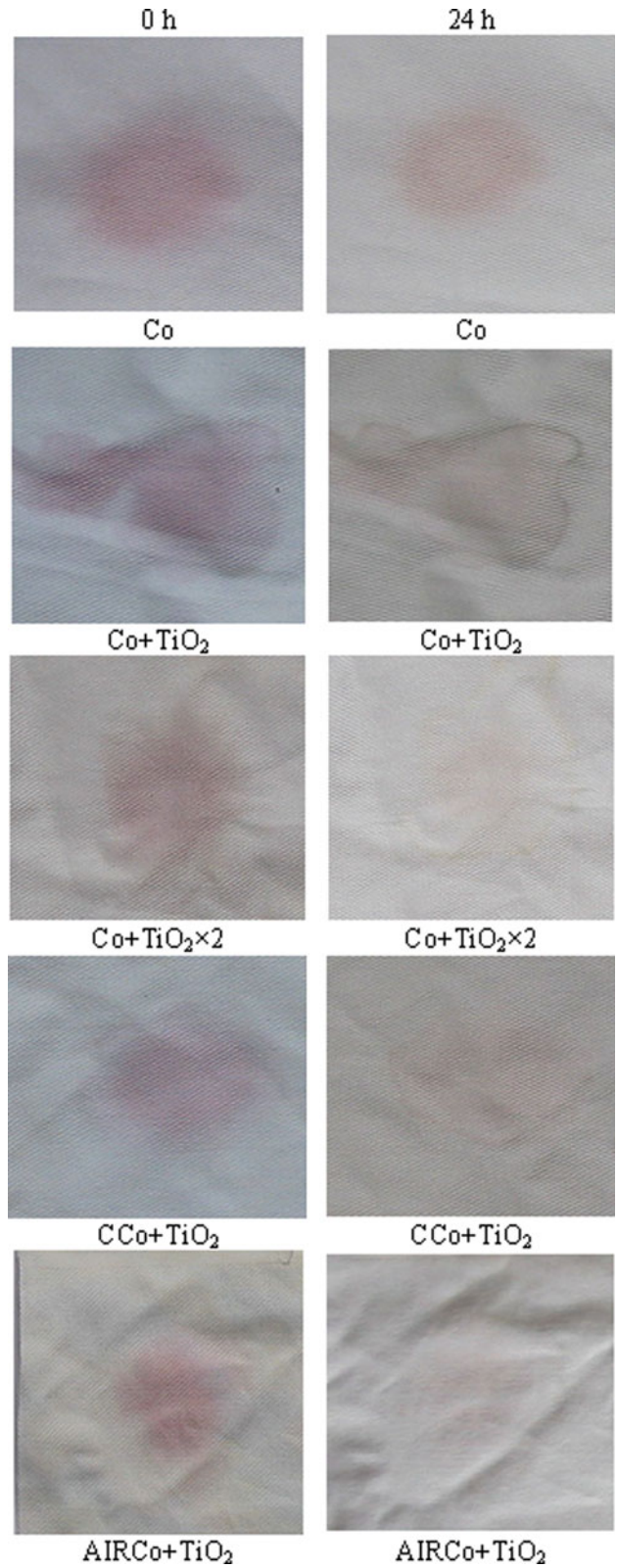

Fig. 5 Blueberry juice stains on untreated and differently modified Co fabrics before and after 24 h of UV illumination

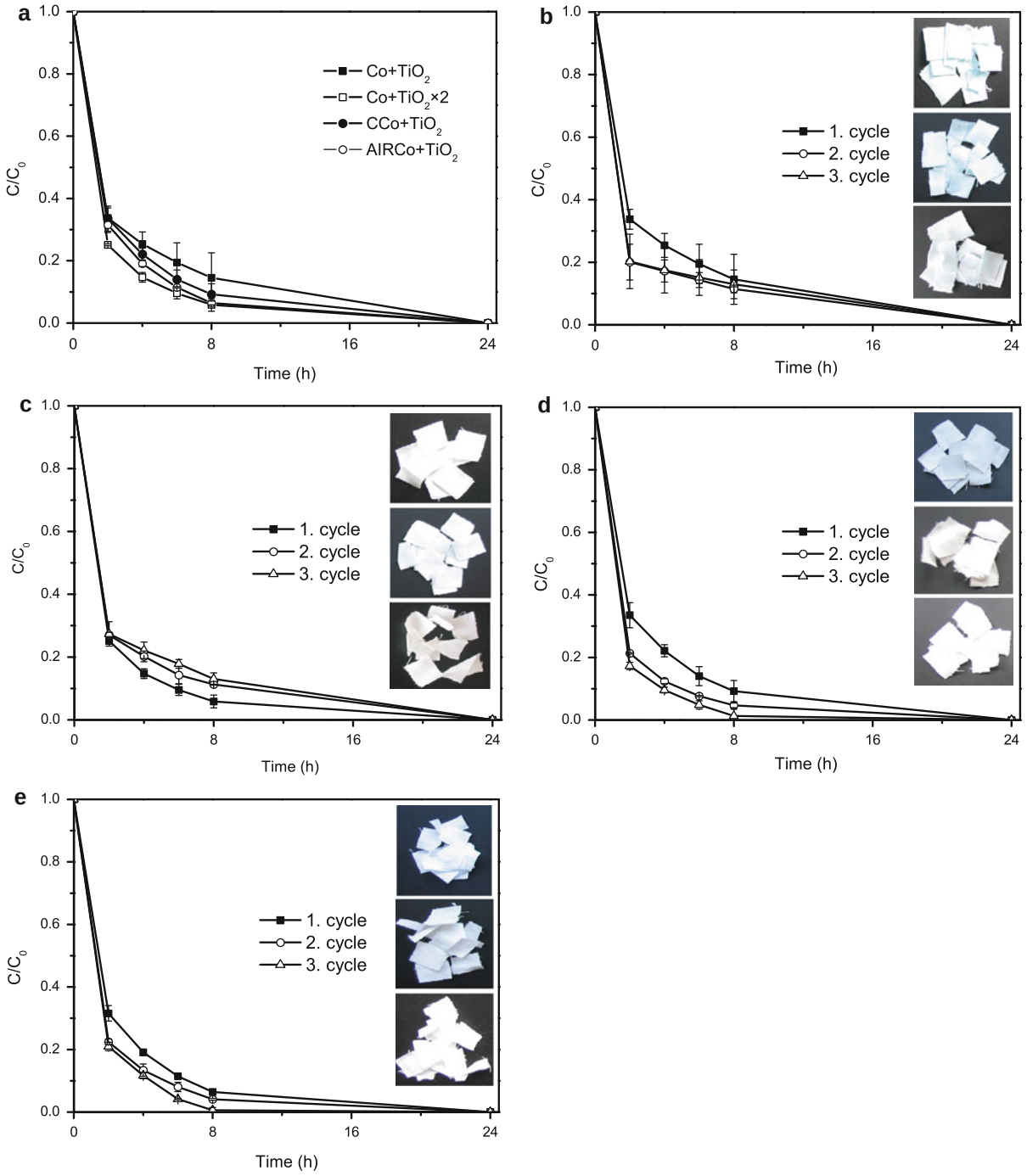

Fig. 6 Changes in relative concentration of MB after 24 h photodegradation under the UV illumination (**a**) and after repeated photodegradation processes for the Co+TiO_2 (**b**), Co+TiO_2×2 (**c**), CCo+TiO_2 (**d**) and AIRCo+TiO_2 fabrics (**e**)

decolourised after 24 h of UV lamp exposure, but this method cannot answer whether some extent of the MB remained on the fabrics. Therefore, the images of differently modified fabrics (dried at room temperature) after each photodegradation cycle were recorded (insets in Fig. 6) and corresponding colour

Table 4 Colour difference between untreated Co fabric and differently treated fabrics that were exposed to MB solution for 24 h after three photodegradation cycles

Sample	Cycle	ΔL^*	Δa^*	Δb^*	ΔE^*	Description
Co	1	−20.5	−13.5	−17.0	29.9	Darker, less red, bluer
	2	−25.4	−13.2	−18.0	33.8	Darker, less red, bluer
	3	−30.0	−13.0	−19.3	37.9	Darker, less red, bluer
Co + TiO_2	1	−10.1	−9.2	−6.6	15.2	Darker, less red, bluer
	2	−10.7	−6.2	−2.7	12.6	Darker, less red, bluer
	3	−7.8	−5.6	−1.8	9.7	Darker, less red, bluer
Co + TiO_2 × 2	1	−0.8	−1.1	2.5	2.8	Darker, less red, less blue
	2	−0.8	−0.9	1.8	2.2	Darker, less red, less blue
	3	−0.7	−0.9	1.8	2.1	Darker, less red, less blue
CCo+TiO_2	1	−1.9	−2.1	0.4	2.9	Darker, less red, less blue
	2	−1.0	−1.1	2.1	2.6	Darker, less red, less blue
	3	−1.1	−1.1	1.8	2.4	Darker, less red, less blue
AIRCo+TiO_2	1	−1.5	−1.4	1.1	2.3	Darker, less red, less blue
	2	−1.9	−1.6	1.1	2.8	Darker, less red, less blue
	3	−2.1	−1.1	1.6	2.9	Darker, less red, less blue

differences (ΔE^*) between the untreated Co (as supplied) and certain Co fabrics after 24 h of UV illumination were determined (Table 4). As expected, untreated Co fabric did not display any photocatalytic activity and the fabric was completely blue coloured even after 24 h of UV illumination. The fabric became significantly darker, less red and bluer. Consequently, compare to other samples, the highest ΔE^* was reached and it increased in each subsequent cycle as more dye was absorbed by the fabric.

The deposition of TiO_2 NPs onto Co fabrics resulted in the reduction of ΔE^*, particularly on the Co + TiO_2 × 2, CCo + TiO_2 and AIRCo + TiO_2 fabrics. The fabrics turned to be darker, less red and less blue. In the cases of Co + TiO_2, Co + TiO_2 × 2 and CCo + TiO_2 fabrics ΔE^* decreased in each following cycle since the MB photodegraded due to presence of TiO_2. Paralely, absolute values of lightness difference (ΔL^*) decreased in every subsequent cycle indicating that fabrics became successively lighter. On the contrary, in the case of AIRCo + TiO_2 fabric, ΔE^* slightly increased after the second photodegradation cycle and in fact, it remained almost the same after the third cycle. Such behaviour might be attributed to uneven deposition of TiO_2 NPs.

The results also imply that these samples did not show full discoloration even after 24 h of UV illumination. In other words, spectrophotometric measurements proved that no more MB remained in the solution, but obviously small amount of MB retained on the samples that did not entirely degrade. Despite the fact that ΔE^* greater than one is eye visible, calculated ΔE^* values are acceptable and they indicate that MB almost totally photodegraded also on the fabric. Presented colour changes can be considered even as a lower since the colour of the Co fabric exposed to UV lamp for 24 h in water was altered and it became redder and bluer ($\Delta E^* = 1.2$; $\Delta L^* = -0.08$; $\Delta a^* = 0.4$; $\Delta b^* = -1.1$). Additionally, the results from Fig. 6 and Table 4 also reveal that the Co + TiO_2 × 2 fabric not only completely removed the MB from the solution after 24 h of UV illumination, but it provided the lowest ΔE^* demonstrating excellent photodegradation efficacy. Hence, it can be assumed that slightly lower rate of MB photodegradation in the second and the third cycle (Fig. 6d) was likely due to slower absorption of the MB.

Conclusion

Corona discharge at atmospheric pressure and air RF plasma at low pressure can be efficiently exploited for the activation of cotton fibre surface prior to

deposition of colloidal TiO_2 nanoparticles. XPS analysis confirmed the presence of TiO_2 nanoparticles on the surface of cotton fibres. Elemental mapping indicated that TiO_2 nanoparticles were uniformly distributed across the surface of untreated and corona pre-treated fabrics unlike the air RF plasma pre-treated fabric. AAS measurements showed that corona and RF plasma pre-treated fabrics had the same content of TiO_2 which was by 31% higher compared to sample that was only modified with TiO_2 nanoparticles. The larger amount of deposited TiO_2 nanoparticles provided bactericidal activity against Gram-negative bacteria *E. coli*. The same effect can be achieved with the fabric that underwent double loading of TiO_2 nanoparticles without any pre-treatment. All the samples modified with TiO_2 provided UPF rating of 50+, which designates the maximum UV-protection. Maximum bacteria reduction and UPF rating were preserved after five washing cycles, indicating good laundering durability. Excellent photocatalytic activity of deposited TiO_2 nanoparticles was confirmed by efficient self-cleaning of blueberry juice stain on the cotton fabric as well as by discolouration of methylene blue in the aqueous solution in the presence of the fabric under the UV illumination. Obtained results clearly demonstrate that both corona discharge and air RF plasma can be efficiently used for the activation of the cotton fibre surface, increasing the binding efficiency of TiO_2 nanoparticles.

Acknowledgments The financial support for this work was provided by the Ministry of Science of Republic of Serbia 45020 and 172056.

References

Bozzi A, Yuranova T, Kiwi J (2005a) Self-cleaning of wool-polyamide and polyester textiles by TiO_2-rutile modification under daylight irradiation at ambient temperature. J Photochem Photobio A 172:27–34

Bozzi A, Yuranova T, Guasaquillo I, Laub D, Kiwi J (2005b) Self-cleaning of modified cotton textiles by TiO_2 at low temperatures under daylight irradiation. J Photochem Photobio A 174:156–164

Cai Z, Qiu Y, Zhang C, Hwang YH, McCord M (2003) Effect of atmospheric plasma treatment on desizing of PVA on cotton. Text Res J 73:670–674

Chung C, Lee M, Kyung Choe E (2004) Characterization of cotton fabric scouring by FTIR ATR spectroscopy. Carbohyd Polym 58:417–420

Clemencic D, Simoncic B, Tomsic B, Orel B (2010) Biodegradation of silver functionalised cellulose fibres. Carbohyd Polym 80:426–435

Daoud WA, Xin JH (2004) Low temperature sol-gel processed photocatalytic Titania coating. J Sol-Gel Sci Techn 29: 25–29

Daoud WA, Xin JH, Zhang YH (2005) Surface functionalization of cellulose fibres with titanium dioxide nanoparticles and their combined bactericidal activities. Surf Sci 599:69–75

Fras L, Johansson LS, Stenius P, Laine J, Stana-Kleinschek K, Ribitsch V (2005) Analysis of the oxidation of cellulose fibres by titration and XPS. Colloid Surf A 260:101–108

Ghoranneviss M, Bahareh M, Shahidi S, Anvari A, Rashidi A (2006) Decolourization of denim fabrics with cold plasmas in the presence of magnetic field. Plasma Proc Polym 3:316–321

Johansson K (2007) Plasma modification of natural cellulosic fibres. In: Shishoo R (ed) Plasma technologies for textiles. Woodhead publishing in textiles, Cambridge, pp 251–260

Johansson LS, Campbell JM (2004) Reproducible XPS on biopolymers: cellulose studies. Surf Interface Anal 36: 1018–1022

Karahan HA, Özdoğan E (2008) Improvements of surface functionality of cotton fibres by atmospheric plasma treatment. Fiber Polym 9:21–26

Kiwi J, Pulgarin C (2010) Innovative self-cleaning and bactericide textiles. Catal Today 151:2–7

Kontturi E, Thüne PC, Niemantsverdriet JW (2003) Novel method for preparing cellulose model surfaces by spin coating. Polymer 44:3621–3625

Lee HJ, Yeo SY, Jeong SH (2003) Antibacterial effect of nanosized silver colloidal solution on textiles fabrics. J Mater Sci 38:2199–2204

Mejía MI, Marín JM, Restrepo G, Pulgarín C, Mielczarski E, Mielczarski J, Arroyo Y, Lavanchy JC, Kiwi J (2009) Self-cleaning modified TiO_2 cotton pre-treated by UVC-light (185 nm) and RF-plasma in vacuum and also under atmospheric pressure. Appl Catal B 91:481–488

Mihailović D, Šaponjić Z, Radoičić M, Molina R, Radetić T, Jovančić P, Nedeljković J, Radetić M (2010a) Novel properties of PES fabrics modified by corona discharge and colloidal TiO_2 nanoparticles. Polym Advan Technol. doi:10.1002/pat.1568

Mihailović D, Šaponjić Z, Molina R, Radoičić M, Esquena J, Jovančić P, Nedeljković J, Radetić M (2010b) Multifunctional properties of polyester fabrics modified by corona discharge/air RF plasma and colloidal TiO_2 nanoparticles. Polym Composit. doi:10.1002/pc.21053

Mihailović D, Šaponjić Z, Radoičić M, Radetić T, Jovančić P, Nedeljković J, Radetić M (2010c) Functionalization of polyester fabrics with alginates and TiO_2 nanoparticles. Carbohyd Polym 79:526–532

Morent R, De Geyter N, Verschuren J, De Clerck K, Kiekens P, Leys C (2008) Non-thermal plasma treatment of textiles. Surf Coat Tech 202:3427–3449

Navaneetha Pandiyaraj K, Selvarajan V (2008) Non-thermal plasma treatment for hydrophilicity improvement of grey cotton fabrics. J Mater Process Tech 199:130–139

Paul R, Bautista L, De la Varga M, Botet JM, Casals E, Puntes V, Marsal F (2010) Nano-cotton fabrics with high ultraviolet protection. Text Res J 80:454–462

Qi K, Daoud WA, Xin JH, Mak CL, Tang W, Cheung WP (2006) Self-cleaning cotton. J Mater Chem 16:4567–4574

Qi K, Xin JH, Daoud WA, Mak CL (2007) Functionalizing polyester fiber with a self-cleaning property using anatase TiO_2 and low-temperature plasma treatment. Int J Appl Ceram Tec 4:554–563

Radetić M, Jovančić P, Puač N, Petrović ZLj, Šaponjić Z (2009) Plasma induced decolorization of indigo dyed denim fabrics related to mechanical properties and fiber surface morphology. Text Res J 79:558–565

Sun D, Stylios GK (2006) Fabric surface properties affected by low temperature plasma treatment. J Mater Process Tech 173:172–177

Sun D, Stylos G (2004) The effect of low temperature plasma treatment on the scouring and dyeing processes of natural fabrics. Text Res J 74:751–756

Thomas H (2007) Plasma modification of wool. In: Shishoo R (ed) Plasma technologies for textiles. Woodhead publishing in textiles, Cambridge, pp 228–246

Topalovic T, Nierstrasz VA, Bautista L, Jocic D, Navarro A, Warmoeskerken MMCG (2007) XPS and contact angle of cotton surface oxidation by catalytic bleaching. Colloid Surf A 296:76–85

Tourrette O, De Geyterb N, Jocic D, Morent R, Warmoeskerken MMCG, Leys C (2009) Incorporation of poly(N-isopropylacrylamide)/chitosan microgel onto plasma functionalized cotton fibre surface. Colloid Surf A 352:126–135

Tung WS, Daoud WA (2009) Photocatalytic self-cleaning keratines: a feasibility study. Acta Biomater 5:50–56

Uddin MJ, Cesano F, Bonino F, Bordiga S, Spoto G, Scarano D, Zecchina A (2007) Photoactive TiO_2 films on cellulose fibres: synthesis and characterization. J Photochem Photobio A 189:286–294

Ueda M, Tokino S (1996) Physico-chemical modifications of fibres and their effect on coloration and finishing. Rev Progress Color 26:9–19

Wakida T, Tokino S (1996) Surface modification of fibre and polymeric materials by discharge treatment and its application to textile processing. Ind J Fibre Text Res 21:69–78

Wu D, Long M, Zhou J, Cai W, Zhu X, Chen C, Wu Y (2009) Synthesis and characterization of self-cleaning cotton fabrics modified by TiO_2 through a facile approach. Surf Coat Tech 203:3728–3733

Xin JH, Daoud WA, Kong YY (2004) A new approach to UV-blocking treatment for cotton fabrics. Text Res J 74:97–100

Yuen CWM, Kan CW (2007) Influence of low-temperature plasma on the ink-jet-printed cotton fabric. J Appl Polym Sci 104:3214–3219

Yuranova T, Mosteo R, Bandara J, Laub D, Kiwi J (2006) Self-cleaning cotton textiles surfaces modified by photoactive SiO_2/TiO_2 coating. J Molec Catal A 244:160–167

Yuranova T, Laub D, Kiwi J (2007) Synthesis, activity and characterization of textiles showing self-cleaning activity under daylight irradiation. Catal Today 122:109–117

MASS SPECTROSCOPY OF AN ATMOSPHERIC PRESSURE PLASMA BULLET

Conference Paper · August 2013

READS
33

6 authors, including:

Gordana Malovic
Institute of Physics Belgrade
157 PUBLICATIONS **932** CITATIONS
SEE PROFILE

Zoran Lj Petrović
Institute of Physics Belgrade
510 PUBLICATIONS **5,652** CITATIONS
SEE PROFILE

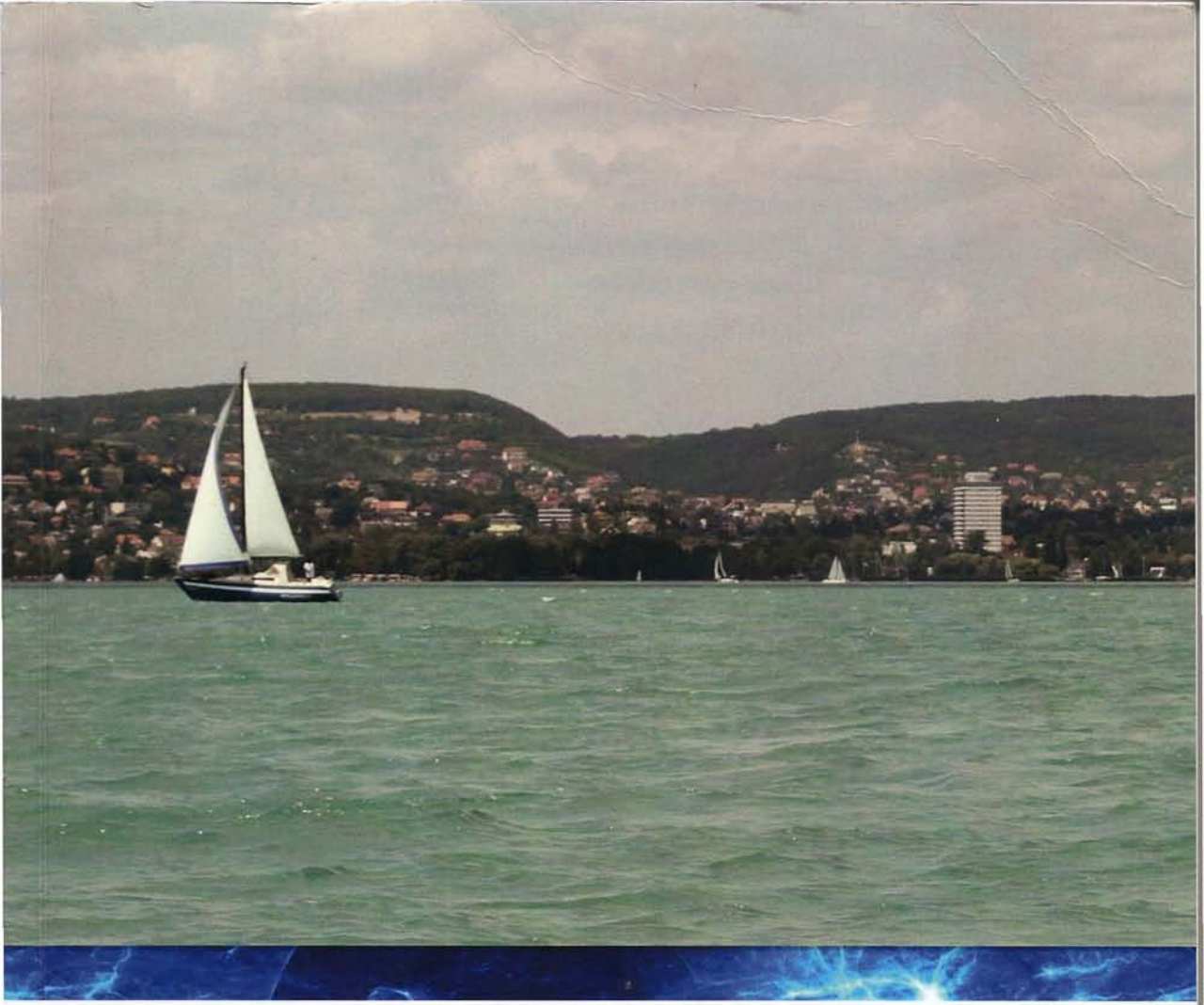

5th Central European Symposium on Plasma Chemistry

Balatonalmádi, Hungary, 25-29 August 2013

Final scientific programme & Book of abstracts

ISBN 978-615-5270-04-8

5th Central European Symposium on Plasma Chemistry

Final scientific programme
&
Book of abstracts

Balatonalmádi, Hungary, 25-29 August 2013

Published by:

Research Centre for Natural Sciences, Hungarian Academy of Sciences
H-1025 Budapest, Pusztaszeri út 59-67., HUNGARY

Wigner Research Centre for Physics, Hungarian Academy of Sciences
H-1121 Budapest, Konkoly Thege Miklós út 29-33. , HUNGARY

Diamond Congress Ltd., Conference Secretariat
H-1012 Budapest, Vérmező út 8., HUNGARY
www.diamond-congress.hu

Lectored by: Kinga Kutasi, Klára Szentmihályi, Zoltán Donkó
Edited by: Róbert Hohol, Zsuzsanna Heiszler

ISBN 978-615-5270-04-8

O-BM9
MASS SPECTROSCOPY OF AN ATMOSPHERIC PRESSURE PLASMA BULLET

N. Selaković, D. Maletić[1], N. Puač, S. Lazović, G. Malović, Z. Lj. Petrović

Institute of Physics, University of Belgrade, Belgrade, Serbia

nele@ipb.ac.rs

Wide range of potential applications of plasma sources operating at atmospheric pressure, particularly in medicine and biology, has led to a large expansion in their development. Before using a new plasma source for treatment of bio-samples it is necessary to make detailed diagnostics of the plasma and, most importantly, examine its chemical composition. We have used Hiden HPR 60 mass-energy analyzer for the time-resolved measurements of the ionic species originated from atmospheric-pressure plasma jet.

Plasma jet was made of Pyrex glass tube with two transparent electrodes (15 mm wide) made of polyester (PET) foil. The gap between the electrodes was 15 mm. This source operated at excitation frequency of 80 kHz and applied voltage was in the range of 6-10 $kV_{peak\text{-}to\text{-}peak}$. The feeding gas was helium with flow rate of 4 slm. In all experiments distance between the plasma source and HPR60 orifice was 15 mm. We also used plastic side-covers around plasma source to prevent plasma flickering due to ambient air disturbance. The applied current and voltage signal and HPR 60 internal gate signal have been synchronized. The internal gate width of HPR60 analyzer was 0.5 μs.

Mass spectrometer was operated in ion mass spectroscopy mode and we have measured positive and negative ion species coming from the plasma. The detected positive species from the plasma plume are N_2^+(36%), N^+(20%), O_2^+(18.5%), O^+(16.8%), H_2O^+(6.1%) and a few percentage of OH^+, NO^+, N_2H^+ and Ar^+ (see Fig.1). In case of negative ions we have detected O^-(34.3%), OH^-(24.2%), O_2^-(10.5%) and a few percentage of CO_2^-, NO_3^- and NO_2^-. The signal of detected ions was also tracked in time for the duration of 5 periods (5x12.5 μs) of current and voltage signal.

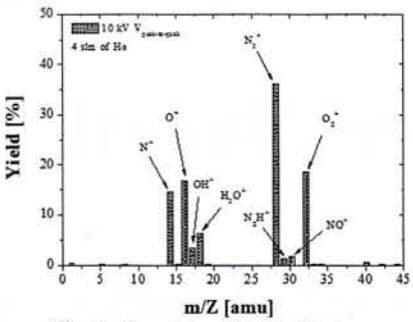

Fig. 1: Mass spectra plot of positive ions

Acknowledgements

This research has been supported by the MESTD, Serbia, under projects ON171037 and III41011.

References

1 *N. Puač, D. Maletić, S. Lazović, G. Malović, A. Đorđević and Z. Lj. Petrović, Applied Physics Letters, 101(2), (2012), 24103.*

Sterilization of bacteria suspensions and identification of radicals deposited during plasma treatment

Article *in* Open Chemistry · January 2015

Impact Factor: 1.33 · DOI: 10.1515/chem-2015-0041

11 authors, including:

Milicic Biljana
University of Belgrade
119 PUBLICATIONS **2,181** CITATIONS
SEE PROFILE

Saša Lazović
Institute of Physics Belgrade
70 PUBLICATIONS **212** CITATIONS
SEE PROFILE

Gordana Malovic
Institute of Physics Belgrade
157 PUBLICATIONS **932** CITATIONS
SEE PROFILE

Zoran Lj Petrović
Institute of Physics Belgrade
510 PUBLICATIONS **5,652** CITATIONS
SEE PROFILE

Research Article **Open Access**

Nevena Puač*, Maja Miletić, Miloš Mojović, Ana Popović-Bijelić, Dragana Vuković, Biljana Miličić, Dejan Maletić, Saša Lazović, Gordana Malović, Zoran Lj. Petrović

Sterilization of bacteria suspensions and identification of radicals deposited during plasma treatment

Abstract: In this paper we will present results for plasma sterilization of planktonic samples of two reference strains of bacteria, *Pseudomonas aeruginosa* ATCC 27853 and *Enterococcus faecalis* ATCC 29212. We have used a plasma needle as a source of non-equilibrium atmospheric plasma in all treatments. This device is already well characterized by OES, derivative probes and mass spectrometry. It was shown that power delivered to the plasma is bellow 2 W and that it produces the main radical oxygen and nitrogen species believed to be responsible for the sterilization process. Here we will only present results obtained by electron paramagnetic resonance which was used to detect the OH, H and NO species. Treatment time and power delivered to the plasma were found to have the strongest influence on sterilization. In all cases we have observed a reduction of several orders of magnitude in the concentration of bacteria and for the longest treatment time complete eradication. A more efficient sterilization was achieved in the case of gram negative bacteria.

Keywords: plasma needle, sterilization, spin-trap, Electron Paramagnetic Resonance, radicals

DOI: 10.1515/chem-2015-0041
received January 31, 2014; accepted May 29, 2014.

***Corresponding author: Nevena Puač:** Institute of Physics, University of Belgrade, 11080 Belgrade, Serbia, E-mail: nevena@ipb.ac.rs
Dejan Maletić, Saša Lazović, Gordana Malović, Zoran Lj. Petrović: Institute of Physics, University of Belgrade, 11080 Belgrade, Serbia
Maja Miletić, Biljana Miličić: Faculty of Dental Medicine, University of Belgrade, 11000 Belgrade, Serbia
Miloš Mojović, Ana Popović-Bijelić: Faculty of Physical Chemistry, University of Belgrade, University of Belgrade, 11000 Belgrade, Serbia
Dragana Vuković: Institute of Microbiology and Immunology, Faculty of Medicine, University of Belgrade, 11000 Belgrade, Serbia

1 Introduction

Atmospheric non-equilibrium low temperature plasmas have proven their usefulness in many applications involving living cells, tissue and bacteria. In spite of the fact that ignition and sustaining of atmospheric non-equilibrium plasmas are much harder than for low pressure plasmas, the former have taken over the leading place in plasma applications in biology and medicine. This is because such plasmas fulfil the most important requirements such as low gas and substrate temperature (must be below 42°C to avoid thermal necrosis), they provide abundance of chemical species and do not pose any electrical and chemical hazards. In addition, the composition and plasma-chemical processes can be controlled, even tailored, depending on the desired effect.

Results of previous studies have shown that the low-temperature plasma can be used for modification of biomaterials and, at the same time, as an alternative to conventional methods of sterilization [1-3]. The majority of the latest research has focused on the possible use of low-temperature plasma *in vivo*. Given that low-temperature plasma exerts a strong lethal effect on microorganisms, in recent years a possibility of applying it *in vivo* for disinfection and antimicrobial therapy has been extensively examined [4-9].

One of the non-thermal atmospheric pressure plasma sources, operating in the mixture of ambient air and rare gas, convenient for biomedical applications is the plasma needle [10]. We have redesigned and improved the plasma needle and performed detailed investigation of the properties of the discharge. To achieve an effective and safe treatment it is necessary to optimize the conditions under which it would be possible to implement it. The derivative probe measurements of power delivered to the plasma and mass spectrometry of the plasma generated by the needle have already been presented in our previous work [11,12]. Plasma needle generates radical oxygen species (ROS) and radical nitrogen species (RNS) radicals

like N, O, O_3, OH and NO that may play a role in metabolism of cells, triggering different biological processes and in sterilization. When the samples are in direct contact with the discharge all these radicals easily reach the surface of the sample. However, when bacteria are suspended in liquid it is needed to additionally investigate whether and which radicals originated from the plasma can penetrate into the solution. Electron Paramagnetic Resonance (EPR) is one of the diagnostic methods that can be used to detect presence of radicals in the solutions.

In the present study, the antimicrobial potential of low-temperature atmospheric plasma, generated by a plasma needle, was tested on two bacterial species, notorious for their growing resistance to various antimicrobial agents. EPR was used in order to detect the OH, H and NO species in solutions that were used to prepare suspensions of bacteria.

2 Experimental procedure

2.1 Bacterial suspensions

In this study we used the reference strains *Pseudomonas aeruginosa* ATCC 27853 and *Enterococcus faecalis* ATCC 29212.

Bacterial suspensions were prepared at the Laboratory of Microbiology, Faculty of Dental Medicine, University of Belgrade. Standard strains of bacteria were kept in a deep freezer at -76°C. They were inoculated into dextrose broth (Torlak Institute of Immunology and Virology, Serbia), and incubated aerobically for 20 h at 37°C. The strains were then subcultured in solid nutritional media under the same conditions. *E. faecalis* on blood agar (Torlak) and *P. aeruginosa* on Müller-Hinton agar (Torlak). The next step was preparation of bacterial suspensions. The initial bacterial concentration was determined using a spectrophotometer, so that the optical density corresponded to 1.5×10^8 CFU mL^{-1} of bacterial cells. From this initial suspension, 1:10, 1:100 and 1:1000 dilutions were made, and inoculated into 96-well microtiter plates, 0.2 mL per well.

2.2 Plasma system

The plasma needle that was used in these experiments consisted of long central electrode made of thin tungsten wire (0.5 mm in diameter) covered by a ceramic tube. Both were placed inside a glass tube with outer diameter of 6 mm. The purpose of the ceramic tube was to isolate central electrode from helium flow in order to avoid creation of plasma inside the glass tube and the Teflon body of the plasma needle. In the experiments helium was used as the feeding gas. The flow rates were adjusted to 0.5 and 1 sLm (standard litres per minute) by mass flow controller (OmegaFMA5400/5500). Sinusoidal signal at the frequency of 13.56 MHz was used for powering the plasma needle. In all experiments home-made calibrated derivative probes were used for measuring and controlling the power. Both probes were placed inside a metal case, as close as possible to the tip of the plasma needle. These probes were connected to the oscilloscope (Agilent DSO3202A) by the cables of equal length in order to acquire current and voltage signals. Obtained signals were converted from time to frequency domain by Fast Fourier Transform (FFT) and then multiplied by calibration curves. Finally, signals were converted back to the time domain using an Inverse Fast Fourier Transform (IFFT). We chose mean power as the main plasma parameter that was used to monitor and calculate from the calibrated signal. Powers transmitted to the plasma, obtained from the difference of calculated powers with and without plasma (no helium flow), were used to monitor plasma treatment conditions. In all treatments power delivered to the plasma did not go above few watts. Plasma was created in the mixture of helium and gas components from the surrounding atmosphere that can diffuse into helium plasma and produce more radicals such as atomic oxygen, nitrogen, nitrogen oxides and ozone. Plasma was generated only on the plane tip of the powered central electrode.

The plasma needle was placed vertically above the microtiter plate at the edge of each well containing bacterial cells. To examine the antibacterial effect of non-thermal plasma, the treatments were performed for three different powers of plasma (0.15, 0.9, 1.6 W), two flows of helium (0.5 and 1 sLm) and three exposure times (60, 120 and 180 s). To be sure that the helium flow has no influence on the treated cell samples we also treated samples in helium flow without ignition of plasma for the same exposure times. Untreated wells containing bacteria were used as control samples.

After exposing the bacterial suspensions to low-temperature atmospheric plasma, 0.05 mL of each suspension were taken and inoculated onto appropriate solid media, *E. faecalis* on blood agar (Torlak) and *P. aeruginosa* on Müller-Hinton agar (Torlak). After an incubation period of 20 h at 37°C in aerobic conditions, the effect of the plasma treatment was evaluated based on the number of bacterial colonies. Arbitrary units (0-6) were used to assess the bacterial growth: 0 - absence of

colony growth, 1 – number of colonies ≤ 50, 2 - number of colonies 51-100, 3 - number of colonies 101-300, 4 - number of colonies 301-500, 5- number of colonies > 500, fields with confluent growth; 6 - confluent growth.

2.3 Electron paramagnetic resonance

The spin-trap DEPMPO (5-(diethoxyphosphoryl)-5-methyl-1-pyrroline-N-oxide) was purified and tested for hydroxylamine impurities, as previously described [13]. The final concentration of DEPMPO in samples was 50 mM. The Fe(II)$(DTCS)_2$ complex was prepared by dissolving DTCS (N-(dithiocarboxy) sarcosine, diammonium salt) and $FeSO_4 \bullet 7H_2O$ in 18 MΩ deionized water. The final concentration of the complex in samples was 20 mM.

The samples for EPR measurements (60 μL) were drawn into 10 cm long gas-permeable Teflon tubes (wall thickness 0.025 mm and internal diameter 0.6 mm; Zeus industries, Raritan, USA). EPR spectra were recorded at room temperature using a Varian E104-A EPR spectrometer operating at X-band (9.51 GHz) with the following settings: modulation amplitude, 2 G; modulation frequency, 100 kHz; microwave power, 10 mW; time constant, 0.032 s; field center, 3410 G; scan range, 200 G. The spectra were processed using EW software (Scientific Software, Bloomington, IL, USA). Spectral simulation was performed using EasySpin program for MATLAB environment [14].

3 Results and discussion

3.1 EPR measurements of plasma treated samples

In our previous work we have shown that plasma needle produces significant amounts of ROS, RNS and ions [12]. Similar results were obtained by Stofells and coworkers [15]. The radical which is of most interest in biological processes is NO followed by the singlet delta ($^1\Delta$) metastable O_2 molecule and hydrogen peroxide. All of these ROS can be detected in the plasma needle discharge. When the discharge is in direct contact with the sample we can be sure that ROS reaches the membranes of the treated cells or bacteria, but when the samples are in suspensions it is unclear which radicals enter the suspension and are responsible for the sterilization of the sample containing bacteria. In order to get a clearer picture about the role of ROS, we have evaluated the existence of free radicals in plasma-irradiated water samples by using DEPMPO spin trap and Fe(II)$(DTCS)_2$ complex. DEPMPO is the most efficient spin trap for the detection of various short lived free radicals, which could be generated in the same system [16]. The DEPMPO free radical adducts give rise to characteristic EPR spectra as shown in [17]. The Fe(II)$(DTCS)_2$ complex traps nitric oxide radicals (NO•) and forms the ferrous nitrosyl complex Fe(NO)$(DTCS)_2$ which gives a characteristic three line EPR spectrum [18].

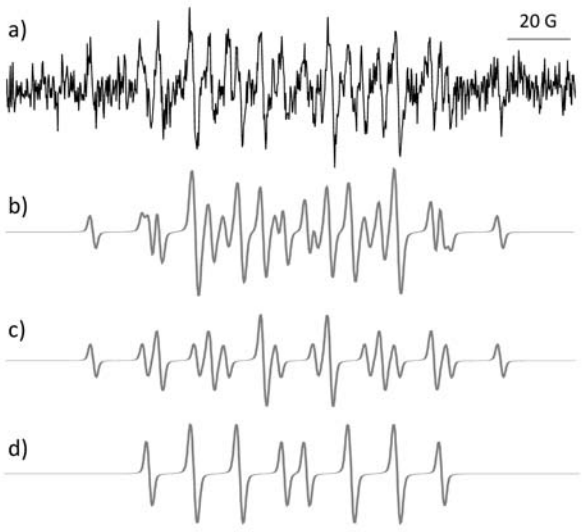

Figure 1: a) EPR spectrum of a water sample containing 50 mM DEPMPO irradiated with plasma for 9 min, power 1.6 W. b) Simulation of spectrum in a) obtained by spectral addition of simulations of 50% DEPMPO/OH and 50% DEPMPO/H adduct signals. c) Simulation of the DEPMPO/H adduct signal, hyperfine splitting constants (in Gauss); a^P=50.7; a^N=15.4; a^H_β (1H)=19.5, a^H_β (1H)=20, d) Simulation of the DEPMPO/OH adduct signal, hyperfine splitting constants (in Gauss); a^P=46.7; a^N=13.64, a^H_β (1H)=12.78.

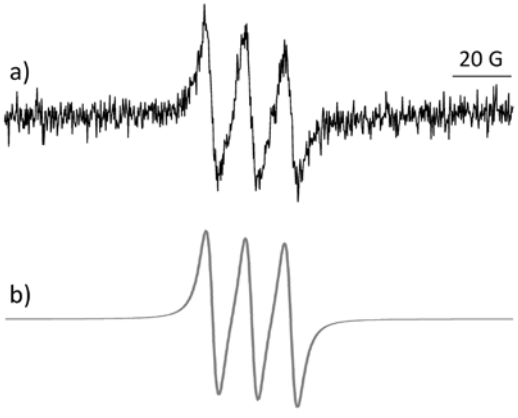

Figure 2: a) Experimental EPR spectrum of the Fe(NO)$(DTCS)_2$ complex obtained after plasma irradiation of a water sample containing Fe$(DTCS)_2$ for 9 min, power 1.6 W. b) Simulated EPR spectrum of Fe(NO)$(DTCS)_2$, nitrogen hyperfine splitting constant (in Gauss) a^N=12.7.

The samples that contained DEPMPO or Fe(II)(DTCS)$_2$ complexes in water but were not irradiated by plasma did not exhibit EPR spectra at room temperature. However, after plasma irradiation (1.6 W power, 9 min exposure) the samples that contained the DEPMPO spin trap, gave rise to an EPR spectrum shown in Fig. 1a. By spectral simulation (Fig. 1b) it was determined that this spectrum is composed of two components, one that arises from the DEPMPO/H adduct (Fig. 1c) and the other that arises from the DEPMPO/OH adduct (Fig. 1d). From additions of the simulated spectra (Figs. 1c and d), we could estimate the contributions of adducts to be ~ 50% for DEPMPO/H and ~ 50% for DEPMPO/OH. It should also be noted that the same EPR signal was observed even after 2-10 min irradiation with powers less than 1.6 W. In the experiments with Fe(II)(DTCS)$_2$, it was observed that after plasma irradiation (1.6 W power, 9 min exposure), an EPR signal characteristic of the Fe(NO)(DTCS)$_2$ is detected (Fig. 2a). This indicates that NO$^\bullet$ is produced during plasma irradiation as well.

3.2 Sterilization of planktonic samples of E. faecalis and P. aeruginosa

The plasma needle was used for sterilization of several species of Gram positive and Gram negative bacteria. Here, we will present results of plasma treatments of *E. faecalis* ATCC 29212 and *P. aeruginosa* ATCC 27853 in more detail. The samples for both bacterial strains were prepared in a form of suspensions of four different concentrations. Apart from concentration of bacteria in suspensions, we have varied flow of buffer gas, power delivered to the plasma and time of treatment. In Figs. 3a, 3b results of sterilization of *E. faecalis* for the helium flows 0.5 and 1 slm are shown. We can see that better results were obtained for the higher flow of 1 sLm (Fig. 3b). This could be explained by higher input of the radicals created in the plasma into the suspension that contains bacteria. As expected, the reduction in colonies increased with the increase in treatment time. In case of the lowest concentration we have obtained complete sterilization of the samples, *i.e.*, after the treatment no bacterial colonies were formed. In all other cases reduction was several orders of magnitude.

In Figs. 4a, 4b results for the longest treatment time are shown comparing different powers and initial concentrations. We can see that for the lowest power we did not observe any significant reduction in bacterial colonies compared to the untreated positive control. On the other hand, with an increase of the power delivered to the plasma, sterilization effect increases. As expected,

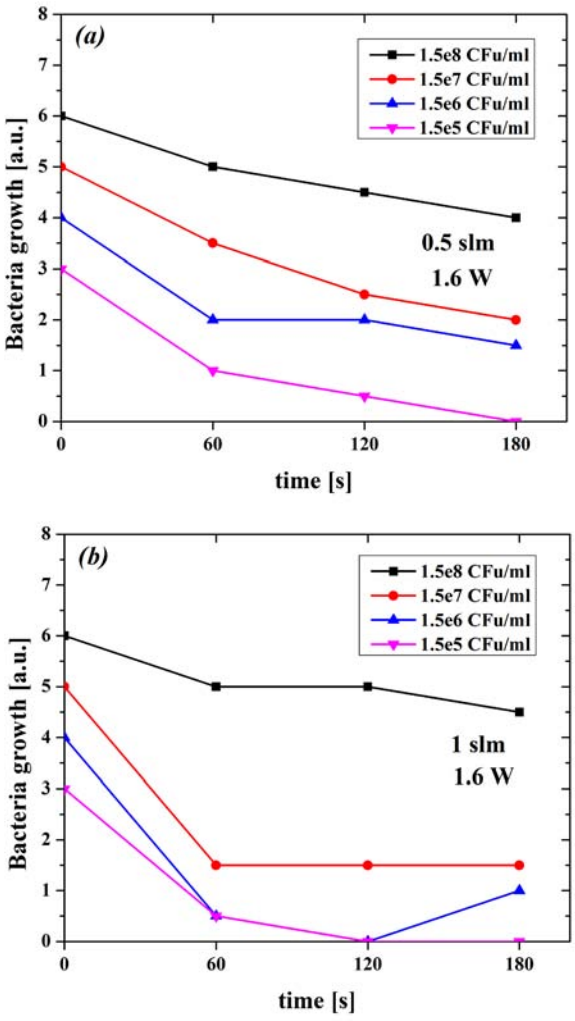

Figure 3: Sterilization of *Enterococcus faecalis* ATCC 29212. The samples contained four different concentrations of bacteria. Treatment power was 1.6 W. (a) He flow 0.5 sLm; (b) He flow 1 sLm. Values for 0 s correspond to the values of positive untreated control.

the higher power resulted in better sterilization effects. However, the final result was highly dependent on the initial concentration of bacteria. We can see that for the highest concentration of 1.5×10^8 CFU mL^{-1} the reduction was only one to two orders of magnitude. Again, higher flow of 1 sLm yielded better results.

The second strain of bacteria used in experiments was gram negative *P. aeruginosa* ATCC 27853. In Figs. 5a, 5b we show the results of plasma treatments of four different concentrations for two flows of buffer gas. Presented results were obtained for the highest power delivered to the plasma. As with *E. faecalis*, a better sterilization was achieved with the higher flow of helium. We can see that for the concentrations of 1.5×10^6 CFU mL^{-1} and 1.5×10^5 CFU mL^{-1} a complete sterilization of samples was

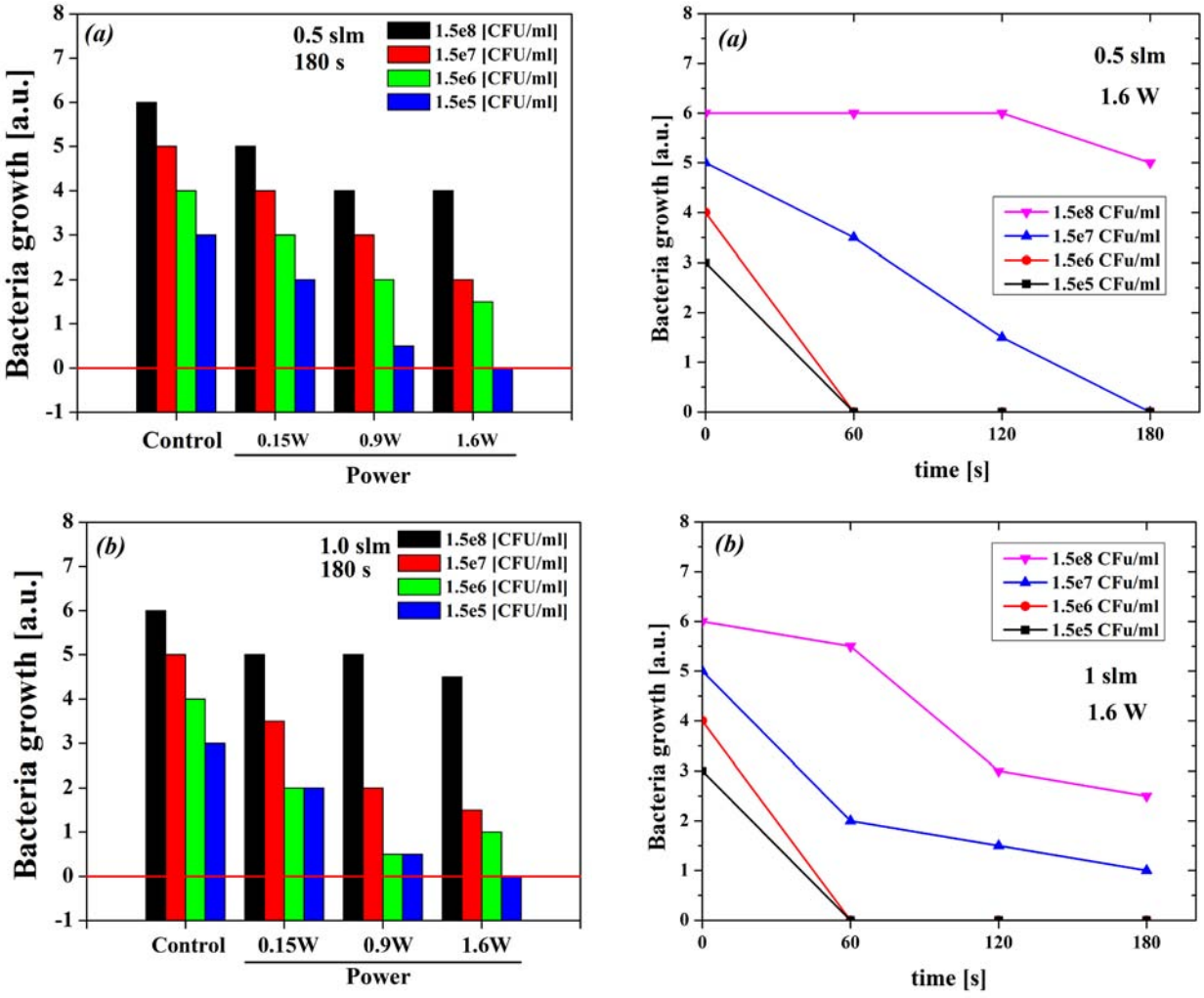

Figure 4: Sterilization of *Enterococcus faecalis* ATCC 29212. The samples contained four different concentrations of bacteria. The untreated control values for bacterial growth are 6(1.5×10^{8} CFU mL^{-1}), 5(1.5×10^{7} CFU mL^{-1}), 4(1.5×10^{6} CFU mL^{-1}) and 3(1.5×10^{5} CFU mL^{-1}). Treatment time was 180 s. (a) He flow 0.5 sLm; (b) He flow 1 sLm. The red line represents complete sterilization of the sample.

Figure 5: Sterilization of *Pseudomonas aeruginosa* ATCC 27853. The samples contained four different concentrations of bacteria. Treatment power was 1.6 W. (a) He flow 0.5 sLm; (b) He flow 1 sLm. Values for 0 s correspond to the values of positive untreated control.

already achieved for the treatment time of 60 s. For higher concentrations the reduction in bacteria was 4-5 orders of magnitude. The dependence of the sterilization on power delivered to the plasma is shown in Figs. 6a, 6b. With an increase in power delivered to the plasma we achieved a better sterilization.

We can see that the two main parameters in sterilization of planktonic samples of bacteria are power delivered to the plasma and duration of treatment. The flow of buffer gas had some influence on the results of sterilization, but not that pronounced as power or treatment time. The importance of power delivered to the plasma can be explained by chemistry in the discharge. If more power is delivered to the plasma, reactive species responsible for the sterilization are produced more effectively and in higher concentrations (unless there is some chemical reaction promoted at higher densities of other constituents). Similarly, the duration of treatment is responsible for the total amounts of radicals and other species involved in process of sterilization delivered to the samples. The combination of these two parameters provides a possibility for a wider range of optimal sterilization conditions. One can reduce the treatment time and increase the power delivered to the plasma or increase the duration of treatments and work with lower power and still have a similar sterilization effect.

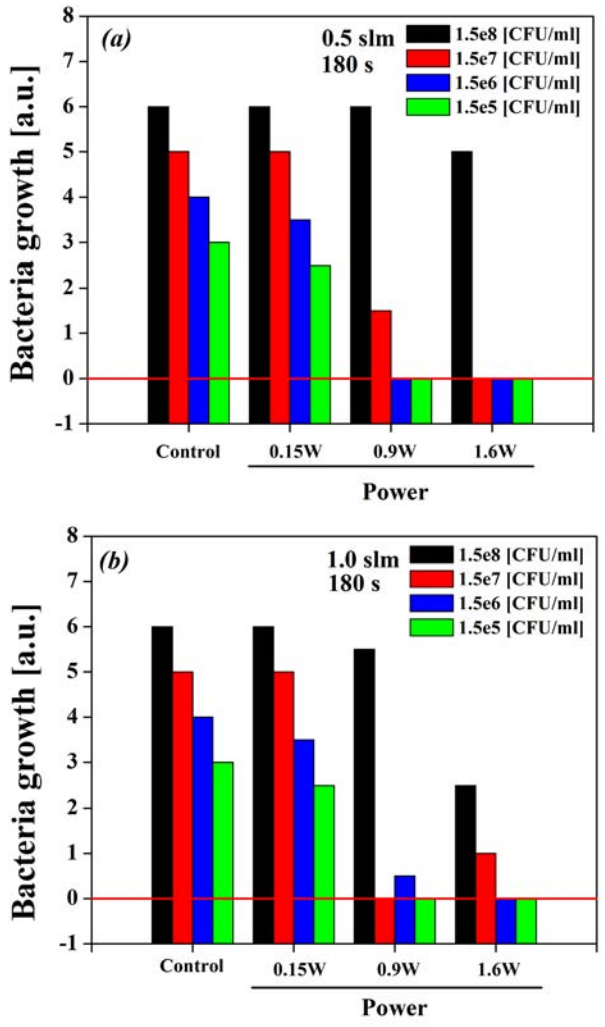

Figure 6: Sterilization of *Pseudomonas aeruginosa* ATCC 27853. The samples contained four different concentrations of bacteria. The untreated control values are 6(1.5×10^8 CFU mL^{-1}), 5(1.5×10^7 CFU mL^{-1}), 4(1.5×10^6 CFU mL^{-1}) and 3(1.5×10^5 CFU mL^{-1}). Treatment time was 180 s. (a) He flow 0.5 sLm; (b) He flow 1 sLm. The red line represents complete sterilization of the sample.

Apart from these two important parameters, the effect mostly depends on concentration of bacteria and on the bacterial strain. Broadly speaking, there are two types of bacteria, Gram positive and Gram negative. This division is due to the difference in the cell wall structure. In Gram positive bacteria the cell wall consists of multiple layers of peptidoglycan, forming a thick, rigid structure. Gram negative cell wall contains only a thin layer of peptidoglycan and an outer membrane composed of lipolysaccharide. In Figs. 7a, 7b we have shown results of plasma treatment of two Gram negative (*P. aeruginosa*, *Escherichia coli*) and two Gram positive (*E. faecalis*, *Staphylococcus aureus*) strains of bacteria. We can see that better results were obtained in the treatments of Gram negative bacteria. It seems reasonable to assume that either the thinner wall or the chemical composition of the wall of the Gram negative bacteria leaves them more exposed to the extracellular influence. The main conclusion that can be drawn here is that major actors in sterilization mechanism are radicals coming from the plasma. Also, the sterilization mechanism is closely connected to the interaction of these radicals (NO, OH, $^1O_2$, H, H_2O_2 *etc.*) with the lypopolysaccharides in the outer membrane of the bacterial cell wall. The absence of the lipopolysaccharides in the cell walls of the Gram positive bacteria, on the other hand, may be responsible for lower sterilization effect. Although we obtained the sterilization effect of low temperature atmospheric plasma generated by a plasma needle source on Gram positive bacteria, it was not that pronounced as the sterilization effect on Gram negative bacteria. The difference in susceptibility to the cold plasma treatment between Gram positive and Gram negative bacteria has already been reported [5,19]. However, a number of studies demonstrated excellent effects of low temperature atmospheric plasma against Gram positive bacteria [4,8], including eradication of their extremely resistant biofilms [7,9]. Nevertheless, one has to take care when generalizing the conclusion of the plasma influence on all strains in one type of bacteria (for example Gram negative). Even within the same type of bacteria there are differences in the results of sterilization treatments. We can see in Fig. 7 that much better results are obtained for *E. coli* as compared to the results obtained for *P. aeruginosa*. This implies that in addition to the general properties of the cell wall other characteristics of bacteria also have an important role in plasma-cell interaction.

4 Conclusion

We have presented the results of plasma sterilization of Gram positive and Gram negative strains of bacteria. The sterilization was performed by using atmospheric pressure plasma device and treated samples were in form of a suspension. Electron paramagnetic resonance was used in order to detect radicals deposited in the solution. We have detected H, OH and NO radicals deposited in the solution after the plasma treatment. In this case the most important radical is NO which is a potent antimicrobial agent effective against a range of Gram-negative and Gram-positive bacteria [21]. In experiments we have used four initial concentrations of bacteria (10^5-10^8 CFU mL^{-1}). For higher concentrations we have observed reduction of several orders of magnitude and for the lower ones

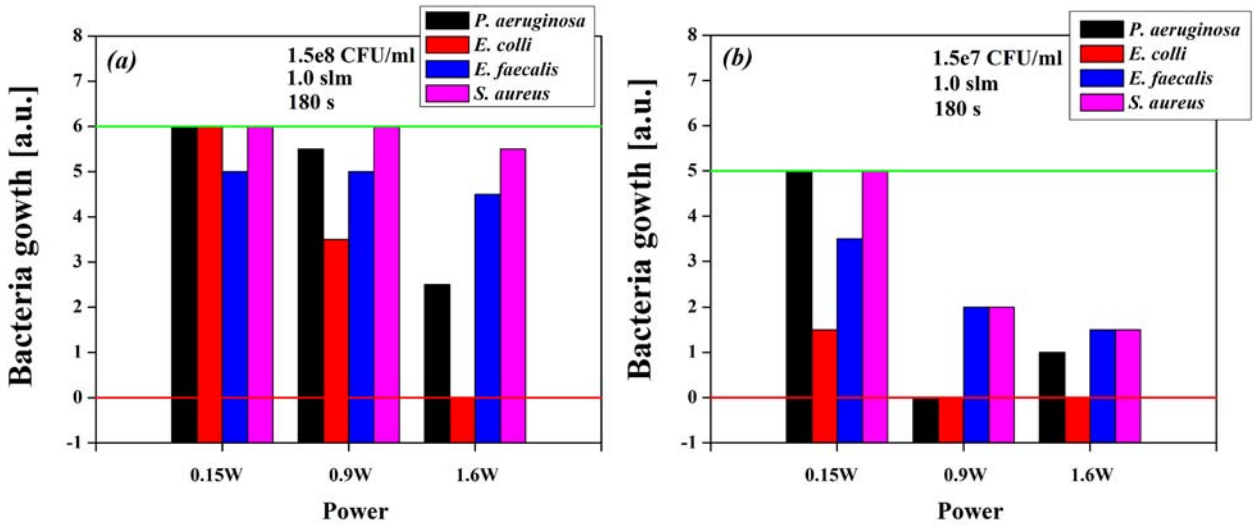

Figure 7: Sterilization of four different strains of bacteria: *Enterococcus faecalis* ATCC 29212, *Pseudomonas aeruginosa* ATCC 27853, *Escherichia coli* ATCC 25922 and *Staphylococcus aureus* ATCC 25923. More detailed data for the *Escherichia coli* and *Staphylococcus aureus* are given in [20]. Here, a part of the data from [20] are given for clearer comparison between plasma effect on Gram positive and Gram negative bacteria. The flow of helium was 1 sLm and the treatment time 180 s. Green line represents untreated control values and red line represents complete sterilization of the sample. (a) concentration 1.5×10^{8} CFU mL^{-1}; (b) concentration 1.5×10^{7} CFU mL^{-1}.

a complete eradication of the bacteria. It was shown that power delivered to the plasma and duration of the treatment are closely interlinked. One can reduce the treatment time and increase the power delivered to the plasma or increase the duration of treatments and work with lower power and still have a similar sterilization effect. The sterilization effect also depends on the type of bacterial strain. Gram negative bacteria appear more sensitive to the plasma treatment, which can be partially explained by their thinner wall and/or presence of lipopolysaccharides in their envelopes.

Acknowledgments: This work was supported by Grants No. III41011, ON175039 and ON171037 from the Ministry of Education, Science and Technological Development of the Republic of Serbia. The authors would like to thank Prof. Pavle Milenković for useful discussions, Prof Dušan Pavlica for providing ATCC strains of *Pseudomonas aeruginosa* and *Enterococcus faecalis*, and Dr Milena Jovanović and Dr Emilija Grego for technical assistance.

References

[1] Cheruthezhekatt S., Černak M., Slaviček P., Havel J., J. Appl. Biomed., 2010, 8, 55
[2] Shintani H., Sakudo A., Burke P., McDonnell G., Exp. Ther. Med., 2010, 1, 731
[3] Kim C.H. et al., J. Biotechnol., 2010, 150, 530
[4] Hong Y.F. et al., Lett. Appl. Microbiol., 2009, 48, 33
[5] Lee K., Peak K.H., Ju W.T., Lee Y., J. Microbiol., 2006, 44, 269
[6] Yu H. et al., J. Appl. Microbiol., 2006, 101, 1323
[7] Cotter J.J. et al., J. Hosp. Infect., 2011, 78, 204
[8] Maisch T. et al., Plos one, 2012, 7, e34610
[9] Jiang C. et al., ISRN Dentistry, 2012, 2012, Article ID 295736
[10] Stoffels E., Flikweert A.J., Stoffels W.W., Kroesen G.M.W., Plasma Sources Sci. T., 2002, 11, 383
[11] Puač N. et al., J. Phys. D. Appl. Phys., 2006, 39, 3514
[12] Malović G., Puač N., Lazović S., Petrović Z., Plasma Sources Sci. T., 2010, 19, 034014
[13] Jackson S.K., Liu K.J., Liu M., Timmins G.S., Free Radical Bio. Med., 2002, 32, 228
[14] Stoll S., Schweiger A., J. Magn. Reson., 2006, 178, 42
[15] Stoffels E. et al., Plasma Sources Sci. Technol., 2007, 16, 549
[16] Frejaville C. et al., J. Med. Chem. 1995, 38, 258
[17] Karoui H., Chalier F., Finet J.P., Tordo P., Org. Biomol. Chem., 2011, 9, 2473
[18] Fujii S., Yoshimura T., Coordin. Chem. Rev., 2000, 198, 89
[19] Ermolaeva S.A. et al., J. Med. Microbiol., 2011, 60, 75
[20] Lazović S. et al. New J. Phys., 2010, 12, 083037
[21] Ghaffari A., Miller C.C., McMullin B., Ghahary A., Nitric oxide, 2006, 14, 21

Detection of atomic oxygen and nitrogen created in a radio-frequency-driven micro-scale atmospheric pressure plasma jet using mass spectrometry

Article *in* Plasma Physics and Controlled Fusion · November 2012

Impact Factor: 2.19 · DOI: 10.1088/0741-3335/54/12/124046

7 authors, including:

Saša Lazović
Institute of Physics Belgrade
70 PUBLICATIONS **212** CITATIONS
SEE PROFILE

Gordana Malovic
Institute of Physics Belgrade
157 PUBLICATIONS **932** CITATIONS
SEE PROFILE

Timo Gans
The University of York
134 PUBLICATIONS **1,558** CITATIONS
SEE PROFILE

Zoran Lj Petrović
Institute of Physics Belgrade
510 PUBLICATIONS **5,652** CITATIONS
SEE PROFILE

Detection of atomic oxygen and nitrogen created in a radio-frequency-driven micro-scale atmospheric pressure plasma jet using mass spectrometry

2012 Plasma Phys. Control. Fusion 54 124046

(http://iopscience.iop.org/0741-3335/54/12/124046)

Plasma Phys. Control. Fusion **54** (2012) 124046 (8pp) doi:10.1088/0741-3335/54/12/124046

Detection of atomic oxygen and nitrogen created in a radio-frequency-driven micro-scale atmospheric pressure plasma jet using mass spectrometry

D Maletić[1], N Puač[1], S Lazović[1], G Malović[1], T Gans[2], V Schulz-von der Gathen[3] and Z Lj Petrović[1]

[1] Institute of Physics, University of Belgrade, Pregrevica 118, 11080 Belgrade, Serbia
[2] York Plasma Institute, Department of Physics, University of York, Heslington, York YO10 5DD, UK
[3] Institut für Experimentalphysik, Ruhr-Universität Bochum, 44780 Bochum, Germany

E-mail: dejan_maletic@ipb.ac.rs

Received 5 July 2012, in final form 4 October 2012
Published 21 November 2012
Online at stacks.iop.org/PPCF/54/124046

Abstract
In this paper we show mass spectrometry results for a radio-frequency-driven micro-atmospheric pressure plasma jet (μ-APPJ) discharge obtained using a mass analyzer with triple differential pumping allowing us to sample directly in ambient atmospheric pressure environment (Hiden HPR-60). The flow of the buffer gas (mixture of helium and 1% oxygen) was 2 slm and 3 slm and the excitation frequency was 13.56 MHz. We monitored production of atomic oxygen and nitrogen in the plasma for different flows and powers given by the RF power supply. These measurements were made for energies of electrons emitted from the ionization filament below the threshold for dissociation of O_2 and N_2. In addition to oxygen and nitrogen atoms, yields for O_2, N_2, NO and O_3 are recorded for different powers and gas flows. It is shown that the μ-APPJ is symmetrical and operates in α-mode. The power transmitted to the discharge was below 5 W in all measurements.

(Some figures may appear in colour only in the online journal)

1. Introduction

When plasmas are applied to organic materials and other materials that cannot survive high temperatures, it is essential to use non-equilibrium (low temperature or even cold) plasmas [1, 2]. In such systems, one can control, by application of an external field and other discharge parameters, the energy of electrons while maintaining the ion and gas temperatures close to room temperature. Achieving non-equilibrium conditions is comparatively easy at low pressures where breakdown voltages are the lowest since the operation is close to the minimum of the Paschen curve [3]. On the other hand, with standard gaps between electrodes (and pressures) (1 cm^{-1} Torr) operation at higher and atmospheric pressures is far from the Paschen minimum. As a result, apart from a higher breakdown voltage, it is difficult to achieve uniform glow discharges in large volumes [4] and due to high rates of ionization over short distances thermal plasmas are formed.

In recent years the development of new sources of non-equilibrium (low-temperature) atmospheric plasmas has been a topical issue with a goal to provide cheaper and more convenient alternatives for implementation of low-temperature plasma technology and also to open possibilities for treatment of living tissues. It was found that plasmas may be easily operated under atmospheric pressure at radio-frequencies in a flow of rare gases which mix with atmospheric gases in the region of the discharge [5]. Apart from this, many different configurations and applications of non-equilibrium atmospheric plasmas have been developed and studied [6–17].

The concept of radio-frequency-driven atmospheric pressure plasma jets (APPJs) was introduced by Selwyn and co-workers in 1998 [18]. Several experiments have been

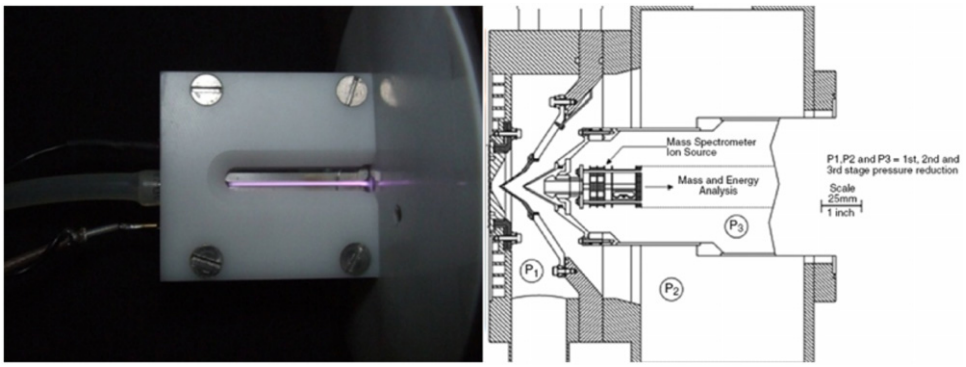

Figure 1. μ-APPJ with formed plasma at the orifice of the mass spectrometer.

performed by Selwyn and co-workers demonstrating the ability of APPJ to clean surfaces from biological contamination, to deposit and remove silicon oxide layers and to remove tungsten layers [18]. Based on this a similar device, the micro-atmospheric pressure plasma jet (μ-APPJ), was developed by Schulz-von der Gathen and co-workers [19]. A mixture of helium and oxygen is fed to the discharge through a glass cuvette. For sufficiently high powers and flow rates of gas feed mixture, a plasma effluent at the end of the electrodes appears. This is one of the reasons why the μ-APPJ is suitable for different kinds of localized treatments and can be used as one of the alternative plasma sources in biomedical applications. Rectangular geometry allows spatial scans of optical emission and different versions of laser and optical spectroscopy inside and outside the discharge volume.

The critical aspect of plasmas for any application (medical in particular), at any but especially at atmospheric pressure, is the production of different radicals and new stable molecules because ions and electrons have very small mean free paths. At the same time implementation of both spectroscopy and mass analysis is more difficult at high pressures. Recently commercial systems for atmospheric pressure mass analysis have been developed enabling studies of active molecules and ions at higher pressures all the way to ambient atmospheric pressure [20, 21].

In this paper we present mass spectrometry on products created by a μ-APPJ discharge. Mass spectra are obtained using a Hiden HPR-60 mass spectrometer. Measurements at energies lower than the dissociation energies for oxygen and nitrogen generated in the discharge were made. Moreover, O and N atoms, yields for oxygen and nitrogen molecules, were determined. In order to be able to compare the μAPPJ with other cold atmospheric pressure plasma sources being used in treatments of biological samples we have measured NO and O_3. In this paper we will show voltage-current characteristics of the discharge as well as the spectrum of its harmonics in the frequency domain. A preliminary report of this work was presented in [20]. Similar studies were made in the same system [22] with a different focus. Finally it is worth noting that the results of this work could be used to compare with plasma chemical models [23] and to support measurements of dissociated species by laser spectroscopy [24].

2. Experimental setup

The μ-APPJ consists of two symmetrical electrodes of equal length (34 mm) made of stainless steel. The distance between the electrodes can be adjusted with good precision from a few mm up to several hundred micrometers. In all our experiments the distance between the powered and grounded electrodes was 1 mm. One of the electrodes was powered by a radio-frequency generator at 13.56 MHz through a matching network while the other electrode was grounded. Measurements were made for powers from 40 to 80 W as indicated by the RF power supply.

Plasma is ignited along the entire length of the electrodes (figure 1) and for certain combinations of power/gas flow parameters the effluent of plasma coming out of the cuvette can be formed. The main advantage of such a construction is that both discharge volume (plasma core) and effluent region are accessible for optical diagnostics such as optical emission spectroscopy (OES) and two-photon absorption laser-induced fluorescence (TALIF) [24]. Also, plan parallel geometry of the electrodes adds to simplicity when it comes to modeling of this type of discharge [25–27].

In our experiments we have used a 1% oxygen–helium mixture as a buffer gas. The flows of buffer gas mixtures were 2 and 3 slm. The μ-APPJ was placed right in front of the sampling orifice of the mass spectrometer and it was carefully aligned with the orifice in order to gain maximum signal. Before starting the measurements it was necessary to wait until the pressures in all three stages (P1, P2, P3 in figure 1) were reduced to minimum values and were stabilized. The pressures in different stages along the line of the molecular beam were 7.9×10^{-1}, 4.4×10^{-5} and 3.5×10^{-7} Torr during all measurements.

Each stage has its own orifice and all three orifices are aligned to minimize losses of particles from the molecular beam through collisions to walls and to other particles in the beam. We have used the following set of orifices with the diameters of 0.3 (entering orifice), 0.3 (orifice between P1 and P2 stage) and 0.7 mm (orifice between P2 and P3 stage). A relative calibration was performed using gas mixtures including the measurement of the composition of air [20].

Several problems occurred during the setting up of the experiment. The front plate of the mass spectrometer which is made of stainless steel acted as a second grounded electrode (see figure 2(*a*)). When placing the μ-APPJ in front of the

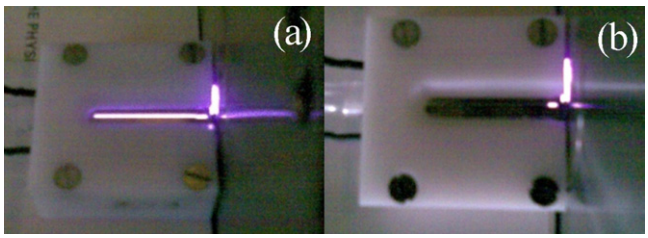

Figure 2. Photograph of the μ-APPJ: (*a*) energy–mass analyzer off; (*b*) energy–mass analyzer on.

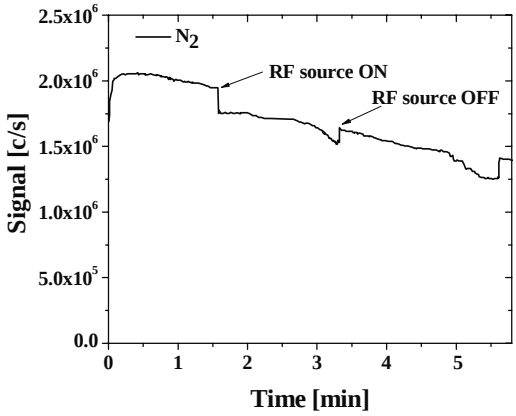

Figure 3. Demonstration of undesirable influence of the RF electric field generated by the μ-APPJ to the mass spectrometer electronics—changes of N_2 count without the plasma (no He flow) in cases when RF source is on and off.

orifice and after ignition of the discharge between the two electrodes, an additional discharge was ignited between the front plate of the mass spectrometer and the powered electrode. This discharge was facilitated by its passage through the region of reduced pressures at the front end of the differentially pumped system.

One of the solutions to this problem could be by placing the plasma source at longer distances, but that meant lower count rates and lower sensitivities. To solve this problem we had to put a Teflon plate ($d = 1$ mm) on the front plate of the mass spectrometer. The Teflon plate also served as spacer between the μ-APPJ and the orifice and this distance of 1 mm was kept constant during the measurements.

The second problem appeared as soon as voltages of the analyzer were set to the proper values causing the discharge between the electrodes to quench and develop toward the inside of the mass analyzer through the orifice (see figure 2(*b*)). Often, the discharge between the two blades of the μ-APPJ reactor was extinguished and the discharge was initiated from the corner of the powered electrode. Setting the zero potential for the first set of cones inside the analyzer solved this problem without any significant reduction of the signal.

Finally, the third problem was that a decrease in count rates was observed in the presence of strong RF sources in the proximity of the mass spectrometer (figure 3). A significant decrease in count rate appears when the RF source is turned on even when there is no ignition of plasma (no helium flow). When the strong RF source is turned off the signal needs some time to get back to its initial value. This problem was solved by shielding the mass analyzer from the influence of external strong RF sources and by additional grounding between the metal front plate and the grounded electrode of the μ-APPJ [20].

After solving all of the above-mentioned problems, we were able to analyze the mass spectra of the neutrals generated by the μ-APPJ. The sampling was carried out in the effluent formed by mixing the plasma ignited in the feed gas (1%O_2/He) and ambient air. The oxygen is added with the aim to regulate the concentrations and ratios of reactive biomedical species such as NO or O_3.

The mass spectrometer can be used for detecting both ions and neutrals coming from the plasma. Neutrals have to be ionized in the device and then are detected as ions. There are two filaments that can be used for ionization with controllable electron energies in the range from 0.1 eV to 70 eV. In order to record the background signal a valve was placed between the first and the second pumping stage to cut off the signal from the atmospheric plasma while keeping all signals from the ionization of gases in the ionizer. In all measurements the background signal was removed from the total signal. Homemade derivative probes [9, 28] were used for measurements of instantaneous current and voltage waveforms. Voltage–current characteristics and the power transmitted to the plasma were obtained for several flows of buffer gas.

Mass-spectrometry measurements are performed after the system reached the stationary operation regime and both derivative probe and count rates provided stable results. In this case the recorded mass spectra scans were only slightly different. The presented spectra are averages of (at least) three scans. Furthermore, we have decided to use presentation of the results as yields to reduce the influence of short and long term variations in plasma and on surfaces. The origin of the systematic errors can be related to the mass spectrometer device and to the system generating the plasma. The principal problem is in the transmission of particles that may be mass dependent. This was tested on known gas mixtures covering the range of masses used here. We obtained air composition in excellent agreement (better than 5% uncertainty) for all major constituents and their isotopes. The discrepancies occurred only for rare gases and their isotopes which could be expected in a laboratory with several plasma jets releasing argon and helium into the air. So we could claim that uncertainty in the data is less than 10% in relative values over the range covered by the main molecules.

3. Results and discussion

3.1. Electrical properties

μ-APPJ is a symmetrical system since only main harmonics at 13.56 MHz are present in voltage and current signals. With increased power the amplitude of the main harmonics also increases, but higher harmonics do not emerge. For one value of the mixture flow the discharge was ignited for the same values of power given by the RF power supply during all experiments. Voltage–current characteristic for the flow

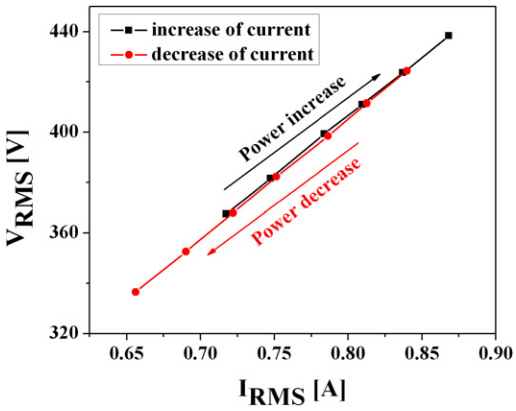

Figure 4. RMS voltage–current characteristic of the μ-APPJ discharge for a flow rate of 2 slm and 1%O_2/He mixture. Measurements of the characteristics were made by increasing (solid squares) and decreasing (solid circles) current and they show a small hysteresis.

of 2 slm (1%O_2/He) is shown in figure 4. One can see that after ignition of the discharge the RMS values of the voltage and current were ∼360 V and ∼0.7 A, respectively and they increased with power. The power at the RF generator is increased until voltages above 360 V are achieved when the gas breakdown occurs and the plasma is formed between the electrodes. For low values of transmitted power, plasma covers just a part of the volume between the electrodes which is closer to the gas feedthrough. With an increase in the power, the entire volume between the electrodes is homogeneously filled with plasma. Further increase leads to the formation of plasma effluent outside of the quartz cuvette and the plasma source and its length is depending on the applied power. Mass-spectrometry measurements are performed with the effluent formed. In all these cases discharge operates in α mode. Arcing/sparking occurs with a further increase in the power but only for a very short time, presumably due to the overheating and possible intensive damage of the electrodes. We were not able to perform any measurements in this mode. During all the experiments power was kept below the values at which arcing occurred, which were dependent on flow and abundances of O_2 in He.

The V–I dependence of the discharge is linear which indicates that the discharge is running in α-mode. We could not observe any mode change (α to γ) below the voltage where arcing occurs. The second curve in figure 4 represents the V–I characteristics in the case when the power was decreased. When decreasing the power, plasma remained ignited for the values of voltage and current which are lower than the initial values when plasma is formed (330 versus 360 V and 0.66 versus 0.72 A), which clearly demonstrates a hysteresis albeit a weak one. Power transmitted to the discharge was measured using derivative probes which were placed as close as possible to the powered electrode. In all measurements power transmitted to the plasma was below 5 W. For easier representation and possible comparison with other similar plasma systems values for the power released by the source are given to label the data while probe results are shown in figures with volt ampere characteristics.

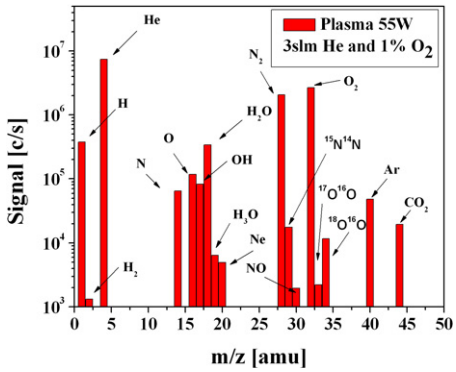

Figure 5. Neutral spectra for 55 W plasma and 3 slm of helium with 1% of oxygen.

3.2. Mass spectroscopy

The Hiden HPR-60 mass spectrometer was used to acquire yield of neutrals coming from the plasma. Figure 5 shows the neutral spectrum that is obtained for filament electron energy of 70 eV and 55 W plasma. The feeding gas was a 1%O_2/He mixture and we have used two different flow rates (2 and 3 slm). We can see that the highest count rates are for He, O_2 and N_2. High signals for H_2O and H are also detected and expected. Radicals which are essential to numerous biomedical applications [29, 30] of atmospheric pressure plasmas in general, such as N, O and NO, are also present in μ-APPJ in significant amounts. Peak 2 atomic masses heavier than the O_2 signal is associated with H_2O_2.

The results are presented using yields of specific masses (relative contribution to the total signal) instead of counts per second obtained directly from the MBMS to reduce noise due to temporal variations of the plasma. The yield was calculated as

$$Y = \frac{Y^i_{\text{mass}}}{\sum_i Y^i_{\text{mass}}}[\%], \qquad (1)$$

where Y^i_{mass} is the count due to the specific species and this was divided by the sum of counts for all recorded masses (1–100 amu). Here we can point out that the total signal corresponds only to the neutrals and not to the sum of neutrals and ions created in the plasma. This fact was confirmed by turning the filament off and then checking the signal of ions for the same mass analyzer setup. No ions coming from the plasma were detected under these conditions.

Total measured signals that correspond to N and O atoms are produced both by the reactions in plasma and by the mass spectrometer filament. Atomic oxygen ions are produced in two reactions:

(1) $O + e \rightarrow O^+ + 2e$, threshold 13.6 eV,
(2) $O_2 + e \rightarrow O^+ + O + 2e$, threshold 20 eV.

Atomic nitrogen ions are also produced in direct and dissociative ionization:

(1) $N + e \rightarrow N^+ + 2e$, threshold 14.5 eV,
(2) $N_2 + e \rightarrow N^+ + N + 2e$, threshold 24 eV.

To obtain the number of atomic species created in the plasma, first the contributions due to direct atomic ionization

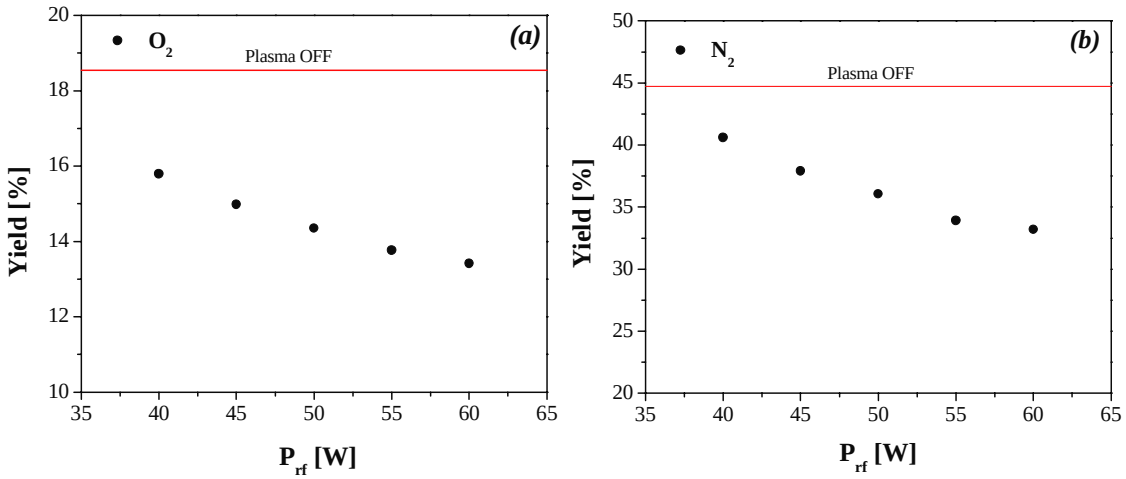

Figure 6. Depletion of O_2 (*a*) and N_2 (*b*) molecules as a function of the power at the RF power supply. The He/O_2 admixture flow rate was 2 slm. The percentage of O_2 in the admixture was 1%.

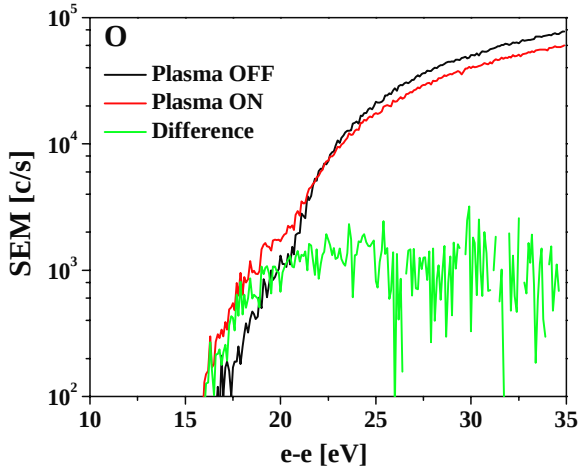

Figure 7. Filament electron energy dependence of the oxygen signal (2 slm 1% O_2 70 W).

(reaction (1)) should be isolated. In the neutral gas (plasma OFF), N and O signals are only due to dissociative ionization of N_2 and O_2 (i.e. reaction (2)) in the ionizer.

It is obvious that if we wish to understand the chemistry in the plasma it is not enough to measure only the yield of radicals of interest. We also have to measure the contributions of the species that take part in the reactions with those radicals and other relevant species. Therefore, yields for O_2 and N_2 are also shown in figure 6. The decrease in yields for O_2 and N_2 when the plasma is on is due to dissociation of those molecules in the plasma itself prior to ionization by the electrons from the device filament. The depletion of oxygen molecules increases with the increase in the applied voltages in the range from 2% up to the 5%. In the case of nitrogen, the percentage of depletion is much higher and goes up to 10%.

We have recorded electron energy dependences for total O and N signals in order to define the number of oxygen and nitrogen atoms created in the discharge. Measurements of the atmosphere without plasma are presented in figure 7 by the black line (plasma OFF). The contribution to this signal is only through the second reaction. When plasma is on, both reactions take part but the main contribution is still through the second reaction (dissociation). The signal of interest to us is obtained for energies between 13.6 and 20 eV (first reaction). That is why the signal obtained without plasma is scaled to the 'plasma on' signal for high electron energies (35 eV) and then subtracted [21]. This difference is presented by the green line in figure 7.

The signal of plasma produced O atoms is obtained by integrating the difference line (figure 7 green line) for electron energies from 13.6 to 19 eV. The same procedure described before has been used for nitrogen but integration was carried out for the electron energy range from 14.5 to 23 eV. The results obtained for O and N atoms are presented in figures 8(*a*) and (*b*).

The amount of O increases linearly with the applied power (indicated by the RF power supply). While we have a reading of the actual power transmitted to the plasma we show data as a function of the reading at the power supply as there is a linear relationship. The observed increase can be explained by increased dissociation of the O_2 molecules with an increase in the applied RF power that is followed by an increase in electron density [31–33]. Similar results were obtained in independent experiments using a slightly different μAPPJ device [22, 34]. In the case of atomic nitrogen there is no increase in the number of created atoms in the plasma with an increase in the applied voltages. Both in the cases of O and N atoms a significant increase can be achieved by increasing the flow rate of the He/O_2 admixture.

Interaction of plasma and living tissue is an open subject and much effort is being made trying to put some light to this problem. It is known that NO plays crucial role in a number of cell processes [35]. If one would like to compare the μAPPJ with other cold atmospheric pressure plasma sources being used in treatments of biological samples knowledge of NO and O_3 yields would be highly desirable.

Figures 9(*a*) and (*b*) show yields of NO and O_3 for 1% O_2/He admixture flow rates of 2 slm and 3 slm. Yields of NO and O_3 presented in these figures are obtained as the difference of signals with and without plasma. In both cases we have used electron energy of 70 eV. The yield for NO increases with the applied power as well as with an increase in the flow

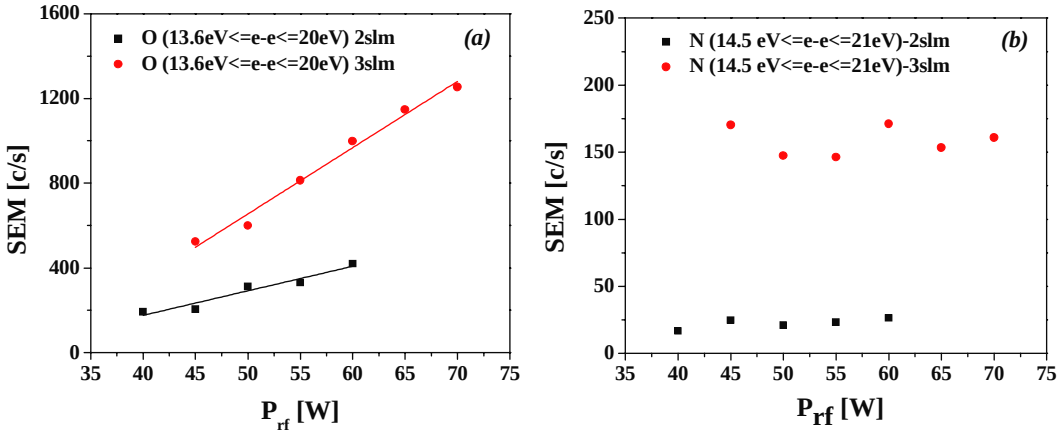

Figure 8. Oxygen (*a*) and nitrogen (*b*) count rates for different powers and two different feed gas flow rates.

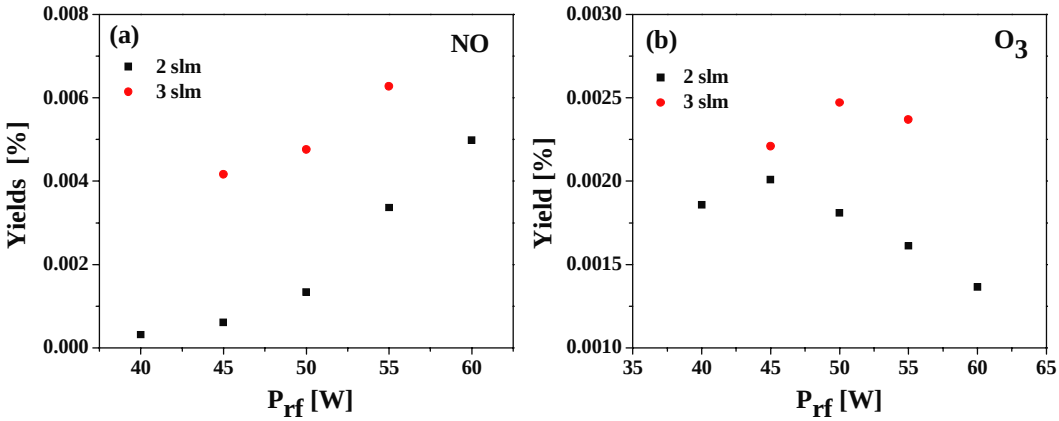

Figure 9. Concentrations of NO (*a*) and O_3 (*b*) radicals for feed gas flow rates of 2 slm and 3 slm (1% of O_2).

rate. On the other hand the yield for O_3 molecules increases with the applied power and after reaching a maximum value it starts to drop. The same behavior is observed when the admixture flow rate was increased. Also, with an increase in the buffer gas flow, yields for both NO and O_3 increase.

The increase in ozone yield with an increase in the applied power can be explained by the increase in atomic oxygen (see figure 8(*a*)). Dissociation of the O_3 molecules becomes significant at higher powers resulting in decreased ozone yields. For a smaller abundance (0.5%) of the O_2 in the buffer gas mixture the measured yield for O_3 decreases by a factor of 2. At the lower concentration of O_2 (∼0.5%) production of ozone is smaller than in the case of higher percentages (∼1%) of O_2 in the gas mixture due to the fact that atomic oxygen is generated by the dissociation of oxygen molecules and is lost by the recombination in three-body collisions with the oxygen molecules and helium atoms producing the ozone [31, 32]. Under the same time changing conditions in the plasma (e.g. increasing power or flow) may affect different production channels such as $O + 2O_2 = O_3 + O_2$, which is strongly dependent on temperature. Most processes will be strongly dependent on the internal energy of the participating molecules. However, we have no evidence of a significant heating of the gas and certainly a couple of centimeters beyond the discharge the temperature does not increase above 42 °C. Having this in mind the most plausible interpretation of the decrease of ozone density at a higher power is due to increased dissociation of O_3 in plasma. The signal of ozone (this is valid for other molecules as well) may be affected by the electrons in the ionizer. It is quite possible that dissociative ionization will lead to production of several molecular ions. The likelihood of this will decrease as energy approaches the threshold from higher energies. Yet for our analysis that is predominantly relative we should point out that there are no reasons why this process would be non-linear and affect relative results. On the other hand it is possible that electrons in the ionizer could destroy the molecular ions [36]. This process is, however, less likely than the ionization of neutral molecule (non dissociative or dissociative) as density of ions is considerably smaller than the density of neutrals. As ionizers are not adjusted to operate in single collision mode this process is, however, possible but again for a fixed pressure it would not affect relative values. Processes influencing the ozone production and destruction in mass analyzer are manifold and complicated so more detailed measurements and modeling should be performed.

4. Conclusion

In this paper we have presented electrical characterization and mass-spectrometry measurements of a μ-APPJ. We have used

derivative probes to record current and voltage waveforms. When transferring adjusted signals (due to the calibration curves) to the frequency domain we could see that only the main harmonic is present for all plasma parameters. As shown in the V–I curve our experiment was running in α-mode and we did not observe an α–γ mode transition for higher applied powers covered here.

The mass-spectrometry measurements were made using a Hiden HPR-60. Some of the problems that occurred during setting up the experiments were described as well as solutions that we applied. The additional discharge between the powered electrode and the front plate of the mass spectrometer was removed by inserting a Teflon plate between the μ-APPJ and the front plate. Quenching of the discharge between the plates and ignition of a discharge through the orifice of the mass spectrometer was solved by setting the first mass spectrometer cones to zero potential. The problem of recording RF signal induced by the external RF power supply was resolved by additional grounding of the mass spectrometer front plate.

The presence of different radicals, atoms and other reactive species created in the discharge is very important information for understanding their effects in treatment of living tissues. Here we have reported measurements of atomic oxygen and nitrogen created in the discharge. Measurements were made for electron energies below the threshold for dissociation of O_2 and N_2 molecules. The counts for atomic O increase with the applied power as well as the buffer gas flow. This can be explained by the increase in the electron densities with the applied power [6, 31, 32]. Depletion of molecular oxygen also increases with applied power. In the case of atomic nitrogen, counts stay almost constant with increasing applied power. Based on the results presented in this paper and on our previous work [20] we can discuss some of the distinctive features of two plasma sources convenient for biomedical applications—μ-APPJ and the plasma needle. We were able to record only neutral spectra in the case of μ-APPJ while both ions and neutrals generated in the plasma are recorded in the case of the plasma needle. The cause for this is the difference in the electrode configurations: ions are localized between the plan parallel electrodes of the μ-APPJ and the measurements are performed in the effluent region free of ions. On the other hand, the needle-like electrode provides extremely localized plasma of small volume also containing ions and neutrals. Another important difference is in the power delivered to the plasma which is typically in the range 0.1 W to 1 W for the plasma needle and few watts for the μ-APPJ.

In treatments of living tissues two radicals play very important roles. It is shown that NO is active in majority of the mechanisms in cell biochemistry. Therefore, we measured NO yields for two different gas flows. It is shown that the yields for NO increase with the applied power and with the flow of the buffer gas. The second important molecule in plasma–cell interactions is ozone, which desirability depends of the aspired result. In the case of sterilization higher concentration of O_3 is welcome. On the other hand, when treating living cells, high O_3 concentrations can be harmful, even fatal. The yields of O_3 measured by μ-APPJ are low and can be adjusted to the desired values by changing applied power or flow of the buffer gas.

Acknowledgments

This research has been supported by the Ministry of Science and Technological Development, Serbia, under the contract numbers ON171037 and III41011. VSvdG gratefully acknowledges the support by the Deutsche Forschungsgemeinschaft within the frame of research unit POR 1123 ‘Physics of Microplasmas’.

References

[1] Lieberman M A and Lichtenberg A J 2005 *Principles of Plasma Discharges and Materials Processing* 2nd edn (Hoboken, NJ: Wiley)
[2] Makabe T and Petrović Z Lj 2006 *Plasma Electronics* (New York: Taylor and Francis)
[3] Radmilović-Radjenović M, Petrović Z Lj, Malović G, Marić D and Rađenović B 2006 *Czech. J. Phys.* **56** B996–1001
[4] Petrović Z Lj, Škoro N, Marić D, Mahony C M O, Maguire P D, Radmilović-Rađenović M and Malović G 2008 *J. Phys. D: Appl. Phys.* **41** 194002
[5] Park J, Henins I, Herrmann H W, Selwyn G S and Hicks R F 2001 *J. Appl. Phys.* **89** 15
[6] Knake N, Reuter S, Niemi K, Schulz-von der Gathen V and Winter J 2008 *J. Phys. D: Appl. Phys.* **41** 194006
[7] Iza F, Kim G J, Lee S M, Lee J K, Walsh J L, Zhang Y T and Kong M G 2008 *Plasma Process. Polym.* **5** 322–44
[8] Laroussi M and Akan T 2007 *Plasma Process. Polym.* **4** 777–88
[9] Puač N, Petrović Z Lj, Malović G, Đorđević A, Živković S, Giba Z and Grubišić D 2006 *J. Phys. D: Appl. Phys.* **39** 3514–9
[10] Kieft I E, Laan E P and E Stoffels 2004 *New J. Phys.* **6** 149
[11] Weltmann K D, Brandenburg R, Woedtke T, Ehlbeck J, Foest R, Stieber M and Kindel E 2008 *J. Phys. D: Appl. Phys.* **41** 194008
[12] Rajasekaran P, Mertmann P, Bibinov N, Dirk W, Viöl W and Awakowicz P 2009 *J. Phys. D: Appl. Phys.* **42** 225201
[13] Khacef A, Cormier J M and Pouvesle J M 2002 *J. Phys. D: Appl. Phys.* **35** 1491–8
[14] Ayan H, Staack D, Fridman G, Gutsol A, Mukhin Y, Starikovskii A, Fridman A and Friedman G 2009 *J. Phys. D: Appl. Phys.* **42** 125202
[15] O’Connell D, Cox L J, Hyland W B, McMahon S J, Reuter S, Graham W G, Gans T and Currell F J 2011 *Appl. Phys. Lett.* **98** 043701
[16] Sousa J S, Niemi K, Cox L J, Algwari Q T H, Gans T and O’Connell D 2011 *J. Appl. Phys.* **109** 123302
[17] Mahony C M O, Gans T, Graham W G, Maguire P D and Petrovic Z LJ 2008 *Appl. Phys. Lett.* **93** 011501
[18] Schütze A, Jeong J Y, Babayan S E, Park J, Selwyn G S and Hicks R F 1998 *IEEE Trans. Plasma Sci.* **26** 1685
[19] Niemi K, Reuter S, Schaper, Knake N, Schulz-von der Gathen V and Gans T 2007 *J. Phys.: Conf. Ser.* **71** 012012
[20] Malović G, Puač N, Lazović S and Petrović Z Lj 2010 *Plasma Sources Sci. Technol.* **19** 034014
[21] Stoffels E, Aranda-Gonzalvo Y, Whitmore T D, Seymour D L and Rees J A 2007 *Plasma Sources Sci. Technol.* **16** 549–56
[22] Ellerweg D, Benedikt J, Keudell A, Knake N and Schulz-von der Gathen V 2010 *New J. Phys.* **12** 013021
[23] Murakami T, Gans T, O’Connell D and Graham W G 2010 *Bull. Am. Phys. Soc.* BAPS. GEC.ET1.7
[24] Gathen V S, Schaper L, Knake N, Reuter S, Niemi K, Gans T and Winter J 2008 *J. Phys. D: Appl. Phys.* **41** 194004

[25] Niemi K, Waskoenig J, Sadeghi N, Gans T and O'Connell D 2011 *Plasma Sources Sci. Technol.* **20** 055005
[26] Waskoenig J and Gans T 2010 *Appl. Phys. Lett.* **96** 181501
[27] Niemi K, Reuter S, Graham L M, Waskoenig J and Gans T 2009 *Appl. Phys. Lett.* **95** 151504
[28] Puač N, Petrović Z Lj, Živković S, Giba Z, Grubišić D and Đorđević A 2005 *Plasma Processes and Polymers* ed R d'Agostino, P Favia, C Oehr and M R Wertheimer *et al* (New York: Wiley) chapter 15 (Low-Temperature Plasma Treatment of Dry Empress-Tree Seeds)
[29] Graves D 2012 *J. Phys. D: Appl. Phys.* **45** 263001
[30] Giba Z, Grubišić D and Konjević R 2007 *Plant Cell Monogr.* **5** 91–111
[31] Park G Y, Lee H, Kim G and Lee J K 2008 *Plasma Process. Polym.* **5** 569–76
[32] Park G Y, Hong Y J, Lee H W, Sim J Y and Lee J K 2010 *Plasma Process. Polym.* **7** 281–7
[33] Knake N, Niemi K, Reuter S, Schulz-von der Gathen V and Winter J 2008 *Appl. Phys. Lett.* **93** 131503
[34] Waskoenig J, Niemi K, Knake N, Graham L M, Reuter S, Schulz-von der Gathen V and Gans T 2010 *Plasma Sources Sci. Technol.* **19** 045018
[35] Wendehenne D, Pugin A, Klessig D F and Durner J 2001 *Trends Plant Sci.* **6** 177–83
[36] Deng S, Vane C and Bannister M 2010 *Phys. Rev.* A **82** 062715

Time-resolved images of plasma bullet for different electrode geometries

Conference Paper · July 2012

READS
6

7 authors, including:

Dejan Maletic
Institute of Physics Belgrade
53 PUBLICATIONS **97** CITATIONS
SEE PROFILE

Saša Lazović
Institute of Physics Belgrade
70 PUBLICATIONS **212** CITATIONS
SEE PROFILE

Gordana Malovic
Institute of Physics Belgrade
157 PUBLICATIONS **932** CITATIONS
SEE PROFILE

Zoran Lj Petrović
Institute of Physics Belgrade
510 PUBLICATIONS **5,652** CITATIONS
SEE PROFILE

Time-resolved images of plasma bullet for different electrode geometries

D. Maletić[(*)1], N. Puač[1], N. Selaković[1], S. Lazović[1, 2], G. Malović[1], A. Đorđević[3] and Z. Lj. Petrović[1]

[1]*Institute of Physics, University of Belgrade, Pregrevica 118, 11080 Belgrade, Serbia*
[2]*Institute Jožef Stefan, Jamova cesta 39, 1000 Ljubljana, Slovenia*
[3]*Faculty of Electrical Engineering, University of Belgrade, Bulevar kralja Aleksandra 73, 11000 Belgrade, Serbia*
[(*)] dejan_maletic@ipb.ac.rs

In this paper we will present time-resolved images of atmospheric pressure plasma jet obtained by using fast ICCD camera for several electrode settings. It will be shown that formation and position of the plasma bullet strongly depends on the electrode geometry. The main purpose of our investigation was the possibility of applying plasma bullet for the treatment of thermo-sensitive samples.

A possibility to obtain the discharges of various geometries at low gas/ion temperatures and at atmospheric pressure would be a good basis for numerous applications in the industry, biology and medicine [1-5]. Here we study properties of an atmospheric pressure plasma jet (APPJ) operating with sinusoidal voltage excitation at a frequency of 80 kHz. Construction of plasma jet [6, 7] allowed easy ICCD camera capturing of the time-resolved images of the discharge between and inside the electrodes, as well as, of the plasma bullet that is formed outside the tube/electrode system. Experimental setup is given in Fig. 1. We will use the common term "plasma bullet" for visible manifestations of plasma because these ionization fronts create appearance of a motion of a bullet even though plasma itself may have a very different motion.

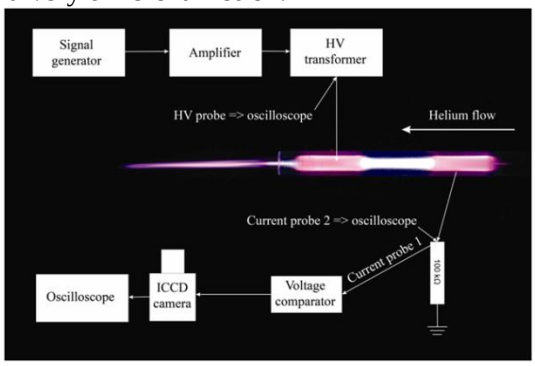

Fig. 1. Experimental setup

The body of a plasma jet was made of Pyrex glass tube 6 mm outer diameter and 4 mm inner diameter. The length of the coated PET electrodes was 15 mm and the distance between them was 15 mm. The distance between the electrodes was kept constant during all measurements. The right electrode was grounded and the other electrode, closer to the end of the glass tube, was the powered one (see Fig. 1.). The calculated mean power transmitted to the plasma was 4 W and the flow rate of the feeding gas (He) was 4 slm. The distance between the powered electrode and the end of the glass tube was varied and ICCD images were taken for distances of 7, 10, 30 and 50 mm. Voltage – current signals are shown in Fig. 2. with trigger position of 11.2 μs.

In order to obtain the time-resolved images we have used integration on the chip because the light emission in a single shot is not always sufficient to obtain clear images with gate widths of less than 25 ns. In Fig. 3. (A, B, C and D) we can see time-resolved image of plasma jet obtained by ICCD camera for 4 different electrode distances to the end of the tube while the rest of the geometry is unchanged. All images were obtained for the same parameters of electrical circuit and ICCD camera settings. It is shown that, when the distances of electrodes to the edge of the tube are shorter, the

plasma bullet is formed (see Fig. 3. – A, B and C). At the same time there is no visible discharge in the powered electrode.

When plasma is moving through the tube, including both electrodes, it is at a much lower speed then the speed of the bullet. With an increase of the distance of the electrodes from the edge of the tube plasma bullet is formed but with lower emission intensity (Fig. 3. – C). For the longest distance bullet is not emerging from the plasma jet body throughout the whole cycle period of 12.5 μs. (Fig. 3. – D) and it simply dissipates.

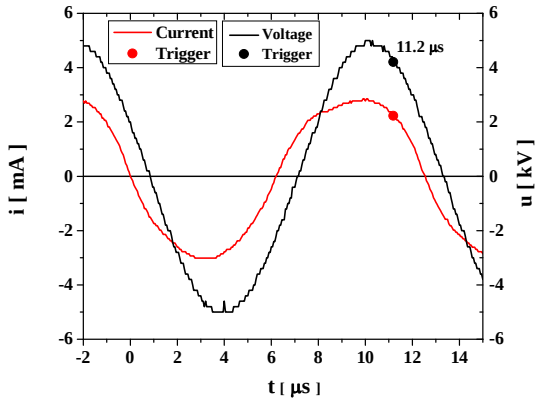

Fig. 2. Current – Voltage signals with 11.2 μs trigger position

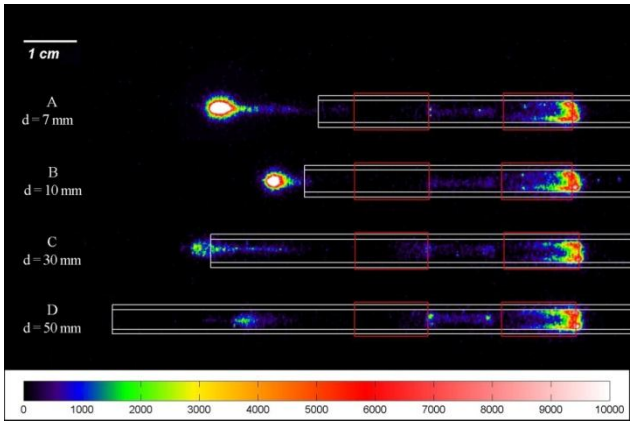

Fig. 3. Time resolved ICCD images for different geometry, delay of 11.2 μs, helium flow rate of 4 slm and average applied power of 4 W. Color bar represents intensities of emission.

This research has been supported by the Ministry of Education and Science Serbia, project III41011 and ON171037.

References

[1] G. Fridman, G. Friedman, A. Gutsol, A. B. Shekhter, V. N. Vasiletsm and A. Fridman, *Plasma Process. Polym.* 5 (2008) 503–533.
[2] M. Laroussi, *IEEE T. Plasma Sci*. 37-6 (2009) 714-725.
[3] E. Robert, E. Barbosa, S. Dozias, M. Vandamme, C. Cachoncinlle, R. Viladrosa, J. M. Pouvesle, *Plasma Process. Polym.* 6 (2009) 795–802.
[4] N. Puač, Z.Lj. Petrović, G. Malović, A. Đorđević, S. Živković, Z. Giba and D. Grubišić, *J. Phys. D Appl. Phys.* 39 (2006) 3514-3519.
[5] S. Lazović, N. Puač, M. Miletić, D. Pavlica, M. Jovanović, D. Bugarski, S. Mojsilović, D. Maletić, G. Malović, P. Milenković and Z. Petrović, *New J. Phys* 12 (2010) 083037.
[6] M. Kong, J. Walsh., *IEEE T. Plasma Sci. 36-4* (2008) 954-955.
[7] J. Shi, F. Zhong, J. Zhang, D. W. Liu and M. G. Kong, *Phys. Plasmas* 15 (2008) 013504.

Time resolved ICCD images of an atmospheric pressure plasma jet

Conference Paper · November 2011

READS
19

6 authors, including:

Dejan Maletic
Institute of Physics Belgrade
53 PUBLICATIONS **97** CITATIONS
SEE PROFILE

Saša Lazović
Institute of Physics Belgrade
70 PUBLICATIONS **212** CITATIONS
SEE PROFILE

Gordana Malovic
Institute of Physics Belgrade
157 PUBLICATIONS **932** CITATIONS
SEE PROFILE

Zoran Lj Petrović
Institute of Physics Belgrade
510 PUBLICATIONS **5,652** CITATIONS
SEE PROFILE

BULLETIN

OF THE AMERICAN PHYSICAL SOCIETY

64th Annual Gaseous Electronics Conference

November 2011

Salt Lake City, Utah

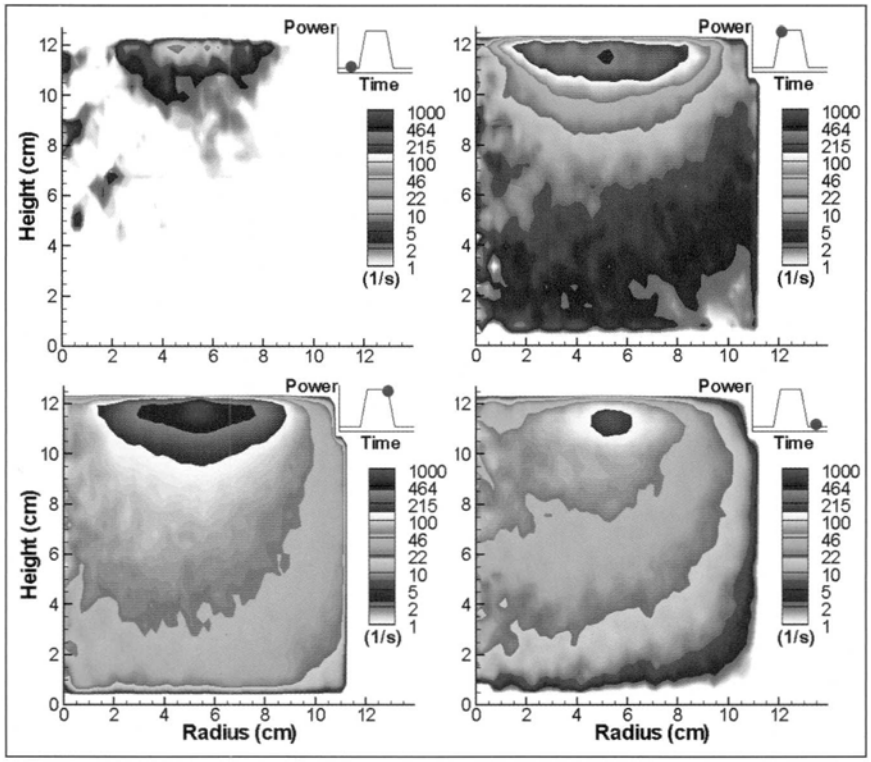

Volume 56, Number 15

APS physics

QRP1 75 A study on floating harmonic method in non-Maxwellian plasmas KYOUNG YOO, *Department of Nanoscale Semiconductor Engineering, Hanyang University* JIN-YOUNG BANG, YU-SIN KIM, CHIN-WOOK CHUNG, *Department of Electrical Engineering, Hanyang University* Electron energy distribution function (EEDF) is an important parameter to understand electron kinetics. Floating harmonic method provides the real-time measurement of plasma density and electron temperature at a floating potential with little perturbation to plasma. However, this method assumes a Maxwellian electron distribution and cannot measure the EEDF. In this study, we suggest a estimation method for the EEDF using the floating harmonic method without scanning an entire electron energy region. A theoretical study was also performed to calculate harmonic currents flowing through the probe in various EEDFs. According to theoretical results, the type of the EEDF was able to estimate by the ratio of the harmonic currents. Experiment results were in good agreement with the theoretical results in the various EEDFs. In conclusion, this method is expected to complement the conventional floating harmonic method in non-Maxwellian electron distributions.

QRP1 76 Measurement of the plasma density and electron temperature uniformities in inductively coupled plasmas using 2D real time measurement method YOUNG-CHEOL KIM, YU-SIN KIM, SE-JIN OH, HYO-CHANG LEE, CHIN-WOOK CHUNG, *Hanyang University* Recently, two-dimensional (2D) wafer-type probe sensor for the measurement of spatial distribution of plasma parameters was developed based on the floating harmonic method by Chung and co-workers [1, 2]. In this study, the 2D plasma density profile and electron temperature were measured in inductively coupled plasma (ICP) with various external parameters such as RF power, gas pressure, gas mixing ratio. It was found that the plasma uniformity was significantly changed with external parameters, such as gas pressure, He gas mixing, and ICP power. These results are closely related to the electron kinetics, plasma diffusion neutral depletion and ionization process and give guide lines for plasma uniformity control method by changes in the external parameters.

[1]M. H. Lee, S. H. Jang, and C. W. Chung, J. Appl. Phys. **101**, 033305 (2007).
[2]Y. C. Kim, S.H. Jang, G.H. Kim, and C. W. Chung, "Real time two-dimensional spatial distribution measurement method of electron temperature and plasma density," 62nd Gaseous Electronic Conference, 2009.

QRP1 77 Catalytic probe measurements in a large scale CCP reactor* SASA LAZOVIC, KOSTA SPASIC, NEVENA PUAC, GORDANA MALOVIC, *Institute of Physics, University of Belgrade, Serbia* UROS CVELBAR, MIRAN MOZETIC, *Jozef Stefan Institute, Ljubljana, Slovenia* ZORAN LJ. PETROVIC, *Institute of Physics, University of Belgrade, Serbia* A large scale cylindrical asymmetric CCP reactor is suitable for efficient treatment of materials like polymers, textile and plant seeds. Plasma is homogeneous and stable from transitions to streamers. For many biomedical and textile treatment effects, role of extremely reactive atomic oxygen species is very important. For instance, the formation of new oxygen-containing groups on the fiber surface is suggested to be due to the presence of extremely reactive atomic oxygen species in discharge during the air plasma processing and/or post-plasma chemical reactions when the activated fiber surface reacts with environmental species. Measurements were performed using nickel catalytic probe placed side-on to the powered electrode. Concentrations of neutral oxygen atoms were measured for a range of powers given by the RF generator, at several different distances from the powered electrode, in air at two different pressures. Oxygen atom concentrations coming to the surface of the samples can be controlled by adjusting the pressure, distance from the powered electrode and RF power.

*Projects III41011 and ON171037, MES Republic of Serbia.

QRP1 78 Time resolved ICCD images of an atmospheric pressure plasma jet* NEVENA PUAC, DEJAN MALETIC, SASA LAZOVIC, GORDANA MALOVIC, *Institute of Physics, University of Belgrade, Serbia* ANTONIJE DJORDJEVIC, *Faculty of Electrical Engineering, University of Belgrade, Serbia* ZORAN LJ. PETROVIC, *Institute of Physics, University of Belgrade, Serbia* Plasma bullet is a relatively new plasma source with a large field of potential applications, from biomedical to material processing and surface activation. Our plasma bullet was made of Pyrex glass tube with two electrodes. The width of the electrodes and distance between them was 15 mm. The buffer gas was helium with a flow of 4 slm. High voltage probe was used to obtain voltage waveforms while current waveforms were measured at the resistor. Working frequency was 80 kHz and the power transmitted to the plasma was less than 5 W. Time-resolved images obtained by fast ICCD camera show that the plasma is not continuous, but consisted of small packages of plasma traveling at high speeds. The velocity of these packages outside of the tube is much larger (~15 km/s) than the speed of the feed gas (~7 m/s). On the other hand, the velocities in the zone of the electrodes are smaller (~5 km/s) than the speed of the bullet, but still much higher than the speed of the flowing gas.

*Projects III41011 and ON171037, MES Republic of Serbia.

QRP1 79 Determination of Electron and Ion Energy Distribution Functions in a Plasma Ion Assisted Deposition (PIAD) Process* J. HARHAUSEN, R. FOEST, A. OHL, *Leibniz Institute for Plasma Science and Technology* High performance optical coatings are commonly produced by PIAD in order to achieve comparably high deposition rates. Here, the plasma source is a hot cathode direct current discharge with an auxiliary magnetic field (APS). Its design is such to generate a population of fast ions to be released into the deposition chamber. A detailed understanding of the plasma properties in the chamber is mandatory to increase the level of uniformity and reproducibility of the deposition process. In order to determine the electron and ion energy distribution functions (EEDF, IEDF) the concepts of the Langmuir probe, the retarding field energy analyzer and optical emission spectroscopy are employed. Fundamental findings are that the EEDF can be described in the framework of the non-local approximation and that the degree of ionization inside the APS is close to unity. The shape of the IEDF and its evolution along the beam path can be described consistently by considering charge exchange reactions with the background neutral gas and the profile of the plasma potential.

*Funded by the German Ministry for Education and Research (BMBF, Fkz. 13N10462).

QRP1 80 Tomographic Reconstruction of Local Parameters of a Plasmoid in the Afterglow of a Supersonic Flow Microwave Discharge ANA SAMOLOV, MILKA NIKOLIC, ALEXANDER GODUNOV, SVETOZAR POPOVIC, LEPOSAVA VUSKOVIC, *Old Dominion University, Department of Physics, Center for Accelerator Science, Norfolk, VA 23529* FILIP CUCKOV, *Old Dominion*

Spectroscopic ellipsometry of few-layer graphene

Article *in* Journal of Nanophotonics · June 2011

Impact Factor: 1.69 · DOI: 10.1117/1.3598162

Spectroscopic Ellipsometry of Few Layer Graphene

Goran Isić,[a,b] Milka Jakovljević,[a] Marko Filipović,[a] Djordje Jovanović,[a] Borislav Vasić,[a] Saša Lazović,[a] Nevena Puač,[a] Zoran Lj. Petrović,[a] Radmila Kostić,[a] Radoš Gajić,[a] Iris Bergmair,[c] Kurt Hingerl,[d] Tom Oates,[e] Karsten Hinrichs,[e] Jozef Humlicek,[f] Maria Losurdo,[g] Giovanni Bruno,[g]

[a]Institute of Physics,University of Belgrade, Pregrevica 118, 11080 Belgrade, Serbia
isicg@ipb.ac.rs
[b]School of Electronic and Electrical Engineering, University of Leeds, Leeds LS2 9JT, United Kingdom
[c]Functional Surfaces and Nanostructures, Profactor GmbH, Steyr-Gleink, Austria
[d]Center for Surface- and Nanoanalytics, Johannes Kepler University Linz, Linz, Austria
[e]Leibniz - Institut für Analytische Wissenschaften - ISAS - e.V., Department Berlin, Berlin, Germany
[f]Department of Condensed Matter Physics, Faculty of Science, Masaryk University Brno, Brno, Czech Republic
[g]Institute of Inorganic Methodologies and of Plasmas, IMIP-CNR, Department of Chemistry, University of Bari, Bari, Italy

Abstract. The optical properties of few layer graphene (FLG) films are studied in the ultraviolet and visible spectrum using a spectroscopic ellipsometer equipped with a 50 micron nominal microspot size. The FLG thickness is found by atomic force microscopy. The spot size measurements revealed that it is larger than the FLG flake. The ellipsometric measurements on FLG films are interpreted using the island film model. Comparison with graphite and recently published graphene data has shown reasonable agreement but with some features that could not be explained. The error margin for the optical constants is estimated to be $\pm 10\%$.

Keywords: graphene, ellipsometry, island film model

1 INTRODUCTION

Graphene has been recognized as an exciting new material since the first report on its electronic properties [1]. This is mostly due to the peculiar behaviour of electrons in graphene and due to the fact that it has been the missing two-dimensional allotrope of carbon. Recently, however, the optical properties of graphene are receiving considerable attention both due to potential applications in photonics [2] and the fact that the optical spectra of graphene provide the grounds to observe some fundamental features of two-dimensional physics [3, 4].

The optical response of graphene has been theoretically predicted [5, 6] to be well described by the sheet conductance $\sigma_0 = e^2/4\hbar$. Recent experimental results on graphite [7] and graphene [8, 9] have confirmed the validity of the σ_0 model in the infrared and visible parts of the spectrum. Some differences have, however, been observed the theoretical explanation of which is a topic of considerable interest [3].

It was not until very recently, [10, 11], that spectroscopic ellipsometric measurements of graphene have been reported. The main reason is that the minimal size of an ellipsometric spot in the visible part of spectrum is usually $50\mu\mathrm{m}$ or more while it is hard to prepare high-quality mechanically exfoliated graphene flakes with features larger than few tens of microns.

Send correspondence to G. I.

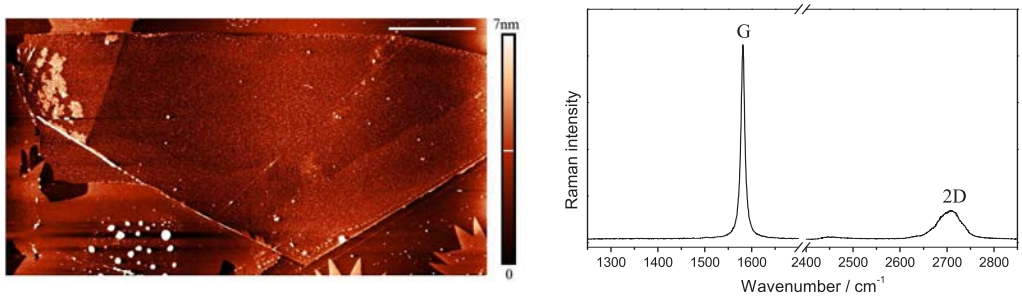

(a) (b)

Fig. 1. AFM and Raman spectroscopy characterization of the sample. (a) AFM tapping mode topography map of the sample. The middle part shows the FLG while some glue residue is seen around it. The size of the white scale bar in the upper right corner is $20\mu\mathrm{m}$. (b) Raman spectrum of the sample. It proves the quality of the FLG while the structure of the 2D peak indicates that more than one layer is present.

In Ref. [12] this problem has been resolved by using an imaging ellipsometer with a resolution better than $1\mu\mathrm{m}$. The optical properties of graphene grown by chamical vapor deposition on copper and transferred to a glass substrate have also recently been measured by ellipsometry in Ref. [13]. While the data obtained by ellipsometric measurements are in general agreement, there are still clearly seen differences. Perhaps this is not unexpected considering that even the graphite optical data differ amongst various sources [14, 15].

In this paper we report on ellipsometric measurements of a few layer graphene (FLG) flake in the $250 - 650\mathrm{nm}$ spectral range. Since the ellipsometric spot size is found to be larger than the FLG flake, we use the island film model in extracting the optical constants and compare the results with the recently published graphene data.

2 SAMPLE PREPARATION AND CHARACTERIZATION

The FLG films are prepared by means of micromechanical exfoliation [16] of graphite on n-doped (As, $10^{-3} - 10^{-2}\mathrm{ohm\,cm}$) silicon substrates with a $300\mathrm{nm}$ (nominal) thickness of thermal silicon-dioxide on top. The sample was characterized by atomic force microscopy (AFM) and Raman spectroscopy, as shown in Fig. 1 (a) and (b), respectively.

The AFM measurements of the sample have been carried out on NT-MDT NTEGRA Prima system in the AFM tapping mode. Figure 1 (a) shows the sample topography. The apparent FLG thickness in the tapping mode has been found to be $2.3\mathrm{nm}$. In retrieving the optical constants of graphene from the ellipsometric spectra, we have assumed that the FLG thickness is $d_{\mathrm{FLG}} = 2\mathrm{nm}$ while the remaining $0.3\mathrm{nm}$ are ascribed to the AFM artifact comming from the difference between the tip adhesion to graphene and the SiO_2 surface [17]. The uncertainty in d_{FLG} is estimated to be below $\pm 5\%$. The glue residue seen around the sample has been found to have a few nanometer thickness most. The refractive index of glue is around 1.5 (around two times smaller than graphite) while the relative portion of the illuminated area covered by glue is small as seen in Fig. 2 (a). Consequently the effect of glue has been neglected.

The micro-Raman scattering measurements were performed at room temperature using the Jobin-Yvon T64000 triple spectrometer system with $0.7\mathrm{cm}^{-1}$ spectral resolution, equipped with a liquid-nitrogen cooled CCD detector and a nominal spot size of the order of $1\mu\mathrm{m}$. The $\lambda = 514.5\mathrm{nm}$ line of an Ar+ laser was used as an excitation source with laser power $P = 10\mathrm{mW}$. The Raman spectra shown in Fig. 1 (b) was collected from the middle of the FLG, corresponding to the center of the ellipse shown in Fig. 2 (a).

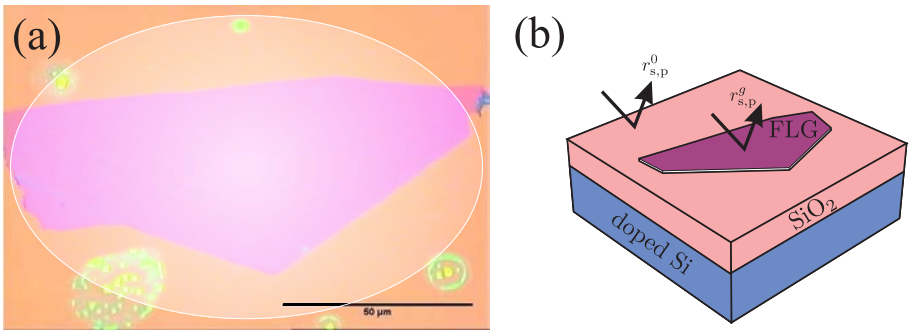

Fig. 2. Figure 2. (a) Image of the FLG sample on which the ellipsometric measurements have been made taken by an optical microscope. The transparent ellipse is drawn to schematically show the ellipsometric spot size relative to the sample and, also, the light intensity variation within the spot. Traces of glue residue are also visible. While we are unsure of the precise influence of the glue residue on our measurements, its effective area and thickness found from AFM is sufficiently small to assume it is negligible. (b) Explaining the island-film model: the complex reflection coefficient of the FLG island on the SiO_2 surface (r_s for s-polarization and r_p for p-polarization) is assumed to be a weighted average of the complex reflection coefficients of the bare substrate (r^0_s and r^0_p) and the substrate completely covered by the FLG film (r^g_s and r^g_p).

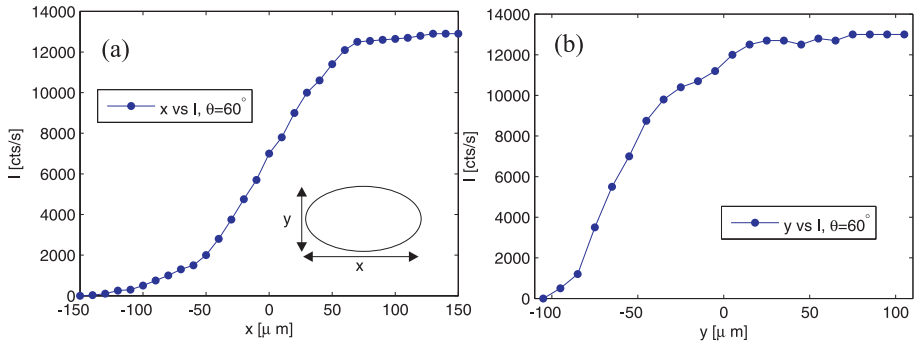

Fig. 3. Knife-edge measurements of the ellipsometric micro-spot at the incidence angle of $60°$. (a) and (b) show the measured intensity of the reflected light vs the sharp edge displacement along x and y direction, respectively, see the inset of (a).

3 ELLIPSOMETRIC MEASUREMENTS

3.1 Measurement setup

The optical properties of the few layer graphene (FLG) sample are studied in the ultraviolet and visible ($200 - 650\mathrm{nm}$) spectrum using a SOPRA spectroscopic ellipsometer equipped with a $50\mu\mathrm{m}$ microspot (nominal) size.

Since the size of the sample is comparable to the ellipsometric spot size, an accurate knowledge of the spot size was required. The spot intensity profile has been measured using the knife-edge technique as shown in Fig. 3. The spot size established from these measurements is $110 \times 60\mu\mathrm{m}^2$. Taking into account that the light flux is not uniform across the spot, the fraction of the total flux falling on the FLG flake has been estimated to be $s = 0.35$ with an uncertainty of ± 0.05.

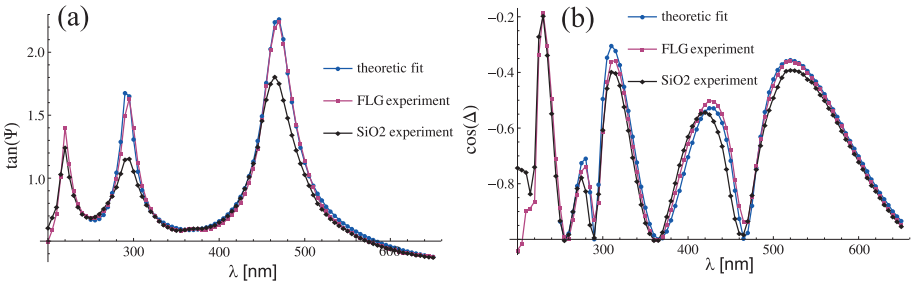

Fig. 4. The ellipsometric spectra (a) $\tan\Psi$ and (b) $\cos\Delta$ of FLG and the bare SiO_2 film measured at the nominal angle of $\theta = 60°$. The spectral range below 250nm is found to be unreliable so it was not considered in the determination of optical constants. The figure also shows that the 2nm thin layer of FLG makes a noticeable difference in $\tan\Psi$ only around the Fabri-Perot resonances of the silicon-dioxide film.

The ellipsometric spectra have been found to be very sensitive on the relative position of the FLG flake and light spot. The area around the FLG is monitored using a CCD camera with a magnifying lens providing a resolution of around $10\mu\text{m}$. However the light spot itself is not seen because the surface is very flat (specular reflection). Its approximate position is determined by covering the sample with a thin paper. A large bright spot appears which tells us roughly where the spot is. However, to define and find the exact position the following idea has been used: the height of the Fabri-Perot peak in $\tan\Psi$ at $\lambda = 480\text{nm}$ (corresponding to the 300nm silicon-dioxide film at $\theta = 60°$ incidence angle) is known to be very sensitive to the presence of thin absorbents on the surface. This has been observed in [10] and is seen in calculations based on Fresnel formulas. The spot is positioned approximately over the FLG flake after which the exact position is found by moving around the sample within a $100\mu\text{m}$-diameter circle until a maximum value of the $\tan\Psi$ at $\lambda = 480\text{nm}$ is found. Knowing that this maximum occurs when most of the light flux falls onto the FLG we knew that this is the correct position. The spectra measured this way, Fig. 4, have been found to be reproducible in the $250 - 650\text{nm}$ range, i.e. after removing the sample and repeating the procedure, the same spectra has been measured.

3.2 Retrieval of FLG optical constants

The main difficulty in interpreting the measured data is that the ellipsometric spot size is larger than the FLG flake. For this reason the island-film model (see [18] and references therein) has been used in data modelling. The idea, as explained in Fig. 2 (b), is that the reflection coefficient r is a weighted average of the reflection coefficient r^0 of the bare substrate and the reflection coefficient r^g with graphene on top

$$r = (1 - s)r^0 + sr^g, \tag{1}$$

where s is the fraction of the surface covered by the FLG. It is suitable for surfaces covered by thin flakes whose lateral dimensions are much smaller than the lateral correlation length. This is assumed to hold since the flake lateral dimensions are measured in tens of micrometers.

By measuring the bare substrate at multiple places around the FLG flake, the SiO_2 thickness is found to be $d_{SiO_2} = 307\text{nm}$ and the angle of incidence $\theta = 61.5°$. Using these parameters and assuming a polynomial model

$$n(\lambda) = a_0 + a_1\lambda + a_2\lambda^2 + a_3\lambda^3, \quad k(\lambda) = b_0 + b_1\lambda_1 + b_2\lambda^2 + b_3\lambda^3 + b_4\lambda^4, \tag{2}$$

for the FLG dispersion, a numerical fitting procedure has been performed. The best fit is found for $a_0 = 2.775$, $a_1 = -3.6$, $a_2 = 5.6$, $a_3 = -4.1$, $b_0 = 9.8$, $b_1 = -51$, $b_2 = 115$, $b_3 = -113$,

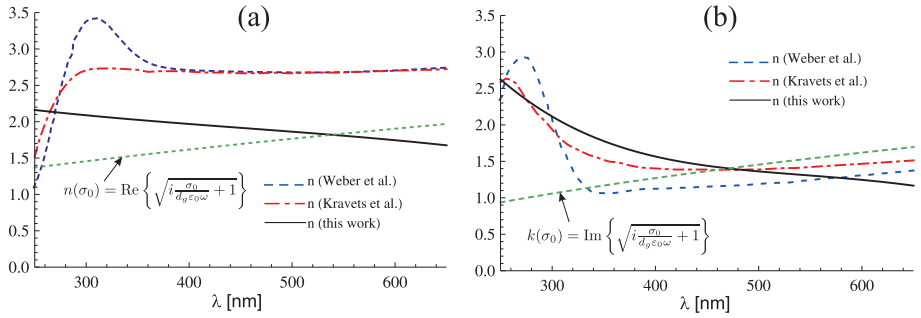

Fig. 5. Retrieved optical constants of FLG represented as the real (a) and imaginary (b) part of the refractive index. The blue dashed line is the graphene data taken from [11], the red dash-dotted is the graphene data from [10]. The green dotted line shows the values expected from the σ_0 model.

$b_4 = 39$ (for λ in nm). This n and k spectra is shown in Fig. 5 where a comparison is made with the recently published data for graphene [10, 11]. The green dotted line shows the optical constants calculated assuming that the optical response of each graphene layer is equal to $\sigma_0 = e^2/4\hbar$. The graphite data from [14] is not shown since it is practically the same as the one found for graphene in [10].

The uncertainty of the optical constants shown in Fig. 5 is determined by two dominant factors:

1) d_{FLG}, the measured thickness of the FLG Since we are well within the thin film limit, $d_{\mathrm{FLG}} \ll \lambda$, a relative error in of $\pm 5\%$ in d_{FLG} will produce the same relative error in the retrieved dielectric function implying that the relative error in the refractive index will be two times smaller, $\pm 2.5\%$;

2) spot placement uncertainty the light spot intensity profile found by differentiating the data in Fig. 3 enabled us to estimate that that the fraction s of the light flux falling onto the FLG is $s = 0.35 \pm 0.05$ which is a relative uncertainty of around $\pm 15\%$. Using the thin film argument, it is seen that this implies the same relative uncertainty in ε and $\pm 7.5\%$ in the refractive index.

Therefore we estimate the retrieved data for n and k should both have an error margin of around $\pm 10\%$.

In comparing the FLG n and k spectra with graphene data in Fig. 5 a very good agreement is expected because these are dominated by the electronic response while the energy scale at which the graphene and FLG bandstructures differ is few hundreds of milielectronvolts, the energy of the inter-layer coupling in FLGs [19].

The n data reported in this paper is found to be around 30% lower than the graphene data. While the disagreement in magnitude could be partially explained by various sources of error that we mentioned (even though it is outside the estimated error range), the decreasing trend in n (seen in both [10, 11] and predicted by the σ_0 model) remains unclear. The k spectra shown in Fig. 5 (b) is found to be in good agreement with [10, 11] but here also an opposite slope for wavelengths above $450\mathrm{nm}$ is observed.

4 SUMMARY

The use of spectroscopic ellipsometry for measuring the optical constants of a FLG flake has been considered. The FLG thickness and its quality have been established from AFM and Raman measurements. The problem of the sample being smaller than the ellipsometric spot

(but still much larger than the wavelength) has been circumvented by the use of the island-film model which allowed the recovery of optical constants of the FLG film with a scale uncertainty that is estimated to be around $\pm 10\%$. The data for the extinction coefficient has been found to be in good agreement with the previously published data for graphene and graphite including the rising trend in the UV. The refractive index data has been found to be around 30% lower and missing the sharp decrease in the UV.

Acknowledgments

This work is supported by the Serbian Ministry of Science through Projects OI 171005, OI 171037, III 45018, III 41011, and by the EU FP7 projects NIM_NIL (gr. a. no 228637 NIM_NIL: www.nimnil.org). We are grateful to K. Novoselov and S. Anisimova for their help regarding graphene exfoliation.

References

[1] K. S. Novoselov, A. K. Geim, S. V. Morozov, D. Jiang, Y. Zhang, S. V. Dubonos, I. V. Grigorieva, and A. A. Firsov, "Electric Field Effect in Atomically Thin Carbon Films," *Science* **306**(5696), 666–669 (2004).

[2] F. Bonaccorso, Z. Sun, T. Hasan, and A. C. Ferrari, "Graphene photonics and optoelectronics," *Nat. Photonics* **4** (2010).

[3] N. M. R. Peres, "Colloquium: The transport properties of graphene: An introduction," *Rev. Mod. Phys.* **82**(3), 2673–2700 (2010).

[4] K. F. Mak, J. Shan, and T. F. Heinz, "Seeing many-body effects in single- and few-layer graphene: Observation of two-dimensional saddle-point excitons," *Phys. Rev. Lett.* **106**(4), 046401 (2011).

[5] T. Ando, Y. Zheng, and H. Suzuura, "Dynamical conductivity and zero-mode anomaly in honeycomb lattices," *J. Phys. Soc. Jpn.* **71**(5), 1318–1324 (2002).

[6] V. P. Gusynin, S. G. Sharapov, and J. P. Carbotte, "Unusual microwave response of dirac quasiparticles in graphene," *Phys. Rev. Lett.* **96**(25), 256802 (2006).

[7] A. B. Kuzmenko, E. van Heumen, F. Carbone, and D. van der Marel, "Universal optical conductance of graphite," *Phys. Rev. Lett.* **100**(11), 117401 (2008).

[8] R. R. Nair, P. Blake, A. N. Grigorenko, K. S. Novoselov, T. J. Booth, T. Stauber, N. M. R. Peres, and A. K. Geim, "Fine Structure Constant Defines Visual Transparency of Graphene," *Science* **320**(5881), 1308 (2008).

[9] Z. Q. Li, E. A. Henriksen, Z. Jiang, M. C. Hao, Z. Martin, P. Kim, H. L. Stormer, and D. N. Basov, "Dirac charge dynamics in graphene by infrared spectroscopy," *Nat. Phys.* **4**, 532 (2008).

[10] V. G. Kravets, A. N. Grigorenko, R. R. Nair, P. Blake, S. Anissimova, K. S. Novoselov, and A. K. Geim, "Spectroscopic ellipsometry of graphene and an exciton-shifted van hove peak in absorption," *Phys. Rev. B* **81**(15), 155413 (2010).

[11] J. W. Weber, V. E. Calado, and M. C. M. van de Sanden, "Optical constants of graphene measured by spectroscopic ellipsometry," *Appl. Phys. Lett.* **97**(9), 091904 (2010).

[12] U. Wurstbauer, C. Roling, U. Wurstbauer, W. Wegscheider, M. Vaupel, P. H. Thiesen, and D. Weiss, "Imaging ellipsometry of graphene," *Appl. Phys. Lett.* **97**(23), 231901 (2010).

[13] F. J. Nelson, V. K. Kamineni, T. Zhang, E. S. Comfort, J. U. Lee, and A. C. Diebold, "Optical properties of large-area polycrystalline chemical vapor deposited graphene by spectroscopic ellipsometry," *Appl. Phys. Lett.* **97**(25), 253110 (2010).

[14] A. Borghesi and G. Guizzetti, "Graphite (C)," in *Handbook of optical constants of solids II*, E. D. Palik, Ed., 449, Academic Press (1991).

[15] G. E. Jellison, J. D. Hunn, and H. N. Lee, "Measurement of optical functions of highly oriented pyrolytic graphite in the visible," *Phys. Rev. B* **76**(8), 085125 (2007).

[16] K. S. Novoselov, D. Jiang, F. Schedin, T. J. Booth, V. V. Khotkevich, S. V. Morozov, and A. K. Geim, "Two-dimensional atomic crystals," *Proc. Natl. Acad. Sci. USA* **102**(30), 10451–10453.

[17] P. Nemes-Incze, Z. Osvth, K. Kamars, and L. Bir, "Anomalies in thickness measurements of graphene and few layer graphite crystals by tapping mode atomic force microscopy," *Carbon* **46**(11), 1435 – 1442 (2008).

[18] H. Fujiwara, *Spectroscopic Ellipsometry - Principles and Applications*, John Wiley & Sons, Ltd, Tokyo (2007).

[19] H. Min and A. H. MacDonald, "Origin of universal optical conductivity and optical stacking sequence identification in multilayer graphene," *Phys. Rev. Lett.* **103**(6), 067402 (2009).

ICAPT2009
iPlasmaNanoSym

2ND INTERNATIONAL CONFERENCE ON ADVANCED PLASMA TECHNOLOGIES WITH 1ST INTERNATIONAL PLASMA NANOSCIENCE SYMPOSIUM

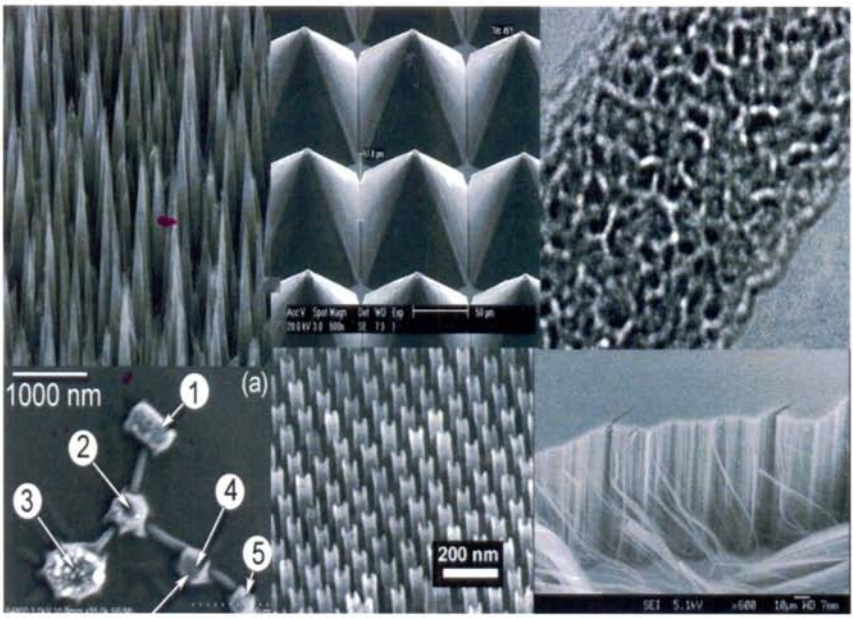

CONFERENCE PROCEEDINGS

Sep 29th - Oct 2nd 2009 | Piran, Slovenia, EU

2 nd International Conference on Advanced Plasma Technologies (iCAPT-II)

&

1 st International Plasma Nanoscience Symposium (iPlasmaNanoSym-I)

CONFERENCE PROCEEDINGS

September 29th — October 2nd 2009, Piran, Slovenia

Mass spectrometry analysis of atmospheric plasma discharge

N. Puač, D. Maletić, S. Lazović, G. Malović, Z. Lj. Petrović
Institute of physics, Pregrevica 118, 11080 Belgrade, Serbia

nevena@phy.bg.ac.rs

In order to understand the chemistry in the gas phase and at the surface of the sample knowledge of the composition of plasma, i.e. of the active species, is needed. Mass spectrometry (MS) is a popular method to analyze chemical composition of gases and plasmas [1, 2]. The results are particularly relevant for surface treatment, because the mass spectrometer samples the species which arrive at and potentially interact with the surface. At the same time, until recently MS was not applicable to atmospheric pressure plasmas which are required for numerous applications with living tissues or cells.

The objective of the experiment was to analyze products, molecule and atomic radicals which are formed in RF plasma, by using Hiden mass spectrometer HPR-60. This spectrometer has triple differential pumping and allows direct contact with the gas at atmospheric pressure. Radicals and other active species are important for the treatment and modification of the sensitive surfaces. We have analyzed Micro Atmospheric Pressure Plasma Jet (μ-AAPJ) [3]. The main parts of this device are two parallel stainless steel electrodes. The gap between electrodes was 1 mm and the electrodes are placed in the quartz cuvette. One electrode was grounded and the other was powered with excitation frequency of 13.56 MHz.

The plasma was operating in homogeneous glow mode in the mixture of noble gas helium and small percent of oxygen (1 %) and the flow rate was 3 slm (standard liter per minute). μ-AAPJ was placed at the distance of 1 mm from the orifice of the mass spectrometer. Between the mass spectrometer and μ-AAPJ we placed a sheet of Teflon, 0.8 mm thick. This Teflon sheet served as

isolation between powered electrode and mass spectrometer. Species created in the plasma are sampled using a three stage differentially pumped molecular beam inlet system.

The mass spectrometer has capability of collecting and counting both neutrals and ions coming from the plasma. In case of detecting neutrals, ionization filament, which is placed in the third stage of mass spectrometer, has to be turned on. Ionization filament serves as electron source with electron energies between 0.4 and 70 eV. In this third stage of mass spectrometer ions are created from the neutrals coming from plasma and detected by analyzer.

In this experiment we scanned masses of neutrals from 1-50 amu at the fixed electron energy of 70 eV and, also, we scanned distribution of neutral atoms for electron energies from 5 to 35eV. From these distributions one can identify all processes that are present in creation of neutral atoms. After identifying which process takes place densities of N and O atoms and other neutrals created in the plasma are determined. In Figures 1 and 2 number of O and N atoms, respectively, created in the discharge for different powers given by RF power supply are shown. We can see that number of oxygen atoms created by the plasma is increasing with an increase of the power given by the reading from the RF power supply. On the other hand number density of nitrogen atoms stays almost constant with an increase of power.

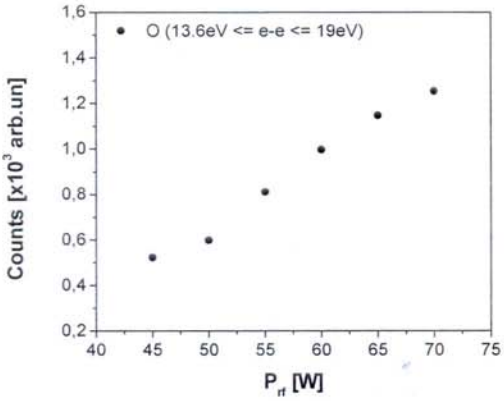

Figure 1: Number of oxygen atoms created in plasma for different powers given by RF supply.

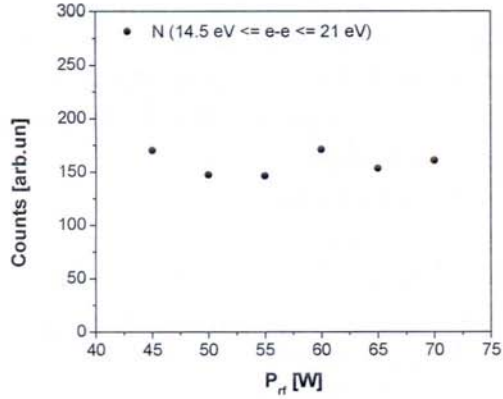

Figure 2: Number of nitrogen atoms created in plasma for different powers given by RF supply.

References:

[1] E. Stoffels, Y. Aranda Gonzalvo, T. D. Whitmore, D. L. Seymour and J. A. Rees. Mass spectrometric detection of short-living radicals produced by a plasma needle, *Plasma Sources Sci. Technol.*, 16, 549-556, 2007

[2] S. Lazović, N. Puač, G. Malović, A. Đorđević and Z. Lj. Petrović. Diagnostic of plasma needle properties by using mass spectrometry, *Chem. Listy* **102,** s1383-s1387, 2008

[3] V. Schulz-von der Gathen, V. Buck, T. Gans, N. Knake, K. Niemi, St. Reuter, L. Schaper, and J.Winter. Optical Diagnostics of Micro Discharge Jets. *Contrib. Plasma Phys.*, 47(7), 510–519, 2007

ECM 112
ICAPT2011

112 IUVSTA Executive Council Meeting and 4th International Conference on Advanced Plasma Technologies with Workshop

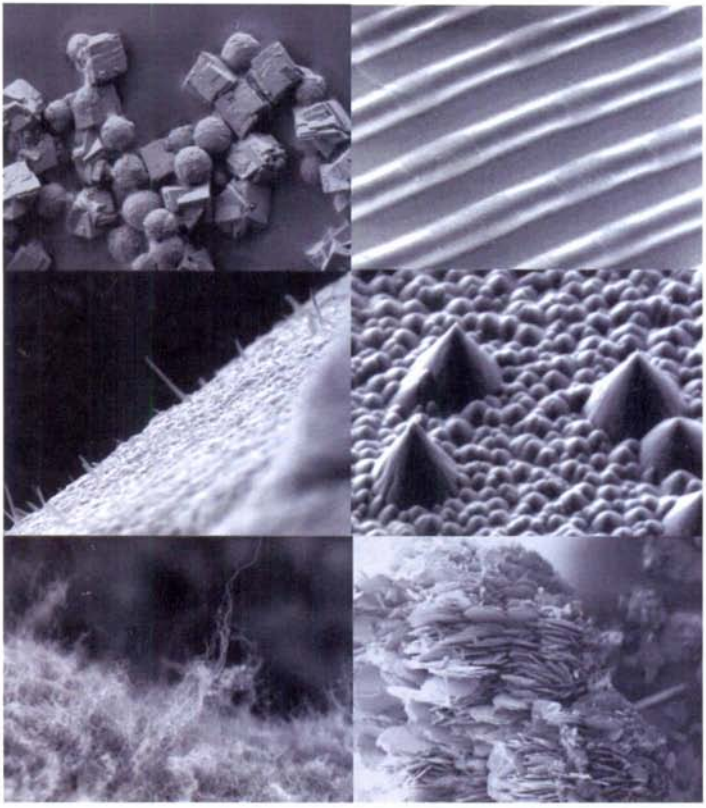

CONFERENCE PROCEEDINGS

Sep 9th-13th 2011 | Strunjan, Slovenia, EU

Editors of Proceedings: Miran Mozetič and Uroš Cvelbar

Published by: Slovenian Society for Vacuum Technique (DVTS Društvo za vakuumsko tehniko Slovenije), Teslova 30, SI-1000 Ljubljana, Slovenia

Graphic design: Kristina Eleršič

Printed by: Infokart d.o.o., Ljubljana

Ljubljana, September 2011

CIP - Kataložni zapis o publikaciji
Narodna in univerzitetna knjižnica, Ljubljana

533.9(082)
620.3(082)

INTERNATIONAL Conference on Advanced Plasma Technologies (4 ; 2011 ; Strunjan)

Conference proceedings / 4th International Conference on Advanced Plasma Technologies (iCAPT-IV), September 11th - Aeptember 13th 2011, Strunjan, Slovenia ; [editor Miran Mozetič]. - Ljubljana : Slovenian Society for Vacuum Technique = DVTS - Društvo za vakuumsko tehniko Slovenije, 2011

ISBN 978-961-92989-3-0
1. Mozetič, Miran, 1961-

257634560

P-29	*ICCD images of plasma bullets for two different electrode configurations*	D. Maletić, N. Puač, S. Lazović, G. Malović, A. Đorđević and Z. Lj. Petrović
P-30	*Automatisation of Processing of Fibre Optics Catalytic Probe Signals*	A. Drenik, A. Tomeljak, R. Zaplotnik and M. Mozetič
P-31	*Photocatalytically active printing ink based on the redox dye 2,6-dichloroindophenol*	A. Pondelak, A. Sever Škapin, R. Urbas, M. Klanjšek Gunde
P-32	*Encapsulation of nano-dimensional organic pigments by silica*	E. Švara Fabjan, A. Sever Škapin, M. Otoničar, M. Gaberšček
P-33	*Diagnostics of a large scale CCP reactor suitable for textile treatments*	S. Lazović, N. Puač, K. Spasić, G. Malović, U. Cvelbar, M. Mozetič and Z. Lj. Petrović
P-34	*Study of the effect of firing process on photocatalytic activity of external self-cleaning ceramic tiles*	A. Sever Škapin, V. Ducman

ICCD images of plasma bullets for two different electrode configurations

D. Maletić[1], N. Puač[1], S. Lazović[1], G. Malović[1], A. Đorđević[2] and Z.Lj. Petrović[1]

[1]Institute of Physics, University of Belgrade, Pregrevica 118, 11000 Belgrade, Serbia
[2]School of Electrical Engineering, University of Belgrade, Bulevar kralja Aleksandra 73, 11000 Belgrade, Serbia

dejan_maletic@ipb.ac.rs

In the last decade, many atmospheric pressure plasma sources have been constructed and analyzed because of wide range of applications. Most of these plasmas are in a form of jets. The important characteristic of these jets is low gas temperature and power transmitted to the plasma. These plasmas can be generated in many different gases and using different types of electrical excitation. For biomedical applications, gas temperature should not exceed 40 °C, and high concentration of radicals and ions are desirable. The field of biomedical applications and plasma medicine are constantly growing and encourage the development of new plasma sources [1-4].

Plasma bullets are a new topic of considerable interest. Characteristic of plasma bullet is that the plasma is not continuous but it actually consists of fast moving train of highly luminous but discrete plasma packages. Several theories of bullet formation have been proposed [5-7]; however, to date a definite explanation of the physical mechanisms driving the plasma bullet phenomenon remains unexplained. This line of current research would benefit from a more detailed characterization of plasma bullet behavior. In this paper we will present images obtained by using fast ICCD camera for two different configurations of the electrodes.

The atmospheric pressure plasma bullet that we used was made of a Pyrex glass tube (I.D. 4 mm and O.D. 6 mm). We have used two different electrode configurations, the first set-up of electrodes were made of a thin copper foil wrapped around the glass tube. The distance between the powered and the

grounded electrode was 10 mm. The width of both electrodes was 13 mm. The experimental scheme is given in Figure 1.

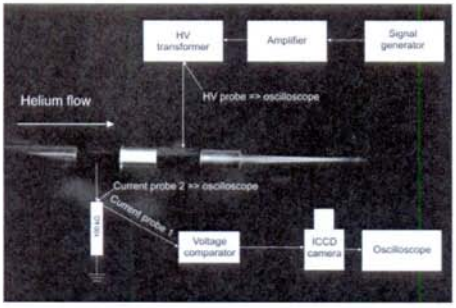

Figure 4. Experimental setup.

In the second configuration we used two electrodes made of copper wire (d=0.5 mm), the distance between them was 20 mm, and the distance from the end of glass tube and powered electrode was 25 mm. The feeding gas was helium and the flow rates used in this work were 1-5 slm, adjusted with a mass flow controller.

Plasma jet was powered by a signal generator connected to a custom-made amplifier and to an additional homemade step-up transformer. For delaying camera gating and for external triggering of the oscilloscope we have used camera's internal delay generator. The applied frequency was 80 kHz and the voltage was in the range 7-11 kVpp. The power transmitted to the plasma did not exceed 2 W during all measurements in the configuration with copper wires and somewhat higher for the copper foil electrodes (<10 W).

In order to see how the shape of the electrodes influences the bullet formation we used these two different electrode setups. For the first set of electrodes, made of copper foil, we observed the bullet at the positive half cycle of the current. Fig 2 shows the influence of flow for two different delays. We can see that for delay of 10 μs bullet has low intensity and for the delay of 10.8 μs intensity increase and bullet propagate downstream the helium flow. We can also see that the influence of the flow on bullet speed is very small.

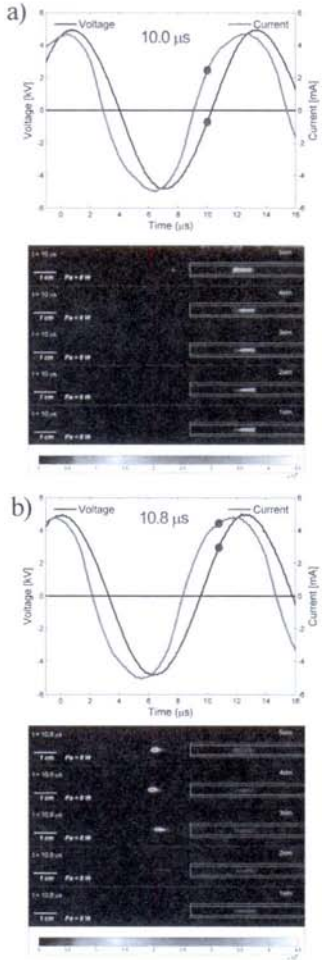

Fig.2. Plasma jet at 1, 2, 3, 4 and 5 slm. Exposure time 2 ms, gate width 25 ns, gate delay a) 10.0 and b) 10.8 μs. Obtained with wide electrodes.

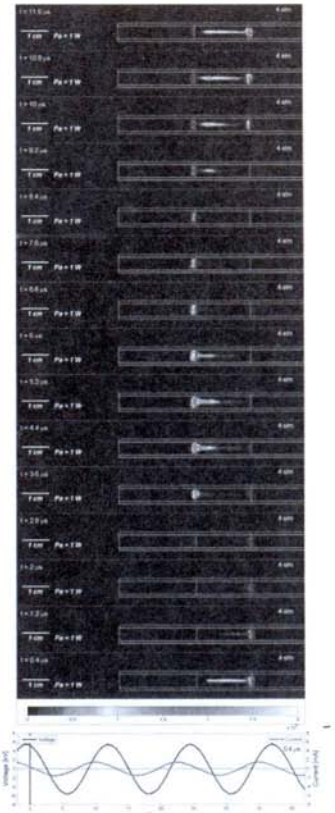

Fig.3. Plasma jet at 4 slm, exposure time 6 ms, gate width 25 ns and gate delay from 0 to 11.6 μs. Obtained with narrow electrodes.

ICCD images of the discharge formation for the set of electrodes made of copper wire are shown on fig.3. We used integration on chip and gate width of

25 ns to record the images. We did not observe formation of plasma bullet for this set of electrodes. The discharge moves from one electrode to the other. Presented ICCD images show that shape of the electrode has great influence on the formation of the bullet. Increasing the flow of helium gives the intense plasma jet but has almost no influence on its velocity. Controlling the shape of jet by changing the dimensions of electrodes can be interesting for possible applications.

Acknowledgements

This research has been supported by the MNTR, Serbia, under the contract numbers ON171037 and III41011 and bilateral projects Serbia-Slovenia.

Reference

[1] A. Fridman and L. A. Kennedy. "Plasma Physics and Engineering", Taylor and Francis, 2004.

[2] F. Iza, G. J. Kim , S. M. Lee, J. K. Lee, J. L. Walsh, Y. T. Zhang and M. G. Kong, "Microplasmas: sources, particle kinetics, and biomedical applications", Plasma Process. Polym., 5 (2008) 322.

[3] E. Stoffels, A. J. Flikweert, W. W. Stoffels, and G. M. W. Kroesen, "Plasma needle: a non-destructive atmospheric plasma source for fine surface treatment of (bio) materials", Plasma Sources Sci. Technol., 11 (2002) 383.

[4] N. Puač, Z.Lj. Petrović, G. Malović, A. Đorđević, S. Živković, Z. Giba and D. Grubišić, "Measurements of voltage–current characteristics of a plasma needle and its effect on plant cells", Journal of Physics D: Applied Physics, 39 (2006) 3514.

[5] Lu X and Laroussi M, "Dynamics of an atmospheric pressure plasma plume generated by submicrosecond voltage pulses", 2006 J. Appl. Phys. 100 063302

[6] Shi J, Zhong F, Zhang J, Liu D W and Kong M G, "Three distinct modes in a cold atmospheric pressure plasma jet", 2008 Phys.Plasmas 15 013504

[7] Mericam-Bourdet N, Laroussi M, Begum A and Karakas E, "Experimental investigations of plasma bullets", 2009 J. Phys. D: Appl. Phys. 42 055207

Images of plasma jet/bullet formation for different electrode configurations

Conference Paper · August 2011

READS
11

6 authors, including:

Dejan Maletic
Institute of Physics Belgrade
53 PUBLICATIONS **97** CITATIONS
SEE PROFILE

Saša Lazović
Institute of Physics Belgrade
70 PUBLICATIONS **212** CITATIONS
SEE PROFILE

Gordana Malovic
Institute of Physics Belgrade
157 PUBLICATIONS **932** CITATIONS
SEE PROFILE

Zoran Lj Petrović
Institute of Physics Belgrade
510 PUBLICATIONS **5,652** CITATIONS
SEE PROFILE

Topic number C10

Images of plasma jet/bullet formation for different electrode configurations

D. Maletić[1], S. Lazović[1], N. Puač[1], G. Malović[1], A. Đorđević[2] and Z.Lj. Petrović[1]

[1] *Institute of Physics, University of Belgrade, Pregrevica 118, 11000 Belgrade, Serbia*
[2] *School of Electrical Engineering, University of Belgrade, Bulevar kralja Aleksandra 73, 11000 Belgrade, Serbia*

Plasma jet operating in plasma bullet mode is a relatively new plasma source with a large range of potential applications, from biomedical to material processing and surface activation. Our plasma source was made of Pyrex glass tube with inner diameter of 4 mm and outer diameter of 6 mm. The frequency that we used was 80 kHz and the applied voltage was in the range of 7-11 $kV_{peak\text{-}to\text{-}peak}$. The power supply was a waveform generator connected to an HF amplifier and custom-made HV transformer. In this paper, we will show time-resolved ICCD images of our plasma bullet device for two different electrode configurations. The power transmitted to the plasma was calculated and it was lower than 2 W for both used sets of electrodes.

1. Introduction

In the last few years atmospheric microplasmas drew considerable attention because of the wide spectra of their applications. The necessity to use plasma for *in-vivo* treatments/procedures has led to several requirements for plasma sources to meet. The most obvious one is that biomedical plasmas have to operate at atmospheric pressure in most cases. The other requirement is that the gas temperature should not exceed 40^{o}C. The secret of generating atmospheric pressure non-equilibrium plasma is in control of ionization before density of the charged particles grows sufficiently to favor momentum and energy transfer from electrons to heavy particles through Coulomb interaction.

This constantly growing field of biomedical applications is now a new frontier that drives the development of plasma sources [1-3]. Special branch of atmospheric pressure plasmas which are being developed for various applications are atmospheric plasma jets. These plasmas can be generated in many different gases and using different types of electrical excitation.

A major topic of current interest in plasma jets has been plasma bullets, a fast moving train of highly luminous but discrete clusters of plasma. Several theories of bullet formation have been proposed [5-7]; however, to date a definite explanation of the physical mechanisms driving the plasma bullet phenomenon remains elusive. This line of current research would benefit from a more detailed characterization of plasma bullet behaviour and indeed from exploring whether the regime of plasma bullets may border with other discharge regimes. In this paper we will present images obtained by using fast ICCD camera for two different configurations of the electrodes.

2. Experimental set-up

The atmospheric pressure plasma jet/bullet that we used was made of a Pyrex glass tube (I.D. 4 mm and O.D. 6 mm). We have used two different electrode configurations. In the first set-up electrodes were made of a thin copper foil wrapped around the glass tube. The distance between the powered and the grounded electrode was 10 mm. The width of both electrodes was 13 mm. The experimental scheme is given in Figure 1.

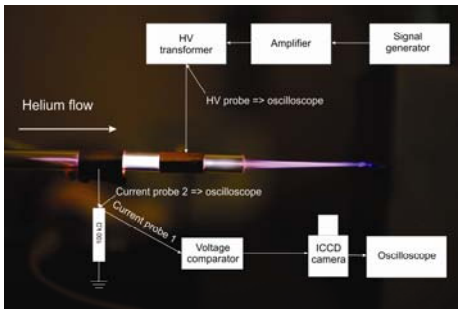

Figure 1. Experimental setup.

In the second configuration we used two electrodes made of copper wire (d=0.5 mm), the distance between them was 20 mm, and the distance from the end of glass tube and powered electrode was 25 mm. The feeding gas was helium and the flow rates used in this work were 4 slm, adjusted with a mass flow controller (Omega FMA5400/5500).

Plasma jet was powered with a signal generator (Peak Tech DDS function generator 4025) connected to a custom-made amplifier and to an additional homemade step-up transformer. We used two commercial probes and oscilloscope (Agilent DSO3202A), for the current and voltage measurements. For delaying camera gating and for

external triggering of the oscilloscope we have used camera's internal delay generator. The applied frequency was 80 kHz and the voltage was in the range 7-11 $kV_{peak\text{-}to\ peak}$. The power transmited to the plasma did not exceed 2 W during all measurements in the configuration with copper wires and somewhat hier for the copper foil electrodes (<10 W).

3. Results and discussion

We have used two different electrode configurations in order to see how the shape of the electrodes influences plasma bullet formation. In the case of thin copper foil electrodes plasma bullet was formed in the positive parts of current and voltage waveforms. Figure 2 shows the plasma bullet images obtained for different flows of working gas. We can see that with the decrease in the He flow, the plasma bullet starts to be elongated, deformed and its intensity is much smaller. On the other hand there seems to be very little difference in the velocity of the bullet.

Furthermore we replaced wide copper foil electrodes with two copper wires whose diameter was 0.5 mm and images of the formed discharge obtained by fast ICCD camera are shown in Figure 3.

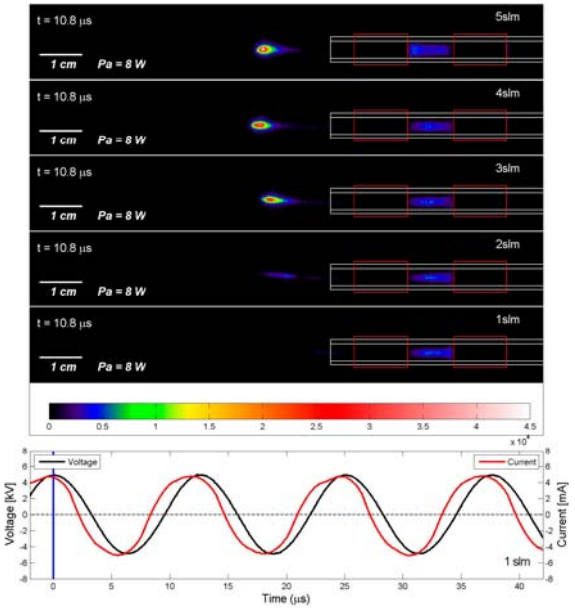

Figure 2. Plasma jet at 1, 2, 3, 4 and 5 slm. Exposure time 2 ms, gate width 25 ns, gate delay 10.8 µs. Obtained with wide electrodes.

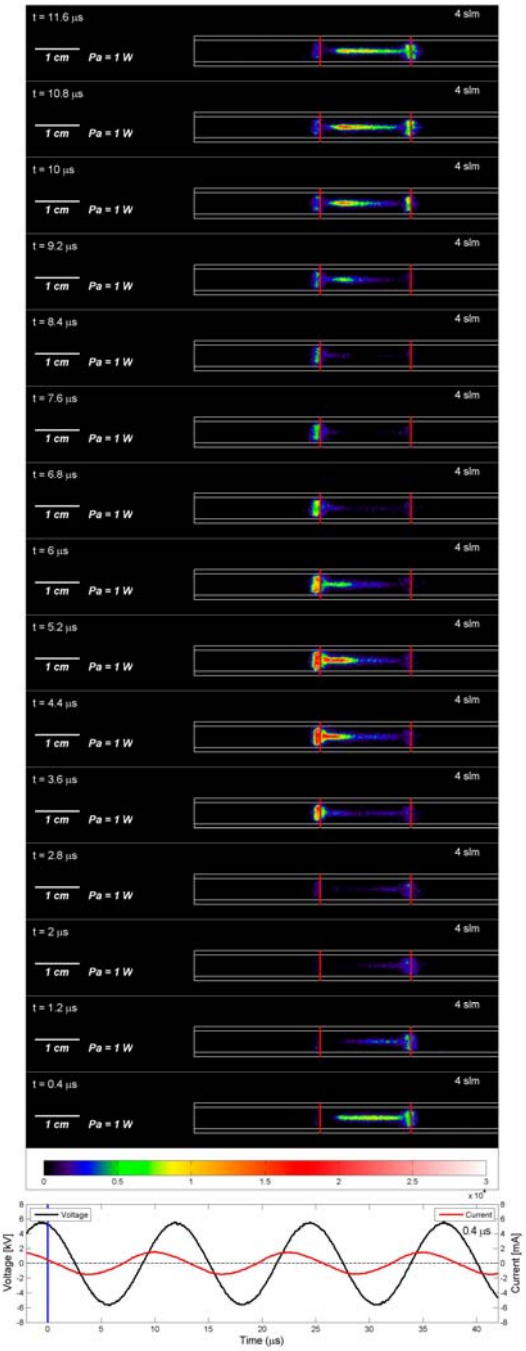

Figure 3. Plasma jet at 4 slm, exposure time 6 ms, gate width 25 ns and gate delay from 0 to 11.6 µs. Obtained with narrow electrodes.

We have used gate width of 25 ns and exposure times of 2 and 6 ms. Integration was done on the chip. As we can see plasma bullet was not formed for narrow electrodes and there was no plasma effluent even for the larges applied voltages. We have tried to move both electrodes closer to the end

of the glass tube, but in this case discharge was unstable and in some cases there was arcing between plasma and the closest electrode.

3. Conclusion

In this paper we have presented images of plasma bullet formation obtained by fast ICCD camera for two different sets of electrodes. In the case of copper wire electrodes bullet was not formed for any given sets of parameters.

For the copper foil electrodes the results show that our plasma source was not continuous, but it consisted of very small plasma packages that traveled at high speed. By varying the plasma parameters, the length and intensity of the plasma coming out of the tube can be adjusted.

Acknowledgements

This research has been supported by the MNTR, Serbia, under the contract numbers ON171037 and III41011.

4. References

[1] A. Fridman and L. A. Kennedy. Plasma Physics and Engineering, Taylor and Francis, 2004.

[2] F. Iza, G. J. Kim , S. M. Lee, J. K. Lee, J. L. Walsh, Y. T. Zhang and M. G. Kong, Plasma Process. Polym., 5 (2008) 322.

[3] E. Stoffels, A. J. Flikweert, W. W. Stoffels, and G. M. W. Kroesen, Plasma Sources Sci. Technol., 11 (2002) 383.

[4] N. Puač, Z.Lj. Petrović, G. Malović, A. Đorđević, S. Živković, Z. Giba and D. Grubišić, Journal of Physics D: Applied Physics, 39 (2006) 3514.

[5] Lu X and Laroussi M 2006 *J. Appl. Phys.* **100** 063302

[6] Shi J, Zhong F, Zhang J, Liu D W and Kong M G 2008 *Phys.Plasmas* **15** 013504

[7] Mericam-Bourdet N, Laroussi M, Begum A and Karakas E 2009 *J. Phys. D: Appl. Phys.* **42** 055207

Diagnostics and applications of high frequency discharges with focus on plasma treatment of human periodontal stem cells

Conference Paper · July 2013

READS
43

8 authors, including:

Slavko Mojsilović
University of Belgrade
59 PUBLICATIONS **298** CITATIONS
SEE PROFILE

Gordana Malovic
Institute of Physics Belgrade
157 PUBLICATIONS **932** CITATIONS
SEE PROFILE

Diana Bugarski
Institute for Medical Research - Belgrade
60 PUBLICATIONS **421** CITATIONS
SEE PROFILE

Zoran Lj Petrović
Institute of Physics Belgrade
510 PUBLICATIONS **5,652** CITATIONS
SEE PROFILE

Diagnostics and applications of high frequency discharges with focus on plasma treatment of human periodontal stem cells

N. Puač[1], D. Maletić[1], M. Miletić[2], S. Mojsilović[3], S. Lazović[1], G. Malović[1], D. Bugarski[3] and Z. Lj. Petrović[1]

[1] *Institute of Physics, University of Belgrade, Pregrevica 118, 11080 Zemun, Serbia*
[2] *Faculty of Dental Medicine, University of Belgrade, Serbia*
[3] *Institute for Medical Research, University of Belgrade, Serbia*

The non thermal atmospheric pressure plasmas are recently used for the treatment of the diverse thermo sensitive biological samples. Their design and diagnostics are of the key importance in obtaining desired effects on cells and tissues. Here we will present in more detail the influences of non-thermal atmospheric plasma on human mesenchymal stem cells isolated from periodontal ligament (hPDL-MSCs). The data regarding interaction of plasma with hPDL-MSCs demonstrated that plasma treatment of hPDL-MSCs does not affect their viability. Additionally, plasma significantly inhibited hPDL-MSCs proliferation, but promoted their osteogenic differentiation. The results of this study indicated that non-thermal plasma offers specific activity with non-destructive properties that can be advantageous for future dental application.

1. Introduction

Biomedical applications of the low temperature, non-thermal plasmas are at the moment the forefront of future technologies and the most active front of present day research [1-3]. The key feature that ensures this leading place of non-thermal plasmas is that it is possible to produce huge amount of chemically active species at low temperatures. If the gas composition is chosen properly, if applied fields are designed efficiently and appropriately, desired effects may be achieved while at the same time fulfilling the criteria of maintaining temperature of the background gas below 42°C [4]. Until now various types of plasma sources operating at atmospheric pressure were used for sterilization [5-7], wound healing and dermatology [6-8], cancer cell removal [9, 10] and even in dental application such as caries removal or tooth bleaching [11].

In our laboratory we have several atmospheric pressure non-equilibrium plasmas: plasma needle, micro atmospheric pressure plasma jet, plasma jet (operating in a plasma bullet mode) and corona. For all these plasma sources it was necessary to perform detailed diagnostics in order to efficiently use them in biomedical applications. The electrical properties were mainly obtained by using current and voltage probes. In case of MHz discharges homemade probes, capable of measuring powers below 1 W delivered to the plasma, were used. Time and spatial profiles of emission coming from the discharge were recorded by an ultra fast ICCD. Finally, we have employed two types of mass analyzers to determine chemical composition of plasma. One of the used systems is Hiden HPR60 mass-energy analyzer capable of sampling ions, neutrals and radicals originated in plasma. The other is Proton Transfer Mass Spectrometer (PTR-MS) which enabled us to detect non-fragmented molecules (VOCs) which were the result of plasma treatment of samples.

One of the plasma sources that we have extensively used in biomedical applications is plasma needle. In our previous work it was redesigned and improved [12, 13] to be suitable for interactions with living cells and tissues. In this paper we will present in more detail only the results of plasma needle treatment of human periodontal ligament mesenchymal stem cells.

To our knowledge, there are no reports on applications of non-thermal atmospheric plasma in periodontal therapy, and therefore in this study we aimed at investigating its influence on the periodontal tissue. Hence, the human periodontal ligament-derived mesenchymal stem cells (hPDL-MSCs) were isolated and characterized and the influence of non-thermal plasma on different cell functions, such as viability and proliferation was evaluated. Additionally, related to the potential application in periodontal therapy, we examined the capability of plasma to modulate the hPDL-MSCs differentiation toward osteogenic lineage.

2. Experimental set-up

We have used atmospheric pressure plasma source (plasma needle) for treatments of hPDL-M stem cells. This source was previously used in treatments of planctonic samples containing bacteria [14]. It consists of powered central electrode (tungsten wire) placed in ceramic tube, glass tube

and body of the plasma needle made of Teflon. The glass tube serves to convey flow of the feeding gas (helium) and plasma is created in the mixture of helium and gas components from the surrounding atmosphere that can diffuse into plasma and produce radicals such as atomic oxygen, nitrogen, nitrogen oxides and ozone [13]. The plasma needle is powered through signal generator (13.56 MHz), amplifier and matching box. Mean power is calculated from the calibrated derivative probe signals and in all experiments it serves as the main plasma parameter. In all treatments presented here power delivered to the plasma did not go above two watts. In a separate measurement these powers were shown not to generate an increase of temperature beyond 40^{o}C which would lead to thermal necrosis.

Normal impacted third molars were extracted for orthodontic purposes at the Department of Oral Surgery of the Faculty of Dental Medicine, University of Belgrade, according to the approved ethical guidelines set by the Ethics Committee of the Faculty of Dental Medicine, University of Belgrade. Human MSCs derived from the alveolar crestal and horizontal fibers of human periodontal ligament were characterized following the minimal criteria for defining MSCs [15].

The hPDL-MSCs were plated in triplicates in 96-well microtiter flat-bottomed plates with 200 µl of medium per well. The plasma needle was placed vertically above the microtiter plate in line with the upper edge of each well. The cells were treated using three different powers of plasma (0.15, 0.9, and 1.6 W), two flows of helium (0.5 and 1 slm) and four exposure times (10, 30, 60, and 120 s). We had two control groups in all experiments. Untreated samples were first control group and the samples treated only with helium flow (no plasma) were the second one.

After the treatment, viability of the cells was tested using 3-(4,5-dimethylthiazol-2-yl)-2,5-diphenyltetrazolium bromide (MTT) assay. After dyeing of the samples absorbance was measured at 540 nm by a spectrophotometer.

Proliferation assay consisted of detaching the cells on days 0, 2, 4, and 6 after the treatment and enumerating them by the Trypan blue exclusion test. After that the population doubling time (PDT) was determined. We measured the ALP (Alkaline phosphatase) activity in culture supernatants in order to show differentiation of the stems cells into the osteogenic line. To overcome the problem of unequal number of the cells per well, the absorbance values were normalized to the total amount of cellular proteins.

3. Results and discussion

The results of the MTT assay demonstrated that the non-thermal atmospheric-pressure plasma generated showed no significant effect on cell viability at all three tested powers as compared to both non-treated and the He-only-treated control cells (see Figure 1.). This finding regarding the effect on the MSCs viability is consistent with the results of our previous study, in which we showed that non-thermal plasma applied under the same conditions, was not cytotoxic for the peripheral blood-derived MSCs, although exhibited strong antibacterial effect [Lazovic].

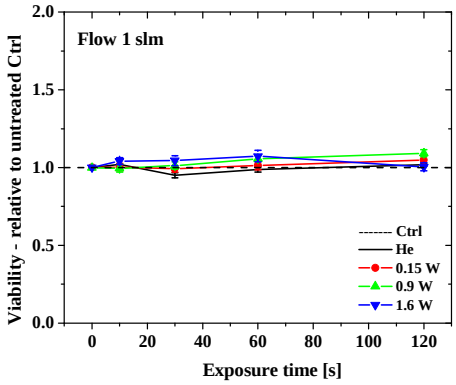

Figure 1. Effects of non-thermal plasma on viability of hPDL-MSCs. The viability test was performed using MTT assay.

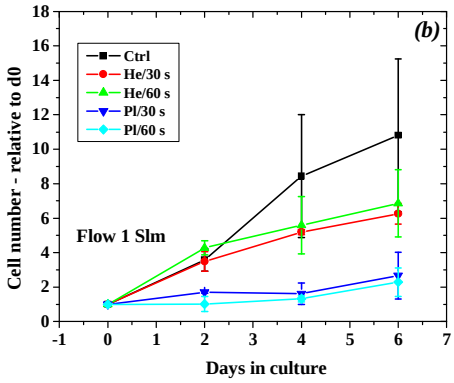

Figure 2. Effects of non-thermal plasma on hPDL-MSCs proliferation. After treatment with 1.6 W plasma (Pl) or gas only (He) for 30 s and 60 s, the cells were cultured for further 6 days and enumerated on days 0, 2, 4, and 6. Control cells were left untreated. The results are presented as mean number of cells ± SEM of three separate experiments.

In a control group untreated hPDL-MSCs exhibited high proliferation rate. At the day 6 after plating the number of these cells was increased more than 10-fold. However, after the same period of time, the cell population merely doubled in

plasma-treated cultures, disregarding the different gas flow or exposure time applied (Figure 2).

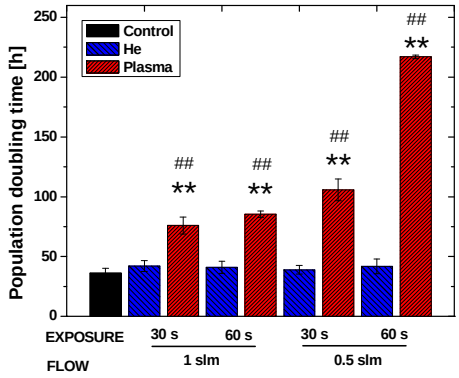

Figure 3. Population doubling time of hPDL-MSCs for the power of 1.6 W. The population doubling times are given as mean ± SEM of three separate experiments. Notation in figure is: ** p<0.01 compared to untreated control, ## p<0.01 compared to He-only control (Mann-Whitney's U-test).

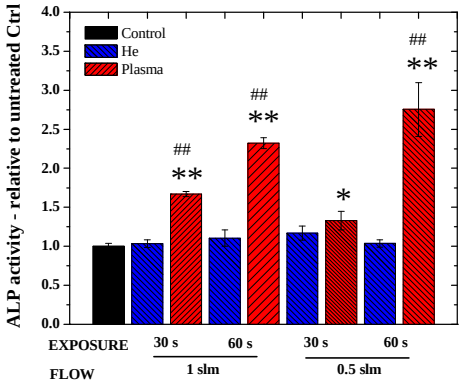

Figure 4. Alkaline phosphatase (ALP) activity of hPDL-MSCs after non-thermal plasma treatment. The ALP activity was measured in a 3-day condition medium of 1.6 W plasma-treated, He-only-treated and the non-treated cells after 10 days of culture in osteogenic medium. The results were normalized to the total cell protein concentration and presented as mean fold-change related to control cells ± SEM of three separate experiments. Notation in figure is: * p<0.05, ** p<0.01 compared to untreated control, ## p<0.01 compared to He-only control (Student's t-test).

When PDTs were calculated, the results confirmed that plasma treatment lead to significant delay in cell proliferation, as PDT values for plasma-treated hPDL-MSCs were significantly higher in comparison to non-treated controls (Figure 3). Although the cells treated by He-only did show somewhat slower proliferation, the PDTs for these cells were not significantly prolonged, as compared to non-treated hPDL-MSCs.

In order to analyze the effect of non-thermal plasma on hPDL-MSCs differentiation potential, we measured the activity of ALP in cell culture supernatants. The results demonstrated that plasma treatment increased the osteogenic potential of hPDL-MSCs, since for all experimental conditions applied significant enhancement in the ALP activity was observed in plasma-treated cells, as compared to non-treated cells (Figure 4). Moreover, He flow without plasma ignition did not significantly alter the ALP activity in the analyzed samples.

3. Conclusion

The results presented here demonstrated that the treatment of the hPDL-MSCs with our plasma needle device significantly decreased their proliferation. Interestingly, under the same conditions, plasma treatment induced significant increase in the ALP activity in these cells. Since ALP is known as an early marker for osteoblastic differentiation, this finding suggests that plasma treatment can enhance osteogenic differentiation of the hPDL-MSCs. Moreover, as the differentiation process is a sequential event that follows attenuated cell proliferation, we can suppose that the plasma-induced decrease in the rate of cell growth resulted in the increasing level of differentiation. Although more extensive studies are required to investigate the mechanisms associated with the plasma-mediated osteogenic differentiation of hPDL-MSCs, these results point to new possible applications of low-temperature plasmas at atmospheric pressure and provide new insights into the establishment of cell-based therapeutic strategy for periodontal defects.

Acknowledgements This study was supported by Grant No ON171037, III 41011 and ON175062, Ministry of Education and Science, Republic of Serbia.

4. References

[1] M. A. Lieberman, A. J. Lichtenberg, Principles of Plasma Discharge and Materials Processing.Wiley Place (2005)

[2] T. Makabe, Z. L. Petrović, Plasma electronics: applications in microelectronic device fabrication.Taylor and Francis Place (2006)

[3] M. G. Kong, G. Kroesen, G. Morfill, T. Nosenko, T. Shimizu, J. Van Dijk, J. L. Zimmermann, New J. Phys. **11** (2009) 115012

[4] Z. L. Petrović, N. Puač, S. Lazović, D. Maletić, K. Spasić, G. Malović, Journal of Physics: Conference Series **356** (2012) 012001

[5] G. E. Morfill, T. Shimizu, B. Steffes and H-U. Schmidt, New J. Phys. **11** (2009) 115019–115029

[6] J. Heinlin, G. Isbary, W. Stolz, G. Morfill, M. Landthaler, T. Shimizu, B. Steffes, T. Nosenko, J. L. Zimmermann and S. Karrer, J. Eur. Acad. Dermatol. Venereol **25** (2011)1–11

[7] G. Lloyd, G. Friedman, S. Jafri, G. Schultz, A. Fridman and K. Harding, Plasma Process. Polym **7** (2010) 194–211

[8] T. Nosenko, T. Shimizu and G. E. Morfill, New J. Phys. **11 (**2009) 115013–115032

[9] M. Vandamme, E. Robert, S. Dozias, J. Sobilo, S. Lerondel, A. Le Pape and J-M. Pouvesle, Plasma Medicine, **1** (2011) 27–43

[10] G. Fridman, A. Shereshevsky, M. M. Jost, A. D. Brooks, A. Fridman, A. Gutsol, V. Vasilets and G. Friedman, Plasma Chem. Plasma Process. **27** (2007) 163 -176

[11] H. W. Lee, G. J. Kim, J. M. Kim, J. K. Park, J. K. Lee and G. C. Kim, J. Endodont. **35** (2009) 587–591

[12] N. Puač, Z. Petrović, G. Malović, A. Đorđević, S. Živković, Z. Giba and D. Grubišić, J. Phys. D: App. Phys. **39 (**2006) 3514-3519

[13] G. Malović, N. Puač, S. Lazović and Z.Lj. Petrović, Plasma Sources Sci. Technol. **19 (**2010) 034014

[14] S. Lazović, N. Puač, M. Miletić, D. Pavlica, M. Jovanović, D. Bugarski, S. Mojsilović, D. Maletić, G. Malović, P. Milenković and Z.Lj. Petrović, New J. Phys. **12** (2010) 083037

[15] M. Dominici, K. Le Blanc, I. Mueller, I. Slaper-Cortenbach, F. Marini, D. Krause, R. Deans, A. Keating, D.J. Prockop and E. Horwitz Cytotherapy **8** (2006) 315-317

Mass analysis of atmospheric pressure discharges

Conference Paper · July 2009

READS
10

4 authors:

Gordana Malovic
Institute of Physics Belgrade
157 PUBLICATIONS **932** CITATIONS
SEE PROFILE

Nevena Puač
Institute of Physics Belgrade
98 PUBLICATIONS **390** CITATIONS
SEE PROFILE

Saša Lazović
Institute of Physics Belgrade
70 PUBLICATIONS **212** CITATIONS
SEE PROFILE

Dejan Maletic
Institute of Physics Belgrade
53 PUBLICATIONS **97** CITATIONS
SEE PROFILE

XXIX
INTERNATIONAL CONFERENCE ON PHENOMENA IN IONIZED GASES

Cancún, México

12-17 July, 2009

Sponsored by

International Union of Pure and Applied Physics
Universidad Nacional Autónoma de México
Universidad Autónoma Metropolitana
Universidad Autónoma Metropolitana-A
Institute of Physics Publishing
Instituto de Ciencias Físicas, UNAM
Consejo Mexiquense de Ciencia y Tecnología
Instituto de Ciencia y Tecnología del Distrito Federal
Wiley VCH
Aeroméxico

BOOK OF ABSTRACTS

J. de Urquijo, Editor
Logo by Carolina de Urquijo-Isoard

The ICPIG 2009 Book of Abstracts is intended to provide the participants a quick guide to the subject matters of all *Invited General, Topical, and Prize lectures*, as well as all to all the *Contributed Papers* presented in this conference in poster form.

We hope this book of abstracts will also be a useful piece of timely information for all scientists and engineers working or interested in the topics covered by the ICPIG 2009.

HINT: Browsing this book is very easy with the SEARCH TOOL of Adobe Acrobat

GENERAL INDEX*

* This Index can also be found preceding the List of Authors on page 127

Thanks are due to Carolina and Javier de Urquijo-Isoard for their help in assembling the list of authors.

power generator. Hydrodynamic simulations showed that using relatively moderate pulsed power generators with stored energy of several hundreds of kJ, the pressure of several Mbar can be achieved at the axis of implosion.

TB-1

Mass analysis of atmospheric pressure discharges

G. Malović, N. Puač, S. Lazović, D. Maletić

[1]*Institute of Physics, P.O. Box 68, 11080, Belgrade, Serbia*

malovic@phy.bg.ac.yu

There has been and increased interest in atmospheric pressure discharges, as they provide advantages of non-equilibrium low temperature plasmas at the atmospheric pressure which may be used in many practical applications such as material processing, surface treatment, and chemical and biological agent destruction without the need for the expensive and complicated vacuum systems. In particular these discharges open a possibility for medical applications. In this paper we show results of different diagnostic techniques applied to such discharges, above all measurements of the composition of neutral radicals and complex molecules and also of ions and their energy distribution. For that purpose we have applied three stage pumping system with mass-energy analyzer manufactured by Hiden HPR 60.

The first plasma source that was studied was the plasma needle [1]. While similar work of Stoffels et al. [2] has been done on a similar system in their papers they had to use larger dimensions and flow because pumping of the mass analyzer perturbed and even turned off the discharge [3]. These authors found that atmospheric plasma operated in air and helium is a good source of active oxygen and nitrogen radicals. This could explain the efficiency of such plasma in (among others) bacterial inactivation.

Our measurements were performed on a standard size plasma needle. After some efforts the mass analyzer could be operated under conditions that would not greatly affect the discharge itself. However, we had to increase the gas flow from several 100 sccm to more than 1000 sccm. We have detected radicals produced in plasma (NO, N_2O etc.) as well as ions (N^+, O^+, NO^+ etc) and we could follow the changes in composition with variation of plasma parameters and changing regimes of operation.

We have also performed measurements in Atmospheric pressure plasma jet (μ-APPJ) developed by Schulz-von der Gathen and coworkers [4]. The μ-APPJ is homogenous non-equilibrium rf discharge at the ambient pressure. Measurements were performed for the flow of pure He and 0.5% O_2 in He. Discharge volume was about 1x1x30 mm^2 and this allows detailed investigations of the discharge dynamics from the discharge to the effluent [5]. In both cases we have applied derivative probes to control the power (current and voltage) deposited to plasma.

.

1. N. Puač, Z.Lj. Petrović, G. Malović, A. Đorđević, S. Živković, Z. Giba and D. Grubišić, J.of Phys.D: Appl. Phys. **39** 3514 (2006).
2. E. Stoffels, A J Flikweert, W W . Stoffels and G M W .Kroesen, Plasma Sources Sci. Technol. **11** p 383 (2002).
3. E. Stoffels, Y .Aranda Gonzalvo, T D .Whitmore, D L .Seymour , J A .Rees, Plasma Sources Sci. Technol. **16** p 549 (2007).

4. K. Niemi, St. Reuter, L. Schaper, N. Knake, V. Schulz-von der Gathen, T. Gans, Journal of Physics: Conference Series **71** 012012 (2007).
5. V. Schulz-von der Gathen, V. Buck, T. Gans, N. Knake, K. Niemi, St. Reuter, L. Schaper, and J.Winter, Contrib. Plasma Phys. **47**, No. 7, 510 (2007).

TB-2

Plasma-assisted conversion of greenhouse gases

S. Paulussen[1], B. Verheyde[1], X. Tu[2], C. De Bie[3], T. Martens[3], D. Petrovic[3], A. Bogaerts[3], B. Sels[2]

[1]*VITO, Vlaamse Instelling voor Technologisch Onderzoek, Materials Technology, Boeretang 200, B-2400 Mol, Belgium*
[2] *Center for Surface Chemistry and Catalysis, Katholieke Universiteit Leuven, Kasteelpark Arenberg 23, B-3001 Heverlee, Belgium*
[2] *University of Antwerp, Research Group PLASMANT, Universiteitsplein 1, B-2600 Wilrijk Belgium*
sabine.paulussen@vito.be

The catalytic conversion of methane to more useful chemicals is generally renowned as a challenge for the 21st century. Today, methane is a greatly underutilized resource for chemicals and liquid fuels, mainly because it is one of the most stable molecules. Direct synthesis of hydrocarbons starting from methane is not feasible and the conventional indirect methods for partial or total oxidation of methane have poor yields and require high amounts of energy. It is clear that a process which circumvents the energy intensive syngas step would offer a distinct economic advantage. The enormous reserves of natural gas worldwide, even rivalling those of petroleum make from natural gas an interesting alternative for crude oil as a feedstock for the chemical industry in the near future, providing methane can be converted in an economical and environment friendly way. In addition, methane of relatively high purity is burned or released in the atmosphere during the production of liquid petroleum and therefore conversion of this greenhouse gas would represent significant benefits, both economically and with respect to sustainability.
In this work, atmospheric pressure, low temperature dielectric barrier discharges are evaluated for the selective conversion of methane to base chemicals like methanol, formaldehyde and syngas. Greenhouse gases like CO_2 or N_2O, and environment friendly oxidants like O_2 or H_2O are applied as co-reagent. It is clear that plasma processes offer a unique way to induce gas phase reactions at significantly lower temperatures compared to classical catalytic processes, although the yield and selectivity obtained so far in the plasma-assisted conversion of methane are relatively low. Catalytic processes on the other hand can be very selective, but often require a certain gas composition and a sufficiently high temperature. By combining both heterogeneous catalysts and atmospheric plasma processing, a synergistic effect is aimed at. For example, the conversion of CH_4 and CO_2 to CO and H_2 (syngas) below a temperature of 400 °C is negligible in a classical catalytic process. In contrast to this, conversions as high as 40 % can be achieved in a dielectric barrier discharge configuration at temperatures below 100 °C, in the absence of a catalyst. By comparing different reaction conditions, both with and without a heterogeneous catalyst, the possibility of shifting a thermodynamic equilibrium by applying a dielectric barrier discharge is evaluated. The partial oxidation of methane to methanol by using O_2 as an oxidant in a dielectric barrier discharge is studied to determine the effect of an atmospheric plasma on the initiation of classical radical chemistry at low temperature.
Plasma parameters like frequency, applied voltage, power input and reactor geometry are evaluated as well as the effect of a catalyst on the discharge properties.

Plasma needle treatments of the human peripheral blood-derived multipotent mesenchymal stem cells (hPB-MSC)

Conference Paper · March 2010

READS
26

9 authors, including:

Gordana Malovic
Institute of Physics Belgrade
157 PUBLICATIONS **932** CITATIONS
SEE PROFILE

Diana Bugarski
Institute for Medical Research - Belgrade
60 PUBLICATIONS **421** CITATIONS
SEE PROFILE

Slavko Mojsilović
University of Belgrade
59 PUBLICATIONS **298** CITATIONS
SEE PROFILE

Zoran Lj Petrović
Institute of Physics Belgrade
510 PUBLICATIONS **5,652** CITATIONS
SEE PROFILE

IC-PLANTS 2010

The 3rd International Conference on PLAsma-NanoTechnology & Science

March 11-12, 2010
Meijo University, Nagoya, Japan

Sponsored by
Plasma Nanotechnology Research Center (PLANT), Nagoya University

Co-Sponsored by
Meijo University
Aichi Science and Technology Foundation (Tokai Region Knowledge Cluster Headquarters)
International Training Program, Japan Society for the Promotion of Science

Supported by
Scientific Research on Innovative Areas "Frontier science of interactions between plasmas and nano-interfaces"
Tokai division of the Japan Society of Applied Physics
Tokai Branch of the Institute of Electrical Engineers of Japan
Plasma Electronics Division, the Japan Society of Applied Physics
Plasma Center for Industrial Applications, Nagoya Urban Industrial Promotion Corporation
The Surface Science Society of Japan
Japan Vacuum Industry Association

The 3rd International Conference on PLAsma NanoTechnology & Science (IC-PLANTS 2010)

March 11-12, 2010

Meijo University, Nagoya, Japan

Sponsored by

- **Plasma Nanotechnology Research Center (PLANT), Nagoya University**

Co-Sponsored by

- **Meijo University**
- **Aichi Science and Technology Foundation (Tokai Region Knowledge Cluster Headquarters)**
- **International Training Program, Japan Society for the Promotion of Science**

Supported by

- **Scientific Research on Innovative Areas "Frontier science of interactions between plasmas and nano-interfaces"**
- **Tokai division of the Japan Society of Applied Physics**
- **Tokai Branch of the Institute of Electrical Engineers of Japan**
- **Plasma Electronics Division, the Japan Society of Applied Physics**
- **Plasma Center for Industrial Applications, Nagoya Urban Industrial Promotion Corporation**
- **The Surface Science Society of Japan**
- **Japan Vacuum Industry Association**

Coffee Break (15:05-15:25)

Contributed Talks 1 (15:25-16:45)

15:25 O-01 **Bacterial inactivation using atmospheric pressure capillary tube based micro-plasma system with hollow inner electrode**
C.-C. Weng[1], T.-Y. Lin[1], H.-H. Chen[1], J.-D. Liao[1], C.-C. Ho[2], and Y.-T. Ho[2]
[1]National Cheng Kung University, Taiwan, [2]Taiwan Plasma Corp., Taiwan

15:45 O-02 **Plasma needle treatments of the human peripheral blood-derived multipotent mesenchymal stem cells (hPB-MSC)**
S. Lazović[1], N. Puač[1], M. Miletić[2], D. Maletić[1], G. Malović[1], D. Bugarski[3], S. Mojsilović[3], P. Milenković[2], and Z. Lj. Petrović[1]
[1]Institute of Physics, Serbia, [2]Faculty of Stomatology, Serbia, [3]Institute for the Medical Research, Serbia

16:05 O-03 **Computer simulation of 3C-SiC powder production at initial stage of nucleation**
A. Bondareva, and G. Zmievskaya
M.V. Keldysh institute of applied mathematics of Russian Academy of Sciences, Russia

16:25 O-04 **Raman and AFM studies of fabricated Graphitic Carbon Nanostructures on n-Si <111> With Extremely Non-Equilibrium Plasma conditions**
Y. Malhotra, S. Roy, and M.P. Srivastava
University of Delhi, India

Poster Session (17:00-18:40)

P-01 **In-situ growth of a single nano needle on a metal whisker induced by periodically scanning electron beam and its field emission property**
B. Liang, C. Chen, A. Ogino, and M. Nagatsu
Shizuoka University, Japan

P-02 **Non-isothermal Growth of Carbon Nanotubes**
F.-L. Lu, W.-Y. Chen, and J.-M. Ting
National Cheng Kung University, Taiwan

P-03 **Synthesis and Fabrication of Functional Nanomaterials**
J. Hahm
Penn State University, USA

Plasma needle treatments of the human peripheral blood-derived multipotent mesenchymal stem cells (hPB-MSC)

S. Lazović[1], N. Puač[1], M[1] Miletić[2], D. Maletić[1], G. Malović[1], D. Bugarski[3], S. Mojsilović[3], P. Milenković[2] and Z. Lj. Petrović[1]

[1] *Institute of Physics, Pregrevica 118, 11080 Belgrade, Serbia*

[2] *Faculty of Stomatology, Dr Subotića 8, 11000 Belgrade, Serbia*

[3] *Institute for the Medical Research, Dr Subotića - starijeg 4, 11000 Belgrade, Serbia*

Email: lazovic@ipb.ac.rs

1 Introduction

There are many types of plasmas that can be generated under ambient pressure and temperature conditions, the need for precise and localized treatments qualifies plasma needle to be a good match [1]. Because of its mild plasma, low gas temperature and geometry, the plasma needle is especially convenient for medical applications. This device can be used for non-contact disinfection of dental cavities and wounds, minimum-destructive precise treatment, as well as the removal of damaged tissue. Our measurements were performed on a standard size plasma needle that we originally used for the treatment of plant cells [2].

In this paper we will present results of plasma needle treatments on the human peripheral blood-derived multipotent mesenchymal stem cells (hPB-MSC) (fibroblast cells). We have treated cells in two conditions, i.e. with and without liquid environment (suspension). Results from the MTT viability and Crystal Violet adhesion tests performed with the hPB-MSC will be presented. These results represent the first step of the route of developing, optimizing, understanding and using plasma needle for the *in-vivo* treatment of periodontal pockets.

2 Experimetal setup

Non-equilibrium plasma generated by a plasma needle was used for treatment of cells. The cells used in the experiments for cell toxicity were hPB-MSC obtained from a healthy volunteer. Human MSC were isolated from mononuclear peripheral blood cells, using methodology described by Kuznetsov et al. [3] and characterized as plastic adherent cells that display fibroblastic morphology.

The needle consists of the central electrode made of wolfram 0.5 mm in diameter covered almost to the tip by slightly larger ceramic tube and both placed into the glass tube with 6 mm inside diameter. Needle body is made of Teflon. Helium is flowing between ceramic and glass tubes. We have used flow rates of 0.5 slm and 1 slm (standard liters per minute). Central electrode is powered by 13.56 MHz signal generator (Agilent N9310A) through amplifier (Barthel RFA-0.1/50-100 B00) and matching network. Grounded electrode was copper foil placed beneath the plastic plate. After the treatments, MSC viability and adhesion were tested using the MTT and Crystal Violet assays, respectivelly

3 Results and discussion

The results of the viability tests (MTT) performed are presented in Fig. 1. for cells covered with 100 µl of medium and in Fig 2. for directly exposed cells. From the Fig 1. and from photographs of the wells, in which the cells were covered with 100 µl of medium, after plasma treatment and MTT test coloring, we could notice that more cells were dead with the increase of the applied power and treatment time. Control sample with only He flow shows no changes at all.

On the other hand, when cells were directly exposed (see Fig. 2.) we can see that with increasing of the power and the treatment time a drastic change in viability percentage occurs. Again He flow control was done and with the increase in treatment time more cell were destroyed even if no plasma was ignited.

4 Conclusion

For human hPB-MSC measurements were made when the cells were covered with medium, as well as when the cells were without medium. In the case of direct cell exposure, without medium cover, some small effect of plasma was observable, but its impact was diminished in the context of the desiccation caused by the gas flow. When the cells were covered by medium, gas flow did not affect the results, and the effect of plasma was more obvious.

As far as plasma goes some further optimization may be made for localized accurate treatment of cells or sterilization. Further work needs to be done in achieving optimal operation and uniformity over large areas. With good knowledge of the power deposited into the plasma, and control of radicals that are produced together

with spatial emission profiles indicating changing of the regime of operation sufficient control of reproducibility of plasma needle operation is achieved. Other sources may be sought for more refined and localized interaction with the living cells.

[1] E. Stoffels, A. J. Flikweert, W. W. Stoffels, and G. M. W. Kroesen, Plasma Sources Sci. Technol., **11**(4), 383 (2002)

[2] N. Puač, Z.Lj. Petrović, G. Malović, A. Đorđević, S. Živković, Z. Giba and D. Grubišić, Journal of Physics D: Applied Physics, **39**, 3514 (2006)

[3] S.A. Kuznetsov, M.H. Mankani, S. Gronthos, K. Satomura, P. Bianco, P.G. Robey, J Cell Biol., 153, 1133 (2001)

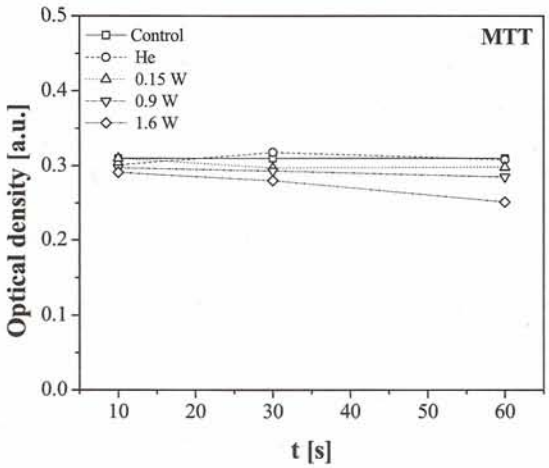

Fig. 1 Optical densities of treated cells covered by 100 µl of medium obtained by spectrophotometer at 540 nm after (MTT test).

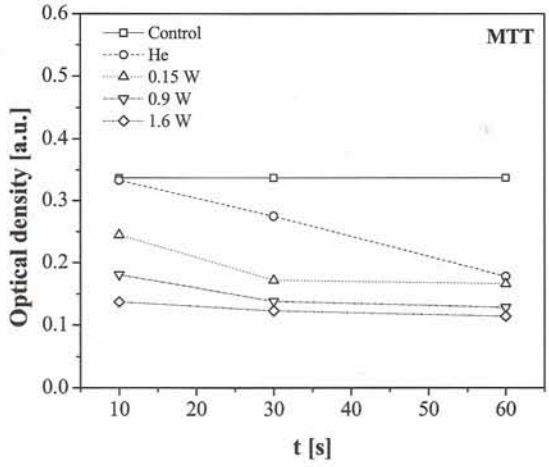

Fig. 2 Optical densities of directly treated cells obtained by spectrophotometer at 540 nm (MTT tests).

IC-PLANTS 2010 Time Table

Thursday, March 11

8	45		Registration
9	20		Opening remarks
	30	I-1	**Kiyoshi Yasutake** (Osaka University, Japan) *New formation process of solar-grade Si from metallurgical-grade Si by chemical transport in near atmospheric-pressure hydrogen plasma*
10	05	I-2	**Bill Graham** (Queen's University, Belfast, UK) *PLASMAS IN LIQUIDS AND THEIR APPLICATIONS*
	40		Coffee break
11	00	I-3	**Olivier Joubert** (LTM-CNRS, France) *Future prospects in plasma etching*
	35	I-4	**Kostya Ostrikov** (CSIRO Materials Science and Engineering and University of Sydney, Australia) *Plasma nanoscience: synergies and opportunities*
12	10		Lunch
13	20	I-5	**Michael Kong** (Loughborough University, UK) *Plasma Biology: What happens when cells meet plasma molecules?*
14	55	I-6	**Yoshinobu Baba** (Nagoya University, Japan) *Nanobiodevice from Single Biomolecule and Cell Analysis to Biomedical Applications*
	30	I-7	**Alexander Fridman** (Drexel University, USA) *PLASMA MEDICINE*
15	05		Coffee break
	25	O-1	**C.-C. Weng, J.-D. Liao** (National Cheng Kung University, Taiwan) *Bacterial inactivation using atmospheric pressure capillary tube based micro-plasma system with hollow inner electrode*
	45	O-2	**Zoran Lj. Petrović, S. Lazović, N. Puač, M. Miletić, D. Maletić, G. Malović, D. Bugarski, S. Mojsilović, P. Milenković** (Institute of Physics, Serbia) *Plasma needle treatments of the human peripheral blood-derived multipotent mesenchymal stem cells (hPB-MSC)*
16	05	O-3	**A. Bondareva, G. Zmievskaya** (M.V. Keldysh institute of applied mathematics of Russian Academy of Sciences, Russia) *Computer simulation of 3C-SiC powder production at initial stage of nucleation*
	25	O-4	**M.P. Srivastava, Yashi Malhotra** (University of Delhi, India) *Raman and AFM studies of fabricated Graphitic Carbon Nanostructures on n-Si <111> With Extremely Non-Equilibrium Plasma conditions*
	45		Break
17:00 ~ 18:40			Poster Session

19:00 ~ 20:30 Banquet

Friday, March 12

8	30		Registration
9	00	S-1	**Masaharu Shiratani** (Kyushu University, Japan) *Frontier science of interactions between plasmas and nano-interfaces*
	30	S-2	**Kazuo Terashima, Sven Stauss** (The University of Tokyo, Japan) *Nano-interface plasmas generated in supercritical fluids and their application to nanomaterials processing*
10	00	S-3	**Tatsuru Shirafuji** (Nagoya University, Japan) *Plasmas Involving Liquid Media, and Their Applications*
	30		Coffee break
11	50	S-4	**Koichi Sasaki** (Nagoya University, Japan) *Physical control of plasma and cavitation bubble in liquid-phase laser ablation*
	20	S-5	**Fumiyoshi Tochikubo** (Tokyo Metropolitan University, Japan) *Atmospheric Glow Discharges with Liquid Electrode – Toward Understanding of Plasma-Liquid Interface –*
12	50		Lunch
13	00	I-8	**Pascal Chabert** (Ecole Polytechnique, France) *Modelling of chlorine inductive discharges*
	35	I-9	**Nae Eung Lee** (Sungkyunkwan University, Korea) *Plasma functionalized carbon nanomaterials for nanocomposite bio-scaffolds and cell viability effects*
14	10	O-5	**W.E.N. van Harskamp, O. Gabriel, D.C. Schram, M.C.M. van de Sanden, R. Engeln** (Eindhoven University of Technology, The Netherlands) *Population inversion in a magnetized thermal plasma investigated by active and passive spectroscopy*
	30	O-6	**David Z. Pai, Gabi D. Stancu, Farah Kaddouri, Deanna A. Lacoste, Christophe O. Laux** (Ecole Centrale Paris, France) *Ultrafast heating in air at atmospheric pressure for nanotechnology applications*
	50	O-7	**Lukas Hoferek, Rutul Trivedi, Jan Mistrik, Vladimir Cech** (Brno University of Technology, Czech Republic) *Anisotropic film construction using plasma nanotechnology (atomic polymerization)*
15	10		Coffee break
	30	I-10	**Uros Cvelbar** (Jozef Stefan Institute, Slovenia) *Tailoring nanostructures with low-temperature plasmas*
16	05	I-11	**Rod Boswell** (Australian National University, Australia) *Focused Inert Ion Beam systems for 3D rock tomography on the nano-scale*
	40	I-12	**Jin-Hyo Boo** (Sungkyunkwan University, Korea) *ZnO nano-materials: Synthesis, Characteristic, and Application*
17	15	I-13	**Hiroshi Amano** (Meijo University, Japan) *With the aim of establishing low-cost fabrication technology for high-performance nitride-based light emitters*
	50		Closing remarks

Invited talk : 25 min. presentation, 10 min. discussions,
Special session : 25 min. talk, 5 min. discussions,
Contributed talk : 15-min. presentation, 5 min. discussions

3rd International Conference on Plasma Medicine (ICPM-3)

19th-24th September 2010

ERNST MORITZ ARNDT
UNIVERSITÄT GREIFSWALD

Wissen
lockt.
Seit 1456

INP
Greifswald

BOOK OF ABSTRACTS

ISPM
INTERNATIONAL SOCIETY
FOR•PLASMA•MEDICINE

INTERNATIONAL SOCIETY
FOR•PLASMA•MEDICINE

BOOK OF ABSTRACTS

3rd International Conference for Plasma Medicine (ICPM-3)

19th-24th September 2010

INP Greifswald

Leibniz Institute for Plasma Science and Technology (INP Greifswald)

ERNST MORITZ ARNDT UNIVERSITÄT GREIFSWALD

Ernst-Moritz-Arndt-University Greifswald (IfP)

Editor: Prof K.-D. Weltmann

Supported by:

DOT

neoplas

Sparkasse - Vorpommern

International Scientific Committee (ISC)

Prof David B. Graves
Berkley, USA
Prof Pietro Favia
Bari, Italy
Prof Alexander Fridman
Philadelphia, USA
Prof Gary Friedman
Philadelphia, USA
Prof Satoshi Hamaguchi
Osaka, Japan
Prof Mounir Laroussi
Norfolk, USA
Prof Jae Koo Lee
Pohang, Rep. Korea
Prof Michel Moisan
Montreal, Kanada
Prof Gregor Morfill
Garching, Germany
Prof Jean-Michel Pouvesle
Orleans, France
Prof Richard Satava
Seattle, USA
Prof Victor Vasilets
Moscow, Russia
Dr Thomas v. Woedtke
Greifswald, Germany
Prof Klaus-Dieter Weltmann
Greifswald, Germany
Prof (emer.) Michael Wertheimer
Montreal, Canada

Management Board ISPM

(International Society for Plasma Medicine)

Dr Alexander Dolgopolsky
Prof Alexander Fridman
Prof Gary Friedman
Prof Klaus-Dieter Weltmann

Local Organizing Committee

Prof Klaus-Dieter Weltmann
Prof Michael Juenger
Prof Thomas Kocher
Prof Ulrike Lindequist
Prof Juergen Meichsner
Dr Thomas v. Woedtke

Secretariat and Support Staff

Nadja Dahlhaus, Anne Paepke (Secretary)
Cornelia Krcka (Finance and Registration Secretary)

Sterilization of bacteria containing liquids and biofilms

[1] Saša S Lazović, [1] Nevena Puač, [2] Maja Miletić, [1] Dejan Maletić, [2] Milena Jovanović, [2] Dušan Pavlica, [2] Dragana Vuković, [1] Gordana Malović, [2] Pavle Milenković, [1] Zoran Lj Petrović

[1] Intitute of Physics Belgrade, Serbia and Montenegro: lazovic@ipb.ac.rs, nevena@ipb.ac.rs, majamilet@eunet.rs, dejan.maletic@ipb.ac.rs, gordana.malovic@ipb.ac.rs, zoran@ipb.ac.rs

[2] Faculty of Stomatology Belgrade, Serbia and Montenegro: majamilet@eunet.rs

To investigate possible applications of plasma needle in biomedicine we performed experiments studying effects of plasma needle on different species of bacteria in a planctonic form and staphylococcus aureus biofilms. In this study standard strains of four species were used: Staphylococcus aureus (ATCC 25923), Escherichia coli (ATCC 25922), Pseudomonas aurigi-nosa (ATCC 27853) and Enterococcus faecalis (ATCC 29212) in order to study deactivation of harmful bacte-ria. Possible plasma needle application in treatments of light bacterial infections, such as in-vivo sterilization of skin and dental cavities was our main motivation. Most importantly the study is made to see the effects when the living cells are in liquid medium which nor-mally acts as a protection against many agents that may be released by plasmas. It was found that a goods effect may be expected for a wide range of initial cell densities and operating conditions giving destruction of several orders of magnitude even under protection of a liquid. It was established independently that tem-perature increase did not affect the cells under condi-tions of our experiment so the effect could only origi-nate from the active species produced by the plasma. Further optimization of the operation may be sought opening a possibility of a localized in-vivo sterilization.

Bactericidal Efficiency of Ag Nanoparticles Deposited onto RF Plasma Pre-treated Polyester Fabrics

Article *in* Industrial & Engineering Chemistry Research · January 2010

Impact Factor: 2.59

7 authors, including:

Zoran Saponjic
Vinča Institute of Nuclear Sciences
79 PUBLICATIONS **935** CITATIONS
SEE PROFILE

Vesna V Vodnik
Vinča Institute of Nuclear Sciences
79 PUBLICATIONS **696** CITATIONS
SEE PROFILE

Suzana I, Dimitrijevic-Brankovic
University of Belgrade
103 PUBLICATIONS **1,043** CITATIONS
SEE PROFILE

Maja Radetić
University of Belgrade
89 PUBLICATIONS **1,083** CITATIONS
SEE PROFILE

Bactericidal Efficiency of Silver Nanoparticles Deposited onto Radio Frequency Plasma Pretreated Polyester Fabrics

Vesna Ilić,[†] Zoran Šaponjić,[‡] Vesna Vodnik,[‡] Saša Lazović,[§] Suzana Dimitrijević,[||] Petar Jovančić,[†] Jovan M. Nedeljković,[‡] and Maja Radetić*,[†]

Textile Engineering Department, Faculty of Technology and Metallurgy, University of Belgrade, Karnegijeva 4, 11120 Belgrade, Serbia, Vinča Institute of Nuclear Sciences, P. O. Box 522, 11001 Belgrade, Serbia, Institute of Physics, Pregrevica 118, 11080 Zemun, Serbia, and Department of Bioengineering and Biotechnology, Faculty of Technology and Metallurgy, University of Belgrade, Karnegijeva 4, 11120 Belgrade, Serbia

The potential application of low-temperature radio frequency (RF) plasma for fiber surface activation in order to enhance the binding efficiency of colloidal silver nanoparticles onto the polyester fabrics and improve the stability of antibacterial effects was studied. Antibacterial activity and laundering durability were tested against gram-negative bacterium *Escherichia coli* and gram-positive bacterium *Staphylococcus aureus.* Plasma treatment positively affected the loading of silver nanoparticles as well as antibacterial activity and laundering durability of these textile nanocomposite materials. In spite of good laundering durability after five washing cycles, it was found that silver leached from the fabric into the bath during washing. Released silver from the washing effluent was efficiently removed by recycled wool-based nonwoven sorbent modified with hydrogen peroxide and biopolymer alginate.

1. Introduction

Textile materials have been recognized as media that can easily support the growth of different microbes.[1] Hence, the growing production of advanced medical, protective, and hygiene textiles requires efficient antimicrobial finishing. A wide range of antimicrobial agents have been employed so far in the antimicrobial finishing of textile materials: metals and metal compounds, quaternary ammonium salts, poly(hexamethylene biguanide), triclosan, chitosan, dyes, regenerable *N*-halamine compounds, and peroxyacids.[1] Relatively poor efficiency and/or high toxicity made most of them unsuitable for long-term use. However, silver in different forms exhibits outstanding antimicrobial activity with low toxic impact to mammalian cells.[2] It is a powerful biocide for more than 650 various microbes.[3] In particular silver nitrate has been widely used as an antimicrobial agent.[4,5] Despite its excellent antimicrobial properties, silver nitrate is not convenient for the treatment of textile materials as it stains to black-brown when exposed to air and light, due to uncontrolled reduction processes.[6] On the other hand, the deposition of engineered silver nanoparticles (Ag NPs) onto textile materials can provide an adequate level of antimicrobial efficiency without considerable color change.[3]

Recently developed simple procedures for synthesis of Ag NPs and their high antimicrobial efficiency make them a viable substitute to conventional antimicrobial agents. Consequently, the treatment of different textile materials with Ag NPs is receiving remarkable, not only scientific but also industrial, attention.[2,7–11] Numerous methods have been developed for the loading of textile substrates with Ag NPs. In addition to the most commonly applied dip-coating methods,[7,8,10,11] sonochemical coating using ultrasound irradiation[12,13] as well as the sputter deposition[14,15] of Ag NPs onto textile surfaces, were performed. Vigneshwaran et al. proposed in situ synthesis of Ag NPs on cotton fabrics where the aldehyde terminal of starch made possible the reduction of the silver nitrate to silver metal, simultaneously stabilizing the NPs on the fabric.[9] Durán et al. reported that good antibacterial efficiency can be achieved using the Ag NPs produced by a fungal process on cotton fabrics.[16] Ag NPs can be also efficiently incorporated into fibers by electrospinning.[17]

However, the latest trends are more oriented toward obtaining stable and durable nanocomposite textile materials with Ag NPs.[2,18] Plasma activation of textile materials, in particular hydrophobic polyester (PES) fabrics, appears to be beneficial for Ag NPs loading from colloids.[2,18] Conventional chemical treatments that can increase the surface energy of PES fibers, and, hence, improve their wettability and adhesion properties, are recognized as ecologically unacceptable as they require huge amounts of water and chemicals.[19] Unlike them, plasma processing is dry, clean, simple, multifunctional, environmentally friendly, and an economically feasible treatment. Additionally, it is not time-consuming, and it provides superficial modification of a fiber surface, leaving the bulk properties unaltered. The desired surface chemistry, i.e., plasma functionalization, can be achieved by adequate control of plasma parameters (treatment time, power, gas type, pressure, and gas flow).

It has been shown that pretreatment of PES fabrics by corona discharge at atmospheric pressure improves the loading of Ag NPs, providing the enhanced antimicrobial activity and laundering durability.[20–22] The main advantage of corona systems is that they operate at atmospheric pressure. Although corona systems principally meet the demands of the textile industry from the standpoint of speed and width, generated type of plasma cannot provide the desired spectrum of surface functionalizations on textile materials.[23] Plasma particles cannot penetrate deeply into yarns, and, hence, achieved effects are short-lived. Additionally, the thickness of the textile materials is limited due to small interelectrode spacing.[23] However, low-pressure devices, in particular radio frequency (RF) powered plasma sources, allow easier control of properties and provide

* To whom correspondence should be addressed. Fax: +381 11 3370387. Tel.: +381 11 3303 857. E-mail: maja@tmf.bg.ac.rs.
[†] Textile Engineering Department, University of Belgrade.
[‡] Vinča Institute of Nuclear Sciences.
[§] Institute of Physics.
[||] Department of Bioengineering and Biotechnology, University of Belgrade.

10.1021/ie1001313
Published on Web 07/12/2010

a greater stability and uniformity at the cost of a more complex handling of fabric through the vacuum system.[24–26] Therefore, the first part of this study discusses the potential application of low-temperature air RF plasma for fiber surface activation that can facilitate the deposition of colloidal Ag NPs onto the PES fabrics and, thus, enhance their antibacterial properties. Antibacterial activity and laundering durability were tested against gram-negative bacterium *Escherichia coli* (*E. coli*) and gram-positive bacterium *Staphylococcus aureus* (*S. aureus*).

In spite of growing commercialization of Ag NPs in general, little is known about the environmental impact of the products containing these species.[27] It is well-established that ionic silver is very toxic to aquatic organisms, and its concentration in water is strictly regulated by water quality criteria.[28,29] In contrast, data corresponding to toxicity and exposure of Ag NPs are still lacking.[28] To our knowledge, there are only a few studies on silver release during washing of textile materials and possible treatments of these effluents.[28–30] Benn and Westerhoff analyzed the form and amount of silver released from different sorts of commercial socks into water and its fate in wastewater treatment plants.[28] This study clearly indicates that silver is released either in the form of NPs or as ions. Additionally, the amount and rate of silver release strongly depends on the sock type, suggesting that the manufacturing process may control silver release.[28] Durán et al. studied the bioremediation process of Ag NPs released from cotton fabrics with the bacterium *Chromobacterium violaceum* (*C. violaceum*).[29] This treatment based on biosorption seems to be efficient for removal of released Ag NPs in water. However, both studies reported the leaching of silver in ultrapure or tap water; i.e., the effect of washing agents on silver release from textile materials into the washing effluents was not addressed in their work. Geranio et al. followed the effect of pH, surfactants, and oxidizing agents on the amount and the form of released silver during washing from nine different fabrics with silver bound to the fiber surface or incorporated into the fiber.[30] Again, they came to the same conclusion that the release of silver either in ionic or particulate form varies remarkably among the products (from less than 1 to 45%). However, particulate silver seems to be the predominant form of silver released under conditions relevant to washing.

Hence, the second part of this study considers silver release from the PES fabrics during washing in the presence of washing agent and the possibility of silver removal by recycled wool-based nonwoven sorbent from washing effluent. Extensive research on potentials of this sorbent for removal of metal ions (Pb^{2+}, Cu^{2+}, and Zn^{2+}), different dyes, and oils from water indicated its multifunctionality and high sorption efficiency.[31–33] It is well-known that Ag^{+} is bound to the wool primarily via carboxylic groups.[34] Thus, in order to introduce new carboxylic groups to the wool fiber surface, the recycled wool-based nonwoven sorbent was modified with hydrogen peroxide and biopolymer alginate.

2. Materials and Methods

2.1. Materials. 2.1.1. Treatment of PES Fabrics. Desized and bleached polyester (PES, 115 g/m^2) fabrics were cleaned in a bath containing 0.50% nonionic washing agent Felosan RG-N (Bezema) at a liquor-to-fabric ratio of 50:1.[20] After 15 min of washing at 50 °C, the fabrics were rinsed once with warm water (50 °C) for 3 min and three times (3 min) with cold water. The samples were dried at room temperature.

Low-temperature plasma treatment of fabrics was carried out in capacitively coupled, radio frequency (13.56 MHz) air induced plasma. This capacitively coupled plasma (CCP) reactor was previously used for treatment of polymers and different textile materials.[24,26,35] The apparatus consisted of a constant RF power supply (Dressler Caesar 1010), matching box (Variomatch matching network), vacuum pump, chamber, gas supply with appropriate pressure gauges, current and voltage probes, digital oscilloscope, and a computer. To keep the reflected power at the minimum, the impedance was adjusted by tuning the matching box. With reduction of the reflected power, the power transmitted to the system increased and a stable operation was achieved.

The chamber was cylindrical (37 cm in diameter, 50 cm in length) with a central electrode (14 mm in diameter) that was powered through the matching box. Plasma formed between the central electrode and the wall of the chamber that was grounded. The samples were placed on the platform at the bottom of the chamber. Such an asymmetric system was intentionally constructed in order to provide operating conditions under which the sheath potential is not too high[36] but sufficient for optimum modification of different textile materials, avoiding their permanent damage. Preliminary studies indicated that plasma parameters which showed optimum effects in previous work seemed to be also adequate for PES fabrics. Therefore, the power applied to the CCP reactor was 100 W; treatment time was 2.5 min, while the pressure was maintained at a constant level of 0.27 mbar.

$AgNO_3$ (Kemika) and $NaBH_4$ (Fluka) of p.a. grade were used without any further purification for the synthesis of colloidal Ag NPs. Briefly, 8.5 mg of $AgNO_3$ was dissolved in 250 mL of water purged by argon for 30 min.[37,38] Under vigorous stirring, reducing agent $NaBH_4$ (125 mg) was added to the solution and left for 1 h in argon atmosphere. The concentration of Ag colloid was 50 ppm.

A 1 g amount of PES fabric was immersed in 65 mL of colloid of Ag NPs for 5 min and dried at room temperature. After 5 min of curing at 100 °C, the samples were rinsed twice (5 min) with deionized water and dried at room temperature. To investigate the influence of the colloid concentration, the whole procedure was repeated on certain fabrics.

2.1.2. Treatment of Sorbent. The possibility of silver removal from the washing effluent by sorption was tested on the recycled wool-based nonwoven material (78/22 wool/polyester). This sorbent was produced from second-hand military knitted pullovers. A procedure for the production of recycled wool-based nonwoven material is described elsewhere in detail.[32]

The recycled wool-based nonwoven material was treated with hydrogen peroxide and biopolymer alginate in order to improve its sorption properties. Hydrogen peroxide treatment (H_2O_2, 20 mL/L; $Na_4P_2O_7$, 1.5 g/L; NH_3(aq), 2.5 mL/L) was carried out in static conditions (without shaking). Samples were treated in the solution for 1 h (liquor ratio, 30:1) at 70 °C and pH 9.4, washed with water, and dried at room temperature.

Low-viscosity sodium alginate (CHT-alginat NVS, Bezema) was used for the preparation of 0.5% alginate solution. Sodium alginate was dissolved in deionized water and stirred for 30 min. A 1 g amount of sorbent was dipped into 50 mL of freshly prepared 0.5% alginate solution for 10 min. After 10 min of curing at 100 °C, the fabrics were rinsed twice (5 min) with deionized water and dried at room temperature.

2.2. Methods. 2.2.1. Scanning Electron Microscopy. Fiber morphology was investigated by scanning electron microscopy (SEM, JEOL JSM 6460 LV). A golden layer was deposited on the samples before the analysis.

2.2.2. Atomic Absorption Spectroscopy. The content of silver in the washing bath after each washing cycle and in the fabrics after the fifth washing cycle was determined by a Perkin-Elmer 403 atomic absorption spectrometer.

2.2.3. Antibacterial Efficiency. The antibacterial efficiency of PES fabrics was quantitatively assessed using a gram-negative bacterium *E. coli* ATCC 25922 and gram-positive bacterium *S. aureus* ATCC 25923. Bacterial inoculum was prepared in the Tryptone soya broth (Torlak, Serbia), which was used as a growing medium for bacteria, and potassium hydrogen phosphate buffer solution (pH 7.2) as a testing medium. Bacteria were cultivated in 3 mL of Tryptone soya broth at 37 °C and left overnight (late exponential stage of growth). Sterile potassium hydrogen phosphate buffer solution (70 mL) was added to a sterile Erlenmeyer flask (300 mL), which was then inoculated with 0.7 mL of bacterial inoculum. A 1 g amount of sterile fabric cut into small pieces (1×1 cm^2) was placed in the flask and shaked for 1 h.

Time zero counts were made by removing 1 mL aliquots from the inoculum which were diluted with physiological saline solution (8.5 g of NaCl in 1 L of water). A 0.1 mL aliquot of the solution was placed onto a Tryptone soya agar, and after 24 h of incubation at 37 °C, the zero time counts (initial number of bacterial colonies) of viable bacteria were made. Counts of 1 h each were made in accordance with the previously described procedure.

The percentage of bacterial reduction (R, %) was calculated using the following equation:

$$R = \frac{C_0 - C}{C_0} \times 100\% \quad (1)$$

where C_0 (CFU, colony forming units) is the number of bacterial colonies on the control fabric (untreated fabric without Ag) and C (CFU) is the number of bacterial colonies on the fabric loaded with Ag NPs.[7,8,39]

2.2.4. Laundering Durability. Laundering durability of antibacterial effects was evaluated after five washing cycles in Polycolor (Werner Mathis AG) laboratory beaker dyer at 45 rpm. The fabrics were washed in the bath containing 0.5% Felosan RG-N (Bezema) at a liquor-to-fabric ratio of 40:1. After 30 min of washing at 40 °C, the fabrics were rinsed once with warm water (40 °C) for 3 min and three times (3 min) with cold water. Afterward, the fabrics were dried at 70 °C.[8] The percentage of bacterial reduction after five washing cycles was determined in accordance with eq 1.

2.2.5. Sorption of Silver. The effluents collected after the first two cycles of washing of all studied samples were mixed, and silver concentration was measured by atomic absorption spectroscopy (AAS). The measured pH value of the effluent was pH 4.5. Subsequently, 0.50 g of recycled wool-based nonwoven material was shaken in 25 mL of effluent for 3 and 24 h. Ag concentration after the sorption was also followed by AAS.

3. Results and Discussion

3.1. Characterization of PES Fabrics Modified by Plasma Treatment and Ag NPs. To enhance the interaction between hydrophilic colloidal Ag NPs and hydrophobic PES fibers, the surface of the substrate was modified by air RF plasma. Plasma induced morphological changes of PES fibers were analyzed by SEM. SEM images of untreated (UPES) and plasma treated PES (PPES) fibers are shown in Figure 1. Figure 1a reveals the smooth surface of the UPES fiber. The topography

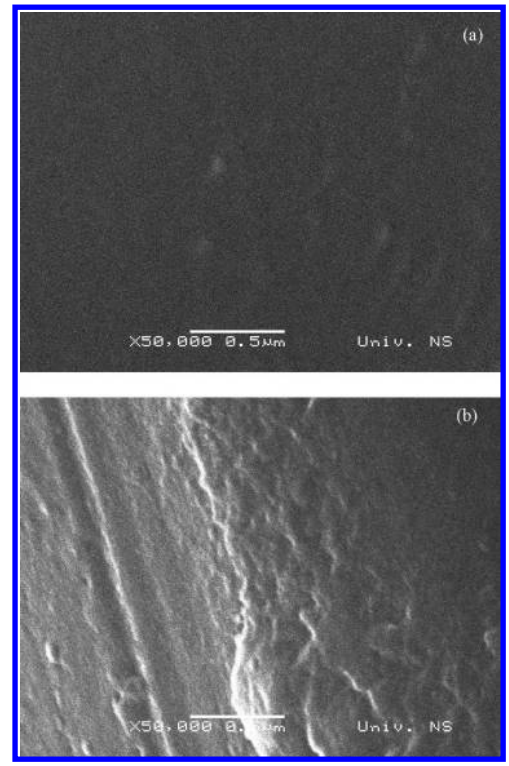

Figure 1. SEM images of UPES (a) and PPES fibers (b).

of the fiber was considerably altered after plasma treatment due to plasma etching (Figure 1b). Namely, energetic and highly reactive plasma species attacked the fiber surface and triggered the fiber ablation. Consequently, uneven cracks, pits, and striations running parallel to the fiber axis appeared, inducing the increase in fiber surface roughness.[20,40,41]

In addition to morphological changes, the chemical composition of the outer layers of the PES fibers was significantly altered. The XPS measurements in our previous study showed that air plasma treatment of PES fabrics resulted in an increase of the O/C ratio.[42] The formation of new oxygen-containing groups on the fiber surface is suggested to be due to the presence of extremely reactive atomic oxygen species in discharge during the air plasma processing and/or post-plasma chemical reactions when the activated fiber surface reacts with environmental species.[43–45] The rise of oxygen content ensures the improvement of PES fiber surface hydrophilicity and better accessibility of hydrophilic species.

UPES and PPES fabrics were loaded once or twice with colloidal Ag NPs. For this purpose, uniform nearly spherical Ag NPs with an average diameter of approximately 10 nm, synthesized without using any stabilizer, were applied.[20] The changes in fiber surface morphology after deposition of Ag NPs was also followed by SEM. SEM images of the PES fabrics loaded once and twice with Ag NPs (UPES + Ag and UPES + Ag × 2) as well as of the PPES fabrics loaded once and twice with Ag NPs (PPES + Ag and PPES + Ag × 2) are shown in Figure 2. Only a few almost spherical aggregates of Ag NPs with dimensions around 100 nm are observed on the surface of the UPES + Ag fiber (Figure 2a). On the contrary, a higher amount of smaller aggregates of Ag NPs with dimensions ranging from 40 to 70 nm was deposited on the surface of the UPES + Ag × 2 fibers (Figure 2b). As expected, plasma treatment positively affected the deposition of Ag NPs onto PES fibers (Figure 2c,d). Aggregates of Ag NPs (from 40 to 70 nm) were more uniformly distributed particularly over the surface of the PPES + Ag × 2 fibers (Figure 2d). Namely,

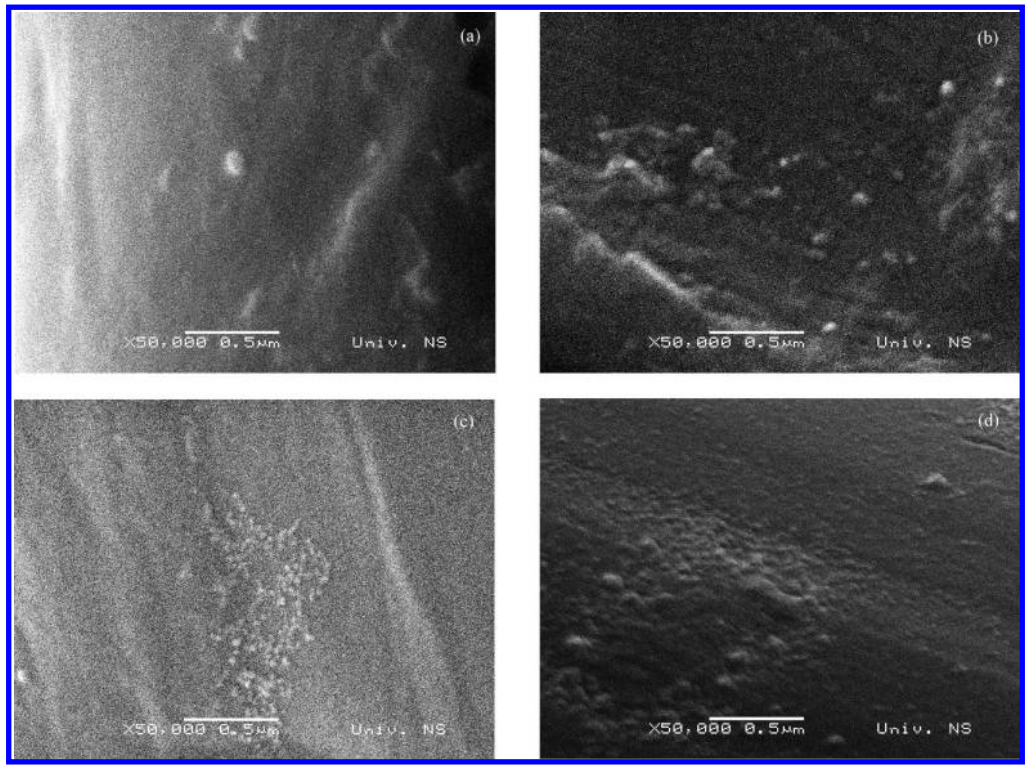

Figure 2. SEM images of UPES fabrics loaded with Ag NPs once (a) and twice (b) and PPES fabrics loaded with Ag NPs once (c) and twice (d).

Table 1. Antibacterial Efficiency of Ag Loaded UPES and PPES Fabrics

sample	bacteria	initial no. of bacterial colonies (CFU)	no. of bacterial colonies on the fabric (CFU)	*R* (%)
control	*E. coli*	5.6×10^5	3.4×10^4	
UPES + Ag			<10	99.9
UPES + Ag × 2			<10	99.9
PPES + Ag			<10	99.9
PPES + Ag × 2			<10	99.9
control	*S. aureus*	1.7×10^5	1.0×10^4	
UPES + Ag			<10	99.9
UPES + Ag × 2			<10	99.9
PPES + Ag			<10	99.9
PPES + Ag × 2			<10	99.9

Table 2. Antibacterial Efficiency of Ag Loaded UPES and PPES Fabrics after Five Washing Cycles

sample	bacteria	initial no. of bacterial colonies (CFU)	no. of bacterial colonies on the fabric (CFU)	*R* (%)
control	*E. coli*	2.4×10^5	1.7×10^4	
UPES + Ag			2.0×10^2	98.9
UPES + Ag × 2			10	99.9
control		5.6×10^5	7.4×10^4	
PPES + Ag			<10	99.9
PPES + Ag × 2			<10	99.9
control	*S. aureus*	1.4×10^5	4.0×10^4	
UPES + Ag			2.8×10^2	99.3
UPES + Ag × 2			55	99.9
control		1.0×10^4	4.5×10^3	
PPES + Ag			<10	99.9
PPES + Ag × 2			<10	99.9

plasma-induced hydrophilicity of PES fiber surface in conjunction with increased fiber surface roughness makes the PES fibers remarkably more accessible to colloidal Ag NPs. Hence, better deposition of Ag NPs is provided on PPES fabrics.

AAS measurements also confirmed higher Ag content in the PPES fabrics. It was found that 1 g of the UPES + Ag, UPES + Ag × 2, PPES + Ag, and PPES + Ag × 2 contains 79.7, 61.8, 155.7, and 145.5 μg of Ag, respectively. Unlike plasma pretreatment, double loading of colloidal Ag NPs did not enhance the deposition of Ag NPs onto the UPES and PPES fabrics.

3.2. Antibacterial Efficiency and Laundering Durability of PES Fabrics Loaded with Ag NPs. Antibacterial activity of UPES and PPES fabrics loaded with Ag NPs was tested against gram-negative bacterium *E. coli* and gram-positive bacterium *S. aureus*. The values of bacterial reduction of the UPES and PPES fabrics loaded once and twice with Ag NPs are given in Table 1. All PES fabrics loaded with Ag NPs reached the maximum bacterial reduction, independently of treatment. The results in Table 2 demonstrate that after five washing cycles the PPES fabrics loaded with Ag NPs once and twice, preserved the initial antibacterial activity, indicating an excellent laundering durability. A similar effect was achieved by corona treatment at atmospheric pressure in our previous work.[20] To obtain the same level of antibacterial efficiency after five washing cycles, the UPES fabrics have to be loaded with Ag NPs twice. In other words, the UPES + Ag fabric exhibited poorer laundering durability. It is interesting to note that laundering durability of the UPES + Ag × 2 fabrics in our previous study[20] was not as good as the data in Table 2 imply. The discrepancy between previous and current results is very likely due to different construction of the studied PES fabrics. Obtained results reveal that the fabric parameters should be also taken into consideration since they indirectly determine the macroscopic accessibility of fibers to colloidal Ag NPs.

The exact mechanism by which Ag NPs interact with bacteria is not totally clear yet. One approach relies on the hypothesis that Ag ions released from Ag NPs are responsible for killing the bacteria[46–48] Lok et al. suggested that antibacterial activity of Ag NPs depends on the chemisorbed Ag^+ that is formed on the nanoparticle surface.[49] However, another approach is oriented toward the work of Morones et

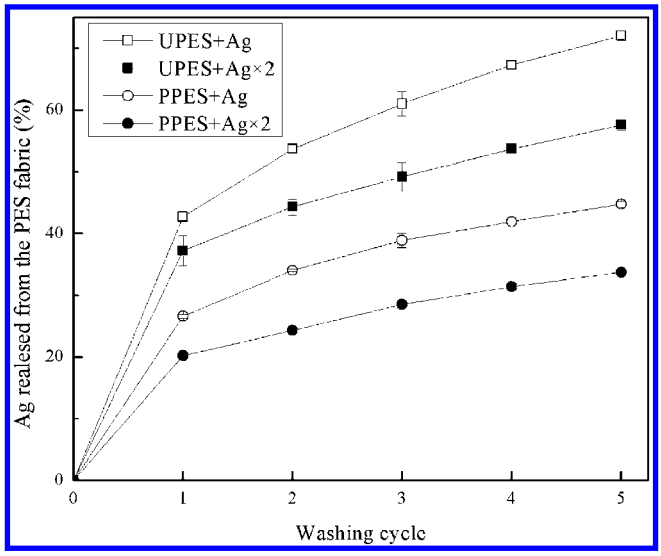

Figure 3. Silver release from the PES fabrics loaded with Ag NPs during washing.

al. who reported the presence of small-sized Ag NPs attached to the cell membrane and inside the bacteria that are crucial findings for understanding the bactericidal mechanism of Ag NPs.[46] Because silver shows high affinity to react with sulfur and phosphorus compounds,[50] it can be expected that Ag NPs react with sulfur reach protein in the bacteria cell membrane and interior of the cell or with phosphorus-containing compounds such as DNA.[51,52] Therefore, the morphological changes in the cell membrane of bacteria and possible damage of DNA triggered by reaction with Ag NPs negatively affect the respiratory chain or cell division processes, inducing a cell death.[46]

The amount of Ag released from the PES fabrics loaded with Ag NPs into the washing bath after each washing cycle was evaluated by AAS measurements. The total amount of Ag initially deposited onto PPES fabrics was approximately two times higher compared to equivalent UPES fabrics. As predicted, Ag leaching from the PES fabrics occurred during the washing. The results in Figure 3 indicate that the amount of Ag released from the PES fabrics decreases in each subsequent washing cycle. After a high initial rate of Ag release, the Ag leaching slowed down already in the second washing cycle for all samples. A similar trend of Ag release was observed on cotton fabrics.[3] The fabrics were burned after the last washing cycle, and the amount of Ag retained on the fabrics was determined. It was found that 22.3, 26.2, 86.1, and 96.4 μg of Ag is left in 1 g of the UPES + Ag, UPES + Ag × 2, PPES + Ag and PPES + Ag × 2 fabric, respectively. It can be noticed that Ag contents in the UPES + Ag and UPES + Ag × 2 after washing only slightly differ. Taking into account that the UPES + Ag fabric exhibited poor laundering durability unlike UPES + Ag × 2, it could be assumed that the critical amount of Ag necessary to provide desirable antibacterial activity in our systems should be within 22.3 and 26.2 μg/(g of fabric). It is also evident that a larger amount of Ag is left on the double-loaded PES fabrics compared to single-loaded PES fabrics. It appears that PPES fabrics retained almost four times more Ag compared to equivalent UPES samples. These results along with obtained antibacterial effects clearly confirm the positive effect of air RF plasma treatment on the deposition of Ag NPs onto PES fibers.

This study implies that silver leaching occurs during washing, but it cannot answer in what form silver is released from the PES fabrics. One assumption relies on the simple detachment of Ag NPs from the fiber surface and release into the washing bath. Another one involves the oxidation of silver since it was found out that, in contact with water and dissolved oxygen, Ag NPs release small amounts of silver ions according to[53]

$$O_2(aq) + 4H_3O^+ + 4Ag(s) \rightarrow 4Ag^+(aq) + 6H_2O \quad (2)$$

Benn and Westerhoff reported the presence of both forms of silver in the ultrapure water after simulated washing of commercial socks.[28] However, it is known that colloidal Ag NPs oxidize in aqueous medium on a long time scale (days).[37]

3.3. Sorption of Silver on the Recycled Wool-Based Nonwoven Material. To diminish the possible risk of ionic silver impact on the aquatic environment, the sorption of silver from the effluent collected after the first two washing cycles was tested using the recycled wool-based nonwoven material. AAS measurement indicated that the initial concentration of silver in the effluent was 0.5 mg/L. This value is in excellent agreement with the one calculated on the basis of results from Figure 3 corresponding to the amount of released silver in a certain volume of effluent. After 3 h of sorption about 70% of silver was removed from the effluent. The removal of silver increased to 84% after 24 h of sorption. Modification of sorbent with hydrogen peroxide and particularly biopolymer alginate positively influenced the removal of silver from the effluent. Already after 3 h of sorption, material modified with hydrogen peroxide removed 90% while with alginate 92% of silver. The good sorption properties of the material treated with hydrogen peroxide are likely due to modification of the surface of the wool fibers, i.e., oxidation and formation of appropriate groups that are potential sites for the binding of metal cations.[54,55] The abundance of carboxylic groups existing in alginates[56,57] makes this biopolymer a potential modifier of textile fiber surfaces, which may provide additional sites for complexation of ionic silver.

Presented results along with published data clearly imply that silver in concentrations existing in the washing effluents can be successfully treated.

4. Conclusions

Untreated and air RF plasma treated polyester fabrics loaded with silver nanoparticles once or twice from 50 ppm colloid exhibited excellent antibacterial activity against gram-negative bacterium *E. coli* and gram-positive bacterium *S. aureus*. Plasma pretreated polyester fabrics preserved excellent antibacterial activity even after five washing cycles. Untreated polyester fabric has to be loaded twice with silver nanoparticles to reach the equal antibacterial activity after washing. For the same goal, plasma pretreated PES fabric required only one loading of silver nanoparticles. Greater antibacterial efficiency of plasma treated fabrics is attributed to a larger amount of deposited silver. On the other hand, double loading did not improve the deposition of the silver nanoparticles. The results also demonstrated that a similar amount of silver was released from both untreated and plasma treated fabrics during washing. However, a much higher amount of silver was retained on the plasma pretreated fabrics after five washing cycles, indicating that plasma pretreatment positively affected the silver nanoparticle deposition, but it did not provide enhanced stability of the textile nanocomposite system. Released silver from the washing effluent was

efficiently removed by recycled wool-based nonwoven sorbent modified with hydrogen peroxide and biopolymer alginate.

Acknowledgment

This study was supported by the Ministry of Science of the Republic of Serbia—Project TR19007, 142066 and Eureka Project E !4043—NANOVISION. We gratefully acknowledge M. Bokorov (University of Novi Sad, Serbia) for performing SEM measurements.

Literature Cited

(1) Gao, Y.; Cranston, R. Recent Advances in Antimicrobial Treatments of Textiles. *Text. Res. J.* **2005**, *78*, 60.

(2) Yuranova, T.; Rincon, A. G.; Bozzi, A.; Parra, S.; Pulgarin, C.; Alberts, P.; Kiwi, J. Antibacterial Textiles Prepared by RF-plasma and Vacuum-UV Mediated Deposition of Silver. *J. Photochem. Photobiol., A* **2003**, *161*, 27.

(3) Ilić, V.; Šaponjić, Z.; Vodnik, V.; Potkonjak, B.; Jovančić, P.; Nedeljković, J.; Radetić, M. The Influence of Silver Content on Antimicrobial Activity and Color of Cotton Fabrics Functionalized with Ag Nanoparticles. *Carbohydr. Polym.* **2009**, *78*, 564.

(4) Feng, Q. L.; Wu, J.; Chen, G. Q.; Cui, F. Z.; Kim, T. N.; Kim, J. O. A Mechanism Study of Antibacterial Effect of Silver Ions on Escherichia coli and Staphylococcus aureus. *J. Biomed. Mater. Res.* **2000**, *52*, 662.

(5) Kostić, M.; Radić, N.; Obradović, B. M.; Dimitrijević, S.; Kuraica, M. M.; Škundrić, P. Silver Loaded Cotton/Polyester Fabric Modified by Dielectric Barrier Discharge Treatment. *Plasma Process. Polym.* **2009**, *6*, 58.

(6) Vigneshwaran, N.; Kumar, S.; Kathe, A. A.; Vradarajan, P. V.; Prasad, V. Functional Finishing of Cotton Fabrics Using Zinc Oxide-Soluble Starch Nanocomposites. *Nanotechnology* **2006**, *17*, 5087.

(7) Jeong, H. S.; Hwang, Y. H.; Yi, S. C. Antibacterial Properties of Padded PP/PE Nonwovens Incorporating Nano-Sized Silver Colloids. *J. Mater. Sci.* **2005**, *40*, 5413.

(8) Lee, H. J.; Yeo, S. Y.; Jeong, S. H. Antibacterial Effect of Nanosized Silver Colloidal Solution on Textiles Fabrics. *J. Mater. Sci.* **2003**, *38*, 2199.

(9) Vigneshwaran, N.; Kathe, A. A.; Varadarajan, P. V.; Nachane, R. P.; Balasubramanya, R. H. Functional Finishing of Cotton Fabrics Using Silver Nanoparticles. *J. Nanosci. Nanotechnol.* **2007**, *7*, 1893.

(10) Lee, H. J.; Jeong, S. H. Bacteriostasis of Nanosized Colloidal Silver on Polyester Nonwovens. *Text. Res. J.* **2004**, *74*, 442.

(11) Yuranova, T.; Rincon, A. G.; Pulgarin, C.; Laub, D.; Xantopoulos, N.; Mathieu, H. J.; Kiwi, J. Performance and Characterization of Ag-cotton and Ag/TiO_2 Loaded Textiles During the Abatement of *E. coli*. *J. Photochem. Photobiol., A* **2006**, *181*, 363.

(12) Perelshtein, I.; Applerot, G.; Perkas, N.; Guibert, G.; Mikhailov, S.; Gedanken, A. Sonochemical Coating of Silver Nanoparticles on Textile Fabrics (Nylon, Polyester and Cotton) and Their Antibacterial Activity. *Nanotechnology* **2008**, *19*, 255705.

(13) Hadad, L.; Perkas, N.; Gofer, Y.; Calderon-Moreno, J.; Hule, A.; Gedanken, A. Sonochemical Deposition of Silver Nanoparticles on Wool Fibers. *J. Appl. Polym. Sci.* **2007**, *104*, 1732.

(14) Wang, H. B.; Wei, Q. F.; Wang, J. Y.; Hong, J. H.; Zhao, X. Y. Sputter Deposition of Nanostructured Antibacterial Silver on Polypropylene Non-wovens. *Surf. Eng.* **2008**, *24*, 70.

(15) Mejia, M. I.; Restrepo, G.; Marin, J. M.; Sanjines, R.; Pulgarin, C.; Mielzarski, E.; Mielzarski, J.; Kiwi, J. Magnetron-Sputtered Ag Surfaces. New Evidence for the Nature of the Ag Ions Intervaning in Bacterial Inactivation. *ACS Appl. Mater. Interfaces* **2010**, *2*, 230.

(16) Durán, N.; Marcato, P. D.; De Souza, G. I. H.; Alves, O. L.; Esposito, E. Antibacterial Effect of Silver Nanoparticles Produced by Fungal Process on Textile Fabrics and Their Effluent Treatment. *J. Biomed. Nanotechnol.* **2007**, *3*, 203.

(17) Xu, X.; Yang, Q.; Wang, Y.; Yu, H.; Chen, X.; Jing, X. Biodegradable Electrospun Poly (L-lactide) Fibers Containing Antibacterial Silver Nanoparticles. *Eur. Polym. J.* **2006**, *42*, 2081.

(18) Jiang, S. Q.; Yuen, C. W. M.; Tao, X. M.; Kan, C. W.; Choi, P. S. R. Low-Temperature Plasma Pre-treatment of Polyester Fabric for Chemical Silver Plating. Presented at the 6th AUTEX Conference, Raleigh, NC, June 2006.

(19) Morent, R.; De Geyter, N.; Leys, C.; Gengembre, L.; Payen, E. Surface Modification of Non-woven Textiles using a Dielectric Barrier Discharge Operating in Air, Helium and Argon at Medium Pressure. *Text. Res. J.* **2007**, *77*, 471.

(20) Radetić, M.; Ilić, V.; Vodnik, V.; Dimitrijević, S.; Jovančić, P.; Šaponjić, Z.; Nedeljković, J. Antibacterial Effect of Silver Nanoparticles Deposited on Corona Treated Polyester and Polyamide Fabrics. *Polym. Adv. Technol.* **2008**, *19*, 1816.

(21) Ilić, V.; Šaponjić, Z.; Vodnik, V.; Mihailović, D.; Jovančić, P.; Nedeljković, J.; Radetić, M. The Study of Coloration and Antibacterial Efficiency of Corona Activated Dyed Polyamide and Polyester Fabrics Loaded with Ag Nanoparticles. *Fiber Polym.* **2009**, *10*, 650.

(22) Ilić, V.; Šaponjić, Z.; Vodnik, V.; Molina, R.; Dimitrijević, S.; Jovančić, P.; Nedeljković, J.; Radetić, M. Antifungal Efficiency of Corona Pretreated Polyester and Polyamide Fabrics Loaded with Ag Nanoparticles. *J. Mater. Sci.* **2009**, *44*, 3983.

(23) Shishoo, R. Introduction—The Potential of Plasma Technology in the Textile Industry. In *Plasma Technologies for Textiles*; Shishoo, R., Ed.; Woodhead: Cambridge, U.K., 2007.

(24) Radetić, M.; Jocić, D.; Jovančić, P.; Trajković, R.; Petrović, Z. Lj. The Effect of Low-Temperature Plasma Pretreatment on Wool Printing. *Text. Chem. Color. Am. Dyest. Rep.* **2000**, *32*, 55.

(25) Riccardi, C.; Barni, R.; Fontanesi, M.; Marcandalli, B.; Massafra, M.; Selli, E.; Mazzone, G. ASF6 RF Plasma Reactor for Research on Textile Treatment. *Plasma Sources Sci. Technol.* **2001**, *10*, 92.

(26) Puač, N.; Petrović, Z. Lj.; Radetić, M.; Djordjević, A. Low Pressure RF Capacitively Coupled Plasma Reactor for Modification of Seeds, Polymers and Textile Fabrics. *Mater. Sci. Forum* **2005**, *494*, 291.

(27) Morris, J.; Willis, J. *U.S. Environmental Protection Agency Nanotechnology White Paper*, EPA 100/B-07/001; Science Policy Council, U.S. Environmental Protection Agency: Washington, DC, 2007.

(28) Benn, T. M.; Westerhoff, P. Nanoparticle Silver Released into Water from Commercially Available Sock Fabrics. *Environ. Sci. Technol.* **2008**, *42*, 4133.

(29) Durán, N.; Marcato, P. D.; Alves, O. L.; Da Silva, J. P. S.; De Souza, G. I. H.; Rodrigues, F. A.; Esposito, E. Ecosystem Protection by Effluent Bioremediation: Silver Nanoparticles Impregnation in a Textile Fabrics Process. *J. Nanopart. Res.*, in press.

(30) Geranio, L.; Heuberger, M.; Nowack, B. The Behavior of Silver Nanotextiles during Washing. *Environ. Sci. Technol.* **2009**, *43*, 8113.

(31) Radetić, M.; Ilić, V.; Radojević, D.; Miladinović, R.; Jocić, D.; Jovančić, P. Efficiency of Recycled Wool-Based Nonwoven Material for the Removal of Oils from Water. *Chemosphere* **2008**, *70*, 525.

(32) Radetić, M.; Radojević, D.; Ilić, V.; Jocić, D.; Povrenović, D.; Potkonjak, B.; Puač, N.; Jovančić, P. Removal of Metal Cations from Wastewater Using Recycled Wool-Based Non-woven Material. *J. Serb. Chem. Soc.* **2007**, *72*, 605.

(33) Radetić, M.; Radojević, D.; Ilić, V.; Mihailović, D.; Jovančić, P. Recycled Wool-Based Nonwoven Material for Decolorisation of Dyehouse Effluents. *Int. J. Cloth. Sci. Tech.* **2009**, *21*, 109.

(34) Masri, M. S.; Friedman, M. Effect of Chemical Modification of Wool on Metal Ion Binding. *J. Appl. Polym. Sci.* **1974**, *18*, 2367.

(35) Tomčik, B.; Popović, D. R.; Jovanović, I. V.; Petrović, Z. Lj. Modification of Wettability of Polymer Surface by Microwave Plasma. *J. Polym. Res.* **2001**, *8*, 259.

(36) Lieberman, M. A.; Lichtenberg, A. J. *Principles of Plasma Discharge and Materials Processing*; Wiley: Hoboken, NJ, and New York, 2005.

(37) Vuković, V. V.; Nedeljković, J. M. Surface Modification of Nanometer-Scale Silver Particles by Imidazole. *Langmuir* **1993**, *9*, 980.

(38) Šaponjić, Z. V.; Csencsits, R.; Rajh, T.; Dimitrijević, N. Self-Assembly of Topo-Derivatized Silver Nanoparticles Into Multilayered Film. *Chem. Mater.* **2003**, *15*, 4521.

(39) Ki, H. Y.; Kim, J. H.; Kwon, S. C. Antibacterial Activity of Ag^+ Ion-Containing Silver Nanoparticles Prepared Using the Alcohol Reduction Method. *J. Mater. Sci.* **2007**, *42*, 8020.

(40) Qi, K.; Xin, J. H.; Daoud, W. A. Functionalizing Polyester Fiber with a Self-Cleaning Property Using Anatase TiO_2 and Low-Temperature Plasma Treatment. *Int. J. Appl. Ceram. Technol.* **2007**, *4*, 554.

(41) Zhang, C.; Fang, K. Surface Modification of Polyester Fabrics for Inkjet Printing with Atmospheric-Pressure Air/Ar plasma. *Surf. Coat. Technol.* **2009**, *203*, 2058.

(42) Mihailović, D.; Radetić, M.; Radoičić, M.; Molina, R.; Puač, N.; Jovančić, P.; Nedeljković, J.; Šaponjić, Z. *Specific Properties of Polyester Fabrics Functionalized by RF Plasma and Colloidal TiO_2 Nanoparticles*. Presented at the International Conference: Latest Advances in High Tech Textiles and Textile-Based Materials, Ghent, Belgium, September 2009, 213.

(43) Pappas, D.; Bujanda, A.; Demaree, J. D.; Hirvonen, J. K.; Kosik, W.; Jensen, R.; McKnight, S. Surface Modification of Polyamide Fibers and Films Using Atmospheric Plasmas. *Surf. Coat. Technol*. **2006**, *201*, 4384.

(44) Dai, X. J.; Hamberger, S. M.; Bean, R. A. Reactive Plasma Species in the Modification of Wool Fibre. *Aust. J. Phys*. **1995**, *48*, 939.

(45) De Geyter, N.; Morent, R.; Leys, C. Penetration of a Dielectric Barrier Discharge Plasma into Textile Structures at Medium Pressure. *Plasma Sources Sci. Technol*. **2006**, *15*, 78.

(46) Morones, J. R.; Elechiguerra, J. L.; Camacho, A.; Holt, K.; Kouri, J. N.; Ramirez, J. T.; Yacaman, M. J. The Antibactericidal Effect of Silver Nanoparticles. *Nanotechnology* **2005**, *16*, 2346.

(47) Xu, X.; Yang, Q.; Wang, Y.; Yu, H.; Chen, X.; Jing, X. Biodegradable Electrospun Poly(L-lactide) Fibers Containing Antibacterial Silver Nanoparticles. *Eur. Polym. J*. **2006**, *42*, 2081.

(48) Damm, C.; Muenstedt, H.; Roesch, A. Long-Term Antimicrobial Polyamide 6/Silver-Nanocomposites. *J. Mater. Sci*. **2007**, *42*, 6067.

(49) Lok, C. N.; Ho, C. M.; Chen, R.; He, Q. Y.; Yu, W. Y.; Sun, H.; Tam, P. K. H.; Chiu, J. F.; Che, C. M. Silver Nanoparticles: Partial Oxidation and Antibacterial Activities. *J. Biol. Inorg. Chem*. **2007**, *12*, 527.

(50) Hatchett, D. W.; Henry, S. Electrochemistry of Sulfur Adlayers on the Low-Index Faces Silver. *J. Phys. Chem*. **1996**, *100*, 9854.

(51) Feng, Q. L.; Wu, J.; Chen, G. Q.; Cui, F. Z.; Kim, T. N.; Kim, J. O. A Mechanism Study of Antibacterial Effect of Silver Ions on Escherichia coli and Staphylococcus aureus. *J. Biomed. Mater. Res*. **2000**, *52*, 662.

(52) Kim, J. S. Antibacterial Activity of Ag^{+} Ion-Containing Silver Nanoparticles Prepared Using the Alcohol Reduction Method. *J. Ind. Eng. Chem*. **2007**, *13*, 718.

(53) Hoskins, J. S.; Karanfil, T.; Serkiz, S. M. Removal and Sequestation of Iodide Using Silver-Impregnated Activated Carbon. *Environ. Sci. Technol*. **2002**, *36*, 784.

(54) Jovančić, P.; Jocić, D.; Molina, R.; Juliá, M. R.; Erra, P. Shrinkage Properties of Peroxide-Enzyme-Biopolymer Treated Wool. *Text. Res. J*. **2001**, *71*, 948.

(55) Julià, M. R.; Erra, P.; Jocić, D.; Canal, J. M. The Use of Chitosan on Hydrogen Peroxide Pretreated Wool. *Text. Chem. Color*. **1998**, *30*, 78.

(56) Mihailović, D.; Šaponjić, Z.; Radoičić, M.; Radetić, T.; Jovančić, P.; Nedeljković, J.; Radetić, M. Functionalization of Polyester Fabrics with Alginates and TiO_2 Nanoparticles. *Carbohydr. Polym*. **2010**, *79*, 526.

(57) Fernandez, J.; Dhananjeyan, M. R.; Kiwi, J.; Senuma, Y.; Hilborn, J. Evidence for Fenton Photoassisted Processes Mediated by Encapsulated Fe Ions at Biocompatible pH Values. *J. Phys. Chem. B* **2000**, *104*, 5298.

Received for review January 20, 2010
Revised manuscript received June 28, 2010
Accepted June 28, 2010

IE1001313

Effect of dissipated power due to antenna resistive heating on E- to H-mode transition in inductively coupled oxygen plasma

Article *in* Indian Journal of Physics · June 2015

Impact Factor: 1.38 · DOI: 10.1007/s12648-014-0615-2

6 authors, including:

Saša Lazović

Institute of Physics Belgrade

70 PUBLICATIONS **212** CITATIONS

SEE PROFILE

Rok Zaplotnik

Jožef Stefan Institute

41 PUBLICATIONS **129** CITATIONS

SEE PROFILE

Miran Mozetic

Jožef Stefan Institute

287 PUBLICATIONS **3,708** CITATIONS

SEE PROFILE

Zoran Lj Petrović

Institute of Physics Belgrade

510 PUBLICATIONS **5,652** CITATIONS

SEE PROFILE

Indian J Phys
DOI 10.1007/s12648-014-0615-2

ORIGINAL PAPER

Effect of dissipated power due to antenna resistive heating on *E*- to *H*-mode transition in inductively coupled oxygen plasma

N Puač[1,2], S Lazović[1,2], R Zaplotnik[1], M Mozetič[1], Z Lj Petrović[2] and U Cvelbar[1]*

[1]Jozef Stefan Institute, Jamova cesta 39, 1000 Ljubljana, Slovenia

[2]Institute of Physics, University of Belgrade, Pregrevica 118, 11080 Belgrade, Serbia

Received: 24 July 2014 / Accepted: 13 October 2014

Abstract: The problem of the effective power input into plasma is investigated for the inductively coupled RF oxygen discharge operated at 13.56 MHz. The power significantly deviates especially at the *E*- to *H*-mode transition. In order to enlighten this phenomenon the *U–I* characteristics of the discharge are recorded. With these data, we have recalculated the power deposited into plasma and determined the effective power losses due to the resistive antenna heating. The *E–H* mode transition is investigated in the pressure range from 10 to 200 Pa. With an increase of the working gas pressure, the threshold for the *E–H* transition moves towards the higher powers. The transition exhibits a hysteresis for the pressures higher than 10 Pa. When the dissipated power due to the antenna resistive heating is taken into account, the characteristic hysteresis profile skews towards lower power as compared to the case of taking generator power as a relevant parameter. This means that the *E*-mode is strongly affected by the way the power is obtained, while for the *H*-mode the generator power can be considered as a relatively good external parameter.

Keywords: Oxygen; Inductively coupled plasma; Mode transitions; Discharge power

PACS Nos.: 52.25.-b; 52.40.Fd; 52.50.-b

1. Introduction

Modern plasma processing systems often contain a combination of two or more capacitively (CCP) and/or inductively coupled (ICP) multi-frequency plasma reactors. The complex designs are introduced to provide independent control of important etching parameters like ion energies and charged particle concentrations in order to achieve high aspect ratios with minimum damage to the device [1–3]. The complexity of plasma systems made plasma diagnostics very challenging, due to multi-parameter control. High chemical reactivity of non-thermal plasma is exploited for processing of materials like polymers, composites, textiles, and for biomedical applications [3–16].

Inductively coupled plasma reactors operate in two regimes. The *E*-mode is sustained at lower powers and is characterized by low electron densities but high mean electron energies with non-equilibrium distribution. In the *H*-mode, the electron densities are high, while mean electron energy is lower.

A special feature of mode transition is the hysteresis [2]. ICP is usually initiated locally by the capacitive coupling between the RF coil and surroundings, known as *E*-mode. Next, electrons are accelerated in induced electric field, which results from oscillating magnetic field inside the coil (*H*-mode) providing the power given by the RF power supply is large enough. There is always a threshold power or induced voltage below, which no *H*-mode can be formed. Hysteresis occurs as the transition back to the *E*-mode at a lower power/induced voltage. This effect is observed in plasmas sustained at different frequencies (13.56 MHz [17, 18], 0.56 MHz [19] and 0.5 MHz [20]).

The difference in modes can in principle be observed from electrical properties [deposited power, Volt-Ampere (U–I) characteristics] [19–23] and plasma brightness (or measurements of densities of excited states) [17, 18, 24]. Besides the optical emission spectroscopy (OES), where the significant difference of line intensities is recorded for the two modes. The transition of modes is also easily

*Corresponding author, E-mail: uros.cvelbar@ijs.si

Published online: 09 November 2014

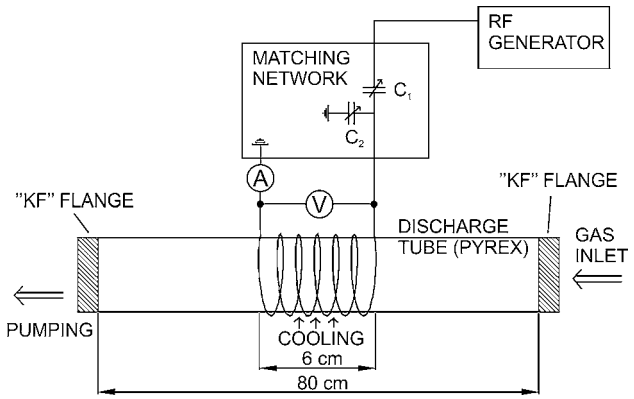

Fig. 1 Experimental set-up for the ICP RF discharge

detectable by using Langmuir probes to record the changes in electron densities and/or electron temperature [25, 26]. Mode transitions are mostly reported in noble gases. The transition between two modes is studied using different types of diagnostics, but recently the most useful results may be obtained by observing 2D emission profiles, which reveal directly difference between the two modes [27, 28].

Recent measurements on oxygen plasma have been reported [29]. The increase in atomic oxygen concentrations has been recorded during the transition from *E*- to *H*-mode [30], where an increase of the factor of 3 has been reported at elevated pressure (160 Pa). A key and relevant external parameter has been proven to be a generator power. In most studies of *E–H* transition power measured at the power supply is used. Sometimes reflected power is subtracted. However, for the more complete understanding of the observed phenomena (*E–H* transition power and hysteresis effect) it is necessary to include other losses, such as the power emitted by the radio waves and the heating of the coil due to the resistance.

In this paper, we study the effects of dissipated power due to antenna resistive heating on the *E–H* mode transition and the hysteresis effect. We also discuss in details the power efficiency during the mode transition in oxygen plasma in both directions (*E–H* and *H–E*). We unfold the influence of the coil/reactor wall temperature on the dissipated power, measure, calculate and compare effective power losses in the RF coil. Furthermore, we define the regions, where plasma does not operate in a stable regime and elaborate on hysteresis effect [21]. Commercial current and voltage probes and the procedure for the determination of the plasma power and electrical properties of the system can be applied to complex plasma processing systems as well. Herein we present also results of electrical properties of the discharge.

2. Experimental details

Experimental set-up of the ICP reactor was used in the experiments as presented in Fig. 1. The system was composed from an RF power supply (Dressler CESAR 1312D), matching box and discharge tube made of Pyrex. The discharge tube was 80 cm long with the diameter of 4 cm. The pressure in the reactor was measured by an absolute pressure transducer MKS Baratron 722A positioned at the chamber gas outlet. The experimental vessel was evacuated using a two-stage oil rotary pump with an ultimate pressure of approximately 0.5 Pa. After evacuating the vacuum chamber to the base pressure, oxygen feedstock gas was continuously let into the chamber.

Plasma glow discharge was created by an inductively coupled RF generator that operates at 13.56 MHz with maximum output power of 1,200 W. The L-type matching network was employed with two vacuum variable tuning capacitors, $C_1 = 5$–500 pF and $C_2 = 5$–500 pF and was connected directly to the inductive coil to reduce resistive losses. The capacitors were tuned to achieve the minimal value of the reflected power, while plasma was operated in the *H*-mode. The values were kept constant throughout the measurements. Power supply was coupled to the discharge by a coil (six turns) made of copper. The applied power was recorded as the difference between the forward and reflected power as read from the power supply meter. IR-pyrometer Raytek Raynger MX4+ was used to measure the temperature and determine the heat loss in the coil. After a certain period of plasma operation the temperature increased and became close to the melting temperature of the glass chamber. Therefore, coil and the discharge area had to be air cooled during all the measurements in order to prevent the overheating. Besides the temperature measurements, we used commercial current and voltage probes (Tektronix A6302, Tektronix P6015A) in order to obtain current and voltage characteristic. Oxygen was used as a feeding gas in the pressure range from 10 to 200 Pa. Power used to create discharge by RF power supply was varied in small increments and characteristics were measured between 10 and 1,000 W.

3. Results and discussion

We now discuss the influence of the antenna resistive heating on power transmission, stable regimes of plasma operation, power transfer efficiency, Volt-Ampere characteristics of the discharge and hysteresis effect of *E*- and *H*-mode transitions. Finally, we compare the results, when the generator power is used as a relevant parameter with the results obtained in this study, when the power dissipation is taken into account.

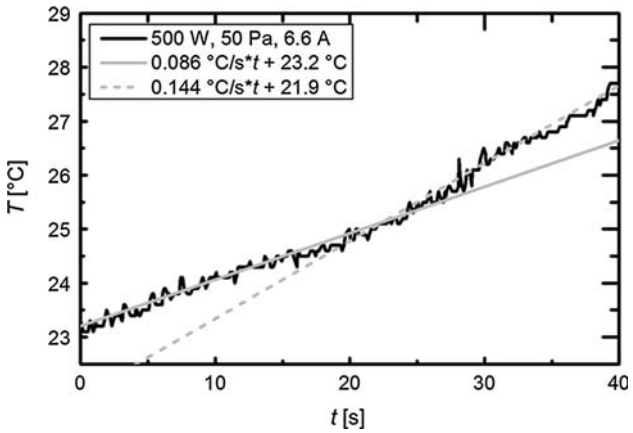

Fig. 2 Time dependence of the coil temperature after the plasma ignition

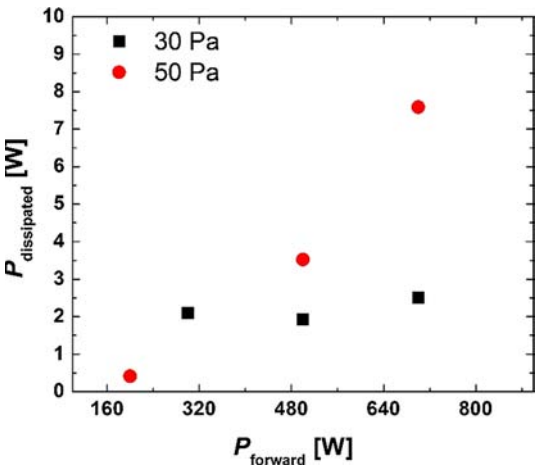

Fig. 3 Power dissipated as coil heating for two different pressures while plasma was ignited

Coil heating can significantly influence the transmission efficiency of the power given by the power supply to the discharge. In order to determine the heat loss in the coil, we have measured the temperature and the power dissipated as the heat loss has been calculated. During temperature measurements, we have implied no coil cooling with convective air or running water. The temperature dependence of the coil after plasma ignition is presented in Fig. 2 for the case of RF power supply at 500 W and operating pressure 50 Pa. The coil temperature behavior typically shows two regimes characterized by different slopes of temperature versus time. At first, the temperature of the coil increases with the time only due to resistive heating. However, after a certain period of time, the temperature curve steepens probably due to the heating coming from the discharge itself, which starts to heat up chamber walls. The position of the inflection point depends on the pressure and the power input by the power supply. At higher powers and lower pressures the heating due to the ignited discharge

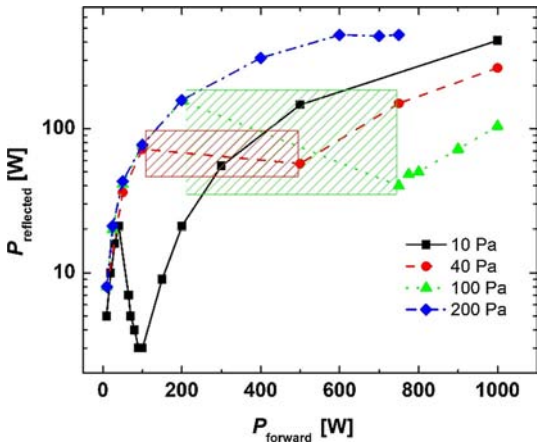

Fig. 4 Dependence of the reflected power for different pressures on forward power of the RF power supply

is more pronounced as compared to the lower powers and/or higher pressures.

The power dissipated in the coil is shown in Fig. 3. It is calculated as $P_{diss} = m \cdot c_{Cu} \cdot dT/dt$, where m is coil mass, c_{Cu} is specific heat coefficient for copper and dT/dt is the slope of the first part of the temperature curve, due to the resistive heating, as shown in Fig. 2. At 30 Pa, dissipated power does not change with forward power. For 50 Pa the dissipated power increases linearly with forward power, where the dissipation at 700 W is about 8 W. Since there is an additional constant heating coming from discharge, the temperature of the coil as well as the glass chamber itself increases linearly with time. At the same time, the overheating of the discharge area leads to the decrease in power transmission efficiency.

Besides the influence of resistive antenna heating on power transmission, the transition from *E*- to *H*-mode is clearly visible as a decrease in reflected power, as shown in Fig. 4. Threshold point (forward power where transition occurs) for the *E*- to *H*-mode transition moves towards higher powers with an increase of working gas pressure. However, at 200 Pa we do not observe this threshold point because at this pressure the transition is out of the power range of our RF power supply. In order to observe this transition, we would need forward power higher than 800 W. All power–pressure dependences show 'the gaps' in the power range, where no stable discharge can be obtained. This occurs due to the unstable transition between the two modes of operation. Even more so, in this range, we have significant power oscillations. These oscillation areas are marked in Fig. 4 for pressures of 40 and 100 Pa with red and green shaded area, respectively. The range of power oscillations, where no stable discharge could be obtained, becomes wider when increasing the working pressure.

The applied power P_a is determined as the difference between the forward and reflected power. Both are

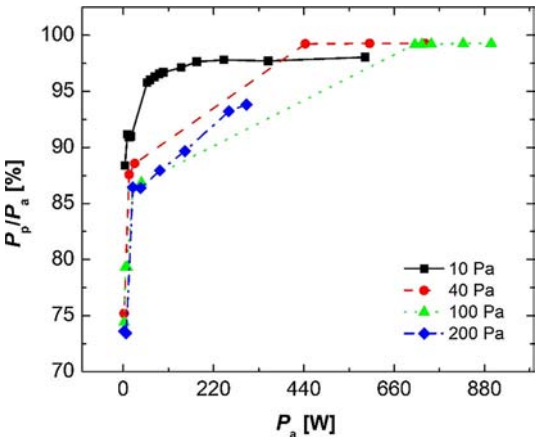

Fig. 5 Power transfer efficiency for four different pressures shown as a function of applied power

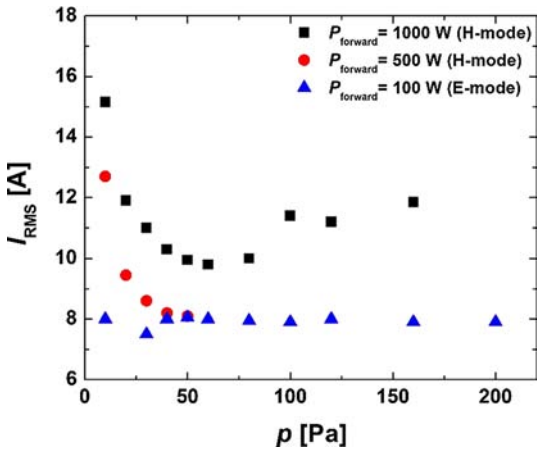

Fig. 6 RMS current values shown as a function of working pressure

measured by the RF power supply meter. The resolution of the RF generator power meter is ± 1 W. In order to determine the "real" power transmitted to the plasma, we need to determine the effective power losses in the antenna. The effective power loss is calculated as I^2R_{eff}, where R_{eff} represents the resistance in the antenna and associated hardware [20, 31, 32]. The effective coil resistance is determined from dissipating a known power in the matching circuit with no plasma present. Based on the power dissipated in the matching circuit and the current, the effective coil resistance has been measured to be 0.05 Ω during the reported measurements. From the obtained value, lower than 0.1 Ω, we could assume that the coupling efficiency of the system is very good and above 90 % for most of the used discharge parameters [33].

Plasma power is then determined as

$$P_p = P_a - I^2 R_{eff}, \tag{1}$$

where I is the RMS current flowing in the circuit and R_{eff} is the effective resistance of the coil and associated hardware. Here it should be noted that if the plasma significantly alters the current distribution in the chamber, then R_{eff} and the power transmitted into the plasma would change.

R_{eff} can be calculated using the resistivity of copper ($\rho_{Cu} = 1.59 \times 10^{-8}$ Ωm), the theoretical skin depth of 13.56 MHz current in the conductors ($\delta = 18$ μm) at the given length ($l = 0.91$ m) and circumference ($O = 0.14$ m) of the six-turn coil with interconnects:

$$R_{eff} = \rho_{Cu} \cdot \frac{l}{O \cdot \delta} = 0.006\ \Omega \tag{2}$$

However it is worth noting that this effective resistance does not include contributions from the tuning capacitors. In order to calculate R_{eff}, we also need to assume that the current distribution around the cross section circumference of the coil is uniform. More realistic situation of the non-uniform current distribution leads to an increase in effective resistance. Eq. (2) gives only the lower bound of the actual resistance, so in further analysis the experimentally obtained value of resistance has been used.

The measured power transfer efficiency P_p/P_a is presented in Fig. 5 as a function of applied power. The power transfer efficiency rises steeply from about 75 % in E-mode to a nearly constant efficiency in H-mode, with values from 95 to 98 % at different pressures. We have not observed the E–H mode transition at 200 Pa, due to the limitations of the power supply. For lower pressures, the power transfer efficiency rises faster than for higher pressures. At lower pressures, the maximal power efficiency is reached at lower applied powers. Moreover, at high pressures, the transition to H-mode can be expected at higher applied power values.

It is interesting to note how the coil current behaves at different pressures. From Fig. 6, we observe that the decrease of the pressure increases the current significantly, especially for the H-mode. This occurs due to the increase of the electric field and therefore the increase of the RF magnetic flux. At the same time, at 100 W, the current is almost constant throughout the measured pressure range, when the discharge is in the E-mode.

The E–H transition is also clearly seen from the U–I characteristics of the discharge presented in Fig. 7. When the discharge is in the E-mode, RMS values of the voltage linearly increase up to the threshold values, where transition occurs. After the transition, RMS values of voltage drop suddenly and again start to increase with the increase of the power transmitted into the plasma. In our discharge, RMS values of the voltage are in the range between 200 and 1250V, whereas the RMS values of current lie in the range 2.5–20 A. After the transition (inflection point), the RMS voltage still increases, but in a slower manner compared to the previous E-mode. Two

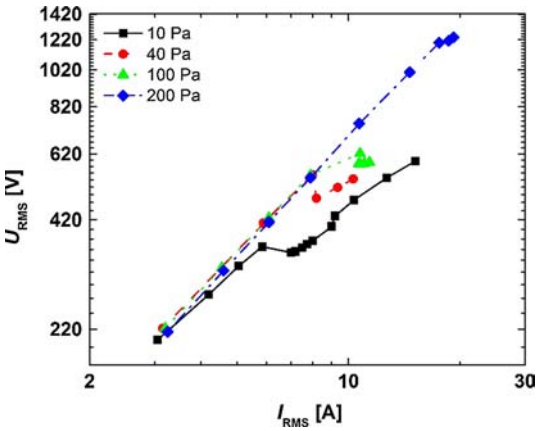

Fig. 7 U_{rms}–I_{rms} characteristics of the discharge

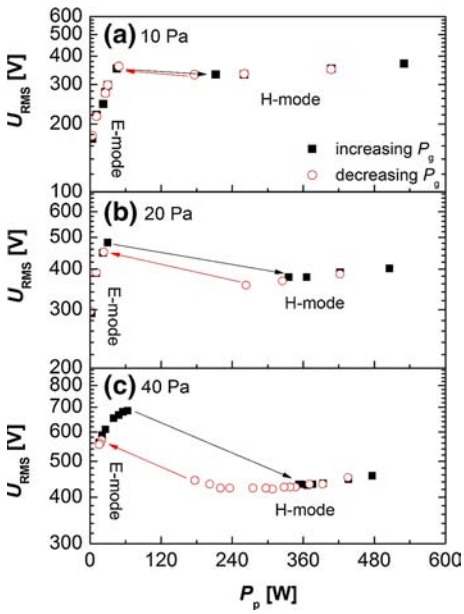

Fig. 8 Dependence of the U_{rms} values on the power deposited to the plasma for different preassures: (**a**) 10 Pa, (**b**) 20 Pa, (**c**) 40 Pa. Measurements were made for an increase of the power given by RF power supply (increasing P_g) and after that, a decreasing power (decreasing P_g) in order to detect hysteresis

distinct slopes show the change of the effective plasma impedance. In the *E*-mode, the slope is steeper leading to the conclusion that the plasma impedance is higher than in the *H*-mode.

The transition between *E*- and *H*-modes has already been reported to exhibit hysteresis [17–19, 31]. The threshold power for *H* to *E* transition is normally lower than in the case of *E* to *H* transition. Plasma stays in the *H*-mode even for lower powers, when applied power is decreased. Several authors [19, 21] have suggested that this threshold point for the *H*-mode and the hysteresis originates from the electron energy balance in the discharge. It is necessary that the power absorbed by the electrons is balanced by the power

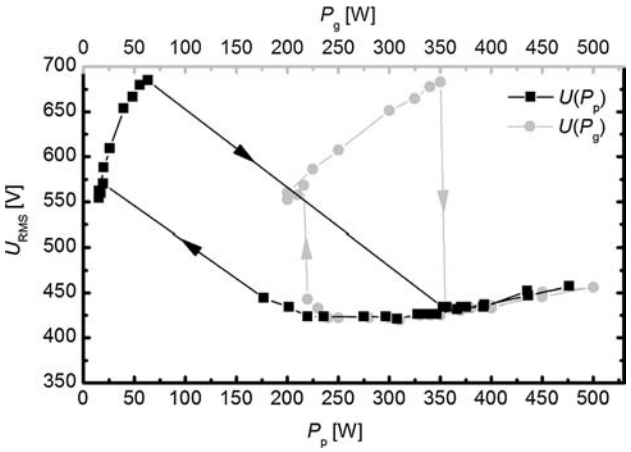

Fig. 9 Influence of the resistive antenna heating on the hysteresis for *E*- and *H*-mode at 40 Pa (generator power vs. plasma power)

dissipated in the discharge for a stable discharge to exist (both *E*- and *H*-mode). To obtain the transition between the two modes, we need to assume a nonlinearity in the power absorbed or dissipated in the plasma [34]. RMS voltages are presented in Fig. 8, as a function of the power deposited into the ICP plasma for (a) 10 Pa, (b) 20 Pa and (c) 40 Pa in Fig. 8. At the lowest pressure of 10 Pa, the effect of hysteresis is minimal. However, when we increase the working pressure, the hysteresis becomes more pronounced, as in the case of 40 Pa, as shown in Fig. 8(c).

In most of the cases, the hysteresis is demonstrated as a function of the generator power. However, Fig. 9 clearly demonstrates that if the antenna dissipated power due to the resistive heating and the generator reflected power are taken into account the hysteresis skews and slightly shifts towards lower power.

The change in the shape profile shows that the recalculated power is strongly affecting the *E*-mode. If the generator power is taken as a relevant external parameter, the *E*- to *H*-mode transition occurs in only a few watt span in the power. On the other hand, if the dissipated and reflected power is included, the *E*- to *H*-mode is having a power span of several hundred watts. Unlike the *E*-mode, the *H*-mode is only slightly affected by the way the power is determined. While outside the realm of our facilities, spatial profiles of negative ions in *E* and *H* modes cannot be easily measured for our experiment and should be sought from plasma modelling. It is also known that the negative ion energies are far less than those of electrons. However, electrons need to gain enough energy to produce the excited states that are observed in measurements. In addition to the negative ions, density of excited states such as oxygen metastables also plays an enhanced role in the transition from *E* to *H*.

4. Conclusions

This paper presents the power measurements, electrical characterization and plasma behavior obtained in an inductively coupled RF oxygen discharge that operates at 13.56 MHz. We include the effects of dissipated power due to the resistive antenna heating (together with the generator reflected power) and study the *E*- to *H*-mode transition and its hysteresis effect. Furthermore, we compare the results in two cases: when generator power is used as a relevant external parameter and when the recalculated so called "plasma power" is used. We find that if the power dissipation is taken into account the difference in the power values is pronounced for the *E*-mode. In the case of *H*-mode, the generator power can be considered as a satisfactory parameter.

We also investigate transition from the low density capacitive *E*-mode to the inductive *H*-mode for the range of pressures from 10 to 200 Pa. We find that the increase in the working gas pressure requires higher powers deposited into plasma in order to observe the mode transition. Moreover, in all mode transitions the oscillations of discharge occur. This is explained by a rapid change in plasma density and topography during *E–H* transition, which results in an unstable plasma system. The power transfer efficiency is in the range of 70–85 % for the *E*-mode, whereas it is much higher and constant for the *H*-mode ($\sim$95 %). Additionally, the hysteresis effects have to be accounted for when the pressure is above 10 Pa, since the transition point is significantly shifted. All of these have to be taken into account when reporting power input into plasma during material processing, but is mostly unaccounted for in scientific reports.

Acknowledgments This research has been supported by the Ad-Futura and Slovenian Research Agency (ARRS), Slovenia and by the Ministry of Education and Science Serbia through project III41011 and ON171037.

References

[1] M A Lieberman and A J Lichtenberg *Principles of plasma discharge and materials processing* (Hoboken: Wiley) (2005)
[2] T Makabe and Z L Petrović *Plasma electronics: applications in microelectronic device fabrication* (New York: Taylor and Francis) (2006)
[3] U Cvelbar et al. *Appl. Surf. Sci.* **253** 8669 (2007)
[4] U Cvelbar, S Pejovnik, M Mozetic and A Zalar *Appl. Surf. Sci.* **210** 255 (2003)
[5] B Denis, S Steves, E Semmler, N Bibinov, W Novak and P Awakowicz *Plasma Process. Polym.* **9** 619 (2012)
[6] V Ilic et al. *Ind. Eng. Chem. Res.* **49** 7287 (2010)
[7] M Laroussi *Plasma Process. Polym.* **2** 391 (2005)
[8] D Mihailović et al. *Cellulose* **18** 811 (2011)
[9] N Puač, Z Lj Petrović, S Živković, Z Giba, D Grubišić and A Đorđević *Plasma Process. Polym.* (Weinheim: WILEY-VCH Verlag GmbH & Co. KGaA) Chapter 15 p 193 (2005)
[10] N Puač et al. *J. Phys. D Appl. Phys.* **39** 3514 (2006)
[11] M Modic, I Junkar, A Vesel and M Mozetic *Surf. Coat. Technol.* **213** 98 (2012)
[12] J Vasiljević et al. *Cellulose* **20** 277 (2012)
[13] Z Peršin, M Devetak, I Drevenšek-Olenik, A Vesel, M Mozetič and K Stana-Kleinschek *Carbohydr. Polym.* **97** 143 (2013)
[14] K H Karstensen et al. *Environ. Sci. Policy* **9** 577 (2006)
[15] G Mandal and T Ganguly *Indian J. Phys.* **85** 1229 (2011)
[16] A Kaplan, H Büyükuslu, E Tel, A Aydin and M H Bölükdemir *Indian J. Phys.* **85** 1615 (2011)
[17] U Kortshagen, N D Gibson and J E Lawler *J. Phys. D Appl. Phys.* **29** 1224 (1996)
[18] Y Miyoshi, Z L Petrovic and T Makabe *J. Phys. D Appl. Phys.* **35** 454 (2002)
[19] I M El-Fayoumi, I R Jones and M M Turner *J. Phys. D Appl. Phys.* **31** 3082 (1998)
[20] K N Ostrikov, S Xu and M Y Yu *J. Appl. Phys.* **88** 2268 (2000)
[21] K Suzuki, K Nakamura, H Ohkubo and H Sugai *Plasma Sources Sci. Technol.* **7** 13 (1998)
[22] G Cunge, B Crowley, D Vender and M M Turner *Plasma Sources Sci. Technol.* **8** 576 (1999)
[23] N Nimje, S Dubey and S Ghosh *Indian J. Phys.* **84** 1567 (2010)
[24] Y C Wang, E C Benck, M Misakian, M Edamura and J K Olthoff *J. Appl. Phys.* **87** 2114 (2000)
[25] S Xu, K N Ostrikov, W Luo and S Lee *J. Vac. Sci. Technol. A* **18** 2185 (2000)
[26] Y Chen, Z G Guo, X M Zhu, Z G Mao and Y K Pu *J. Phys. D Appl. Phys.* **40** 5112 (2007)
[27] Y Hayashi, Y Mitsui, T Tatsumi and T Makabe *New J. Phys.* **13** 073025 (2011)
[28] M Satoshi, H Yuichiro and M Toshiaki *Plasma Sources Sci. Technol.* **19** 055007 (2010)
[29] M Zaka-Ul-Islam, K Niemi, T Gans and D O'Connell *Appl. Phys. Lett.* **99** 041501 (2011)
[30] R Zaplotnik, A Vesel and M Mozetic *EPL* **95** 55001 (2011)
[31] A M Daltrini, S A Moshkalev, T J Morgan, R B Piejak and W G Graham *Appl. Phys. Lett.* **92** 061504 (2008)
[32] P A Miller, G A Hebner, K E Greenberg, P D Pochan and B P Aragon *J. Res. Natl. Inst. Stan.* **100** 427 (1995)
[33] J Hopwood *Plasma Sources Sci. Technol.* **3** 460 (1994)
[34] M M Turner and M A Lieberman *Plasma Sources Sci. Technol.* **8** 313 (1999)

Time resolved images of an atmospheric pressure plasma bullet

Conference Paper · July 2011

READS
21

6 authors, including:

Dejan Maletic
Institute of Physics Belgrade
53 PUBLICATIONS **97** CITATIONS
SEE PROFILE

Saša Lazović
Institute of Physics Belgrade
70 PUBLICATIONS **212** CITATIONS
SEE PROFILE

Gordana Malovic
Institute of Physics Belgrade
157 PUBLICATIONS **932** CITATIONS
SEE PROFILE

Zoran Lj Petrović
Institute of Physics Belgrade
510 PUBLICATIONS **5,652** CITATIONS
SEE PROFILE

Time resolved images of an atmospheric pressure plasma bullet

Dejan Maletić[1,3], Saša Lazović[1,3], Nevena Puač[1,3], Gordana Malović[1,3],
Antonije Đorđević[2] and Zoran Lj. Petrović[1,3]

[1]*Institute of Physics, Pregrevica 118, 11080 Belgrade, Serbia*
[2]*School of Electrical Engineering, University of Belgrade, Bulevar kralja Aleksandra 73, 11000 Belgrade, Serbia*
[3]*University of Belgrade, Studentski trg 1, 11000 Belgrade, Serbia*
e-mail: dejan_maletic@ipb.ac.rs

Abstract: Plasma bullet is a relatively new plasma source with a large field of potential applications, from biomedical to material processing and surface activation. Our plasma source was made of Pyrex glass tube with inner diameter of 4 mm and outer diameter of 6 mm. Electrodes were made of thin copper foil (13 mm wide) and the gap between the electrodes was 10 mm. The power supply was a waveform generator connected to an HF amplifier and custom-made HV transformer. The frequency that we used was 80 kHz and the applied voltage was in the range of 6-10 $kV_{peak\text{-}to\text{-}peak}$. In this paper, we will show time-resolved ICCD images of our plasma bullet device and how the emission changes with the applied power and flow of working gas. The power transmitted to the plasma was calculated and it was lower than 10 W.

Keywords: plasma, atmospheric, bullet, ICCD camera, time resolved

1. Introduction

In the last few decades, there has been a huge advance in plasma research; many atmospheric pressure plasma devices have been constructed and analyzed using various diagnostic techniques [1, 2, 3]. There is large potential use of atmospheric pressure plasmas in surface modification, plasma etching, thin film deposition, medicine and cosmetology. The low gas temperature is suitable for the treatment of thermo-sensitive samples like polymer materials and biological samples. Dimensions of plasma can be very different, from a few millimeters, suitable for microsurgery and stomatology, to large plasmas appropriate for treatment of large surfaces like wounds, textile and plant seeds [4, 5, 6].

Some of the well-known small-size plasma sources are: plasma needle [3, 7], μAPPJ [8], plasma bullet [9], plasma torch [10] and floating electrode dielectric barrier discharge plasma [11]. Their electrode configuration, voltages and excitation frequencies are very different; some of them work at 13.56 MHz and other at 5-120 kHz in sine or pulse regime. Some authors recently reported that the plasma jet that is formed with low excitation frequency is not continuous, but instead consisted of small plasma packages that are formed in positive and negative half cycle of the period [12]. The velocity of these packages is much larger than the speed of the flowing feed gas. In this paper, we will present our results of time-resolved images of plasma bullet obtained by using ICCD camera.

2. Experimental setup

The atmospheric pressure plasma jet that we used is made of a Pyrex glass tube (I.D. 4 mm and O.D. 6 mm). Electrodes were made of a thin copper foil wrapped around the glass tube. The distance between the powered and the grounded electrode was 10 mm. The width of both electrodes was 13 mm. The experimental scheme is given in figure 1. The left electrode was grounded and the second electrode, closer to the end of the glass tube, was powered. The distance between the powered electrode and the end of the glass tube was 5.6 mm. The feeding gas was helium and the flow rates used in this work were 2, 3, 4 and 5 slm. The flow rate is adjusted with a mass flow controller (Omega FMA5400/5500).

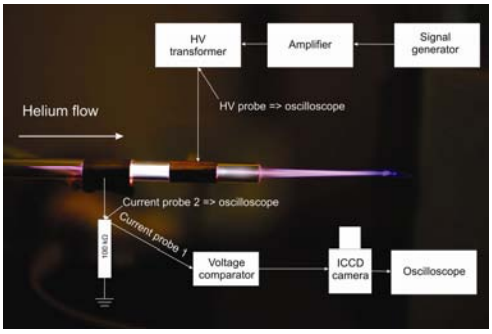

Figure 1. Experimental setup.

For powering the plasma jet, we used a signal generator (Peak Tech DDS function generator 4025) connected to a custom-made amplifier connected to an additional homemade step-up transformer.

For the current and voltage measurements, we used two commercial probes and two oscilloscopes (Agilent DSO3202A). The first probe, a high-voltage probe (Agilent N2771A), was connected to the HV-output and used for obtaining voltage waveforms. For the current waveforms we used the second probe (Agilent 10076A) which measured the voltage drop on a 100 kΩ resistor placed in the grounded branch of the electrical circuit (see Fig. 1). At the same place the third probe was connected (Agilent 10076A) for external triggering of the ICCD camera (Andor iStar DH734I). We have used camera's internal delay generator for delaying camera gating and for external triggering of the oscilloscope. The working frequency was 80 kHz and the applied voltage was in the range 6-10 $kV_{peak\text{-}to\ peak}$. The power tranmited to the plasma did not exceed 8 W during all measurements.

3. Results and discussion

Current and voltage waveforms when the plasma is formed and without discharge are shown in figure 2. When the plasma is off, the phase difference between the current and voltage is close to 90˚. In this case, we have a capacitive impedance of several MΩ, corresponding to the capacitance of about 0.5 pF. On the other hand, when plasma is formed, the current signal is larger, deformed and shifted in phase towards the voltage signal. The plasma ignition introduces a parallel nonlinear load into the electrical circuit and in this case the slopes of the V_{RMS}–I_{RMS} curves are lower (see Fig. 3.).

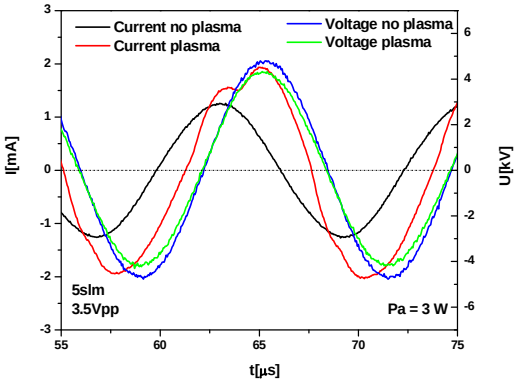

Figure 2. Signals of the current and voltage without plasma and when the plasma is formed for 5slm and 3.5Vpp at the signal generator (Pa = 3W).

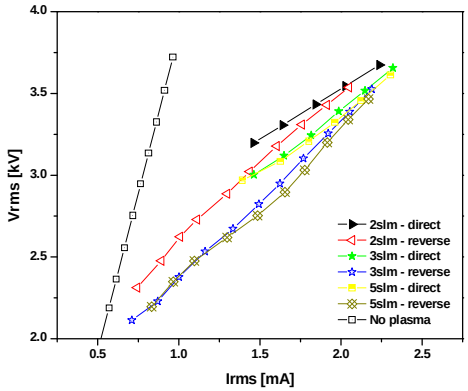

Figure 3. V_{rms} as the function of I_{rms} for different flows of helium.

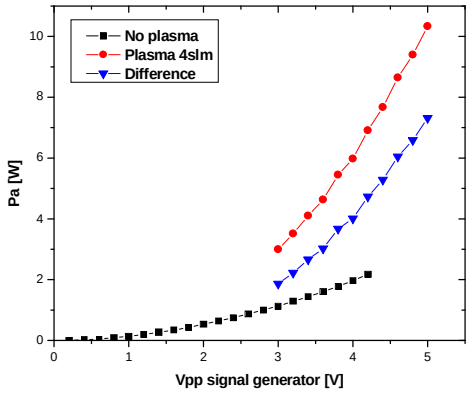

Figure 4. Dependence of the average power and the power difference when the plasma is on and off as the function of voltage at the signal generator.

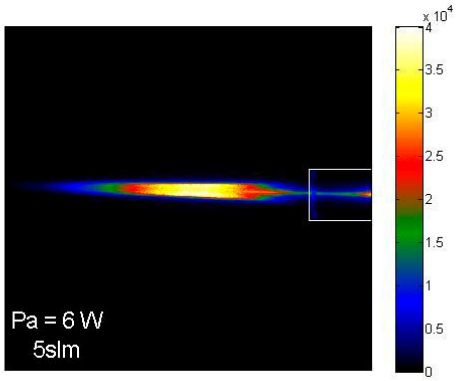

Figure 5. Plasma jet at 5 slm of helium, 6 W, exposure time 6 ms, gate width 5 ms.

We calculated average powers from signal waveforms when the plasma is on and off and difference between them (see fig. 4). The mean power increases with the increase of the applied voltage. One can see (fig 4.) that power transmitted to the plasma was in the range from 1 to 8 W.

For the exposure times larger than the cycle period (12.5 μs), the plasma looks continuous, like a plume (see fig. 5). The length of the plasma plume is up to five centimeters, depending of the flow rate and applied voltage.

For the time-resolved images, we have used integration on the chip because the light emission in a single shot is not always sufficient to obtain clear images with gate widths less than 25 ns. In figure 7 we show the propagation of the plasma for the entire period of excitation signal (12.5 μs). All images are scaled to the same maximum intensity and they can be compared to each other. We can see that when the current and voltage signals are close to zero, the plasma is not visible. In the negative part of the current and voltage waveforms, the plasma is confined between the electrodes. During the positive part of the waveforms, the plasma is first confined between the electrodes (rising slope) and then, near the maximum of the curves, it leaves the glass tube in the form of a bullet. The dimensions of the bullet are very small, on the order of a few millimeters. We calculated the speed of the bullet at ~20 km/s, depending on the position from the end of the glass tube. The plasma bullet is much faster than the speed of the buffer gas flow (1 to 7 m/s).

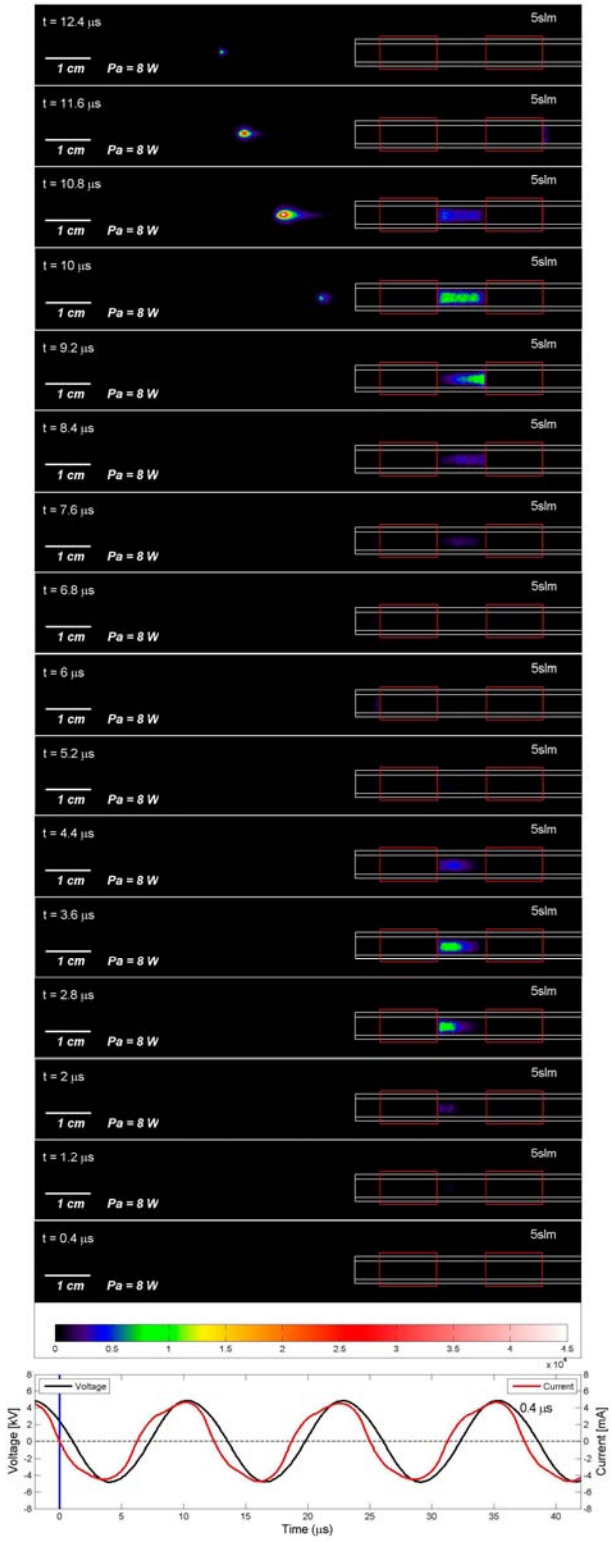

Figure 7. Plasma jet at 5 slm, exposure time 2 ms, gate width 25 ns and gate delay from 0.4 to 12.4 μs.

Fig. 8 shows plasma bullet images obtained for several different flows of gas. We can see that with

the decrease in the He flow, the plasma bullet starts to be elongated, deformed and its intensity is much smaller.

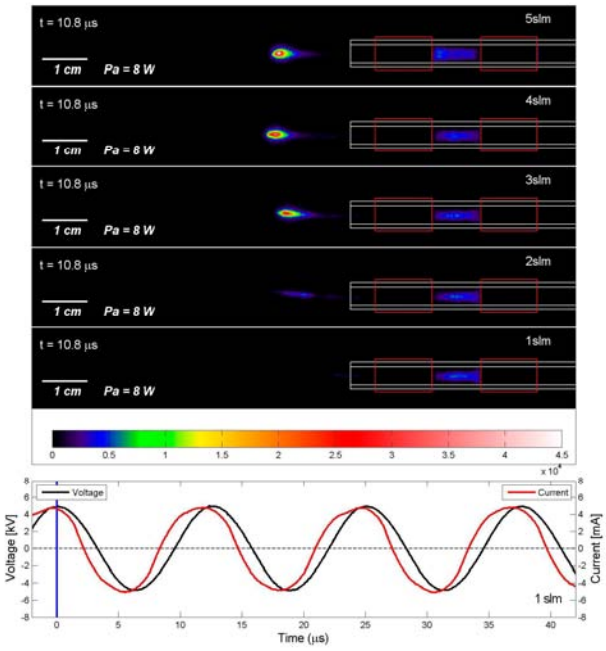

Figure 8. Plasma jet at 1, 2, 3, 4 and 5 slm. Exposure time 2 ms, gate width 25 ns, gate delay 10.8 µs.

4. Conclusion

In this paper we have presented current-voltage characteristics and ICCD images of the atmospheric plasma jet. The results show that our plasma source was not continuous, but it consisted of very small plasma packages that traveled at high speed. By varying the plasma parameters, the length and intensity of the plasma coming out of the tube can be adjusted.

5. Acknowledgement

This research has been supported by the MNTR, Serbia, under the contract numbers ON171037 and III41011.

References

[1] V Schulz-von der Gathen, V Buck, T Gans, N Knake, K Niemi, St Reuter, L Schaper and J Winter, Contrib. Plasma Phys. 47 (2007) 7, 510

[2] E Stoffels, Y A Gonzalvo, T D Whitmore, D L Seymour and J A Rees, Plasma Sources Sci. Technol. 15 (2006) 501

[3] I E Kieft, E P v d Laan and E Stoffels, New J. Phys. 6 (2004) 149

[4] G Fridman, G Friedman, A Gutsol, A B Shekhter, V N Vasiletsm and A Fridman, Plasma Processes and Polymers 5 (2008) 503–533

[5] N Puač, Z Lj Petrović, M Radetić, A Djordjević, Materials Science Forum, 494 (2005) 291-296

[6] S Živković, N Puač, Z Giba, D Grubišić, Z Lj Petrović, Seed Science and Technology 32 (2004) 3, 693-701

[7] N Puač, Z Lj Petrović, G Malović, A Đorđević, S Živković, Z Giba and D Grubišić,J. Phys. D: Appl. Phys. 39 (2006) 3514–3519

[8] V Schulz-von der Gathen, L Schaper, N Knake, S Reuter, K Niemi, T Gans and J Winter, J. Phys. D: Appl. Phys. 41 (2008) 194004

[9] J Shi, F Zhong, J Zhang, D W Liu and M G Kong, Physics Of Plasmas 15 (2008), 013504

[10] S Yonson, S Coulombe, V Leveille and R L Leask, J. Phys. D: Appl. Phys. 39 (2006) 3508–3513

[11] G Fridman, A Shereshevsky, M M Jost, A D Brooks, A Fridman, A Gutsol, V Vasilets , G Friedman, Plasma Chem. And Plasma Process 27 (2007) 163–176

[12] James L. Walsh and Michael G. Kong, IEEE Trans. On Plasma Science, 36 (2008) 4

Mass spectrometric detection of N, O and NO radicals and ions generated by a plasma needle

Conference Paper · July 2009

READS
35

5 authors, including:

Saša Lazović
Institute of Physics Belgrade
70 PUBLICATIONS **212** CITATIONS
SEE PROFILE

Dejan Maletic
Institute of Physics Belgrade
53 PUBLICATIONS **97** CITATIONS
SEE PROFILE

Gordana Malovic
Institute of Physics Belgrade
157 PUBLICATIONS **932** CITATIONS
SEE PROFILE

Zoran Lj Petrović
Institute of Physics Belgrade
510 PUBLICATIONS **5,652** CITATIONS
SEE PROFILE

Mass spectrometric detection of N, O and NO radicals and ions generated by a plasma needle

S. Lazović[1], N. Puač[1], D. Maletić[1], G. Malović[1], Z. Lj. Petrović[1]

[1]*Institute of Physics, Pregrevica 118, 11080 Belgrade, Serbia*

Abstract: Mass spectrometric measurements of atmospheric pressure plasma needle were done both for neutrals (RGA) and ions (SIMS). Yields of N, O and NO radicals were determined for different powers of RF source and helium flow rates. Positive ions generated by plasma needle itself were also measured. Significant conversion of feed gases (nitrogen and oxygen) into radicals N and O, and NO was observed.

Keywords: Atmospheric discharge, plasma needle, mass spectrometry, neutrals, ions

1. Introduction

Interest in the non-thermal atmospheric pressure plasmas began to grow rapidly in the late 1980s and different kinds of atmospheric pressure plasma sources have been developed for various types of applications [1, 2]. Such discharges have drawn considerable attention due to their enormous potential for technological applications mostly in surface modifications. This is especially true for organic materials or living tissues that would be damaged or destroyed by putting them into vacuum chambers.

One of atmospheric pressure devices recently developed is plasma needle. This device is especially convenient for medical applications because of its mild plasma and geometry. Non contact disinfection of dental cavities and wounds and minimum-destructive precise treatment and removal of diseased tissue can be done by a plasma needle [3]. The treatment can be done with less than 0.1 mm accuracy. Biological samples like plant tissue can also be easily treated [4].

For the purpose of successful treatment and comparison of different samples by plasma needle it is necessary to characterize the plasma itself the best way possible. One needs to determine optimal conditions for different types of treatment. Plasma needle can be used both for 'positive' and 'negative' (destructive) treatment. By positive treatment we refer to plasma treatment of cells of mammalian or plant origin where results would be faster growth of cells [4] or programmed death of cells (apoptosis). The same device, but under harsher conditions, can be used for sterilization (bacteria from periodontal pocket).

The standard parameters for treatment of samples are duration of treatment, power transmitted to the plasma and distance of the sample to the tip of the needle. For the power measurements the derivative probes were used. The total power distributed to plasma itself was determined from the recorded voltage and current waveforms.

In order to understand the chemistry in the gas phase and at the surface of the sample a knowledge of the composition of plasma, i.e. of the active species, is needed. Mass spectrometry (MS) is the best method to analyze chemical composition of gases and plasmas. The results are particularly relevant for surface treatment, because mass spectrometer samples the species which arrive at and potentially interact with the surface.

The advance of the differential pumping/evacuating has been already used for mass spectrometric study of atmospheric plasma operated in mixture of helium, nitrogen and oxygen. Stoffels and coworkers investigated various short living nitrogen and oxygen species and their threshold ionization [5] as well as nitric oxide generation by the plasma needle [6]. As the pumping of the mass analyzer affected (turned off) their standard plasma needle these authors have used a significantly larger model of the plasma needle.

Mass spectrometry (HIDEN HPR60) was also used for detection of ions produced both in positive and negative point-to-plane corona discharges in nitrous oxide containing traces of water vapor at atmospheric pressure [7, 8].

In this paper we will present some of the properties of our low temperature atmospheric pressure discharge (plasma needle). We have achieved mass analysis with the standard geometry albeit with a somewhat increased gas flow rate.

2. Experimental set-up

Plasma needle is atmospheric pressure plasma source powered by 13.56 MHz RF generator that operates in a mixture of air and helium. The needle consists of a central tungsten wire (0.5 mm in diameter) placed intside a ceramic tube with slightly larger diameter and both placed inside the glass tube with 6 mm diameter. We have used configuration with the grounded copper ring placed at the tip of the glass tube. The central wire represents the powered electrode and the grounded electrode is the surface

in the vicinity of the plasma needle tip.

The rest of the electrical circuit is the same that we have already used [4] and is shown in Figure 1. Low-temperature RF discharge at 13.56 MHz is generated using a Dressler Caesar 1010 power supply, in combination with Variomatch matching network. In order to increase the peak-to-peak voltage, we have used a custom-made transformer and inserted it between the plasma needle and the RF matching network. Additional element of the circle was dummy load which served as 'power divider' .

Instantaneous voltage and current are monitored using two derivative probes [9] somewhat different from the probes already proposed in the literature. Both probes were placed inside a stainless steel box opposite to each other and as close as possible to the plasma needle. The output of the probes was connected to a digital oscilloscope (Agilent DSO6052A) with the cables of equal length. All waveforms were collected by the computer for further manipulation.

The MBMS (Molecular Beam Mass Spectrum) system incorporates a Hiden EQP mass/energy analyzer. This system consists of two parts: pumping section that has three different pumping stages which makes it possible to work at atmospheric pressures and the detector section which itself works at low pressures. The sampling orifice is the entrance to the first pumping stage and plasma needle is positioned against the orifice. Species created in the discharge are sampled using a triple stage differentially pumped molecular beam inlet system. The sampling orifices are carefully aligned to produce a molecular beam which minimizes the collisions of the sampled particles with each other and with surfaces.

The mass spectrometer is equipped with an internal electron source with variable electron energy, which allows ionization of neutral species (radicals) inside the mass spectrometry device. We have made our measurements of plasma needle discharge in this mode. The recorded positive ion signal in this case is directly proportional to the radical number density.

HPR60 can also operate in the so-called SIMS (Secondary ion mass spectrometry as labeled by manufacturer although the label has very little meaning) mode. In this mode no ions are created in the HPR60 device, in other words all collected ion species come directly from the plasma.

Our measurements were performed on a standard size plasma needle. After some efforts it was possible to operate the mass analyzer under conditions that would not greatly affect the discharge itself. However, we had to increase the gas flow from several 100 sccm to more than 1000 sccm.

3. Results and discussion

We were able to obtain stable plasmas in air-helium atmospheres containing down to 10 % of helium. However, we had to increase the gas flow from several 100 sccm to more than 1000 sccm in order to sustain plasma in the close vicinity of mass spectrometer. Data were collected for different values of plasma parameters such as power, various distances between the needle and the QMS and flow.

When presenting results we have used yields of specific masses (relative contribution to the total signal) instead of counts per second obtained directly from the MBMS to reduce noise induced by temporal variations of the plasma.

The yield was calculated as:

$$Y = \frac{Y^i_{mass}}{\sum_i Y^i_{mass}} [\%] \quad (1)$$

where Y^i_{mass} is the count due to the specific positive species (like N^+, O^+, etc.) and this was divided by the sum of counts for all recorded masses (1–100 amu). Same formula (1) for calculations of yields are used for neutrals and ions created by the plasma.

Neutrals

Neutral radicals formed in the plasma may be detected in the mass analyzer by ionizing them by electron beam. Unfortunately ionization also causes fragmentation of molecules and thus the signal of neutrals is dominated by the ions produced through dissociative ionization. In Fig. 1-3 we show energy dependence of the signal that may be associated with the neutral radicals. As, typically the energy threshold for dissociative ionization of molecules is higher than the threshold for ionization of fragments we may detect the signal between the two energies as the one originating from radicals produced by the plasma. These signals are shown in **Fig.** 1 for N, **Fig.** 2 for O and **Fig.** 3 for NO. We can see that there is a significant dissociation of molecular gases and also that NO radical is formed.

Two possible reactions for forming of NO are:

$$N + O + X \rightarrow NO + X \quad (2)$$

with the recombination rate at temperatures close to the ambient temperature about 10^{-45} m^6s^{-1} [10] and

$$N + O_2 \rightarrow NO + O \quad (3)$$

with rate coefficient of 1.56×10^{-21} m^3s^{-1} at 400 K [11].

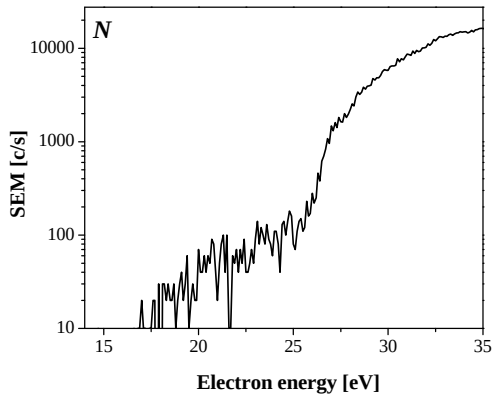

Fig. 1 Electron energy dependence for nitrogen

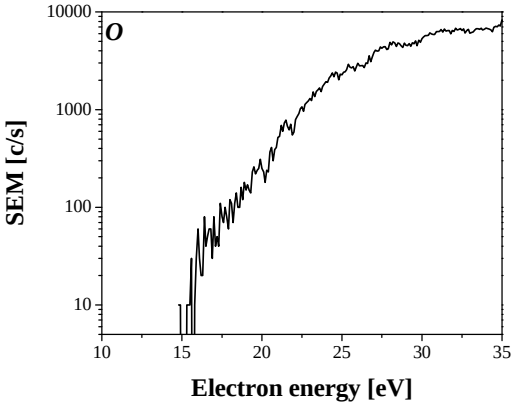

Fig. 2 Electron energy dependence for oxygen

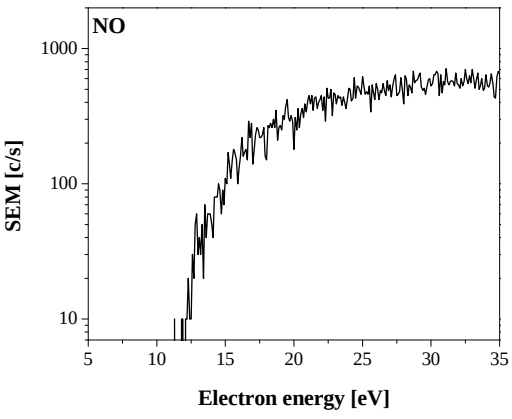

Fig. 3 Electron energy dependence for nitric oxide

Yields for molecular nitrogen and oxygen decrease when the discharge is ignited and these values continue to decrease with the increase of the power transmitted to the plasma (see **Fig.** 4) thus indicating significant depletion of the molecular gases due to dissociation in the plasma.

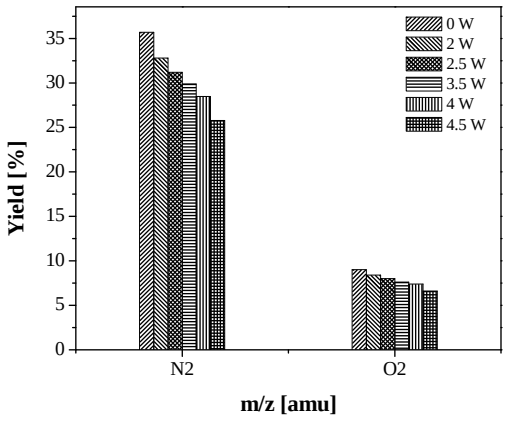

Fig. 4 Yields of N_2 and O_2 for different powers. Distance between tip of the needle and orifice of mass spectrometer was 1.5 mm.

Ions

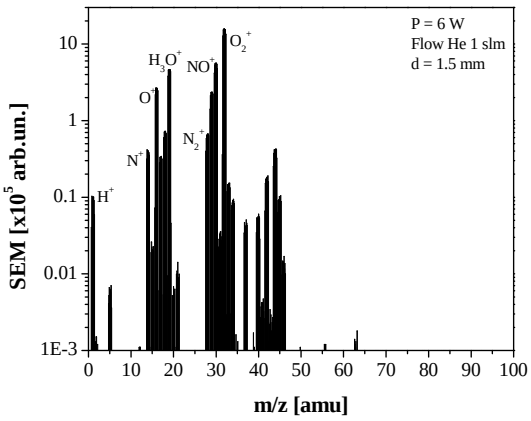

Fig. 5 Ion spectra (ions created in the discharge)

HPR60 mass-energy spectrometer, can operate in the mode without ionization by electron beam which means that collected species in this mode are ions created by the discharge and no ions are created inside the HPR60 device. In **Fig.** 5 ion spectra is shown. We can see that predominant ions created by the plasma are O_2^+, O^+, H_3O^+, N_2^+, N^+, NO^+.

When it comes to plasma treatment of samples of biological origin ions that are of interest are O^+, N^+ and NO^+. We can see that the most abundant ions created in the plasma are NO^+ ions which are believed to be the key

factor in treatment of cells or tissues.

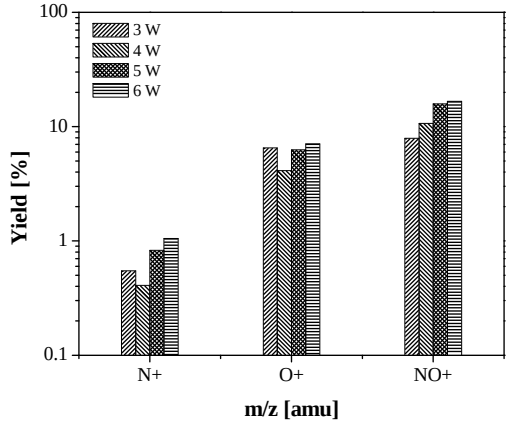

Fig. 6 Yields of N^+, O^+ and NO^+ ions created in the discharge for 4 different powers. Distance between tip of the needle and orifice of mass spectrometer was 1.5 mm.

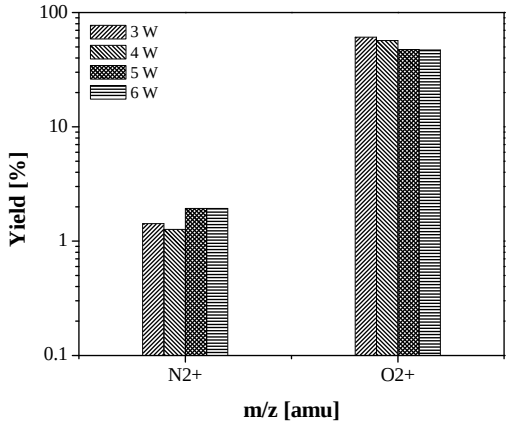

Fig. 7 Yields of N_2^+ and O_2^+ ions created in the discharge for 4 different powers. Distance between tip of the needle and orifice of mass spectrometer was 1.5 mm.

In **Fig.** 6 we show ions measured from the plasma source. One can see that yields for all three ions increase with the increase of the power. Total contribution of NO^+ ion in plasma is about 10-20 %, while the contribution of N^+ and O^+ ions oscillate between 0.5-1 % and 4-7 %, respectively.

When it comes to the molecular ions of N_2^+ and O_2^+ their yields are in the range 1-2 % and 50-60 %, respectively (see **Fig.** 7). While the yield for N_2^+ doesn't change significantly with the increase of the power transmitted to the plasma, yield for O_2^+ decrease with the power increase.

4. Conclusion

Mass spectrometric measurements show significant conversion of feed gases (nitrogen and oxygen) into radicals N and O, and NO molecule which is found to be the dominant reaction product of these reactions. With the increase of helium flow rate the decrease in yields for all three ions was noticed. Transition from unipolar to bipolar mode that was observed by CCD detection of the profile of emission is confirmed through observation of a sudden increase in the yields of the measured species.

References

[1] E. E. Kunhart, IEEE Trans. Plasma Sci. 28, 189 (2000).
[2] A. Fridman, A. Chirokov. A. and Gutsol, Journal of Physics D : Applied Physics, 38(2), R1 (2005).
[3] R.E.J. Sladek and E. Stoffels, J. Phys. D: Appl. Phys., 38, 1716 (2005).
[4] N. Puač, Z.Lj. Petrović, G. Malović, A. Đorđević, S. Živković, Z. Giba and D. Grubišić, Journal of Physics D: Applied Physics, 39, 3514 (2006).
[5] E. Stoffels, Y. Aranda Gonzalvo, T.D. Whitmore, D. L.Seymour and J. A. Rees, Plasma Sources Sci. Technol.,16 , 549 (2007).
[6] E. Stoffels, Y. Aranda-Gonzalvo, T.D. Whitmore, D. L. Seymour and J.A. Rees, Plasma Sources Sci. Technol., 15, 501 (2006).
[7] J.D. Skalny, J. Orszagh, N.J. Mason, J.A. Rees, Y. Aranda-Gonzalvo and Whitmore, Journal of Physics D: Applied Physics, 41, 085202 (2008).
[8] J.D. Skalny, J. Orszagh, N.J. Mason, J.A. Rees, Y. Aranda-Gonzalvo, T.D. Whitmore, International Journal of Mass Spectrometry 272, 12 (2008).
[9] N. Puač, Z.Lj. Petrović, S. Živković, Z. Giba, D. Grubišić and A. Đorđević, Plasma Processes and Polymers, Chap. 15, p. 193. John Wiley, NY (2005).
[10] http://kinetics.nist.gov
[11] J. C. Hewson and F. A.Williams Combust. Flame 117, 441, (1999).

69TH IUVSTA WORKSHOP ON OXIDATION OF ORGANIC MATERIALS BY EXCITED RADICALS CREATED IN NON-EQUILIBRIUM GASEOUS PLASMA

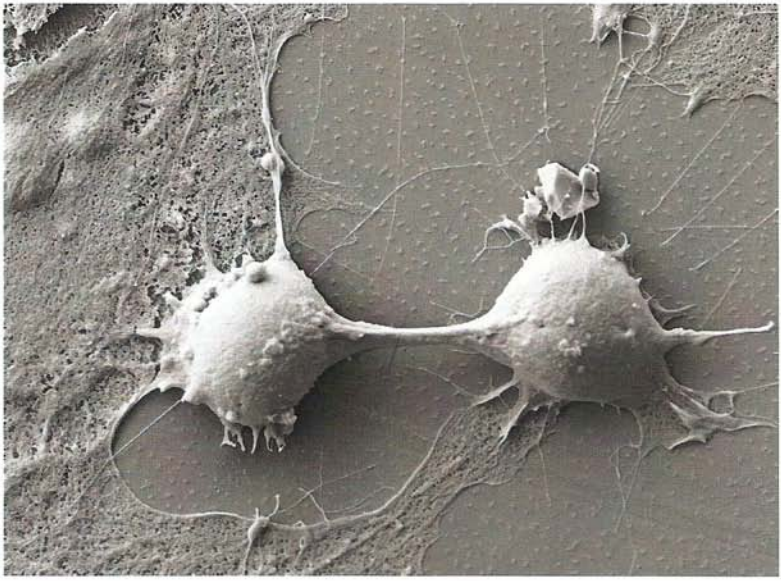

Book of abstracts

69TH IUVSTA WORKSHOP ON OXIDATION OF ORGANIC MATERIALS BY EXCITED RADICALS CREATED IN NON-EQUILIBRIUM GASEOUS PLASMA

ABSTRACTS

December 9th — December 13th 2011, Crklje na Gorenjeskem, Slovenia

Editors of Proceedings: Miran Mozetič and Uroš Cvelbar

Published by: Slovenian Society for Vacuum Technique (DVTS Društvo za vakuumsko tehniko Slovenije), Teslova 30, SI-1000 Ljubljana, Slovenia

Conference Chair:

Miran Mozetič (Slovenia)

Program Committee :

Miran Mozetič, Slovenia (Program chair)
Giorgos Evangelakis, Greece (Program vice chair)
Igor Levchenko, Australia
Primoz Eiselt, Austria
Xiaoxia Zhong, PR China
Masaharu Shiratani, Japan
Mohan R. Sankaran, USA
Mahendra K. Sunkara, USA
Francisco Tabares, Spain
Slobodan Milosevic, Croatia
JJ Shi, PR China
Petr Slobodian, Czech Republic
Shuyan Xu, Singapore

Organizing Committee:

Uroš Cvelbar, Slovenia (Organizing chair)
Ita Junkar , Slovenia (Secretary)
Kristina Eleršič, Slovenia
Saša Lazović, Slovenia
Gregor Filipič, Slovenia
Martina Modic, Slovenia
Gregor Primc, Slovenia
Aleksander Drenik, Slovenia

Organizer:

Društvo za vakuumsko tehniko slovenije (DVTS) - Slovenian Society for Vacuum Technique, Teslova 30, SI-1000 Ljubljana, Slovenia

Sponsors:

International Union for Vacuum Science, Technique and Applications (IUVSTA)
Slovenian Research Agency (ARRS)
Jožef Stefan Institute, Ljubljana, Slovenia
Plasmait

Properties and bio-medical applications of non-thermal plasma

S. Lazović[1,2], N. Puač[1], S. Živković[3], S. Jevremović[3], D. Maletić[1], N. Selaković[1], G. Malović[1], J. Kovač[2], T. Filipič[2], M. Mozetič[2], U. Cvelbar[2] and Z. Lj. Petrović[1]

[1]Institute of Physics, University of Belgrade, Pregrevica 118, Belgrade, Serbia [2]Jožef Stefan Institute, Jamova cesta 39, 1000 Ljubljana, Slovenia [3]Institute for Biological Research 'Siniša Stanković', Bulevar despota Stefana 142, 11060 Belgrade, Serbia

lazovic@ipb.ac.rs

Understanding of the complex mechanisms of interaction between the plasma reactive species and cells is among the major tasks in plasma medicine [1, 2]. Results show that treatment with atmospheric plasma can either improve the growth and development of cells and in some cases induces cells death [3, 4]. In order to investigate this phenomenon, we have used plant callus cells as a model of eukaryotic cells, due to their distinctive features and simplicity in handling. After the plasma treatment with different combination of discharge parameters which yield different plasma parameters (densities of charged species and neutrals, electron energies, UV radiation intensity), we have performed surface analyses (XPS) in order to determine plasma effects on the surface. Consequently we have monitored growth and viability of the callus cells (fresh weight increase, MTT test, fluorescent vital staining techniques).

Plasma treatment of plant tissue is demonstrated on fresh plant calli of Iris germanica var. "HP" (fam. Iridaceae), about 3 mm diameter in size. Calli were grown on Murashige and Skoog (MS) solid medium [5], containing 30 gl-1 sucrose, 7 gl-1 agar, 0.1 gl-1 myo-inositol, 0.1 mgl-1 2.4-dichlorophenoxyacetic acid (2.4-D), 0.1 mgl-1 1-naphthaleneacetic acid NAA, 1 mgl-1 kinetin, 0.25 gl-1 proline and 0.25 gl-1 casein. Callus is a distinctively organized mass of proliferating cells, with specific morphology and anatomy, and may be obtained from almost any type of plant. According to the explants origin (and type of medium) compact or friable calli may be formed [6].

Plasma needle setup used in our previous research [7] was used to treat calli cells. Temperature was monitored not to exceed 40°C and it was found that there is no influence of the helium gas flow and plasma generated UV light (through the quartz window).

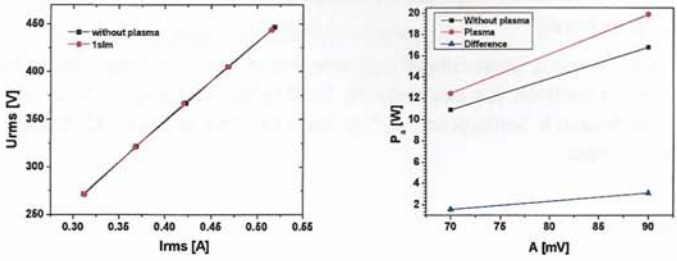

Fig.2. a) V_{rms} as the function of I_{rms}; b) Average power delivered to the plasma (blue line).

Voltage-current characteristics show that the discharge is operating in alpha regime. Derivative probes were used to determine the power delivered to the plasma (see Fig.2. b) blue line). Low powers were used in order to avoid the sample overheating to more than 40°C. It was also found that there is no influence of the helium gas flow and plasma generated UV light.

After the plasma treatment, calli were stained or transferred to fresh half strength MS solid medium (½ of MS salts and vitamins) medium without growth regulators, in order to determine the plasma influence on the fresh weight of the calli. Fresh weight increase of the samples was measured every 7 days during six weeks. Evans blue stain was used for determination of cell death. Calli were transferred to a 2 ml plastic Eppendorf tube and submerged in 0.5 ml of 0.25% Evans blue for 20 min. This led to nonpermeating or exclusion dye leak through ruptured membranes and stained the content of the death cells. Calli were drained and rinsed by distilled water until no further dye eluted from the cells. Untreated plants and calli treated by absolute ethyl alcohol for 6 h represented control and negative control, respectively. Stained calli were observed using light microscopy. Staining of the plant material were repeated six weeks after the plasma treatment using the same protocol. Calli were grown under 16 h day/8 h night photoperiod, light intensity 50 (mol m−2 s−1, and

temperature 25 ± 1 °C. Each treatment was performed in 3 replicates and each experiment was replicated twice.

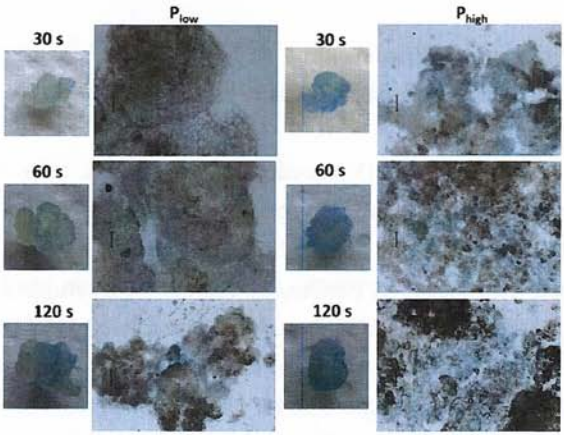

Figure 2. Plasma treatment of iris calli. Samples were stained with 0.25% Evans blue solution for 20 minutes, washed and observed using light microscopy. (Bar = 100 μm).

Parameters such as the power delivered to the plasma, temperature, distance, gas flow rate were measured and optimized so that the treatment of calli of Iris germanica var. "HP" induced minimal injury of the surface plant cells layer, and calli continued their growth. Plasma needle treatment causes enhancement of the fresh weight of the iris calli. Moreover, values of the measured parameter significantly increased with the longer exposure times compared with the untreated samples. Increase of the fresh weight is an implication of calli growth accomplished by a combination of cell division and enlargement. Plasma treatment triggered the enhanced growth of the calli, probably influencing the cell division processes. The cells that divide repeatedly remains essentially meristematic (undifferentiated). These cells are small and oval, forming specific meristematic zones or centers. These zones were not observed in control samples. Furthermore, the XPS results show the increase of O/C ratio which is a sign of surface oxidation of calluses.

Reference

[1] M. G. Kong, G. Kroesen, G. Morfill, T. Nosenko, T. Shimizu, J. van Dijk and J. L. Zimmermann 2009 "Plasma medicine: an introductory review", New J. Phys. Vol. 11, 115012.

[2] D. Dobrynin, G. Fridman, G. Friedman and A. Fridman 2009 "Physical and biological mechanisms of direct plasma interaction with living tissue", New J. Phys. Vol. 11, 115020.

[3] Z. L. Petrović, N. Puač, S. Lazović, D. Maletić, K. Spasić and G. Malović 2012 "Biomedical applications and diagnostics of atmospheric pressure plasma", Journal of Physics: Conference Series Vol. 356, 012001.

[4] S. Lazović, N. Puač, M. Miletić, D. Pavlica, M. Jovanović, D. Bugarski, S. Mojsilović, D. Maletić, G. Malović, P. Milenković and Z. Petrović 2010 "The effect of a plasma needle on bacteria in planktonic samples and on peripheral blood mesenchymal stem cells", New J. Phys. Vol. 12, 083037.

[5] T. S. Murasnige, Folke 1962 "A Revised Medium for Rapid Growth and Bio Agsays with Tohaoco Tissue Cultures", Vol. 15, 473.

[6] K. R. a. Ć. L. Nešković M 2003 Plant Physiology (NNK International) Vol. 387.

[7] N. Puač, Z. L. Petrović, G. Malović, A. Dordević, S. Živković, Z. Giba and D. Grubišić 2006 "Measurements of voltage–current characteristics of a plasma needle and its effect on plant cells", J. Phys. D: Appl. Phys. Vol. 39, 3514-9.

Treatment of Paulownia tomentosa seeds in the low pressure CCP reactor

Conference Paper · June 2012

READS
14

11 authors, including:

Suzana Živković
University of Belgrade
35 PUBLICATIONS **180** CITATIONS
SEE PROFILE

Miran Mozetic
Jožef Stefan Institute
287 PUBLICATIONS **3,708** CITATIONS
SEE PROFILE

Gordana Malovic
Institute of Physics Belgrade
157 PUBLICATIONS **932** CITATIONS
SEE PROFILE

Zoran Lj Petrović
Institute of Physics Belgrade
510 PUBLICATIONS **5,652** CITATIONS
SEE PROFILE

Treatment of *Paulownia tomentosa* seeds in the low pressure CCP reactor

Saša Lazović[1,3], Nevena Puač[1], Dejan Maletić[1], Suzana Živković[2], Zlatko Giba[2], Uroš Cvelbar[3], Miran Mozetič[3], Janez Kovač[3], Tatjana Filipič[3], Gordana Malović[1] and Zoran Lj. Petrović[1]

[1] *Institute of Physics, Univesity of Belgrade, Belgrade, 11070, Serbia*
[2] *Institute for Biological Research 'Siniša Stanković', Univesity of Belgrade, Belgrade, 11060, Serbia*
[3] *Jozef Stefan Institute, Ljubljana, 1000, Slovenia*
E-mail: lazovic@ipb.ac.rs

Previous studies of the effects of non-thermal low pressure plasma on seeds as well as detailed experimental setup can be found elsewhere [1]. In order to learn how plasmas affect human tissues full elucidation of mechanisms of plasma effects on simpler living systems would be helpful. Here we present results of air plasma treatment of *Paulownia tomentosa* seeds in the cylindrical asymmetric CCP reactor at 200 mTorr. Significant improvement of germination is observed and the effect is strongly depending on the duration of plasma exposure. After the treatment XPS and SEM EDXS analysis were performed. From the SEM EDXS images we can see the porous structure of the seeds (see Figure 1).

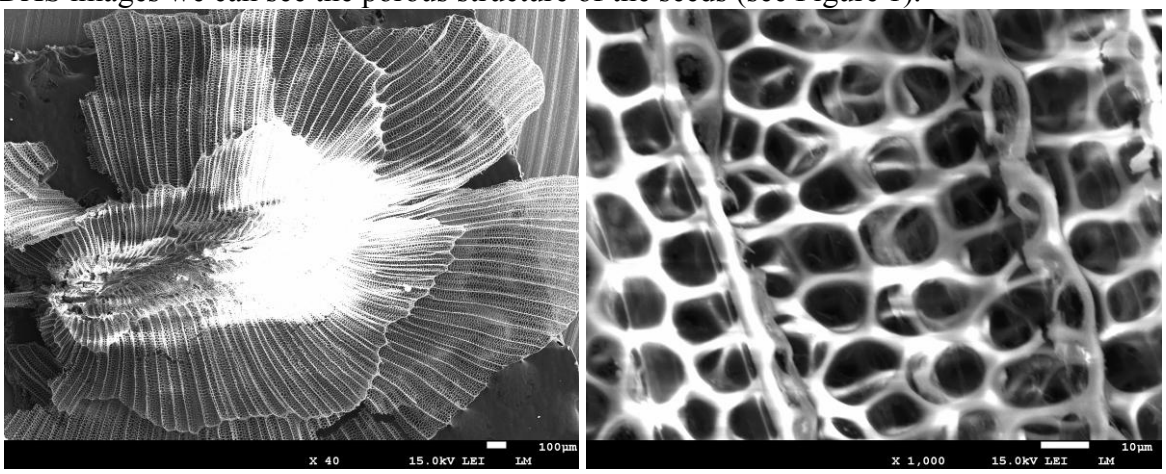

Figure 1: *SEM EDXS on Paulownia tomentosa seeds (*x*40 left,* x*1000 right, 15 kV)*

Based on the XPS results we can see that O/C ratio is increasing with the treatment time which leads to the conclusion that the air plasma is inducing the surface oxidation of the seeds. For shorter treatment times (1, 5 min) N concentration at the surface is increased, as well as, potassium concentration which cannot be observed in control samples. The effect on the germination increase can be explained by increase in N and O concentrations on the seed's surface after plasma treatment. Further optimization of the plasma effects on the seed can be achieved by adjusting the power, pressure, gas composition and the distance of the samples from the powered electrode.

This research has been supported by the MES Serbia, project III41011 and ON171037.

References

[1] Puač N., Petrović Z.Lj., Živković S., Giba Z., Grubišić D. and Đorđević A.R., Plasma Processes and Polymers, Eds. R. d'Agostino, P. Favia, C. Oehr and M.R. Wertheimer, Whiley (2005) p 193-203,

Time-resolved optical emission imaging of an atmospheric plasma jet for different electrode positions with a constant electrode gap

Article *in* Plasma Sources Science and Technology · February 2015

Impact Factor: 3.59 · DOI: 10.1088/0963-0252/24/2/025006

7 authors, including:

Dejan Maletic
Institute of Physics Belgrade
53 PUBLICATIONS **97** CITATIONS
SEE PROFILE

Saša Lazović
Institute of Physics Belgrade
70 PUBLICATIONS **212** CITATIONS
SEE PROFILE

Gordana Malovic
Institute of Physics Belgrade
157 PUBLICATIONS **932** CITATIONS
SEE PROFILE

Zoran Lj Petrović
Institute of Physics Belgrade
510 PUBLICATIONS **5,652** CITATIONS
SEE PROFILE

Time-resolved optical emission imaging of an atmospheric plasma jet for different electrode positions with a constant electrode gap

2015 Plasma Sources Sci. Technol. 24 025006

(http://iopscience.iop.org/0963-0252/24/2/025006)

IOP Publishing Plasma Sources Science and Technology

Plasma Sources Sci. Technol. **24** (2015) 025006 (9pp) doi:10.1088/0963-0252/24/2/025006

Time-resolved optical emission imaging of an atmospheric plasma jet for different electrode positions with a constant electrode gap

D Maletić[1], N Puač[1], N Selaković[1], S Lazović[1], G Malović[1], A Đorđević[2,3] and Z Lj Petrović[1,2,3]

[1] Institute of Physics, University of Belgrade, Pregrevica 118, 11080 Belgrade, Serbia
[2] School of Electrical Engineering, University of Belgrade, Bul. kralja Aleksandra 73, 11000 Belgrade, Serbia
[3] Serbian Academy of Sciences and Arts, Knez Mihajlova 35, 11001 Belgrade, Serbia

E-mail: dejan_maletic@ipb.ac.rs

Received 13 August 2014, revised 4 November 2014
Accepted for publication 5 January 2015
Published 3 February 2015

Abstract

The aim of this paper is to determine the influence of the position of the electrodes on the range of a plasma jet, for specific experimental conditions, by using time-resolved optical emission spectroscopy. The optimal position of the electrodes is determined for a fixed gas flow rate and applied excitation voltage. We characterize the helium plasma jet for different distances from the end of the glass tube, showing detailed results for four different electrode positions from the jet nozzle (7, 15, 30 and 50 mm). It was found that at the distance of 15 mm, the length of the plasma jet is at its maximum. The highest speeds of the plasma package travelling outside the glass tube of the atmospheric plasma jet are obtained for the same electrode configuration (15 mm from the jet nozzle). With the electrodes positioned at smaller distances from the nozzle, the plasma plume was much shorter, and at the larger distances the plasma did not even leave the glass tube.

Keywords: plasma jet, ICCD, time resolved, optical emission spectroscopy

(Some figures may appear in colour only in the online journal)

1. Introduction

Interest in plasma jets that operate at atmospheric pressure has been increasing in research literature in the last decade because of possible applications and also because of their unique characteristics and interesting physics. The most important characteristic of these atmospheric pressure plasma jets (APPJs) is low gas and ion temperature and abundant plasma chemistry. Atmospheric plasma jets produce relatively high concentrations of reactive chemical species, such as atomic oxygen and nitrogen, OH radicals, NO_x and ozone [1].

It is important to understand plasma jets because of their wide range of possible application in the new, fast developing field of plasma medicine [2] and treatment of organic materials [3]. In stomatology, plasma was used in the removal of biofilms of bacteria responsible for the formation of dental plaque and caries [4–7] and also for the sterilization of bacteria responsible for periodontitis [8, 9]. Plasma sterilization of surgical instruments and heat sensitive implants [10, 11] is more efficient than using classical methods such as thermal and chemical sterilization. It is shown that the plasma can also accelerate blood coagulation, speeding up wound healing. It can also kill and remove cancer cells [2, 12–14]. Because of the fungicidal and antimicrobial properties of plasmas, low temperature plasmas may be used in dermatology for healing some chronic skin diseases that are non-sensitive to standard drugs [15].

Some of the pioneering work in the field has been done using a plasma needle, which, although it appears to be similar to plasma jets, has a different electrode configuration [3] and

regime of operation. Still, a large, perhaps even the largest, percentage of activities in plasma medicine are currently based on plasma jets. Many authors have reported results obtained by using various types of plasma jets. These jets can be divided into several groups using several criteria: operating gas, excitation frequency, type of excitation signal, electrode type and geometry. A noble gas, such as helium or argon, is usually used as the operating gas [16, 17] to reduce the breakdown voltage. Gas mixtures were used in order to control the concentration of desirable active species. Usually a small amount (∼1%) of oxygen or nitrogen is added to pure argon or helium. Multiple bullets can appear in a single tube configuration too, by adding small amounts of nitrogen to helium feed gas. In this case, up to eight bullets are reported [18]. Air impurities such as water vapour can also affect plasma propagation and the production of reactive species [19, 20]. The operating frequency can be in the kilohertz, megahertz (13.56 or 27.12 MHz) or gigahertz domain, while the driving signal can be pulsed or sine wave [21, 22]. There are three main groups of electrodes that are typically used in plasma jet devices. The first type is with the electrodes separated from the buffer gas by an insulator, usually a glass tube [23] or capillary [24]; the second type is when they are in contact with the buffer gas [25]; and the third type is when the powered electrode is in contact with the buffer gas and the grounded electrode is isolated from the gas [26]. The electrodes can be cylindrical [27], flat [28], ring shaped [29], needle like [30], etc. Apart from results on systems with different electrode geometries, in the literature results obtained using different geometries of the glass tubes/gas flow may be found. While it has not been reported in most papers that a discharge may go beyond the grounded electrode (as observed by us), in [31] it is reported that in a T-shaped configuration, bullets appear at two ends of the tube asynchronously. This is, however, in both cases, motion of the bullet downstream. The electrode gap, geometry, frequency and type of gas used determine the behaviour of the plasma jet. These parameters have a large impact on the breakdown voltage, operating mode (chaotic, bullet or continuous [26]), voltage–current characteristics, dissipated power in plasma and the effluent length.

Several well-known techniques, such as optical emission spectroscopy, absorption spectroscopy, mass spectrometry, laser spectroscopy and electrical probes, can be used for the characterization and diagnostics of plasma jets. Fast time resolved ICCD imaging is the easiest way to investigate time/space development of plasma. From these high-speed images, it can be seen that plasmas in plasma jets are not always continuous. They sometimes appear to travel in a form of small plasmas that propagate from the glass tube filled with a flow of helium into the surrounding atmosphere [23]. These plasma packages, the so-called 'plasma bullets' or PAPS (pulsed atmospheric pressure streamers) [32], are not yet fully understood. Several theories explaining the formation of these fast travelling plasma packages have been proposed [23, 29, 33]. There have been some attempts to simulate the 'plasma bullets' as positive streamers [34], but there is some discrepancy between the simulation and experimental data [35–38]. It is assumed that photons and Penning ionization [39, 40] play the main role in the propagation of 'plasma bullets'.

In our previous paper, we have presented formation and time/space development of 'plasma bullets'. The powered electrode was 5 mm from the edge of the glass tube and the electrode gap was 15 mm [40]. The point of that paper was to show the operation of a plasma jet with transparent electrodes, so that the development of the plasma could be followed at all times. The aim of this study is to take advantage of the technique presented earlier and provide systematic experimental data over a wider range of configurations and operating conditions. Apart from providing such data in order to provide theory with well-defined data that may be used for qualitative and even quantitative comparisons, we also try to determine the optimal distance of the electrodes from the edge of the glass tube at a constant electrode gap in order to obtain the largest plasma range for the conditions of our plasma source.

2. Experimental setup

A low temperature atmospheric plasma jet that can operate in the 'bullet mode' has been briefly described in [40]. The plasma jet consists of a Pyrex glass tube (inner diameter 4 mm and outer diameter 6 mm) and two transparent electrodes that allow the observation of plasma development inside the electrodes. The electrodes were made of polyethylene terephthalate (PET) covered with a thin conducting film of indium tin oxide. The electrodes were 15 mm wide with the inter-electrode gap of 15 mm. These dimensions were kept constant in the measurements. The electrode closer to the end of the glass tube was connected to the power source (powered electrode). The second electrode was connected through a resistor of 100 kΩ to the ground. Figure 1 shows an ignited plasma jet with the instruments used in the experiment. The parameter that was varied was the distance between the powered electrode and the external edge of the glass tube. We have followed the development of the plasma plume by varying the geometry for many geometries with 1 mm steps; we chose to only present the data for the four dimensions as selected in the text. Above 30 mm, the plasma did not leave the glass tube. Below 30 mm it did, and the maximum range occurred at 15 mm. Here we will show results for distances of 7, 15, 30 and 50 mm.

The operating frequency of the plasma jet was 80 kHz, adjusted by a signal generator. In order to power the plasma jet, the signal generator was connected to a custom built amplifier. The amplifier can produce voltages up to 1 kVpp, which is insufficient for plasma ignition. Therefore, an additional HV transformer was connected after the amplifier so that the voltage was increased up to more than 7 kVpp. Two commercial voltage probes were used for the current and voltage characterization of the system. The average power was calculated from the current and voltage signals obtained by these two probes. In all measurements, the amplifier power was kept at the constant value of 4 W. A very important note is that using a sinusoidal voltage simplifies the electrical power

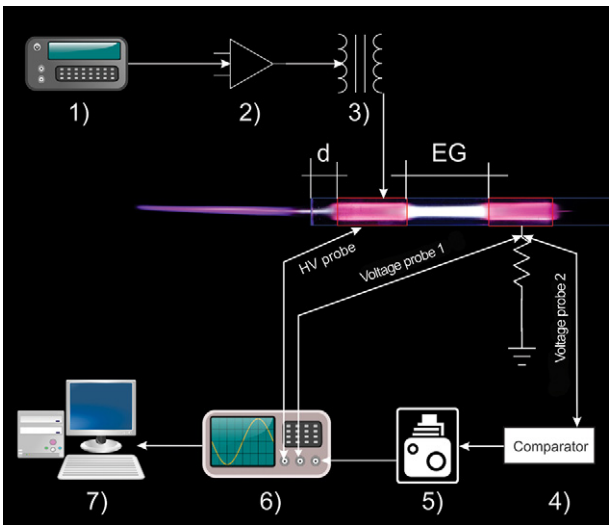

Figure 1. Experimental setup: (1) signal generator; (2) amplifier; (3) high-voltage transformer; (4) voltage comparator; (5) ICCD camera; (6) oscilloscope; (7) computer. EG = electrode gap (15 mm) and d = distance between the powered electrode and the edge of the glass tube (d = 7, 15, 30 and 50 mm).

supply and most measurements, but it also limits the range of plasma bullets (ionization fronts).

We had to introduce the third voltage probe in order to synchronize the ICCD camera (Andor iStar DH734I) with the driving signal of the plasma jet. This probe was connected at the same point in the electrical circuit as the probe for measuring the voltage on the 100 kΩ resistor (voltage probe 2 in figure 1). The signal taken from this probe was introduced in a custom built voltage comparator. The voltage comparator enables triggering of the camera in each cycle (12.5 μs) of the signal while keeping the relative time within the cycle. The stability of the voltage comparator is important since the ICCD camera has to record 160 images during the adjusted exposure time of 2 ms, while keeping the 25 ns gate width. All these single images were then integrated at the chip of the ICCD camera and transferred to the computer by Andor software. The position of the gate was scanned over the whole period of 12.5 μs using the camera's internal delay generator. Thus, the emission over the duration of the entire period was recorded. We have checked our integration and timing jitter by comparing the single shot and the averaged recordings and looked for a change in shape or timing, which turned out to be negligible. In our experimental conditions presented in this paper we have always had only one PAPS formed during one cycle. The moment of formation corresponded to the voltage maximum. The results were experimentally reproducible and there was no evidence of the formation of multiple bullets. In all experiments, helium was flowing through the glass tube at the constant rate of 4 slm (standard litre per minute).

3. Results and discussion

3.1. Images for different distances between the electrodes and the edge of the tube

In this section, we show ICCD images for four different distances between the electrodes and the edge of the glass tube,

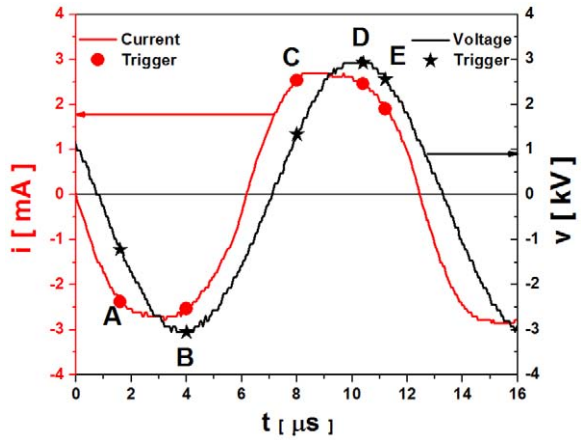

Figure 2. Current–voltage signals with trigger positions (for the distance of 15 mm). One period is 12.5 μs.

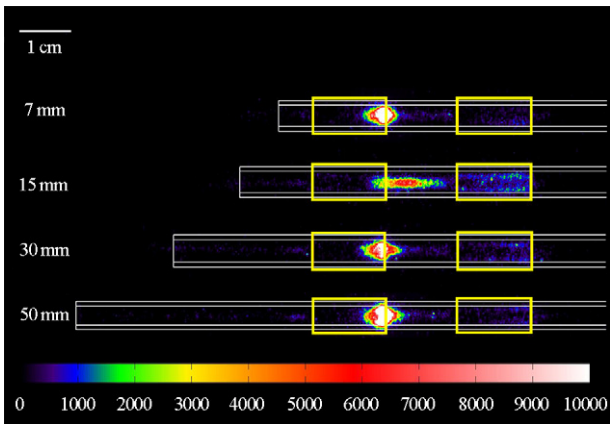

Figure 3. Time-resolved ICCD images at A (1.6 μs).

along with the current and voltage signals with the triggering positions marked that correspond to the timing of those images. The current and voltage signals with the triggering positions A (1.6 μs), B (4.0 μs), C (8.0 μs), D (10.4 μs) and E (11.2 μs) for the gap of 15 mm are shown in figure 2. The beginning of the period is chosen to be in the downward slope of the current and the voltage, when current is close to zero and the voltage is about 1 kV. The voltage signal is a pure sine wave, while the current signal is slightly deformed due to the superimposing of the plasma jet current on the displacement current. (The displacement current is observed directly when there is no plasma.) The peak-to-peak values of the voltage and current are 7 kV and 6 mA, respectively.

In figure 3 we show the emission intensities taken for the triggering time of 1.6 μs after the beginning of the period (point A in figure 2). For this trigger time, the voltage signal is negative and at about one half of its amplitude, while the current signal reaches its maximum negative value. For all cases except for the distance of 15 mm, plasma is formed at the right edge of the powered electrode and fills the tubes almost uniformly. For the distance of 15 mm, however, plasma is somewhat shifted towards the grounded electrode and the main emission originates between the electrodes. It almost appears that the development at 15 mm is slightly ahead of those for other distances.

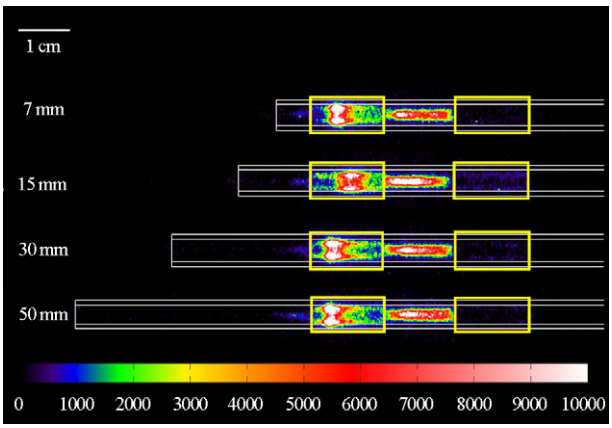

Figure 4. Time-resolved ICCD images at B (4.0 μs).

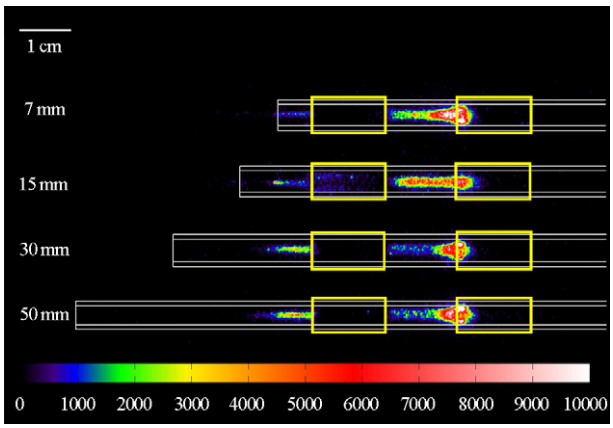

Figure 5. Time-resolved ICCD images at C (8.0 μs).

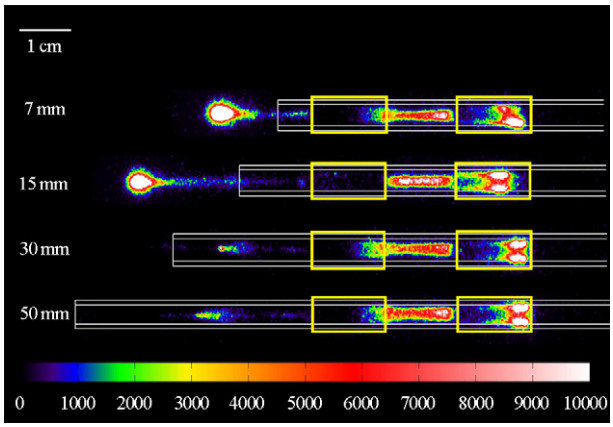

Figure 6. Time-resolved ICCD images at D (10.4 μs).

If we move further along the voltage/current cycle, the ionization wave indicated by the light emission starts propagating inside the powered electrode from its right edge to the left one (downstream of the helium flow and towards the exit of the tube). These images are shown in figure 4 and correspond to the triggering point B in figure 2. For this current/voltage combination, the plasma (as indicated by light emission) inside the powered electrode peaks close to the inner surface of the glass tube and has a ring-like shape. At the same time, the emission intensities originated from between the electrodes indicate that the plasma (emission) is confined at the axis of the glass tube. Comparing the images shown in figure 4, we can see that the plasma behaviour is again similar for all distances except for 15 mm. In the latter case, the position of the maximum emission inside the powered electrode is lagging compared to the results for the distances of 7, 30 and 50 mm. At the same time, the discharge for 15 mm appears to be ahead of other discharges in between the electrodes.

At 8.0 μs (C in figure 2), the voltage is at one half of its amplitude and the current is almost at the maximum in the positive half-cycle. Plasma in the inter-electrode gap reaches the left edge of the grounded electrode (see figure 5) and extends inside. At the same time, inside the powered electrode there is almost no light emission (for 7, 30 and 50 mm) except for the distance of 15 mm, where emission is detected inside the powered electrode. At this point, a PAPS precursor is being formed. We can see that there is a plasma channel connecting the tip of the plasma with the powered electrode. This channel is much stronger when the electrodes are further away from the edge of the glass tube and the ambient air. For the two smaller distances (7 and 15 mm), this channel produces weaker emission, but we can see that plasma is already in contact with ambient air, and PAPS are being formed. At the same time, for the distance of 15 mm, one can see a transition from a hollow emission distribution (peaking close to the wall–wall hugging) to the single peak on the axis in the transition when plasma leaves the electrode. In other words, the wall-hugging emission profile occurs when there is a conducting electrode on the other side of the glass.

When the voltage signal reaches its maximum, the PAPS is already formed and for the distances of 7 and 15 mm it is already travelling outside of the glass tube (see figure 6). For longer distances (30 and 50 mm), we only see the precursor inside the tube travelling downstream of the helium flow. It is also obvious that at the moment of departure of the plasma from the tube, it starts moving faster and becomes brighter. Whatever the explanation for the brighter glow of the plasma (Penning ionization mentioned in [40] and elaborated on in [39] or field distribution [41, 42]), the formation of the brighter region requires some time after the departure from the tube and it appears to be connected to the origin of plasma, thus supporting the streamer-like explanation. In the grounded electrode, the wall-hugging plasma propagates with varying velocities and a possible breakdown of symmetry occurs in one case.

Finally, the plasma reaches its maximum range when the voltage and current start to drop. This case is denoted by the point E (11.2 μs) in figure 2. ICCD images for this triggering time are presented in figure 7. The two bullets formed for shorter distances are progressing further away and dimming. We can see that for a distance of 30 mm, the plasma reached the edge of the glass tube with an indication of growth in brightness, whereas for 50 mm it is still inside the tube. For both these distances, the bright plasma ball (bullet) did not form as a separate plasma package outside the glass tube at any moment during the whole period of 12.5 μs, although a continuous development inside the tube is observable. As for the grounded electrode, the discharge has reached its end, but it does not seem to penetrate any further.

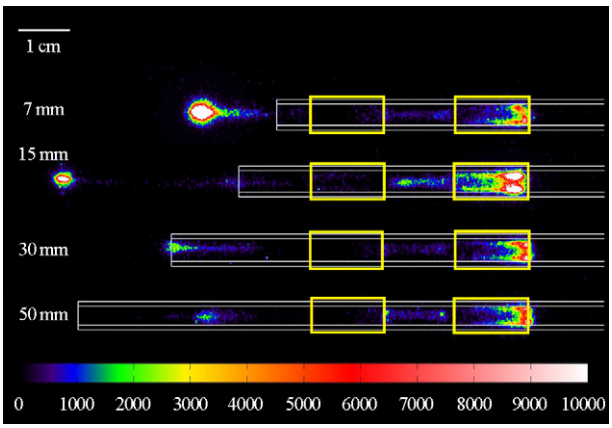

Figure 7. Time-resolved ICCD images at E (11.2 μs).

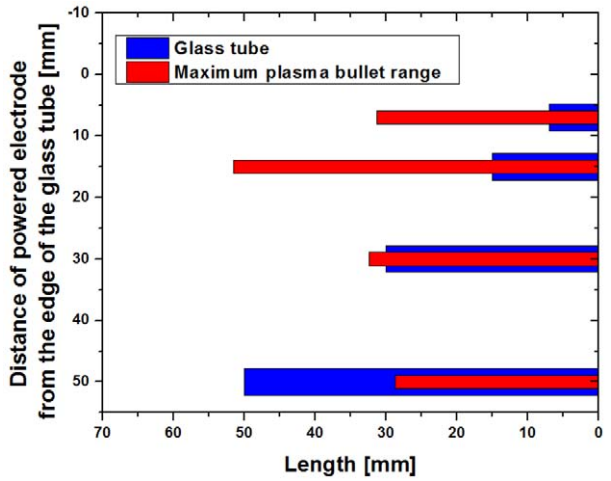

Figure 8. Maximum plasma bullet range.

The maximum ranges that plasma packages can reach are shown in figure 8. We repeat that the development of the bullet may be extended further by a pulsed dc power supply that would allow the existence of the potential gradient at the edge for a longer time. For clearer presentation, we present a histogram graph showing the maximum ranges of the plasma package and the positions of the glass tube. The maximum ranges are obtained from the corresponding ICCD images at 11.2 μs (point E in figure 2). The range is measured as the distance from the left edge of the powered electrode to the left edge of the plasma bullet. The left edge of the bullet was determined in such a way that the intensity of the measured points was not below 2000 a.u. The maximum range reached by the plasma bullet is almost the same when the distances are 7, 30 and 50 mm, and it is about 30 mm. For the distance of 15 mm, the plasma reaches a radically larger range of approximately 50 mm.

The main difference in results among all presented configurations is the maximum travelling range of PAPS. As can be seen from figure 8, the optimal distance of the powered electrode for the maximal plasma range is at 15 mm from the edge of the glass tube. Hence, this particular case will be presented in more detail.

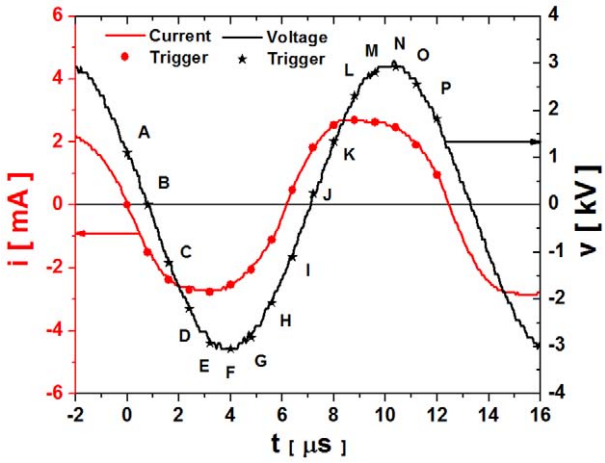

Figure 9. Current–voltage signals with trigger positions.

3.2. The optimal position of the electrodes

Current and voltage waveforms with marked triggering positions of the ICCD camera are shown in figure 9. The ICCD images (figure 10, left column) were taken for the delays from 0.0 to 12.0 μs, with a step of 0.8 μs, to provide detailed time development of the plasma jet. Each image and profile correspond to the letters (A–P) on the current–voltage signal. Axial profiles (figure 10, right column) of the plasma light emission along the glass tube axis were calculated from the obtained ICCD images. The presented profiles are calculated as a sum of the light emission coming from the plasma along the axis of the glass tube. The right edge of the grounded electrode was used as the zero distance. The position of the edge of the glass tube was at 6 cm.

In the downward slope of the current and voltage signal (A–E in figures 9 and 10), the plasma emission is mainly originating from within the electrode gap. As current reaches its maximum negative value, the discharge enters the powered electrode, taking the form of a ring shape. From the emission intensity profiles (figure 10, axial profiles A–E), we can see that the highest intensity inside the powered electrode is at the moment when the plasma is forming at the right edge of the electrode ($D = 2.4\,\mu$s in figure 10). After that moment, the plasma starts to move inside the powered electrode along the surface of the glass tube in the same direction as the helium gas flow. One should bear in mind that the transparency of the electrode film is less than 100%. With the movement of the plasma inside the powered electrode, the emission intensity is decreasing both inside the electrode and in the electrode gap (figure 10, $E = 3.2\,\mu$s to $I = 6.4\,\mu$s). This coincides with the increase of the current and voltage in the negative part of the period (see figure 9).

The positive part of the period of the voltage starts with the point J in figure 9. Now the discharge is almost extinguished inside the powered electrode and the main emission originates from the electrode gap. With the increase in the voltage signal, the discharge is formed at the left edge of the grounded electrode (figure 10, $K = 8.0\,\mu$s). The discharge inside the grounded electrode behaves similarly at some points as in the powered electrode. It is ring-shaped and travels through the

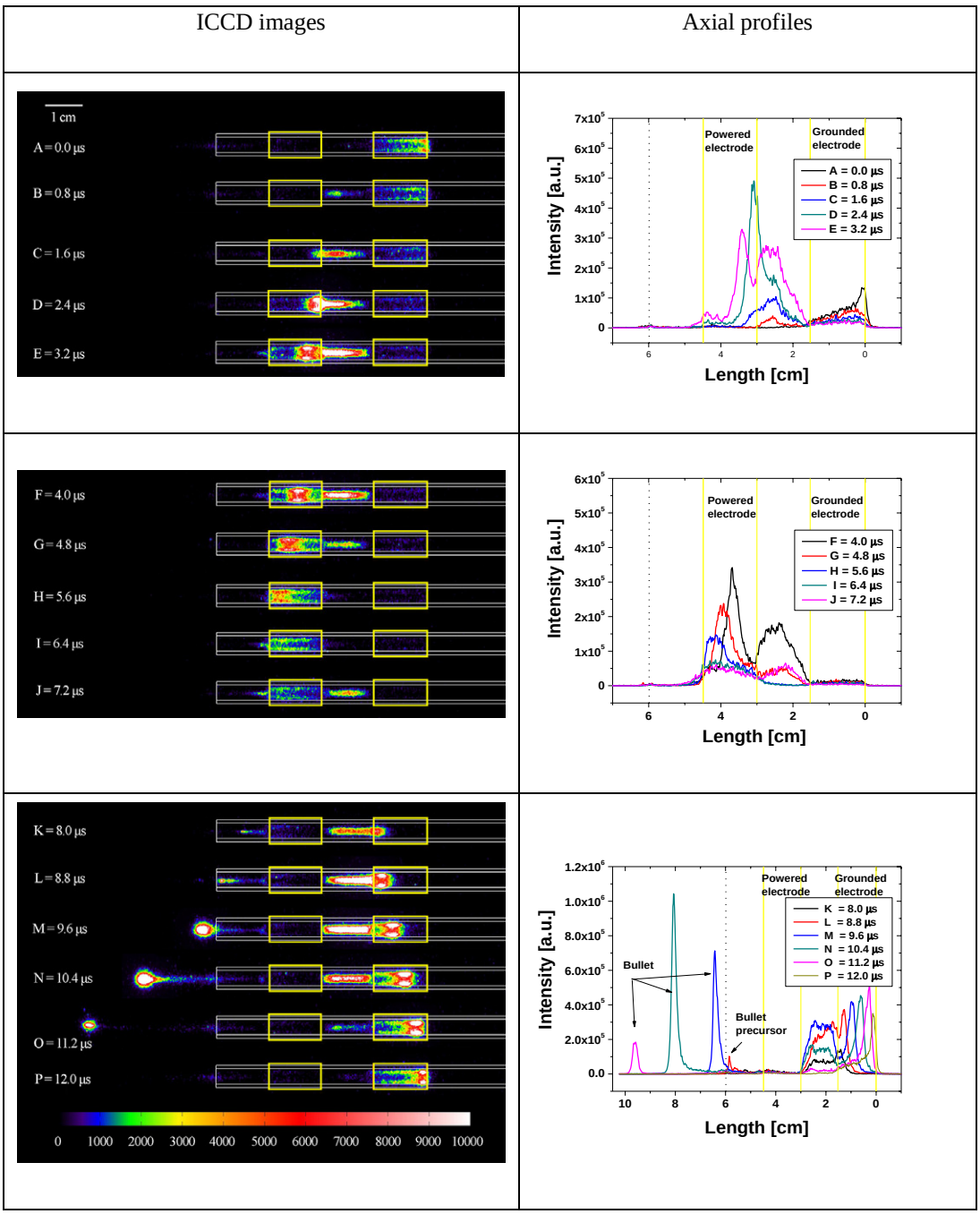

Figure 10. Time-resolved ICCD images for delays 0–12.0 μs (left) and axial light emission profiles for delays 0.0–12.0 μs (right), for 4 slm and power of 4 W.

electrode along the wall of the glass tube. The differences are that in the case of the grounded electrode, the discharge moves contrary to the gas flow and the maximal intensity of the discharge profile increases with the movement (figure 10, K–P axial profiles). In the case of both electrodes, the maximum emission intensity is always at the edge that is further away from the edge of the glass tube. At the same time, when the discharge enters the grounded electrode, a part of the discharge starts to travel away from the powered electrode and towards the exit of the tube (figure 10, $K = 8\,\mu$s). While it travels through the glass tube, we can see that the highest emission is originating from the head of the formed plasma with a low-intensity tail behind (figure 10, K, L images and profiles). We could say that a precursor is formed which will turn into the high-speed travelling package of plasma when it leaves the glass tube. Only upon exiting the glass tube, the plasma significantly expands in volume and the light intensity rises by several orders of magnitude. It appears that the main reason for a fast increase in the emission and volume of the plasma is the contact of excited helium atoms and metastables with molecules of nitrogen and oxygen from the ambient air [38, 39]. However, it appears that the field distribution outside the tube provides a greater potential drop at the front and thus increases ionization considerably.

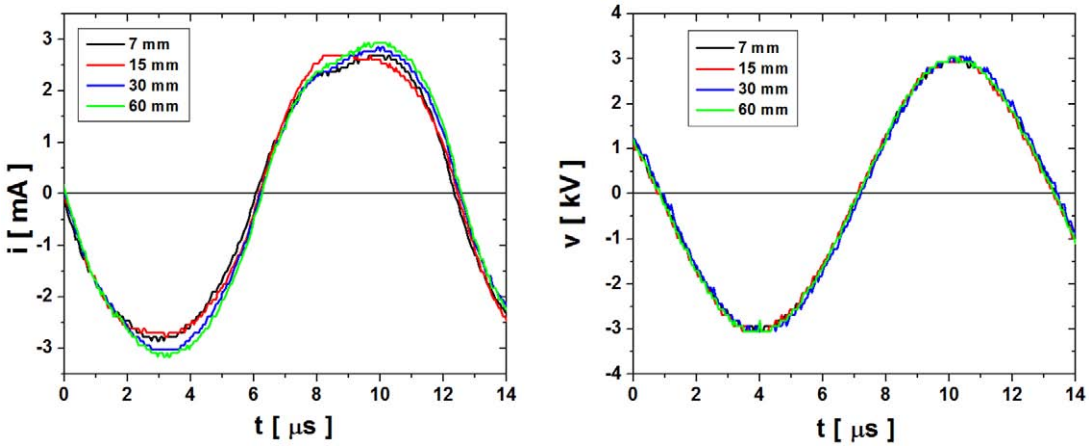

Figure 11. Comparison of current (left) and voltage (right) waveforms for different distances between the electrode and the edge for the glass tube. The flow of the helium was 4 slm.

The propagation of the plasma package in the open air can be explained as propagation of a positive streamer [19, 34]. The peak emission intensity of the propagating streamer is obtained for the delay of $N = 10.4\,\mu$s. We can see that the highest intensity position corresponds to one half of the maximum distance travelled by the plasma. At this point, it is clearly seen that the ionization front is still connected to the main discharge inside the jet tube with a thin, hardly visible and apparently conductive, tail (figure 10, N). With further movement of the ionization front, this conductive tail is diminishing, accompanied by the diminishing intensity of the emission coming from the travelling plasma package. When the ionization front is at the maximal distance from the tube, the emission intensity is low and the plasma tail is thin. We have to point out that from the moment when the plasma package leaves the glass tube and enters surrounding air until the extinguishing of the package, the package appears to be constantly connected to the main discharge inside the tube with a long, streamer-like plasma tail.

The main difference that we have observed between the 15 mm configuration and other configurations is in the current waveform. It is smaller in amplitude during the negative part of the waveform compared to the signal for the other three configurations (see figure 11). Also, the positive peak of this waveform leads the other peaks (obtained for 7, 30 and 50 mm). This difference can be seen in more detail in the frequency domain. For the case of 15 mm, the 2nd and 4th harmonics are smaller in intensity compared to the same harmonics for other configurations. We can see that there is no significant difference between the voltage signals for different configurations. The main conclusion that can be drawn here is that the characteristics of the plasma jet and the plasma packages are influenced by the configuration of the electrodes, i.e., their dimensions and the distance from the mixing point of working noble gas with air. Also, the same system can be tuned by adjusting the electrode configuration with no need to change any component in the power supply system.

3.3. Velocities

The velocities of the emission peaks were determined (calculated from the ICCD spatial emission profiles at different times) for the propagation of plasma through the powered, grounded electrode and outside the glass tube (figure 12). The velocity of the ionization front in the powered electrode starts to rise from the right edge of the electrode. At about 4 mm from the edge it reaches the speed of 4 km s^{-1}. The velocity is almost constant until the ionization front reaches the left edge of the electrode. The propagation direction of the ionization wave is downstream of the helium flow. When the electrode is grounded, the ionization wave starts to accelerate from the left edge of the electrode and reaches the speed of 4 km s^{-1} at 2 mm from the edge of the electrode. The velocity is almost constant until the plasma reaches the centre of the electrode. Thereafter, it starts to accelerate again and reaches the maximal speed of 5 km s^{-1}. Near the edge of the grounded electrode, the ionization front starts to rapidly slow down. The propagation of the ionization wave inside the grounded electrode is upstream of the helium flow. We have performed several experiments where we varied the helium flow while keeping the electrode geometry constant. These results are not in the scope of this paper. We have seen that helium flow does not influence the propagation velocity of PAPS outside the glass tube, but greatly influences its range.

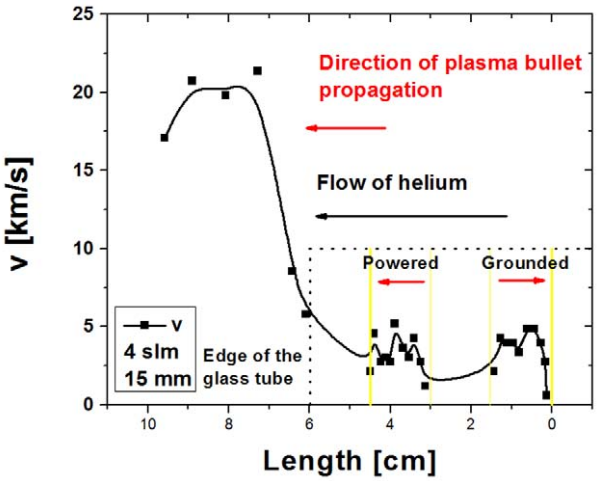

Figure 12. Plasma velocity inside and outside glass tube.

Velocity outside the glass tube rises from the edge of the glass tube and reaches its maximum of approximately 20 km s^{-1} at the distance approximately 15 mm from the edge of the glass tube. The velocity is constant from 15 to 30 mm and thereafter it starts decreasing. The larger velocities outside the glass tube than inside may be due to the changes in the composition of the medium through which the plasma propagates. In the tube, we have pure helium, and outside the tube components of air diffuse into the stream of helium that leads to new and complex reactions in the plasma. Nevertheless, studies like this one, and quantitative comparison of models with the experimental data may be the best way to investigate these plasmas.

4. Conclusion

In this paper, we have shown results of optical emission spectroscopy for four different configurations of a plasma jet. In all configurations, the distance between the powered and grounded electrode was kept constant, while the distance of the electrodes from the edge of the glass tube was varied. Measurements were taken for distances of 7, 15, 30 and 50 mm from the edge of the glass tube.

Several conclusions can be drawn from the presented data that can be applied to all electrode configurations:

- while inside the electrodes, the plasma has a ring-like shape and it is mainly travelling along the walls of the glass tube;
- inside the glass tube (not in the electrode region) plasma is confined to the central axis of the tube and the main emission originates from that volume;
- only when the plasma comes into contact with the ambient air does the volume of discharge increase and the plasma form a sphere-like shape before it starts to travel in the open air;
- in all cases when PAPS is formed, we have seen that it has a trail of very small emission that 'connects' it with the main discharge inside the tube; the connection through the weakly lit plasma to the point of origin resembles streamer-like propagation and is consistent with proposed theoretical explanations.

The main difference between the configurations used in these experiments occurred in the maximum range that PAPS can reach before extinction. For the distances of 7 and 15 mm, PAPS is formed and it starts travelling outside the glass tube. In the case of 30 mm, the plasma reaches the edge of the tube, starts to increase in volume, but does not detach from the tube in order to start travelling in the open air. For 50 mm, the plasma stays inside the tube throughout the whole period of 12.5 μs. Nevertheless, even if plasma does not leave the glass tube, the maximum distance that it can reach is around 30 mm, which corresponds to the ranges obtained for 7 and 30 mm. Only in the case when electrodes are 15 mm away from the edge of the glass tube, is the maximum travelling range of PAPS 50 mm. However, the travelling speed of PAPS for all configurations is almost the same and in open air it reaches about 20 km s^{-1} (for the 15 mm case, and 17 km s^{-1} for the 7 mm case). One should bear in mind that we can measure the velocity only when the PAPS departs from the edge of the tube. It appears that the propagation of the plasma PAPS for the 7 mm case is slow when the plasma leaves the tube and forms the bullet, which could be related to the distribution of the electric field beyond the edge of the tube.

One could argue that the distribution of the field along the glass tube beyond the powered electrode is a key consideration in establishing the range of plasma bullets. In addition, one should consider that for 15 mm the transit time allows the plasma to leave the tube just when the voltage waveform goes through the maximum at a phase of 1.5π. All of these aspects, and other considerations, may be interpreted as the basis for an explanation within some plasma model that is sufficiently detailed and comprehensive. We hope that our results will promote and support such an analysis and its conclusions.

Acknowledgments

This research has been supported by the Ministry of Education, Science and Technological Development, Republic of Serbia, under projects ON171037 and III41011. ZLjP, NP, GM and SL are also grateful for the support from the NATO SfP 984555. AĐ is grateful for the support from SASA project number F-133 for the provision of additional funds to purchase measurement equipment and generators.

References

[1] Oh J-S, Aranda-Gonzalvo Y and Bradley J W 2011 Time-resolved mass spectroscopic studies of an atmospheric-pressure helium microplasma jet *J. Phys. D: Appl. Phys.* **44** 365202

[2] Fridman G, Friedman G, Gutsol A, Shekhter A B, Vasilets V N and Fridman A 2008 Applied plasma medicine *Plasma Process. Polym.* **5** 503–33

[3] Stoffels E, Flikweert A J, Stoffels W W and Kroesen G M W 2002 Plasma needle: a non-destructive atmospheric plasma source for fine surface treatment of (bio)materials *Plasma Sources Sci. Technol.* **11** 383–8

[4] Latha S 2011 Reviews plasma therapy: an overview *J. Health Sci. Res.* **2** 33–6

[5] Sladek R E J and Stoffels E 2005 Deactivation of *Escherichia coli* by the plasma needle *J. Phys. D: Appl. Phys.* **38** 1716–21

[6] Stoffels E, Sakiyama Y and Graves D B 2008 Cold atmospheric plasma: charged species and their interactions with cells and tissues *IEEE Trans. Plasma Sci.* **36** 1441–57

[7] Kim G C, Lee H W, Byun J H, Chung J, Jeon Y C and Lee J K 2013 Dental applications of low-temperature nonthermal plasmas *Plasma Process. Polym.* **10** 199–206

[8] Lazović S *et al* 2010 The effect of a plasma needle on bacteria in planktonic samples and on peripheral blood mesenchymal stem cells *New J. Phys.* **12** 083037

[9] Miletić M, Mojsilović S, Okić Đorđević I, Maletić D, Puač N, Lazović S, Malović G, Milenković P, Petrović Z L and Bugarski D 2013 Effects of non-thermal atmospheric plasma on human periodontal ligament mesenchymal stem cells *J. Phys. D: Appl. Phys.* **46** 345401

[10] Huang H-M, Hsieh S-C, Teng N-C, Feng S-W, Ou K-L and Chang W-J 2011 Biological surface modification of titanium surfaces using glow discharge plasma *Med. Biol. Eng. Comput.* **49** 701–6

[11] Cao Z, Nie Q, Bayliss D L, Walsh J L, Ren C S, Wang D Z and Kong M G 2010 Spatially extended atmospheric plasma arrays *Plasma Sources Sci. Technol.* **19** 025003

[12] Nastuta A V, Topala I, Grigoras C, Pohoata V and Popa G 2011 Stimulation of wound healing by helium atmospheric pressure plasma treatment *J. Phys. D: Appl. Phys.* **44** 105204

[13] Dobrynin D, Wasko K, Friedman G, Fridman A A and Fridman G 2011 Fast Blood coagulation of capillary vessels by cold plasma: a rat ear bleeding model *Plasma Med.* **1** 241–7

[14] Kim C-H, Bahn J H, Lee S-H, Kim G-Y, Jun S-I, Lee K and Baek S J 2010 Induction of cell growth arrest by atmospheric non-thermal plasma in colorectal cancer cells *J. Biotechnol.* **150** 530–8

[15] Heinlin J, Morfill G, Landthaler M, Stolz W, Isbary G, Zimmermann J L, Shimizu T and Karrer S 2010 Plasma medicine: possible applications in dermatology *J. Dtsch. Dermatol. Ges.* **8** 968–76

[16] Topala I, Nastuta A V, Grigoras C and Dumitrascu N 2011 Helium atmospheric pressure plasma jet: diagnostics and application for burned wounds healing *Plasma for Bio-Decontamination, Medicine and Food Security (NATO Advanced Research Workshop, 15–18 March 2011, Slovakia)* pp 53–4

[17] Kim H, Brockhaus A and Engemann J 2009 Atmospheric pressure argon plasma jet using a cylindrical piezoelectric transformer *Appl. Phys. Lett.* **95** 211501

[18] Park S, Moon S Y and Choe W 2013 Multiple (eight) plasma bullets in helium atmospheric pressure plasma jet and the role of nitrogen *Appl. Phys. Lett.* **103** 224105

[19] Naidis G V 2013 Modelling of OH production in cold atmospheric-pressure He–H_2O plasma jets *Plasma Sources Sci. Technol.* **22** 035015

[20] Murakami T, Niemi K, Gans T, O'Connell D and Graham W G 2014 Afterglow chemistry of atmospheric-pressure helium–oxygen plasmas with humid air impurity *Plasma Sources Sci. Technol.* **23** 025005

[21] Stoffels E 2007 'Tissue processing' with atmospheric plasmas *Contrib. Plasma Phys.* **47** 40–8

[22] Xiong Q, Lu X P, Ostrikov K, Xian Y, Zou C, Xiong Z and Pan Y 2010 Pulsed dc- and sine-wave-excited cold atmospheric plasma plumes: a comparative analysis *Phys. Plasmas* **17** 043506

[23] Shi J, Zhong F, Zhang J, Liu D W and Kong M G M 2008 A hypersonic plasma bullet train traveling in an atmospheric dielectric-barrier discharge jet *Phys. Plasmas* **15** 013504

[24] Oh J, Bryant P M and Bradley J W 2011 Discharge and plasma bullet formation in a capillary DBD atmospheric-pressure microplasma jet *IEEE Trans. Plasma Sci.* **39** 2352–3

[25] Cho G, Lim H, Kim J, Jin D J, Kwon G C, Choi E and Uhm H S 2011 Cold plasma jets made of a syringe needle covered with a glass tube *IEEE Trans. Plasma Sci.* **39** 1234–8

[26] Walsh J L, Iza F, Janson N B, Law V J and Kong M G 2010 Three distinct modes in a cold atmospheric pressure plasma jet *J. Phys. D: Appl. Phys.* **43** 075201

[27] Sands B L, Ganguly B N and Tachibana K 2008 A streamer-like atmospheric pressure plasma jet *Appl. Phys. Lett.* **92** 151503

[28] Knake N, Reuter S, Niemi K, Schulz-von der Gathen V and Winter J 2008 Absolute atomic oxygen density distributions in the effluent of a microscale atmospheric pressure plasma jet *J. Phys. D: Appl. Phys.* **41** 194006

[29] Lu X and Laroussi M 2006 Dynamics of an atmospheric pressure plasma plume generated by submicrosecond voltage pulses *J. Appl. Phys.* **100** 063302

[30] Pipa a V, Bindemann T, Foest R, Kindel E, Röpcke J and Weltmann K-D 2008 Absolute production rate measurements of nitric oxide by an atmospheric pressure plasma jet (APPJ) *J. Phys. D: Appl. Phys.* **41** 194011

[31] Algwari Q Th and O'Connell D 2011 Electron dynamics and plasma jet formation in a helium atmospheric pressure dielectric barrier discharge jet *Appl. Phys. Lett.* **99** 121501

[32] Robert E, Sarron V, Riès D, Dozias S, Vandamme M and Pouvesle J-M 2012 Characterization of pulsed atmospheric-pressure plasma streams (PAPS) generated by a plasma gun *Plasma Sources Sci. Technol.* **21** 034017

[33] Shashurin A, Shneider M N, Dogariu A, Miles R B and Keidar M 2009 Temporal behavior of cold atmospheric plasma jet *Appl. Phys. Lett.* **94** 231504

[34] Naidis G V 2011 Simulation of streamers propagating along helium jets in ambient air: polarity-induced effects *Appl. Phys. Lett.* **98** 141501

[35] Naidis G V 2010 Modelling of streamer propagation in atmospheric-pressure helium plasma jets *J. Phys. D: Appl. Phys.* **43** 402001

[36] Naidis G and Walsh J 2013 The effects of an external electric field on the dynamics of cold plasma jets—experimental and computational studies *J. Phys. D: Appl. Phys.* **46** 095203

[37] Xiong Z and Kushner M J 2012 Atmospheric pressure ionization waves propagating through a flexible high aspect ratio capillary channel and impinging upon a target *Plasma Sources Sci. Technol.* **21** 034001

[38] Breden D, Miki K and Raja L L 2012 Self-consistent two-dimensional modeling of cold atmospheric-pressure plasma jets/bullets *Plasma Sources Sci. Technol.* **21** 034011

[39] Li Q, Zhu W-C, Zhu X-M and Pu Y-K 2010 Effects of Penning ionization on the discharge patterns of atmospheric pressure plasma jets *J. Phys. D: Appl. Phys.* **43** 382001

[40] Puač N, Maletić D, Lazović S, Malović G, Đorđević A and Petrović Z L 2012 Time resolved optical emission images of an atmospheric pressure plasma jet with transparent electrodes *Appl. Phys. Lett.* **101** 24103

[41] Boeuf J P 2011 personal communication

[42] Sakiyama Y, Graves D B, Jarrige J and Laroussi M 2010 Finite element analysis of ring-shaped emission profile in plasma bullet *Appl. Phys. Lett.* **96** 041501

Plasma needle treatment of Staphylococcus Aureus (ATCC 25923) biofilms

Conference Paper · June 2012

READS
47

9 authors, including:

Dejan Maletic
Institute of Physics Belgrade
53 PUBLICATIONS **97** CITATIONS
SEE PROFILE

Saša Lazović
Institute of Physics Belgrade
70 PUBLICATIONS **212** CITATIONS
SEE PROFILE

Gordana Malovic
Institute of Physics Belgrade
157 PUBLICATIONS **932** CITATIONS
SEE PROFILE

Zoran Lj Petrović
Institute of Physics Belgrade
510 PUBLICATIONS **5,652** CITATIONS
SEE PROFILE

Plasma needle treatment of Staphylococcus Aureus *(ATCC 25923)* biofilms

Dejan Maletić[1], Maja Miletić[3], Nevena Puač[1], Nenad Selaković[1], Saša Lazović[1,2], Dragana Vuković[4], Pavle Milenković[3], Gordana Malović[1] and Zoran Lj. Petrović[1]

[1]*Institute of Physics,University of Belgrade, Pregrevica 118, 11080 Belgrade, Serbia*
[2]*Institute Jožef Stefan, Jamova cesta 39, 1000 Ljubljana, Slovenia*
[3]*Faculty of Stomatology, Dr Subotića 8, 11000 Belgrade, Serbia*
[4]*Faculty of Medicine, Dr Subotića 8, 11000 Belgrade, Serbia*

E-mail: nevena@ipb.ac.rs

New atmospheric pressure plasma sources opened a wide range of biomedical applications, such as sterilization of wounds and medical equipment, treatment of dental caries, faster coagulation of blood, etc. In this paper we will present results obtained in plasma treatment of formed and unformed (MRSA) biofilms. Plasma source used for these treatments was plasma needle that was previously used in treatments of planctonic samples containing bacteria [1]. Treatments were carried out on unformed biofilm for three different powers, two different flow rates of helium (0.5 and 1 slm) and several treatment times (10, 30, 60 and 120 s). The mean power was calculated and it did not exceed 2 W in all treatments (which in our experience does not heat the substrate by more than 6-7 degrees). Figure 1. shows comparison of absorbance after treated samples were allowed sufficient time to develop the fully formed biofilm. We can see that the longer exposure times and higher transmitted power to the plasma reduced biofilm production. Plasma treatment is more efficient on unformed than on formed biofilm. For presentation of results we used four categories of biofilm production: no biofilm, weak, medium and strong biofilm [2].

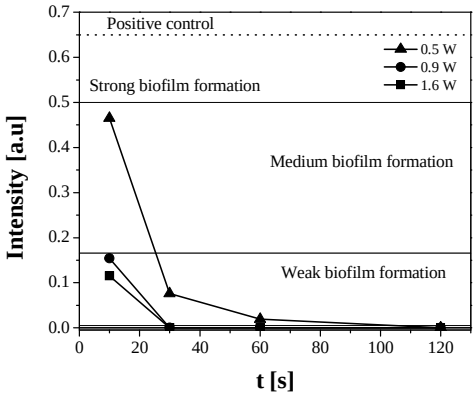

Figure 1: *Optical density apsorbances of biofilm formation after plasma treatment of the biofilm during formation for three different applied powers. The initial concentration of unformed biofilm was 10^6 CFU/ml and flow of working gas was 1 slm.*

This research has been supported by the MES Serbia, project III41011 and ON171037.

References

[1] Lazović S., Puač N., Miletić M., Pavlica D., Jovanović M., Bugarski D., Mojsilović S., Maletić D., Malović G., Milenković P. and Petrović Z., New Journal of Physics (2010), **12**, 083037 (21pp).
[2] Stepanović S., Vuković D., Hola V., Di Bonaventura G., Đukić S., Ćirković I. and Ruzicka F., APMIS (2007), **115**, 891–899.

Development of biomedical applications of non-equilibrium plasmas and possibilities for atmospheric pressure nanotechnology applications

Article · May 2012

DOI: 10.1109/MIEL.2012.6222791

9 authors, including:

Zoran Lj Petrović

Institute of Physics Belgrade

510 PUBLICATIONS **5,652** CITATIONS

SEE PROFILE

Kosta Spasic

University of Belgrade

10 PUBLICATIONS **12** CITATIONS

SEE PROFILE

Nikola D Skoro

University of Belgrade

9 PUBLICATIONS **25** CITATIONS

SEE PROFILE

Gordana Malovic

Institute of Physics Belgrade

157 PUBLICATIONS **932** CITATIONS

SEE PROFILE

Development of Biomedical Applications of Non-equilibrium Plasmas and Possibilities for Atmospheric Pressure Nanotechnology Applications

Z.Lj. Petrović, N. Puač, D. Marić, D. Maletić, K. Spasić, N. Škoro, J. Sivoš, S. Lazović, G. Malović

Abstract - In this paper we discuss the synergisms between different realms of plasma supported nanotechnologies. First the developments in plasma etching for micro and later nanoelectronics have fueled immense growth of knowledge and tools in describing non-equilibrium plasmas. This has led to detailed predictive codes and that knowledge has been used to develop a large number of new sources of non-equilibrium plasmas operating at atmospheric pressure, even in air. With those tools a new front of plasma medicine has opened wide with new possibilities and a number of promising techniques for sterilization, cancer treatment, oral cavity treatment, dermatology and in a range of applications where deposition of thin films for biocompatibility is necessary. This new front opens new possibilities in the realm of nanotechnologies with atmospheric pressure deposition of nano-structures allowing direct application of new techniques in medicine and in cheaper technologies for other purposes.

I. INTRODUCTION

Non-equilibrium plasma etching and related plasma processes [1] have proven to be the key to achieving manufacturing of integrated circuits, adherence to Moore's law and fueling of the global economy through explosion of all fields of economy that may benefit or even be generated with a strong dependence on processing power. The most important steps in developing of modern micro-electronic technology were achieved by empirical industry based research and science came in later to explain. Having said that, we must acknowledge a lot of successes in continuous improvements of the technology that were made, based on scientific development of diagnostics, modeling and fine tuning of key steps, such as multi frequency [2] and pulsed operation [3]. Finally science has made a significant contribution to understanding and removal of defects caused by the plasma itself or by the ever increasing demands in miniaturization. The contribution of science nevertheless boils down mainly to BETTER UNDERSTANDING of non-equilibrium (low temperature, cold...) plasmas. Most directly this understanding spills over to predictive models [1,4,5] that have been developed for complex geometries, complex chemistries and powering sequences and may represent realistically most of the low pressure industry devices.

Z.Lj. Petrović, N. Puač, D. Marić, D. Maletić, K. Spasić, N. Škoro, J. Sivoš, S. Lazović, G. Malović are with the Institute of Physics, University of Belgrade, Pregrevica 118, 11080 Belgrade, Serbia, E-mail: zoran@ipb.ac.rs

At the same time there are constant reminders from the cost aware practitioners that operation of plasma devices is expensive, partly because of the need to have low pressure operation with vacuuming system to ensure the purity of gases. Operating pressures in industry are typically from few to 200 mTorr and purity of the gas that has to be achieved requires pumping down to very low pressures before the gas flow is started. Thus plasma devices operating at atmospheric pressure have been the holy grail of the industry, although some processes are not much cheaper and also cleanliness of substrates may require operation in pure gases maintained in sealed vacuum tight systems (albeit with somewhat smaller restrictions on pumping). Finally vacuum systems make production line manufacturing more complicated. In any case high pressure operation of plasma devices would be a welcome addition to the existing battery of plasma devices that micro-electronics industry has at its disposal.

Nano-particles worthy of scientific interest have been discovered first in atmospheric pressure thermal plasmas, but later non-equilibrium plasmas were shown to give some advantages and additional features [6,7]. While there are other processes that produce nano-particles, still one out of five significant papers in this field comes from the plasma background in one form or the other. Thus nanotechnologies are strongly connected to plasmas, especially non-equilibrium, and in all cases operation at atmospheric pressure would be beneficial.

Atmospheric pressure discharges and plasmas have been known in nature and have been generated by humans for the last 200 and more years. However, most of these plasmas are thermal which in principle means that electrons, ions and gas molecules tend to have the same temperature. When we calculate what is needed for ionization in order to maintain plasma, those are enormous temperatures. Yet maintaining plasma does not require all

978-1-4673-0238-8/12/$31.00 © 2012 IEEE

free electrons to have excessive energies, only a small group in the high energy end of the distribution function needs to have such energies (> 150 000 K), just enough to compensate the losses. Even such "reduced" requirement means that typical atmospheric pressure plasmas have a temperature of 5000 K- 10000 K. In that case, most of the energy invested into plasma goes to heating of gas and walls of the vessel. On the other hand such plasma is very productive, as every collision has a good chance to lead to dissociation needed to initiate chains of chemical reactions [8,9]. In any case, one cannot envisage application of a welding arc for treatment of organic materials or even treatment of living organisms. If applied for plasma etching, thermal plasmas would not provide selective anisotropic etching which is the foundation of our micro-electronics industry.

On the other hand, non-equilibrium plasmas have natural tendency to occur at low pressure, but they allow complete separation of electron kinetics from that of the ions and gas molecules [8]. This allows us to have the former at extremely high temperatures while the latter are essentially at the room temperature. Thus we may treat thermally unstable materials [10,11]. However there is no chance to apply such plasmas on living organisms, as pressures required for such plasmas do not allow living organisms to survive (with exception of some dry seeds and spores) [11,12].

Present is thus a very interesting time in plasma physics as, partly due to saturation of research motivated by micro electronics industry (read draining of the funds), a new front of applications is being developed. This time it is the science that leads the way, fueled by the achievements of the previous period and supported by a promise of significant discoveries albeit in completely different fields [13-17]. Plasma scientists have almost single-mindedly focused on developing new and more practical plasma sources operating at atmospheric pressure and mainly in atmospheric gases [16,17]. At the same time, new fronts of applications open and also the new possibilities in the existing fronts.

First of the two most important motivations stem from a broad range of different, completely different in nature and in the required technology, applications associated with the nano-science (i.e. nanotechnologies). The second, the field of medical and biological (and biotechnical) applications has always been at a back of everybody's mind but little has been initiated from the plasma side. In this paper we shall discuss how motivation to develop new non-equilibrium plasma sources operating mainly in the air has propelled new application fronts in the medicine, biology and what it may offer to nanotechnologies. Finally we shall address possible connections and interdependencies between the two.

II. Non-equilibrium Plasmas at Low and High Pressures

Gas is ionized by applying an external source of energy, typically electric field (although often chemical or nuclear energy may do the trick). In external field a randomly produced electron will initiate an avalanche which may lead to the self sustained discharge and formation of plasmas if all conditions are met. Typically electrons cannot heat up the gas as their momentum transfer in collisions is small due to their low mass. When, however, charged particles have high density, the Coulomb force couples electrons and ions and through a continuous interaction (that may be described as a large number of momentum transfer collisions) ions get accelerated and they heat up the background gas.

At low pressures electrons have a relatively small number of collisions (proportional to the scaling parameter *pd*, where *p* is the pressure and *d* is the characteristic dimension along which field is effective). Electrons gain their energy based on the external field (normalized by the gas number density) *E/N* so that they may ionize (by a very small part of the ensemble from the high energy tail of the distribution) Thus if we plot the breakdown voltage V_B as a function of *pd* (Paschen curve) we have a minimum which gives the electrons, that have just the right number of collisions sufficient to maintain the discharge and the plasma. At lower pressures insufficient number of collisions requires a higher voltage and at higher pressures higher voltage is needed as, in spite of increased number of collisions at that particular *E/N*, the energy of electrons may not be sufficient to ionize.

Plasmas at atmospheric pressure have a tendency to have high densities of charged particles because, at such high pressure, every ionization avalanche produces very rapidly a large degree of ionization, changing completely the conditions and the field distribution. Usually those modes at higher degrees of ionization have more effective production and thus lower operating voltage and they take over above pressures of 100 Torr.

In Figure 1 we show Paschen curve [18] for the breakdown in water vapour. At the upper right end, conditions have been met for a streamer breakdown, which first requires a Townsend like avalanche, but then it has a lower breakdown voltage and dominates the breakdown at higher pressures, including the atmospheric pressure. Breakdown of water is of interest for both, plasma medical applications but also for special treatment of organic materials and related modeling of discharges in realistic atmospheric gas mixtures.

Streamers have sufficient density of charged particles to turn off the external field in its center completely and the ionization is due to the extremely high fields at the plasma edges due to separation of ions and electrons. Photo ionization is supporting the development under some conditions. The plasma channel that develops is highly conductive and once it connects two electrodes large

current flows which again heats up the gas further, heats the cathode and completely changes conditions.

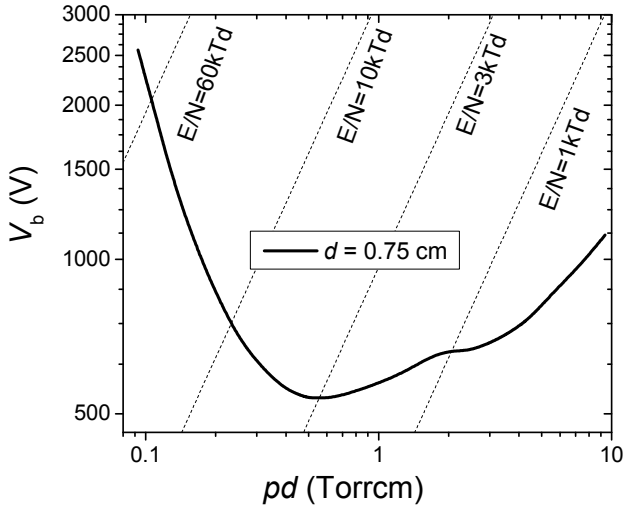

Fig. 1. Paschen curve for parallel plate discharge in water vapour, for standard gaps/pressures. At the right corner the breakdown by streamers is observed, limiting the ability to determine Paschen curve [18].

Even without developing a streamer, a standard non-equilibrium glow discharge first makes transition to the abnormal glow, where effects of excited molecules, heating of the gas and other effects become apparent and when surface of the cathode is heated sufficiently to produce new electrons more efficiently than the standard Townsend's mechanisms. Then, a transition is made to an arc plasma.

All efforts to create atmospheric pressure non-equilibrium plasmas are focused on controlling the excessive ionization growth. Following strategies may be employed:

A. Reduce the Distance

This in essence means that you may move the operating point to *pd* values that do not allow streamers but one needs also to limit the current by a resistor in the external circuit. Thus one may still operate close to the minimum of the Paschen curve [13,14,18].

This is the idea behind micro discharges, a fast growing field of plasma physics that is yet to show its full potential, although judging by Plasma TV cells it has already proved its value. Achieving desirable operation in micro discharges is not easy as the optimum distance for the atmospheric pressure would be around 12 μm. Of course, one may pursue larger gaps of the order of 500 μm, while still being in the optimum range and avoiding unwanted high ionization modes.

Apart from the difficulty to control and properly diagnose such discharges, one has to be aware of the new possible effects due to small distances, such as field emission and even quantum effects (e.g. tunneling) [19].

B. Reduce the Time

Reducing the time allowed to develop the ionization is also a possibility that has been shown to work either on its own (capacitively coupled atmospheric pressure discharge) or in combination with other techniques. Turning the field on and off or using a more practical approach of using RF fields, in both cases give a possibility to use scaling with time ω/N to control ionization. One however enters a different realm of physics, such as RF breakdown, which has its own characteristics and also an option to achieve breakdown without production of secondary electrons at surfaces, (i.e. without electrodes) [20,21].

C. Inhomogeneous Field

The non-equilibrium plasma that has always been present in human experience is corona which is often observed in different forms (St. Elmo's fire). It is formed around a sharp peak or a wire, where field is very inhomogeneous. Thus ionization occurs over a limited gap and, at the same time, a low field is maintained elsewhere to carry the charges and close the current loop. Corona has been discharging our capacitors and all charged objects but has also found a lot of applications, including the purification of air and ion wind which, while potentially useful, is often observed as a kind of a circus attraction.

Normally around the sharp peak a discharge develops (see Figure 2) which is in its properties very much like swarms or Townsend's discharges. It is too weakly ionized to be regarded a plasma. However, often streamers are formed randomly and they consist of real plasma. Both parts of the discharge may be useful in producing charged particles and active species.

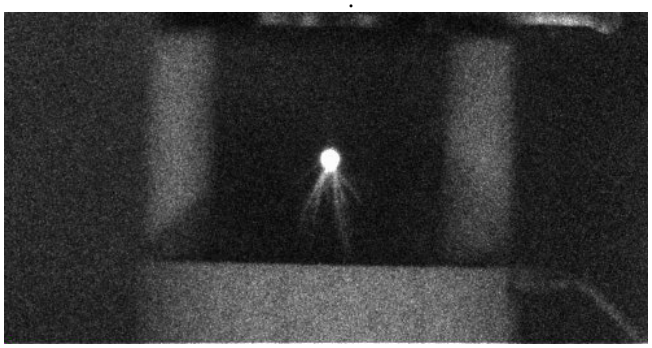

Fig. 2. A point to plane corona discharge developed for sterilization of air.

D. Block the Discharge

The technique employed in the so called Dielectric Barrier Discharges (DBD) is to cover one or both electrodes by a dielectric. Thus, when discharge arrives at the surface, it deposits its charge there and shields the electric field, thereby stopping the discharge altogether. This discharge has been shown to operate in other modes as well, glow and filamentary depending on the conditions.

E. Reduce the Breakdown Voltage

Part of the problem in the air is that it contains oxygen, a very electronegative gas that attaches electrons both at low and moderate energies. This increases the breakdown voltage and the discharge operates at high *E/N* that is prone to fast ionization. When breakdown occurs, it is when ionization overcomes attachment (and other) losses and under such conditions production of electrons can be very fast and lead to sparks, streamers and transition to the arc. The rare gases have lower breakdown voltage as they have no attachment. At the same time, they have no inelastic processes at lower energies and electrons get easily heated to high energies, where they lose energy in electronic excitation. Typically molecular gases present in the air have a lower ionization potential than argon or helium and thus one benefits from starting a discharge in the rare gas and then to mix it with the air [22,23].

F. Remote processing

It is also always possible to use the afterglow, the diffusion (and in some cases combined with flow) that brings active species from the discharge to the region of the treated sample [24]. Nevertheless, one has the same issues about producing and maintaining the plasma at the atmospheric pressure. While this works for deposition of thin films it is of limited use for plasma medical applications except in the case of sterilization.

G. Available plasma Sources for Atmospheric Pressures

In addition to earlier mentioned sources, most other sources apply several principles at the same time. Atmospheric pressure plasma jets and plasma needle use this principle combined with temporal modulation (which is more important for the plasma needle that achieves lower breakdown voltages by operating at RF frequency). In those sources discharge is produced in rare gas and it extends to the region where it is mixed with the air thus producing active radicals. Microwave sources often have spatial limitation in addition to temporal modulation, but also often are used through their afterglow.

In general, atmospheric pressure non-equilibrium discharges are often smaller than desirable, may require additional flow of rare gases and may have higher breakdown voltages and likelihood of sparks than low pressure discharges. Still they produce the same effects as the low pressure discharges; most importantly they produce chemically active plasma without heating of the gas.

Finally a note, even if a discharge operates at atmospheric pressure but in a rare gas for example, the procedure still requires a vacuum tight vessel and also techniques to pass the production line through that. Thus if a low pressure is an option at all, it should be exercised. For example, passage of samples through vacuum chambers has been made extremely efficient in case of plasma nitriding of steel sheaths or treatment of cling foils. However once we developed atmospheric pressure non-equilibrium plasmas, new possibilities of application open and those will be discussed later in this paper.

III. New Results with Atmospheric Pressure Plasma Jet

One of the atmospheric pressure plasma sources has yielded a lot of new, unforeseen effects that warranted detailed, still incomplete, fundamental studies. This source consists of a glass tube which in one end is connected to the source of a rare gas helium (usually). At the other end it is open to the atmosphere and gas flows freely into the air. Close to the open end is a pair of electrodes that have to have sufficient length and gap between them. When a low frequency RF is applied, a plume of plasma is produced that is 5-10 cm in length, that is a non-equilibrium plasma and that, more often than not, actually consists of small plasma bullets passing through the air, i.e. outside the field applied to form the plasma, very rapidly, much faster than the flow of air [25-27]. Voltages required to achieve plasma for APPJ are typically several kV while frequencies vary from 30 kHz to 250 kHz.

The bullets were "shot" towards the air and never against the flow towards the source of gas. On the other hand, it was often found that the bullet's appearance coincided with the establishment of the discharge at the electrode opposite to the exit from the tube, something that could not be easily explained.

In order to follow this phenomenon at all times we have applied transparent electrodes made of Indium Tin Oxide. The observed development of the plasma is shown in Figure 3.

The results show that there is a full continuity of plasma which is formed at the electrode closer to the edge (when it is instantaneous cathode). The discharge expands towards the anode but at the same time hollow cathode like plasma travels along the electrode. It has a circular shape and is close to the walls. When it leaves the electrode plasma reforms at the axis of the tube and proceeds to the edge. Only at the edge a plasma bullet is formed, a much brighter, well defined plasma that begins to move with speed up to 20 km/s which is five time faster than the speed inside the electrode. The coincidence of appearance of the bullet at the same time when plasma develops at the further electrode is due to a slower motion of plasma inside the electrode and tube. Clearly further diagnostics and modeling are required to fully understand the formation and development of plasma bullets, although the first results seem to associate it with the streamers.

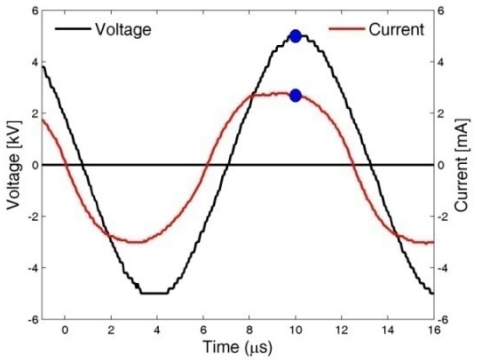

a)

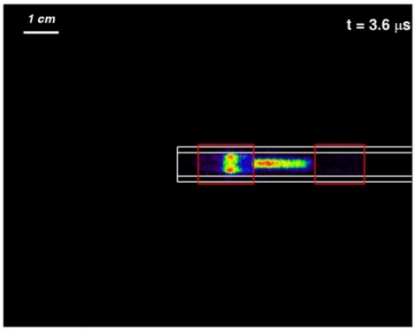

b)

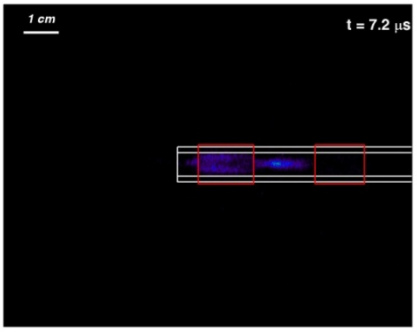

c)

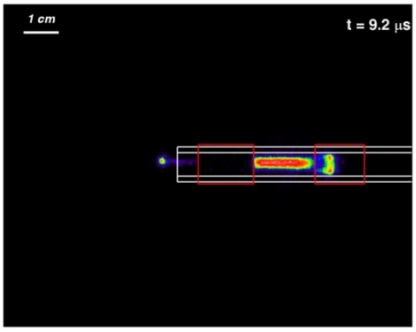

d)

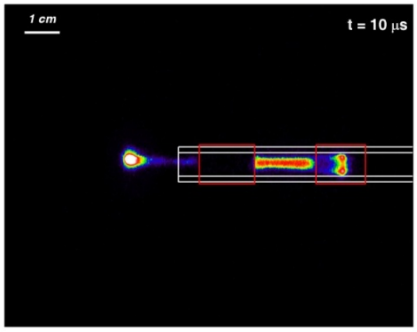

e)

Fig. 3. Development of voltage and current waveforms, the current shows conductive part in phase with the voltage (a) and motion of plasma between two electrodes and inside the powered (closer to the edge of the tube) (b-c), formation of the plasma bullet (d) and its motion outside the tube (e) [28].

IV. Plasma Medicine

In addition to its interesting basic physics APPJ has a potential for medical applications [29]. The field of plasma medicine has exploded in the last 10 years from a trickle to hundreds of publications per year. Number of new group and new directions is also breathtaking. As mentioned above the whole field is fueled by the fundamental advances in development of atmospheric pressure plasma sources, that have been founded on the knowledge on non-equilibrium plasmas developed for the previous round of applications in micro electronics. We will leave a comprehensive literature review for a later publication as this one does not allow enough space.

The first well established application was in sterilization i.e. in destruction of micro organisms. In addition to bacteria [12,29,30], plasmas are equally efficient in removing spores, fungi, viruses and prions. Results of sterilization by using plasma needle of planktonic samples containing 4 different concentrations of *S. aureus* are shown in Figure 4. Also, no form of resistance has been observed. Sterilization may be applied to medical equipment or environment in contact with patients (e.g. surgical equipment, catheters, purification of air, ...). Plasma sterilization is the only technique to remove antibiotic resistant bacteria. One should also be aware that this type of sterilization is quite different from plasma assisted H_2O_2 sterilization where plasma has a secondary role in removing some of the toxic products.

The sterilization has also another important aspect. It has been show that the effect on human cells is much more modest. One can speak of distinct selectivity. This aspect allows application of plasmas for in vivo sterilization, i.e. to treatment of wounds.

Fig. 4. Planktonic samples of S. aureus treated by plasma and afterwards cultivated on growth medium. Flow of He was 1 slm and the power was 1.6 W. Four different initial concentrations of bacteria were used: (1) $12 \cdot 10^8$ CFU/ml; (2) $12 \cdot 10^7$ CFU/ml; (3) 12 10^6 CFU/ml; (4) $12 \cdot 10^5$ CFU/ml.

Wound treatment also has other aspects like a much (40 times) faster blood coagulation. This property is already used in surgery to close the bleeding from blood vessels. Plasma treatment has been shown to be very effective in treatment of wounds, even chronic wounds like those associated with the diabetes. Some of the diseases have been shown to be completely cured (in dermatology), for some standard treatment is facilitated and success rate increased.

A significant success has been achieved in applying plasma to the oral cavity. First it was shown that plasma may remove anaerobic bacteria that lead to the tooth decay without drilling of the healthy tissue. Later it was shown that sterilization of the root canal is very effective and so is fighting against plaque [12] and even ulcers. Finally plasma was shown to be an effective tool for bleaching.

In addition to the oral ulcers, intestinal ulcers have also been successfully treated on laboratory animals. These treatments however require operation. The biggest goal and hope for plasma is the treatment of cancer. It is supported by the achievement of controlled plasma induced apoptosis of cells. These effects were shown again to be selective and affect cancer cells more than healthy cells. Cell cultures were shown to be removed efficiently, even grafted cancers on laboratory animals were shown to be significantly reduced, even cured. Currently the effect of plasma on cancer stem cells is studied with great hope of controlling the secondary tumors.

Surgical application of plasmas that are in non-equilibrium is also of considerable importance. A number of commercial products exist with potential for surgery with minimal blood loss, with the accuracy that rivals or exceeds that of laser surgery. Important advantage of plasma is that it generally leads to less necrosis of cells thus reducing the risks of inflammations. Several devices for specific applications are available including the tool for inducing plasmas in liquids for knee operations [31].

Surgical applications are not exhausted by surgical tools. One may use plasma for efficient tool sterilization and application of such systems to plastic tools extends their life due to reduced thermal strain. Even a hand sterilizer has been developed that is effective in tens of seconds replacing minutes of scrubbing.

Medical applications have a much wider scope than direct use of plasmas directly on the tissue.

For example modeling of radiation damage due to electrons and positrons may be accomplished by the same tools used to model plasmas and following similar principles [32,33]. In fact models of electrons in liquids that are a good model of a tissue are akin to models of ionized gas albeit with slightly modified cross sections in order to take into account scattering of low energy particles on multiple targets.

Treatment of food may be regarded as a prevention, but the principles are the same, from sterilization of packaging to the actual sterilization of the meat or eggs.

Diagnostic tools based on plasmas include proton transfer mass spectroscopy that is able to detect volatile organic compounds in real time without dissociation (and resulting fragment analysis). Analysis of breath may give direct reading of disruptions of metabolism, effects of smoking and pollution, smoking and analysis of food may reduce chances of infection. Finally analysis of toxic fumes due to industrial accidents, war, fires or car accidents helps save humans from possible ill effects of pollutants. A similar method of analysis of fumes is based on Paschen curves [7] for different gases and operation of micro discharges.

Finally one should be aware that plasma may induce unwanted effects such as strand and double strand breaks in DNA [34] and possible toxicity of plasma treatment should be investigated vigorously though no effects have been reported so far.

V. Potential of Atmospheric Pressure Plasmas in Nanotechnologies and Related Applications in Medicine

Plasma treatment of materials has a wide potential for applications in medicine. Reducing the hidrophobicity of polymer surfaces improves sampling in laboratory analysis. On the other hand, hyper hydrophobic surfaces are achieved by nanostructuring. The hydrophobic surface and such materials are difficult to soil and to provide basis for a spread of germs.

Biocompatible coatings are essential for a number of treatments. We would like to draw attention here to two applications. First is treatment of stents by biocompatible coatings, where one requires a micro discharge to deposit the material inside the stent [7].

Another related activity is functionalization of surfaces providing a basis for better adhesion of desired chemicals or particles. For example plasma treated textiles [10] allow binding of large numbers of nano-particles of silver or TO_2 that are bactericidal. Thus textile for surgeons, soldiers or people in food industry may be produced. Same is true for other surfaces and applications.

Functionalization of surfaces is a very wide spread technique in nanotechnologies. In addition to providing bonds between nanotubes or different weakly bound materials, functionalized surfaces may be activated to provide specific tasks. For example treatment of the substrate by plasma increases by a large factor (10 fold) the area of graphene samples produced by a sticky tape technique [35]. At the same time the graphene maybe subsequently coated by specific atoms or radicals using plasma. This would make it sensitive to different organic molecules and could be the basis of sensors, especially sensors for scanning of DNA [36].

By combining nanotechnology and medicine a quest is open for viable biocompatible sensors for human response and nanotubes are the front runners [37]. In that respect plasmas and especially low temperature plasmas may be the best option for growing arrays of nanotubes [38-40] that are coated and functionalized to reduce toxicity and favour certain applications.

Plasma enhanced chemical vapour deposition [PECVD] has been on the forefront of plasma applications in nano-technologies [38]. Mostly PECVD is done at low pressure plasmas and thermal atmospheric pressure plasmas (arcs) have been mostly confined to employing arcs. Applications for small size sensors and targeting of individual cells will require further development of non-equilibrium atmospheric pressure plasmas that would operate within the PECVD scheme or even in a broader context of plasmas used to grow nanotubes or other nano sized structures [41].

ACKNOWLEDGEMENT

This research has been supported by the MES Serbia, under projects ON171037 and III41011.

.

REFERENCES

[1] T. Makabe, Z Lj Petrović, "Plasma Electronics: Application in Microelectronic Device Fabrication", *New York: Taylor and Francis*, 2006.

[2] T. Kitajima, Y. Takeo, Z. Lj. Petrović, and T. Makabe, "Functional separation of biasing and sustaining voltages in two-frequency capacitively coupled plasma", *Applied Physics Letters*, vol. 77, no. 4, pp. 489-491, 2000.

[3] M. Osiac, T. Schwarz-Selinger, D. O'Connell, B. Heil, Z. Lj. Petrović, M. M. Turner, T. Gans and U. Czarnetzki, "Plasma boundary sheath in the afterglow of a pulsed inductively coupled RF plasma" *Plasma Sources Sci. Technol*. vol. 16 pp. 355–363, 2007.

[4] F. Hamaoka, T. Yagisawa, T. Makabe, "Modeling of Si Etching Under Effects of Plasma Molding in Two-Frequency Capacitively Coupled Plasma in SF_6/O_2 for MEMS Fabrication", *IEEE Transactions on Plasma Science*, vol. 35, pp. 1350 –1358, 2007.

[5] P. L. G. Ventzek, R. J. Hoekstra, M. J. Kushner, "Two-dimensional modeling of high plasma density inductively coupled sources for material processing", *J. Vac. Sci. Technol. B*, vol. 12, pp. 461-477, 1994.

[6] K. H. Becker, K. H. Schoenbach, and J. G. Eden, "Microplasmas and applications", *J. Phys. D: Appl. Physics*, vol. 39, pp. R55–R70, 2006.

[7] Z. Lj. Petrović, P. D. Maguire, M. Radmilović-Rađenović, M. Radetić, N. Puač, D. Marić, C. Mahony, and G. Malović, "On Application of Plasmas in Nanotechnologies", in *Nanotechnology for Electronics, Photonics, and Renewable Energy*, A. Korkin, P. S. Krstić and J. C. Wells, Eds., pp. 85-130, New York: Springer, 2010.

[8] Z Lj Petrović, S Dujko, D Marić, G Malović, Ž Nikitović, O Šašić, J Jovanović, V Stojanović and M Radmilović-Radenović, "Measurement and interpretation of swarm parameters and their application in plasma modeling", *J. Phys. D: Appl. Phys.*, vol. 42, 194002 (33pp), 2009.

[9] Z Lj Petrović, M Šuvakov, Ž Nikitović, S Dujko, O Šašić, J Jovanović, G Malović and V Stojanović, "Kinetic phenomena in charged particle transport in gases, swarm parameters and cross section data",*Plasma Sources Sci. Technol*., vol.16, pp. S1–S12, 2007.

[10] M. Gorenšek, M. Gorjanc, V. Bukošek, J. Kovač, Z. Lj. Petrović and N. Puač, "Functionalization of Polyester Fabric by Ar/N2 Plasma and Silver" *Textile Research Journal*, vol. 80, no.16, pp.1633–1642, 2010.

[11] N. Puač, Z. Lj. Petrović, S. Živković, Z. Giba, D. Grubišić and A. R. Đorđević, "Low temperature plasma treatment of dry Empress-tree seeds", *Plasma Processes and Polymers*, Eds. R. d'Agostino, P. Favia, C. Oehr and M.R. Wertheimer, Whiley, pp. 193-203, 2005.

[12] S. Lazović, N. Puač, M. Miletić, D. Pavlica, M. Jovanović, D. Bugarski, S. Mojsilović, D. Maletić, G. Malović, P. Milenković, and Z. Lj. Petrović, "The effect of a plasma needle on bacteria in planktonic samples and on peripheral blood mesenchymal stem cells", *New J. Phys.*, vol. 12, 083037 (21pp), 2010.

[13] D. Marić, N. Škoro, P. D. Maguire, C. M. O. Mahony, G. Malović, and Z. Lj. Petrović, "On the possibility of long path breakdown affecting the Paschen curves for microdischarges", accepted for publication in *Plasma Sources Sci. Technology*, 2012.

[14] Z. Lj. Petrović, N. Škoro, D. Marić, C. M. O. Mahony, P. D. Maguire, M. Radmilović-Rađenović, and G. Malović, "Breakdown, scaling and volt–ampere characteristics of low current micro-discharges", *J. Phys. D: Appl. Physics*, vol. 41, 194002 (5pp), 2008,.

[15] F. Iza, A. Gon Jun Kim , A. Seung Min Lee, A. Jae Koo Lee, A. James L Walsh, A. Yuantao T. Zhang, and A. Michael G. Kong, "Microplasmas: Sources, particle kinetics, and biomedical applications", *Plasma Process. Polym.*, vol. 5, pp. 322–344, 2008.

[16] T. Sato, T. Miyahara, A. Doi, S. Ochiai, T. Urayama, T. Nakatani, "Sterilization mechanism for Escherichia coli by plasma flow at atmospheric pressure", *Appl. Phys. Letters*, vol. 89, pp. 073902, 2006.

[17] M. Laroussi, "Nonthermal Decontamination of Biological Media by Atmospheric-Pressure Plasmas: Review, Analysis, and Prospects", *IEEE Trans. Plasma Sci*, vol. 30, no. 4, 1409-1415, 2002.

[18] N. Škoro, D. Marić, G. Malović, W. G. Graham, and Z. Lj. Petrović, "Electrical Breakdown in Water Vapor", *Phys. Rev. E*, vol. 84, 055401 (4pp), 2011.

[19] M. Radmilović-Radjenović and B. Radjenović, "Theoretical study of the electron field emission phenomena in the generation of a micrometer scale discharge" *Plasma Sources Sci. Technol.*, vol. 17, 024005 (5pp), 2008.

[20] A. V. Lisovskiy and V. D. Yegorenkov, “RF breakdown of low-pressure gas and a novel method for determination of electron-drift velocities in gases” *J. Phys. D, Appl. Phys*., vol. 31, no. 23, pp. 3349–3357, 1998.

[21] M.Savić, M. Radmilović-Radjenović, M. Šuvakov, S. Marjanović, D. Marić, Z.Lj. Petrović, “On Explanation of the Double-Valued Paschen-Like Curve for RF Breakdown in Argon”, *IEEE Trans. Plasma Sci*., vol. 39, no. 11, pp. 2556 - 2557, 2011.

[22] E. A. Sosnin, E. Stoffels, M. V. Erofeev, I. E. Kieft, and S. E. Kunts, “The effects of UV irradiation and gas plasma treatment on living mammalian cells and bacteria: A comparative approach”, *IEEE Trans. Plasma Sci*., vol. 32, no. 4, pp. 1544–1550, 2004.

[23] V Schulz-von der Gathen, L Schaper, N Knake, S Reuter, K Niemi, T Gans and J Winter, “Spatially resolved diagnostics on a microscale atmospheric pressure plasma jet”, *J. Phys. D: Appl. Phys.* vol. 41 pp.194004, 2008

[24] K. Kutasi and J. Loureiro, “Role of the wall reactor material on the species density distributions in an N_2–O_2 post-discharge for plasma sterilization”, *J. Phys. D: Appl. Phys*., vol. 40, pp. 5612-5623, 2007.

[25] J. Shi, F. Zhong, J. Zhang, D. W. Liu and M. G. Kong, “A hypersonic plasma bullet train traveling in an atmospheric dielectric-barrier discharge jet”, *Phys. Plasmas*, vol. 15, no. 1, 013504 (5pp), 2008.

[26] N. M. Bourdet, M. Laroussi, A. Begum and E. Karakas, “Experimental investigations of plasma bullets”, *J. Phys. D: Appl. Phys*., vol. 42, no. 5, 055207 (7pp) , 2009.

[27] G. V. Naidis, “Simulation of streamers propagating along helium jets in ambient air: Polarity-induced effects”, *Appl. Phys. Lett.*, vol. 98, no. 14, 141501(3pp), 2011.

[28] N.Puač, D. Maletić, S. Lazović, G. Malović, A. Đorđević and Z. Lj. Petrović, “Time resolved ICCD images of an atmospheric pressure plasma jet with transparent electrodes” submitted 2012.

[29] M. Laroussi, D. A. Mendis, and M. Rosenberg, “Plasma interaction with microbes”, *New J. Phys*., vol. 5, no. 1, pp. 41.1-41.10, 2003.

[30] M. Laroussi, “Low Temperature Plasma-Based Sterilization: Overview and State-of-the-Art”, *Plasma Process. Polym.*, vol. 2, pp. 391-400, 2005.

[31] K. R. Stalder, G. Nersisyan, and W. G. Graham, “Spatial and temporal variation of repetitive plasma discharges in saline solutions”, *J. Phys. D: Appl. Physics*, vol. 39, pp. 3457–3460, 2006.

[32] A Banković, S Dujko, R D White, J P Marler, S J Buckman, S Marjanović, G Malović, G Garcıa and Z Lj Petrović, “Positron transport in water vapour” *New Journal of Physics*, vol. 14, 035003 (23pp), 2012.

[33] G.Garcia, Z Lj Petrović, R White, S Buckman “Monte Carlo Model of Positron Transport in Water: Track Structures Based on Atomic and Molecular Scattering Data for Positrons” *IEEE Trans. Plasma Sci*., vol. 39, pp. 2962 - 2963, 2011.

[34] D. O’Connell, L. J. Cox, W. B. Hyland, S. J. McMahon, S. Reuter, W. G. Graham, T. Gans, and F. J. Currell "Cold atmospheric pressure plasma jet interactions with plasmid DNA". *Appl. Phys. Lett.*, vol. 98, pp.043701, 2011.

[35] G. Isić, M. Jakovljević, M. Filipović, D. Jovanović, B. Vasić, S. Lazović, N. Puač, Z. Lj. Petrović, R. Kostić, R. Gajić, J. Humliček, M. Losurdo, G. Bruno, I. Bergmair, and K. Hingerl, “Spectroscopic Ellipsometry of Few-Layer Graphene”, *J. Nanophoton*., vol. **5**, pp.051809, 2011.

[36] S. Joseph,W. Guan, M. A Reed, and P. S Krstic, “A long DNA segment in a linear nanoscale Paul trap”, *Nanotechnology*, vol. 21, pp. 015103 (10pp), 2010.

[37] K. Balasubramanian, M. Burghard, “Biosensors based on carbon nanotubes”, *Anal. Bioanal. Chem*., vol. 385, no. 3, pp. 452-468, 2006.

[38] M. Meyyappan, L. Delzeit, A. Cassell and D. Hash, “Carbon nanotube growth by PECVD: a review”, *Plasma Sources Sci. Technol*., vol. 12, pp. 205–216, 2003.

[39] B. K. Kenneth Teo, D. B. Hash, R. G. Lacerda, N. L. Rupesinghe, M. S. Bell, S. H. Dalal, D. Bose, T. R. Govindan, B. A. Cruden, M. Chhowalla, G. A. J. Amaratunga, M. Meyyappan and W. I. Milne, “The Significance of Plasma Heating in Carbon Nanotube and Nanofiber Growth”, *Nano Letters*, vol. 4, no. 5, pp. 921-926, 2004.

[40] M. Meyyappan, “Carbon Nanotubes: Science and Applications”, New York CRC Press 2004.

[41] K. Ostrikov, U. Cvelbar and A. B Murphy, “Plasma nanoscience: setting directions, tackling grand challenges”, *J. Phys. D: Appl. Phys*., vol.44, 174001 (29 pp), 2011.

Time resolved optical emission images of an atmospheric pressure plasma jet with transparent electrodes

Article *in* Applied Physics Letters · July 2012

Impact Factor: 3.3 · DOI: 10.1063/1.4735156

6 authors, including:

Dejan Maletic
Institute of Physics Belgrade
53 PUBLICATIONS **97** CITATIONS
SEE PROFILE

Saša Lazović
Institute of Physics Belgrade
70 PUBLICATIONS **212** CITATIONS
SEE PROFILE

Gordana Malovic
Institute of Physics Belgrade
157 PUBLICATIONS **932** CITATIONS
SEE PROFILE

Zoran Lj Petrović
Institute of Physics Belgrade
510 PUBLICATIONS **5,652** CITATIONS
SEE PROFILE

AIP | Applied Physics Letters

Time resolved optical emission images of an atmospheric pressure plasma jet with transparent electrodes

N. Puač, D. Maletić, S. Lazović, G. Malović, A. Đorđević et al.

Citation: Appl. Phys. Lett. **101**, 024103 (2012); doi: 10.1063/1.4735156
View online: http://dx.doi.org/10.1063/1.4735156
View Table of Contents: http://apl.aip.org/resource/1/APPLAB/v101/i2
Published by the American Institute of Physics.

Time resolved optical emission images of an atmospheric pressure plasma jet with transparent electrodes

N. Puač,[1] D. Maletić,[1] S. Lazović,[1] G. Malović,[1] A. Đorđević,[2] and Z. Lj. Petrović[1]
[1]*Institute of Physics, University of Belgrade, Pregrevica 118, 11080 Belgrade, Serbia*
[2]*School of Electrical Engineering, University of Belgrade, Bul. kralja Aleksandra 73, 11000 Belgrade, Serbia*

(Received 5 April 2012; accepted 25 June 2012; published online 11 July 2012)

We study development of plasma packages in atmospheric pressure plasma jet from their formation as a discharge close to the instantaneous cathode, following their motion between and inside the electrodes up to their emergence at the edge of the glass tube and formation of a plasma bullet. Inside both electrodes, plasma is concentrated close to the walls and is bright, while outside it is located at the axis. This paper opens issues of the geometry of electrodes, fields, and atomic processes, allowing some predictions to be made about pertinent mechanisms. © *2012 American Institute of Physics*. [http://dx.doi.org/10.1063/1.4735156]

Recent advances in developing atmospheric pressure non-equilibrium (low temperature) plasma have yielded several sources[1–5] and opened much more widely the realm of plasma medical applications.[4,6–8] One of the most promising sources is the atmospheric pressure plasma jet (APPJ) that is formed with low excitation frequency (few tens of kHz) albeit at higher voltages.[9,10] It was very quickly found that the plasma of the APPJ is not continuous, but instead consists of small plasma packages that are formed in positive and/or negative half cycles of the period[11] (plasma bullets). Plasma jet consists of a glass tube with two external electrodes of certain length (along the axis of the tube) and some gap in-between. Plasma is formed in the flowing rare gas (usually helium). These packages travel within the tube and outside in the air, where they form bullets even though there is no external field. The apparent speed of visible plasma packages, ionization fronts, and plasma bullet is much larger than the speed of the flowing feed gas.

Several basic explanations of the bullet formation have been proposed[2,9,12–14] and a large number of measurements have been made.[15–18] Nevertheless, a detailed explanation of the physical mechanisms involved in creation and propagation of plasma bullets is still eluding us.

The issues that have to be understood include: how the formation of the bullet is connected to the processes between the two electrodes, what is the role of the geometry of the electrodes and their gap, as well as the role of the distance from the electrode to the end of the glass tube, how plasma interacts with walls, and most importantly what the basic physical mechanism is that allows forming of the bullet and its propagation at a very high velocity. Initial theoretical models seem to focus on a streamer like mechanism.[19–21] It is also important to note that Kushner and coworkers[22] mainly have explained the propagation of plasma inside narrow tubes (catheters) as ionization waves interacting strongly with the walls. In this paper, we will present results of time-resolved images of plasma bullets obtained using intensified charge coupled device (ICCD) camera for all phases throughout the period of excitation.

Our atmospheric pressure plasma jet source was made of a Pyrex glass tube (inner diameter 4 mm and outer diameter 6 mm). In this paper, we employ transparent conductive electrodes (polyethylene terephthalate, PET, foil with a thin film of indium tin oxide, Rs $\leq$ 10 Ω) to be able to follow the continuous development of the bullet at all phases. The transparent electrodes were introduced instead of non-transparent electrodes so that we could follow the development of the discharge inside of the electrodes. It was established earlier in a study with non-transparent electrodes[23] that if the electrodes are not long enough, the bullets do not develop. The length of the coated PET electrodes was 15 mm and the distance between them was also 15 mm. Schematics of the experimental setup is given in Figure 1. The electrode to the right was grounded and the other electrode, closer to the end of the glass tube, was powered. The distance between the powered electrode and the end of the glass tube was typically 6 mm. The feeding gas was helium and the flow rate used in this work was 4 slm, which was found earlier to be the optimum for creating plasma bullets.

We used a commercial signal generator connected to a custom-made amplifier with upper voltage limit of 1 kV to power the plasma jet. A homemade step-up transformer was also employed in order to obtain high enough voltages for igniting and maintaining the discharge. A high voltage (HV) probe was connected to the HV-output and used for voltage waveforms. The second probe was used for the current waveforms by measuring the voltage drop on a 100 kΩ resistor placed in the grounded branch of the electrical circuit (see Figure 1). The third probe was connected to the same resistor for external triggering of the ICCD camera (Andor iStar DH734I). We have used camera's internal delay generator for delaying camera gating and for external triggering of the oscilloscope. The frequency was chosen to be 80 kHz and the applied voltage was in the range 6–10 kV (peak-to-peak values). The power transmitted to the plasma was determined by integrating the product of the voltage and current waveforms and did not exceed 6 W during all measurements.

Current and voltage waveforms are presented in Figure 2. The signals obtained without the discharge are shown by dashed lines. In this case, there was no flow of feeding gas, so the tube is filled with air. Thus, we could be sure that the discharge is not ignited by the applied voltage selected to induce

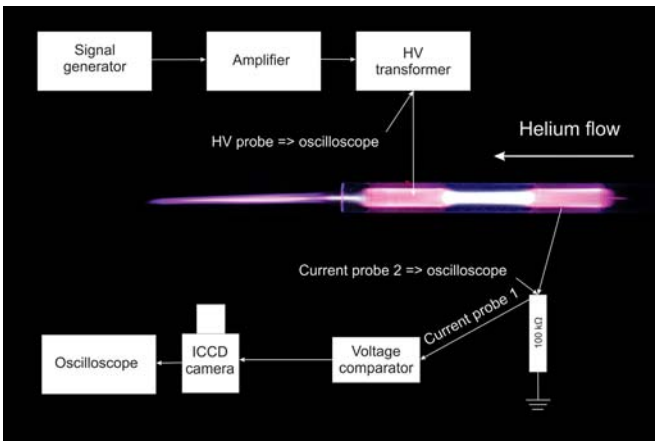

FIG. 1. Experimental setup.

only breakdown in helium and not in air. Nevertheless, ICCD image was taken as an additional crosscheck. In this case, the phase difference between the current and voltage waveforms is close to 90° and the current sinusoid precedes the voltage. When there is no discharge, we have an impedance of several MΩ, which corresponds to a stray capacitance of about 0.5 pF.

On the other hand, when the discharge is ignited, current waveforms increase in amplitude and become deformed, developing a large component that is in the phase with the voltage and resulting in considerably increased 2nd and 3rd harmonics (see Figure 2). At the same time, the voltage is decreased because the voltage needed to sustain the discharge is lower than the ignition voltage (red dashed and solid curves in Figure 2). The plasma introduces a parallel nonlinear load into the electrical circuit.

When camera exposure times are larger than the cycle period (12.5 μs), plasma appears to be continuous, shaped like a plume (see Figure 1) upon emergence from the tube. The length of the visible plasma plume, with the present tube radius, can be up to five centimeters, depending on the flow rate and the applied voltage. When exposure times are shorter, we could detect plasma bullets under a wide range of conditions. We could obtain spatial emission recordings both in the single shot and in the repetitive mode. Integration

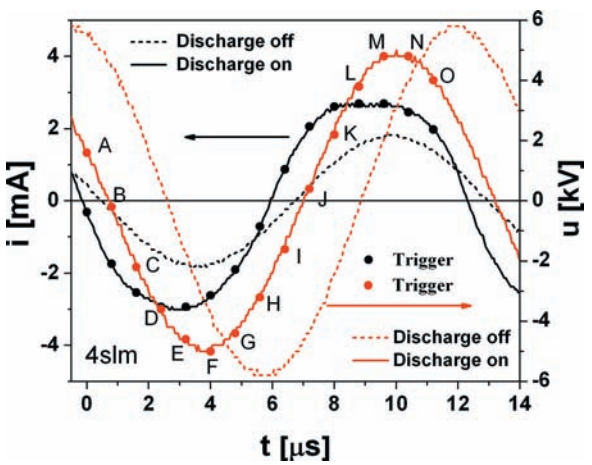

FIG. 2. Current (black lines) and voltage (red lines) waveforms with (solid line-symbols showing triggering of ICCD camera) and without (dashed) the ignited discharge. In both cases, the same voltage at the signal generator was applied.

on the chip (over a large number of bullets) was used for the time resolved images because the light emission in a single shot is not always sufficient to obtain clear images with gate widths less than 25 ns. Nevertheless, the single shot recordings could be used to verify that integration did not skew the profiles and thus the jitter was shown to be small.

We show development of plasma for the entire period of excitation (12.5 μs) in Figure 3. The selection of the colors for the layers in all images is scaled to the same maximum intensity. The points A–O in the waveforms of Figure 2 correspond to the timing of the recordings of the spatial emission profiles shown in Figure 3. When the current and voltage signals are

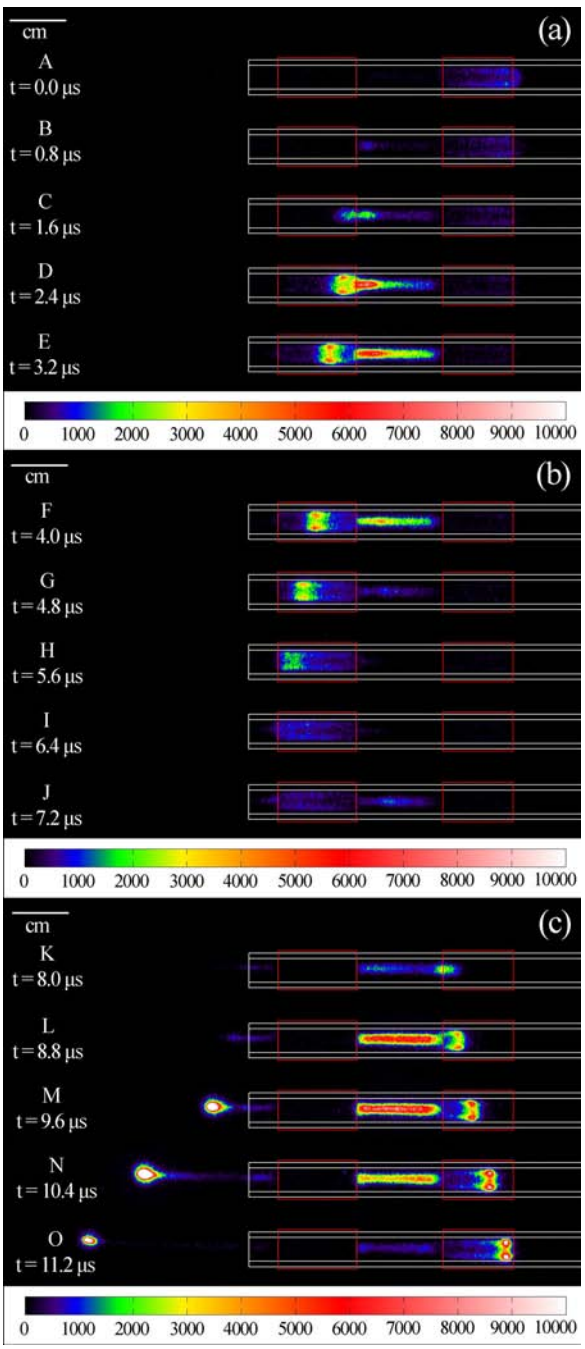

FIG. 3. Time-resolved images of the plasma bullet: (a) formation of the discharge between electrodes, (b) movement of the discharge behind the electrodes, and (c) emergence of the plasma bullet and breakdown at the opposite electrode. Red boxes denote the positions of transparent electrodes. The grounded electrode is on the right.

close to zero (as shown in point A in Figure 3(a)), plasma is not visible between the electrodes. The afterglow of the previous discharge is confined inside the grounded electrode and has very low emission intensity. As long as the voltage signal is small, there is no visible discharge between the electrodes. Only when both current and voltage become negative, one can see low-intensity emission close to the powered electrode (see Figure 3(a); B). With an increase of the current and voltage, the emission intensity of the discharge increases with appearance of a hollow cathode discharge. The discharge is also expanding away from the instantaneous cathode in the direction of the grounded electrode (C–E).

At the same time, the discharge begins traveling through the powered electrode with a constant apparent ionization front speed of around 4 km/s towards the end of the glass tube. The shape of this emission (see Figures 3(a) and 3(b); D–H) suggests that this plasma package is "ring-shaped" (moving in the direction of the gas flow). Some authors report that the bullet coming out of the tube is not homogenous in volume, but it has a shape of a "donut."[13] We have only noticed (from the side of observation) the "ring-shape" of the plasma when it travels through both electrodes.

At the same time, between the electrodes, plasma is confined to the center of the glass tube traveling towards the grounded electrode (against He gas flow). The discharge spreads at the same or somewhat lower speeds of ionization front (1–5 km/s) as compared to the plasma inside the grounded electrode.

The propagation of the plasma inside the powered electrode continues even when the discharge between two electrodes appears to have been extinguished (Figure 3(b); H–I) because the absolute value of the voltage is too small. As the plasma reaches the farther edge of the powered electrode and, later, the edge of the tube, it appears to have almost disappeared between the electrodes. Yet, it is sufficiently visible to ascertain that it is located at the center of the tube.

Under some circumstances, however, there is much brighter emission at all times indicating continuity of plasma motion. So, we can conclude that the ionized gas is still moving and only the potential distribution does not favor heating of electrons that can lead to emission.

Upon reaching the edge of the tube, a small emission can be observed (see Figure 3(c); L), which shows the initial part of the bullet (re)formation. From that moment on, the bullet is formed at the edge of the glass tube (Figure 3(c); M–O) and continues to move very fast. The apparent speed of plasma bullet is variable, peaking at 17.5 km/s, which is much faster than the speed of the buffer gas flow (~7 m/s) and considerably faster than the speed of the ionization front inside the tube. While the bullet is well defined, its size also changes as it travels away from the edge of the tube. Its motion outside the tube seems to be unrelated to the voltage distribution inside the tube and the status of the discharge.

As the current and voltage rise again, emission of the discharge can be observed at the edge of grounded electrode and between the electrodes. With the increase of the amplitudes, the discharge between the electrodes becomes more intense, spreading towards the powered electrode.

The discharge also forms a plasma ring traveling inside the grounded electrode (Figure 3(c); L–O), but it only reaches its edge and does not extend much beyond the electrode, so no bullet is formed.

The most important conclusion of this work is that there is a continuity of plasma development. The plasma forms at the edge of the electrode (cathode) facing the other electrode. The glow between the two electrodes expands towards the anode. The plasma also moves inside the electrode, while its emission weakens. In one or two frames, it is almost unobservable, but one can follow the continuity to the point when it reaches the edge of the tube.

Inside the tube, plasma is donut-shaped and travels while clinging close to the walls.[24] A "wall hugging" constriction moving rapidly around a large diameter tube was observed in Ref. 25 resulting in time-averaged donut-shaped emission from the end on observation. Here, however, the donut shape (hollow cathode like) is maintained even with very short recording times. The difference between ring-shaped plasma and plasma formed at the axis of the tube is due to the presence of the conducting material right behind the glass walls and in the resulting field profiles.

While the dimming of emission as the plasma moves towards the edge of the tube is consistent with thermalization of electrons and lack of high fields (it coincides with low external voltage), the rejuvenation (and reforming of the plasma) is something that needs to be explained by modeling. Two possible causes come to mind, the first being a burst of Penning ionization of molecules from the air by helium metastables. The increase of emission only occurs when abundance of air molecules becomes significant. Another possible explanation[26] is that the ionized gas of the air is effective at the ground potential, and the field at the front increases as the bullet leaves the tube and is subject to the external potential distribution.

In any case, at the edge of the tube, a spherical bullet (plasma) is formed (or perhaps reformed) at the axis and it moves very fast. It carries all the properties of a low-temperature plasma including its ability to produce reactive species, UV photons, and high energy ions, and selectively apply them to the surface. While plasma bullets look like a smaller version of ball lightning,[27] only further studies will reveal whether the explanations could be similar. In any case, further diagnostics of the bullet itself will reveal the properties needed for plasma medical application and detailed quantitative explanation of this regime of atmospheric non-equilibrium plasmas. Recording of the properties of the plasma bullets with transparent electrodes[16,17] will allow a detailed modeling of the development of the bullets and with that knowledge facilitate their potential applications in different fields.

This research has been supported by the Ministry of Education and Science, Serbia, under Projects ON171037 and III41011.

[1]V. S. Gathen, V. Buck, T. Gans, N. Knake, K. Niemi, S. Reuter, L. Schaper, and J. Winter, Contrib. Plasma Phys. **47**, 510 (2007).
[2]J. L. Walsh, F. Iza, N. B. Janson, V. J. Law, and M. G. Kong, J. Phys. D: Appl. Phys. **43**, 075201 (2010).
[3]E. Stoffels, Y. A. Gonzalvo, T. D. Whitmore, D. L. Seymour, and J. A. Rees, Plasma Sources Sci. Technol. **15**, 501 (2006).
[4]G. C. Kim, G. J. Kim, S. R. Park, S. M. Jeon, H. J. Seo, F. Iza, and J. K. Lee, J. Phys. D: Appl. Phys. **42**, 032005 (2009).

[5]J. Jarrige, M. Laroussi, and E. Karakas, Plasma Sources Sci. Technol. **19**, 065005 (2010).
[6]G. Fridman, A. Shereshevsky, M. M. Jost, A. D. Brooks, A. Fridman, A. Gutsol, V. Vasilets, and G. Friedman, Plasma Chem. Plasma Process. **27**, 163 (2007).
[7]S. A. Ermolaeva, A. F. Varfolomeev, M. Y. Chernukha, D. S. Yurov, M. M. Vasiliev, A. A. Kaminskaya, M. M. Moisenovich, J. M. Romanova, A. N. Murashev, I. I. Selezneva, T. Shimizu, E. V. Sysolyatina, I. A. Shaginyan, O. F. Petrov, E. I. Mayevsky, V. E. Fortov, V. E. Fortov, B. S. Naroditsky, and A. L. Gintsburg, J. Med. Microbiol. **60**, 75 (2011).
[8]M. G. Kong, G. Kroesen, G. Morfill, T. Nosenko, T. Shimizu, J. Dijk, and J. L. Zimmermann, New J. Phys. **11**, 115012 (2009).
[9]X. P. Lu and M. Laroussi, J. Appl. Phys. **100**, 063302 (2006).
[10]J. L. Walsh, J. J. Shi, and M. G. Kong, Appl. Phys. Lett. **88**, 171501 (2006).
[11]J. L. Walsh and M. G. Kong, IEEE Trans. Plasma Sci. **36**, 954 (2008).
[12]J. Shi, F. Zhong, J. Zhang, D.W. Liu, and M. G. Kong, Phys. Plasmas **15**, 013504 (2008).
[13]N. M. Bourdet, M. Laroussi, A. Begum, and E. Karakas, J. Phys. D: Appl. Phys. **42**, 055207 (2009).
[14]A. Shashurin, M. N. Shneider, A. Dogariu, R. B. Miles, and M. Keidar, Appl. Phys. Lett. **94**, 231504 (2009).
[15]J. S. Oh, Y. A. Gonzalvo, and J. W. Bradley, J. Phys. D: Appl. Phys. **44**, 365202 (2011).
[16]J. L. Walsh and M. G. Kong, IEEE Trans. Plasma Sci. **39**, 2306 (2011).
[17]J. S. Oh, P. M. Bryant, and J. W. Bradley, IEEE Trans. Plasma Sci. **39**, 2352 (2011).
[18]E. Karakas, M. A. Akman, and M. Laroussi, IEEE Trans. Plasma Sci. **39**, 2308 (2011).
[19]G. V. Naidis, Appl. Phys. Lett. **98**, 141501 (2011).
[20]Y. Sakiyama, D. B. Graves, J. Jarrige, and M. Laroussi, Appl. Phys. Lett. **96**, 041501 (2010).
[21]J. P. Boeuf and L. C. Pitchford, in 6th International Workshop on Microplasmas, France, Paris, 2011.
[22]Z. Xiong and M. J. Kushner, IEEE Trans. Plasma Sci. **39**, 2320 (2011).
[23]D. Maletić, S. Lazović, N. Puač, G. Malović, A. Đorđević, and Z. Lj. Petrović, in ISPC20, USA, Philadelphia, 2011.
[24]B. Niermann, T. Hemke, N. Y. Babaeva, M. Boke, M. J. Kushner, T. Mussenbrock, and J. Winter, J. Phys. D: Appl. Phys. **44**, 485204 (2011).
[25]Z. Lj. Petrovic and A.V. Phelps, Phys. Rev. E **56**, 5920 (1997).
[26]J. P. Boeuf, personal communication (2011).
[27]J. J. Lowke, J. Phys. D: Appl. Phys. **29**, 1237 (1996).

Application of non-equilibrium plasmas in medicine

Conference Paper · September 2012

5 authors, including:

Zoran Lj Petrović
Institute of Physics Belgrade
510 PUBLICATIONS **5,652** CITATIONS
SEE PROFILE

Gordana Malovic
Institute of Physics Belgrade
157 PUBLICATIONS **932** CITATIONS
SEE PROFILE

BOOK OF ABSTRACTS

FIRST INTERNATIONAL CONFERENCE
PROCESSING, CHARACTERISATION AND
APPLICATION OF NANOSTRUCTURED
MATERIALS AND NANOTECHNOLOGY
NANOBELGRADE 2012

SEPTEMBER 26-28, 2012,
BELGRADE, SERBIA

www.nanobelgrade.tmf.bg.ac.rs

FP7-REGPOT-2009-1

First International Conference

PROCESSING, CHARACTERIZATION AND APPLICATION OF NANOSTRUCTURED MATERIALS AND NANOTECHNOLOGY

PROGRAMME

&

BOOK of ABSTRACTS

The Conference is organized within the scope of the FP7 NANOTECH FTM project "Reinforcing of Nanotechnology and Functional Materials Centre" (No: 245916).

SEVENTH FRAMEWORK PROGRAMME

FP7-REGPOT-2009-1

NANOTECH FTM

CMF

PROCESSING, CHARACTERIZATION AND APPLICATION OF NANOSTRUCTURED MATERIALS AND NANOTECHNOLOGY
First International Conference, NanoBelgrade 2012
PROGRAMME & BOOK of ABSTRACTS

Izdavač:
Tehnološko-metalurški fakultet
Univerziteta u Beogradu
Beograd, Karnegijeva 4

Za izdavača:
Prof. dr Ivanka Popović, dekan

Glavni i odgovorni urednik:
Prof. dr Karlo Raić

Priredili:
Prof. dr Bojana Obradović,
Prof dr Petar Uskoković,
Prof dr Đorđe Janaćković

Tiraž:
150 primeraka

Štampa:
Razvojno-istraživački centar grafičkog inženjerstva
Tehnološko-metalurškog fakulteta
Beograd, Karnegijeva 4

ISBN 978-86-7401-285-7

PROGRAMME

Tuesday
September 25

19.00 – 20.00	**Registration**
20.00 – 22.00	**Welcome cocktail, Hotel Moskva**

Wednesday
September 26

9.30 – 10.00	**Opening ceremony**

Nanomaterials for Biomedical and Pharmaceutical Applications

10.00 – 10.30	Nanocomposites, nanospheres, nanocapsules and nanostructured surfaces of biodegradable polymers for biomedical applications, **Josè M. Kenny***, N. Rescignano, E. Fortunati, S. Mattioli, I. Armentano, **University of Perugia, Italy and Institute of Polymer Science and Technology, Madrid, Spain*
10.30 – 11.00	Biomaterial nanostructures obtained by advanced pulsed laser techniques for applications in nanomedicine, **Ion Mihailescu**, *National Institute for Laser, Plasma, and Radiation Physics, Romania*
11.00 – 11.20	***Coffee break***
11.20 – 11.50	Application of non-equilibrium plasmas in medicine, **Zoran Petrović***, N. Puač, G. Malović, S. Lazović and D. Maletić, **Institute of Physics, University of Belgrade, Serbia*

Application of non-equilibrium plasmas in medicine

Zoran Lj. Petrović, N. Puač, G. Malović, S. Lazović and D. Maletić

Institute of Physics, University of Belgrade POB 68 11080 Zemun
zoran.petrovic@ipb.ac.rs

Recent advances in plasma medical applications have left very little doubt that this application will be the main driving force for the future developments of non-equilibrium collisional plasmas. We shall review the potential of such applications, the connections to nanotechnologies and the results obtained by our group.

A special issue in plasma medicine is the development of the plasma sources that would achieve non-equilibrium at atmospheric pressure in atmospheric gas mixture with no or only marginal heating of the gas, and with desired properties and mechanisms that may be controlled. The main trick in achieving the non-equilibrium operation and no gas heating is in control of the electron multiplication. For that purpose one may use inhomogeneous fields (corona), dielectric barrier, RF and pulsed operation and breakdown in rare gas flow.

Our studies have shown that control of radicals or chemically active products of the discharge such as ROS (reactive oxygen species) and/or NO may be used to control the growth of the seeds. At the same time specially designed plasma needle and other sources were shown to be efficient to sterilize not only colonies of bacteria but also planctonic samples (micro organisms protected by water) or bio films. Finally we have shown that plasma may induce differentiation of stem cells.

Non-equilibrium plasmas may used in detection of different specific markers in medicine. For example proton transfer mass spectroscopy may be employed n detection of volatile organic compounds without their dissociation and thus as a technique for instantaneous measurement of the presence of markers for numerous diseases.

The same techniques employed modeling of collisional plasmas may be modified to study positrons in gases and even human body as a part of positron diagnostic or therapy.

CIP - Каталогизација у публикацији
Народна библиотека Србије, Београд

66.017/.018(048)
544.2(048)

INTERNATIONAL Conference Processing, Characterization and Applications of Nanostructured Materials and Nanotechnology (1 ; 2012 ; Beograd)
Programme & Book of Abstracts / First International Conference Processing, Characterization and Applications of Nanostructured Materials and Nanotechnology, [NanoBelgrade 2012] ; [priredili Bojana Obradović, Petar Uskoković, Đorđe Janaćković]. - Beograd : Tehnološko-metalurški fakultet, 2012 (Beograd : Razvojno-istraživački centar grafičkog inženjerstva TMF). - 127 str. ; 24 cm

"The Conference is organized within the scope of the FP7 NANOTECH FTM project 'Reinforcing of Nanotechnology and Functional Materials Centre' (No: 245916)." --> nasl. str. -
Tiraž 150.

ISBN 978-86-7401-285-7

a) Наука о материјалима - Апстракти b) Нанотехнологија - Апстракти c) Наноструктуре - Апстракти
COBISS.SR-ID 193577996

MASS-ENERGY SPECTROMETRY DETECTION OF MOLECULE AND ATOMIC RADICALS FORMED BY μ-APPJ

Conference Paper · July 2010

READS
9

5 authors, including:

Dejan Maletic
Institute of Physics Belgrade
53 PUBLICATIONS **97** CITATIONS
SEE PROFILE

Saša Lazović
Institute of Physics Belgrade
70 PUBLICATIONS **212** CITATIONS
SEE PROFILE

Gordana Malovic
Institute of Physics Belgrade
157 PUBLICATIONS **932** CITATIONS
SEE PROFILE

Zoran Lj Petrović
Institute of Physics Belgrade
510 PUBLICATIONS **5,652** CITATIONS
SEE PROFILE

MASS-ENERGY SPECTROMETRY DETECTION OF MOLECULE AND ATOMIC RADICALS FORMED BY μ-APPJ

D. Maletić[(1,*)], S. Lazović[(1)], N. Puač[(1)], G. Malović[(1)] and Z. Lj. Petrović[(1)]

[(1)] Institute of Physics, Pregrevica 118, 11080 Belgrade, Serbia

[(*)]**dejan_maletic@ipb.ac.rs**

In the last few years atmospheric microplasmas draw considerable attention because of the wide spectra for their application. Large concentrations of radicals, low gas temperatures, absence of vacuum systems and possibility of localized treatment make these plasmas suitable for modification of sensitive surfaces and for biomedical applications [1, 2, 3]. Here we will present results obtained by mass spectrometry measurements of micro atmospheric pressure plasma jet. This device was previously developed by Schultz van der Gathen and coworkers [4]. One of our guidelines was to investigate possibility of applying μ-APPJ for treatment of biological samples. We have analyzed plasma products like O, N, NO, O_3 formed by μ-APPJ.

First we had to determine the calibration, reproducibility and sensitivity of our mass spectrometer. As a preliminary measure in place of a more systematic study we measured the composition of the atmosphere in our laboratory by using Hiden HPR-60 mass-energy spectrometer. Results are compared with the results of other researchers with similar systems and the data taken from the literature (Table 1.). Measured yields of atmospheric compounds agree reasonably though not perfectly with literature values. Reproducibility of the device was checked by doing the measurements consecutively during several days. Sensitivity of the mass analyzer was confirmed by measuring isotopes from the atmosphere which can be found only in traces.

Table 1. Percentages of different compounds in the atmosphere [5].

	1st day	2nd day	3rd day	4th day	Standard atmosphere	Other systems [6]
H	0.0409	0.0407	0.0465	0.0393		
H_2	0.0080	0.0189	0.0115	0.0163		
^{14}N	1.4458	1.5015	1.4279	1.4040		
^{15}N	0.0085	0.011	0.0137	0.015		
^{16}O	0.4162	0.4385	0.3945	0.3947		
OH	0.1309	0.1555	0.1548	0.1529		
H_2O	0.55	0.52	0.59	0.79	0.4	
$^{28}N_2$	74.16	73.72	73.36	73.20	78.08	68.71
$^{29}N_2$	0.57	0.59	0.649	0.636	0.566	
O_2	20.50	20.83	21.16	21.03	20.94	30.11
^{36}Ar	0.0086	0.0088	0.0438	0.0085	0.0031	0.0054
^{38}Ar	0.0033	0.0052	0.0027	0.0046	0.0006	0.0006
^{40}Ar	1.6158	1.6808	1.6704	1.7106	0.93	1.10
^{84}Kr	0.0977	6.82E-4	0.00102	0.0574	0.65E-4	1.62E-4

In our diagnostics of the μ-APPJ we scanned masses of neutrals from 1-50 amu at fixed electron energy of 70 eV and, also, we scanned distribution of neutral atoms for electron energies from 5 to 35 eV [6]. From these distributions one can identify processes that are pertinent in creation of neutral atoms. In order to eliminate contribution of atoms produced by dissociation of O_2 inside the mass analyzer, the electron energy range was varied from 13.6 eV (required for direct ionization of O) up to 19 eV (less then O_2 dissociation threshold). Total concentrations of atomic oxygen were obtained by integrating electron energy dependent curves in this range. The results are presented in Fig. 1. for different values of power given by RF source and two feed gas flow rates (2 slm and 3 slm of 99% He and 1% O_2). An increase in concentrations can be seen resulting both from increases of power and unexpectedly the flow rate.

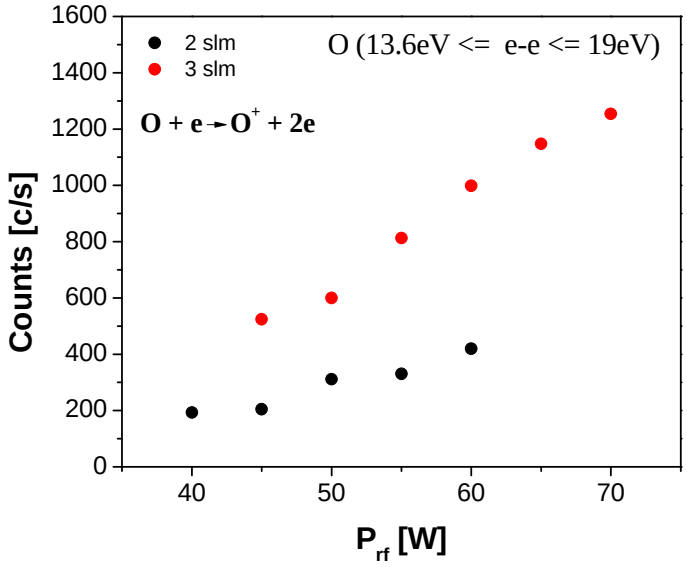

Fig. 1: Number of oxygen atoms as function of power given by RF power supply for two different flow rates of a mixture containing 99% of He and 1% of O_2.

Reference

[1] M. G. Kong, G. Kroesen, G. Morfill, T. Nosenko, T. Shimizu, J. van Dijk and J. L. Zimmermann, 2009 *New J. Phys.* **11** 115012

[2] G. Fridman, G. Friedman, A. Gutsol, A. B. Shekhter, V. N. Vasilets and Alexander Fridman, 2008 *Plasma Process. Polym.* **5** 000

[3] N. Puač, Z. Lj. Petrović, G. Malović, A. Đorđević, S. Živković, Z. Giba and D. Grubišić, 2006 *J. Phys.* D*: Applied Physics* **39** 3514

[4] V. Schulz-von der Gathen, V. Buck, T. Gans, N. Knake, K. Niemi, St. Reuter, L. Schaper, and J.Winter, 2007 *Contrib.Plasma Phys.*, **47** 7 510

[5].Malović *et.al.*, PSST submitted

[6] Jan Benedikt, *personal communication*

CURRENT –VOLTAGE CHARACTERISTICS OF μ–APPJ OBTAINED BY USING DERIVATIVE PROBES

Conference Paper · July 2010

READS
32

6 authors, including:

Saša Lazović
Institute of Physics Belgrade
70 PUBLICATIONS **212** CITATIONS
SEE PROFILE

Dejan Maletic
Institute of Physics Belgrade
53 PUBLICATIONS **97** CITATIONS
SEE PROFILE

Gordana Malovic
Institute of Physics Belgrade
157 PUBLICATIONS **932** CITATIONS
SEE PROFILE

Zoran Lj Petrović
Institute of Physics Belgrade
510 PUBLICATIONS **5,652** CITATIONS
SEE PROFILE

CURRENT - VOLTAGE CHARACTERISTICS OF μ-APPJ OBTAINED BY USING DERIVATIVE PROBES

S. Lazović [1,*], D. Maletić [1], N. Puač[1], G. Malović[1], A. Đorđević[2] and Z. Lj. Petrović[1]

[1] Institute of Physics, Belgrade, Pregrevica 118, 11080 Belgrade, Serbia

[2] Faculty of Electrical Engineering, Bul. Kralja Aleksandra 73, 11000 Belgrade, Serbia

[*]**lazovic@ipb.ac.rs**

In this paper we present results of derivative probe measurements made on micro atmospheric pressure plasma jet previously developed by Schultz van der Gathen and coworkers [1]. This technically relatively simple capacitively coupled device is typically operated at an excitation frequency of 13.56 MHz. μ-APPJ plasma source is interesting both for applications as well as for the study of fundamental processes. Capability of applying μ-APPJ for different treatments is due to mild non thermal plasma generated at atmospheric pressure in a mixture of a noble gas and a small amount of molecular gas (in our case 99% of He and 1% of O2).

Determining adequate set of parameters in order to properly describe plasma is a very important task when it comes to reproducibility of desired plasma properties. Unpredictable changes in plasma properties can be caused by non-linearity of plasma impedance. For example, apparently neglectable change in matching network auto-set reflected power minima can cause significant variations in plasma properties due to this non-linearity [2]. This is manifested by drive frequency harmonics generation at external circuitry leads and by different amounts of power that are delivered to plasma. Therefore, power measured directly at power supply is not a representative parameter. On the other hand, derivative probes can provide us with the information about mean power delivered to the plasma and with harmonic composition of our signals. Until recently derivative probes have been applied for discharges of higher powers (i.e. currents and voltages) but we were able to develop probes with sufficient sensitivity to make their application in micro discharges possible.

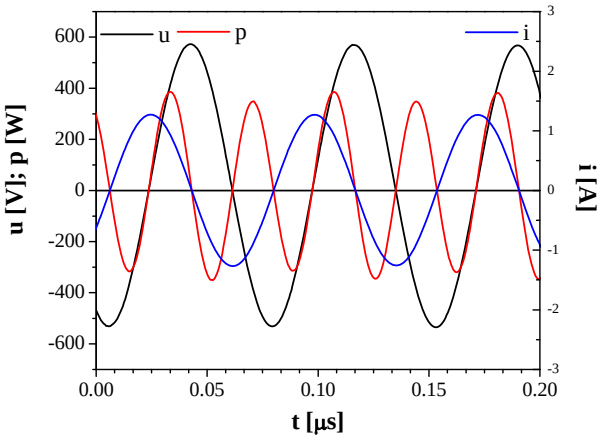

Fig. 1. Instantaneous current, voltage and power values for input power of 70 W and gas mixture flow rate of 1 slm.

We have used derivative probes [3, 4] to analyze volt-ampere characteristics of μ-APPJ for three different gas flow rates (1 slm, 2 slm and 3 slm). Current, voltage and power waveforms after the numerical procedure has been performed are shown in Figure 1. Numerical procedure consists of Fast Fourier Transform of current and voltage probe signals, followed by multiplication with adequate calibration curves in the frequency domain and finally of an Inverse Fast Fourier Transform. Power waveform is obtained by multiplying final current and voltage waveforms and mean power is calculated as an integral of this waveform (45 periods of 13.56 MHz).

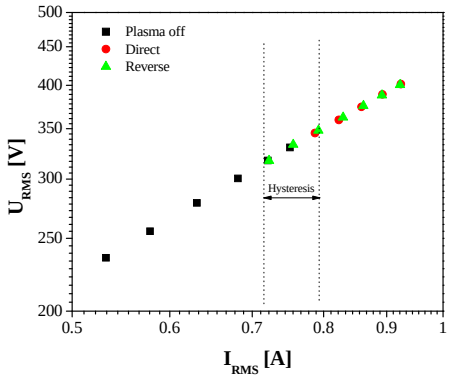

Fig. 2. U_{RMS}-I_{RMS} characteristics of the μ-APPJ when increasing (Direct) and decreasing (Reverse) power given by RF power supply. Gas flow was 2 slm.

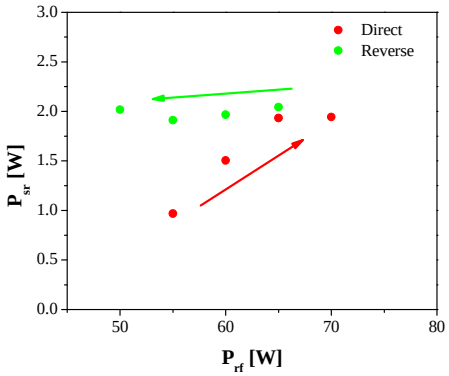

Fig. 3. Mean power values when increasing and decreasing input power. Gas mixture (1% O2 – 99% He) flow was 2 slm.

In Figure 2. U_{RMS}-I_{RMS} characteristics of the discharge are shown. We can see that the discharge operates in alpha mode. When decreasing the power we have observed that plasma remains ignited even for the input powers lower than the powers needed for its initial ignition. In case when hysteresis occurs we can see that more power is transmitted to the plasma (see Figure 3.)

Reference

[1] V. Schulz-von der Gathen, V. Buck, T. Gans, N. Knake, K. Niemi, St. Reuter, L. Schaper, and J.Winter, 2007 *Contributions to Plasma Physics*, **47** 7 510

[2] P.A. Miller, H. Anderson, M.P. Splichal, 1992 *J. App. Phys.* **71** 1171

[3] N. Puač, Z.Lj. Petrović, S. Živković, Z. Giba, D. Grubišić and A.R. Đorđević, Plasma Processes and Polymers, Eds. R. d'Agostino, P. Favia, C. Oehr and M.R. Wertheimer, (Whiley: (2005) p 193-203

[4] N. Puač, Z. Lj. Petrović, G. Malović, A. Đordević, S. Živković, Z. Giba and D. Grubišić, 2006 *J. Phys. D: Applied Physics* **39** 3514

Effects of non-thermal atmospheric plasma on human periodontal ligament mesenchymal stem cells

Article *in* Journal of Physics D Applied Physics · August 2013

Impact Factor: 2.72 · DOI: 10.1088/0022-3727/46/34/345401

Effects of non-thermal atmospheric plasma on human periodontal ligament mesenchymal stem cells

2013 J. Phys. D: Appl. Phys. 46 345401

(http://iopscience.iop.org/0022-3727/46/34/345401)

J. Phys. D: Appl. Phys. **46** (2013) 345401 (9pp) doi:10.1088/0022-3727/46/34/345401

Effects of non-thermal atmospheric plasma on human periodontal ligament mesenchymal stem cells

M Miletić[1], S Mojsilović[2], I Okić Đorđević[2], D Maletić[3], N Puač[3], S Lazović[3], G Malović[3], P Milenković[1,2], Z Lj Petrović[3] and D Bugarski[2]

[1] Faculty of Dental Medicine, University of Belgrade, Belgrade, Serbia
[2] Institute for Medical Research, University of Belgrade, Belgrade, Serbia
[3] Institute of Physics, University of Belgrade, Pregrevica 118, 11080 Zemun, Serbia

E-mail: maja.miletic@stomf.bg.ac.rs

Received 17 March 2013, in final form 21 June 2013
Published 7 August 2013
Online at stacks.iop.org/JPhysD/46/345401

Abstract
Here we investigate the influences of non-thermal atmospheric plasma on human mesenchymal stem cells isolated from periodontal ligament (hPDL-MSCs). A specially redesigned plasma needle was used as the source of low-temperature plasma and its effects on different hPDL-MSC functions were investigated. Cell cultures were obtained from extracted normal impacted third molars and characterized for their phenotype and multi-potential differentiation. The hPDL-MSCs possessed all the typical MSC properties, including clonogenic ability, high proliferation rate, specific phenotype and multilineage differentiation. The data regarding the interaction of plasma with hPDL-MSCs demonstrated that plasma treatment inhibited the migration of hPDL-MSCs and induced some detachment, while not affecting their viability. Additionally, plasma significantly attenuated hPDL-MSCs' proliferation, but promoted their osteogenic differentiation. The results of this study indicated that a non-thermal plasma offers specific activity with non-destructive properties that can be advantageous for future dental applications.

(Some figures may appear in colour only in the online journal)

1. Introduction

Non-thermal atmospheric plasmas have received much attention in biomedicine during the past decade, offering precise and localized treatment in various therapeutic fields. In dentistry, due to their efficient bactericidal effect, plasmas can treat dental cavities resulting from caries and periodontal pockets, but can also affect the surrounding cells. In this paper we study the influence of low-temperature (non-equilibrium) atmospheric-pressure plasma on human mesenchymal stem cells isolated from periodontal ligaments (hPDL-MSCs) with the treatment of peridontitis and its resulting effects in mind.

Periodontitis is one of the most prevalent oral diseases in adults, caused by pathogenic microflora in the dental plaque [1]. Bacterial infection induces an inflammatory response of the alveolar bone and soft periodontal tissues, and the inflammation cascade often leads to the irreversible destruction of the tooth supporting tissue and eventually causes the loss of the tooth [2]. The regeneration of lost periodontal tissue has always been the ultimate goal of periodontal therapy, but current regenerative procedures remain limited and unpredictable [3]. Stem-cell therapy is a novel and promising option for periodontal tissue regeneration, since these cells have been used for the repair and/or regeneration of defective tissues and organs such as bone [4], cartilage [5], heart [6] and spinal cord [7]. The identification and isolation of dental-derived mesenchymal stem cells (MSCs) have presented exciting possibilities for applications in tissue engineering, as well as gene-based therapies in reconstructive dentistry [8]. Recently, multipotent stem-cell populations have been isolated from the periodontal ligament of extracted human third molar teeth [9], and the data reported has suggested that these cells can be ideal candidates for potential therapeutical applications in periodontal regeneration [10–12].

The biomedical application of atmospheric-pressure gas plasma dates from the beginning of the 20th century, when

mainly heat was used for tissue removal. The rapid expansion in this field was brought by the development of low-temperature atmospheric-pressure plasma sources in the 1990s [13, 14]. Sterilization and the treatment of wounds and dental caries are only small segments of the fast growing field of biomedical applications of atmospheric-pressure plasmas. The heat generated by non-thermal atmospheric-pressure plasma sources designed for biomedical applications usually does not increase the temperature of the treated samples to more than 40 °C. This makes them highly suitable for *in vitro* and *in vivo* treatments. Until now, various types of plasma sources operating at atmospheric pressure were used for sterilization [15–20], wound healing and dermatology [16, 20, 21], cancer cell removal [22, 23] and even in dental application such as caries removal or tooth bleaching [24]. Here we have mentioned only a small part of the studies into the biomedical applications of plasma sources.

The plasma needle is one of the non-thermal atmospheric-pressure plasma sources that can be particularly convenient for biomedical applications [25]. In our previous work, we redesigned and improved our device [26, 27] to be suitable for interactions with living cells and tissues. In order to optimize and develop a new technique for possible *in vivo* antimicrobial therapy in medicine and dentistry, we also tested the effect of our plasma needle on bacteria and peripheral blood-derived MSCs and demonstrated its antimicrobial potential, as well as its non-cytotoxicity on normal human primary cells [28].

The plasma needle is especially convenient for localized and precise treatments due to its mild plasma and geometry, so the bactericidal, non-destructive treatment of periodontal pockets appears to be one of the promising applications. However, beside the fast and efficient bactericidal effect, plasma treatment can affect other cells in the periodontal region. To our knowledge, there are no reports of the applications of non-thermal atmospheric plasma in periodontal therapy, and therefore in this study we aimed at investigating its influence on periodontal tissue. Hence, human periodontal ligament-derived mesenchymal stem cells (hPDL-MSCs) were isolated and characterized, and the influence of a non-thermal plasma on different cell functions, such as viability, adhesion, motility and proliferation, was evaluated. Additionally, related to the potential application in periodontal therapy, we examined the capability of plasma to modulate the hPDL-MSCs' differentiation towards osteogenic lineage.

Independent of our work, similar results indicating a strong differentiation of stem cells towards osteogenic linage was shown by the collaboration between the groups of Friedman and Freeman [29]. A different plasma source was used in that study, and results showed impressive plasma-induced limb growth in embryos.

2. Experimental setup

The plasma source used in this study was the plasma needle previously used in treatments of planktonic samples containing bacteria [28]. It consists of a long central electrode made of thin tungsten wire covered with a ceramic tube, that is placed in a glass tube with an outer diameter of 6 mm. Helium was used as the feeding gas and it was flowing between the glass and ceramic tubes with flow rates adjusted to 0.5 or 1 standard litres per minute (slm) by the mass flow controller (Omega FMA5400/5500). The purpose of the ceramic tube is to isolate the central electrode from the helium in order to generate a very small plasma, only on the plane tip of the electrode. The central electrode and ceramic and glass tubes were placed in the body of a plasma needle made of Teflon. Plasma was created in the mixture of helium and gas components from the surrounding atmosphere that can diffuse into plasma and produce radicals such as atomic oxygen, nitrogen, nitrogen oxides and ozone [27].

A sinusoidal signal with the frequency of 13.56 MHz was used to power the plasma needle. The signal was generated by a signal generator (Agilent N9310A) and amplified by a linear amplifier (Barthel RFA-0.1/50–100 B00). The mean power was calculated from the calibrated derivative probe signals and was monitored as the main plasma parameter. Calibrated probes enabled the accurate determination of the power transmitted to the plasma which was tested by our ability to remove the displacement current. Powers transmitted to the plasma, obtained from the difference of calculated powers with and without plasma (no helium flow) were used to monitor plasma treatment conditions. In all treatments the power delivered to the plasma did not go above two watts. In a separate measurement these powers were shown not to generate an increase in temperature beyond 40 °C, which would lead to thermal necrosis.

2.1. Cell culture and assays

Normal impacted third molars were extracted for orthodontic purposes at the Department of Oral Surgery of the Faculty of Dental Medicine, University of Belgrade, according to the approved ethical guidelines set by the Ethics Committee of the Faculty of Dental Medicine, University of Belgrade. Immediately after extraction, the periodontal ligament was gently separated from the middle third of the tooth root surface, minced into small pieces, transferred to a tissue culture flask with Dulbecco's modified Eagle's medium (DMEM; PAA Laboratories, Pasching, Austria) supplemented by 20% fetal bovine serum (FBS; PAA Laboratories), 100 U/ml penicillin and 100 μg ml^{-1} streptomycin (PAA Laboratories), and cultured at 37 °C in a humidified atmosphere containing 5% CO_2. Adherent cells that morphologically resembled characterized MSCs could be seen as early as 4 days post-plating, while after approximately 7 days, the first colonies were observed, when the remnants of the tissue fragments were removed. After 3–4 weeks of culture, when the 80% to 90% confluence was reached, the cells were detached by using 0.05% trypsin with 1mM EDTA (PAA Laboratories). Following the first confluence (P0), the cells were passaged regularly in a growth medium (GM–DMEM with 10% FBS). Human MSCs derived from the alveolar crestal and horizontal fibres of human periodontal ligament were characterized following the minimal criteria for defining MSCs, including plastic adherence, the expression of characteristic markers, and multilineage differentiation [30]. For this study passages P3–P6 were used.

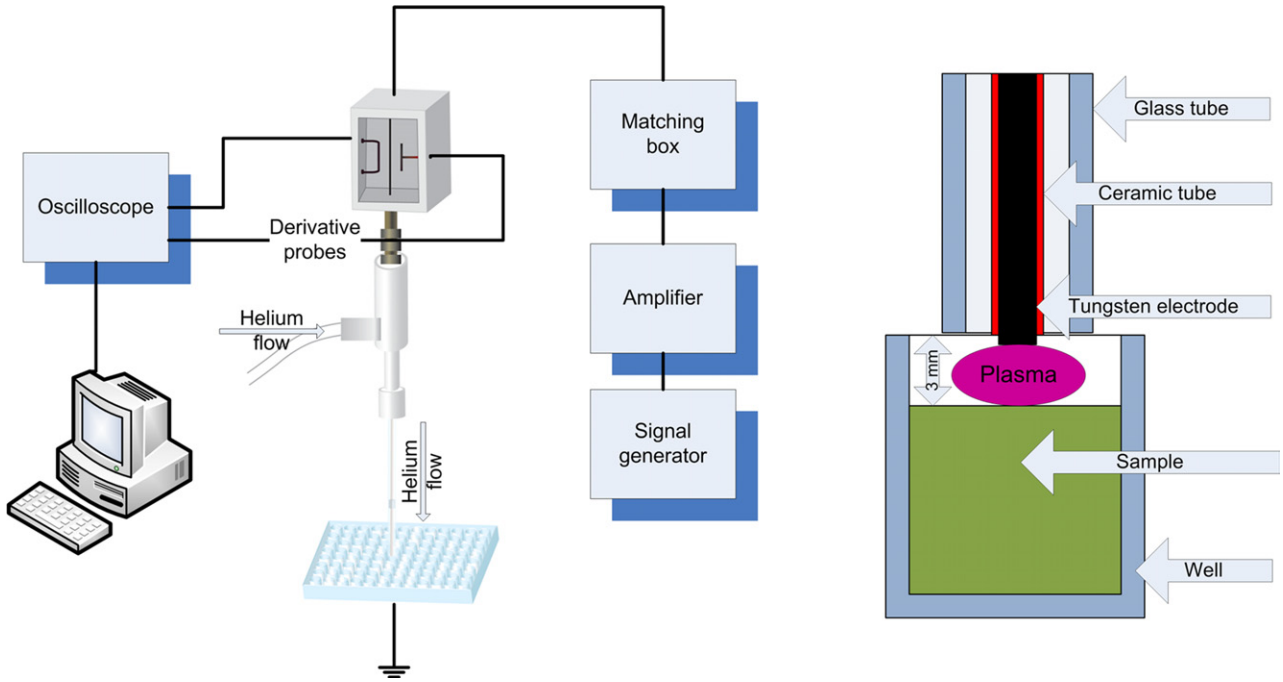

Figure 1. Schematic presentation of the non-thermal atmospheric plasma device used in the study.

The hPDL-MSCs were plated in triplicates in 96-well microtiter flat-bottomed plates with 200 μl of medium per well. The plasma needle was placed vertically above the microtiter plate in line with the upper edge of each well (figure 1). To examine the influence of the non-thermal plasma on the viability and the adhesion of hPDL-MSCs, the cells were treated using three different powers of plasma (0.15, 0.9 and 1.6 W), two flows of helium (0.5 and 1 slm) and four exposure times (10, 30, 60 and 120 s). Consequently, for the next treatments the highest power of plasma (1.6 W) combined with two flows of helium (0.5 and 1 slm) during two exposure times (30 and 60 s) were chosen. To be sure that the helium flow has no influence on the treated cell samples, we also treated the samples in a helium flow without the ignition of plasma for the same exposure times. Additionally, as control samples, untreated cells were used.

2.2. Viability assay

The viability of hPDL-MSCs, i.e. the survival of cells after the plasma treatment, was assessed using a 3-(4,5-dimethylthiazol-2-yl)-2,5-diphenyltetrazolium bromide (MTT) assay. After the treatments, the medium was replaced and the MTT substrate (Sigma, MO, USA) was added to the final concentration of 0.5 mg ml^{-1}. The cells were incubated for 3 h in culture conditions and formazan salts dissolved with 10% SDS/0.1N HCl during overnight incubation. The absorbance was measured at 540 nm by a spectrophotometer [31].

2.3. Adhesion assay

To test the plasma needle effect on the cells' detachment, an adhesion assay was performed. After the treatments, the wells were washed and the remaining adherent cells were stained with crystal violet. The stain was dissolved in 33% acetic acid and the absorbance was measured at 540 nm by a spectrophotometer [32].

2.4. Migration assay

The migration activity of the hPDL-MSCs was analysed using the *in vitro* scratch assay as previously described [33]. A scratch was made in the hPDL-MSCs' confluent monolayer using a sterile pipette tip and the remaining hPDL-MSCs were treated by plasma or He only, and cultured for a further 24 h. The cells were then stained with crystal violet. The migration of the cells into the scratch area was documented and quantified as a percentage of the cell-free area by TScratch® software (Computational Science and Engineering Laboratory, Swiss Federal Institute of Technology, ETH Zurich, Zurich, Switzerland).

2.5. Proliferation assay

The hPDL-MSCs were seeded at a density of 5×10^3/200 μl/well, and cultured overnight. On days 0, 2, 4 and 6 after the treatment cells were detached, they were counted and their number was determined by a Trypan blue exclusion test. The population doubling times (PDTs), were calculated according to the formula $\mathrm{PDT} = (T - T_0)\lg 2/(\lg N_T - \lg N_0)$, where T_0 is starting time of cell culture and T is ending time of cell culture, while N_0 and N_T respectively represent the cell number at the start and at the end of each culture.

2.6. ALP activity

To analyse the effect on the hPDL-MSCs' differentiation potential, we measured the activity of alkaline phosphatase

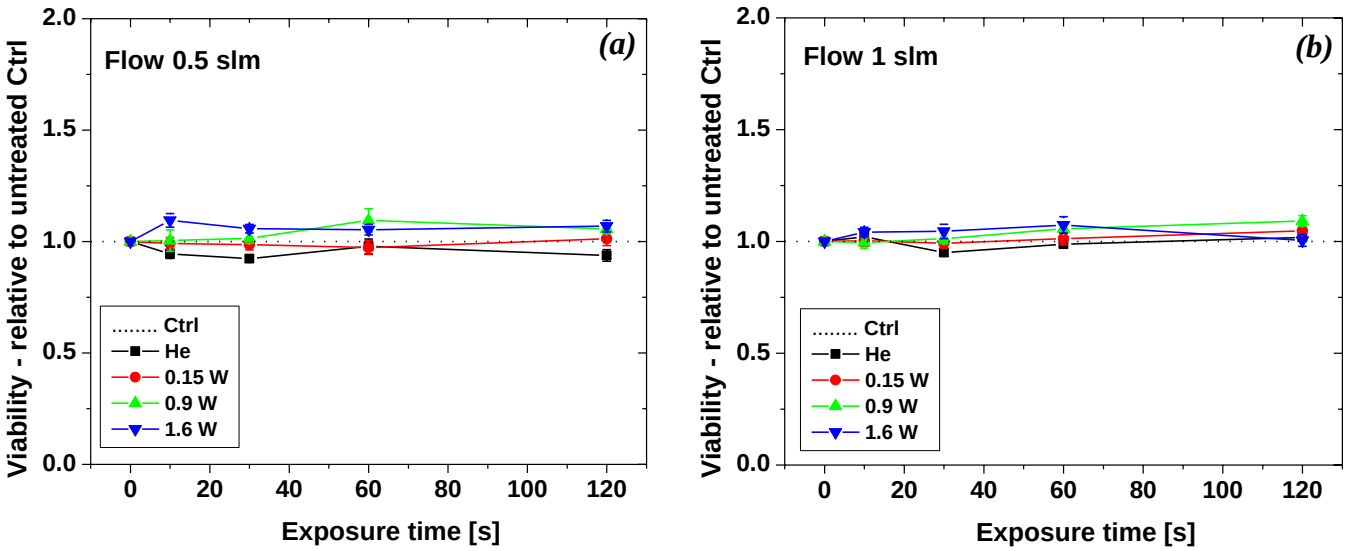

Figure 2. Effects of non-thermal plasma on the viability of hPDL-MSCs. The cells were treated by three different plasma powers (0.15, 0.9 and 1.6 W) or gas only (He), combined with two different He flows (0.5 and 1 slm) and four exposure times (10, 30, 60 and 120 s). The viability test was performed using MTT assay (*a*), (*b*). The data are expressed as mean fold changes of optical density values relative to the corresponding mean values of the untreated control cells from the same time point ± SEM of three separate experiments.

(ALP) in the cell culture supernatants using a commercial kit (Behringwerke AG, Marburg, Germany). After exposure, the hPDL-MSCs were cultured for 10 days in an osteogenic medium. In the condition medium collected during the last three days of culture, the ALP activity was assessed by measuring the absorbance of a p-nitrophenol product from a p-nitrophenylphosphate substrate at a wavelength of 405 nm by a spectrophotometer. To overcome the problem of an unequal number of the cells per well, the absorbance values were normalized to the total amount of cellular proteins. It was determined by a Micro BCA™ Protein Assay Kit (Pierce Biotechnology, Rockford, IL, USA) after lysing the cells.

2.7. Statistical analysis

To evaluate the probability of significant differences between two groups, a Student's t-test was used for parametric homogenous data, and a Mann–Whitney's U-test was used for non-homogenous data (CV $>$ 30%). Values of $p < 0.05$ were considered statistically significant.

3. Results and discussion

3.1. Effects of non-thermal plasma on the viability of hPDL-MSCs

The hPDL-MSCs isolated for these studies shared the features of other postnatal MSCs derived from various sources [30], as well as of the hPDL-MSCs reported in previous studies [34, 35], including plastic adherence, typical fibroblastic morphology, formation of colony-formatting units, extensive proliferation *in vitro*, MSC-specific surface antigen expression, as well as multipotent differentiation potential (manuscript in preparation).

To determine whether the non-thermal plasma affected the viability of the hPDL-MSCs, primary cells isolated from periodontal ligament were cultured and treated by three different powers of plasma (0.15, 0.9 and 1.6 W), and two flows of helium (0.5 and 1 slm), during four exposure times (10, 30, 60 and 120 s).

The results of the MTT assay demonstrated that at both gas flows, the non-thermal atmospheric-pressure plasma generated showed no significant effect on cell viability at all three tested powers as compared to both the non-treated and the He-only-treated control cells (figures 2(*a*) and (*b*)). This finding regarding the effect on the MSCs' viability is consistent with the results of our previous study, in which we showed that a non-thermal plasma applied under the same conditions was not cytotoxic for the peripheral blood-derived MSCs, although it exhibited a strong antibacterial effect [28]. This non-cytotoxic activity of plasma is of great importance if non-thermal plasma is going to be considered for potential applications in periodontal therapy.

3.2. Effect of non-thermal plasma on the detachment and migration of hPDL-MSCs

The adhesion assay data showed that the treatment with a non-thermal plasma did not significantly affect the hPDL-MSCs' adhesion, although some detachment of the cells was observed when the higher powers of plasma were combined with 0.5 slm flow (figures 3(*a*) and (*b*)).

The *in vitro* scratch assay was performed in order to investigate the plasma effect on the motility of the hPDL-MSCs. As shown in figure 4(*a*), plasma treatment considerably decreased the migration capacity of the hPDL-MSCs. Moreover, when the percentage of the cell-free area was quantified, significant differences were documented compared to both non-treated and He-only-treated control cells (figure 4(*b*)).

These findings were in a way unexpected, since no harmful effect on the hPDL-MSCs' viability was observed.

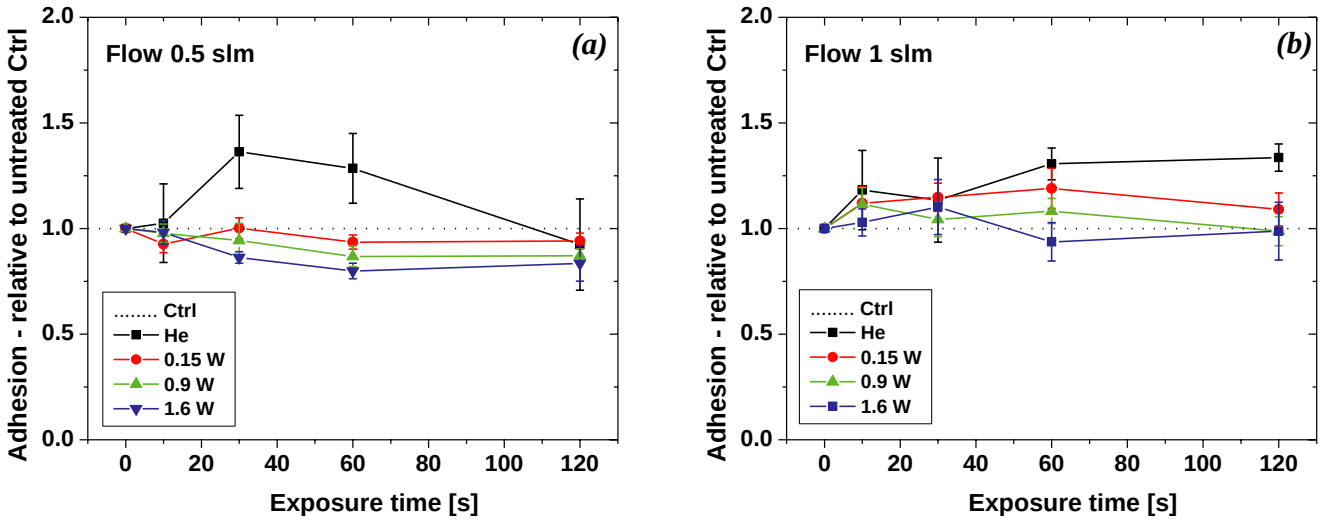

Figure 3. Effects of the non-thermal plasma on the adhesion of the hPDL-MSCs. Adhesion was assessed by colorimetric assay after staining with crystal violet (*a*), (*b*). The data are expressed as mean fold changes of optical density values relative to the corresponding mean values of the untreated control cells from the same time point ± SEM of three separate experiments.

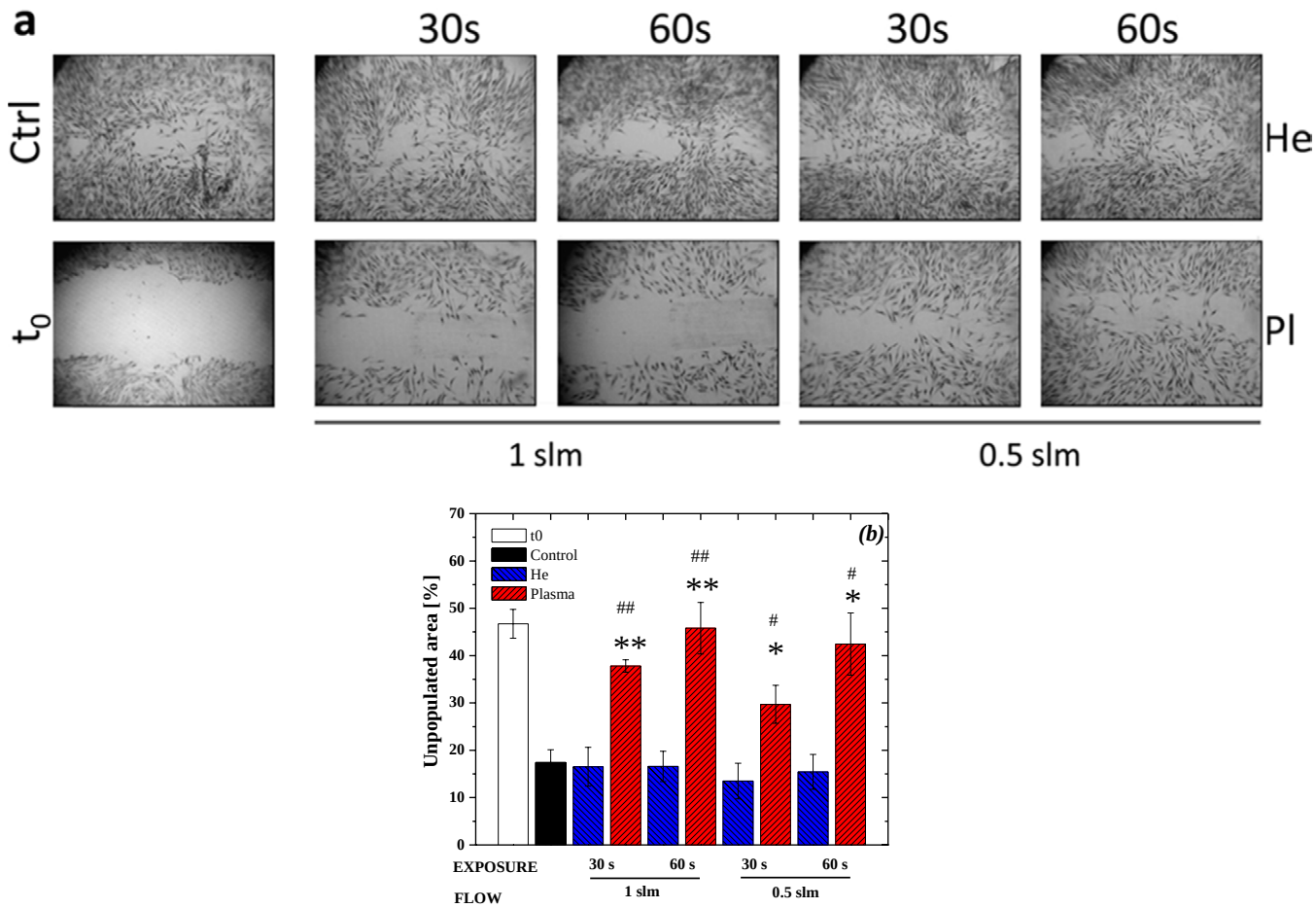

Figure 4. The effect of non-thermal plasma on hPDL-MSCs' migration. After reaching confluence, a scratch was made in the monolayer (t0) and the cells were treated by 1.6 W plasma (Pl) or gas only (He), at two different He flows (1 or 0.5 slm) for 30 s and for 60 s. Control cells were left untreated. After a further 24 h of culture, the cells were stained with crystal violet and the scratch area was photographed. The representative panels from three experiments are presented (*a*). The scratch area left unpopulated was measured using TScratch® software and is presented as the mean percentage of the cell-free area ± SEM of three separate experiments (*b*). The notation in the figure is: * $p < 0.05$, ** $p < 0.01$ compared to the untreated control, # $p < 0.05$, ## $p < 0.01$ compared to the He-only control (Mann–Whitney's U-test).

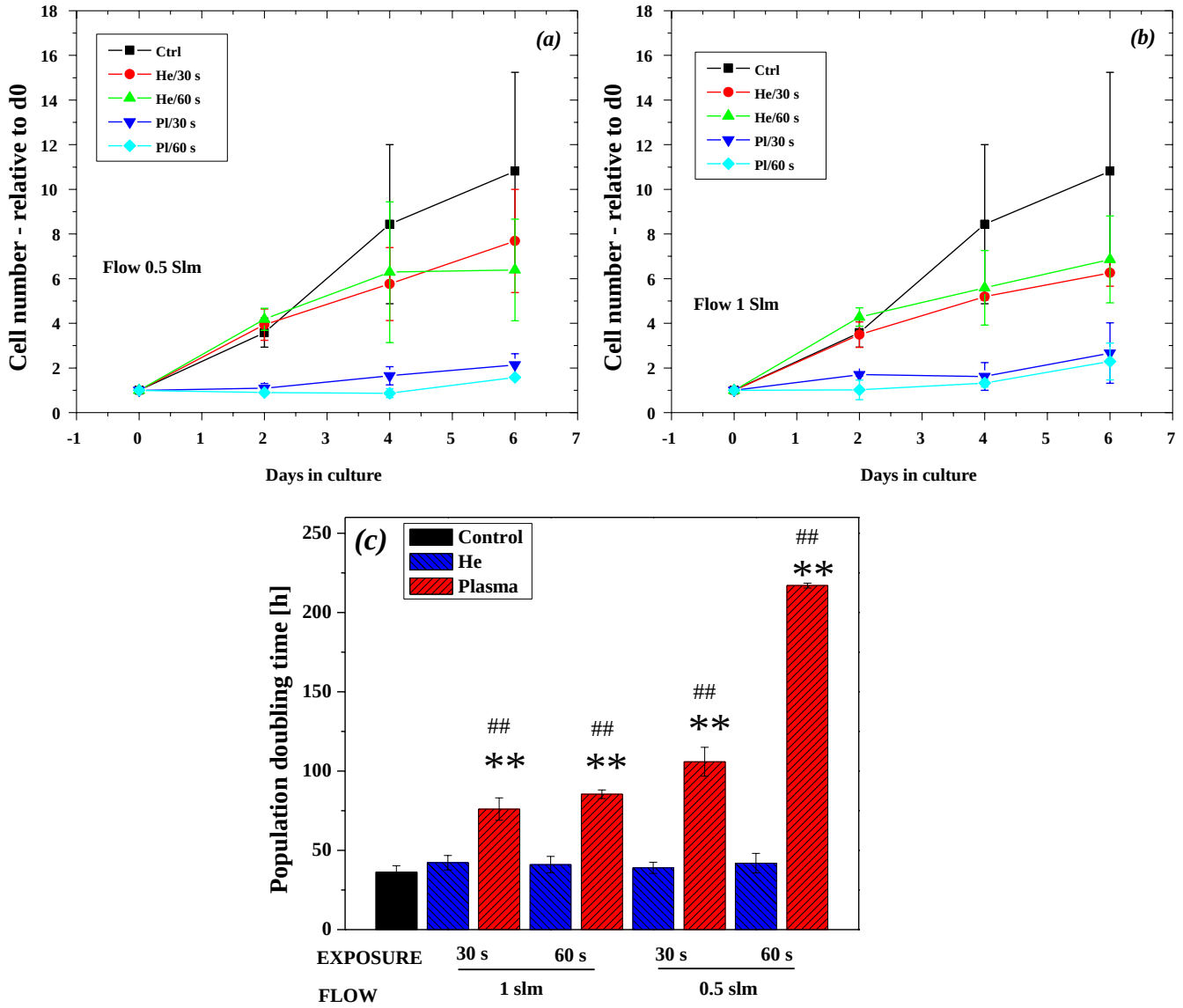

Figure 5. The effects of non-thermal plasma on the hPDL-MSCs' proliferation. (*a*), (*b*) After treatment with a 1.6 W plasma (Pl) or gas only (He) at two different He flows (1 slm or 0.5 slm) for 30 and 60 s, the cells were cultured for a further 6 days and enumerated on days 0, 2, 4 and 6. Control cells were left untreated. The results are presented as the mean number of cells ± SEM of three separate experiments. (*c*) The PDTs are given as the mean ± SEM of three separate experiments. The notation in the figure is: ** $p < 0.01$ compared to the untreated control, ## $p < 0.01$ compared to the He-only control (Mann–Whitney's U-test).

However, similar observations regarding the effects of plasma on the adhesion and migration of various adherent cells were previously reported. Namely, several studies demonstrated that low-intensity helium plasmas affect cells, such as fibroblasts and endothelial and smooth muscle cells, by inducing the disruption of cell-to-cell adhesion and subsequent cell detachment from the substrates, acting in a dosage-dependent manner [36–38]. More importantly, the observed effects were reversible, since after the plasma treatment, the detached cells remained viable, reattached to the plate surface and continued proliferating after a short incubation time. It is worth mentioning that the plasmas themselves are difficult to fully compare, since the working parameters for the application of different low-temperature sources of the atmospheric-pressure plasma are almost impossible to be standardized, and are defined separately for every single source, which, at present, additionally hinders the interpretation of the plasma-induced effects. Thus it would be very interesting to carry out similar studies in several different laboratories using the same standardized source.

3.3. Effect of non-thermal plasma on the proliferation and differentiation of hPDL-MSCs

Non-treated hPDL-MSCs exhibited a high proliferation rate, as the number of these cells increased more than 10-fold at day 6 after plating (figure 5). However, after the same period of time, the cell population merely doubled in the plasma-treated cultures, disregarding the different gas flow or exposure time applied (figures 5(*a*) and (*b*)). When PDTs were calculated, the results confirmed that plasma treatment lead to significant delay in cell proliferation, as PDT values for plasma-treated

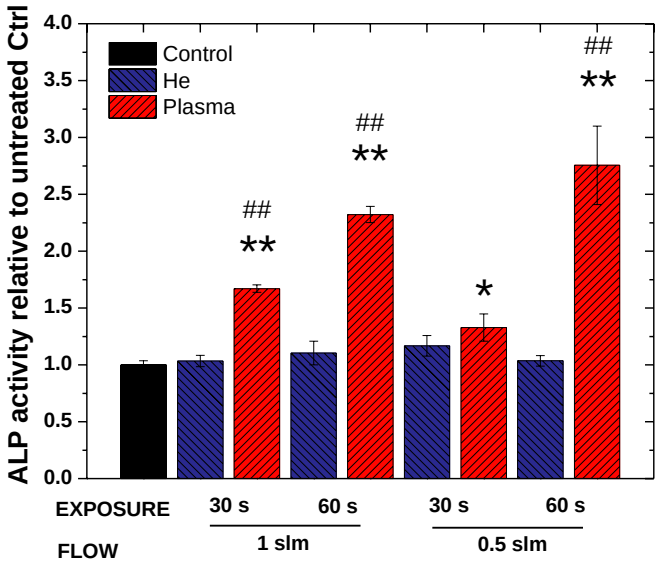

Figure 6. The alkaline phosphatase (ALP) activity of the hPDL-MSCs after non-thermal plasma treatment. The ALP activity was measured in a 3-day condition medium of 1.6 W plasma-treated, He-only-treated and the control, non-treated cells after 10 days of culture in an osteogenic medium. The results were normalized to the total cell protein concentration and presented as a mean fold-change related to the control cells ± SEM of three separate experiments. The notation in figure is: * $p < 0.05$, ** $p < 0.01$ compared to the untreated control, ## $p < 0.01$ compared to the He-only control (Student's t-test).

hPDL-MSCs were significantly higher in comparison to non-treated controls (figure 5(*c*)). Although the cells treated by He-only did show somewhat slower proliferation, the PDTs for these cells were not significantly prolonged, as compared to the non-treated hPDL-MSCs.

In order to analyse the effect of the non-thermal plasma on the hPDL-MSCs' differentiation potential, we measured the activity of ALP in the cell culture supernatants of the plasma-treated, He-only-treated and the control, non-treated cells. The results demonstrated that plasma treatment increased the osteogenic potential of the hPDL-MSCs, since for all experimental conditions applied significant enhancement in the ALP activity was observed in the plasma-treated cells, as compared to the non-treated cells (figure 6). Moreover, an He flow without plasma ignition did not significantly alter the ALP activity in the analysed samples.

The hPDL-MSCs have themselves already generated much attention in periodontal tissue engineering because of their multilineage differentiation potential, while the application of plasma treatment in the field of bone, as well as periodontal tissue engineering, has not yet been described. The results presented here suggest that plasma application may determine the status of the growth and osteogenic differentiation of hPDL-MSCs that may prove both useful and advantageous in bone regeneration and tissue engineering with hPDL-MSCs. Namely, treatment of the hPDL-MSCs with our plasma needle device significantly decreased their proliferation. However, growth-arrested hPDL-MSCs retained their ability to differentiate as plasma treatment induced a significant increase in the ALP activity in these cells. Since ALP is known as an early marker for osteoblastic differentiation, this finding suggests that plasma treatment can enhance osteogenic differentiation of the hPDL-MSCs. Generally, proliferation and differentiation are poorly consistent and the differentiation process is defined as a sequential event that follows attenuated cell proliferation. Namely, when progenitor/stem cells differentiate into specialized cells during the regeneration or reconstruction of damaged tissues, the factors and intracellular signals involved in cell growth are evenly inhibited. Therefore, we can suppose that the plasma-induced decrease in the rate of the hPDL-MSCs growth was probably a prerequisite for their subsequent induction of differentiation. At present, with the exception of the recently discovered effects of indirect plasma treatment on cell apoptosis [39], necrosis [36] and detachment [40], very little is known regarding the influence of plasma treatment on other cell functions, especially on human MSCs and their proliferation and differentiation capacity. Recent reported data only demonstrates the ability of plasma technology to modify the physicochemical properties of biomaterial surfaces, as a potentially efficacious strategy to control and influence either the response of human MSCs [41] or pre-osteoblast proliferation and differentiation [42]. Independent studies very impressively [29] confirm our observations on the ability of plasma to promote the osteogenic differentiation of human MSCs while suppressing their proliferation, i.e. to control and direct the MSCs' osteogenic differentiation. Further extensive studies need to be performed in order to specify these growth-suppressive and differentiation-inducing properties of non-thermal atmospheric-pressure plasma, as well as the underlying mechanisms.

As noted earlier, plasmas themselves are difficult to fully characterize, model and compare. Additionally, their biologically active targets are even more complex and therefore it is hard to investigate their effects, and even more difficult to elucidate the mechanisms involved. Reactive oxygen species (ROS) and the closely related reactive nitrogen species (RNS) are often generated in applications of atmospheric-pressure plasmas intended for biomedical purposes, and it is believed that these species influence many cellular responses [13, 43]. A recent study implicated the involvement of plasma-derived ROS in endothelial cell proliferation [44], so it can be presumed that these species are involved in plasma-induced effects on hPDL-MSCs' proliferation and differentiation. As for our plasma, NO was shown to be the dominant chemically active molecule [27]. Nitric oxide is involved in various cellular functions in all mammalian cells [45], including the proliferation and differentiation of neural [46] and hematopoietic [47–49] stem cells. Moreover, NO was suggested as an important factor in the induction of MSCs' [50] and hPDL cells' [51] differentiation into osteoprogenitor cells, with specific influence on the enhancement of ALP activity and mineralized nodule formation [52].

4. Conclusion

The hPDL-MSCs were isolated, expanded and characterized, and how their treatment with a non-thermal atmospheric

plasma affects their growth and differentiation status was analysed. The data obtained indicates that our plasma device combines specific activity with non-destructive properties on the hPDL-MSCs, since while reducing the proliferation, migration and adhesion of the hPDL-MSCs, the plasma did not affect their viability. Moreover, the plasma increased the ALP activity of hPDL-MSCs, strongly suggesting that plasma treatment may promote their osteogenic differentiation. Although more extensive studies are required to investigate the mechanisms associated with the plasma-mediated osteogenic differentiation of hPDL-MSCs, these results point to new possible applications of low-temperature plasmas at atmospheric pressure and provide new insights into the establishment of cell-based therapeutic strategies for periodontal defects.

Acknowledgments

This study was supported by Grant No ON175062, ON171037 and III 41011, Ministry of Education, Science and Technological Development, Republic of Serbia. The authors declare that there are no conflicts of interest in this study. The authors would like to thank M Andrić and A Pucar for supplying the periodontal ligament material and J F Santibañez for his valuable comments and suggestions.

References

[1] Savage A, Eaton K A, Moles D R and Needleman I 2009 A systematic review of definitions of periodontitis and methods that have been used to identify this disease *J. Clin. Periodontol.* **36** 458–67
[2] Pihlstrom B L, Michalowicz B S and Johnson N W 2005 Periodontal diseases *Lancet* **366** 1809–20
[3] Chen F M, Zhang J, Zhang M, An Y, Chen F and Wu Z F 2010 A review on endogenous regenerative technology in periodontal regenerative medicine *Biomaterials* **31** 7892–927
[4] Horwitz E M, Gordon P L, Koo W K, Marx J C, Neel M D, McNall R Y, Muul L and Hofmann T 2002 Isolated allogeneic bone marrow-derived mesenchymal cells engraft and stimulate growth in children with osteogenesis imperfecta: implications for cell therapy of bone *Proc. Natl Acad. Sci. USA* **99** 8932–7
[5] Murphy J M, Fink D J, Hunziker E B and Barry F P 2003 Stem cell therapy in a caprine model of osteoarthritis *Arthritis Rheum.* **48** 3464–74
[6] Stamm C, Westphal B, Kleine H D, Petzsch M, Kittner C, Klinge H, Schumichen C, Nienaber C A, Freund M and Steinhoff G 2003 Autologous bone-marrow stem-cell transplantation for myocardial regeneration *Lancet* **361** 45–6
[7] Mezey E, Key S, Vogelsang G, Szalayova I, Lange G D and Crain B 2003 Transplanted bone marrow generates new neurons in human brains *Proc. Natl Acad. Sci. USA* **100** 1364–9
[8] Rodriquez-Lozano F J, Bueno C, Insausti C L, Mesequer L, Ramirez M C, Blanquer M, Marin N, Martinez S and Moraleda J M 2011 Mesenchymal stem cells derived from dental tissues *Int. Endodont. J.* **44** 800–6
[9] Seo B M, Miura M, Gronthos S, Bartold P M, Batouli S, Brahim J, Young M, Robey P G, Wang C Y and Shi S 2004 Investigation of multipotent postnatal stem cells from human periodontal ligament *Lancet* **364** 149–55
[10] Ivanovski S, Gronthos S, Shi S and Bartold P M 2006 Stem cells in the periodontal ligament *Oral. Dis.* **12** 358–63
[11] Shi S, Bartold P M, Miura M, Seo B M, Robey P G and Gronthos S 2005 The efficacy of mesenchymal stem cells to regenerate and repair dental structures *Orthod. Craniofac. Res.* **8** 191–9
[12] Park J Y, Jeon S H and Choung P H 2011 Efficacy of periodontal stem cell transplantation in the treatment of advanced periodontitis *Cell Transplantation* **20** 271–85
[13] Morfill G E, Kong M G and Zimmermann J L 2009 Focus on plasma medicine *New J. Phys.* **11** 115011–9
[14] Fridman A 2008 *Plasma Chemistry* (Cambridge: Cambridge University Press)
[15] Morfill G E, Shimizu T, Steffes B and Schmidt H-U 2009 Nosocomial infections-a new approach towards preventive medicine using plasmas *New J. Phys.* **11** 115019–29
[16] Heinlin J, Isbary G, Stolz W, Morfill G, Landthaler M, Shimizu T, Steffes B, Nosenko T, Zimmermann J L and Karrer S 2011 Plasma applications in medicine with a special focus on dermatology *J. Eur. Acad. Dermatol. Venereol.* **25** 1–11
[17] Joshi S G, Paff M, Friedman G, Fridman G, Fridman A and Brooks A D 2010 Control of methicillin-resistant *Staphylococcus aureus* in planktonic form and biofilms: a biocidal efficacy study of nonthermal dielectric-barrier discharge plasma *Am. J. Inf. Control* **38** (4) 293–301
[18] Dobrynin D, Fridman G, Friedman G and Fridman A 2009 Physical and biological mechanisms of direct interaction with living tissue *New J. Phys.* **11** 115020–46
[19] Sato T, Miyahara T, Doi A, Ochiai S, Urayama T and Nakatani T 2006 Sterilization mechanism for *Escherichia coli* by plasma flow at atmospheric pressure *Appl. Phys. Lett.* **89** 073902
[20] Lloyd G, Friedman G, Jafri S, Schultz G, Fridman A and Harding K 2010 Gas plasma: medical uses and developments in wound care *Plasma Process. Polym.* **7** 194–211
[21] Nosenko T, Shimizu T and Morfill G E 2009 Designing plasmas for chronic wound disinfection *New J. Phys.* **11** 115013–32
[22] Vandamme M, Robert E, Dozias S, Sobilo J, Lerondel S, Le Pape A and Pouvesle J-M 2011 Response of human glioma U87 xenografted on mice to non thermal plasma treatment *Plasma Med.* **1** 27–43
[23] Fridman G, Shereshevsky A, Jost M M, Brooks A D, Fridman A, Gutsol A, Vasilets V and Friedman G 2007 Floating electrode dielectric barrier discharge plasma in air promoting apoptotic behavior in melanoma skin cancer cell lines *Plasma Chem. Plasma Process.* **27** 163–76
[24] Lee H W, Kim G J, Kim J M, Park J K, Lee J K and Kim G C 2009 Tooth bleaching with nonthermal atmospheric pressure plasma *J. Endodont.* **35** 587–91
[25] Stoffels E, Flikweert A J, Stoffels W W and Kroesen G M W 2002 Plasma needle: a non-destructive atmospheric plasma source for fine surface treatment of (bio)materials *Plasma Sources Sci. Technol.* **11** 383–8
[26] Puač N, Petrović Z, Malović G, Đorđević A, Živković S, Giba Z and Grubišić D 2006 Measurements of voltage–current characteristics of a plasma needle and its effect on plant cells *J. Phys. D: Appl. Phys.* **39** 3514–9
[27] Malović G, Puač N, Lazović S and Petrović Z 2010 Mass analysis of an atmospheric pressure plasma needle discharge *Plasma Sources Sci. Technol.* **19** 034014
[28] Lazović S *et al* 2010 The effect of a plasma needle on bacteria in planktonic samples and on peripheral blood mesenchymal stem cells *New J. Phys.* **12** 083037
[29] Freeman T A, Steinbeck M J, Fridman G, Zhang J, Shainsky N, Friedman G and Fridman A 2012 Nonthermal dielectric barrier discharge plasma enhances skeletal cell

differentiation and autopad development *Book of Abstracts, Invited Talk on ICPM4 (Orleans, France)*
[30] Dominici M, Le Blanc K, Mueller I, Slaper-Cortenbach I, Marini F, Krause D, Deans R, Keating A, Prockop D J and Horwitz E 2006 Minimal criteria for defining multipotent mesenchymal stromal cells The International Society for Cellular Therapy position statement *Cytotherapy* **8** 315–7
[31] Mosmann T 1983 Rapid colorimetric assay for cellular growth and survival: application to proliferation and cytotoxicity assay *J. Immunol. Methods* **65** 55–63
[32] Oez S, Welte K, Platzer E and Kalden J R 1990 A simple assay for quantifying the inducible adherence of neutrophyls *Immunobiology* **180** 308–15
[33] Kocić J, Santibañez F J, Krstić A, Mojsilović S, Okić Đorđević I, Trivanović D, Ilić V and Bugarski D 2012 Interleukin 17 inhibits myogenic and promotes osteogenic differentiation of C2C12 myoblasts by activating ERK1,2 *Biochim. Biophys. Acta* **1823** 838–49
[34] Nagatomo K, Komaki M, Sekiya I, Sakaguchi Y, Naguchi K, Oda S, Muneta T and Ishikawa I 2006 Stem cell properties of human periodontal ligament cells *J. Periodont. Res.* **41** 303–10
[35] Iwata T, Yamato M, Zhang Z, Mukobata S, Washio K, Ando T, Feijen J, Okano T and Ishikawa I 2010 Validation of human periodontal ligament-derived cells as a reliable source for cytotherapeutic use *J. Clin. Periodontol.* **37** 1088–99
[36] Kieft I E, Darios D, Roks A J M and Stoffels E 2005 Plasma treatment of mammalian vascular cells: a quantitative description. *IEEE Trans. Plasma Sci.* **33** 771–5
[37] Shashurin A, Keidar M, Bronnikov S, Jurjus R A and Stepp M A 2008 Living tissue under treatment of cold plasma atmospheric jet *Appl. Phys. Lett.* **93** 181501
[38] Yonson S, Coulombe S, Leveille V and Leask R L 2006 Cell treatment and surface functionalization using a miniature atmospheric pressure glow discharge plasma torch *J. Phys. D: Appl. Phys.* **39** 3508–13
[39] Kieft I E, Kurdi M and Stoffels E 2006 Reattachment and apoptosis after plasma needle treatment of cultures cells *IEEE Trans. Plasma Sci.* **34** 1331–6
[40] Stoffels E, Roks A J M and Deelman L E 2008 Delayed effects of cold atmospheric plasma on vascular cells *Plasma Process. Polym.* **5** 599–605
[41] Tan F, O'Neill F, Naciri M, Dowling D and Al-Rubeai M 2012 Cellular and transcriptomic analysis of human mesenchymal stem cell response to plasma-activated hydroxyapatite coating *Acta Biomater.* **8** 1627–38
[42] Barradas A M *et al* 2012 Surface modifications by gas plasma control osteogenic differentiation of MC3T3-E1 cells *Acta Biomater.* **8** 2969–77
[43] Graves D B 2012 The emerging role of reactive oxygen and nitrogen species in redox biology and some implications for plasma applications to medicine and biology *J. Phys. D: Appl. Phys.* **45** 263001
[44] Kalghatgi S, Friedman G, Friedman A and Clyne A M 2010 Endothelial cell proliferation is enhanced by low dose non-thermal plasma through fibroblast growth factor-2 release *Ann. Biomed. Eng.* **38** 748–57
[45] MacMicking J, Xie Q W and Nathan C 1997 Nitric oxide and macrophage function *Annu. Rev. Immunol.* **15** 323–50
[46] Cheng A, Wang S, Cai J, Rao M S and Mattson M P 2003 Nitric oxide acts in a positive feedback loop with BDNF to regulate neural progenitor cell proliferation and differentiation in the mammalian brain *Dev. Biol.* **258** 319–33
[47] Epperly M W, Cao S, Yhang X, Franicola D, Shen H, Greenberger E E, Epperly L D and Greenberger J S 2007 Increased longevity of hematopoiesis in continuous bone marrow cultures derived from NOS1 (nNOS, mtNOS) homozygous recombinant negative mice correlates with radioresistance of hematopoietic and marrow stromal cells *Exp. Hematol.* **35** 137–45
[48] Krasnov P, Michurina T, Packer M A, Stasiv Y, Nakaya N, Moore K A, Drazan K E and Enikolopov G 2008 Neuronal nitric oxide synthase contributes to the regulation of hematopoiesis *Mol. Med.* **14** 141–9
[49] Krstić D A, Santibanez F J, Okić I, Mojsilović S, Kocić J, Jovčić G S, Milenković B P and Bugarski S D 2010 Combined effect of IL-17 and blockade of nitric oxide biosynthesis on haematopoiesis in mice *Acta. Physiol.* **199** 31–41
[50] Ocarino N M, Boeloni J N, Goes A M, Silva J F, Marubayashi U and Serakides R 2008 Osteogenic differentiation of mesenchymal stem cells from osteopenic rats subjected to physical activity with and without nitric oxide synthase inhibition *Nitric Oxide* **19** 320–5
[51] Orciani M, Trubiani O, Vignini A, Mattioli-Belmonte M, Di Primio R and Salvolini E 2009 Nitric oxide production during the osteogenic differentiation of human periodontal ligament mesenchymal stem cells *Acta Histochem.* **111** 15–24
[52] Mei Y F, Yamaza T, Atsuta I, Danjo A, Yamashita Y, Kido M A, Goto M, Akamine A and Tanaka T 2007 Sequential expression of endothelial nitric oxide synthase, inducible nitric oxide synthase, and nitrotyrosine in odontoblasts and pulp cells during dentin repair after tooth preparation in rat molars *Cell Tissue Res.* **328** 117–27

Plasma functionalization of titanium surface for repulsion of blood platelets

Article *in* Surface and Coatings Technology · October 2012

Impact Factor: 2 · DOI: 10.1016/j.surfcoat.2012.01.017

12 authors, including:

Martina Modic
Jožef Stefan Institute
24 PUBLICATIONS **108** CITATIONS
SEE PROFILE

Ita Junkar
Jožef Stefan Institute
62 PUBLICATIONS **687** CITATIONS
SEE PROFILE

Cristina Canal
Polytechnic University of Catalonia
54 PUBLICATIONS **724** CITATIONS
SEE PROFILE

Miran Mozetic
Jožef Stefan Institute
287 PUBLICATIONS **3,708** CITATIONS
SEE PROFILE

Surface & Coatings Technology 211 (2012) 200–204

Contents lists available at SciVerse ScienceDirect

Surface & Coatings Technology

journal homepage: www.elsevier.com/locate/surfcoat

Plasma functionalization of titanium surface for repulsion of blood platelets

U. Cvelbar [a,b,*], M. Modic [a,b], J. Kovač [a,b], S. Lazović [a,c], G. Filipič [a], D. Vujošević [d], I. Junkar [b], K. Eleršič [a,b], S.P. Brühl [e], C. Canal [f], T. Belmonte [g], M. Mozetič [b]

[a] Department F4, Jozef Stefan Institute, Jamova cesta 39, SI-1000 Ljubljana, Slovenia
[b] Centre of Excellence for Polymer Materials and Technologies, Tehnološki park 24, SI-1000 Ljubljana, Slovenia
[c] Institute of Physics Belgrade, Pregrevica 118, 11080 Belgrade, Serbia
[d] Institute for Public Health, Ljubljanska bb, MNE-81000 Podgorica, Montenegro
[e] National University of Technology, Regional Faculty of Concepcion del Uruguay, Ing. Pereira 676, Concepcion del Uruguay, Argentina
[f] Biomaterials, Biomechanics and Tissue Engineering Group, Materials Science and Metallurgy, Department, Technical University of Catalonia (UPC), Av. Diagonal 647, 08028 Barcelona, Spain
[g] Institute Jean Lamour, Equipe ESPRITS (201), Department CP2S, Ecole des Mines de Nancy, Parc de Saurupt, CS 14234, France

ARTICLE INFO

Available online 15 January 2012

Keywords:
Oxygen plasma
Titanium
Platelet adhesion
Stents

ABSTRACT

Thrombosis and restenosis are the most common problems during insertion of biocompatible implants like titanium stents into human blood, due to aggregation of platelets on their surfaces. Because of this reason, we studied the response of blood platelets to a plasma treated titanium surface. The aim was to design a functionalized surface which would repel blood platelets or prevent their adhesion. Therefore, we functionalized surfaces with low-temperature inductively coupled oxygen plasma treatment, which in the first stage cleaned the surface of titanium, and in the second promoted incorporation of oxygen functional groups as well as the growth of a titanium dioxide film. In this paper we show that oxygen atoms or oxygen containing groups play an important role in the repulsion of platelets and their deactivation. At the same time, increased surface temperature of samples either through sequential thermal deactivation in oven at 150 °C or heating the surface with ion bombardment during the treatment, lowers the oxygen content and the surface repulsion for platelets.

1. Introduction

Titanium is an important material for biocompatible artificial implants e.g. coronary stents in human blood, which is comparable in characteristics to polymer materials that have been recently increasing due to low cost and flexibility [1–3]. The advantage in using titanium for stents instead of poly(ethylene terephthalate) (PET) or poly(tetrafluoroethylene) (PTFE) polymer materials is increased durability and wear resistance to circulating and eroding human blood [4]. However, when vein diameters are smaller than 6 mm, thrombosis and restenosis can occur after stent implantation [1,5,6]. The predominant reason for this is the adhesion of blood platelets to the stent which become activated. Attached and activated platelets attract other platelets from the circulating blood, leads to platelet aggregation on the stent. This can eventually lead to agglomeration, which leads to health problems, e.g. clogged veins. The aim, in this paper, is to prepare artificial implant surfaces, (including stents) in such a way that they will mimic the original biological components (e.g. veins) [1,4]. In this case, the best stent would be one that is coated with endothelial cells (the building units of veins) which naturally prevent adhesion of blood platelets. The platelets, however, can adhere to the surface during the growth process of endothelial cells from human blood. Due to this limitation, we are investigating new ways to prevent adhesion and activation of platelets on the implant surface, which in our case is a titanium stent.

One of the best ways how to prepare titanium stent surfaces is with an oxygen plasma. A typical low-temperature oxygen plasma can be used in many ways during processing of the stent surface, for example; it can clean the surface from organic impurities, sterilize the surface and possibly prevent adhesion of platelets. It has already been proven that plasma surface cleaning [7–9] and sterilization processes [10–12] are effective in oxygen plasmas, generated either with microwave, radiofrequency, DC discharges or similar sources [13–16]. However despite this, the link between plasma functionalized titanium surfaces and the behaviour of blood platelets has been explored only to a very limited extent. It has been found that ion implantation of oxygen can improve the repulsion of platelets [17,18]. Moreover it was reported that the layer of titanium dioxide prepared by wet chemical treatment in H_2O_2 increased the probability for the adhesion of platelets. Extensive heating of the same samples was shown to reduce the probability for adhesion [19], however, when the TiO_2 was prepared by thermal heating only, the probability for adhesion of platelets reduced with oxide layer thickness. The adhesion of platelets was reported to be influenced also by composition of oxide layer [20].

* Corresponding author at: Department F4, Jozef Stefan Institute, Jamova cesta 39, SI-1000 Ljubljana, Slovenia.
E-mail address: uros.cvelbar@ijs.si (U. Cvelbar).

0257-8972/$ – see front matter © 2012 Elsevier B.V. All rights reserved.
doi:10.1016/j.surfcoat.2012.01.017

Motivated by this observation, we explored the repulsion and adhesion of platelets to a modelled titanium surface after different plasma treatment procedures. Moreover, we tried to link the surface properties of plasma treated samples with platelet activity near their surfaces.

2. Experimental

The experiments were performed using an industrial grade titanium (96 at.% Ti and 4 at.% impurities) sheet with a thickness of 0.25 mm. The sheet was cut into 0.5×2 cm^2 sized pieces, which were washed ultrasonically for 2 min in demineralized water and air dried. The samples were then exposed to an oxygen plasma in the discharge chamber shown in Fig. 1. The system was pumped down using a two-stage oil rotary pump with a pumping speed of $16.7 \cdot 10^{-3}$ m^3/s. The discharge chamber was a Pyrex cylinder with a length of 270 mm and an inner diameter of 320 mm. The plasma was created using an inductively coupled RF generator, operating at a frequency of 27.12 MHz and a maximum output power of approximately 1.5 kW. The plasma parameters were measured with a double Langmuir probe and a catalytic probe. Commercially available oxygen was introduced into the discharge chamber. The pressure was measured by an absolute vacuum gauge and adjusted during continuous pumping by a precise leak valve. In our experiments, the pressure was fixed at 100 Pa, with plasma discharge parameters, the ion and neutral atom densities (close to the holder) of the plasma discharge were $7 \cdot 10^{15}$ m^{-3} and $1 \cdot 10^{22}$ m^{-3}, respectively. The samples were placed into the discharge chamber on a stainless steel holder with aluminum hook which was also connected to a RF coil for biasing as shown in Fig. 1. The samples were treated in the oxygen plasma for varied treatment times. When a bias was applied to a holder, the titanium samples could be heated up to 450–550 °C. Thermal treatment of samples was performed after the plasma treatment in the dry heat oven at 150 °C for 1 h, in order to study influence of temperature on deactivation of the surface. These samples were marked as plasma pre-treated samples.

Prior to and after the plasma treatment, the samples were analysed though wettability contact angle (WCA) measurements and X-ray photoelectron spectroscopy (XPS). Wettability was investigated using See System Advex Instruments immediately after plasma treatment by measuring the water contact angle with a demineralised water droplet of volume 1 μl. Each determination was obtained by averaging results of 7 measurements. The relative humidity (45%) and the room temperature (25 °C) were monitored continuously and were found not to vary significantly during the contact angle measurements. The measurement error of wettability angle was 1°.

The surface of the sample was analyzed using an XPS instrument TFA XPS Physical Electronics. The base pressure in the XPS analysis chamber was approximately $6 \cdot 10^{-8}$ Pa. The samples were excited with X-rays over a 400 μm spot area with monochromatic Al $K_{\alpha\ 1,2}$ radiation at 1486.6 eV. The photoelectrons were detected with a hemispherical analyzer positioned at an angle of 45° with respect to the normal to the sample surface. The energy resolution was about 0.5 eV. Survey-scan spectra were made at a pass energy of 187.85 eV and a 0.4 eV energy step, while for C 1s, O 1s and Ti 2p individual high-resolution spectra were taken at a pass energy of 29.35 eV and a 0.125 eV energy step. The XPS spectra were measured on both the pristine and oxygen plasma treated samples. The spectra were fitted using MultiPak software from Physical Electronics. A Shirley-type background subtraction was used.

The plasma treated surfaces at room temperature were then tested for repulsion of blood platelets. The blood from a healthy human volunteer was collected into a vacutainer containing sodium citrate as an anticoagulant. Six samples were prepared for single plasma treatment and an untreated control, which was used as a control, were incubated in 1 ml of human blood in a 24-well cell culture plate at ambient conditions at a shearing rate of 300 rpm. After 1 h of incubation, the samples were taken out and dip-rinsed several times with 1 ml PBS (phosphate buffer saline) in order to remove platelets which were not attached to the surface, and fixed with 2,5 (v/v) glutaraldehyde for 30 min. Subsequently, the samples were washed with distilled water and dried. Samples were then examined using a confocal light microscope (Axio CSM 700). The platelets were counted on 5 samples with at least 5 counted areas of size 234 μm × 188 μm per treated sample. Parallel to counting, we also performed control with in vitro Sulforhodamine B based toxicology assay. This is a colorimetric assay originally developed for the cytotoxicity screening of the cancer drugs based on the incorporation of sulforhodamine B on intracellular proteins. The quantity of incorporated colour is proportional to a total cell mass, and is measured with absorbance at 564 nm with UV/VIS spectrophotometer.

3. Results and discussion

Surface functionalization or modification in a plasma treatment can normally be directly observed by simple wettability contact angle measurements. Due to this, we tested titanium samples for surface wettability after different treatment times in an oxygen plasma. The samples were either treated only with an inductively coupled plasma or they were additionally biased in order to increase the effective ion flux to the surface, which could rapidly heat the surface to temperatures around 450 °C. Since the increased temperature after the plasma treatment is expected to reduce the surface functionalization and deactivate the surface, the samples were treated in a dry heat oven at 150 °C for 1 h. From Fig. 2, we can clearly see the activation

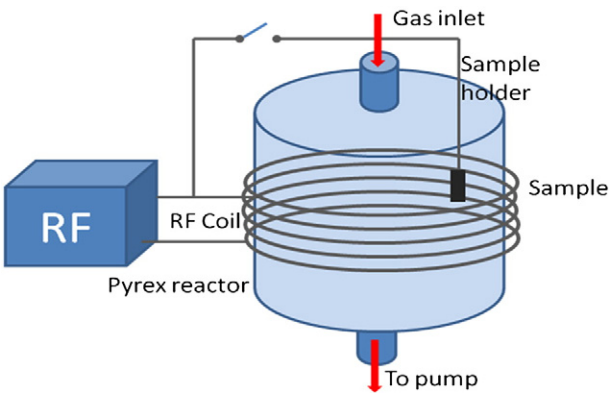

Fig. 1. Schematic of plasma system with different configurations.

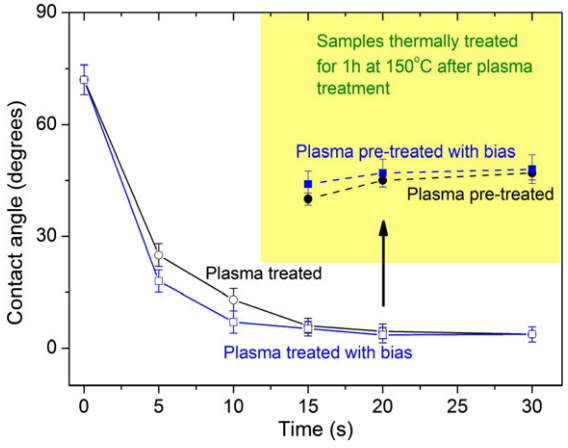

Fig. 2. Wettability contact angle (WCA) measurements of demineralized 1 μm water drop for different plasma treatment times, where samples were subjected to O_2 plasma with floating (-○-) or biasing (-□-) sample holder. Both types of plasma treated samples were additionally subjected to heating in the dry heat oven for 1 h at 150 °C (-●- floating, --■-- biased samples).

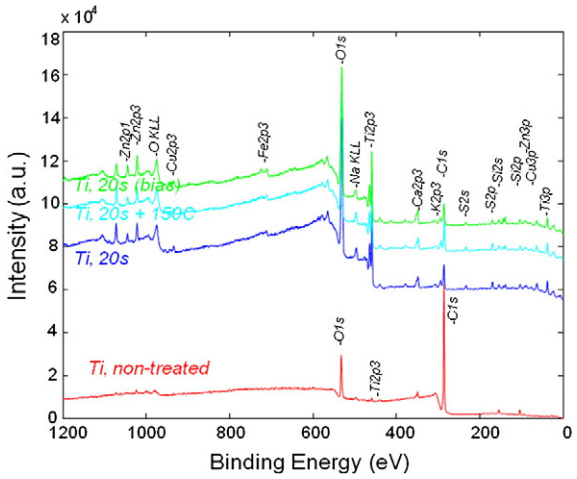

Fig. 3. XPS survey spectra with characteristic peaks for different treatment type of industrial grade titanium; a) non-treated surface, b) 20 s oxygen plasma treated surface, c) 20 s oxygen plasma treated surface with sample on biased stage, and d) prepared surface with 20 s oxygen plasma treatment and then subjected to 1 h thermal heating at 150 °C.

process of the surfaces, where the wettability of the demineralised water drop increases rapidly in seconds after plasma treatment. The wettability curve drop is slightly more pronounced for biased sample, due to more intensive interaction of ions with the surfaces. After 15 min the wettability reaches values around 5° and stabilizes around this value for both types of treatment. In the second step, the same samples were exposed to heat treatment and tested again afterwards for wettability properties. As seen in Fig. 2, the contact angle in both cases increases to 40–50°, depending on the first plasma treatment time. From this we can conclude that something occurred on the surface which lowered the surface energy.

Following the wettability measurements showing surface energy modifications, surface characterization with XPS was performed. From the XPS survey spectra, seen in Fig. 3, we determined that the pristine (non-treated) sample has a high amount of carbon, and small amounts of titanium. This suggests that pristine samples are highly contaminated with carbon like impurities. As shown in Fig. 3 a short 20 s exposure to oxygen plasma removes contaminants and reveals Ti as well as other elements contained in the industrial grade titanium, such as C, Na, K, Ca, Zn, Cu, S, Si, and Fe. More importantly, there is a strong increase in the oxygen content. This can be seen also in Fig. 4 which shows the atomic concentration of elements on the surface. The pristine sample is highly contaminated with carbon, which is removed after the 20 s oxygen plasma treatment. Moreover, there is very little variation between the 20 s sample and 20 s (150 °C) which was subjected to thermal heating. The only difference is seen in oxygen and carbon content which can be linked to reduced

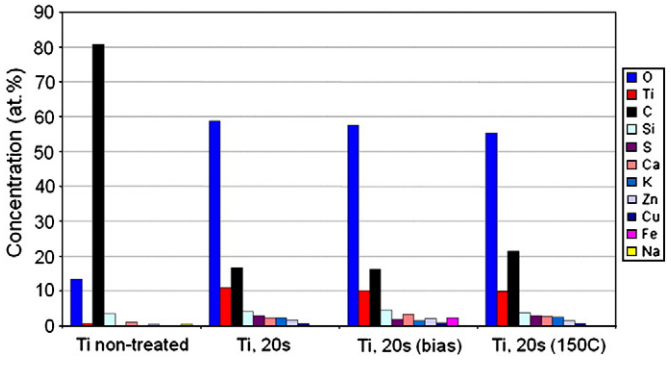

Fig. 4. The elemental composition of the surfaces measured from XPS survey spectra after different treatments.

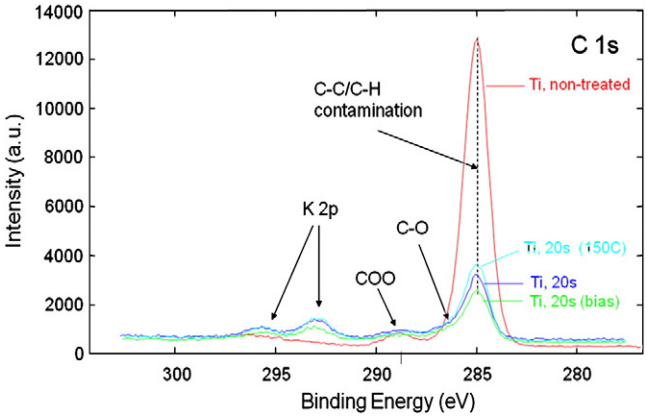

Fig. 5. High-resolution XPS peak of carbon C1s after different treatments.

contact angle. The oxygen content is also slightly lower for the biased treated titanium the compared to 20 s treatment, and slightly higher than for the 20 s thermally treated samples. The content of carbon for the biased sample, namely, is lower than for the thermally treated sample. Interestingly, there are small variations in the other element impurity concentrations, which suggest that there is a segregation process taking place under changed electrical conditions. However the major role surface activation plays is the removal of carbon contaminants and adsorption of oxygen. To check this argument, we performed high-resolution XPS analysis, shown in Figs. 5, 6 and 7. In Fig. 5 the HR XPS spectra of carbon C 1s peaks are shown. The carbon C 1s peak at 285 eV and contains C–C and C–H bonds, whereas the peak at 289 eV has COO bonds. Both peaks can be linked to strong surface contamination which is typical for organic materials. Therefore, prior to plasma treatment the surface is contaminated with carbon-like impurities or organic materials. A short treatment with an oxygen plasma lowered the C 1s peak as well as the COO peak, but increased the C–O bond peak at 285.6 eV. This indicates that the carbon impurities have been removed, and the oxygen bonded to carbon. There is no significant difference between the different treatments (plasma-only, plasma biased or additionally thermally treated samples), except in carbon content. The most efficient removal of carbon was on the biased samples, where ions were used more extensively.

Oxygen plasma treatment of titanium also creates a thin TiO_2 layer. This can be seen in Fig. 6, from the Ti^{4+} peak at 458.6 eV. The non-treated sample has almost no visible TiO_2 layer and a very low surface concentration of Ti. After activation with 20 s plasma treatment, the TiO_2 thin layer is created. This is comparable with both, plasma with biased substrate or additional thermal heating of 20 s treated sample. Surprisingly, there are no expected Ti^{3+} or Ti^{2+} peaks, which are characteristic for less stable titanium oxide

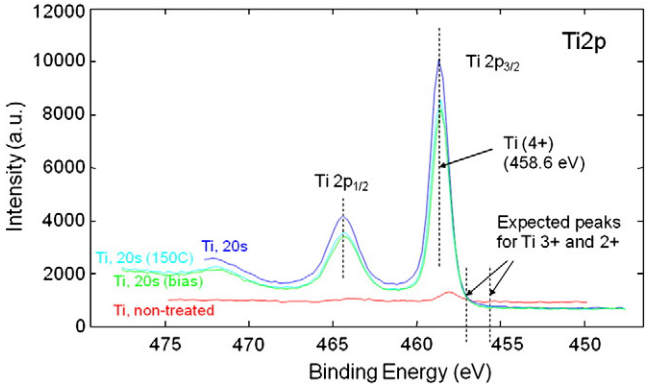

Fig. 6. High-resolution XPS peak of titanium Ti2p after different treatments.

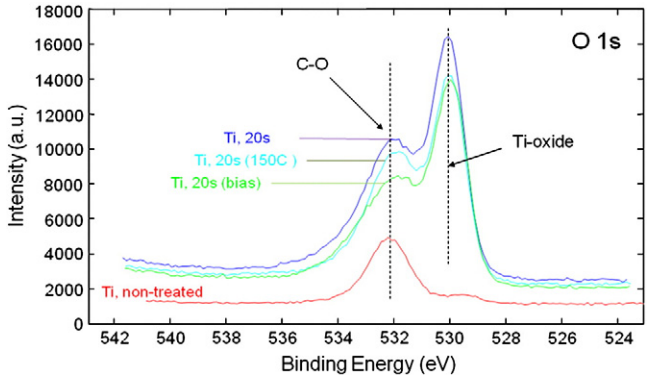

Fig. 7. High-resolution XPS peak of oxygen O1s after different treatments.

compounds. From this we can conclude that a stable TiO_2 layer has been created during surface activation. The O1s peak in Fig. 7 confirms that plasma created the TiO_2 layer and added large amounts of oxygen to the surface, either interstitial or through bonding with Ti, C (through C–O bond at 532.4 eV) or even absorption of water molecules from the surrounding air (H–O peak at 534.5 eV), when taken out of vacuum.

The functionalization of titanium in a plasma treatment can be explained with removal of surface contamination by carbon or organic deposits, which adhered to the surface during sample preparation or exposure to air. Removal of such contamination enables better water contact angle and increased surface energy. It is well known that the created TiO_2 layer, which is activated, exhibits superhydrophilic properties with WCA lower than 5°. Normally, such a surface is prepared by UV irradiation, but can be also done in a plasma irradiation by photons and interaction of neutral oxygen atoms, oxygen ions and other oxygen plasma species (excited O atoms, O_2 molecules in 1st and 2nd excited state, etc.) [21–25]. Since plasma treatment including biasing the sample, enhances the interactions with oxygen ions, the cleaning is performed in a faster manner until all impurities are removed from the surface. The oxidation process creates a thin TiO_2 layer (approximately 100–200 nm), and consequently influences the wettability of demineralized water. If the surface of titanium is put into the heat oven at 150 °C, the most significant drop is in the oxygen content. For the 20 s plasma treatment, the concentration drops to 3.5 at.%. Given that XPS analysis depth is 5 nm, representing approximately 20 atomic mono-layers, this concentration probably represents the weakly bonded oxygen based molecules (H_2O/OH) which have been removed from the surface. On the top of oxygen loss, the carbon content rises, since it is likely that more organic vapours from the surrounding air are attached to the surface over the 1 h treatment. Therefore, the increased wettability contact angle can be attributed to loss of oxygen as well as deposition of carbon-containing material from the surrounding air on the surface.

Given the above results, we were able to determine how our surface properties have changed under different treatment procedures. The samples were then inserted into human blood. After the adhesion of platelets from blood took place, the samples were dried and surface analysed with confocal light microscope. From Fig. 8a, we can see that a number of platelets along with other residuals from blood are to the non-treated surface. Generally, the platelets can be found in various non-activated to activated forms, ranging from round to discoid form sizes from 1 to 3 μm (Fig. 8d), which is non-active and normal in circulating blood. The next activated form is dendritic or early pseudopodial (Fig. 8e), or spread-dendritic or intermediate pseudopodial (Fig. 8f), and both are characterized with a round shape and different spread stage of dendritic part. The most activated forms are spreading or late pseudopodial and fully spread, where the round shape fully disappears. Knowing this, Fig. 8a, doesn't show many active forms of platelets, whereas the small round and discoid forms are distributed through blood residuals. When titanium is functionalized with oxygen plasma for 20 s, no blood residuals can be observed on the surface, except for a number of micrometer sized round and discoid forms of platelets, and some separate cases of early pseudopodial stage (Fig. 8b). However, when the surface is thermally deactivated, the number of activated platelets increases (Fig. 8c). So, on the surface we found a large number of round or discoid forms as well as activated dendritic, spread dendritic and some spreading.

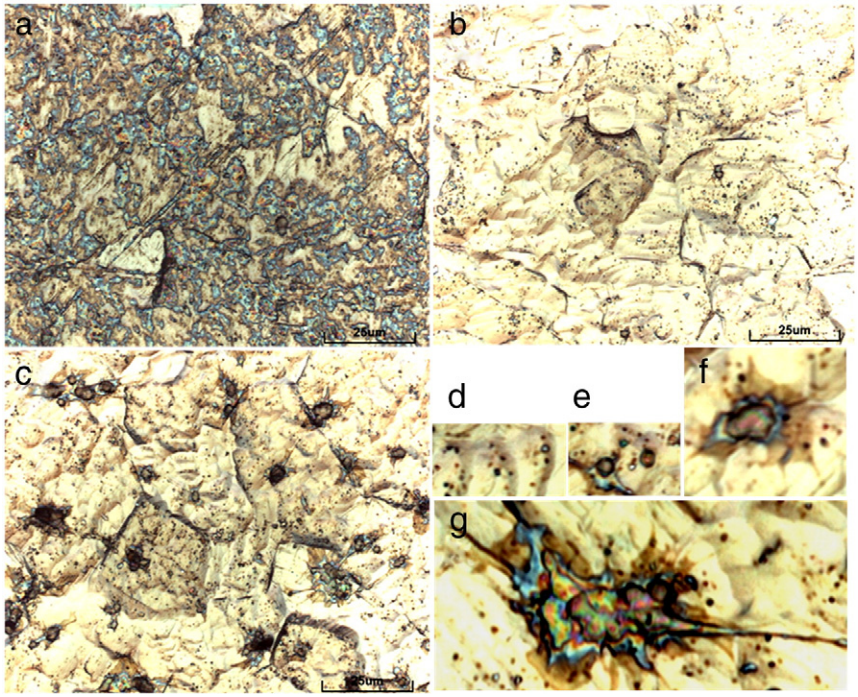

Fig. 8. Optical microscope images with platelets of a) non-treated, b) 20 s oxygen plasma treated sample and c) the same with 1 h thermally treated sample at 150 °C. Platelets on the surface have developed different forms, depending on the treatment. The image d) shows non-activated round or discoid form, e) activated dendritic or early pseudopodial, f) spread-dendritic or intermediate pseudopodial and g) spreading or late pseudopodial form.

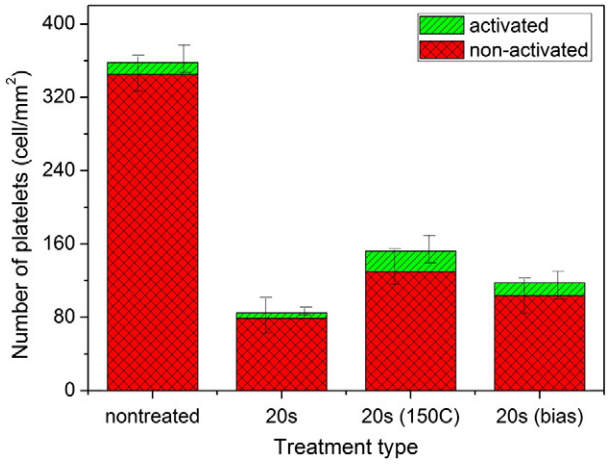

Fig. 9. The density of non-activated or activated attached platelets cells per mm^2 of titanium substrate for non-treated and different 20 s oxygen plasma treatment procedures.

From Fig. 8g we can also see the aggregate of platelets in the first stage of good adhesion to the substrate. Later, the newly attached platelets start activating and bonding between themselves as well as creating such aggregates. However no fully spread form of platelet was found on any sample, treated or non-treated. All samples were also investigated with scanning electron microscope (SEM), but there were no significant changes in surface morphology compared to the confocal light microscope.

When we look at the adhesion of platelets to the surface for different treatment times in Fig. 9, we can see that the highest adhesion is to the non-treated surface. The activation with oxygen and removal of carbon-containing material already lowers the probability for adhesion of platelets four-fold. The density of platelets drops from an average value of 358 cells/mm^2 to 85 cells/mm^2. Moreover, the number of activated forms lowers from an average value of 13 to 4 cells/mm^2. If such an activated surface is subjected to thermal deactivation, the number of cells grows back to 152.2 cells/mm^2, whereas the number of activated increases to 22.4 cells/mm^2. On the other hand, the plasma biased sample shows 117.3 cells/mm^2 with 14.2 cells/mm^2 activated. The control of these results was done with in vitro. Sulforhodamine B based toxicology assay counting which was comparable to a microscope counting within 5% measurement error. Since plasma biased samples have been heated to approximately 450 °C during the treatment the number of weakly bonded (interstitial) oxygen atoms is lower than plasma treated only samples, and higher than the secondarily heated samples. At the same time the plasma biased samples have lower concentrations of carbon compared to the heat treated sample, and slightly lower than plasma only treated sample. This suggests that the major repulsion factor for platelets could be attributed to oxygen atoms, either as weakly bonded atoms or oxygen containing groups on the surface.

4. Conclusions

We treated titanium surfaces as a model of stent implants in order to get better repulsion of blood platelets and prevent their aggregation as well as potential thrombosis. The samples were treated with inductively coupled oxygen plasma and additional biasing of substrates to increase surface temperature. Samples were cleaned and functionalized with oxygen which increase surface energy, we also thermally deactivated surfaces with the heat. It has been proven that predominantly interstitial oxygen atoms as well as oxygen containing groups influence repulsion of platelets. Increased concentration of oxygen prevents deactivation of platelets and aggregation on titanium surfaces. Therefore using our approach, the stents can be better protected against clogging, since the adhesion of undesired platelets can be minimized through plasma treatment.

Acknowledgments

The authors would like to acknowledge the support from FP7 COST Action “BioPlasma”.U.C. and D.V. would acknowledge the Slovenian Research Agency (ARRS) for Bi-CG-SLO grant. J.K., I.J. and M.M. grant given to CO PoliMat by the Slovenian Ministry for Higher Education, Science and Technology. C.C. would like to acknowledge financial support of the Spanish Ministry of Science and Innovation within the MAT2010-12022-E network.

References

[1] G. Mani, M.D. Feldman, D. Patel, C.M. Agrawal, Biomaterials 28 (9) (2007) 1689.
[2] O.F. Bertrand, R. Sipehia, R. Mongrain, J. Rodés, J.C. Tardif, L. Bilodeau, G. Côté, M.G. Bourassa, J. Am. Coll. Cardiol. 32 (1998) 562.
[3] J. Hong, A. Azens, K.N. Ekdahl, C.G. Granqvist, B. Nilsson, Biomaterials 26 (12) (2005) 1397.
[4] V. Biehl, T. Wach, S. Winter, U.T. Seyfert, J. Breme, Biomol. Eng. 19 (2-6) (2002) 97.
[5] J. Choi, D. Bogdanski, M. Koller, S.A. Esenwein, D. Muller, G. Muhr, M. Epple, Biomaterials 24 (21) (2003) 3689.
[6] G. Tepe, J. Schmehl, H.P. Wendel, S. Schaffner, G. Tepe, J. Schmehl, H.P. Wendel, S. Schaffner, S. Heller, M. Gianotti, C.D. Claissen, S.H. Duda, Biomaterials 27 (4) (2006) 643.
[7] U. Cvelbar, M. Mozetič, A. Zalar, Vacuum 71 (2003) 207.
[8] A. Vesel, M. Mozetič, A. Drenik, S. Miošević, N. Krstulovic, M. Balat-Pichelin, I. Poberaj, D. Babič, Plasma Chem. Plasma Process. 26 (2006) 577.
[9] A. Drenik, A. Vesel, M. Mozetic, J. Nucl. Mater. 386–388 (2009) 893.
[10] U. Cvelbar, M. Mozetič, N. Hauptman, M. Klanjšek-Gunde, J. Appl. Phys. 106 (2009) 103303.
[11] U. Cvelbar, D. Vujošević, Z. Vratnica, M. Mozetič, J. Phys. D: Appl. Phys. 39 (2006) 3487.
[12] R. Rossi, O. Kylian, M. Hasiwa, Plasma Processes Polym. 3 (2006) 431.
[13] Y. Hayashi, S. Hirao, Y. Zhang, T. Gans, D. O'Connell, Z.Lj. Petrović, T. Makabe, J. Phys. D: Appl. Phys. 42 (2009) 145206.
[14] M. Mafra, T. Belmonte, F. Poncin-Eppaillard, A. Maliska, U. Cvelbar, Plasma Processes Polym. 6 (10) (2009) 667.
[15] T. Gyergyek, J. Kovačič, M. Čerček, Phys. Plasmas 17 (2010) 1.
[16] A. Vesel, M. Mozetič, P. Panjan, N. Hauptman, M. Klanjšek-Gunde, M. Balat-Pichelin, Surf. Coat. Technol. 204 (6/7) (2010) 1503.
[17] N. Huang, P. Yang, Y.X. Leng, J. Wang, H. Sun, J.Y. Chen, G.J. Wan, Surf. Coat. Technol. 186 (1–2) (2004) 218.
[18] I. Tsyganov, M.F. Maitz, E. Wieser, F. Prokert, E. Richter, A. Rogozin, Surf. Coat. Technol. 174–175 (2003) 591.
[19] S. Takemoto, T. Yamamoto, K. Tsuru, S. Hayakawa, A. Osaka, S. Takashima, Biomaterials 25 (2004) 3485.
[20] Y. Tanaka, K. Kurashima, H. Saito, A. Nagai, Y. Tsutsumi, H. Doi, N. Nomura, T. Hanawa, J. Artif. Organs 12 (3) (2009) 182.
[21] R. Wang, K. Hashimoto, A. Fujishima, M. Chikuni, E. Kojima, A. Kitamura, M. Shimohigoshi, T. Watanabe, Nature 388 (1997) 431.
[22] V. Rico, P. Romero, J.L. Hueso, J.P. Espinós, A.R. González-Elipe, Catal. Today 143 (2009) 347.
[23] T. Watanabe, A. Nakajima, R. Wang, M. Minabe, S. Koizumi, A. Fujishima, K. Hashimoto, Thin Solid Films 351 (1999) 260.
[24] N.P. Mellott, C. Durucan, C.G. Pantano, M. Guglielmi, Thin Solid Films 502 (2006) 112.
[25] C.H. Kwon, Je.H. Kim, I.S. Jung, H. Shin, K.H. Yoon, Ceram. Int. 29 (2003) 851.

Diagnostics and biomedical applications of radiofrequency plasmas

2012 J. Phys.: Conf. Ser. 399 012015

(http://iopscience.iop.org/1742-6596/399/1/012015)

Diagnostics and biomedical applications of radiofrequency plasmas

Saša Lazović[1,2]

[1]Institute of Physics, University of Belgrade, Pregrevica 118, 11080 Belgrade, Serbia

[2]Jozef Stefan Institute, Jamova cesta 39, 1000 Ljubljana, Slovenia

lazovic@ipb.ac.rs

Abstract. In this paper we present spatial profiles of ion and atomic oxygen concentrations in a large scale cylindrical 13.56 MHz capacitively coupled plasma low pressure reactor suitable for indirect biomedical applications (like treatment of textile to increase antibacterial properties) and direct (treatment of seeds of rare and protected species). Such reactor can easily be used for the sterilization of medical instruments by removing bacteria, spores, prions and fungi as well. We also discuss electrical properties of the system based on the signals obtained by the derivative probes and show the light emission profiles close to the sample platform. In the case of seeds treatment, the desired effect is to plasma etch the outer shell of the seed which will lead to the easier nutrition and therefore increase of the germination. In the case of textile treatment the functionalization is done by bounding atomic oxygen to the surface. It appears that antibacterial properties of the textile are increased by incorporating nanoparticles to the fibres which can successfully be done after the plasma treatment. From these two examples it is obvious that the balance of ion and atomic oxygen concentrations as well as proper choice of ion energy and power delivered to the plasma direct the nature of the plasma treatment.

1. Introduction

Non-thermal plasmas are widely used in many industrial processes due to high and controllable chemical reactivity at low gas temperatures [1, 2]. This enables treatment of sensitive materials like cells, polymers, textile and seeds [3, 4, 5, 6, 7, 8]. It is much easier to achieve non-equilibrium conditions at low pressure compared to atmospheric pressure (due to lower ionization growth) and uniformity over the large volumes [9]. Of course, this comes at the cost of using a pumping system and not being able to apply plasma directly to patients.

The specifics of material that we wanted to treat with plasma led us to develop a large scale, low-cost reactor of simple design. Sensitive materials like textile and seeds were treated in air plasma [10, 11]. After the treatment of textile, the surface became hydrophilic leading to increased wettability and therefore easier dying of the samples. Plasma treatment also makes it possible to incorporate nanoparticles like that of silver or TiO_2 which increases antibacterial properties of the textile [3, 4]. Plasma treated textile can be used in hospitals, surgery, military, food production facilities to lower the chance of bacterial infections. In the case of seeds, plasma improves the nutrition of the seeds by etching the outer shell. In nature it is done mechanically, usually by the birds and it also can be done chemically. Nevertheless, plasma shows good results in increasing the seeds germination which is especially important for the rare and protected species. Similar effects can be achieved with the atmospheric pressure plasma [12] but the advantage of a low pressure plasma reactor is the uniform

covering of large treatment area. Damaging or even destruction of the seeds is inevitable if the plasma is too aggressive so the proper optimization of the discharge parameters in necessary.

In this paper we will discuss plasma properties of the asymmetric cylindrical reactor and discuss characteristic features introduced by using such geometry. Ion and atomic oxygen concentrations were radially measured using Langmuir and catalytic probes. Development of plasma light emission was recorded using ICCD camera. Derivative probes that we have used to measure the power delivered to the plasma can be used for all sources in the MHz range regardless of the operating pressure (low or atmospheric). Finally, plasma influence to the germination of *Gentiana asclepiadea* L. seeds will be shown.

2. Experimental setup

The discharge is developed in a cylindrical vessel made of stainless steel, 2.5 m long and 1.17 m in diameter. The powered electrode made of aluminium (1.5 m long) is placed axially in the chamber. The reactor is powered at 13.56 MHz using a Dressler Cesar 1310 together with Variomatch matching network. The chamber wall is grounded. Low pressure is maintained using a mechanical pump.

The samples are placed beneath the powered electrode on a platform which can be moved closer or away from the electrode. Derivative probes are placed as close as possible to the powered electrode as shown at Figure 1. The signals form the probes are collected using an oscilloscope and a PC and then processed [13, 14].

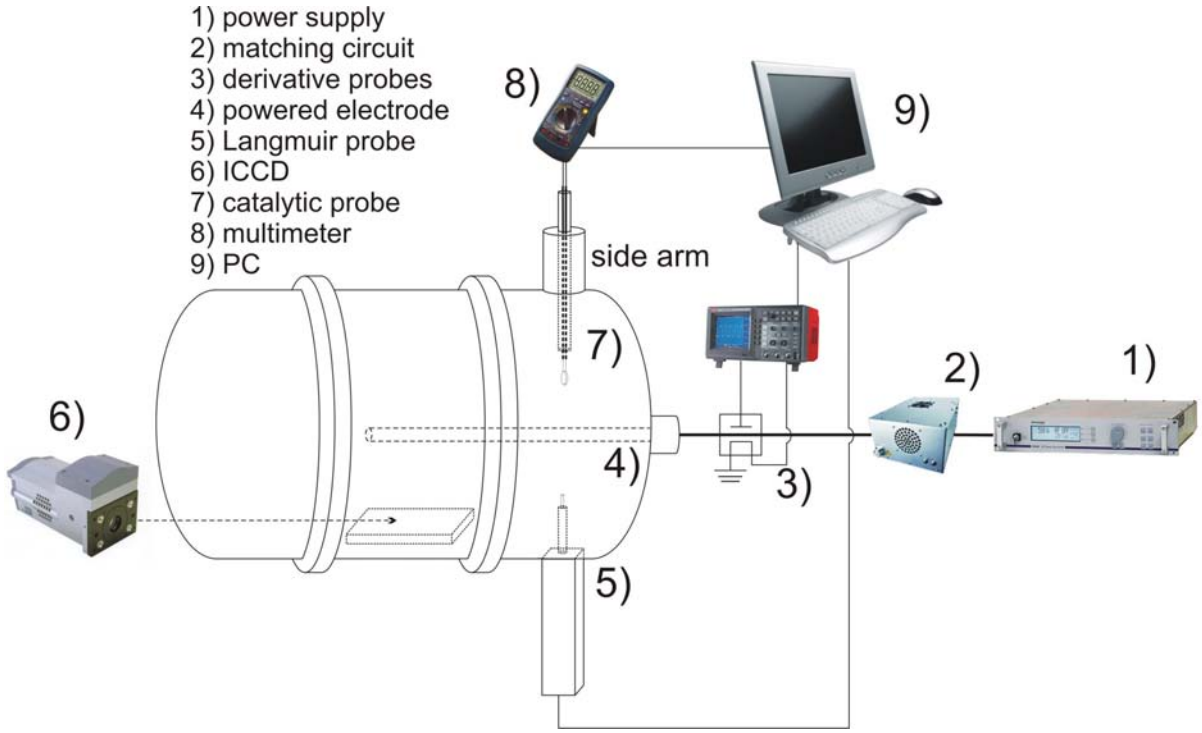

Figure 1. Experimental setup.

Radial profiles of ion and atomic oxygen concentrations are recorded using Langmuir probe (Hiden ESPION) and a nickel catalytic probe [15, 16, 17] respectively. ICCD camera (Andor iStar DH720-18U-03) placed end on to the sample platform was used to record the light emission in the vicinity at the location where sample are to be placed.

3. Plasma diagnostics

3.1. Electrical properties

Signals from the derivative probes were recorded for the range of pressures from 100 to 800 mTorr and the results are presented at Figure 2. The working gas was air.

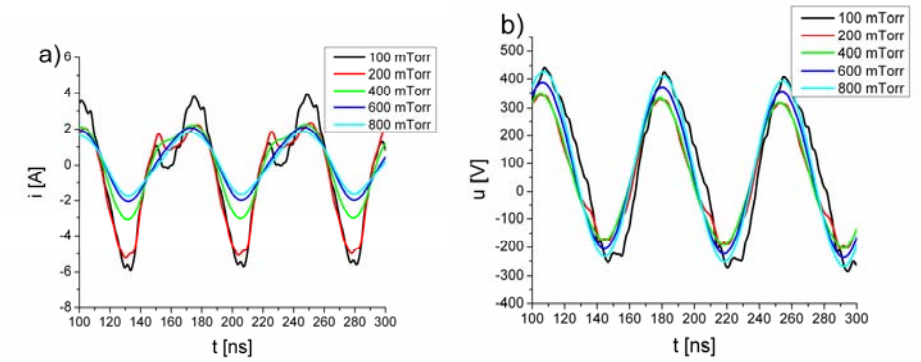

Figure 2. Current a) and voltage b) signals obtained by derivative probes in air at 100, 200, 400, 600 and 800 mTorr. RF generator power was 200 W.

We can see that the shape of both current and voltage are influenced by the working pressure. With the increase of the pressure, the amplitudes of current signals are decreasing and starting to be sine-like. At low pressures the voltage signals are less distorted compared to the current signals. Their shape is changing from the triangle-like to the sine-like when increasing the pressure.

The changes of current and voltage with pressure lead to the change in the power calculated as the integral of their product as shown at Figure 3. We can see that the power transmitted to the plasma is actually higher than 75% in all cases. At 600 mTorr this percent is even higher meaning that the power transfer efficiency is slightly higher compared to 100 mTorr.

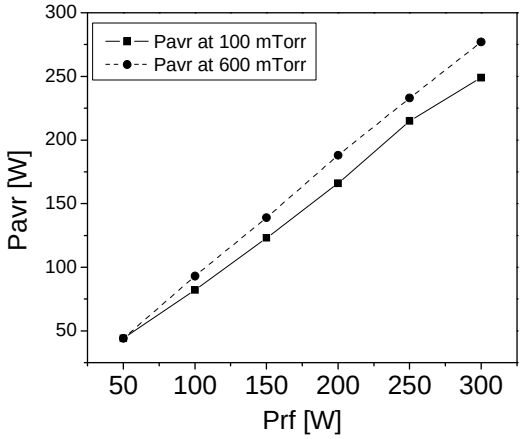

Figure 3. Average power delivered to the plasma at 100 and 600 mTorr.

Measuring of the power delivered to the plasma represents a good parameter for characterizing the treatment procedures and insures its reproducibility. Derivative probes are capable of measuring small powers (less than 1 W) achieving good accuracy of 0.1 W.

3.2. Light emission profiles

Light emission profiles were recorder using ICCD camera placed end-on to the sample platform underneath the powered electrode (see the top picture at Figure 4.). The generator power was increased from 20 to 400 W. The maximum intensity is moving towards the platform, more intensive light emission starts to develop across the surface of the platform where samples are to be placed.

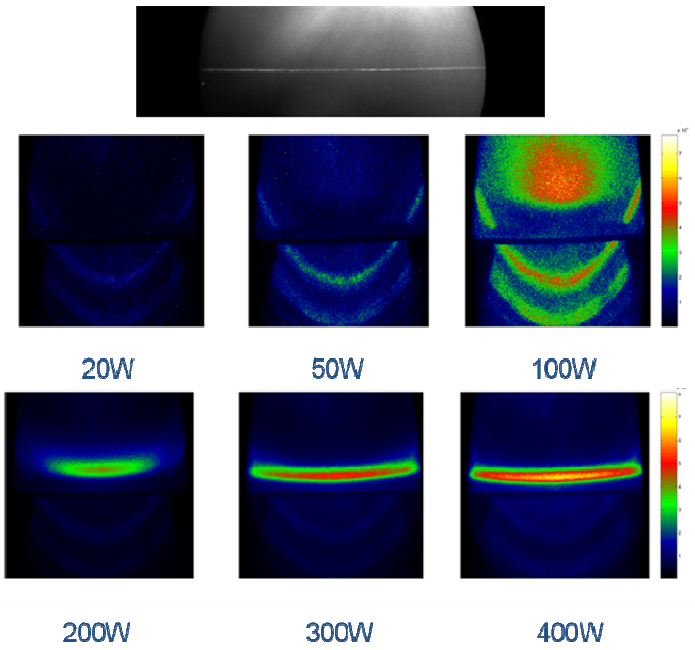

Figure 4. Light emission profile recorded end-on to the sample platform. The gas was air at 100 mTorr.

For smaller powers, after the plasma ignition, light emission intensity is maximal around the powered electrode. With the power increase emission intensity is also increasing around the powered electrode, but at the same time another region of increased intensity can be observed between the powered electrode and sample platform (Fig. 4. - 100W). With further increase in power, the maximum of emission moves towards the sample platform and for powers higher than 200 W the emission is centered on the platform. The light emission is uniform across the large area of the platform for high powers.

3.3. Ion and atomic oxygen concentrations

As mentioned before in the text, the nature of the treatment is strongly dependent on the choice of plasma parameters where concentrations of ions and reactive atomic oxygen represent one of the key players for many of the biomedical applications. Radial profiles were investigated using Langmuir and catalytic probes for the discharge in air by placing the probes on several distances from the powered electrode.

Figure 5. shows the results of ion concentrations which are of the order of 10^{15} m^{-3} to 10^{16} m^{-3}. The measurements are made close to the grounded chamber wall (50.5 cm from the powered electrode), at 20.5 cm from the powered electrode and in-between at 35.5 cm. With the increase of rms voltage (by increasing the power given by the generator) the concentrations increase but the changes are much less pronounced compared to the changes introduced by moving the probes closer to the electrode.

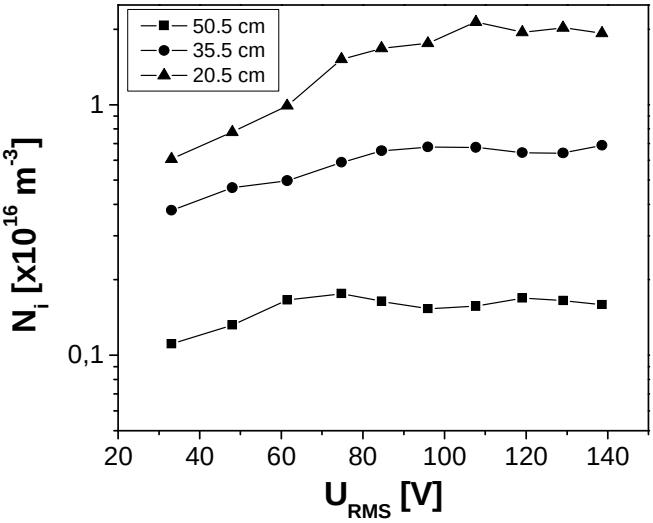

Figure 5. Ion concentrations as a function of rms voltage recorded radially for three distances from the powered electrode (air at 100 mTorr).

This leads to the conclusion that a specific value of ion concentration can be achieved either by increasing the power or by moving closer to the electrode. The results also show that is more practical to obtain higher concentrations by adjusting the distance of the treated sample than to increase the power.

The last conclusions can also be made for the atomic oxygen concentrations. These concentrations are of the order of 10^{19} m^{-3} which is less than in the ICP reactors by 1 to 2 orders of magnitude [18, 19].

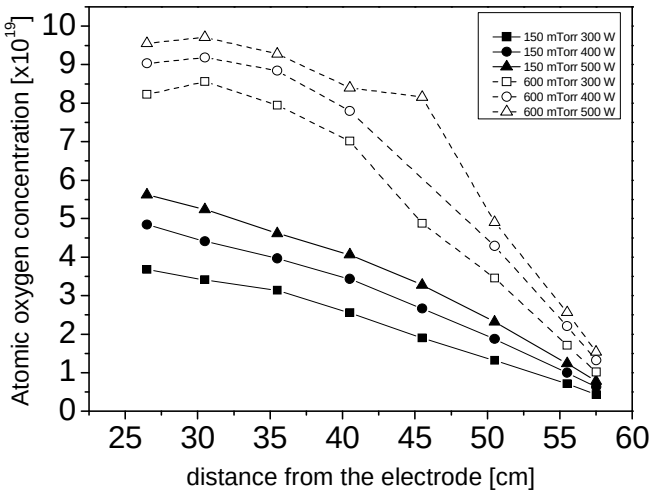

Figure 6. Radial profiles of atomic oxygen concentrations recorded in air at 150 and 500 mTorr.

We can see that the concentrations are decreasing when moving towards the stainless steel wall which also recombines atomic oxygen and contributes to its loss term. At higher pressure the concentrations are higher as expected.

3.4. Biomedical application

Here we present the effects of the plasma to the germination of the *Gentiana asclepiadea* L. (see Figure 7.). The seeds were treated in air plasma at 200 mTorr for the generator power of 100 W. Depending on the treatment time the germination can be increased but if the treatment is too long, the seeds are damaged and the germination is decreased (20 min exposure).

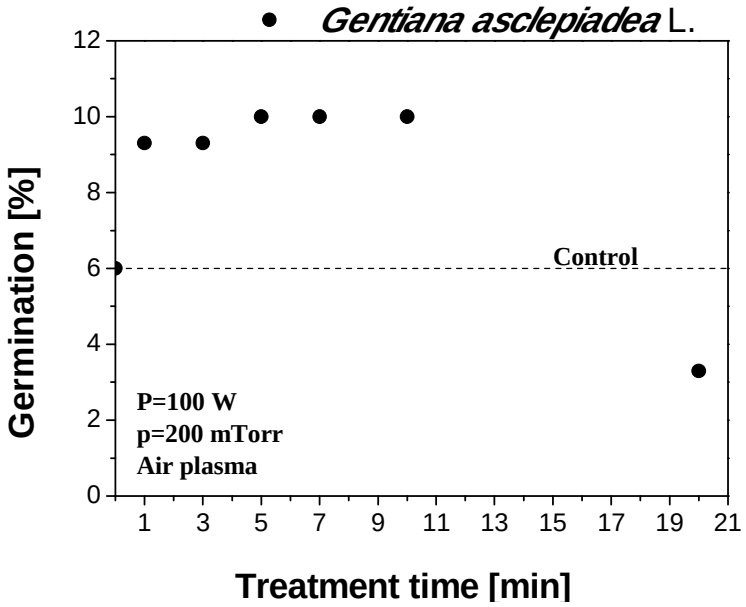

Figure 7. Effects of the plasma to the germination of the *Gentiana asclepiadea* L. seeds..

4. Conclusions

We have shown the properties of the low pressure cold plasma capable of indirect (textile treatment) and direct (seeds treatment) biomedical applications. Antibacterial properties of textile and increased germination of seeds are accomplished due to the functionalization of fiber surface by oxygen atoms and then incorporating the nanoparticles and plasma etching of the seed outer shell, respectively [3, 4, 6]. The advantages of cylindrical geometry of the reactor are shown by presenting the ion and atomic oxygen concentrations at different distances from the powered electrode making it possible to adjust their ratio to the certain amount and achieve different effects. The ion energy is also strongly dependent on the position where the sample is placed.

The uniformity of plasma light emission at the location where samples are to be placed is demonstrated for higher powers. The power delivered to the plasma is measured with good accuracy providing proper treatment characterization and reproducibility. The low pressure cold plasma is not an alternative to atmospheric plasma sources when it comes to biomedical applications but is the preferred tool for all materials that may be treated under low pressure including organic materials and even some biological samples such as seeds. Full understanding of the processes and phenomena occurring in such plasmas as well as optimization of new applications may be achieved by using swarm based data [20, 21], plasma models [21,22] and possibly known scaling [23] to connect to other types of discharges.

Acknowledgments
This work was performed as a part of requirement for a PhD thesis which was completed under the supervision of Dr. Nevena Puač and Prof. Zoran Lj. Petrović. I would also like to express gratitude to my co-supervisor Dr. Gordana Malović, Kosta Spasić and colleagues from the Biological institute "Siniša Stanković". This research has been supported by the Ministry of Education, Republic of Serbia, project numbers III41011 and ON171037.

References

[1] Makabe T and Petrovic Z Lj 2006 Plasma Electronics (Taylor and Francis:New York); Lieberman M A and Lichtenberg A J 2005 Principles of Plasma Discharge and Materials Processing, (Wiley:Hoboken)
[2] Roth J R 1995 Industrial Plasma Engineering (Institute of Physics:Bristol, UK); Kelly-Wintenberg K, Hodge A, Montie T C, Deleanu L, Sherman D, Roth J R, Tsai P and WadsworthL 1999 *J. Vac. Sci. Technol.* A **17** p 1539
[3] Ilic V, Saponjic Z, Vodnik V, Lazovic S, Dimitrijevic S, Jovancic P, Nedeljkovic J M and Radetic M 2010 *Ind Eng Chem Res* **49** p 7287
[4] Mihailovic D, Saponjic Z, Radoicic M, Lazovic S, Baily C J, Jovancic P, Nedeljkovic J and Radetic M 2011 *Cellulose* **18** p 811
[5] Lazović S, Puač N, Miletić M, Pavlica D, Jovanović M, Bugarski D, Mojsilović S, Maletić D, Malović G, Milenković P and Petrović Z 2010 *New Journal of Physics* **12** p 083037
[6] Zivkovic S, Puac N, Giba Z, Grubisic D and Petrovic Z L 2004 *Seed Sci Technol* **32** p 693
[7] Junkar I, Vesel A, Cvelbar U, Mozetič M, and Strnad S 2009 *Vacuum*, **84**(1) p 83
[8] Vesel A, Junkar I, Cvelbar U, Kovač J, and Mozetič M 2008 *Surf. Interface Anal.*,**40**(11) p 1444
[9] Petrović Z Lj, Puač N, Lazović S, Maletić D, Spasić K and Malović G 2012 *J. of Phys.:Conf. Ser.* **356** p 012001
[10] Radetić M 2012 *Journal of Materials Science* DOI 10.1007/s10853-012-6677-7
[11] Gorensek M, Gorjanc M, Bukosek V, Kovac J, Petrovic Z and Puac N 2010 *Textile Research Journal* **80** p 1633
[12] Puač N 2008 *Journal of Physics: Conference Series* **133** p 012007
[13] Puač N, Petrović Z Lj, Malović G, Đorđević A, Živković S, Giba Z and Grubišić D 2006 *J. Phys. D: Appl. Phys.* **39** p 3514
[14] Puač N, Petrović Z Lj, Živković S, Giba Z, Grubišić D and Đorđević A 2005 Plasma Processes and Polymers ed. R d'Agostino, P Favia, C Oehr, M R Wertheimer (Wiley-VCH:Berlin) p 193
[15] Drenik A, Vesel A and Mozetic M 2005 *Inform. Midem* **35** p 85.
[16] Mozetic M, Vesel A, Cvelbar U and Ricard A 2006 *Plasma Chem. and Plasma Proc.* **26** (2) p 103
[17] Vrlinic T, Mille C, Debarnot D and Poncin-Epaillard F 2009 *Vacuum* **83** p 792
[18] Primc G, Zaplotnik R, Vesel A and Mozetic M 2011 *AIP Advances* **1** p 022129
[19] Zaplotnik R, Vesel A and Mozetic M 2011 *EPL (Europhysics Letters)* **95** p 55001
[20] Dujko S, Ebert U, White R D and Petrović Z Lj 2011 *Japanese Journal of Applied Physics* **50** p 08JC01
[21] Petrović Z Lj, Dujko S, Marić D, Malović G, Nikitović Ž, Šašić O, Jovanović J, Stojanović V and Radmilović-Radenović M 2009 *J. Phys. D: Appl. Phys.* **42** p 194002
[22] Savić M, Radmilović-Radjenović M, Šuvakov M, Marjanović S, Marić D and Petrović Z Lj 2011 *IEEE Trans. Plasma Sci.* **39** (11) p 2556
[23] Petrović Z Lj, Škoro N, Marić D, Mahony C M O, Maguire P D, Radmilović-Rađenović M and Malović G 2008 *J. Phys. D: Appl. Phys.* **41** p 194002

Applications of nonequilibrium plasmas in biology and medicine

Conference Paper · September 2012

READS
43

11 authors, including:

Slavko Mojsilović
University of Belgrade
59 PUBLICATIONS **298** CITATIONS
SEE PROFILE

Gordana Malovic
Institute of Physics Belgrade
157 PUBLICATIONS **932** CITATIONS
SEE PROFILE

Diana Bugarski
Institute for Medical Research - Belgrade
60 PUBLICATIONS **421** CITATIONS
SEE PROFILE

Zoran Lj Petrović
Institute of Physics Belgrade
510 PUBLICATIONS **5,652** CITATIONS
SEE PROFILE

RBC 2012

Relax-Be snooping-Carpe diem

Regional Biophysics Conference 2012

Kladovo-Belgrade, Serbia

September 03-07, 2012

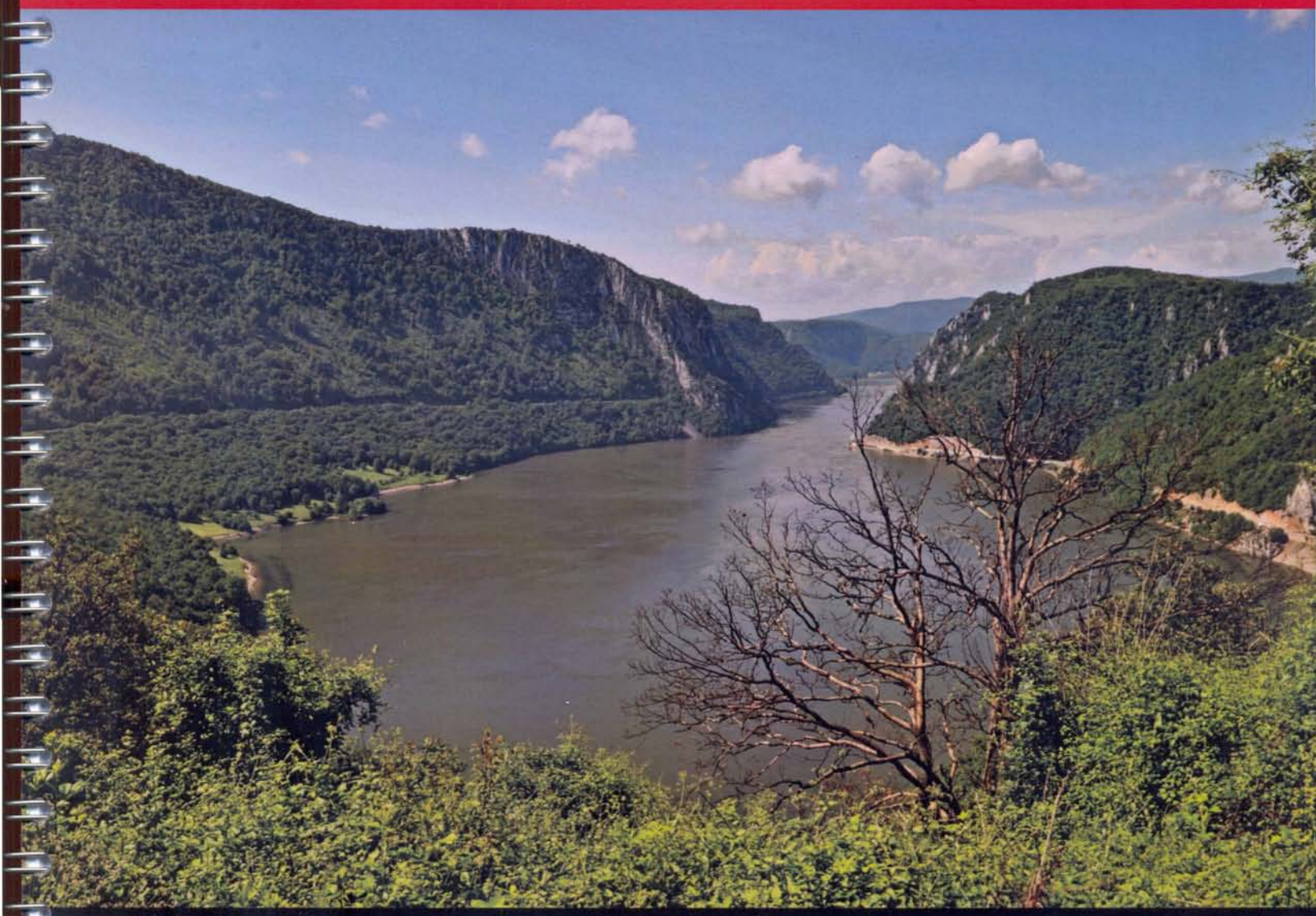

BOOK OF ABSTRACTS

Organized by Biophysical Society of Serbia

EBSA Biophysics in Europe

IUPAB Connecting the World of Biophysics

ESN European Society for Biochemistry

CMJ Croatian Medical Journal

RBC 2012

Relax-Be snooping-Carpe diem

Regional Biophysics Conference 2012
Kladovo-Belgrade, Serbia
September 03-07, 2012

BOOK OF ABSTRACTS

Organized by Biophysical Society of Serbia

EBSA
Biophysics in Europe

European Biophysical Societies' Association (EBSA)

IUPAB
Connecting the World of Biophysics

International Union for Pure and Applied Biophysics

Ministry of Education and Science, Serbia

ESN
European Society for Neurochemistry

European Society for Neurochemistry

CMJ
Croatian Medical Journal

Croatian Medical Journal

RBC 2012 Principal organizer
Biophysical Society of Serbia

President:
Professor Pavle Andjus, Institute of Physiology and Biochemistry, Faculty of Biology, University of Belgrade

Secretary
Dr Miroslav Živić, Institute of Physiology and Biochemistry, Faculty of Biology, University of Belgrade

Steering Committee
Dr Pavle Andjus
Dr Miroslav Živić
Dr Ksenija Radotić, Institute for Multidisciplinary Research, Belgrade
Dr Joanna Zakrzewska, Institute of General and Physical Chemistry, Belgrade
Dr Miloš Mojović, Facuty of Physical Chemistry, University of Belgrade, Belgrade

RBC 2012 Organizing Committee
Pavle Andjus, Chair
Goran Bačić
Joanna Zakrzewska
Ksenija Radotić
Miroslav Živić
Miloš Mojović
Nataša Todorović
Ana Popović-Bjelić
Marina Stanić

RBC 2012 Scientific advisory board
Peter Pohl (Austia)
Georg Pabst (Austia)
Vesna Svetličić (Croatia)
Sanja Tomić (Croatia)
Laszlo Zimanyi (Hungary)
Péter Závodszky (Hungary)
László Mátyus (Hungary)
Mauro Dalla Serra (Italy)
Giorgio M. Giacometti (Italy)
Silvia Morante (Italy)
Pavle Andjus (Serbia)
Goran Bačić (Serbia)
Miroslav Zivić (Serbia)
Marjeta Šentjurc (Slovenia)
Janez Štrancar (Slovenia)
Milan Brumen (Slovenia)
Tibor Hianik (Slovakia)
Pavol Miskovsky (Slovakia)

The RBC is a series of biennial symposia intended to bring together biophysics researchers from Austria, Croatia, Hungary, Italy, Serbia, Slovenia and Slovakia and also includes internationally renowned guest speakers. The first such meeting took place in March 2005 in Terme Zrece, Slovenia. The language of the conference is English.

http://rbc2012.biofizikasrbija.com/

Thursday, 6/9

Section S4: Modeling and instrumental techniques in biophysics

09:30-09:50 **Vladana Vukojević** (Sweden), *Quantitative study of transcription factor binding kinetics in living cells.*

09:50-10:10 **Lóránd Kelemen** (Hungary), *Optically-driven microtool for microfluidic and biological applications.*

10:10-10:30 **Aleš Fajmut** (Slovenia), *Modelling of smooth muscle contraction in normal and pathological conditions and its coherence with pharmacology and medicine.*

10:30-10:50 **Tanja Dučić** (Germany), *X-ray microscopy on cellular level.*

10:50-11:30 Coffee break

11:30-11:50 **Janez Štrancar** (Slovenia), *Confocal fluorescence microspectroscopy: powerful biophysical tool to resolve molecular environment.*

11:50-12:10 **Francesco Stellato** (Germany), *Serial X-ray nanocrystallography with Free Electron Laser radiation.*

12:10-12:30 **Nevena Puač** (Serbia), *Applications of nonequilibrium plasmas in biology and medicine.*

12:30–12:50 **Miloš Mojović** (Serbia), *Proposing some new biomarking tools for cancer and ALS.*

12:50–13:10 **Tilen Koklič** (Slovenia), *Effect of perifosine on liposome membrane characteristics, transcytosis and liposome contents leakage.*

13:10-14:45 Lunch.

Section S5: Medical biophysics

14:45-15:05 **Brana Jelenković** (Serbia), *The use of laser technology in biomedicine.*

15:05-15:25 **Božidar Casar** (Slovenia), *Stereotactic radiosurgery (SRS) with linear accelerator for treatment of intracranial lesions.*

15:25-15:45 **Aleš Iglič** (Slovenia), *Electrostatics and mechanics of the interactions between osteoblasts and titanium implants.*

15:45-16:15 Coffee break

16:15-16:35 **Pavol Miskovsky** (Slovakia), *Towards increased selectivity of cancer treatment by Photodynamic therapy*

16:35-16:55 **Lenart Giradon** (Slovenia), *Using cells and biomaterials for regeneration of diseased and damaged tissues.*

16:55 -17:15 **Sofija Andjelić** (Slovenia) *Calcium changes and contractions of human anterior lens epithelial cells*

17:15-17:35 **Petar Marinković** (Germany) *Imaging axonal transport in health and disease*

17:45-19:45 **Poster session S4 & S5**

20:00 **Farewell Dinner**

Friday, 7/9

Departure

31.S4

Applications of nonequilibrium plasmas in biology and medicine

N. Puač[1]
M. Miletić[2]
S. Mojsilović[3]
S. Živković[4]
D. Maletić[1]
S. Lazović[1]
G. Malović[1]
D. Bugarski[3]
Z.Giba[4]
P. Milenković[2]
Z. Lj. Petrović[1]

[1] *Institute of Physics, University of Belgrade, Pregrevica 118, 11080 Belgrade, Serbia*
[2] *Faculty of Stomatology, University of Belgrade, Dr Subotića 8, 11000 Belgrade, Serbia*
[3] *Institute for Medical Research, University of Belgrade, Dr Subotića-starijeg 4, 11000 Belgrade, Serbia*
[4] *Institute for Biological Research „Siniša Stanković", University of Belgrade, Bulevar Despota Stefana 142, 11060 Belgrade, Serbia*

Constantly growing field of biomedical applications is a new frontier that drives the development of plasma sources. The choice of the plasma system used for treatment is usually guided by the type of samples that are treated and effect these plasmas are intended to have on the samples. Some of the samples cannot undergo vacuum and due to this fact non-thermal atmospheric pressure plasmas lately have drawn considerable attention with their enormous potential for technological applications in surface modifications and biomedical applications. The necessity to use plasma for *in-vivo* treatments/procedures has led to several requirements for plasma sources to meet. Because of its mild plasma, low gas temperature and geometry, the plasma needle is especially convenient for medical applications. We have studied effect of the plasma needle on different living cells, from plants through bacteria such as Escherichia coli and Staphylococcus aureus to the human peripheral blood mesenchymal stem cells (hPB-MSC), as a model system to predict the degree of possible damage to the human cells. The results support application of the plasma needle in treatments of light bacterial infections, such as in vivo sterilization of skin and dental cavities.

This research has been supported by the MES Serbia, project III41011 and ON171037.

Regional Biophysics Conference 2012, Book of Abstracts

Izdavač
Društvo biofizičara Srbije, Beograd

Štampa
MST Gajić, Beograd

Tiraž
130 primeraka, 30cm

ISBN
978-86-904161-2-7

Urednici
Dr Joanna Zakrzewska
Dr Miroslav Živić
Prof. dr Pavle Andjus

CIP - Каталогизација у публикацији
Народна библиотека Србије, Београд

577.3(048)

REGIONAL Biophysics Conference (2012 ; Kladovo, Belgrade)
Book of Abstracts / Regional Biophysics Conference 2012, Kladovo-Belgrade, Serbia, September 03-07, 2012 ; [organized by Biophysical Society of Serbia ; urednici Joanna Zakrzewska, Miroslav Živić, Pavle Andjus]. - Beograd : Društvo biofizičara Srbije, 2012 (Beograd : MST Gajić). - 140 str. ; 30 cm

Tiraž 130. - Registar.

ISBN 978-86-904161-2-7
1. Društvo biofizičara Srbije
a) Биофизика - Апстракти
COBISS.SR-ID 193043980

AXIAL PROFILES OF PLASMA BULLET WITH DIFFERENT ELECTRODE GAPS

Conference Paper · August 2012

READS
19

7 authors, including:

Gordana Malovic
Institute of Physics Belgrade
157 PUBLICATIONS **932** CITATIONS

SEE PROFILE

Zoran Lj Petrović
Institute of Physics Belgrade
510 PUBLICATIONS **5,652** CITATIONS

SEE PROFILE

ISBN 978-86-7031-242-5

SPIG 2012

26th Summer School and International Symposium on the Physics of Ionized Gases

August 27th -31st, 2012, Zrenjanin Serbia

CONTRIBUTED PAPERS & ABSTRACTS OF INVITED LECTURES AND PROGRESS REPORTS

Editors
M. Kuraica, Z. Mijatović

University of Novi Sad, Faculty of Sciences
Department of Physics
Novi Sad, Serbia

ISBN 978-86-7031-242-5

CONTRIBUTED PAPERS & ABSTRACTS
OF INVITED LECTURES AND PROGRESS REPORTS
of the
26th SUMMER SCHOOL AND INTERNATIONAL
SYMPOSIUM ON THE PHYSICS OF IONIZED GASES

August 27th - 31st, Zrenjanin, Serbia

Editors: Milorad Kuraica
Zoran Mijatović

Publisher:

University of Novi Sad
Faculty of Sciences
Department of Physics
Trg Dositeja Obradovića 3
21000 Novi Sad, Serbia

CIP - Каталогизација у публикацији
Библиотека Матице Српске, Нови Сад

537.56(082)
539.186.2(082)
539.121.7(082)
533.9(082)

SUMMER School and International Symposium on the Physics of Ionized Gases (26 ; 2012 ; Zrenjanin)
Contributed papers & abstracts of invited lectures and progress reports / SPIG 2012 - 26th Summer School and International Symposium on the Physics of Ionized Gases, August 27th-31st, 2012, Zrenjanin Serbia ; editor Z. Mijatović. - Novi Sad : Faculty of sciences, Department of physics, 2012 (Novi Sad : Stojkov). - XVII, 403 str. : ilustr. ; 24 cm

Str. III: Preface / editors. - Napomene i bibliografske reference uz tekst. - Bibliografija uz svaki rad. - Registar.

ISBN 978-86-7031-242-5
I. SPIG (26 ; 2012 ; Zrenjanin) v. Summer School and International Symposium on the Physics of Ionized Gases (26 ; 2012 ; Zrenjanin)
a) Јонизовани гасови - Зборници b) Атоми - Интеракција - Зборници c) Плазма - Зборници
COBISS.SR-ID 272861703

Printed by:
Štamparija "Stojkov", Novi Sad, Serbia

AXIAL PROFILES OF PLASMA BULLET WITH DIFFERENT ELECTRODE GAPS

Nenad Selaković[1], Dejan Maletić[1], Nevena Puač[1], Saša Lazović[1], Gordana Malović[1], Antonije Đordjević[2] and Zoran Lj. Petrović[1]

[1]Institute of Physics, University of Belgrade, Pregrevica 118, 11080 Belgrade, Serbia
[2]School of Electrical Engineering, University of Belgrade, Bulevar kralja Aleksandra 73, 11000 Belgrade, Serbia

Abstract. We used fast ICCD imaging in order to record time evolution of plasma bullet formation. Plasma jet was made of Pyrex glass tube with two transparent electrodes made of polyester (PET) foil whose position can be easily adjusted. The excitation voltage was approximately 10 kVpp at frequency of 80 kHz. The power transmitted to the plasma in all measurements was 4 W. The working gas was helium with constant flow rate of 4 slm. In this paper we shall show the total axial light emission profiles of plasma jet bullets obtained for three different electrode gaps, of 10, 15 and 20 mm.

1. INTRODUCTION

One of the main reasons for the development of new low temperature plasma sources which are working at atmospheric pressure is their simple, non-expensive design with great potential for possible applications. These plasma sources are used for treatment of polymers, cells, tissues, etc. [1-3]. One of the newest scientific fields developed from this high-end research is plasma medicine [4]. Achieving high temperatures of electrons, much higher than the temperatures of ions and ambient gas, is crucial for sustaining stabile non-equilibrium plasmas. In order to reduce the breakdown voltage in these discharges, noble gases are used, usually helium or argon [5]. For powering plasma jets, various types of signals at high frequencies are used [6], as well as different geometries [7, 8]. By choosing different materials for the electrodes, different electrode gaps and sizes, one can significantly change the behavior of plasma jets and control if the plasma jet will form bullets or not. The optimal geometry parameters can be found in order to maximize the distance that plasma bullets can reach. In this paper we present axial profiles for several gaps between the powered and the grounded electrode.

2. EXPERIMENTAL SETUP

The atmospheric pressure plasma jet used in these experiments is shown in Fig. 1. Its body was made of a Pyrex glass tube (O. D. of 6 mm and I. D. of 4 mm) with two transparent thin conductive PET foil electrodes (width of 15 mm) wrapped around the glass tube. The copper foil was used to connect electrodes to an external electrical circuit. The electrode closer to the edge of the glass tube was the powered one, and the other electrode was grounded (see Fig. 1). A resistor of 100 kΩ between the grounded electrode and the ground was connected for current measurements. During all measurements, the helium flow rate was 4 slm. As the power supply, a signal generator was used, and it was connected to a home-made amplifier. The excitation signal was sinusoidal and the working frequency was 80 kHz. Since the maximum value of the voltage at the output of the amplifier is around 1 kV, it was necessary to make a high-voltage transformer to increase the signal from the amplifier up to 10 kV peak-to-peak. The calculated power transmitted to plasma in all measurements was 4 W. The gap between electrodes was 10, 15 and 20 mm. The distance between the powered electrode and the edge of the glass tube was kept constant at 7 mm for all measurements.

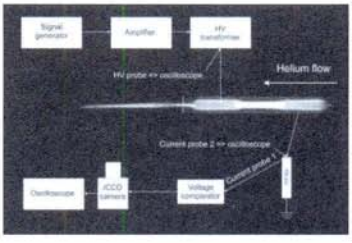

Figure 1. Experimental setup

3. RESULTS AND DISCUSSION

Signals of current and voltage, with trigger positions, are presented in Fig. 2 (left). The voltage signal has pure sine waveform, while the current signal is a somewhat deformed. Three triggering positions of ICCD imaging were selected to present behavior of plasma at different time positions of the whole cycle. The first trigger position is close to the minimum, the second one is near the zero and the third is right after the maximum of the voltage signal. Axial (along the glass tube axis) profiles of plasma emission were calculated from the obtained ICCD images (see Fig. 2 (right)-3). The presented profiles are calculated as a sum of the emission intensity coming from plasma along the axis of the glass tube diameter. In Fig. 2 (right)-3, the right edge of the grounded electrode is chosen to be the reference (zero) position, the positions of the powered and the grounded electrode are marked by vertical solid lines and the edge of the glass tube by a vertical dashed line. The direction of helium flow is from the grounded toward the powered electrode (as shown in Fig. 2 (right)-3).

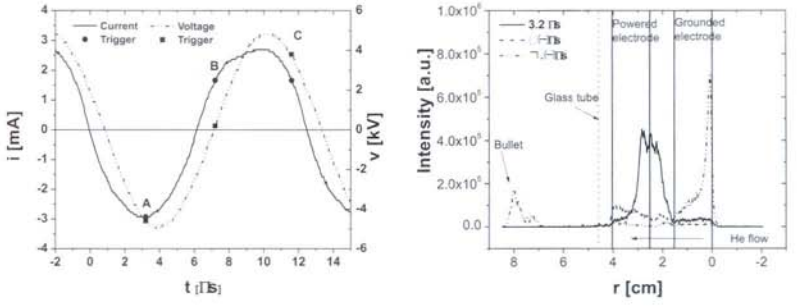

Figure 2. Current and voltage signals with trigger positions for 15 mm electrode gap (left); Axial light emission profiles for 10 mm electrode gap for three different trigger delays (3.2 μs, 7.2 μs and 11.6 μs), 4 slm flow of helium and power of 4 W

Axial profiles of light emission for the gap of 10 mm between electrodes are shown in Fig. 2 (right). For the minimum of the voltage and current signal, the maximum emission intensity coming from the discharge is on the right edge of the powered electrode (Fig. 2 (right), black solid curve). At the same time, the emission intensity in other areas is several orders of magnitude smaller. With increase of the voltage and current signals, plasma is moving towards the left edge of the powered electrode and the emission intensity decreases.

For the delay of 7.2 μs (Fig. 2 (right), black dashed curve) the intensity is very small with the maximum near the left edge of the powered electrode. A plasma bullet is formed at the maximum values of current and voltage signals and it reaches the maximum distance of 3.5 cm from the edge of the glass tube for the delay time 11.6 μs. Also, there is another well-defined maximum at the right edge of the grounded electrode.

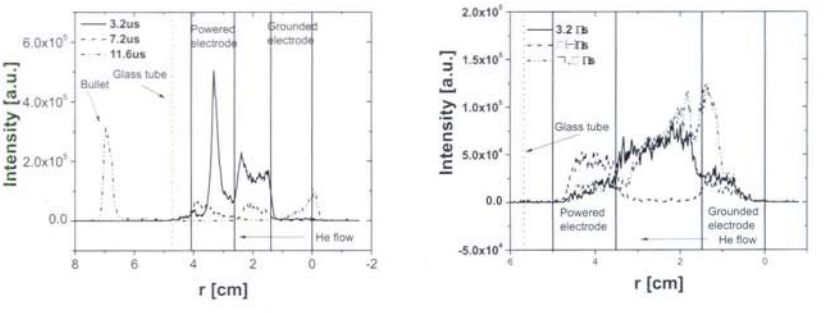

Figure 3. Axial light emission profiles for 15 mm (left) and 20 mm (right) electrode gap for three different trigger delays (3.2 μs, 7.2 μs and 11.6 μs), 4 slm flow of helium and power of 4 W

Axial profiles for the gap of 15 mm are presented in Fig. 3 (left). A well-defined peak of light emission can be seen in the powered electrode, as

well as significant emission between electrodes (for the delay of 3.2 μs, solid black curve). For the delay of 7.2 μs, the intensity significantly drops in and between the electrodes (dashed black curve). For the delay of 11.6 μs, there are two distinct peaks: one inside the grounded electrode and the second one outside the tube approximately at 2.2 cm from the edge of the glass tube. For the 15 mm gap, the bullet is better defined than in the case of other electrode gaps used in this paper.

For the largest electrode gap in Fig. 3 (right), the emission intensity is much smaller than in other two cases. For the delays of 3.2 μs and 7.2 μs, there are no well-defined peaks. For the delay of 11.6 μs, there is no light emission outside the glass tube. This electrode gap is not suitable for treatment of surfaces because plasma does not leave the glass tube.

4. CONCLUSION

Using ICCD imaging it has been shown that the light emission is highly dependent of the electrode geometry. In this study it is has been shown that if it is needed to obtain a well-defined plasma bullet, the most suitable configuration is a gap of 15 mm between the electrodes. In other two configurations, the plasma bullet is distorted or it does not leave the glass tube at all. One of the directions for future research could be to record emission profiles by using filters for different wavelengths.

Acknowledgements

This research has been supported by the Ministry of Education and Science, Serbia, under projects ON171037 and III41011.

REFERENCES

[1] F. Iza, G. J. Kim, S. M. Lee, J. K. Lee, J. L. Walsh, Y. T. Zhang, M. G. Kong, Plasma Process. Polym. 5, 322–344 (2008).
[2] A. Shashurin, M. Keidar, S. Bronnikov, R. A. Jurjus, M. A. Stepp, Appl. Phys. Letters 93, 181501 (2008).
[3] S. J. Kim, T. H. Chung, S. H. Bae, S. H. Leem, Appl. Phys. Letters 97, 023702 (2010).
[4] A. V. Nastuta, I. Topala, C. Grigoras, V. Pohoata, G. Popa, J. Phys. D: Appl. Phys. 44,105204(2011).
[5] H. S. Park, S. J. Kim, H. M. Joh, T. H. Chung, S. H. Bae, S. H. Leem, Phys. Plasmas 17, 033502 (2010).
[6] Q. Xiong, X. P. Lu, K. Ostrikov, Y. Xian, C. Zou, Z. Xiong, Y. Pan, Phys. Plasmas17, 043506 (2010).
[7] E. Karakas, M. Koklu, M. Laroussi, J. Phys. D: Appl. Phys. 43,155202 (2010).
[8] N. Jiang, A.Ji, Z. Cao, J. Appl. Phys. 108, 033302 (2010).

Current-Voltage Characteristics Of Atmospheric Pressure Plasma Jet

Article · July 2010

6 authors, including:

Gordana Malovic
Institute of Physics Belgrade
157 PUBLICATIONS **932** CITATIONS
SEE PROFILE

Zoran Lj Petrović
Institute of Physics Belgrade
510 PUBLICATIONS **5,652** CITATIONS
SEE PROFILE

UDC 537.56(082)
539.186.2(082)
539.121.7(082)
533.9(082)

ISSN 0373-3742

ПУБЛИКАЦИЈЕ АСТРОНОМСКЕ ОПСЕРВАТОРИЈЕ У БЕОГРАДУ
PUBLICATIONS OF THE ASTRONOMICAL OBSERVATORY OF BELGRADE
Св. 89 No. 89

25th Summer School and International Symposium on the Physics of Ionized Gases

Donji Milanovac, Serbia,
August 30 - September 3, 2010

CONTRIBUTED PAPERS

&

ABSTRACTS of INVITED LECTURES,
TOPICAL INVITED LECTURES and PROGRESS REPORTS

Editors:
Luka Č. Popović,
Milorad M. Kuraica

БЕОГРАД
2010

PUBL. ASTRON. OBS. BELGRADE No. 89, 1-405 BELGRADE, JULY 2010

PUBLICATIONS OF THE ASTRONOMICAL OBSERVATORY OF BELGRADE

FOUNDED IN 1947

Published and copyright © by Astronomical Observatory, Volgina 7, 11060 Belgrade 38, Serbia

Director of the Astronomical Observatory: Dr. Zoran Knežević

Typesetting: Tatjana Milovanov

Internet address `http://www.aob.bg.ac.rs`

ISBN 978–86–80019–37–6

The publication of this issue is financially supported by the Serbian Ministry of Science and Technological Development.

Number of copies / тираж : 400

Production: "1909.MINERVA", Karadjordjev put br. 37, Subotica, Serbia

Publ. Astron. Obs. Belgrade No. 89 (2010), 307-310 *Contributed Paper*

CURRENT–VOLTAGE CHARACTERISTICS OF ATMOSPHERIC PRESSURE PLASMA JET

NEVENA PUAČ[1], DEJAN MALETIĆ[1], SAŠA LAZOVIĆ[1], GORDANA MALOVIĆ[1], ANTONIJE ĐORĐEVIĆ[2] and ZORAN Lj. PETROVIĆ[1]

[1]*Institute of Physics University of Belgrade, Pregrevica 118, 11080 Zemun, Serbia*
E-mail: nevena@ipb.ac.rs

[2]*School of Electrical Engineering, University of Belgrade, Bulevar kralja Aleksandra 73, 11000 Belgrade, Serbia*

Abstract. We have constructed a plasma jet that can operate in the frequency range 25-150 kHz and within the range of 5-10 kV of applied peak-to-peak voltages. High voltage probes are used in order to obtain current and voltage waveforms. In this paper, we will show V_{RMS}-I_{MRS} plasma jet characteristics for the working frequency of 80 kHz. Current and voltage measurements were made both for the increase and decrease of the applied voltage in order to see if there is a hysteresis effect.

1. INTRODUCTION

Atmospheric pressure discharges cover a wide range of dimensions, starting from micrometer-scale plasmas convenient for localized and precise treatment, up to dimensions suitable for the treatment of large-scale samples. So far, many different configurations and applications of non-thermal atmospheric plasmas have been developed and studied (see Kundthart et al. 2000, Fridman et al. 2008, Puač et al. 2006, von der Gathen et al. 2007). Recently, several authors have reported on various means of generating cold plasma jets at atmospheric pressure. More interestingly, these jets turned out not to be a continuous plasma, but trains of small high-velocity plasma packets-bullets (see Kong et al. 2008, Teschke et al. 2005).

We have constructed plasma jet that can operate in the frequency range from 25 kHz to 150 kHz and within the range of 5-10 kV of applied peak-to-peak voltages. In this paper, we will show V_{RMS}-I_{MRS} plasma jet characteristics for the working frequency of 80 kHz. High voltage probes are used in order to obtain current and voltage waveforms. Measurements are made for the increase and decrease of the applied voltage in order to see if there is a hysteresis effect.

2. EXPERIMENTAL SETUP

The atmospheric pressure plasma jet is made of a Pyrex glass tube with inner diameter of 4 mm and outer diameter of 6 mm. Electrodes that were used were made of a thin copper foil wrapped around the glass tube. The distance between the powered and the grounded electrode was 13.5 mm. The width of both electrodes was 13 mm. One of the electrodes (the left electrode, see Fig. 1) was grounded. The other electrode, closer to the end of the glass tube, was the powered one (see Fig. 1). The distance between the powered electrode and the end of the glass tube was 11 mm. The feeding gas was helium and the flow rates used in this work were 2, 3 and 4 slm. The flow rate is adjusted with a mass flow controller (Omega FMA5400/5500).

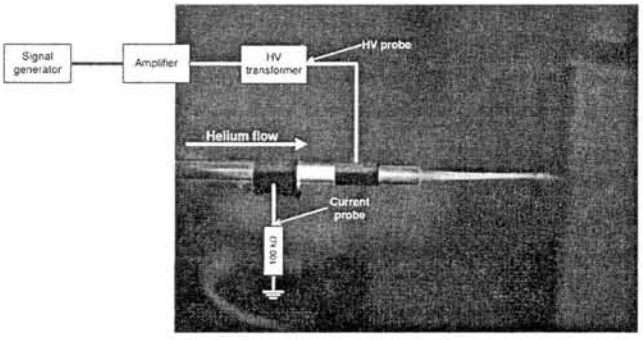

Figure 1: Experimental setup.

For powering the plasma jet, we used a signal generator (Peak Tech DDS FUNCTION GENERATOR 4025) connected to the custom-made amplifier. Highest voltages that we could obtain from the amplifier were up to 1 kV, which was not enough to ignite the plasma. In order to the increase applied voltages to the values higher than 5-6 kV, we had to use an additional homemade transformer.

Current and voltage measurements were made with two commercial probes. The first probe, used for obtaining voltage waveforms, was a high-voltage probe (Agilent N2771A) and it was connected to the HV-output (see Fig. 1). In order to obtain current waveforms, we used the second probe (Agilent 10076A) which measured the voltage drop on a 100 kΩ resistor placed in the grounded branch of the electrical circuit. The working frequency was 80 kHz and the applied voltage was in the range of 6-10 $kV_{peak\text{-}to\text{-}peak}$.

3. RESULTS AND DISCUSSION

The current and voltage waveforms when there is no discharge, and with plasma on, are shown in Fig. 2. We can see that when the plasma is not ignited, the phase difference between the current and the voltage is approximately $\pi/2$. The imped-

ance is practically capacitive (the voltage waveform lags behind the current waveform). When plasma is ignited, the phase difference between the voltage and the current reduces significantly. Signal for the current is increased and deformed, while the peak-to-peak value for the voltage is smaller than in the case when there is no plasma (no He flow). By igniting the discharge we have employed additional nonlinear load into the electrical circuit.

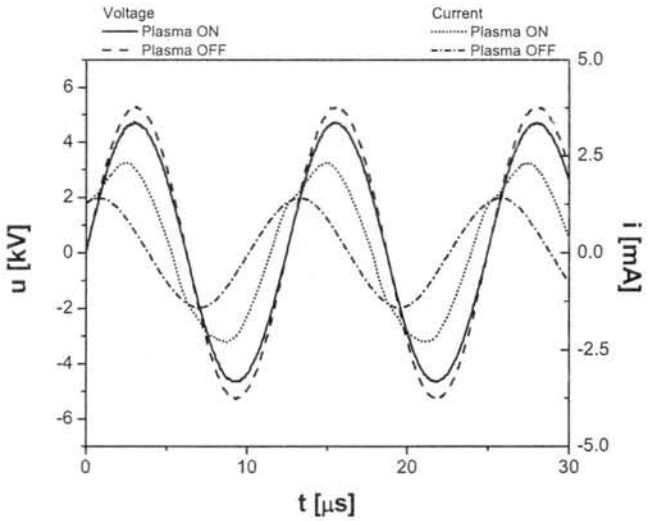

Figure 2: Current and voltage waveforms for the helium flow rate of 3 slm. Dashed lines represent case when discharge is OFF and solid lines when discharge is ignited.

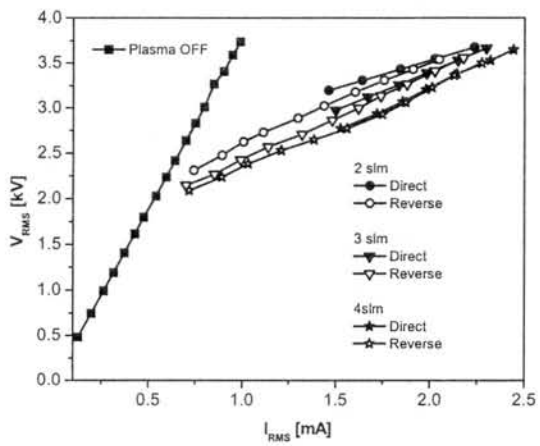

Figure 3: Current-voltage characteristics for three different flows of helium.

In Fig. 3 V_{RMS}–I_{RMS} characteristics are shown for three different flows of the feeding gas. In case when plasma is off, the RMS values of the current are lower than in the case when the plasma is ignited. On the other hand, the voltage is decreased with the plasma ignition.

When the plasma is off, the phase difference between the current and voltage is close to 90°. In this case, we have a capacitive impedance of several MΩ, corresponding to the capacitance of about 0.5 pF. On the other hand, the plasma ignition introduces a parallel nonlinear load into the electrical circuit. and in this case the slopes of the V_{RMS}–I_{RMS} curves are lower (see Fig. 3.).

With the increase of the helium flow, the voltage needed for the ignition of the discharge decreases. When reducing the applied voltage, the plasma stayed on even for lower values than those needed to ignite the discharge, i.e., the plasma exhibited a hysteresis. The mean power in all cases was less than 10 W.

4. CONCLUSION

We have constructed a plasma jet which can operate in a range of frequencies 25-150 kHz. In this paper, we have shown results for the frequency of 80 kHz and several gas flows of the feeding gas (helium). High-voltage probes were used in order to record the current and voltage waveforms. The ignited plasma behaves like a nonlinear load introduced into the electrical circuit. With the increase of the helium flow, the ignition voltages reduce for the same current range. The power in all cases did not exceed 10 W, which makes this device suitable for the applications with biological samples.

Acknowledgement

This research has been supported by the Ministry of Science, Serbia, under the contract number 141025 of the project Physics Fundamentals of Applications of Non-Equilibrium Plasmas in Nanotechnologies and Treatment of Materials.

References

Fridman, G., Friedman, G., Gutsol, A., Shekhter, A. B., Vasilets, V. N. and Fridman, A.: 2008, *Plasma Process. Polym.*, **5**, 503.

Kunhardt, E. E.: 2000, *IEEE Trans. Plasma Sci.*, **28**, 189.

Puač, N., Petrović, Z. Lj., Malović, G., Đorđević, A., Živković, S., Giba, Z. and Grubišić, D.: 2006, *J. Phys. D: Appl. Phys.*, **39**, 3514.

Schulz-von der Gathen, V., Buck, V., Gans, T., Knake, N., Niemi, K., Reuter, St., Schaper, L. and Winter, J.: 2007, *Contrib. Plasma Phys.*, **47**, 510.

Shi, J., Zhong, F., Zhang, J., Liu, D. W. and Kong, M. G.: 2008, *Physics of Plasmas*, **15**, 013504.

Teschke, M., Kedzierski, J., Finantu-Dinu, E. G., Korzec, D. and Engemann, J.: 2005, *IEEE Transactions on plasma science*, **33**, 310.

Current-voltage characteristics of atmospheric pressure plasma jet

Conference Paper · August 2010

READS
38

6 authors, including:

Saša Lazović
Institute of Physics Belgrade
70 PUBLICATIONS **212** CITATIONS

SEE PROFILE

Gordana Malovic
Institute of Physics Belgrade
157 PUBLICATIONS **932** CITATIONS

SEE PROFILE

UDC 537.56(082)
539.186.2(082)
539.121.7(082)
533.9(082)

ISSN 0373-3742

ПУБЛИКАЦИЈЕ АСТРОНОМСКЕ ОПСЕРВАТОРИЈЕ У БЕОГРАДУ
PUBLICATIONS OF THE ASTRONOMICAL OBSERVATORY OF BELGRADE
Св. 89 No. 89

25th Summer School and International Symposium on the Physics of Ionized Gases

Donji Milanovac, Serbia,
August 30 - September 3, 2010

CONTRIBUTED PAPERS

&

ABSTRACTS of INVITED LECTURES,
TOPICAL INVITED LECTURES and PROGRESS REPORTS

Editors:
Luka Č. Popović,
Milorad M. Kuraica

БЕОГРАД
2010

PUBL. ASTRON. OBS. BELGRADE No. 89, 1-405 BELGRADE, JULY 2010

PUBLICATIONS OF THE ASTRONOMICAL OBSERVATORY OF BELGRADE

FOUNDED IN 1947

Published and copyright © by Astronomical Observatory, Volgina 7, 11060 Belgrade 38, Serbia

Director of the Astronomical Observatory: Dr. Zoran Knežević

Typesetting: Tatjana Milovanov

Internet address `http://www.aob.bg.ac.rs`

ISBN 978–86–80019–37–6

The publication of this issue is financially supported by the Serbian Ministry of Science and Technological Development.

Number of copies / тираж : 400

Production: "1909.MINERVA", Karadjordjev put br. 37, Subotica, Serbia

Publ. Astron. Obs. Belgrade No. 89 (2010), 307-310 *Contributed Paper*

CURRENT–VOLTAGE CHARACTERISTICS OF ATMOSPHERIC PRESSURE PLASMA JET

NEVENA PUAČ[1], DEJAN MALETIĆ[1], SAŠA LAZOVIĆ[1], GORDANA MALOVIĆ[1], ANTONIJE ĐORĐEVIĆ[2] and ZORAN Lj. PETROVIĆ[1]

[1]*Institute of Physics University of Belgrade, Pregrevica 118, 11080 Zemun, Serbia*
E-mail: nevena@ipb.ac.rs

[2]*School of Electrical Engineering, University of Belgrade, Bulevar kralja Aleksandra 73, 11000 Belgrade, Serbia*

Abstract. We have constructed a plasma jet that can operate in the frequency range 25-150 kHz and within the range of 5-10 kV of applied peak-to-peak voltages. High voltage probes are used in order to obtain current and voltage waveforms. In this paper, we will show V_{RMS}-I_{MRS} plasma jet characteristics for the working frequency of 80 kHz. Current and voltage measurements were made both for the increase and decrease of the applied voltage in order to see if there is a hysteresis effect.

1. INTRODUCTION

Atmospheric pressure discharges cover a wide range of dimensions, starting from micrometer-scale plasmas convenient for localized and precise treatment, up to dimensions suitable for the treatment of large-scale samples. So far, many different configurations and applications of non-thermal atmospheric plasmas have been developed and studied (see Kundthart et al. 2000, Fridman et al. 2008, Puač et al. 2006, von der Gathen et al. 2007). Recently, several authors have reported on various means of generating cold plasma jets at atmospheric pressure. More interestingly, these jets turned out not to be a continuous plasma, but trains of small high-velocity plasma packets-bullets (see Kong et al. 2008, Teschke et al. 2005).

We have constructed plasma jet that can operate in the frequency range from 25 kHz to 150 kHz and within the range of 5-10 kV of applied peak-to-peak voltages. In this paper, we will show V_{RMS}-I_{MRS} plasma jet characteristics for the working frequency of 80 kHz. High voltage probes are used in order to obtain current and voltage waveforms. Measurements are made for the increase and decrease of the applied voltage in order to see if there is a hysteresis effect.

2. EXPERIMENTAL SETUP

The atmospheric pressure plasma jet is made of a Pyrex glass tube with inner diameter of 4 mm and outer diameter of 6 mm. Electrodes that were used were made of a thin copper foil wrapped around the glass tube. The distance between the powered and the grounded electrode was 13.5 mm. The width of both electrodes was 13 mm. One of the electrodes (the left electrode, see Fig. 1) was grounded. The other electrode, closer to the end of the glass tube, was the powered one (see Fig. 1). The distance between the powered electrode and the end of the glass tube was 11 mm. The feeding gas was helium and the flow rates used in this work were 2, 3 and 4 slm. The flow rate is adjusted with a mass flow controller (Omega FMA5400/5500).

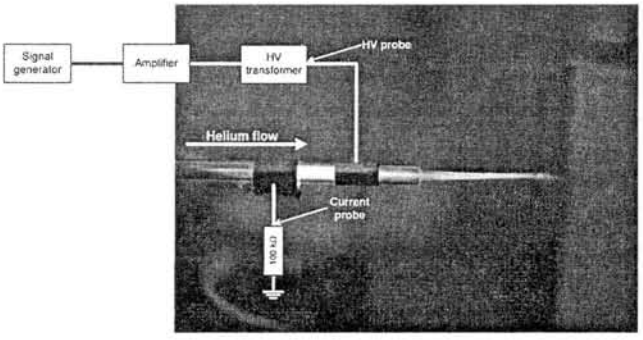

Figure 1: Experimental setup.

For powering the plasma jet, we used a signal generator (Peak Tech DDS FUNCTION GENERATOR 4025) connected to the custom-made amplifier. Highest voltages that we could obtain from the amplifier were up to 1 kV, which was not enough to ignite the plasma. In order to the increase applied voltages to the values higher than 5-6 kV, we had to use an additional homemade transformer.

Current and voltage measurements were made with two commercial probes. The first probe, used for obtaining voltage waveforms, was a high-voltage probe (Agilent N2771A) and it was connected to the HV-output (see Fig. 1). In order to obtain current waveforms, we used the second probe (Agilent 10076A) which measured the voltage drop on a 100 kΩ resistor placed in the grounded branch of the electrical circuit. The working frequency was 80 kHz and the applied voltage was in the range of 6-10 $kV_{peak\text{-}to\text{-}peak}$.

3. RESULTS AND DISCUSSION

The current and voltage waveforms when there is no discharge, and with plasma on, are shown in Fig. 2. We can see that when the plasma is not ignited, the phase difference between the current and the voltage is approximately $\pi/2$. The imped-

ance is practically capacitive (the voltage waveform lags behind the current waveform). When plasma is ignited, the phase difference between the voltage and the current reduces significantly. Signal for the current is increased and deformed, while the peak-to-peak value for the voltage is smaller than in the case when there is no plasma (no He flow). By igniting the discharge we have employed additional nonlinear load into the electrical circuit.

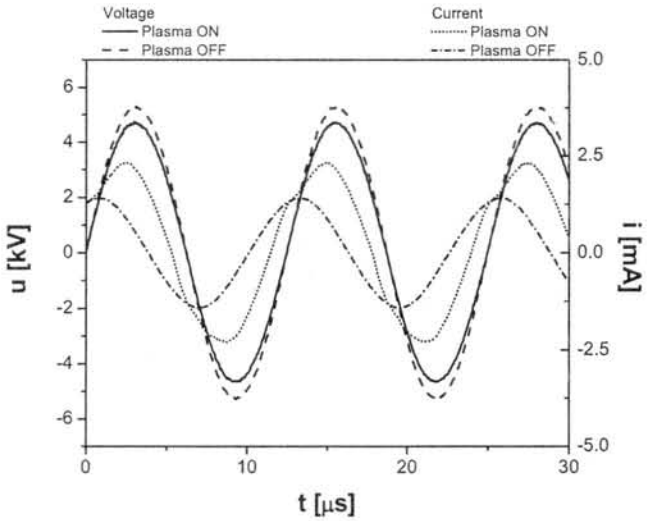

Figure 2: Current and voltage waveforms for the helium flow rate of 3 slm. Dashed lines represent case when discharge is OFF and solid lines when discharge is ignited.

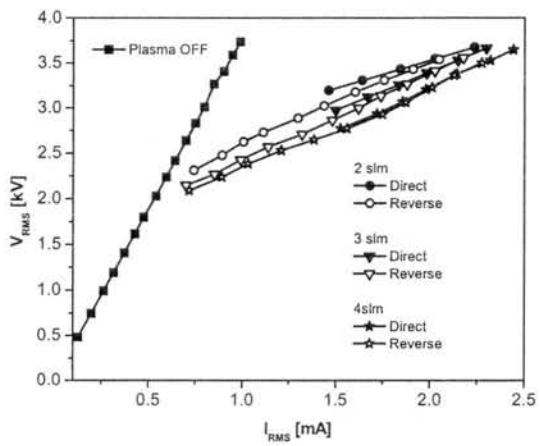

Figure 3: Current-voltage characteristics for three different flows of helium.

In Fig. 3 V_{RMS}–I_{RMS} characteristics are shown for three different flows of the feeding gas. In case when plasma is off, the RMS values of the current are lower than in the case when the plasma is ignited. On the other hand, the voltage is decreased with the plasma ignition.

When the plasma is off, the phase difference between the current and voltage is close to 90°. In this case, we have a capacitive impedance of several MΩ, corresponding to the capacitance of about 0.5 pF. On the other hand, the plasma ignition introduces a parallel nonlinear load into the electrical circuit. and in this case the slopes of the V_{RMS}–I_{RMS} curves are lower (see Fig. 3.).

With the increase of the helium flow, the voltage needed for the ignition of the discharge decreases. When reducing the applied voltage, the plasma stayed on even for lower values than those needed to ignite the discharge, i.e., the plasma exhibited a hysteresis. The mean power in all cases was less than 10 W.

4. CONCLUSION

We have constructed a plasma jet which can operate in a range of frequencies 25-150 kHz. In this paper, we have shown results for the frequency of 80 kHz and several gas flows of the feeding gas (helium). High-voltage probes were used in order to record the current and voltage waveforms. The ignited plasma behaves like a nonlinear load introduced into the electrical circuit. With the increase of the helium flow, the ignition voltages reduce for the same current range. The power in all cases did not exceed 10 W, which makes this device suitable for the applications with biological samples.

Acknowledgement

This research has been supported by the Ministry of Science, Serbia, under the contract number 141025 of the project Physics Fundamentals of Applications of Non-Equilibrium Plasmas in Nanotechnologies and Treatment of Materials.

References

Fridman, G., Friedman, G., Gutsol, A., Shekhter, A. B., Vasilets, V. N. and Fridman, A.: 2008, *Plasma Process. Polym.*, **5**, 503.

Kunhardt, E. E.: 2000, *IEEE Trans. Plasma Sci.*, **28**, 189.

Puač, N., Petrović, Z. Lj., Malović, G., Đorđević, A., Živković, S., Giba, Z. and Grubišić, D.: 2006, *J. Phys. D: Appl. Phys.*, **39**, 3514.

Schulz-von der Gathen, V., Buck, V., Gans, T., Knake, N., Niemi, K., Reuter, St., Schaper, L. and Winter, J.: 2007, *Contrib. Plasma Phys.*, **47**, 510.

Shi, J., Zhong, F., Zhang, J., Liu, D. W. and Kong, M. G.: 2008, *Physics of Plasmas*, **15**, 013504.

Teschke, M., Kedzierski, J., Finantu-Dinu, E. G., Korzec, D. and Engemann, J.: 2005, *IEEE Transactions on plasma science*, **33**, 310.

Removal of Reactive Orange 16 From Water by Plasma Needle

Conference Paper · August 2014

DOI: 10.13140/2.1.3570.6240

9 authors, including:

Saša Lazović
Institute of Physics Belgrade
70 PUBLICATIONS **212** CITATIONS
SEE PROFILE

Gordana Malovic
Institute of Physics Belgrade
157 PUBLICATIONS **932** CITATIONS
SEE PROFILE

Z. Dohčević-Mitrović
Institute of Physics Belgrade
158 PUBLICATIONS **1,112** CITATIONS
SEE PROFILE

Zoran Lj Petrović
Institute of Physics Belgrade
510 PUBLICATIONS **5,652** CITATIONS
SEE PROFILE

27th International Symposium on t

&

Dr

Zor vić

I ade y
Univ ade

www.spig2014.ipb.ac.rs

27th Summer School and International Symposium on the Physics of Ionized Gases

SPIG 2014

CONTRIBUTED PAPERS

&

ABSTRACTS OF INVITED LECTURES,
TOPICAL INVITED LECTURES, PROGRESS REPORTS
AND WORKSHOP LECTURES

Editors

Dragana Marić, Aleksandar R. Milosavljević and
Zoran Mijatović

Institute of Physics, Belgrade
University of Belgrade

Serbian Academy
of Sciences and Art

Belgrade, 2014

CONTRIBUTED PAPERS & ABSTRACTS OF INVITED LECTURES, TOPICAL INVITED LECTURES, PROGRESS REPORTS AND WORKSHOP LECTURES
of the 27th Summer School and International Symposium on the Physics of Ionized Gases

August 26 – 29, 2014, Belgrade, Serbia

Editors:

Dragana Marić, Aleksandar R. Milosavljević and Zoran Mijatović

Publishers:

Institute of Physics,Belgrade
Pregrevica 118, P. O. Box 68
11080 Belgrade, Serbia

Klett izdavačka kuća d.o.o.
Maršala Birjuzova 3-5, IV sprat
11000 Belgrade

Computer processing:

Sanja D. Tošić, Nikola Škoro and Miloš Ranković

Printed by

CICERO
Belgrade

Number of copies

300

ISBN 978-86-7762-600-6

REMOVAL OF REACTIVE ORANGE 16 FROM WATER BY PLASMA NEEDLE

Tatjana Mitrović[1,2], Dejan Maletić[1], Nataša Tomić[1], Saša Lazović[1], Gordana Malović[1], Tanja Nenin[2], Uroš Cvelbar[3], Zorana Dohčević-Mitrović[1] and Zoran Lj. Petrović[1]

[1]*Institute of Physics, University of Belgrade, Pregrevica 118, 11080 Belgrade, Serbia*
[2]*Institute for development of water recources"Jaroslav Černi", Jaroslava Černog 80, 11226 Belgrade, Serbia*
[3]*Jožef Stefan Insitute, Jamova Cesta 39, Ljubljana, SI-1000, Slovenia*
email:lazovic@ipb.ac.rs

Abstract. In this article we present the results of decolourisation and degradation of Reactive Orange 16 dye in the water by a plasma needle. Argon flow rates are varied in order to improve the removal efficiency. We find that the complete decolourization and a considerable percent of mineralization are achieved after 60 min of plasma treatment for the flow rates higher than 4 slm. The decolourisation and mineralization effects are measured by UV/VIS spectrophotometry and total organic carbon content.

1. INTRODUCTION

Plasma technologies are used in wastewater treatment because of a high removal efficiency of organic pollutants. Besides the capability to abundantly generate chemically active species, plasma is used for water decontamination because of convenient operating conditions (atmospheric pressure and relatively low temperature) [1].

There are various types of non-thermal plasma devices such as plasma jets, plasma needle, gliding arc, etc. [2-4]. These plasmas can produce high concentrations of radicals [5]. Plasma generated radicals enable numerous biomedical applications. In our previous research we have used plasma needle for treatment of biological samples like bacteria, human stem cells, plant stem cells (calli) [2, 6-8]. Besides the biomedical applications, radicals are important in advanced oxidation processes [1]. OH radicals have a particularly large oxidation potential. They interact with organic pollutants and can decompose them into less or non-harmful components.

In this paper we present the results of decolourisation of Reactive Orange 16 (RO 16) azo dye recorded using the UV/VIS spectroscopy.

Furthermore, we present degradation curves for two different argon flow rates (4 and 8 slm) obtained by total organic carbon measurements (TOC).

2. EXPERIMENTAL SETUP

The experimental setup is given on Figure 1. Plasma needle consists of a body made of Teflon, a central electrode made of copper, and a glass tube. A dye sample is prepared with distilled water (50 mg/l, 25 ml). The needle tip is immersed into the solution as presented in Figure 1. Magnetic stirrer (300 rpm) preserved the homogeneity of the sample. We use different argon flow rates (1, 4, and 8 slm). Decolourisation is monitored by measuring absorbance after plasma treatments at 493.7 nm (which corresponds to the -N=N- bond). A complete dye spectra and absorbance at a fixed wavelength are measured by UV/VIS spectrophotometry. Degradation is recorded based on the total organic carbon content.

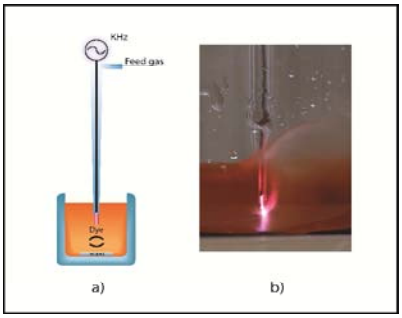

Figure 1. a) Experimental setup, b) Plasma in the dye solution.

3. RESULTS AND DISCUSSION

The degradation rate of RO 16 is determined following two different processes: the colour loss and oxidation. The colour loss gives evidence that the chromophore group which is responsible for the absorption of the dye molecule in the visible region of the spectral range is eliminated. This colorant is characterized by azo group as a chromophore (–N=N–) which has a maximum absorption at 493.7 nm. Decolourisation is presented on Figure 2. For the given set of experimental conditions we observe a decrease of absorbance and that the total decolourisation is achieved after 60 min of plasma treatment for the flow rates of 4 and 8 slm. However, for the lowest flow rate of 1 slm the colour loss is not complete even after 60 min of treatment, but it is obvious that there is a decreasing trend. In this case, longer treatment times could lead to the total decolourisation. It is very interesting to compare the decolourisation kinetics for 4 and 8 slm flow rates in the first 30 min and beyond that time. We can see that when we double the flow rate, the degradation rate significantly increases for the

first 30 min. For example, after 10 min of treatment the absorbance ratio (A/A_o) is reduced to 20 and 40 % for 8 and 4 slm flow rates of argon, respectively. However, after 30 min, the increase in flow rate does not contribute that much to the decolourisation rate as compared to the previous case.

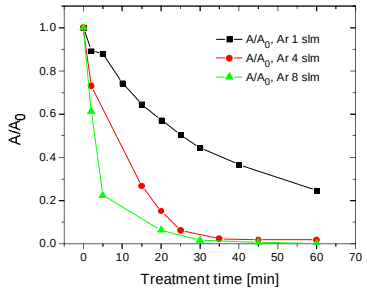

Figure 2. Decolourisation of Reactive orange 16 for three different argon flow rates (1, 4, 8 slm).

In order to demonstrate that the colorant is not just decolourised, but also degraded to some extent, we have performed TOC measurements. Although a full decolourisation is achieved after 60 min of plasma treatment, there is a possibility that hazardous by-products may appear as a result of incomplete decomposition of the molecule. To verify this, total organic carbon content, which concerns bond breaking in the aromatic part of the dye (C–C, C=C, C–N, C–S) is measured.

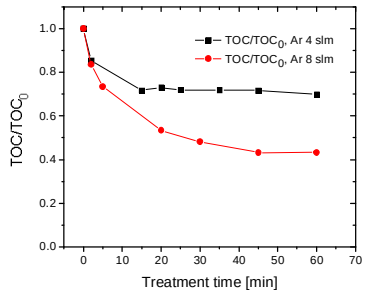

Figure 3. Degradation of Reactive Orange 16 for two different argon flow rates (4 and 8 slm)

We can see that the total organic carbon is reduced by about 60 % for 8 slm and only 30 % for 4 slm after 60 minutes of plasma treatment (Figure 3). As in the case of decolourisation, mineralisation rate also depends on the flow rate. For smaller flow rates the oxidation process is typically slower as compared to the

higher flow rates. Unlike decolourisation, full degradation was not reached after 60 min of plasma treatment.

4. CONCLUSION

In this paper we show the results of decolourisation and degradation of Reactive Orange 16 dye in aqueous solution. We find that complete decolourisation and a considerable percent of degradation are achieved after 1 hour of plasma treatment. As expected, degradation is much slower than decolourisation and both processes are dependent on treatment conditions such as the gas flow rate. We can conclude that the plasma needle can be a promising device for removal of organic pollutants from water and that further optimization of treatment parameters is needed to obtain high removal rates.

Acknowledgements

MESTD, Republic of Serbia, project no. III 41011 and ON 171037.

REFERENCES

[1] B. Jiang, J. Zheng, S. Qiu, M. Wu, Q. Zhang, Z. Yan and Q. Xue, Chem. Eng. J., 236, 348–368 (2014).
[2] S. Lazović, N. Puač, M. Miletić, D. Pavlica, M. Jovanović, D. Bugarski, S. Mojsilović, D. Maletić, G. Malović, P. Milenković and Z. Petrović, New J. Phys., 12, 8, 083037 (2010).
[3] M. R. Ghezzar, F. Abdelmalek, M. Belhadj, N. Benderdouche and a Addou, J. Hazard. Mater., 164, 2–3, 1266–74 (2009).
[4] N. Puač, D. Maletić, S. Lazović, G. Malović, A. Đorđević and Z. Lj. Petrović, Appl. Phys. Lett., 101, 2, 024103 (2012).
[5] G. Malović, N. Puač, S. Lazović and Z. Petrović, Plasma Sources Sci. Technol., 19, 3, 034014 (2010).
[6] M. Miletić, D. Vuković, I. Živanović, I. Dakić, I. Soldatović, D. Maletić, S. Lazović, G. Malović, Z. Lj. Petrović and N. Puač, Cent. Eur. J. Phys., 12, 3, 160–167 (2014).
[7] M. Miletić, S. Mojsilović, I. Okić Đorđević, D. Maletić, N. Puač, S. Lazović, G. Malović, P. Milenković, Z. Lj. Petrović and D. Bugarski, J. Phys. D. Appl. Phys., 46, 34, 345401 (2013).
[8] N. Puač, S. Živković, N. Selaković, M. Milutinović, J. Boljević, G. Malović and Z. Lj. Petrović, Appl. Phys. Lett., 104, 21, 214106 (2014).

Biomedical applications and diagnostics of atmospheric pressure plasma

Conference Paper · September 2011

CITATION
1

READS
27

6 authors, including:

Zoran Lj Petrović
Institute of Physics Belgrade
510 PUBLICATIONS **5,652** CITATIONS
SEE PROFILE

Saša Lazović
Institute of Physics Belgrade
70 PUBLICATIONS **212** CITATIONS
SEE PROFILE

Kosta Spasic
University of Belgrade
10 PUBLICATIONS **12** CITATIONS
SEE PROFILE

Gordana Malovic
Institute of Physics Belgrade
157 PUBLICATIONS **932** CITATIONS
SEE PROFILE

Seventeenth International Summer School
19 – 23 September 2011
Sunny Beach, Bulgaria

VEIT
Vacuum Electron Ion Technologies

PROGRAM ABSTRACTS

IL–2

BIOMEDICAL APPLICATIONS AND DIAGNOSTICS OF ATMOSPHERIC PRESSURE PLASMA

Z.Lj. Petrović, N. Puač, S. Lazović, D. Maletić, K. Spasić and G. Malović

Institute of Physics, Pregrevica 118, 11080 Belgrade, Serbia

Numerous applications of non-equilibrium (cold, low-temperature) plasmas require those plasmas to operate at atmospheric pressure. Achieving non-equilibrium at atmospheric pressure is difficult since the ionization growth is very fast at such a high pressure. The high degree of ionization, on the other hand, enables energy transfer between electrons and ions and heating of the background neutral gas through collisions between ions and neutrals. Thus, all schemes of producing non-equilibrium plasmas revolve around some form of control of the ionization growth. It can be achieved by an inhomogeneous field using a dielectric barrier or by a time varying field. Another approach is to operate at the *pd* value corresponding to the Paschen minimum, i.e. at microscopic dimensions and high pressures. In all cases, however, atmospheric pressure plasmas have small dimensions making it very difficult to perform standard diagnostics.

Diagnostics of atmospheric pressure plasmas is difficult and some of the techniques cannot be employed at all. Optical emission spectroscopy and laser absorption spectroscopy require very high resolution in order to resolve the anatomy of the discharges. Mass analysis is not normally applicable to atmospheric pressure plasmas; systems with triple differential pumping have been developed recently that allow analysis of the plasma chemistry at atmospheric pressures, which is essential for numerous applications. Application of such systems is, however, not free of problems; we will discuss ways of dealing with them. Applications in biomedicine require minimal heating of the ambient air. The gas temperature should not exceed 40 ^{o}C to avoid thermal damage to the living tissues. Thus, plasmas should operate at very low powers and controlling the power is of essential importance. We have developed unique derivative probes that allow control of powers well below 1 W.

We will describe four different sources, including dielectric barrier discharges, a plasma needle, an atmospheric pressure jet and a micro-atmospheric pressure jet. The jet operates in the plasma bullet regime if proper conditions are mėt.

Finally, we will present results on plasma treatment of bacteria, human cells and plants. Localized delivery of active species by plasmas may lead to a number of medical procedures that may also involve removal of bacteria, fungi and spores.

Program

Fundamentals and Applications of Microplasmas

March 1- 6, 2009
Catamaran Resort Hotel, San Diego, California
Tel: 1-858-488-1081

Conference Co-chairs:

J. Gary Eden
University of Illinois, USA

Sung-Jin Park
University of Illinois, USA

Kunihide Tachibana
Kyoto University, Japan

Jörg Winter
Ruhr Universität Bochum, Germany

Engineering Conferences International
32 Broadway, Suite 314
New York, NY 10004, USA
Phone: 1-212-514-6760, Fax: 1-212-514-6030
www.engconfintl.org – info@engconfintl.org

VOLT-AMPERE CHRACTERISTICS AND DIAGNOSTICS OF MICRO DISCHARGES

Zoran Petrovic, Institute of Physics, University of Belgrade
Pregrevica 118 POB 68, Zemun, 11080, Serbia
T: 381628026994, F: 381113162190, zoran@phy.bg.ac.yu
Dragana Maric, Nikola Skoro, Gordana Malovic, Nevena Puac, Sasa Lazovic, Marija Radjenovic-Radmilovic, Dejan Miletic, Institute of Physics, University of Belgrade

Basic breakdown properties of micro discharges should be scalable to standard size/pressure discharges if the same physics persists. We have studies the breakdown in normal size discharges and have used several scaling laws including E/N, pd, jd^2 in order to test the main physics defining the discharge. In addition to the breakdown as represented by the Paschen curve we have employed Volt Ampere characteristics to study the properties of the discharge and also the key processes leading to the breakdown as the secondary yield coefficient has a deciding role on the behavior of the operating voltage as current is changed in dc discharges. Theoretical predictions state that the standard Townsed phenomenology breaks down only below 0.005 mm gaps when field emission becomes the key mechanism affecting the breakdown and deforming the left hand side of the Paschen curve. However it has been often observed that the voltage is constant and equal to the minimum breakdown voltage to the left of the minimum and it may be argued either that the long path breakdown becomes important or that some new processes are introduced. Plasma needle also belongs to a group of micro discharges and it operates supplied by rf power. We have tested how volt ampere characteristics may be related to the real power submitted to the discharge, how modes of operation differ in external properties and we have applied mass spectrometry to see how production of chemically active radicals may be associated with different modes of operation.

Title: WO_3/TiO_2 composite coatings: structural, optical and photocatalytic properties

Author: Zorana Dohčević-Mitrović Stevan Stojadinović Luca Lozzi Sonja Aškrabić Milena Rosić Nataša Tomić Novica Paunović Saša Lazović Marko G. Nikolić Sandro Santucci

PII: S0025-5408(16)30255-0
DOI: http://dx.doi.org/doi:10.1016/j.materresbull.2016.06.011
Reference: MRB 8811

To appear in: *MRB*

Received date: 24-2-2016
Revised date: 19-5-2016
Accepted date: 6-6-2016

Please cite this article as: Zorana Dohčević-Mitrović, Stevan Stojadinović, Luca Lozzi, Sonja Aškrabić, Milena Rosić, Nataša Tomić, Novica Paunović, Saša Lazović, Marko G.Nikolić, Sandro Santucci, WO3/TiO2 composite coatings: structural, optical and photocatalytic properties, Materials Research Bulletin http://dx.doi.org/10.1016/j.materresbull.2016.06.011

Highlights

- WO_3/TiO_2 coatings were fabricated via Plasma Electrolytic Oxidation process.
- With increasing time of PEO process WO_3 and $WO_{2.96}$ phases became dominant.
- Band gap red shift with increasing $WO_3/WO_{2.96}$ content.
- Enhanced visible light photoactivity of composite coatings.
- Catalysts ehxibit increased adsorption affinity and charge separation efficiency.

WO_3/TiO_2 composite coatings: structural, optical and photocatalytic properties

Zorana Dohčević-Mitrović[a*], Stevan Stojadinović[c], Luca Lozzi[d], Sonja Aškrabić[a], Milena Rosić[e], Nataša Tomić[a], Novica Paunović[a], Saša Lazović[b], Marko G. Nikolić[b], Sandro Santucci[d]

[a]Center for Solid State Physics and New Materials, Institute of Physics Belgrade, University of Belgrade, Pregrevica 118, 11080 Belgrade, Serbia

[b]Institute of Physics Belgrade, University of Belgrade, Pregrevica 118, 11080 Belgrade, Serbia

[c]Faculty of Physics, University of Belgrade, Studentski Trg 12-16, 11000 Belgrade, Serbia

[d]Department of Physical and Chemical Sciences, University of L'Aquila, Via Vetoio 67100, L'Aquila, Italy

[e]Laboratory for Material Science, Institute of Nuclear Sciences „Vinča", University of Belgrade, P.O. Box 522, 11001 Belgrade, Serbia

Corresponding author.

E-mail address: zordoh@ipb.ac.rs (Z. Dohčević-Mitrović)

KEYWORDS: A. Nanostructures, A. Oxides, D. Crystal structure, B. Optical properties, D. Catalytic properties

Abstract

WO_3/TiO_2 and TiO_2 coatings were prepared on titania substrates using facile and cost-effective plasma electrolytic oxidation process. The coatings were characterized by X-ray diffraction, scanning electron microscopy, Raman, UV-vis diffuse reflectance spectroscopy, and X-ray photoelectron spectroscopy. With increasing duration of PEO process, the monoclinic WO_3 phase became dominant and new monoclinic $WO_{2.96}$ phase appeared. The optical absorption edge in the WO_3/TiO_2 samples, enriched with $WO_3/WO_{2.96}$ phase, was shifted to the visible region. The photocatalytic efficiency of WO_3/TiO_2 and pure TiO_2 samples was evaluated by performing the photodegradation experiments in an aqueous solution of Rhodamine 6G and Mordant Blue 9 under the visible and UV light. The WO_3/TiO_2 catalysts are much more efficient than pure TiO_2 under visible light and slightly better under UV light. The improvement of photocatalytic activity in the visible region is attributed to better light absorption, higher adsorption affinity and increased charge separation efficiency.

1. Introduction

Among semiconductor materials, titanium dioxide (TiO_2) in anatase phase has been shown as excellent and widely used photocatalyst for the degradation of different organic contaminants, because of its physical and chemical stability, high oxidative power, high catalytic activity, long-term photostability, low cost and ease of production. Many organic compounds can be decomposed in an aqueous solution in the presence of TiO_2, illuminated by photons with energies greater than or equal to the band gap energy of titanium dioxide (3.2 eV for anatase TiO_2) [1–6]. The major drawback for TiO_2 commercial use lies in its wide band

gap, and relatively high recombination rate of photoinduced electron-hole pairs. The modification of TiO_2 by doping with metals and non-metals [7–12] or by Ti^{3+} self-doping [13,14] have been extensively performed in order to improve its photocatalytic activity under the visible irradiation.

Another very promising approach is the combination of TiO_2 with metal oxides like V_2O_5, ZnS, $InVO_4$, WO_3 [15-19] or graphene [20]. Among the metal oxides, WO_3 has smaller band gap (2.8 eV) than TiO_2 and better absorbs visible light. Moreover, WO_3 has a suitable conduction band potential and acts as a trapping site for photoexcited electrons from TiO_2. The photogenerated holes from the valence band of WO_3 move towards and accumulate in the valence band of TiO_2. In such a way the efficiency of charge separation is increased, enhancing at the same time the photocatalytic acivity of TiO_2 [21]. Additionally, the formation of WO_3 monolayer on TiO_2 increases the acidity of the WO_3/TiO_2 surface enabling the adsorption of greater amount of hydroxyl groups and organic reactants on the surface [21, 22]. In recent years, WO_3/TiO_2 composites were synthesized using different methods such as sol-gel, ultrasonic spray pyrolysis, ball milling, hydrothermal, sol-precipitation, and impregnation to improve photocatalytic activity of TiO_2 under the visible light [23–28]. Thin films of TiO_2/WO_3 have also been prepared by dip and spin coating [29, 30] or by one-step oxidation method [31]. In most of these reports it was demonstrated that WO_3/TiO_2 composites were found to have much higher photocatalytic activity under the visible light than pure TiO_2 [24, 26, 28, 31]. Therefore, the combination of these two materials can lead to increased charge carrier lifetime and improved photocatalytic activity under the visible irradiation. Among different synthesis routs, plasma electrolytic oxidation (PEO) process is very facile, cost-effective and environmentally benign process for producing of well-adhered and crystalline oxide films, but the studies on structural and photocatlytic properties of WO_3/TiO_2 films (coatings), produced by PEO process, are limited [32, 33, 34].

In this study WO_3/TiO_2 coatings were synthetized on titanium substrate by using PEO process. Structural and optical properties of the coatings were fully characterized by XRD, SEM, Raman, XPS, and diffuse reflectance spectroscopy. The aim of this work was to tailor the band gap energy of WO_3/TiO_2 coatings towards the visible spectral region, varying the time of PEO process and to explore the photocatalytic properties of the coatings. The photocatalytic efficiency of WO_3/TiO_2 coatings was tested under the visible and UV light irradiation using Rhodamine 6G and Mordant Blue 9 as model pollutants. We demonstrated that this approach provides an efficient route for the formation of cost-effective and improved visible-light-driven photocatalysts.

2. Experimental section

2.1 Preparation of WO_3/TiO_2 coatings

WO_3/TiO_2 coatings were prepared on titanium substrate using plasma electrolytic oxidation (PEO) process. PEO process is an anodizing process of lightweight metals (aluminum, magnesium, zirconium, titanium, etc.) or metal alloys above the dielectric breakdown voltage, when thick, highly crystalline oxide coating with high corrosion and wear resistance, and other desirable properties are produced. During the PEO process, numerous small sized and short-lived discharges are generated continuously over the coating's surface, accompanied by gas evolution. Due to increased local temperature, plasma-chemical reactions are induced at the discharge sites modifying the structure, composition, and morphology of such oxide coatings. The oxide coatings formed by PEO process usually contain crystalline and amorphous phases with constituent species originating both from metal and electrolyte. WO_3/TiO_2 coatings were formed on the rectangular titanium samples (99.5% purity, Alfa

Aesar) of dimensions 25 mm × 10 mm × 0.25 mm, which were used as working electrodes in the experiment. The working electrodes were sealed with insulation resin leaving only an area of 1.5 cm^2 as an active surface. Before starting the PEO process, titanium samples were degreased in acetone, ethanol, and distilled water, using ultrasonic cleaner and dried in a warm air stream. The anodic oxidation process was conducted in an aqueous solution of 10^{-3} M 12-tungstosilicic acid ($H_4SiW_{12}O_{40}$), at constant current density (150 mA/cm^2). During PEO process, the electrolyte circulated through the chamber–reservoir system. The temperature of the electrolyte was kept fixed at (20 ± 1) °C. Detailed description of PEO process is given in the ref. [33].

After plasma electrolytic oxidation, the samples were rinsed in distilled water to prevent additional deposition of electrolyte components during drying. The WO_3/TiO_2 samples were obtained by varying the time of PEO process from 90 s up to 300 s. The pure TiO_2 sample was obtained after 300 s of PEO process.

2.2 Characterization of WO_3/TiO_2 coatings

The crystal structure of WO_3/TiO_2 samples was analyzed by X-ray diffraction (XRD), using a Rigaku Ultima IV diffractometer in Bragg-Brentano geometry, with Ni-filtered CuKα radiation (λ=1.54178 Å). Diffraction data were acquired over the scattering angle 2θ from 15^o to 75^o with a step of 0.02^o and acquisition rate of 2^o/min. The XRD spectra refinement was performed with the software package Powder Cell. The TCH pseudo-Voigt profile function gave the best fit to the experimental data.

Scanning electron microscope (SEM) JEOL 840A equipped with an EDS detector was used to characterize the morphology and chemical composition of formed oxide coatings.

Micro-Raman scattering measurements were performed at room temperature in a backscattering geometry, using a Jobin-Yvon T64000 triple spectrometer system and Nd:YAG laser line of 532 nm as an excitation source. The incident laser power was kept less than 10 mW in order to prevent the heating effects.

UV-vis diffuse reflectance spectra were acquired using the Specord M40 Carl Zeiss spectrometer.

X-ray photoelectron spectroscopy (XPS) was used for the surface composition analysis of WO_3/TiO_2 coatings. XPS was carried out on a VG ESCALAB II electron spectrometer with a base pressure in the analysis chamber of 10^{-8} Pa. The X-ray source was monochromatized AlKα radiation (1486.6 eV) and the instrumental resolution was 1 eV. The spectra were calibrated using the C 1s line (284.8 eV) of the adventitious carbon and corrected by subtracting a Shirley-type background.

2.3 Photocatalytic experiments

The photocatalytic activity of WO_3/TiO_2 samples was evaluated by monitoring the decomposition of Rhodamine 6G (R6G) and Mordant Blue 9 (MB9) under the irradiation of two different light sources: fluorescent and UV lamps. The photocatalytic measurements on R6G solution (initial concentration in water: 10 mg/L) have been performed using a 36 W visible fluorescent lamp (Hyundai eagle), whose emission spectrum, compared to sunlight spectrum, is given in ref. [9]. The cuvette (3 mL) was placed at about 5 cm from the lamp. The evolution of the rhodamine concentration was followed by measuring the variation of the intensity of main absorption peak at ~525 nm. UV-vis absorption measurements as a function of the light exposure time were performed by using USB2000 spectrometer by Ocean Optics.

The solution was placed in the dark for 60 min to reach the adsorption/desorption equilibrium before visible light exposure.

The photocatalytic activity of WO_3/TiO_2 samples under UV light irradiation was evaluated using aqueous solution of MB9 as a model pollutant. Batch type experiments were performed in an open thermostated cell (at 25 °C). The cell was equipped with a water circulating jacket to maintain the solution at room temperature. A mercury lamp (125 W) was used as a light source and was placed 13 cm above the surface of the dye solution. The initial concentration of MB9 in an aqueous suspension was 50 mg/L and the working volume was 25 mL. Before the lamp was switched on, the cell was kept in dark for 60 min in order to achieve the adsorption-desorption equilibrium. At regular time intervals the aliquots were taken and the concentration of the dye was determined by UV-vis spectrophotometer (Super Scan) at λ_{max}=516 nm. The photocatalytic experiments were conducted at the natural pH of the dyes (pH=7 in a case of R6G solution and at pH=6 in a case of MB9 solution). All photocatalytic measurements were repeated at least twice to check their reproducibility.

In order to detect the formation of free hydroxyl radicals ($OH^{\bullet}$) on the UV illuminated WO_3/TiO_2 surface, photoluminescence (PL) measurements were performed using terephthalic acid, which is known to react with $OH^{\bullet}$ radicals and produces highly fluorescent 2-hydroxyterephthalic acid. The experiment was conducted at ambient temperature. The WO_3/TiO_2 photocatalyst (TW300) was placed in open termostated cell filled with 20 mL of the 5×10^{-4} mol L^{-1} terephthalic acid in a diluted NaOH aqueous solution with a concentration of 2×10^{-3} mol L^{-1}. UV lamp (125 W) was used as a light source. Sampling was performed after 15, 30, 60 and 90 min. PL spectra of reaction solution, using excitation wavelength of 315 nm, were measured on a Spex Fluorolog spectrofluorometer system at wavelength of 425 nm for which the 2-hydroxyterephthalic acid exhibits intense PL peak.

3. **Results and discussion**

3.1 Crystal structure and morphology

XRD patterns of the WO_3/TiO_2 samples obtained for 90 (TW90), 120 (TW120), and 300 s (TW300) of PEO process are presented in Fig. 1. The diffraction peaks which appear in TW90 sample at 2θ = 23.3°, 33.4°, 54.2° belong to (002), (022) and (042) planes of monoclinic WO_3 phase, which crystallizes in $P2_1/c$ (No. 14) space group. Besides these XRD peaks, the XRD pattern also shows peak at 25.3° which belongs to TiO_2 anatase crystal phase (space group $I4_1/amd$ (No. 141)) and intense peaks of elemental Ti (space group $P6_3/mmc$ (No. 194)). This indicates that Ti substrate is not completely oxidized to form TiO_2 during the PEO process. With increasing duration of PEO process, for the TW120 and TW300 samples, the XRD peaks of WO_3 phase became more intense. The spectra refinement, using Powder Cell program, showed that besides WO_3 phase a monoclinic $WO_{2.96}$ phase appeared (space group *P2/c* (No. 13)). Furthermore, the intensities of XRD peaks which belong to TiO_2 phase and elemental Ti decreased implying that the WO_3/TiO_2 coatings were enriched with $WO_3/WO_{2.96}$ phase. According to the JCPDS database for WO_3, $WO_{2.96}$, TiO_2, and elemental Ti (JCPDS: 43-1035 (WO_3), 30-1387 ($WO_{2.96}$), 16-0934 (TiO_2) and 44-1294 (elemental Ti)) very good agreement is obtained between experimental and calculated diffraction patterns of the WO_3/TiO_2 samples. In Fig. 1 are marked main XRD peaks of WO_3 and $WO_{2.96}$ phases for clarity. The lattice parameters and the estimated volume fractions (%) of different phases for the WO_3/TiO_2 samples are given in Table 1.

Fig. 1

Table 1

In Fig. 2 are presented SEM images of WO_3/TiO_2 samples. In the TW90 sample produced with shorter PEO time, certain number of microdischarge channels together with molten regions was present because of the rapid cooling of the electrolyte. With increasing time of PEO process, when the thickness of the oxide coating was increased, the number of microdischarge channels and micropores decreased followed by increased roughness of the coating's surface.

Fig. 2

The quantitative elemental analysis confirmed the presence of Ti, O and W and the elemental composition of the samples is shown in Table 2. EDS analysis confirmed the increasing trend of W content with increasing of PEO time.

Table 2

3.2 Raman and diffuse reflectance spectra

The Raman spectra of WO_3/TiO_2 samples produced for different duration of PEO process are shown in Fig. 3a. Several modes originating from two crystalline oxide phases can be identified (marked on Fig. 3a as T and W).

Fig. 3

The Raman modes positions were determined using Lorentzian fit procedure and the deconvoluted spectra of TW90, TW120 and TW300 samples are presented in the Fig. 3b. Besides the modes at about 144 cm^{-1} ($E_{g(1)}$), 197 cm^{-1} ($E_{g(2)}$), 393 cm^{-1} ($B_{1g(1)}$), 516 cm^{-1} (A_{1g}, $B_{1g(2)}$) and 638 cm^{-1} ($E_{g(3)}$) which belong to anatase phase of TiO_2 [35], several modes characteristic for monoclinic WO_3 phase are present [22, 36, 37]. The broad band at ~703 cm^{-1} and strong band at ~793 cm^{-1} are assigned to the stretching (O–W–O) modes of the bridging oxygen of the WO_6 octahedra. The bands observed at ~272 cm^{-1} and at ~316 cm^{-1} are

assigned to the bending (O–W–O) vibrations of bridging oxygen in monoclinic m-WO_3 [22, 37]. The band positioned at ~989 cm^{-1} is assigned to the dioxo $(W=O)_2$ symmetric vibration of the isolated surface WO_4 structure, whereas its weak shoulder at ~942 cm^{-1} represents asymmetric vibration of the same atomic group [22, 37]. The low frequency mode at 58 cm^{-1} belongs to the to lattice modes of monoclinic WO_3 phase [38].

Further, from the Lorentzian fit procedure it was obtained that the ratio between the intensity of the peak positioned at 639 cm^{-1} and the sum of the intensities of the 703 cm^{-1} and 793 cm^{-1} peaks decreased with the increase of PEO time. This fact supports the XRD results that WO_3 content increases with prolonged duration of PEO process.

In Fig. 4 are presented the Raman spectra of TW90, TW120 and TW300 samples in the C–H and O–H region. The Raman band at around 2885 cm^{-1} originates from the overlapped CH_3 and CH_2 stretching vibrations [39]. Broad Raman peak in the 3000-3600 cm^{-1} frequency range can be assigned to the O–H stretching vibration of water molecules adsorbed on the surface of the WO_3/TiO_2 coatings [3, 5].

Fig. 4

The absorption spectra of TW90, TW120 and TW300 samples are given in Fig. 5a. With increasing content of WO_3 phase the absorption edge shifts to higher wavelengths. In the spectra of TW120 a structure around 380-400 nm can be observed, which is very pronounced in the TW300 sample. The appearance of this absorption structure can be attributed to the electronic population of WO_3 conduction band [40]. From the absorption spectra from Fig. 4a, applying the same procedure as Ghobadi in his work [41], the band gap energies for pure TiO_2 and WO_3/TiO_2 samples were estimated. In Fig. 5b are presented the Tauc plots for indirect transition, as TiO_2 and WO_3 are indirect band gap semiconductors [26]. The band gap (E_g) energies are 3.19 eV for pure TiO_2, and 2.84, 2.77 and 2.6 eV for TW90, TW120 and TW300 samples, respectively. It is obvious that with increasing WO_3 content the band gap decreases

compared to pure TiO_2 and shifts to the visible spectral range. Patrocinio et al. [40] have shown that in TiO_2/WO_3 films, the WO_3 conduction band introduces new low lying electronic levels with respect to the conduction band of TiO_2, causing the lowering of the band gap energy of composite samples compared to pure TiO_2. This finding is in accordance with the band gap behavior of our WO_3/TiO_2 samples from Fig. 5b.

Fig. 5

3.3 XPS analysis

The XPS study was further used to confirm the chemical binding states of W 4f. The W 4f XPS spectra of the TW90 and TW300 samples and the results of their decomposition into peaks are shown in Fig. 6. The W 4f spectrum of TW90 sample (Fig. 6a) can be deconvoluted into one doublet with binding energies of 35.8 (W $4f_{7/2}$) and 38.1 eV (W $4f_{5/2}$), respectively. The energy position of this doublet corresponds to the W^{6+} oxidation state [42].

Fig. 6

In the TW300 sample (Fig. 6c) the contribution of W^{5+} states from nonstoichiometric oxide phase can be seen. The W 4f spectrum can be deconvoluted with two doublets. The first two characteristic peaks at 36 (W $4f_{7/2}$) and 38.3 eV (W $4f_{5/2}$) correspond to W^{6+} state as in the case of TW90. The binding energies of these peaks are somewhat higher than that for TW90 sample. The up-shift in binding energy can be ascribed to the presence of defects and OH-groups on the surface [43], existence of which is confirmed by Raman analysis (Fig. 4). The binding energies of the second doublet at 34.5 (W $4f_{7/2}$) and 36.5 eV (W $4f_{5/2}$) correspond to W^{5+} state [42]. These results are in accordance with XRD analysis.

The O 1s spectra of TW90 and TW300 samples (Fig. 6b, d) are decomposed into three peaks. The major peak at binding energy of 531.2 eV can be assigned to the oxygen atoms in

WO_3 and to the OH-groups present on the surface [32, 44]. The second peak observed at 530.6 eV has been attributed to oxygen bound to Ti [26], whereas the binding energy of the third peak at 533.1 eV corresponds to the oxygen in water molecules bound in the coating's structure or adsorbed on its surface [45]. The relative intensity of the XPS peaks at 531.2 eV and 533.1 eV was increased in the TW300 sample. The intensity increase of these peaks can be related to the presence of sub-stoichiometric WO_{3-x} phase ($WO_{2.96}$). Similar behavior was reported in the paper of Shpak et al. [44] in which these peaks were more intense in WO_{3-x} oxides than in stoichiometric WO_3. This finding is also supported by the Raman spectrum of TW300 sample (Fig. 4), for which the intensity of the Raman mode, corresponding to the water molecules adsorbed on the surface, is higher than in TW90 sample.

3.4 Photocatalytic performances of WO_3/TiO_2 coatings

Fig. 7a shows the kinetics of degradation of R6G for pure TiO_2 and WO_3/TiO_2 samples under the visible light. No detectable degradation of R6G was registered without the presence of WO_3/TiO_2 samples (black circles on Fig. 7a). As can be seen from Fig. 7a, both TiO_2 and WO_3/TiO_2 coatings adsorbed the dye in the equilibrium period of 60 min before the exposure to visible light. It is known from the literature that the zero point charge (pH_{zpc}) of TiO_2 lies between 6 and 6.8 [46, 47, 48], whereas the isoelectric point of WO_3 is even lower and lies in the range 1.5-2.5 [49]. At higher pH values than these WO_3 and TiO_2 surfaces should be negatively charged. Therefore, the adsorption of the R6G as cationic dye at pH=7, points out that the surfaces of WO_3/TiO_2 and TiO_2 coatings are negative and attract the positively charged R6G. The dye adsorption ability can be crucial for the high catalytic activity of the catalyst, because it can enhance the electron/hole transfer efficiency and contact with photogenerated active species.

When TiO_2 and WO_3/TiO_2 samples were subjected to visible radiation, composite coatings have shown much better photoefficiency and demonstrated to be far superior than pure TiO_2. The highest activity was observed for the TW90 and TW120 samples for which the photodegradation of R6G reached almost 80% after 60 min. With further increase of WO_3 content, the photocatalytic efficiency slightly decreased, but is still much higher than for pure TiO_2.

Fig. 7

Further, the photocatalytic activity of WO_3/TiO_2 coatings for degradation of MB9 was tested under the UV light. In Fig. 7b is presented the photodegradation of MB9 in the presence of WO_3/TiO_2 samples. In the dark, WO_3/TiO_2 coatings showed no adsorption of MB9. The absence of adsorption can be explained by highly anionic character of MB9 and electrostatic repulsion between the dye and negatively charged surface of WO_3/TiO_2 coatings.

The photocatalytic activity of WO_3/TiO_2 samples was improved with increased content of WO_3 phase, and the TW300 sample exhibited better activity than pure TiO_2. As can be seen from Fig. 7b, after 240 min more than 80% of dye was degraded in the presence of WO_3/TiO_2 coatings.

Photocatalytic degradation of both dyes can be well described by first-order kinetic equation, $ln(C/C_o)=kt$, where C_o is the initial dye concentration and C is the dye concentration at time t. The first order kinetic constant k is obtained from the slope of the $ln(C/C_o)$ versus t for both dyes. In Table 3 are given the first order rate constants for R6G and MB9 (k_{R6G}, k_{MB9}), together with the corresponding linear correlation coefficient (R^2). In a case of R6G degradation under the visible light, the highest k value (k_{R6G}) was obtained for the TW90 sample. In a case of MB9 degradation under UV light, value of k_{MB9} increased with increasing amount of WO_3.

Table 3

The degradation rate constant *k* of WO_3/TiO_2 coatings under visible light is almost five times higher than that of TiO_2, whereas its value under UV light are comparable with TiO_2, suggesting that composite coatings are very efficient photocatalysts under visible light.

3.5 Hydroxyl radical Analysis

The formation of free hydroxyl radicals ($OH^{\bullet}$) was tested on the surface of TW300 photocatalyst under UV irradiation and detected by PL method. Applying similar procedure as described in the paper of Su et al. [50], TW300 sample was placed in terephthalic acid solution and illuminated by UV light. PL spectra of the reaction solution were measured at room temperature after 15, 30, 60 and 90 min, and these spectra are presented in Fig. 8. The terephthalic acid reacts with $OH^{\bullet}$ producing 2-hydroxyterephthalic acid, which exhibits PL peak at 425nm [51]. The intensity of this peak is proportional to the amount of $OH^{\bullet}$ produced in water [50, 51]. As can be seen from Fig. 8, gradual increase of PL intensity at 425nm with prolonged illumination time points at increasing amount of $OH^{\bullet}$ radicals produced at the surface of TW300 sample.

Fig. 8

3.6 Mechanism of the reaction

The photocatalytic degradation of R6G or MB9 is initiated by the photoexcitation of the WO_3/TiO_2 coatings when the electron-hole pairs are formed on the catalyst's surface. According to the generally accepted photoexcitation mechanism, electrons from the conduction band of TiO_2 can easily diffuse into the conduction band of WO_3 [40, 52]. Since

W(VI) can be easily reduced to W(V), WO_3 acts as an acceptor of conduction band electrons from TiO_2, whereas the photogenerated holes migrate in the opposite direction, i.e. from the lower-lying valence WO_3 band to the valence band of TiO_2. In such a way the charge separation efficiency can be increased.

Fig. 9

In Fig. 9 is given an illustration of photo-induced electron-hole separation and reacting radicals formation. The presence of holes in the dye solution permits a direct oxidation of the dye, due to high oxidative potential of the holes (h^+):

$$h^+ + \text{dye} \rightarrow \text{dye}^{\bullet+} \rightarrow \text{oxidation of the dye} \quad (1)$$

Further, hydroxyl radicals ($OH^\bullet$) are usually formed by the reaction between the holes and OH^- or water molecules present on the surface of the catalyst. The $OH^\bullet$ radicals attack the dye in aqueous solution leading to its degradation:

$$OH^\bullet + \text{dye} \rightarrow \text{photodegradation of the dye} \quad (2)$$

The photo-induced electrons can also react with dissolved oxygen to form superoxide ions ($O_2^{-\bullet}$) which in contact with H_2O molecules form OH^- ions and finally $OH^\bullet$ radicals.

It is known from the literature that WO_3 is almost 15 times more acidic than TiO_2 [21, 22, 31], so it is expected that the surface of PEO produced WO_3/TiO_2 coatings is more acidic than that of TiO_2, and has a higher affinity for chemical species having unpaired electrons. Because of higher acidity, the surface of WO_3/TiO_2 coatings can absorb more H_2O and OH^- generating more $OH^\bullet$ radicals. The XPS and Raman spectra of WO_3/TiO_2 composite coatings gave an evidence that adsorbed H_2O and hydroxyls are present on the surface of WO_3/TiO_2 coatings, existence of which is important for the formation of $OH^\bullet$ radicals. PL measurements, performed on TW300 sample, (Fig. 8) clearly demonstrated that with increasing illumination time the increasing amount of $OH^\bullet$ radicals is formed on the surface of photocatalysts, which manifests through higher photocatalytic activity of TW300 sample.

The absorption measurements have shown that the band gap energy of TiO_2 is higher than that of WO_3/TiO_2 coatings. Namely, with prolonged time of PEO process, the WO_3 content increases followed by an appearance of $WO_{2.96}$ phase. As the conduction band of nonstoichiometric WO_{3-x} oxides is lower with respect to WO_3 and TiO_2 (Fig. 9) [53], the presence of $WO_{2.96}$ phase will further reduce the band gap of WO_3/TiO_2 samples towards the visible spectral range, as already noticed from the Tauc plots from Fig. 5. As a result, the electron-hole recombination will be more difficult and more reactive radicals can be produced at the WO_3/TiO_2 surface. Therefore, WO_3/TiO_2 coatings should be more efficient as catalysts under the visible light. The photocatalytic degradation of R6G and kinetics of the reaction confirmed that WO_3/TiO_2 coatings are efficient photocatalysts in the visible region. Slight decrease of photocatalytic activity of TW300 sample in a case of R6G photodegaradation (Fig. 7a) can be explained by the occurrence of photochromism [27, 40]. Namely, the electron accumulation at the WO_3 conduction band can be more pronounced with increased WO_3 content. The accumulated electrons can react with $OH^{\bullet}$ radicals forming OH^- ions or can reduce the number of superoxide radicals [27, 40] degrading at some extent the photocatalytic activity of WO_3/TiO_2 coatings. The presence of pronounced absorption feature around 380-400 nm in the absorbance spectrum of TW300 sample confirms this assumption. Another reason can be found in the formation of small polarons, appearance of which is characteristic for WO_3 and WO_{3-x} phases. The photoexcited electron-hole pairs can be rapidly quenched by recombination of photoexcited holes with electrons from localized polaron states, whereas photoexcited electrons populate polaron states [54], reducing on the other side the photocatalytic efficiency of the catalyst.

4. Conclusion

WO_3/TiO_2 composite and pure TiO_2 coatings have been prepared on titania substrates using facile and cost-effective PEO process. The structural, morphological, optical properties and chemical composition of these samples were investigated by different methods such as XRD, SEM, Raman, UV-vis diffuse reflectance spectroscopy and XPS. XRD and Raman analysis revealed that the coatings are mainly composed of monoclinic WO_3 and anatase TiO_2. With increasing duration of PEO process the crystallinity of the samples was improved, the WO_3 phase become dominant and a certain amount of monoclinic $WO_{2.96}$ phase appeared. XPS analysis confirmed the XRD results and revealed the presence of OH-groups and adsorbed H_2O on the surface of WO_3/TiO_2 coatings. The increasing amount of $WO_3/WO_{2.96}$ phase caused a decrease of optical band gap, i.e. shift from near UV to visible spectral region. The photocatalytic activity of WO_3/TiO_2 samples has been measured by monitoring photodecolouration of two model pollutants in aqueous solution, R6G under visible and MB9 under UV light irradiation. The WO_3/TiO_2 samples have shown enhanced photocatalytic activity compared to pure TiO_2 under the visible light irradiation. Slight decrease of photocatalytic activity under the visible light in the sample enriched with $WO_3/WO_{2.9}$ phase can be ascribed to the occurrence of photochromism and/or small polaron formation. Under the UV light, the WO_3/TiO_2 photocatalysts have shown slightly better photocatalytic activity than pure TiO_2. PL mesurements demonstrated the correlation between photoactivity and the formation rate of $OH^{\bullet}$ radicals under UV light irradiation, i.e. higher amount of $OH^{\bullet}$ radicals formed, the better photoactivity of WO_3/TiO_2 photocatalysts was achieved. The kinetics of the reaction in the case of both azo dyes followed the pseudo-first order. The degradation rate constant k of WO_3/TiO_2 coatings under the visible light is almost five times higher than that of TiO_2. Much better photocatalytic activity of the WO_3/TiO_2 samples compared to pure TiO_2

in the visible range can be attributed to better light absorption, higher adsorption affinity and increased charge separation efficiency with increasing content of $WO_3/WO_{2.96}$ phase.

Acknowledgements

This work was financially supported by the Ministry of Education, Science and Technological Development of the Republic of Serbia under the projects ON171032, III45018 and bilateral project Serbia-Italy No. RS13MO11.

References

[1] L. Ren, Y. Li, J. Hou, X. Zhao, and C. Pan, ACS Appl. Mater. Interfaces 6 (2014) 1608−1615.

[2] F. Ruggieri, A. A. D'Archivio, M. Fanellia, S. Santucci, RSC Adv. 1 (2011) 611–618.

[3] M. Šćepanović, B. Abramović, A. Golubović, S. Kler, M. Grujić-Brojčin, Z. Dohčević-Mitrović, B. Babić, B. Matović, Z. V. Popović, J. Sol-Gel Sci. Technol. 61 (2012) 390–402.

[4] A. Golubović, B. Abramović, M. Šćepanović, M. Grujić-Brojčin, S. Armaković, I. Veljković, B. Babić, Z. Dohčević-Mitrović, Z.V. Popović, Mater. Res. Bull. 48 (2013) 1363‑1371.

[5] S. Watson, D. Beydoun, J. Scott, R. Amal, J. Nanoparticle Res. 6 (2004) 193–207.

[6] A. N. Banerjee, Nanotechnol. Sci. Appl. 4 (2011) 35–65.

[7] M. Xing, D. Qi, J. Zhang, F. Chen, Chem. Eur. J. 17 (2011) 11432–11436.

[8] Y. Niu, M. Xing, J. Zhang, B. Tian, Catal. Today 201 (2013) 159– 166.

[9] F. Ruggieri, D. Di Camillo, L. Maccarone, S. Santucci, L. Lozzi, J. Nanopart. Res. 15 (2013) 1-11.

[10]M. Xing, W. Li, Y. Wu, J. Zhang, X. Gong, J. Phys. Chem. C 115 (2011) 7858–7865.

[11] M. Janus, B. Tryba, E. Kusiak, T. Tsumura, M. Toyoda, M. Inagaki, A. W. Morawski, Catal. Lett. 128 (2009) 36–39.

[12] M. Takeuchi, M. Matsuoka, M. Anpo, Res. Chem. Intermed. 38 (2012) 1261–1277.

[13] X. Chen, L. Liu, P.Y. Yu, S.S. Mao, Science 331 (2011) 746–750.

[14] W. Fang, M. Xing, J. Zhang, Appl. Catal. B: Environ. 160–161 (2014) 240–246.

[15] Y. Wang, J. Zhang, L. Liu, C. Zhu, X. Liu, Q. Su, Mater. Lett. 75 (2012) 95–98.

[16] Y. Xiaodan, W. Qingyin, J. Shicheng, G. Yihang, Mat. Charac. 57 (2006) 333–341.

[17] J. Rashid, M. A. Barakat, S. L. Pettit, J. N. Kuhn, Environ. Technol. 35 (2014) 2153-2159.

[18] B. Gao, Y. Ma, Y. Cao, W. Yang, J. Yao, J. Phys. Chem. B 110 (2006) 14391–14397.

[19] X. Luo, F. Liu, X. Li, H. Gao, G. Liu, Mat. Sci. Semicon. Proc. 16 (2013)1613–1618.

[20] N. R. Khalid, E. Ahmed, Z. Hong, M.Ahmad, Y. Zhang, S. Khalid, Ceram. Int. 39 (2013) 7107–7113.

[21] Y. Li, P. C. Hsu, S. M. Chen, Sensor. Actuat. B-Chem. 174 (2012) 427– 435.

[22] K. K. Akurati, A. Vital, J. P. Dellemann, K. Michalowa, T. Graule, D. Ferri, A. Baiker, Appl. Catal. B: Environ. 79 (2008) 53–62.

[23] D. Ke, H. Liu, T. Peng, X. Liu, K. Dai, Mater. Lett. 62 (2008) 447–450.

[24] H. Song, H. Jiang, X. Liu, G. Meng, J. Photoch. Photobio. A 181 (2006) 421–428.

[25] C. Shifu, C. Lei, G. Shen, C. Gengyu, Powder Technol. 160 (2005) 198–202.

[26] F. Riboni, L. G. Bettini, D. W. Bahnemann, E. Selli, Catal. Today 209 (2013) 28– 34.

[27] J. Yang, X. Zhang, H. Liu, C. Wang, S. Liu, P. Sun, L. Wang, Y. Liu Catal. Today 201 (2013) 195– 202.

[28] S. Bai, H. Liu, J. Sun, Y. Tian, S. Chen, J. Song, R. Luo, D. Li, A. Chen, C.-C. Liu, Appl. Surf. Sci. 338 (2015) 61–68.

[29] A. Rampaul, I. P. Parkin, S. A. O'Neill, J. DeSouza, A, Mills, N. Elliott, Polyhedron 22 (2003) 35-44.

[30] J. H. Pan, W. In Lee, Chem. Mater. 18 (2006) 847-853.

[31] M. Long, B. Tan, P. Hu, B. Zhou, Y. Zhou, J. Mater. Chem. A 3 (2015) 10195–10198.

[32] J. He, Q. Luo, Q. Z. Cai, X. W. Li, D. Q. Zhang, Mater. Chem. Phys. 129 (2011) 242–248.

[33] S. Stojadinović, N. Radić, R. Vasilić, M. Petković, P. Stefanov, Lj. Zeković, B. Grbić, Appl. Catal. B: Environ. 126 (2012) 334– 341.

[34] S. Petrović, S. Stojadinović, Lj. Rožić, N. Radić, B. Grbić, R. Vasilić, Surf. Coat. Tech. 269 (2015) 250–257.

[35] T. Ohsaka, F. Izumi, Y. Fujiki, J. Raman Spectrosc. 7 (1978) 321–324.

[36] Y. Djaoued, S. Balaji, N, Beaudoin, J. Sol-Gel Sci. Technol. 65 (2013) 374–383.

[37] C. Santato, M. Odziemkowski, M. Ulmann, Jan Augustynski, J. Am. Chem. Soc. 123 (2001) 10639-10649.

[38] E. Cazzanelli, C. Vinegoni, G. Mariotto, A. J. Purans, Solid State Ionics 123 (1999) 67–74.

[39] Y. Yu, K. Lin, X. Zhou, H. Wang, S. Liu, X. Ma, J. Phys. Chem. C 111 (2007) 8971-8978.

[40] A. O. T. Patrocinio, L. F. Paula, R. M. Paniago, J. Freitag, D. W. Bahnemann, ACS Appl. Mater. Interfaces 6 (2014) 16859−16866.

[41] N. Ghobadi, Int. Nano Let. 3 (2013) 1-4.

[42] K. Senthil, K. Yong, Nanotechnology 18 (2007) 395604 (1-7).

[43] H. Ling, J. Lu, S. Phua, H. Liu, L. Liu, Y. Huang, D. Mandler, P. S. Lee, X. Lu, J. Mater. Chem. A 2 (2014) 2708-2717.

[44] A. P. Shpak, A. M. Korduban, M. M. Medvedskij, V. O. Kandyba, J. Electron. Spectrosc. Relat. Phenom. 156–158 (2007) 172–175.

[45] H. Y. Wong, C. W. Ong, R. W. M. Kwok, K. W. Wong, S. P. Wong, W. Y. Cheung, Thin Solid Films 376 (2000) 131-139.

[46] A. A. Khodja, A. Boulkamh, C. Richard, Appl. Catal. B: Environ. 59 (2005) 147–154.

[47] C. C. Wang, J. Y. Ying, Chem. Mater. 11 (1999) 3113–3120.

[48] M. D. Hernández-Alonso, F. Fresno, S. Suarez, J. M. Coronado, Energy Environ. Sci. 2 (2009) 1231–1257.

[49] M. Anik,T. Cansizoglu, J. Appl. Electrochem. 36 (2006) 603–608.

[50] T. M. Su, Z. L. Liu, Y. Liang, Z. Z. Qin, J. Liu, Y. Q. Huang, Catal. Comm. 18 (2012) 93–97.

[51] K. Ishibashi, A. Fujishima, T.Watanabe, K. Hashimoto, Electrochem. Commun. 2 (2000) 207-210.

[52] H. Park, A. Bak, T. H. Jeon, S. Kim, W. Choi, Appl. Catal. B: Environ. 115– 116 (2012) 74– 80.

[53] A. K. L. Sajjad, S. Shamaila, B. Tian, F. Chen, J. Zhang, Appl. Catal. B: Environ. 91 (2009) 397–405.

[54] M. B. Johansson, G. A. Niklasson, L. Österlund, J. Mater. Res., 27 (2012) 3130-3140.

Figure captions

Fig. 1. XRD patterns of TW90, TW120 and TW300 samples formed in various stages of PEO process, together with the XRD spectrum of Ti-substrate. In the inset is given XRD spectrum of anatase TiO_2 obtained on Ti-substrate after 300 s of PEO process.

Fig. 2. SEM micrographs of WO_3/TiO_2 samples formed in various stages of PEO process: (a) TW90, (b) TW120 and (c) TW300 sample.

Fig. 3. Room-temperature Raman spectra of WO_3/TiO_2 samples (a). The TiO_2 and WO_3 Raman modes are marked as T and W. Deconvoluted Raman spectra of TW90, TW120 and TW300 samples (b).

Fig. 4. Raman spectra of WO_3/TiO_2 samples in the C-H and O-H spectral region.

Fig. 5. Absorbance spectra (a) and Tauc plots for indirect band gap for WO_3/TiO_2 samples (b). In the inset are given Tauc plots for indirect band gap for pure TiO_2.

Fig. 6. XPS spectra of W 4f and O 1s regions for TW90 and TW300 samples.

Fig. 7. Photocatalytic degradation of R6G under visible light (a) and MB9 under UV light (b) in the presence of WO_3/TiO_2 and TiO_2 coatings.

Fig. 8. PL spectral changes observed during UV illumination of TW300 sample in the solution of terephthalic acid after 15, 30, 60 and 90 min. The PL spectra of pure terephthalic acid is also presented.

Fig. 9. Schematic diagram of electron-hole pairs separation and proposed mechanism of photodegradation over WO_3/TiO_2 photocatalysts.

Table 1. Phase fraction (vol%) and cell parameters (Å) of WO_3/TiO_2 samples.

Phase	TW90	TW120	TW300
WO_3	*a*=7.4060 *b*=7.6400 *c*=7.6455 29.6%	*a*=7.3026 *b*=7.5398 *c*=7.6933 29.1%	*a*=7.4060 *b*=7.5177 *c*=7.5920 54.5%
$WO_{2.96}$	/	*a*=11.9006 *b*=3.8258 *c*=59.6312 36.7%	*a*=11.8000 *b*=3.8098 *c*=59.7400 20.9%
TiO_2	*a*=3.7778, *c*=9.4440, 66.0%	*a*=3.7841, *c*=9.5105, 32.2%	*a*=3.7790 *c*=9.4124 23.8%
Ti	*a*=2.9481 *c*=4.7325 4.3%	*a*=2.9594 *c*=4.7254 2.0%	*a*=3.0510 *c*=4.7820 0.9%

Table 2. EDS analysis of the WO_3/TiO_2 composites.

Sample	EDS data			
	Ti (at%)	W (at%)	O (at%)	W/Ti
TW90	6.98	14.17	78.85	2.03
TW120	6.22	16.12	77.66	2.59
TW300	4.09	17.16	78.75	4.1

Table 3. The pseudo-first rate constants for R6G and MB9 together with R^2.

Sample	$k_{R6G} \times 10^{-2}$ (min^{-1})	R^2	$k_{MB9} \times 10^{-2}$ (min^{-1})	R^2
TW90	1.52	0.975	0.44	0.990
TW120	1.24	0.957	0.47	0.982
TW300	1.20	0.963	0.65	0.966
TiO_2	0.28	0.888	0.41	0.963

Fig.1

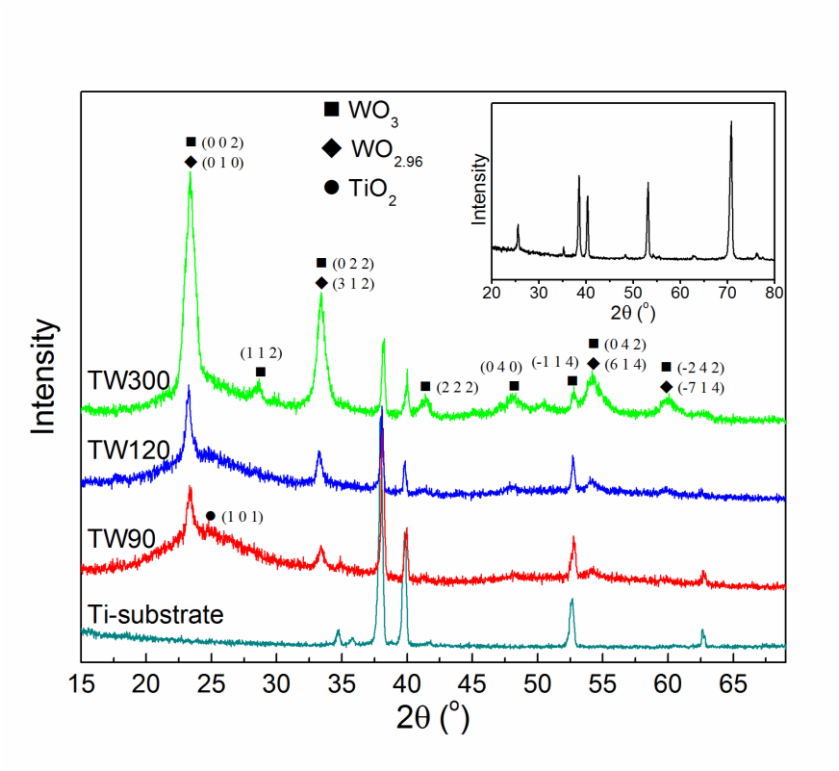

Fig. 2

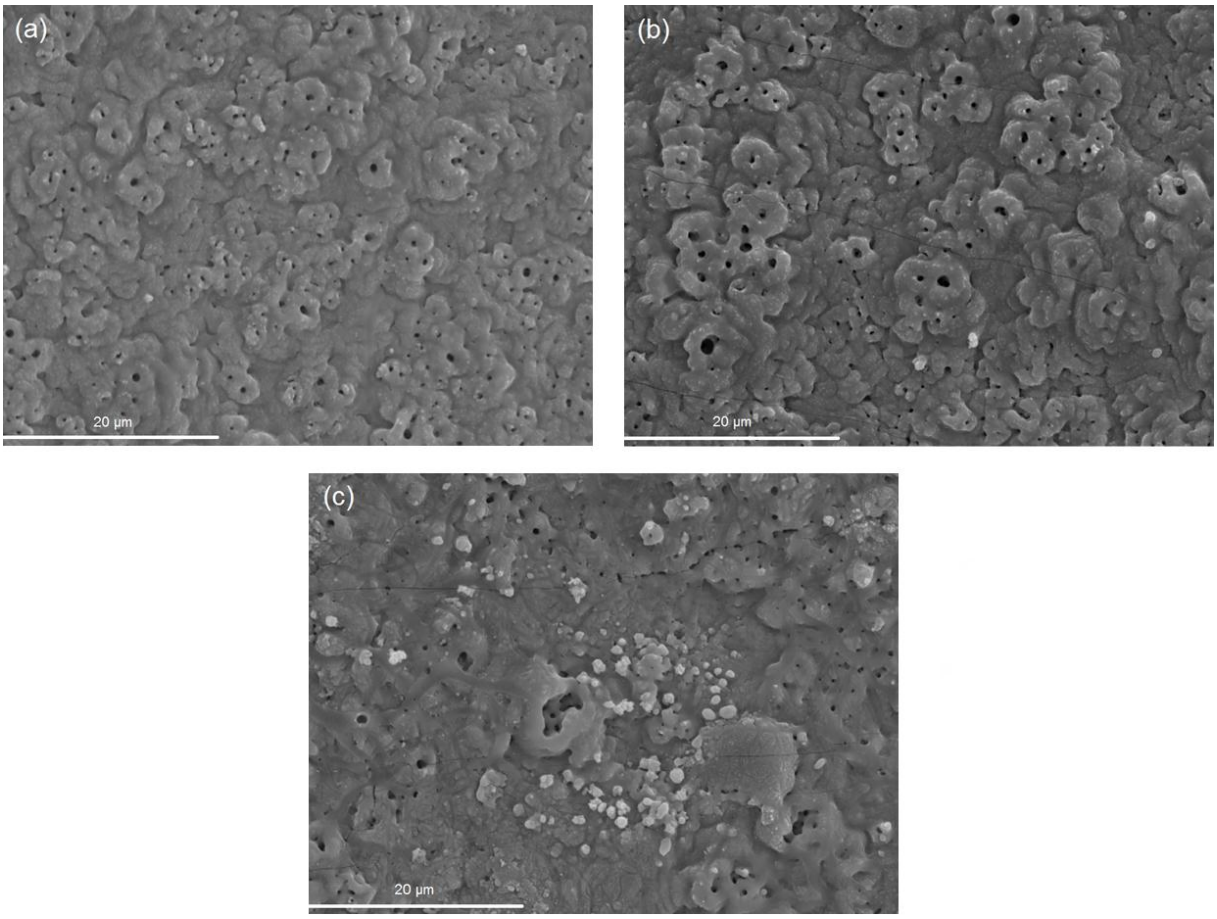

Fig. 3

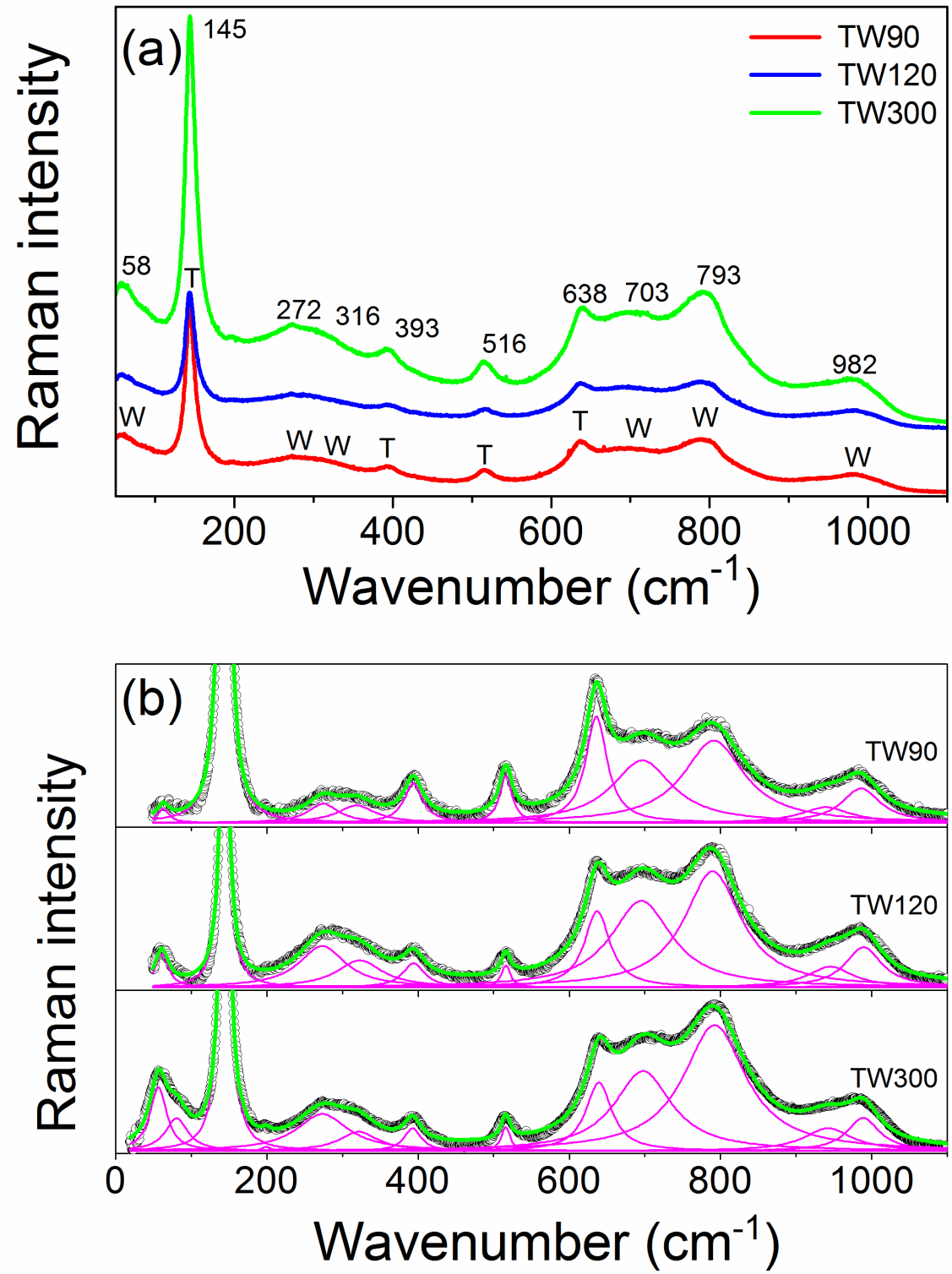

Fig. 4

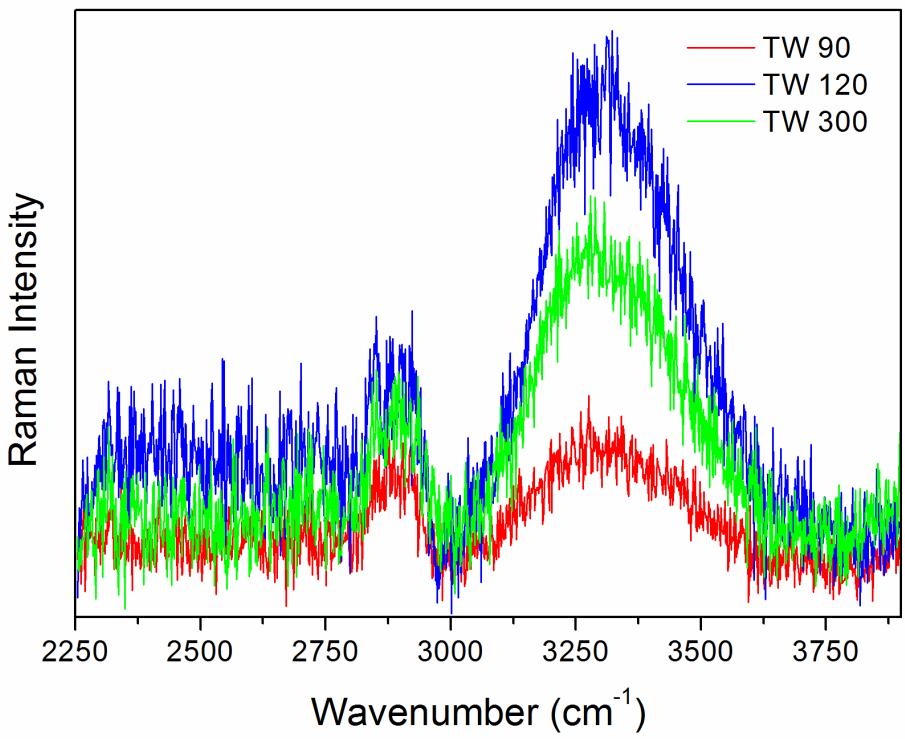

Fig. 5

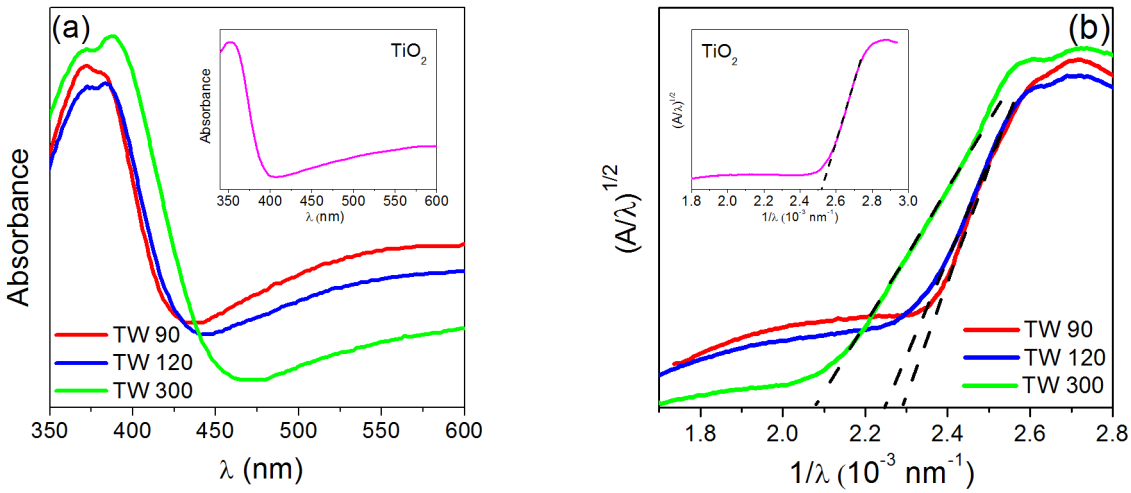

Fig. 6

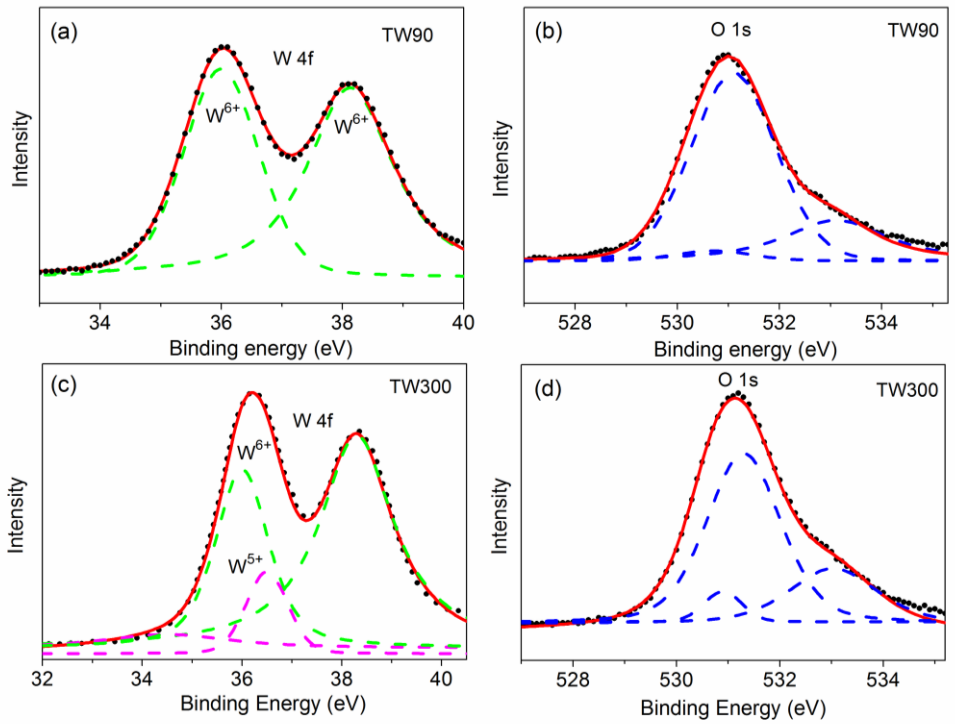

Fig. 7

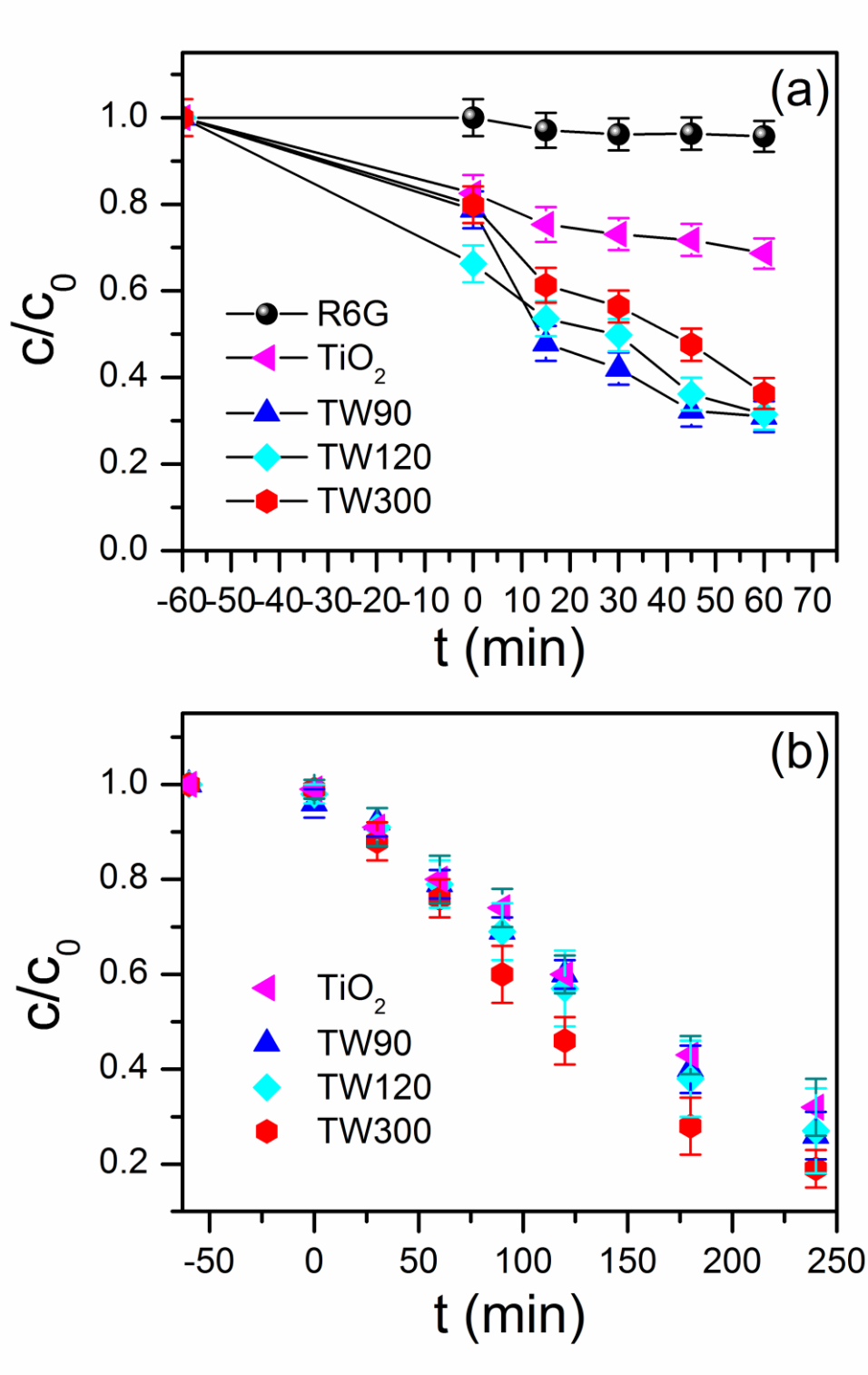

Fig. 8

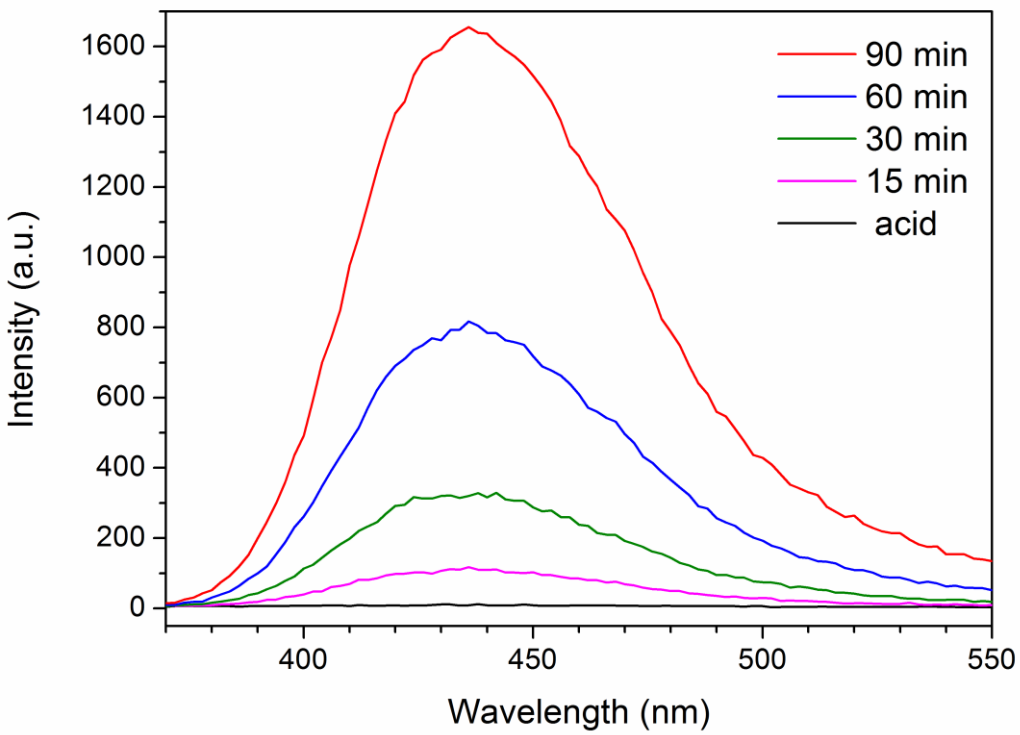

Fig. 9

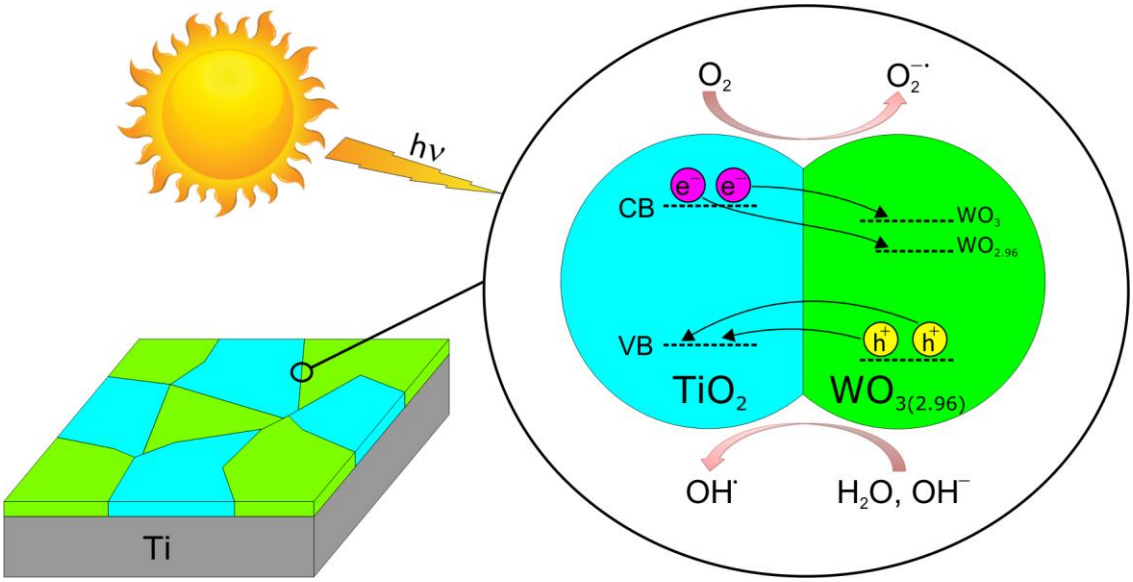

Graphical Abstract

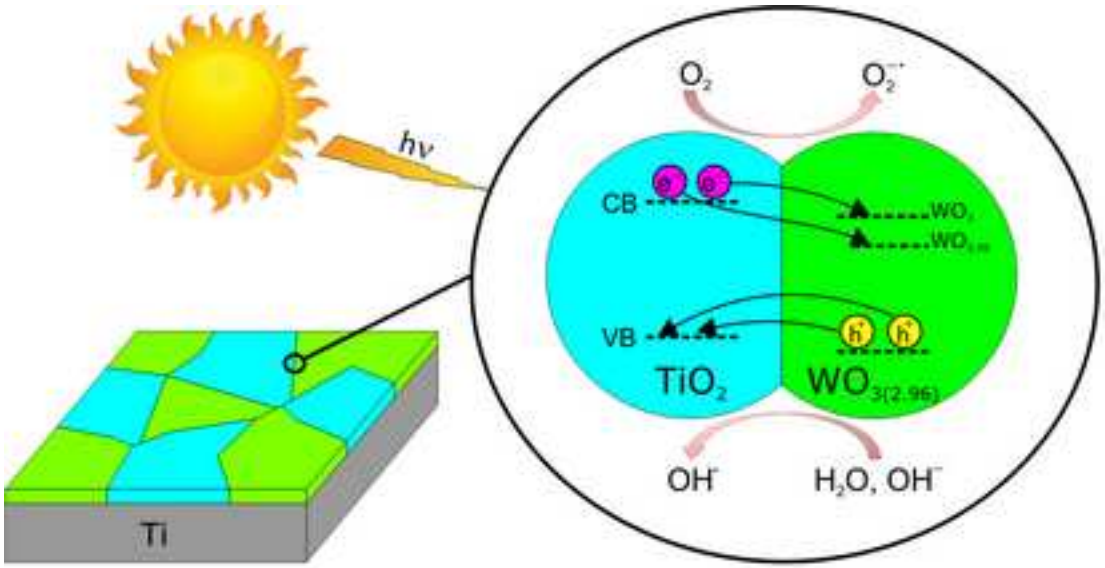

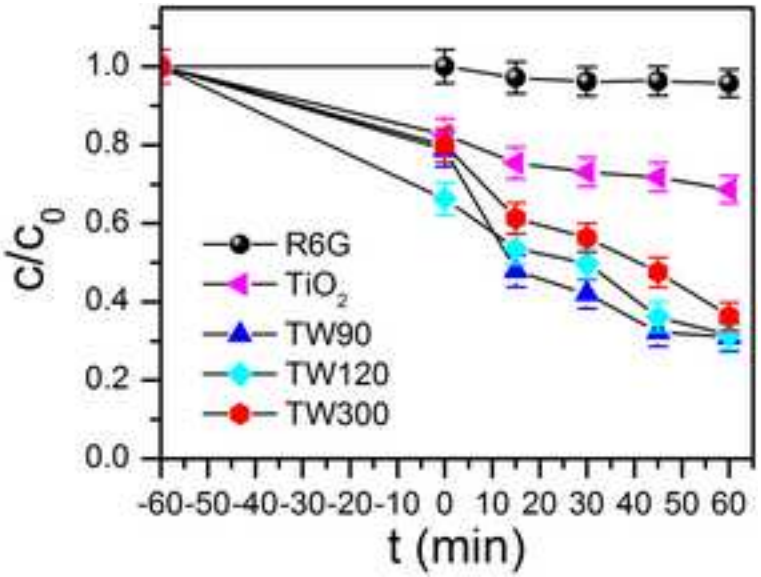

PLOS ONE

RESEARCH ARTICLE

Microplasma Induced Cell Morphological Changes and Apoptosis of *Ex Vivo* Cultured Human Anterior Lens Epithelial Cells – Relevance to Capsular Opacification

Nina Recek[1☯‡], Sofija Andjelić[2☯‡*], Nataša Hojnik[1], Gregor Filipič[1], Saša Lazović[3], Alenka Vesel[1], Gregor Primc[1], Miran Mozetič[1], Marko Hawlina[2], Goran Petrovski[4,5], Uroš Cvelbar[1]

1 Department of Surface Engineering and Optoelectronics (F4), Jožef Stefan Institute, Ljubljana, Slovenia, **2** Eye Hospital, University Medical Centre, Ljubljana, Slovenia, **3** Institute of Physics Belgrade, University of Belgrade, Belgrade, Serbia, **4** Stem Cells and Eye Research Laboratory, Department of Ophthalmology, Faculty of Medicine, University of Szeged, Szeged, Hungary, **5** Centre of Eye Research, Department of Ophthalmology, Oslo University Hospital, University of Oslo, Oslo, Norway

☯ These authors contributed equally to this work.
‡ These authors are joint first authors on this work.
* sofija.andjelic@kclj.si

Citation: Recek N, Andjelić S, Hojnik N, Filipič G, Lazović S, Vesel A, et al. (2016) Microplasma Induced Cell Morphological Changes and Apoptosis of *Ex Vivo* Cultured Human Anterior Lens Epithelial Cells – Relevance to Capsular Opacification. PLoS ONE 11(11): e0165883. doi:10.1371/journal.pone.0165883

Editor: Mohammed Yousfi, Universite Toulouse III Paul Sabatier, FRANCE

Received: November 6, 2015

Accepted: October 19, 2016

Published: November 10, 2016

Data Availability Statement: All relevant data are within the paper and its Supporting Information files.

Funding: The work has been supported by the Slovenian Research Agency (ARRS) programs P3-0333 & P2-0082, EU COST programs MP1101 & TP1208, and NATO grant SPS 984555.

Competing Interests: The authors have declared that no competing interests exist.

Abstract

Inducing selective or targeted cell apoptosis without affecting large number of neighbouring cells remains a challenge. A plausible method for treatment of posterior capsular opacification (PCO) due to remaining lens epithelial cells (LECs) by reactive chemistry induced by localized single electrode microplasma discharge at top of a needle-like glass electrode with spot size ~3 μm is hereby presented. The focused and highly-localized atmospheric pressure microplasma jet with electrode discharge could induce a dose-dependent apoptosis in selected and targeted individual LECs, which could be confirmed by real-time monitoring of the morphological and structural changes at cellular level. Direct cell treatment with microplasma inside the medium appeared more effective in inducing apoptosis (caspase 8 positivity and DNA fragmentation) at a highly targeted cell level compared to treatment on top of the medium (indirect treatment). Our results show that single cell specific micropipette plasma can be used to selectively induce demise in LECs which remain in the capsular bag after cataract surgery and thus prevent their migration (CXCR4 positivity) to the posterior lens capsule and PCO formation.

Introduction

The applications of cold atmospheric pressure plasmas (CAP) in biomedicine has been growing enormously in the recent years.[1, 2] The CAPs have been applied for stem cell manipulation, cancer, skin treatments, wound healing and the like [3–5] To the best of our knowledge, this is the first to report highly selective use of CAP upon lens epithelial cells (LECs). These

cells are responsible for posterior capsular opacification (PCO), which is a major cause of post-operative or secondary visual loss that develops after cataract surgery in approximately 20% of cases within 5 years.[6] Cataract is still the leading cause of blindness worldwide, while PCO is caused by proliferation and migration of LECs remaining in the capsular bag after cataract surgery. The remaining cells can re-colonize the posterior lens capsule which was otherwise cell-free, and therefore, obstruct the visual axis contributing to light scattering and secondary visual loss.

By using *ex vivo* cultured explants from the human anterior portion of the lens capsule (aLC) and visualization by light microscopy, scanning electron microscopy (SEM) and immunofluorescence staining for proliferation and pluripotency markers, we have already shown that human aLC contains LECs that can migrate and proliferate, suggesting a role of aLC-LECs in PCO formation.[7, 8] Such *ex vivo* cultured aLC-LECs may serve as a model for testing different physical and pharmacological agents against PCO development. Herein, the effect of cold atmospheric pressure microplasma jet (μAPPJ) on the LECs morphology and survival is being investigated. LECs have been previously investigated for their mechanical stress-induced contractions.[9] Similar experimental setup was used for the plasma studies as well.

More generally, atmospheric-pressure plasmas (APPs) have become increasingly attractive for different therapies, since plasmas can trigger a complex sequence of biological responses in tissues and cells.[10] Plasma typically contains short-lived free radicals, including reactive oxygen species (ROS) that can induce cell apoptosis, preferably in tumor cells.[11–16] APP is known to abundantly generate radicals [17] and affect the proliferation and migration of human periodontal ligament mesenchymal stem cells. [18] Plasma can also be used without risk of contamination or secondary infection due to their bactericidal properties.[2, 19–26] To move ahead in the further development of actual commercial tools that can be used in hospitals, and in finding novel and perhaps unexpected uses of plasmas, an understanding of the mechanisms of interaction of non-equilibrium gas discharges with living organisms, tissues and cells has become essential.

Dobrynin *et al.* [27] showed that not only ROS generated in plasma are responsible for achieving a desired effect, but also the charged particles (electrons and ions). The mechanism of plasma interaction with cells is complex, owing partially to the complexity of plasma and mainly to the overwhelming complexity of biological processes. Further complexity is added by the presence of medium as well. We hereby describe direct and indirect interaction of microplasma discharge with targeted cells for limitation of secondary effects of plasma to the surrounding cells and environment. The direct plasma treatment is considered, when a single or targeted LEC is treated by microplasma inside a liquid medium, while indirect is when microplasma is positioned outside and on top of the liquid.[10] We hereby treat aLC-LECs directly and indirectly to study the effects plasma particles generated by bulk plasma, created vapours on interfaces and solvated species created by plasma-liquid interactions. For these purpose, the morphological responses of single or targeted cells were monitored immediately after the treatment and after specified incubation times in order to determine the plasma effects on undergoing apoptosis.

Materials and Methods

Microplasma treatment

In order to scale down the plasma volume and achieve a single- or targeted- cell-precision of treatment, modification to the standard APPJ had to be introduced with the electrode configuration.[5, 28, 29] Precision targeted-cell treatment was performed using localized single-electrode microplasma discharge around a needle-like electrode inside the borosilicate glass

tube micropipette (no. TW150F-3, World Precision Instruments, USA) with outside diameter 1.2 mm and inner 0.8 mm which had a tip with end opening diameter of ~3 μm. The glass micropipette tip was made by Flaming/Brown micropipette puller (Model P97 Shutter Instruments Co., USA). The experimental setup for targeted-cell-precision microplasma treatment is schematically shown together with some experimental details in Fig 1. The plasma plume was generated around the powered Teflon insulated microelectrode (outer diameter 0.5 mm) with the striped copper wire end of diameter 0.25 mm positioned 2 mm from micropipette end with opening, but still inside the narrowing tip. The generated plasma plum spread visually into air only for about 10–20 μm and thus was suitable for precise treatment of selected cells or larger groups of cells. When the micropipette tip with inner electrode approached the targeted cell(s) in the liquid, the cell membranes served as a floating counter-electrode, while the plasma was brought in a direct contact with its surface; the upper surface of the liquid represented the interface itself. The plasma source [29] used was then powered at 25 kHz, delivering not more than 1 W of real power in all cases. Pure Helium (Messer, He 5.0) was used as the feeding gas and it was flowing between the glass and the insulated electrode copper wire with flow rates adjusted to 0.2 standard litres per minute (slm) by the Matheson FM-1000 mass flow controller. An adapted electrophysiological micromanipulator (model MP 285, Sutter, USA) was used to control and manipulate the microtip with blowing plasma position with the

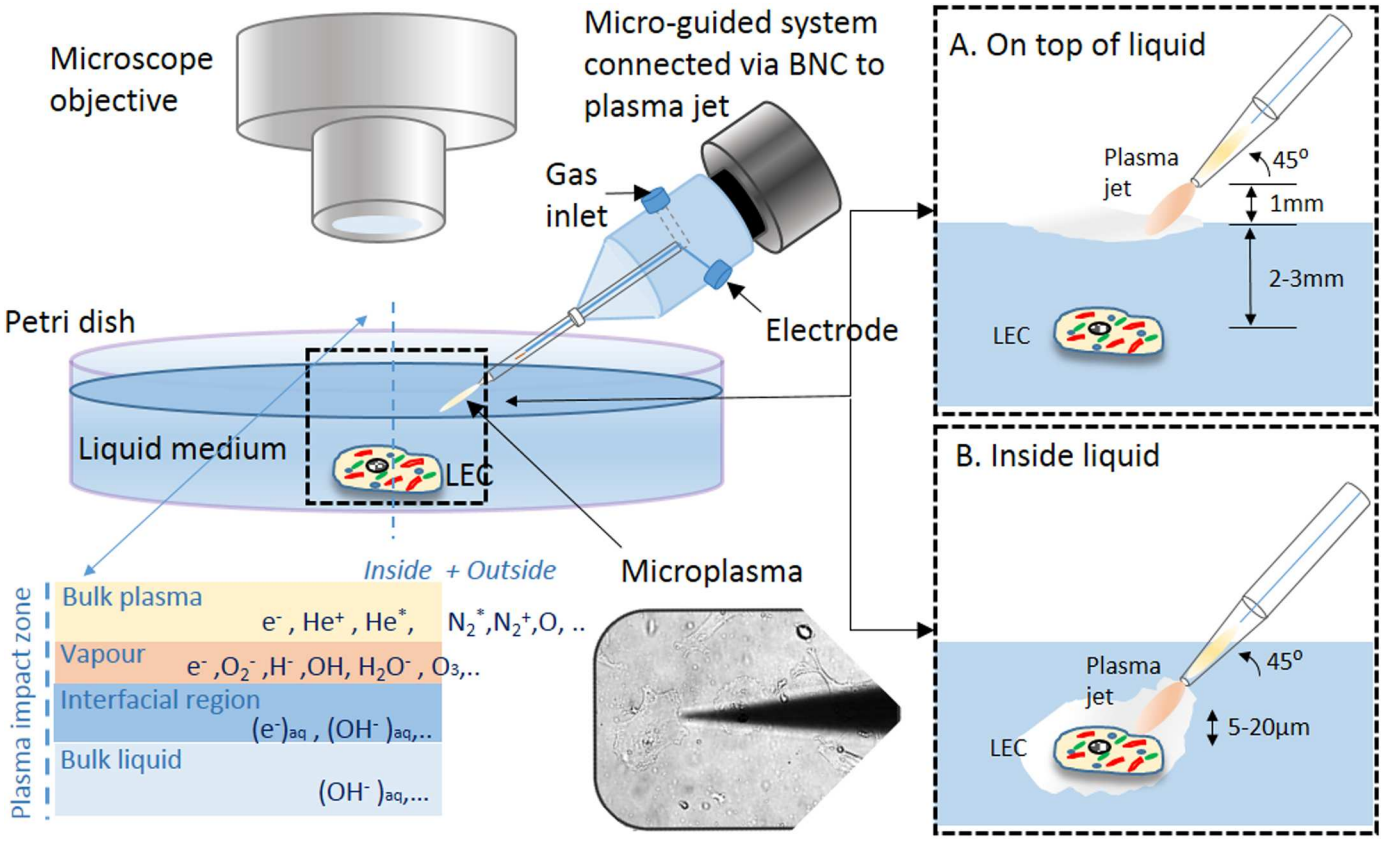

Fig 1. Schematic of the microplasma jet setup with plasma zones and a sketch of the biomedical treatments. A) On the top of the liquid and B) inside the liquid medium.

doi:10.1371/journal.pone.0165883.g001

precision of a few micrometers, which made it possible to potentially agitate selected cell area. Adherent cells were selected after careful observation under the microscope.

Two different ways of targeted cell treatment were performed: (i) the selected cell(s) were treated with the microplasma tip inside the liquid medium several micrometers away from the cell(s) to avoid mechanical damage due to tip—cell membrane surface interaction, and (ii) the targeted cell(s) were treated with the microplasma with the tip positioned outside and on top of the liquid, ~ 1 mm above the surface and about 2–4 mm from the immersed cell (Fig 1). In both cases, the cells were treated for the same plasma treatment times e.g. 10, 30, 60 and 180 s and the effects of the treatment were studied immediately and after incubation for 30 min, 3 and 24 hours afterwards. The samples were then labelled with positions based on underlying grid, so that one could always return to the initial position of the time monitored cell.

During plasma treatment, the environmental properties were monitored by thermal imaging using IR camera FLIR SC5000. The images recorded the tip of the glass tube with a plasma jet and zone of interaction including liquid medium. The thermal images detected were adjusted for glass emissivity (0.92), where the background temperature was adjusted to room temperature (23˚C). This means that the temperature of surrounding air and the liquid shown in Fig 2 can deviate for several degrees. When doing the time evolution of the temperature in selected points, the emission coefficient was adjusted to the materials of each point; again 0.92 for the glass, and 0.96 for the pure water as approximation of the liquid medium being used. Since the liquid medium was not water but it had many additives, the emissivity was again not precise, and thus, the measurements should be taken just as an indication of the temperature change. However, the initial measured temperature of the liquid before plasma ignition was within 10–11˚C of the room temperature.

Tissue collection and processing

All tissue collection complied with the Guidelines of the Helsinki Declaration and was approved by the National Medical Ethics Committee of Slovenia, while patients signed an informed consent before surgery. The aLC-LEC explants were obtained from routine uneventful cataract surgery (20 eyes from 20 patients from Slovenia) performed by M.H. at the Eye Hospital, University Medical Centre (UMC), Ljubljana, Slovenia. All cataracts were done in elderly patients in whom the cataractogenesis was age-related and of progredient type. Lenses were dissected so that the aLC (i.e. basal lamina and associated LECs) were isolated from the fiber cells that form the bulk of the lens. After the surgery, the LEC capsules were transferred [30] to cell culture plastic glass bottom Petri dishes (Mattek Corp., Ashland, MA, USA; 3.5 cm in diameter) and cultivated *ex vivo* under adherent conditions in high glucose-containing medium (DMEM; Gibco®, low glucose, GlutaMAXTM supplement, pyruvate)) supplemented with 10% human serum (Sigma-Aldrich; from human male AB plasma, USA origin, sterile-filtered)and 1% Penicillin-Streptomycin (Sigma-Aldrich; Penicillin-Streptomycin with 10,000 units penicillin and 10 mg streptomycin/mL, sterile-filtered). Detailed description of the aLC tissue attachment, LEC proliferation and migration has been described previously.[7, 8] After 2–3 weeks of aLC incubation, LECs migrated from the capsule to the bottom of the Petri dish, adhered and proliferated. *Ex vivo* cultured human aLC-LECs were used throughout all of the experiments performed.

Real-time monitoring of morphological, apoptotic and migratory changes of the cells

The cell culture medium was treated with the same APP set up as the cells before. After the exposures, Hydrogen Peroxide (H_2O_2) Detection Assay with the ferric-xylenol orange complex

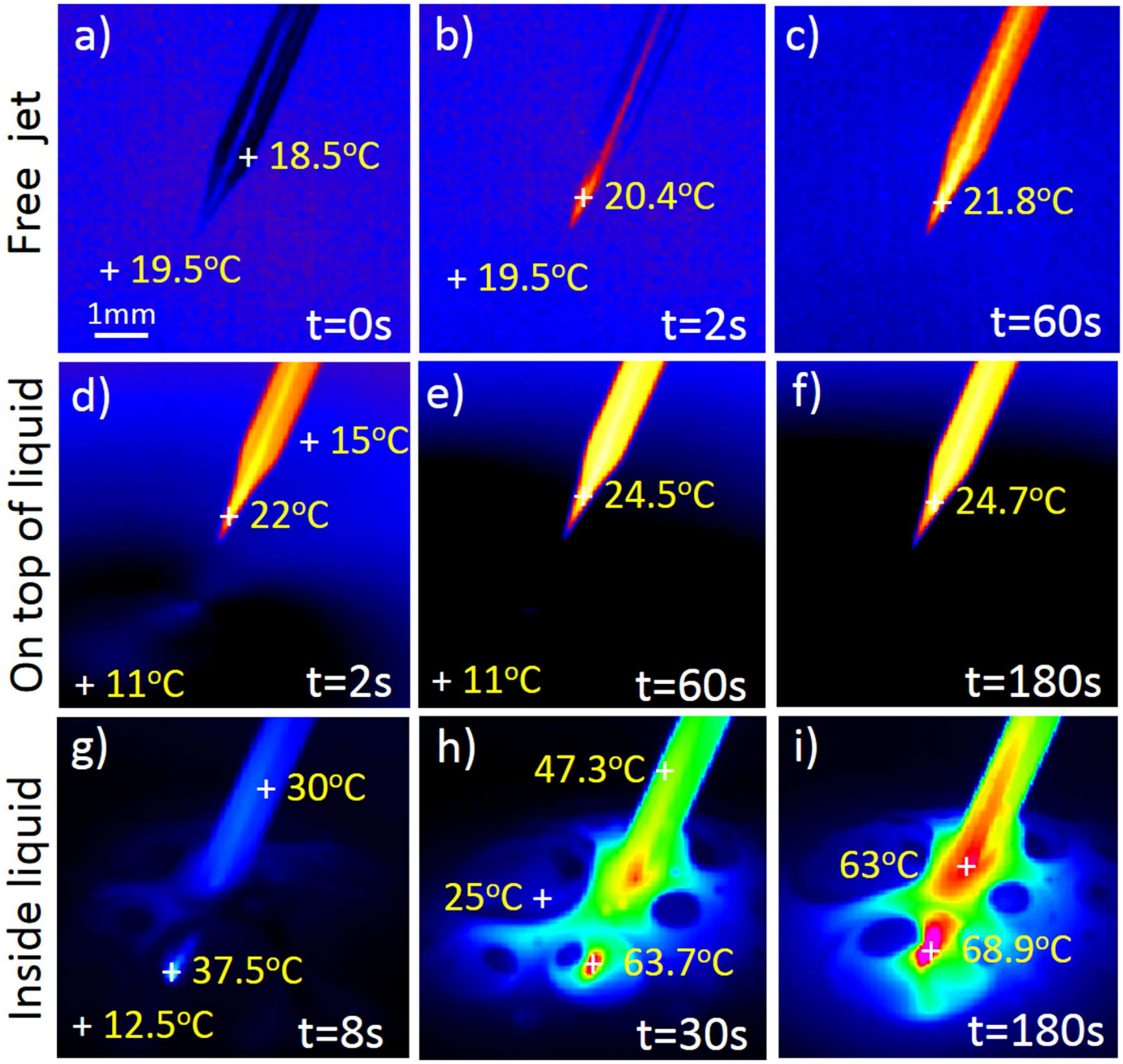

Fig 2. Thermal imaging of microplasma and environment in respect to treatment time. Typical images with marked temperature positions are presented for 3 cases; a)-c) free standing jet spreading into open air, d)-f) microplasma jet on the top of the liquid, and g)-i) microplasma jet inserted into liquid medium.

doi:10.1371/journal.pone.0165883.g002

(xylenole orange, sorbitol and ammonium iron sulfate; all obtained from Sigma-Aldrich) was used with UV-Vis multiplate reader (Biotek Epoch) to determine the concentration of newly produced H_2O_2 in the liquid. Similarly, the nitrite concentrations were measured with standard Griess Reagent Assay (Promega; Griess reagent system). pH levels were determined as well with pH strips (Merck; pH strips).

To asses the apoptotic effect of the microplasma exposure on a treated LEC, real-time morphological observations were performed with an inverted light microscope (Axiovert S100, Carl Zeiss, AG, Oberkochen, Germany). Image acquisition was carried out by a 12-bit cooled CCD camera SensiCam (PCO Imaging AG, Kelheim, Germany). The software used for the acquisition was WinFluor (written by J. Dempster, University of Strathclyde,Glasgow, UK). Microscope objectives used were: 4x/0.10 Achroplan, 10x/ 0.30 Plan-NeoFluar and 40x/0.50 LD A-plan (Zeiss). Real-time observations of the cell morphology changes were carried out and photographed. The surrounding cells were used as controls. The criteria for selecting a region for imaging were the presence of adherent cells and intact cell morphology.

Furthermore DNA fragmentation in apoptotic cells was detected by DAPI staining of LEC samples prefixed in 4% paraformaldehyde (PFA) solution in PBS at room temperature. Immediately after this, the samples were analysed under a fluorescence microscope using standard fluorescein filter set to view 4',6-diamidino-2-phenylindole DAPI fluorescence at 460 nm and counted in three separate visual areas expressed as mean ± SD.

For immunofluorescent staining of the studied cells, fixed samples in 4% PFA were labelled by anti-Caspase 8 (goat polyclonal, Santa Cruz (sc6130), dilution 1:100) apoptosis detecting antibody, and anti-CXCR4 (rabbit polyclonal, Abcam (ab7099), dilution 1:100) cell migration detecting antibody, while nuclear staining was performed using DAPI. Fluorescent images were taken by a ZEISS Axio Observer.Z1 (ZEISS, Oberkochen, Germany) microscope. Due to scarcity of material used for immunocytochemical study and difficulty showing positive and negative controls of the stainings performed on the same cells, only inter-channel fluorescence analysis and differentiation could be performed on a same donor sample, i.e. green-labelled Caspase-8 protein was checked in the red channel for negativity, which was the case; similarly, red labelled CXCR4 protein was checked in the green channel for negativity, and that was also the case.

Results

Morphological changes of the cells

In order to investigate the effect of microplasma on targeted treatment of LECs, the morphological changes were studied. Before the microplasma exposure, all the cells were healthy and spindle-shaped with clear contours. Untreated LEC assumes extensively spread morphology: the cell body and cytoplasm are clearly visible. Cells adhere to the substrate in clusters, with cell extensions (filopodia) projecting toward other cells. The cytoplasm of untreated LEC appear smooth and rounded.

Following plasma treatment, the LEC morphology varied greatly, but was highly dependent on the type and duration of treatment. Immediately after the treatment with the microplasma inside the medium, the affected single cell started shrinking and assumed poor morphology, indicated by a more apoptotic appearance with presence of apoptotic bodies and discernible nucleus. Weak membrane blebs appeared after 30 min, following the 30 s of plasma treatment applied on top of the medium for a twin cell system Fig 3. In comparison, the same morphological changes were observed also at plasma-treatment time of 30 s, after 30 min of incubation, when plasma was applied inside the medium (Fig 4). However, the cell membrane blebbing was also more apparent with prolonged incubation time (Fig 4; 2 h and 24 h), whereas in case the first case of Fig 3 almost no changes are observed in prolonged incubation. On the other hand, the non-treated control cells were unaffected and healthy during the entire incubation periods. These distinctive morphological changes were the simplest indicators of increase in cell death.

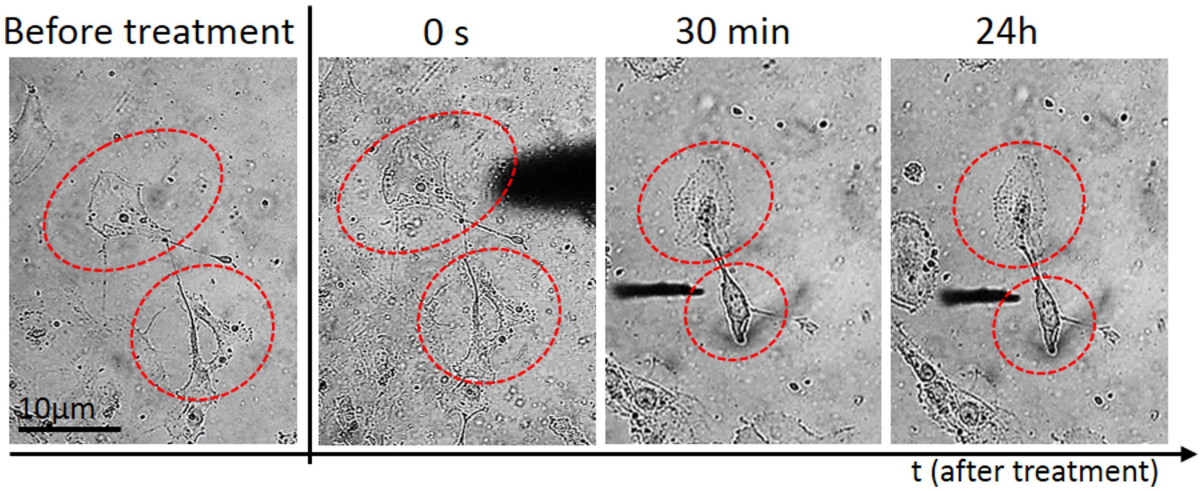

Fig 3. Real-time monitoring of morphological changes of aLC-LEC during indirect plasma treatment. A doublet of adherent LECs were selected and treated by the microplasma on top of the medium for 30 s. The monitored targeted cells in time after the treatment are labeled by the red dotted line.

doi:10.1371/journal.pone.0165883.g003

Typically, Fig 4 where a double-LEC system was present and following plasma treatment for 30 s inside the medium, the large difference in cell morphology appeared after 30 minutes, when compared to control untreated LECs: the cells were both shrunk and more rounded, with predominantly raised nuclear region. The stress bundles of actin filaments could also be seen, particularly around the cell edges and some rounded features corresponding to organelles as seen under the surface by light microscopy. Compared to the untreated LECs, damaged parts of the cell membrane and other cellular components could be observed. The cytoplasm of the cell seemed very rough and dense, which is another consequence of plasma treatment. More pronounced changes like cellular shrinking and alterations of the cytoplasmic structure could be observed on the LEC 3 h after plasma treatment. The targeted-cell treatment with microplasma exhibited multiple perforations on the membrane (which could not be noticed on the untreated cells) and loss of nuclear structures (e.g. nucleoli) (Fig 3). After longer incubation time (24 h following plasma treatment), the observed effects were similar to those after

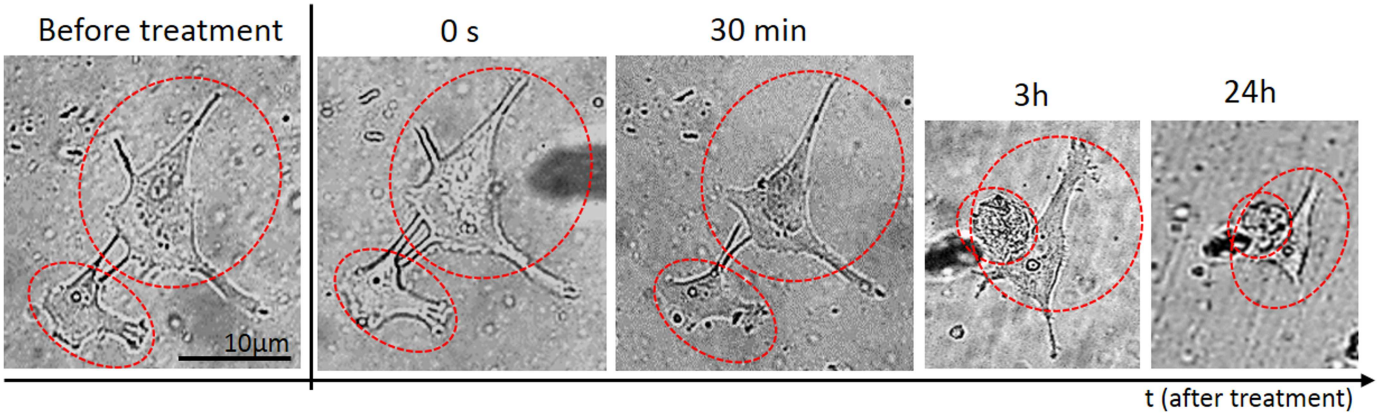

Fig 4. Real-time monitoring of morphological changes of aLC-LEC during direct plasma treatment. A doublet of adherent LECs were selected and treated by the microplasma directly inside the medium for 30 s. The monitored targeted cells in time after the treatment are labeled by the red dotted line.

doi:10.1371/journal.pone.0165883.g004

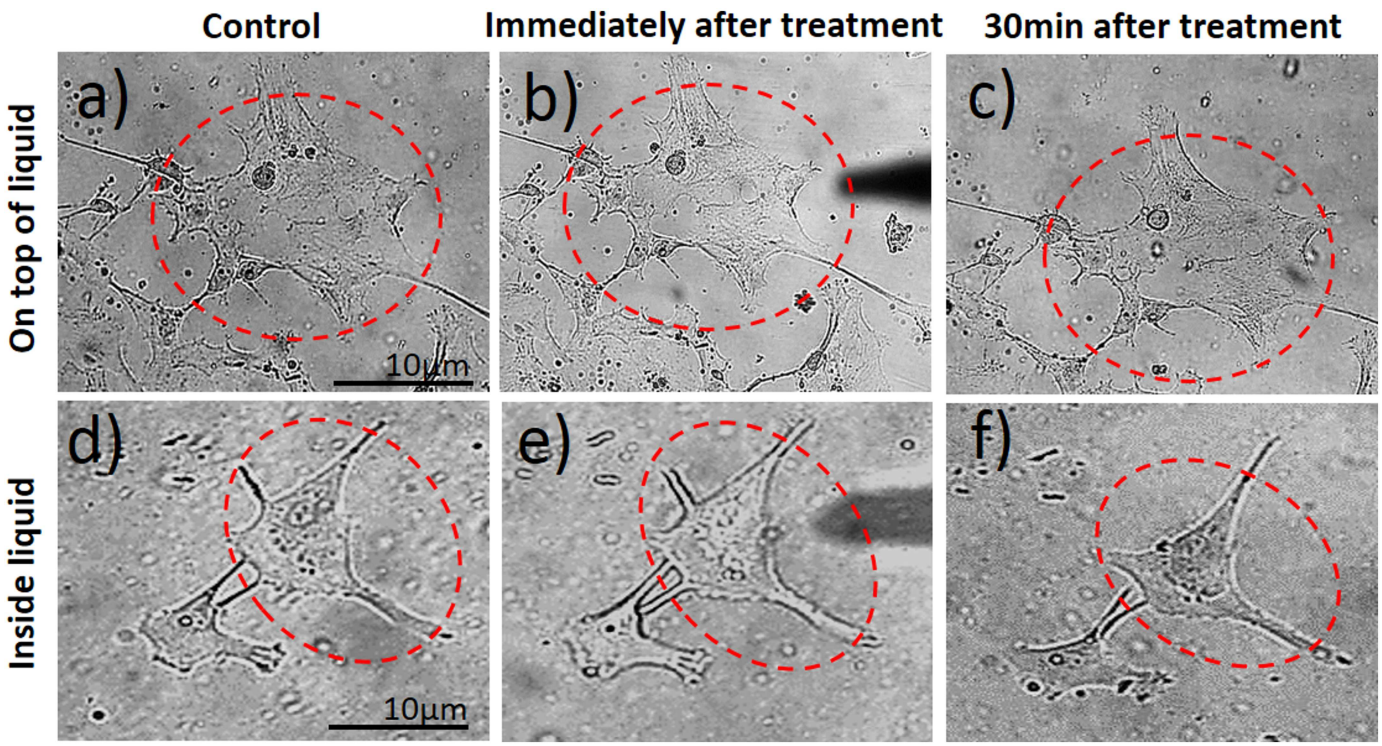

Fig 5. Comparison of the morphological changes evoked in a LEC. Indirectly and directly treated with plasma are being shown for the same plasma treatment time of 30 s.

doi:10.1371/journal.pone.0165883.g005

3 h, although the changes on cell shape, cytoplasmic and nuclear, were even more pronounced Fig 4.

If we compare the same treatment of randomly selected LEC using microplasma with the same microtip, but on top of the medium, delayed and sometimes varied results could be observed (Fig 5). Fig 5b and 5c show that the treated cell were not affected immediately after 30 s exposure to microplasma. The cells maintained healthy morphology after 30 min. The same treatment time of a doublet of cells inside the medium resulted in serious alteration of their morphology (Fig 5e and 5f). However, there are important differences of longer incubation time when compared to control untreated LEC (as observed with the shorter incubation treatment). Differences on the cell membrane could be observed after 30 s indirect plasma treatment of LECs. It is noteworthy that the membrane blebbing was observed 3 h after the plasma exposure (S1 Fig), which is another morphological change reminiscent of apoptosis, thus confirming the occurrence of cell death in the targeted treatment of cells after longer incubation time. Induction of apoptosis could be shown in the targeted LEC by the expression of Caspase 8 (marker of apoptosis) in a population of LECs which showed migrating (CXCR positive) properties (Fig 6). Since the nuclear changes occur relatively late in the process of apoptosis, no obvious difference could be seen even at 3 h after the microplasma treatment. However, 24 h after the plasma exposure, the nucleus of the treated cell became brighter or lense dense compared to the non-treated cell, while nuclear condensation could be observed in the treated cell (S1e Fig).

Cell morphological changes leading to apoptosis, especially after longer incubation time are probably results of changes done by ROS which create H_2O_2 as well as nitrites and nitrates

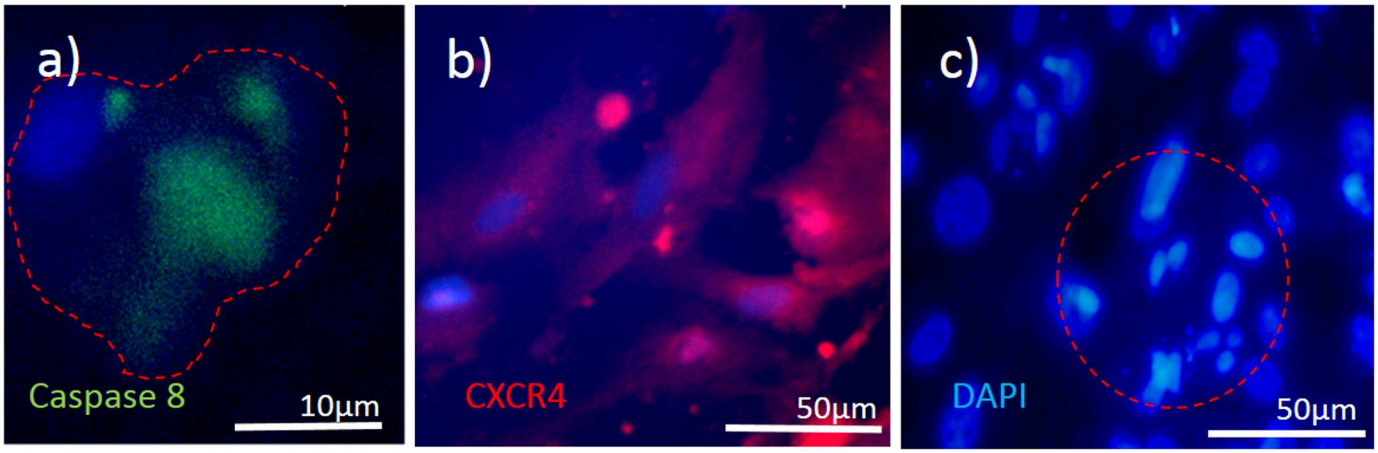

Fig 6. Cell death analysis and migration potential of the treated cells. 3 representative cases are being shown: a) immunostaining againt expression of Caspase 8 (an apoptosis marker), and b) CXCR4 (cell migration marker); c) DAPI stained cells (marker for DNA fragmentation) for assessment of cell death. The red-dotted line presents boundary of a single cell in a). while in c), it presents the treated area of impact with apoptotic bodies being formed.

doi:10.1371/journal.pone.0165883.g006

(Fig 7), which will be discussed later. These changes become more pronounced in longer exposure times of the liquid.

Influence of plasma on the liquid medium

The gaseous plasma which interacts with medium modifies its properties due its interaction with liquid surface interface (on top of the liquid), as well as surrounding environment by creation of vapors (inside the liquid). The products of these reactions are in our case peroxides and nitrites. The concentrations of H_2O_2 progressively increased after the plasma treatments of the liquid medium (Fig 7a). Concentrations obtained after 30 s, 60 s and 180 s of treatment were significantly higher compared to control. However, much different trend was observed when the media was treated on the surface: concentrations first showed increasing tendency, which was later followed by a drop in values. The highest H_2O_2 concentration was observed at 60 s plasma treatment performed in the liquid medium.

On the other hand, when the cell culture medium was treated in the liquid, no nitrites were detected after the exposure, since there was no interaction of plasma with surrounding air (Fig 7b). In contrast, the nitrate concentrations gradually increased with longer exposure times. Concentrations obtained after 60 s and 180 s were significantly higher compared to control. Interestingly, the pH level remained almost constant under all treatment modalities (around value 8).

Plasma versus mechanical effect of the gas flow

In order to make sure that the treatment is the result of ROS generated by the microplasma discharge in comparison to the He gas flow-related effects, a set of control experiments were performed only with He gas. Specifically, to elucidate the effects of the plasma exposure versus the mechanical related effects, the LECs were treated using the same tips as shown in Fig 1 for only mechanical stimulation of gas. Importantly, the single cell treated with He gas exhibited no morphological changes and underwent no apoptosis, when directly or indirectly treated with plasma (Fig 8). Therefore, it can be concluded that the observed apoptotic response in the cells is indeed likely related to the plasma-generated species rather than a mere mechanical effect of moving the fluid on attached cells and due to the gas flow.

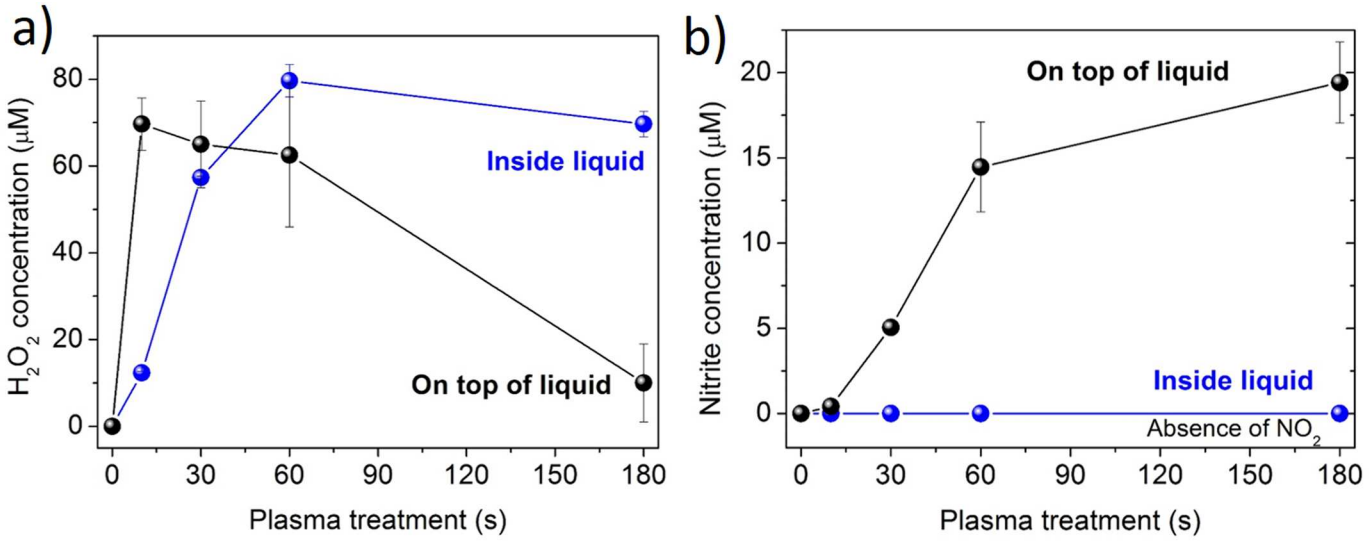

Fig 7. The initiated liquid chemistry with microplasma treatment on top or inside the liquid medium. a) Hydrogen peroxide and b) nitrite concentrations are being shown in respect to different treatment times.

doi:10.1371/journal.pone.0165883.g007

Effect of the plasma dose on targeted treatment of LECs

The results of plasma dose which is directly related to treatment time in respect to direct or indirect cell treatment are summarized in Fig 9. During direct treatments the cell effects were

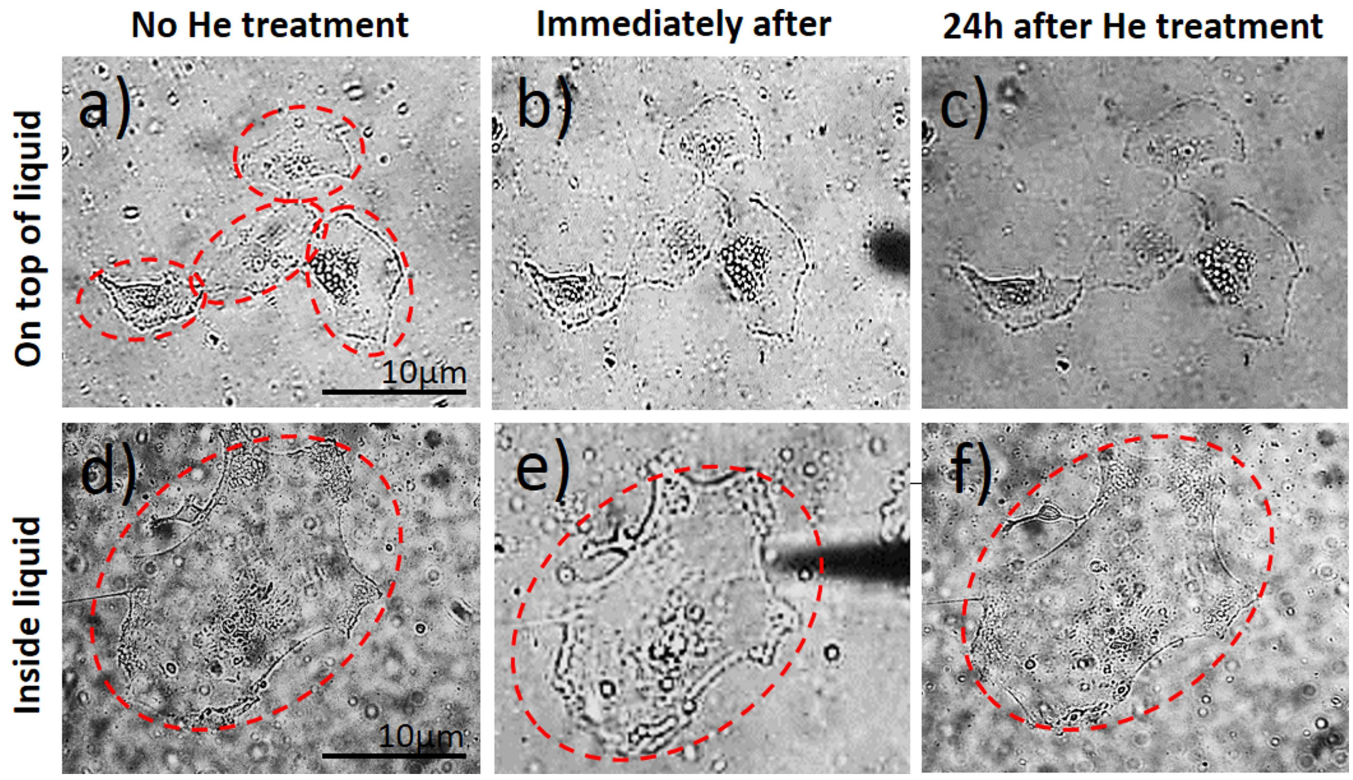

Fig 8. Effect of He gas flow on the cell morphological responses. Indirectly and directly treated with plasma are being shown.

doi:10.1371/journal.pone.0165883.g008

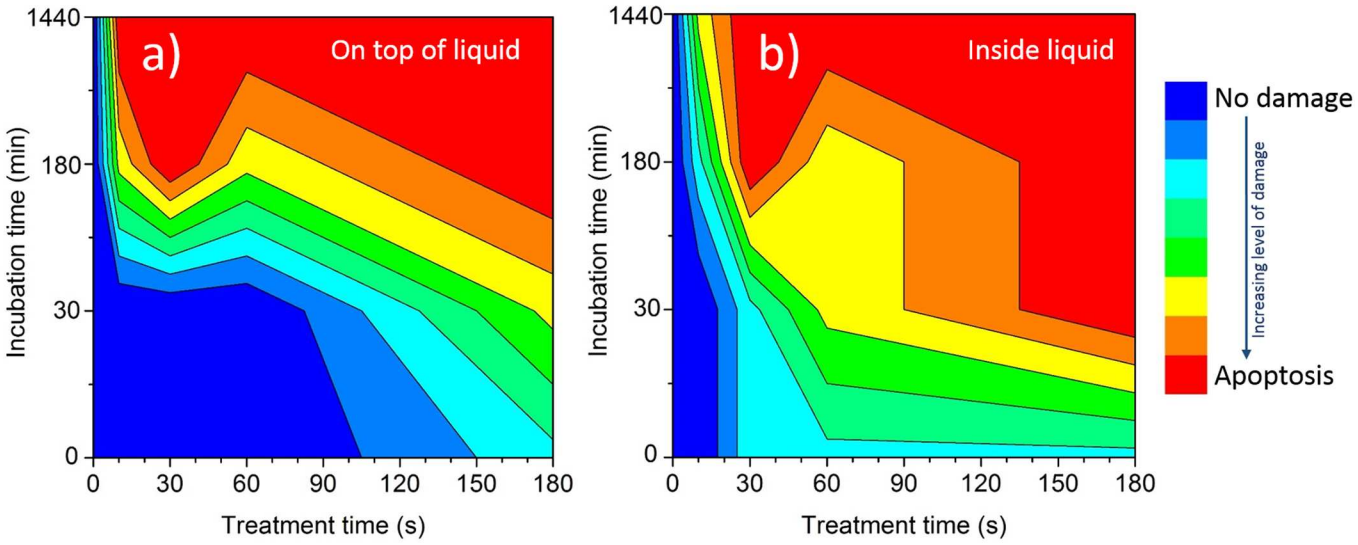

Fig 9. The morphological changes connected to the apoptosis induction in the cells in respect to microplasma treatment over a given time and consequent incubation of cells for a) indirect and b) direct treatments. The legend shows multiple potential apoptosis stages, which are highly likely for certain treatment after 24h, which are medium value of optical and fluorescent observation taking under consideration Gaussian distribution of results.

doi:10.1371/journal.pone.0165883.g009

quickly pronounced and lead to cell damage. However, in the case of indirect treatments the effects on cells are delayed and longer treatments are needed. The longer the plasma exposure, the stronger was the effect on the targeted-cell morphology, immediately after the treatment or later after incubation for 30 min or more. This trend was observed in both cases, when treatment was performed on top of liquid or inside the liquid medium. Moreover, when the targeted-cells were treated inside the medium, the effect of plasma on the treated cells was significantly stronger than when treated on top of the medium.

The results of systematic treatments of cells with the liquid interface, when on top of the liquid medium are shown in S1 and S2 Figs. As can be seen, microplasma induced the LEC to undergo apoptosis in a dose-dependent manner. The effect of plasma on LECs is only observed for incubation times above 3h under current experimental conditions (treatment times of 30 and 60 s).

When treatment was performed inside the medium (S3–S5 Figs) shorter treatment times were needed to observe morphological changes as compared to treatments on top of the medium. Interestingly, already at the short treatment times, the microplasma induced morphological changes in LEC immediately after the treatment.

Effects of plasma on the surrounding LECs

To clarify the effect of the microplasma exposure, the targeted-cells undergoing plasma treatment were compared to the surrounding cells. A well-defined boundary between plasma-treated cells and untreated cells could be observed. The most obvious case for this is seen in Fig 6c: the stained cells with DAPI and a marked region of apoptotic bodies after 30 s treatment inside the liquid can be seen, while the marked region is surrounded by untreated cells. Importantly, just the plasma-treated cells were induced to undergo cell death, while the neighbouring cells were not affected significantly. The effect of plasma on surrounding cells was slightly stronger when treatment was performed on top of the medium: this can clearly be seen from the 3 h long examinations. Although sometimes the surrounding cells were not strongly

affected, some cells in the close vicinity still changed their morphology. However, the major problem is always mixing of the liquid medium during the treatments or after. The mixing is driven by the blowing gas, which enables migration of newly created products from the plasma-liquid interaction. These products might significantly affect the cells after longer incubation times, but their role cannot be confined.

Other physical effects on cells

One of the most significant effects that may influence LECs is localized temperature generated by microplasma. For this reason, a sequence of experiments was performed, where the system was monitored by IR camera, when the microplasma was applied as a free jet plume in open air without any interaction with a surface, as well as the top or inside the liquid. The time series of images were taken for all measurements and most specific cases are presented in Fig 2a–2i. The results for free operating microplasma jet and microplasma on top of the liquid medium are similar: in both cases, following plasma ignition, the temperature of the tip increased to maximum 5˚C for 180 s operation. This is mostly a result of pure He plasma species interacting with the surrounding walls, which are simultaneously cooled by gas flow. The liquid medium temperature is almost constant during indirect microplasma treatment (Fig 2d–2f). On the contrary, the liquid was significantly heated during direct treatment inside the liquid (Fig 2g–2i). Here, the localized area was heated to almost 70˚C after prolonged operations, which probably occurred due to the created vapours when plasma is in contact with liquid. In cellular terms, this means that an already significant influence of temperature upon the cells could be generated, which can lead to their apoptosis.

An important factor that can sometimes influence the cell viability and physiological state is also UV radiation many times released from the plasma source. This should be taken under consideration. The generated microplasma in pure He has typical major emission lines in the range between 388 nm to 667 nm. However, in our case, we deliberately neglected this, especially in light of the temperature effect measured for inside liquid treatments, whereas on the top of the liquid, there is strong absorbing layer of organic fluid with proteins which we believe can reasonable well protect the cells based on UV-VIS measurements spectra of liquid. Another potential effect on the cells vitality can be also created by the electric field around the electrode tip. If electrode wire tip is considered to be a cylinder, then the calculated electric field at top of the electrode is ~$8{\cdot}10^2$ V/cm. However, to observe any apoptotic effects upon the cells from electroporation science point of view, a pulsed electric field above 10^3 V/cm would be needed. Taking into consideration that the nearest cells without liquid interface are at a distance of 2 to 3 mm from the tip, where the electric field falls with the distance, the field can then be taken as negligible to influence the cell vitality.

Discussion

The present study illustrates the interaction of μAPPJ targeted to the cell surface of *ex vivo* cultured aLC-LECs when treated by microplasma inside and on top of the culture medium. The effect of plasma on the cell morphology and cell death is therefore evaluated, as well as its effect on the surrounding cells and the mechanical effects of the gas flow. It is shown that plasma affects only a limited number of treated LECs, which morphology over time changes to apoptotic, while leaving the surrounding LECs unaffected. Furthermore, no mechanical effect of the gas flow on the cell morphology could be observed, which proved that the observed viability changes in the LECs were indeed generated by the ROS species induced by the plasma.

Based on the changes seen in the targeted-cell morphology following plasma treatment, it can be concluded that charged and reactive species produced in the plasma and coming in

direct contact with the treatment target, play a key role in the biological mechanisms, probably initiating and catalysing production of hydroxides, nitrites and nitrates, which might cause induction of apoptosis in later stages. The primary target of the direct plasma treatment is the cell membrane. Past the membrane, the plasma-related or physical mechanisms cease and the biochemical interactions seem to take place such as DNA damage and nuclear condensation. [10]

No change in the pH level is usually observed when plasma treated liquid medium contains a buffer [31], which was the case in our experiments, where the major part of the DMEM culture medium is composed of a phosphate buffered saline (PBS). The contact of plasma with the surrounding air plays a major role in the formation of nitrites, since no concentrations of them could be detected when the treatments were performed inside the liquid. Under such conditions, only H_2O_2 was formed, which is probably a result of the plasma interaction with the water molecules. On the other hand, the interaction between plasma and air results (on top of the liquid) in the formation of nitrogen and oxygen species which are later diluted in the liquid also as peroxides and nitrites. [31]

A careful investigation of the modified liquid and targeted cell changes revealed that most processes occur on the cell membrane, e.g. the phospholipid bilayer of the cell. The key processes occurring on the membrane are probably peroxidation of lipids and polysaccharides due to oxidative species and charges (OH^-, OOH, O_2^-, e^-). However, there are also effects of nitrites and nitrates, which are created in smaller quantities and only during indirect treatments. The effect is chemical and highly dependent on the amount of medium and on the chemical composition of the medium surrounding the cells. The bigger the volume of the medium, a weaker effect on the treated biological species is observed.[10] In our experiments, the volume of the treated medium was constant (~ 2.0 cm^3) for all performed treatments. The influence of medium and their modifications which surrounds the cells plays an important role, especially in later stages, where the much stronger effect of direct plasma treatment is observed on the targeted-cells due to the interaction of plasma helium species (He^* and He^+) with cells and created vapours from the surrounding liquid (O_2^-, H^-, OH^-, H_2O^-) and in comparison to indirect treatment. The treated medium interface may minimize the effect of the plasma due to dispersal of charged particles especially $(e^-)_{aq}$, $(OH^-)_{aq}$ or NO_2^-, NO_3^- as well as some reactive species inside the medium [32]. In this case, the role of plasma species created in bulk plasma or created vapours is reduced, and as result different chemical reactions take place in the liquid phase compared to gas phase. Additional difference between both conditions is also that, in indirect treatments, He bulk plasma interacts with ambient air and creates more nitrogen or nitrogen containing species, which might play important role in the structure or the created vapour or in the penetration into liquid media (Fig 1). Dispersal by the charged particles such as electrons and ions that are generated by the gas discharge, and initially formed near the electrode region, move to the nozzle of the tip and are finally discharged into the ambient air. While the generated plasma and neutral He gas passes through the narrow nozzle of the tip, the linear velocities of their flow abruptly increases with a decrease of the inner diameter of the tip. For this reason, the charged species are better spread into the liquid (by Henry's law) due to diffusion and turbulences occurring at the surface of the medium and due to their velocity difference at the boundary between the tip nozzle and the ambient air [33, 34]. This can make a difference in plasma treatments either influencing larger zone of plasma impact or in indirectly diminishing effects of plasma to targeted cells by dispersion of species through the entire liquid. On the other hand, the discharge created inside the liquid creates vapours which enable better energy-heat transfer and can significantly heat the several mm^2 zone and potentially damage larger number of cells. The temperatures are significant and increased to several tens of degrees Celsius. All these effects have to be considered in the

evaluation of plasma results and prolonged treatments, where H_2O_2, nitrites and nitrates are being generated.

In order to assess the differences in morphology and the effect of plasma treatment time, the morphological appearances of the adherent post-operatively cultured LECs were studied right after the treatment, or 30 min, 3 h and 24 h after plasma treatment. Microscopic images revealed important information on the shape and cell adhesion before and after plasma treatment with substantial differences being observed between the samples. Specific impact of the plasma on the treated cell shape and morphology after longer 3 h and 24 h of incubation could be shown, with cell morphology being significantly changed only after longer treatments, which also suggests limited effects of temperature during direct treatments. On the other hand, the results suggest that surrounding LECs remain unaffected. Furthermore, important differences between direct and indirect treatments could be observed—the plasma exposure time needed to reach observable morphological changes on targeted LECs was 6-times shorter under direct plasma treatment. These results show that differences between direct and indirect treatments are not only important for fast induction of apoptosis, but also suggest the important role the medium has on the viability of plasma treated LECs.

Under direct treatment of targeted LECs inside the medium, the plasma comes in direct contact with the cells and achieves the desired effect in orders of magnitude faster than indirect application, where plasma is separated from the treated target by the medium (plasma treatment of LECs performed on top of the medium). Likely, this effect can be primarily attributed to the bulk He plasma and created vapours along with time dependent heating. Thus, the key role in plasma–cell interaction is played probably by the ions or ionized molecules being generated and specifically, the positive and negative ions which have a relatively similar effect. The charged species being generated pose a chemical effect which is not related to the physical phenomena such as stress (mechanical stress induced by the moving fluid), ion bombardment damage, or thermal effects. Ions catalyze oxidation processes both inside and outside of the cell, which explains why they are able to have greater effect than neutral active species.[18]

In the work by Dobrynin *et al.* [10], the role of water in direct and indirect plasma inactivation of bacteria was studied. The first method was 'direct' application of plasma to bacteria, where the bacteria were used as a second active electrode—plasma was bound between the dielectric surface of the powered electrode and the surface of the bacteria being treated; the second method was 'indirect' application of plasma, where plasma was separated from the bacteria by a grounded metal mesh and gas was blown through the discharge to carry active species outside of the plasma. It was shown that direct application of plasma yields roughly a two orders of magnitude improvement in the rate of bacterial inactivation as compared to indirect application, even when the plasma is removed from the tissue by a fraction of a millimetre.[35] Similarly, we observed that plasma treatment inside the medium, achieved much stronger effect of the plasma on the treated LECs. Although prokaryotic and eukaryotic cells are very different regarding the cell structure and morphology, the effect of plasma treatment on both may be very similar.

A likely mechanism of plasma interaction with cell is through the membrane, as it is the primary cell barrier on its way of penetration. Different mechanism is also possible such as formation of small pores due to high local electric fields proposed by Joshi *et al.* [36, 37], which may lead to either cell leakage or a pathway for entrance of radicals into the cell. These pores, depending on their size, may re-close rapidly and the cell would appear intact under the microscope while the damage done may be permanent and lead to subsequent cell death. Another potential mechanism is through the use of the cell's own enzymes: ions present in the solution, especially ions introduced from plasma, may activate the secondary messenger system that

amplifies any external signal [38]. This way, plasma may be able to alter the behaviour of the cell by simply altering the ionic strength of the solution in the treated media [12, 39].

Interaction of plasma with DNA also should be taken into account. Arjunan *et al*. summarized the effects of APP on both isolated and cellular DNA [40], whereas O'Connell *et al*. reported on cold APPJ interactions with plasmid DNA. In the latter, the atomic oxygen density was correlated to the rates of single and double strand DNA breaks' formation [41]. Moreover, Lazović *et al*. compared the effects of plasma to gamma irradiation in terms of DNA damage [42]. Generally, peroxidation of phospholipid bilayer is also known to cause cellular death through a chain process leading to the formation of DNA adducts [43–45]. Interestingly, these defects in DNA are relatively easily repaired by mammalian cells [46]. Other important mechanism of plasma action on the cell is through formation of ROS directly in the vicinity of the DNA molecules inside the cell nucleus [47, 48]. The ROS of interest are hydroxide (OH^-), H_2O_2 and a superoxide anion (O_2^-). ROS are not generated at the vicinity of a DNA molecule, but are rather transported to it through a series of mechanisms already present in the cells. Hydroxyl radicals can react with nearby organic molecules, leading to chain oxidation and thus destruction of DNA as well as cellular membranes and other cell components [10]. Therefore, charges generated during plasma treatment may have an effect on bacteria and cells in solution due to the oxidation and peroxidation chain reactions they can catalyze; the same may be a reason for the difference in treatment times required to inactivate bacteria versus those needed to achieve cellular damage.

The true mechanism of atmospheric plasma on cells, especially when treated inside the medium, remains to be elucidated. However, the present study provides further data on the effect of cold plasma on a LEC viability by studying the cell morphology before and after plasma treatment inside and on top of the medium. Because of the extreme complexity in plasma-cell interaction, it is difficult to determine which mechanisms the cell uses to protect itself against stress (e.g. plasma treatment) and which signalling pathways are initiated inside the cell, although some implications for what is happening inside LECs after direct and indirect plasma treatment can be assumed. While the response of a single-cell treated inside the medium is significantly faster and more pronounced than that of a single-cell treated on top of the medium, we can speculate different initial signalling pathways get activated after plasma treatment under each condition.

The present data will serve to better define the complex interaction between cold plasma and the cell membrane surface and aid in the design of future experiments. To our knowledge, this is the first report of targeted cell treatment with microplasma inside a medium, which is more effective in inducing cell death when applied directly. A significantly shorter time is needed for a single-cell to undergo apoptosis and thus effective microplama single-cell therapy under such conditions. Moreover, plasma does not influence the large number of surrounding cells, which is of course beneficial and favourable for achieving highly localized-cell therapy.

Our results show that with a precision of a single cell level, plasma needle and plasma treatment can be used to selectively kill LECs that remain in the capsular bag after cataract surgery that can otherwise re-colonize the posterior lens capsule and create PCO, thus, obstruct the visual axis and contribute to light scattering and decreased visual acuity. Even more, our results suggest that μAPPJ application can achieve medically relevant therapeutic effects, which can potentially be applied in wide range of eye and other medical conditions.

Conclusions

Despite the small inner diameter and very low gas flow rate, a microplasma releasing device can induce apoptosis in LECs in a dose-dependent manner under both, direct and indirect

treatment conditions. The microplasma can be confined to the small (~3 μm) volume around the tip of the needle, which can be positioned in any specific area by using a micromanipulator. The power delivered to the cell is very small (1 W) yet sufficient to induce apoptosis, without affecting a large number of neighbouring cells, even within small clusters of closely contacting cells. A boundary region between plasma-treated and untreated cells could be observed on the order of cellular dimensions. We hereby demonstrate that inside the medium, the effect of microplasma on a treated targeted-cells is 6-times stronger than on top of the medium. Immediate morphological changes could be observed already after 30 s of direct treatment with microplasma, in comparison to indirect treatment, when immediate changes in morphology of the treated single-cell were observed only after longer treatment periods. These findings support the notion that direct treatment with microplasma inside the medium is more effective, as the treatment time needed for immediate response of a cell is significantly shortened. This variation allows the direct application of a microplasma jet device for precise use for single cell manipulation to selectively induce demise in LECs.

Although these results are potentially promising, many unanswered questions and gaps in understanding of cell-plasma interaction remain. The interaction mechanisms of microplasma inside and on top of the medium with the cells, and the potential reasons for the observed significant differences presented here, are an open question requiring deeper understanding before microplasma applications *in vivo* or for operative-therapeutic purposes. A logical step to follow in these targeted-cell plasma experiments may be to investigate the communication pathways and critical distances between the cells in different cluster configurations as a ground for testing collective tissue and cluster cell responses to plasma treatments.

Supporting Information

S1 Fig. Real-time monitoring of morphological changes at the cell level in LEC. A targeted adherent LECs were selected and treated by the microplasma *on top of the medium* for **30 s**. The monitored cell in time after treatment is labeled by the red dotted line.
(TIFF)

S2 Fig. Real-time monitoring of morphological changes at the cell level in LEC. A targeted adherent LECs were selected and treated by the microplasma *on top of the medium* for **60 s**. The monitored cell in time after treatment is labeled by the red dotted line.
(TIFF)

S3 Fig. Real-time monitoring of morphological changes at the cell level in LEC. A targeted adherent LECs were selected and treated by the microplasma *inside the medium* for **10 s**. The monitored cell in time after treatment is labeled by the red dotted line.
(TIFF)

S4 Fig. Real-time monitoring of morphological changes at the cell level in LEC. A targeted adherent LECs were selected and treated by the microplasma *inside the medium* for **60 s**. The monitored cell in time after treatment is labeled by the red dotted line.
(TIFF)

S5 Fig. Real-time monitoring of morphological changes at the cell level in LEC. A targeted adherent LECs were selected and treated by the microplasma *inside the medium* for **180 s**. The monitored cell in time after treatment is labeled by the red dotted line.
(TIFF)

Author Contributions

Conceptualization: SA UC.

Data curation: NR SA UC.

Formal analysis: NR NH GF GP.

Funding acquisition: MM MH UC.

Investigation: SA NH GF.

Methodology: SA UC GP.

Project administration: SA UC.

Resources: UC GP MH.

Supervision: SA MH AV MM UC.

Writing – original draft: NR SA.

Writing – review & editing: SA SL MM GP UC.

References

1. Hensel K, Kučerová K, Tarabová B, Janda M, Machala Z, Sano K, et al. Effects of air transient spark discharge and helium plasma jet on water, bacteria, cells, and biomolecules. Biointerphases. 2015; 10(2): 029515. http://dx.doi.org/10.1116/1.4919559. PMID: 25947389
2. Morfill GE, Kong MG, Zimmermann JL. Focus on plasma medicine. New J Phys. 2009; 11. doi: 10.1088/1367-2630/11/11/115011
3. Vandamme M, Robert E, Lerondel S, Sarron V, Ries D, Dozias S, et al. ROS implication in a new antitumor strategy based on non-thermal plasma. International journal of cancer Journal international du cancer. 2012; 130(9):2185–94. Epub 2011/06/28. doi: 10.1002/ijc.26252 PMID: 21702038.
4. Isbary G, Stolz W, Shimizu T, Monetti R, Bunk W, Schmidt HU, et al. Cold atmospheric argon plasma treatment may accelerate wound healing in chronic wounds: Results of an open retrospective randomized controlled study in vivo. Clinical Plasma Medicine. 2013; 1(2):25–30. http://dx.doi.org/10.1016/j.cpme.2013.06.001.
5. Lazović S, Puač N, Miletić M, Pavlica D, Jovanović M, Bugarski D, et al. The effect of a plasma needle on bacteria in planktonic samples and on peripheral blood mesenchymal stem cells. New J Phys. 2010; 12. doi: 10.1088/1367-2630/12/8/083037
6. Duncan G, Wang L, Neilson GJ, Wormstone IM. Lens cell survival after exposure to stress in the closed capsular bag. Investigative ophthalmology & visual science. 2007; 48(6):2701–7. Epub 2007/05/26. doi: 10.1167/iovs.06-1345 PMID: 17525202.
7. Andjelic S, Lumi X, Veréb Z, Josifovska N, Facskó A, Hawlina M, et al. A Simple Method for Establishing Adherent Ex Vivo Explant Cultures from Human Eye Pathologies for Use in Subsequent Calcium Imaging and Inflammatory Studies. Journal of Immunology Research. 2014; 2014. doi: 10.1155/2014/232659 PMID: 25276840
8. Andjelic S, Draslar K, Lumi X, Yan XH, Graw J, Facsko A, et al. Morphological and proliferative studies on ex vivo cultured human anterior lens epithelial cells—relevance to capsular opacification. Acta Ophthalmologica. 2015; 93(6):E499–E506. doi: 10.1111/aos.12655. WOS:000361797700012. PMID: 25631167
9. Andjelic S, Zupancic G, Perovsek D, Hawlina M. Human anterior lens capsule epithelial cells contraction. Acta Ophthalmol. 2011; 89(8):e645–53. Epub 2011/08/02. doi: 10.1111/j.1755-3768.2011.02199.x PMID: 21801334.
10. Dobrynin D, Fridman G, Friedman G, Fridman A. Physical and biological mechanisms of direct plasma interaction with living tissue. New J Phys. 2009; 11. doi: 10.1088/1367-2630/11/11/115020
11. Stoffels E, Sakiyama Y, Graves DB. Cold Atmospheric Plasma: Charged Species and Their Interactions With Cells and Tissues. Plasma Science, IEEE Transactions on. 2008; 36(4):1441–57. doi: 10.1109/TPS.2008.2001084

12. Fridman G, Shereshevsky A, Jost M, Brooks A, Fridman A, Gutsol A, et al. Floating Electrode Dielectric Barrier Discharge Plasma in Air Promoting Apoptotic Behavior in Melanoma Skin Cancer Cell Lines. Plasma Chemistry and Plasma Processing. 2007; 27(2):163–76. doi: 10.1007/s11090-007-9048-4

13. Kim CH, Bahn JH, Lee SH, Kim GY, Jun SI, Lee K, et al. Induction of cell growth arrest by atmospheric non-thermal plasma in colorectal cancer cells. Journal of Biotechnology. 2010; 150(4):530–8. doi: 10.1016/j.jbiotec.2010.10.003 PMID: 20959125

14. Kim GC, Lee HJ, Shon CH. The Effects of a Micro plasma on Melanoma (G361) Cancer Cells. J Korean Phys Soc. 2009; 54(2):628–32. WOS:000263371300012.

15. Kim JY, Kim S-O, Wei Y, Li J. A flexible cold microplasma jet using biocompatible dielectric tubes for cancer therapy. Applied Physics Letters. 2010; 96(20):-. http://dx.doi.org/10.1063/1.3431392.

16. Georgescu N, Lupu AR. Tumoral and Normal Cells Treatment With High-Voltage Pulsed Cold Atmospheric Plasma Jets. Plasma Science, IEEE Transactions on. 2010; 38(8):1949–55. doi: 10.1109/TPS.2010.2041075

17. Malović G, Puač N, Lazović S, Petrović Z. Mass analysis of an atmospheric pressure plasma needle discharge. Plasma Sources Science and Technology. 2010; 19(3). doi: 10.1088/0963-0252/19/3/034014

18. Miletić M, Mojsilović S, Okićorević I, Maletić D, Puač N, Lazović S, et al. Effects of non-thermal atmospheric plasma on human periodontal ligament mesenchymal stem cells. Journal of Physics D: Applied Physics. 2013; 46(34). doi: 10.1088/0022-3727/46/34/345401

19. Park BJ, Lee DH, Park JC, Lee IS, Lee KY, Hyun SO, et al. Sterilization using a microwave-induced argon plasma system at atmospheric pressure. Physics of Plasmas. 2003; 10(11):4539–44. doi: 10.1063/1.1613655

20. Tan X, Zhao S, Lei Q, Lu X, He G, Ostrikov K. Single-Cell-Precision Microplasma-Induced Cancer Cell Apoptosis. PLoS ONE. 2014; 9(6):e101299. doi: 10.1371/journal.pone.0101299. PMC4074162. PMID: 24971517

21. Ohkawa H, Akitsu T, Tsuji M, Kimura H, Kogoma M, Fukushima K. Pulse-modulated, high-frequency plasma sterilization at atmospheric-pressure. Surface and Coatings Technology. 2006; 200(20–21):5829–35. http://dx.doi.org/10.1016/j.surfcoat.2005.08.124.

22. Martines E, Zuin M, Cavazzana R, Gazza E, Serianni G, Spagnolo S, et al. A novel plasma source for sterilization of living tissues. New J Phys. 2009; 11. doi: 10.1088/1367-2630/11/11/115014

23. Selcuk M, Oksuz L, Basaran P. Decontamination of grains and legumes infected with Aspergillus spp. and Penicillum spp. by cold plasma treatment. Bioresource technology. 2008; 99(11):5104–9. Epub 2007/11/13. doi: 10.1016/j.biortech.2007.09.076 PMID: 17993274.

24. Liu F, Sun P, Bai N, Tian Y, Zhou H, Wei S, et al. Inactivation of Bacteria in an Aqueous Environment by a Direct-Current, Cold-Atmospheric-Pressure Air Plasma Microjet. Plasma Processes and Polymers. 2010; 7(3–4):231–6. doi: 10.1002/ppap.200900070

25. Scholtz V, Julák J, Kříha V. The Microbicidal Effect of Low-Temperature Plasma Generated by Corona Discharge: Comparison of Various Microorganisms on an Agar Surface or in Aqueous Suspension. Plasma Processes and Polymers. 2010; 7(3–4):237–43. doi: 10.1002/ppap.200900072

26. Takayama M, Ebihara K, Stryczewska H, Ikegami T, Gyoutoku Y, Kubo K, et al. Ozone generation by dielectric barrier discharge for soil sterilization. Thin Solid Films. 2006; 506–507(0):396–9. http://dx.doi.org/10.1016/j.tsf.2005.08.332.

27. Dobrynin D, Arjunan K, Fridman A, Friedman G, Clyne AM. Direct and controllable nitric oxide delivery into biological media and living cells by a pin-to-hole spark discharge (PHD) plasma. J Phys D-Appl Phys. 2011; 44(7). doi: 10.1088/0022-3727/44/7/075201. WOS:000286883800011.

28. Stoffels E, Kieft IE, Sladek REJ, Van Den Bedem LJM, Van Der Laan EP, Steinbuch M. Plasma needle for in vivo medical treatment: Recent developments and perspectives. Plasma Sources Science and Technology. 2006; 15(4):S169–S80. doi: 10.1088/0963-0252/15/4/s03

29. Zaplotnik R, Bišćan M, Kregar Z, Cvelbar U, Mozetič M, Milošević S. Influence of a sample surface on single electrode atmospheric plasma jet parameters. Spectrochimica Acta Part B: Atomic Spectroscopy. 103–104(0):124–30. http://dx.doi.org/10.1016/j.sab.2014.12.004.

30. Andjelic S, Draslar K, Hvala A, Lopic N, Strancar J, Hawlina M. Anterior lens epithelial cells attachment to the basal lamina. Acta Ophthalmologica. 2014; 92:0-. doi: 10.1111/j.1755-3768.2014.S078.x

31. Laurita R, Barbieri D, Gherardi M, Colombo V, Lukes P. Chemical analysis of reactive species and antimicrobial activity of water treated by nanosecond pulsed DBD air plasma. Clinical Plasma Medicine. 2015; 3(2):53–61. doi: 10.1016/j.cpme.2015.10.001

32. Rumbach P, Bartels DM, Sankaran RM, Go DB. The solvation of electrons by an atmospheric-pressure plasma. Nature communications. 2015; 6:7248. Epub 2015/06/20. doi: 10.1038/ncomms8248 PMID: 26088017; PubMed Central PMCID: PMCPMC4557361.

33. Hao PF, Ding YT, Yao ZH, He F, Zhu KQ. Size effect on gas flow in micro nozzles. Journal of Micromechanics and Microengineering. 2005; 15(11):2069–73. doi: 10.1088/0960-1317/15/11/011

34. Rossi C, Rouhani MD, Estève D. Prediction of the performance of a Si-micromachined microthruster by computing the subsonic gas flow inside the thruster. Sensors and Actuators, A: Physical. 2000; 87(1–2):96–104. doi: 10.1016/s0924-4247(00)00464-7

35. Fridman G, Brooks AD, Balasubramanian M, Fridman A, Gutsol A, Vasilets VN, et al. Comparison of Direct and Indirect Effects of Non-Thermal Atmospheric-Pressure Plasma on Bacteria. Plasma Processes and Polymers. 2007; 4(4):370–5. doi: 10.1002/ppap.200600217

36. Joshi RP, Nguyen A, Sridhara V, Hu Q, Nuccitelli R, Beebe SJ, et al. Simulations of intracellular calcium release dynamics in response to a high-intensity, ultrashort electric pulse. Physical Review E—Statistical, Nonlinear, and Soft Matter Physics. 2007; 75(4). doi: 10.1103/PhysRevE.75.041920 PMID: 17500934

37. Joshi RP, Sridhara V, Schoenbach KH. Microscopic calculations of local lipid membrane permittivities and diffusion coefficients for application to electroporation analyses. Biochemical and Biophysical Research Communications. 2006; 348(2):643–8. doi: 10.1016/j.bbrc.2006.07.144 PMID: 16890913

38. Mukai M, Maruo K, Kikuchi JI, Sasaki Y, Hiyama S, Moritani Y, et al. Propagation and amplification of molecular information using a photoresponsive molecular switch. Supramolecular Chemistry. 2009; 21(3–4):284–91. doi: 10.1080/10610270802468439

39. Kalghatgi SU, Fridman G, Cooper M, Nagaraj G, Peddinghaus M, Balasubramanian M, et al. Mechanism of blood coagulation by nonthermal atmospheric pressure dielectric barrier discharge plasma. IEEE Trans Plasma Sci. 2007; 35(5 II):1559–66. doi: 10.1109/tps.2007.905953

40. Arjunan K, Sharma V, Ptasinska S. Effects of Atmospheric Pressure Plasmas on Isolated and Cellular DNA—A Review. International Journal of Molecular Sciences. 2015; 16(2):2971. doi: 10.3390/ijms16022971 PMID: 25642755

41. O'Connell D, Cox LJ, Hyland WB, McMahon SJ, Reuter S, Graham WG, et al. Cold atmospheric pressure plasma jet interactions with plasmid DNA. Appl Phys Lett. 2011; 98(4). doi: 10.1063/1.3521502

42. Lazović S, Maletić D, Leskovac A, Filipović J, Puač N, Malović G, et al. Plasma induced DNA damage: Comparison with the effects of ionizing radiation. Applied Physics Letters. 2014; 105(12):124101. http://dx.doi.org/10.1063/1.4896626.

43. Li QT, Yeo MH, Tan BK. Lipid peroxidation in small and large phospholipid unilamellar vesicles induced by water-soluble free radical sources. Biochemical and Biophysical Research Communications. 2000; 273(1):72–6. doi: 10.1006/bbrc.2000.2908 PMID: 10873566

44. Ramanathan L, Das NP, Li QT. STUDIES ON LIPID OXIDATION IN FISH PHOSPHOLIPID LIPOSOMES. Biol Trace Elem Res. 1994; 40(1):59–70. doi: 10.1007/bf02916821. WOS: A1994MW32500007. PMID: 7511921

45. Qu B, Li QT, Wong KP, Ong CN, Halliwell B. Mitochondrial damage by the 'pro-oxidant' peroxisomal proliferator clofibrate. Free Radical Biology and Medicine. 1999; 27(9–10):1095–102. doi: 10.1016/s0891-5849(99)00143-4 PMID: 10569642

46. Marnett LJ. Lipid peroxidation—DNA damage by malondialdehyde. Mutation Research—Fundamental and Molecular Mechanisms of Mutagenesis. 1999; 424(1–2):83–95. doi: 10.1016/s0027-5107(99)00010-x PMID: 10064852

47. Wiseman H, Halliwell B. Damage to DNA by reactive oxygen and nitrogen species: Role in inflammatory disease and progression to cancer. Biochem J. 1996; 313(1):17–29.

48. Riley PA. Free radicals in biology: Oxidative stress and the effects of ionizing radiation. International Journal of Radiation Biology. 1994; 65(1):27–33. doi: 10.1080/09553009414550041 PMID: 7905906

Experimental and Toxicologic Pathology xxx (2016) xxx–xxx

Contents lists available at ScienceDirect

Experimental and Toxicologic Pathology

journal homepage: www.elsevier.de/etp

Full length article

Biological effects of bacterial pigment undecylprodigiosin on human blood cells treated with atmospheric gas plasma *in vitro*

Saša Lazović[a,*], Andreja Leskovac[b], Sandra Petrović[b], Lidija Senerovic[c], Nevena Krivokapić[b], Tatjana Mitrović[d,a], Nikola Božović[d,a], Vesna Vasić[b], Jasmina Nikodinovic-Runic[c]

[a] Institute of Physics Belgrade, University of Belgrade, Pregrevica 118, 11080 Belgrade, Serbia
[b] Department of Physical Chemistry, Vinča Institute of Nuclear Sciences, University of Belgrade, M. Petrovica Alasa 12-14, 11001 Belgrade, Serbia
[c] Institute of Molecular Genetics and Genetic Engineering, University of Belgrade, Vojvode Stepe 444a, P.O. Box 23, 11010 Belgrade, Serbia
[d] Institute for Development of Water Resources "Jaroslav Černi", Jaroslava Černog 80, 11226 Belgrade, Serbia

ARTICLE INFO

Article history:
Received 14 August 2016
Received in revised form 31 October 2016
Accepted 7 November 2016

Keywords:
Atmospheric pressure gas plasma
Genotoxicity
Free radicals
Undecylprodigiosin

ABSTRACT

It is known that some bacterial species are more resilient to different kinds of irradiation due to the naturally developed protective mechanisms and compounds such as pigments. On the other hand, reasoned tissue engineering using plasma remains a critical task and requires very precise control of plasma parameters in order to mitigate its potential detrimental effects. Here we isolated a natural protective agent, microbially produced undecylprodigiosin ((5′Z)-4′-methoxy-5′-[(5-undecyl-1H-pyrrol-2-yl)methylene]-1H,5′H-2,2′-bipyrrole), and investigated its effects on human blood cells independently and in combination with plasma. Two approaches were applied; the first, undecylprodigiosin (UP pigment) was added to the blood cultures, which then were exposed to plasma (pre-treatment); and the second- the blood cultures were exposed to plasma and then treated with pigment (post-treatment). The interactions of plasma and UP pigment with blood cells were investigated by conducting a series of biological tests providing the information regarding their genotoxicity, cytotoxicity and redox modulating activities. The exposure of cells to plasma induced oxidative stress as well as certain genotoxic and cytotoxic effects seen as elevated micronuclei incidence, decreased cell proliferation and enhanced apoptosis. In blood cultures treated with UP pigment alone, we found that both cytotoxic and protective effects could be induced depending on the concentration used. The highest UP pigment concentration increased lipid peroxidation and the incidence of micronuclei by more than 70% with maximal suppression of cell proliferation. On the contrary, we found that the lowest UP pigment concentration displayed protective effects. In combined treatments with plasma and UP pigment, we found that UP pigment could provide spatial shielding to plasma exposure. In the pre-treatment approach, the incidence of micronuclei was reduced by 35.52% compared to control while malondialdehyde level decreased by 36% indicating a significant mitigation of membrane damage induced by plasma. These results open perspectives for utilizing UP pigment for protection against overexposures in the field of plasma medicine.

1. Introduction

In everyday life, people are exposed to different agents, which can lead to biological modifications and in some cases irreparable damage. Damage can be characterized at different levels including cellular, molecular, biochemical, and genetic. The effects on human body are mostly cumulative and closely related to production of free radicals. Radicals can be biologically, chemically, and physically created (Valko et al., 2007). Typical physical agents, which create free radicals are different types of irradiation such as

Abbreviations: UP, undecylprodigiosin; CBMN, cytokinesis block micronucleus; BN, binucleated cells; MN, micronuclei; CBPI, cytokinesis-block proliferation index; TBA, thiobarbituric acid; AP, apoptosis; CAT, catalase.

* Corresponding author.
E-mail address: lazovic@ipb.ac.rs (S. Lazović).

http://dx.doi.org/10.1016/j.etp.2016.11.003
0940-2993/

UV, gamma or plasma irradiation (Halliwell and Gutteridge, 2007). Often irradiation of biological systems results in generation of highly reactive oxygen and nitrogen species (ROS, RNS). Consequently, radicals interact with cellular macromolecules such as membranes, DNA, RNA, and proteins causing their dysfunction, damage, and perturb the integrity and survival of cells (Moller and Wallin, 1998; Undeger et al., 2004).

Gas plasma is an efficient source of radicals. Electrical discharges may be generated at atmospheric pressure and used to treat samples that cannot tolerate vacuum, such as cells. Another important feature is that plasma can be produced in such a way that overheating of sensitive samples is avoided. Charged particles – electrons and ions, photons, metastable species and free radicals – are typical plasma constituents. Numerous chemical reactions may occur both in the gas phase and in interactions with surfaces. The literature refers to this type of plasma as atmospheric non-equilibrium or non-thermal plasma or as cold atmospheric plasma (Becker et al., 2004). Since the 1990s, an abundance of biomedical applications has been developed, utilizing the features mentioned above.

Biomedical applications of non-thermal plasma are gaining significant attention due to increasing number of diseases and problems that can be solved by direct therapies (Kong et al., 2009; Petrovic et al., 2012; von Woedtke et al., 2014). Some of the examples are Hailey-Hailey disease and wound treatments (Heinlin et al., 2011; Isbary et al., 2011; Nosenko et al., 2009). Atmospheric pressure plasma is known to abundantly create radicals while maintaining low temperature and is widely used for biomedical applications, such as sterilization (Hensel et al., 2015; Laroussi et al., 2003), blood coagulation (Kalghatgi et al., 2007), tooth bleaching (Lee et al., 2010), and cancer treatment (Cheng et al., 2014; Utsumi et al., 2013). However, the toxicity of plasma is still controversial, and it depends on dose and exposure time; low dose plasma is relatively non-toxic to the cells, but high dose induces apoptotic cell death (Kalghatgi et al., 2011). Low doses of ROS/RNS have been shown to promote cell survival, proliferation and migration, while excessive ROS levels leading to oxidative stress have been associated with cell senescence and the initiation of apoptosis (Arjunan et al., 2015a). Furthermore, atmospheric pressure plasma can even have selective effects – efficient killing of cancer cells without causing damage to surrounding healthy cells (Iseki et al., 2012; Tanaka et al., 2011).

Cellular antioxidative defense system that includes enzymic and nonenzymic antioxidants keeps the cellular redox homeostasis and reduces the level of damage through reduction of oxidative stress. However, there is a substantial interest in the use of natural products in an effort to prevent or reduce the oxidative damages induced by irradiation (Adaramoye et al., 2010; Sandeep and Nair, 2012). It is well known that some bacteria have developed compounds, usually pigments, for protection against irradiation (Abboud and Arment, 2013; Mohammadi et al., 2012). Undecylprodigiosin ((5′Z)-4′-methoxy-5′-[(5-undecyl-1H-pyrrol-2-yl) methylene]-1H,5′H-2,2′-bipyrrole) (UP) is a dark-red pyrrole-based pigment belonging to prodigiosin family of compounds (Furstner, 2003), which have been characterized to be antimicrobial, antimalarial, immunosuppressive and cytotoxic (Pandey et al.,

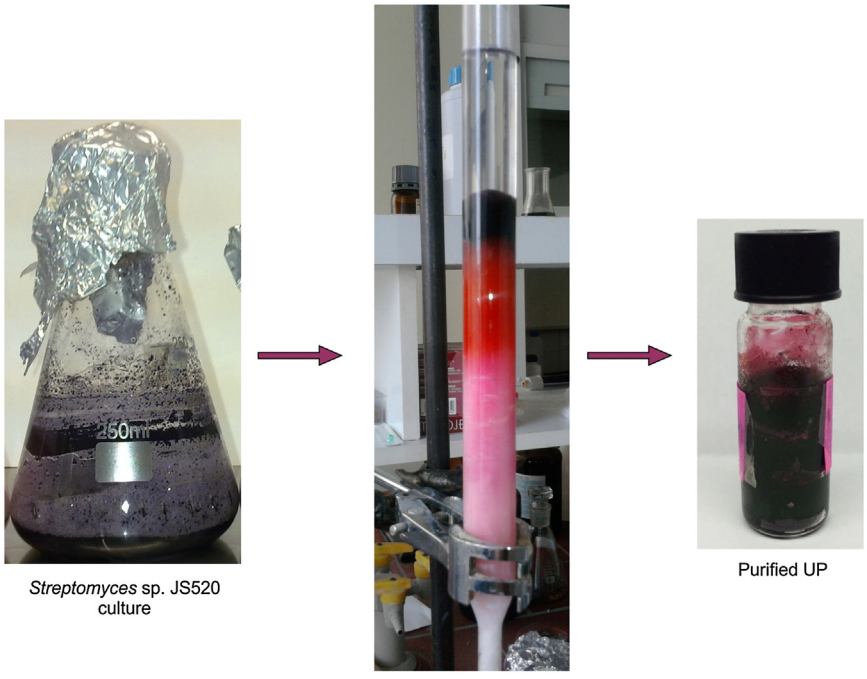

Fig. 1. UP pigment purification process and structural formula.

Please cite this article in press as: S. Lazović, et al., Biological effects of bacterial pigment undecylprodigiosin on human blood cells treated with atmospheric gas plasma *in vitro*, Exp Toxicol Pathol (2016), http://dx.doi.org/10.1016/j.etp.2016.11.003

2009; Perez-Tomas et al., 2003; Williamson et al., 2007). Although the role of undecylprodigiosin is not fully understood, recent studies showed its antimicrobial, UV protective and antioxidative activity (Stankovic et al., 2012). It has been reported that UP pigment inhibits neuronal cytotoxicity by mitochondrial function improvement, ROS production inhibition, and enhancement of antioxidant enzymes activities, thus providing protection against oxidative stress (Leirós et al., 2014).

In our previous work, we have used plasma needle for manipulating different types of stem cells as well as for bacteria and biofilm sterilization (Lazovic et al., 2010; Miletić et al., 2014; Puac et al., 2015). We have shown that plasma treatments can be optimized to sterilize bacteria (*E. coli* and *S. aureus* in planktonic samples) while keeping the stem cells (peripheral blood mesenchymal stem cells) which were used as a model of surrounding healthy tissue practically without significant damage (Lazovic et al., 2010). Several authors have investigated direct and indirect DNA damage induced by plasma treatments (Arjunan et al., 2015b; Lazovic et al., 2014; O'Connell et al., 2011). Arjunan et al. summarize the effects of atmospheric pressure plasmas on isolated and cellular DNA (Arjunan et al., 2015b). In order to determine the effective plasma irradiation doses we have compared the effects on DNA damage of primary human fibroblast cells with gamma irradiation (Lazovic et al., 2014). We found that plasma dose can be tuned to match a standard therapeutically dose for gamma irradiation of 2 Gy. However, even in this case it may be very useful to provide spatial selectivity to treatments by covering only sensitive sample sections by UP pigment obtained from bacteria, thereby physically blocking plasma generated species to reach the covered areas.

In this study, we have investigated the effects of UP pigment on human blood cells exposed to plasma irradiation. The interactions of plasma and UP pigment with blood cells were investigated by conducting a series of biological tests providing the information regarding their genotoxicity, cytotoxicity and redox modulating activities.

2. Materials and methods

2.1. Undecylprodigiosin (UP) pigment preparation

Undecylprodigiosin was synthesized in a shake flask culture of *Streptomyces* sp. JS520 using mannitol-soy-yeast medium supplemented with methyl-oleate (0.2%, v/v) for 6 days at 30 °C and recovered and purified by column chromatography. The process of pigment purification and its structural formula are presented in Fig. 1. The quality of the purified UP was analyzed by liquid chromatography coupled to mass spectroscopy (LC–MS) as described previously (Stankovic et al., 2012).

2.2. Plasma irradiation

Plasma needle operating at 25 kHz was used for all treatments. Detailed characterization of the plasma device is presented elsewhere (Zaplotnik et al., 2015). Furthermore, different authors investigated the influence of frequency on plasma properties, namely temperature and plasma range (Kim et al., 2011; Zaplotnik et al., 2014).

Blood samples were placed in tubes and exposed to plasma (Fig. 2). Argon was used as a feed gas (0.5 slm flow rate). Power supply operated at 25 kHz and provided 2.5 kV (root mean square value). The tip of the powered electrode was placed 5 mm above the surface of the samples. The exposure time for all treatments was 60 s. We distinguished two treatment setups: pre-treatment and post-treatment. In the pre-treatment, UP pigment was used to cover the blood cells before the plasma irradiation. UP pigment was physically blocking the direct exposure of the cells to plasma. We refer to this as to spatial shielding. Furthermore, by covering only certain areas of the plasma treated sample, we can limit the effect of plasma on underneath cells, while the full effect on uncovered areas is preserved (spatial selectivity). In the post-treatment, UP pigment was added upon plasma treatment.

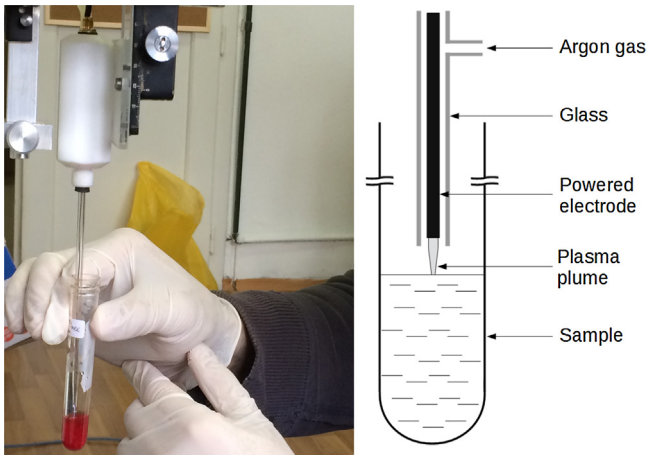

Fig. 2. Plasma treatments.

2.3. Blood sample preparation

Blood sample was obtained from healthy, non-smoking young male volunteer donor in accordance with current Health and Ethical regulations in Serbia. Aliquots of heparinized whole blood (0.5 ml) were added to culture tubes containing 4.5 ml of RPMI-1640 medium supplemented with 15% calf serum (Invitrogen-Gibco, Paisley, UK) and treated with increasing concentration of UP (final concentrations 0.1 μg/ml, 1 μg/ml and 5 μg/ml).

For pre- treatment, UP was added to lymphocyte cultures and incubated at 37° for 1 h. Cultures were subsequently exposed to plasma irradiation. After irradiation, UP was washed out by centrifugation and cultures were reconstituted by adding 4.5 ml of RPMI-1640 medium supplemented with 15% calf serum and 2% phytohemagglutinin, and were incubated at 37 ± 0.05 °C.

For post-treatment, lymphocyte cultures were set up in the absence of phytohemagglutinin and exposed to plasma irradiation. Immediately after irradiation, phytohemagglutinin and UP were added to cultures, which were incubated for 72 h. The untreated cultures served as control. The adequate number of lymphocyte cultures was established to enable examinations of malondialdehyde level, micronuclei, cell proliferation index and catalase activity, respectively. For apoptosis assay, blood aliquots of 0.5 ml were incubated in a RPMI-1640 medium (Invitrogen-Gibco, Paisley, UK) supplemented with 15% calf serum (Invitrogen-Gibco, Paisley, UK) for 24 h. All cultures were set up in triplicate.

2.3.1. Thiobarbituric acid (TBA) assay

After 72 h of incubation, blood cultures were separated on Lymphoprep; lymphocytes were collected by centrifugation, washed in physiological saline, and frozen at −20 °C. A thawed lymphocyte suspension was treated with thiobarbituric acid, and used to determine malondialdehyde levels, spectrophotometrically at 532 nm (Aruoma et al., 1989). Values are expressed as nmol TBA-reactive substance (MDA equivalent)/mg protein, using a standard curve of 1,1,3,3-tetramethoxypropane. Protein concentration was determined according to the method of Lowry et al. (Lowry et al., 1951).

Please cite this article in press as: S. Lazović, et al., Biological effects of bacterial pigment undecylprodigiosin on human blood cells treated with atmospheric gas plasma *in vitro*, Exp Toxicol Pathol (2016), http://dx.doi.org/10.1016/j.etp.2016.11.003

Table 1
Comparison between plasma treated and untreated cells. Results of MDA, MN, CAT, CBPI, and AP tests (mean ± SD).

	Level of malondialdehyde (nmol MDA/mg protein)	Incidence of micronuclei (MN/1000 BN cells)	Catalase activity (min^{-1} mg Hb^{-1})	Cell proliferation potential	Percentage of apoptotic cells
Control	2.95 ± 0.04	14.74 ± 1.04	1.14 ± 0.06	1.59 ± 0.01	5.00 ± 0
Plasma	7.27 ± 0.05	20.67 ± 1.06	1.31 ± 0.05	1.50 ± 0.01	19.95 ± 11.24

2.3.2. Micronucleus assay

For micronuclei preparation, the cytokinesis block micronucleus (CBMN) method of Fenech (Fenech, 1993) was used. Cytochalasin B (Sigma-Aldrich, St. Louis, MO, USA) at a final concentration of 4 μg/ml was added to each culture 44 h after incubation in order to inhibit cytokinesis. The lymphocyte cultures were incubated for a further 28 h. Cells were collected by centrifugation and treated with hypotonic solution (0.56% KCl + 0.90% NaCl, mixed in equal volumes) at 37 °C. Cell suspension was fixed in methanol/acetic acid (3:1), washed three times with fixative and dripped onto clean slides. Slides were air-dried and stained in alkaline Giemsa. For each sample, at least 1000 binucleated cells (BN) were scored and micronuclei were recorded using an Optech microscope (Munich, Germany) with 400× or 1000× magnification.

2.3.3. Cell proliferation index

A cytokinesis-block proliferation index (CBPI) was calculated according to method of Surrallés at al. (Surrallés et al., 1995) as follows: CBPI = MI + 2MII + 3(MIII + MIV)/N, where MI–MIV represent the number of cells with one to four nuclei, respectively, and N is the number of cells scored.

2.3.4. Assay of catalase activity

After 72 h of incubation, blood cultures were separated on Lymphoprep (Lymphocyte separation medium, PAA Laboratories GmbH, Pasching, Austria); erythrocytes were collected by centrifugation, washed in deionised water, and frozen at −20 °C. The catalase activity was measured using the method of Aebi (Aebi, 1974) with minor modifications by following the catalytic reduction of hydrogen peroxide. The decomposition of the substrate H_2O_2 was measured using a Perkin Elmer Lambda 25 Spectrophotometer (PerkinElmer Instruments, Norwalk, CT, USA) at 240 nm. The activity was expressed as K – rate constant of the first-order reaction per minute per mg of Hb (min^{-1} $mgHb^{-1}$). Hemoglobin concentration was determined by the Drabkin's method.

2.3.5. Apoptosis of leukocytes

After 24 h of incubation, cells were gently washed with physiological saline (0.9% NaCl) at 37 °C, and fixed in methanol: acetic acid (3:1). Afterwards, the pellet was fixed in 96% ethanol and stored at +4 °C. Samples were incubated at room temperature for 10–15 min in incubation phosphate buffer. Propidium iodide (PI, Sigma-Aldrich) and Ribonuclease A (RNase A, Sigma-Aldrich) were added 5 min prior to flow cytometric analysis.

Apoptosis was assessed by flow cytometric (Sysmex Partec, Germany) identification of cells displaying apoptosis-associated DNA condensation (Tung et al., 2007). DNA content was assessed by measuring the UV fluorescence of propidium iodide stained DNA. Apoptotic population was calculated using the Flow Max software (Sysmex Partec, Germany). Experiments were set up in triplicate. At least 10 000 cells per sample were analysed.

2.4. Statistics

A statistical analysis was carried out using the statistical software package Statistica 8 and OriginPro 8.5.1 for Microsoft Windows. Statistical analysis was done using the Student's *t* test and product-moment and partial correlations. *P* values less than 0.05 were considered to be significant.

3. Results

Results of the study are presented in order that accommodates the interpretation that the first plasma target is a cell membrane where the level of malondialdehyde (MDA), as an oxidative stress marker, provides information on the lipid peroxidation occurrence; micronuclei incidence (MN) on DNA damage; catalase activity (CAT) on cellular antioxidative potential; cytokinesis-block proliferation index (CBPI) on the ability of cells to divide; and percentage of apoptotic cells (AP) on percentage of cells undergoing apoptosis.

At first, we investigated the interaction of blood cells with plasma. Afterwards, we addressed the role of different concentrations of UP pigment in terms of toxicity and optimal protection. We conducted the two types of treatments. In the first approach, UP pigment was added to the blood cultures and then exposed to plasma irradiation (pre-treatment) while in the second approach, the blood cells were exposed to plasma irradiation and treated with UP pigment immediately after the exposure (post-treatment). We compared the results of these treatments.

3.1. The influence of plasma on blood cells

First, we investigated the influence of plasma alone on blood cells and compared its effects with untreated samples. The results of MDA, MN, CAT, CBPI, and AP tests are presented in Table 1.

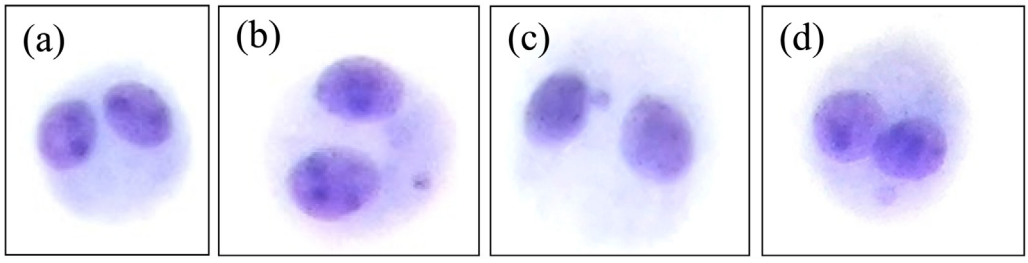

Fig. 3. Binucleated cells without (a) and with micronuclei (b–d).

Please cite this article in press as: S. Lazović, et al., Biological effects of bacterial pigment undecylprodigiosin on human blood cells treated with atmospheric gas plasma *in vitro*, Exp Toxicol Pathol (2016), http://dx.doi.org/10.1016/j.etp.2016.11.003

Table 2
Summary of the results of MDA, MN, CAT, CBPI, and AP tests (mean ± SD) for three UP pigment concentrations (0.1 μg/ml, 1 μg/ml, and 5 μg/ml).

	Level of malondialdehyde (nmol MDA/mg protein)	Incidence of micronuclei (MN/1000 BN cells)	Catalase activity (min^{-1} mg Hb^{-1})	Cell proliferation potential	Percentage of apoptotic cells
Control	2.95 ± 0.04	14.74 ± 1.04	1.14 ± 0.06	1.59 ± 0.01	5.00 ± 0
UP 0.1 μg/ml	4.32 ± 0.23	10.85 ± 1.16	2.61 ± 0.26	1.54 ± 0.02	17.70 ± 11.23
UP 1 μg/ml	7.07 ± 0.26	15.61 ± 0.59	2.02 ± 0.10	1.53 ± 0.01	21.83 ± 8.85
UP 5 μg/ml	10.44 ± 0.19	25.31 ± 1.25	1.25 ± 0.12	1.41 ± 0.01	10.15 ± 8.70

Results have shown that plasma irradiation significantly enhanced MDA level (from 2.95 to 7.27) compared to untreated control ($p < 0.05$). Besides induction of direct damage to the cell membrane, MDA, as the most mutagenic product of lipid peroxidation, can also induce DNA damages. The micronuclei incidence, as a measure of DNA damage, was significantly enhanced (40%) in plasma treated cells compared to control ($p < 0.05$). Thus, the increase of MN incidence represents a sum of two effects, a direct effect of irradiation on DNA and indirect-through MDA. Micrographs of untreated human peripheral blood lymphocytes and lymphocytes treated with UP and plasma are shown in Fig. 3. Cell antioxidative potential is measured by the activity of catalase (CAT). We found a slight increase of the activity (15%), which means that cells have preserved their capacities to defend against oxidative stress.

Measurement of cell proliferation potential (CBPI) is another validation of cell damage. Typically, the reduction of the proliferation potential can be interpreted as cell intention to postpone the cell division in order to gain time to repair the damage, or it can be a sign of cells undergoing apoptosis. Since proliferation potential of cells was significantly decreased ($p < 0.05$), it can be concluded that plasma affects a cell cycle by postponing the cell division. Disabled to repair the damage, the cells underwent apoptosis; the percentage of apoptotic cells increased four times (see Table 1).

3.2. The influence of UP pigment on blood cells

Prior to exposure to plasma, we used different quantities of UP bacterial pigment in order to determine its genotoxicity, cytotoxicity and redox modulating activities in human peripheral blood lymphocytes. The results are summarized in Table 2.

Analysis of MDA level has shown that UP pigment increased lipid peroxidation in all treated samples ($p < 0.01$) compared to control. Furthermore, *in vitro* genotoxic effects of UP pigment determined using the CB-micronuclei assay, have shown a concentration-dependent increase of the incidence of micronuclei. Treatment with UP demonstrated non-toxic effect at the lowest concentration applied (0.1 μg/ml); the incidence of micronuclei was reduced by 26.4%. On the contrary, a high *in vitro* genotoxicity against selected normal human lymphocytes was observed at the highest concentration applied (5 μg/ml); the incidence of micronuclei was enhanced by 71.73% ($p < 0.05$), relative to control. For the concentration of 1 μg/ml the results were similar to control. Considering the influence of UP on catalase activity, results have shown a significant enhancement of catalase activity in cultures treated with 0.1 μg/ml ($p < 0.01$) and 1 μg/ml ($p < 0.005$) of UP pigment. The level of malondialdehyde inversely correlated with a catalase activity of cells ($r = -0.99$, $p < 0.05$). In addition, concentration-dependent decrease of CBPI was observed in all samples treated with UP ($p < 0.01$). The maximal suppression of cell proliferation was observed at the highest UP concentration employed ($p < 0.005$). The percentage of apoptotic cells was increased at all concentrations of UP pigment compared to control. Although the rate of apoptosis at the highest concentration applied seems to be reduced, the high level of MDA and MN and a suppressed cell proliferation suggest that most of the cells are in the stage prior to apoptosis and that majority of them will eventually contribute to the total number of apoptotic cells in time.

3.3. Pre-treatment and post-treatment with UP pigment

Although UP pigment displayed cytotoxic effects in unirradiated cells, our results have shown its protective effects in cells

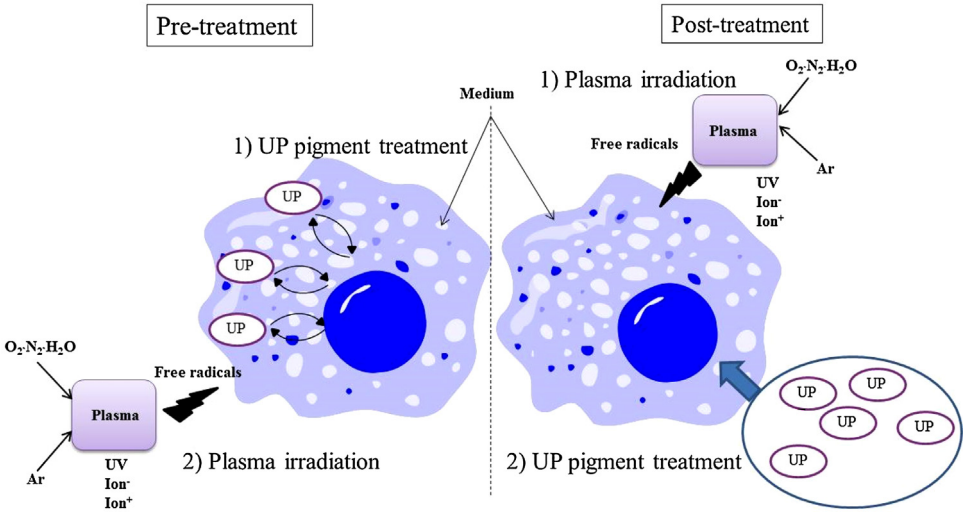

Fig. 4. Schematics of plasma-UP pigment-cells-medium interactions.

Please cite this article in press as: S. Lazović, et al., Biological effects of bacterial pigment undecylprodigiosin on human blood cells treated with atmospheric gas plasma *in vitro*, Exp Toxicol Pathol (2016), http://dx.doi.org/10.1016/j.etp.2016.11.003

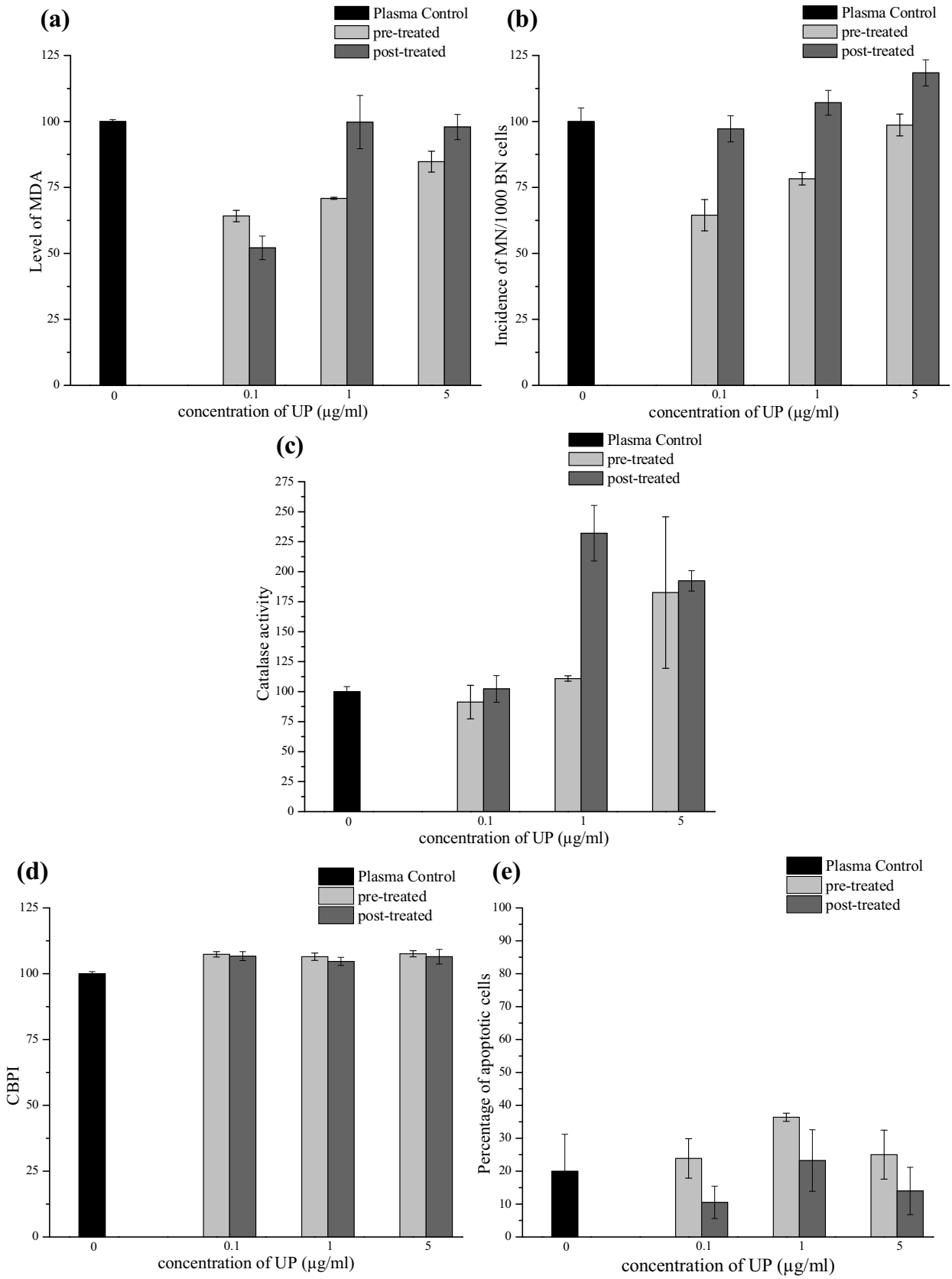

Fig. 5. (a) Level of malondialdehyde (MDA), (b) Incidence of micronuclei (MN), (c) Catalase activity (CAT), (d) Cell proliferation potential (CBPI), (e) Percentage of apoptotic cells (AP); pre-treated and post-treated samples. Results are expressed as mean ± SD.

Please cite this article in press as: S. Lazović, et al., Biological effects of bacterial pigment undecylprodigiosin on human blood cells treated with atmospheric gas plasma *in vitro*, Exp Toxicol Pathol (2016), http://dx.doi.org/10.1016/j.etp.2016.11.003

treated with plasma. As previously described, we investigated two different approaches of blood exposure to plasma and UP pigment (pre-treatment and post-treatment) (Fig. 4).

Results have shown that pre-treatment with UP pigment decreased lipid peroxidation at all concentrations employed ($p < 0.05$) compared to corresponding plasma irradiated cells (plasma-control) (Fig. 5). On the contrary, a post-treatment with UP pigment resulted in decrease ($p < 0.001$) of MDA level only at the lowest concentration applied. Moreover, a pre-treatment of lymphocytes with UP pigment followed by plasma irradiation induced a significant decrease of the micronuclei incidence at concentration 0.1 μg/ml ($p < 0.05$) and 1 μg/ml ($p < 0.05$), compared to plasma-control. The incidences of micronuclei were reduced by 35.52% and 21.70%, respectively. Results obtained for samples in which UP pigment was added after the plasma treatment (post-treatment) have shown no apparent difference in the micronuclei incidence compared to plasma-control except for the enhancement at the highest concentration applied ($p < 0.05$, 18.43%). The catalase activity in cultures pre-treated with UP pigment were increased ($p < 0.005$) only at higher applied concentrations, 1 μg/ml and 5 μg/ml, respectively. The similar results were obtained in cultures treated with UP pigment after the plasma treatment. Pre-treatment and post-treatment of lymphocytes with UP pigment did not significantly influence cell proliferation in all analysed samples compared to plasma-control. The percentage of apoptotic cells was significantly enhanced only at concentration 1 μg/ml of UP pigment in pre-treatment, and decreased at the lowest applied concentration in post-treatment. The proliferation potential of cells and the percentage of apoptotic cells correlated inversely ($r = -0.99$, $p < 0.05$).

Based on the results, we can conclude that the highest general protective effect was obtained in cell cultures treated with 0.1 μg/ml of UP pigment prior to plasma irradiation.

4. Discussion

In this paper, we present the results of plasma treatment of human blood cells, with and without the protection of UP pigment. UP pigment is isolated and utilized as a protective agent to plasma irradiation. Blood cells are exposed to atmospheric pressure plasma, UP pigment, and to both. MDA, MN, CAT, CBPI, and AP tests are used to characterize the levels of toxicity and damage to the cells. Although UP pigment displayed dose dependent cytotoxicity in unirradiated cells, our results have shown its protective effects in cells treated with plasma.

Cell membrane is known to protect the cell, among other functions. A level of damage introduced to the cell membrane by plasma is characterized by MDA, which is one of the products of lipid peroxidation of membrane. When transported to the vicinity of DNA, it can induce damage (Marnett, 2000). In all these processes ROS and RNS species play a major role (Marnett, 1999, 2002). Giving to the high reactivity, plasma creates active short and long lived neutral atoms and molecules, including ozone, NO, OH radicals, and singlet oxygen ($O_2{}^1\Delta_g$), and a significant flux of charged particles, including both electrons and positive and negative ions like super oxide radicals (Fridman, 2008). It is known that free radicals generated by plasma in low levels play an important role in vital physiological processes. Cells can be directly exposed to these species but can also be shielded by the UP pigment. Pigment itself interacts with irradiated cells and depending on the concentration displays more or less protective effects. Another scenario is that plasma modifies pigment and in that case, an open question is how plasma-modified pigment interacts with cells. Another important influence of plasma on cells can be indirect – through modification of medium containing cells. Reactive species can be deposited into the medium. The radical concentrations of hydroxyl (OH) and superoxide anion ($O_2^{\bullet}-$) in cell growth medium for different feed gas settings and plasma treatments can be measured by electron paramagnetic resonance (EPR) (Winter et al., 2014).

It is well known that atmospheric pressure plasmas for biomedical applications dominantly induce apoptosis rather than necrosis (Lazovic et al., 2014; Thiyagarajan et al., 2013). However, if the treatment parameters are not carefully adjusted, necrosis or unacceptably high levels of apoptosis can be reached which is often undesirable. Even in the case when parameters are carefully controlled it is useful to restrict the area of plasma exposure very precisely. UP pigment can be utilized on places that we want to cover from the plasma to reduce or completely avoid its effect. We found that exposure to high concentrations of UP pigment can lead to toxic effects similar to those induced by plasma. Indeed toxic effects have been demonstrated previously for UP on a variety of cell lines in doses above 5 μg/ml (Nikodinovic-Runic et al., 2014). On the other hand, if the concentration of pigment is properly adjusted the pigment has antioxidative and antigenotoxic effects and protects the cells from negative plasma effects, which is the outcome we observed in cell cultures pre-treated with UP pigment.

5. Conclusion

We conclude that plasma alone induces oxidative stress as well as certain genotoxic and cytotoxic effects seen as elevated micronuclei incidence, decreased cell proliferation and enhanced apoptosis. The pigment concentration of 0.1 μg/ml is found to give the best protection for our experimental conditions – we found that incidence of micronuclei was reduced by 35.52% compared to control. In addition, UP pigment mitigated plasma damage to the cell membrane that is confirmed by reduction of MDA level ranging from 15 to 36%. In conclusion, we found that better protection is achieved when samples are covered with UP pigment before the plasma exposure (pre-treatment) as compared to the post-treatment (adding UP pigment after the exposure).

This research opens the perspectives of utilizing natural protective agents in the field of plasma medicine for protection against overexposures. It also opens a question if UP or other pigments can be selective scavengers of ROS/RNS. In order to understand the complex cells-plasma-pigment interaction in liquid environment the plasma modification of UP pigment itself will be investigated in the light of eventual selective scavenging effects of short and long living radicals.

Conflict of interest

The authors declare that they have no conflict of interest.

Acknowledgments

This work has been supported by the Ministry of Education, Science and Technological Development of the Republic of Serbia (Project no. 172023, 173048, 171037, and III41011). Authors would like to acknowledge the support of Uroš Cvelbar (Jozef Stefan Institute, Slovenia) in development of the source of atmospheric pressure plasma. S.L. is grateful for the support from NATO SfP 984555 and would also like to acknowledge COST action TD1208 – Electrical discharges with liquids for future applications.

References

Abboud [4_TD$DIFF]AN, Arment A. The protective effects of the violacein pigment against UV-C irradiation in Chromobacterium violaceum. Ohio J. Sci. 2013;111 (2–5):28–32.

Adaramoye OA, Okiti OO, Farombi EO. Dried fruit extract from Xylopia aethiopica (Annonaceae) protects Wistar albino rats from adverse effects of whole body radiation. Exp. Toxicol. Pathol. 2010;63(7–8):635–43.
Aebi H. Catalase. In: Bergmeyer HU, editor. Methods of Enzymatic Analysis. Weinheim: Verlag Chemie; 1974.
Arjunan KP, Sharma VK, Ptasinska S. Effects of atmospheric pressure plasmas on isolated and cellular DNA-a review. Int. J. Mol. Sci. 2015a;16(2):2971–3016.
Arjunan KP, Sharma VK, Ptasinska S. Effects of atmospheric pressure plasmas on isolated and cellular DNA-a review. Int. J. Mol. Sci. 2015b;16(2):2971–3016.
Aruoma OI, Halliwell B, Laughton MJ, Quinlan GJ, Gutteridge JM. The mechanism of initiation of lipid peroxidation: evidence against a requirement for an iron(II)-iron(III) complex. Biochem. J. 1989;258(2):617–20.
Becker KH, Kogelschatz U, Schoenbach KH, Barker RJ. Non-Equilibrium Air Plasmas at Atmospheric Pressure. New York: Taylor & Francis; 2004.
Cheng X, Murphy W, Recek N, Yan D, Cvelbar U, Vesel A, Mozetič M, Canady J, Keidar M, Sherman JH. Synergistic effect of gold nanoparticles and cold plasma on glioblastoma cancer therapy. J. Phys. D: Appl. Phys. 2014;47(33):335402.
Fenech M. The cytokinesis-block micronucleus technique: a detailed description of the method and its application to genotoxicity studies in human populations. Mutat. Res. 1993;285(1):35–44.
Fridman A. Plasma Biology and Plasma Medicine, Plasma Chemistry. New York, NY: Cambridge University Press; 2008. p. 848–57.
Furstner A. Chemistry and biology of roseophilin and the prodigiosin alkaloids: a survey of the last 2500 years. Angew. Chem. Int. Ed. Engl. 2003;42(31):3582–603.
Halliwell B, Gutteridge J. Free Radicals in Biology and Medicine. 4 ed. Oxford, UK: Oxford University Press; 2007.
Heinlin J, Isbary G, Stolz W, Morfill G, Landthaler M, Shimizu T, Steffes B, Nosenko T, Zimmermann J, Karrer S. Plasma applications in medicine with a special focus on dermatology. J. Eur. Acad. Dermatol. Venereol. 2011;25(1):1–11.
Hensel K, Kucerova K, Tarabova B, Janda M, Machala Z, Sano K, Mihai CT, Ciorpac M, Gorgan LD, Jijie R, Pohoata V, Topala I. Effects of air transient spark discharge and helium plasma jet on water, bacteria, cells, and biomolecules. Biointerphases 2015;10(2):029515.
Isbary G, Morfill G, Zimmermann J, Shimizu T, Stolz W. Cold atmospheric plasma: a successful treatment of lesions in Hailey-Hailey disease. Arch. Dermatol. 2011;147(4):388–90.
Iseki S, Nakamura K, Hayashi M, Tanaka H, Kondo H, Kajiyama H, Kano H, Kikkawa F, Hori M. Selective killing of ovarian cancer cells through induction of apoptosis by nonequilibrium atmospheric pressure plasma. Appl. Phys. Lett. 2012;100(11):113702.
Kalghatgi S[6_TD$DIFF]U, et al. Mechanism of blood coagulation by nonthermal atmospheric pressure dielectric barrier discharge plasma. IEEE Trans. Plasma Sci. 2007;35(5):1559–66, doi:http://dx.doi.org/10.1109/TPS.2007.905953.
Kalghatgi S, Kelly CM, Cerchar E, Torabi B, Alekseev O, Fridman A, Friedman G, Azizkhan-Clifford J. Effects of non-thermal plasma on mammalian cells. PLoS One 2011;6(1):e16270.
Kim DB, Jung H, Gweon B, Moon SY, Rhee JK, Choe W. The driving frequency effects on the atmospheric pressure corona jet plasmas from low frequency to radio frequency. Phys. Plasmas 2011;18(4):043503.
Kong MG, Kroesen G, Morfill G, Nosenko T, Shimizu T, Dijk JV, Zimmermann JL. Plasma medicine: an introductory review. New J. Phys. 2009;11(11):115012.
Laroussi M, Mendis DA, Rosenberg M. Plasma interaction with microbes. New J. Phys. 2003;5(1):1–10.
Lazovic S, Puac N, Miletic M, Pavlica D, Jovanovic M, Bugarski D, Mojsilovic S, Maleti D, Malovic G, Milenkovic P, Petrovic ZL. The effect of a plasma needle on bacteria in planktonic samples and on peripheral blood mesenchymal stem cells. New J. Phys. 2010;12(8):083037.
Lazovic S, Maletic D, Leskovac A, Filipovic J, Puac N, Malovic G, Joksic G, Petrovic ZL. Plasma induced DNA damage: comparison with the effects of ionizing radiation. Appl. Phys. Lett. 2014;105(12):124101.
Lee HW, Nam SH, Mohamed A-AH, Kim GC, Lee JK. Atmospheric pressure plasma jet composed of three electrodes: application to tooth bleaching. Plasma Processes Polym. 2010;7(3–4):274–80.
Leirós M, Alonso E, Sanchez JA, Rateb ME, Ebel R, Houssen WE, Jaspars M, Alfonso A, Botana LM. Mitigation of ROS insults by Streptomyces secondary metabolites in primary cortical neurons. ACS Chem. Neurosci. 2014;5(1):71–80.
Lowry OH, Rosebrough NJ, Farr AL, Randall RJ. Protein measurement with the Folin phenol reagent. J. Biol. Chem. 1951;193(1):265–75.
Marnett LJ. Lipid peroxidation-DNA damage by malondialdehyde. Mutat. Res. 1999;424(1–2):83–95.
Marnett LJ. Oxyradicals and DNA damage. Carcinogenesis 2000;21(3):361–70.
Marnett LJ. Oxy radicals: lipid peroxidation and DNA damage. Toxicology 2002;181–182:219–22.
Miletić M, Vuković D, Živanović I, Dakić I, Soldatović I, Maletić D, Lazović S, Malović G, Petrović ZL, Puač N. Inhibition of methicillin resistant Staphylococcus aureus by a plasma needle. Cent. Eur. J. Phys. 2014;12(3):160–7.
Mohammadi M, Burbank L, Roper MC. Biological role of pigment production for the bacterial phytopathogen Pantoea stewartii subsp. stewartii. Appl. Environ. Microbiol. 2012;78(19):6859–65.
Moller P, Wallin H. Adduct formation, mutagenesis and nucleotide excision repair of DNA damage produced by reactive oxygen species and lipid peroxidation product. Mutat. Res. 1998;410(3):271–90.
Nikodinovic-Runic J, Mojic M, Kang Y, Maksimovic-Ivanic D, Mijatovic S, Vasiljevic B, Stamenkovic VR, Senerovic L. Undecylprodigiosin conjugated monodisperse gold nanoparticles efficiently cause apoptosis in colon cancer cells in vitro. J. Mater. Chem. B 2014;2(21):3271–81.
Nosenko T, Shimizu T, Morfill GE. Designing plasmas for chronic wound disinfection. New J. Phys. 2009;11(11):115013.
O'Connell D, Cox LJ, Hyland WB, McMahon SJ, Reuter S, Graham WG, Gans T, Currell FJ. Cold atmospheric pressure plasma jet interactions with plasmid DNA. Appl. Phys. Lett. 2011;98(4):043701.
Pandey R, Chander R, Sainis KB. Prodigiosins as anti cancer agents: living upto their name. Curr. Pharm. Des. 2009;15(7):732–41.
Perez-Tomas R, Montaner B, Llagostera E, Soto-Cerrato V. The prodigiosins, proapoptotic drugs with anticancer properties. Biochem. Pharmacol. 2003;66(8):1447–52.
Petrovic ZL, Puac N, Lazovic S, Maletic D, Spasic K, Malovic G. Biomedical applications and diagnostics of atmospheric pressure plasma. J. Phys.: Conf. Ser. 2012;356(1):012001.
Puac N, Miletic M, Mojovic M, PopovicBijelic A, Vukovic D, Milicic B, Maletic D, Lazovic S, Malovic G, Petrovic ZL. Sterilization of bacteria suspensions and identification of radicals deposited during plasma treatment. Open Chem. 2015;13(1):332–8.
Sandeep D, Nair CK. Protection from lethal and sub-lethal whole body exposures of mice to gamma-radiation by Acorus calamus L.: studies on tissue antioxidant status and cellular DNA damage. Exp. Toxicol. Pathol. 2012;64(1–2):57–64.
Stankovic N, Radulovic V, Petkovic M, Vuckovic I, Jadranin M, Vasiljevic B, Nikodinovic-Runic J. Streptomyces sp. JS520 produces exceptionally high quantities of undecylprodigiosin with antibacterial, antioxidative, and UV-protective properties. Appl. Microbiol. Biotechnol. 2012;96(5):1217–31.
Surrallés J, Xamena N, Creus A, Catalan J, Norppa H, Marcos R. Induction of micronuclei by five pyrethroid insecticides in whole-blood and isolated human lymphocyte cultures. Mutat. Res. 1995;341(3):169–84.
Tanaka H, Mizuno M, Ishikawa K, Nakamura K, Kajiyama H, Kano H, Kikkawa F, Hori M. Plasma-activated medium selectively kills glioblastoma brain tumor cells by down-regulating a survival signaling molecule. AKT Kinase 2011;1(3–4):265–77.
Thiyagarajan M, Gonzales XF, Anderson H. Regulated cellular exposure to non-thermal plasma allows preferentially directed apoptosis in acute monocytic leukemia cells. Stud. Health Technol. Inf. 2013;184:436–42.
Tung JW, Heydari K, Tirouvanziam R, Sahaf B, Parks DR, Herzenberg LA. Modern flow cytometry: a practical approach. Clin. Lab. Med. 2007;27(3)453–68 (v).
Undeger U, Giray B, Zorlu AF, Oge K, Bacaran N. Protective effects of melatonin on the ionizing radiation induced DNA damage in the rat brain. Exp. Toxicol. Pathol. 2004;55(5):379–84.
Utsumi F, Kajiyama H, Nakamura K, Tanaka H, Mizuno M, Ishikawa K, Kondo H, Kano H, Hori M, Kikkawa F. Effect of indirect nonequilibrium atmospheric pressure plasma on anti-proliferative activity against chronic chemo-resistant ovarian cancer cells in vitro and in vivo. PLoS One 2013;8(12):e81576.
von Woedtke T, Metelmann HR, Weltmann KD. Clinical plasma medicine: state and perspectives of in vivo application of cold atmospheric plasma. Contrib. Plasma Phys. 2014;54(2):104–17.
Valko M, Leibfritz D, Moncol J, Cronin MT, Mazur M, Telser J. Free radicals and antioxidants in normal physiological functions and human disease. Int. J. Biochem. Cell Biol. 2007;39(1):44–84.
Williamson NR, Fineran PC, Gristwood T, Chawrai SR, Leeper FJ, Salmond GP. Anticancer and immunosuppressive properties of bacterial prodiginines. Future Microbiol. 2007;2(6):605–18.
Winter J, Tresp H, Hammer MU, Iseni S, Kupsch S, Schmidt-Bleker A, Wende K, Dunnbier M, Masur K, Weltmann KD, Reuter S. Tracking plasma generated H2O2 from gas into liquid phase and revealing its dominant impact on human skin cells. J. Phys. D: Appl. Phys. 2014;47(28):285401.
Zaplotnik R, Kregar Z, Bišćan M, Vesel A, Cvelbar U, Mozetič M, Milošević S. Multiple vs. single harmonics AC-driven atmospheric plasma jet. EPL (Europhys. Lett.) 2014;106(2):25001.
Zaplotnik R, Bišćan M, Kregar Z, Cvelbar U, Mozetič M, Milošević S. Influence of a sample surface on single electrode atmospheric plasma jet parameters. Spectrochim. Acta Part B: At. Spectrosc. 2015;103–104:124–30.

Please cite this article in press as: S. Lazović, et al., Biological effects of bacterial pigment undecylprodigiosin on human blood cells treated with atmospheric gas plasma *in vitro*, Exp Toxicol Pathol (2016), http://dx.doi.org/10.1016/j.etp.2016.11.003

Original article DOI: 10.1515/aiht-2017-68-2897

The impact of concentration and administration time on the radiomodulating properties of undecylprodigiosin *in vitro*

Sandra Petrović[1], Vesna Vasić[1], Tatjana Mitrović[3], Saša Lazović[2], and Andreja Leskovac[1]

Vinča Institute of Nuclear Sciences[1], Institute of Physics Belgrade[2], University of Belgrade, Institute for Development of Water Resources "Jaroslav Černi"[3], Belgrade, Serbia

[Received in October 2016; Similarity Check in October 2016; Accepted in January 2017]

Undecylprodigiosin pigment (UPP) is reported to display cytotoxic activity towards various types of tumours. Nevertheless, its efficacy in modifying the cellular response to ionising radiation is still unknown. In this study, the radiomodulating effects of UPP were investigated. The effects of UPP were assessed *in vitro* by treating cultures of human peripheral blood with UPP and ionising radiation using two treatment regimens, the UPP pre-irradiation treatment and UPP post-irradiation treatment. The activity of UPP was investigated evaluating its effects on the radiation-induced micronuclei formation, cell proliferation, and induction of apoptosis. The redox modulating effects of UPP were examined measuring the catalase activity and the level of malondialdehyde, as a measure of oxidative stress. The results showed that UPP effects on cellular response to ionising radiation depend on its concentration and the timing of its administration. At low concentration, the UPP displayed radioprotective effects in γ-irradiated human lymphocytes while at higher concentrations, it acted as a radiosensitiser enhancing either mitotic catastrophe or apoptosis depending on the treatment regimen. The UPP modified redox processes in cells, particularly when it was employed prior to γ-irradiation. Our data highlight the importance of further research of the potential of UPP to sensitize tumour cells to radiation therapy by inhibiting pathways that lead to treatment resistance.

KEY WORDS: *apoptosis; mitotic catastrophe; oxidative stress; radiosensitisation; undecylprodigiosin*

The main therapeutic modalities to treat cancer are surgery, radiotherapy, and chemotherapy. Radiotherapy is one of the most effective forms of cancer treatment. However, ionising radiation (IR) used for the elimination of malignant tumours induces persistent DNA double-strand breaks (DSBs) leading to the permanent cell growth arrest, apoptosis, necrosis, or mitotic catastrophe (1). The major difficulties encountered during the treatment of cancer are tumour resistance to therapy and therapy-associated normal tissue toxicity (2). Alternative approaches to enhancing the efficacy of radiotherapy and minimising its harmful side effects focus on a combined treatment with anticancer drug and radiation (2). The potential radiotherapeutic agents are commonly categorised as (i) radioprotectors, which reduce normal tissue toxicity, thus, minimising the side effects of radiotherapy, and (ii) radiosensitisers, which enhance the radiosensitivity of tumour cells, thereby minimising the radiation dosage and damage to surrounding normal tissues (3, 4). Radiosensitisation of tumour cells by different agents is mainly achieved by enhancement of radiation-induced DNA damage in tumour cells compared to surrounding tissues, inhibition of DNA synthesis and cell growth, and enhancement of radiation-induced apoptosis (2, 5). Another approach is to modulate reduction/oxidation reactions within tumour cells (4).

In the last few decades, a wide variety of naturally occurring compounds have been tested in order to identify effective radiosensitisers that could enhance the sensitivity of cancer to the effects of IR and improve the cancer patients' survival rate (6-8). Plant-derived anticancer drugs continue to play a significant role in the development of new therapeutics aimed at modifying the radiobiological response of cells. Plant compounds such as etoposide, pactitaxel, and *Vinca* alkaloids have been recognised as radiosensitisers with low toxicity and high effectiveness whose synergism with radiation therapy increases the likelihood of cancer treatments (9). However, besides plants, microorganisms represent a profuse source of diverse bioactive metabolites with anticancer and possible radiomodulating activities.

Prodigiosins (PGs), produced as secondary metabolites by many terrestrial and marine bacterial strains such as the species of *Serratia* (10) and *Streptomyces* (11, 12), are a family of natural red pigments that are reported to possess antimicrobial, immunosuppressive, and cytotoxic activities (13-15). It has been reported that PGs mainly target cancer cells (hematopoietic, gastrointestinal, breast, and lung

Correspondence to: Dr Andreja Leskovac, Vinča Institute of Nuclear Sciences, University of Belgrade, M. Petrovića Alasa 12-14, 11001 Belgrade, Serbia, e-mail: *andreja@vinca.rs*

cancer) with little or no effects on normal cells (16-18). Numerous studies indicated that PGs displayed selective cytotoxicity against cancer cells, anti-metastatic activity, and p53-independent proapoptotic effects, which points to their potency as anticancer agents (16, 19).

Recent studies put a PG family member, undecylprodigiosin pigment (UPP), in the focus of anticancer investigation based on its proapoptotic potency demonstrated in various types of tumours (20-23). It has been suggested that UPP inhibits cell proliferation by inducing G2/M phase arrest and apoptosis of cancer cells. The tumoricidal action of UPP alone and UPP conjugated to gold nanoparticles was observed in melanoma, lung, breast, and colon cancer cells, enabling the platform for further development of efficient anticancer drugs suitable for clinical application (22). On the other side, it has been shown that UPP provides protection against oxidative stress by delaying the lipid peroxidation process (24) and displaying the antioxidant properties and mitochondrial function improvement (25). Similar findings were obtained in our previous investigation showing that treatment of human lymphocytes with low UPP concentrations (0.1 μg mL^{-1}) significantly reduced DNA damages and maintained the redox homeostasis of cells, indicating its cytoprotective nature. At moderate concentrations (1 μg mL^{-1}), UPP displayed effects similar to that of the untreated control, while the highest applied concentration (5 μg mL^{-1}) was genotoxic (unpublished data). The protective effects of UPP against UV irradiation were described previously (26).

As far as we know, the effect of UPP as a modifier of cellular response to ionising radiation is still unknown. Therefore, in this study, we investigated potential radioprotective/radiosensitising effects of UPP in γ-irradiated human peripheral blood cells using different combined treatment regimens with UPP and IR. The influence of UPP on radiation-induced apoptosis, micronuclei (MNi) induction, and oxidative stress alterations was investigated.

MATERIALS AND METHODS

Undecylprodigiosin pigment (UPP) preparation

Undecylprodigiosin (UP) pigment was synthesised in a shake flask culture of *Streptomyces* sp. JS520 using mannitol-soy-yeast medium supplemented with methyl-oleate (0.2 %, v/v) for six days at 30 °C and recovered and purified by column chromatography. The quality of the purified UP was analysed by liquid chromatography coupled to mass spectroscopy (LC-MS) as described previously (24).

Cell cultures and treatments

Blood sample was obtained from a healthy, non-smoking, 30-year-old male volunteer donor in accordance with current Health and Ethical Regulations in Serbia (27). Aliquots of heparinised whole blood (0.5 mL) were first added to culture tubes containing 4.5 mL of RPMI-1640 medium supplemented with 15 % calf serum (Invitrogen-Gibco, Paisley, UK) and were then treated with an increasing concentration of UPP (final concentrations 0.1 μg mL^{-1}, 1 μg mL^{-1}, and 5 μg mL^{-1}).

The UPP effects were studied employing the experimental set up used in the study of Shukla et al. (28). For each UPP concentration, two treatment regimens were applied: pre-treatment - UPP was added to cell cultures and then exposed to γ-irradiation, and post-treatment - cell cultures were treated with γ-irradiation and then exposed to UPP treatment. γ-irradiated cultures not treated with UPP served as control.

For pre-treatment, UPP was added to cell cultures and incubated at 37 °C for one hour. Cultures were subsequently exposed to 2 Gy of ^{60}Co γ-radiation, at a dose rate of 0.45 Gy min^{-1}. After irradiation, UPP was washed off by centrifugation and cultures were reconstituted by adding 4.5 mL of RPMI-1640 medium supplemented with 15 % calf serum and 2 % phytohemagglutinin (Invitrogen-Gibco, Paisley, UK). They were then incubated at 37 °C for 72 h.

For post-treatment, cell cultures were exposed to γ-irradiation as described above. Immediately after irradiation, phytohemagglutinin and UPP were added to the cultures, which were then incubated for 72 h.

The adequate number of blood cultures was established to enable examinations of the MNi frequency, cytokinesis-block proliferation index (CBPI), catalase activity (CAT), and malondialdehyde (MDA) level.

For the apoptosis (AP) assay, blood aliquots of 0.5 mL were incubated in a RPMI-1640 medium (Invitrogen-Gibco, Paisley, UK) supplemented with 15 % calf serum (Invitrogen-Gibco, Paisley, UK) for 24 h. The treatments with UPP and γ-irradiation were performed as described above.

For each analysis performed, three independent experiments were carried out. The obtained data were pooled and results were expressed as the mean and standard deviation (SD) of the mean.

Micronucleus assay

Radiosensitivity was assessed using the cytokinesis block method of Fenech (29). For MN preparation, Cytochalasin B (Sigma-Aldrich, St. Louis, MO, USA) at a final concentration of 4 μg mL^{-1} was added to each culture 44 h after incubation in order to inhibit cytokinesis. Lymphocyte cultures were incubated for further 28 h. Cells were collected by centrifugation and treated with a hypotonic solution (0.56 % KCl+0.90 % NaCl, mixed in equal volumes) at 37 °C. Cell suspension was fixed in

methanol/acetic acid (3:1), washed three times with a fixative, and dropped onto clean slides. Slides were air-dried and stained in alkaline Giemsa. For each sample, at least 1000 binucleated (BN) cells were scored and MNi were recorded using an Optech microscope (Munich, Germany) with 400x or 1000x magnification.

Cytokinesis-block proliferation index

The ability of cells to proliferate *in vitro* was evaluated by counting the number of cells with one to four nuclei on the same slides. The results of these analyses are presented as a cytokinesis-block proliferation index. CBPI was calculated according to the method of Surrales at al. (30) as follows: CBPI =[MI + 2MII + 3(MIII +MIV)]/N, where MI-MIV represents the number of cells with one to four nuclei, respectively, and N is the number of cells scored.

Apoptosis of leukocytes

After 24 h of incubation, cells were gently washed with physiological saline (0.9 % NaCl) at 37 °C, and fixed in methanol/acetic acid (3:1). Afterwards, the pellet was fixed in 96 % ethanol and stored at +4 °C. Samples were incubated at room temperature for 10-15 min in incubation phosphate buffer. Propidium iodide (PI, Sigma-Aldrich) and Ribonuclease A (RNase A, Sigma-Aldrich) were added 5 min prior to the flow cytometry analysis.

Apoptosis was assessed by flow cytometric (Partec, Germany) identification of cells displaying apoptosis-associated DNA condensation. DNA content was assessed by measuring the UV fluorescence of propidium iodide stained DNA. Apoptotic population was calculated using the Flow Max software (Partec, Germany).

Blood culture preparation

After 72 h of incubation, blood cultures were separated on a Lymphoprep (Lymphocyte separation medium, PAA Laboratories GmbH, Pasching, Austria); lymphocytes were collected by centrifugation, washed in a physiological saline, and frozen at -20 ºC for the TBA assay, while erythrocytes were haemolysed in ice cold deionised water and frozen at -20 ºC for subsequent analyses of the catalase activity.

Assay of the catalase activity

The catalase activity was measured using the method of Aebi (31) with minor modifications by following the catalytic reduction of hydrogen peroxide. The decomposition of the substrate H_2O_2 was measured using a Perkin Elmer Lambda 25 Spectrophotometer (Perkin Elmer Instruments, Norwalk, CT, USA) at 240 nm. The activity was expressed as K – rate constant of the first-order reaction per minute per mg of Hb. Haemoglobin concentration was determined using the Drabkin's method.

Thiobarbituric acid (TBA) assay

A thawed lymphocyte suspension was treated with thiobarbituric acid, and used to determine malondialdehyde levels, spectrophotometrically at 532 nm (32). Values were expressed as nmol TBA-reactive substance (MDA equivalent)/mg protein, using a standard curve of 1,1,3,3-tetramethoxypropane. Protein concentration was determined according to the method of Lowry et al. (33).

Statistics

Statistical analysis was carried out using the Statistica 8 and OriginPro 8.5.1 software packages for Microsoft Windows. Statistical analysis was done using the Mann-Whitney U test. *P* values of less than 0.05 were considered to be significant.

RESULTS

The radiomodulating effects of UPP were assessed *in vitro* by treating human peripheral blood cultures with UPP and IR using two treatment regimens: UPP was added to the cultures one hour prior to γ-irradiation as pre-treatment and immediately after γ-irradiation as post-treatment. The activity of UPP was investigated evaluating its effects on the radiation-induced MNi formation, cell proliferation, and induction of apoptosis. The redox modulating effects of UPP were examined measuring the catalase activity and the level of malondialdehyde, the lipid peroxidation product, as markers of oxidative stress.

Combined treatment with IR and UPP – the UPP pre-treatment regimen

As shown in Table 1, the UPP pre-treatment, at low concentration, induced a significant reduction of the MNi frequency (by 13 %) compared to control (irradiated sample not treated with UPP) ($p<0.05$). At higher applied UPP concentrations, no considerable differences in the MNi frequency compared to control were observed. The proliferation potential of cells was almost unchanged up to the highest applied concentration when significant suppression of cell proliferation was found ($p<0.05$). As shown in Figure 1, the percentage of apoptotic cells was significantly higher (by approximately 50 %) than that in control ($p<0.01$), irrespective of the UPP concentration.

Considering the redox modulating activities of UPP, in cell cultures that were pre-treated with the lowest UPP concentration, a significant decrease in the MDA level (by 32 %) was observed ($p<0.05$), while the subsequent increase in UPP concentrations enhanced MDA level ($p<0.05$), potentiating hence the effects of IR (Figure 2a). As shown in Figure 2b, the catalase activity slightly increased in a dose-dependent manner reaching significant enhancement (by 36 %) at the highest UPP concentration applied ($p<0.05$).

Table 1 *Frequency of micronuclei and proliferation potential of cells (mean±SD) in human lymphocytes treated with UPP and γ-irradiation (UPP pre-irradiation treatment and UPP post-irradiation treatment)*

		Frequency of micronuclei (MN)	Proliferation potential (CBPI)
Unirradiated Control		10.56±1.22	1.82±0.02
γ-irradiated Control		215.87±8.46	1.51±0.04
	UPP concentration		
UPP pre-irradiation treatment	0.1 μg ml^{-1}	189.04±9.41*	1.53±0.01
	1 μg ml^{-1}	203.33±4.55	1.48±0.02
	5 μg ml^{-1}	215.43±8.38	1.40±0.03*
UPP post-irradiation treatment	0.1 μg ml^{-1}	228.30±9.30	1.48±0.01
	1 μg ml^{-1}	231.27±6.81*	1.41±0.02*
	5 μg ml^{-1}	247.52±4.30*	1.38±0.02*

**Comparison with γ-irradiated control, p<0.05*

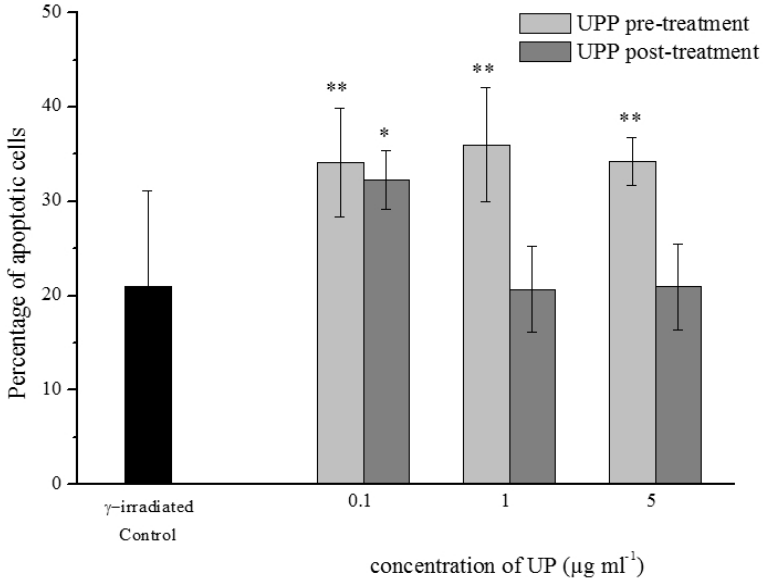

Figure 1 *Apoptosis of leukocytes in a combined treatment with IR and UPP (mean± SD); Comparison with γ-irradiated control, *p<0.05, **p<0.01*

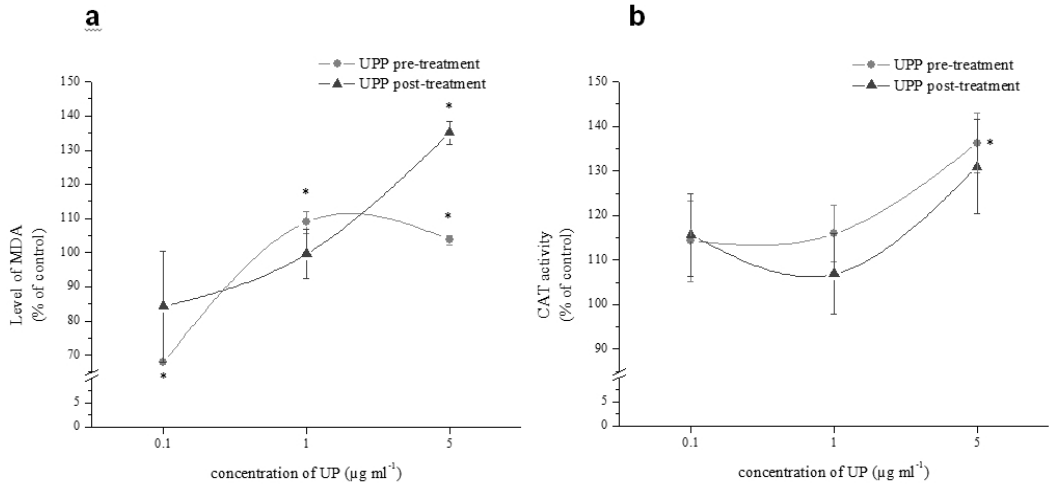

Figure 2 *(a) Level of malondialdehyde and (b) Catalase activity in cell cultures treated with UPP and γ-irradiation (UPP pre-irradiation treatment and UPP post-irradiation treatment), expressed as a percentage of γ-irradiated control set to 100 % (mean±SD); Comparison with γ-irradiated control, *p<0.05*

Combined treatment with IR and UPP – the UPP post-treatment regimen

The UPP post-treatment resulted in significant enhancement of radiation-induced MN (by 15 %) and reduction of cell proliferation in a concentration dependent manner ($p<0.05$) (Table 1).

The percentage of apoptotic cells was significantly enhanced (by approximately 50 %) compared to control only at the lowest applied UPP concentration ($p<0.05$), while a further increase in UPP concentrations decreased apoptosis to control level (Figure 1).

As shown in Figure 2a, the UPP post-treatment caused no significant changes in the MDA level except for the highest UPP concentration, which enhanced radiation-induced lipid peroxidation by 35 % ($p<0.05$).

The UPP post-treatment caused mild, insignificant enhancement of the catalase activity (Figure 2b). Schematic representation of the treatment of human peripheral blood lymphocytes with UPP and γ-irradiation is given in Figure 3.

DISCUSSION

Different classes of natural compounds have been investigated for their potencies to augment the therapeutic index of radiotherapy (1). Although PGs have been found to display anticancer activities, their efficacy in modifying cellular response to IR has not been investigated so far. In this study, we examined the influence of UPP on different end-points of radiation damage. Results of the study clearly indicate that UPP radiomodulating effects depend on its concentration and treatment regimens.

IR is known to cause direct DNA damage and indirect DNA damage is caused by free radicals derived from the ionisation or excitation of the water component of cells (34). Reactive oxygen species (ROS) generated upon irradiation induce DNA strand breaks and structural and functional alterations of biomolecules (35). Some ROS i.e. HO_2^- and H_2O_2 can pass through cell membranes, which results in important changes in cellular functions (36).

Acting on cells before radiation exposure, UPP displayed significant proapoptotic effects enhancing the radiation-induced apoptosis independently of the concentration applied. This result is in accordance with the previously reported propensity of PGs to induce apoptosis. It has been shown that prodigiosins modulate the expression of Bcl-2 family proteins, IAP proteins, and death ligand/receptors involving both mitochondrial and death-receptor apoptotic pathways (19). The influence of UPP on radiation-induced MNi formation appeared to be concentration dependent. Specifically, the low UPP concentration attenuated the radiation-induced MNi frequency while the subsequent increase of UPP concentrations kept the level of MNi similar to that of control. On the other hand, the UPP post-treatment induced enhanced radiation-induced MNi and suppressed cell proliferation in a concentration dependant manner. A dose-dependent increase in the frequency of MNi in the lymphocytes treated with UPP was also observed in our previous study (unpublished data). These results suggest that UPP added to cell cultures after irradiation displayed cytostatic effects and promoted mitotic catastrophe, a type of cell death that results from abnormal mitosis and leads to the formation of cells with multiple MNi (37). In this treatment regimen, the observed decrease in radiation-induced apoptosis is compensated by an

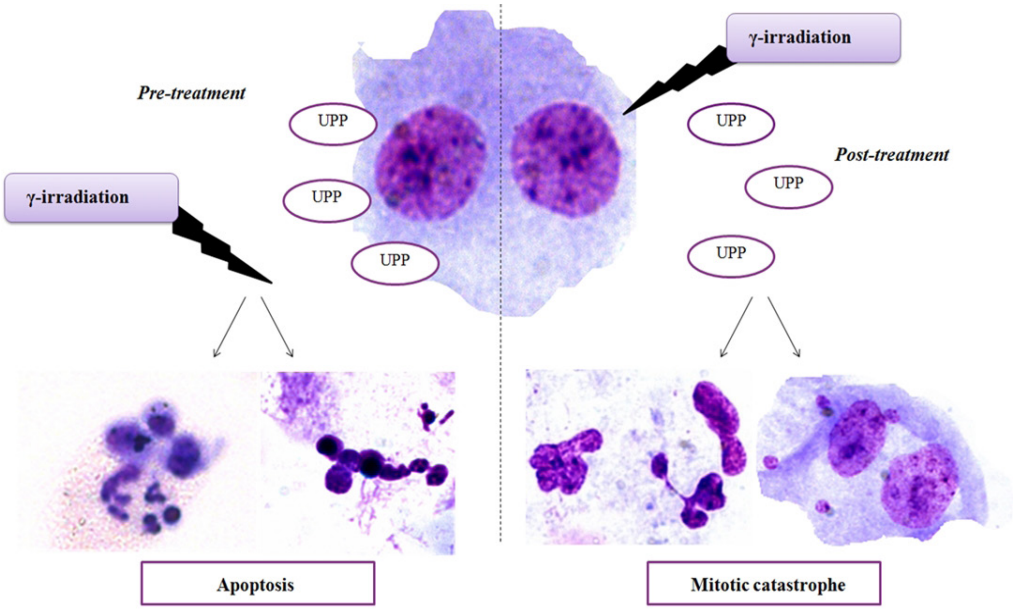

Figure 3 *Schematic representation of the treatment of human peripheral blood lymphocytes with UPP and γ-irradiation. Left panel: Treatment with UPP prior to γ-irradiation enhanced radiation-induced apoptosis; Right panel: The UPP post- irradiation treatment enhanced radiation-induced mitotic catastrophe*

increase in the fractions of cells that die through the process of mitotic catastrophe. Mitotic catastrophe represents the main form of cell death induced by IR (38). Thus, in a post-treatment regimen, UPP contributed to the inappropriate entry of cells into mitosis possibly *via* suppression of multiple central checkpoint proteins or disturbance of the mitotic spindle formation.

The effect of UPP on radiation-induced lipid peroxidation is mainly observed in the UPP pre-treatment; the experimental data showed that high concentration of UPP displayed pro-oxidant effects, while at low concentration UPP possessed antioxidant properties and acted as a scavenger of highly reactive free radicals generated upon irradiation. The attenuation of radiation-induced injury was also seen through the reduction of IR-induced MNi as described above. However, UPP at the same concentration proved to be ineffective as antioxidant if administered at the post-irradiation stage. Augmented levels of intrinsic oxidative stress have been found in a variety of tumours, possibly due to more active metabolism, mitochondrial mutation, cytokines, and inflammation (39). Therefore, modulating the redox status of cancer cells might be critical for their survival (40). In that way, UPP as the IR-induced oxidative stress enhancer may sensitise cancer cells to undergo apoptotic death, which was the scenario observed in cell cultures pre-treated with UPP. It can be assumed that UPP promotes the fixation of IR-induced free radicals and prevents the repair of cellular radiation damage. In addition, the highest UPP concentration added to cells prior to gamma irradiation induced a significant enhancement of the catalase activity. Knowing that many human cancers including melanoma, neuroblastoma, colon carcinoma, and ovarian carcinoma, constitutively generate a high amount of H_2O_2 (41), it can be assumed that UPP may induce cell cycle arrest and apoptosis of these cancer cells through the scavenging of H_2O_2 by overexpressed catalase. It is worth noting that in a post-treatment regimen, the UPP redox modulating activities were attenuated. Radiation-induced lipid peroxidation was potentiated by UPP only at the highest employed concentration.

CONCLUSION

Taken together, the results of this study suggest that UPP effects on cellular response to IR vary from mild radioprotection to radiosensitisation depending on its concentration and the timing of its administration, i.e. pre- or post-irradiation stage. At higher concentrations, the UPP's genotoxic and pro-oxidant behaviour augmented radiation-induced injury and it acted as a radiosensitiser enhancing either mitotic catastrophe or apoptosis depending on the treatment regimen. These findings highlight the importance of further research of UPP effects in cancer cells in terms of its utilisation for sensitising tumour cells to radiation therapy. If proven to be inefficient in killing cancer cells, this kind of exposure and high concentrations of UPP should not be applied. When applied at pre-irradiation stage, UPP, at low concentration, displayed radioprotective effects in gamma-irradiated human lymphocytes reducing MNi formation and acting as an antioxidant, thus exhibiting potential for further research.

Acknowledgments

This work has been supported by the Ministry of Education, Science and Technological Development of the Republic of Serbia (Project no. 172023). The authors are thankful to Dr Branka Vasiljević, Dr Jasmina Nikodinović and Dr Lidija Šenerović from the Institute of Molecular Genetics and Genetic Engineering, Belgrade, Serbia, for providing UPP for the research.

REFERENCES

1. Labay E, Efimova EV, Quarshie BK, Golden DW, Weichselbaum RR, Kron SJ. Ionizing radiation-induced foci persistence screen to discover enhancers of accelerated senescence. Int J High Throughput Screen 2011:2:1-13. doi: 10.2147/IJHTS.S17076
2. Garg AK, Buchholz TA, Aggarwal BB. Chemosensitization and radiosensitization of tumors by plant polyphenols. Antioxid Redox Signal 2005;7:1630-47. doi: 10.1089/ars.2005.7.1630
3. Hazra B, Ghosh S, Kumar A, Pandey BN. The prospective role of plant products in radiotherapy of cancer: a current overview. Front Pharmacol 2012;2:94. doi: 10.3389/fphar.2011.00094
4. Rosenberg A, Knox S. Radiation sensitization with redox modulators: a promising approach. Int J Radiat Oncol Biol Phys 2006;64:343-54. doi: 10.1016/j.ijrobp.2005.10.013
5. Papazisis KT, Zambouli D, Kimoundri OT, Papadakis ES, Vala V, Geromichalos GD, Voyatzi S, Markala D, Destouni E, Boutis L, Kortsaris AH. Protein tyrosine kinase inhibitor, genistein, enhances apoptosis and cell cycle arrest in K562 cells treated with gamma-irradiation. Cancer Lett 2000;160:107-13. doi: 10.1016/S0304-3835(00)00569-3
6. Begg AC, Stewart FA, Vens C. Strategies to improve radiotherapy with targeted drugs. Nat Rev Cancer 2011;11:239-53. doi: 10.1038/nrc3007
7. Joksic G, Leskovac A, Petrovic S. Modulation of radiation-induced damage by Serbian natural plant products: implications for radioprotection. In: Arora R, editor. Herbal radiomodulators: applications in medicine, homeland defence and space. Oxfordshire: CAB International; 2008. p. 67-82.
8. Moding EJ, Kastan MB, Kirsch DG. Strategies for optimizing the response of cancer and normal tissues to radiation. Nat Rev Drug Discov 2013;12:526-42. doi: 10.1038/nrd4003
9. Burris HA, 3rd, Hurtig J. Radiation recall with anticancer agents. Oncologist 2010;15:1227-37. doi: 10.1634/theoncologist.2009-0090
10. Thomson NR, Crow MA, McGowan SJ, Cox A, Salmond GP. Biosynthesis of carbapenem antibiotic and prodigiosin pigment in *Serratia* is under quorum sensing control. Mol Microbiol 2000;36:539-56. doi: 10.1046/j.1365-2958.2000.01872.x

11. Hobbs G, Frazer CM, Gardner DCJ, Flett F, Oliver SG. Pigmented antibiotic production by *Streptomyces coelicolor* A3(2): kinetics and the influence of nutrients. J Gen Microbiol 1990;136:2291-6. doi: 10.1099/00221287-136-11-2291
12. Kawasaki T, Sakurai F, Hayakawa Y. A prodigiosin from the roseophilin producer *Streptomyces griseoviridis*. J Nat Prod 2008;71:1265-7. doi: 10.1021/np7007494
13. Nakamura A, Magae J, Tsuji RF, Yamasaki M, Nagai K. Suppression of cytotoxic T cell induction *in vivo* by prodigiosin 25-C. Transplantation 1989;47:1013-6. doi: 10.1097/00007890-198906000-00019
14. Songia S, Mortellaro A, Taverna S, Fornasiero C, Scheiber EA, Erba E, Colotta F, Mantovani A, Isetta AM, Golay J. Characterization of the new immunosuppressive drug undecylprodigiosin in human lymphocytes: retinoblastoma protein, cyclin-dependent kinase-2, and cyclin-dependent kinase-4 as molecular targets. J Immunol 1997;158:3987-95. PMID: 9103470
15. Tsuji RF, Magae J, Yamashita M, Nagai K, Yamasaki M. Immunomodulating properties of prodigiosin 25-C, an antibiotic which preferentially suppresses induction of cytotoxic T cells. J Antibiot (Tokyo) 1992;45:1295-302. PMID: 1399851
16. Pandey R, Chander R, Sainis KB. Prodigiosins as anti cancer agents: living upto their name. Curr Pharm Design 2009;15:732-41. doi: 10.2174/138161209787582192
17. Yamamoto C, Takemoto H, Kuno K, Yamamoto D, Nakai K, Baden T, Kamata K, Hirata H, Watanabe T, Inoue K. Cycloprodigiosin hydrochloride, a H+/Cl- symporter, induces apoptosis in human colon cancer cell lines *in vitro*. Oncol Rep 2001;8:821-4. PMID: 11410791
18. Yamamoto D, Kiyozuka Y, Uemura Y, Yamamoto C, Takemoto H, Hirata H, Tanaka K, Hioki K, Tsubura A. Cycloprodigiosin hydrochloride, a H+/Cl- symporter, induces apoptosis in human breast cancer cell lines. J Cancer Res Clin Oncol 2000;126:191-7. doi: 10.1007/s004320050032
19. Chang CC, Chen WC, Ho TF, Wu HS, Wei YH. Development of natural anti-tumor drugs by microorganisms. J Biosci Bioeng 2011;111:501-11. doi: 10.1016/j.jbiosc.2010.12.026
20. Ho TF, Ma CJ, Lu CH, Tsai YT, Wei YH, Chang JS, Lai JK, Cheuh PJ, Yeh CT, Tang PC, Tsai Chang J, Ko JL, Liu FS, Yen HE, Chang CC. Undecylprodigiosin selectively induces apoptosis in human breast carcinoma cells independent of p53. Toxicol Appl Pharmacol 2007;225:318-28. doi: 10.1016/j.taap.2007.08.007
21. Liu P, Wang YY, Qi X, Gu Q, Geng M, Li J. Undecylprodigiosin induced apoptosis in P388 cancer cells is associated with its binding to ribosome. PLoS One 2013;8:e65381. doi: 10.1371/journal.pone.0065381
22. Nikodinovic-Runic J, Mojic M, Kang Y, Maksimovic-Ivanic D, Mijatovic S, Vasiljevic B, Stamenkovic VR, Senerovic L. Undecylprodigiosin conjugated monodisperse gold nanoparticles efficiently cause apoptosis in colon cancer cells *in vitro*. J Mater Chem B. 2014;2:3271-81. doi: 10.1039/C4TB00300D
23. Stankovic N, Senerovic L, Ilic-Tomic T, Vasiljevic B, Nikodinovic-Runic J. Properties and applications of undecylprodigiosin and other bacterial prodigiosins. Appl Microbiol Biotechnol 2014;98:3841-58. doi: 10.1007/s00253-014-5590-1
24. Stankovic N, Radulovic V, Petkovic M, Vuckovic I, Jadranin M, Vasiljevic B, Nikodinovic-Runic J. *Streptomyces sp*. JS520 produces exceptionally high quantities of undecylprodigiosin with antibacterial, antioxidative, and UV-protective properties. Appl Microbiol Biotechnol 2012;96:1217-31. doi: 10.1007/s00253-012-4237-3
25. Leiros M, Alonso E, Sanchez JA, Rateb ME, Ebel R, Houssen WE, Jaspars M, Alfonso A, Botana LM. Mitigation of ROS insults by *Streptomyces* secondary metabolites in primary cortical neurons. ACS Chem Neurosci 2014;5:71-80. doi: 10.1021/cn4001878
26. Boric M, Danevcic T, Stopar D. Prodigiosin from *Vibrio sp*. DSM 14379; a new UV-protective pigment. Microb Ecol 2011;62:528-36. doi: 10.1007/s00248-011-9857-0
27. Law on health care. Official Gazette of the Republic of Serbia. Parliament of the Republic of Serbia. 2005. 107:112-161.
28. Shukla S, Anjaria K, Bhat N, Shirsath K, Sreedevi B. Effect of caffeine on radiation induced micronuclei in human lymphocytes. Radiat Protect Environ 2010;33:195-8 [displayed 11 January 2017]. Available at http://www.rpe.org.in/article.asp?issn=0972-0464;year=2010;volume=33;issue=4;spage=195;epage=198;aulast=Shukla
29. Fenech M. The cytokinesis-block micronucleus technique: a detailed description of the method and its application to genotoxicity studies in human populations. Mutat Res 1993;285:35-44. doi: 10.1016/0027-5107(93)90049-L
30. Surralles J, Xamena N, Creus A, Marcos R. The suitability of the micronucleus assay in human lymphocytes as a new biomarker of excision repair. Mutat Res 1995;342:43-59. doi: 10.1016/0165-1218(95)90089-6
31. Aebi H. Catalase. In: Bergmeyer HU, editor. Methods of enzymatic analysis. Weinheim: Verlag Chemie; 1974. p. 673-6.
32. Aruoma OI, Halliwell B, Laughton MJ, Quinlan GJ, Gutteridge JM. The mechanism of initiation of lipid peroxidation. Evidence against a requirement for an iron(II)-iron(III) complex. Biochem J 1989;258:617-20. doi: 10.1042/bj2580617
33. Lowry OH, Rosebrough NJ, Farr AL, Randall RJ. Protein measurement with the Folin phenol reagent. J Biol Chem 1951;193:265-75. PMID: 14907713
34. Baskar R, Lee KA, Yeo R, Yeoh KW. Cancer and radiation therapy: current advances and future directions. Int J Med Sci 2012;9:193-9. doi: 10.7150/ijms.3635
35. Halliwell B, Gutteridge J. Free Radicals in Biology and Medicine. 4 ed. Oxford: Oxford University Press; 2007.
36. Azzam EI, Jay-Gerin JP, Pain D. Ionizing radiation-induced metabolic oxidative stress and prolonged cell injury. Cancer Lett 2012;327:48-60. doi: 10.1016/j.canlet.2011.12.012
37. Roninson IB, Broude EV, Chang B-D. If not apoptosis, then what? Treatment-induced senescence and mitotic catastrophe in tumor cells. Drug Resist Updat 2001;4:303-13. doi: 10.1054/drup.2001.0213
38. Vakifahmetoglu H, Olsson M, Zhivotovsky B. Death through a tragedy: mitotic catastrophe. Cell Death Differ 2008;15:1153-62. doi: 10.1038/cdd.2008.47
39. Gupte A, Mumper RJ. Elevated copper and oxidative stress in cancer cells as a target for cancer treatment. Cancer Treat Rev 2009;35:32-46. doi: 10.1016/j.ctrv.2008.07.004
40. Dröge W. Free radicals in the physiological control of cell function. Physiol Rev 2002;82:47-95. doi: 10.1152/physrev.00018.2001
41. Szatrowski TP, Nathan CF. Production of large amounts of hydrogen peroxide by human tumor cells. Cancer Res 1991;51:794-8. PMID: 1846317

Utjecaj koncentracije i vremena administracije na radiomodulirajuća svojstva undecilprodigozina *in vitro*

Undecilprodigiozin pigment (UPP) pokazuje citotoksičnu aktivnost kod različitih tipova tumora. Međutim, njegova učinkovitost u modulaciji staničnog odgovora na ionizirajuće zračenje i dalje je nepoznata. U ovoj studiji ispitani su radiomodulirajući učinci UPP-a *in vitro* tretiranjem kultura ljudske periferne krvi s UPP-om i ionizirajućim zračenjem. Pri ispitivanju su se koristile dvije vrste tretmana: tretman s UPP-om prije ozračivanja (predtretman) i tretman s UPP-om poslije ozračivanja (posttretman). Djelotvornost UPP-a ispitivana je procjenom njegovih učinaka na zračenjem inducirano formiranje mikronukleusa, staničnu proliferaciju i apoptozu. Redoks-modulirajući učinci UPP-a ispitivani su mjerenjem aktivnosti katalaze i razine malondialdehida kao parametara oksidacijskoga stresa. Rezultati pokazuju da učinci UPP-a na stanični odgovor na ionizirajuće zračenje ovise o njegovoj koncentraciji i vrsti tretmana. Pri niskim koncentracijama UPP pokazuje radioprotekcijski učinak u ozračenim humanim limfocitima, a pri visokim koncentracijama djeluje kao radiosenzibilizator inducirajući ili mitotsku katastrofu ili apoptozu, ovisno o vrsti tretmana. UPP modificira redoks procese u stanici, osobito ako se primjenjuje prije zračenja. Naši rezultati upućuju na značaj daljnjeg ispitivanja UPP-a u cilju njegove primjene za senzibilizaciju tumorskih stanica u terapiji zračenjem inhibicijom puteva koji vode rezistenciji na tretman.

KLJUČNE RIJEČI: *apoptoza; ionizirajuće zračenje; mitotska katastrofa; oksidacijski stres; stanična proliferacija*

THE JOURNAL OF PHYSICAL CHEMISTRY C

Article

pubs.acs.org/JPCC

Realization of Enhanced Magnetoelectric Coupling and Raman Spectroscopic Signatures in 0−0 Type Hybrid Multiferroic Core−Shell Geometric Nanostructures

Ann Rose Abraham,[†] B. Raneesh,[‡] Tesfakiros Woldu,[§] Sonja Aškrabić,[∥] Saša Lazović,[∥] Zorana Dohčević-Mitrović,[∥] Oluwatobi Samuel Oluwafemi,*[,⊥,#] Sabu Thomas,[g] and Nandakumar Kalarikkal*[,†,g]

[†]School of Pure and Applied Physics, Mahatma Gandhi University, Kottayam, Kerala-686560, India

[‡]Department of Physics, Catholicate College, Pathanamthitta, Kerala-689 645, India

[§]Department of Physics, Osmania University, Hyderabad 500007, India

[∥]Institute of Physics Belgrade, University of Belgrade, Pregrevica 118, 11080, Belgrade, Serbia

[⊥]Department of Applied Chemistry, University of Johannesburg, Doornfontein Campus, P.O Box 17011, Doornfontein 2028, South Africa

[#]Centre for Nanomaterials Science Research, University of Johannesburg, Johannesburg, South Africa

[g]International & Inter University Centre for Nanoscience and Nanotechnology, Mahatma Gandhi University, Kottayam, Kerala-686 560, India

ABSTRACT: Multiferroic heterostructures' contribution to the persistent growth of ultrafast wireless communications may pave the way for future 5G technology. In line with this, we herein report the development of an engineered hybrid multiferroic core−shell nanostructure with a soft magnetic core and a ferroelectric shell. In this system, the attributes of the ferromagnetic core were modulated by a ferroelectric coating over it, in order to impart a bifunctionality to it and thus induce magnetoelectric coupling in it for multifunctional device applications. The phase, crystal structure and morphology of these composites have been investigated using X-ray diffraction (XRD), transmission electron microscopy (TEM), scanning electron microscopy (SEM), and confocal Raman spectroscopy. The origin of strain mediated magnetoelectric coupling effect at the ferromagnetic core and ferroelectric shell interface was also investigated. Raman spectroscopy is efficiently utilized to manifest the multiferroism in the core−shell samples. High resolution transmission electron microscopy images and domain structure mapping using confocal Raman microscopy along with Raman images substantiate the core−shell nature of the samples. The findings manifest how tuning of the ferromagnetic phase influences the magnetoelectric coupling at the interface and reveal novel approaches for manipulating the attributes of a ferromagnetic−ferroelectric interface for innovative device applications. The outcome of the experiments indicates an energy efficient move toward the control of the *E*-field by the magnetic field, which demonstrates an enormous prospective for novel low power electronic, magnonic, and spintronic devices.

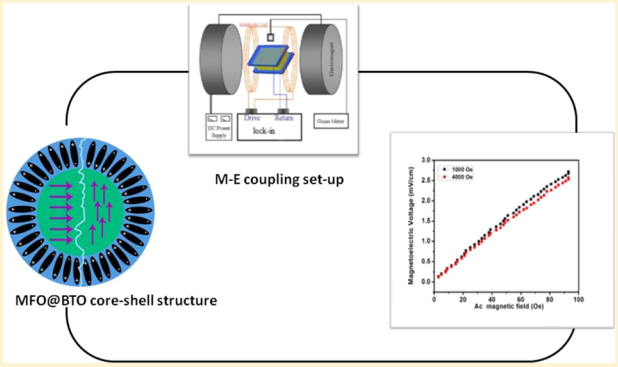

1. INTRODUCTION

The voltage control of magnetism, exhibited by multiferroics, makes them attractive and promising for multifunctional device applications.[1−3] Hence, the exploration of hybrid multiferroic materials or artificial multiferroics in which ferromagnetism and ferroelectricity coexist is highly appealing and of great technological significance.[4−6] Multiferroic materials are rare in nature[7−9] and of great demand due to their potential to conserve power and space and their amazing applications in information technology,[8] data storage,[11] magnetoelectric sensors,[11] multiple-state memories,[12,13] and emerging ultra-low-power spintronics technology.[10−13] The electromagnons[13,14] or the quantized hybrid spin−lattice excitations in multiferroics[15,16] have opened up vast doors in the emerging magnonic and spintronics technology and production of fast, reliable, and low power magnetoelectric devices.

Multiferroics are fascinating for engineering of future generation of fast and nonvolatile hybrid type memories like multiferroic or magnetoelectric memories (MERAMS) with unlimited write-erase cycles and enormous data transfer

Received: December 13, 2016
Revised: January 26, 2017
Published: January 30, 2017

DOI: 10.1021/acs.jpcc.6b12461
J. Phys. Chem. C 2017, 121, 4352−4362

rate.[17−20] They magnificently assist one to realize a highly energy efficient and switchable four-state (+P, + M), (+P, −M), (−P, + M), (−P, −M) memory. The quest for development of engineered hybrid multiferroic structures[4] for energy efficient spintronics and magnetoelectric memories[17−20] was propelled by the enhanced values of magnetoelectric coupling (ME) demonstrated by ferromagnetic−ferroelectric heterostructures[1] at room temperature, rather than that exhibited by the single phase multiferroics that exhibit multiferroicity at cryogenic temperatures.[21−26] Engineered hybrid multiferroic heterostructures[27] with large values of magnetoelectric coupling have been reported in ferromagnetic−ferroelectric composites, such as cobalt ferrite−barium titanate ceramic composites,[28] $BaTiO_3$−$MgFe_2O_4$ composites,[29] $BaTiO_3$−$MgFe_2O_4$ composite powders (synthesized by a Pechini one-pot method),[30] $(x)MgFe_2O_4$−$(1 - x)BaTiO_3$ systems composites[31] and also in hybrid multiferroic core−shell structures like Ni@$BiFeO_3$,[32] $NiFe_2O_4$@$BaTiO_3$,[33−35] $Ni_{0.5}Zn_{0.5}Fe_2O_4$@$BaTiO_3$,[36] and $CoFe_2O_4$@$BaTiO_3$.[37] However, as far as the authors know, the preparation of $MgFe_2O_4$@$BaTiO_3$ core−shell nanocomposites with varying magnetic core sizes has never been reported.

We focus on composite structures of spinel ferrite of AB_2O_4 structure[38] and perovskites of (ABO_3) structure.[39] Ferrites, the most desirable magnetic materials, have wide applications as waveguides for electromagnetic radiation and in high-density data storage, sensors, microwave devices, food pathogen detection, and nanomedicine.[40−42] Furthermore, $MgFe_2O_4$[38] is highly promising in spintronics, owing to its high curie temperature.[40] On the other hand, $BaTiO_3$ (BTO) possesses exceptional ferroelectric attributes at room temperature, in addition to the multiferroic nature at the nanoscale; hence, we found no best candidate other than $BaTiO_3$ (BTO)[43] to realize our objective of achieving ferromagnetic−ferroelectric systems with enhanced multiferroicity.

Functionality of the hybrid multiferroic nanostructures is highly dependent on the morphology of the magnetic and ferroelectric counterparts and could be extensively tailored by playing around with their geometry.[44] As far as the authors know there are no reports that explains how the magnetoelectric coupling gets tuned in a hybrid[45] core−shell multiferroic system by varying the magnetic core sizes. The existence of spin−phonon coupling[12] mediated by the lattice distortion[46] has been investigated by several researchers in multiferroics like $YMnO_3$,[47] $TbMn_2O_5$.[46]

In this work, we have focused our attention on preparing three core−shell systems in which soft magnesium ferrite core of different particle sizes were coated with $BaTiO_3$ shell to study its influence in enhancing the magnetoelectric coupling between the magnetic and ferroelectric phases. Emphasis is given to the development of core−shell multiferroic composite structures with enhanced ME coupling than the individual phases. The sketch map of a ferroelectric shell over a ferromagnetic core (FM@FE) as shown in Figure 1 is attractive because of the interfacial magnetoelectric effects, due to coupling at FE (ferroelectric)/(FM) ferromagnetic interfaces.

The Morphology of the developed core−shell samples were verified using X-ray diffraction, transmission electron microscopy, scanning electron microscopy, and Raman spectroscopy while the coupling between the ferromagnetic and ferroelectric phases was studied by a magnetoelectric coupling setup and confocal Raman spectroscopy.

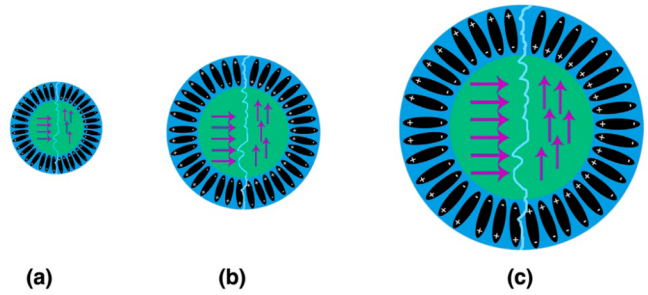

Figure 1. Sketch map of ferromagnetic@ferroelectric core−shell nanocomposites of varying cores sizes.

2. EXPERIMENTAL SECTION

2.1. Materials. Magnesium nitrate, $Mg(NO_3)_2.6H_2O$ (99% purity, Fisher Scientific Chemicals), ferric nitrate $Fe(NO_3)_3 \cdot 9H_2O$ (99.99% purity, Fisher Scientific Chemicals), poly(vinyl alcohol) (PVA) (99.99% purity, Fisher Scientific chemicals), citric acid, barium carbonate, and titanium isopropoxide (Sigma- Aldrich).

2.2. Synthesis. The $MgFe_2O_4$ @ $BaTiO_3$ (MFO@BTO) core−shell nanoparticles were synthesized by a two-step method. Nanoparticles of polycrystalline $MgFe_2O_4$ were prepared by a sol−gel method, using high purity nitrates of magnesium and iron. In a typical reaction, aqueous solution of 0.1 M magnesium nitrate and 0.2 M ferric nitrate was prepared and sonicated. PVA with a weight equal to the weight of the metal ions in the solution was added to the mixed solution. The solution was evaporated until the formation of a viscous sol and dried completely so that it can be powdered. The powder obtained was divided into three and calcined at three different high temperatures to obtain $MgFe_2O_4$ nanoparticles of different particle sizes labeled as MFO1, MFO2, and MFO3. The $MgFe_2O_4$ nanoparticles (MFO1, MFO2, and MFO3) were dispersed under vigorous stirring into the $BaTiO_3$ precursor solution containing a mixture of $BaCO_3$, citric acid, and titanium isopropoxide, probe sonicated, dried, and calcined at 800 °C to obtain $MgFe_2O_4$@$BaTiO_3$ core−shell nanoparticles (MFO@BTO1, MFO@BTO2 and MFO@BTO3).

The $MgFe_2O_4$/$BaTiO_3$ composite samples were synthesized by mixing the two phases, prepared independently, followed by annealing. $MgFe_2O_4$ nanoparticles (MFO3) prepared by sol−gel method, and $BaTiO_3$ prepared by sol−gel method, were mixed at ratio 1:1 in the presence of acetone, grinded and sintered at 800 °C for 2 h. The obtained powder was pressed into pellets at 500 MPa and sintered at 800 °C for 2 h. Silver paste was coated on the sintered pellets to get electrical contacts.

2.3. Characterization. X-ray diffraction (XRD) measurements of the core and core−shell samples were carried out by using X'PERT PRO PANalytical X-ray diffractometer with Cu Kα radiation. The scanning electron microscopy (SEM) study was carried out by an energy-filtered 200 kV JEOL 6390 scanning electron microscope. The transmission electron microscopy (TEM) images were obtained from JEOL GEM 2100 transmission electron microscope equipped with an Oxford energy transmission electron microscope for elemental analysis operated at 200 kV. Confocal Raman spectra and Raman image was acquired using WITEC alpha300 RA confocal Raman microscope with a 100×/NA= 0.9 air objective and an excitation wavelength of 532 nm (600 g/mm grating blazed at 500 nm). The ME coupling studies were performed

DOI: 10.1021/acs.jpcc.6b12461
J. Phys. Chem. C 2017, 121, 4352−4362

by using a dynamic lock-in amplifier ME coupling measurement set up. Micro-Raman spectra were acquired in the back-scattering configuration using the micro-Raman system Jobin Yvon T64000.

3. RESULTS AND DISCUSSION

X-ray diffraction (XRD) patterns of $MgFe_2O_4$ (MFO), $BaTiO_3$ (BTO), and $MgFe_2O_4$@$BaTiO_3$ (MFO@BTO) samples are shown in Figure 2. A well crystallized single phase of

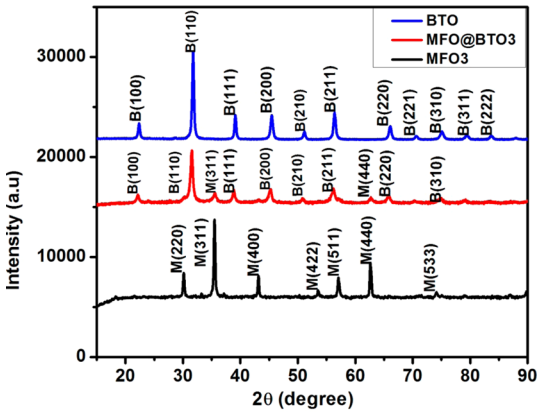

Figure 2. XRD patterns of MFO3 BTO, and MFO@BTO3.

magnesium ferrite with cubic spinel structure was detected. The fundamental peak at $2\theta = 36.45°$ with maximum intensity correspond to the (311) plane of magnesium ferrite (PDF data 71−1232). Peaks corresponding to the reflections from other planes, (220), (400), (440), and (422), are also detected but with weak intensities. The nonexistence of any additional intermediate phases indicates the high purity level of the samples. The crystalline size of the nanoparticle was calculated using the Scherrer equation. The crystalline size increased with increasing annealing temperature. The particle diameter of the core is 5, 14, and 20 nm for MFO1, MFO2, and MFO3, respectively. The formation of cubic perovskite structure of Barium titanate was confirmed from the XRD pattern (PDF 89-2475). The peaks corresponding to the magnesium ferrite with cubic spinel structure and Barium titanate with cubic perovskite structure were observed in the XRD patterns of MFO@BTO. In the XRD pattern of MFO@BTO, the fundamental reflections from the planes (311), (400), (511), and (440) characterizing the cubic spinel structures and from the planes (110), (111), and (211) characterizing the ferroelectric barium titanate were strongly observed.

The SEM images for both pure MFO powder and MFO@BTO composite powders are shown in Figure 3. The SEM images of MFO nanoparticles show that the particles are spherical in shape and are slightly agglomerated. After coating the ferrite particles with ferroelectric shell, the agglomeration decreases and spherical shape particles with uniform particle size are produced.

A typical transmission electron microscopy image of the core is shown in Figure 4. The TEM image shows that the materials are spherical in shape with uniform size distribution. The average grain size is found to be 5−6 nm which should be superparamagnetic in nature. The TEM images confirm the grain size calculations from XRD. The formation of spinel structure of Magnesium ferrite is confirmed by *d*-spacing values. The *d*-spacing of 0.284 nm corresponds to the (110) plane of BTO while the *d*-spacing of 0.295 nm corresponds to the (220) plane of MFO. This confirms the cubic spinel and the perovskite structure of the core−shell samples. (PDF No. 89-3084). The crystal planes identified from the selected area diffraction (SAED) pattern are found to be in conformity with that from XRD pattern.

The TEM images (Figure 5 and 6) confirm the formation of core−shell structure of MFO@BTO samples. The darker core and brighter shell can be clearly seen in the TEM images. Figure 5b shows the HRTEM image of the core−shell sample. The *d*-spacing of 0.284 nm corresponds to the (110) plane of BTO while the *d*-spacing of 0.295 nm corresponds to the (220) plane of MFO. This confirms the cubic spinel and the perovskite structure of the core−shell samples. The SAED patterns of core−shell samples shown in Figure 5 and Figure 6 also confirm the crystallinity of as-synthesized core−shell samples.

Chemical purity and stoichiometry of the $MgFe_2O_4$ sample was confirmed by EDX (Figure 7a) before encapsulating it in ferroelectric matrix. The EDAX spectrum shows strong peaks corresponding to magnesium, oxygen and iron. The elemental composition and atomic concentration is shown in Table. 1. EDAX spectrum of the core−shell sample (Figure 7b) was also studied to confirm the stoichiometry of the prepared sample. The spectrum reveals the presence of elements Mg, Fe, O, Ba, Ti and O in the magnesium ferrite@barium titanate core−shell sample. Their atomic concentrations are given in Table 2.

Raman spectroscopy is reported to be highly promising in studying the spin dynamics and the effect of the spin- phonon coupling in multiferroics at local scale. It has played an important role in the study of spin−phonon coupling in $BiFeO_3$,[48,49] $Ba_{1.6}Sr_{1.4}Co_2Fe_{24}O_{41}$[50] and other compounds.[51] Confocal Raman spectroscopy[52] that probes the vibrational energy levels within a molecule is employed to acquire the molecular fingerprints and high resolution Raman image of the core−shell samples. Confocal Raman image of the MFO@BTO samples shown in Figure 8a−c helps to study the structural

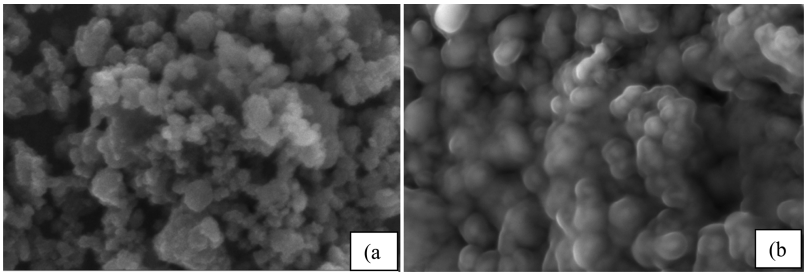

Figure 3. SEM images of (a) MFO3 at 100 nm and (b) MFO@BTO3 core−shell sample: Scale bar = 100 nm.

DOI: 10.1021/acs.jpcc.6b12461
J. Phys. Chem. C 2017, 121, 4352−4362

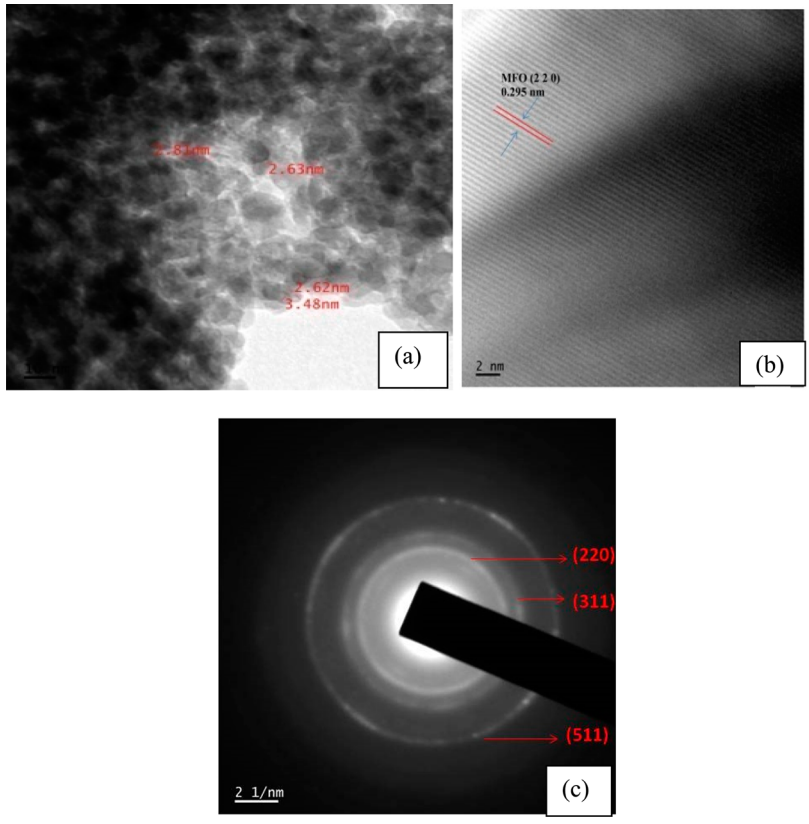

Figure 4. (a) TEM image: scale bar = 2 nm. (b) HRTEM image. (c) SAED pattern of magnesium ferrite (MFO1).

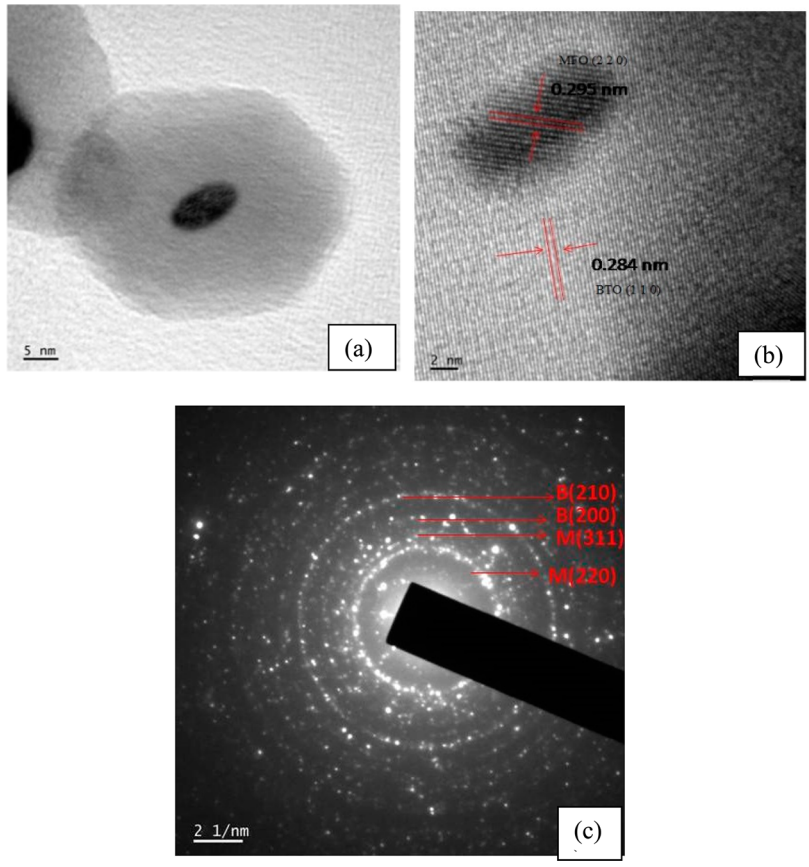

Figure 5. (a) TEM image: scale bar = 5 nm. (b) HRTEM images and (c) SAED pattern of MFO@BTO1.

DOI: 10.1021/acs.jpcc.6b12461
J. Phys. Chem. C 2017, 121, 4352−4362

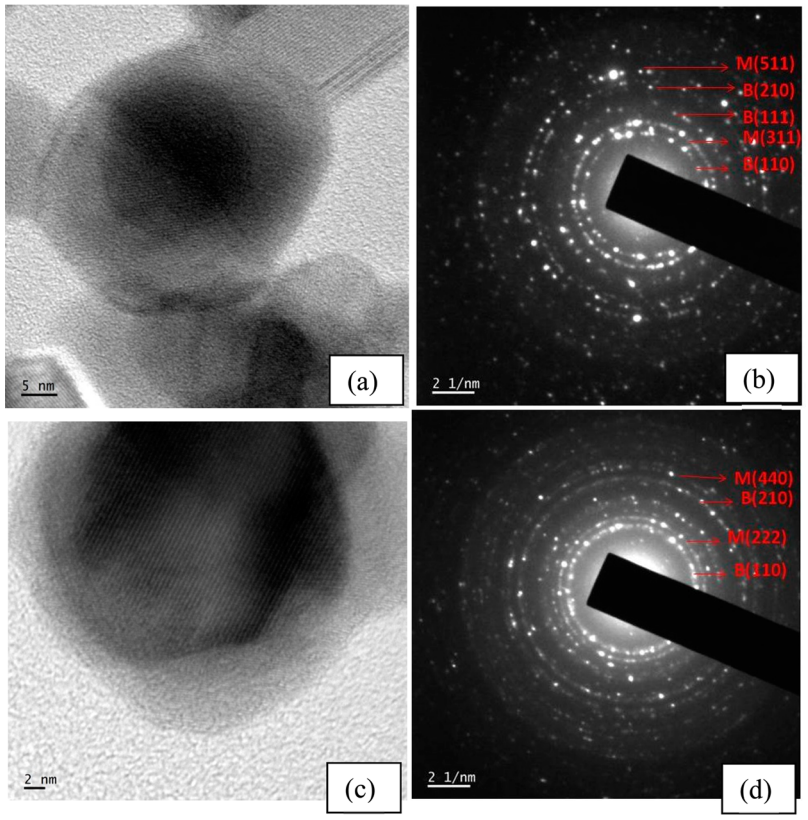

Figure 6. (a) TEM and (b) SAED pattern of MFO@BTO2 and (c) TEM and (d) SAED pattern of MFO@BTO3.

deformations of the sample. Raman image shows the ferromagnetic and ferroelectric domain allocation at the sample surface by color distribution.[53] Contrast in the Raman image confirms the multiferroic nature of the samples. The confocal Raman spectra show characteristic mode at 220 cm^{-1} attributed to the ferroelectric[54] nature of the multiferroic sample. The Raman modes between 300 to 700 cm^{-1} are the two-phonon peaks due to the Fe−O bonding[55] and are assigned to magnetic character of multiferroic MFO@BTO. The band observed at ∼1300−1500 cm^{-1} is associated with two-phonon Raman scattering,[48] and the strong band observed at 1320 cm^{-1} is the two phonon scattering band[54] observed in MFO. Thus, confocal Raman spectroscopy manifest the strong spin−phonon coupling[12] in MFO@BTO samples.

3.1. Magnetoelectric (ME) Coupling Responses. The coexistence of the ferroelectric and magnetic phases in MFO@BTO samples brings about the magnetoelectric (ME) effect, which is characterized by the magnetoelectric voltage coefficient,[53,55,56] $\alpha = dE/dH$. The investigation of the magnetoelectric (ME) coupling of the samples was performed by using a dynamic lock-in amplifier ME coupling[57−60] measurement set up to quantitatively figure out the actual magnitude of α. The details of the experimental setup are mentioned elsewhere.[59]

In multiferroic composites composed of magnetostrictive and ferroelectric phases, the magnetoelectric effect depends on the applied magnetic field. The ac magnetic field (H_{ac}) dependence of the ME voltage developed at room temperature in the BTO (Figure 9), MFO@BTO core−shell samples (Figure 10), and MFO/BTO composite sample (Figure 11) at a fixed frequency of 850 Hz with constant dc bias field of 1000 and 4000 Oe are shown below. The variation of ME voltage as a function of dc magnetic field for the MFO@ BTO core−shell samples is shown in Figure 12.

The magnetoelectric (ME) coupling responses of the BTO and $MgFe_2O_4$@$BaTiO_3$ core−shell samples were investigated. ME voltage coefficient was 5 $mVcm^{-1}Oe^{1-}$ for the synthesized nanomultiferroic $BaTiO_3$ sample (Figure 9). However, an enhanced ME voltage coefficient α_{ME} as high as 25 $mVcm^{-1}$ Oe^{-1} (MFO@BTO1) and 28 $mVcm^{-1}$ Oe^{-1} (MFO@BTO3) was obtained for the artificial multiferroic $MgFe_2O_4$@$BaTiO_3$ core−shell samples (Figure 10), higher than that reported for $MgFe_2O_4$/$BaTiO_3$ composite samples[31] (Figure 11). Thus, the results can be summarized as the magnetoelectric (ME) coupling response of the samples follows the trend $ME_{BTO} < ME_{MFO/BTO} < ME_{MFO@BTO}$.

The higher ME coefficient of the $MgFe_2O_4$@$BaTiO_3$ core−shell samples may be attributed to better coupling between the two phases at the ferromagnetic−ferroelectric interface. This can be elucidated by the proximity effects and larger interfacial area offered by the core−shell structure. The core−shell structure guarantee firm and compact coupling between ferroelectric and ferromagnetic phases to a great extent and hence, an improved magnetoelectric coupling response was achieved in ferromagnetic−ferroelectric core−shell nanoparticles as expected.[26] It can be clearly seen that the spin-dependent transport mechanism in multiferroics is highly influenced by the interface between the two phases and core−shell geometry has an appreciable role to play in significantly enhancing the magnetoelectric effect. The enhanced ME voltage coefficient displayed by the core−shell samples (Figure 10) indicate the strong spin−lattice correlations in the synthesized samples. Strain mediated elastic coupling at the core (ferromagnetic)−shell (ferroelectric) interface is attributed

DOI: 10.1021/acs.jpcc.6b12461
J. Phys. Chem. C 2017, 121, 4352−4362

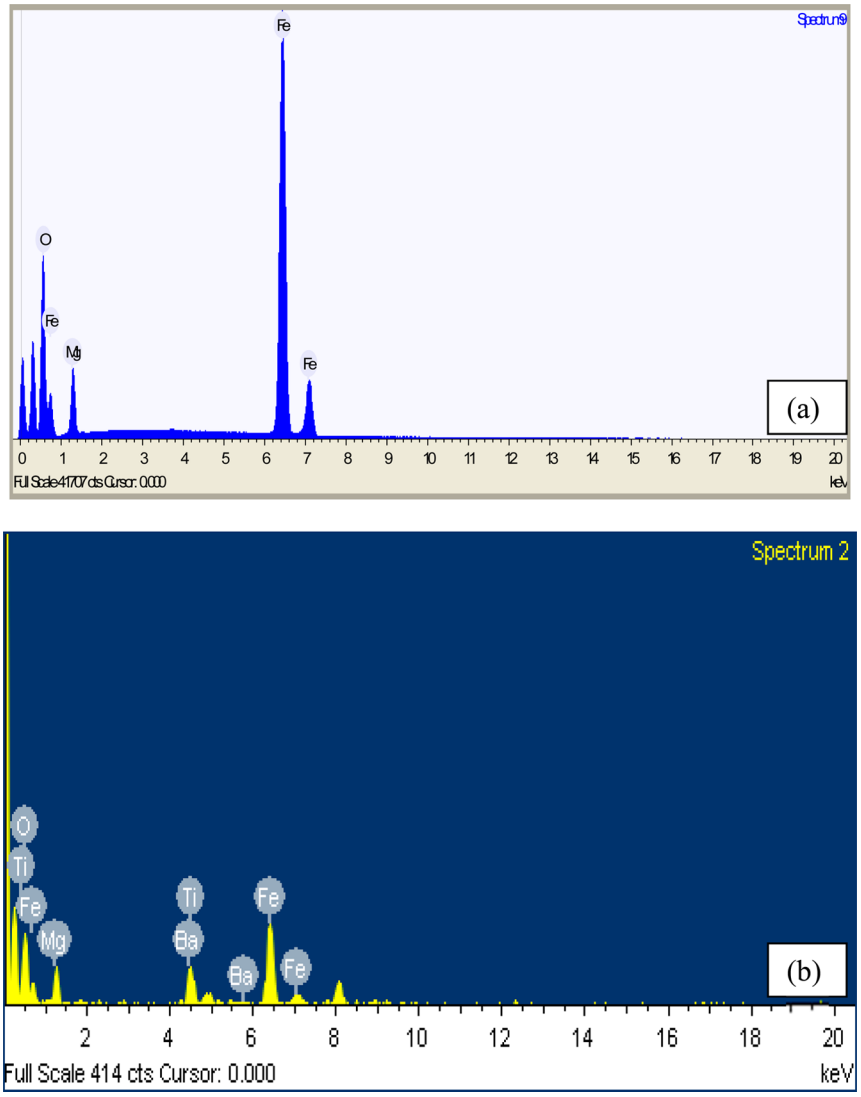

Figure 7. EDAX spectrum of (a) MFO3 and (b) MFO@BTO3.

Table 1. Elemental Composition and Atomic Concentration of MFO from EDAX Spectrum

element	weight (%)
magnesium	3.113
iron	73.719
oxygen	23.168

Table 2. Elemental Composition and Atomic Concentration of MFO@BTO from EDAX Spectrum

element	weight (%)	atomic (%)
O	24.28	50.40
Mg	10.20	13.93
Fe	39.79	23.66
Ti	12.81	8.88
Ba	12.93	3.13
totals	100	100

to account for the magnetoelectric coupling in the core−shell samples. Comparing the magnetoelectric response of the core−shell structured samples, it can be observed that, $ME_{MFO@BTO1} < ME_{MFO@BTO2} < ME_{MFO@BTO3}$. The underlying reason may be basically that, due to the smaller size of MFO grains in sample MFO@BTO1, reduced magnetic properties is expected as a result of the size effect which is influenced by the sintering temperature and consequently a weaker ME coupling. In addition, the comparatively larger size of $MgFe_2O_4$ grains in sample MFO@BTO3 yields superior magnetic properties that couple with ferroelectric properties of BTO and contribute to the large value of observed ME coupling coefficient, which indicate a strong ME coupling between the phases. Thus, the somewhat superior ME response of the MFO@BTO3 sample, compared to the MFO@BTO1 sample, may be due to the improved ferromagnetic and ferroelectric functionalities of the constituent phases that contribute to a larger piezoelectric strain at the MFO@BTO interface. The noticed variations in the magnetoelectric coefficients is indicative of the probable domain structure modification[8] that occurs in the in these hybrid systems.

These findings pave the way for experimental achievement for the development of system with strong ME coupling[59] responses, and they provide important implications for the design and performance optimization of related devices comprising of this kind of core−shell magnetoelectric[60] materials.

DOI: 10.1021/acs.jpcc.6b12461
J. Phys. Chem. C 2017, 121, 4352−4362

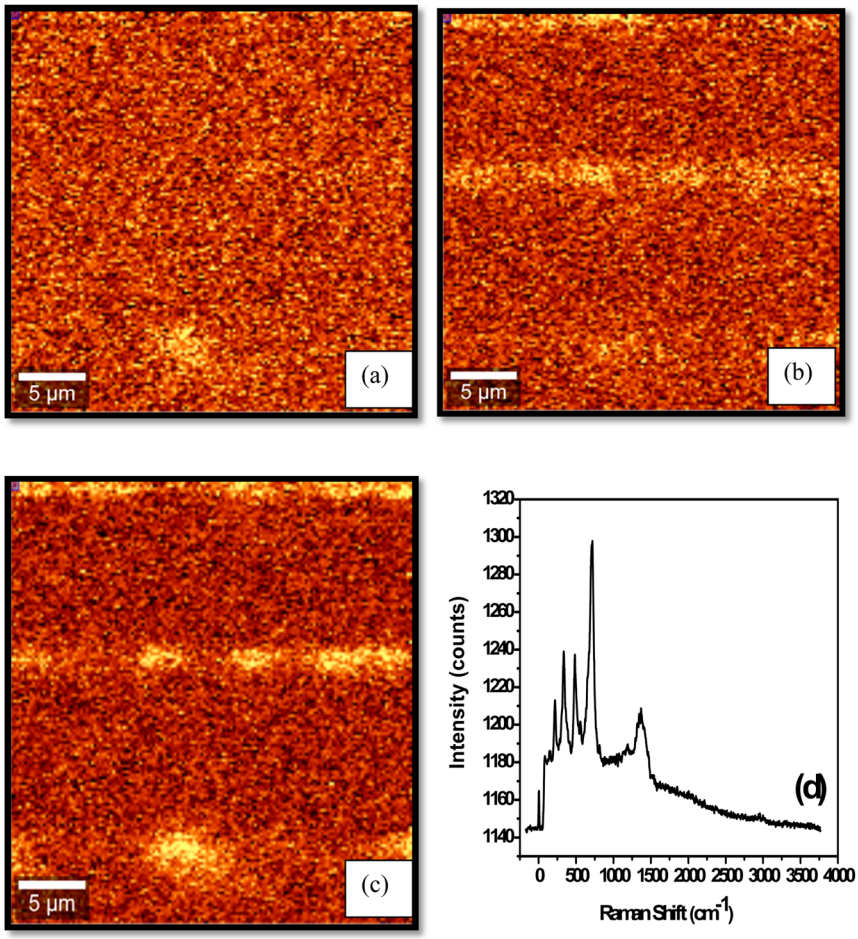

Figure 8. Domain structure mapping of (a) MFO@BTO1, (b) MFO@BTO2, and (c) MFO@BTO3 by confocal Raman spectroscopy. (d) Confocal Raman spectra of MFO@BTO3 Raman image.

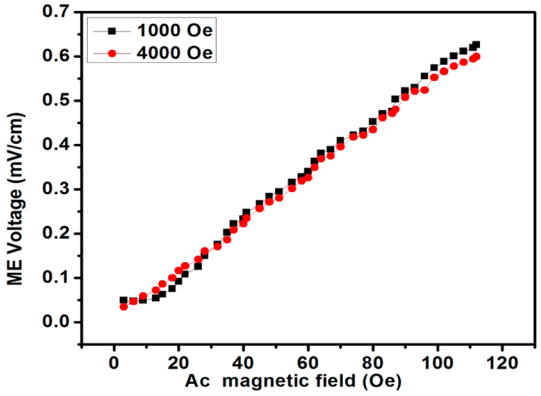

Figure 9. ME voltage vs ac magnetic field with constant dc bias magnetic field for BTO.

3.2. Raman Spectroscopic Studies. $MgFe_2O_4$ is a spinel ferrite with $Fd\bar{3}m$ crystal symmetry. It is a partially inverse spinel;[40] i.e., some of the Mg^{2+} ions are not positioned on tetrahedral sites only but also appear on the octahedral sites. The crystal symmetry $Fd\bar{3}m$ defines five Raman active modes in the center of Brillouine zone: $\Gamma = A_{1g} + E_g + 3F_{2g}$. Observed Raman spectra of $MgFe_2O_4$, $BaTiO_3$, and core−shell particles with $MgFe_2O_4$ core and $BaTiO_3$ shell (MFO@BTO3) are shown in Figure 13. The spectra of core−shell nanoparticles (Figure 13a) are almost identical to the spectrum of their core material, $MgFe_2O_4$ (Figure 13b). The assignation of the modes was performed according to the literature data for $MgFe_2O_4$ and similar spinels.[61] Three F_{2g} modes present in the pure $MgFe_2O_4$ and core−shell particles are positioned at 212, 487, and 550 cm^{-1}. The mode positioned at 329 cm^{-1} was assigned to the E_g vibration, whereas the mode positioned at ~706 cm^{-1} with a broad shoulder at ~654 cm^{-1} was assigned to the A_{1g} vibration. Correlation of the highest wavenumber mode, A_{1g}, with particular atomic movements is not consistent with the literature data reported so far. This mode represents symmetric breathing vibration of oxygen atoms around cation on the tetrahedral position,[62] but the question of whether the cation positioned on the octahedral site influences the wavenumber of this mode remains opened. Hosterman[63] in his thesis compared the literature A_{1g} mode wavenumber values for a normal spinel ZnB_2O_4 (B = Cr, Fe), where trivalent B cations are positioned on octahedral sites only and concluded that the discrepancy between the wavenumber values of A_{1g} mode in $ZnCr_2O_4$ and $ZnFe_2O_4$ is too large if it is presumed that octahedral site cations do not influence A_{1g} mode.[63] Furthermore, splitting of the Raman A_{1g} mode in several inverse or partially inverse spinels was reported by Errandonea,[64] and this was explained by the fact that, both types of cations are present on the octahedral sites which results in different wavenumbers of A_{1g} vibrational modes. Such splitting was observed in $MgFe_2O_4$@$BaTiO_3$ core−shell particles. Weak intensity modes positioned at 223, 298, and 411 cm^{-1} were also observed in the Raman

DOI: 10.1021/acs.jpcc.6b12461
J. Phys. Chem. C 2017, 121, 4352−4362

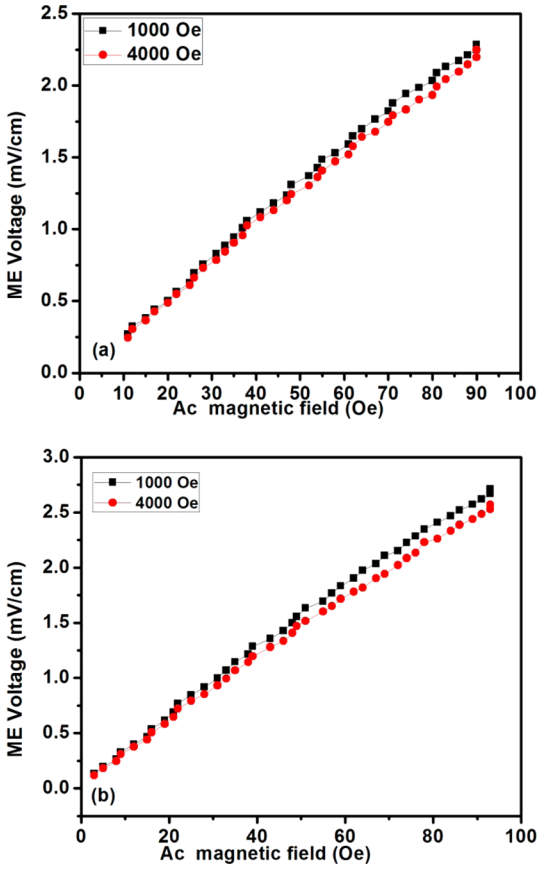

Figure 10. ME voltage vs ac magnetic field with constant dc bias magnetic field for (a) MFO@BTO1 and (b) MFO@BTO3.

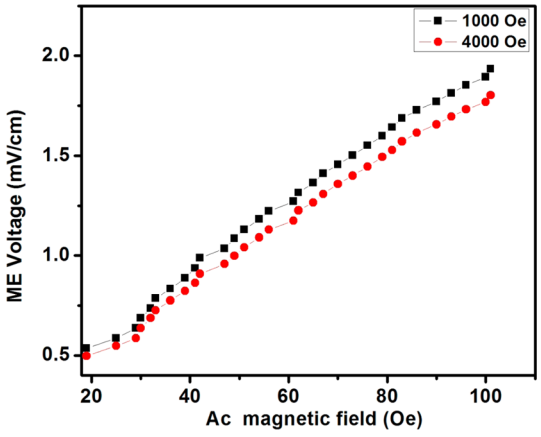

Figure 11. ME voltage vs ac magnetic field with constant dc bias magnetic field for MFO/BTO3 composite.

spectra of pure $MgFe_2O_4$ and $MgFe_2O_4$@$BaTiO_3$ core−shell particles (Figure 13a). These modes are marked with arrows in Figure 13a and represent hematite vibrations.[65] The appearance of these modes leads to the conclusion that hematite phase is present in small amounts and randomly distributed in the shell. Positions of the A_{1g} higher wavenumber mode differ slightly in the spectrum obtained from the hematite−containing surrounding (blue curve) and the hematite free surrounding (pink curve) shown in Figure 13a. This can be ascribed to the decrease in Fe^{3+} concentration in the shells due to the formation of iron oxide phase.

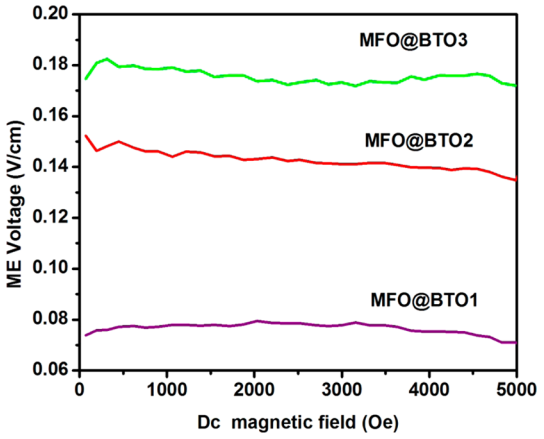

Figure 12. Variation of ME voltage as a function of dc magnetic field.

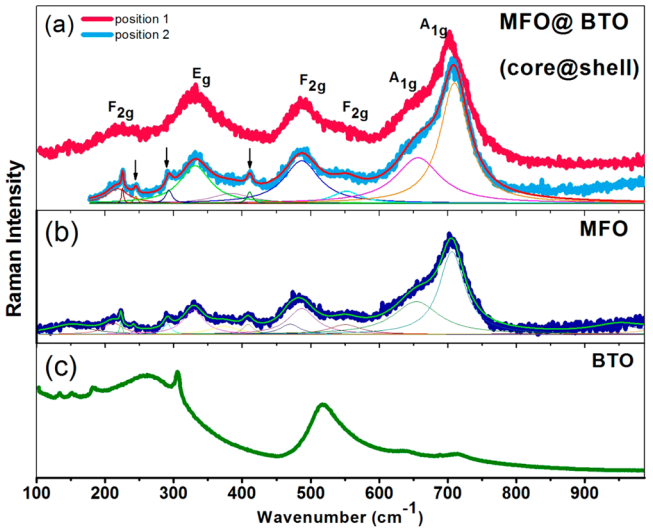

Figure 13. Raman spectra of (a) core−shell $MgFe_2O_4$@$BaTiO_3$ (MFO@BTO3) particles, (b) $MgFe_2O_4$ (MFO), and (c) $BaTiO_3$ (BTO).

Pink and blue curves from the graph (Figure 13a) represent spectra obtained from two different positions on the sample. The blue spectrum is deconvoluted with Lorentzian profile and the fit (red curve) is shown in graph a. The arrows present the modes of the hematite phase.

Raman active phonons of the $BaTiO_3$ tetragonal phase which belong to *P4 mm* crystal symmetry are $\Gamma = 3A_1+B+4E$.[66] In $BaTiO_3$ (Figure 13c), the most intense modes of tetragonal phase are positioned at 260, 305, 519, and 715 cm^{-1}. A broad peak at 264 cm^{-1} belong to the A_1 (TO) mode, whereas sharper peaks at 305, 519, and 715 cm^{-1} belong to the [B_1, E(TO + LO)], [A_1(TO), E(TO)], and [A_1(LO), E(LO)] modes.[66]

Data presented in Table 3 show that some of the vibrational modes in the spectrum of $MgFe_2O_4$,[67] positioned at 329 and 706 cm^{-1} were shifted in the spectra of core−shell particles and broadened. This is due to the influence of $BaTiO_3$ modes positioned at 260, 305, and 715 cm^{-1}. Unfortunately, the latter $BaTiO_3$ modes are broad and of low intensity which is why they could not be modeled in order to obtain meaningful results; their existence is confirmed by the broadening of $MgFe_2O_4$ modes. The narrowing of the mode at 649 cm^{-1} is probably caused by the higher crystallinity in the spots where less of

DOI: 10.1021/acs.jpcc.6b12461
J. Phys. Chem. C 2017, 121, 4352−4362

Table 3. Fit-Obtained Values of the Characteristic Peak Wavenumbers and the Widths in the Spectra of $MgFe_2O_4$ and $MgFe_2O_4/BaTiO_3$ Core−Shell Particles at Two Different Positions

$MgFe_2O_4$		$MgFe_2O_4/BaTiO_3$ position 1		$MgFe_2O_4/BaTiO_3$ position 2	
ω (cm^{-1})	fwhm (cm^{-1})	ω (cm^{-1})	fwhm (cm^{-1})	ω (cm^{-1})	fwhm (cm^{-1})
212	34	218	39	219	53
329	36	331	55	329	56
487	48	487	50	488	45
550	50	552	50	535	53
654	80	656	80	649	56
706	45	709	50	704	55

hematite is present and therefore less iron vacancies in the original lattice.

4. CONCLUSION

The 0−0 type multiferroic magnesium ferrite @ barium titanate core−shell structure, with enhanced coupling between the electric and magnetic phases was proficiently developed. The vibrational modes in the spectrum of $MgFe_2O_4$ and the shift in the spectra of core−shell particles was efficiently studied by micro Raman spectra. Raman spectroscopy indicated the encapsulation of ferrite inside the ferroelectric particles. The Raman spectrum of the core−shell particles was excitingly found to be almost identical to the spectrum of their core material, $MgFe_2O_4$. Confocal Raman mapping was used to identify the domain arrangement within the core−shell structure. Existence of strong spin−phonon coupling and mapping of ferromagnetic and ferroelectric domains within the core−shell structure was made possible through confocal Raman spectroscopy. The clear indication of strong magnetoelectric coupling realized in the developed core−shell hybrid structures, which is not present in any of the parent phases (MFO or BTO) and is greater than that achieved in the multiferroic composite sample at room temperature, highlights the significance of the core−shell architecture. Remarkably, among the developed core−shell structures, enhanced coupling with a large magnetoelectric coupling coefficient value is identified in the multiferroic core−shell structure with a comparatively larger ferromagnetic core (diameter ∼20 nm) within the ferroelectric BTO shell. It is worth finding out that, the magnetoelectric coupling effects in hybrid multiferroic structures are dependent on the geometry of magnetic phase and is enhanced by enrichment of the ferromagnetic phase (increasing magnetic core sizes). The observations unearthed in this study are promising in the deeper perception of the dynamics of magnetoelectric coupling that originate between ferromagnetic and ferroelectric phases in hybrid multiferroic systems and proves helpful when employing these materials for futuristic device applications.

AUTHOR INFORMATION

Corresponding Authors

*(O.S.O.) E-mail: oluwafemi.oluwatobi@gmail.com.
*(N.K.) E-mail: nkkalarikkal@mgu.ac.in.

ORCID

Oluwatobi Samuel Oluwafemi: 0000-0001-8964-5646
Sabu Thomas: 0000-0003-4726-5746

Notes

The authors declare no competing financial interest.

ACKNOWLEDGMENTS

The authors acknowledge the DST-Sophisticated Analytical Instruments Facility (SAIF), Mahatma Gandhi University, and the financial support from the DST-Government of India for funding through Nano Mission, FIST, and PURSE programs and the UGC-Government of India through the SAP program. N.K. also acknowledges the KSCSTE-Government of Kerala for funding. B.R. acknowledges SERB- Govt. of India (ECR/2015/000536) for providing financial assistance. S.A. and Z.D.M. acknowledge the support from the project OI 171032, and S.L. from the projects OI171037 and III41011, Ministry of Education, Science and Technological Development of the Republic of Serbia.

REFERENCES

(1) Kim, T. Y.; Song, S.; Jang, H. M.; Peters, J. A.; Jeong, Y. K. Piezoelectrically Enhanced Exchange Bias in Multiferroic Heterostructures. *J. Mater. Chem. C* **2014**, *2*, 8018−8022.

(2) Fernandes Vaz, C. A.; Staub, U. Artificial Multiferroic Heterostructures. *J. Mater. Chem. C* **2013**, *1*, 6731−6742.

(3) Jones, S. P.; Gaw, S. M.; Doig, K. I.; Prabhakaran, D.; Hétroy Wheeler, E. M.; Boothroyd, A. T.; Lloyd-Hughes, J. High-Temperature Electromagnons in the Magnetically Induced Multiferroic Cupric Oxide Driven by Intersublattice Exchange. *Nat. Commun.* **2014**, *5*, 3787.

(4) Scott, J. F. Applications of Magnetoelectrics. *J. Mater. Chem.* **2012**, *22*, 4567.

(5) Van Aken, B. B.; Rivera, J. P.; Schmid, H.; Fiebig, M. Observation of Ferrotoroidic Domains. *Nature* **2007**, *449*, 702−705.

(6) Lee, J. H.; Fang, L.; Vlahos, E.; Ke, X.; Jung, Y. W.; et al. A Strong Ferroelectric Ferromagnet Created by Means of Spin-Lattice Coupling. *Nature* **2010**, *466*, 954−958.

(7) Ramesh, R. Materials Science: Emerging Routes to Multiferroics. *Nature* **2009**, *461*, 1218−1219.

(8) Naik, V. B.; Mahendiran, R. Magnetic and Magnetoelectric Studies in Pure and Cation Doped $BiFeO_3$. *Solid State Commun.* **2009**, *149*, 754−758.

(9) Naik, V. B.; Mahendiran, R. Electrical, Magnetic, Magnetodielectric, and Magnetoabsorption Studies in Multiferroic $GaFeO_3$. *J. Appl. Phys.* **2009**, *106* (12), 123910.

(10) Gilioli, E.; Ehm, L. High Pressure and Multiferroics Materials: A Happy Marriage. *IUCrJ* **2014**, *1*, 590−603.

(11) Trassin, M. Low Energy Consumption Spintronics Using Multiferroic Heterostructures. *J. Phys.: Condens. Matter* **2016**, *28* (3), 033001.

(12) Scott, J. F. Room-Temperature Multiferroic Magnetoelectrics. *NPG Asia Mater.* **2013**, *5*, e72.

(13) Popov, M.; Sreenivasulu, G.; Petrov, V. M.; Chavez, F. A.; Srinivasan, G. High Frequency Magneto-Dielectric Effects in Self-Assembled Ferrite-Ferroelectric Core-Shell Nanoparticles. *AIP Adv.* **2014**, *4*, 097117.

(14) Cano, A.; Kats, E. I. Electromagnon Excitations in Modulated Multiferroics. *Phys. Rev. B: Condens. Matter Mater. Phys.* **2008**, *78* (1), 012104.

DOI: 10.1021/acs.jpcc.6b12461
J. Phys. Chem. C 2017, 121, 4352−4362

(15) Morelli, A.; Johann, F.; Burns, S. R.; Douglas, A.; Gregg, J. M. Deterministic Switching in Bismuth Ferrite Nanoislands. *Nano Lett.* **2016**, *16* (8), 5228−5234.
(16) Bahoosh, S. G.; Wesselinowa, J. M.; Trimper, S. Modified Heisenberg Model for the Zig-Zag Structure in Multiferroic RMn_2O_5. *J. Appl. Phys.* **2015**, *118* (8), 084102−1.
(17) Jeong, D. S.; Thomas, R.; Katiyar, R. S.; Scott, J. F.; Kohlstedt, H.; Petraru, A.; Hwang, C. S. Emerging Memories: Resistive Switching Mechanisms and Current Status. *Rep. Prog. Phys.* **2012**, *75*, 076502.
(18) Bibes, M.; Barthélémy, A. Multiferroics: Towards a Magnetoelectric Memory. *Nat. Mater.* **2008**, *7*, 425−426.
(19) Scott, J. F. Data Storage Multiferroic memories. *Nat. Mater.* **2007**, *6*, 256.
(20) Chung, A.; Deen, J.; Lee, J. S.; Meyyappan, M. Nanoscale Memory Devices. *Nanotechnology* **2010**, *21*, 412001.
(21) Wang, J.; Fu, Z.; Liu, M.; Sun, S.; Huang, H.; Li, L.; et al. Low Magnetic Field Response Single-Phase Multiferroics under High Temperature. *Mater. Horiz.* **2015**, *2*, 232−236.
(22) Martin, L. W. Engineering Functionality in the Multiferroic $BiFeO_3$− Controlling Chemistry to Enable Advanced Applications. *Dalt. Trans.* **2010**, *39*, 10813.
(23) Rao, C. N. R.; Serrao, C. R. New Routes to Multiferroics. *J. Mater. Chem.* **2007**, *17*, 4931−4938.
(24) Wang, W.; Zhao, J.; Wang, W.; Gai, Z.; Balke, N.; Chi, M.; Lee, H. N.; Tian, W.; Zhu, L.; Cheng, X.; Keavney, D. J.; et al. Room-Temperature Multiferroic Hexagonal $LuFeO_3$ Films. *Phys. Rev. Lett.* **2013**, *110*, 237601.
(25) Chang, C. M.; Mani, B. K.; Lisenkov, S.; Ponomareva, I. Thermally Mediated Mechanism to Enhance Magnetoelectric Coupling in Multiferroics. *Phys. Rev. Lett.* **2015**, *114*, 177205.
(26) Sun, D.; Fang, M.; Xu, X.; Jiang, L.; Guo, H.; Wang, Y.; Yang, W.; Yin, L.; Snijders, P. C.; Ward, T. Z.; Gai, Z.; et al. Active Control of Magnetoresistance of Organic Spin Valves Using Ferroelectricity. *Nat. Commun.* **2014**, *5*, 1−12.
(27) Pradhan, D. K.; Puli, V. S.; Kumari, S.; Sahoo, S.; Das, P. T.; Pradhan, K.; Katiyar, R. S.; et al. Studies of Phase Transitions and Magnetoelectric Coupling in PFN-CZFO Multiferroic Composites. *J. Phys. Chem. C* **2016**, *120* (3), 1936−1944.
(28) Etier, M.; Schmitz-Antoniak, C.; Salamon, S.; Trivedi, H.; Gao, Y.; Nazrabi, A.; Landers, J.; Gautam, D.; Winterer, M.; Schmitz, D.; et al. Magnetoelectric Coupling on Multiferroic Cobalt Ferrite−Barium Titanate Ceramic Composites with Different Connectivity Schemes. *Acta Mater.* **2015**, *90*, 1−9.
(29) Tadi, R.; Kim, Y. I.; Sarkar, D.; Kim, C.; Ryu, K. S. Magnetic and Electrical Properties of Bulk $BaTiO_3$+$MgFe_2O_4$ Composite. *J. Magn. Magn. Mater.* **2011**, *323*, 564−568.
(30) Koferstein, R.; Walther, T.; Hesse, D.; Ebbinghaus, S. G. Fine-Grained $BaTiO_3$-$MgFe_2O_4$ Composites Prepared by a Pechini-Like Process. *J. Alloys Compd.* **2015**, *638*, 141−147.
(31) Tan, S. Y.; Shannigrahi, S. R.; Tan, S. H.; Tay, F. E. H. Synthesis and Characterization of Composite $MgFe_2O_4$−$BaTiO_3$ Multiferroic System. *J. Appl. Phys.* **2008**, *103*, 094105.
(32) Shi, D. W.; Javed, K.; Ali, S. S.; Chen, J. Y.; Li, P. S.; Zhao, Y. G.; Han, X. F. Exchange-Biased Hybrid Ferromagnetic−Multiferroic Core−Shell Nanostructures. *Nanoscale* **2014**, *6*, 7215.
(33) Sreenivasulu, G.; Popov, M.; Chavez, F. A.; Hamilton, S. L.; Lehto, P. R.; Srinivasan, G. Controlled Self-Assembly of Multiferroic Core-Shell Nanoparticles Exhibiting Strong Magneto-Electric Effects. *Appl. Phys. Lett.* **2014**, *104*, 052901.
(34) Srinivasan, G.; Sreenivasulu, G.; Benoit, C.; Petrov, V. M.; Chavez, F. Magnetic Field Directed Assembly of Superstructures of Ferrite-Ferroelectric Core-Shell Nanoparticles and Studies on Magneto-Electric Interactions. *J. Appl. Phys.* **2015**, *117*, 17B904.
(35) Verma, K. C.; Kotnala, R. K. Nanostructural and Lattice Contributions to Multiferroism in $NiFe_2O_4$/$BaTiO_3$. *Mater. Chem. Phys.* **2016**, *174*, 120−128.
(36) Curecheriu, L. P.; Buscaglia, M. T.; Buscaglia, V.; Mitoseriu, L.; Postolache, P.; Ianculescu, A.; Nanni, P. Functional Properties of $BaTiO_3$−$Ni_{0.5}Zn_{0.5}Fe_2O_4$ Magnetoelectric Ceramics Prepared from Powders with Core-Shell Structure. *J. Appl. Phys.* **2010**, *107*, 104106.
(37) Chaudhuri, A.; Mandal, K. Large Magnetoelectric Properties in $CoFe_2O_4$:$BaTiO_3$ Core−Shell Nanocomposites. *J. Magn. Magn. Mater.* **2015**, *377*, 441−445.
(38) Koferstein, R.; Walther, T.; Hesse, D.; Ebbinghaus, S. G. Preparation and Characterization of Nanosized Magnesium Ferrite Powders by a Starch-Gel Process and Corresponding Ceramics. *J. Mater. Sci.* **2013**, *48*, 6509−6518.
(39) Rao, C. N. R.; Sundaresan, A.; Saha, R. Multiferroic and Magnetoelectric Oxides: The Emerging Scenario. *J. Phys. Chem. Lett.* **2012**, *3*, 2237−2246.
(40) Wu, H. C.; Mauit, O.; Coileáin, C. O.; Syrlybekov, A.; et al. Magnetic and Transport Properties of Epitaxial Thin Film $MgFe_2O_4$ Grown on MgO (100) by Molecular Beam Epitaxy. *Sci. Rep.* **2014**, *4*, 7012.
(41) Frey, N. A.; Peng, S.; Cheng, K.; Sun, S. Magnetic Nanoparticles: Synthesis, Functionalization, and Applications in Bioimaging and Magnetic Energy Storage. *Chem. Soc. Rev.* **2009**, *38* (9), 2532−2542.
(42) Augustine, R.; Abraham, A. R.; Kalarikkal, N.; Thomas, S. Monitoring and Separation of Food-Borne Pathogens using Magnetic Nanoparticles. *Novel Approaches of Nanotechnology in Food* **2016**, 271−312.
(43) Smith, M. B.; Page, K.; Siegrist, T.; Redmond, P. L.; Walter, E. C.; Seshadri, R.; Brus, L. E.; Steigerwald, M. L. Crystal Structure and the Paraelectric-to-Ferroelectric Phase Transition of Nanoscale $BaTiO_3$. *J. Am. Chem. Soc.* **2008**, *130*, 6955−6963.
(44) Wang, B. Y.; Wang, H. T.; Singh, S. B.; Shao, Y. C.; Wang, Y. F.; Chuang, C. H.; Yeh, P. H.; Chiou, J. W.; Pao, C. W.; Tsai, H. M.; et al. Effect of Geometry on the Magnetic Properties of $CoFe_2O_4$−$PbTiO_3$ Multiferroic Composites. *RSC Adv.* **2013**, *3*, 7884.
(45) Stroppa, A.; Picozzi, S. Hybrid Functional Study of Proper and Improper Multiferroics. *Phys. Chem. Chem. Phys.* **2010**, *12*, 5405−16.
(46) Dela Cruz, C. R.; Yen, F.; Lorenz, B.; Park, S.; Cheong, S. W.; Gospodinov, M. M.; Ratcliff, W.; Lynn, J. W.; Chu, C. W. Evidence for Strong Spin-Lattice Coupling in Multiferroic RMn_2O_5 (R= Tb, Dy, Ho) via Thermal Expansion Anomalies. *J. Appl. Phys.* **2006**, *99*, 08R103.
(47) Gupta, M. K.; Mittal, R.; Zbiri, M.; Sharma, N.; Rols, S.; Schober, H.; Chaplot, S. L. Spin-Phonon Coupling and High-Temperature Phase Transition in Multiferroic Material $YMnO_3$. *J. Mater. Chem. C* **2015**, *3*, 11717−11728.
(48) Ramirez, M. O.; Krishnamurthi, M.; Denev, S.; Kumar, A.; Yang, S. Y.; Chu, Y. H.; Saiz, E.; Seidel, J.; Pyatakov, A. P.; Bush, A.; et al. Two-Phonon Coupling to the Antiferromagnetic Phase Transition in Multiferroic $BiFeO_3$. *Appl. Phys. Lett.* **2008**, *92*, 022511.
(49) Jaiswal, A.; Das, R.; Maity, T.; Vivekanand, K.; Adyanthaya, S.; Poddar, P. Temperature-Dependent Raman and Dielectric Spectroscopy of $BiFeO_3$ Nanoparticles: Signatures of Spin-Phonon and Magnetoelectric Coupling. *J. Phys. Chem. C* **2010**, *114*, 12432−12439.
(50) Santos, Y. P.; Andrade, B. C.; Machado, R.; Macêdo, M. A. Spin−Phonon Coupling in Multiferroic $Ba_{1.6}Sr_{1.4}Co_2$ $Fe_{24}O_{41}$. *J. Magn. Magn. Mater.* **2014**, *364*, 95−97.
(51) Sklyadneva, I. Y.; Heid, R.; Bohnen, K. P.; Echenique, P. M.; Benedek, G.; Chulkov, E. V. The Effect of Spin−Orbit Coupling on the Surface Dynamical Properties and Electron−Phonon Interaction of Tl (0001). *J. Phys. Chem. A* **2011**, *115* (25), 7352−7355.
(52) Trivedi, H.; Shvartsman, V. V.; Lupascu, D. C.; Medeiros, M. S. A.; Pullar, R. C.; Kholkin, A. L.; Shur, V. Y.; et al. Local Manifestations of a Static Magnetoelectric Effect in Nanostructured $BaTiO_3$−$BaFe_{12}$ O_9 Composite Multiferroics. *Nanoscale* **2015**, *7* (10), 4489−4496.
(53) Rubio-Marcos, F.; Del Campo, A.; Marchet, P.; Fernández, J. F. Ferroelectric Domain Wall Motion Induced by Polarized Light. *Nat. Commun.* **2015**, *6*, 6594.
(54) Ummer, R. P.; B, R.; Thevenot, C.; Rouxel, D.; Thomas, S.; Kalarikkal, N. Electric, Magnetic, Piezoelectric and Magnetoelectric Studies of Phase Pure ($BiFeO_3$−$NaNbO_3$)−(P(VDF-TrFE)) Nano-

DOI: 10.1021/acs.jpcc.6b12461
J. Phys. Chem. C 2017, 121, 4352−4362

composite Films Prepared by Spin Coating. *RSC Adv.* **2016**, *6*, 28069−28080.
(55) Muneeswaran, M.; Jegatheesan, P.; Gopiraman, M.; Kim, I. S.; Giridharan, N. V. Structural, Optical, and Multiferroic Properties of Single Phased $BiFeO_3$. *Appl. Phys. A: Mater. Sci. Process.* **2014**, *114*, 853−859.
(56) Nguyen, T. H. L.; Laffont, L.; Capsal, J. F.; Cottinet, P. J.; Lonjon, A.; Dantras, E.; Lacabanne, C. Magnetoelectric Properties of Nickel Nanowires-P(VDF−TrFE) Composites. *Mater. Chem. Phys.* **2015**, *153*, 195−201.
(57) Stephanovich, V. A.; Laguta, V. V. Transversal Spin Freezing and Re-entrant Spin Glass Phases in Chemically Disordered Fe-Containing Perovskite Multiferroics. *Phys. Chem. Chem. Phys.* **2016**, *18*, 7229−7234.
(58) Meher, K. R. S. P.; Martin, C.; Caignaert, V.; Damay, F.; Maignan, A. Multiferroics and Magnetoelectrics: A Comparison Between Some Chromites and Cobaltites. *Chem. Mater.* **2014**, *26*, 830−836.
(59) Woldu, T.; Raneesh, B.; Reddy, M. V. R.; Kalarikkal, N. Grain Size Dependent Magnetoelectric Coupling of $BaTiO_3$ Nanoparticles. *RSC Adv.* **2016**, *6*, 7886−7892.
(60) Nuraje, N.; Su, K. Perovskite Ferroelectric Nanomaterials. *Nanoscale* **2013**, *5*, 8752−80.
(61) Wang, Z.; Lazor, P.; Saxena, S. K.; O'Neill, H. St. C. High Pressure Raman Spectroscopy of Ferrite $MgFe_2O_4$. *Mater. Res. Bull.* **2002**, *37* (8), 1589−1602.
(62) Wang, Z.; Schiferl, D.; Zhao, Y.; O'Neill, H. St. C. High Pressure Raman Spectroscopy of Spinel-Type Ferrite $ZnFe_2O_4$. *J. Phys. Chem. Solids* **2003**, *64*, 2517−2523.
(63) Hosterman, B. D. *Raman Spectroscopic Study of Solid Solution Spinel Oxides*. Thesis. University of Nevada, Las Vegas: 2011.
(64) Errandonea, D.; Kumar, R. S.; Manjón, F. J.; Ursaki, V. V.; Rusu, E. V. Post-Spinel Transformations and Equation of State in $ZnGa_2O_4$: Determination at High Pressure by in situ X-ray Diffraction. *Phys. Rev. B: Condens. Matter Mater. Phys.* **2009**, *79*, 024103.
(65) De Faria, D. L. A.; Venâncio Silva, S. V.; De Oliveira, M. T. Raman Microspectroscopy of Some Iron Oxides and Oxyhydroxides. *J. Raman Spectrosc.* **1997**, *28*, 873−878.
(66) Shiratori, C.; Pithan, J.; Dornseiffer; Waser, R. Raman Scattering Studies on Nanocrystalline $BaTiO_3$ Part II—consolidated polycrystalline ceramics. *J. Raman Spectrosc.* **2007**, *38* (10), 1300−1306.
(67) Perumbilavil, S.; Sridharan, K.; Abraham, A. R.; Janardhanan, H. P.; Kalarikkal, N.; Philip, R. Nonlinear Transmittance and Optical Power Limiting in Magnesium Ferrite Nanoparticles: Effects of Laser Pulsewidth and Particle Size. *RSC Adv.* **2016**, *6*, 106754−106761.

DOI: 10.1021/acs.jpcc.6b12461
J. Phys. Chem. C 2017, 121, 4352−4362

Non-thermal plasma for revalorization of a complex waste substrate in open lactic acid fermentation

Aleksandra Djukić-Vuković[1], Saša Lazović[2], Dragana Mladenović[1], Zorica Knežević-Jugović[1], Jelena Pejin[3], Ljiljana Mojović[1]

[1]Department of Biochemical Engineering and Biotechnology, Faculty of Technology and Metallurgy, University of Belgrade, Serbia
[2]Institute of Physics Belgrade, University of Belgrade, Zemun, Serbia
[3]Faculty of Technology, University of Novi Sad, Novi Sad, Serbia

Correspondence: Dr. Aleksandra Djukić-Vuković (adjukic@tmf.bg.ac.rs). Department of Biochemical Engineering and Biotechnology, Faculty of Technology and Metallurgy, University of Belgrade, Karnegijeva 4, 11120 Belgrade, Serbia.

Abstract

Purpose: Stillage is the main by-product of bioethanol production and cost of its treatment significantly affects the economy of bioethanol production. Utilization of stillage for fermentative lactic acid (LA) and biomass production improves sustainability of bioethanol production. Standard process of thermal sterilization of stillage for biorefinery purposes is energy demanding and is causing deterioration of valuable compounds present in stillage. Modern biorefinery processes require energy efficient recovery of nutrients from stillage at different scales.

Methods: We replaced standard sterilization with ultrasound (UT) and plasma (PT) treatments and observed a significant reduction in number of viable microorganisms in the stillage after PT and UT. After applied treatment, we initiated lactic acid fermentation (LAF) by *Lactobacillus rhamnosus* ATCC 7469. Concentration of LA is used to quantify the efficiency of stillage revalorization.

Results: We find that the highest LA productivity of 1.21 g/Lh and yield of 0.82 g/g are obtained after PT. While, UT of 10 min provides productivity of 1.02 g/Lh and LA yield of 0.69 g/g. The results are benchmarked against closed LAF. We achieved 20% better revalorization of stillage by PT when compared with conventional sterilization. An excellent L (+) LA stereoselectivity of 95.5% is achieved after PT LAF. From the aspect of energy efficiency, PT was three times lower than UT and almost ten times lower than thermal sterilization.

Conclusions: This way we achieved a simpler and energy efficient process for LA production on stillage in „open" fermentation. These are new findings in fermentative treatment of stillage or similar by-products and wastes for the benefit of industry, academia and policy making.

Keywords: biorefinery, non-thermal plasma, open lactic acid fermentation, stillage, ultrasound

1. Introduction

Distillery stillage is the main by-product of bioethanol production on renewable feedstock. It remains after distillation of bioethanol and depending on the feedstock used for bioethanol production COD values of stillage can reach up to 100 g/L [1,2]. Approximately 20L of stillage are produced per every liter of bioethanol and environmental burden of stillage disposal is high [2]. Stillage has to be treated in order to decrease its organic load and its revalorization through production of chemicals is increasing competitiveness of bioethanol [3,4]. Besides anaerobic digestion, stillage is most often used after drying for animal nutrition, as dried distillers' grains with solubles (DDGS) [2,5]. Nutrients from stillage could be recovered through other processes also, including its utilization as fertilizer [6] or as substrate for fermentative production of bacterial cellulose, fungal biomass, 1,3–propanediol, malic and lactic acid (LA) [7–12]. Among proposed fermentative processes on stillage, almost all are „closed" fermentations which include thermal sterilization of substrate [7,9–11]. Thermal sterilization is energy demanding, costly treatment; it is difficult to apply in large scale processes and part of the nutrients is lost after thermal treatment [13]. Alternative to these are „open" fermentations when substrate is used without prior sterilization and fermented under unsterile conditions by a mixed culture of microorganisms [14]. Open fermentations are simpler, lower in energy consumption than conventional closed fermentations on sterilized substrates and could be adapted to various renewable and waste substrates due to the evolution capacity of microbiota, if process is well controlled [14]. Lower productivities, lower optical purity of product and contamination are still challenges in open fermentations [14,15] in parallel with necessary improvements in extraction techniques [16]. Control of fermentation conditions and possibility to manipulate substrate microbiota are crucial for efficient open fermentations.

Non-thermal treatments are an alternative to standard thermal sterilization for control of microorganisms in agricultural and wastewater substrates [17]. These treatments should enable selective inactivation of undesired microorganisms from complex microbial communities like those in stillage [18,19] but also preserve species capable of producing desired chemicals, like lactic acid for example. Non-thermal plasmas generate abundance of highly reactive species at low temperatures thus enabling processing of sensitive materials [20] and avoidance of thermal degradation of the compounds present in treated media. Beside reactive oxidative species, the UV photons and pulsed electric field generated during plasma treatment (PT) could contribute to the overall effect [21,22]. In a complex media with high dry matter content like stillage, the effects of non-thermal plasma treatment have not been thoroughly examined since most of the studies were performed in water, water based media with low dry matter content or on solid surfaces [22–26].

The high-power ultrasound treatment (UT) can be used for decontamination due to the mechanical disruption and cavitation effects induced in samples [27]. The microbial inactivation by UT is highly dependent on substrate composition, types of microorganisms present in media and treatment conditions [26,27].

LAFs on cheap substrates like stillage attract great interest since the LA market size was valued at 2.08 billion US $ in 2016 and is expected to grow by annual growth rate of 16.3% until 2025

[28]. The demand for LA is mainly driven by increasing utilization of LA as a platform chemical and for poly-lactides – biocompatible and biodegradable polymers suitable for pharmaceutical and food applications [15,28]. The concentration of LA produced in LAF on stillage is used in our work to quantify the efficiency of stillage revalorization.

The main objective of this study is to investigate plasma and ultrasound in LAF on stillage as an alternative to standard sterilization processes. The mechanism of non-thermal plasma inactivation of *Lactobacillus acidophilus* and *Escherichia coli* in water and stillage as media is thoroughly studied. Furthermore, non-thermal plasma inactivation of indigenous stillage microbiota was compared with inactivation by ultrasound treatment. The stillage after different treatments was subjected to open or closed LAF to assess its revalorization potential through LA production with high-LA producing strain of *Lactobacillus rhamnosus* [29]. The parameters of LAFs in terms of LA concentration, optical purity, yield and productivity were studied and compared for various applied treatments. In addition, all treatments were compared from the aspect of energy efficiency.

2. Materials and Methods

2.1. Preparation of distillery stillage

The distillery stillage remained after bioethanol production on wasted bread was obtained from ethanol producing facility (Reahem d.o.o., Serbia) and used for preparation of media for LAF. Chemical composition of the stillage was determined as following: dry matter content (12.79 ± 0.31%), sugar concentration (11.19 ± 0.83 g/L), protein (63.91 ± 2.81 g/L), free amino-nitrogen (295.6 ± 1.5 mg/L), ash (31.2 ± 0.1 g/L), lipids (17.36 ± 1.84 g/L). The pH value in all samples was adjusted to 6.5. The stillage was subjected to various decontamination treatments: PT, UT and thermal sterilization and it was used as the substrate for LAFs. The standard thermal sterilization was performed in an autoclave (Sutjeska, Serbia, device power 5.25 kW) at 121 ^{o}C for 20 min.

2.2. Microorganism

Lactobacillus rhamnosus ATCC 7469 and *Lactobacillus acidophilus* ATCC 4356, homofermentative LA producing strains and *Escherichia coli* ATCC 25922 were obtained from American Type Culture Collection. The *L. rhamnosus* and *L. acidophilus* cultures were propagated at 37 °C in Man Rogosa Sharpe broth (MRS) under microaerophilic static conditions. *E. coli* culture was propagated at 37 °C in nutrient broth, under aerobic static conditions. Overnight cultures were used as an inoculum in experiments.

2.3. Non-thermal plasma treatment

2.3.1. The effect of non-thermal plasma on G (+) and G (-) bacteria in water and distillery stillage

These experiments were undertaken at the beginning of the study in order to determine how non-thermal plasma acts towards *E. coli* (a representative of G (-) bacteria) and *L. acidophilus* (a representative of G (+) bacteria) in water and stillage media.

In the first set of experiments, the samples of water and stillage (6 ml) were sterilized by autoclaving (Sutjeska, Serbia) at 121 ^{o}C for 20 min and inoculated by overnight cultures of *E. coli* and *L. acidophilus* in order to set initial number of viable cells in samples at around 10^5 CFU/ml. Immediately

after inoculation, the samples were transferred in glass Petri dishes and subjected to PT for 30 min (duration of treatment was selected after preliminary studies) by using plasma needle jet. All treatments were conducted using a plasma needle operating at 25 kHz in ambient air. Argon was used as a feed gas (2 slm flow rate) in order to reduce the breakdown voltage through Penning ionization. The operating power was 2 W. The distance between the needle tip and the samples was 1 cm. Detailed description of the plasma device is provided by [30]. No significant increase of temperature in samples has been observed during treatments. During the treatments, the samples were mixed. The schematic presentation is shown in **Fig.1a**.

The second set of experiments was performed in order to determine effect of plasma generated UV photons on microbial inactivation in water and stillage. The samples were prepared and treated in the same way as previously, but quartz glass was placed between plasma jet and sample to prevent other effects of PT except UV light. Graphical presentation is provided in **Fig.1b**. The samples of sterilized water and stillage inoculated by *E. coli* and *L. acidophilus* were subjected to the same procedure but without PT, as a control.

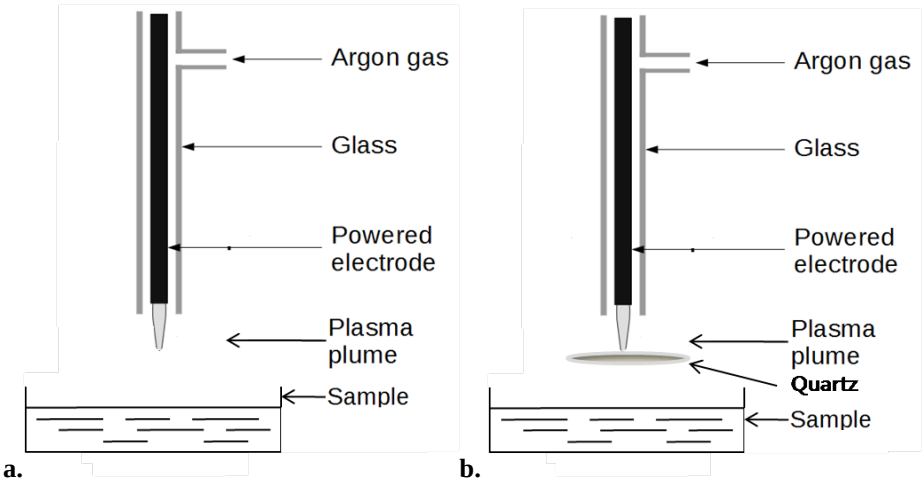

Fig.1 Schematic presentation of experimental setup for non-thermal PT (**a**) and assessment of contribution of the UV photons generated by plasma (**b**)

A number of viable cells in samples was determined using pour plate counting method on nutrient agar (for *E. coli*) and MRS agar (for *L. acidophilus*). Reduction in the number of viable microorganisms was presented as log reduction, log (N/N_0), where N - number of viable cells in samples and N_0- number of viable cells in control.

2.3.2. Non-thermal plasma treatment of distillery stillage for lactic acid fermentation

The samples of non-sterile stillage in 6 ml batches were placed in glass Petri dishes and treated by non-thermal plasma needle for 30 min (duration of treatment was selected after preliminary studies). The PT details are explained in Section 2.3.1. After the treatments and prior to LAF the samples were incubated under microaerophilic conditions at 41 ˚C (the same conditions which were used for LAF, studied in the second set of experiments and explained in section 2.5.) for 24 h in order to assess effect of

PT on the stillage microbiota. A number of total aerobic mesophilic bacteria in samples was determined using pour plate counting method as previously described on MRS agar as substrate [31].

2.4. High-power ultrasound treatment of distillery stillage

The stillage samples (60 ml) placed in 200 ml glass were treated by high-power ultrasound (Sonopuls HD 2200, Bandelin, Berlin, Germany, device power 200 W) with sonotrode TT 13 for 10 min (duration of treatment was selected after preliminary studies) at actual value of amplitude 75% and frequency of 20 kHz. After the treatment, in the first set of experiments, the samples were incubated under microaerophilic conditions at 41 ˚C for 24 h in order to examine the effect of treatment on the number of viable bacterial cells in the stillage. A number of total aerobic mesophilic bacteria in all samples was determined using pour plate counting method as previously described on MRS agar as plate substrate [31]. In the second set of experiments, the samples after the treatment were subjected to LAF (explained in section 2.5.).

2.5. Lactic acid fermentation

Stillage samples (60 ml per sample) treated by PT, UT and sterilized were subjected to fermentation for LA and probiotic biomass production. Untreated stillage was also subjected to LAF in the same way as treated samples. Initial glucose concentration in all samples was adjusted at around 35 g/L by addition of a 70% glucose solution and pH value was adjusted to 6.5. The LAFs were inoculated by 5% (v/v) *L. rhamnosus* ATCC 7469 while the untreated stillage was fermented by indigenous microbiota and considered as a control sample. The fermentations were performed as batch cultures with shaking in 200 ml flasks (100 rpm, KS 4000i control, IKA®, Germany), at 41 °C, under microaerophilic conditions maintained by using gas-pack system. These conditions were previously selected for the fermentation of stillage by *L. rhamnosus* ATCC 7469 [32]. During the LAF, the pH value in media was maintained at 6.5 by addition of 30% NaOH, in 4 h intervals.

2.6. Energy consumption calculations

The calculation of energy consumption of different treatments was performed by using manufacturers' information for lab scale equipment applied in experiments, taking into account a volume of samples subjected to the treatment. Energy of different treatments was calculated according to formula [33]:

$$E=P\times t, \quad (1)$$

where E is energy, P is power of device used for treatment and t is for duration of treatment.

The actual power of ultrasound treatment of stillage was calculated according to the procedure based on calorimetry and the following formula [26]:

$$P=m_s\times C_p\times \partial T/\partial t, \quad (2)$$

where m_s is mass of stillage media, C_p is specific heat at a constant pressure (J/gK), and $\partial T/\partial t$ is the slope at the origin of the curve (T is temperature, t is time). This equation is used to calculate the actual power of UT with a presumption that all of the power entering the system is dissipated as heat.

2.7. Methods of analysis

Chemical composition of the stillage was determined using methods described in our previous work [32]. The antioxidative activity of the stillage before and after the treatment against 2,2-Diphenyl-1-

picrylhydrazyl radical (DPPH, Sigma Aldrich, USA, CAS No. 1898-66-4) was determined as in the study of Jovanović et al. [34]. The stereoselectivity of produced LA was determined by enzymatic method (L(+)/D(-) LA assay, Megazyme®, Ireland). The LA and glucose concentrations during LAFs were determined by HPLC analysis. The samples were withdrawn from fermentation media, filtered through 0.22 μm filters (Minisart® syringe filters, Sartorius AG, Germany) and analysed by adapted HPLC method of Srivastava et al. [35]. In brief, the HPLC analysis was performed on the Dionex Ultimate 3000 Thermo Scientific (Waltham, USA) system. A reverse phase column (Hypersil gold C18, 150 mm × 4.6 mm, 5 μmL; Thermo Scientific, USA) at 65 ˚C was employed. Mobile phase was 5 mM H_2SO_4 (JT Baker, USA) with an elution rate 0.6 ml/min. Detection was performed by UV/VIS detector at 210 nm. All data acquisition and processing were done using Chromeleon Software. All chemicals used in experiments were of analytical grade and obtained from Sigma Aldrich, USA.

2.8. Statistical analysis

The experiments were done in duplicates, in three independent experiments. All values are expressed as means ± standard deviation. Mean values of treatments were compared by the analysis of variance (one-way ANOVA) followed by Tukey test for mean differences testing. Differences were considered significant at $p < 0.05$.

3. Results and Discussion

3.1. Interaction of non-thermal plasma and stillage – effect on chemical composition

The major challenge in processing of a complex medium such as stillage and similar wastewater is to achieve inactivation of specific microorganisms while preserving valuable compounds. Uchiyama *et al.* [36] report that argon cold atmospheric plasma as one used in our study can generate enormous amounts of $^{\cdot}OH$ radicals and H_2O_2 - the combination product of $^{\cdot}OH$ radicals in the aqueous phase even at distances of approximately 1 cm from the plasma source nozzle [36]. Superoxide $O_2^{\cdot -}$ can be present in the liquid phase in significant amounts, also [37,38]. Besides reactive oxygen species, plasma source is generating UV photons [39]. UV light has direct negative effect on bacteria and it can initiate photo dissociation of water and additional chemical reactions in treated media, therefore, interaction of non-thermal plasma with substrate like stillage is complex.

For effective fermentative processes, contents of reducing sugars and free amino-nitrogen are crucial and C/N ratio is most often determining productivity of the processes with LAB [32,40]. After the longest studied plasma treatment of 30 min, only a slight decrease in antioxidant activity was observed, from 93.5 ± 1.3% before to 90.1 ± 1.2% after the treatment. In other antioxidant rich substrates exposed to non-thermal plasma, no significant change in antioxidant activity was noted and it was confirmed using array of methods [41]. Some studies reported that antioxidants can act as scavengers for reactive species generated during PT [42]. Therefore, decrease in the antioxidant activity, as observed in our study, can be explained by a similar decrease in the concentration of enzymes and molecules associated to oxidative stress (vitamin C, polyphenol oxidase, peroxidase) which acted like scavengers in radical reactions initiated by PT [43].

The changes in the contents of reducing sugars and free amino nitrogen after the PT were not significant as confirmed by HPLC and spectrophotometric methods. Unlike other thermal methods, where

Millard reaction is occurring causing a loss of proteins and sugars by generation of melanoidins which are toxic for bacteria [44,45], non-thermal PT did not change the content of the most important compounds for stillage revalorization in LAF. Therefore, the effects of non-thermal PT on survival of different microorganisms in stillage were further examined.

3.2. Inactivation of model G (+) and G (-) bacteria in water and stillage by non-thermal plasma treatment

The effects of non-thermal PT on the survival of *E. coli*, G (-) bacteria, and *L. acidophilus*, G (+) bacteria, in different media were studied first. *E. coli*, being the most studied G (-) bacteria from the sanitary perspective [23], was used as a model of undesired G (-) microorganism in substrates. *L. acidophilus* was a representative of G (+) lactic acid bacteria (LAB) belonging to *Lactobacillus* sp. which are main constituents of indigenous stillage and food waste microbiota and responsible for LAF and silage of these substrates in uncontrolled conditions [18,19]. PTs were performed in water and stillage inoculated with the model G (-) and G (+) microorganisms.

The reduction in the number of viable *E. coli* and *L. acidophilus* in water and stillage by PT is presented in **Fig.2**. Reactive oxygen species ($^{\cdot}OH$, H_2O_2, $O_2^{\cdot -}$), reactive nitrogen species and UV photons created during PT all contribute to the antimicrobial effects of plasma [36–38]. We examined total microbial inactivation by PT and also isolated effects of UV photons generated by plasma on inactivation of bacteria (**Fig.2**).

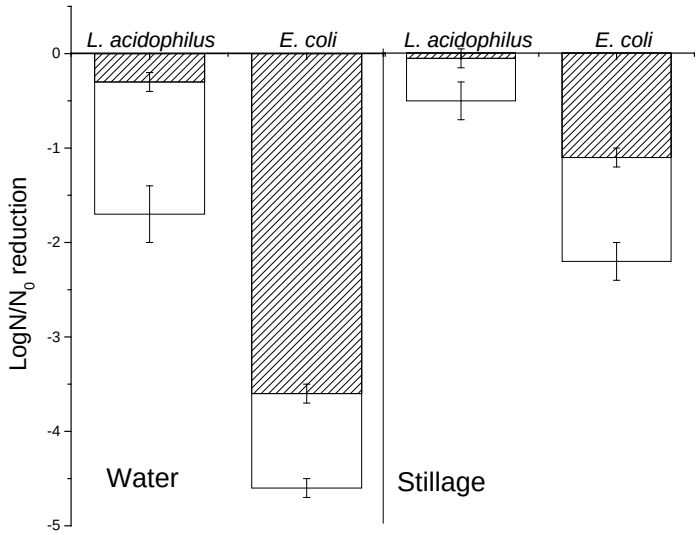

Fig.2 LogN reduction in the number of viable *E. coli* and *L. acidophilus* cells in different media. Symbols: white bars – inactivation by plasma generated radicals, patterned bars – inactivation by plasma generated UV photons

The higher reduction in viable cell number was obtained in water for both studied bacteria but in general *E. coli* was more sensitive to PT than *L. acidophilus* regardless of the media (**Fig.2**). The UV dependent inactivation of *E. coli* in water comprised up to 78% of the total logN reduction while in the

stillage it represented around 50% of the total inactivation. The dissimilarity in inactivation in different media is predominantly due to the UV dependent inactivation, especially for *E. coli*. Also, observed presence of scavengers in stillage (section 3.1.) could inactivate oxidative species produced by plasma source leading to lower microbial inactivation in stillage than in water. For *E. coli*, in absolute values, logN reduction mediated by UV photons decreased three times in stillage in comparison to water as media. The remaining contribution of reactive species to overall logN reduction has not been altered significantly with a change of media for stillage (**Fig.2**).

Because of turbidity of the stillage, the effect of UV radiation was less pronounced in stillage. These results emphasize the importance of penetration depth of UV photons and therefore a significance of the treatment chamber shape and overall treatment conditions, beside the most often reported volume of sample [39].

The inactivation of plankatonic *E. coli* cells in water obtained in this study was similar to results of Purevdorj et al. [46] and Puač et al. [23] but in more efficient time/volume ratio [23,46]. Geveke [47], Arrange et al. [48] and Mai-Prochnow et al. [49] reported higher susceptibility of G (-) bacteria to both UV light and cold PT in general. Boudam et al. [39] pointed that a fine adjustment of plasma operating conditions could increase the participation of UV light or radicals in overall bactericidal activity of PT. In this study, *E. coli* was found more susceptible to UV light component of PT compared to *L. acidophilus.* Therefore, PT in stillage enabled significant decrease in the number of *E. coli* while growth *L. acidophilus,* a representative of LAB, was minimally affected. This way, PT provided some selectivity in microbial inactivation in stillage, qualifying it as a promising strategy for treatment of stillage for revalorization in LAF.

3.3. Comparison of the effect of non-thermal plasma and ultrasound treatment on microorganisms in stillage

In the next set of experiments, PT was compared with high-power ultrasound. As an alternative non-thermal treatment, the UT method is already proven for microbial inactivation in less complex media like juices [26] and found effective in disintegration of fresh distillery spentwash [50]. The effects of non-thermal PT and UT on the growth of indigenous stillage microbiota were studied and the results are presented in **Fig.3**. The non-thermal PT caused higher reduction in viable cell number than UT. The number of viable cells did not increase during 24 h after the PT resulting in around 3 logN lower number of viable cells in PT than in control, untreated sample (**Fig.3**). Possible reason could be a slow growth and recovery of bacteria which survived the treatment. The lifetime of reactive species generated by plasma is extremely short but they initiate numerous reactions in media causing prolonged effects [51,52]. The application of plasma-activated water, water subjected to PT and then used for sanitation purposes, is based on this effect [53].

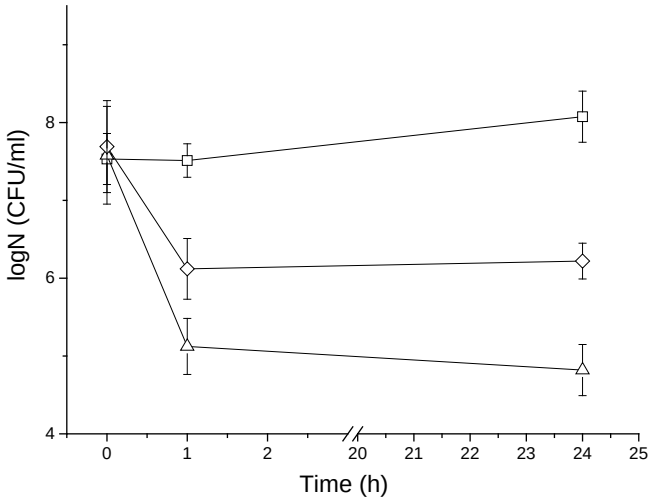

Fig.3 Number of viable cells of stillage microbiota in time after different treatments. Symbols: square – untreated stillage, romb – ultrasound treated stillage, triangle – plasma treated stillage

The decrease in the number of microorganisms achieved after PT (**Fig.3**) could be very useful for the control of contamination of the stillage. This provides longer storage time of stillage and more versatility in its utilizations. On the other hand, the presence of reactive species in stillage after PT can maybe negatively affect growth of LAB responsible for LA production and limit valorization potential of stillage for fermentation. Therefore, we inoculated stillages subjected to different treatments with a high L (+) LA producing strain *Lactobacillus rhamnosus* ATCC 7469 [7] and compared number of viable bacteria 24h after different treatments against untreated stillage also inoculated with *L. rhamnosus*. These results are presented in **Fig.4**.

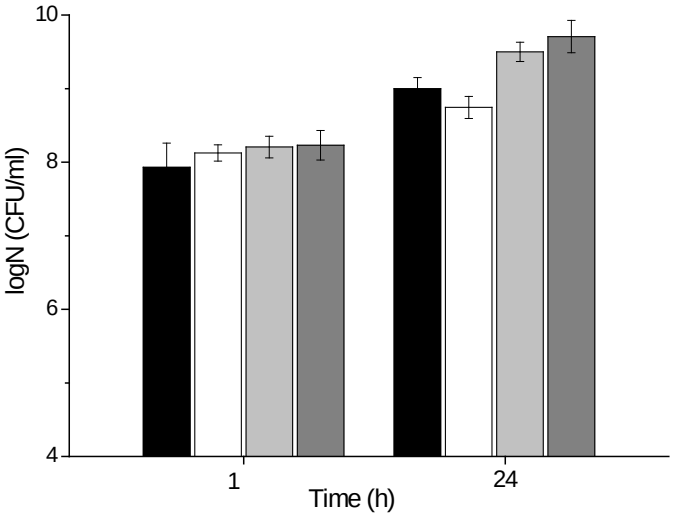

Fig.4 Number of viable cells in stillage after different treatments and inoculation with high LA producing strain *Lactobacillus rhamnosus* ATCC 7469. Symbols: black bars-untreated stillage, white bars- sterilized stillage, light grey bars- plasma treated stillage, dark grey stillage- ultrasound treated stillage.

When we compare the number of viable microorganisms after 24h with *L. rhamnosus* (**Fig.4**) and without *L. rhamnosus* (**Fig.3**), the higher number of bacteria was obtained with addition of *L. rhamnosus* than without it. Also, the growth was enhanced in PT and UT samples over untreated or sterilized (**Fig.4**). However, LAF performance of bacterial populations in PT and UT samples has to be benchmarked against untreated and conventional thermally treated samples in order to evaluate their potential for effective LA production.

3.4. Lactic acid fermentation of treated stillage by *Lactobacillus rhamnosus* ATCC 7469

The concentration of LA produced in LAF is used to quantify the efficiency of stillage revalorization. Additionally, optical purity of the produced LA is very important criteria for selection of the most promising process. *L. rhamnosus* ATCC 7469 is a high L (+) LA producing strain in mono culture, while in open fermentations on a complex media with mixed populations it can be difficult to achieve desired optical purity because different LAB produce different LA isomers. Two key factors have to be taken into account to achieve best treatment results - high sugar to LA conversion rate and stereoselective LA production.

After performing the treatments of the stillage (UT, PT, sterilization), all treated stillage samples and untreated control were inoculated with *L. rhamnosus* ATCC 7469 and subjected to LAF. The LA concentrations during open LAF, performed on PT, UT stillage and untreated stillage as substrates, and closed LAF, performed on sterilized stillage, are presented in **Fig.5**. In Table 1. the most important parameters of all studied LAFs are presented.

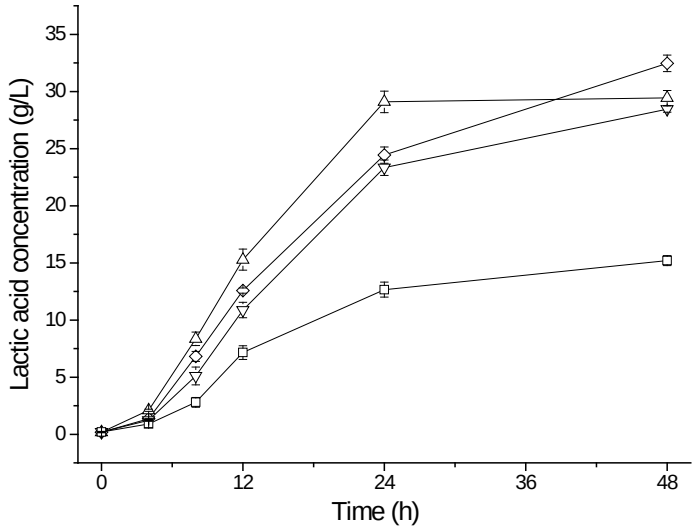

Fig.5 Kinetics of LA production during closed and open LAF on stillage subjected to different treatments. Symbols: square – untreated stillage, non-inoculated, open LAF; up triangle – non-thermal PT, inoculated by *L. rhamnosus* ATCC 7469, open LAF; diamond – non-thermal UT, inoculated by *L. rhamnosus* ATCC 7469, open LAF; down triangle – sterilized stillage, inoculated by *L. rhamnosus* ATCC 7469, closed LAF.

The most productive LAF was in PT samples directly followed by LAF in UT sample (**Fig.5**). Obviously, indigenous LAB preserved after treatments enhanced LA production. The highest LA

productivity in PT sample is a result of minimal deterioration of substrate because of absence of substrate heating during the treatment (section 3.1.) and significant suppression of competition of microorganisms in the substrate (**Fig.3**, **Fig.4**). Competition between indigenous microbiota of stillage and inoculated *L. rhamnosus* in untreated samples resulted in very low productivity of 0.57 g/Lh (Tab.1.) although this is still higher than the values reported for open LAF of kitchen waste [19] implying suitability of stillage as a substrate for LAF. Higher final LA concentration (in 48h) after UT can be explained by the presence of higher number of microorganisms in samples after UT (**Fig.4**). Although UT is often considered as non-thermal technique, ultrasound (10 min) elevated the temperature of stillage to 70˚C similarly to the reported UT of other substrates [26]. This plays additional role in microbial inactivation, deterioration of stillage and finally results in very similar productivities achieved in closed fermentation on sterilized stillage (0.97 g/Lh) and open fermentation on UT stillage (1.02 g/Lh). Besides yields and productivities, stereoselectivity of obtained LA is very important issue to be addressed.

In closed LAF, 97.2% of produced LA was L (+) isomer, while in the open LAF with PT, 95.5% of produced LA was L (+) LA, suggesting the prevalence of L (+) LA producing species after PT. Stereoselectivity of produced LA was lower in other samples. Although the final concentration was higher after UT, the diversity of LA producing strains (**Fig.4**) resulted in less stereoselective LA production, which is not desired. The highest values of LAF parameters were obtained in an open LAF performed after PT, being around 20% higher than in closed LAF with sterilized media. Therefore, PTs could be recommended as a good alternative to sterilization in order to achieve higher overall LA production with still high stereoselectivity. Inoculation by *L. rhamnosus* was necessary at the beginning of fermentation; otherwise the productivities on the stillage fermented solely by stillage microbiota were very low (Tab.1.).

The interaction of PT and UT with the stillage used for LAF was not previously studied, especially in the context of substrate pretreatments for open fermentations. The open LAF but without any physical treatment of substrate were studied with *Bacillus* sp., *Lactobacillus* sp. or *Streptococcus* sp. until now [13,19,54]. The highest LA productivities of around 2 g/Lh have been obtained in open LAF on food waste by *Streptococcus* sp. [13] and on synthetic substrate by *Enterococcus mundtii* QU 25 [55]. The average LA productivity of 1.04 g/Lh on lignocellulosic hydrolyzates by *Bacillus* sp. NL01, in an open fed-batch fermentation was reported [54] while on mixed restaurant food waste maximal reported LA productivity by *Lactobacillus* sp. was between 0.27–0.53 g/ Lh [13]. These are significantly lower values than the LA productivity of 1.2 g/Lh obtained in batch LAF on stillage after PT (**Fig.5**,Tab.1).

L. rhamnosus ATCC 7469 used in our study to produce LA has a proven probiotic potential [7]. After the separation of liquid fermentation broth with dissolved LA for extraction, solid remains with probiotic biomass of *L. rhamnosus* ATCC 7469 could be used as valuable additive for feed. It is demonstrated that in open LAF, the selected PT can significantly decrease the number of undesired G (-) microorganisms (**Fig.2**). Therefore, the PT could be a valuable tool to increase the safety of biomass and solid remains for utilization in animal nutrition.

3.4. Comparison of energy efficiency of different treatments

The estimated values of energy inputs of the performed pretreatments as well as amounts of LA

produced are presented in **Fig.6**. After different treatments all samples were subjected to LAF in the same way, therefore only energy consumption of pretreatments was included in calculation.

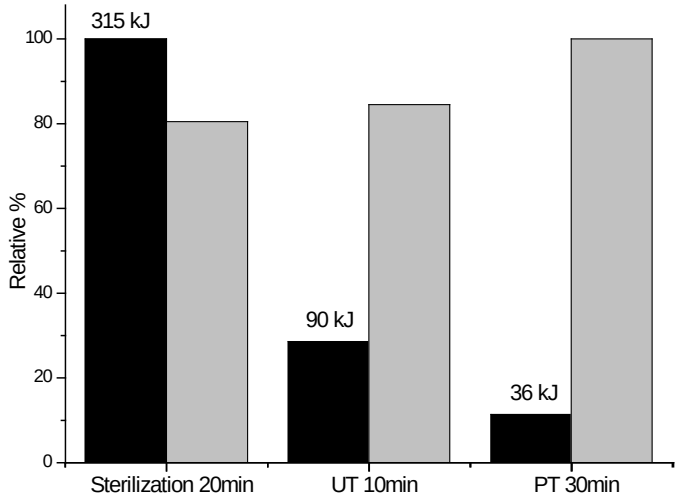

Fig.6 Estimate of required energy for different processes at laboratory level and mass of LA produced. Symbols: black bars – energy consumption of treatment in relative %, above bars is actual energy of treatment; grey bars – amount of LA produced in LAF after treatments in relative %

The lowest in energy consumption is non-thermal PT while, as expected, sterilization is the highest energy-consuming treatment. The actual values of energy consumption of PT, UT and sterilization amounted 36 kJ, 90 kJ and 315 kJ, respectively. The productivity of closed LAF solely by *L. rhamnosus* strain did not justify a high cost of energy for media sterilization. In the case of UT, only the part of energy spent during the treatment was actually delivered to the sample and this part is called actual energy of UT which is calculated based on calorimetric data for every studied sample [26]. Hence, although the UT was the second best regarding LA productivity, actual energy of UT delivered to stillage media is lower than the energy spent for UT (90 kJ) and amounts around 29.5 kJ. Therefore, only one third of spent energy was used in the process for improvement of LAF.

4. Conclusion

The microbial inactivation by non-thermal PT is highly influenced by substrate. We find that there are two reasons for lower reduction in stillage than in water. The turbidity of the stillage is causing a lower penetration of plasma generated agents decreasing their microbial inactivation efficiency. The high concentration of antioxidants in the stillage is also explaining lower logN reduction noticed in the stillage in comparison to water.

E. coli was more susceptible to PT than *L. acidophilus,* regardless of substrate. PT has shown selectivity towards G (-) microorganism and a resistance of G (+) LAB. This recommends the PT as a promising technique for the control of microorganisms present in distillery wastewater.

By comparing PT and UT we find that a 30 min long PT shows superior characteristics of up to 2.5 logN reduction, while UT also induced a decrease in the number of viable microorganisms in stillage

but to lower extent. A 20% higher LA productivity was achieved in open LAF by *L. rhamnosus* ATCC 7469 after PT than in open LAF after UT of distillery stillage. Besides being the most effective, the PT was the lowest in energy consumption and maintains stereoselectivity of LA production.

The PT provided the most effective revalorization of stillage through LAF with the highest LA productivity and the lowest energy consumption. This was achieved in the open fermentation mode which is much simpler process. Further adaptations for PT in larger scale could significantly influence effectiveness and improve the economy of process with integrated PT.

5. Acknowledgement

This work was supported by Serbian Ministry of Education, Science and Technological development, project number TR 31017, Project #I-1/2018 of Scientific and Technological Collaboration of Republic of Serbia and PR China and III 43007. Authors also want to acknowledge Milica Carević, PhD and Prof. Dejan Bezbradica, PhD for their help in HPLC analysis of samples.

6. References

[1] Noukeu, N.A., Gouado, I., Priso, R.J., Ndongo, D., Taffouo, V.D., Dibong, S.D., Ekodeck, G.E.: Characterization of effluent from food processing industries and stillage treatment trial with *Eichhornia crassipes* (Mart.) and *Panicum maximum* (Jacq.), Water Resour. Ind. 16, 1–18 (2016)

[2] Wilkie, A.C., Riedesel, K.J., Owens, J.M.: Stillage characterization and anaerobic treatment of ethanol stillage from conventional and cellulosic feedstocks, Biomass and Bioenergy. 19, 63–102 (2000)

[3] Baral, N.R., Shah, A.: Techno-economic analysis of utilization of stillage from a cellulosic biorefinery, Fuel Process. Technol. 166, 59–68 (2017)

[4] Moestedt, J., Påledal, S., Schnürer, A., Nordell, E.: Biogas Production from Thin Stillage on an Industrial Scale—Experience and Optimisation, Energies. 6, 5642–5655 (2013)

[5] Semenčenko, V.V., Mojović, L.V., Dukić-Vuković, A.P., Radosavljević, M.M., Terzić, D.R., Milašinović Šeremešić, M.S.: Suitability of some selected maize hybrids from Serbia for the production of bioethanol and dried distillers' grains with solubles, J. Sci. Food Agric. 93, 811–818 (2013)

[6] Fuess, L.T., Garcia, M.L.: Implications of stillage land disposal: A critical review on the impacts of fertigation, J. Environ. Manage. 145, 210–229 (2014)

[7] Djukić-Vuković, A.P., Mojović, L.V., Semenčenko, V.V., Radosavljević, M.M., Pejin, J.D., Kocić-Tanackov, S.D.: Effective valorisation of distillery stillage by integrated production of lactic acid and high quality feed, Food Res. Int. 73, 75–80 (2015)

[8] Pleissner, D., Qi, Q., Gao, C., Rivero, C.P., Webb, C., Lin, C.S.K., Venus, J.: Valorization of organic residues for the production of added value chemicals: A contribution to the bio-based economy, Biochem. Eng. J. 116, 3–16 (2016)

[9] West, T.P.: Malic acid production from thin stillage by *Aspergillus* species, Biotechnol. Lett. 33, 2463–2467 (2011)

[10] Wu, J.M., Liu, R.H.: Cost-effective production of bacterial cellulose in static cultures using distillery wastewater, J. Biosci. Bioeng. 115, 284–290 (2013)

[11] Kang, T.S., Korber, D.R., Tanaka, T. : Bioconversion of glycerol to 1,3-propanediol in thin stillage-based media by engineered *Lactobacillus panis* PM1, J. Ind. Microbiol. Biotechnol. 41, 629–635 (2014)

[12] Ghosh Ray, S., Ghangrekar, M.M.: Enhancing organic matter removal, biopolymer recovery and electricity generation from distillery wastewater by combining fungal fermentation and microbial fuel cell, Bioresour. Technol. 176, 8–14 (2015)

[13] Pleissner, D., Demichelis, F., Mariano, S., Fiore, S., Navarro Gutiérrez, I.M., Schneider, R., Venus, J.: Direct production of lactic acid based on simultaneous saccharification and fermentation of mixed restaurant food waste, J. Clean. Prod. 143, 615–623 (2017)

[14] Li, T., Chen, X., Chen, J., Wu, Q., Chen, G.-Q.: Open and continuous fermentation: Products, conditions and bioprocess economy, Biotechnol. J. 9, 1503–1511 (2014)

[15] Abdel-Rahman, M.A., Tashiro, Y., Sonomoto, K.: Recent advances in lactic acid production by microbial fermentation processes, Biotechnol. Adv. 31, 877–902 (2013)

[16] Dai, J.-Y., Sun, Y.-Q., Xiu, Z.-L.: Separation of bio-based chemicals from fermentation broths by salting-out extraction, Eng. Life Sci. 14, 108–117 (2014)

[17] Yusaf, T., Al-Juboori, R.A.: Alternative methods of microorganism disruption for agricultural applications, Appl. Energy. 114, 909–923 (2014)

[18] Sakai, K., Murata, Y., Yamazumi, H., Tau, Y., Mori, M., Moriguchi, M., Shirai, Y.: Selective Proliferation of Lactic Acid Bacteria and Accumulation of Lactic Acid during Open Fermentation of Kitchen Refuse with Intermittent pH Adjustment., Food Sci.Technol. Res. 6, 140–145 (2000)

[19] Tang, J., Wang, X., Hu, Y., Zhang, Y., Li, Y.: Lactic acid fermentation from food waste with indigenous microbiota: Effects of pH, temperature and high OLR, Waste Manag. 52, 278–285 (2016)

[20] Krásný, I., Lapčík, L., Lapčíková, B., Greenwood, R.: The effect of low temperature air plasma treatment on physico-chemical properties of kaolinite/polyethylene composites, Compos. Part B. Eng. 59, 293-299 (2014)

[21] Moreau, M., Orange, N., Feuilloley, M.G.J.: Non-thermal plasma technologies: New tools for bio-decontamination, Biotechnol. Adv. 26, 610–617 (2008)

[22] Surowsky, B., Schlüter, O., Knorr, D.: Interactions of Non-Thermal Atmospheric Pressure Plasma with Solid and Liquid Food Systems: A Review, Food Eng. Rev. 7, 82–108 (2015)

[23] Puač, N., Miletić, M., Mojović, M., Popović-Bijelić, A., Vuković, D., Miličić, B., Maletić, D., Lazović, S., Malović, G., Petrović, Z.L.: Sterilization of bacteria suspensions and identification of radicals deposited during plasma treatment, Open Chem. 13, 332–338 (2015)

[24] Liao, X., Liu, D., Xiang, Q., Ahn, J., Chen, S., Ye, X., Ding, T.: Inactivation mechanisms of non-thermal plasma on microbes: A review, Food Control. 75, 83–91 (2017)

[25] Ho, G.S., Faizal, H.M., Ani, F.N.: Microwave induced plasma for solid fuels and waste processing: A review on affecting factors and performance criteria, Waste Manag. 69, 423–430

(2017)

[26] Herceg, Z., Jambrak, A.R., Vukušić, T., Stulić, V., Stanzer, D., Milošević, S.: The effect of high-power ultrasound and gas phase plasma treatment on *Aspergillus* spp. and *Penicillium* spp. count in pure culture, J. Appl. Microbiol. 118, 132–141 (2015)

[27] Feng, H., Barbosa-Canovas, G., Weiss, J. (Eds.): Ultrasound Technologies for Food and Bioprocessing, Food Engineering Series. Springer New York, New York (2011)

[28] Research Grand View, Lactic Acid Market & Polylactic Acid (PLA) Market, Industry Report 2025. http://www.grandviewresearch.com/industry-analysis/lactic-acid-and-poly-lactic-acid-market (2017). Accessed 16 May 2018

[29] Djukić-Vuković, A.P., Mojović, L.V., Jokić, B.M., Nikolić, S.B., Pejin, J.D.: Lactic acid production on liquid distillery stillage by *Lactobacillus rhamnosus* immobilized onto zeolite, Bioresour. Technol. 135, 454–458 (2013)

[30] Zaplotnik, R., Bišćan, M., Kregar, Z., Cvelbar, U., Mozetič, M., Milošević, S.: Influence of a sample surface on single electrode atmospheric plasma jet parameters, Spectrochim. Acta - Part B At. Spectrosc. 103–104 124–130 (2015)

[31] Issa-Zacharia, A., Kamitani, Y., Miwa, N., Muhimbula, H., Iwasaki, K.: Application of slightly acidic electrolyzed water as a potential non-thermal food sanitizer for decontamination of fresh ready-to-eat vegetables and sprouts, Food Control. 22, 601–607 (2011)

[32] Djukić-Vuković, A., Mladenović, D., Radosavljević, M., Kocić-Tanackov, S., Pejin, J., Mojović, L., Wastes from bioethanol and beer productions as substrates for l(+) lactic acid production - A comparative study, Waste Manag. 48, 478–482 (2016)

[33] Hulsmans, A., Joris, K., Lambert, N., Rediers, H., Declerck, P., Delaedt, Y., Ollevier, F., Liers, S.: Evaluation of process parameters of ultrasonic treatment of bacterial suspensions in a pilot scale water disinfection system, Ultrason. Sonochem. 17, 1004–1009 (2010)

[34] Jovanović, J.R., Stefanović, A.B., Žuža, M.G., Jakovetić, S.M., Šekuljica, N.Ž., Bugarski, B.M., Knežević-Jugović, Z.D.: Improvement of antioxidant properties of egg white protein enzymatic hydrolysates by membrane ultrafiltration, Hem. Ind. 70, 419–428 (2016)

[35] Srivastava, A., Poonia, A., Tripathi, A.D., Singh, R.P., Srivastava, S.K.: Optimization of nutritional supplements for enhanced lactic acid production utilizing sugar refinery by-products, Ann. Microbiol. 64, 1211–1221 (2014)

[36] Uchiyama, H., Zhao, Q.L., Hassan, M.A., Andocs, G., Nojima, N., Takeda, K., Ishikawa, K., Hori, M., Kondo, T., EPR-spin trapping and flow cytometric studies of free radicals generated using cold atmospheric argon plasma and X-ray irradiation in aqueous solutions and intracellular milieu, PLoS One. 10, e0136956 (2015)

[37] Tresp, H., Hammer, M.U., Winter, J., Weltmann, K.D., Reuter, S.: Quantitative detection of plasma-generated radicals in liquids by electron paramagnetic resonance spectroscopy, J. Phys. D. Appl. Phys. 46, 435401 (2013)

[38] Gorbanev, Y., O'Connell, D., Chechik, V.: Non-Thermal Plasma in Contact with Water: The Origin of Species, Chem. - A Eur. J. 22, 3496–3505 (2016)

[39] Boudam, M.K., Moisan, M., Saoudi, B., Popovici, C., Gherardi, N., Massines, F.: Bacterial spore inactivation by atmospheric-pressure plasmas in the presence or absence of UV photons as obtained with the same gas mixture, J. Phys. D. Appl. Phys. 39, 3494–3507 (2006)

[40] Koutinas, A., Vlysidis, A., Pleissner, D., Kopsahelis, N., Lopez Garcia, I., Kookos, I.K., Papanikolaou, S., Kwan, T.H., Lin, C.S.K.: Valorization of industrial waste and by-product streams via fermentation for the production of chemicals and biopolymers. Chem. Soc. Rev. 43, 2587–627 (2014)

[41] Ramazzina, I., Berardinelli, A., Rizzi, F., Tappi, S., Ragni, L., Sacchetti, G., Rocculi, P.: Effect of cold plasma treatment on physico-chemical parameters and antioxidant activity of minimally processed kiwifruit, Postharvest Biol. Technol. 107, 55–65 (2015)

[42] Caderby, E., Baumberger, S., Hoareau, W., Fargues, C., Decloux, M., Maillard, M.-N.: Sugar Cane Stillage: A Potential Source of Natural Antioxidants, J. Agric. Food Chem. 61, 11494–11501 (2013)

[43] Surowsky, B., Schlüter, O. Knorr, D.: Interactions of Non-Thermal Atmospheric Pressure Plasma with Solid and Liquid Food Systems: A Review, Food Eng. Rev. 7, 82–108 (2015)

[44] Pagliaccia, P., Gallipoli, A., Gianico, A., Montecchio, D., Braguglia, C.M., Single stage anaerobic bioconversion of food waste in mono and co-digestion with olive husks: Impact of thermal pretreatment on hydrogen and methane production, Int. J. Hydrogen Energy. 41, 905–915 (2016)

[45] Tampio, E., Ervasti, S., Paavola, T., Heaven, S., Banks, C., Rintala, J.: Anaerobic digestion of autoclaved and untreated food waste, Waste Manag. 34, 370–377 (2014)

[46] Purevdorj, D., Igura, N., Hayakawa, I., Ariyada, O.: Inactivation of *Escherichia coli* by microwave induced low temperature argon plasma treatments, J. Food Eng. 53, 341–346 (2002)

[47] Geveke, D.J.: UV Inactvation of bacteria in Apple Cider, J. Food Prot. 68, 1739–1742 (2005)

[48] Arrange, A.A., Phelps, T.J., Benoit, R.E., Palumbo, A.V., White, D.C.: Bacterial sensitivity to UV light as a model for ionizing radiation resistance, J. Microbiol. Methods. 18, 127–136 (1993)

[49] Mai-Prochnow, A., Clauson, M., Hong, J., Murphy, A.B.: Gram positive and Gram negative bacteria differ in their sensitivity to cold plasma. Sci. Rep. 6, 38610 (2016)

[50] Sangave, P.C., Pandit, A.B.: Ultrasound pre-treatment for enhanced biodegradability of the distillery wastewater, Ultrason. Sonochem. 11, 197–203 (2004)

[51] Graves, D.B., The emerging role of reactive oxygen and nitrogen species in redox biology and some implications for plasma applications to medicine and biology, J. Phys. D Appl. Phys. 45, 263001–42 (2012)

[52] Traylor, M.J., Pavlovich, M.J., Karim, S., Hait, P., Sakiyama, Y., Clark, D.S., Graves, D.B., Long-term antibacterial efficacy of air plasma-activated water, J. Phys. D. Appl. Phys. 44, 472001 (2011)

[53] Ma, R., Wang, G., Tian, Y., Wang, K., Zhang, J., Fang, J.: Non-thermal plasma-activated water inactivation of food-borne pathogen on fresh produce, J. Hazard. Mater. 300, 643–651 (2015)

[54] Ouyang, J., Ma, R., Zheng, Z., Cai, C., Zhang, M., Jiang, T.: Open fermentative production of l-

lactic acid by *Bacillus* sp. strain NL01 using lignocellulosic hydrolyzates as low-cost raw material, Bioresour. Technol. 135, 475–480 (2013)

[55] Abdel-Rahman, M.A., Tashiro, Y., Zendo, T., Sonomoto, K.: Improved lactic acid productivity by an open repeated batch fermentation system using *Enterococcus mundtii* QU 25, RSC Adv. 3, 8437 (2013)

Tables

Table 1. Important parameters of open and closed LAFs performed on distillery stillage media

Characteristics of LAF	Distillery stillage treatment	LA concentration [c] (g/L)	LA yield (g/g)	LA volumetric productivity [c] (g/Lh)
Open LAFs [d]	non-thermal PT [a]	29.09±0.94	0.82±0.03	1.21±0.04
	UT [b]	24.43±0.71	0.69±0.02	1.02±0.03
Closed LAF [d]	sterilization	23.33±0.68	0.66±0.02	0.97±0.03
Open LAF	untreated	13.66±0.65	0.38±0.02	0.57±0.03

[a] 30 min PT, [b] 10 min UT, [c] after 24 h of LAF, [d] Samples inoculated by *L. rhamnosus* ATCC 7469 after treatments

Plasma Sci. Technol. **19** (2017) 075504 (8pp) https://doi.org/10.1088/2058-6272/aa656b

Plasma effects on the bacteria *Escherichia coli* via two evaluation methods

Danijela VUJOŠEVIĆ[1], Uroš CVELBAR[2], Urška REPNIK[2], Martina MODIC[2], Saša LAZOVIĆ[3], Tina ZAVAŠNIK-BERGANT[2], Nevena PUAČ[3], Boban MUGOŠA[1], Evangelos GOGOLIDES[4], Zoran Lj PETROVIĆ[3] and Miran MOZETIČ[2]

[1] Institute of Public Health, Ljubljanska bb, 81000 Podgorica, Montenegro
[2] Jozef Stefan Institute, Jamova cesta 39, 1000 Ljubljana, Slovenia, EU
[3] Institute of Physics, University of Belgrade, Pregrevica 118, 11080 Belgrade, Serbia
[4] Institute of Nanoscience and Nanotechnology (INN), National Center for Scientific Research NCSR Demokritos, Aghia Paraskevi, Attiki, Greece

E-mail: uros.cvelbar@ijs.si

Received 23 September 2016, revised 25 February 2017
Accepted for publication 3 March 2017
Published 24 May 2017

Abstract

The degradation of *Escherichia coli* bacteria by treatment with cold, weakly ionised, highly dissociated oxygen plasma, with an electron temperature of 3 eV, a plasma density of 8×10^{15} m^{-3} and a neutral oxygen atom density of 3.5×10^{21} m^{-3} was studied. To determine the 'real' plasma effects, two methods were used for evaluation and determination, as well as a comparison of the number of bacteria that had survived: the standard plate count technique (PCT) and advanced fluorescence-activated cell sorting (FACS). Bacteria were deposited onto glass substrates and kept below 50 °C during the experiments with oxygen plasma. The results showed that the bacteria had fully degraded after about 2 min of plasma treatment, depending slightly on the amount of bacteria that had been deposited on the substrates. The very precise determination of the O flux on the substrates and the two-method comparison allowed for the determination of the critical dose of oxygen atoms required for the destruction of a bacterial cell wall—about 6×10^{24} m^{-2}—as well as deactivation of the substrates—about 8×10^{25} m^{-2}. These results were taken in order to discuss other results obtained by comparable studies and scientific method evaluations in the determination of plasma effects on bacteria.

Keywords: oxygen plasma, bacteria, degradation, PCT, FACS

(Some figures may appear in colour only in the online journal)

1. Introduction

Plasma treatment is an advanced technique for the sterilization or removal of organic materials, like proteins, from delicate materials that cannot withstand autoclaving [1–9]. The method is based on the exposure of materials to plasma created in different gases, and with different electrical discharges. Both low pressure and atmospheric pressure discharges are popular [10–18]. While aggressive (often moderately ionized) plasma created in oxygen is extremely effective in the destruction of any bacteria or their spores, such plasma has a huge disadvantage, as it usually causes irreversible modifications of the materials (polymers) that are to be cleaned or sterilized [19–22]. Most researchers have therefore been focusing on the application of mild plasma for the sterilization of delicate biomedical materials. 'Mild plasmas' are commonly realized in 'cold' or non-equilibrium collisional plasmas, or in other words, in 'weakly ionised, highly dissociated plasmas' with the bulk kinetic temperature of the ions and background gas close to room temperature. However, even these plasmas often cause some modifications of the organic materials [23–29]. Interaction of the reactive plasma particles (in the case of oxygen or nitrogen plasma, the major reactants are neutral O or N atoms, as well as their metastables) cause, at least, the modification of the surface free energy by functionalization of the

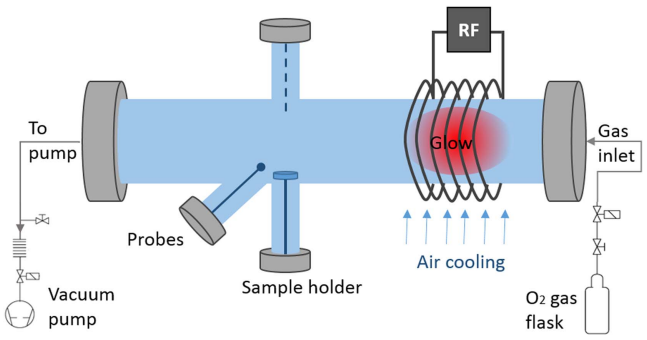

Figure 1. A schematic of the experimental setup along with a detailed presentation of the plasma reactor.

polymers with polar functional groups, if not degradation of the polymer [30–34]. In order to estimate critically the applicability of the plasma for the sterilization of a given medical device made from or containing polymers—or better said the degradation of the bacterial material—one should know the reaction probabilities for both the bacteria and the substrate. Since the major reactants are neutral atoms, the probabilities should be expressed in terms of the critical dose of atoms suitable for the degradation of all bacteria (or, rather, the dose required for decreasing the initial number of live bacteria by six orders of magnitude). Obviously, the plasma should be well characterized, and the number of surviving bacteria should be precisely measured, possibly by two independent techniques. However, it has come to our attention that the results vary between the different reports published. With this in mind, we designed the experiment in such a way that viability could be re-tested by two independent methods, where the dynamics of degradation can also be observed and the mechanism studied.

2. Experiment

2.1. Experimental plasma reactor

In order to avoid the stray effects caused by interaction between the ions from plasma with bacteria, plasma with a very small ionization fraction and a very high dissociation fraction should be used. Such plasma is often created in electrode-less discharges, such as microwave [22, 35–37] and radiofrequency discharges. For our experiments, we used radiofrequency plasma in a glass chamber, as presented in detail elsewhere [23]. Such plasma is suitable for various applications, from activation of the polymer materials to synthesis of the nanomaterials [38–40]. The RF generator was operated at 27.12 MHz, and the power was estimated at 180 W. The plasma was generated by an inductively coupled discharge inside a borosilicate glass tube with an inner diameter of 36 mm and a length of 65 cm, as seen in figure 1. The tube was first evacuated to a pressure base pressure of 3 Pa and then filled with oxygen to 75 Pa, where maximal dissociation of the oxygen molecules is achieved in the system. The samples were positioned 10 cm downstream from the discharge coil and plasma glow, where no ions were present. The plasma parameters were measured with a double Langmuir probe and a catalytic probe [41, 42]. At a pressure of 75 Pa, the electron temperature was 3 eV, the plasma density was $8 \times 10^{15}\,\mathrm{m}^{-3}$ and the neutral oxygen atom density was $3.5 \times 10^{21}\,\mathrm{m}^{-3}$. In addition, bacteria were exposed to pure vacuum conditions at base pressure for 2 min and untreated, as set for experiments following the same procedure, only without the plasma and 75 Pa O_2 flow rate, in order to detect possible changes in their viability.

2.2. Sample preparation and analyses

2.2.1. Bacteria preparation. The inactivation effect of the oxygen plasma was tested on *E. coli* ATCC no. 25922 (Gram-negative bacteria). These bacteria were obtained from MicroBioLogics CE (MN, USA). The bacterial cultures were grown overnight on Colombia agar plates (Difco Laboratories, MI, USA) at 37 °C. The cells were transferred from plates with a loop and re-suspended in sterile but not distilled water, directly prior to sample preparation and experiments. Of this initial bacterial suspension, 100 μl was evenly distributed onto the surface of a sterile glass substrate with a dimension of 4 cm × 1.25 cm, and air dried in a laminar-flow hood. The bacteria on the substrate triplicates were then either exposed to low-pressure oxygen plasma or control samples, vacuum-treated at base pressure and untreated following the same procedure as for plasma treatment.

2.2.2. Plate count technique (PCT). The plate count is one of the standard means of enumeration of viable microbes, because it allows a visual indication of every cell in the specimen. One major disadvantage of the viable plate count is the assumption that each colony arises from one cell. In species where cells grow together in clusters, a gross underestimation of the true population results. This is why the term *CFUs per ml* is used instead of *bacteria per ml* for the results of such an analysis. It is a constant reminder that one colony does not equal one cell. Great care must also be taken during dilution and plating to avoid errors. Even a small error in dilution can have a large effect on the final counting numbers. The rate at which bacteria give rise to an observable colony can also vary, depending on the incubation time. If the incubation time is too short, then some colonies may not arise. The temperature of the incubation and medium conditions must also be optimized to achieve the largest colonies possible, in order to make counting easier. Last but not least, the disadvantage of this technique is that it is very time consuming. Depending on the organism, one day to several weeks are needed to determine the number of CFUs. Therefore, results obtained via the plate count should be taken with some critical reservations.

Before and after each treatment, the samples (bacteria on carriers) were aseptically placed in sterile containers with a 2 ml 0.85% NaCl saline solution. The containers were then briefly vortexed in order to wash the bacterial cells from the carriers. The suspension was serially diluted (1/10) in saline to the required concentration range. A sample of 100 μl

of the diluted suspension was inoculated onto a Colombia agar plate and spread evenly with a sterile glass hockey stick. The plates were than incubated at 37 °C for 24 h. The colony forming units were finally counted to determine the number of survivors of bacteria. Also, 100 μl of bacterial suspension (before dilution) was transferred to a 5 ml tryptic glucose yeast broth, incubated for 7 days, and monitored daily for growth. When turbidity occurred in a container, we sub-cultivated it on Columbia agar plates and searched for any nominated (or any other, in the case of contamination) bacteria. After 7 days, the contents of all the containers had been sub-cultivated on Columbia agar plates, proving the absence of growth. The samples were thereafter declared sterile if no positive growth was observed.

2.2.3. Flow cytometry. Flow cytometry is a technique for counting, examining and sorting microscopic particles suspended in a stream of fluid. The technique allows for simultaneous multiparametric analysis of the physical and/or chemical characteristics of single cells flowing through an optical and/or electronic detection apparatus. Modern flow cytometers are able to analyse several thousand particles every second, in real time, and can actively separate and isolate particles with specified properties. A flow cytometer is similar to a microscope, except that instead of producing an image of the cell, flow cytometry offers the 'high-throughput' (for a large number of cells) automated quantification of set parameters.

A fluorescence-activated cell sorting (FACS) instrument, as used in our experiments, is a specialized type of flow cytometry. It provides a method for sorting a heterogeneous mixture of biological cells into two or more containers, one cell at a time, based upon the specific light scattering and fluorescent characteristics of each cell. It is a useful scientific instrument as it provides fast, objective and quantitative recording of fluorescent signals from individual cells as well as the physical separation of cells of particular interest.

The viability of the bacteria was determined with a LIVE/DEAD BacLight bacterial viability kit for microscopy and quantitative assay (Molecular Probes, L7012). Alternatively, the viability, as well as the concentrations of live and dead bacteria, were determined using a LIVE/DEAD BacLight bacterial viability and counting kit (Molecular Probes, L34856). Both kits contain two stains: green-fluorescent SYTO9 and red-fluorescent propidium iodide (PI). SYTO9 stains both live and dead bacteria, whereas PI only enters dead bacteria. Live bacteria fluorescence is thus green, while dead bacteria have strong red fluorescence and also a weak green fluorescence. In addition, the counting kit contains a microsphere standard (beads), by which the volume of the analysed sample can be determined, and the concentration of bacteria in the sample can thereby be calculated. In this way, all initial concentrations of bacteria in the suspension were determined in prior experiments and deposited on the sample carriers as well as counted after the experiments. The counted bacterial cells in the initial suspension, before deposition on the carriers, is marked in the latter text as an initial suspension, whereas the deposited and dried bacteria on the sample holders is labelled as untreated.

After plasma treatment, glass carriers coated with a layer of bacteria were transferred to a 50 ml tube containing 2 ml of 0.85% NaCl, and the bacteria were released from the carriers into a suspension by gentle shaking. To prepare a 1 ml sample for simple viability analysis, 1.5 μl of each dye was added to 997 μl of the bacteria suspension. To prepare the 1 ml sample for quantitative analysis, 10 μl of the microsphere standard diluted ten times (1.0×10^7 beads ml^{-1}; final concentration thus 1.0×10^5 beads ml^{-1}) and 1.5 μl of each dye was added to 987 μl of bacteria suspension. Before the analysis, the samples were incubated for 15 min at room temperature. If necessary, the bacteria suspension was diluted 10, 50 or 100 times to prepare the samples for analysis.

The samples were analysed using an FACS Calibur flow cytometer (Becton Dickinson), with CellQuest software, version 3.3 (Becton Dickinson). Gates for the beads and for the bacteria were set using green or red fluorescence and side scatter parameters. The percentages of live and dead bacteria within the gate were calculated from a green fluorescence versus a red fluorescence plot upon three runs for each treated sample.

All experiments were performed with an untreated cell suspension, which served as the live cell control, as well as with 70% isopropyl-alcohol-treated bacterial suspension, which served as the dead cell control.

2.3. Statistical analysis

All the experiments were performed in at least three sample replicates. The results are presented as a mean $\pm$ standard deviation. The efficiency of the bacterial inactivation was statistically analysed using a one-way analysis of variance (ANOVA) and IBM SPSS statistics software (New York, USA). Probability values lower than 0.05 were considered as significant.

3. Results

3.1. Results with the PCT method

After treatment, the results were obtained by the PCT method. The result of oxygen plasma treatment on the survival of the *E. coli* bacteria as a function of the plasma treatment time is presented in figure 2. As can be seen from figure 2, the number of CFUs decreases with an increasing treatment time. During the first 30 s, a very rapid drop in the concentration of live bacteria is exhibited. The complete inactivation of the substrate was accomplished within approximately 120 s.

An identical experiment to the previous one was performed with the 8×10^7 *E. coli* cells on the carrier (two-fold lower concentration). The results with the mean values of the surviving bacteria for both concentrations can be seen in figure 2. The inactivation dynamics is very similar for both

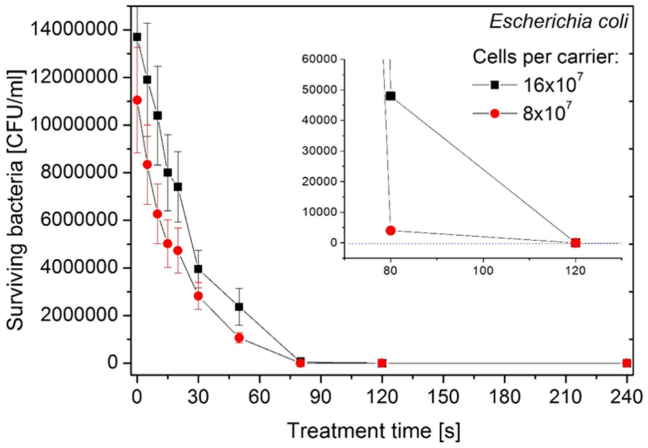

Figure 2. Survival curves of *E. coli* by PCT. The graph represents the CFUs of *E. coli* versus the treatment time by an oxygen plasma glow discharge at a pressure of 75 Pa. The concentrations of bacteria cells on the glass substrate were 16×10^7 and 8×10^7.

curves. The bacteria killing time is somehow shortened, with a decrease of the original concentration of cells, and in this case sterilization was accomplished within 90 s.

3.2. Results with FACS

To see how oxygen plasma interacts with bacteria *E. coli*, we used two different concentrations of bacteria deposited on the carrier, and the plasma parameters for a pressure of 75 Pa. The results of the live and dead bacteria after plasma treatment, as well as after the control experiments, were quantified using kit L34856. The results of this quantitative viability analysis are presented in figures 3–5, in addition to figure 6, which shows the dynamics of time-dependent bacteria inactivation.

As can be seen from figures 3 and 4, there were already a large number of dead *E. coli* bacteria on the untreated samples. This occurred during the sample preparation process. However, there were no notable changes in the number of live bacteria exposed to the vacuum (2 min at 3 Pa) in comparison to the untreated bacteria (at 75 Pa following the same procedure, only without plasma), which would have been caused directly by the influence of the vacuum. The dead cell control was in accordance with the test. Furthermore, the number of living cells measured by the flow cytometry decreased rapidly with an increasing plasma treatment time. As expected, this reduction of viable counts was matched by a parallel increase in the number of dead cells. However, a decrease in the amount of dead cells was observed with an increasing plasma treatment time. So, the amount of live and dead *E. coli* cells decreased with prolonged exposure to the plasma. Similar results were obtained for a halved concentration of cells per carrier, presented in figure 5.

In the case of a two-fold lower concentration of *E. coli* cells per carrier, the experimental results demonstrated that for lower concentrations, the bacteria killing time shortens. After 80 s plasma treatment, the total number of cells (live and dead) declined significantly, and almost all the *E. coli* cells were killed. Already, after 120 s, there were no live *E. coli* cells left. In addition, the total number of cells was significantly reduced. For longer treatment times, almost no cells are detected.

Three flow cytometry measurements for a single plasma exposure time, made in triplicate, were performed to obtain some statistics. The average results are presented in a flow cytometry count graph, where both concentrations (8×10^7 and 16×10^7) are shown with the time scale (figure 6). Here, both the survival curves as well as the dead cell counts are presented. The samples with 8×10^7 cells per carrier are characteristically inactivated at 80 s, whereas samples 16×10^7 are deactivated at 120 s of oxygen plasma exposure. The total number of (dead and live) bacteria declined significantly, which indicates the plasma degradation process and the final removal of bacteria from the surface of the carrier.

4. Discussion

Let us now discuss the results obtained with the *E. coli*. The results of the bacterial survival, as determined by FASC, are summarized in figures 4–6. The first three columns in figure 4 represent the number of bacteria, as detected by FACS after treatment by isopropyl alcohol, bacteria exposed to a vacuum at 3 Pa for 2 min, and for untreated bacteria (2 min at 75 Pa with O_2 flow), respectively. The original number of bacteria per carrier should be 1.6×10^8. In a short treatment time of 5 s, the number of surviving bacteria is lowered by a factor of $3.9/4.8 = 0.81$, so we can conclude that about 20% of bacteria has been killed in 5 s. Surprisingly enough, the number of dead bacteria is lowered even more: $4/12 = 0.33$. This rapid drop in dead bacteria cannot be attributed to the experimental uncertainty of the FACS technique, which has been established with reasonable certainty to be at about 20%. Furthermore, the SEM images presented in figure 7 did not show the complete degradation of any bacterium after 5 s of plasma treatment. This rapid drop in the number of dead bacteria after a few seconds of treatment by oxygen plasma cannot be simply attributed to a general error, but should be explained. The handiest explanation is the charging effect caused by plasma treatment. As long as bacteria are alive, they can stick to the surface with their pili. Once dead, they do not stick so actively, but rather by electrostatic forces. When such bacteria are placed into plasma for a short time, both the bacteria and the carrier are charged negatively. The electrostatic force between the bacteria and the carrier is thus repelling, so the dead bacteria can just be detached from the substrate in a short time of plasma treatment. Of course, not all dead bacteria can be removed, since this force is weak. Apparently, this is a possible explanation for the quick drop in dead bacteria after the plasma treatment of *E. coli* for 5 s.

Further exposure of the bacteria to plasma leads to a continuous decrease of the number of dead bacteria. This observation is attributed to the destruction of the bacteria, because the size as well as the shape of the dead bacteria has changed so much that FASC cannot detect them—the remains of the bacteria are rather detected as debris. This explanation is sound, with SEM images of the bacteria

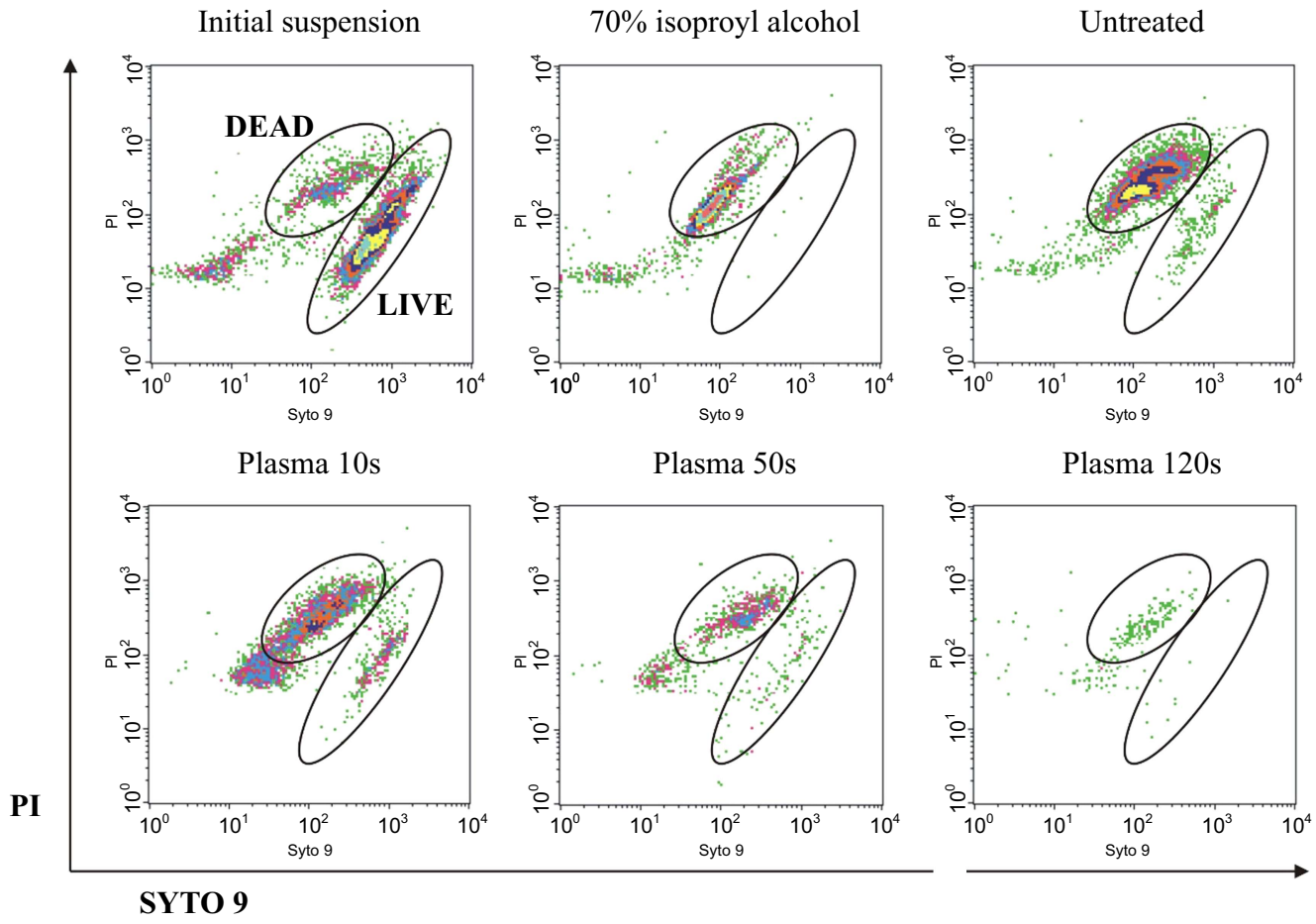

Figure 3. A flow cytometric plot analysis of *E. coli* after plasma treatment. The *E. coli* was analysed by flow cytometry after staining with the LIVE/DEAD BacLightTM bacterial viability kit (L7012) of the initial bacterial suspension, the dead cell control by 70% isopropyl alcohol, the untreated samples, and the oxygen plasma treated samples for 10 s, 50 s and 120 s.

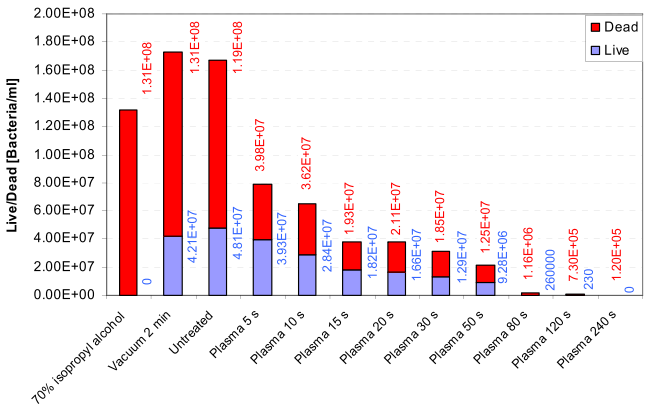

Figure 4. Quantitative viability analysis of *E. coli* after plasma treatment. The number of live/dead *E. coli* cells measured for various oxygen plasma treatment times at 75 Pa, as well as in a vacuum and 70% isopropyl alcohol by a flow cytometer. The concentration of bacteria cells per carrier was 16×10^7.

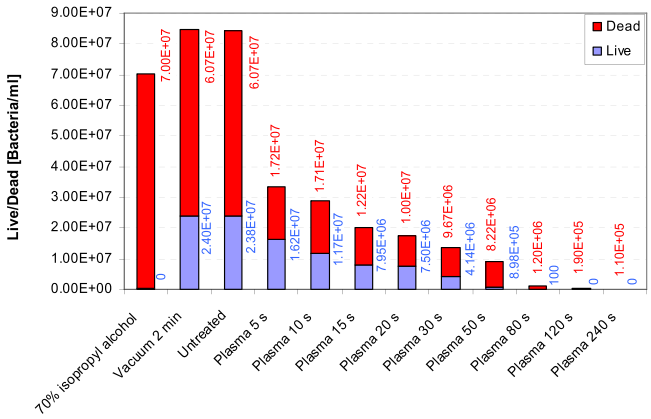

Figure 5. A quantitative viability analysis of *E. coli* after plasma treatment. The number of live/dead *E. coli* cells (with a two-fold lower initial concentration) measured for various oxygen plasma treatment times at 75 Pa, as well as in a vacuum and 70% isopropyl alcohol by a flow cytometer. The initial number of bacteria cells per carrier was 8×10^7.

showing damage after about a minute of plasma treatment. Let us now consider the number of live *E. coli*. As expected, the bacteria exposed to isopropyl alcohol are all dead. Interestingly enough, the number of live bacteria for the untreated sample is pretty low—only about 28% of bacteria is found alive on the untreated sample. This is the result of improper handling of such delicate experimental materials. The number of surviving bacteria after exposure to a vacuum or exposure to plasma for 5 s further decreases by

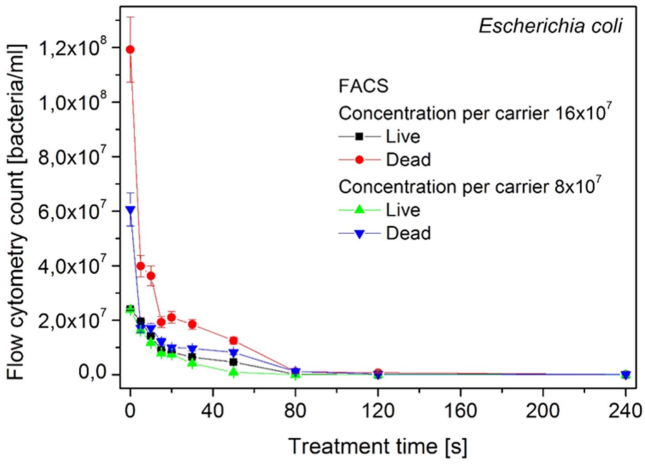

Figure 6. A quantitative viability analysis of *E. coli* for two concentrations after plasma treatment. The number of live/dead *E. coli* cells with two different concentrations on the sample glass carriers is plotted versus the oxygen plasma treatment times at 75 Pa. The initial amount of bacteria cells per carrier was 8×10^7 and 16×10^7.

about 25%. There is a small difference between the number of live bacteria for the vacuum- and plasma-treated samples. This difference cannot be attributed to the action of the plasma, since the SEM images do not any show serious damage to the *E. coli* after 5 s of plasma treatment either. The first substantial fall in the number of live bacteria is observed after 10 s of plasma treatment. This appears to be due to damage to the bacterial cell wall [43]. Knowing the plasma parameters, it is possible to calculate the dose of O atoms required for substantial damage to the cell wall. The O atom density at 75 Pa is $3.5 \times 10^{21}\,\mathrm{m}^{-3}$. The flux of O atoms on the surface of the bacteria is $j = \frac{1}{4}nv$, where n is the density of neutral oxygen atoms as measured by the catalytic probe, and v is average of the absolute velocity of the thermalized oxygen atoms: $v = \sqrt{\frac{8kT}{\pi m}}$. Here, T is the kinetic temperature of neutral gas in the vicinity of our sample (measured in Kelvin), k is the Boltzmann constant, and m is the mass of oxygen atoms. Taking into account the numerical values, i.e. $k = 1.38 \times 10^{-23}\,\mathrm{JK}^{-1}$, $T = 300\,\mathrm{K}$, $m = 16\,\mathrm{emu} = 2.66 \times 10^{-26}\,\mathrm{kg}$, the velocity is: $v = 6.3 \times 10^2\,\mathrm{ms}^{-1}$.

The flux of oxygen atoms onto the bacteria during treatment with the plasma at a pressure of 75 Pa is thus: $j = 5.5 \times 10^{23}\,\mathrm{m}^{-2}\,\mathrm{s}^{-1}$. The dose that the bacteria receive during the plasma treatment for a period of t is: $D = jt$. For the case of bacteria treated at a pressure of 75 Pa for 10 s, the dose is $5.5 \times 10^{24}\,\mathrm{m}^{-2} = 5.5 \times 10^{12}\,\mu\mathrm{m}^{-2}$.

Prolonged treatment of *E. coli* by oxygen plasma causes damage to the bacteria, and eventually their inactivation. Prolonged treatment at 55 s leads to even stronger plasma etching effects on the envelope, by the destruction of the cell wall and cytoplasmatic membrane. At the same time, cytoplasm is released and etched from the surface by oxygen atoms and ions. This probably causes the certain death of the bacteria, which can be seen from the debris and cell deformation. After the cytoplasm is released, the etching continues by removal of the bacterial residuals from the surface until the surface is virtually free of any bacterial material. The treatment time, needed for the detection of an immeasurably low number of bacteria, depends slightly on the concentration of bacteria in the samples, and is approximately 2 min. The absolute inactivation of the plasma-treated samples cannot be determined precisely by FACS, but it can be by PCT. Happily enough, both techniques give similar results, so we can conclude that absolute sterility is obtained after (to be on the safe side) about 150 s. The required dose of oxygen atoms to obtain the full destruction of *E. coli* is calculated using the dose equation, and is found to be: $D_{\mathrm{EC}} = 8.25 \times 10^{25}\,\mathrm{m}^{-2} = 8.25 \times 10^{13}\,\mu\mathrm{m}^{-2}$.

This is, as mentioned, the recommended dose of oxygen atoms that the bacteria should receive to obtain a sterile substrate. Of course, as mentioned above, the particular dose that can be calculated from our results depends on both the technique (PCT of FACS) as well as the number of originally deposited bacteria. The number of surviving bacteria is plotted on a logarithmic scale versus the dose of oxygen atoms for the case of PCT and FACS in figures 8 and 9, respectively. The total inactivation of *E. coli* is achieved after a dose of $6.6 \times 10^{25}\,\mathrm{m}^{-2}$ or at most after $1.3 \times 10^{26}\,\mathrm{m}^{-2}$ for a double concentration of bacteria cells.

There are some discrepancies in the surviving bacteria results obtained by the PCT and FACS method (see figures 8 and 9). The reason for this may be that under certain conditions, bacteria with compromised membranes may recover and reproduce, even though such bacteria may score as 'dead' in the LIVE/DEAD BacLight assay, due to staining with PI. However, more often, bacteria with compromised membranes are unable to reproduce in a nutrient medium, and are scored 'dead' by the PCT method.

As mentioned earlier, oxygen atoms also interact with substrates (carriers). Materials with a high coefficient for heterogeneous surface recombination tend to heat up during prolonged plasma treatment [44–46]. Let us now perform a simple calculation for a rough estimation of the required properties of materials that would be heated by less than 30 K after receiving a dose which is fatal for *E. coli*, i.e. $D_{\mathrm{EC}} = 8.25 \times 10^{25}\,\mathrm{m}^{-2} = 8.25 \times 10^{13}\,\mu\mathrm{m}^{-2}$. In the following calculation, the substrate to be sterilized is of a spherical shape. A sphere of radius r made from a material with a density of ρ, a specific heat capacity of c_{p}, and a heterogeneous surface recombination coefficient of γ, is heated at a rate of:

$$P = \frac{1}{2}\gamma j W_{\mathrm{D}} 4\pi r^2 = \rho \frac{4}{3}\pi r^3 c_{\mathrm{p}} \frac{\Delta T}{\Delta t}. \qquad (1)$$

The critical radius of the sample to be heated by $\Delta T = 30\,\mathrm{K}$ depends on the recombination coefficient:

$$r = \frac{3\gamma D W_{\mathrm{D}}}{2\rho c_{\mathrm{p}} \Delta T}. \qquad (2)$$

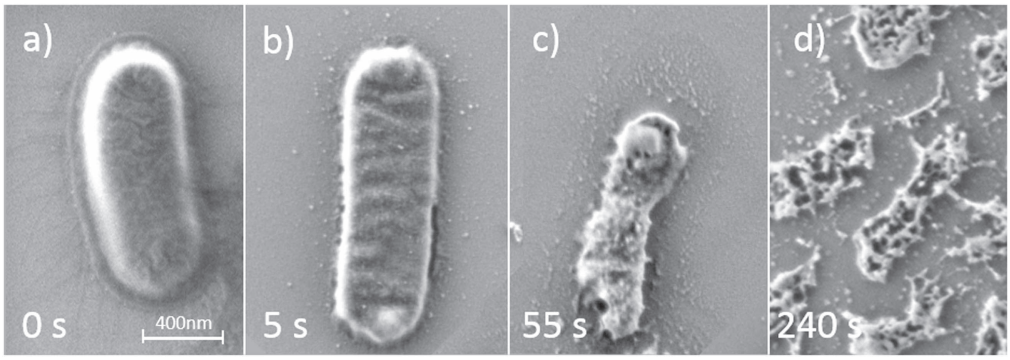

Figure 7. SEM micrographs of *E. coli* bacteria on the substrate: (a) untreated; (b) treated with low-pressure highly dissociated oxygen plasma for 5 s, (c) 55 s, and (d) 240 s.

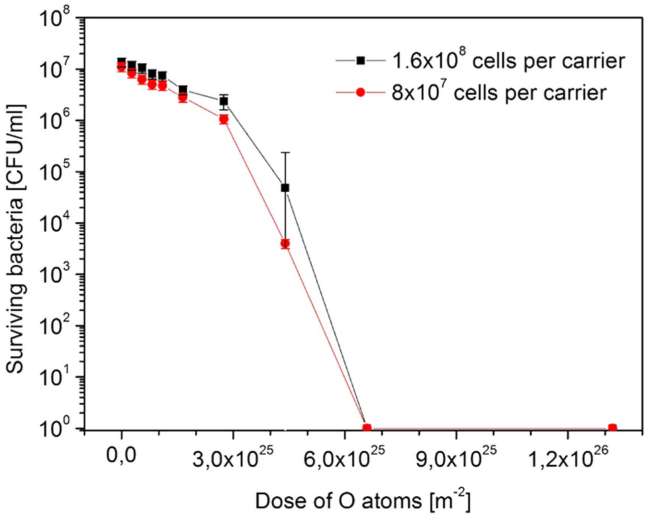

Figure 8. Survival curve of *E. coli* for a received dose of O atoms (measured by PCT). The number of surviving CFUs of the *E. coli* bacteria with respect to the received dose of neutral oxygen atoms. The two initial concentrations were used: 8×10^7 and 16×10^7 cells per carrier.

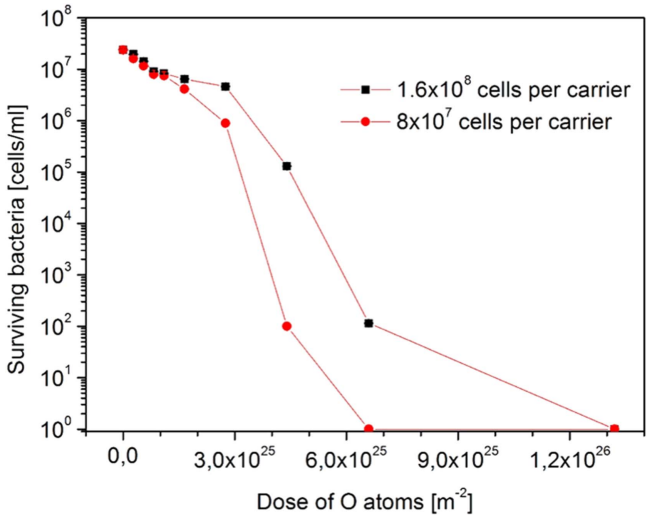

Figure 9. The survival curve of *E. coli* for the received dose of O atoms (measured by FACS). The number of surviving *E. coli* bacteria cells with respect to the received dose of neutral oxygen atoms. The two initial concentrations were used: 8×10^7 and 16×10^7 cells per carrier.

Taking into account the measured values as well as the typical values of constants for delicate organic materials, i.e. $\gamma = 0.005$, $D_{EC} = 8.25 \times 10^{25}\,m^{-2}$, $W_D = 8.3 \times 10^{-19}\,J$, $\rho = 2 \times 10^3\,kg\,m^{-3}$, $c_p = 1000\,J\,kg^{-1}\,K^{-1}$ and $\Delta T = 30\,K$, the minimum radius that our sample can have to avoid substantial heating is 0.017 m. Spherical samples with a radius larger than 1.7 cm are therefore suitable for sterilization with our plasma, as long as they are contaminated with *E. coli*. In the upper calculation, we did not take into account the cooling of the sample by thermal conductivity of the surrounding gas. On the other hand, actual samples are not usually spherical, so the overestimation of the critical radius due to neglecting the cooling is compensated for by a less favourable actual sample shape. The upper calculation, therefore, just gives some directions about the possible application of sterilization with our plasma source: large samples can be effectively sterilized without bothering about the heating effects; smaller samples, on the other hand, would overheat after receiving the lethal dose of oxygen atoms, so they should be kept in cooled holders to avoid this.

The upper calculation takes into account a typical value for the recombination coefficient of oxygen atoms on polymer materials, i.e. $\gamma = 5 \times 10^{-3}$. If our sample is made from a metal with moderate catalytic activity (i.e. $\gamma = 5 \times 10^{-2}$), the required radius is 10 times larger, i.e. $r = 17$ cm. For highly catalytic materials, the required radius to avoid overheating is even larger than that, so active cooling during plasma sterilization is required.

5. Conclusion

Two different techniques were used for studying bacteria degradation, with weakly ionized highly dissociated oxygen plasma: the plate count technique (PCT) and fluorescence-activated cell sorting (FACS). The difference between the techniques goes up to an order of magnitude, which is not much taking into account the peculiarities of both methods. In any case, full scale degradation was obtained after about 2 min of plasma treatment. Since the survival curves are usually presented in log scales in international literature, it can be concluded that the differences between both methods are small. Since the plasma was well characterized, it was possible to

determine the required dose of oxygen atoms suitable for the destruction of the bacteria; this was found to be a bit lower than $1 \times 10^{26}\,\mathrm{m}^{-2}$. This result depends slightly on the number of bacteria deposited on the glass substrates, and represents a valuable recommendation for scientists working on the sterilization of biomedical devices contaminated with *E. coli*. Different results are expected for other types of bacteria. In particular, sporulating bacteria may require much larger doses. The heating effects caused by the heterogeneous recombination of neutral oxygen atoms on the surface of substrates were addressed. Simple but reliable calculations revealed that sterilization using weakly ionized highly dissociated oxygen plasma is only suitable for materials with a low recombination coefficient. Materials with catalytic properties in the surface recombination of O atoms are heated to an elevated temperature before sterilization is accomplished, so they should be cooled effectively in order to avoid unwanted heat effects.

Acknowledgments

The financial support from the Slovenian Research Agency (ARRS), NATO CLG/SPS.984555 and EU COST grant MP1101 is gratefully acknowledged. NP, SL and ZLP are grateful to the MESS 171037 and 41011 projects for partial support.

References

[1] Canal C *et al* 2006 *Eur. Phys. J. Appl. Phys.* **36** 35
[2] d'Agostino R *et al* 2005 *Plasma Processes and Polymers* (Weinheim: Wiley)
[3] Kylián O and Rossi F 2009 *J. Phys. D: Appl. Phys.* **42** 085207
[4] Pintassilgo C D, Loureiro J and Guerra V 2005 *J. Phys. D: Appl. Phys.* **38** 417
[5] Laroussi M 2005 *Plasma Process. Polym.* **2** 391
[6] Kong M G *et al* 2009 *New J. Phys.* **11** 115012
[7] Kutasi K *et al* 2006 *J. Phys. D: Appl. Phys.* **39** 3978
[8] Scholtz V *et al* 2015 *Biotechnol. Adv.* **33** 1108
[9] Guo J, Huang K and Wang J P 2015 *Food Control* **50** 482
[10] Ayan H *et al* 2009 *J. Phys. D: Appl. Phys.* **42** 125202
[11] Antao D S *et al* 2009 *Plasma Sources Sci. Technol.* **18** 035016
[12] Puač N *et al* 2006 *J. Phys. D: Appl. Phys.* **39** 3514
[13] Kylián O, Sasaki T and Rossi F 2006 *Eur. Phys. J. Appl. Phys.* **34** 139
[14] Stoffels E *et al* 2006 *Plasma Sources Sci. Technol.* **15** S169
[15] Krstulović N *et al* 2006 *J. Phys. D: Appl. Phys.* **39** 3799
[16] Lazović S *et al* 2010 *New J. Phys.* **12** 083037
[17] Bayliss D L *et al* 2009 *New J. Phys.* **11** 115024
[18] Laroussi M 2014 *Plasma Process. Polym.* **11** 1138
[19] Shen J *et al* 2014 *Jpn. J. Appl. Phys.* **53** 110310
[20] Vatansever F *et al* 2013 *FEMS Microbiol. Rev.* **37** 955
[21] Shintani H 2016 *Biocontrol Sci.* **21** 1
[22] Taghizadeh L *et al* 2015 *Plasma Process. Polym.* **12** 75
[23] Cvelbar U *et al* 2007 *Appl. Surf. Sci.* **253** 8669
[24] Junkar I *et al* 2009 *Plasma Process. Polym.* **6** 667
[25] Grulich O *et al* 2012 *Plasma Chem. Plasma Process.* **32** 1075
[26] Chvátalová L *et al* 2012 *Eur. Polym. J.* **48** 866
[27] Gorjanc M *et al* 2010 *Text. Res. J.* **80** 557
[28] Shimizu K, Fukunaga H and Blajan M 2014 *Curr. Appl. Phys.* **14** S154
[29] Delgado L M, Pandit A and Zeugolis D I 2014 *Expert Rev. Med. Devic.* **11** 305
[30] Vesel A *et al* 2015 *Appl. Surf. Sci.* **357** 1325
[31] Kostov K G *et al* 2014 *Appl. Surf. Sci.* **314** 367
[32] Borcia C, Punga I L and Borcia G 2014 *Appl. Surf. Sci.* **317** 103
[33] De Geyter N 2013 *Surf. Coat. Technol.* **214** 69
[34] De Geyter N and Morent R 2014 Cold plasma surface modification of biodegradable polymer biomaterials *Biomaterials for Bone Regeneration: Novel Techniques and Applications* (Cambridge: Elsevier) pp 202–24
[35] Arnoult G *et al* 2008 *Appl. Phys. Lett.* **93** 191507
[36] Ricard A *et al* 2001 *Surf. Coat. Technol.* **142–144** 333
[37] Deng X L *et al* 2013 *J. Appl. Phys.* **113** 023305
[38] Canal C *et al* 2007 *Plasma Process. Polym.* **4** 445
[39] Ostrikov K, Cvelbar U and Murphy A B 2011 *J. Phys. D: Appl. Phys.* **44** 174001
[40] Pintassilgo C D, Kutasi K and Loureiro J 2007 *Plasma Sources Sci. Technol.* **16** S115
[41] Valencia-Alvarado R *et al* 2009 *Vacuum* **83** S264
[42] Mozetic M and Cvelbar U 2009 *Plasma Sources Sci. Technol.* **18** 034002
[43] Elersic K *et al* 2011 *IEEE Trans. Plasma Sci.* **39** 2972
[44] Cvelbar U *et al* 2006 *J. Phys. D: Appl. Phys.* **39** 3487
[45] Cartry G, Duten X and Rousseau A 2006 *Plasma Sources Sci. Technol.* **15** 479
[46] Canal C *et al* 2007 *Plasma Chem. Plasma Process.* **27** 404

Science of the Total Environment 654 (2019) 1000–1009

Contents lists available at ScienceDirect

Science of the Total Environment

journal homepage: www.elsevier.com/locate/scitotenv

Virtual water quality monitoring at inactive monitoring sites using Monte Carlo optimized artificial neural networks: A case study of Danube River (Serbia)

Tatjana Mitrović [a], Davor Antanasijević [b,*], Saša Lazović [c], Aleksandra Perić-Grujić [d], Mirjana Ristić [d]

[a] Jaroslav Cerni Institute for Development of Water Resources, Jaroslava Cernog 80, 11226 Belgrade, Serbia
[b] Innovation Center of the Faculty of Technology and Metallurgy, Karnegijeva 4, 11120 Belgrade, Serbia
[c] Institute of Physics Belgrade, University of Belgrade, Pregrevica 118, 11080 Belgrade, Serbia
[d] University of Belgrade, Faculty of Technology and Metallurgy, Karnegijeva 4, 11120 Belgrade, Serbia

HIGHLIGHTS

- WQPs at inactive monitoring sites were estimated by ANN models.
- The selection of input sites for spatial interpolation was done by similarity index.
- MCS routine for the selection of inputs was modified to fit simultaneous models.
- The best modeling strategy for study area was determined.

GRAPHICAL ABSTRACT

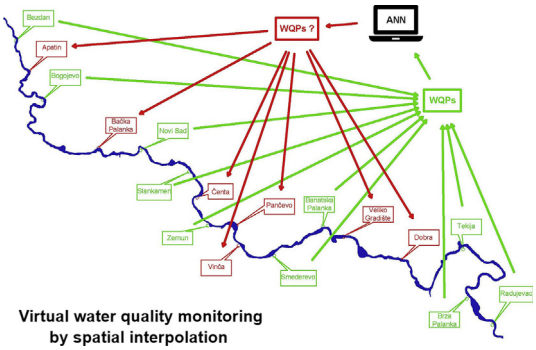

ARTICLE INFO

Article history:
Received 15 August 2018
Received in revised form 6 November 2018
Accepted 13 November 2018
Available online 14 November 2018

Editor: Damia Barcelo

Keywords:
ANNs
Monte Carlo simulations
River water monitoring
Water quality prediction
Inactive monitoring sites

ABSTRACT

Rationalization of water quality monitoring stations nowadays is applied in many countries. In some cases, missing data from abandoned/inactive stations, spatial and temporal, could be very important, hence the use of artificial neural networks (ANNs) for virtual water quality monitoring at inactive monitoring sites was investigated. The aim was to develop single-output and simultaneous ANNs for the spatial interpolation of 18 water quality parameters at single- and multi-inactive monitoring sites on Danube River course through Serbia. Those different modeling approaches were considered in order to determine the most suitable combination of models. The variable selection and sensitivity analysis in the case of simultaneous models were performed using a modified procedure based on Monte Carlo Simulations (MCS). In general, the multi-target models tend to be more accurate than single target ones, while single output models outperform the simultaneous ones. Hence, for particular monitoring network and set of water quality parameters the optimal combination of models must be defined based on model's accuracy and computational effort needed. The MCS selection procedure has proved to be efficient only in the case of simultaneous multi-target model. MCS based analysis of input-output interactions has shown all significant interactions in the case of simultaneous single-target are grouped as a complex cluster of interactions, where majority of inputs influence on several outputs. In the case multi-target model those interactions were portioned in five separate clusters, there majority of them mimic the input-output interactions that are present in single output models. The modeling strategy for study area was proposed on the basis of the performance of created models (mean average percentage error < 10%): simultaneous multi-target model for pH,

* Corresponding author.
E-mail address: dantanasijevic@tmf.bg.ac.rs (D. Antanasijević).

https://doi.org/10.1016/j.scitotenv.2018.11.189

alkalinity, conductivity, hardness, dissolved oxygen, HCO_3^-, SO_4^{2-} and Ca, single-output multi-target models for temperature and Cl^-, simultaneous single-target models for Mg and CO_2, single output single target models for NO_3^-.

1. Introduction

River water quality is on one hand influenced by natural as well as anthropogenic factors, like population growth and industrialization, but on another hand it strongly determines the use of fresh water, aquatic ecosystem status, and even human health. An inevitable step in ensuring good quality of river water is monitoring. In this way, continuous collection of data on status of surface water is ensured, as well as taking measures for the elimination of potential hazards. One of the potential problems, linked to monitoring stations, is missing data, caused by different reasons.

The current tendency is to reduce the number of monitoring sites wherever possible, in order to reduce costs (Chapman et al., 2016). Typically, monitoring stations that have been observed to have similar impacts like one chosen as representative, or have a similar trend in data analysis are abolished (abandoned). In this case, studies and research were focused on number of water quality monitoring stations optimization. For example, Chapman et al. (2016) have used combined cluster and discriminant analysis (Kovács et al., 2014) to estimate the efficiency of monitoring network at Austrian and Hungarian section of the Danube River, while Antanasijević et al. (2018) have proposed self-organizing network based similarity index for the optimization of sampling locations in an existing river water quality monitoring network of the River Danube on its stretch through Serbia.

Excluding some stations from monitoring program could have significant implications in future, for different reasons: necessity of activation of some inactive station and comparison with past data; the emergence of a new source of pollution near inactive monitoring station, indicating serious pollution, the occurrence of invasive species, or their extinction.

Regarding the water quality parameters (WQPs) prediction, artificial neural networks (ANNs) (Peleato et al., 2018) have been successfully applied for the estimation of temperature (Sahoo et al., 2009), chloride (Salami and Ehteshami, 2015; Barzegar et al., 2016), fluoride (Barzegar et al., 2017), electrical conductivity (Barzegar et al., 2018), alkalinity (Salami and Ehteshami, 2015), total hardness (Salami and Ehteshami, 2015), salinity (Huang and Foo, 2002; Salami Shahid and Ehteshami, 2016; Barzegar and Moghaddam, 2016), total dissolved solids (Salami et al., 2016), sodium adsorption ratio (Salami et al., 2016), ammonia nitrogen (Wang et al., 2013), bicarbonate (Salami et al., 2016), chemical and biological oxygen demand (COD and BOD) (Ay and Kisi, 2014; Dogan et al., 2009; Salami et al., 2016; Salami Shahid and Ehteshami, 2016; Verma and Singh, 2013), dissolved oxygen (DO) (Antanasijević et al., 2014; Keshtegar and Heddam, 2017; Salami et al., 2016; Salami and Ehteshami, 2015; Salami Shahid and Ehteshami, 2016; Wang et al., 2013), DO percentage (Salami and Ehteshami, 2015), etc.

An ANN can be described as an information process system which consists of many nonlinear and densely interconnected processing units. With this parallel-distributed processing architecture, ANNs have been proven to be an efficient alternative to traditional methods for hydrological modeling (Chang et al., 2007). As Rigol et al. (2001) have noted, the advantage of ANNs for spatial interpolation is that the input variables are not assumed necessarily to be linearly related with the data being interpolated, and that combinative effects are taken into account during modeling. ANNs have been effectively applied for various spatial interpolation tasks, e.g. surface air temperatures (Li et al., 2004; Snell et al., 2000), solar radiation (Li et al., 2004), wind speed (Philippopoulos and Deligiorgi, 2012), soil salinity (Shahabi et al., 2017) etc. Even an integrated ANN-kriging approach was recently proposed for spatial prediction of saline and sodic soils in rice–shrimp farming land (Dinh et al., 2017).

The focus of this study is on a monitoring network of Danube River course through Serbia, namely on the prediction of common water quality parameters (WQPs) at monitoring sites (MSs) that have become non-operational (inactive) since 2012 network rationalization (Antanasijević et al., 2018). This virtual monitoring can be performed by spatial interpolation using measured WQPs data from neighboring MSs. For this task, ANNs was selected, since simplicity and robustness of their application are more important than an accurate description of the various internal sub-processes (Lima et al., 2016). Also, it was proven that ANNs can provide similar or better performance models in comparison with alternative techniques, such as various kriging methods (universal, ordinary, etc.) or partial thin plate splines (Rigol, 2003).

The novelty of this work lies is the fact that single output and simultaneous ANNs for the spatial interpolation of common 18 WQPs at single inactive MS on Danube River course through Serbia, as well as at multi inactive MSs were developed by the variable selection and sensitivity analysis performed using procedure based on Monte Carlo Simulations (MCS) that was previously applied for single output ANN models (Gao et al., 2018; Šiljić et al., 2015), and which is modified in this work to fit simultaneous models.

2. Materials and methods

2.1. Study area and water quality data

The Danube River with its length of 2857 km (588 km through Serbia) is the second largest watercourse in Europe and thus very important International River. About 16% of its total drainage basin (817,000 km^2) belongs to the Serbian territory. It is the main source for domestic and industrial water supply and irrigation in Serbia. In addition, it serves as an international waterway and as receiving waters for wastewater effluents. The major municipal pollution sources come from the cities of Belgrade (1.7 million inhabitants) and Novi Sad (300,000 inhabitants), which do not have satisfying wastewater purification treatment plants. These untreated wastewaters, which are discharged into the river directly, are sources of significant organic and nutrient pollution (The International Commission for the Protection of the Danube River (ICPDR), 2018).

Two hydroelectric power plants (Iron Gate I and II) with their reservoir systems are located at the Serbian territory. These reservoirs change the Danube regime and trap millions of tons of sediment per year which are considerable deposit for nutrients and hazardous pollutants originating upstream of the dam. As a result, the water residence time and temperature increase thermal stratification changes, primary production in situ enhance etc. Considering these facts, there is a big impact of the dams on the river aquatic life as well as on the environment at all (Mitrović et al., 2010).

The dataset used in this study was generated through monitoring of the water quality of Danube River (Serbia). Monthly and semi-monthly

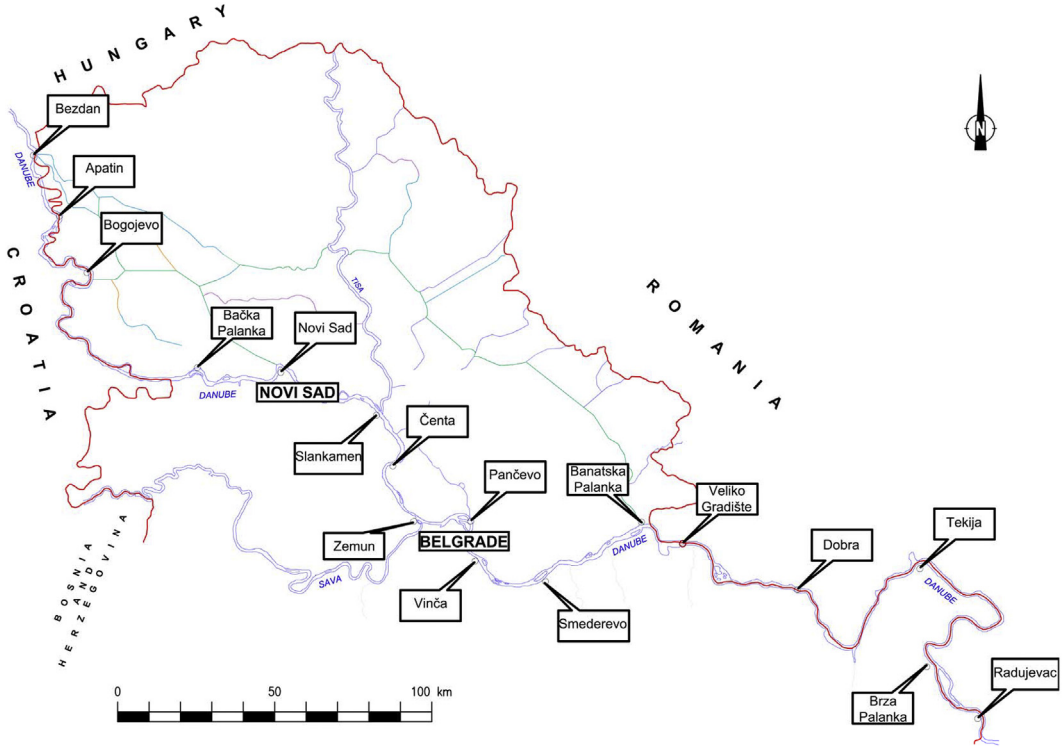

Fig. 1. Danube River course through The Republic of Serbia.

sampling was carried out during ten years (2002–2011) at 17 monitoring sites (Fig. 1). A dataset consisted of 18 WQPs:

a) 8 non-specific WQPs, namely temperature (T), pH, total suspended solids (TSS), hardness, alkalinity, electrical conductivity, biological oxygen demand (BOD), chemical oxygen demand (COD), and
b) 10 specific WQPs, whereby

i. two gaseous WQPs, i.e. dissolved oxygen (DO) and CO_2,
ii. two cations, i.e. Ca and Mg,
iii. five anions, namely HCO_3^-, NO_3^-, PO_4^{3-}, Cl^-, SO_4^{2-}, and
iv. total phosphorus (P).

For model generation, available dataset was split into three sub-sets: training, validation and testing in ratio 8:1:1, respectively.

2.2. Modeling approaches

If a monitoring network of few dozen monitoring sites is considered, then its rationalization will yield at least several inactive monitoring sites. This allows the development of two types of ANN prediction models (Fig. 2), which have been already compared in studies related to the modeling of water quality monitoring data (e.g. (Nevers and Whitman, 2011)):

1) single-target (ST) models, i.e. for each inactive monitoring site (target) separate model can be created, and
2) multi-target (MT) model, i.e. data for all inactive monitoring sites are combined to create a single prediction model. The MT model discussed in this section should not be confused with multi-output regression (Borchani et al., 2015) that is often labeled in the same way.

Although ST models are more frequently used, MT models can be suitable alternative because of the obvious reduction of computational

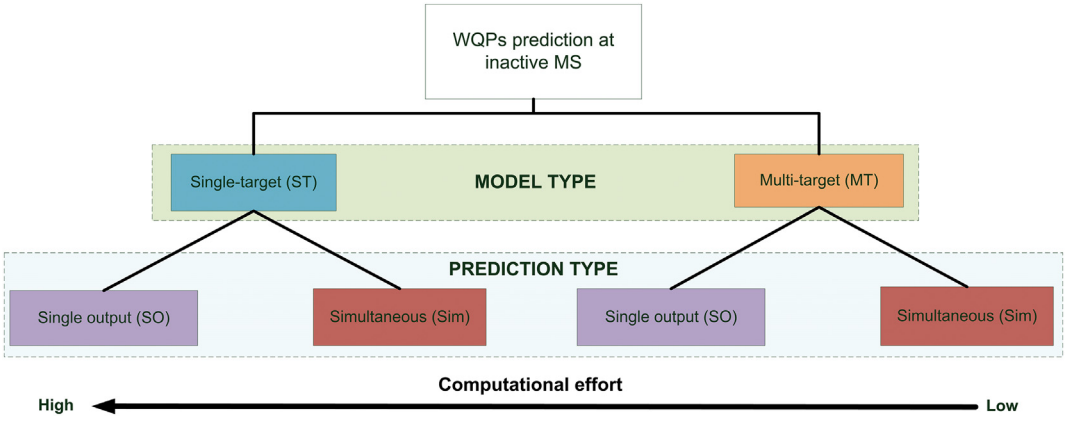

Fig. 2. Modeling approaches.

cost. Also a MT model is smaller than the total size of the ST models and it explains dependencies between different targets (Kocev et al., 2009).

Further, ANN models can be produced to be single output (SO) and simultaneous (Sim), which defines not only the computational efficiency, but also their accuracy, since simultaneous model is obtained by a compromising optimization of all outputs, hence there is no guarantee that minimum error for each output is reached (Chang et al., 2007). While SO ANN models are the most commonly used, several studies have shown that ANNs can simultaneously predict several outputs with desired accuracy, e.g. simultaneous prediction of: five traffic-related pollutants at the national level (Antanasijević et al., 2017), seven meteorological parameters in a weather station (Raza and Jothiprakash, 2014), physical and chemical properties prediction (Ghaedi, 2015), as well as multi-output time series forecasting of electricity prices (Gareta et al., 2006) and demand (An et al., 2013).

The issue related to the computational effort, which can be expressed in the number of models, is more pronounced in the current study, concerning that the number of WQPs that should be predicted for a single inactive monitoring site can be very large (≥20). As can be observed in Fig. 2a, the creation of theoretically most accurate SO-ST models actually means that up to several hundred models are needed to cover each inactive monitoring site (MS), since its number depends both on the number of inactive MS, as well as on the number of WQPs that should be predicted. Therefore, other modeling approaches appear to be more practical since they demand the creation of model(s) which number ranges from 1 to up to the number of WQPs that are subject of prediction (Fig. S1 in the Supplement). Regarding that their accuracy is questionable, it should be empirically verified and benchmarked using SO-ST models, which is one of the aims of current study.

2.3. ANN modeling

ANNs are data-driven methods capable to fit highly nonlinear relations between several input and output variables, which is typically achieved by training performed using iterative algorithms. They are consisted of layers of neurons, usually three, and their training implies (i) random initialization of the weights, (ii) iterative adjustment of the weights, and (iii) the determination of the optimal value of weights based on external criterion, e.g. sum-of-squares error or mean squared error.

In this study, three-layered feed-forward neural network was used for the creation of prediction models. The BFGS algorithm, a quasi-Newton iterative method proposed independently by Broyden–Fletcher–Goldfarb–Shanno (Borsato et al., 2011; Zounemat-Kermani et al., 2016), was used for ANN training, since it is regarded as one of the most powerful methods to solve unconstrained optimization problem (Dai, 2013). Although, BFGS has high memory requirements, due to storage of the Hessian matrix, its fast convergence makes it more efficient in comparison with standard back-propagation algorithm (Nawi et al., 2006). Different types of activation functions (Identity, Logistic sigmoid, Hyperbolic tangent and Exponential) were tested in the hidden and output layers to achieve the best model setup. The complexity of models was determined empirically by testing models with predefined lower and upper limits of hidden neurons. Overtraining has been prevented by stopping the network training at the point where errors for the validation set started to increase. The generalization capability of final models is evaluated on their performance on testing set. All ANN models were generated using STATISTICA Automated Neural Networks module (TIBCO Software Inc., 2017).

As it was already stated, two types of models were constructed: single- and multi-target (Fig. 3). The ST models are generated by coupling historical monitoring data from three monitoring sites: upper neighboring active monitoring site (NAMS) and down NAMS, where both serve as "input" sites, and inactive monitoring site. The selection of representing input sites is discussed in Section 2.5.

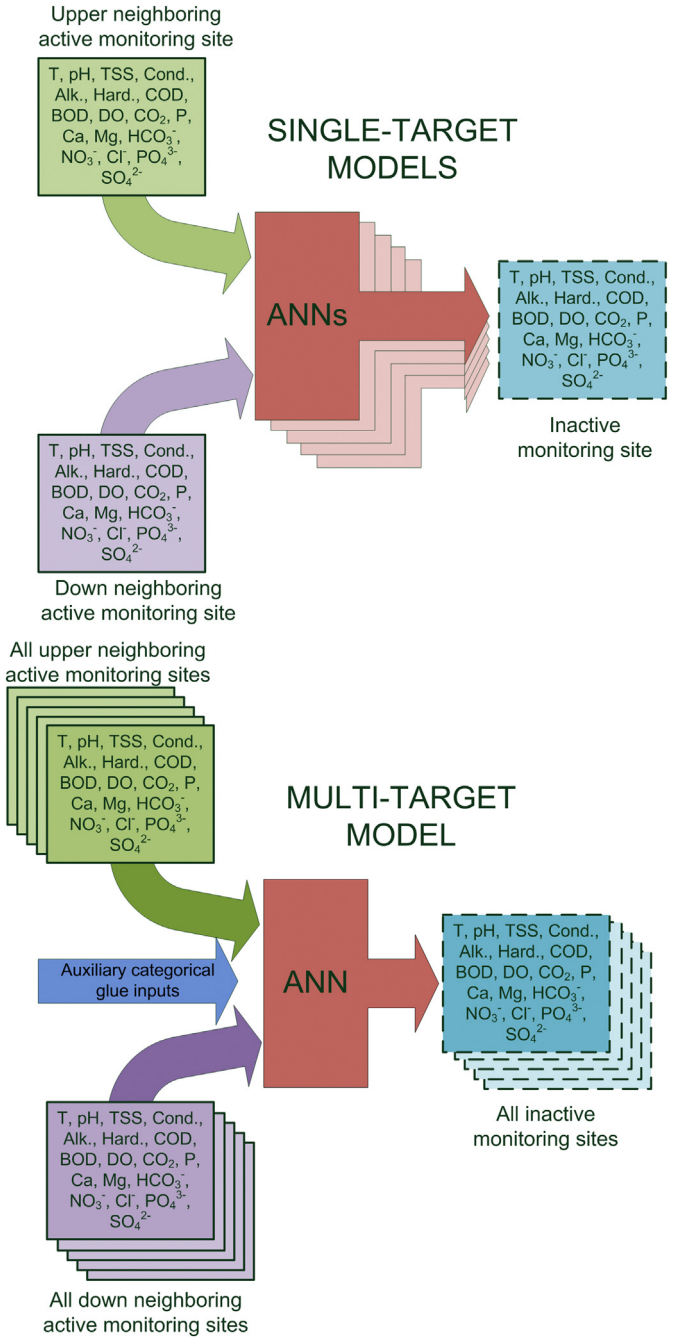

Fig. 3. Single- and multi-target ANN models.

Since seven monitoring sites are not operational on Danube section through Serbia, based on the principles of data fusion (Fosdick et al., 2016), the monitoring data for all those sites are gathered in a single MT model using auxiliary (categorical) "glue" inputs. In this case, three glue inputs are needed, each labeling one of sites that are coupled: upper glue variable (UGV) that marks upper NAMS, down glue variable (DGV) that marks down NAMS, and inactive glue variable (IGV) that is related to the inactive MS.

In the case of single output models, only corresponding WQP from upper and down NAMS are used as inputs, e.g. temperature (T) at inactive MS is predicted using only T measure at upper and down NAMS. In the case of simultaneous models, all available input WQPs are used for the prediction of corresponding WQPs at inactive MS. But concerning that the selection of the best subset of measured input variables is

vital for the performance of an ANN model, additional (optimized) simultaneous models are created based on MCS input selection procedure (Šiljić et al., 2015). The reduction of the number of inputs should reduce the number of free parameters in the model, hence improving its generalization and computational efficiency (Fernando et al., 2005). This particular selection procedure was used since as a model-based approach provide the real influence of inputs on the output results, and also it allows analysis for all outputs in a single run of initial model.

2.4. MCS input selection for simultaneous models

MCS input selection procedure has been previously applied for the selection of the best subset of inputs for single output model, yielding model with better performance which has used 25% less inputs (Šiljić et al., 2015). This procedure comprises of several steps:

1. estimation of probability density functions (PDFs) for each input,
2. selection of the most significant PDF based on the Kolmogorov-Smirnov non-parametric test,
3. re-sampling of inputs according to the selected PDFs,
4. construction of MCS dataset that contains blocks of *n* patterns per input, where each block had one input with re-sampled values, while other inputs were set to the median of measured values,
5. application of initial ANN model to MCS dataset,
6. quantification of a specific input significance based on difference between maximum and minimum predicted output value (Δ) for each block in the MCS dataset,
7. generation of new ANN model with selected inputs and it's evaluation, and
8. sensitivity analysis based on Δ values obtained for final model.

In the case of simultaneous models, additional operations in step 6 are required:

6.1. comparison of particular input significance for different output variables based on normalized Δ (Δ_{norm})
6.2. selection of most significant inputs for each output variable based on predefined number of significance levels (e.g. 1st and 2nd) and/or Δ_{norm} threshold (e.g. $\Delta_{norm} \geq 0.90$).

Application of this procedure is presented in details in Section 3.1.

2.5. Created models

The selection of the pair of active MSs, which WQPs data were used for the prediction of WQPs at particular inactive MS, was performed using two criterions: geographical position and statistical similarity of measured WQPs at target and input sites.

In the first step, active MS are classified into upper and down MS based on their geographical position relative to the particular inactive MS. Namely, all active MS located in the section presiding the target inactive MS are labeled as upper MS, while others are labeled as down MS. This is done under the assumption that MS at Danube river entry and exit point will remain active after rationalization of monitoring network.

In the second step, the one active MS that have highest WQPs pattern similarity with target MS, from both groups, is selected and used for the creation of model. In the current study, similarity between two MSs is determined using location similarity index (LSI) (Antanasijević et al., 2017), which is based on the self-organizing network classification. The LSI values ranges from 0 to 100%, where higher value indicate higher similarity. The LSI for studied monitoring network was published in our previous study (Antanasijević et al., 2017).

The selected pairs of active MSs for each of seven inactive MS with corresponding LSI values are presented in Table 1. As it can be observed, the LSI values in the majority of cases were higher than 80%, indicating high patterns similarity, and supporting the creation of ANN models with satisfactory performance.

Table 1
Combination of MS used for model creation.

Inactive MS	IGV[a]	LSI (upper NAMS)	UGV[b]	LSI (down NAMS)	DGV[c]
Apatin	2	89% (Bezdan)	1	95% (Bogojevo)	3
Bačka Palanka	4	88% (Bezdan)	1	84% (Novi Sad)	5
Čenta	7	95% (Slankamen)	6	73% (Banatska Palanka)	12
Pančevo	9	91% (Slankamen)	6	74% (Banatska Palanka)	12
Vinča	10	81% (Zemun)	8	87% (Smederevo)	11
Veliko Gradište	13	81% (Smederevo)	11	90% (Brza Palanka)	16
Dobra	14	83% (Smederevo)	11	91% (Tekija)	15

[a] Upper glue variable.
[b] Down glue variable.
[c] Inactive glue variable.

To reduce the computational effort needed, the SO-ST and Sim-ST models were created only for one inactive MS, i.e. Apatin (Table S1 in the Supplement). Concerning that 18 WQPs are measured at each site, 18 separate SO- and two Sim-ST (initial and MCS optimized) were created and evaluated.

In the case of MT models, monitoring data for all inactive MS are combined yielding dataset of 466 patterns (Table S2 in the Supplement). Again, 18 separate SO- and two Sim-MT were created and evaluated.

3. Results and discussion

3.1. Optimization and performance of models

In case of single target modeling, i.e. prediction of WQPs at Apatin using Bezdan and Bogojevo data, the models selected based on error obtained on validation data with their topology and testing performance are presented in Table S3 in the Supplement, while performance metrics are defined in Table 2. It can be observed that single output models (SO-ST) were superior (overall NSE = 0.64) in comparison with the initial simultaneous (Sim-ST) model (overall NSE = 0.41), as well as that this simultaneous model is a good starting point for further optimization, concerning that 2/3 of WQPs are predicted with satisfactory accuracy (Fig. 4), according to NSE ratings (Table 2).

In further step, MCS procedure for the selection of inputs was applied. Table S4 in the Supplement shows the PDFs obtained for 36 inputs used in Sim-ST model and the values of Kolmogorov-Smirnov test, which was used for the selection of the best fitting PDF, based on its significance (*p*). The examples of fitted PDFs are presented in Fig. S2 in the Supplement. The MCS dataset was assembled of blocks of inputs with 100 re-sampled values.

The Δ values obtained for the each output of Sim-ST model are presented in the Supplement (see Table S5). In addition, the Δ_{norm} values were calculated by scaling Δ values in the range 0 to 1 (see Table S6 in the Supplement), in order to allow the comparison of the significance of each input-output combination. Finally, the selection of most significant inputs for each output variable, based on 1st and 2nd significance level and Δ_{norm} threshold of 0.90, was performed (Fig. 5a). Hence, the number of inputs has been reduced for 50%, from 36 to only 18, and new simultaneous ST model (labeled as MCS-Sim-ST) was created. Its testing performance is given in Table S3, and it can be noted that prediction result has not been enhanced by MCS, regarding the low NSE (Fig. 4) and overall NSE values (0.30).

It can be concluded that limited number of data point impedes the development of accurate simultaneous single target model. It seems that only possibility for the accurate simultaneous prediction at single location is the reduction of the number of outputs that are

Table 2
Performance metrics with guides on their values, where n is the number of cases and Y_o, Y_p and Y_m are observed, predicted and mean observed output values, respectively.

Metrics	Calculation	Ratings	Short description (Moriasi et al. 2007)
Coefficient of determination (R^2)		Acceptable $R^2 > 0.50$	It describes the proportion of the observed variance explained by the model. R^2 ranges from 0 to 1, with higher values indicating less error variance.
Mean absolute error (MAE)	$\frac{1}{n}\sum\lvert Y_o - Y_p\rvert$		RMSE and MAE are frequently reported because they indicate error in the unit of outputs. Their values of 0 indicate a perfect fit.
Root mean squared error (RMSE)	$\sqrt{\frac{1}{n}\sum(Y_o - Y_p)^2}$		
Nash-Sutcliffe efficiency (NSE)	$1 - \frac{\sum(Y_o - Y_p)^2}{\sum(Y_o - Y_m)^2}$	Very good[a] 0.75 <NSE ≤ 1 Good 0.65 <NSE ≤ 0.75 Satisfactory 0.50 <NSE ≤ 0.65 Unsatisfactory NSE ≤ 0.50	Normalized metrics that determines the relative magnitude of the residual variance (noise) compared to the measured data variance (information). It ranges between - ∞ and 1.0, where 1 is the optimal value, while values < 0.0 indicates that the mean observed value is a better predictor than the model.
Mean absolute percentage error (MAPE)	$\frac{100\%}{n}\sum\frac{\lvert Y_o - Y_p\rvert}{Y_o}$	Highly accurate[b] MAPE ≤ 10% Good 10 < MAPE ≤ 20% Reasonable 20 < MAPE ≤ 50% Inaccurate MAPE > 50%	Frequently used metrics that gives overall relative error, where low values are preferable.

[a]Indicative ratings recommended for a monthly time step (Moriasi et al., 2007).
[b]According to Lewis interpretation the MAPE results (Pao et al., 2012).

simultaneously modeled, and finding their most efficient combination, which is out of the scope of this study.

xThe selected multi-target models with their topology and testing performance are presented in Table S7 in the Supplement. Again, the single output models (SO-MT) were superior (overall NSE = 0.68) in comparison with the initial simultaneous (Sim-MT) model (overall NSE = 0.48). Also, those multi-target models have shown better performance in comparison with single target ones (Fig. 4). This confirms the benefits of data fusion that yields significantly higher number of data patterns available for model development.

Data related to the optimization of Sim-MT models are presented in Table S4 in the Supplement (the best fitting PDFs), Table S8 in the Supplement (the obtained Δ values), Table S9 in the Supplement (the Δ_{norm} values) and Fig. 5b (highly significant inputs with their interactions).

The MCS-Sim-MT has been created with only 19 inputs (plus three glue ones) which makes a reduction of 44% in comparison with the

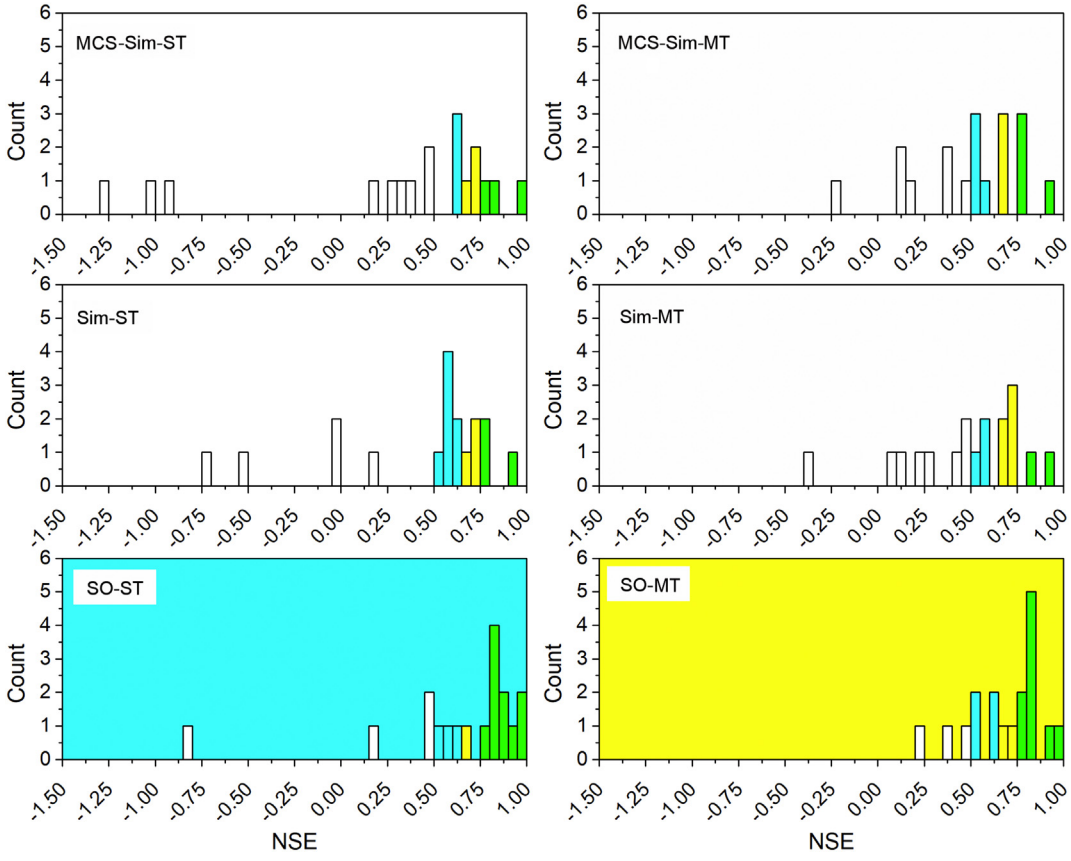

Fig. 4. Histograms of NSE values (for colors see Table 2). (For interpretation of the references to color in this figure legend, the reader is referred to the web version of this article.)

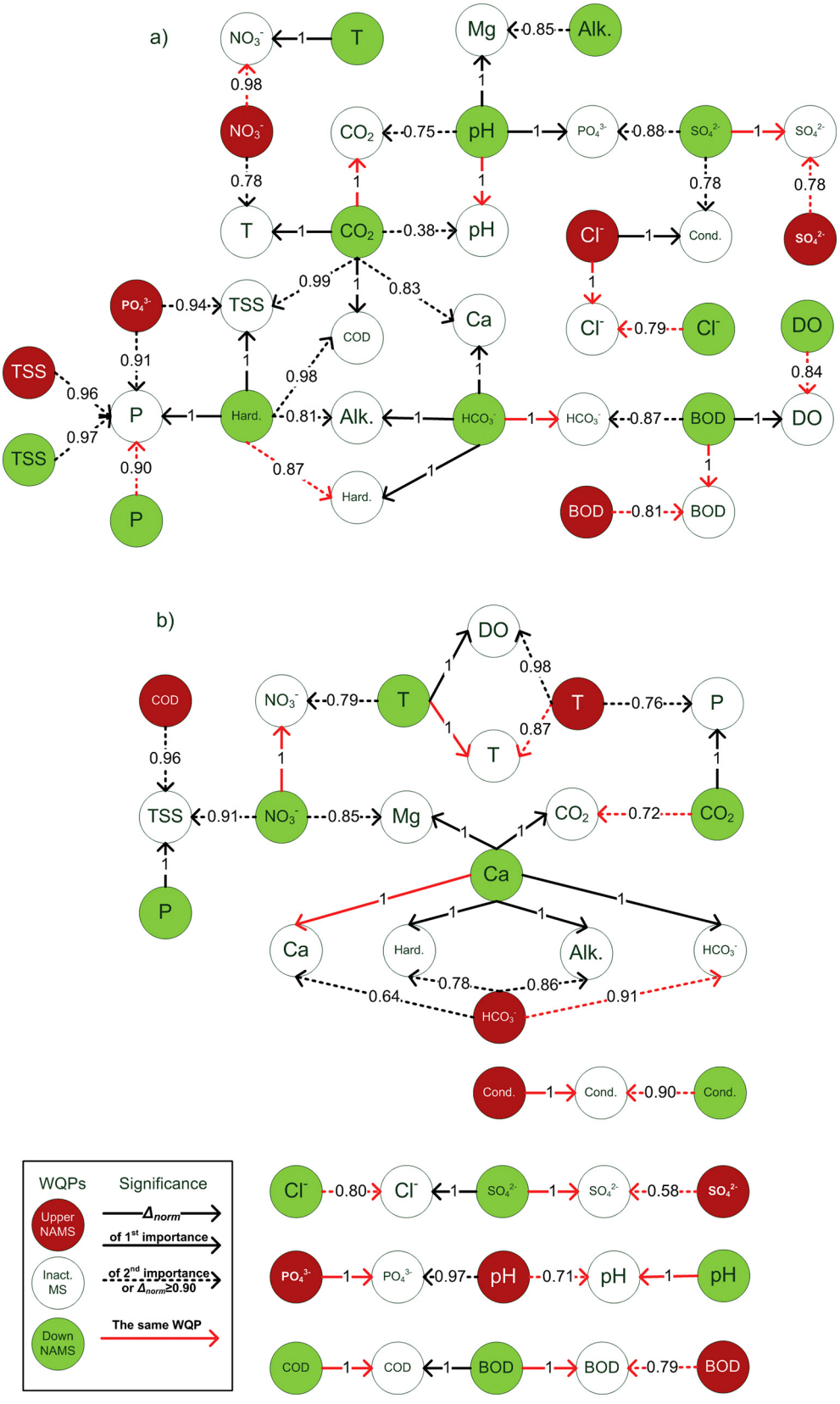

Fig. 5. Highly significant interaction between WQPs for a) Sim-ST and b) Sim-MT.

initial Sim-MT model. The optimized model performance was slightly better with overall NSE = 0.50, which is a threshold for satisfactory performance (Table 2), but still, it had poor performance in comparison with corresponding single output models.

3.2. Overview of input-output interactions

From the above results it can be observed that best performance is obtained when spatial interpolation of particular WQP was performed

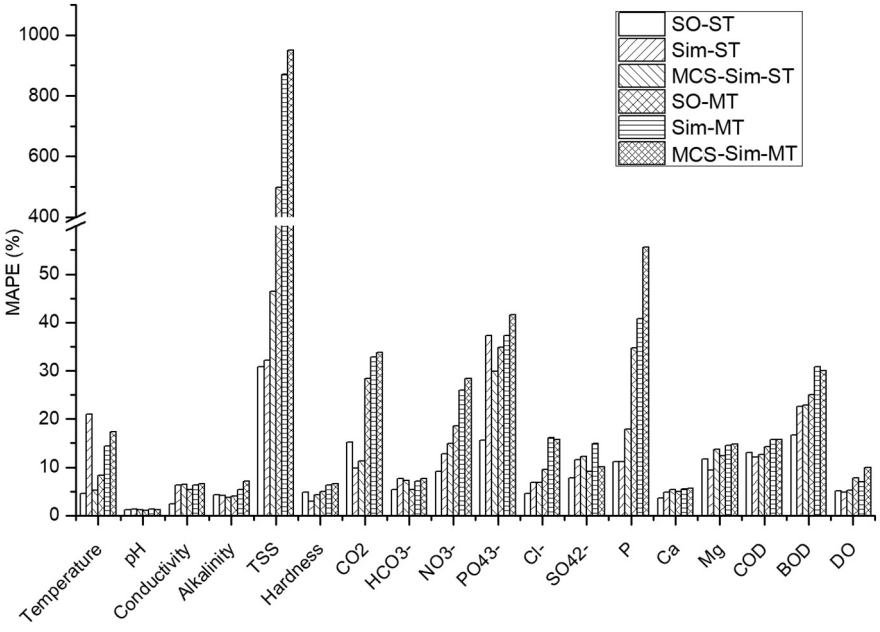

Fig. 6. MAPE depending modeling approach.

with the same WQP measured at similar neighboring locations. This is the case in all single target models, where by default input-output interactions at 1st and 2nd significance level are made by the same WQPs. In the case of simultaneous single-target model (Fig. 5a) one can be observed that BOD, Cl^- and SO_4^{2-} were only WQPs determined at 1st and 2nd significance level determined only by the same input WQPs, while in the case of pH, CO_2, P, DO, Hardness, NO_3^- and HCO_3^- one of the 1st or 2nd significance level was determined by the same WQP. Moreover, all significant interactions in this case present the complex cluster of interactions, where the majority of inputs has the influence on several outputs. In order to quantify the suitability of input-output interactions, to each input-output interaction made by the same WQPs, the weight 1 was given, while the others had 0. For the single output models, the overall suitability index has value that equals two times the number of inputs, i.e. 36, while Sim-ST has index value of only 13.

In the case of simultaneous multi-target model this suitability index is higher (17), and it should be noted that Sim-MT (Table S3) had better performance than Sim-ST (Table S6). From Fig. 5b it can be noted that in the case of Sim-MT(i) T, Conductivity, pH, BOD, SO_4^{2-}were determined only by the same WQPs at the 1st and 2nd significance level, while (ii) COD, CO_2, NO_3^-, Ca, HCO_3^-, Cl^-, PO_4^{3-} were determined by the same WQP at one of the 1st or 2nd significance level. More important, the single cluster of interactions that was observed in the case of single-target model, was portioned in five separate clusters (Fig. 5b) and majority of them mimic the input-output interactions that are present in single output models.

Table 3
Proposed modeling strategy for study area.

Relative error	Model type	Parameters	Number of models
Single-target			
MAPE < 10%	Single output	NO_3^-	7
	Simultaneous	Mg, CO_2	7
Multi-target			
MAPE < 10%	Single output	Temperature, Cl^-	2
	Simultaneous	pH, Alkalinity, Conductivity, Hardness, DO, HCO_3^-, SO_4^{2-}, Ca	1
10% < MAPE < 30% (SO-ST)		TSS, COD, BOD, P, PO_4^{3-}	

3.3. Modeling strategy for studied area

In order to resolve two (opposite) goals, i.e. high accuracy and low computational cost, suitable modeling strategy for studied area has been determined based on MAPE for each modeled WQP. The aim was to define a set of models that will give highly accurate predictions (MAPE ≤ 10%) with lowest possible computational cost. After MAPE for each modeling approach and WQP was assessed (Fig. 6), the combination of models was determined (Table 3). These results indicate that TSS, COD, BOD, P and PO_4^{3-} cannot be predicted with such high accuracy, while the concentration of most other WQPs, all except NO_3^-, Mg, CO_2, can be obtained using multi-target models.

4. Conclusion

The prediction of 18 common water quality parameters (WQPs) on inactive monitoring station/stations on the Danube River at the territory of Republic of Serbia was performed by developing and testing of single output and simultaneous artificial neural network (ANNs) for spatial interpolation of these WQPs at single- and multi-inactive monitoring sites. Monthly and semimonthly data collected during ten years (2002–2011) were used for models development and testing. Monte Carlo Simulation was applied for the variable selection and the analysis of input-output interactions.

Results presented in this study have shown that single output models have outperformed simultaneous ones in the case of majority WQPs. The benefit of data fusion in the case of multi-target models has been observed, concerning that overall Nash-Sutcliffe efficiency (NSE) has increased in comparison with single target models, i.e. from 0.64 to 0.68 in case of single output models and from 0.41 to 0.48 in the case of simultaneous ones. Also, only in the case of simultaneous multi-target model the Monte Carlo Simulation based selection of inputs was successful in providing model with enhanced performance.

After the performance of all type of ANN models had been analyzed, it was determined that the majority of studied WQPs (13/18) were predicted with relative error <10%, which makes the virtual monitoring highly accurate alternative to the field measurements of those WQPs. Moreover, ¾ of studied WQPs can be predicted with desired accuracy using multi-target models which significantly reduce the computational effort and time.

Acknowledgements

The authors are grateful to the Ministry of Education, Science and Technological Development of the Republic of Serbia for financial support (project number 172007).

Appendix A. Supplementary data

Supplementary data to this article can be found online at https://doi.org/10.1016/j.scitotenv.2018.11.189.

References

An, N., Zhao, W., Wang, J., Shang, D., Zhao, E., 2013. Using multi-output feedforward neural network with empirical mode decomposition based signal filtering for electricity demand forecasting. Energy 49, 279–288. https://doi.org/10.1016/j.energy.2012.10.035.

Antanasijević, D., Pocajt, V., Perić-Grujić, A., Ristić, M., 2014. Modelling of dissolved oxygen in the Danube River using artificial neural networks and Monte Carlo simulation uncertainty analysis. J. Hydrol. 519, 1895–1907. https://doi.org/10.1016/j.jhydrol.2014.10.009.

Antanasijević, D., Pocajt, V., Perić-Grujić, A., Ristić, M., 2017. Multiple-input-multiple-output general regression neural networks model for the simultaneous estimation of traffic-related air pollutant emissions. Atmos. Pollut. Res. 9, 388–397. https://doi.org/10.1016/j.apr.2017.10.011.

Antanasijević, D., Pocajt, V., Antanasijević, J., Perić-Grujić, A., Ristić, M., 2018. A novel SON2-based similarity index and its application for the rationalization of river water quality monitoring network. River Res. Appl. 34, 144–152. https://doi.org/10.1002/rra.3231.

Ay, M., Kisi, O., 2014. Modelling of chemical oxygen demand by using ANNs, ANFIS and k-means clustering techniques. J. Hydrol. 511, 279–289. https://doi.org/10.1016/j.jhydrol.2014.01.054.

Barzegar, R., Moghaddam, A.A., 2016. Combining the advantages of neural networks using the concept of committee machine in the groundwater salinity prediction. Model. Earth Syst. Environ. 2, 26.

Barzegar, R., Adamowski, J., Moghaddam, A.A., 2016. Application of wavelet-artificial intelligence hybrid models for water quality prediction: a case study in Aji-Chay River, Iran. Stoch. Env. Res. Risk A. 30, 1797–1819.

Barzegar, R., Moghaddam, A.A., Adamowski, J., Fijani, E., 2017. Comparison of machine learning models for predicting fluoride contamination in groundwater. Stoch. Env. Res. Risk A. 31, 2705–2718.

Barzegar, R., Moghaddam, A.A., Adamowski, J., Ozga-Zielinski, B., 2018. Multi-step water quality forecasting using a boosting ensemble multi-wavelet extreme learning machine model. Stoch. Env. Res. Risk A. 32, 799–813.

Borchani, H., Varando, G., Bielza, C., Larrañaga, P., 2015. A survey on multi-output regression. Wiley Interdiscip. Rev. Data Min. Knowl. Discov. 5, 216–233. https://doi.org/10.1002/widm.1157.

Borsato, D., Pina, M.V.R., Spacino, K.R., dos Santos Scholz, M.B., Filho, A.A., 2011. Application of artificial neural networks in the geographical identification of coffee samples. Eur. Food Res. Technol. 233, 533–543. https://doi.org/10.1007/s00217-011-1548-z.

Chang, F.J., Chiang, Y.M., Chang, L.C., 2007. Multi-step-ahead neural networks for flood forecasting. Hydrol. Sci. J. 52, 114–130. https://doi.org/10.1623/hysj.52.1.114.

Chapman, D.V., Bradley, C., Gettel, G.M., Hatvani, I.G., Hein, T., Kovács, J., Liska, I., Oliver, D.M., Tanos, P., Trásy, B., Várbíró, G., 2016. Developments in water quality monitoring and management in large river catchments using the Danube River as an example. Environ. Sci. Pol. 64, 141–154. https://doi.org/10.1016/j.envsci.2016.06.015.

Dai, Y.-H., 2013. A perfect example for the BFGS method. Math. Program. 138, 501–530. https://doi.org/10.1007/s10107-012-0522-2.

Dinh, Q.T., Liang, D., Thi Anh Thu, T., Le, T.D.H., Dinh Vuong, N., Pham, V.T., 2017. Spatial prediction of saline and sodic soils in rice–shrimp farming land by using integrated artificial neural network/regression model and kriging. Arch. Agron. Soil Sci. https://doi.org/10.1080/03650340.2017.1352088.

Dogan, E., Sengorur, B., Koklu, R., 2009. Modeling biological oxygen demand of the Melen River in Turkey using an artificial neural network technique. J. Environ. Manag. 90, 1229–1235. https://doi.org/10.1016/j.jenvman.2008.06.004.

Fernando, T.M.K.G., Maier, H.R., Dandy, G.C., May, R., 2005. Efficient selection of inputs for artificial neural network models. In: Zerger, A., Argent, R.M. (Eds.), Modsim 2005: International Congress on Modelling and Simulation: Advances and Applications for Management and Decision Making: Advances and Applications for Management and Decision Making. MSSANZ, Melbourne, Victoria, pp. 1806–1812.

Fosdick, B.K., Deyoreo, M., Reiter, J.P., 2016. Categorical data fusion using auxiliary information. Ann. Appl. Stat. 10, 1907–1929.

Gao, M., Yin, L., Ning, J., 2018. Artificial neural network model for ozone concentration estimation and Monte Carlo analysis. Atmos. Environ. https://doi.org/10.1016/j.atmosenv.2018.03.027.

Gareta, R., Romeo, L.M., Gil, A., 2006. Forecasting of electricity prices with neural networks. Energy Convers. Manag. 47, 1770–1778. https://doi.org/10.1016/j.enconman.2005.10.010.

Ghaedi, A., 2015. Simultaneous prediction of the thermodynamic properties of aqueous solution of ethylene glycol monoethyl ether using artificial neural network. J. Mol. Liq. 207, 327–333. https://doi.org/10.1016/j.molliq.2015.04.015.

Huang, W., Foo, S., 2002. Neural network modeling of salinity variation in Apalachicola River. Water Res. 36, 356–362. https://doi.org/10.1016/S0043-1354(01)00195-6.

Keshtegar, B., Heddam, S., 2017. Modeling daily dissolved oxygen concentration using modified response surface method and artificial neural network: a comparative study. Neural Comput. Appl., 1–12 https://doi.org/10.1007/s00521-017-2917-8.

Kocev, D., Džeroski, S., White, M.D., Newell, G.R., Griffioen, P., 2009. Using single- and multi-target regression trees and ensembles to model a compound index of vegetation condition. Ecol. Model. 220, 1159–1168. https://doi.org/10.1016/j.ecolmodel.2009.01.037.

Kovács, J., Kovács, S., Magyar, N., Tanos, P., Hatvani, I.G., Anda, A., 2014. Classification into homogeneous groups using combined cluster and discriminant analysis. Environ. Model. Softw. 57, 52–59. https://doi.org/10.1016/j.envsoft.2014.01.010.

Li, B., McClendon, R.W., Hoogenboom, G., 2004. Spatial interpolation of weather variables for single locations using artificial neural networks. Trans. ASAE 47, 629–637.

Lima, A.R., Cannon, A.J., Hsieh, W.W., 2016. Forecasting daily streamflow using online sequential extreme learning machines. J. Hydrol. 537, 431–443. https://doi.org/10.1016/j.jhydrol.2016.03.017.

Mitrović, T., Obradović, V., Golobočanin, D., Ogrinc, N., Miljević, N., 2010. Spatial and temporal variability of stable isotopes and biological parameters for the Danube River in Serbia. Isot. Environ. Health Stud. 46, 166–179.

Moriasi, D.N., Arnold, J.G., Van Liew, M.W., Bingner, R.L., Harmel, R.D., Veith, T.L., 2007. Model evaluation guidelines for systematic quantification of accuracy in watershed simulations. Trans. ASABE 50, 885–900.

Nawi, N.M., Ransing, M.R., Ransing, R.S., 2006. An improved learning algorithm based on the Broyden-Fletcher-Goldfarb-Shanno (BFGS) method for back propagation neural networks. Proceedings of the Sixth International Conference on Intelligent Systems Design and Applications (ISDA'06). IEEE, Jinan, China, pp. 152–157 https://doi.org/10.1109/ISDA.2006.95.

Nevers, M.B., Whitman, R.L., 2011. Efficacy of monitoring and empirical predictive modeling at improving public health protection at Chicago beaches. Water Res. 45, 1659–1668. https://doi.org/10.1016/j.watres.2010.12.010.

Pao, H.-T., Fu, H.-C., Tseng, C.-L., 2012. Forecasting of CO_2 emissions, energy consumption and economic growth in China using an improved grey model. Energy 40, 400–409. https://doi.org/10.1016/j.energy.2012.01.037.

Peleato, N.M., Legge, R.L., Andrews, R.C., 2018. Neural networks for dimensionality reduction of fluorescence spectra and prediction of drinking water disinfection by-products. Water Res. 136, 84–94. https://doi.org/10.1016/j.watres.2018.02.052.

Philippopoulos, K., Deligiorgi, D., 2012. Application of artificial neural networks for the spatial estimation of wind speed in a coastal region with complex topography. Renew. Energy 38, 75–82. https://doi.org/10.1016/j.renene.2011.07.007.

Raza, K., Jothiprakash, V., 2014. Multi-output ANN model for prediction of seven meteorological parameters in a weather station. J. Inst. Eng. Ser. A 95, 221–229. https://doi.org/10.1007/s40030-014-0092-9.

Rigol, J.P., 2003. Neural networks for spatial interpolation of meteorological data. 3rd Conference on Artificial Intelligence Applications to the Environmental Science. American Meteorological Society, Boulder, Colorado.

Rigol, J.P., Jarvis, C.H., Stuart, N., 2001. Artificial neural networks as a tool for spatial interpolation. Int. J. Geogr. Inf. Sci. 15, 323–343. https://doi.org/10.1080/13658810110038951.

Sahoo, G.B., Schladow, S.G., Reuter, J.E., 2009. Forecasting stream water temperature using regression analysis, artificial neural network, and chaotic non-linear dynamic models. J. Hydrol. 378, 325–342. https://doi.org/10.1016/j.jhydrol.2009.09.037.

Salami, E.S., Ehteshami, M., 2015. Simulation, evaluation and prediction modeling of river water quality properties (case study: Ireland Rivers). Int. J. Environ. Sci. Technol. 12, 3235–3242. https://doi.org/10.1007/s13762-015-0800-7.

Salami Shahid, E., Ehteshami, M., 2016. Application of artificial neural networks to estimating DO and salinity in San Joaquin River basin. Desalin. Water Treat. 57, 4888–4897. https://doi.org/10.1080/19443994.2014.995713.

Salami, E.S., Salari, M., Ehteshami, M., Bidokhti, N.T., Ghadimi, H., 2016. Application of artificial neural networks and mathematical modeling for the prediction of water quality variables (case study: southwest of Iran). Desalin. Water Treat. 3994, 1–12. https://doi.org/10.1080/19443994.2016.1167624.

Shahabi, M., Jafarzadeh, A.A., Neyshabouri, M.R., Ghorbani, M.A., Valizadeh Kamran, K., 2017. Spatial modeling of soil salinity using multiple linear regression, ordinary kriging and artificial neural network methods. Arch. Agron. Soil Sci. 63, 151–160. https://doi.org/10.1080/03650340.2016.1193162.

Šiljić, A., Antanasijević, D., Perić-Grujić, A., Ristić, M., Pocajt, V., 2015. Artificial neural network modelling of biological oxygen demand in rivers at the national level with input selection based on Monte Carlo simulations. Environ. Sci. Pollut. Res. Int. 22, 4230–4241. https://doi.org/10.1007/s11356-014-3669-y.

Snell, S.E., Gopal, S., Kaufmann, R.K., 2000. Spatial interpolation of surface air õ-temperatures using artificial neural networks: evaluating their use for downscaling GCMs. J. Clim. 13, 886–895. https://doi.org/10.1175/1520-0442(2000)013<0886:SIOSAT>2.0.CO;2.

The International Commission for the Protection of the Danube River (ICPDR), 2018. River Basin [WWW Document]. URL. http://www.icpdr.org/.

TIBCO Software Inc, 2017. STATISTICA Automated Neural Networks (SANN) - Neural Networks: An Overview [WWW Document]. URL. http://documentation.statsoft.com/STATISTICAHelp.aspx?path=SANN/Overview/SANNNeuralNetworksAnOverview.

Verma, a.K., Singh, T.N., 2013. Prediction of water quality from simple field parameters. Environ. Earth Sci. 69, 821–829. https://doi.org/10.1007/s12665-012-1967-6.

Wang, Y., Zheng, T., Zhao, Y., Jiang, J., Wang, Y., Guo, L., Wang, P., 2013. Monthly water quality forecasting and uncertainty assessment via bootstrapped wavelet neural networks under missing data for Harbin, China. Environ. Sci. Pollut. Res. Int. 20, 8909–8923. https://doi.org/10.1007/s11356-013-1874-8.

Zounemat-Kermani, M., Kişi, Ö., Adamowski, J., Ramezani-Charmahineh, A., 2016. Evaluation of data driven models for river suspended sediment concentration modeling. J. Hydrol. 535, 457–472. https://doi.org/10.1016/j.jhydrol.2016.02.012.

7th INTERNATIONAL SYMPOSIUM ON INDUSTRIAL ENGINEERING

INDUSTRIAL ENGINEERING DEPARTMENT,
FACULTY OF MECHANICAL ENGINEERING,
UNIVERSITY OF BELGRADE, SERBIA
&
STEINBEIS ADVANCED RISK TECHNOLOGIES,
STUTTGART, GERMANY
&
INNOVATION CENTER OF THE FACULTY OF MECHANICAL ENGINEERING,
UNIVERSITY OF BELGRADE

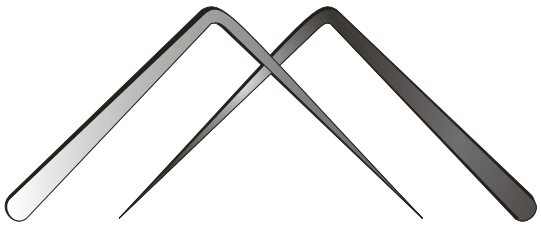

SIE 2018 PROCEEDINGS

Editors:

Vesna Spasojević-Brkić
Mirjana Misita
Dragan D. Milanović

27th-28th September 2018
Belgrade, Serbia

Editors
Vesna Spasojević-Brkić
Mirjana Misita
Dragan D. Milanović

7th INTERNATIONAL SYMPOSIUM ON INDUSTRIAL ENGINEERING - SIE 2018, PROCEEDINGS

Publisher
Faculty of Mechanical Engineering, Belgrade

Printing firm
"PLANETA PRINT" d.o.o. Beograd

Published 2018
ISBN 978-86-7083-981-6

CIP - Каталогизација у публикацији -
Народна библиотека Србије, Београд

INTERNATIONAL Symposium of Industrial Engineering
(7th; 2018; Beograd)
Proceedings / 7th International Symposium of Industrial Engineering - SIE 2018, 27th-28th September, 2018, Belgrade ; [organizers] Industrial Engineering Department, Faculty of Mechanical Engineering, University of Belgrade [and] Steinbeis Advanced Risk Technologies, Stuttgart, Germany [and] Innovation Center of The Mechanical Engineering, University of Belgrade; editors Vesna Spasojević-Brkić, Mirjana Misita, Dragan D. Milanović. - Belgrade: Faculty of Mechanical Engineering, 2018 (Beograd: Planeta PRINT d.o.o.). - [9], 271 str. : ilustr. ; 30 cm

Tekst štampan dvostubačno. - Tiraž 100. - Str. [4]: Preface / editors. - Bibliografija uz svaki rad.

ISBN 978-86-7083-981-6

1. Spasojević-Brkić, Vesna [уредник] [аутор додатног текста], 1971-
2. Faculty of Mechanical Engineering (Beograd). Industrial Engineering Department
a) Производња - Организација - Зборници b) Индустријски менаџмент - Зборници c) Индустрија - Систем квалитета - Зборници

Sponzored by
Government of the Republic of Serbia
Ministry of Education, Science and Technological Development

Organizers of SIE 2018:

INDUSTRIAL ENGINEERING DEPARTMENT, FACULTY OF MECHANICAL ENGINEERING, UNIVERSITY OF BELGRADE, SERBIA & STEINBEIS ADVANCED RISK TECHNOLOGIES, STUTTGART, GERMANY & INNOVATION CENTER OF THE FACULTY OF MECHANICAL ENGINEERING, UNIVERSITY OF BELGRADE

Program Advisory Committee

Chairperson: Spasojević-Brkić Vesna, FME, Belgrade, SERBIA; Jovanović Aleksandar, Stuttgart University, Stuttgart, GERMANY

- Babić Bojan, FME, UB (SRB)
- Bragatto Paolo, INAIL (ITA)
- Buchmeister Borut, University of Maribor (SLO)
- Bugarić Uglješa, FME, UB (SRB)
- Casadesus Marti, Universidad de Girona (ESP)
- Csetverikov Dmitrij, Hungarian Academy of Sciences, Institute for Computer Science and Control (HUN)
- Cockalo Dragan, TF "Mihajlo Pupin", UNS (SRB)
- Dondur Nikola, FME, UB (SRB)
- Dźwiarek Marek, Central Institute for Labour Protection – National Research Institute (POL)
- Engh Erik, Web-Dev, Oslo (NOR)
- Ferreira Pedro, Instituto Superior Técnico, Lisbon & FEES (PRT)
- Filipović Jovan, FOS, UB (SRB);
- Francalanza Emmanuel, FE, University of Malta (MLT)
- Gane Patrick, OY, Oftringen (CHE)
- Karapetrovic Stanislav, University of Alberta (CAN)
- Klarin Milivoj, TF "Mihajlo Pupin", UNS (SRB)
- Kreiner Jesa, California State Universitiy, Fullerton (USA)
- Lalić Bojan, FTS, UNS (SRB)
- Majstorović Vidosav, FME, UB (SRB)
- Milanović D. Dragan, FME, UB (SRB)
- Milazzo Francesca Maria, UM (ITA)
- Milosavljevic Pedja, FME, UN (SRB)
- Mitrović Radivoje, FME, UB (SRB)
- Minovski Robert, FME, Skoplje (MKD)
- Misic Dimic Katarina, Aalto University (FIN)
- Misita Mirjana, FME, UB (SRB)
- Nunes Lopes Isabel, FCTUNL, Lisbon (PRT)
- Petrović Dušan, FME, UB (SRB)
- Popović Predrag, Institute Vinča (SRB)
- Putnik Goran, Universidade de Minho (PRT)
- Radenovic Stojan, FME, UB (SRB)
- Radojević Slobodan, FME, UB (SRB)
- Rakonjac Ivan, Serbian Innovation Fund (SRB)
- Rožić Tomislav, FTTS, Zagreb (CRO)
- Shuman Rutar Teodora, Seattle University (USA)
- Sibalija Tatjana, MU, Belgrade (SRB)
- Tadic Danijela, FEM, Kragujevac (SRB)
- Tanović Ljubodrag, FME, UB (SRB)
- Uzunovic-Zaimovic Nermina, FME, Zenica (BIH)
- Valis David, UD (CZE)
- Váncza József, MTA SZTAKI (HUN)
- Veljković Zorica, FME, UB (SRB)
- Mihajlović Ivan, TFB, Bor (SRB)
- Zajac Mateusz, PW, Wroclaw (POL)
- Živković Živan, TFB, Bor (SRB)
- Žunjić Aleksandar, FME, UB (SRB)
- Xiao-Guang Yue, IETI, Hong Kong (CHN)
- Weiss John, University of Bradford, Bradford (UK)

Organizing Committee

- Vesna Spasojevic-Brkic, PhD, Full Professor, FME, Belgrade, Serbia, Chairperson
- Mirjana Misita, PhD, Full Professor, FME, Belgrade, Serbia
- Sonja Josipović, PhD, FME, Belgrade, Assistant, Serbia
- Tamara Golubović, PhD, FME, Belgrade, Assistant, Serbia

PREFACE

Since the first symposium in Belgrade, Serbia more than two decades ago, in 1996, International Symposium on Industrial Engineering - SIE has been held regularly every 3 years. It represents an opportunity for researchers in the Industrial Engineering community to review and evaluate their scientific achievements over the period since the previous SIE, share their most recent results and ideas, and discuss possibilities for new directions in research, joint experiments and observing campaigns.

The aim of the 7th International Symposium on Industrial Engineering – SIE 2018 is to contribute to a better comprehension of the role and importance of Industrial Engineering and to point out to the future trends in the field of Industrial Engineering. The Symposium is also expected to foster networking, collaboration and joint effort among the conference participants to advance the theory and practice as well as to identify major trends in Industrial Engineering today. According to these goals the Symposium addresses itself to all experts in all fields of Industrial Engineering to make their contribution to success and show capabilities achieved in the work that has been done are very welcomed. SIE 2018 provides an international forum for the dissemination and exchange of scientific information in industrial engineering fields through the large number of multidisciplinary topics.

The book brought together 58 papers and more than 170 authors from 12 countries, namely from Serbia, Portugal, Finland, Switzerland, FR Macedonia, Italy, United Kingdom, Thailand, Slovakia, Canada, Poland and Bosnia and Herzegovina. The submitted full length manuscripts were peer-reviewed, and selected for publication by experts in their respective fields. The authors ranged from senior and renowned scientists to young researchers. Only unpublished papers were accepted and the first author is responsible for the originality of the paper. All papers are classified into six chapters, including opening and closing plenary lectures.

We expect that papers and discussions will contribute to better comprehension the role and importance of Industrial Engineering in this and other countries, both in domain of scientific work and everyday practice.

Our efforts in organizing would not succeed without the considerable help of the members of Scientific Program and the financial help of Ministry of Education, Science and Technological Development was greatly supportive for the success of the entire project.

At the end, the editors hope, and would like, that this book to be useful, meeting the expectation of the authors and wider readership and to incentive further scientific development and creation of new papers in the field of Industrial Engineering.

Welcome to the 7th International Symposium on Industrial Engineering – SIE 2018! We wish to all participants a pleasant stay in Belgrade and are looking forward to seeing you all together at the 8th Symposium on Industrial Engineering – SIE 2021.

Belgrade, September 2018

EDITORS

- CONTENTS –

OPENING PLENARY SESSION - CHAIRPERSONS: Maria Francesca Milazzo, John Weiss, Paolo Bragatto, Ivan Rakonjac

SESSION A1 - CHAIRPERSONS: Dragan D. Milanović, Sanja Stanisavljev, Dragan Ćoćkalo

SESSION A2 - CHAIRPERSONS: Zorica Veljković, Nikola Dondur, Aleksandar Žunjić

SESSION B1 - CHAIRPERSONS: Katarina Dimic-Misic, Danijela Tadić, Tatjana Šibalija

SESSION B2 - CHAIRPERSONS: Mirjana Misita, Andrea Sütőová, Pedja Milosavljevic

CLOSING PLENARY SESSION - CHAIRPERSONS: Patrick Gane, Kristína Zgodavová, Ernest Barceló

7 th International Symposium on Industrial Engineering
SIE2018
IE
Supported by: STEINBEIS ADVANCED RISK TECHNOLOGIES & INNOVATION CENTER OF THE FACULTY OF MECHANICAL ENGINEERING

NITROGEN PLASMA SURFACE TREATMENT ON MICRO NANOFIBRILLATED CELLULOSE FILMS

Katarina Dimić-Misić[1], Mirjana Kostić[2], Ana Kramar[2], Miodrag Kuraica[3], Bratislav Obradović[3], Stevan Jovanović[4], Sasa Lazović[4], Dimitrije Stepanenko[4], Marija Mitrović Dankulov[4] , Thad Maloney[1], Patrick Gane[1]

[1] School of Chemical Engineering, Department of Bioproducts and Biosystems, Aalto University, 00076 Aalto, Helsinki, Finland
[2] Faculty of Technology and Metallurgy, University of Belgrade, Karnegijeva 4, Belgrade 11000, Serbia
[3] Faculty of Physics, University of Belgrade, Studentski trg 12, 11001 Belgrade, Serbia
[4] Institute of Physics, Pregrevica 118, 11080 Belgrade, Serbia

ABSTRACT

Micro-nanofibrillated cellulose (MNFC) films were formed from aqueous suspensions of progressively enzymatic pretreated wood-free cellulose fibres. The mechanical properties of each film are highly dependent on the enzymatic pretreatment time. The films were surface modified by exposure to dielectric-barrier discharge (DBD) nitrogen plasma, seen to increase wettability by both polar (water) and non-polar (hexadecane) liquids, but the increase is proportionally greater for the polar liquid. The change in surface chemistry is revealed using X-ray photoelectron spectroscopy (XPS). An increase in surface roughness acts to link the increase in both polar and dispersive components. The relative change between the polar and dispersive surface energy components favoured trapping of organic-based polar-solvent inks, such as are used in the production of printed solar cells.

Keywords: DBD plasma, nitrogen plasma surface treatment, nanocellulose films, enzymatic nanocellulose, printing of organic-based polar inks

INTRODUCTION AND BACKGROUND

Sustainability is one of the key targets for industrial practice today, and related research aimed at new biobased materials derived from renewable sources, is considered highly relevant in the emergent bioeconomy. In the bioproducts industry, micro nanofibrillated cellulose (MNFC) has attracted attention due to a number of potential applications, not only in forest products, such as paper and board manufacturing, but also in a broad range of industrial value chains, such as biodegradable packaging films, laminates for paper/board. MNFC has interesting intrinsic properties derived from high specific surface area, regions of crystallinity and hydroxylated surface chemistry, ideal for possible chemical modification. Films formed from MNFC are considered smart materials and are being researched for functional materials applications. One such application is as a substrate for printed solar cells using organic-based inks [1].

Enzymatically treated fibres used to produce cellulose nanofibrils provide higher crystallinity in the resulting nanocellulose, as enzymes digest amorphous cellulose. The surface properties of nanocellulose films, such as wettability, topography, chemistry, surface charge, the presence of hydrophobic and hydrophilic domains, density and conformation of functional groups, all play a crucial role in printability and barrier properties. Their ability to support controlled migration of solvent ink vehicle and chromatographic differentiation of ink components is important in the printing of IP inks, and especially for production of bio-based printed functionality in a wide range of applications, such as printed electronics and printed diagnostics [2, 3].

Solar panel inkjet printable (IP) photovoltaic (PV) inks contain a complex mix of materials, including the organic electron acceptor (p-type) and negative electron donor (n-type) suspended in solvent together with specific surfactant(s) intended to keep the p-type and n-type components de-mixed. Although especially drop-on-demand (DoD) IP is a

very competitive candidate for printing PV inks on film substrates, there are some limitations in respect to mutual compatibility between highly hydrophilic surface MNFC films and mixed polar-dispersive solvents constituting the PV ink [4-9]. This complexity of polar-dispersive surface energy balance is, therefore, critical.

The plasma technique is a convenient method to modify the surface properties of polymeric materials, keeping intact their bulk properties. Furthermore, it is an easy way to introduce the desired groups or chains onto the surface of materials with increased roughness. Surface properties of paper and cellulose based materials also may be altered by plasma treatment techniques using careful control of operational parameters, including the gas used, reaction conditions (power, pressure and exposure time) and the reactor geometry [10].

In this work, we aim at modifying the MNFC film surfaces using nitrogen plasma to enhance their amphiphilic surface affinity to polar and non-polar IP PV inks. Surface energy (sessile drop method), surface roughness (atomic force microscopy (AFM)) and X-ray photoelectron spectroscopy (XPS) were used to parameterise the MNFC film surface before and after plasma treatment. The affinity for IP PV ink was assessed visually after inkjet printing.

The mechanical properties of the obtained films were studied to ensure satisfactory film strength.

MATERIALS AND METHODS

Preparation of MNFC

For the manufacture of short MNFC fibrils, the pulp was first washed to create the sodium form by adding sodium hydroxide to a 2 w/w% fibre suspension until the pH reached 10, and then re-washed with deionised water to a conductivity of 8.2 µS. The enzymatic treatment was performed with a commercial enzyme ECOPULP® R (Ecopulp Finland Oy), a genetically modified strain of Trichoderma reesei fungus. An amount of 3 mg of enzyme per gram of pulp fibre was added to a 2.5 w/w% suspension and the temperature was increased to 57 °C at pH 5.5 during hydrolysis, whilst keeping under constant agitation. The period of digestion was increased for each subsequent sample in 30 min steps, Table 1. The enzymatic activity was terminated by adjusting the pH to 9-10 by sodium carbonate and increasing the temperature to 90 °C. After cooling the suspension overnight in cold storage, the samples were refined through an homogeniser (model M-110P, Microfluidics, USA) under a pressure of 2 000 bar through a 100 µm flow gap. The solids content of the MNFC suspension after the fluidisation was 1.65 w/w%.

Enzymatic hydrolysis of pulp as a route for production of low-charged MNFC results in production of short fibrils, which have much lower aspect ratio than MFC and NFC produced via chemical oxidative pretreatment or mechanical refining alone, as presented in Fig. 1, observed with imaging comparing MNFC/300/ and MNFC/0/ suspensions, i.e. Fig. 1a) reveals much shorter fibrils obtained upon 300 min of enzymatic hydrolysis.

Enzymatic treatment time / min	0 (reference)	30	60	90	120	150	180	210	240	270	300
Sample label	MNFC /0/	MNFC /30/	MNFC /60/	MNFC /90/	MNFC /120/	MNFC /150/	MNFC /180/	MNFC /210/	MNFC /240/	MNFC /270/	MNFC /300/

Table 1. Materials used in this study: bleached hardwood Kraft pulp treated with enzymes under controlled conditions, with progressive increase in enzymatic digestion time by 30 min steps for each subsequent sample.

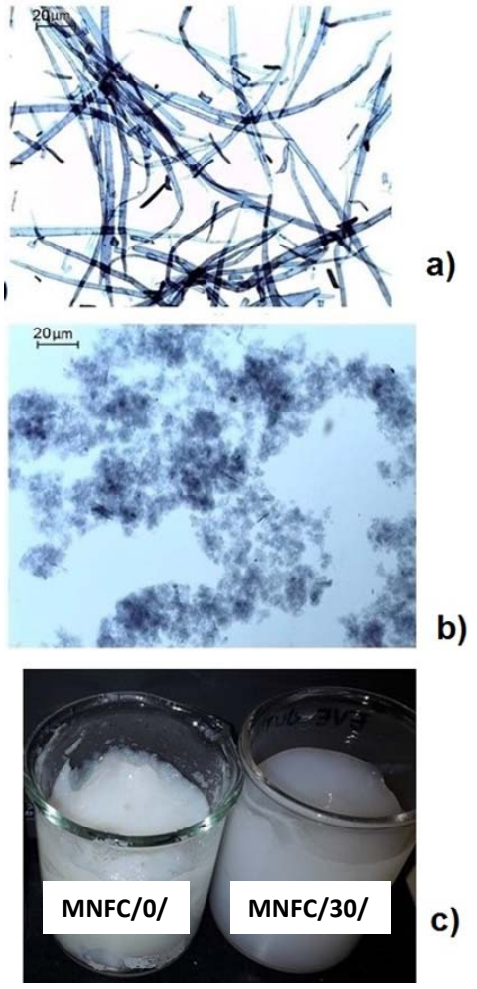

Fig 1. Images of fibrils sample suspensions obtained with optical microscopy revealing the effect of processing conditions on the fibril size and aspect ratio: a) without enzymatic treatment produced MNFC/0/ yielding long fibrils, b) MNFC/300/ short, low aspect ratio fibrils, and c) displaying the corresponding 2 w/w% MNFC suspensions of MFC/0/ and MNFC/300/, showing the difference in gelation strength due to the different size of fibrils and corresponding water dispersed within the fibrillar matrix.

MNFC film preparation

Depending on enzymatic treatment time, the resulting MNFC suspension viscosity decreased significantly, and so the solid content for preparation of the respective films ranged from 0.6 w/w% to 1.9 w/w% to meet the target film grammage of 60 gm^{-2} produced under conditions of 23 °C and relative humidity (RH) 50 %. Films were made on a sheet-former according to ISO standard 5269-1, with some modification of the screen to aid fines retention. The system was pressurised to 0.3 bar and the sealing lid was used on the sheet-former, with a 10 µm mesh supplemented nylon screen in addition to metallic wire screen, so that the slurry of pulp was poured at high viscosity onto the former without adding water or stirring the slurry. Double-sided adhesive tape, width of 5 mm, was attached to the edges of the drying plate between plate and formed film, with purpose of fixing the edge of the film to prevent it shrinking during drying.

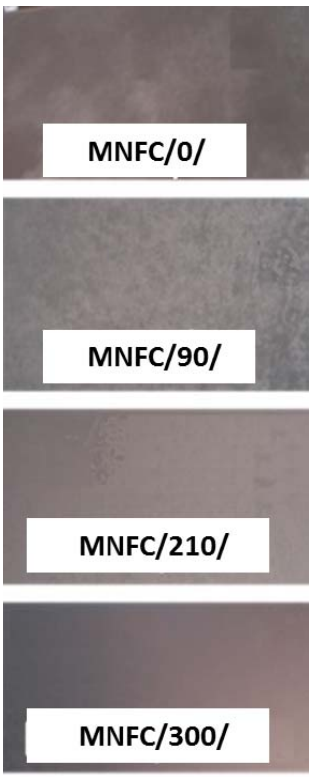

Fig. 2 Samples of cut-offs (60 x 15 mm^2) from MNFC films produced from pulp refined with different enzymatic pretreatment time (Table 1). Transparency and uniformity of films increases with hydrolysis time.

Material treatment and characterisation

Optical microscopy was used to study the fibrillar sample suspensions and films using an Olympus BX 61 microscope equipped with a ColorView 12 camera. The water retention value (WRV) of the MNFC was determined in accordance to the standard SCAN-C 102XE with a slight modification in that a polyamine monofilament open mesh fabric SEFAR NITEX® 03-1/1 with a pore size of 1µm was placed on top of a 125 µm metal screen. The experiment was performed in triplicate for each sample.

Plasma treatment

Dielectric Barrier Discharge (DBD) plasma operates in a thermodynamically non-equilibrium condition (so-called cold plasma) in which the ion

and molecular translational temperature is much lower than the electron temperature, such that excessive gas heating can be suppressed. The advantage is that the plasma can be generated at atmospheric pressure, both in open or closed environment. In an open atmosphere the plasma discharges can be produced with a gas flow between the electrodes. A further attractive characteristic of the DBD plasma at atmospheric pressure is that it can be used to modify or activate surfaces of a wide range of materials, from polymers, textile fibres to biological tissues, without damaging them. To generate the DBD plasma we used a home-made device built at the Faculty of Physics, University Belgrade, Fig. 3. The DBD is assembled in a chamber with nitrogen gas injected into the discharge volume (6 dm^3min^{-1}) through ten equidistant holes to ensure homogeneous gas flow. MNFC films were treated for 0 s, 30 s and 60 s, respectively. The device was operated at 300 electric field pulses per second (Hz) for the prescribed durations of time.

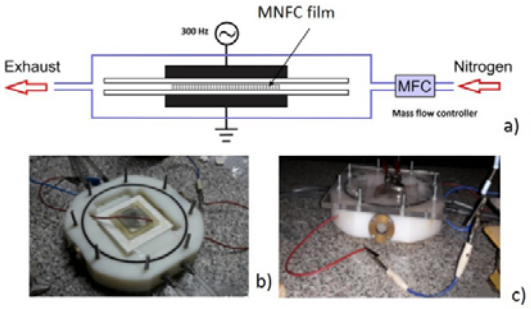

Fig. 3. DBD device with two electrodes and sample placed between them: a) schematic illustration of DBD plasma devise, b) plasma chamber housing the sample placed 1 mm from the upper electrode, and c) closed plasma set up with glass lid placed above the top of the upper electrode.

Free surface energy (FSE)

Measurement of high energy surfaces

Most liquids are rapidly spreading on a high energy surface, and so a representative contact angle (CA) cannot be readily measured. Schultz (1977) [11] developed a method where CA can be measured by submerging the surface in one liquid and using a second liquid to measure the contact angle. In this case a hydrocarbon n-hexadecane is used as the submerging liquid having the purely dispersive liquid-vapour surface tension of $\gamma_{LV}^{h} = 27.4$ $mJ.m^{-2}$, much lower than the expected surface free energy of the MNFC samples, and water as the contact angle liquid with the highly polar liquid-vapour surface tension $\gamma_{LV}^{w} = 59.4$ $mJ.m^{-2}$. A sessile drop of water is lowered into contact with the horizontal film immersed under hexadecane using a precise pipette delivering 70 µl of liquid and the progressive change in drop shape due to the change in CA recorded with a Nikon camera (D5000) in time steps of 1 ms. The CA of water is also recorded separately to represent the print challenge of a highly polar ink. For each given MNFC sample and given liquid data variation is within 10 %. The identification of contact line geometry and evaluation of CA uses numeric software tools, as presented visually in Fig. 4. For a parallel optimal method for polar FSE determination with water alone, the Girifalco and Good approach [12], combined with the Neumann equation of state was used. This latter allowed the polar contribution to SFE be estimated and thus can be added to the formerly measured dispersive component. Each measurement was conducted five times.

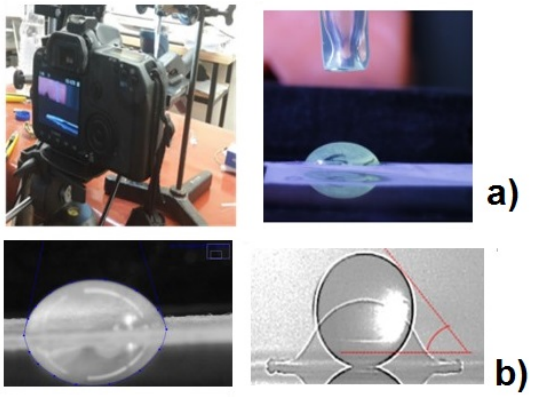

Fig. 4. Contact angle (CA) measurements as made at the Belgrade Institute for Physics: a) set-up for evaluating water CA under n-hexadecane with camera, b) determination of CA with use of image processing software and Java program for calculation.

Surface topography

Plasma action on the film surface can lead to a degree of debonding of fibrils as well as electrostatic charging and potential for subsequent additional moisture adsorption. Such changes can lead to re-conformation of the surface, even though no mechanical forces have been applied. The change in topography of the MNFC films was investigated by Atomic Force Microscopy (AFM) (Veeco Instruments, model Dimension V). using a MultiMode 8 with Bruker NanoScope V controller. Each MNFC film sample was dry-cast onto a Mica support for AFM imaging. Micrographs were obtained in trapping mode under ambient conditions, using TAP 300 tips (resonant frequency 300 kHz, line force being kept constant at 40 Nm^{-1} and the AFM images were processed and analysed with the Bruker NanoScope Analysis 1.5 software.

Mechanical properties

Mechanical properties of the MNFC films were measured by a MTS 400/M vertical tensile tester equipped with a 20 N load cell. The instrument was controlled by a TestWorks 4.02 program. Specimen strips with dimensions of 60 x 15 mm^2 were clipped from the MNFC films with a lab paper cutter. The thickness of the strips was separately measured with an L&W micrometer SE 250. The gauge length was 40 mm and the testing velocity was 0.5 $mm.min^{-1}$. The results are presented as an average value obtained from five parallel specimens. The suspension was filtered subsequently using a Britt Dynamic Drainage Jar (DDJ), stirred by an overhead stirrer at 200 min^{-1} (rpm), based on Tappi test method T261cm-00, to collect fibres retained on the 200-mesh screen (105 μm).

Surface chemical composition

Surface composition of the MNFC films was evaluated with X-ray photoelectron spectroscopy (XPS), using a Kratos AXIS Ultra electron spectrometer, with monochromatic Al Kα irradiation at 100 W and under charge neutralisation. Both the untreated MNFC films and plasma treated specimens were analysed. For the preparation, samples were pre-evacuated for at least 12 h, after which wide area survey spectra (for elemental analysis) as well as high resolution regions of C1s and O1s were recorded from several locations, and an in-situ reference of pure cellulose was recorded for each sample batch (Johansson and Campbell 2004). With the parameters used, XPS analysis was recorded on an area of 1 mm^2 and the analysis depth is less than 10 nm. Carbon high resolution data were fitted using CasaXPS and a four component Gaussian fit tailored for celluloses.

Printing

The photovoltaic (PV) inkjet printing inks (IP) contain a complex mix of materials, solvent and surfactants that keep the p-type and n-type components de-mixed. A piezoelectric laboratory scale drop-on-demand (DoD) materials inkjet printer (Dimatix 2831-DMP) was used to test the printability of the plasma treated MNFC films. The solvent of the IP ink is 3-methoxypropionitrile, which is highly polar and non-volatile (boiling point 164 ºC), viscosity 1.2 mPa.s and density 0.937 gcm^{-3}, as stated by the supplier, Sigma Aldrich. The surface tension measurement was performed on the ink with an optical tensiometer (CAM 200 from KSV instruments) in pendant drop mode, giving a value of 29.2 $mN.m^{-1}$ ($mJ.m^{-2}$)

RESULTS AND DISCUSSION

The change in dewatering of the MNFC suspensions and change in fibre morphology, expressed as the fines content using the dynamic drainage jar (DDJ), are given in Table 2.

It is clear to see that with increase in enzymatic hydrolysis time, dewatering decreases as fibrils become thinner and smaller, and suspensions become more gel-like. At the same time, crystallinity of fibrils increases.

The *mechanical and optical* properties of MNFC films are presented in Table 3 where it is evident that the sheet density of the films increases with increase in hydrolysis time, while the packing density of the smaller crystalline particles increases. The permeability of those films created with the finer nanofibrils obtained after 120 min hydrolysis in turn falls rapidly, and it was not possible to measure using air flow techniques. The light scattering coefficient decreases also as the packing density is increased and the amorphous parts of the cellulose fibres were reduced, while, due also to higher packing density, the elasticity modulus increases, showing that films had improved strength.

Table 2. Properties of MNFC suspensions

MNFC suspensions properties		
Enzymatic treatment time / min	WRV / cm^3g^{-1}	DDJ fines value / %
0	1.25	93.8
30	1.61	88.8
60	1.83	79.5
90	2.19	62.4
120	2.55	27.0
150	2.85	21.0
180	2.98	11.8
210	3.33	9.6
240	3.37	6.5
270	3.32	1.5
300	3.34	0.2

Table 3. Mechanical and optical properties of MNFC films

Film properties					
Enzymatic treatment time / min	film weight / gm^{-2}	density / gcm^{-3}	permeability / $\mu m(Pa\ s)^{-1}$	light scattering coefficient / m^2kg^{-1}	E-Modulus / GPa
0	73.91	0.637	69.86	37.43	2.53
30	76.12	0.794	9.96	22.83	4.16
60	71.35	0.910	1.06	16.12	5.12
90	72.31	1.016	NA	9.94	7.02
120	70.53	1.090	NA	6.93	8.59
150	70.81	1.127	NA	5.81	9.13
180	69.57	1.145	NA	4.48	8.95
210	71.08	1.178	NA	3.74	11.26
240	70.10	1.179	NA	3.08	9.17
270	71.18	1.226	NA	3.11	9.76
300	65.27	1.187	NA	3.31	10.03

Roughness colour contour and profile plots of the surface of MNFC/30/150/300 films before and after plasma treatment are presented in Fig. 5. Before plasma treatment, the roughness of the films is directional, being different in in the two measured directions (red and blue profile lines). The map for MFC/30/ indicates that there are voids present between 1-2 µm wide, while in the case of MFC/300/ the surface is flatter with less voids and of much smaller size. This means that the degree of enzyme hydrolysis directly increases the resulting smoothness due to the ever finer fibrillar elements produced, as the crystalline parts are separated due to breakdown of the amorphous constituent. After plasma treatment, the amorphous material containing surfaces, e.g. MNFC/30/, are also seen to become relatively rougher than the highly hydrolysed crystalline films, e.g. MNFC/300/. The action of the plasma is to increase voidage in the courser particulate systems, as previously described, due to effects of charge, fibril debonding etc. In MFC/30/, it is possible to identify irregular both small and large voids appearing after plasma treatment, while in MFC/300/, the surface of the film has almost no such jagged appearance with only voids smaller than 1 µm. Nitrogen plasma treatment, thus, obviously changes the morphology of the films, on both the micro (nano) and macro level, which is likely also to have an influence on the wetting behaviour and decrease in CA due to the increased meniscus liquid-solid wetting line length.

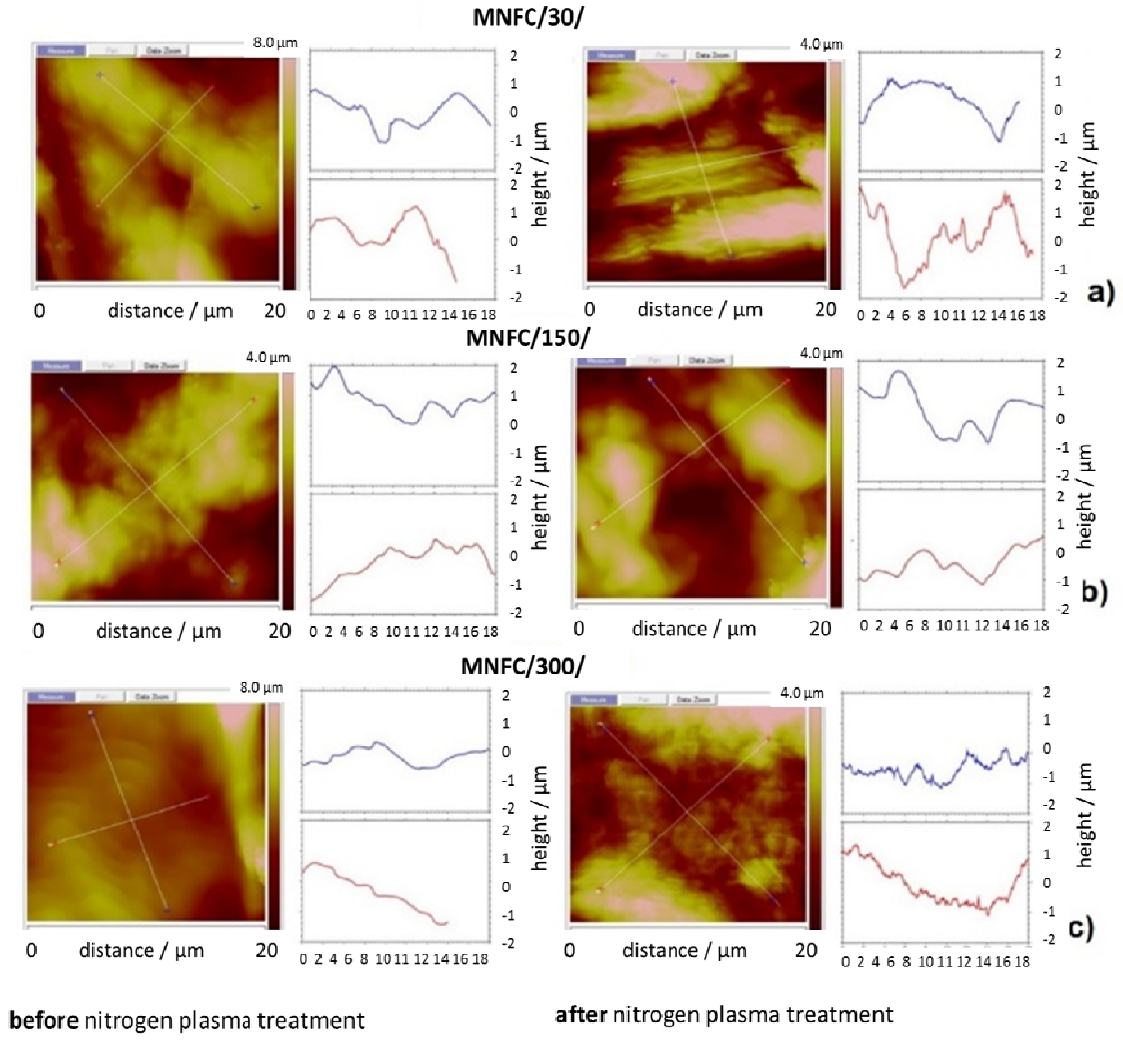

Fig. 5. Surface morphology and roughness of (a) MNFC/30/, (b) MNFC/150/ and (c) MNFC/300/ before and after nitrogen plasma treatment

The *surface chemical species* are revealed by the XPS spectra, from which the atomic % of C-C, C-O, O-C=O and N can be derived, Fig. 6. The effect of surface modification after nitrogen plasma can be clearly seen as the level of N attachment increasing as a function of the enzymatic removal of

amorphous content [13, 14]. The samples with increased crystalline proportion after longer enzymatic treatment nonetheless show similar C-C bond content. Similarly, with reduction of the amorphous part with increased hydrolysis, the amount of C-O groups decreases while C=O groups are formed, and other groups, having C atoms, form with N atoms.

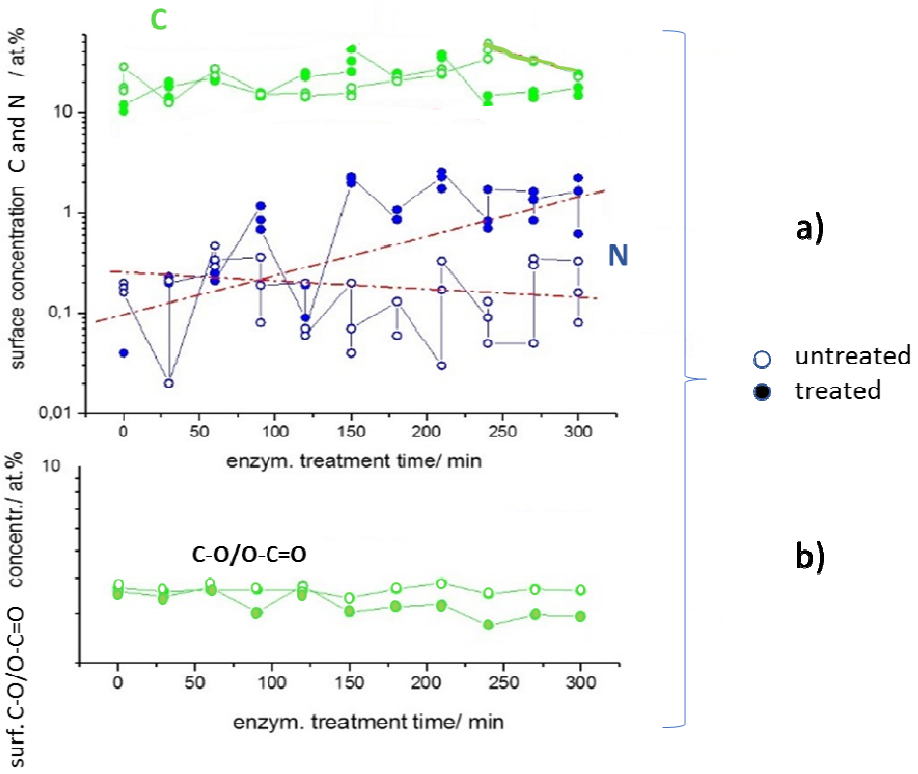

Fig. 6 Surface modification obtained through XPS data showing (a) increase in N atoms at constant carbon content, and (b) change in ratio of C-O/O-C=O groups.

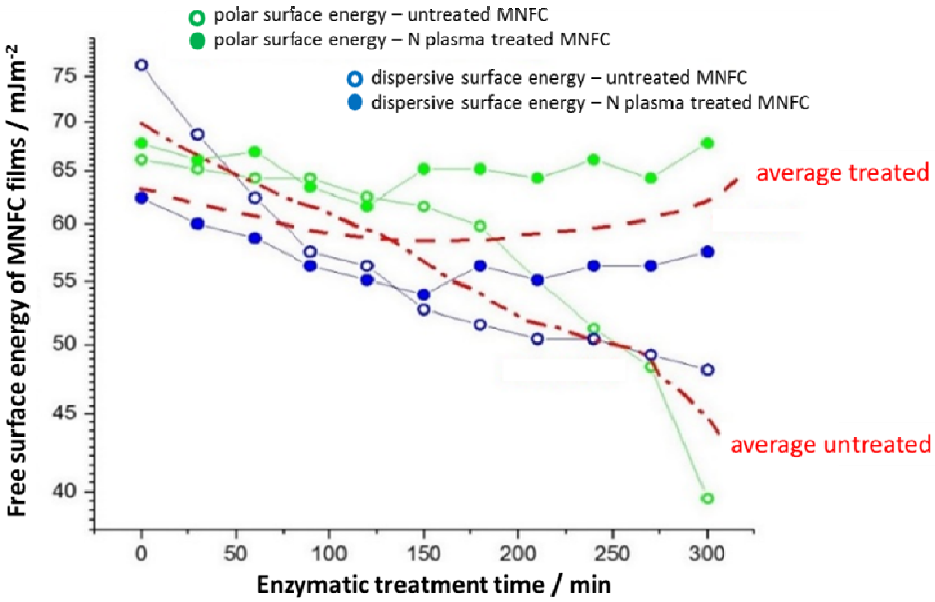

Fig. 7 Free surface energy (FSE) of MNFC films as a function of the treatment time (Table 1).

Results from Fig. 7 reveal that with the increase in enzymatic treatment of the raw material pulp, there is a reduction of total FSE in the corresponding MNFC films, corresponding with a reduction in both polar and dispersive energy of the untreated samples (green and blue unfilled symbols, respectively) [15, 16]. A reversal of the decline in FSE as a function of enzymatic treatment can be observed resulting from nitrogen plasma treatment, showing compensating increases in both polar and dispersive measured components (green and blue filled symbols, respectively). Thus, an increase in wettability for water and n-hexadecane is reflected by a decrease in CA as the plasma treatment acts on the more crystalline samples [17-19]. However, as the roughness is also seen to increase as a function of plasma treatment for the lower crystalline samples (less exposure to enzymatic breakdown), one would expect from the Wenzel model that the wettability would increase. That we see a recorded increase in n-hexadecane CA, and thus decrease in dispersive FSE, we can conclude that the action of the plasma discharge on the amorphous part is initially to reduce the dispersive energy component, and so likely act, at least partially, to breakdown first the amorphous content resulting in debonding and hence roughening [20-22]. This effective etching of amorphous parts of fibrils, is then replaced by the action of nitrogen attachment, such that the higher average FSE values regained in the more crystalline samples after plasma treatment are significantly higher than the theoretical FSE 59.4 $mJ.m^{-2}$ of cellulose, and this is achieved via the major contribution of the plasma-induced increase in polar component.

The increased contribution of the polar component in the FSE donated by the cationic N adsorption under plasma exposure is, therefore, expected to enhance the compatibility with the application of highly polar inks, especially if their components are anionic. The images in Fig. 8 confirm this expectation, where the improved wetting of the surface by water as a function of plasma exposure time is paralleled by the greater pick-up of ink colorant.

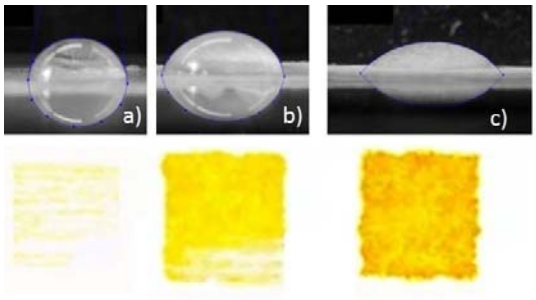

Fig. 8 IP ink printed on MNFC/300/ film showing the dependence on wettability of the surface after nitrogen plasma treatment; lower water droplet CA on the film corresponds with a significant increase in print colour density: (a) untreated film, (b) plasma treated for 30 s and (c) plasma treated for 60 s.

SUMMARY AND CONCLUSIONS

Micro nanofibrillated cellulose films formed from aqueous suspension can be made stronger by pretreatment of the raw fibre using enzymatic hydrolysis. However, the wettability by ionic liquids, including functional inkjet printing inks, such as are used for printed electronics, solar cells etc., decreases as a result, limiting the use of such films in practice. Nitrogen plasma treatment, however, enables wettability by such formulations to be improved. The mechanism by which this occurs has been studied in this work presented in this paper and the following conclusions can be drawn:

- Total surface energy increases with nitrogen plasma treatment of highly enzymatically hydrolysed fibrillar films (contact angle decreases), with a major increase in the polar component.

- Dispersive surface energy initially decreases on unpretreated or low enzymatic treated films on exposure to nitrogen plasma, whereas the polar surface energy component remains relatively unchanged.
    - This effect is related to the interaction of the nitrogen plasma with the amorphous cellulose component in the non-hydrolysed fibrils.
    - The dispersive energy component can once again be increased by exposure to nitrogen plasma in the case of the more crystalline fibrillar material derived from increased hydrolysis via enzymatic pretreatment

- Highly ionic liquids, water and solvents typically used to disperse surfactant-containing organic-based inks, wet MNFC film better as hydrolysing pretreatment of fibres is increased and subsequent nitrogen plasma is applied.

References

1. Zhou, Y., Fuentes-Hernandez, C., Khan, T.M., Liu, J-C., Hsu, J., Shim, J.W., Dindar, A., Youngblood, J.P., Moon, R.J., and Kippelen, B. "Recyclable organic solar cells on cellulose nanocrystal substrates." Nature, Scientific Reports, Scientific Reports, (2013) Vol 3, Article number: 1536: http://dx.doi.org/10.1038/srep01536

https://www.nature.com/articles/srep01536#supplementary-information
2. Hoeng, F., Denneulin, A., and Bras, J. “Use of nanocellulose in printed electronics: a review.” Nanoscale, 2016,8, 13131-13154: http://dx.doi.org/10.1039/C6NR03054H
3. Jutila, E., Koivunen, R., Kiiski, I., Bollström, R., Sikanen, T., and Gane, P. “Microfluidic Lateral Flow Cytochrome P450 Assay on a Novel Printed Functionalized Calcium Carbonate-Based Platform for Rapid Screening of Human Xenobiotic Metabolism.” (2018), Adv. Funct. Mater. 2018, 1802793-1802804: DOI: 10.1002/adfm.201802793
4. Ma, H. Yip, H-L., Huang, F., and Jen, A.K-Y. “Interface engineering for organic electronics.” Advanced Functional Materials 2010, 20, 1371.
5. Kumar, P., and Chand, S. “Recent progress and future aspects of organic solar cells.” Progress in Photovoltaics: Research and Applications 2012, 20, 377.
6. Singh, M., Haverinen, H.M., Dhagat, P., and Jabbour, G.E. “Inkjet Printing-Process and its Applications.” Advanced Materials 2010, 22, 673.
7. Hoth, C.N., Schilinsky, P., Choulis, S.A., and Brabec, C.J. “Printing highly efficient organic solar cells.” Nano Letters 2008, 8, 2806.
8. Möllera, M., Leylanda, N., Copelanda, G. and Cassidya, M. “Self-powered electrochromic display as an example for integrated modules in printed electronics applications.” The European Physical Journal Applied Physics 2010, 51, 33205.
9. Galagan, Y., Rubingh, J-E.J.M., Adrriessen, R., Fan, C.C., Blom, P.W.M., Veenstra, S.C., Kroon, J.M. “ITO-free flexible organic solar cells with printed current collecting girds.” Solar Energy Materials & Solar Cells 2011, 95, 1339.
10. Èernáková, Ł., Sahel, P., Kováèik, D., Johansson, K., and Èernák, M. “Low Cost High-Speed Plasma Treatment of Paper Surfaces.” 2006 TAPPI Advanced Coating Fundamentals Symposium, proceedings, Tappi Press, Atlanta.
11. Schultz, J., Tsutsumi, K., and Donnet, J.-B. “Surface properties of high-energy solids: I. Determination of the dispersive component of the surface free energy of mica and its energy of adhesion to water and n alkanes.” (1977) J. Colloid lnterface Sci. 59, 272-276: “II. Determination of the nondispersive component of the surface free energy of mica and its energy of adhesion to polar liquids.” (1977) J. Colloid Interface Sci 59, 272 and 277-282
12. Girifalco, L.A., and Good, R.J. “Theory for the Estimation of Surface and Interfacial Energies. I. Derivation and Application to Interfacial Tension.” The Journal of Physical Chemistry 1957 61 (7), 904-909; DOI: 10.1021/j150553a013
13. Prysiazhnyi, V., A. Kramar, B. Dojcinovic, A. Zekic, B. M. Obradovic, M. M. Kuraica, and M. Kostic. "Silver incorporation on viscose and cotton fibers after air, nitrogen and oxygen DBD plasma pretreatment." *Cellulose* 20, no. 1 (2013): 315-325.
14. Hashmi, S.G., Özkan, M., Halme, J., Dimic-Misic, K., Zakeeruddin, S.M., Paltakari, J., Grätzel, M., and Lund, P.D. "High performance dye-sensitized solar cells with inkjet-printed ionic liquid electrolyte." *Nano Energy* 17 (2015): 206-215.
15. Özkan, M., Dimic-Misic, K., Karakoc, A., Hashmi, S.G., Lund, P., Maloney, T., and Paltakari, J., 2016. “Rheological characterization of liquid electrolytes for drop-on-demand inkjet printing.” *Organic Electronics*, *38*, pp.307-315.
16. Relvas, C., Castro, G., Rana, S., and Fangueiro, R., 2015. “Characterization of physical, mechanical and chemical properties of quiscal fibres: the influence of atmospheric DBD plasma treatment.” *Plasma Chemistry and Plasma Processing*, *35*(5), pp.863-878.
17. Jun, W., Fengcai, Z., and Bingqiang, C. "The solubility of natural cellulose after DBD plasma treatment." *Plasma Science and Technology* 10, no. 6 (2008): 743.
18. Chu, P.K., Chen, J.Y., Wang, L.P., and Huang, N. "Plasma surface modification of biomaterials." *Materials Science and Engineering: R: Reports* 36, no. 5-6 (2002): 143-206.
19. Van de Vyver, S., Geboers, J., Jacobs, P.A., and Sels, B.F. “Recent advances in the catalytic conversion of cellulose.” *ChemCatChem* 3, no. 1 (2011): 82-94.
20. Vanneste, J., Ennaert, T., Vanhulsel, A. and Sels, B. “Unconventional Pretreatment of Lignocellulose with Low-Temperature Plasma.” *ChemSusChem* 10, no. 1 (2017): 14-31.
21. Pertile, R.A.N., Andrade, F.K., Alves, C. Jr, and Gama, M. “Surface modification of bacterial cellulose by nitrogen-containing plasma for improved interaction with cells.” *Carbohydrate Polymers* 82, no. 3 (2010): 692-698.
22. Kostić, M., Radić, N., Obradović, B.M., Dimitrijević, S., Kuraica, M.M. and Škundrić, P., 2009. “Silver-Loaded Cotton/Polyester Fabric Modified by Dielectric Barrier Discharge Treatment.” *Plasma Processes and Polymers*, *6*(1), pp.58-67.

INTERNATIONAL CONFERENCE ON ADVANCED NANOSTRUCTURES (ICAN-2018)

12-14 March 2018

Organized by

Post Graduate and Research Department of Physics

Catholicate College, Pathanamthitta, Kerala, 689645

(NAAC 'A' Grade) (CGPA 3.60)

In association with

IIUCNN, Mahatma Gandhi University, Kerala, INDIA

&

International Society for Optics and Photonics (SPIE), Washington, USA

Supported By

Patrons : **Prof. Dr. Sabu Thomas**
(Pro-Vice Chancellor, Mahatma Gandhi University, Kottayam, Kerala)

H. H. Baselios Marthoma Paulose II
(Catholicos and Malakara Metropolitan)

Co- patrons : **H. G (Dr) Thomas Mar Athanasius Metropolitan**
(Manger, MOC Colleges)

H.G Kuriakose MarClemis Metropolitan
(Local Manger, Catholicate College)

Dr. M E Kuriakose
(Secretary, MOC Colleges)

Dr. Mathew P Joseph
(Principal, Catholicate College)

Convener : **Dr. Raneesh B.**
(Department of Physics, Catholicate College, Pathanamthitta)

Co-Conveners: **Dr. George Thomas**
(HOD, Department of Physics, Catholicate College, Pathanamthitta)

Prof. Dr. Nandakumar Kalarikkal
(Director, IIUCNN, Mahatma Gandhi University, Kottayam, Kerala)

International Advisory Committee

Prof. Didier Rouxel, France
Prof. Sasa Lazovic, Serbia
Prof. Murukeshan Vadakke Matham, Singapore
Prof. Tesfakiros Woldu, Ethiopia
Prof. Oluwafemi oluwatobi, South Africa
Prof. Ichiro Terasaki, Japan
Prof. Andrey Aleshin, Russia
Prof. Hafedh Kochkar, Tunisia
Prof. Gideon Grader, ISRAEL
Prof. Sajid Alavi, USA
Prof. Yves Grohens, France
Prof. Józef T. Haponiuk, Poland
Prof. Alexey Goncharov, Ukraine
Prof. Manfred Stamm, Germany
Prof. Maya Jacob John, South Africa
Prof. Paula Moldenaers, Belgium
Prof. Minn-Tsong Lin, Taiwan
Prof. Harald Brune, Switzerland

National Advisory Committee

Prof. Abhijit Saha, UGC-DAE-CSR, Kolkata
Prof.P. S Anil Kumar, IISC, Bangalore
Prof. Jacob Philip, AJC, Kottayam
Prof. P.M.G. Nambissan, SINP, Kolkata
Prof. M.K Jayaraj, CUSAT, Cochin
Prof. P. Preedep, NIT, Calicut
Prof. P.S Anil kumar, IISC, Bangalore
Dr. M.M Shijumon, IISER, Trivandrum
Prof. Sudhakar Yarlagadda, SINP, Kolkata
Dr. Swapna S. Nair, CUK, Kasaragod
Dr. Pramod P.Pillai, IISER, Pune
Prof. Arul Manual Stephen, CECRI, Karaikudi
Dr. V.G. Geethamma, UCE, Thodupuzha
Prof. Ranjith Ramadurai, IIT, Hyderabad
Prof. Kuruvilla Joseph, IIST, Trivandrum
Dr. P.V Rajeesh, UGC-DAE-CSR, Kolkata
Dr. M.S Latha, SNC, Kollam
Dr. George Varughese (Former Principal)
Dr. Achamma Kurian (Former HOD)
Dr. M.J Kurien (Former HOD)

Local Organizing committee

Dr. Soosan Samuel M.
Dr. Raji Koshi
Dr. Dhanya I.
Dr. Anoop P. D.
Ms. Jini K. Jose
Ms. Asitha C. Nair
Mr. Sajith Babu S.
Dr. Achamma George
Dr. Karthika S.
Mr. Sibi Chandran C. S.
Ms. Reshmi P.
Ms. Priya Elizabeth Thomas
Ms. Keerthana C. S.
Mr. Rahul M. T.

PROGRAMME AT A GLANCE

Day - 1 (12th March 2018)	
Hall - 1	
08.00-08.40	Registration
09.00-10.00	Inauguration
10.00-10.10	Tea Break
10.10-11.00	Plenary Lecture
11.00-13.00	Invited Lectures
13.00-13.45	Lunch Break
13.45-15.45	Invited Lectures
15.45-16.00	Tea Break
16.00-17.00	Invited Lectures
17.00-18.00	Poster Session
18.00-19.30	Cultural Programme
19.30- 20.00	Conference Dinner
Day - 2 (13th March 2018)	
Hall - 1	
09.00-9.50	Plenary Lecture
09.50-10.00	Tea Break
10.00-12.40	Invited Lectures
12.40-13.40	Lunch Break
13.40-15.00	Invited Lectures
15.00-15.10	Tea Break
15.10-19.00	Conference Tour
19.00-20.00	Conference Dinner
Day - 2 (13th March 2018)	
Hall - 2	
10.00 -12.00	Invited Lectures
12.00-12.40	Oral Presentation Competition
12.40-13.40	Lunch Break
13.40-15.00	Oral Presentation Competition
Day - 3 (14th March 2018)	
Hall - 1	
09.00-09.50	Plenary Lecture
09.50-10.00	Tea Break
10.00-13.00	Invited Lectures
13.00-13.45	Lunch Break
13.45-14.00	KSCSTE Presentation
14.00- 15.20	Invited Lectures
15.20-15.30	Tea Break
15.30-16.00	Concluding Session

SCHEDULE

INTERNATIONAL CONFERENCE ON ADVANCED NANOSTRUCTURES (ICAN-2018)

12-14 March 2018

Venu: Auditorium, Catholicate College, Pathanamthitta, Kerala

(PL-Plenary Lecture**, IL-**Invited Lecture**, SIL-**Short Invited Lecture**, OP-**Oral Presentation**, PP-**Poster Presentation)

1st Day of the Conference 12th March 2018			
SL. No.	Name of Speaker	Title of the talk	Time
	Registration		8.00-8.40
	Opening Remarks		9.00-10.00
	Tea Break		10.00-10.10
PL-1	**Prof. Dr. E. Carolina Sañudo**, Universitat de Barcelona, Spain	Coupling SMMs to a Substrate: Understanding Molecule-Surface Interaction in Molecular Spintronic Devices	10.10-11.00
Chairpersons: Prof. Dr. Jean-Pierre Leburton, University of Illinois, USA **Prof. Dr. Nandakumar Kalarikkal,** Mahatma Gandhi University			
IL-1	**Prof. Dr. Jacob Philip**, Amal Jyothi College of Engineering, India	Magneto-electric coupling in multiferroic nanocomposites of the type NKLN-MFO: Role of ferrite phase	11.00-11.40
IL-2	**Prof. Dr. P.M.G. Nambissan**, Saha Institute of Nuclear Physics, India	The importance of focusing on defects in nanocrystalline systems	11.40-12.20
IL-3	**Prof. Dr. Pramod P. Pillai**, Indian Institute of Science and Education Research, India	Advanced nanoparticle functions through interplay of forces	12.20-13.00
	Lunch Break		13.00-13.45
Chairpersons: Prof. Dr. P.M.G. Nambissan, Saha Institute of Nuclear Physics, India **Prof. Dr. Józef T. Haponiuk**, Gdansk University of Technology, Poland			
IL-4	**Prof. Dr. M K Jayaraj,** Cochin University of Science and Technology, India	Fabrication of cost effective and reproducible SERS substrates	13.45-14.25

IL-5	**Prof. Dr. Lamouroux Emmanuel**, Université de Lorraine, France	Transparent nanostructured indium tin oxide electrodes: preparation and characterization	14.25-15.05
IL-6	**Prof. Dr. Ramana Murthy Sarabusity**, Osmania University, India	Microwave absorption properties of NiCuZn ferrite-PANI nanocomposites	15.05-15.45
	Tea Break		15.45-16.00
Chairpersons: Prof. Dr. S.K. Musharaf Ali, Bhabha Atomic Research Centre, India **Prof. Dr. Sony C George,** Amal jyothi College of Engineering, India			
IL-7	**Prof. Dr. Chaitanya Lekshmi Indira**, CMR Institute of Technology, India	Metal oxide nanocrystal functionalization of graphite electrodes for catechol biosensing in aqueous solutions	16.00-16.40
SIL-1	**Dr. Achu Chandran**, Central Electronics Engineering Research Institute, India	Liquid crystal-nanocomposites; a promising candidate for next generation optical device	16.40-17.00
	Poster Session		17.00-18.00
	Cultural Programme		18.00-19.30
	Conference Dinner		19.30- 20.00
2nd Day of the Conference 13th March 2018 **Hall-1: Auditorium, Catholicate College, Pathanamthitta, Kerala**			
PL-2	**Prof. Dr. Aleshin Andrei**, Ioffe Physical-Technical Institute, Russia	Light-emitting field-effect transistors based on polyfluorene – cesium lead halide nanocrystals films with small hysteresis of output and transfer characteristics	09.00-9.50
	Tea Break		09.50-10.00
Chairpersons: Prof. Dr. Henrich H Paradies, Jacobs-University Bremen, Germany **Prof. Dr. M K Jayaraj**, Cochin University of Science and Technology, India			
IL-8	**Prof. Dr. P. Pradeep**, National Institute of Technology, India	Green material strategies for organic and hybrid electronics	10.00-10.40
IL-9	**Prof. Dr. Sony C George,** Amal Jyothi College of Engineering, India	Graphene nanocomposites: Multifunctional materials for the future	10.40-11.20

IL-10	**Prof. Dr. S.K. Musharaf Ali,** Bhabha Atomic Research Centre, India	Computational and Experimental Molecular Engineering of the Nanomaterials	11.20-12.00
IL-11	**Prof. Dr. Darja Lisjak,** Jožef Stefan Institute, Slovenia	Upconverting Nanoparticles: Dissolution Problem and a Potential Solution towards Biomedical Applications	12.00-12.40
	Lunch Break		12.40-13.30
Chairpersons: Prof. Dr. Gonzalo Vallejo Fernandez, University of York, United Kingdom **Prof. Dr. P. Pradeep**, National Institute of Technology, India			
IL-12	**Prof. Dr. Ivan Zulim,** University of Split, Croatia	A gas-phase model of cluster formation based on van der Waals-London interaction betweenneutral silicon atoms	13.30-14.10
IL-13	**Prof. Dr. Józef T. Haponiuk**, Gdansk University of Technology, Poland	Polyurethane Nanocomposite Elastomers, Foams and Blends	14.10-14.50
	Conference Tour		14.50-19.00
	Conference Dinner		19.00-20.00
2nd Day of the Conference 13th March 2018 **Hall-2: Mar Clemis Hall, Catholicate College, Pathanamthitta, Kerala**			
Chairpersons: Prof. Dr. Sasa Lazovic, University of Belgrade, Serbia **Dr. Pramod Avti,** Postgraduate Institute of Medical Education and Research, India			
SIL-2	**Dr.Pratibha Kumari,** University of Delhi Delhi, India	Calixarene modified magnetite nanomaterials for the Removal of pyridinium based pollutants from aquous solution	10.00-10.20
SIL-3	**Dr. K. Pattabiraman**, Annamalai University, India	Topological Descriptors of Some Nanostructures	10.20-10.40
SIL-4	**Dr. P Nuja S John**, CMS College, India	Synthesis of luminescent PVA/SBN nanofiber	10.40-11.00
SIL-5	**Dr. Sherin Reju**, St. Xavier's College, India	Electrochemical study of nanostructured Mn_3O_4 synthesized through a single step auto igniting combustion technique	11.00-11.20

SIL-6	**Dr. Sankar S**, Sree Narayana College, India	Biological reduction of AgNPs with anti-fungal activity using aloe barbadensismiller	11.20-11.40
SIL-7	**Dr. M. Seenivasan,** Annamalai University, India	Batch arrival retrial queueing model with matrix geometric analysis	11.40-12.00
Chairpersons: Prof. Dr. P.M.G. Nambissan, Saha Institute of Nuclear Physics, India **Prof. Dr. E. Carolina Sañudo,** Universitat de Barcelona, Spain **Prof. Dr. Jacob Philip,** Amal Jyothi College of Engineering, India			
OP (1 - 4)	Oral Presentation Competition for Young Researchers		12.00-12.40
	LUNCH BREAK		12.40-13.30
Chairpersons: Prof. Dr. P.M.G. Nambissan, Saha Institute of Nuclear Physics, India **Prof. Dr. E. Carolina Sañudo,** Universitat de Barcelona, Spain **Prof. Dr. Jacob Philip,** Amal Jyothi College of Engineering, India			
OP (5 -12)	Oral Presentation Competition for Young Researchers		13.30-14.50
3nd Day of the Conference 14th March 2018 **Hall1: Auditorium, Catholicate College, Pathanamthitta.**			
PL-3	**Prof. Dr. Jean-Pierre Leburton,** University of Illinois, USA	2D Nanoscale Materials for Genetic Applications	09.00-9.50
	TEA BREAK		09.50-10.00
Chairpersons: Prof. Dr. Aleshin Andrei, Ioffe Physical-Technical Institute, Russia **Prof. Dr. E. Carolina Sañudo**, Universitat de Barcelona, Spain			
IL-14	**Prof. Dr. Henrich HParadies,** Jacobs-University Bremen, Germany	Ordering and liquid-crystalline lipid A-phosphate complexes controlling the immunological defense.	10.00-10.40
IL-15	**Prof. Dr. Gonzalo Vallejo Fernandez,** University of York, United Kingdom	Factors affecting the measurement of magnetic hyperthermia	10.40-11.20
IL-16	**Prof. Dr. Kuruvila Joseph,** Indian Institute of Space Science and Technology, India	Surface Engineered Nanosystems for Bio-Medical Applications	11.20-12.00
IL-17	**Prof. Dr. Sasa Lazovic**, University of Belgrade, Serbia	Biomedical applications of gas plasma and natural pigments	12.00-12.40

SIL-8	**Dr. Pramod Avti**, Postgraduate Institute of Medical Education and Research, India	Advanced nanomaterials as emerging tools for Biomedical Applications	12.40-13.00
	Lunch Break		13.00-13.45
	KSCSTE Presentation		13.45-14.00
Chairpersons: **Prof. Dr. Darja Lisjak**, Jožef Stefan Institute, Slovenia **Prof. Dr. Ivan Zulim**, University of Split, Croatia			
IL-18	**Prof. Dr. Nandakumar Kalarikkal**, Mahatma Gandhi University, India	Carbon Based Nanostructured Materials for Energy Applications	14.00-14.40
IL-19	**Prof. Dr. E. S. Rajendran,** Vinayaka Mission's University, India	Homeopathy - Nanopharmacology and a Personalized Nanomedicine – Nanoparticle Characterization of Aurum Metallicum and Lycopodium 6c To Cm	14.40-15.20
	Tea break		15.20-15.30
	Concluding Remarks, Valedictory Function and Farewell Photo Session		15.30-16.00

and grafting with nano reinforcing agent, we can improve the compatibility with matrix and thereby tailor the material for specific applications.

♣□□□□□□♣

IL-17

Biomedical applications of gas plasma and natural pigments

Saša Lazović

Institute of Physics Belgrade, University of Belgrade,
Pregrevica 118, 11080, Belgrade, Serbia
lazovic@ipb.ac.rs

Abstract

Development of nonthermal plasma at atmospheric pressure has led to an expansion of biomedical applications in the past few decades. The fact that we are able to control ionization growth at high pressure and without vacuum enables direct exposure of cells and tissues togas plasma [1]. Gas plasma is being used for wound healing, enhanced blood coagulation, sterilization of bacteria, cancer treatment, stem cell manipulation, etc. [2]. However, some of the most important challenges remain open. As the field of plasma medicine matures in clinical applications the questions of plasma selectivity, treatment doses, damage control, and efficient delivery of reactive species to cells and tissues require more attention.

We will discuss selectivity by studying the effects of plasma on Staphylococcus aureus (ATCC 25923), Escherichia coli (ATCC 25922), and on human peripheral bloodmesenchymal stem cells. Therapeutic plasma doses and optimization of treatments will be discussed by comparing plasma with ionizing radiation in terms of induced DNA damage[3]. Finally, we will elaborate on biological effects of bacterial pigment undecylprodigiosin on humanblood cells treated with atmospheric gas plasma in vitro [4].

References:

[1] Biomedical applications and diagnostics of atmospheric pressure plasma, J. of Phys:Conf. Ser, **356**, p 012001-012009, (2012)

[2] Clinical Plasma Medicine: State and Perspectives ofin VivoApplication of ColdAtmospheric Plasma, Contrib. to Plasma Phys, **54**(2), p 104-117, (2014)

[3] Plasma induced DNA damage: Comparison with the effects of ionizing radiation, Appl.Phys. Lett, **105**(12), p 124101-124105, (2014)

[4] Biological effects of bacterial pigment undecylprodigiosin on human blood cells treated with atmospheric gas plasma in vitro, Exp.Toxicol.Pathol, **69**(1), p 55-62, (2017)

♣□□□□□□♣

Non-thermal plasma for revalorization of a complex waste substrate in open lactic acid fermentation

Aleksandra Djukić-Vuković[1], Saša Lazović[2], Dragana Mladenović[1], Zorica Knežević-Jugović[1], Jelena Pejin[3], Ljiljana Mojović[1]

[1]Department of Biochemical Engineering and Biotechnology, Faculty of Technology and Metallurgy, University of Belgrade, Serbia
[2]Institute of Physics Belgrade, University of Belgrade, Zemun, Serbia
[3]Faculty of Technology, University of Novi Sad, Novi Sad, Serbia

Correspondence: Dr. Aleksandra Djukić-Vuković (adjukic@tmf.bg.ac.rs). Department of Biochemical Engineering and Biotechnology, Faculty of Technology and Metallurgy, University of Belgrade, Karnegijeva 4, 11120 Belgrade, Serbia.

Abstract

Purpose: Stillage is the main by-product of bioethanol production and cost of its treatment significantly affects the economy of bioethanol production. Utilization of stillage for fermentative lactic acid (LA) and biomass production improves sustainability of bioethanol production. Standard process of thermal sterilization of stillage for biorefinery purposes is energy demanding and is causing deterioration of valuable compounds present in stillage. Modern biorefinery processes require energy efficient recovery of nutrients from stillage at different scales.

Methods: We replaced standard sterilization with ultrasound (UT) and plasma (PT) treatments and observed a significant reduction in number of viable microorganisms in the stillage after PT and UT. After applied treatment, we initiated lactic acid fermentation (LAF) by *Lactobacillus rhamnosus* ATCC 7469. Concentration of LA is used to quantify the efficiency of stillage revalorization.

Results: We find that the highest LA productivity of 1.21 g/Lh and yield of 0.82 g/g are obtained after PT. While, UT of 10 min provides productivity of 1.02 g/Lh and LA yield of 0.69 g/g. The results are benchmarked against closed LAF. We achieved 20% better revalorization of stillage by PT when compared with conventional sterilization. An excellent L (+) LA stereoselectivity of 95.5% is achieved after PT LAF. From the aspect of energy efficiency, PT was three times lower than UT and almost ten times lower than thermal sterilization.

Conclusions: This way we achieved a simpler and energy efficient process for LA production on stillage in „open" fermentation. These are new findings in fermentative treatment of stillage or similar by-products and wastes for the benefit of industry, academia and policy making.

Keywords: biorefinery, non-thermal plasma, open lactic acid fermentation, stillage, ultrasound

1. Introduction

Distillery stillage is the main by-product of bioethanol production on renewable feedstock. It remains after distillation of bioethanol and depending on the feedstock used for bioethanol production COD values of stillage can reach up to 100 g/L [1,2]. Approximately 20L of stillage are produced per every liter of bioethanol and environmental burden of stillage disposal is high [2]. Stillage has to be treated in order to decrease its organic load and its revalorization through production of chemicals is increasing competitiveness of bioethanol [3,4]. Besides anaerobic digestion, stillage is most often used after drying for animal nutrition, as dried distillers' grains with solubles (DDGS) [2,5]. Nutrients from stillage could be recovered through other processes also, including its utilization as fertilizer [6] or as substrate for fermentative production of bacterial cellulose, fungal biomass, 1,3–propanediol, malic and lactic acid (LA) [7–12]. Among proposed fermentative processes on stillage, almost all are „closed" fermentations which include thermal sterilization of substrate [7,9–11]. Thermal sterilization is energy demanding, costly treatment; it is difficult to apply in large scale processes and part of the nutrients is lost after thermal treatment [13]. Alternative to these are „open" fermentations when substrate is used without prior sterilization and fermented under unsterile conditions by a mixed culture of microorganisms [14]. Open fermentations are simpler, lower in energy consumption than conventional closed fermentations on sterilized substrates and could be adapted to various renewable and waste substrates due to the evolution capacity of microbiota, if process is well controlled [14]. Lower productivities, lower optical purity of product and contamination are still challenges in open fermentations [14,15] in parallel with necessary improvements in extraction techniques [16]. Control of fermentation conditions and possibility to manipulate substrate microbiota are crucial for efficient open fermentations.

Non-thermal treatments are an alternative to standard thermal sterilization for control of microorganisms in agricultural and wastewater substrates [17]. These treatments should enable selective inactivation of undesired microorganisms from complex microbial communities like those in stillage [18,19] but also preserve species capable of producing desired chemicals, like lactic acid for example. Non-thermal plasmas generate abundance of highly reactive species at low temperatures thus enabling processing of sensitive materials [20] and avoidance of thermal degradation of the compounds present in treated media. Beside reactive oxidative species, the UV photons and pulsed electric field generated during plasma treatment (PT) could contribute to the overall effect [21,22]. In a complex media with high dry matter content like stillage, the effects of non-thermal plasma treatment have not been thoroughly examined since most of the studies were performed in water, water based media with low dry matter content or on solid surfaces [22–26].

The high-power ultrasound treatment (UT) can be used for decontamination due to the mechanical disruption and cavitation effects induced in samples [27]. The microbial inactivation by UT is highly dependent on substrate composition, types of microorganisms present in media and treatment conditions [26,27].

LAFs on cheap substrates like stillage attract great interest since the LA market size was valued at 2.08 billion US $ in 2016 and is expected to grow by annual growth rate of 16.3% until 2025

[28]. The demand for LA is mainly driven by increasing utilization of LA as a platform chemical and for poly-lactides – biocompatible and biodegradable polymers suitable for pharmaceutical and food applications [15,28]. The concentration of LA produced in LAF on stillage is used in our work to quantify the efficiency of stillage revalorization.

The main objective of this study is to investigate plasma and ultrasound in LAF on stillage as an alternative to standard sterilization processes. The mechanism of non-thermal plasma inactivation of *Lactobacillus acidophilus* and *Escherichia coli* in water and stillage as media is thoroughly studied. Furthermore, non-thermal plasma inactivation of indigenous stillage microbiota was compared with inactivation by ultrasound treatment. The stillage after different treatments was subjected to open or closed LAF to assess its revalorization potential through LA production with high-LA producing strain of *Lactobacillus rhamnosus* [29]. The parameters of LAFs in terms of LA concentration, optical purity, yield and productivity were studied and compared for various applied treatments. In addition, all treatments were compared from the aspect of energy efficiency.

2. Materials and Methods

2.1. Preparation of distillery stillage

The distillery stillage remained after bioethanol production on wasted bread was obtained from ethanol producing facility (Reahem d.o.o., Serbia) and used for preparation of media for LAF. Chemical composition of the stillage was determined as following: dry matter content (12.79 ± 0.31%), sugar concentration (11.19 ± 0.83 g/L), protein (63.91 ± 2.81 g/L), free amino-nitrogen (295.6 ± 1.5 mg/L), ash (31.2 ± 0.1 g/L), lipids (17.36 ± 1.84 g/L). The pH value in all samples was adjusted to 6.5. The stillage was subjected to various decontamination treatments: PT, UT and thermal sterilization and it was used as the substrate for LAFs. The standard thermal sterilization was performed in an autoclave (Sutjeska, Serbia, device power 5.25 kW) at 121 ^{o}C for 20 min.

2.2. Microorganism

Lactobacillus rhamnosus ATCC 7469 and *Lactobacillus acidophilus* ATCC 4356, homofermentative LA producing strains and *Escherichia coli* ATCC 25922 were obtained from American Type Culture Collection. The *L. rhamnosus* and *L. acidophilus* cultures were propagated at 37 °C in Man Rogosa Sharpe broth (MRS) under microaerophilic static conditions. *E. coli* culture was propagated at 37 °C in nutrient broth, under aerobic static conditions. Overnight cultures were used as an inoculum in experiments.

2.3. Non-thermal plasma treatment

2.3.1. The effect of non-thermal plasma on G (+) and G (-) bacteria in water and distillery stillage

These experiments were undertaken at the beginning of the study in order to determine how non-thermal plasma acts towards *E. coli* (a representative of G (-) bacteria) and *L. acidophilus* (a representative of G (+) bacteria) in water and stillage media.

In the first set of experiments, the samples of water and stillage (6 ml) were sterilized by autoclaving (Sutjeska, Serbia) at 121 ^{o}C for 20 min and inoculated by overnight cultures of *E. coli* and *L. acidophilus* in order to set initial number of viable cells in samples at around 10^5 CFU/ml. Immediately

after inoculation, the samples were transferred in glass Petri dishes and subjected to PT for 30 min (duration of treatment was selected after preliminary studies) by using plasma needle jet. All treatments were conducted using a plasma needle operating at 25 kHz in ambient air. Argon was used as a feed gas (2 slm flow rate) in order to reduce the breakdown voltage through Penning ionization. The operating power was 2 W. The distance between the needle tip and the samples was 1 cm. Detailed description of the plasma device is provided by [30]. No significant increase of temperature in samples has been observed during treatments. During the treatments, the samples were mixed. The schematic presentation is shown in **Fig.1a**.

The second set of experiments was performed in order to determine effect of plasma generated UV photons on microbial inactivation in water and stillage. The samples were prepared and treated in the same way as previously, but quartz glass was placed between plasma jet and sample to prevent other effects of PT except UV light. Graphical presentation is provided in **Fig.1b**. The samples of sterilized water and stillage inoculated by *E. coli* and *L. acidophilus* were subjected to the same procedure but without PT, as a control.

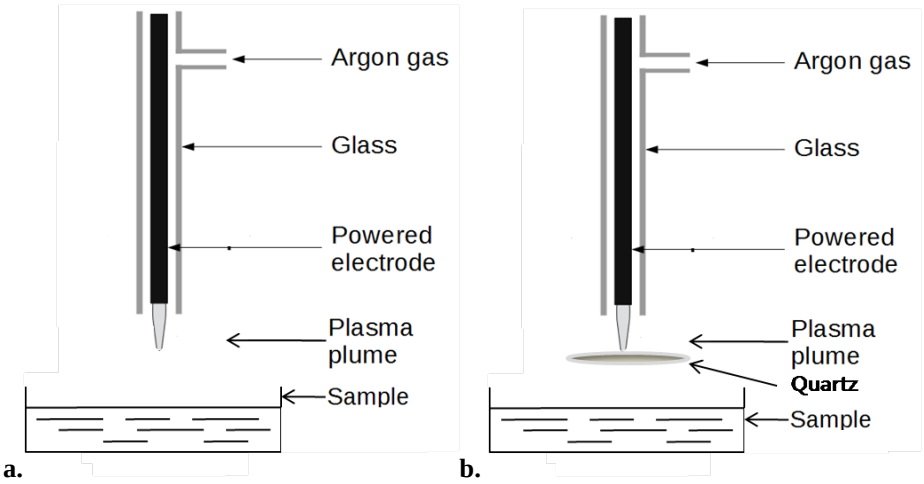

Fig.1 Schematic presentation of experimental setup for non-thermal PT (**a**) and assessment of contribution of the UV photons generated by plasma (**b**)

A number of viable cells in samples was determined using pour plate counting method on nutrient agar (for *E. coli*) and MRS agar (for *L. acidophilus*). Reduction in the number of viable microorganisms was presented as log reduction, log (N/N_0), where N - number of viable cells in samples and N_0- number of viable cells in control.

2.3.2. Non-thermal plasma treatment of distillery stillage for lactic acid fermentation

The samples of non-sterile stillage in 6 ml batches were placed in glass Petri dishes and treated by non-thermal plasma needle for 30 min (duration of treatment was selected after preliminary studies). The PT details are explained in Section 2.3.1. After the treatments and prior to LAF the samples were incubated under microaerophilic conditions at 41 ˚C (the same conditions which were used for LAF, studied in the second set of experiments and explained in section 2.5.) for 24 h in order to assess effect of

PT on the stillage microbiota. A number of total aerobic mesophilic bacteria in samples was determined using pour plate counting method as previously described on MRS agar as substrate [31].

2.4. High-power ultrasound treatment of distillery stillage

The stillage samples (60 ml) placed in 200 ml glass were treated by high-power ultrasound (Sonopuls HD 2200, Bandelin, Berlin, Germany, device power 200 W) with sonotrode TT 13 for 10 min (duration of treatment was selected after preliminary studies) at actual value of amplitude 75% and frequency of 20 kHz. After the treatment, in the first set of experiments, the samples were incubated under microaerophilic conditions at 41 ˚C for 24 h in order to examine the effect of treatment on the number of viable bacterial cells in the stillage. A number of total aerobic mesophilic bacteria in all samples was determined using pour plate counting method as previously described on MRS agar as plate substrate [31]. In the second set of experiments, the samples after the treatment were subjected to LAF (explained in section 2.5.).

2.5. Lactic acid fermentation

Stillage samples (60 ml per sample) treated by PT, UT and sterilized were subjected to fermentation for LA and probiotic biomass production. Untreated stillage was also subjected to LAF in the same way as treated samples. Initial glucose concentration in all samples was adjusted at around 35 g/L by addition of a 70% glucose solution and pH value was adjusted to 6.5. The LAFs were inoculated by 5% (v/v) *L. rhamnosus* ATCC 7469 while the untreated stillage was fermented by indigenous microbiota and considered as a control sample. The fermentations were performed as batch cultures with shaking in 200 ml flasks (100 rpm, KS 4000i control, IKA®, Germany), at 41 °C, under microaerophilic conditions maintained by using gas-pack system. These conditions were previously selected for the fermentation of stillage by *L. rhamnosus* ATCC 7469 [32]. During the LAF, the pH value in media was maintained at 6.5 by addition of 30% NaOH, in 4 h intervals.

2.6. Energy consumption calculations

The calculation of energy consumption of different treatments was performed by using manufacturers' information for lab scale equipment applied in experiments, taking into account a volume of samples subjected to the treatment. Energy of different treatments was calculated according to formula [33]:

$$E=P\times t, \quad (1)$$

where E is energy, P is power of device used for treatment and t is for duration of treatment.

The actual power of ultrasound treatment of stillage was calculated according to the procedure based on calorimetry and the following formula [26]:

$$P=m_s\times C_p\times \partial T/\partial t, \quad (2)$$

where m_s is mass of stillage media, C_p is specific heat at a constant pressure (J/gK), and $\partial T/\partial t$ is the slope at the origin of the curve (T is temperature, t is time). This equation is used to calculate the actual power of UT with a presumption that all of the power entering the system is dissipated as heat.

2.7. Methods of analysis

Chemical composition of the stillage was determined using methods described in our previous work [32]. The antioxidative activity of the stillage before and after the treatment against 2,2-Diphenyl-1-

picrylhydrazyl radical (DPPH, Sigma Aldrich, USA, CAS No. 1898-66-4) was determined as in the study of Jovanović et al. [34]. The stereoselectivity of produced LA was determined by enzymatic method (L(+)/D(-) LA assay, Megazyme®, Ireland). The LA and glucose concentrations during LAFs were determined by HPLC analysis. The samples were withdrawn from fermentation media, filtered through 0.22 μm filters (Minisart® syringe filters, Sartorius AG, Germany) and analysed by adapted HPLC method of Srivastava et al. [35]. In brief, the HPLC analysis was performed on the Dionex Ultimate 3000 Thermo Scientific (Waltham, USA) system. A reverse phase column (Hypersil gold C18, 150 mm × 4.6 mm, 5 μmL; Thermo Scientific, USA) at 65 ˚C was employed. Mobile phase was 5 mM H_2SO_4 (JT Baker, USA) with an elution rate 0.6 ml/min. Detection was performed by UV/VIS detector at 210 nm. All data acquisition and processing were done using Chromeleon Software. All chemicals used in experiments were of analytical grade and obtained from Sigma Aldrich, USA.

2.8. Statistical analysis

The experiments were done in duplicates, in three independent experiments. All values are expressed as means ± standard deviation. Mean values of treatments were compared by the analysis of variance (one-way ANOVA) followed by Tukey test for mean differences testing. Differences were considered significant at $p < 0.05$.

3. Results and Discussion

3.1. Interaction of non-thermal plasma and stillage – effect on chemical composition

The major challenge in processing of a complex medium such as stillage and similar wastewater is to achieve inactivation of specific microorganisms while preserving valuable compounds. Uchiyama *et al.* [36] report that argon cold atmospheric plasma as one used in our study can generate enormous amounts of $^{\cdot}OH$ radicals and H_2O_2 - the combination product of $^{\cdot}OH$ radicals in the aqueous phase even at distances of approximately 1 cm from the plasma source nozzle [36]. Superoxide $O_2^{\cdot -}$ can be present in the liquid phase in significant amounts, also [37,38]. Besides reactive oxygen species, plasma source is generating UV photons [39]. UV light has direct negative effect on bacteria and it can initiate photo dissociation of water and additional chemical reactions in treated media, therefore, interaction of non-thermal plasma with substrate like stillage is complex.

For effective fermentative processes, contents of reducing sugars and free amino-nitrogen are crucial and C/N ratio is most often determining productivity of the processes with LAB [32,40]. After the longest studied plasma treatment of 30 min, only a slight decrease in antioxidant activity was observed, from 93.5 ± 1.3% before to 90.1 ± 1.2% after the treatment. In other antioxidant rich substrates exposed to non-thermal plasma, no significant change in antioxidant activity was noted and it was confirmed using array of methods [41]. Some studies reported that antioxidants can act as scavengers for reactive species generated during PT [42]. Therefore, decrease in the antioxidant activity, as observed in our study, can be explained by a similar decrease in the concentration of enzymes and molecules associated to oxidative stress (vitamin C, polyphenol oxidase, peroxidase) which acted like scavengers in radical reactions initiated by PT [43].

The changes in the contents of reducing sugars and free amino nitrogen after the PT were not significant as confirmed by HPLC and spectrophotometric methods. Unlike other thermal methods, where

Millard reaction is occurring causing a loss of proteins and sugars by generation of melanoidins which are toxic for bacteria [44,45], non-thermal PT did not change the content of the most important compounds for stillage revalorization in LAF. Therefore, the effects of non-thermal PT on survival of different microorganisms in stillage were further examined.

3.2. Inactivation of model G (+) and G (-) bacteria in water and stillage by non-thermal plasma treatment

The effects of non-thermal PT on the survival of *E. coli*, G (-) bacteria, and *L. acidophilus*, G (+) bacteria, in different media were studied first. *E. coli*, being the most studied G (-) bacteria from the sanitary perspective [23], was used as a model of undesired G (-) microorganism in substrates. *L. acidophilus* was a representative of G (+) lactic acid bacteria (LAB) belonging to *Lactobacillus* sp. which are main constituents of indigenous stillage and food waste microbiota and responsible for LAF and silage of these substrates in uncontrolled conditions [18,19]. PTs were performed in water and stillage inoculated with the model G (-) and G (+) microorganisms.

The reduction in the number of viable *E. coli* and *L. acidophilus* in water and stillage by PT is presented in **Fig.2**. Reactive oxygen species ($^{\cdot}OH$, H_2O_2, $O_2^{\cdot -}$), reactive nitrogen species and UV photons created during PT all contribute to the antimicrobial effects of plasma [36–38]. We examined total microbial inactivation by PT and also isolated effects of UV photons generated by plasma on inactivation of bacteria (**Fig.2**).

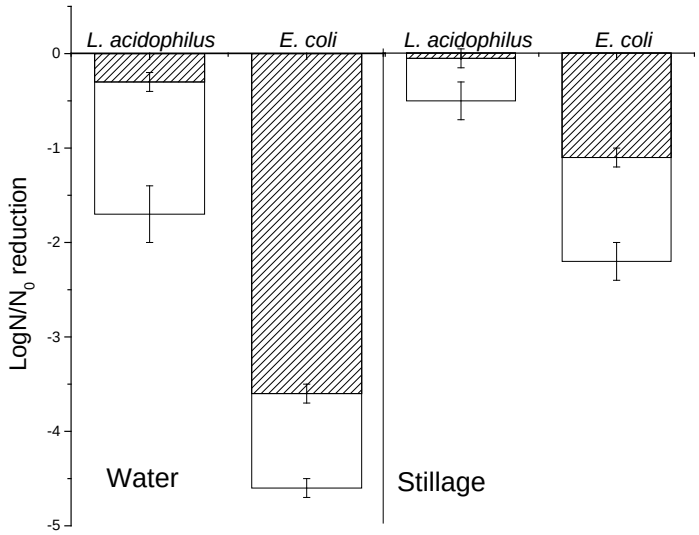

Fig.2 LogN reduction in the number of viable *E. coli* and *L. acidophilus* cells in different media. Symbols: white bars – inactivation by plasma generated radicals, patterned bars – inactivation by plasma generated UV photons

The higher reduction in viable cell number was obtained in water for both studied bacteria but in general *E. coli* was more sensitive to PT than *L. acidophilus* regardless of the media (**Fig.2**). The UV dependent inactivation of *E. coli* in water comprised up to 78% of the total logN reduction while in the

stillage it represented around 50% of the total inactivation. The dissimilarity in inactivation in different media is predominantly due to the UV dependent inactivation, especially for *E. coli*. Also, observed presence of scavengers in stillage (section 3.1.) could inactivate oxidative species produced by plasma source leading to lower microbial inactivation in stillage than in water. For *E. coli*, in absolute values, logN reduction mediated by UV photons decreased three times in stillage in comparison to water as media. The remaining contribution of reactive species to overall logN reduction has not been altered significantly with a change of media for stillage (**Fig.2**).

Because of turbidity of the stillage, the effect of UV radiation was less pronounced in stillage. These results emphasize the importance of penetration depth of UV photons and therefore a significance of the treatment chamber shape and overall treatment conditions, beside the most often reported volume of sample [39].

The inactivation of plankatonic *E. coli* cells in water obtained in this study was similar to results of Purevdorj et al. [46] and Puač et al. [23] but in more efficient time/volume ratio [23,46]. Geveke [47], Arrange et al. [48] and Mai-Prochnow et al. [49] reported higher susceptibility of G (-) bacteria to both UV light and cold PT in general. Boudam et al. [39] pointed that a fine adjustment of plasma operating conditions could increase the participation of UV light or radicals in overall bactericidal activity of PT. In this study, *E. coli* was found more susceptible to UV light component of PT compared to *L. acidophilus.* Therefore, PT in stillage enabled significant decrease in the number of *E. coli* while growth *L. acidophilus,* a representative of LAB, was minimally affected. This way, PT provided some selectivity in microbial inactivation in stillage, qualifying it as a promising strategy for treatment of stillage for revalorization in LAF.

3.3. Comparison of the effect of non-thermal plasma and ultrasound treatment on microorganisms in stillage

In the next set of experiments, PT was compared with high-power ultrasound. As an alternative non-thermal treatment, the UT method is already proven for microbial inactivation in less complex media like juices [26] and found effective in disintegration of fresh distillery spentwash [50]. The effects of non-thermal PT and UT on the growth of indigenous stillage microbiota were studied and the results are presented in **Fig.3**. The non-thermal PT caused higher reduction in viable cell number than UT. The number of viable cells did not increase during 24 h after the PT resulting in around 3 logN lower number of viable cells in PT than in control, untreated sample (**Fig.3**). Possible reason could be a slow growth and recovery of bacteria which survived the treatment. The lifetime of reactive species generated by plasma is extremely short but they initiate numerous reactions in media causing prolonged effects [51,52]. The application of plasma-activated water, water subjected to PT and then used for sanitation purposes, is based on this effect [53].

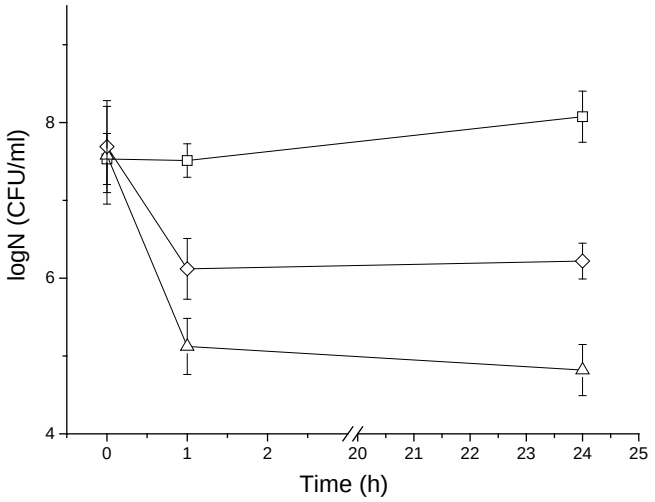

Fig.3 Number of viable cells of stillage microbiota in time after different treatments. Symbols: square – untreated stillage, romb – ultrasound treated stillage, triangle – plasma treated stillage

The decrease in the number of microorganisms achieved after PT (**Fig.3**) could be very useful for the control of contamination of the stillage. This provides longer storage time of stillage and more versatility in its utilizations. On the other hand, the presence of reactive species in stillage after PT can maybe negatively affect growth of LAB responsible for LA production and limit valorization potential of stillage for fermentation. Therefore, we inoculated stillages subjected to different treatments with a high L (+) LA producing strain *Lactobacillus rhamnosus* ATCC 7469 [7] and compared number of viable bacteria 24h after different treatments against untreated stillage also inoculated with *L. rhamnosus*. These results are presented in **Fig.4**.

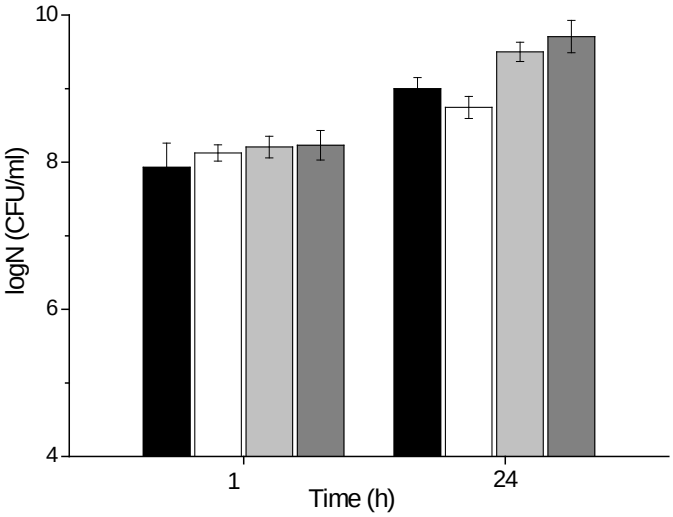

Fig.4 Number of viable cells in stillage after different treatments and inoculation with high LA producing strain *Lactobacillus rhamnosus* ATCC 7469. Symbols: black bars-untreated stillage, white bars- sterilized stillage, light grey bars- plasma treated stillage, dark grey stillage- ultrasound treated stillage.

When we compare the number of viable microorganisms after 24h with *L. rhamnosus* (**Fig.4**) and without *L. rhamnosus* (**Fig.3**), the higher number of bacteria was obtained with addition of *L. rhamnosus* than without it. Also, the growth was enhanced in PT and UT samples over untreated or sterilized (**Fig.4**). However, LAF performance of bacterial populations in PT and UT samples has to be benchmarked against untreated and conventional thermally treated samples in order to evaluate their potential for effective LA production.

3.4. Lactic acid fermentation of treated stillage by *Lactobacillus rhamnosus* ATCC 7469

The concentration of LA produced in LAF is used to quantify the efficiency of stillage revalorization. Additionally, optical purity of the produced LA is very important criteria for selection of the most promising process. *L. rhamnosus* ATCC 7469 is a high L (+) LA producing strain in mono culture, while in open fermentations on a complex media with mixed populations it can be difficult to achieve desired optical purity because different LAB produce different LA isomers. Two key factors have to be taken into account to achieve best treatment results - high sugar to LA conversion rate and stereoselective LA production.

After performing the treatments of the stillage (UT, PT, sterilization), all treated stillage samples and untreated control were inoculated with *L. rhamnosus* ATCC 7469 and subjected to LAF. The LA concentrations during open LAF, performed on PT, UT stillage and untreated stillage as substrates, and closed LAF, performed on sterilized stillage, are presented in **Fig.5**. In Table 1. the most important parameters of all studied LAFs are presented.

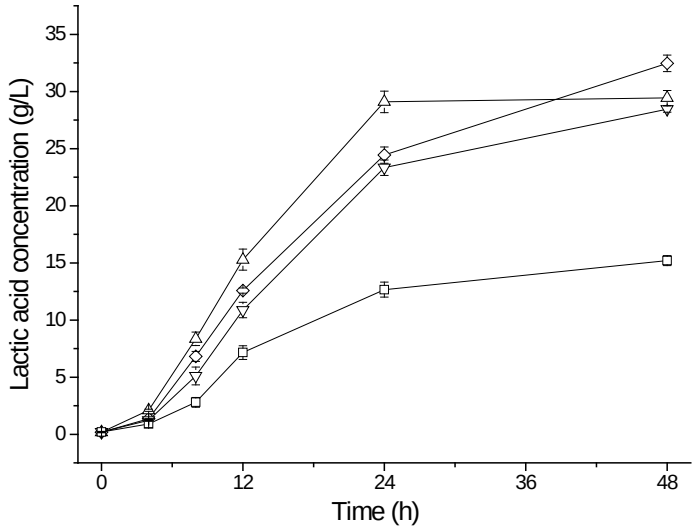

Fig.5 Kinetics of LA production during closed and open LAF on stillage subjected to different treatments. Symbols: square – untreated stillage, non-inoculated, open LAF; up triangle – non-thermal PT, inoculated by *L. rhamnosus* ATCC 7469, open LAF; diamond – non-thermal UT, inoculated by *L. rhamnosus* ATCC 7469, open LAF; down triangle – sterilized stillage, inoculated by *L. rhamnosus* ATCC 7469, closed LAF.

The most productive LAF was in PT samples directly followed by LAF in UT sample (**Fig.5**). Obviously, indigenous LAB preserved after treatments enhanced LA production. The highest LA

productivity in PT sample is a result of minimal deterioration of substrate because of absence of substrate heating during the treatment (section 3.1.) and significant suppression of competition of microorganisms in the substrate (**Fig.3**, **Fig.4**). Competition between indigenous microbiota of stillage and inoculated *L. rhamnosus* in untreated samples resulted in very low productivity of 0.57 g/Lh (Tab.1.) although this is still higher than the values reported for open LAF of kitchen waste [19] implying suitability of stillage as a substrate for LAF. Higher final LA concentration (in 48h) after UT can be explained by the presence of higher number of microorganisms in samples after UT (**Fig.4**). Although UT is often considered as non-thermal technique, ultrasound (10 min) elevated the temperature of stillage to 70˚C similarly to the reported UT of other substrates [26]. This plays additional role in microbial inactivation, deterioration of stillage and finally results in very similar productivities achieved in closed fermentation on sterilized stillage (0.97 g/Lh) and open fermentation on UT stillage (1.02 g/Lh). Besides yields and productivities, stereoselectivity of obtained LA is very important issue to be addressed.

In closed LAF, 97.2% of produced LA was L (+) isomer, while in the open LAF with PT, 95.5% of produced LA was L (+) LA, suggesting the prevalence of L (+) LA producing species after PT. Stereoselectivity of produced LA was lower in other samples. Although the final concentration was higher after UT, the diversity of LA producing strains (**Fig.4**) resulted in less stereoselective LA production, which is not desired. The highest values of LAF parameters were obtained in an open LAF performed after PT, being around 20% higher than in closed LAF with sterilized media. Therefore, PTs could be recommended as a good alternative to sterilization in order to achieve higher overall LA production with still high stereoselectivity. Inoculation by *L. rhamnosus* was necessary at the beginning of fermentation; otherwise the productivities on the stillage fermented solely by stillage microbiota were very low (Tab.1.).

The interaction of PT and UT with the stillage used for LAF was not previously studied, especially in the context of substrate pretreatments for open fermentations. The open LAF but without any physical treatment of substrate were studied with *Bacillus* sp., *Lactobacillus* sp. or *Streptococcus* sp. until now [13,19,54]. The highest LA productivities of around 2 g/Lh have been obtained in open LAF on food waste by *Streptococcus* sp. [13] and on synthetic substrate by *Enterococcus mundtii* QU 25 [55]. The average LA productivity of 1.04 g/Lh on lignocellulosic hydrolyzates by *Bacillus* sp. NL01, in an open fed-batch fermentation was reported [54] while on mixed restaurant food waste maximal reported LA productivity by *Lactobacillus* sp. was between 0.27–0.53 g/ Lh [13]. These are significantly lower values than the LA productivity of 1.2 g/Lh obtained in batch LAF on stillage after PT (**Fig.5**,Tab.1).

L. rhamnosus ATCC 7469 used in our study to produce LA has a proven probiotic potential [7]. After the separation of liquid fermentation broth with dissolved LA for extraction, solid remains with probiotic biomass of *L. rhamnosus* ATCC 7469 could be used as valuable additive for feed. It is demonstrated that in open LAF, the selected PT can significantly decrease the number of undesired G (-) microorganisms (**Fig.2**). Therefore, the PT could be a valuable tool to increase the safety of biomass and solid remains for utilization in animal nutrition.

3.4. Comparison of energy efficiency of different treatments

The estimated values of energy inputs of the performed pretreatments as well as amounts of LA

produced are presented in **Fig.6**. After different treatments all samples were subjected to LAF in the same way, therefore only energy consumption of pretreatments was included in calculation.

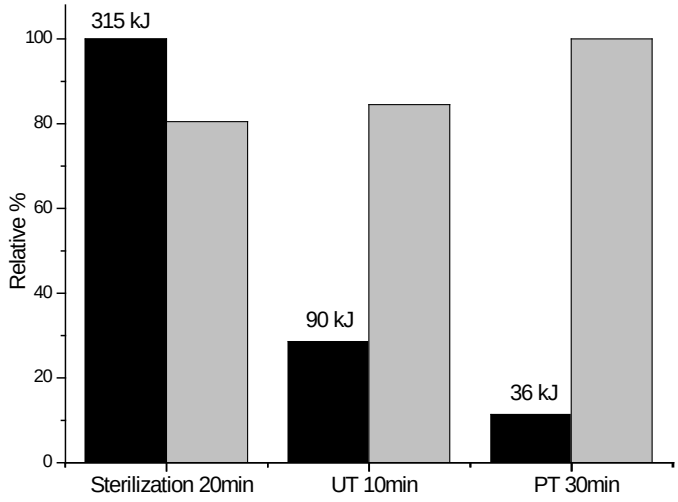

Fig.6 Estimate of required energy for different processes at laboratory level and mass of LA produced. Symbols: black bars – energy consumption of treatment in relative %, above bars is actual energy of treatment; grey bars – amount of LA produced in LAF after treatments in relative %

The lowest in energy consumption is non-thermal PT while, as expected, sterilization is the highest energy-consuming treatment. The actual values of energy consumption of PT, UT and sterilization amounted 36 kJ, 90 kJ and 315 kJ, respectively. The productivity of closed LAF solely by *L. rhamnosus* strain did not justify a high cost of energy for media sterilization. In the case of UT, only the part of energy spent during the treatment was actually delivered to the sample and this part is called actual energy of UT which is calculated based on calorimetric data for every studied sample [26]. Hence, although the UT was the second best regarding LA productivity, actual energy of UT delivered to stillage media is lower than the energy spent for UT (90 kJ) and amounts around 29.5 kJ. Therefore, only one third of spent energy was used in the process for improvement of LAF.

4. Conclusion

The microbial inactivation by non-thermal PT is highly influenced by substrate. We find that there are two reasons for lower reduction in stillage than in water. The turbidity of the stillage is causing a lower penetration of plasma generated agents decreasing their microbial inactivation efficiency. The high concentration of antioxidants in the stillage is also explaining lower logN reduction noticed in the stillage in comparison to water.

E. coli was more susceptible to PT than *L. acidophilus,* regardless of substrate. PT has shown selectivity towards G (-) microorganism and a resistance of G (+) LAB. This recommends the PT as a promising technique for the control of microorganisms present in distillery wastewater.

By comparing PT and UT we find that a 30 min long PT shows superior characteristics of up to 2.5 logN reduction, while UT also induced a decrease in the number of viable microorganisms in stillage

but to lower extent. A 20% higher LA productivity was achieved in open LAF by *L. rhamnosus* ATCC 7469 after PT than in open LAF after UT of distillery stillage. Besides being the most effective, the PT was the lowest in energy consumption and maintains stereoselectivity of LA production.

The PT provided the most effective revalorization of stillage through LAF with the highest LA productivity and the lowest energy consumption. This was achieved in the open fermentation mode which is much simpler process. Further adaptations for PT in larger scale could significantly influence effectiveness and improve the economy of process with integrated PT.

5. Acknowledgement

This work was supported by Serbian Ministry of Education, Science and Technological development, project number TR 31017, Project #I-1/2018 of Scientific and Technological Collaboration of Republic of Serbia and PR China and III 43007. Authors also want to acknowledge Milica Carević, PhD and Prof. Dejan Bezbradica, PhD for their help in HPLC analysis of samples.

6. References

[1] Noukeu, N.A., Gouado, I., Priso, R.J., Ndongo, D., Taffouo, V.D., Dibong, S.D., Ekodeck, G.E.: Characterization of effluent from food processing industries and stillage treatment trial with *Eichhornia crassipes* (Mart.) and *Panicum maximum* (Jacq.), Water Resour. Ind. 16, 1–18 (2016)

[2] Wilkie, A.C., Riedesel, K.J., Owens, J.M.: Stillage characterization and anaerobic treatment of ethanol stillage from conventional and cellulosic feedstocks, Biomass and Bioenergy. 19, 63–102 (2000)

[3] Baral, N.R., Shah, A.: Techno-economic analysis of utilization of stillage from a cellulosic biorefinery, Fuel Process. Technol. 166, 59–68 (2017)

[4] Moestedt, J., Påledal, S., Schnürer, A., Nordell, E.: Biogas Production from Thin Stillage on an Industrial Scale—Experience and Optimisation, Energies. 6, 5642–5655 (2013)

[5] Semenčenko, V.V., Mojović, L.V., Dukić-Vuković, A.P., Radosavljević, M.M., Terzić, D.R., Milašinović Šeremešić, M.S.: Suitability of some selected maize hybrids from Serbia for the production of bioethanol and dried distillers' grains with solubles, J. Sci. Food Agric. 93, 811–818 (2013)

[6] Fuess, L.T., Garcia, M.L.: Implications of stillage land disposal: A critical review on the impacts of fertigation, J. Environ. Manage. 145, 210–229 (2014)

[7] Djukić-Vuković, A.P., Mojović, L.V., Semenčenko, V.V., Radosavljević, M.M., Pejin, J.D., Kocić-Tanackov, S.D.: Effective valorisation of distillery stillage by integrated production of lactic acid and high quality feed, Food Res. Int. 73, 75–80 (2015)

[8] Pleissner, D., Qi, Q., Gao, C., Rivero, C.P., Webb, C., Lin, C.S.K., Venus, J.: Valorization of organic residues for the production of added value chemicals: A contribution to the bio-based economy, Biochem. Eng. J. 116, 3–16 (2016)

[9] West, T.P.: Malic acid production from thin stillage by *Aspergillus* species, Biotechnol. Lett. 33, 2463–2467 (2011)

[10] Wu, J.M., Liu, R.H.: Cost-effective production of bacterial cellulose in static cultures using distillery wastewater, J. Biosci. Bioeng. 115, 284–290 (2013)

[11] Kang, T.S., Korber, D.R., Tanaka, T. : Bioconversion of glycerol to 1,3-propanediol in thin stillage-based media by engineered *Lactobacillus panis* PM1, J. Ind. Microbiol. Biotechnol. 41, 629–635 (2014)

[12] Ghosh Ray, S., Ghangrekar, M.M.: Enhancing organic matter removal, biopolymer recovery and electricity generation from distillery wastewater by combining fungal fermentation and microbial fuel cell, Bioresour. Technol. 176, 8–14 (2015)

[13] Pleissner, D., Demichelis, F., Mariano, S., Fiore, S., Navarro Gutiérrez, I.M., Schneider, R., Venus, J.: Direct production of lactic acid based on simultaneous saccharification and fermentation of mixed restaurant food waste, J. Clean. Prod. 143, 615–623 (2017)

[14] Li, T., Chen, X., Chen, J., Wu, Q., Chen, G.-Q.: Open and continuous fermentation: Products, conditions and bioprocess economy, Biotechnol. J. 9, 1503–1511 (2014)

[15] Abdel-Rahman, M.A., Tashiro, Y., Sonomoto, K.: Recent advances in lactic acid production by microbial fermentation processes, Biotechnol. Adv. 31, 877–902 (2013)

[16] Dai, J.-Y., Sun, Y.-Q., Xiu, Z.-L.: Separation of bio-based chemicals from fermentation broths by salting-out extraction, Eng. Life Sci. 14, 108–117 (2014)

[17] Yusaf, T., Al-Juboori, R.A.: Alternative methods of microorganism disruption for agricultural applications, Appl. Energy. 114, 909–923 (2014)

[18] Sakai, K., Murata, Y., Yamazumi, H., Tau, Y., Mori, M., Moriguchi, M., Shirai, Y.: Selective Proliferation of Lactic Acid Bacteria and Accumulation of Lactic Acid during Open Fermentation of Kitchen Refuse with Intermittent pH Adjustment., Food Sci.Technol. Res. 6, 140–145 (2000)

[19] Tang, J., Wang, X., Hu, Y., Zhang, Y., Li, Y.: Lactic acid fermentation from food waste with indigenous microbiota: Effects of pH, temperature and high OLR, Waste Manag. 52, 278–285 (2016)

[20] Krásný, I., Lapčík, L., Lapčíková, B., Greenwood, R.: The effect of low temperature air plasma treatment on physico-chemical properties of kaolinite/polyethylene composites, Compos. Part B. Eng. 59, 293-299 (2014)

[21] Moreau, M., Orange, N., Feuilloley, M.G.J.: Non-thermal plasma technologies: New tools for bio-decontamination, Biotechnol. Adv. 26, 610–617 (2008)

[22] Surowsky, B., Schlüter, O., Knorr, D.: Interactions of Non-Thermal Atmospheric Pressure Plasma with Solid and Liquid Food Systems: A Review, Food Eng. Rev. 7, 82–108 (2015)

[23] Puač, N., Miletić, M., Mojović, M., Popović-Bijelić, A., Vuković, D., Miličić, B., Maletić, D., Lazović, S., Malović, G., Petrović, Z.L.: Sterilization of bacteria suspensions and identification of radicals deposited during plasma treatment, Open Chem. 13, 332–338 (2015)

[24] Liao, X., Liu, D., Xiang, Q., Ahn, J., Chen, S., Ye, X., Ding, T.: Inactivation mechanisms of non-thermal plasma on microbes: A review, Food Control. 75, 83–91 (2017)

[25] Ho, G.S., Faizal, H.M., Ani, F.N.: Microwave induced plasma for solid fuels and waste processing: A review on affecting factors and performance criteria, Waste Manag. 69, 423–430

(2017)

[26] Herceg, Z., Jambrak, A.R., Vukušić, T., Stulić, V., Stanzer, D., Milošević, S.: The effect of high-power ultrasound and gas phase plasma treatment on *Aspergillus* spp. and *Penicillium* spp. count in pure culture, J. Appl. Microbiol. 118, 132–141 (2015)

[27] Feng, H., Barbosa-Canovas, G., Weiss, J. (Eds.): Ultrasound Technologies for Food and Bioprocessing, Food Engineering Series. Springer New York, New York (2011)

[28] Research Grand View, Lactic Acid Market & Polylactic Acid (PLA) Market, Industry Report 2025. http://www.grandviewresearch.com/industry-analysis/lactic-acid-and-poly-lactic-acid-market (2017). Accessed 16 May 2018

[29] Djukić-Vuković, A.P., Mojović, L.V., Jokić, B.M., Nikolić, S.B., Pejin, J.D.: Lactic acid production on liquid distillery stillage by *Lactobacillus rhamnosus* immobilized onto zeolite, Bioresour. Technol. 135, 454–458 (2013)

[30] Zaplotnik, R., Bišćan, M., Kregar, Z., Cvelbar, U., Mozetič, M., Milošević, S.: Influence of a sample surface on single electrode atmospheric plasma jet parameters, Spectrochim. Acta - Part B At. Spectrosc. 103–104 124–130 (2015)

[31] Issa-Zacharia, A., Kamitani, Y., Miwa, N., Muhimbula, H., Iwasaki, K.: Application of slightly acidic electrolyzed water as a potential non-thermal food sanitizer for decontamination of fresh ready-to-eat vegetables and sprouts, Food Control. 22, 601–607 (2011)

[32] Djukić-Vuković, A., Mladenović, D., Radosavljević, M., Kocić-Tanackov, S., Pejin, J., Mojović, L., Wastes from bioethanol and beer productions as substrates for l(+) lactic acid production - A comparative study, Waste Manag. 48, 478–482 (2016)

[33] Hulsmans, A., Joris, K., Lambert, N., Rediers, H., Declerck, P., Delaedt, Y., Ollevier, F., Liers, S.: Evaluation of process parameters of ultrasonic treatment of bacterial suspensions in a pilot scale water disinfection system, Ultrason. Sonochem. 17, 1004–1009 (2010)

[34] Jovanović, J.R., Stefanović, A.B., Žuža, M.G., Jakovetić, S.M., Šekuljica, N.Ž., Bugarski, B.M., Knežević-Jugović, Z.D.: Improvement of antioxidant properties of egg white protein enzymatic hydrolysates by membrane ultrafiltration, Hem. Ind. 70, 419–428 (2016)

[35] Srivastava, A., Poonia, A., Tripathi, A.D., Singh, R.P., Srivastava, S.K.: Optimization of nutritional supplements for enhanced lactic acid production utilizing sugar refinery by-products, Ann. Microbiol. 64, 1211–1221 (2014)

[36] Uchiyama, H., Zhao, Q.L., Hassan, M.A., Andocs, G., Nojima, N., Takeda, K., Ishikawa, K., Hori, M., Kondo, T., EPR-spin trapping and flow cytometric studies of free radicals generated using cold atmospheric argon plasma and X-ray irradiation in aqueous solutions and intracellular milieu, PLoS One. 10, e0136956 (2015)

[37] Tresp, H., Hammer, M.U., Winter, J., Weltmann, K.D., Reuter, S.: Quantitative detection of plasma-generated radicals in liquids by electron paramagnetic resonance spectroscopy, J. Phys. D. Appl. Phys. 46, 435401 (2013)

[38] Gorbanev, Y., O'Connell, D., Chechik, V.: Non-Thermal Plasma in Contact with Water: The Origin of Species, Chem. - A Eur. J. 22, 3496–3505 (2016)

[39] Boudam, M.K., Moisan, M., Saoudi, B., Popovici, C., Gherardi, N., Massines, F.: Bacterial spore inactivation by atmospheric-pressure plasmas in the presence or absence of UV photons as obtained with the same gas mixture, J. Phys. D. Appl. Phys. 39, 3494–3507 (2006)

[40] Koutinas, A., Vlysidis, A., Pleissner, D., Kopsahelis, N., Lopez Garcia, I., Kookos, I.K., Papanikolaou, S., Kwan, T.H., Lin, C.S.K.: Valorization of industrial waste and by-product streams via fermentation for the production of chemicals and biopolymers. Chem. Soc. Rev. 43, 2587–627 (2014)

[41] Ramazzina, I., Berardinelli, A., Rizzi, F., Tappi, S., Ragni, L., Sacchetti, G., Rocculi, P.: Effect of cold plasma treatment on physico-chemical parameters and antioxidant activity of minimally processed kiwifruit, Postharvest Biol. Technol. 107, 55–65 (2015)

[42] Caderby, E., Baumberger, S., Hoareau, W., Fargues, C., Decloux, M., Maillard, M.-N.: Sugar Cane Stillage: A Potential Source of Natural Antioxidants, J. Agric. Food Chem. 61, 11494–11501 (2013)

[43] Surowsky, B., Schlüter, O. Knorr, D.: Interactions of Non-Thermal Atmospheric Pressure Plasma with Solid and Liquid Food Systems: A Review, Food Eng. Rev. 7, 82–108 (2015)

[44] Pagliaccia, P., Gallipoli, A., Gianico, A., Montecchio, D., Braguglia, C.M., Single stage anaerobic bioconversion of food waste in mono and co-digestion with olive husks: Impact of thermal pretreatment on hydrogen and methane production, Int. J. Hydrogen Energy. 41, 905–915 (2016)

[45] Tampio, E., Ervasti, S., Paavola, T., Heaven, S., Banks, C., Rintala, J.: Anaerobic digestion of autoclaved and untreated food waste, Waste Manag. 34, 370–377 (2014)

[46] Purevdorj, D., Igura, N., Hayakawa, I., Ariyada, O.: Inactivation of *Escherichia coli* by microwave induced low temperature argon plasma treatments, J. Food Eng. 53, 341–346 (2002)

[47] Geveke, D.J.: UV Inactvation of bacteria in Apple Cider, J. Food Prot. 68, 1739–1742 (2005)

[48] Arrange, A.A., Phelps, T.J., Benoit, R.E., Palumbo, A.V., White, D.C.: Bacterial sensitivity to UV light as a model for ionizing radiation resistance, J. Microbiol. Methods. 18, 127–136 (1993)

[49] Mai-Prochnow, A., Clauson, M., Hong, J., Murphy, A.B.: Gram positive and Gram negative bacteria differ in their sensitivity to cold plasma. Sci. Rep. 6, 38610 (2016)

[50] Sangave, P.C., Pandit, A.B.: Ultrasound pre-treatment for enhanced biodegradability of the distillery wastewater, Ultrason. Sonochem. 11, 197–203 (2004)

[51] Graves, D.B., The emerging role of reactive oxygen and nitrogen species in redox biology and some implications for plasma applications to medicine and biology, J. Phys. D Appl. Phys. 45, 263001–42 (2012)

[52] Traylor, M.J., Pavlovich, M.J., Karim, S., Hait, P., Sakiyama, Y., Clark, D.S., Graves, D.B., Long-term antibacterial efficacy of air plasma-activated water, J. Phys. D. Appl. Phys. 44, 472001 (2011)

[53] Ma, R., Wang, G., Tian, Y., Wang, K., Zhang, J., Fang, J.: Non-thermal plasma-activated water inactivation of food-borne pathogen on fresh produce, J. Hazard. Mater. 300, 643–651 (2015)

[54] Ouyang, J., Ma, R., Zheng, Z., Cai, C., Zhang, M., Jiang, T.: Open fermentative production of l-

lactic acid by *Bacillus* sp. strain NL01 using lignocellulosic hydrolyzates as low-cost raw material, Bioresour. Technol. 135, 475–480 (2013)

[55] Abdel-Rahman, M.A., Tashiro, Y., Zendo, T., Sonomoto, K.: Improved lactic acid productivity by an open repeated batch fermentation system using *Enterococcus mundtii* QU 25, RSC Adv. 3, 8437 (2013)

Tables

Table 1. Important parameters of open and closed LAFs performed on distillery stillage media

Characteristics of LAF	Distillery stillage treatment	LA concentration [c] (g/L)	LA yield (g/g)	LA volumetric productivity [c] (g/Lh)
Open LAFs [d]	non-thermal PT [a]	29.09±0.94	0.82±0.03	1.21±0.04
	UT [b]	24.43±0.71	0.69±0.02	1.02±0.03
Closed LAF [d]	sterilization	23.33±0.68	0.66±0.02	0.97±0.03
Open LAF	untreated	13.66±0.65	0.38±0.02	0.57±0.03

[a] 30 min PT, [b] 10 min UT, [c] after 24 h of LAF, [d] Samples inoculated by *L. rhamnosus* ATCC 7469 after treatments

Title: Apoptosis time window induced by cold atmospheric plasma: comparison with ionizing radiation

Authors: Gordana Joksic[1*], Ana Valenta Sobot[1], Jelena Filipovic Trickovic[1], Nevena Puac[2], Dejan Maletić[2] , Gordana Malovic[2], Zoran Lj. Petrovic[2], Sasa Lazovic[2]

[1]Department of Physical Chemistry, Vinca Institute of Nuclear Sciences, University of Belgrade, Mike Petrovica Alasa 12-14, 11001 Belgrade, Serbia

[2]Institute of Physics, University of Belgrade, Pregrevica 118, 11080 Belgrade, Serbia

Corresponding author: Gordana Joksic, Department of Physical Chemistry, Vinca Institute of Nuclear Sciences, Mike Petrovica Alasa 12-14, University of Belgrade, 11001 Belgrade, Serbia.

Email: gjoksic@vin.bg.ac.rs

Abstract

We perform γ-H2AX phosphorylation assay and flow cytometry to establish apoptosis time window of primary human fibroblasts treated with cold atmospheric plasma (CAP) for 30 seconds with power ranged 0.4-1.4 W. In parallel, set of cultures are γ-irradiated for tailoring the effects of CAP. γ-H2AX foci reaches maximum values 2 hours upon treatment with CAP power of 0.4 and 0.6 W, while γ-irradiated cells display maximum foci level 30 minutes after irradiation. Number of cells carrying >60 foci/cell and percentage of apoptotic cells correlate positively. CAP power greater than 0.6 W induces necrosis. Our results indicate that CAP treatment with power of 0.4-0.6 W induces irreparable lesions which activate massive apoptosis. Apoptosis time window is estimated to be 2 hours.

Key words: primary human fibroblasts**,** cold atmospheric plasma, ionizing radiation, repair kinetics, apoptosis

Introduction

Double strand breaks (DSBs) of the DNA represent the most significant damage of the DNA. In complex reactions between stressor, cellular DNA and repair processes, DNA lesion may be repaired back to the original state, or miss-repaired making chromosomal aberrations or inducing the frame of chromatin structure to activate other cell functions beyond canonical DNA damage response.

Phosphorylated histone H2AX (namely – γ-H2AX) represents the first signal molecule in the pathway that activates DSBs repair[1]. The role of γ-H2AX foci is to amplify DSB signaling to facilitate cell cycle arrest at distinct points of the cell cycle, consecutively enabling sufficient time for repair, namely to prevent entry of damaged cells into mitosis[2]. During the arrest, cell either activates a cascade of proteins needed to complete repair or it commits suicide by apoptosis. Phosphorylation of histone H2AX takes place in both processes[3,4], representing a universal cellular response to DSBs. Although a body of evidence shows that DSBs could occur after exposure to different exogenous agents, it is also discovered that their molecular structure could be very complex, and strongly relates to their origin, suggesting that their repair and final fate of cell survival could be strictly related to their complexity[5,6].

Cold atmospheric plasma (CAP) produces different kinds of reactive oxygen and nitrogen species (hydroxyl radical ($^{\bullet}OH$), hydrogen peroxide (H_2O_2), ozone (O_3), atomic oxygen (O), superoxide anion (O_2^-), nitric oxide (NO) and peroxynitrite ($ONOO^-$)), consequently triggering various signaling pathways including DNA repair, cell cycle control, apoptosis, and other types of cell death[7,8].

Our previous work[9], has shown that the effects of plasma doses can be tuned to match the typical therapeutic doses of ionizing radiation, inducing mainly apoptosis of human

primary cells. In this work, we used previously established experimental conditions to further investigate the repair kinetic of plasma induced DSBs as well as to approximate the time window when apoptotic outcome of the cells occurs. Repair kinetics was assessed using γ-H2AX phosphorylation assay and, in parallel, apoptosis was assessed by flow cytometry. The level of lipid peroxidation was monitored as well.

Methodology

Primary fibroblast cell lines preparation

Primary fibroblasts were obtained from skin biopsies of three healthy volunteers undergoing plastic surgery. All subjects signed informed consents regarding this investigation. The study conformed to Declaration of Helsinki and was approved by Ethical Committee of the Vinca Institute of Nuclear Sciences. A total of three primary fibroblast cell lines have been established. Cells were grown in Chang Amnio medium (Irvine Scientific, USA) at 37 ºC in humidity atmosphere and 10 % of CO_2. Each sample was set up in duplicate: one set was used for γ-irradiation whereas the second one was used for plasma treatment.

Plasma treatment

Plasma needle was placed above the samples as presented on Figure 1. The needle is powered at 13.56 MHz. Helium flow rate of 1 SLM (Standard Liter per Minute) was used for all treatments. Derivative probes were used to measure the power delivered to the plasma. Grounded electrode made of copper foil is placed beneath the sample containing vessel. The

distance between the needle tip and the samples was 5 mm. Plasma power of 0.4 W, 0.6 W and 1.4 W was used in the experiment. The monolayer of cells was covered with 5 μL of Chang medium; afterwards, cells were put in incubator to recover. On different incubation times slide by slide was processed employing the γ-H2AX phosphorylation assay to assess the repair kinetic of induced damages.

Gamma irradiation

Samples were irradiated using ^{60}Co γ-rays source (the most explored therapeutic dose of 2 Gy at dose-rate 0.45 Gy/min). The dimensions of the radiation field were 20 x 20 cm and the distance from the source was 74 cm. After irradiation, cells were returned to the tissue culture incubator. Cells were processed according to the method of Rogakau and coworkers[10]. Afterwards, cells were put in incubator to recover. On different incubation times (30 minutes, 2 hours, 5 hours and 24 hours) slide by slide was processed in the same way as after the plasma treatment employing γ-H2AX phosphorylation assay. Parallel samples were used for flow cytometry and lipid peroxidation analysis.

γ-H2AX assay

For immunostaining exponentially growing cells were seeded on polylysine glass-slides (Sigma-Aldrich, USA) and allowed to attach to the slide surface for 24 h before treatment with ionizing radiation or cold plasma. At various time points after the treatment, the cells were fixed in 4 % formaldehyde, permeabilized with 0.2 % triton X-100 and stained

with the γ-H2AX primary antibody (Merck Millipore, USA) and a FITC-labeled secondary antibody (Sigma-Aldrich, USA). The slides were mounted with 4′,6′-diamidino-2-phenylindole (DAPI)-containing Vectashield solution (Vector Laboratories Ltd, UK), covered with coverslips and sealed. Foci positive for γ-H2AX were counted using an epifluorescent Axiomager A1 microscope (Carl Zeiss, Germany) and the computer software ISIS (Metasystem, Germany) according to the method of Kinner and coworkers[11].

Apoptosis and cell cycle analysis

For apoptosis assay, at each time point after irradiation and plasma treatment, cells were washed with pre-warmed phosphate buffer saline (PBS), at 37 °C and fixed in 96 % ethanol. Apoptosis was monitored by flow cytometry (Becton Dickinson, Germany). DNA content was assessed by measuring the UV fluorescence of propidium iodide stained DNA (PI, 10 mg/mL, Sigma-Aldrich, USA). Apoptotic population and cell cycle analysis was performed using CellQuest software (Becton Dickinson, Germany), according to method of Holmes and colleagues[12].

Lipid peroxidation products-Thiobarbituric acid (TBA) assay

For the determination of lipid peroxidation, by measuring of thiobarbituric acid reactive substances (TBARS) spectrophotometrically, we followed the method of Jainero[13]: 0.1 mL of pellet and 0.1 mL of medium of the same culture were used for analysis. Briefly, 0.4 mL of 50 mM Tris-HCl buffer containing 180mM KCl and 10mM EDTA was added to 0.1 mL of pellet lysate or defrosted medium, 0.5 mL of 2-thiobarbituric acid (Merck; 1%

wt/vol) in 0.05 M NaOH and 0.5 mL of HCl (25% wt/vol in water). The mixture was heated in boiling water for 10 minutes, reaction was stopped by cooling samples on ice, and afterwards the chromogen was extracted in 3 mL of n-butanol in the organic phase separated by centrifugation at 5000 rpm for 10 min. The absorbance of the organic phase was measured spectrophotometrically (Tecan Sunrise absorbance microplate reader, Tecan group LTD, Switzerland), at 532 nm wavelength. The value is expressed as nmol TBARS (malondialdehide, MDA equivalents)/mg of proteins, using a standard curve of 1,1,3,3-tetramethoxypropane. Proteins were determined according to Lowry using bovine serum albumin as standard[14].

2.7. Statistics

Statistical analysis was performed in statistical program SPSS 10 for Windows. Differences between the groups were assessed using nonparametric Mann Whitney U test, while correlation between different parameters was assessed by Pearson correlation. Differences at $p<0.05$ were accepted as the level of significance.

3. Results and Discussion

Results obtained in the experiment where cells where directly exposed to non thermal plasma are presented in Table 1 and Figure 2.

Previously established experimental parameters such as power delivered to plasma of 0.4 W, 0.6 W and 1.4 W and exposure time of 30 seconds, were used to investigate repair kinetic of DSBs (visualized by γ-H2AX histone), apoptosis and lipid peroxidation biomarker - malondialdehyde (MDA) at different recovery periods of time after treatment. Results are compared with the effects of γ-rays (^{60}Co) - acute irradiation. The powers of 0.4, 0.6 and 1.4 W correspond to voltage 337, 357 and 393 V, respectively. At exposure time of 30 seconds calculated corresponding equivalent radiation dose in Gy ranged from 0.96 Gy (0.4 W and 30 sec) to 2.2 Gy[9].

The base-line level of γ-H2AX in unexposed control cells was 3.9 per cell, whereas 30 minutes after the plasma treatment (power 0.4 W) the yield of γ-H2AX reached 16.2 foci per cell. Further increase of power (0.6 W) induces 46.6 foci per cell, whereas power of 1.4 W momentarily induces cell death seen as misshapen nuclei (Figure 2e and f) or as a "track" (Figure 2e) where all the cells closest to the powered electrode were detached from the polylysine surface (Figure 2e and f).

A maximum of foci induction after non thermal plasma treatment with power 0.4 and 0.6 W occurred 2 hours after the treatment (1.5 hour later when compared with ionizing radiation) indicating that most of treated cells will die via apoptosis (Table 1, Figure 2c). Initial DNA damages are non-reparable and determine early apoptosis. This observation is confirmed by flow cytometry data, which show that apoptosis occurred at dose (power) dependent manner, i.e., the highest power induces necrosis, power of 0.6 W induces apoptosis

with maximum pick of apoptosis between 30 minutes and 2 hours after the treatment; whereas 0.4 W induces apoptosis 2 hours after the exposure and lasts continuously for up to 5 hours (Figure 2a). Interestingly, beside power-dependent time shift in apoptosis induction, apoptosis time window is the same and lasts for two hours.

A positive correlation between number of cells carrying 60 signals per cell and percentage of cells displaying apoptotic granulation was found for cold plasma treatments of power 0.4 and 0.6 W (Pearson correlation, $p<0.01$, $r=0.967$ and $p<0.05$, $r=0.934$, respectively). In samples treated with the power of 1.4W, high number of misshapen nuclei was observed, as well as elevated concentration of MDA. Bulky phosphorylation of γ-H2AX seen as more than 60 signals per nuclei, correlates with apoptotic fragmentation. It has been previously reported that H2AX phosphorylation that leads to apoptosis mainly occurred by DNA-PKcs kinases[4], although phosphorylation of H2AX via c-Jun N terminal kinases (JNK) can't be neglected due to UV irradiation in plasma source. However, DNA-PKs are predominant kinases that phosphorylates H2AX when unrepairable lesions are induces, activating apoptosis, as normal fibroblast cell lines that we used in the experiment revealed. In cells irradiated with ionizing radiation phosphorylation of H2AX occurs via ATM kinase that leads to activation of cascade molecules involved in DSBs repair. H2AX is the most important molecule in switch between apoptosis versus repair response following DNA damage[15,16]. According to the results obtained in this study we can conclude that non-thermal atmospheric plasma power of (0.4 – 0.6 W) predominantly induces apoptosis, whereas power of 1.4 W predominantly induces necrosis (Figure 2e and f).

Treatment with ionizing radiation (^{60}Co γ-rays) induces maximum γ-H2AX foci formation 30 minutes after irradiation, 19.79 (Table 1, Figure 2c and g). Induced DSBs are mostly repaired within 24 hours. During recovery period a portion of cells are faced with

unsuccessful repair outcome, and they are removed from cell population via apoptosis. Apoptosis starts 30 minutes after irradiation (37.25 %) and continuously occurs during the next 5 hours almost at the same extent, suggesting that all cells that enter S-phase of the cell cycle with unrepaired DSBs are directed toward apoptosis. The maximum pick of apoptosis takes place 24 hours after irradiation (51.51 %), restoring γ-H2AX foci mostly to the base-line level. Residual foci, after recovery period of 24 hours represent the main concern about possible side effects after irradiation with ionizing radiation, because unrepaired DSBs can interact with other lesions creating hybrid genes, deletion or duplication that can lead to genomic instability and transformation of cells[8,17].

In contrast to ionizing radiation, treatment with cold plasma power of 0.4 W and 0.6 W induces maximum formation of γ-H2AX foci 2 hours after the treatment, accompanied by massive apoptosis of treated cells (Table 1, Figure 2a and c). The highest power (1.4 W) induces necrosis of cells, characterized with misshapen, sparkling, partly detached nuclei, as seen microscopically. MDA levels were also elevated in these cells, statistically significant comparing to other treatments ($p<0.05$), indicating increased lipid peroxidation (Figure 2b). Lipid peroxidation, depending on its' extent, may endorse cellular survival or lead to cell death. High peroxidation rates that overcome repair capacities result in cell death[18,19], which, accompanied with exhausted energetic capacities, direct cells to necrosis[20]. After recovery period of 24 hours the number of cells surviving after treatment with non-thermal plasma power of 1.4 W is low, suggesting that initially induced bulky lesions determine lethal fate of treated cells.

4. Conclusion

Non-thermal plasma is very promising method to be used for treatment of small tissue areas. Further investigations of non-thermal plasma should be directed towards investigation of possible bystander effects on the surrounding of target tissues, since extracellular liquid of treated tissue carry newly created chemical compounds that can be stabile for certain period of time and induce adverse effects to surrounding tissue acting as chemical messengers.

Acknowledgements

This work is financially supported by The Ministry of Education, Science and Technological Development of the Republic of Serbia, Grant No 173046.

Conflict of interests: Authors have no conflicts of interest to disclose.

References

1. Downs, J. A., Lowndes, N. F., and Jackson, S. P., A role for Saccharomyces cerevisiae histone H2A in DNA repair. *Nature,* 2000, **408**, 1001-1004.
2. Downs, J. A., Allard, S., Jobin-Robitaille, O., Javaheri, A., Auger, A., Bouchard, N., Kron, S. J., Jackson, S. P., and Cote, J., Binding of chromatin-modifying activities to phosphorylated histone H2A at DNA damage sites. *Mol. Cell,* 2004, **16**, 979-990.
3. Rogakou, E. P., Nieves-Neira, W., Boon, C., Pommier, Y., and Bonner, W. M., Initiation of DNA fragmentation during apoptosis induces phosphorylation of H2AX histone at serine 139. *J. Biol. Chem.,* 2000, **275**, 9390-9395.
4. Yuan, J., Adamski, R., and Chen, J., Focus on histone variant H2AX: to be or not to be. *FEBS Lett.,* 2010, **584**, 3717-3724.

5. Schipler, A., Iliakis, G., DNA double-strand-break complexity levels and their possible contributions to the probability for error-prone processing and repair pathway choice. *Nucleic Acids Res.,* 2013, **41**, 7589-7605.
6. Shibata, A., et al., Factors determining DNA double-strand break repair pathway choice in G2 phase. *EMBO J.,* 2011, **30**, 1079-1092.
7. Dezest, M., et al., Mechanistic insights into the impact of Cold Atmospheric Pressure Plasma on human epithelial cell lines. *Scientific Reports,* 2017, **7**, 41163.
8. Noda, A., Radiation-induced unrepairable DSBs: their role in the late effects of radiation and possible applications to biodosimetry. *J. Radiat. Res.,* 2018, **59**, ii114-ii120.
9. Lazović, S., Maletić, D., Leskovac, A., Filipović, J., Puač, N., Malović, G., Joksić, G., and Petrović, Z. L., Plasma induced DNA damage: Comparison with the effects of ionizing radiation. *Appl. Phys. Lett.,* 2014, **105**, 124101.
10. Rogakou, E. P., Pilch, D. R., Orr, A. H., Ivanova, V. S., and Bonner, W. M., DNA double-stranded breaks induce histone H2AX phosphorylation on serine 139. *J. Biol. Chem.,* 1998, **273**, 5858-5868.
11. Kinner, A., Wu, W., Staudt, C., and Iliakis, G., Gamma-H2AX in recognition and signaling of DNA double-strand breaks in the context of chromatin. *Nucleic Acids Res.,* 2008, **36**, 5678-5694.
12. Holmes, K. L., Otten, G., and Yokoyama, W. M., Flow cytometry analysis using the Becton Dickinson FACS Calibur. *Current protocols in immunology*, 2002, **49**, 5.4.1-5.4.22.
13. Janero, D. R., Malondialdehyde and thiobarbituric acid-reactivity as diagnostic indices of lipid peroxidation and peroxidative tissue injury. *Free Radic. Biol. Med.,* 1990, **9**, 515-540.
14. Lowry, O. H., Rosebrough, N. J., Farr, A. L., and Randall, R. J., Protein measurement with the Folin phenol reagent. *J. Biol. Chem.,* 1951, **193**, 265-275.
15. Cook, P. J., Ju, B. G., Telese, F., Wang, X., Glass, C. K., and Rosenfeld, M. G., Tyrosine dephosphorylation of H2AX modulates apoptosis and survival decisions. *Nature,* 2009, **458**, 591.
16. Xiao, A., et al., WSTF regulates the H2A.X DNA damage response via a novel tyrosine kinase activity. *Nature,* 2009, **457**, 57-62.

17. Fenech, M., The cytokinesis-block micronucleus technique: a detailed description of the method and its application to genotoxicity studies in human populations. *Mutat. Res.,* 1993, **285**, 35-44.
18. Ayala, A., Munoz, M. F., and Arguelles, S., Lipid peroxidation: production, metabolism, and signaling mechanisms of malondialdehyde and 4-hydroxy-2-nonenal. *Oxid. Med. Cell. Longev.,* 2014, **2014**, 360438.
19. Haghdoost, S., Sjolander, L., Czene, S., and Harms-Ringdahl, M., The nucleotide pool is a significant target for oxidative stress. *Free Radic. Biol. Med.,* 2006, **41**, 620-626.
20. Vairetti, M., Ferrigno, A., Bertone, R., Richelmi, P., Berte, F., and Freitas, I., Apoptosis vs. necrosis: glutathione-mediated cell death during rewarming of rat hepatocytes. *Biochim. Biophys. Acta,* 2005, **1740**, 367-374.

Tables

Table 1. Repair kinetics and apoptosis of human primary fibroblasts exposed to non thermal plasma and ionizing radiation.

Treatment	Analysis	0 min	0.5 h	2 h	5 h	24 h
Ionizing radiation	Number of f/c[a)]	0.39	19.79	14.53	5.23	1.12
	% of >60 f/c	0.41	8.89	3.47	1.86	0.16
	% of apoptotic cells	9.1	37.25	33.42	25.16	51.51
	MDA[b)] (nmol/mg of proteins)	0.54	0.68	0.55	0.33	0.67
CAP[c)] power of 0.4 W	Number of f/c	1.39	16.22	39.85	21.8	0.16
	% of >60 f/c	0	1.72	3.9	2.85	0.59
	% of apoptotic cells	8.22	14.43	41.8	31.4	5.82
	MDA (nmol/mg of proteins)	0.54	0.68	0.69	0.8	0.67
CAP power of 0.6 W	Number of f/c	0.4	46.59	47.59	29.27	7.35
	% of >60 f/c	0	42.65	84.9	11.45	0
	% of apoptotic cells	9.14	58.5	68.14	27	0
	MDA (nmol/mg of proteins)	0.59	0.81	0.88	0.74	0.92
CAP power of 1.4 W	Number of f/c	4	13.55	7.88	0	0
	% of >60 f/c	0	36.15	76.08	0	0
	% of apoptotic cells	9.4	36.1	68	0	0
	MDA (nmol/mg of proteins)	0.79	1.47	1.45	1.23	1.3

[a)] f/c - γ-H2AX focus per cell
[b)] MDA - Malondialdehyde
[c)] CAP - Cold atmospheric plasma

Figure legends

Figure 1. Plasma treatment experimental setup.

Figure 2. Percentage of apoptotic cells (a); MDA concentration (b); Number of γ-H2AX foci per cell (c); Percentage of cells with >60 foci per cell in cold plasma and ionizing radiation treated cells (d); detached and necrotic cells in cold plasma treated samples, power 1.4 W visualized by immunostaining (e, f), scale bar 150 μm; γ-H2AX foci in ionizing radiation treated cells (g), scale bar 30 μm.

Figures

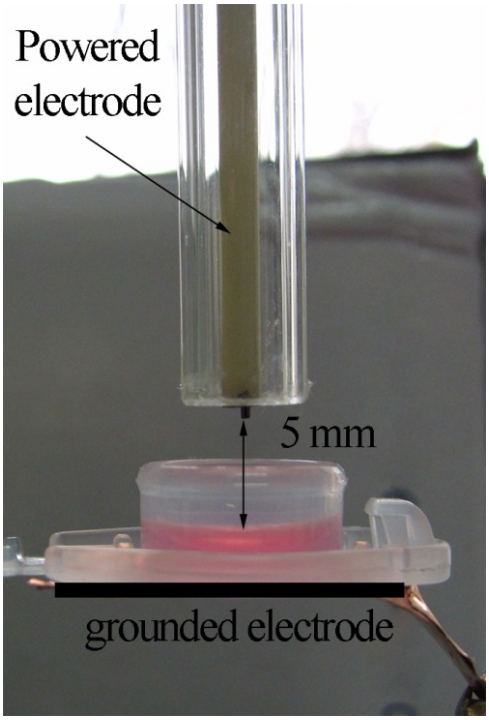

Figure 1.

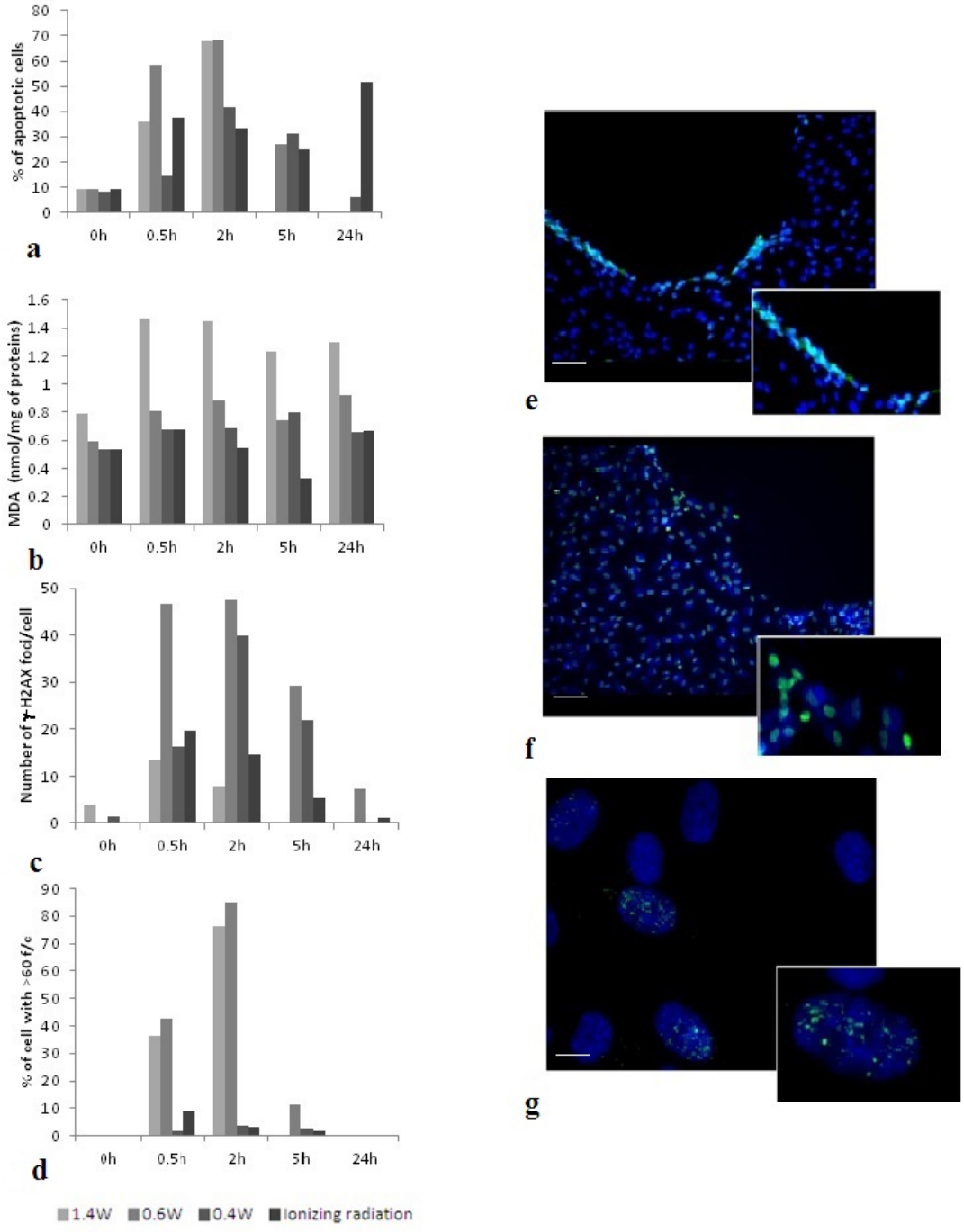
% of apoptotic cells
0h
0.5h
2h
5h
24h
a
MDA (nmol/mg of proteins)
b
Number of γ-H2AX foci/cell
c
% of cell with >60 f/c
d
1.4W
0.6W
0.4W
Ionizing radiation
e
f
g

Figure 2.

Cellulose

Nitrogen plasma surface treatment for improving polar ink adhesion on micro/nanofibrillated cellulose films

--Manuscript Draft--

Manuscript Number:	CELS-D-18-01104
Full Title:	Nitrogen plasma surface treatment for improving polar ink adhesion on micro/nanofibrillated cellulose films
Article Type:	Original Research
Keywords:	DBD plasma; nitrogen plasma surface treatment; nanocellulose films; enzymatic nanocellulose; printing of organic-based polar inks
Corresponding Author:	katarina mirko dimic misic, Dr. (tech) Aalto University Espoo, Espoo FINLAND
Corresponding Author Secondary Information:	
Corresponding Author's Institution:	Aalto University
Corresponding Author's Secondary Institution:	
First Author:	katarina mirko dimic misic, Dr. (tech)
First Author Secondary Information:	
Order of Authors:	katarina mirko dimic misic, Dr. (tech)
	Mirjana Kostic
	Bratislav Obradovic
	Ana Kramar
	Stevan Jovanovic
	Dimitrije Stepanenko
	Marija Mitrovic-Dankulov
	Sasa Lazovic
	Leena-Sisko Johansson
	Thad Maloney
	Patrick Gane
Order of Authors Secondary Information:	
Funding Information:	
Abstract:	We find that nitrogen plasma treatment of micro/nanofibrillated cellulose films increases wettability of the surface by both liquid polar water and nonpolar hexadecane. The increased wetting effect is more pronounced in the case of polar liquid, favouring the use of plasma treated micro/nanofibrillated cellulose films as substrates for a range of inkjet printing including organic-based polar-solvent inks. The films were formed from aqueous suspensions of progressively enzymatic pretreated wood-free cellulose fibres, resulting in increased removal of amorphous species producing novel nanocellulose surfaces displaying increasing crystallinity. The mechanical properties of each film are shown to be highly dependent on the enzymatic pretreatment time. The change in surface chemistry arising from exposure to nitrogen plasma is revealed using X-ray photoelectron spectroscopy (XPS). That both polar and dispersive surface energy components become increased, as measured by contact angle, is also linked to an increase in surface roughness. The change in surface free energy is exemplified to favour the trapping of photovoltaic inks.

Suggested Reviewers:	Patrice Mangin, Dr. professor, Université du Québec, Trois Rivières, Canada patrice.mangin@uqtr.ca Prof. Mangin has been working in last decade in the filed of rheological characterization of nanocellulosic materials . He has a great expertise in the filed of surface treatment of paper and fulm.
	Per Claesson, Dr. professor, KTH, Stockholm, Sweden. percl@kth.se Porf. Claesson has a great exp.ertise in the filed of nanocellulose suspensions, nanocellulose based products and their surface treatment
	Martin Hubbe, Dr. professor, North Carolina University hubbe@ncsu.edu Prof. Hubbe has been for many years working in the firld of nanocellulose base suspensions and film forming. He has a great expertice in surface tretamnet of cellulose fibers and plasma methodology .
	Li Yang, Dr. RISE Research Institutes of Sweden AB li.yang@ri.se Dr. Yang has a very broad knowledge about nanocellulose materials, porous surface and plasma treatement.

graphical abstract

Click here to download attachment to manuscript graphical abstract .jpg

Click here to view linked References

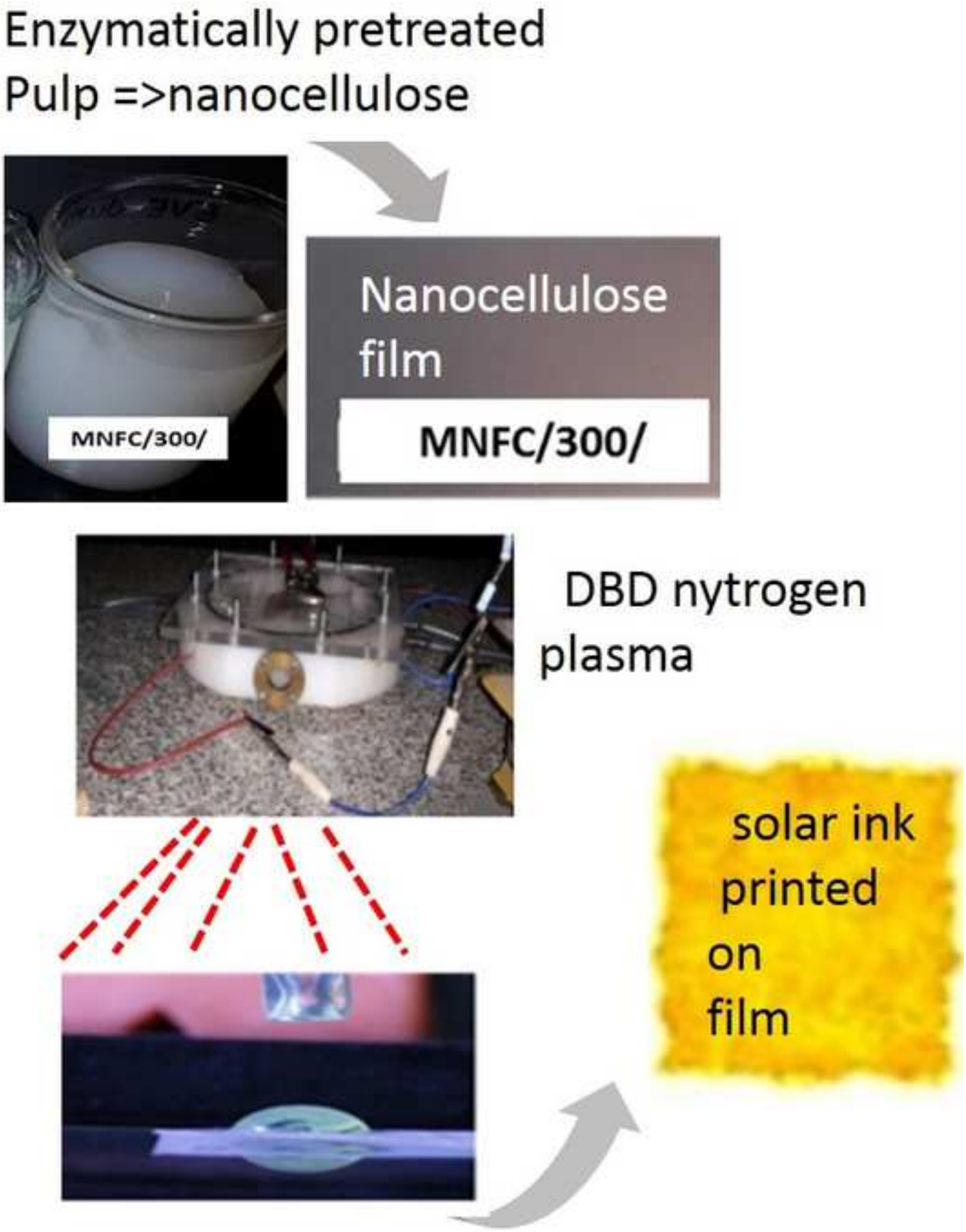

Dear Editor,

We submit manuscript with title “Nitrogen plasma surface treatment for improving polar ink adhesion on micro/nanofibrillated cellulose films”, in which we present novel mechanism which enables improved printability of micro/nanocellulose films, especially for high end application of solar cells printing. .

Due to climate change and overall pollution caused by the excessive use of fossil fuels and fossil fuel-derived chemicals in industry, sustainable technologies are continuously being sought-after. This trend is accompanied by the replacement of current unsustainable fuel and materials sources by biobased raw materials. The need for functional high strength composites is a topic of much research, and micronanocellulose is identified as a strong contender to replace both fossil carbon-based polymeric derivatives and to provide novel materials ranging from substrate films to high tensile construction elements in vehicles, buildings and even aircraft. Driving the need to improve the viability of nanocellulose production, is the realisation that the molecular structure of cellulose renders it relatively easy to modify its surface to generate specific functional properties and compatibility with liquids in industrial applications, such as textiles, moulded articles and advanced technologies as printed electronics and dye-based solar cells. Amongst surface modification methods, plasma treatment has been the subject of intense research, given its use in commonly applied fields such printing and gluing of sheet-like materials. Micro nanofibrillated cellulose films formed from aqueous suspension can be made stronger by environmentally friendly and economically feasible pre-treatment of the raw fibre using enzymatic hydrolysis. However, wettability of such films, which have highly crystalline structure by ionic liquids used for printed electronics, solar cells limits the use of such films in practice. Nitrogen plasma treatment, however, enables wettability by such formulations to be improved. The novel mechanism by which this occurs has been studied in this work presented in this paper. We believe that this research will be interesting for publication in Cellulose.

In the name of authors,

Katarina Dimic-Misic

NITROGEN PLASMA SURFACE TREATMENT FOR IMPROVING POLAR INK ADHESION ON MICRO/NANOFIBRILLATED CELLULOSE FILMS

Katarina Dimic-Misic[1], Mirjana Kostić[2], Bratislav Obradović[3], Ana Kramar[2], Stevan Jovanović[4], Dimitrije Stepanenko[4], Marija Mitrović-Dankulov[4], Saša Lazović[4], Leena-Sisko Johansson[1], Thad Maloney[1], Patrick Gane[1]

[1] School of Chemical Engineering, Department of Bioproducts and Biosystems, Aalto University, 00076 Aalto, Helsinki, Finland

[2] Faculty of Technology and Metallurgy, University of Belgrade, Karnegijeva 4, Belgrade 11000, Serbia

[3] Faculty of Physics, University of Belgrade, Studentski trg 12, 11001 Belgrade, Serbia

[4] Institute of Physics Belgrade, Pregrevica 118, 11080 Belgrade, Serbia

ABSTRACT

We find that nitrogen plasma treatment of micro/nanofibrillated cellulose films increases wettability of the surface by both liquid polar water and nonpolar hexadecane. The increased wetting effect is more pronounced in the case of polar liquid, favouring the use of plasma treated micro/nanofibrillated cellulose films as substrates for a range of inkjet printing including organic-based polar-solvent inks. The films were formed from aqueous suspensions of progressively enzymatic pretreated wood-free cellulose fibres, resulting in increased removal of amorphous species producing novel nanocellulose surfaces displaying increasing crystallinity. The mechanical properties of each film are shown to be highly dependent on the enzymatic pretreatment time. The change in surface chemistry arising from exposure to nitrogen plasma is revealed using X-ray photoelectron spectroscopy (XPS). That both polar and dispersive surface energy components become increased, as measured by contact angle, is also

linked to an increase in surface roughness. The change in surface free energy is exemplified to favour the trapping of photovoltaic inks.

Keywords: DBD plasma, nitrogen plasma surface treatment, nanocellulose films, enzymatic nanocellulose, printing of organic-based polar inks

INTRODUCTION AND BACKGROUND

Sustainability is one of the key targets for industrial practice today. The related research aimed at new biobased materials derived from renewable sources, is relevant for the sustainable economy. In the bioproducts industry, micro/nanofibrillated cellulose (MNFC) has attracted attention in a number of potential applications (Hubbe *et al*. 2017a,). It can be used in standard wood products, such as paper and boards. However, most of the benefits derived from MNFC stem from its wider uptake in a range of industrial value chains, such as biodegradable packaging films and laminates. MNFC has interesting intrinsic properties derived from large specific surface area and its alternate regions of crystallinity. The hydroxylated surface chemistry is readily suitable for chemical modification. Films formed from MNFC are considered smart materials and studied for functional materials applications. Enzyme-treated fibres used to produce cellulose nanofibrils provide higher crystallinity in the resulting nanocellulose, as enzymes digest amorphous cellulose, which acts as the glue between crystalline cellulose regions. Direct hydrogen bonding of crystalline cellulose, therefore, gives a stronger material film. An example of an important application of MNFC is as a substrate for printed solar cells based on organic inks (Zhou *et al*. 2013). The surface properties of MNFC films, such as wettability by liquid, topography, chemistry, surface charge, the presence of hydrophobic and hydrophilic domains, density and conformation of functional groups, all play a crucial role in printability and barrier properties. Their ability to support controlled migration of solvent ink vehicle and chromatographic differentiation of ink components is important in the printing of inkjet printable (IP) inks, and especially for production of bio-based printed functionality in a wide range of applications, such as printed electronics and printed diagnostics (Hieng *et al*. 2016, Jutila *et al*. 2018).

Solar panel IP photovoltaic (PV) inks contain a complex mix of materials, including the organic electron acceptor (p-type) and negative electron donor (n-type) suspended in solvent together with specific surfactant(s) intended to keep the p-type and n-type components de-mixed (Kumar and Chand 2012). Although drop-on-demand (DoD) inkjet printing is a very competitive candidate for printing PV inks on film substrates, there are limitations in respect to mutual compatibility between the surface of MNFC films and mixed polar-dispersive solvents constituting the PV ink (Sing *et al*. 2010, Yinhua *et al*. 2013). Electrolyte is highly polar, for example, and so sufficient wettability is needed by providing a polar surface, despite the parallel requirement for wettability by organic species (Schultz *et al*. 1977, Özkan *et al*. 2016). This complex polar-dispersive surface energy balance is, therefore, critical (Hansson *et al*. 2011).

Exposure to plasma is a convenient method to modify the surface properties of polymeric materials, while keeping their bulk properties intact, making a material better adapted for printing (Möller *et al*. 2010, Kramer *et al*. 2006, Catia *et al*. 2015). Furthermore, as we demonstrate, it is a convenient way to introduce desired groups onto the surface of materials (Mihailovic *et al*. 2011). Surface properties depend on parameters of plasma treatment such as applied electrical field energy, type of feed gas, pressure, exposure time, and reactor geometry (van de Vyer *et al*., 2011, Jun *et al*. 2008).

In this work, we modify enzyme pretreated fibre-derived MNFC film surfaces using nitrogen plasma to enhance their amphiphilic surface affinity to polar and non-polar IP PV inks. Measurements of the surface free energy, surface roughness (atomic force microscopy (AFM)) and material composition (X-ray photoelectron spectroscopy (XPS)) were used to characterise the MNFC film surface before and after plasma treatment. The affinity for IP PV ink was assessed visually after inkjet printing. We link the observation of the level of change in free surface energy of the plasma treated MNFC films with the increase in crystallinity arising from enzymatic pretreatment (Galagan *et al*. 2011, Cernakova *et al*. 2006, Pertile *et al*. 2010, Vammeste *et al*. 2017).

To meet the requirement of sufficient tensile strength of MNFC films for the application exemplified, the rheological properties of enzymatically pretreated MNFC fibrillar suspensions were compared with the mechanical properties of corresponding obtained films, so that rheology can be used as a predictor of film strength (Maloney 2015, Zhou *et al*. 2013).

MATERIALS AND METHODS

Preparation of MNFC

For the manufacture of short MNFC fibrils, the pulp was first washed to create the sodium form by adding sodium hydroxide to a 2 w/w% fibre suspension until the pH reached 10, and then re-washed with deionised water to a conductivity of 8.2 µS. The enzymatic treatment was performed with a commercial enzyme ECOPULP® R (Ecopulp Finland Oy), produced by a genetically modified strain of Trichoderma reesei fungus (Rantanen *et al*. 2015). An amount of 3 mg of enzyme per gram of pulp fibre was added to a 2.5 w/w% suspension and the temperature was increased to 57 °C at pH 5.5 during hydrolysis, whilst keeping under constant agitation. The period of digestion was increased for each subsequent sample in 30 min steps, Table 1. The enzymatic activity was terminated by adjusting the pH to 9-10 by sodium carbonate and increasing the temperature to 90 °C. After cooling the suspension overnight in cold storage, the samples were refined using an homogeniser (model M-110P, Microfluidics, USA), passing the material under a pressure of 2 000 bar through a 100 µm flow gap. The solids content of the MNFC suspension after the fluidisation was 1.65 w/w%.

Enzymatic pretreatment of pulp as a route for producing low-charged MNFC results in an economically feasible production of short fibrils, which have much lower aspect ratio than MFC and NFC produced via chemical oxidative pretreatment or mechanical refining alone, as illustrated in Fig. 1 comparing MNFC/300/ and MNFC/0/ suspensions (Table 1), revealing much shorter fibrils obtained upon 300 min of enzymatic hydrolysis.

Table 1. Materials used in this study: bleached hardwood Kraft pulp treated with enzymes under controlled conditions, with progressive increase in enzymatic digestion time by 30 min steps for each subsequent sample.

Enzymatic treatment time	0 (reference)	30	60	90	120	150	180	210	240	270	300

/ min											
Sample label	MNFC /0/	MNFC /30/	MNFC /60/	MNFC /90/	MNFC /120/	MNFC /150/	MNFC /180/	MNFC /210/	MNFC /240/	MNFC /270/	MNFC /300/

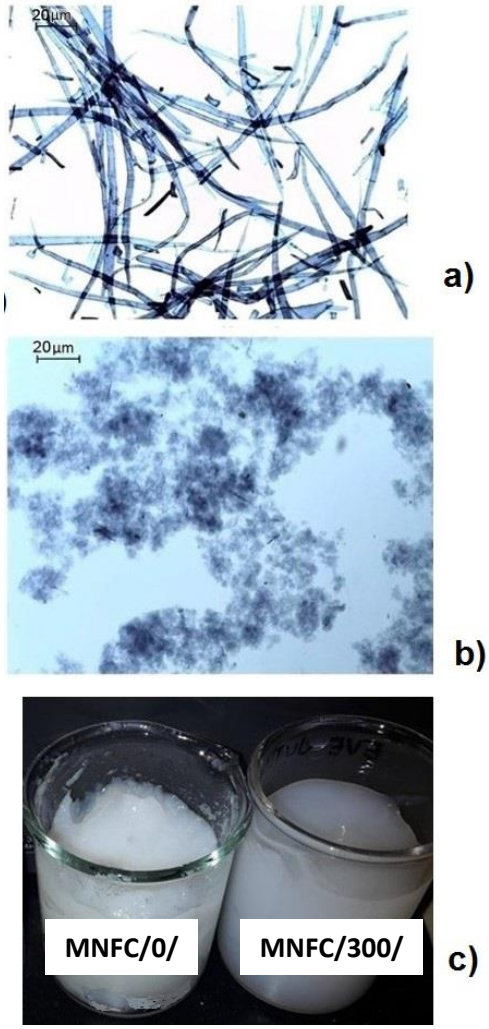

Fig 1. Images of fibrils sample suspensions obtained with optical microscopy revealing the effect of processing conditions on the fibril size and aspect ratio: a) without enzymatic treatment produced MNFC/0/ yielding long fibrils, b) MNFC/300/ short, low aspect ratio fibrils, and c) displaying the corresponding 2 w/w% MNFC suspensions of MFC/0/ and MNFC/300/. The difference in gelation strength is due to the different size of fibrils and corresponding amount of water dispersed within the fibrillar matrix.

MNFC film preparation

With increasing enzymatic treatment time, the resulting MNFC suspension viscosity decreased significantly, and the solid content for preparation of the respective films ranged from 0.6 w/w% to 1.9 w/w% to meet the target film grammage of 60 gm^{-2} produced under conditions of 23 °C and relative humidity (RH) 50 %.

Films were made on a sheet-former according to ISO standard 5269-1, with some modification of the screen to aid fines retention. The system was pressurised to 0.3 bar and the sealing lid was used on the sheet-former, with a 10 µm mesh supplemented nylon screen in addition to metallic wire screen, so that the slurry of pulp was poured at high viscosity onto the former without adding water or stirring the slurry. Double-sided adhesive tape, of 5 mm width, was attached to the edges of the drying plate between plate and formed film, with purpose of fixing the edge of the film to prevent it shrinking during drying. Due to the very strong water retention of MNFC, and its fine size, a polyamide monofilament open mesh fabric SEFAR NITEX® 03-1/1 with a pore size of 1 µm was placed on top of a 125 µm metal screen.

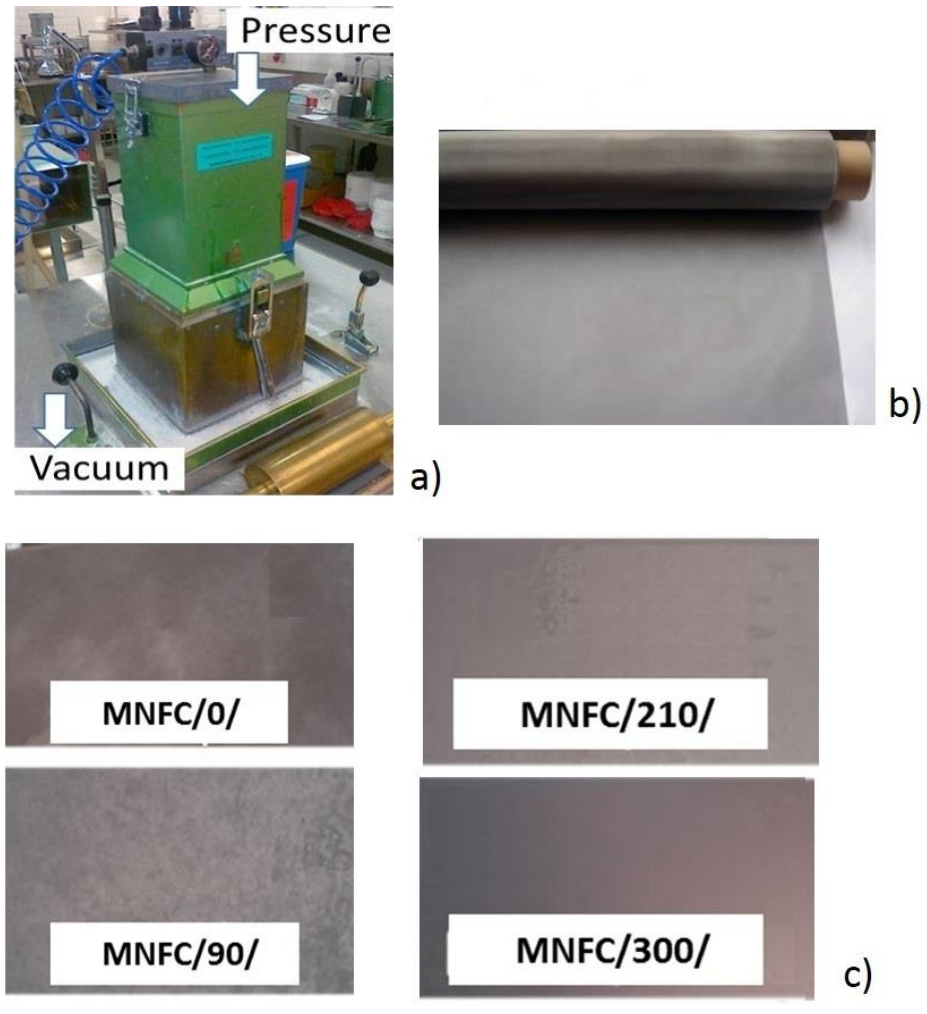

Fig. 2 MNFC film preparation: a) sheet forming device with b) 10 µm mesh supplemented nylon screen, and c) samples of cut-offs (60 x 15 mm^2) from MNFC films produced from pulp refined with different enzymatic pretreatment time (Table 1). Transparency and uniformity of films increases with hydrolysis time.

Material treatment and characterisation

Optical microscopy was used to study the fibrillar sample suspensions and films using an Olympus BX 61 microscope equipped with a DP12 camera.

Water retention – the water retention value (WRV) of the MNFC was determined in accordance to the standard SCAN-C 102XE with a slight modification in that 10 w/w% suspension of the MNFC was added in various ratios to a suspension of bleached unrefined pulp. The pulp matrix helps the MNFC dewater and remain retained on the screen. The WRV of neat MNFC can be evaluated by extrapolating to zero pulp, not including the swelling of the pulp fibres (Möller *et al*. 2010). The experiment was performed in triplicate for each sample.

Dielectric Barrier Discharge (DBD) plasma operates in a thermodynamically non-equilibrium condition (so-called cold plasma) in which the ion and molecular translational temperature is much lower than the electron temperature, such that excessive gas heating can be suppressed (Kostic *et al*. 2009, Prysiazhnyi *et al*. 2013). The advantage is that the plasma can be generated at atmospheric pressure, either in open or closed environment. In an open atmosphere, the plasma discharges can be produced with a gas flow between the electrodes (Mihailovic *et al*. 2011, Chu *et al*. 2002, Jens *et al*. 2017).

A further attractive characteristic of the DBD plasma at atmospheric pressure is that it can be used to modify or activate surfaces of a wide range of materials, from polymers, textile fibres to biological tissues, without damaging them (Kostic *et al*. 2009, Pertile *et al*. 2010, Mihailovic *et al*. 2011). To generate the DBD plasma we used a home-made device built at the Faculty of Physics, University Belgrade, Fig. 3. The DBD is assembled in a chamber with nitrogen gas injected into the discharge volume (6 dm^3min^{-1}) through ten equidistant holes to ensure homogeneous gas flow. MNFC films were treated for 0 s, 30 s and 60 s, respectively. The device was operated at 60 kV **[Katarina, please check this value – you had 60 V at one crazy time!]** and 300 electric field pulses per second (Hz) for the prescribed durations of time.

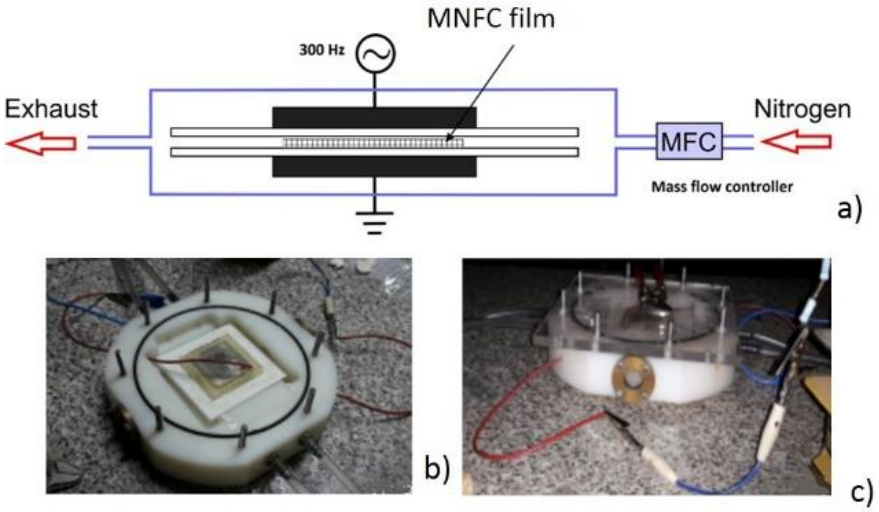

Fig. 3. DBD device with two electrodes and sample placed between them: a) schematic illustration of DBD plasma devise, b) plasma chamber housing the sample placed 1 mm from the upper electrode, and c) closed plasma set up with glass lid placed above the top of the upper electrode.

Determination of free surface energy (FSE) components

For the evaluation of any change in free surface energy of MNFC films arising from nitrogen plasma treatment, the contact angle (CA) is determined.

Most liquids are rapidly spreading on a high energy surface, and so a representative contact angle (CA) cannot be readily measured, Schultz and coworkers (Schultz *et al*. 1977) developed a method where CA can be measured by submerging the surface in one liquid and using a second liquid to measure the contact angle. In this case a hydrocarbon n-hexadecane is used as the submerging liquid having the purely dispersive liquid-vapour surface tension of γ_{LV}^{h} = 27.4 mJ.m^{-2}, much lower than the expected surface free energy of the MNFC samples, and water as the contact angle liquid with the highly polar liquid-vapour surface tension γ_{LV}^{w} = 72.8 mJ.m^{-2} (Hansson *et al*. 2011). A sessile drop of water is lowered into contact with the horizontal film immersed under hexadecane using a precise pipette delivering 70 µl of liquid and the progressive change in drop shape due to the change in CA recorded with a Nikon camera (D5000) in time steps of 1 ms. The CA of water is also recorded separately to represent the print challenge of a highly polar ink (Özkan *et al*. 2016, Dimic-Misic *et al*. 2015). For each given MNFC sample and given liquid data variation is within 10 %. The identification of contact line geometry and evaluation of CA uses numeric software tools, as presented visually in Fig. 4. For a parallel optimal method for polar FSE determination with water alone, the Girifalco and Good approach (GiRifalco and Good 1957), combined with the Neumann equation of state was used. This latter allowed the polar contribution to FSE be estimated and thus can be added to the formerly measured dispersive component. Each measurement was conducted five times. For each given MNFC sample, the relative error of measured FSE was shown to be ~ 10 %.

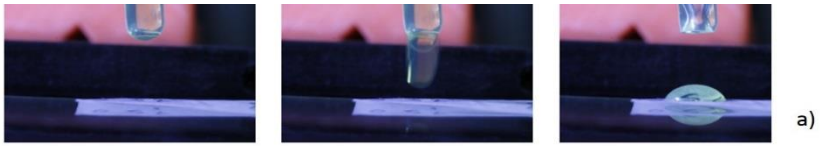

a)

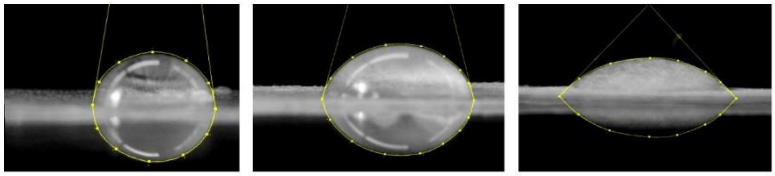

b)

Fig. 4 Set-up for evaluating water CA under n-hexadecane with high speed camera, (Nikon D5000): a) images of films on camera viewfinder, and b) image processing of drop spreading (see also Fig. 8).

Surface topography

Plasma action on the film surface can lead to a degree of debonding of fibrils as well as electrostatic charging and potential for subsequent additional moisture adsorption. Such changes can lead to re-conformation of the surface, even though no mechanical forces have been applied (Kostic *et al*. 2009, Chu *et al*. 2002). The change in topography of the MNFC films was investigated by Atomic Force Microscopy (AFM) (Veeco Instruments, model Dimension V). Using a MultiMode 8 with Bruker NanoScope V controller. Each MNFC film sample was dry-cast onto a Mica support for AFM imaging. Micrographs were obtained in trapping mode under ambient conditions, using TAP 300 tips (resonant frequency 300 kHz, line force being kept constant at 40 Nm^{-1} and the AFM images were processed and analysed with the Bruker NanoScope Analysis 1.5 software.

Mechanical properties

Mechanical properties of the MNFC films were measured by an MTS 400/M vertical tensile tester equipped with a 20 N load cell. The instrument was controlled by a TestWorks 4.02 program. Specimen strips with dimensions of 60 x 15 mm^2 were clipped from the MNFC films with a lab paper cutter (Ghazaleh *et al*. 2017). The thickness of the strips was separately measured with an L&W micrometer SE 250. The gauge length was 40 mm and the testing velocity was 0.5 $mm.min^{-1}$. The results are presented as an average value obtained from five parallel specimens.

Surface chemical composition

Surface composition of the MNFC films was evaluated with X-ray photoelectron spectroscopy (XPS), using a Kratos AXIS Ultra electron spectrometer, with monochromatic Al Kα irradiation at 100 W and under charge neutralisation. Both the untreated MNFC films and plasma treated specimens were analysed. For the preparation, samples were pre-evacuated for at least 12 h, after which wide area survey spectra (for elemental analysis) as well as high resolution regions of C1s and O1s were recorded from several locations, and an in-situ reference of pure cellulose was recorded for each sample batch (Johansson and Campbell 2004). With the parameters used, XPS analysis was recorded on an area of 1 mm^2 and the analysis depth is less than 10 nm. Carbon high resolution data were fitted using CasaXPS and a four component Gaussian fit tailored for celluloses.

MNFC suspension rheology

The rheological properties of MNFC suspensions were analysed at 2 w/w% concentration at 23 °C with an Anton Paar MCR 300 shear rheometer. The dynamic viscosity (η) was determined by steady shear-flow measurements, using the bob-in-cup geometry (Mohtaschemi *et al*. 2014). Due to the potential for wall depletion (apparent slip) and thixotropic behaviour of MNFC suspensions, the "bob" was a four-bladed vane spindle with a diameter of 10 mm and a length of 8.8 mm, while the metal cup had a diameter of 17 mm. A pre-shear protocol was applied using constant shear at a shear rate $\dot{\gamma}$ = 100 s^{-1} for 5 min, followed by a rest time of 10 min prior to recording the flow curves. Flow curves of MNFC suspensions were constructed under decreasing shear rate of $\dot{\gamma}$ = 1 000–0.01 s^{-1}, with a logarithmic spread of data points (Dimic-Misic *et al*. 2013). To distinguish the MNFC suspensions in terms of their colloidal interactions as an effect of hydrolysis time, aspect ratio, crystallinity and friction between nanofibrils during the flow (Pääkkonen *et al*. 2015, Dimic-Misic *et al*. 2017), the log-log plot flow curves were fitted to a power law according to the Oswald-de Waele empirical model, as shown in Equation (1)

$$\eta = k\,\dot{\gamma}^{\,1-n} \quad (1)$$

where k and n are the flow index and the power-law exponent, respectively: $n = 1$ indicates a Newtonian fluid and $n > 1$ indicates pseudo-plastic (shear thinning) behaviour.

The Herschel-Bulkley equation describes the dynamic yield stress τ_d^0 as

$$\tau = \tau_d^0 + k\dot{\gamma}^n \quad (2)$$

where τ is the shear stress.

Printing

The photovoltaic (PV) inkjet printing inks (IP) contain a complex mix of materials, solvent and surfactants that keep the p-type and n-type components de-mixed (Hashmi *et al*, Özkan *et al*. 2015). A piezoelectric laboratory scale drop-on-demand (DoD) materials inkjet printer (Dimatix 2831-DMP) was used to test the printability of the plasma treated MNFC films (Dimic.Misic *et al*. 2015). The solvent of the IP ink is 3-methoxypropionitrile, which is highly polar and non-volatile (boiling point 164 ºC), viscosity 1.2 mPa.s and density 0.937 gcm^{-3}, as stated by the supplier, Sigma Aldrich. The surface tension measurement was performed on the ink with an optical tensiometer (CAM 200 from KSV instruments) in pendant drop mode, giving a value of 29.2 $mN.m^{-1}$ ($mJ.m^{-2}$)

RESULTS AND DISCUSSION

The *rheological properties* of the MNFC suspensions are given in Table 2, showing the change in dewatering, dynamic yield point and flocculation/water trapping gel-like structure (consistency coefficient, *k*) and shear thinning properties (index, *n*, expressed as the positive difference *n* - 1) and change in fibre morphology expressed as the fines content using the dynamic drainage jar (DDJ).

It is clear to see that with increase in enzymatic hydrolysis time, dewatering decreases as fibrils become thinner and smaller, and suspensions become more gel-like rheologically (Rantanen *et al*. 2015). At the same time, crystallinity of fibrils increases and water trapping structure/flocculation within the matrix with contrasting increased mobility in the flow regime once the structure is broken (Pääkkonen *et al*. 2015). The dynamic yield point, the minimum stress needed to be induced to set the suspension into flow increases as the suspensions become more gel like, but, also, breakage of that suspension induces greater shear thinning as fibrils are smaller and more crystalline, orienting easily in the flow direction (Pääkkonen *et al*. 2015, Hubbe *et al*. 2017).

Table 2. Properties of MNFC suspensions

MNFC suspensions properties					
Enzymatic treatment time / min	WRV / cm^3g^{-1}	Yield point, τ_d^0 / Pa	Consistency coefficient, k / $Pa.s^{-n}$	Shear thinning coefficient, $\|(1-n)\|$	DDJ fines value / %
0	1.25	34.12	431.23	0.82	93.8
30	1.61	47.34	241.3	0.81	88.8
60	1.83	54.23	139.65	0.81	79.5
90	2.19	68.45	89.67	0.81	62.4
120	2.55	91.45	69.45	0.84	27.0
150	2.85	438.34	57.23	0.84	21.0
180	2.98	29.82	35.15	0.86	11.8
210	3.33	19.64	19.67	0.86	9.6
240	3.37	12.67	14.34	0.87	6.5
270	3.32	8.99	9.97	0.89	1.5
300	3.34	4.74	5.45	0.91	0.2

The *mechanical and optical* properties of MNFC films are presented in Table 3, where it is evident that the sheet density of the films increases with increase in hydrolysis time, while the packing density of the smaller crystalline particles increases. The permeability of those films created with the finer nanofibrils obtained after 120 min hydrolysis in turn falls rapidly, and it was not possible to measure using air flow techniques. The light scattering coefficient decreases also as the packing density is increased and the amorphous parts of the cellulose fibres were reduced, while, due also to higher packing density, the elasticity modulus increases, showing that films had improved strength.

284 Table 3. Mechanical and optical properties of MNFC films

285

Film properties					
Enzymatic treatment time / min	film weight / gm^{-2}	density / gcm^{-3}	permeability / $\mu m(Pa\ s)^{-1}$	light scattering coefficient / m^2kg^{-1}	E-Modulus / GPa
0	73.91	0.637	69.86	37.43	2.53
30	76.12	0.794	9.96	22.83	4.16
60	71.35	0.910	1.06	16.12	5.12
90	72.31	1.016	NA	9.94	7.02
120	70.53	1.090	NA	6.93	8.59
150	70.81	1.127	NA	5.81	9.13
180	69.57	1.145	NA	4.48	8.95
210	71.08	1.178	NA	3.74	11.26
240	70.10	1.179	NA	3.08	9.17
270	71.18	1.226	NA	3.11	9.76
300	65.27	1.187	NA	3.31	10.03

286

287 *Roughness* colour contour and profile plots of the surface of MNFC/30/150/300 films before and after
288 plasma treatment are presented in Fig. 5. Before plasma treatment, the roughness of the films is
289 directional, being different in in the two measured directions (red and blue profile lines). The map for
290 MFC/30/ indicates that there are voids present between 1-2 µm wide, while in the case of MFC/300/ the
291 surface is flatter with less voids and of much smaller size. This means that the degree of enzyme
292 hydrolysis directly increases the resulting smoothness due to the ever finer fibrillar elements produced,
293 as the crystalline parts are separated due to breakdown of the amorphous constituent. After plasma

treatment, the amorphous material containing surfaces, e.g. MNFC/30/, are also seen to become relatively rougher than the highly hydrolysed crystalline films, e.g. MNFC/300/. The action of the plasma is to increase voyage in the courser particulate systems, as previously described, due to effects of charge, fibril debonding etc. (Jun *et al*. 2008). In MNFC/30/, it is possible to identify irregular both small and large voids appearing after plasma treatment, while in MNFC/300/, the surface of the film has almost no such jagged appearance with voids only smaller than 1 µm. Nitrogen plasma treatment, thus, obviously changes the morphology of the films, on both the micro (nano) and macro level, which is likely also to have an influence on the wetting behaviour and decrease in CA due to the increased meniscus liquid-solid wetting line length (Prysiazhnyi *et al*. 2013, Pertile *et al*. 2010).

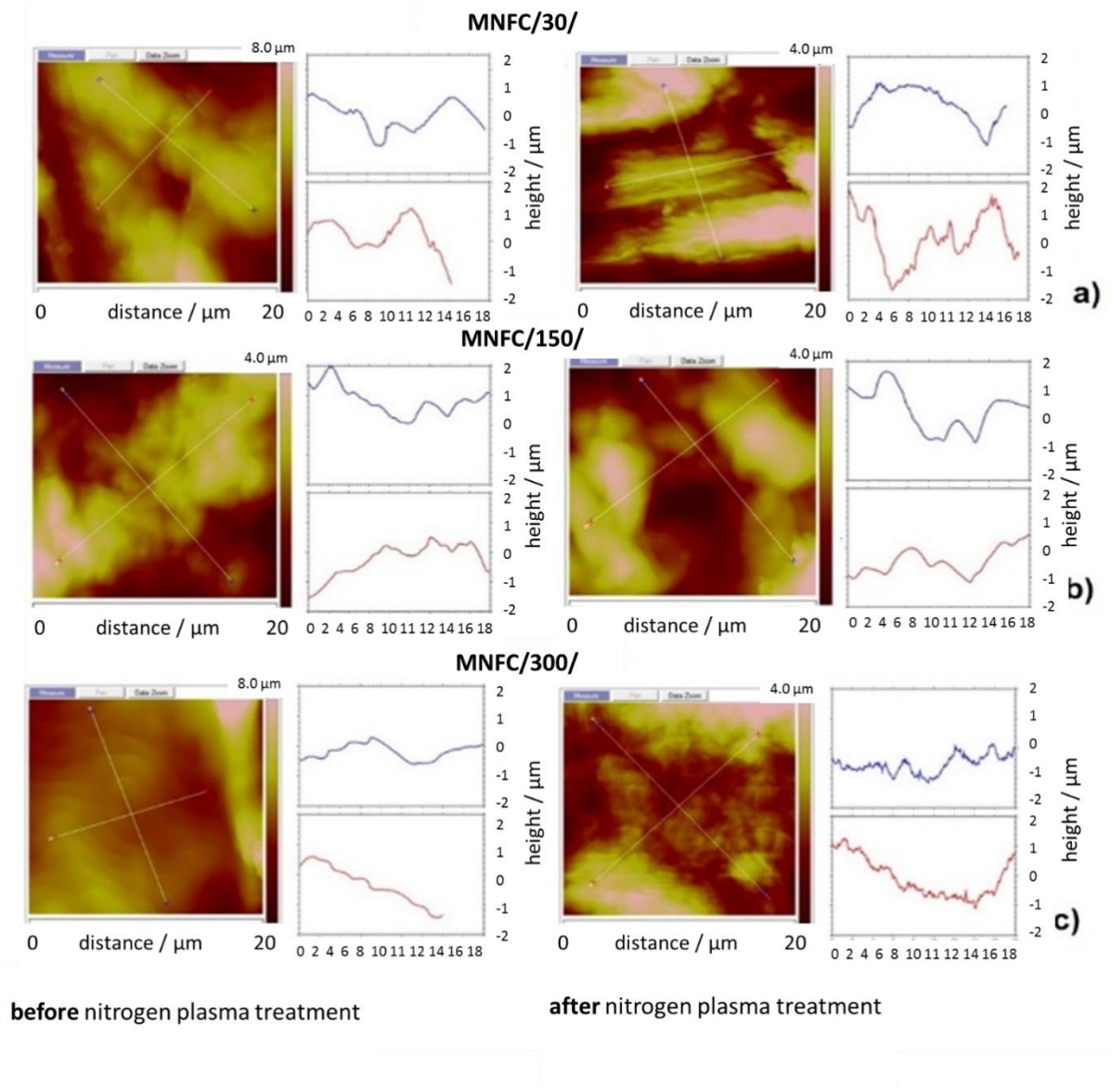

Fig. 5. Surface morphology and roughness of (a) MNFC/30/, (b) MNFC/150/ and (c) MNFC/300/ before and after nitrogen plasma treatment

The *surface chemical species* are revealed by the XPS spectra, from which the atomic % of C-C, C-O, O-C=O and N can be derived, Fig. 6. The effect of surface modification after nitrogen plasma can be clearly seen as the level of N attachment increasing as a function of the enzymatic removal of amorphous content (Johansson and Campbell 2004). The samples with increased crystalline proportion after longer enzymatic treatment nonetheless show similar C-C bond content. Similarly, with reduction of the

amorphous part with increased hydrolysis, the number of C-O groups decreases while C=O groups and other C and N containing groups are formed.

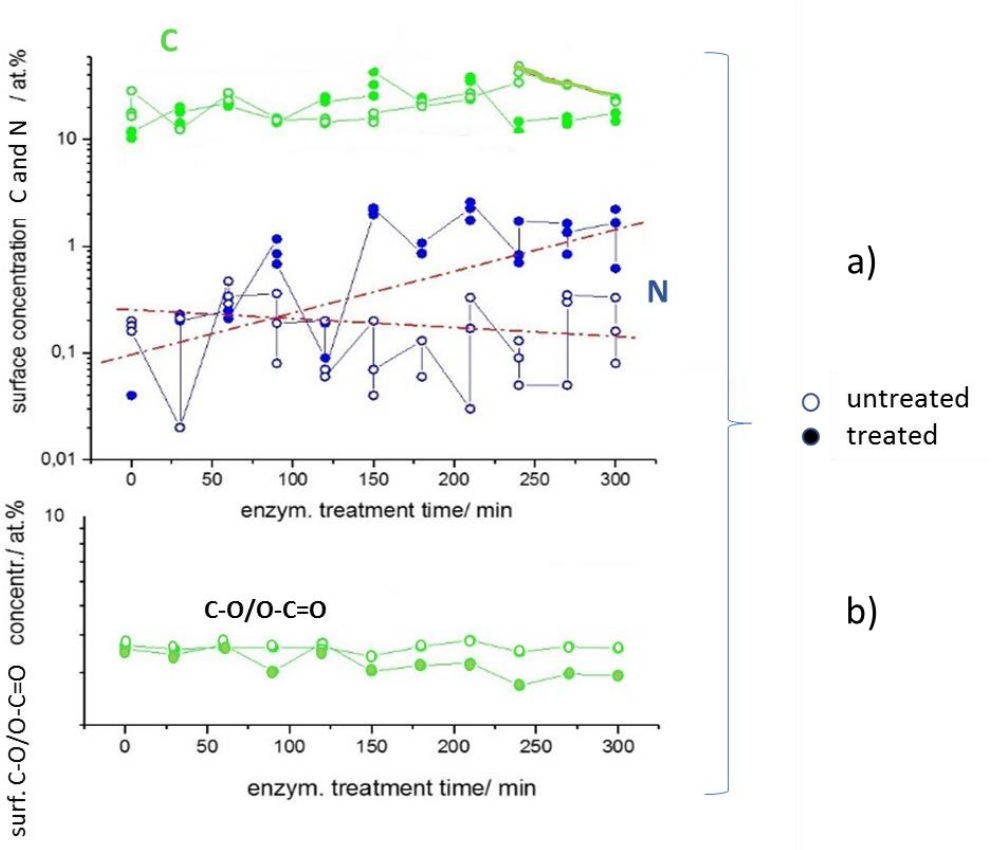

Fig. 6 Surface modification obtained through XPS data showing (a) increase in N atoms at constant carbon content, and (b) change in ratio of C-O/O-C=O groups.

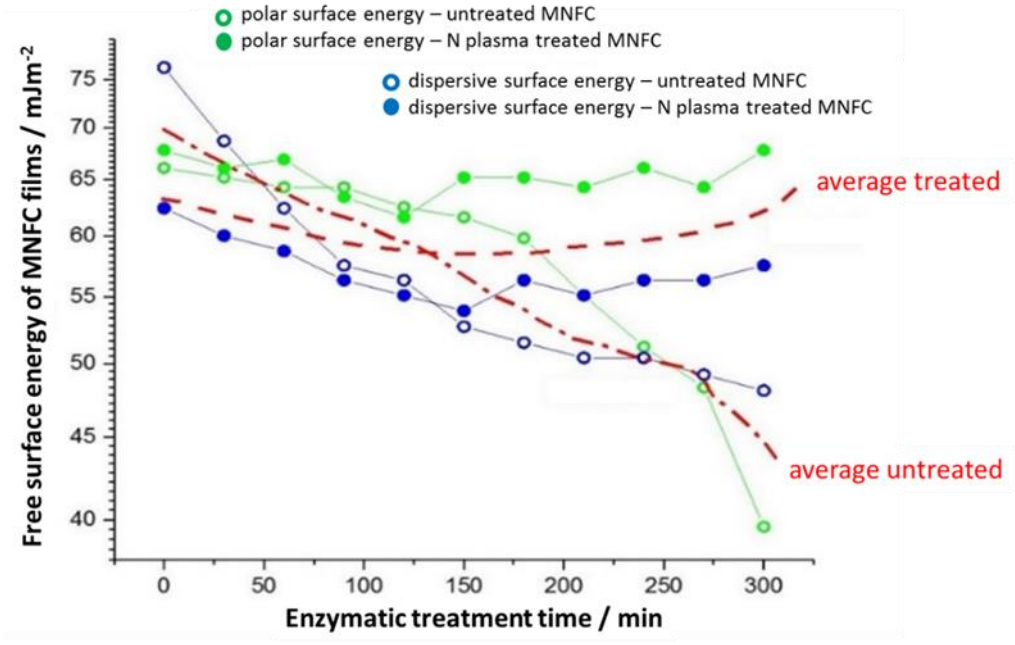

Fig. 7 Surface free energy (SFE) of MNFC films as a function of the treatment time (Table 1).

The results shown in Fig. 7 reveal that with the increase in enzymatic treatment of the raw material pulp there is a reduction of total FSE in the corresponding MNFC films in both polar and dispersive energy (green and blue unfilled symbols, respectively). A reversal of the decline in FSE as a function of enzymatic treatment can be observed resulting from nitrogen plasma treatment, showing compensating increases in both polar and dispersive measured components (green and blue filled symbols, respectively). Thus, an increase in wettability for water and n-hexadecane is reflected by a decrease in CA as the plasma treatment acts on the more crystalline samples (Johansson and Campbell *et al*. 2011). However, as the roughness is also seen to increase as a function of plasma treatment for the lower crystalline samples (less exposure to enzymatic breakdown), one would expect from the Wenzel model that the wettability would increase. That we see a recorded increase in n-hexadecane CA, and thus decrease in dispersive FSE, we can conclude that the action of the plasma discharge on the amorphous part is initially to reduce the dispersive energy component, and so likely act, at least partially, to breakdown first the amorphous content resulting in debonding and hence roughening (Hansson *et al*. 2011). This effective etching of amorphous parts of fibrils, is then replaced by the action of nitrogen attachment, such that the higher average FSE values regained in the more crystalline samples after plasma treatment are significantly higher than the theoretical FSE 59.4 $mJ.m^{-2}$ of cellulose, and this is achieved via the major contribution of the plasma-induced increase in polar component.

The increased contribution of the polar component in the FSE donated by the cationic N adsorption under plasma exposure is, therefore, expected to enhance the compatibility with the application of highly polar inks, especially if their components are anionic (Vanneste *et al*. 2017, Ma *et al*. 2010, Hoth *et al*. 2008). The images in Fig. 8 confirm this expectation, where the improved wetting of the surface by water as a function of plasma exposure time is paralleled by the greater pick-up (trapping) of ink colorant (Hoeng *et al*. 2016).

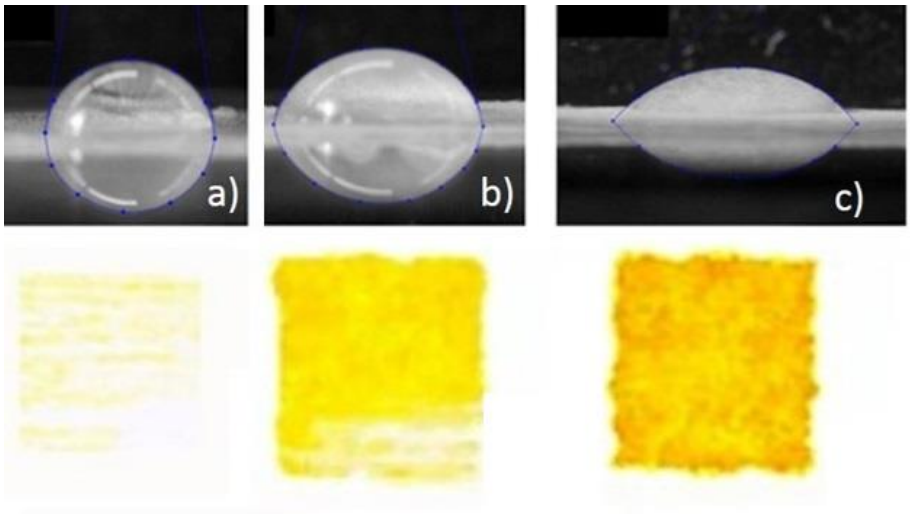

Fig. 8 IP ink printed on MNFC/300/ film showing the dependence on wettability of the surface after nitrogen plasma treatment (see also Fig. 4); lower water droplet CA on the film corresponds with a significant increase in print colour density: (a) untreated film, (b) plasma treated for 30 s and (c) plasma treated for 60 s.

SUMMARY AND CONCLUSIONS

Micro nanofibrillated cellulose films formed from aqueous suspension can be made stronger by pretreatment of the raw fibre using enzymatic hydrolysis. However, the wettability by ionic liquids, including functional inkjet printing inks, such as are used for printed electronics, solar cells etc., decreases as a result, limiting the use of such films in practice. Nitrogen plasma treatment, however, enables wettability by such formulations to be improved. The mechanism by which this occurs has been studied in this work presented in this paper and the following conclusions can be drawn:

- Total free surface energy increases with nitrogen plasma treatment of highly enzymatically hydrolysed fibrillar films (contact angle decreases), with a major increase in the polar component.

- Dispersive surface energy initially decreases on unpretreated or low enzymatic treated films on exposure to nitrogen plasma, whereas the polar surface energy component remains relatively unchanged.

    - This effect is related to the interaction of the nitrogen plasma with the amorphous cellulose component in the non-hydrolysed fibrils.

    - The dispersive energy component can once again be increased by exposure to nitrogen plasma in the case of the more crystalline fibrillar material derived from increased hydrolysis via enzymatic pretreatment.

- Highly ionic liquids, water and solvents typically used to disperse surfactant-containing organic-based inks, wet MNFC film better as hydrolysing pretreatment of fibres is increased and subsequent nitrogen plasma is applied.

Perspectives and future work arising from these findings include the need to study the origins of the surface roughening effect. Is this a random generation of surface disruption or is there a material transfer mechanism at play? The impact on the amorphous component by plasma treatment could offer a means to induce a phase change at the material surface. Similarly, other gas plasma treatments should be investigated in the longer term to understand whether the role of atomic substitution versus the application of energy discharge has the greater treatment potential.

Acknowledgements

The authors from the Institute of Physics Belgrade gratefully acknowledge financial help from the Ministry of Education, Science and Technological Development of the Republic of Serbia. The authors wish to thank to Prof. Milorad M. Kuraica from the Faculty of Physics, Laboratory for Plasma Physics, University of Belgrade, for his patience and skill in assisting with plasma experiments.

References

Afsahi G, Dimic-Misic K, Gane P, Budtova T, Maloney T, Vuorinen T (2018) The investigation of rheological and strength properties of NFC hydrogels and aerogels from hardwood pulp by short catalytic bleaching (H cat). Cellulose 25:1637-1655.

Catia R, Castro G, Rana S, Fangueiro R (2015) Characterization of physical, mechanical and chemical properties

of quiscal fibres: The influence of atmospheric DBD plasma treatment. Plasma Chemistry and Plasma Processing 35: 863-878.

Cernakova L, Stahel P, Kovacik C, Johansson K, Cernak M (2006) Low-Cost High-Speed Plasma Treatment of Paper Surfaces. In 9th TAPPI Advanced Coating Fundamentals Symposium, Turku, Finland: 8-10.

Chu PK, Chen JY, Wang LP, Huang N (2002) Plasma-surface modification of biomaterials. Materials Science and Engineering: R: Reports 36: 143-206.

Dimic-Misic K, Puisto A, Gane P, Nieminen K, Alava M, Paltakari J, Maloney T (2013) The role of MFC/NFC swelling in the rheological behavior and dewatering of high consistency furnishes. Cellulose 20: 2847-2861.

Dimic-Misic K, Karakoc A, Özkan M, Ghufran HS, Maloney T, Paltakari J (2015) Flow characteristics of ink-jet inks used for functional printing. Journal of Applied Engineering Science 13:207-212.

Galagan Y, Rubingh JEJ, Andriessen R, Fan CC, Blom PW, Veenstra SC, Kroon JM (2011) ITO-free flexible organic solar cells with printed current collecting grids. Solar Energy Materials and Solar Cells 95:1339-1343.

Girifalco LA, Good RJ (1957) A theory for the estimation of surface and interfacial energies. I. Derivation and application to interfacial tension. The Journal of Physical Chemistry 61 :904-909.

Hansson PM, Skedung L, Claesson PM, Swerin A, Schoelkopf J, Gane PAC, Rutland MW, Thormann, E (2011) Robust hydrophobic surfaces displaying different surface roughness scales while maintaining the same wettability. Langmuir 27:8153-8159.

Hashmi SG, Özkan M, Halme J, Dimic-Misic, K, Zakeeruddin SM, Paltakari J, Grätzel M, Lund PD (2015) High performance dye-sensitized solar cells with inkjet printed ionic liquid electrolyte. Nano Energy, 17: 206-215.

Hoeng F, Denneulin A, Bras J (2016) Use of nanocellulose in printed electronics: a review. Nanoscale. 8 :13131-54.

Hoth CN, Schilinsky P, Choulis SA, Christoph J. Brabec CJ (2008) Printing highly efficient organic solar cells. Nano Letters 8: (2008): 2806-2813.

Hubbe MA, Ferrer A, Tyagi P, Yin Y, Salas C, Pal L, Rojas O J (2017a) Nanocellulose in thin films, coatings, and plies for packaging applications: A review. BioResources, 12: 2143-2233.

Hubbe MA, Tayeb P, Joyce M, Tyagi P, Kehoe M, Dimic-Misic K, Pal L (2017b) Rheology of nanocellulose-rich aqueous suspensions: a review. BioResources 12: 9556-9661.

Jens V, Ennaert T, Vanhulsel A, Sels B (2017) Unconventional Pretreatment of Lignocellulose with Low-Temperature Plasma. ChemSusChem 10: 14-31.

Johansson LS, Campbell JM (2004) Reproducible XPS on biopolymers: cellulose studies. Surface and Interface Analysis, 36: 1018-1022.

Jun W, Fengcai Z, Bingqiang C (2008) The solubility of natural cellulose after DBD plasma treatment. Plasma Science and Technology 10: 743.

Jutila E, Koivunen R, Kiiski I, Bollström R, Sikanen T, Gane PAC (2018) Microfluidic Lateral Flow Cytochrome

P450 Assay on a Novel Printed Functionalized Calcium Carbonate-Based Platform for Rapid Screening of Human Xenobiotic Metabolism. Advanced Functional Materials: 1802793-1802803.

Kramer F, Klemm D, Schumann D, Heßler N, Wesarg F, Fried W, Stadermann D (2006) Nanocellulose polymer composites as innovative pool for (bio) material development. In Macromolecular Symposia, WILEY-VCH Verlag 244: 136-148.

Kostić M, Radić N, Obradović BM, Dimitrijević S, Kuraica MM, Škundrić P (2009). Silver-Loaded Cotton/Polyester Fabric Modified by Dielectric Barrier Discharge Treatment. Plasma Processes and Polymers, 6(1), 58-67.

Kumar P, Chand S (2012) Recent progress and future aspects of organic solar cells. Progress in Photovoltaics: Research and applications, 20: 377-415.

Ma H, Yip HL, Huang F, Jen AKY (2010) Interface engineering for organic electronics. Advanced Functional Materials 20:1371-1388.

Maloney TC (2015) Network swelling of TEMPO-oxidized nanocellulose. Holzforschung, 69: 207-213.

Mihailović D, Šaponjić Z, Radoičić M, Lazović S, Baily CJ, Jovančić P, Nedeljković J, Radetić M (2011) Functionalization of cotton fabrics with corona/air RF plasma and colloidal TiO2 nanoparticles. Cellulose, 18: 811-825,

Mohtaschemi M, Dimic-Misic K, Puisto A, Korhonen M, Maloney T., Paltakari J, Alava MJ (2014) Rheological characterization of fibrillated cellulose suspensions via bucket vane viscometer. Cellulose 21: 1305-1312.

Möller M, Leyland N, Copeland G, Cassidy M (2010) Self-powered electrochromic display as an example for integrated modules in printed electronics applications. The European Physical Journal Applied Physics, 5: 33205.

Özkan M, Dimic-Misic K, Karakoc A, Hashm, SG, Lund P, Maloney T, Paltakari J (2016) Rheological characterization of liquid electrolytes for drop-on-demand inkjet printing. Organic Electronics, 38: 307-315.

Pertile RA, Andrade FK, Alves J C, Gama M (2010) Surface modification of bacterial cellulose by nitrogen-containing plasma for improved interaction with cells. Carbohydrate Polymers, 82: 692-698.

Prysiazhnyi V, Kramar A, Dojcinovic B, Zekic A. Obradovic BM, Kuraica MM, Kostic M (2013) Silver incorporation on viscose and cotton fibers after air, nitrogen and oxygen DBD plasma pretreatment. Cellulose 20: 315-325.

Rantanen J, Dimic-Misic K, Kuusisto J, Maloney TC (2015) The effect of micro and nanofibrillated cellulose water uptake on high filler content composite paper properties and furnish dewatering. Cellulose 22: 4003-4015.

Schultz J, Tsutsumi K, Donnet JB (1977) Surface properties of high-energy solids: II. Determination of the nondispersive component of the surface free energy of mica and its energy of adhesion to polar liquids. Journal of Colloid and Interface Science, 59: 277-282.

Singh M, Haverinen HM, Dhagat P, Jabbour GE (2010) Inkjet printing—process and its applications. Advanced materials, 22: 673-685.

van de Vyver S, Geboers J, Jacobs PA, Sels BF (2011) Recent advances in the catalytic conversion of cellulose. ChemCatChem, 3: 82-94.

Yinhua Z, Fuentes-Hernandez C, Khan TM, Liu JC, Hsu J, Shim JW, Dindar A, Youngblood JP, Moon RJ, Kippelen B (2013) Recyclable organic solar cells on cellulose nanocrystal substrates. Scientific reports 3: 1536.

Figure

Click here to download Figure Figure 1.jpg

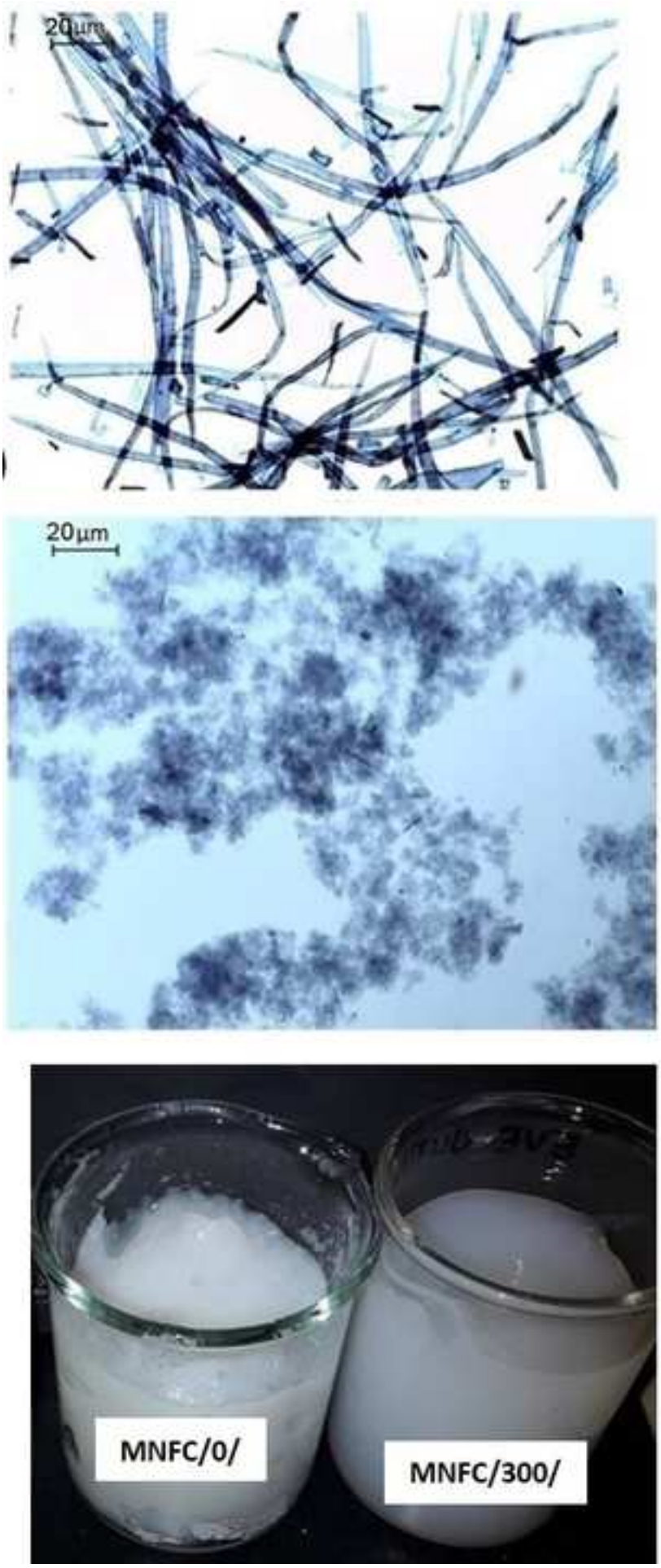

Figure

Click here to download Figure Figure.2.jpg

a)

b)

c)

Figure

Click here to download Figure Fig.3.jpg

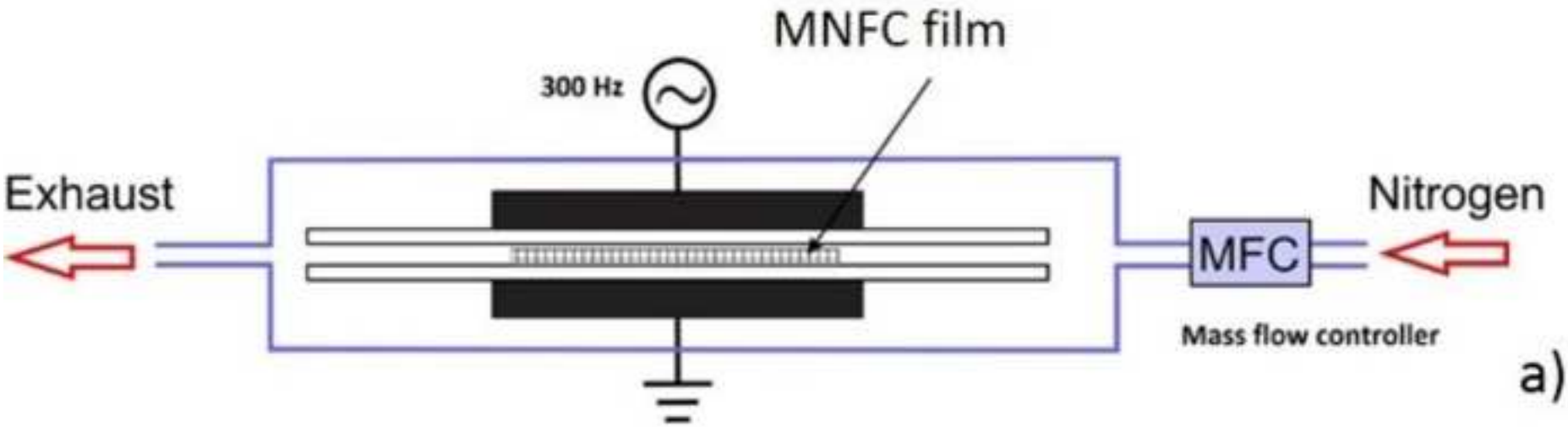

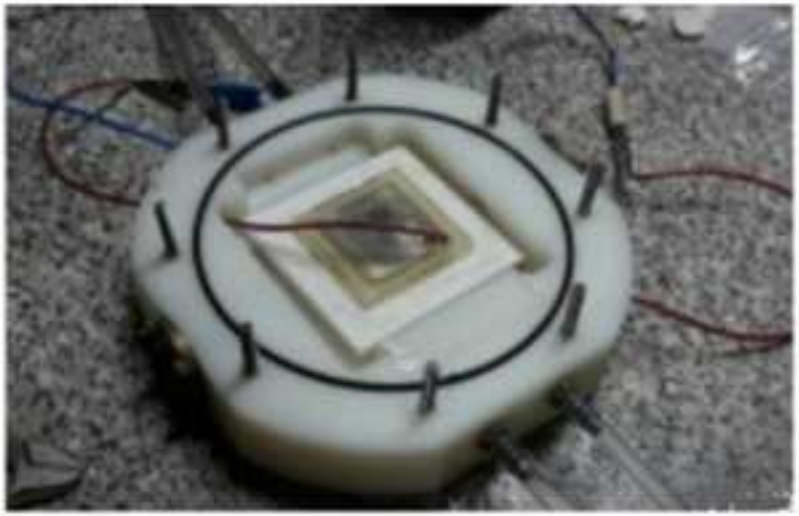

b)

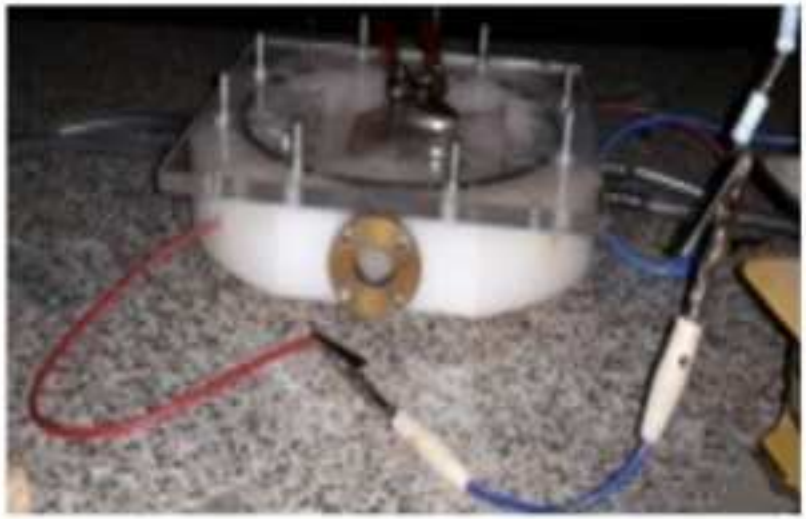

c)

Figure

Click here to download Figure Figure 4.jpg

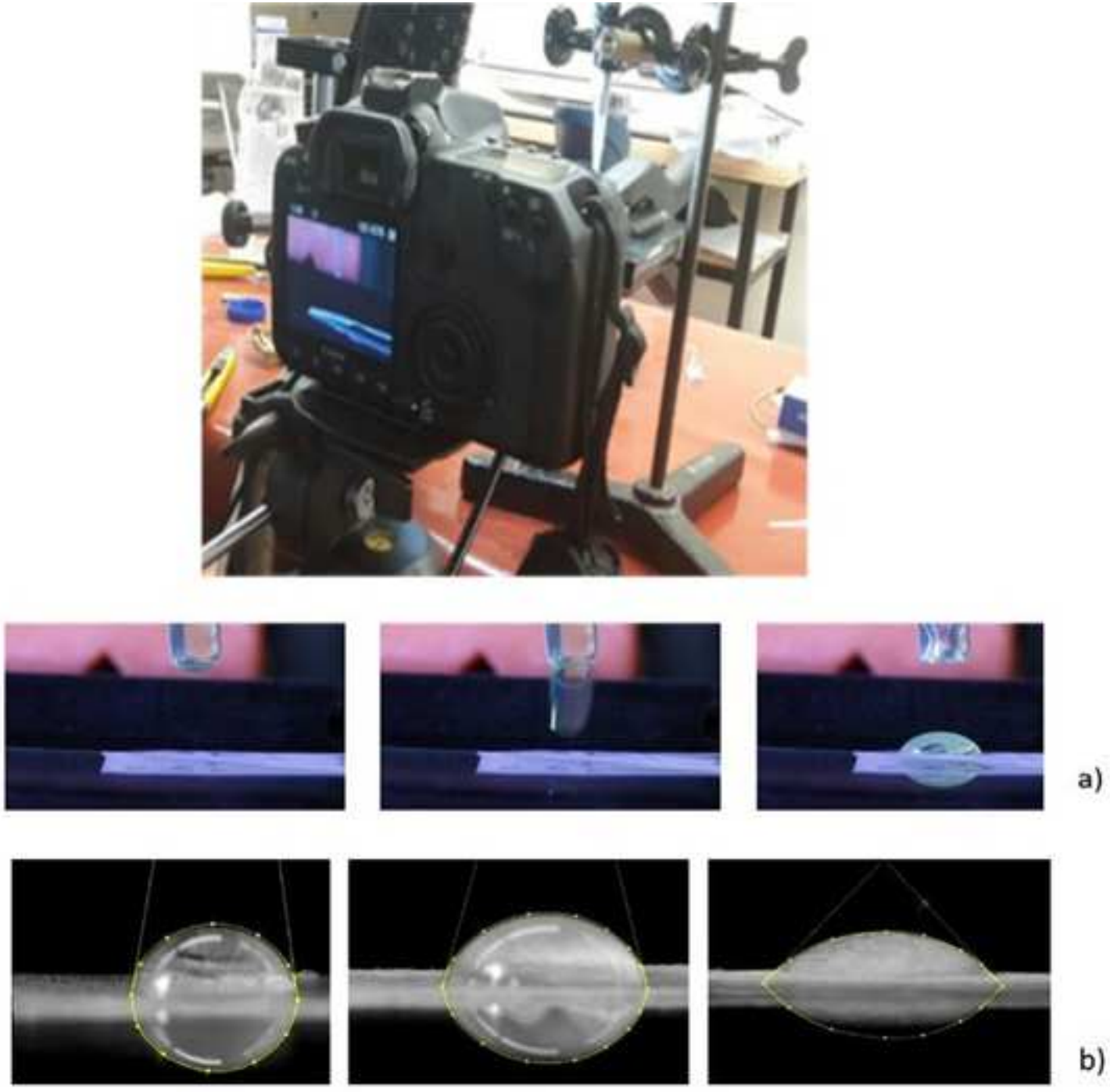

Figure

Click here to download Figure Figure 5.jpg

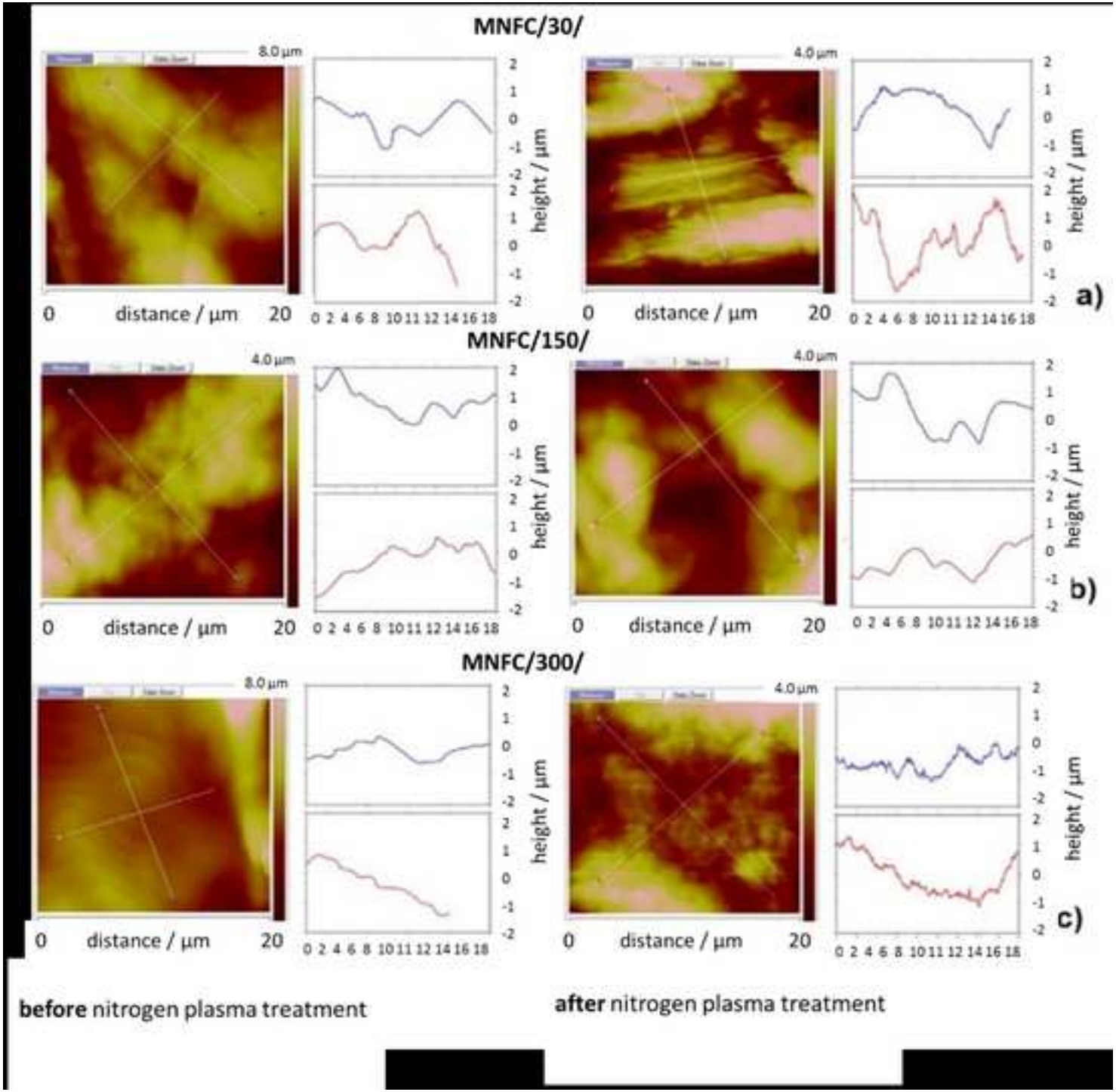

Figure

Click here to download Figure Figure.6.jpg

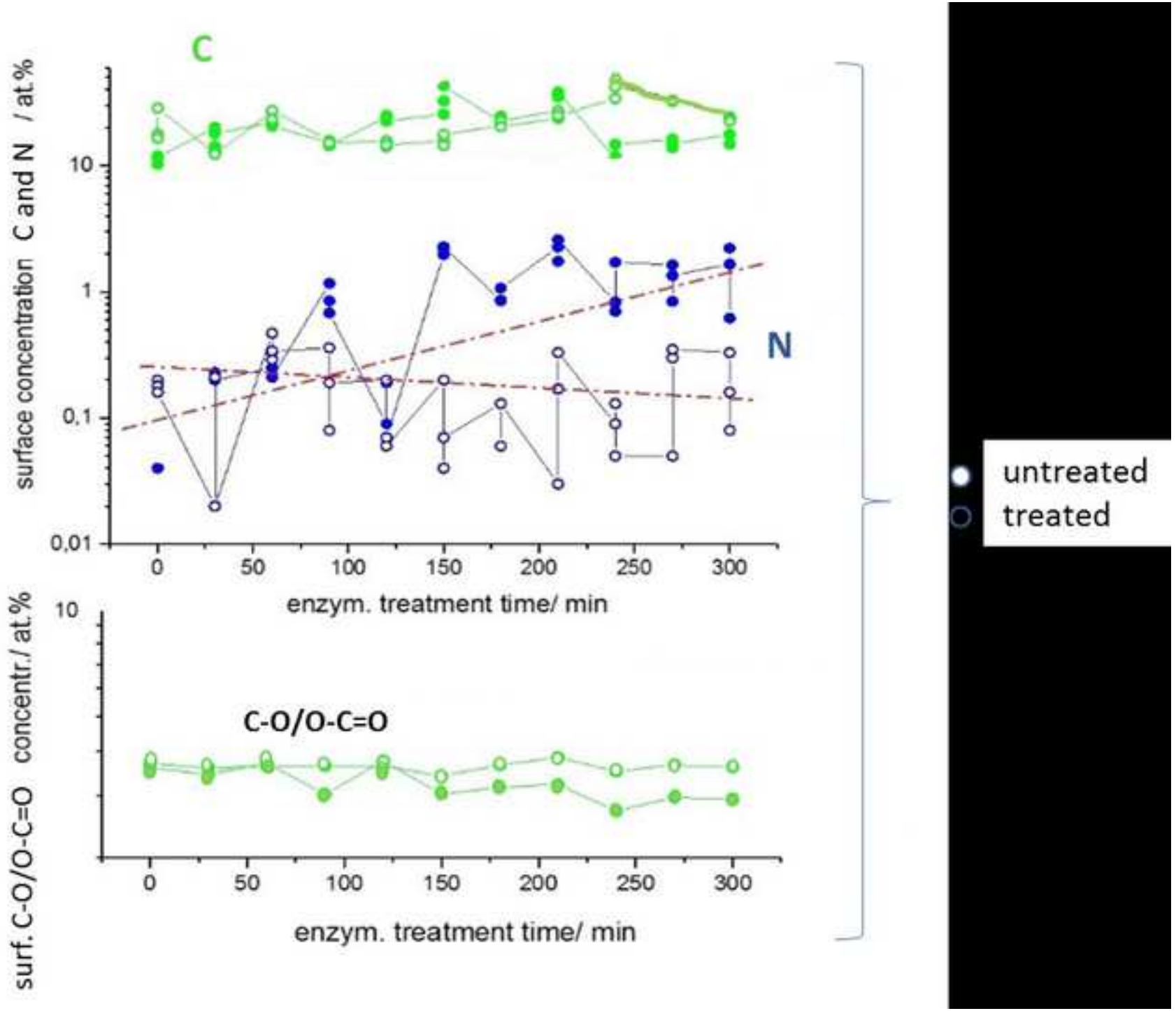

Figure

Click here to download Figure Figure 7.jpg

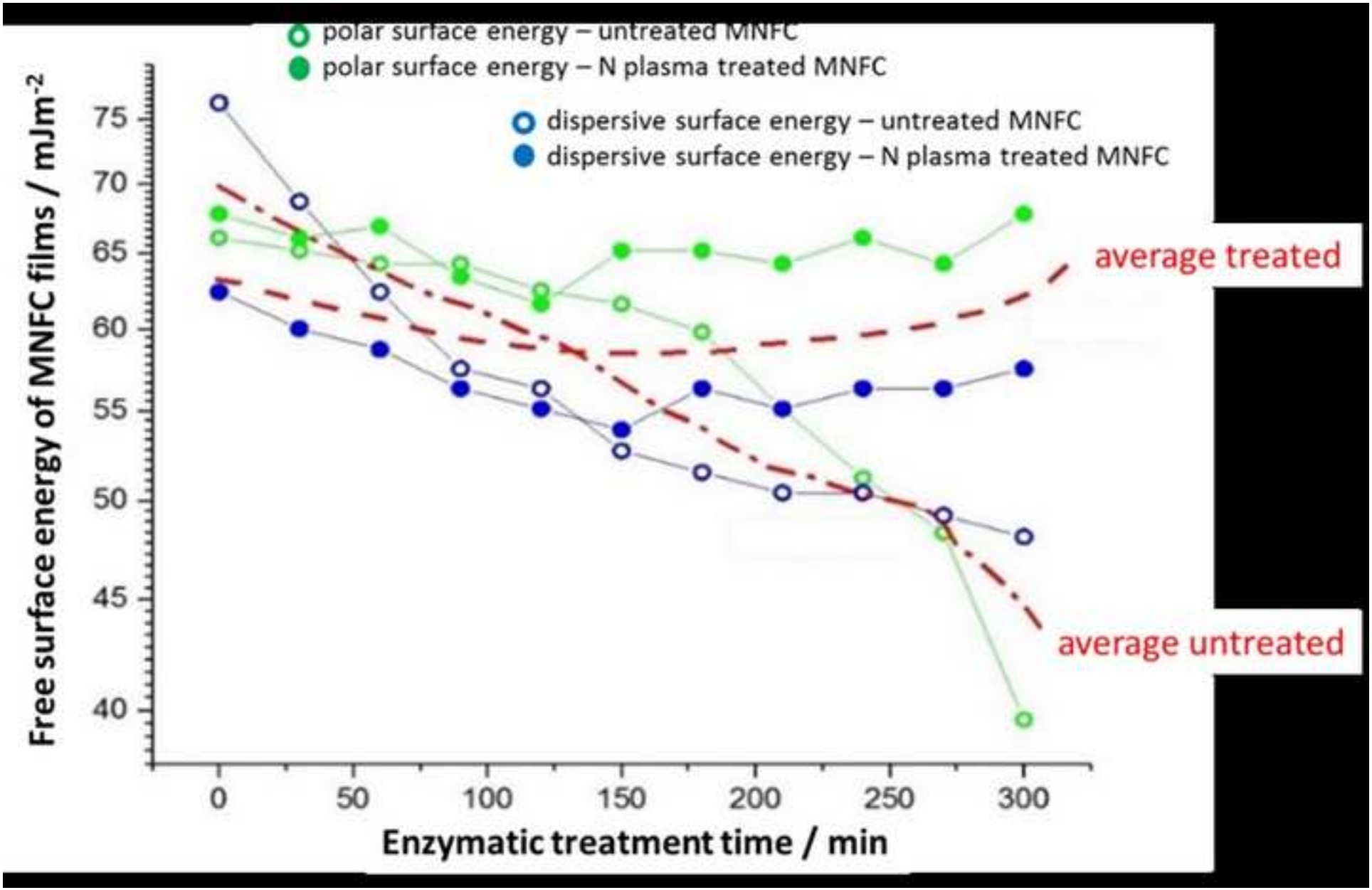

Figure

Click here to download Figure Fig.8.jpg

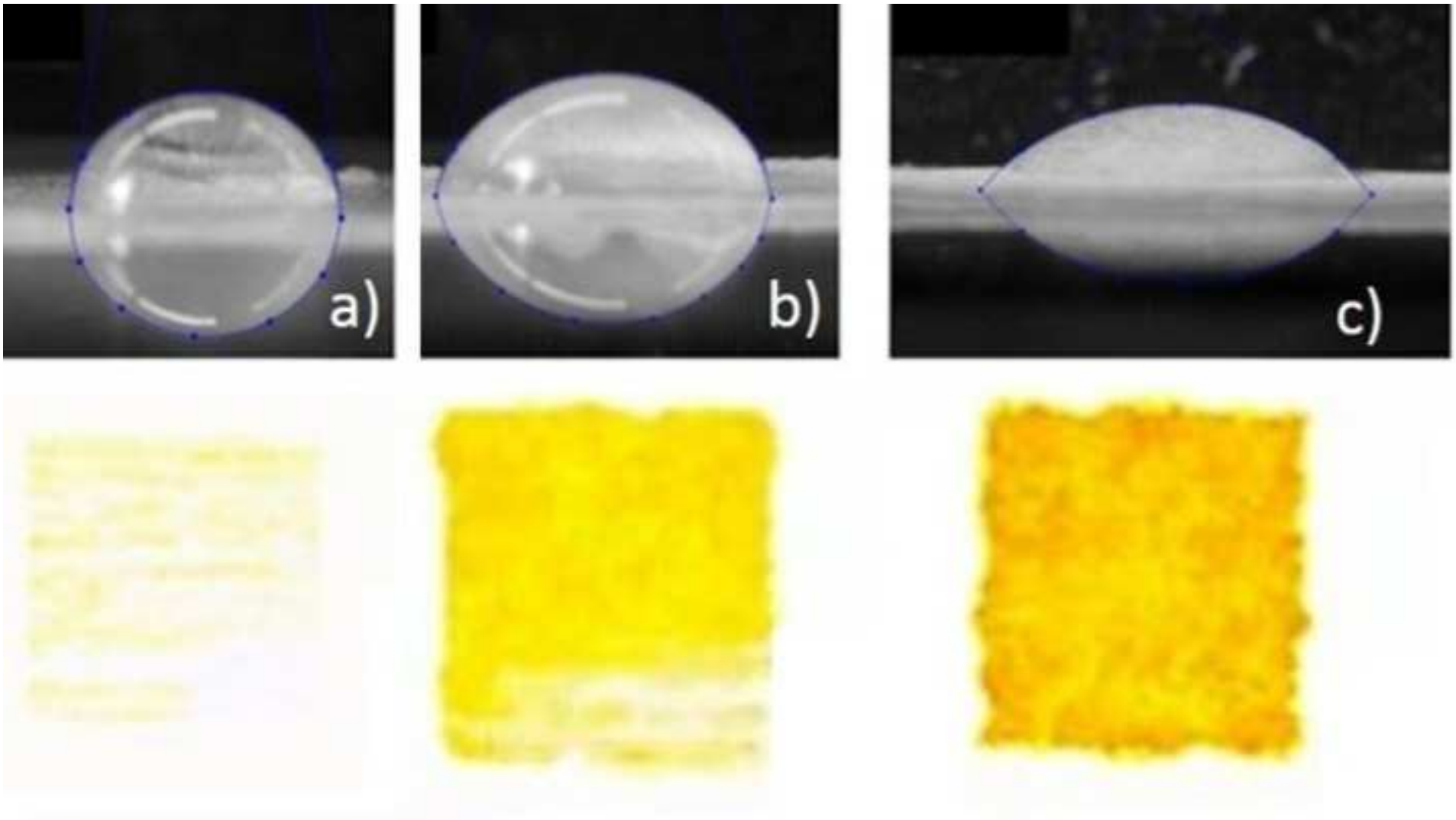

Enzymatic treatment time / min	0 (reference)	30	60	90	120	150	180	210	240	270	300
Sample label	MNFC /0/	MNFC /30/	MNFC /60/	MNFC /90/	MNFC /120/	MNFC /150/	MNFC /180/	MNFC /210/	MNFC /240/	MNFC /270/	MNFC /300/

MNFC suspensions properties					
Enzymatic treatment time / min	WRV / cm^3g^{-1}	Yield point, τ_d^0 / Pa	Consistency coefficient, k / $Pa.s^{-n}$	Shear thinning coefficient, $\|(1-n)\|$	DDJ fines value / %
0	1.25	34.12	431.23	0.82	93.8
30	1.61	47.34	241.3	0.81	88.8
60	1.83	54.23	139.65	0.81	79.5
90	2.19	68.45	89.67	0.81	62.4
120	2.55	91.45	69.45	0.84	27.0
150	2.85	438.34	57.23	0.84	21.0
180	2.98	29.82	35.15	0.86	11.8
210	3.33	19.64	19.67	0.86	9.6
240	3.37	12.67	14.34	0.87	6.5
270	3.32	8.99	9.97	0.89	1.5
300	3.34	4.74	5.45	0.91	0.2

Table

Film properties					
Enzymatic treatment time / min	film weight / gm^{-2}	density / gcm^{-3}	permeability / $\mu m(Pa\ s)^{-1}$	light scattering coefficient / m^2kg^{-1}	E-Modulus / GPa
0	73.91	0.637	69.86	37.43	2.53
30	76.12	0.794	9.96	22.83	4.16
60	71.35	0.910	1.06	16.12	5.12
90	72.31	1.016	NA	9.94	7.02
120	70.53	1.090	NA	6.93	8.59
150	70.81	1.127	NA	5.81	9.13
180	69.57	1.145	NA	4.48	8.95
210	71.08	1.178	NA	3.74	11.26
240	70.10	1.179	NA	3.08	9.17
270	71.18	1.226	NA	3.11	9.76
300	65.27	1.187	NA	3.31	10.03